

THE 24TH EUROPEAN MODELING & SIMULATION SYMPOSIUM

SEPTEMBER 19-21 2012

VIENNA, AUSTRIA



EDITED BY

FELIX BREITENECKER

AGOSTINO G. BRUZZONE

EMILIO JIMENEZ

FRANCESCO LONGO

YURI MERKURYEV

BORIS SOKOLOV

PRINTED IN RENDE (CS), ITALY, SEPTEMBER 2012

ISBN 978-88-97999-01-0 (Paperback)

ISBN 978-88-97999-09-6 (PDF)

© 2012 DIME UNIVERSITÀ DI GENOVA

RESPONSIBILITY FOR THE ACCURACY OF ALL STATEMENTS IN EACH PAPER RESTS SOLELY WITH THE AUTHOR(S). STATEMENTS ARE NOT NECESSARILY REPRESENTATIVE OF NOR ENDORSED BY THE DIME, UNIVERSITY OF GENOVA. PERMISSION IS GRANTED TO PHOTOCOPY PORTIONS OF THE PUBLICATION FOR PERSONAL USE AND FOR THE USE OF STUDENTS PROVIDING CREDIT IS GIVEN TO THE CONFERENCES AND PUBLICATION. PERMISSION DOES NOT EXTEND TO OTHER TYPES OF REPRODUCTION NOR TO COPYING FOR INCORPORATION INTO COMMERCIAL ADVERTISING NOR FOR ANY OTHER PROFIT - MAKING PURPOSE. OTHER PUBLICATIONS ARE ENCOURAGED TO INCLUDE 300 TO 500 WORD ABSTRACTS OR EXCERPTS FROM ANY PAPER CONTAINED IN THIS BOOK, PROVIDED CREDITS ARE GIVEN TO THE AUTHOR(S) AND THE CONFERENCE.

FOR PERMISSION TO PUBLISH A COMPLETE PAPER WRITE TO: DIME UNIVERSITY OF GENOVA, PROF. AGOSTINO BRUZZONE, VIA OPERA PIA 15, 16145 GENOVA, ITALY. ADDITIONAL COPIES OF THE PROCEEDINGS OF THE EMSS ARE AVAILABLE FROM DIME UNIVERSITY OF GENOVA, PROF. AGOSTINO BRUZZONE, VIA OPERA PIA 15, 16145 GENOVA, ITALY.

ISBN 978-88-97999-01-0 (Paperback)

ISBN 978-88-97999-09-6 (PDF)

THE 24TH EUROPEAN MODELING & SIMULATION SYMPOSIUM

September 19-21 2012, Vienna, Austria

ORGANIZED BY



DIME - UNIVERSITY OF GENOA



LIOPHANT SIMULATION



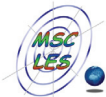
SIMULATION TEAM



IMCS - INTERNATIONAL MEDITERRANEAN & LATIN AMERICAN COUNCIL OF SIMULATION



DIMEG, UNIVERSITY OF CALABRIA



MSC-LES, MODELING & SIMULATION CENTER, LABORATORY OF ENTERPRISE SOLUTIONS



MODELING AND SIMULATION CENTER OF EXCELLENCE (MSCOE)



LATVIAN SIMULATION CENTER - RIGA TECHNICAL UNIVERSITY



LOGISIM



LSIS - LABORATOIRE DES SCIENCES DE L'INFORMATION ET DES SYSTEMES



MIMOS - MOVIMENTO ITALIANO MODELLAZIONE E SIMULAZIONE



MITIM PERUGIA CENTER - UNIVERSITY OF PERUGIA



BRASILIAN SIMULATION CENTER, LAMCE-COPPE-UFRJ



MITIM - MCLEOD INSTITUTE OF TECHNOLOGY AND INTEROPERABLE MODELING AND SIMULATION - GENOA CENTER



M&SNET - MCLEOD MODELING AND SIMULATION NETWORK



LATVIAN SIMULATION SOCIETY



ECOLE SUPERIEURE D'INGENIERIE EN SCIENCES APPLIQUEES

FACULTAD DE CIENCIAS EXACTAS. INGENIERIA Y AGRIMENSURA



UNIVERSITY OF LA LAGUNA



CIFASIS: CONICET-UNR-UPCAM



INSTICC - INSTITUTE FOR SYSTEMS AND TECHNOLOGIES OF INFORMATION, CONTROL AND COMMUNICATION



NATIONAL RUSSIAN SIMULATION SOCIETY



CEA - IFAC

TECHNICALLY CO-SPONSORED



IEEE - CENTRAL AND SOUTH ITALY SECTION CHAPTER

I3M 2012 INDUSTRIAL SPONSORS



CAL-TEK SRL



LIOTECH LTD



MAST SRL

I3M 2012 MEDIA PARTNERS



INDERSCIENCE PUBLISHERS - INTERNATIONAL JOURNAL OF SIMULATION AND PROCESS MODELING



INDERSCIENCE PUBLISHERS - INTERNATIONAL JOURNAL OF CRITICAL INFRASTRUCTURES



IGI GLOBAL - INTERNATIONAL JOURNAL OF PRIVACY AND HEALTH INFORMATION MANAGEMENT



HALLDALE MEDIA GROUP: MILITARY SIMULATION AND TRAINING MAGAZINE



HALLDALE MEDIA GROUP: THE JOURNAL FOR HEALTHCARE EDUCATION, SIMULATION AND TRAINING



EUROMERCI

EDITORS

FELIX BREITENECKER

VIENNA UNIVERSITY OF TECHNOLOGY, AUSTRIA
Felix.Breitenecker@tuwien.ac.at

AGOSTINO BRUZZONE

MITIM-DIME, UNIVERSITY OF GENOA, ITALY
agostino@itim.unige.it

EMILIO JIMENEZ

UNIVERSITY OF LA RIOJA, SPAIN
emilio.jimenez@unirioja.es

FRANCESCO LONGO

MSC-LES, UNIVERSITY OF CALABRIA, ITALY
f.longo@unical.it

YURI MERKURYEV

RIGA TECHNICAL UNIVERSITY, LATVIA
merkur@itl.rtu.lv

BORIS SOKOLOV

ST. PETERSBURG INSTITUTE FOR INFORMATICS AND AUTOMATION OF RAS, RUSSIA
sokol@iias.spb.su

**THE INTERNATIONAL MULTIDISCIPLINARY MODELING AND SIMULATION
MULTICONFERENCE, I3M 2012**

GENERAL CO-CHAIRS

*AGOSTINO BRUZZONE, MITIM DIME, UNIVERSITY OF GENOA, ITALY
YURI MERKURYEV, RIGA TECHNICAL UNIVERSITY, LATVIA*

PROGRAM CHAIR

FRANCESCO LONGO, MSC-LES, MECHANICAL DEPARTMENT, UNIVERSITY OF CALABRIA, ITALY

THE 24TH EUROPEAN MODELING & SIMULATION SYMPOSIUM, EMSS 2012

GENERAL CO-CHAIRS

*FRANCESCO LONGO, MSC-LES, UNIVERSITY OF CALABRIA, ITALY
FELIX BREITENECKER, VIENNA UNIVERSITY OF TECHNOLOGY, AUSTRIA*

PROGRAM CO-CHAIRS

*EMILIO JIMENEZ, UNIVERSITY OF LA RIOJA, SPAIN
BORIS SOKOLOV, ST. PETERSBURG INSTITUTE FOR INFORMATICS AND AUTOMATION OF RAS,
RUSSIA*

EMSS 2012 INTERNATIONAL PROGRAM COMMITTEE

MICHAEL AFFENZELLER, *UPPER AUSTRIAN UNIV. OF AS, AUSTRIA*
MAJA ATANASIJEVIC-KUNC, *UNIVERSITY OF LJUBLJANA, SLOVENIA*
ANDREAS BEHAM, *UPPER AUSTRIAN UNIV. OF AS, AUSTRIA*
ENRICO BOCCA, *SIMULATION TEAM, ITALY*
FELIX BREITENECKER, *TECHNICAL UNIVERSITY OF WIEN, AUSTRIA*
AGOSTINO BRUZZONE, *UNIVERSITY OF GENOA, ITALY*
JOHN CARTLIDGE, *UNIVERSITY OF BRISTOL, UK*
JUNWEI CAO, *TSINGHUA UNIVERSITY, CHINA*
YING CHENG, *BEIHANG UNIVERSITY, CHINA*
PRISCILLA ELFREY, *NASA-KSC, USA*
MARIA PIA FANTI, *POLYTECHNIC UNIVERSITY OF BARI, ITALY*
IDALIA FLORES, *UNIVERSITY OF MEXICO, MEXICO*
CLAUDIA FRYDMAN, *LSIS, FRANCE*
LUCA GAMBARDILLA, *IDSIA, SWITZERLAND*
WITOLD JACAK, *UPPER AUSTRIAN UNIV. OF AS, AUSTRIA*
EMILIO JIMÉNEZ, *UNIVERSITY OF LA RIOJA, SPAIN*
GORAZD KARER, *UNIVERSITY OF LJUBLJANA, SLOVENIA*
ANDREAS KÖRNER, *VIENNA UNIVERSITY OF TECHNOLOGY, AUSTRIA*
GABRIEL KRONBERGER, *UPPER AUSTRIAN UNIV. OF AS, AUSTRIA*
JUAN IGNACIO LATORRE BIEL, *UNIV. PÚBLICA DE NAVARRA, SPAIN*
FRANCESCO LONGO, *MSC-LES, UNIVERSITY OF CALABRIA, ITALY*
YONGLIANG LUO, *BEIHANG UNIVERSITY, CHINA*
MARINA MASSEI, *LIOPHANT SIMULATION, ITALY*
YURI MERKURYEV, *RIGA TECHNICAL UNIVERSITY, LATVIA*
LETIZIA NICOLETTI, *UNIVERSITY OF CALABRIA, ITALY*
MIGUEL MÚJICA MOTA, *UAB, SPAIN*
GASPER MUSIC, *UNIVERSITY OF LJUBLJANA, SLOVENIA*
GABY NEUMANN, *TECH. UNIV. APPL. SCIENCES WILDAU, GERMANY*
TUDOR NICULIU, *UNIVERSITY OF BUCHAREST, ROMANIA*
TUNCER ÖREN, *M&SNET, UNIVERSITY OF OTTAWA, CANADA*
MIQUEL ANGEL PIERA, *UAB, SPAIN*
CESAR DE PRADA, *UNIVERSIDAD DE VALLADOLID, SPAIN*
CHUMMING RONG, *UNIVERSITY OF STAVANGER, NORWAY*
BORIS SOKOLOV, *RUSSIAN ACADEMY SCIENCE, RUSSIA*
CHRYSOSTOMOS STYLIOS, *TECHNOLOGICAL EDUCATIONAL INSTITUTE OF EPIRUS, GREECE*
FEI TAO, *BEIHANG UNIVERSITY, CHINA*
ALBERTO TREMORI, *UNIVERSITY OF GENOA, ITALY*
WALTER UKOVICH, *UNIVERSITY OF TRIESTE, ITALY*
STEFAN WAGNER, *UPPER AUSTRIAN UNIV. OF AS, AUSTRIA*
ANN WELLENS, *UNAM, MEXICO*
THOMAS WIEDEMANN, *UNIVERSITY OF APPLIED SCIENCES AT DRESDEN, GERMANY*
STEPHAN WINKLER, *UPPER AUSTRIAN UNIV. OF AS, AUSTRIA*
GUENTHER ZAUNER, *VIENNA UNIVERSITY OF TECHNOLOGY, AUSTRIA*
LIN ZHANG, *BEIHANG UNIVERSITY, CHINA*
LEVENT YILMAZ, *AUBURN UNIVERSITY, USA*
XUESONG ZHANG, *JILIN UNIVERSITY, CHINA*
YING ZUO, *QUEEN'S UNIVERSITY, CANADA*

TRACKS AND WORKSHOP CHAIRS

DISCRETE AND COMBINED SIMULATION

CHAIR: GASPER MUSIC, UNIVERSITY OF LJUBLJANA, SLOVENIA

INDUSTRIAL PROCESSES MODELING & SIMULATION

CHAIR: CESAR DE PRADA, UNIVERSIDAD DE VALLADOLID, SPAIN

INDUSTRIAL ENGINEERING

CHAIR: FRANCESCO LONGO, MSC-LES, UNIVERSITY OF CALABRIA, ITALY

AGENT DIRECTED SIMULATION

CHAIRS: TUNCER ÖREN, UNIVERSITY OF OTTAWA, CANADA;
LEVENT YILMAZ, AUBURN UNIVERSITY, USA

PETRI NETS BASED MODELLING & SIMULATION

CHAIRS: EMILIO JIMÉNEZ, UNIVERSITY OF LA RIOJA, SPAIN;
JUAN IGNACIO LATORRE, PUBLIC UNIVERSITY OF NAVARRA, SPAIN

SIMULATION AND ARTIFICIAL INTELLIGENCE

CHAIR: TUDOR NICULIU, UNIVERSITY "POLITEHNICA" OF BUCHAREST, ROMANIA

WORKSHOP ON CLOUD MANUFACTURING

CHAIRS: PROF. LIN ZHANG, BEIHANG UNIVERSITY, CHINA;
PROF. FEI TAO, BEIHANG UNIVERSITY, CHINA, ENRICO BOCCA, MAST SRL, ITALY

SIMULATION OPTIMIZATION APPROACHES IN INDUSTRY, SERVICES AND LOGISTICS PROCESSES

CHAIRS: IDALIA FLORES, UNAM, MEXICO; MIGUEL MÚJICA MOTA, UNIVERSITAT AUTONOMA DE BARCELONA, SPAIN

HUMAN-CENTRED AND HUMAN-FOCUSED MODELLING AND SIMULATION

CHAIRS: GABY NEUMANN, TECHNICAL UNIVERSITY OF APPLIED SCIENCES WILDAU, GERMANY; AGOSTINO BRUZZONE, MITIM-DIME, UNIVERSITY OF GENOA, ITALY

WORKSHOP ON SOFT COMPUTING AND MODELLING & SIMULATION

CHAIRS: MICHAEL AFFENZELLER, UPPER AUSTRIAN UNIVERSITY OF APPLIED SCIENCES, AUSTRIA; WITOLD JACAK, UPPER AUSTRIAN UNIVERSITY OF APPLIED SCIENCES, AUSTRIA

WORKSHOP ON CLOUD COMPUTING

CHAIRS: ALBERTO TREMORI, SIMULATION TEAM, ITALY;
CHUNMING RONG, UNIVERSITY OF STAVANGER, NORWAY

SIMULATION APPROACHES IN LOGISTICS SYSTEMS

CHAIRS: MARIA PIA FANTI, POLYTECHNIC OF BARI, ITALY;
CHRYSOSTOMOS STYLIOS, TECHNOLOGICAL EDUCATIONAL INSTITUTE OF EPIRUS, GREECE; WALTER UKOVICH, UNIVERSITY OF TRIESTE, ITALY

MODELLING AND SIMULATION IN AND FOR EDUCATION

CHAIRS: MAJA ATANASIJEVIC-KUNC, UNIV. LJUBLJANA, SLOVENIA;; ANDREAS KÖRNER, VIENNA UNIV. OF TECHNOLOGY, AUSTRIA

MODELLING AND SIMULATION IN PHYSIOLOGY AND MEDICINE (COMMON TRACK EMSS-IWISH)

CHAIRS: MAJA ATANASIJEVIC-KUNC, UNIV. LJUBLJANA, SLOVENIA; FELIX BREITENECKER, VIENNA UNIV. OF TECHNOLOGY, AUSTRIA

GENERAL CO-CHAIRS' MESSAGE

WELCOME TO EMSS 2012!

One more year, after 23 successful editions, the 24th European Modeling and Simulation Symposium constitutes a reference for all the people involved in M&S, as a great forum to share, discuss, and advance on theories, practices and experiences in this field, bringing together people from Academia, Industry and Agencies.

Modeling and Simulation constitutes a transversal discipline, a knowledge more and more important in science and technology, with great interaction with other areas: among others, artificial intelligence, control theory, discrete event systems, industrial engineering, design, business, etc. to cite a small sample of the possibilities. Therefore tracks, special sessions and workshops of EMSS2012 mainly focus on these areas providing a summary of the main ongoing activities in the M&S domain.

Similarly, the plenary speeches of EMSS 2012 show some advanced views from the main experts in their respective specialities related to M&S. Furthermore, this year again, EMSS will be co-located with the 9th International Multidisciplinary Modelling & Simulation Multiconference, I3M2012, the ideal framework where sharing ideas and experiences and attending other thematic M&S international conferences (HMS 2012, MAS 2012, IMAACA 2012, DHSS 2012, IWISH 2012).

EMSS is historically called the traditional Simulation appointment in Europe only because of the locations where the symposium is usually held; as already happened in previous years, people from all over the world attend the symposium (the 2012 edition hosts representatives from 30 countries).

EMSS 2012 is held in the heart of Europe, Vienna; you are all welcome to enjoy the history and cultural background of this fantastic venue.

And, as tradition, all the members of the International Program Committee have worked very hard to assure the high scientific quality of the selected papers. Therefore, we would like to thank each member of the IPC as well as each reviewer. Last but not least, a special thanks goes to the authors, the success of EMSS is the main result of their work.

On behalf of all the people who have made it possible: welcome to EMSS2012.



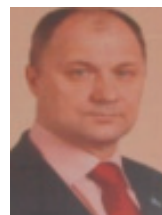
Francesco Longo
MSC-LES University of
Calabria, Italy



Felix Breitenecker
Vienna University of
Technology, Austria



Emilio Jimenez
University of La Rioja,
Spain



Boris Sokolov
St. Petersburg Institute
for Informatics and
Automation of RAS,
Russia

ACKNOWLEDGEMENTS

The EMSS 2012 International Program Committee (IPC) has selected the papers for the Conference among many submissions; therefore, based on this effort, a very successful event is expected. The EMSS 2012 IPC would like to thank all the authors as well as the reviewers for their invaluable work.

A special thank goes to all the organizations, institutions and societies that have supported and technically sponsored the event.

LOCAL ORGANIZATION COMMITTEE

AGOSTINO G. BRUZZONE, *MISS-DIPTM, UNIVERSITY OF GENOA, ITALY*

ENRICO BOCCA, *SIMULATION TEAM, ITALY*

ALESSANDRO CHIURCO, *MSC-LES, UNIVERSITY OF CALABRIA, ITALY*

FRANCESCO LONGO, *MSC-LES, UNIVERSITY OF CALABRIA, ITALY*

FRANCESCA MADEO, *UNIVERSITY OF GENOA, ITALY*

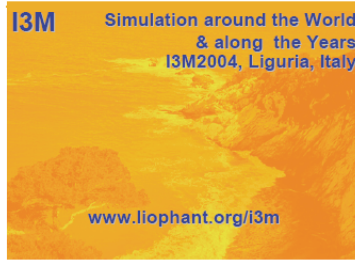
MARINA MASSEI, *LIOPHANT SIMULATION, ITALY*

LETIZIA NICOLETTI, *CAL-TEK SRL, ITALY*

ALBERTO TREMORI, *SIMULATION TEAM, ITALY*



This International Workshop is part of the I3M Multiconference: the Congress leading Simulation around the World and Along the Years



Index

Stability of the convex linear combination of fractional positive discrete-time linear systems Tadeusz Kaczorek	1
A simulation tool for high-fidelity modeling of complex logistical networks Reejo Mathew, Thomas W. Mastaglio, Andrew Lewis	6
On the incorporation of parameter uncertainty for inventory management David F. Muñoz, David G. Muñoz	15
Retrieving the performance overhead of synchronization mechanisms of various popular operating systems Michael Bogner, Johannes Schütz, Franz Wiesinger	21
Modeling and simulation based on inverse finite element method for unfolding large and thick blades of francis turbines Zhengkun Feng, Henri Champlaud, Michel Sabourin, Sebastien Morin	27
Optimization of production ramp-up by using a simulation for personnel requirements planning Gisela Lanza, Anna Sauer	32
Study on the description method of manufacturing capability based on description logics in cloud manufacturing Yongliang Luo, Lin Zhang, Fei Tao, Yongkui Liu, Lei Ren	38
An integrated binary-tabu search approach for the buffer allocation problem: an industrial case study Leyla Demir, Simge Yelkenci Kose, Semra Tunali, Deniz Tursel Eliiyi	44
Comprehensive protocol for artificial intelligence development Bruce L. Toy	50
A new practical approach to asset liability management for BASEL III and SOLVENCY II Vojo Bubevski	59
Spectral approach to reliability evaluation of flow networks Ilya Gertsbakh, Yoseph Shpungin	68
Analysis of the thread assignment behaviour of parallel programs on chip multiprocessors Michael Bogner, Markus Ematinger, Franz Wiesinger	74
The study of a deteriorating manufacturing system using simulation and response methodology Annie Francie Kouedeu, Jean-Pierre Kenne, Pierre Dejax, Victor Songmene	80
Simulating innovation adoption behavior: Lessons learned for modelers and programmers Christian Stummer, Elmar Kiesling	90
The high speed train interior noise reduction using multi-channel ANC system	97

Young Min Kim, Jong Il Bae, Kwon Soon Lee

Multi-actors distributed control systems: reinforcement signal by shannon's entropy Youcef Zennir, Denis Pomorski	103
Simulation of grass phenophases in Inner Mongolia, China Yurong Wei, Xuebiao Pan, Yanfang Cao, He Zhou	109
Capability of today's program verification: a practical approach for better quality and reliability in industrial applications Michael Bogner, Johannes Schiller, Franz Wiesinger	115
The cloud manufacturing services platform structure and key technologies research in the mould industry Songxin Shi, Youmin Rong, Guojun Zhang, Wang Shi	121
Monte Carlo ray-tracing approach to effectively design the ellipsoidal reflector of solar simulators Marco Bortolini, Mauro Gamberi, Alessandro Graziani, Riccardo Accorsi, Emilio Ferrari	129
Development and evaluation of visualization system of global container flow for international manufacturers Hisashi Takizawa, Hiromichi Akimoto, Kenji Tanaka, Jing Zhang	138
AEMOS: an agent-based electronic market simulator with ontology-services and social network support Maria João Viamonte, Virgínia Nascimento, Nuno Silva, Paulo Maio	144
A decision support system for intermodal transportation networks management Maria Pia Fanti, Giorgio Iacobellis, George Georgoulas, Chrysostomos Stylios, Walter Ukovich	150
Electric field and strain effects on surface roughness induced spin relaxation in silicon field-effect transistors Dmitri Osintsev, Oskar Baumgartner, Zlatan Stanojevic, Viktor Sverdlov, Siegfried Selberherr	156
Detecting thin bones and modeling COD skeleton Thordur Helgason, Rannveig Ása Gudundsdottir, Kristín Líf Valtýsdóttir, Kristinn Andersen	163
Analysis of agents' behavior in multiagent system Katerina Slaninova, Jan Martinovic, Pavla Drazdilova, Dominik Vymetal, Roman Sperka	169
Using graphic processors for highspeed simulations and other high performance computations Thomas Wiedemann	176
Project management games using high level architecture Ronald Ekyalimpa, Simaan Abourizk, Yasser Mohamed, Farzaneh Saba	180
Performance of earliest completion strategy in order sortation systems Fahrettin Eldemir, Elif Karakaya	189
Reconfigurable and layout-aware storage system for network-based simulation models in the simulator D³FACT Hendrik Renken, Felix Eichert, Markus Monhof	198

Towards the implementation of a handball player agent framework Joao Jacob, Rosaldo Rossetti, António Coelho, Rui Rodrigues	204
Modelling the effect of sugar refinery pollution in a rural area in central Mexico Ann Wellens, Julio González, Ricardo Torres-Jardón, Hugo Barrera	210
Enriching a DEVS meta-model with OCL constraints Stéphane Garredu, Evelyne Vittori, Jean-François Santucci, Dominique Urbani	216
Simulation optimisation and monitoring in tactical and operational planning of deliveries Galina Merkuryeva, Vitaly Bolshakov	226
Unsupervised learning approach to feature selection in biological data analysis Witold Jacak, Karin Proell	232
Improved linearity CMOS multifunctional structure using computational circuits Cosmin Popa	237
The impacts of data inaccuracy on retailer's perishable inventory Mert Bal, Alp Ustundag	241
Simulation for assessing security-based policies in import/export operations Pasquale Legato, Rina Mary Mazza	248
Traffic light simulation with time-varying traffic distribution at junctions Carmine De Nicola, Rosanna Manzo, Vincenzo Moccia, Vincenza Tufano	256
Variable interaction networks in medical data Stephan Winkler, Michael Affenzeller, Gabriel Kronberger, Michael Kommenda, Stefan Wagner, Witold Jacak, Herbert Stekel	265
Identification of patterns in microscopy images of biological samples using evolution strategies Daniela Borgmann, Julian Weghuber, Susanne Schaller, Jaroslaw Jacak, Stephan Winkler	271
Agent-monitored anticipatory multisimulation: a systems engineering approach for threat-management training Tuncer Oren, Levent Yilmaz	277
Motivation problems in the process of mass reduction through modelling and simulation Maja Atanasijevic-Kunc, Tina Sentocnik, Simon Tomažič, Jože Drinovec	283
Research on simplified modelling strategy for virtual commissioning Peter Hoffmann, Reimar Schumann, Talal M.A. Maksoud, Giuliano C. Premier	293
Optimal ambulance location, at University of Mexico, employing simulation Jose Vindel	303
Simulation of the operation of a metro station Jorge Andres Garcia, Idalia Flores	309
Automated verification of cardiovascular models with continuous integration tools Martin Bachler, Bernhard Hametner, Christopher Mayer, Johannes Kropf, Matthias Gira,	316

Siegfried Wassertheurer

Optimizing ventricular work: a matter of constraints	322
Bernhard Hametner, Stephanie Parragh, Christopher Mayer, Johannes Kropf, Siegfried Wassertheurer	
Optimal control strategies for low fuel consumption in a GDI engine under single and multiple injection	328
Michela Costa, Luigi Allocca, Paolo Sementa	
Production scheduling on multiple lines with shared resources	334
Francesco Costantino, Giulio Di Gravio, Fabio Nonino, Matteo Cappannoli, Tommaso Silvestri	
Enhanced confidence interpretations of GP based ensemble modeling results	340
Michael Affenzeller, Stephan M. Winkler, Stefan Forstenlechner, Gabriel Kronberger, Michael Kommenda, Stefan Wagner, Herbert Stekel	
Multidimensional modelling of the in-cylinder processes in a GDI engine	346
Alessandro Montanaro, Ugo Sorge, Francesco Catapano, Bianca Maria Vaglieco	
Automotive processes simulated by an ODE - PDE model	352
Nicola Pasquino, Luigi Rarità	
Evolution tracking in genetic programming	362
Bogdan Burlacu, Michael Affenzeller, Michael Kommenda, Stephan Winkler, Gabriel Kronberger	
On the analysis, classification and prediction of metaheuristic algorithm behavior for combinatorial optimization problems	368
Andreas Scheibenpflug, Stefan Wagner, Erik Pitzer, Bogdan Burlacu, Michael Affenzeller	
Cloud manufacturing platform architecture	373
Lei Ren	
Symbolic regression using tabu search in a neighborhood of semantically similar solutions	379
Gabriel Kronberger, Andreas Beham	
Customizing Code Of Devs Models According To User Requirements Using LSIS_DME	385
Maamar Hamri, Rabah Messouci	
Simulation of hydrocarbon sales services of the National University of Mexico for the scenario analysis that improves return on equity	390
Israel Andrade Canades, Citlalli Dorantes Bolanos	
Designing PID controller for 4th order system by means of enhanced PSO algorithm with discrete chaotic dissipative standard map	396
Michal Pluhacek, Roman Senkerik, Donald Davendra, Ivan Zelinka	
Operations by forklifts in warehouses	402
Aurelija Burinskiene	
Simulation of dynamically adaptive bandwidth allocation protocols using coloured Petri nets	408
Julija Asmuss, Viktors Zagorskis, Gunars Lauks	

Simulation models to support GALB heuristic algorithms and to evaluate multi objective performance index	414
Sergio Amedeo Gallo, Giovanni Davoli, Andrea Govoni, Riccardo Melloni, Gabriele Pattarozzi	
Using UWB for human trajectory extraction	428
Gonçalo Vasconcelos, Marcelo Petry, João Almeida, Rosaldo Rossetti, António Coelho	
Studies on the thermodynamical coupling of a machine tool and its environment using the object-oriented modelling approach of MODELICA	434
Matthias Rößler, Michael Landsiedl, Friedrich Bleicher, Christian Salvatori, Wolfgang Kastner, Felix Breitenecker	
Sequence of decisions on discrete event systems with structural alternative configurations	440
Juan Ignacio Latorre-Biel, Emilio Jiménez-Macías, Mercedes Pérez-Parte	
Automatic design based on the Petri nets paradigm	446
Juan Ignacio Latorre-Biel, Emilio Jiménez-Macías	
Decision making in the Rioja wine production sector	452
Juan Ignacio Latorre-Biel, Emilio Jiménez-Macías, Julio Blanco-Fernandez, Juan Carlos Sáenz-Díez	
Utilization of analytic programming for the stabilization of high order oscillations of chaotic logistic equation	458
Roman Senkerik, Zuzana Oplatkova, Ivan Zelinka, Donald Davendra, Michal Pluhacek	
Transformation algorithm from an alternatives aggregation Petri net to a compound Petri net. Two representations of an undefined Petri net with a non-empty set of exclusive entities.	465
Juan Ignacio Latorre-Biel, Emilio Jiménez-Macías	
Object-oriented multi-domain modelling of machine tools: a case study	471
Bernhard Heinzl, Michael Landsiedl, Niki Popper, Alexandros-Athanassios Dimitriou, Fabian Dür, Friedrich Bleicher, Christian Reinisch, Felix Breitenecker	
Dynamic analysis of a workpiece deformation in the roll bending process by FEM simulation	477
Tran Hoang Quan, Henri Champliaud, Zhengkun Feng, Dao Thien-My	
Process mining of production management data for improvement of production planning and manufacturing execution	483
Gasper Music, Primoz Rojec	
Achievements in results visualization with the computer numeric e-learning system MMT	489
Irene Hafner, Martin Bicher, Thomas Peterseil, Stefanie Winkler, Ursula Fitsch, Nicole Nagele, Wolfgang Wild, Felix Breitenecker	
Possibilities and limits of co-simulating discrete and continuous models via the building controls virtual test bed	495
Irene Hafner, Matthias Rössler, Bernhard Heinzl, Andreas Körner, Michael Landsiedl, Felix Breitenecker, Christian Reinisch	
Improvement of advanced mathematical skills and abilities using the computer algebra based e-learning system MAPLE T.A.	501

Stefanie Winkler, Andreas Körner, Vilma Urbonaite

Modelling and simulation e-learning set of hydraulic models	507
Martin Bicher, Ursula Fitsch, Maja Atanasijevic-Kunc, Nicole Nagele, Wolfgang Wild, Felix Breitenecker	
A modular architecture for modelling obesity in inhomogeneous populations in Austria with system dynamics - first step: a population model and how to integrate it in a disease model	513
Barbara Glock, Patrick Einzinger, Felix Breitenecker	
Data independent model structure for simulation within Vienna UT more space project	519
Benjamin Rozsenich, Salah Alkilani, Martin Bruckner, Stefan Emrich, Gabriel Wurzer	
About the integration of simulink into the matlab-based simulation and experiment server MMT	525
Andreas Körner, Irene Hafner, Martin Bicher, Stefanie Winkler, Ursula Fitsch	
Change of independent variable for state event detection in system simulation - evaluation with ARGESIM benchmarks	531
Felix Breitenecker, Horst Ecker, Bernhard Heinzl, Andreas Körner, Matthias Rößler, Niki Popper	
Developing a multihybrid system to simulate a university campus	537
Shabnam M. Tauböck, Felix Breitenecker, Dietmar Wiegand, Nikolas Popper, Gerald Hodecek	
A simulation model for analysing unmanned aerial vehicle flight paths	543
Halil Cicibas, Kadir Alpaslan Demir, Murat M. Gunal, Nafiz Arica	
Mathematical modelling for experimental archaeology: case studies for mechanical tools in Hallstatt salt mines	549
Bernhard Heinzl, Erik Auer, Benedikt Slowacki, Kerstin Kowarik, Hans Reschreiter, Niki Popper, Felix Breitenecker	
The translation of CPN into NETLOGO environment for the modelling of political issues: FUPOL project	555
Miguel Mujica, Miquel Angel Piera	
The effects of transit corridor developments on the healthcare access of medically fragile vulnerable populations	565
Rafael Diaz, Asad Khattak, Joshua Behr, Anna Jeng, Francesco Longo, Jun Duanmu	
Innovative C2 and simulation for crowdsourcing as force multiplier	573
Agostino Bruzzone, Henrique C. Marques, Giovanni Cantice, Michele Turi	
Serious games for developing intuition and agile thinking for decision makers	584
Agostino Bruzzone, Alberto Tremori, Claudia Baisini	
An advanced framework for inventory management in reverse logistics	591
Francesco Longo	
Simulation based analysis of a manufacturing system devoted to produce hazelnut based products	602
Agostino Bruzzone, Francesco Longo	

Modeling and simulation of a one-warehouse, N-retailer inventory System: reassessing a negative binomial approximation	610
Adriano O. Solis, Francesco Longo, Pietro Caruso, Elisa Fazzari	
FPGA, physics-based modeling of IGBT and PIN diode for hardware co-simulation of complex power electronic converters and systems	616
Philippos Aristidou, Patrick Palmer	
Authors' Index	626

STABILITY OF THE CONVEX LINEAR COMBINATION OF FRACTIONAL POSITIVE DISCRETE-TIME LINEAR SYSTEMS

Tadeusz Kaczorek

Bialystok University of Technology
 Faculty of Electrical Engineering
 Wiejska 45D, 15-351 Bialystok
kaczorek@isep.pw.edu.pl

ABSTRACT

The asymptotic stability of the convex linear combination of fractional positive discrete-time linear systems is addressed. Necessary and sufficient conditions for the asymptotic stability of the convex linear combination are established. The notion of diagonal dominant matrices for nonnegative real matrices is introduced. It is shown that the convex linear combination is asymptotically stable if its matrices are diagonal dominant.

Keywords: Asymptotic stability, convex linear combination, Metzler matrix, nonnegative matrix, positive systems

1. INTRODUCTION

A dynamical system is called positive if its trajectory starting from any nonnegative initial state remains forever in the positive orthant for all nonnegative inputs. An overview of state of the art in positive theory is given in the monographs (Farina and Rinaldi 2000, Kaczorek 2002). Variety of models having positive behavior can be found in engineering, economics, social sciences, biology and medicine, etc..

New stability conditions for positive discrete-time linear systems have been proposed by Buslowicz (2008a) and next have been extended to robust stability of fractional discrete-time linear systems in (Buslowicz 2010). The practical stability of positive fractional discrete-time linear systems has been investigated in (Buslowicz and Kaczorek 2009). The stability of positive continuous-time linear systems with delays of the retarded type has been addressed in (Buslowicz 2008b). The independence of the asymptotic stability of positive 2D linear systems with delays of the number and values of the delays has been shown in (Kaczorek 2009b). The asymptotic stability of positive 2D linear systems without and with delays has been considered in (Kaczorek 2009a, 2010a). The stability and stabilization of positive fractional linear systems by state-feedbacks have been analyzed in (Kaczorek 2010b, 2011d). The Hurwitz stability of Metzler matrices has been investigated in (Narendra and Shorten 2010) and some new tests for checking the asymptotic stability of positive 1D and 2D linear systems have been proposed

in (Kaczorek 2011b, 2011c). The asymptotic stability of the convex linear combination of positive linear systems has been addressed in (Kaczorek 2012).

In this paper the asymptotic stability of the convex linear combination of fractional positive discrete-time linear systems will be addressed. It will be shown that the convex linear combination is asymptotically stable if its matrices are diagonal dominant.

The paper is organized as follows. In section 2 the basic definition and theorems concerning fractional positive discrete-time linear systems are recalled. The problem is formulated for this class of fractional positive systems in section 3. The problem solution is presented in section 4. Concluding remarks are given in section 5.

The following notation will be used: \mathfrak{R} - the set of real numbers, $\mathfrak{R}^{n \times m}$ - the set of $n \times m$ real matrices, $\mathfrak{R}_+^{n \times m}$ - the set of $n \times m$ matrices with nonnegative entries and $\mathfrak{R}_+^n = \mathfrak{R}_+^{n \times 1}$, M_n - the set of $n \times n$ Metzler matrices (real matrices with nonnegative off-diagonal entries), I_n - the $n \times n$ identity matrix.

2. PRELIMINARIES

Consider the fractional discrete-time linear system

$$\Delta^\alpha x_{i+1} = Ax_i, \quad 0 \leq \alpha \leq 1 \quad (2.1)$$

where $\alpha \in \mathfrak{R}$ is the order, $x_i \in \mathfrak{R}^n$ is the state vector and $A \in \mathfrak{R}^{n \times n}$.

Substituting the fractional difference

$$\Delta^\alpha x_i = \sum_{k=0}^i (-1)^k \binom{\alpha}{k} x_{i-k} \quad (2.2a)$$

where

$$\binom{\alpha}{k} = \begin{cases} 1 & \text{for } k = 0 \\ \frac{\alpha(\alpha-1)\dots(\alpha-k+1)}{k!} & \text{for } k = 1, 2, \dots \end{cases} \quad (2.2b)$$

into (2.1), we obtain

$$x_{i+1} = A_\alpha x_i + \sum_{k=2}^{i+1} (-1)^{k+1} \binom{\alpha}{k} x_{i-k+1}, \quad A_\alpha = A + I_n \alpha \quad (2.3)$$

Theorem 2.1. (Kaczorek 2011d) The solution of equation has the form

$$x_i = \Phi_i x_0 \quad (2.4)$$

where

$$\Phi_{i+1} = \Phi_i A_\alpha + \sum_{k=2}^{i+1} (-1)^{k+1} \binom{\alpha}{k} \Phi_{i-k+1}, \quad \Phi_0 = I_n. \quad (2.5)$$

Definition 2.1. The system (2.1) is called (internally) positive fractional system if $x_i \in \mathfrak{R}_+^n$, $i \in Z_+$ for every initial condition $x_0 \in \mathfrak{R}_+^n$.

Theorem 2.2. (Kaczorek 2011d) The fractional system (2.1) is positive if and only if $A_\alpha \in \mathfrak{R}_+^{n \times n}$.

Definition 2.2. The fractional positive system (2.1) is called asymptotically stable if

$$\lim_{i \rightarrow \infty} x_i = 0 \text{ for all } x_0 \in \mathfrak{R}_+^n \quad (2.6)$$

From (2.4) and (2.6) it follows that the positive fractional system (2.1) is asymptotically stable if and only if

$$\lim_{i \rightarrow \infty} \Phi_i = 0 \quad (2.7)$$

Using (2.5) and (2.7) it is easy to show the following theorem (Kaczorek 2011d).

Theorem 2.3. The fractional positive system (2.1) is asymptotically stable if and only if :

1. The matrix $A + I_n \in \mathfrak{R}_+^{n \times n}$ is asymptotically stable (Schur matrix),
2. The matrix $A_\alpha \in M_n$ is asymptotically stable (Hurwitz Metzler matrix).

Let $\bar{A} = [a_{ij}] \in \mathfrak{R}^{n \times n}$ be a Metzler matrix with negative diagonal entries ($a_{ii} < 0$, $i = 1, \dots, n$) and define

$$\begin{aligned} \bar{A}_n^{(0)} = \bar{A} &= \begin{bmatrix} a_{11}^{(0)} & \dots & a_{1,n}^{(0)} \\ \vdots & \dots & \vdots \\ a_{n,1}^{(0)} & \dots & a_{n,n}^{(0)} \end{bmatrix} = \begin{bmatrix} a_{11}^{(0)} & b_{n-1}^{(0)} \\ c_{n-1}^{(0)} & A_{n-1}^{(0)} \end{bmatrix}, \\ \bar{A}_{n-1}^{(0)} &= \begin{bmatrix} a_{22}^{(0)} & \dots & a_{2,n}^{(0)} \\ \vdots & \dots & \vdots \\ a_{n,2}^{(0)} & \dots & a_{n,n}^{(0)} \end{bmatrix}, \\ b_{n-1}^{(0)} &= [a_{12}^{(0)} \quad \dots \quad a_{1,n}^{(0)}], \quad c_{n-1}^{(0)} = \begin{bmatrix} a_{21}^{(0)} \\ \vdots \\ a_{n,1}^{(0)} \end{bmatrix} \end{aligned} \quad (2.8a)$$

and

$$\begin{aligned} \bar{A}_{n-k}^{(k)} &= \bar{A}_{n-k}^{(k-1)} - \frac{c_{n-k}^{(k-1)} b_{n-k}^{(k-1)}}{a_{k+1,k+1}^{(k-1)}} = \begin{bmatrix} a_{k+1,k+1}^{(k)} & \dots & a_{k+1,n}^{(k)} \\ \vdots & \dots & \vdots \\ a_{n,k+1}^{(k)} & \dots & a_{n,n}^{(k)} \end{bmatrix} \\ &= \begin{bmatrix} a_{k+1,k+1}^{(k)} & b_{n-k-1}^{(k)} \\ c_{n-k-1}^{(k)} & A_{n-k-1}^{(k)} \end{bmatrix}, \\ \bar{A}_{n-k-1}^{(k)} &= \begin{bmatrix} a_{k+2,k+2}^{(k)} & \dots & a_{k+2,n}^{(k)} \\ \vdots & \dots & \vdots \\ a_{n,k+2}^{(k)} & \dots & a_{n,n}^{(k)} \end{bmatrix}, \\ b_{n-k-1}^{(k)} &= [a_{k+1,k+2}^{(k)} \quad \dots \quad a_{k+1,n}^{(k)}], \quad c_{n-k-1}^{(k)} = \begin{bmatrix} a_{k+2,k+1}^{(k)} \\ \vdots \\ a_{n,k+1}^{(k)} \end{bmatrix} \end{aligned} \quad (2.8b)$$

for $k = 1, \dots, n-1$.

It is well-known (Kaczorek 2011c, 2011d) that using the elementary operations we may reduce the matrix

$$\bar{A} = \begin{bmatrix} a_{11} & a_{12} & \dots & a_{1,n} \\ a_{21} & a_{22} & \dots & a_{2,n} \\ \vdots & \vdots & \dots & \vdots \\ a_{n,1} & a_{n,2} & \dots & a_{n,n} \end{bmatrix} \quad (2.9)$$

to the lower triangular form

$$\tilde{A} = \begin{bmatrix} \tilde{a}_{11} & 0 & \dots & 0 \\ \tilde{a}_{21} & \tilde{a}_{22} & \dots & 0 \\ \vdots & \vdots & \ddots & \vdots \\ \tilde{a}_{n,1} & \tilde{a}_{n,2} & \dots & \tilde{a}_{n,n} \end{bmatrix}. \quad (2.10)$$

To check the asymptotic stability of the matrix $\bar{A} = A_\alpha - I_n$ the following theorem is recommended (Kaczorek 2011c, 2011d).

Theorem 2.4. The fractional positive linear system (2.1) for $0 < \alpha < 1$ is asymptotically stable if and only if one of the equivalent conditions is satisfied:

1. All coefficients of the characteristic polynomial

$$\det[I_n \lambda - \bar{A}] = \lambda^n + a_{n-1} \lambda^{n-1} + \dots + a_1 \lambda + a_0 \quad (2.11)$$

are positive, i.e. $a_i > 0$ for $i = 1, \dots, n-1$,

2. All principal minors Δ_i , $i = 1, \dots, n$ of the matrix $-\bar{A} = [-a_{ij}]$ are positive, i.e.

$$\Delta_1 = -a_{11} > 0, \quad \Delta_2 = \begin{vmatrix} -a_{11} & -a_{12} \\ -a_{21} & -a_{22} \end{vmatrix} > 0, \dots, \quad (2.12)$$

$$\Delta_n = \det[-\bar{A}] > 0$$

3. The diagonal entries of the matrices (2.8)

$$\bar{A}_{n-k}^{(k)} \text{ for } k = 1, \dots, n-1 \quad (2.13)$$

are negative,

4. The diagonal entries of the lower triangular matrix (2.10) are negative, i.e.

$$\tilde{a}_{kk} < 0 \text{ for } k = 1, \dots, n \quad (2.14)$$

Proof is given in (Kaczorek 2011c, 2011d).

3. PROBLEM FORMULATION

Consider q positive discrete-time linear systems (2.1) with the matrices

$$A_i = \begin{bmatrix} -a_{11}^{(i)} & a_{12}^{(i)} & \dots & a_{1,n}^{(i)} \\ a_{21}^{(i)} & -a_{22}^{(i)} & \dots & a_{2,n}^{(i)} \\ \vdots & \vdots & \dots & \vdots \\ a_{n,1}^{(i)} & a_{n,2}^{(i)} & \dots & -a_{n,n}^{(i)} \end{bmatrix} \in \mathfrak{R}_+^{n \times n}, \quad i = 1, \dots, q \quad (3.1)$$

Definition 3.1. The matrix (3.1) is called diagonal dominant if

$$1 - a_{k,k}^{(i)} > \sum_{\substack{j=1 \\ j \neq k}}^n a_{k,j}^{(i)} \text{ and } a_{k,j}^{(i)} \geq 0$$

for $k, j = 1, \dots, n; i = 1, \dots, q$ (3.2)

From Definition 3.1 it follows the following lemma.

Lemma 3.1. If the matrices (3.1) are diagonal dominant for $i = 1, \dots, q$ then the matrix

$$A = \sum_{i=1}^q A_i \quad (3.3)$$

is also diagonal dominant.

Definition 3.2. The matrix

$$\hat{A} = \sum_{i=1}^q c_i A_i \text{ for } \sum_{i=1}^q c_i = 1, \quad c_i \geq 0, \quad i = 1, \dots, q \quad (3.4)$$

is called the convex linear combination of the matrices (3.1).

The following question arises: Under which conditions the convex linear combination (3.4) is asymptotically stable nonnegative matrix if the matrices (3.1) are asymptotically stable?

Remark 3.1. The convex linear combination (3.4) of asymptotically stable matrices $A_i, i = 1, \dots, q$ may be unstable.

For example the convex linear combination

$$\begin{aligned} \hat{A} &= cA_1 + (1-c)A_2 = c \begin{bmatrix} 0.2 & 2 \\ 0 & 0.3 \end{bmatrix} \\ &+ (1-c) \begin{bmatrix} 0.1 & 0 \\ 3 & 0.2 \end{bmatrix} = \begin{bmatrix} 0.1+0.1c & 2c \\ 3-3c & 0.2+0.1c \end{bmatrix} \end{aligned} \quad (3.5)$$

of two asymptotically stable matrices A_1 and A_2 is unstable for $c_1 \leq c \leq c_2$ since for these values of c the characteristic polynomial

$$\begin{aligned} \det[I_n(z+1) - \hat{A}] &= \begin{vmatrix} z+0.9-0.1c & -2c \\ 3c-3 & z+0.8-0.1c \end{vmatrix} \\ &= z^2 + (1.7-0.2c)z + 6.01c^2 - 6.17c + 0.72 \end{aligned} \quad (3.6)$$

has one nonpositive coefficient. Note that

$$c_1 = 0.1342, \quad c_2 = 0.8924 \quad (3.7)$$

are the zeros of the polynomial $6.01c^2 - 6.17c + 0.72$.

4. PROBLEM SOLUTION

Theorem 4.1. The convex linear combination (3.4) is asymptotically stable if and only if one of the conditions of Theorem 2.4 is satisfied.

Proof. It is well-known (Kaczorek 2011d, 2012) that the matrix A of positive discrete-time linear systems has eigenvalues in the unit circle if and only if the matrix $A - I_n$ has eigenvalues in the open half of the complex plane. By Theorem 2.4 the convex linear combination (3.4) is asymptotically stable if and only if one of its conditions is satisfied. \square

Checking the conditions of Theorem 2.4 for all $c_i \geq 0$

and $\sum_{i=1}^q c_i = 1$ is numerically complicated.

Theorem 4.2. The convex linear combination (3.4) is asymptotically stable only if all matrices $A_i \in \mathfrak{R}_+^{n \times n}$ $i = 1, \dots, q$ of (3.4) are asymptotically stable.

Proof. The asymptotic stability of convex linear combination (3.4) for $c_i = 1$ and $c_1 = \dots = c_{i-1} = c_{i+1} = \dots = c_q = 0$ implies the asymptotic stability of the matrix $A_i, i = 1, \dots, q$. \square

Lemma 4.1. Every diagonal dominant nonnegative matrix is asymptotically stable.

Proof. This follows immediately from Gershgorin's theorem since if the condition (3.2) is met for $\hat{A} - I_n$ then all Gershgorin's circles are located in the left half of complex plane. \square

Lemma 4.2. If a nonnegative matrix A is asymptotically stable then the matrix cA is also asymptotically stable for $0 < c < 1$.

Proof. Let λ be an eigenvalue of the matrix A and z be an eigenvalue of the matrix cA . Then from the equality

$$\det[I_n z - cA] = \det \left[c \left(I_n \frac{z}{c} - A \right) \right] = c^n \det \left[I_n \frac{z}{c} - A \right] \quad (4.1)$$

we have $z = c\lambda$ and $|z| < 1$ if and only if $|\lambda| < 1$ and $0 < c < 1$. Therefore, the matrix cA is asymptotically stable if and only if the matrix A is asymptotically stable. \square

Theorem 4.3. The convex linear combination (3.4) of the upper (or lower) triangular matrices

$$\bar{A}_i = \begin{bmatrix} \bar{a}_{11} & \bar{a}_{12} & \dots & \bar{a}_{1,n} \\ 0 & \bar{a}_{22} & \dots & \bar{a}_{2,n} \\ \vdots & \vdots & \dots & \vdots \\ 0 & 0 & \dots & \bar{a}_{n,n} \end{bmatrix} \in \mathfrak{R}_+^{n \times n},$$

$$\left(\bar{A}_i = \begin{bmatrix} \bar{a}_{11} & 0 & \dots & 0 \\ \bar{a}_{21} & \bar{a}_{22} & \dots & 0 \\ \vdots & \vdots & \dots & \vdots \\ \bar{a}_{n,1} & \bar{a}_{n,2} & \dots & \bar{a}_{n,n} \end{bmatrix} \in \mathfrak{R}_+^{n \times n} \right), \quad i = 1, \dots, q$$
(4.2)

is asymptotically stable if and only if the diagonal entries of (4.2) satisfies the condition

$$\bar{a}_{j,j} < 1 \text{ for } j = 1, \dots, n. \quad (4.3)$$

Proof. The matrices (4.2) and $c_i \bar{A}_i$ for $0 < c_i < 1$, $i = 1, \dots, q$ are asymptotically stable if and only if (4.3) holds. Therefore, the convex linear combination (3.4) of upper (lower) triangular matrices (4.2) is asymptotically stable if and only if (4.3) holds. \square

From Theorem 4.3 we have the following remark.

Remark 4.2. The convex linear combination (3.4) of the upper (lower) triangular matrices (4.2) is asymptotically stable if and only if the matrices (4.2) are asymptotically stable.

Theorem 4.4. The convex linear combination (3.4) is asymptotically stable if the matrices A_i , $i = 1, \dots, q$ are diagonal dominant.

Proof. Note that if the nonnegative matrix A_i , $i = 1, \dots, q$ is diagonal dominant then the matrix $c_i A_i$, $c_i > 0$, $i = 1, \dots, q$ is also diagonal dominant for $0 < c_i < 1$; $i = 1, \dots, q$. By Lemma 4.1, and 4.2 the convex linear combination (3.4) is asymptotically stable if the matrices A_i , $i = 1, \dots, q$ are diagonal dominant. \square

Example 4.1. Consider the convex linear combination (3.4) for $q = 2$ and the matrices

$$A_1 = \begin{bmatrix} 0.2 & 0.5 \\ 0.1 & 0.3 \end{bmatrix}, \quad A_2 = \begin{bmatrix} 0.1 & 0.3 \\ 0.4 & 0.2 \end{bmatrix}. \quad (4.4)$$

The matrices (4.4) are diagonal dominant. The convex linear combination (3.4) of (4.4) has the form

$$\hat{A} = cA_1 + (1-c)A_2 = \begin{bmatrix} 0.1 + 0.1c & 0.3 + 0.2c \\ 0.4 - 0.3c & 0.2 + 0.1c \end{bmatrix} \quad (4.5)$$

and its characteristic polynomial

$$\det[I_2(z+1) - \hat{A}] = \begin{vmatrix} z+0.9-0.1c & -0.3-0.2c \\ -0.4+0.3c & z+0.8-0.1c \end{vmatrix} \quad (4.6)$$

$$= z^2 + (1.7 - 0.2c)z + 0.07c^2 - 0.16c + 0.6$$

has positive coefficients for $0 < c < 1$.

Therefore, by Theorem 2.4 the convex linear combination (4.5) is asymptotically stable.

Remark 4.3. Note that the convex linear combination (3.4) of the asymptotically stable matrices

$$A_1 = \begin{bmatrix} 0.2 & 2 \\ 0 & 0.3 \end{bmatrix}, \quad A_2 = \begin{bmatrix} 0.1 & 0 \\ 3 & 0.2 \end{bmatrix}. \quad (4.7)$$

is unstable for $c_1 \leq c \leq c_2$ (c_1, c_2 are given by (3.7)) since the matrices are not diagonal dominant.

5. CONCLUDING REMARKS

The asymptotic stability of the convex linear combination of asymptotically stable matrices for fractional positive discrete-time linear systems has been addressed. The notion of diagonal dominant matrices for nonnegative matrices has been introduced. Necessary and sufficient conditions for the asymptotic stability of the convex linear combinations for fractional positive discrete-time linear systems have been established (Theorem 4.2). Checking the conditions is numerically complicated. It has been shown that the convex linear combinations are asymptotically stable if its matrices are diagonal dominant. The considerations has been illustrated by numerical examples. These considerations can be extended to positive and fractional 2D linear systems.

ACKNOWLEDGMENTS

This work was supported by National Science Centre in Poland under work No. N N514 6389 40.

REFERENCES

- Busłowicz, M. 2008. Simple stability conditions for positive discrete-time linear systems with delays, *Bull. Pol. Acad. Sci. Techn.*, vol. 56, no. 4, 325-328.
- Busłowicz, M. 2010. Robust stability of positive discrete-time linear systems of fractional order, *Bull. Pol. Acad. Sci. Techn.*, vol. 58, no. 4, 567-572.
- Busłowicz, M. 2008. Stability of linear continuous-time fractional order systems with delays of the retarded type, *Bull. Pol. Acad. Sci. Techn.*, vol. 56, no. 4, 319-323.
- Busłowicz, M. and Kaczorek, T. 2009. Simple conditions for practical stability of positive fractional discrete-time linear systems, *Int. J. Appl. Math. Comput. Sci.*, vol. 19, no. 2, 263-269.
- Farina, L. and Rinaldi, S., 2000. *Positive Linear Systems; Theory and Applications*, J. Wiley, New York.
- Kaczorek, T., 2002. *Positive 1D and 2D Systems*, Springer Verlag, London.
- Kaczorek, T., 2009. Stability of positive continuous-time linear systems with delays, *Bull. Pol. Acad. Sci. Techn.*, vol. 57, no. 4, 395-398.
- Kaczorek, T., 2010. Stability and stabilization of positive fractional linear systems by state-

- feedbacks, *Bull. Pol. Acad. Sci. Techn.*, vol. 58, no. 4, 517-554.
- Kaczorek, T., 2009. Asymptotic stability of positive 2D linear systems with delays, *Bull. Pol. Acad. Sci. Techn.*, vol. 57, no. 2, 133-138.
- Kaczorek, T., 2010. Asymptotic stability of positive 2D linear systems, *Computer Applications in Electrical Engineering*, Poznan, Poland.
- Kaczorek, T., 2009. Independence of asymptotic stability of positive 2D linear systems with delays of their delays, *Int. J. Appl. Math. Comput. Sci.*, vol. 19, no. 2, 255-261.
- Kaczorek, T., 2011. New stability tests of positive 1D and 2D linear systems, *Proc. 25th European Conf, Modelling and Simulation*, Krakow, June 7-10, Poland, 237-243.
- Kaczorek, T., 2011. New stability tests of positive standard and fractional linear systems, *Circuits and Systems*, vol. 4, no. 2, 261-268.
- Kaczorek, T., 2011. Necessary and sufficient conditions of fractional positive continuous-time linear systems, *Acta Mechanica et Automatica*, vol. 5, no. 2, 52-58.
- Kaczorek, T., 2012. Stability of the convex linear combination of positive linear systems, *Asian Journal of Control* (in Press).
- Kaczorek, T., 2011. *Selected Problems of Fractional System Theory*, Springer Verlag, Berlin.
- Narendra, K.S. and Shorten, R. 2010. Hurwitz Stability of Metzler Matrices, *IEEE Trans. Autom. Contr.*, Vol. 55, no. 6, 1484-1487.

AUTHORS BIOGRAPHY

Tadeusz Kaczorek, born 27.04.1932 in Poland, received the MSc., PhD and DSc degrees from Electrical Engineering of Warsaw University of Technology in 1956, 1962 and 1964, respectively. In the period 1968 - 69 he was the dean of Electrical Engineering Faculty and in the period 1970 - 73 he was the prorector of Warsaw University of Technology. Since 1971 he has been professor and since 1974 full professor at Warsaw University of Technology. In 1986 he was elected a corresponding member and in 1996 full member of Polish Academy of Sciences. In the period 1988 - 1991 he was the director of the Research Centre of Polish Academy of Sciences in Rome. In June 1999 he was elected the full member of the Academy of Engineering in Poland. In May 2004 he was elected the honorary member of the Hungarian Academy of Sciences. He was awarded by the University of Zielona Gora (2002) by the title doctor honoris causa, the Technical University of Lublin (2004), the Technical University of Szczecin (2004), Warsaw University of Technology (2004), Bialystok University of Technology (2008), Lodz University of Technology (2009), Opole University of Technology (2009) and Poznan University of Technology (2011).

His research interests cover the theory of systems and the automatic control systems theory, specially, singular multidimensional systems, positive multidimensional

systems and singular positive 1D and 2D systems. He has initiated the research in the field of singular 2D, positive 2D linear systems and positive fractional 1D and 2D systems. He has published 24 books (7 in English) and over 1000 scientific papers.

He supervised 69 Ph.D. theses. More than 20 of this PhD students became professors in USA, UK and Japan. He is editor-in-chief of Bulletin of the Polish Academy of Sciences, Techn. Sciences and editorial member of about ten international journals.

A SIMULATION TOOL FOR HIGH-FIDELITY MODELING OF COMPLEX LOGISTICAL NETWORKS

Reejo Mathew^(a), Thomas W. Mastaglio^(b), Andrew Lewis^(c)

^(a)Senior Research Scientist, MYMIC LLC, 1040 University Boulevard, Ste. 100, Portsmouth, VA 23704, USA

^(b)CEO, MYMIC LLC, 1040 University Boulevard, Ste. 100, Portsmouth, VA 23704, USA

^(c)Software Engineer, MYMIC LLC, 1040 University Boulevard, Ste. 100, Portsmouth, VA 23704, USA

^(a)reejo.mathew@mymic.net, ^(b)tom.mastaglio@mymic.net, ^(c)andrew.lewis@mymic.net

ABSTRACT

Ports are a vital component of the nation's transportation system. It is vital for ports to address the various security risks associated with port operations, by analyzing these risks, adopting strategies to prevent incidents and developing mitigation strategies to deal with incidents if they do occur. Simulation presents an ideal opportunity to model current port operations, and then to perform what-if analyses by improving/adding infrastructure and resources to determine its effectiveness on improving cargo throughput and relieving bottlenecks. Simulation also provides a cost-effective and non-invasive method to study the impact of disruptive incidents. A simulation tool is presented here that enables the Virginia Port Authority (VPA) to have a system-level view of cargo operations for the entire Hampton Roads region. It also allows planners in determining the cause and effect relationships between disruptive events (natural catastrophes or terrorist acts) and port and transportation infrastructure, to plan for threat contingencies.

Keywords: Decision-support system, Discrete-event simulation, security analysis, programmable processes.

1. INTRODUCTION

Ports form a vital component of the national transportation infrastructure. They are a logistical focal point of the system that, if disrupted, will greatly slow commerce and have significant effects on the quality of life of the citizens, due to the unavailability of items that we require in our daily life. Ports need to investigate and adopt security strategies both to prevent disruptive incidents, and to mitigate their effect, if incidents do occur. It is also important for ports to maintain, if not increase the volume of cargo flowing through them in these times of economic downturn. The security strategies should ideally have minimal effect on the flow of cargo through a port, so that normal operations flow smoothly.

Simulation presents the opportunity to comprehensively model the current state of operations in a complex logistical network. The Virginia Port

Authority (VPA) required a simulation tool to model cargo flow operations within the Port of Virginia (POV). It also required the tool to model the impact of security measures and operational disruptions (natural catastrophes or terrorist acts) from a regional perspective.

The simulation tool presented here, the Port Analysis Simulation (PAS), models the complete multimodal logistical network for the Port of Hampton Roads. PAS connects together relevant cargo terminals (seaside and inland ports, rail yards, etc.) and the transportation infrastructure between these terminals, thereby presenting a system-level view of cargo operations for the entire Hampton Roads region. It allows VPA operational planners to observe cargo flow activity within the entire system as part of the current state of operations and study the potential impact of changes to operations before actually implementing the changes. PAS also enables planners in analyzing the cause and effect relationships between disruptive events (natural catastrophes or terrorist acts) and port and transportation infrastructure. Stakeholders can use the analyses for collaboration and maritime security awareness, risk management and planning, studying the economic impact of potential disruptions and to plan for threat contingencies.

PAS is a customized instantiation of MYMIC's Scalable End-to-End Logistics Simulation (SEELSTM) architecture. The PAS application consists of a Graphical User Interface (GUI) that enables a user to design and design and configure a solution, execute the solution using the SEELS Simulation Core, and view the simulation output for analysis. This interaction is shown in Figure 1.

Section 2 and 3 provide a complete description of the PAS tool. Section 4 describes the SEELS simulation core architecture and capabilities. Section 5 provides some example analyses performed using PAS, including the superior performance of PAS. Section 6 describes related work and Section 7 provides conclusions for this work.

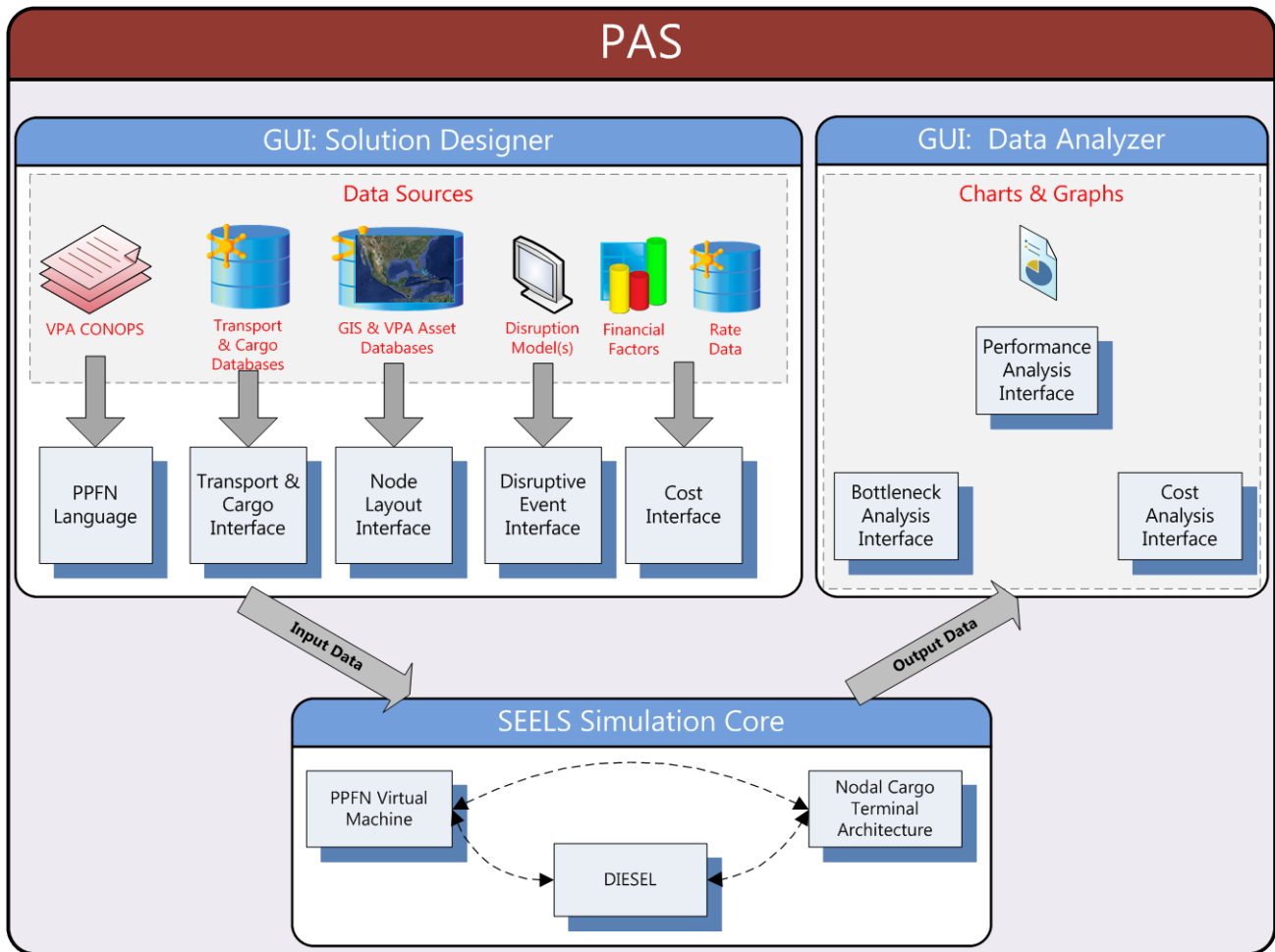


Figure 1: Port Analysis Simulation (PAS)

2. PORT ANALYSIS SIMULATION (PAS)

The Port Analysis Simulation (PAS) models commercial cargo flow operations through all of the facilities belonging to the Virginia Port Authority (VPA), including the Port of Virginia (POV) and the Virginia Inland Port, and presents a system-level view of cargo operations. Terminals within the POV that are modeled within PAS include:

- Norfolk International Terminal (NIT)
- APM Terminals Virginia (APMT)
- Newport News Marine Terminal (NNMT)
- Portsmouth Marine Terminal (PMT)

VPA uses PAS to model their current operations across all of its terminals to study the normal state of operations and validate current cargo throughput. PAS is capable of determining cargo throughput capability using current assets, resources, and business processes. It tracks utilization of critical resources as identifies potential bottlenecks and limiting resources to cargo movement through the network.

2.1. Operational Analyses

Once a baseline model has been established using current infrastructure and resources, VPA can perform

what-if analysis on the impact of adding new infrastructure (new berths, or increases in staging capacity) and/or new resources (straddle carriers, container cranes, etc.). VPA can use this analysis to determine the impact that the increased capability has on performance metrics such as, cargo throughput and truck turnaround times. The analysis can also be used to calculate Return on Investment (ROI) metrics before significant investment decisions are made. VPA can also model proposed changes to its business processes and determine the impact (positive or negative) on the same performance metrics, before actually implementing the changes. VPA can also use PAS to model the planned Craney Island Terminal scheduled to be operational after 2020 (Virginia Port Authority 2010) using its proposed resources and infrastructure to simulate the flow of projected cargo through the terminal to validate current assumptions and identify future requirements.

VPA is also preparing for the Panama Canal expansion, when the capacity of the Canal will be doubled enabling the mega container ships to call on ports on the East Coast. VPA aims to draw a large portion of this container traffic to POV, and has plans to use PAS to model the flow of cargo arriving by the large ships, offloading most if not all of the cargo at

POV, and then transporting the cargo via rail and trucks to their destinations without requiring the ships to make additional ports of call on the East Coast.

2.2. Security Analyses

PAS supports two types of security analyses and assists VPA operational planners to develop contingency plans for various disruptive scenarios and plan for new security measures. First is proactive or preventive, where areas and operations within the ports and the transportation infrastructure are analyzed to identify their impact on operations should they be disrupted. Planners then develop efforts to protect those capabilities using different methods such as new security measures, increased container and truck inspections, etc. PAS allows planners to insert proposed inspection stations anywhere within the port facilities (between berth and staging, or between staging and the gates) and determine the slowdown impact that it has on cargo flow. Planners can also use PAS to determine capability requirements for inspection stations (e.g. 40 inspections per hour) to minimize the impact on cargo flow.

The second type is to analyze responses to disruptive incidents if they do occur. PAS models a disruption in the operations of a terminal by appropriately reducing the allocation and number of resources, available infrastructure, and processing capabilities of that particular terminal, either permanently or for a specific duration of time within the

simulation. The impact of response strategies to alleviate slowdown in cargo flow can then be analyzed including cleanup/recovery procedures and rerouting of cargo to maintain operational effectiveness. This demonstrates the effect on a terminal and the potential ripple effect on other terminals within the region as the logistical network adapt to sustain cargo flow.

PAS can also be integrated with other models (traffic models, weather models, etc.) to form a complete federation that includes all ports and transportation networks in the region and accounts for the man-made and natural variables that can impact port operations. It can also be interfaced with validated disruption models that can automatically inject stimuli to modify the behavior of the simulation.

3. PAS INTERFACE

The PAS Graphical User Interface (GUI) is a standalone windows application that enables a user to design a solution (including scenarios and profiles), execute the solution using the SEELS Simulation Core, and view the simulation output for analysis. The PAS GUI provides an intuitive graphical interface using maps, GIS data and rich, interactive charts. It is implemented using Windows Presentation Foundation (WPF), and follows the Model-View-View Model (MVVM) design pattern (Smith 2009) as shown in Figure 2. The GUI is designed to match the scalability of the SEELS simulation core by utilizing a highly configurable model that is defined by user provided data.

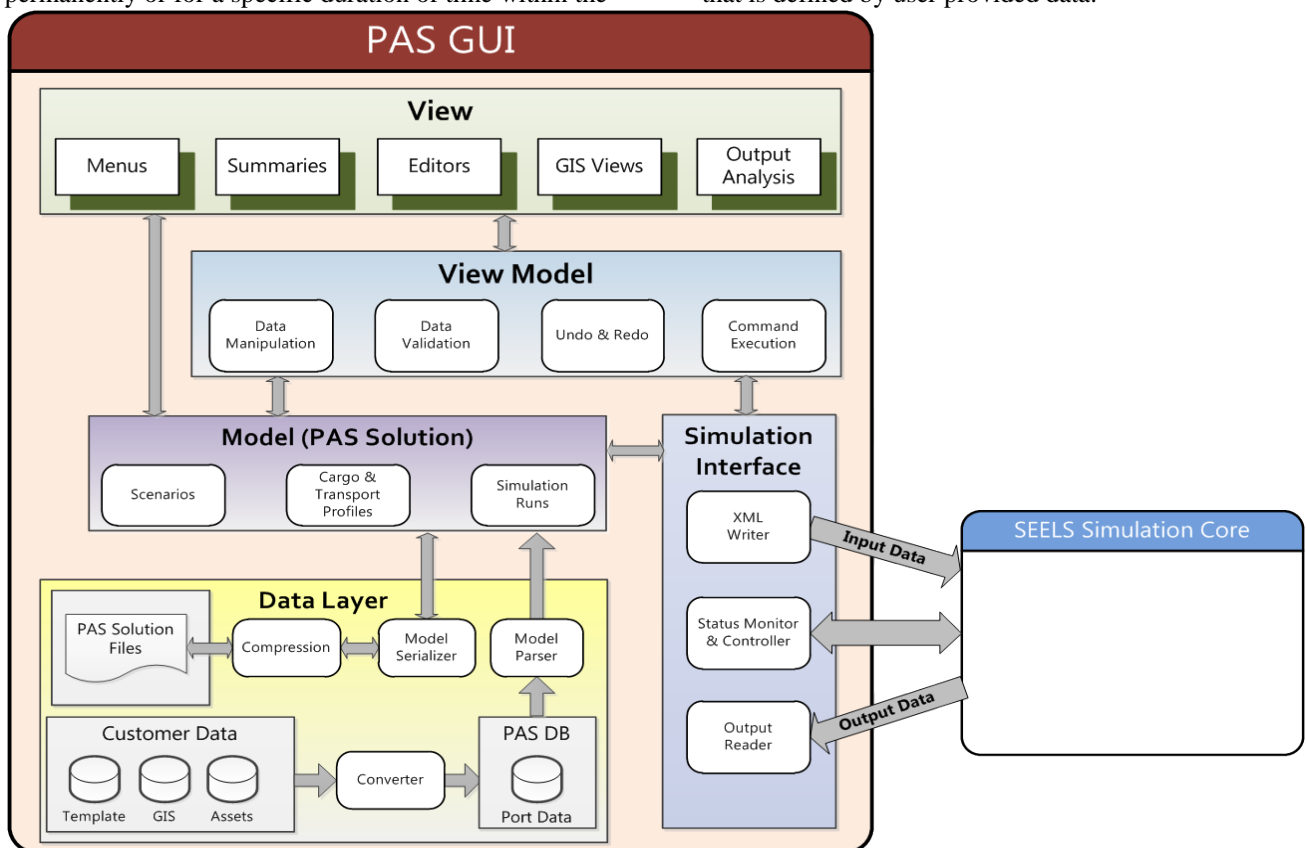


Figure 2: PAS GUI Design

3.1. Solution Designer

The GUI uses a variety of data sources including GIS data on current port infrastructure, asset data on current resources as well as cargo and transport classes that are handled by the logistical network. The GUI also includes a template that defines the structure of the different types of nodes (inland ports, seaports, automated container terminals, etc.). All this data is then used to create PAS Solutions. Solutions are made up of scenarios, cargo/ transport profiles, and simulation runs. Solutions are stored as compressed XML files and can be easily copied and shared between users.

Scenarios are a model of a complete logistical network, consisting of any number of ports, terminals, operational areas, and resources. Scenarios also define the time it takes to travel between each node (transit times) and the time it takes to complete each port operation (processing times). Maps of ports are provided using an ArcGIS map provider and polygons representing infrastructure are generated within the interface using the ESRI Shapefile format. Polygons can also be created and modified in the GUI, enabling a user to create new areas, terminals, ports, etc.

Cargo and transport profiles define the cargo and transports that flow through the logistical network during the simulation. This data can either be created in the GUI or can be ingested from data sources, such as cargo manifests. This generates arrival events, which define the arrival time, quantity, and cargo load of each individual transport. Transports can arrive empty or loaded with a mix of cargo headed for different destinations.

A simulation run consists of a single scenario and one or more transport profiles that are executed by the SEELS Simulation Core. The output data generated by the SEELS Simulation Core are stored as part of the simulation run.

3.2. Output Analysis

PAS models cargo and transports at the individual entity level and the output data collected during a simulation run (or iteration) can be used for extensive after-action reporting and visualization. Output data can be captured for every node within the logistical network for any measurable metric. Typical output includes infrastructure and resource cost and utilization, as well as cargo and transport throughput and timing. The data can be analyzed and compared to previous runs in rich charts and graphs that visualize and filter the data. Users can also easily drill down from a high level view of the entire logistical network to data on a specific operational area within a terminal.

4. SEELS SIMULATION CORE

The Scalable End-to-End Logistics Simulation (SEELS™) technology supports the modeling of complex logistical networks for commercial, military, and government customers for use in planning, analysis, and experimentation. For every customer, SEELS models their unique end-to-end logistical network and

functions as a decision-support tool to quickly analyze different what-if scenarios. SEELS is a scalable, nodal, and programmable architecture that allows a user to:

- Define the item (cargo/bulk/person) entity level used in the simulation
- Scale level of fidelity (as required) to model a node
- Define the handling processes for a node

SEELS can model people, containers, medicinal equipment or any variety of material as cargo flowing through a logistical network. SEELS also enables planning a complete logistical network at a local, regional, or global level. A network can be composed of any number of logistical nodes of any type. The definition of a node is limited only by the user's requirements; thus, a node may be an entire seaport or a single fueling point along a highway. Typical types include seaports, airports, warehouses, distribution centers, intermediate staging bases, etc. The nodes can be defined at any level of fidelity depending on a customer's unique requirements or availability of data.

A set of nodes can be connected by a variety of transportation links, such as air, sea road, rail, or other means of transportation to model a complete, multimodal end-to-end logistical operation. Further, separate logistical operations can be linked to form an integrated, highly scalable, network-of-networks model. SEELS applies a single-model solution to the end-to-end logistics problem, as a viable alternative to the complexity of a federated solution.

SEELS captures a customer's business rules as processes for the different nodes. The processes dictate how cargo and transports are handled within each node. Processes are not part of the SEELS simulation software; rather they are provided as input just like any other data to the software during a simulation run. This allows processes to be modified easily to support experimentation with changes to business rules.

4.1. Nodal Cargo Terminal Architecture

The architecture is defined as a network of nodes, with the flow of cargo and transports through each node defined by processes. A node can be an inland port, seaport, a terminal within a seaport, or an operational area within either the seaport or a terminal. A node could also potentially represent a whole other network of nodes. This allows a hierarchical structure where individual nodes are defined by the internal processes performed within the node on the cargo and transports and possibly by a new network (network nodes). Multiple network nodes, each modeling a complete seaport, airport or inland port in itself, can be connected together to model an end-to-end cargo flow from a point of origin to a destination (Mathew 2002, Mathew, Leathrum, Mazumdar, Frith and Joines 2005).

For example, PAS defines the Port of Hampton Roads as a seaport node. The seaport node has a network of terminals, including Norfolk International

Terminal, APM Terminals Virginia, Portsmouth Marine Terminal, Newport News Marine Terminal, etc. Each terminal itself is defined in terms of operational areas: the berths, staging, loading areas, etc. The Virginia Inland Port (VIP) is also a network node, without terminals, but has a network of operational areas such as staging areas, rail spurs, loading areas, etc.

The capacities and capabilities of individual nodes are programmable, and so are the processes within them. The architecture is configurable to support different port types, different individual ports, different cargo types, and different transport types. The architecture also supports routing entities through the network. A route is defined by a starting node, a destination node, and a sequence of nodes traversed en route. An important approach to avoid infinite queuing in the interconnection segments is that a node must request the next node in the route before advancing. This provides a level of flow control to aid in the avoidance of deadlock.

4.2. Programmable Processes

Processes for the SEELS simulation are programmable, unlike many applications where processes are hard coded within the simulation. The Programmable Process Flow Network (PPFN) supports defining processes that are input to the SEELS simulation core during simulation run-time (Mathew and Leathrum 2008). PPFN is a process flow programming language that describes the process activities at a cargo terminal. PPFN provides an intuitive approach for an analyst to capture processes by providing the ability to define/edit/modify processes independent of the simulation and provide it as an input to the simulation in the same way other data is input; this makes the tool more responsive to changes in requirements. Moreover, port Subject Matter Experts (SMEs) view operations within a cargo terminal in terms of processes that must be performed in a given situation. PPFN provides a process-oriented interface (in terms of flowcharts) for a discrete-event simulation, with processes being defined as sequences of activities and decisions.

4.3. Programmatic Events

SEELS provides a capability to impact simulation behavior, both negatively and positively at run-time called Programmatic Events. Programmatic events allow an analyst or an external disruption model to program unusual events to occur at specific simulation times, thereby modeling the effect disruptive events such as a chemical, or biological weapon attack into a scenario. These events can change the processing, available resources, capacities, and capabilities of a node or transit times between nodes during simulation run-time. For example, an analyst can program a new berth to become available on day 7, instead of day 0, or a berth and associated resources like cranes to be unavailable from days 2-10 due to a disruptive incident. SEELS can also be interface with other disruption models, to portray the effects of disruptive events on

seaport operations, i.e., allowing the capability of the seaport to be degraded as a result of a disruptive event and then be gradually restored over time (Leathrum, Mathew, and Mastaglio 2009).

5. EXAMPLE ANALYSES

A baseline scenario for current cargo operations is developed. This baseline scenario models the container flow through two terminals at POV: NIT and APMT during a week. On an average, 22000 containers (import and export) flow through each terminal during a week. The baseline scenario clears all cargo at NIT by 9 days and at APMT by 10 days. Then different analyses are performed by defining 3 unique use-cases which are described in the following sub-sections.

5.1. Proactive Security Analyses

PAS allows planners to proactively implement security strategies by inserting proposed inspection stations anywhere within the port facilities and assess the impact that it has on cargo flow. In this case, an inspection is inserted right after the gate within the NIT terminal, requiring each truck coming into the terminal to be inspected before proceeding to pick up or drop off containers in the terminal (Figure 3). If 10 concurrent inspections can be performed at the station, using an inspection time (Triangular distribution with a minimum time of 2 minutes, maximum time of 3 minutes and most likely time of 4 minutes), then cargo clearance at NIT is delayed by approximately 3 days compared to the baseline scenario. The comparison between cargo clearances is shown in Figure 4. However, if the number of concurrent inspections that can be conducted is increased to 40, then cargo clearances at NIT is delayed by just 1 day.

Planners can then determine capability requirements for inspection stations and make decisions on whether extra investments are required to improve cargo clearances. Planners can also analyze other data such as area and resource utilization and transport turnaround times in their decision-making process.

5.2. Reactive Analyses

PAS also supports planners in developing response strategies to disruptive incidents if and when they do occur. In this use-case, an incident occurs at APMT that damages a crane rendering another adjacent crane and 2000 feet of berth space unusable for 6 days. This reflects an actual incident that occurred at APMT, where the disruption lasted for longer than 6 days (McCabe 2011). The disruption only delays cargo clearance at APMT by 2 days, even with reduced cargo handling capacity (Figure 5) indicating that APMT has the ability to deal with the disruption. However, if the disruption lasts longer, VPA can use PAS to develop mitigation plans by developing scenarios to analyze the impact of diverting traffic to its other terminals. This would allow other VPA terminals to pick up the slack, while APMT is brought back to its full operational capacity.

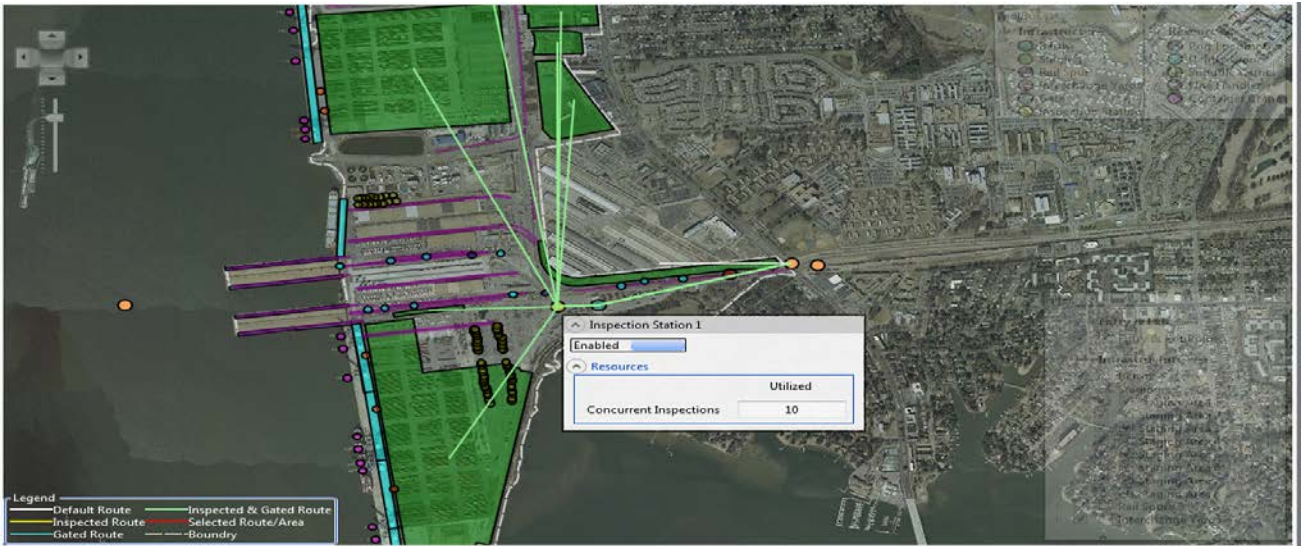


Figure 3. Security Inspection at NIT

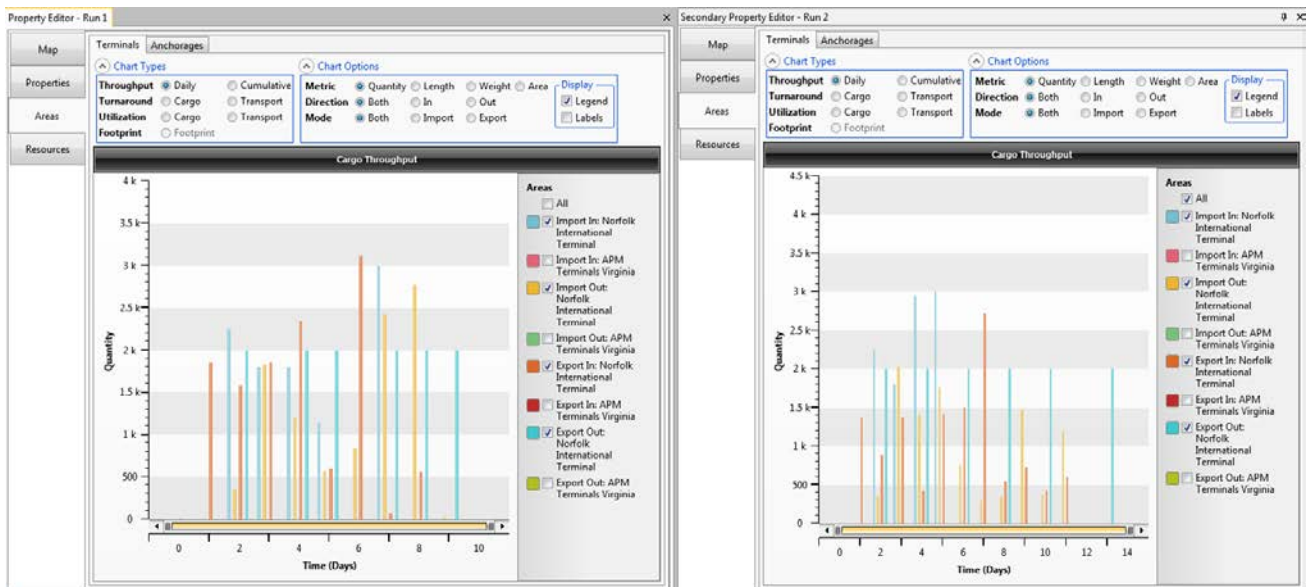


Figure 4. Cargo clearance comparison between baseline scenario and scenario with inspection

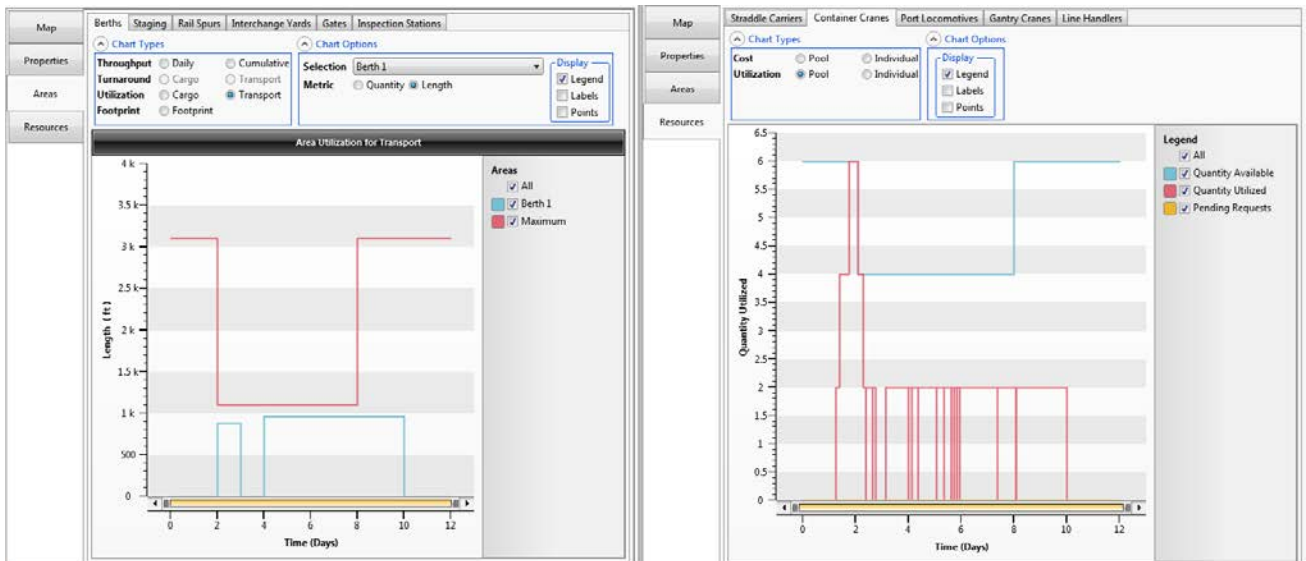


Figure 5. Crane accident scenario at APMT



Figure 6. Proposed Craney Island Terminal next to APMT and NIT

5.3. Craney Island Terminal

PAS can also support VPA in modeling its proposed Craney Island Terminal scheduled to be operational after 2020 (Virginia Port Authority 2010). Planners can use proposed designs including resources and infrastructure to create a complete model of the terminal. PAS provides a simple, intuitive, click-and-drag interface to design new infrastructure, including the ability to create areas (berths, staging areas, rail spurs, etc.) and add resources (straddle carriers, cranes, forklifts, etc.). Planners can then simulate the flow of projected cargo through the terminal and analyze the results to validate current assumptions, detect bottlenecks, and identify future requirements. The model can be refined along with design changes to continuously analyze and validate the design and investment decisions. It also provides VPA with independent and validated analytics to use in discussions with different stakeholders.

5.4. Simulation Performance

The SEELS simulation core has been designed and developed for portability across alternative computing systems. The software code is written as an ANSI Standard C++ implementation, with a key focus on execution speed and low memory usage. It also uses a high-performance, C++ implementation of the Distributed, Independent-platform, Event-driven, Simulation Engine Library (DIESEL) (Mathew 2007), as its underlying simulation executive.

Due to the high-performance of the SEELS simulation core, PAS is capable of simulating the flow of over 40000 pieces of cargo through the VPA network in under 20 seconds, executing approximately 1.6 million events in that time. PAS is also capable of simulating the flow of over a million pieces of cargo at an individual entity level of detail in under 30 minutes.

6. RELATED WORK

There exist a plethora of commercial cargo terminal simulation models and tools modeling ports all over the world (Ballis and Abacoumkin 1996; Bruzzone and Signorile 1998; Dzielinski, Amborski, Kowalczyk, Sukiennik, and Pawlowski 2002; Gambardella, Rizzoli, and Zaffalon 1998; Hayuth, Pollatschek, and Roll 1994; Kia, Shayan, and Ghotb 2002; Kozan 1997; Merkurjev, Tolujew, Blymel, Novitsky, Ginters, Viktorova, Merkurjeva, and Pronins 1998; Merkurjeva, Merkurjev, and Tolujew 2000; Ramani 1996; Shabayek and Yeung 2002; Van Hee and Wijbrands 1988; Yun and Choi 1999). These tools differ widely in their objectives, complexity, level of detail and operational factors taken into consideration due to the variation in the questions that a particular model attempts to answer as well as the model's fidelity. There are also custom tools developed by ports or logistics consulting firms operating on behalf of ports using software such as Arena, ProModel, etc. Most of these tools are limited as they are designed around the commercial activities of a specific port/terminal with very limited capabilities to adapt it to another port without needing significant development. PAS. Developed for VPA, can be easily adapted to any port in the world by populating the tool with GIS data (for infrastructure), asset data (for port resources), business rules for cargo handling, and cargo data. The underlying technology supports modeling any port without requiring software changes.

7. CONCLUSION

The Port Analysis Simulation (PAS) tool presented here supports VPA in modeling cargo operations across all of its terminals. PAS provides capabilities to model VPA facilities and assets at a high level of fidelity and supports analyzing different performance metrics for

improving the efficiency of current VPA operations. PAS also supports VPA in performing operational what-if analyses on the impact of adding new infrastructure or resources and calculate Return on Investment (ROI) metrics before significant investment decisions are made. PAS also enables VPA to adequately prepare for major operational changes such as building the new Craney Island Terminal and the arrival of larger ships after the Panama Canal expansion, by providing a robust, configurable, and high-performance modeling and analysis capability. PAS can be easily adapted to other ports all around the world by populating the tool with appropriate data about the port, without requiring any software development.

ACKNOWLEDGEMENTS

This work is funded by the Virginia Port Authority (VPA) under the Port Security Grant Program (PSGP), administered by the US Federal Emergency Management Agency (FEMA).

The authors would like to acknowledge the contributions of Mr. Taylor Frith, Software Engineer at MYMIC in developing the PAS GUI.

REFERENCES

- Ballis A., Abacoumkin C., 1996. A container terminal simulation model with animation capabilities. *Journal of Advanced Transportation*, 30 (1), 37–57.
- Bruzzone A.G., Signorile R., 1998. Simulation and Genetic Algorithms for Ship Planning and Shipyard Layout. *Simulation*, 71 (2), 74–83.
- Dzielinski A., Amborski K., Kowalczyk P., Sukiennik J., Pawlowski A., 2002. Simulation of operation of a medium sized seaport. Case study: port of Gdansk. *Proceedings of 14th European Simulation Symposium*, pp. 313-317, October 12-16, Dresden (Germany).
- Gambardella L.M., Rizzoli A.E., Zaffalon M., 1998. Simulation and Planning of an Intermodal Container Terminal. *Simulation*, 71 (2), 107–116.
- Hayuth Y., Pollatschek M.A., Roll Y., 1994. Building a Port Simulator. *Simulation*. 63 (3), 179–189.
- Kia M., Shayan E., Ghotb F., 2002. Investigation of port capacity under a new approach by computer simulation. *Computers and Industrial Engineering*, 42 (1), 533–540.
- Kozan E., 1997. Increasing the operational efficiency of container terminals in Australia. *Journal of the Operational Research Society*, 48 (2), 151–161.
- Leathrum, J.F., Mathew, R., Mastaglio, T., 2009. Modeling & Simulation Techniques for Maritime Security. *Proceedings of IEEE International Conference on Technologies for Homeland Security*, May 11–12, Waltham (Massachusetts, USA).
- Mathew, R., 2002. *An Object-oriented Architecture for Concurrent Processes in a Port Simulation*. Thesis (MS). Old Dominion University.
- Mathew, R., 2007. *The Distributed Independent-Platform Event-Driven Simulation Engine Library (DIESEL)*. Thesis (PhD). Old Dominion University.
- Mathew, R., Leathrum, J.F., Mazumdar, S., Frith, T., and Joines, J., 2005. An Object-Oriented Architecture for the Simulation of Networks of Cargo Terminal Operations. *Journal of Defense Modeling and Simulation (JDMS)*, 2 (2), 101–116.
- Mathew, R. and Leathrum, J.F., 2008. Programmable Process Language for Modeling Cargo Logistics. *Proceedings of MODSIM World 2008*, September 15–18, Virginia Beach (Virginia, USA).
- Merkuryev Y., Tolujew J., Blymel E., Novitsky L., Ginters E., Viktorova E., Merkurjeva G., Pronins J., 1998. A Modeling and Simulation Methodology for Managing the Riga Harbour Container Terminal. *Simulation*, 71 (2), 84–95.
- Merkurjeva G., Merkurjev Y., Tolujew J., 2000. Computer Simulation and Metamodelling of Logistics Processes at a Container Terminal. *Studies in Informatics and Control*, 9 (1), 53–59.
- Ramani K.V., 1996. An Interactive Simulation Model for the Logistics Planning of Container Operations in Seaports. *Simulation*, 66 (5), 291–300.
- Shabayek A.A., Yeung W.W., 2002. A simulation model for the Kwai Chung container terminals in Hong Kong. *European Journal of Operational Research*, 140 (1), 1–11.
- Smith, J., 2009. *Patterns: WPF Apps with the Model-View-ViewModel Design Pattern*. MSDN Magazine. Available from: <http://msdn.microsoft.com/en-us/magazine/dd419663.aspx> [accessed 29 March 2012].
- Van Hee K.M., Wijbrands R.J., 1988. Decision support system for container terminal planning. *European Journal of Operational Research*, 34 (3), 264–272.
- Virginia Port Authority, 2010. *The Craney Island Eastward Expansion*. Available from: <http://www.craneyisland.info/overview.html> [accessed 29 March 2012].
- McCabe, R. 2011. *New crane in Portsmouth damaged as ship leaves*. Available from: <http://hamptonroads.com/2011/02/new-crane-portsmouth-damaged-ship-leaves> [accessed 15 April 2012].
- Yun W.Y., Choi Y.S., 1999. A simulation model for container-terminal operation analysis using an object-oriented approach. *International Journal of Production Economics*, 59 (1), 221–230.

AUTHORS BIOGRAPHY

Dr. Reejo Mathew is a Senior Research Scientist at MYMIC LLC, Portsmouth, VA. He is the Program Manager for developing simulation analyses and training tools for the Virginia Port Authority (VPA). He received his PhD in Electrical and Computer Engineering in 2007 and his MS degree in Computer Engineering in 2002, both from Old Dominion

University. His research interests include Simulation Executives, Parallel and Distributed Simulation and Cargo Logistics Simulations.

Dr. Thomas W. Mastaglio is the CEO of MYMIC LLC. Dr. Mastaglio holds MS and PhD degrees in Computer Science from the University of Colorado. He has worked in the computer simulation industry for over 20 years at the technical, program, and corporate management levels. Dr. Mastaglio has served as a Director for the Society for Computer Simulation, member of the U.S. Army Science Board, and an advisor to the Virginia Legislature Joint Committee on Technology and Science.

Andrew Lewis is a Software Engineer at MYMIC LLC. He received his MS degree in Computer Engineering in 2010 from Old Dominion University. His research interests include modeling and simulation and computer architecture.

ON THE INCORPORATION OF PARAMETER UNCERTAINTY FOR INVENTORY MANAGEMENT

David F. Muñoz^(a), David G. Muñoz^(b)

^(a) Departamento de Ingeniería Industrial y Operaciones, Instituto Tecnológico Autónomo de México, Río Hondo #1, Mexico City, Mexico

^(b) Research and Development, AOL Advertising, 395 Page Mill Road, Palo Alto, California

^(a)davidm@itam.mx, ^(b)davidmm82@gmail.com

ABSTRACT

The main purpose of this paper is to discuss how a Bayesian framework is appropriate to incorporate the uncertainty on the parameters of the model that is used for demand forecasting. We first present a general Bayesian framework that allows us to consider a complex model for forecasting. Using this framework we specialize (for simplicity) in the continuous-review (Q, R) system to illustrate how the main performance measures that are required for inventory management can be estimated from the output of simulation experiments. We discuss the use of sampling from the posterior distribution (SPD) and show that, under suitable regularity conditions, the estimators obtained from SPD satisfy a corresponding Central Limit Theorem, so that they are consistent, and the accuracy of each estimator can be assessed by computing an asymptotically valid halfwidth from the output of the simulation experiments.

Keywords: inventory simulation, reorder points, parameter uncertainty, output analysis

1. INTRODUCTION

Most of the proposed techniques to compute service levels and reorder points assume that the parameters of the model that is used for demand forecasting are known with certainty (see, e.g., Nahmias 2008). However in practice, parameters are estimated from available information (data and/or expert judgment), and there exists a certain degree of uncertainty in the value of these parameters. In this article, we use a Bayesian framework that allows us to incorporate parameter uncertainty that is induced from the estimation procedure. This framework is particularly useful when using a complex model for demand forecasting, in the sense that analytical expressions to obtain service levels and/or reorder points may not be available, so that the application of estimation procedures based on stochastic simulation is recommended.

Although it is not our intention to review the abundant literature on inventory simulation (see Jahangirian et al. 2010 for a recent survey), we mention that simulation has been extensively used to analyze inventory policies in a supply chain (see Tako and

Robinson 2012 for a recent survey). Simulation has also been used as a tool to compare different forecasting procedures for inventory management (see, e.g., Syntetos et al. 2009, Bartezzaghi et al. 1999). Furthermore, simulation-based methodologies such as importance sampling (see, e.g., Glasserman and Liu 1996) and simulation optimization (see, e.g., Fu 2002) have been applied to inventory models. However, to the best of our knowledge, parameter uncertainty has not been considered in the related bibliography.

The Bayesian approach described in this article allows us to incorporate parameter uncertainty through a probability distribution, and it is in the spirit of the approach described, e.g., in Chick (2001) and Bermúdez et al. (2010), where the authors discuss the incorporation of parameter uncertainty in a forecasting model using stochastic simulation. In this article, we show how this approach can be extended to the estimation of Bayesian reorder points, and our main contribution is the development of a Central Limit Theorem (CLT) for each of the proposed point estimators. As is well known in the simulation literature, a CLT for an estimator allows us to construct an asymptotic confidence interval (ACI) to assess the accuracy of the point estimator obtained using simulation. We extend the results of Muñoz and Galindo (2010) to include the estimation of three measures of service level and corresponding reorder points.

The remainder of this article is organized as follows. In Section 2 we present a Bayesian framework under which performance measures for inventory management can be precisely defined, we illustrate the derivation of performance measures under this framework by considering the continuous-review (Q, R) system. In Section 3 we discuss how SPD can be used to estimate the performance measures defined in Section 2 as well as to assess the accuracy of the point estimators. Finally, in Section 4 we provide a simple example to illustrate our Bayesian Framework.

2. THEORETICAL FRAMEWORK

2.1. Notation and Model Assumptions

We assume that $W = g(Y(s), 0 \leq s \leq T; \Theta)$ is the demand for an item, where $Y = \{Y(s), s \geq 0; \Theta\}$ is a

stochastic process (possibly multivariate), T is a stopping time that represents the planning horizon, and Θ is a vector of parameters. This notation is general enough to include most forecasting models that are used in practice (e.g., ARIMA and regressions), and in particular, a discrete-time stochastic process can be incorporated into this framework by setting $Y(s) = Y(\lfloor s \rfloor)$ (where $\lfloor s \rfloor$ denotes the integer part of s).

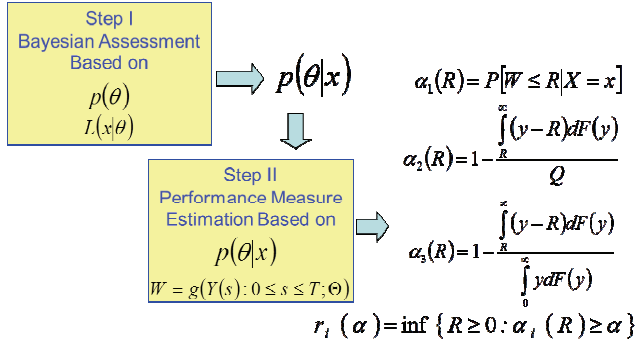


Figure 1: Main Steps to Compute Performance Measures for Inventory Management

A Bayesian approach for inventory management is summarized in two steps, as illustrated in Figure 1. In the first step parameter uncertainty is assessed by constructing the posterior density $p(\theta|x)$ from the available data x and a prior density $p(\theta)$. In the second step $W = g(Y(s), 0 \leq s \leq T; \Theta)$ and the posterior density $p(\theta|x)$ are used to compute the performance measures that are required for inventory management. Input data on the model parameters is available through a vector of observations $x \in \mathfrak{R}^d$ that satisfies a likelihood function $L(x|\theta)$. If $p(\theta)$ is a prior density function for the vector of parameters Θ , then the posterior (given the data x) density function of Θ becomes

$$p(\theta|x) = \frac{p(\theta)L(x|\theta)}{\int_{S_0} p(\theta)L(x|\theta)d\theta}, \quad (1)$$

for $x \in \mathfrak{R}^d$ and $\theta \in S_0$.

Note that we can consider an input $x \in \mathfrak{R}^d$ with correlated data, and for the special case where $x = (x_1, \dots, x_n)$ is a set of observations of a random sample $X = (X_1, \dots, X_n)$ from a density function $f(y|\theta)$, the likelihood function takes the form of

$$L(x|\theta) = f(x_1|\theta)f(x_2|\theta)\dots f(x_n|\theta). \quad (2)$$

The prior density $p(\theta)$ reflects the initial uncertainty on the vector of parameters Θ , and there are essentially

two points of view to proposing a prior density $p(\theta)$. The first approach consists of using a non-informative prior, which is appropriate when we wish to consider a prior density that does not “favor” any possible value of Θ over others. This can be considered as an “objective” point of view (for a discussion on this subject see, e.g., Berger et al. 2008). The second approach is a “subjective” point of view, and consists in the establishment of a prior density based on expert judgment.

2.2. Performance Measures for Inventory Management

Although our previous notation can be useful to consider different inventory control policies, multi-item and/or multi-period systems, a definition of the appropriate performance measures for inventory management may be problem-dependent, and this is why we restrict our discussion to a single-item, single-period inventory system subject to a continuous-review (Q, R) policy. We set $T = T^* + L^*$, where T^* is the time at which the inventory level reaches the reorder point R , and L^* is the (possibly random) lead time for an order. A suitable definition for the output process is $Y(s) =$ cumulative demand of the single item on the interval $[0, s]$, so that $W = Y(T) + Y(T^*)$ is the demand during the lead time.

In general, a forecast for demand W is completely defined by its cumulative distribution function (c.d.f.) $F(w) = P[W \leq w | X = x]$, which allows us to define the following important performance measures for inventory management. The expected demand

$$\mu = E[W | X = x] = \int_0^{\infty} ydF(y) \quad (3)$$

is usually regarded as the point forecast. We assume that demand W is non-negative (i.e., $F(w) = 0$ for $w < 0$). Note that, although F or μ might depend on x , in order to simplify the notation, we denote (on purpose) F or μ not depending on x , and remark that the results of Section 3 can also be applied to the case where parameter uncertainty is not considered.

A performance measure that is of practical importance in inventory management is the probability of no stock-out

$$\alpha_1(R) = P[W \leq R | X = x] = F(R), \quad (4)$$

where $R \geq 0$. Thus, we say that the type-1 service level (T1SL) corresponding to a reorder point $R \geq 0$ is $100\alpha_1(R)\%$, and given $0 < \alpha < 1$, a reorder point for a $100\alpha\%$ T1SL is defined as

$$r_1(\alpha) = \inf \{R \geq 0 : \alpha_1(R) \geq \alpha\}, \quad (5)$$

where $\alpha_1(R)$ is defined in (4).

Another measure of service is the proportion of demands that are met from stock,

$$\alpha_2(R) \stackrel{def}{=} 1 - \frac{\int_R^\infty (y-R)dF(y)}{Q}, \quad (6)$$

where $R \geq 0$, and $Q > 0$. We say that the type-2 service level (T2SL) corresponding to a reorder point $R \geq 0$ is $100\alpha_2(R)\%$, and given $0 < \alpha < 1$, a reorder point for a $100\alpha\%$ T2SL is defined as

$$r_2(\alpha) \stackrel{def}{=} \inf\{R \geq 0 : \alpha_2(R) \geq \alpha\}, \quad (7)$$

where $\alpha_2(R)$ is defined in (6). According to Nahmias (2008), the term ‘‘fill rate’’ is often used to describe T2SL, and is generally what most managers mean by service.

Finally, note that T1SL considers the probability of stock-out only during the lead time, so that we might also consider a measure of fill rate during the lead time,

$$\alpha_3(R) \stackrel{def}{=} 1 - \frac{\int_R^\infty (y-R)dF(y)}{\mu}, \quad (8)$$

where $\mu > 0$ is defined in (3). Similarly, we say that the type-3 service level (T3SL) corresponding to a reorder point $R \geq 0$ is $100\alpha_3(R)\%$, and given $0 < \alpha < 1$, a reorder point for a $100\alpha\%$ T3SL is defined as

$$r_3(\alpha) \stackrel{def}{=} \inf\{R \geq 0 : \alpha_3(R) \geq \alpha\}, \quad (9)$$

where $\alpha_2(R)$ is defined in (8).

When analytical expressions for the performance measures defined in this section cannot be obtained (or they are too complicated), simulation can be applied to estimate these parameters, as we explain in the next Section.

3. ESTIMATION USING SIMULATION

As illustrated in Figure 2, under the SPD algorithm we first sample from the posterior density $p(\theta|x)$ to obtain independent and identically distributed (i.i.d.) observations of the uncertain parameter Θ (given the data x), and then we simulate demand W to estimate μ , $\alpha_i(R)$ and $r_i(\alpha)$, by $\hat{\mu}$, $\hat{\alpha}_i(R)$ and $\hat{r}_i(\alpha)$, $i = 1, 2, 3$, respectively. The algorithm of Figure 2 is based on the algorithm proposed in Chick (2001) for the estimation of μ , and we also show how to produce consistent estimators for $\alpha_i(R)$ and $r_i(\alpha)$, $i = 1, 2, 3$. Furthermore,

each of the point estimators defined in Figure 2 satisfies a corresponding CLT, as we explain below.

For the sake of completeness, we first show, using the case of the estimation of μ , how an ACI is obtained from a CLT. As is well known from the standard CLT, when $E[W_1^2|X = x] < \infty$ we have

$$\frac{m^{1/2}(\hat{\mu} - \mu)}{\sigma_W} \Rightarrow N(0,1), \quad (10)$$

where ‘‘ \Rightarrow ’’ denotes weak converge (as $m \rightarrow \infty$), $N(0,1)$ is a standard normal distribution, and σ_W^2 is the variance of W_1 (given the data x , i.e., $\sigma_W^2 = E[\sigma_1^2|X = x] - \mu^2$). Also, from a Weak Law of Large Numbers we also know that $S_W / \sigma_W \Rightarrow 1$, where

$$S_W = (m-1)^{-1/2} \sqrt{\sum_{j=1}^m W_j^2 - m^{-1} \left(\sum_{j=1}^m W_j \right)^2}$$

is the sample standard deviation, so that it follows from (10) and a converging together argument that

$$\frac{m^{1/2}(\hat{\mu} - \mu)}{S_W} \Rightarrow N(0,1), \text{ and the interval}$$

$$I_m = [\hat{\mu} - z_\beta m^{-1/2} S_W, \hat{\mu} + z_\beta m^{-1/2} S_W]$$

tends (as $m \rightarrow \infty$) to cover the parameter μ with probability $(1 - \beta)$, where $0 < \beta < 1$ is a given constant and $P[N(0,1) < z_\beta] = 1 - \beta/2$. The interval I_m is called a $100(1 - \beta)\%$ ACI for μ , and the corresponding halfwidth

$$H_{\hat{\mu}} = z_\beta m^{-1/2} S_W, \quad (11)$$

is used in the simulation literature to assess the accuracy of $\hat{\mu}$ as an estimator of parameter μ . Similarly, $\alpha_1(R) = E[V_{11}|X = x]$, and $\alpha_2(R) = E[V_{21}|X = x]$, where $V_{11} = I[W_1 \leq R]$ and $V_{21} = 1 - Q^{-1}(W_1 - R)I[W_1 > R]$, so that CLT’s for $\hat{\alpha}_1(R)$ and $\hat{\alpha}_2(R)$ are easily obtained from the standard CLT, and the halfwidths corresponding to a $100(1 - \beta)\%$ ACI for $\alpha_i(R)$, $i = 1, 2$ are given by

$$H_{\hat{\alpha}_i(R)} = z_\beta m^{-1/2} S_i, \quad (12)$$

where $S_i = (m-1)^{-1/2} \sqrt{\sum_{j=1}^m V_{ij}^2 - m^{-1} \left(\sum_{j=1}^m V_{ij} \right)^2}$, $V_{1j} = I[W_j \leq R]$, $V_{2j} = 1 - Q^{-1}(W_j - R)I[W_j > R]$, for $i = 1, 2$, $j = 1, \dots, m$, and the W_j ’s are defined in Figure 2.

Finally, note that $\alpha_3(R) = 1 - \mu_R / \mu$, where $\mu_R = E[\max\{0, W_1 - R\}|X = x]$, so that a CLT for

$\hat{\alpha}_3(R)$ can be obtained by applying the Delta method (see, e.g., Lemma 1 of Muñoz and Glynn 1997), and the halfwidth corresponding to a $100(1-\beta)\%$ ACI for $\alpha_3(R)$ is given by

$$H_{\hat{\alpha}_3(R)} = z_\beta m^{-1/2} S_3, \quad (13)$$

where $S_3 = \hat{\mu}^{-1} \sqrt{S_3^2 - 2(\hat{\mu}_3 - \hat{\mu})S_{WV_3} + (\hat{\mu}_3 - \hat{\mu})^2 S_W^2}$,

$$\hat{\mu}_3 = m^{-1} \sum_{j=1}^m V_{3j}, \quad V_{3j} = \max\{0, W_j - R\}, j = 1, \dots, m,$$

$$S_3^2 = (m-1)^{-1} \left(\sum_{j=1}^m V_{3j}^2 - m \hat{\mu}_3^2 \right), \text{ and}$$

$$S_{WV_3} = (m-1)^{-1} \left(\sum_{j=1}^m W_j V_{3j} - m \hat{\mu} \hat{\mu}_3 \right).$$

When W is discrete, the value of a reorder point can be investigated from the estimation of the corresponding service levels $\alpha_i(R)$ for different values of R , and thus we assume that W is continuous when discussing how to compute a halfwidth for a reorder point. In particular, for the estimation of $\eta_1(\alpha)$, we assume that F is differentiable at $\eta_1(\alpha)$ with $F'(\eta_1(\alpha)) > 0$, so that it follows from Bahadur's representation for quantiles (Bahadur 1966) that $\hat{\eta}_1(\alpha)$ satisfies a CLT, and a halfwidth corresponding to a $100(1-\beta)\%$ ACI for $\eta_1(\alpha)$ is given by

$$H_{\hat{\eta}_1(\alpha)} = (Z_{m_{11}} + Z_{m_{12}}) / 2, \quad (14)$$

where $m_{11} = \lfloor m\alpha - z_\beta [m\alpha(1-\alpha)]^{1/2} \rfloor$,

$m_{12} = \lceil m\alpha + z_\beta [m\alpha(1-\alpha)]^{1/2} \rceil$, and the Z_i 's are

defined in Figure 2. The validity of the ACI corresponding to (14) relies on a CLT for $\hat{\eta}_1(\alpha)$ and is established in Section 2.6.3 of [29]. We remark that the asymptotic variance of the CLT for $\hat{\eta}_1(\alpha)$ depends on the density $F'(\eta_1(\alpha))$, and to avoid a density estimation we are using a halfwidth in the form of (14).

In order to establish a CLT for $\hat{r}_2(\alpha)$ and $\hat{r}_3(\alpha)$, we need to introduce some notation. For $R \geq 0$, set

$$\lambda_{21}(R) = (1-\alpha)Q - \int_R^\infty (y-R)dF(y),$$

$$\lambda_{22}(R) = (1-\alpha)^2 Q^2 - 2Q(1-\alpha) \int_R^\infty (y-R)dF(y) + \int_R^\infty (y-R)^2 dF(y), \quad (15)$$

and

$$\lambda_{31}(R) = (1-\alpha)\mu - \int_R^\infty (y-R)dF(y),$$

$$\lambda_{32}(R) = (1-\alpha)^2 \int_0^R y^2 dF(y) + \int_R^\infty (R-\alpha y)^2 dF(y). \quad (16)$$

Proposition 1. Let us suppose that $\int_0^\infty y^2 dF(y) < \infty$ and $0 < \alpha < 1$. Then

- (i) If $\int_0^\infty y^2 dF(y) > (1-\alpha)^2 Q^2$, $\lambda_{21}(R)$ is differentiable at $R = r_2(\alpha)$ and $\lambda_{22}(R)$ is continuous at $R = r_2(\alpha)$, we have

$$m^{1/2} [\hat{r}_2(\alpha) - r_2(\alpha)] \Rightarrow \sigma_2 N(0,1),$$

where $\lambda_{21}(R)$ and $\lambda_{22}(R)$ are defined in (15), and

$$\sigma_2^2 = \frac{\int_{r_2(\alpha)}^\infty (y - r_2(\alpha))^2 dF(y) - (1-\alpha)^2 Q^2}{(1 - F(r_2(\alpha)))^2}.$$

- (ii) If $\mu > 0$, $\lambda_{31}(R)$ is differentiable at $R = r_3(\alpha)$ and $\lambda_{33}(R)$ is continuous at $R = r_3(\alpha)$, we have

$$m^{1/2} [\hat{r}_3(\alpha) - r_3(\alpha)] \Rightarrow \sigma_3 N(0,1),$$

where $\lambda_{31}(R)$ and $\lambda_{32}(R)$ are defined in (16), and

$$\sigma_3^2 = \frac{(1-\alpha)^2 \int_0^{r_3(\alpha)} y^2 dF(y) + \int_{r_3(\alpha)}^\infty (r_3(\alpha) - \alpha y)^2 dF(y)}{(1 - F(r_3(\alpha)))^2}.$$

For $j = 1$ to the number of replications m :

a. Generate (independently) a value θ_j by sampling from $p(\theta|x)$.

b. Run a simulation experiment with $\Theta = \theta_j$ to obtain an independent replication W_j of $W = g\{Y(s), 0 \leq s \leq T; \Theta\}$

End Loop

Compute $\hat{\mu} = \frac{1}{m} \sum_{j=1}^m W_j, \hat{\alpha}_1(R) = \frac{1}{m} \sum_{j=1}^m I[W_j \leq R]$

$$\hat{\alpha}_2(R) = 1 - \frac{\sum_{j=1}^m (W_j - R) I[W_j > R]}{mQ}, \hat{\alpha}_3(R) = 1 - \frac{\sum_{j=1}^m (W_j - R) I[W_j > R]}{\sum_{j=1}^m W_j}.$$

Sort the W_j 's: $Z_1 \leq \dots \leq Z_m$ and set $f_1(\alpha) = Z_{k_1}, f_2(\alpha) = Z_{k_2}, f_3(\alpha) = Z_{k_3}$,

where $Z_0 = 0$, and

$$k_1 = \lceil m\alpha \rceil, k_2 = \min\left\{0 \leq j \leq m : \sum_{i=j}^m (Z_i - Z_j) \leq Qm(1-\alpha)\right\},$$

$$k_3 = \min\left\{0 \leq j \leq m : \sum_{i=j}^m (Z_i - Z_j) \leq (1-\alpha) \sum_{i=1}^m Z_i\right\}.$$

Figure 2: Estimation of Performance Measures Using SPD

Using Proposition 1 we can establish the following halfwidths, corresponding to a $100(1-\beta)\%$ ACI for $r_2(\alpha)$ and $r_3(\alpha)$, respectively,

$$H_{\hat{r}_2(\alpha)} = z_\beta m^{-1/2} \hat{\sigma}_2 \text{ and } H_{\hat{r}_3(\alpha)} = z_\beta m^{-1/2} \hat{\sigma}_3, \quad (17)$$

where

$$\hat{\sigma}_2^2 = m(m - k_2)^{-2} \left[\sum_{j=k_2}^m (W_j - \hat{r}_2(\alpha))^2 - mQ^2(1-\alpha)^2 \right],$$

$$\hat{\sigma}_3^2 = m(m - k_3)^{-2} \left[(1-\alpha)^2 \sum_{j=1}^{k_3-1} W_j^2 + \sum_{j=k_3}^m (\hat{r}_3(\alpha) W_j)^2 \right],$$

k_2, k_3 and the W_j 's are defined in the algorithm of Figure 2.

4. AN ILLUSTRATIVE EXAMPLE

In order to illustrate our notation, we present a model that is inspired in the ideas of Silver (1965) and Croston (1972) to forecast intermittent demand. Suppose that the arrival of clients at a retailer occurs according to a Poisson process, however there is uncertainty on the arrival rate Θ_0 , so that given $[\Theta_0 = \theta_0]$, the time between customers arrivals are i.i.d. according to the exponential density function

$$f(y|\theta_0) = \begin{cases} \theta_0 e^{-\theta_0 y}, & y > 0, \\ 0, & \text{otherwise,} \end{cases}$$

where $\theta_0 \in S_{00} = (0, \infty)$. In addition, every customer orders j items (independently of each other) with probability Θ_{1j} , $j = 1, \dots, q$, $q \geq 2$.

Set $\Theta_1 = (\Theta_{11}, \dots, \Theta_{1(q-1)})$ and $\Theta_{1q} = 1 - \sum_{j=1}^{q-1} \Theta_{1j}$, then $\Theta = (\Theta_0, \Theta_1)$ denotes the parameter vector, and the parameter space is $S_0 = S_{00} \otimes S_{01}$, where

$$E_{01} = \left\{ (\theta_{11}, \dots, \theta_{1(q-1)}) : \sum_{j=1}^{q-1} \theta_{1j} < 1; \theta_{1j} > 0, j = 1, \dots, q-1 \right\}.$$

We are interested in the total demand (W) during a lead time of length L^* ,

$$W = \begin{cases} \sum_{i=1}^{N(T^*+L^*)-N(T^*)} U_i, & N(T^*+L^*)-N(T^*) > 0, \\ 0, & \text{otherwise,} \end{cases} \quad (18)$$

where T^* is as in (3), $L^* > 0$ is a constant, $N(s)$ is the number of clients that arrived on $[0, s]$, $s \geq 0$, and U_1, U_2, \dots are the individual demands (assumed conditionally independent relative to Θ). Information on Θ is available from (i.i.d.) observations of past clients $v = (v_1, \dots, v_n)$ and $u = (u_1, \dots, u_n)$ where v_i is the interarrival time of client i , and u_i is the number of items ordered by client i . Note that, according to (2), the likelihood functions for v and u take the form of

$$L(v|\theta_0) = \theta_0^n e^{-\theta_0 \sum_{i=1}^n v_i}, \text{ and } L(u|\theta_1) = \left(1 - \sum_{j=1}^{q-1} \theta_{1j}\right)^{c_q} \prod_{j=1}^{q-1} \theta_{1j}^{c_j},$$

respectively, where $\theta_1 = (\theta_{11}, \dots, \theta_{1(q-1)})$, and $c_j = \prod_{i=1}^n I[u_i = j]$ is the number of past clients that ordered j items.

If we adopt an objective point of view, we may wish to consider a non-informative prior density for Θ , and using Jeffrey's prior may be appropriate. As is well known, Jeffrey's prior density for the exponential model is $p(\theta_0) = \theta_0^{-1}$, $\theta_0 \in S_{00}$, so that it follows from (1) that

$$p(\theta_0|v) = \frac{\theta_0^{n-1} \left(\sum_{i=1}^n v_i\right)^n e^{-\theta_0 \sum_{i=1}^n v_i}}{(n-1)!}, \quad (19)$$

which corresponds to the Gamma($n, \sum_{i=1}^n v_i$) distribution, where, for $\beta_1, \beta_2 > 0$, $Gamma(\beta_1, \beta_2)$ denotes a Gamma distribution with expectation $\beta_1 \beta_2^{-1}$. Similarly, Jeffrey's prior density for the multinomial model (see, e.g., Berger and Bernardo 1992) is

$$p(\theta_1) = \frac{\left(1 - \sum_{j=1}^{q-1} \theta_{1j}\right)^{-1/2} \prod_{j=1}^{q-1} \theta_{1j}^{-1/2}}{B(1/2, \dots, 1/2)},$$

where $B(1/2, \dots, 1/2) = \left(\sum_{j=1}^q a_j\right)^{-1} \prod_{j=1}^q a_j$, for $a_1, \dots, a_n > 0$, so that it follows from (1) and (19) that

$$p(\theta_1|u) = \frac{\left(1 - \sum_{j=1}^{q-1} \theta_{1j}\right)^{c_q-1/2} \prod_{j=1}^{q-1} \theta_{1j}^{c_j-1/2}}{B(c_1+1/2, \dots, c_q+1/2)}, \quad (20)$$

which corresponds to a Dirichlet($c_1+1/2, \dots, c_q+1/2$) distribution. Thus, if we set $x_i = (z_i, u_i)$, $i = 1, \dots, n$, $x = (x_1, \dots, x_n)$, and $\theta = (\theta_0, \theta_1)$, under an appropriate independence assumption, the posterior density becomes $p(\theta|x) = p(\theta_0|z)p(\theta_1|u)$, where $p(\theta_0|z)$ and $p(\theta_1|u)$ are defined in (19) and (20), respectively.

Note that in this example we can obtain an analytical expression for the point forecast $\mu = E[W|X = x]$, since from (19) and (20) we have

$$E[\Theta_0|V = v] = n \left(\sum_{i=1}^n v_i\right)^{-1}, \text{ and}$$

$$E[\Theta_{1j}|U = u] = c^{-1} (c_j + 1/2)$$

(where $c = \sum_{j=1}^n (c_j + 1/2) = n + q/2$), so that from (18) we have

$$\begin{aligned} \mu &= E[E[W|\Theta, X = x]|X = x] \\ &= E\left[E\left[N(T^* + L^*) - N(T^*)\right] \Theta \mid E[U_1|\Theta] X = x\right] \\ &= L^* E\left[\Theta_0 \sum_{j=1}^q j \Theta_{1j} \mid X = x\right] \\ &= L^* E[\Theta_0|V = v] \sum_{j=1}^q j E[\Theta_{1j}|U = u] \\ &= L^* n \left(\sum_{i=1}^n v_i\right)^{-1} (n + q/2)^{-1} \sum_{j=1}^q j (c_j + 1/2), \end{aligned}$$

which allows us to compute the point forecast μ from the available data x . However in this case, analytic expressions for a service level or a reorder point may not be easy to obtain, and the SPD algorithm described in Section 3 may be useful to compute, via simulation, the other performance measures defined in Section 2. It is worth mentioning that Muñoz and Muñoz (2011) applied a simplified version of this model to the estimation of reorder points for a TISL using data from a car dealer.

5. CONCLUSIONS

We discussed how performance measures for inventory management (service levels and reorder points) can be suitably defined under a Bayesian framework, and how these performance measures can be estimated from the output of simulation experiments.

In the case where the sample data has the form of $x = (x_1, \dots, x_n)$ and the likelihood has the form of (2), this approach is particularly relevant when the sample size n is small, since in that case parameter uncertainty should be relatively large. It is worth mentioning that, as $n \rightarrow \infty$, this approach is consistent with the classical approach of ignoring parameter uncertainty and fixing the value of the parameter at the maximum likelihood estimator, since under regularity conditions (see e.g., Theorem 5.14 of Bernardo 2000), $p(\theta|x)$ has an asymptotically (as $n \rightarrow \infty$) normal distribution, with mean equal to the estimator $\hat{\theta}_n$ that maximizes $p(\theta|x)$.

Finally, note that SPD can be applied when a valid algorithm to generate samples from $p(\theta|x)$ is available. If this is not the case, methodologies based on Markov Chain Monte Carlo (see, e.g., Robert 2007) can be applied, and, under regularity conditions, a valid ACI for any of the performance measures defined in Section 2 can still be obtained (see, e.g., Muñoz and Glynn 1997 and Muñoz 2010 for regularity conditions of ACI's based on the batch means method).

ACKNOWLEDGMENTS

This research has been supported by the Asociación Mexicana de Cultura AC.

REFERENCES

- Bahadur, R.R., 1966. A note on quantiles in large samples. *The Annals of Mathematical Statistics* 37 (3), 577-580.
- Bartezzaghi, E., Verganti, R., Zotteri, G., 1999. A simulation framework for forecasting uncertain lumpy demand. *International Journal of Production Economics*, 59 (3), 499-510.
- Berger, J.O., Bernardo, J.M., 1992. Ordered group reference priors with application to the multinomial problem. *Biometrika*, 79 (1), 25-37.
- Berger, J.O., Bernardo, J.M., Sun, D., 2008. The formal definition of reference priors. *The Annals of Statistics*, 37 (2), 905-938.
- Bernardo, J.M., Smith, A.F.M., 2000. *Bayesian Theory*, England: John Wiley.
- Bermúdez, J.D., Segura, J.V., Vercher, E., 2010. Bayesian forecasting with the Holt-Winters model. *Journal of the Operational Research Society*, 61 (1), 164-171.
- Chick, S.E., 2001. Input distribution selection for simulation experiments: accounting for input uncertainty. *Operations Research*, 49 (5), 744-758.
- Croston, J.D., 1972. Forecasting and stock control for intermittent demands. *Operations Research Quarterly*, 23 (3), 289-303.

- Fu, M.C., 2002. Optimization for simulation: Theory vs practice. *Inform Journal on Computing*, 14 (3), 192-215.
- Glasserman, P., Liu T.W., 1996. Rare-event simulation for multistage production-inventory systems. *Management Science*, 42 (9), 1292-1307.
- Jahangirian, M., Eldavi, T., Naser, A., Stergioulas, L.K., Young, T., 2010. Simulation in manufacturing and business: A review, *European Journal of Operational Research*, 203 (1), 1-13.
- Muñoz, D.F., Glynn, P.W., 1997. A batch means methodology for estimation of a nonlinear function of a steady-state mean. *Management Science*, 43 (8), 1121-1135.
- Muñoz, D.F., Galindo, R., 2010. Incorporating parameter uncertainty for inventory management. *Proceedings of the 2010 IIE Annual Conference*, A. Johnson & J. Miller (eds.), Institute of Industrial Engineers.
- Muñoz, D.F., 2010. On the validity of the batch quantile method in Markov chains. *Operations Research Letters*, 38 (3), 223-226.
- Muñoz, D.F., Muñoz, D.F., 2011. Bayesian forecasting of spare parts using simulation. In: Altay, N. and Litteral, L. A. (Eds.), *Service Parts Management: Demand Forecasting and Inventory Control*, NY: Springer, 105-124.
- Nahmias, S., 2008. *Production and Operations Analysis*, 6th ed. NY: McGraw-Hill.
- Robert, C.P., 2007. *The Bayesian Choice: From Decision-Theoretic Foundations to Computational Implementations*, NY: Springer.
- Silver, E.A., 1965. Bayesian determination of the reorder point of a slow moving item, *Operations Research*, 13 (6), 989-997.
- Syntetos, A.A., Boylan, J.E., Disney S.M., 2009. Forecasting for inventory planning: A 50-year review. *Journal of the Operational Research Society*, 60 (1), 149-160.
- Tako, A.A., Robinson, S., 2012. The application of discrete event simulation and system dynamics in the logistics and supply chain context. *Decision Support Systems*, 52 (4), 802-815.

AUTHORS BIOGRAPHY

David Fernando Muñoz is Head of the Department of Industrial & Operations Engineering at the Instituto Tecnológico Autónomo de México. He received his PhD in Operations Research from Stanford University, and is an Edelman Laureate for participating in the project that received the 2010 Franz Edelman Award. His research interests include the statistical analysis of simulation output.

David Gonzalo Muñoz is an Analyst at the R&D Department of AOL Advertising. He received his MSC degree in Management Science and Engineering from Stanford University. His research interests include stochastic modeling and yield management.

RETRIEVING THE PERFORMANCE OVERHEAD OF SYNCHRONIZATION MECHANISMS OF VARIOUS POPULAR OPERATING SYSTEMS

Michael Bogner ^(a), Johannes Schütz ^(b), Franz Wiesinger ^(c)

^(a, b, c) University of Applied Sciences Upper Austria,
Hardware/Software Design & Embedded Systems Design

^(a) michael.bogner@fh-hagenberg.at, ^(b) johannes.schuetz@fh-hagenberg.at, ^(c) franz.wiesinger@fh-hagenberg.at

ABSTRACT

The importance of multi-core processors increases every day. So multi-threaded programming also becomes more important. Due to data consistency it is necessary to synchronize specific parts of the code. These synchronizing methods cause an overhead during program execution. This paper analyses this overhead based on time on different operating systems. On the one hand, the paper gives a short introduction to the most important synchronization methods, on the other hand a test application is introduced to determine the delay time of each of these methods. All tests are designed to give real world examples of how much overhead is produced. Following the given data of the test application, the delay times of different operating systems are compared to each other. The paper shows that some methods perform better on one system and others perform better on the other systems.

Keywords: synchronization methods, synchronization performance, multi-threaded performance, decision support

1. INTRODUCTION

1.1. Motivation

The development of new processors, such as faster single-core processors and multi-core processors, resulted in new opportunities in software development. On multi-core processors it is now possible to achieve real parallelism of software by running various software components on different cores.

Alongside these new opportunities also new difficulties came. One primary difficulty is the synchronization of software components which run independently. Synchronization refers to controlling the application flow of paralleled software components.

There are certain techniques required to perform synchronization. Because of the various implementations of these techniques, different overhead is produced depending on the way of the implementation.

This paper analyses the overhead on the popular operating systems Windows XP, Windows 7 and Ubuntu 10.04 LTS in each case 32-bit edition.

1.2. Objective

The primary objective is to accomplish a comparison of various synchronization techniques on different operating systems. This is achieved by measuring the delay time by modelling real-world usage of the different techniques and simulating their real-world behaviour in the test environment.

The paper is divided into two main sections. The first section gives an overview to the basics of each synchronization method. Especially the usage of the methods using Win32-API and using POSIX (IEEE 1003.1-2008, 2008) is described.

The second section describes the test scenario, the implementation and the analysis of the results. Both, modelling and simulation of the test scenario is done with industrial applications in mind.

1.3. Related work

A similar approach of analysing synchronization techniques can be found in the paper “A new Look at the Roles of Spinning and Blocking” (Johnson, 2009). There the trade-off between spinning and blocking synchronization is analysed and observed that the trade-off can be simplified by isolating the load control aspects of contention management.

Another approach can be found in the article “Multi-threaded Performance” (Asche, 1996) where strategies for rewriting single-threaded applications to be multi-threaded applications are discussed. It analyses the performance of multi-threaded computations over compatible single-threaded ones in terms of throughput and response.

2. THE BASICS

2.1. Multi-threaded programming

Multi-threaded programming allows the creation of parallel software. Since C++ does not provide mechanisms for multi-threaded applications until C++11 (ISO, 2011), operating system functions have to be accessed. The problem with these functions is that they are implemented differently on various operating systems and also provide different results in regard to performance. C++11 already provides multi-threaded mechanisms on the basis of POSIX-threads, but there

are hardly any compilers or commercial software since it was released in August 2011.

Multi-threaded code is program code which is executed simultaneously by the operating system.

On Linux systems these functions are defined by the POSIX standard and implemented in the kernel. On Windows systems they are defined by the Win32-API and also implemented in the kernel.

Because of parallel execution of software components, which also share resources and communicate with each other, the control flow is synchronized. But this synchronized execution also causes problems in the form of deadlocks, race conditions, starvation and live-locks. These problems occur when synchronization methods are used carelessly.

Further discussions on multi-threaded programming can be found in (Akhter & Roberts, 2006), (Williams, 2012) and (Johnson, Athanassoulis, Stoica, & Ailamaki, 2009).

2.2. Why synchronization?

Due to the previously mentioned problems with multi-threaded programming a synchronization of the control flow is needed.

Synchronization is always needed when parallel reading and writing on memory occurs and when a specific sequence of the control flow has to be guaranteed. Also synchronization is needed when only writing parallel on memory but reading sequential. No synchronization is needed when the memory is written sequential.

In general, synchronization is always necessary when several threads write to a specific memory area.

2.3. POSIX-standard

The POSIX-standard defines a consistent standard system interface for UNIX-systems and Windows-systems. POSIX is the abbreviation for *Portable Operating System Interface for UNIX*. POSIX has been created to enable portable code for various UNIX-systems. POSIX includes the PThread-library for programming multi-threaded applications for UNIX-systems.

2.4. Synchronization mechanisms

There are various synchronization primitives, depending on the operating system and the underlying CPU. Each primitive has its special purpose:

- Critical Sections: atomic areas within a process for exclusive access.
- Events: signal that a certain state of the application occurred.
- Wait-functions: blocked waiting for an event or other signal.
- Mutex: similar to critical sections which work outside process boundaries.
- Semaphore: similar to mutex with an internal counter for handling several threads.

- Spin-lock: similar to critical sections but with short active waiting before passive waiting.
- Interlocked functions: hardware depended atomic operations which directly execute CPU-instructions

Further discussions on these techniques can be found in (Hart, 2010) and (Jones, 2008).

3. TEST SCENARIO

3.1. Introduction

As basis for the tests the Microsoft operating systems Windows XP and Windows 7, as well as the UNIX based free operating system Ubuntu 10.04 LTS are used. Windows XP and Windows 7 have been taken because they are the most commonly used Microsoft operating systems in industry. Ubuntu 10.04 LTS is used because it's one of the most commonly used UNIX based operating systems. The test environment is built with C++ and uses its object oriented capabilities.

3.2. Time measurement

The time measurement is carried out by operating system internal time measurement operations with high accuracy. The measurement uses an accuracy of 1 us which is accurate enough for our real world measurement approach.

Not the absolute time delay is measured, but the delay relative to the current CPU-tick count. This allows a better comparison by disregarding the blur of each operating system because their similar scheduling algorithms.

To keep the source code compatible between Windows and UNIX the Win32-API functions *QueryPerformanceCounter* and *QueryPerformanceFrequency* were implemented using *gettimeofday* (Linux High-Resolution Timer, 2009). The functions have the same interface like the Win32-API functions and are implemented using compiler directives.

3.3. Test flow

Given that the different synchronization techniques primarily differ in their field of application and therefore similar in usage also the test flow is structured similar for each technique.

Basically a test consists of initialization, start of the components, time measurement and analysis.

1. Initialization: The synchronization mechanisms and program components are initialized according to their usage.
2. Execution: The execution and time measurement are carried out in parallel and are repeated to generate a more accurate median.
3. Analysis: The median is calculated and written into an Excel file for further processing.

3.4. Constraints

Given that there are a lot of multi-core processors with various numbers of cores and clock frequencies and the different operating systems, it needs to be ensured that the average result is only exposed to low deviation.

It has to be ensured that the whole program inclusive all its components is executed on only one CPU core. This is needed because the switch of the execution to another CPU core also produces overhead and to avoid inter-core communication influence.

Also it has to be ensured that the overhead of context switches between parallel executed components is minimized. This is done by setting the process priority to the highest priority available.

4. IMPLEMENTATION

4.1. Introduction

This section describes the architecture and implementation of the test application for each synchronization technique.

4.1.1. Software architecture

The architecture is built up from two base classes, one for the test flow and one for threads. Derived from this base classes are all classes needed for testing each synchronization technique. Classes are named after the technique they are used for with the suffixes 'Test' and 'Thread' to differentiate between the test flow and the threads.

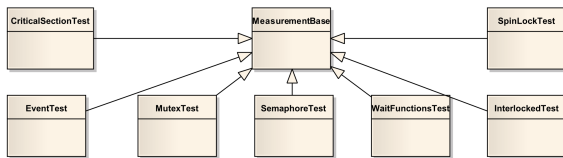


Figure 1: Test Classes

Figure 1 shows the class hierarchy of the test classes. Each test class implements methods for controlling the test flow and interpreting the test results.

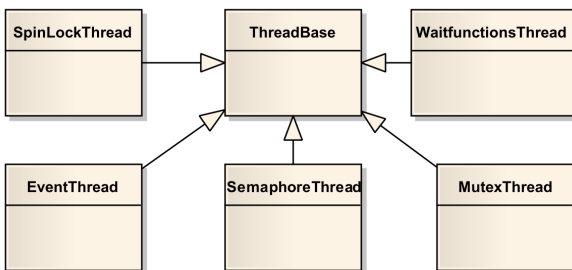


Figure 2: Thread Classes

Figure 2 shows the class hierarchy of the thread classes. The base class is used for controlling the typical thread flow such as creating, starting or suspending. The derived classes implement the specific methods for each synchronization technique and the control flow. The threads are implemented as fire-and-forget threads so

there is no need to stop and delete them. They are used for calculating the overhead of the various synchronization techniques.

Because the POSIX-standard doesn't provide an implementation for manual-reset-events, they are self-implemented using a conditional variable and a mutex. There are methods and a structure realized which implement the functionality.

4.1.2. Test flow

Figure 3 shows the typical test flow with the help of the base classes. The user creates a new test class and initializes it. The test class then creates the corresponding thread class and starts the testing. The testing is repeated as often as *MEASURES* declares. After the tests are completed the average overhead is calculated and written to a file for further processing.

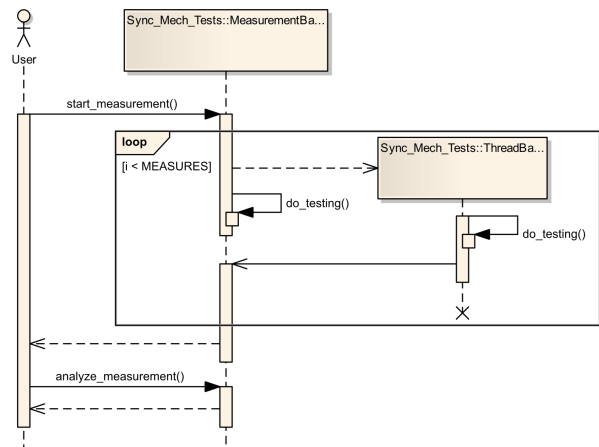


Figure 3: Test flow

4.1.3. Choosing processor core and process priority

As described in section 3.4 the overhead of context switches and switching to another core needs to be reduced so the results don't get falsified.

To reduce the number of context switches the process priority is set to real-time. To block core switching the process affinity mask has to be set. It doesn't matter on which core the program is executed as long as it is only one core.

Listing 1 and Listing 2 show the Windows implementation and respectively the UNIX implementation of setting process priority and affinity mask.

Listing 1: Windows Process Priority and Affinity Mask (without error handling)

```
HANDLE h_process = GetCurrentProcess();
// set process priority to high
SetPriorityClass(h_process, REALTIME_PRIORITY_CLASS);
// set process affinity mask to only use core 0
SetProcessAffinityMask(h_process, AFFINITY_MASK);
```

Listing 2: UNIX Process Priority and Affinity Mask (without error handling)

```
cpu_set_t mask;
CPU_ZERO(&mask);
CPU_SET(0, &mask);
```



```
// set process priority to high
setpriority(PRIO_PROCESS,0,-20);
//set process affinity mask to only use core 0
sched_setaffinity(0, sizeof(mask), &mask);
```

4.2. Synchronization techniques

All tests are designed to give real world examples of how much overhead is produced by the various techniques and not just laboratory values.

4.2.1. Critical sections

The test flow is shown in Figure 4. The delay time measured is the delay from entering and respectively leaving the critical section. This way of measurement is done because critical sections are used for short sections only so there is not much overhead.

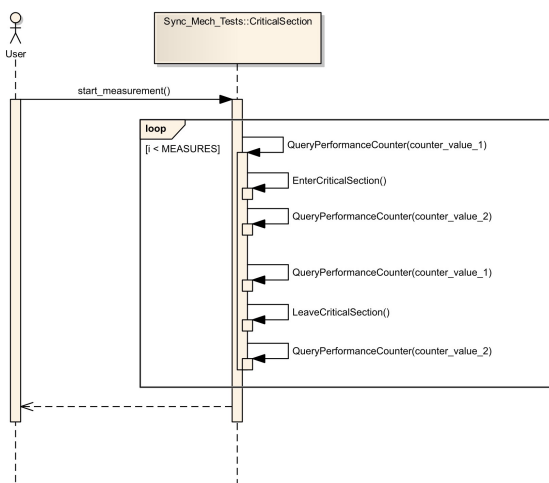


Figure 4: Measuring Critical Sections

4.2.2. Events

The test flow is shown in Figure 5. After starting the test a thread is created which initially waits for an event to continue execution. In the test method this event is signalled and the thread continues its execution. After signalling the event the test method waits for an event signalled by the thread. After continuing execution the thread sets the event and finishes its work. The delay of events is calculated by measuring the time from signalling the event to recognizing the signalled event. With this method of measurement not only the execution time of the technique is measured but also the overhead produced by context switches which gives a real world example of the overhead.

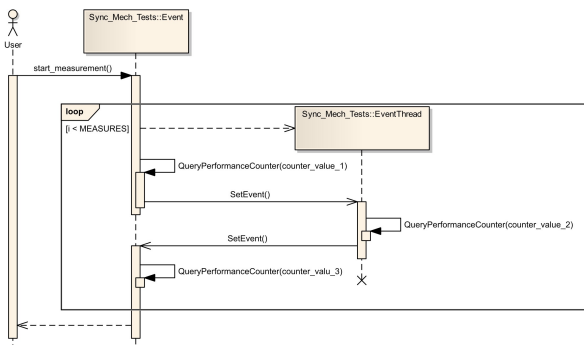


Figure 5: Measuring Events

4.2.3. Wait-functions

Because there are no directly equivalent functions in the POSIX-standard this tests measures the delay of recognizing the exiting of a thread. And also wait-functions from Win32-API which are used to wait for signals of mutex, semaphores and events are measures in the corresponding tests.

Figure 6 shows the test flow of measuring the wait-functions. After the test is started a thread is created and started and the test method waits for it to complete. The time is measured after the thread was started and after the thread completed execution.

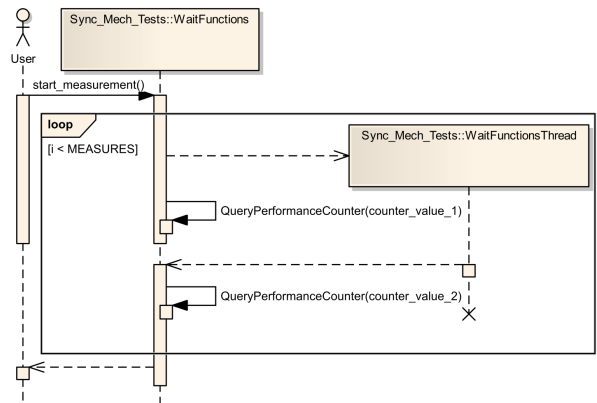


Figure 6: Measuring Wait-functions

4.2.4. Mutex

The test flow of testing mutex is similar to that of testing critical sections with the difference that there is a thread to communicate with.

Figure 7 shows the test flow. After starting the test a mutex is created in blocked mode and a thread is created and started. The thread opens the mutex and waits for it to be released. After the thread owns the mutex the test method waits for it to be released. The overhead is calculated by measuring the time from releasing the mutex in the test method and respectively in the thread and getting to own the mutex in the thread and respectively the test method.

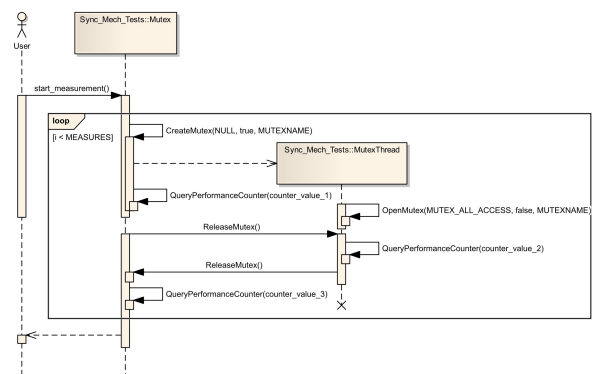


Figure 7: Measuring Mutex

4.2.5. Semaphore

The test flow of the semaphore test, shown in Figure 8, works corresponding to the mutex test with the difference that more threads are used.

4.2.6. Spin-locks

The test flow of the spin-locks test is corresponding to that of testing critical sections with the only difference being spin-locks in testing instead of critical sections. Because of this nearly equivalent test flow there is now explicit figure given to illustrate it.

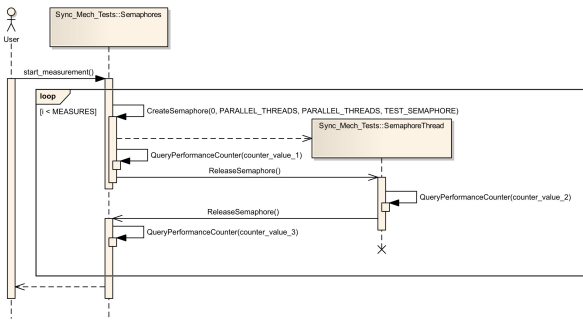


Figure 8: Measuring Semaphore

4.2.7. Interlocked functions

The test flow of measuring interlocked functions, shown in Figure 9, is very simple. Each function is executed and its execution time is measured.

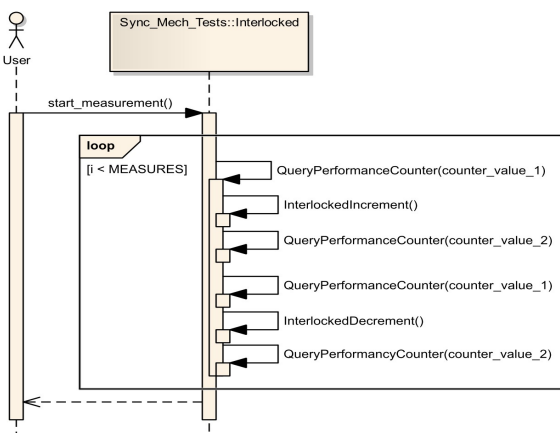


Figure 9: Measuring Interlocked Functions

5. ANALYSIS

5.1. General Findings

Through the evaluation of the test results insights could be gained on how the performance of synchronization techniques differs on different operating systems. When viewing the test results it is important to differ between synchronization techniques, which are influenced by the operating system and those without. Influenced by the operating system are mutex, semaphore, events and wait-functions. Without influence are critical sections, spin-locks and interlocked functions.

If synchronization does not depend on the operating system, less overhead can clearly be

recognized. In general, for process-internal synchronization critical sections should be used and for calculations interlocked functions if available. Spin-locks are particularly well suited for synchronization of small areas which are divided among multiple processor cores, but produce more overhead if the number of critical areas exceeds the number of processor cores.

If synchronization depends on the operating system, wait-functions cause the least overhead because they only wait for a certain signal, usually in a blocked manner. Because of the operating system influenced token system of mutexes they produce more overhead than critical sections. Semaphores produce similar overhead to mutex but have even more impact due to the internal counter. The overhead of events exists of operating system influence and the expense to signal the wait-function to continue execution.

Table 1 shows the results of the tests on Windows 7, Windows XP and Ubuntu 10.04 LTS. As it can be seen clearly, synchronization techniques without the influence of the operating system are by far, the fastest. Values of 1us indicate that the measurement is near or beyond its precision, which doesn't mind as the high values are important in real-world applications. That confirms the knowledge that for process internal synchronization critical sections and for calculations interlocked functions should be used. Also recognizable is that wait-functions produce nearly the same overhead regardless of whether they are waiting on one or more signals. Mutex, semaphore and events produce very different overhead on the several operating systems; this will be illustrated in the next section.

Looking at the results of operating system influenced synchronization techniques it can be said, that semaphores should be avoided when possible. If synchronization is needed outside of process boundaries use events or mutex under Windows but try to avoid events under UNIX.

Table 1: Results Windows XP, Windows 7, Ubuntu 10.04 LTS (time in us)

Synchronization technique	Win 7	Win XP	Ubuntu
EnterCriticalSection	1	1	1
Interlocked Decrement	1	1	1
Interlocked Increment	1	1	1
LeaveCriticalSection	1	1	1
Lock Spinlock	1	1	1
ReleaseMutex	21	59	14
ReleaseSemaphore	39	27	11
SetEvent	32	20	51
Unlock Spinlock	1	1	1
WaitForMultipleObjects	18	20	19
WaitForSingleObject	18	19	15
Waiting for Mutex	24	26	42
Waiting for Semaphore	145	105	106

5.2. Differences between Windows XP, Windows 7 and Ubuntu 10.04 LTS

In a direct comparison of windows and UNIX it can be seen that in general the mechanisms require less effort under UNIX than under Windows.

On all systems critical sections, spin-locks and interlocked functions only produce such a small overhead that no difference is recognizable. The same can be seen by looking at wait-functions, which produce nearly the same overhead on the several operating systems. A big difference can be seen when looking at mutex, which produces more than twice the overhead when it is released on Windows XP than on Windows 7 or Ubuntu. Acquiring a mutex produces more overhead on Ubuntu than on Windows XP or Windows 7 which produce similar overhead. Another big difference can be seen at semaphores. Acquiring a semaphore on Windows XP or Ubuntu produces nearly the same overhead but produces a lot more overhead on Windows 7. This could be explained due to the internal implementation of the semaphore counter. In general, acquiring a semaphore produces the most overhead of all synchronization techniques. Releasing a semaphore produces very different overhead on all operating systems. On Windows XP the overhead is twice as much as on Ubuntu and on Windows 7 three times as much overhead. Also events produce different overhead on each operating system. The least overhead is produced on Windows XP, a little more overhead is produced on Windows 7 but on Ubuntu the overhead is more than twice the overhead produced on Windows XP. This can be explained by looking at the implementation of the manual-reset-event on Ubuntu which uses a mutex and a conditional variable, so the overhead of two mechanisms is included in this test.

In general, it can be seen beside a few exceptions that Ubuntu operating system produces less overhead than both Windows operating systems. With the Windows operating systems it is more complicated, because some mechanisms produce less overhead on Windows XP and some on Windows 7.

A visual representation of these differences can be seen in Figure 10.

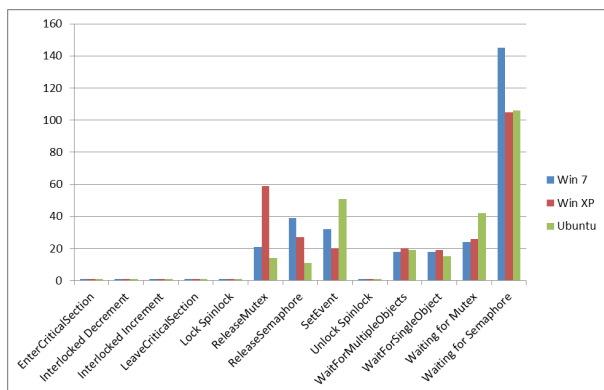


Figure 10: Difference between Windows and Linux

CONCLUSION

The performed tests have shown what average overhead is expected on the various operating systems. Also it was pointed out that UNIX comparing all mechanism produces less overhead than Windows operating systems. It can be seen that each operating system has its strengths and weaknesses in the implementation of synchronization techniques.

Based on these measurements it can now be shown which operating systems are the better option for each synchronization technique, provided a free selection is an option. In the field of synchronization Linux would be in almost every field the better option, except for events which have less overhead under Windows than under Linux.

On UNIX-systems it cannot be assumed, despite the POSIX-standard that the overhead on average is the same, since different UNIX-derivatives also have different kernel implementations. But in general it can be assumed that different Linux-distributions with the same kernel produce the same overhead.

Due to the different performance of synchronization techniques it is important to analyse in advance which mechanisms will be needed to not slowing down a multi-threaded application unnecessarily.

REFERENCES

- Akhter, S., Roberts, J., 2006. *Multi-Core Programming: Increasing Performance through Software Multi-threading*. Intel Press.
- Asche, R. R., 1996. *Multithreaded Performance*. Available from: <http://msdn.microsoft.com/en-us/library/ms810437.aspx> [accessed April 2012]
- Hart, J. M., 2010. *Windows System Programming*. Addison-Wesley Professional.
- IEEE 1003.1-2008., 2008. 1003.1-2008 - IEEE Standard for Information Technology - Portable Operating System Interface (POSIX(R)). IEEE.
- ISO, 2011. *ISO/IEC 14882:2011, Information technology - Programming languages - C++*. Available from: www.iso.org [accessed April 2012]
- Johnson, R., et al. 2009. *A new look at the roles of spinning and blocking*. In Proceedings of the Fifth International Workshop on Data Management on New Hardware (DaMoN '09). ACM, New York
- Jones, M. T., 2008. *GNU/Linux Application Programming*. Charles River Media.
- Williams, A., 2012. *C++ Concurrency in Action: Practical Multithreading*. Available from: <http://www.manning.com/williams/> [accessed April 2012]

MODELING AND SIMULATION BASED ON INVERSE FINITE ELEMENT METHOD FOR UNFOLDING LARGE AND THICK BLADES OF FRANCIS TURBINES

Zhengkun Feng^(a), Henri Champlaud^(b), Michel Sabourin^(c), Sebastien Morin^(d)

^{(a)(b)(d)}Department of Mechanical Engineering, École de technologie supérieure, University of Quebec
1100 Notre-Dame Street West, Montreal, Quebec, H3C 1K3, Canada

^(c)Alstom Renewable Power, Hydro, Global Technology Centre, Alstom Hydro Canada Inc.
1350 St-Roch Road, Sorel-Tracy, Quebec, J3P 5P9, Canada

^(a)zhengkun.feng@etsmtl.ca, ^(b)henri.champlaud@etsmtl.ca,
^(c)michel.sabourin@power.alstom.com, ^(d)sebastien.morin.3@ens.etsmtl.ca

ABSTRACT

The metal pressing process is widely used in industries, such as energy, civil, automotive and shipbuilding engineering. For the design of the process, blank design is firstly performed to determine the dimension of the flat blank. Traditionally, the trial and error approach is used. However, this approach wastes much time and raw materials, especially in manufacturing the blades of large Francis turbines. The rapid development of the computing technology makes it possible to get optimum blanks by numerical modeling and simulations. In this paper, the multi-step inverse finite element approach is investigated for the blank design and an elasto-plastic model has been built using the well-known software ANSYS. Unfolding tests with simple geometries have been carried out and the numerical results agree well with the results obtained by analytical analyses. Finally, a large and thick blade of Francis turbines for hydropower plants has been successfully unfolded.

Keywords: finite element method, inverse approach, pressing forming, blade, blank design, Francis turbine

1. INTRODUCTION

A runner is one of the fundamental components of a Francis turbine for hydropower plants and the manufacturing of its blades using pressing process from a flat blank has many advantages (Casacci, Bosc, Moulin, and Sauron 1977; Casacci and Caillot 1983). This process is widely applied in other industries, such as automotive, shipbuilding and civil engineering. For the design of the process, firstly, blank design is performed to determine the dimension of the flat blank. Traditionally, the trial and error approach is used in blank design. However, this approach wastes much time and raw materials, especially in manufacturing the blades of large Francis turbines. Hydraulic conditions and cost of energy make design of Francis turbines very variable from site to site. Therefore the blade design is custom and not standard, the raw material trimmed away and the trimming time after the pressing process are very costly due to the over dimensioned blank to

ensure the machining for the final shapes or the pressed blades. With the powerful development of the computing technology, numerical modeling and simulation are widely applied (Feng, Champlaud, and Dao 2009). Several methods were attempted to obtain the optimum blank, such as the slip line method (Kuwabara and Si 1997; Chen and Sowerby 1996), the roll-back method (Kim, Kim, and Huh 2000), the sensibility analysis method (Shim, Son, and Kim 2000), the initial velocity of boundary nodes methods (Son and Shim 2003) and the geometric mapping method (Blount and Stevens 1990; Ryu and Shin 2006). The most popular method is the inverse approach (IA) method. Some varieties of this method can be found in publication, such as the updated inverse approach (Zhang, Liu, and Du 2010); the one-step inverse approach with energy-based algorithm (Tang, Zhao Hagenah, and Lu 2007; Zhang, Hu, Lang, Guo, and Hu 2007), the multi-step inverse approach with membrane elements (Guo, Batoz, Detraux, and Duroux 1990; Lee and Huh 1998; Lan, Dong, and Li 2005; Nguyen and Bapanapalli 2009) and the multi-step inverse approach with shell elements to take consideration of bending effect (Guo, Batoz, Naceur, Bouabdallah, Mercier, and Barlet 2000; Lee and Cao 2001; Azaouzi, Belouettar, and Rauchs 2011).

There are so many papers involving in inverse finite element approach; however the data is not easily accessible. In this paper, the multi-step inverse approach is investigated through the well-known and easily accessible software ANSYS. The approach is applied to the blank design of large and thick blades of Francis turbines for hydropower plants. The flat blank is obtained from the desired blade which is the finally deformed shape of the pressing process.

2. FORMULATION

In inverse finite element approach, the initial state of the model is the deformed shape obtained in the pressing process and the final state is the flat blank. The given variables are the constant thickness and the geometry of the deformed shape and the unknowns are the thickness

and the strain/stress of the flat blank, the coordinates of the flat blank in the working plane. Figure 1 shows the principle of the inverse approach, where the 3D deformed shape C passes to the 2D flat blank C⁰. Each point P on C has an orthogonal projecting point P* on the working plane defined by the flat blank. The vertical displacement of point P is forced to be the distance between the two points P and P*. The process is characterized by geometry and material nonlinearities. The actions of the die and the punch are simplified by external forces. The principle of virtual work is established on the 3D deformed shape C as follows:

$$W = \sum_e W^e = \sum_e W_{int}^e - \sum_e W_{ext}^e = 0 \quad (1)$$

where the virtual internal work is given by

$$\sum_e W_{int}^e = \sum_e \int_{V_e} \varepsilon^{*T} \sigma dV \quad (2)$$

and the virtual external work is given by

$$\sum_e W_{ext}^e = \sum_e \int_{V_e} u^{*T} f dV \quad (3)$$

where ε^* and u^* denote the virtual strain and the virtual displacement, respectively. σ and f denote the Cauchy stress and the external forces which represent the tool actions, respectively. e denotes the sum of the elements. V_e denotes element volume.

Nonlinear equation (1) is solved by the following Newton-Raphson method (Ansys 2010):

$$[K_T^i] \{\Delta U\} = \{F_{ext}(U^i)\} - \{F_{int}(U^i)\} \quad (4)$$

$$[K_T^i] = \left[-\frac{\partial \{R(U)\}}{\partial \{U\}} \right] \quad (5)$$

$$\{U^{i+1}\} = \{U^i\} + \{\Delta U\} \quad (6)$$

where $[K_T^i]$ denotes the Jacobian matrix or the tangent matrix. i denotes the current iteration. $R(U)$ represents the residual vector. $\{F_{ext}(U^i)\}$ represents the vector for the external loads and $\{F_{int}(U^i)\}$ represents the vector for the internal loads. The solution $\{U^{i+1}\}$ contains the displacements of the projecting points of the nodes in the working plane which defines the flat blank.

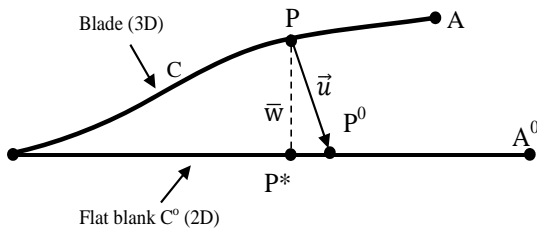


Figure 1: Schematic description of inverse approach

3. MODELING AND SIMULATIONS

The model represented by equation 1 is modeled with static analysis method under ANSYS environment. Inertial and damping effects, except of the static acceleration, are ignored.

3.1. Unfolding tests of Cylindrical Sections

Stainless steel was used in the models in this paper and the material properties (Table 1) were represented by a bilinear isotropic material model (Figure 2), where E denotes the elastic modulus, E_T denotes the tangent modulus, σ_Y denotes the yield stress. Elasto-plastic model with large displacement was established under ANSYS environment. 4-node shell elements were used to take account of the bending effect of thick blank. There was only one element with five integration points in the thickness direction. The nodes were located at the middle surface of the blank. Each node had six degrees of freedom (translations in the x , y , and z directions, and rotations about the x , y , and z axes).

Table 1: Material properties of stainless steel

Elastic modulus (GPa)	200
Yield stress (MPa)	754
Tangent modulus (GPa)	2.0
Poisson's ratio	0.3
Density (kg/m ³)	7850

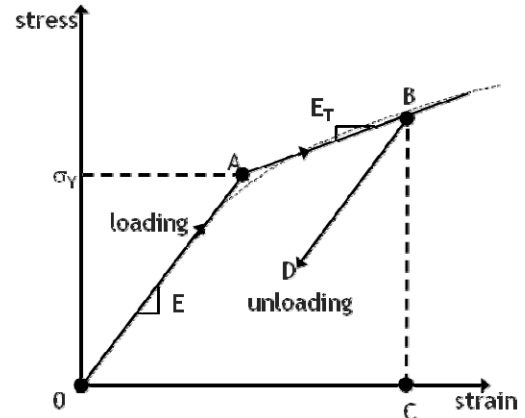


Figure 2: Bilinear material model

A cylindrical section meshed with shell elements for the unfolding tests is shown in Figure 3. In the figure, r was 1.5 m which was the radius of the middle surface of the cylindrical section. The width of the cylindrical section was 2 m and the thickness was 13 cm. In the tests, Angle θ was selected as 15°, 30°, 45°, respectively. The models had the following boundary conditions: locked translation degrees of freedom in X , Y and Z directions for node 1, locked translation degrees of freedom Y and Z directions for node 2 and locked translation degree of freedom in Y direction for node 3, the other nodes had predefined displacements in Y direction. These predefined values were the distances of

each node to the working plane for unfolded geometry or the flat blank which defined by nodes 1, 2, and 3. The simulation gave the displacement of each node in X and Z directions in the working plane. As the motion of node 2 presented the motion of the free edge, the length of the cylindrical section L was determined by the following equation:

$$L = 2r \sin \frac{\theta}{2} + u_x \quad (7)$$

where u_x denotes the displacement of node 2 in X direction; r denotes the radius of the cylindrical section.

The theoretical length was calculated by the following equation:

$$L_{theoretical} = r\theta \quad (8)$$

In Table 2, the lengths obtained by the numerical simulations are compared with the values calculated by equation (8). The maximal error was 0.03% which indicated that the inverse approach gave satisfactory prediction of the flat blank.

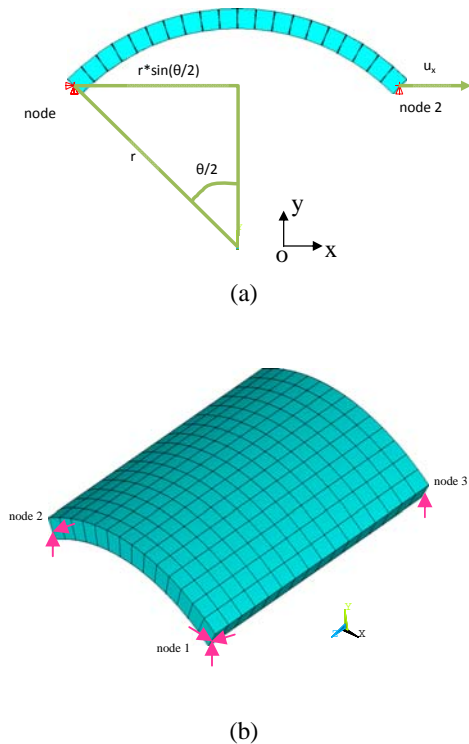


Figure 3: Schematic description of inverse FE approach for a cylindrical section: (a) inverse FE model of a cylindrical section and its boundary conditions; (b) Geometrical setup for unfolding a cylindrical section

Table 2: Lengths of unfolded cylindrical sections compared with theoretical lengths

Angle θ (deg)	Theoretical length (m)	Length obtained by simulation (m)	Error (%)
30	0.7854	0.7853	-0.02
60	1.5708	1.5704	-0.02
90	2.3562	2.3556	-0.03

3.2. Unfolding of a Blade of Francis Turbine

The blades of large Francis turbines have complex geometries with different thicknesses and curvatures at different locations. This complex geometry is obtained by machining a pressed shape from pressing process. In such a process, a flat blank with constant thickness is firstly pressed to form a shape with little difference of thickness comparing to the flat blank. Then, the deformed shape is machined by a 5-axis CNC milling machine to obtain the desired curvature and thickness at each location of the blade (Sabourin, Paquet, Hazel, Cote, and Mongenot 2010).

During the unfolding of the blade with the inverse approach, it is supposed that the model for the unfolding of Francis turbine blades had also a constant thickness of 13 cm (Figure 4). At first, a working plane was defined by 3-point set: one point was located at the apex of the blade which coincided with the origin of the coordinate system, and two other points on the blade with reasonable distances from this apex (Figure 5). The material properties and element type were as the same as those used for the tests with simple geometries of the previous section. The unfolding procedure was also similar as the one used for the tests with simple geometries described in the same section. The boundary conditions were defined by the three points which defined a new coordinate system as follows: locked translation degrees of freedom in X , Y and Z directions for the point at the origin of the coordinate system (point 1), locked translation degrees of freedom in Y and Z directions for the second point (point 2), locked translation degree of freedom in Z direction for the third point (point 3). The displacements of the other nodes in Z direction were predefined. These predefined values were the distances of each node to the working plane. For ensuring the computational convergence, multi-step approach was applied to divide the total predefined displacement of each node by the number of steps and a loop was used to compute the predefined displacements of each node.

The elasto-plastic model had a structural mesh with 1480 nodes and 1404 elements. A numerical simulation took about 96 seconds of CPU time. The middle surface of the flat blank obtained from the simulation had an area of 3.66 mm². The flat blank and a blade of Francis turbines presented in dotted mesh are shown in Figure 6. Figure 7 illustrates the Von Mises stress distribution of the flat blank. The maximal Von Mises stress was 1003 MPa which was located at the highly deformed zone where the blade had the maximal curvature (Figure 8). In this zone, the mechanical strain in the normal

direction of the flat blank had the maximal value (Figure 9) which indicated that the maximal thickness change occurred in the zone with maximal curvature. However, the thickness changes at any location were very small. Taking consideration of the element of the maximal value in Figure 9, the distribution of total mechanical strain in thickness direction of the element with maximal value is illustrated in Figure 10. Since the deformation beside the middle surface had nearly equal values and opposite signs, therefore, the thickness change during the unfolding was neglected.

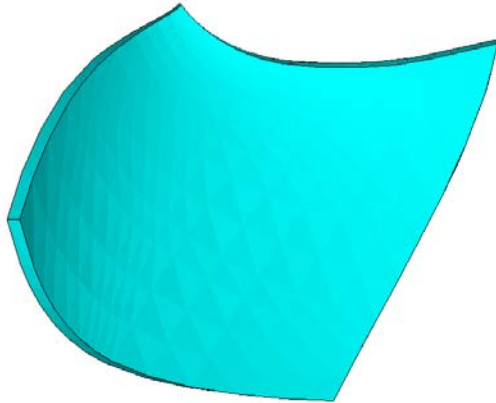


Figure 4: Geometry of Francis turbine blades

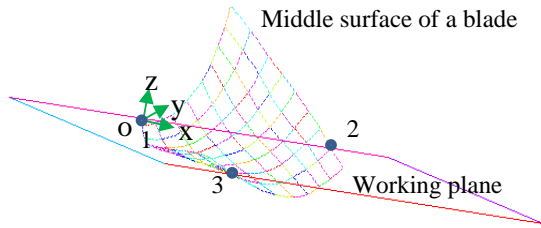


Figure 5: Middle surface of a blade of Francis turbine

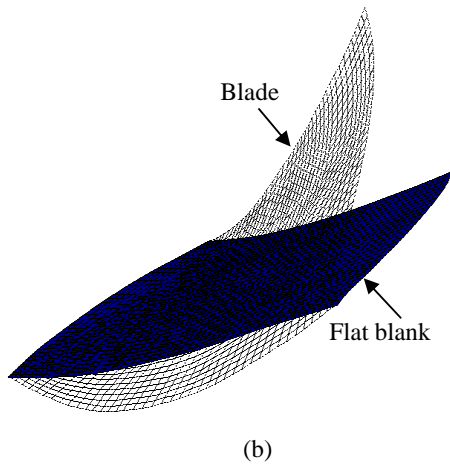


Figure 6: Comparison between the flat blank and the blade

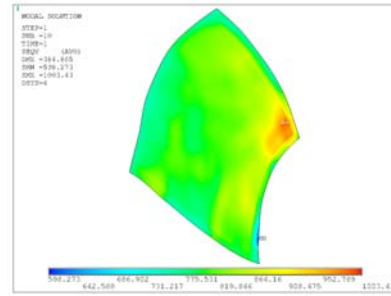


Figure 7: Von Mises stress distribution in the flat blank

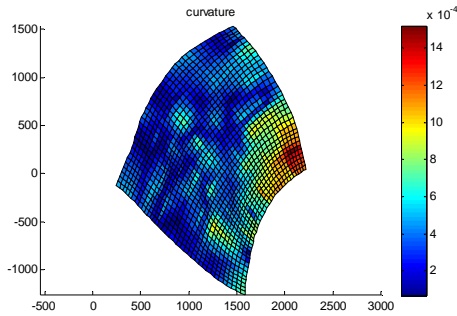


Figure 8: Distribution of residual stress of the flat blank compared with the curvature of the blade

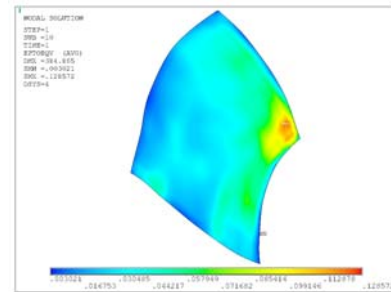


Figure 9: Von Mises total mechanical strain distribution in the flat blank

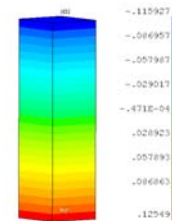


Figure 10: Distribution of total mechanical strain in thickness direction of the element with maximal value

CONCLUSIONS

Unfolded blank for thick and large blades of Francis turbine is obtained using finite element method under the easily accessible and common used software ANSYS environment. Unfolding tests with simple geometry with multi-step inverse approach are carried out and results shown that the error compared with analytical ones are less than 0.03%. The results show that the maximal thickness change occurred in the zone with maximal curvature. Future works will concentrate on adding automatically a minimum extra contour for machining purpose at the edges, on running simulations of the pressing process with the obtained blank to produce the desired blade and on validating the procedure with upcoming experiments.

ACKNOWLEDGMENTS

The authors thank the Natural Sciences and Engineering Research Council (NSERC), Alstom Hydro Canada Inc. and Hydro Quebec for their financial supports to this research.

REFERENCES

- Anslys, inc., 2010. *ANSYS Mechanical APDL and Mechanical Applications Theory Reference*. Release 13.0.
- Azaouzi, M., Belouettar, S., Rauchs, G., 2011. A numerical method for the optimal blank shape design. *Materials and Design*, 32(2), 756-765.
- Blount, G.N., Stevens, P.R., 1990. Blank shape analysis for heavy gauge metal forming. *Journal of Materials Processing Technology*, 24, 65-74.
- Casacci, S., Bosc, J., Moulin, C., Sauron, A., 1977. Conception et construction des turbomachines hydrauliques de grandes dimensions. *La houille blanche*, 7-8, 591-616.
- Casacci, S., Caillot, G., 1983. Le développement des turbomachines hydrauliques de grandes puissances. *La houille blanche*, 7-8, 475-484.
- Chen, X., Sowerby, R., 1996. Blank development and the prediction of earing in cup drawing. *International Journal of Mechanical Sciences*, 38(5), 509-516.
- Feng Z., Champlaud H., Dao T.M., 2009. Numerical Studying of Non-Kinematical Conical Bending with Cylindrical Rolls. *Simulation Modelling Practice and Theory*, 17(10), 1710-1722.
- Guo, Y.Q., Batoz, J.L., Detraux, J.M., Duroux, P., 1990. Finite element procedures for strain estimations of sheet metal forming parts. *International Journal for Numerical Methods in Engineering*, 30(8), 1385-1401.
- Guo, Y.Q., Batoz, J.L., Naceur, H., Bouabdallah, S., Mercier, F., Barlet, O., 2000. Recent developments on the analysis and optimum design of sheet metal forming parts using a simplified inverse approach. *Computers and Structures*, 78(1-3), 133-148.
- Kim, J.Y., Kim, N., Huh, M.S., 2000. Optimum blank design of an automobile sub-frame. *Journal of Materials Processing Technology*, 101(1-3), 31-43.
- Kuwabara, T., Si, W.H., 1997. PC-based blank design system for deep-drawing irregularly shaped prismatic shells with arbitrarily shape flange. *Journal of Materials Processing Technology*, 63(1-3), 89-94.
- Lan, J., Dong, X., Li, Z., 2005. Inverse finite element approach and its application in sheet metal forming. *Journal of Materials Processing Technology*, 170(3), 624-631.
- Lee, C.H., Huh, H., 1998. Three dimensional multi-step inverse analysis for the optimum blank design in sheet metal forming processes. *Journal of Materials Processing Technology*, 80-81, 76-82.
- Lee, C., Cao, J., 2001. Shell element formulation of multi-step inverse analysis for axisymmetric deep drawing process. *International Journal for Numerical Methods in Engineering*, 50(3), 681-706.
- Nguyen, B.N., Bapanapalli, S.K., 2009. Forming analysis of AZ31 magnesium alloy sheets by means of a multistep inverse approach. *Materials and Design*, 30(4), 992-999.
- Ryu, C., Shin, J.G., 2006. Optimal approximated unfolding of general curved shell plates based on deformation theory. *Transactions of the ASME, Journal of Manufacturing Science and Engineering*, 128(1), 261-9.
- Sabourin, M., Paquet, F., Hazel, B., Cote, J., Mongenot, P., 2010. Robotic approach to improve turbine surface finish. *1st International Conference on Applied Robotics for the Power Industry (CARPI 2010)*, October 5-7, Montreal, Canada.
- Shim, H., Son, K., Kim, K., 2000. Optimum blank shape design by sensitivity analysis. *Journal of Materials Processing Technology*, 104(3), 191-199.
- Son, K., Shim, H., 2003. Optimal blank shape design using the initial velocity of boundary nodes. *Journal of Materials Processing Technology*, 134(1), 92-98.
- Tang, B.T., Zhao, Z., Hagenah, H., Lu, X.Y., 2007. Energy based algorithms to solve initial solution in one-step finite element method of sheet metal stamping. *Computer Methods in Applied Mechanics and Engineering*, 196(17-20), 2187-2196.
- Zhang, X., Hu, S., Lang, Z., Guo, W., Hu, P., 2007. Energy-based initial guess estimation method for one-step simulation. *International Journal of Computational Methods in Engineering Science and Mechanics*, 8(6), 411-417.
- Zhang, Z., Liu, Y., Du, T., 2010. Design and quick formability analysis of autpanel at preliminary design stage. *Journal of Manufacturing Science and Engineering*, 132(2), 0245011-0245015.

OPTIMIZATION OF PRODUCTION RAMP-UP BY USING A SIMULATION FOR PERSONNEL REQUIREMENTS PLANNING

Gisela Lanza^(a), Anna Sauer^(a)

^(a) Karlsruhe Institute of Technology, wbk Institute of Production Science, Kaiserstraße 12, 76131 Karlsruhe

^(a) Anna.Sauer@kit.edu

ABSTRACT

Today there is a strong innovation competition; this is why the number of product models constantly increases and the reduction of product life cycles causes a more frequent occurrence of production ramp-ups. Therefore, it is inevitable that the existing resources, especially human resources should be used efficiently in order to ensure an ideal ramp-up. Hence, the planning of these resources has become an important challenge also in a ramp-up. This paper presents an approach developed at the Institute of Production Science (wbk) of the Karlsruhe Institute of Technology to optimize the forecast of personnel requirements during ramp-up. It describes a method providing support to the calculation of the necessary manpower for every single ramp-up phase in order to realize an economic optimum. Therefore, the paper focuses on the simulation of the ramp-up process within its dynamic planning variables, organizational basic conditions, its verification and results.

Keywords: simulation, ramp-up management, personnel planning

1. INTRODUCTION

Companies have to accelerate the development, production and supply of their products in order to be internationally successful on a competitive basis in the current economic situation. The increasing number of models and versions of products can be ascribed to the enormous pressure of innovation, in order to ensure the companies' market shares in the long run (Schuh, Riedel, Abels and Desoi 2002). This leads to shorter product life cycles, implicating an increasing number of production ramp-ups in a set time interval (Abel, Elzenheimer and Rüstig 2003). Especially resource management plays a decisive role for the earliest possible market entry timing, which can be traced back to the so-called lost sales. These are missed sales, which are caused by a delayed market entry. Due to shorter product life cycles it will hardly be possible to recover lost profits (Kuhn, Wiendahl, Eversheim and Schuh 2002). Due to the fact that the capability of responding quickly is an important issue during ramp-ups, the correct planning of resources is essential. Moreover, the exact personnel requirement planning is an outstanding

feature and regarding to the amount of unforeseen situations it is difficult to handle. Therefore, the Institute of Production Science (wbk) of the Karlsruhe Institute of Technology has developed a method to optimize the planning of personnel requirements during a production ramp-up by using a simulation.

2. PRODUCTION RAMP-UP

The production ramp-up can be described as the transfer phase from the stage of product development to a stable series production (Clark and Fujimoto 1991). The primary ramp-up objective is represented by the achievement of production quantity objectives in due time, the so called "time to market". This primary objective is based on the performance goal and the efficiency goal of the ramp-up. Whereas the performance goal evaluates the achievement of the planned efficiency of the whole plant, the efficiency goal describes the best possible employment of resources or costs concerning the performance goal. Therefore, the reduction of the personnel costs is also important. The performance goal optimization to maximize the overall equipment effectiveness (OEE) includes an improvement of every single parameter, such as availability or quality rate (Nakajima 1988). The OEE is a key performance indicator, which quantifies how effectively a manufacturing plant is utilized. It is defined as the product of availability, performance and quality (Lanza 2005).

3. STATE OF THE ART

To justify the developed simulation's approach some existing models are described in their characteristics: First there are forecast and simulation based methods. *Winkler* (2007) presents a ramp-up project management based on an operational network, which should realize control and mastery of the ramp-up processes (Winkler 2007). *Lanza* (Lanza 2005), *Rottinger* (Rottinger 2005) and *Coordes* (Coordes and Spieckermann 2001) developed simulation based methods considering the quality of the production processes or the personal structure. These methods are not able to implement improvement processes which are very important during production ramp-up. Furthermore, they do not consider any time-variant effects and are only partially suitable for the ability to plan resources especially for highly complex problems. Second there are ramp-up

supporting controlling systems. The method developed by Laick (2003) is able to guide and design production process systems (Laick 2003), but still does not consider any time-variant effects and machine models as well as processes. Third there are learning curve models to map ramp-up curves, but they have in general the same deficits as the models described so far. As an example of a model in the department of knowledge management to support the ramp-up, the model developed by Zeugträger (Zeugträger 1998) may be mentioned based on aspects of the learning organization and on the provision of information. Additionally to the deficits depicted in the other departments the models in this sector are not suitable to map connected systems and interactions. Furthermore, there are models based on the ramp-up supporting in networks. Weinzierl for example focused on the support of the decision making process in the field of strategy ramp-up management (Weinzierl 2006). Nevertheless, these model types have apart from other deficits no control loop character.

The general target of the developed method should be to shorten the ramp-up phase by using a simulation (Verein Deutscher Ingenieure 2000). During the ramp-up phase the simulation can predict the order flow, to plan the work in process, to evaluate troubleshooting measures and to predict resource requirements. In contrast, former ramp-up simulation methods focused more on material flow and were not able to illustrate the personnel aspects adequately (Coordes and Spieckermann 2001). Therefore, it is necessary to develop a new approach meeting all of the following requirements: Regarding the production system it has to deal with different machine models and processes. The method should consider time-variant effects as well as interactions. Moreover, it should include exact improvement procedures. It is also necessary to prove if the method fulfils the character of a control loop. Therefore, it should be able to plan resources, to make some forecasts and to evaluate preventively.

4. DESCRIPTION OF THE METHOD

The developed method to support the personnel requirements planning during a production ramp-up is divided into four phases where the essential step is described by the simulation. First of all every phase will be introduced before the simulation itself will be explained in detail. The method is described by the exhibition of dependencies between resources and target figures during the production ramp-up.

Figure 1 shows the methods' software architecture. The model can be divided into three levels. The lowest level, the data level, includes essential configuration data and functional data. Also the planning results will be saved at this level to make them available at any time. The second level, the logical level, is responsible for the execution of functions and methods during the planning run. It supports partial aspects of the model, for example the model configuration, the opening procedure, the improvement process and the preparation

of decision for the optimization of human resources, which are part of the interactive level.

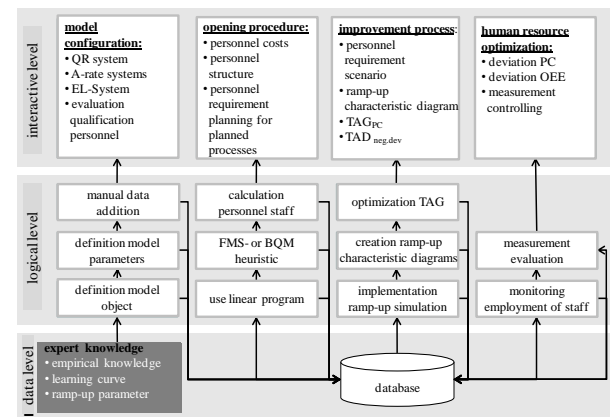


Figure 1: overview software architecture

The interactive level is responsible for the systematic documentation of the model parameters. First it contains the configuration of the planning method, including the OEE-values and the evaluation of existing personal regarding the ramp-up tasks. The second stage of the interactive level, the opening procedure, contains the setup of a linear program, providing an initial solution as a launch setting for the simulation. The complexity of the calculations and the number of variables related to this problem decide whether a linear program can be used or if an initial solution can only be reached with the help of heuristics (Sotskov 1991). Therefore, a heuristic is used to solve problems with a high complexity and a large number of variables. Two alternatives are possible as heuristics, which lead to different initial solutions for the planning of human resources, depending on the special circumstances. There are the FMS-heuristic (heuristic fixed-member set) and the BQM-heuristic (heuristic best qualified member of staff). These heuristics are aiming at the processing of all accumulating operations with a firmly defined number of staff members. Subsequently, the heuristic method's results serve as initial variables for the improvement process, representing the third stage of the model. This process consists of a simulation and a feedback loop, reflecting a target-performance comparison. The improvement process, which is based on the ramp-up simulation, enables the identification, the evaluation and the removal of shortage of staff with the help of ramp-up control loops. The personnel planning scenarios will be measured by the target figures "personnel costs" and "negative deviation of the optimal OEE". During every single phase of the ramp-up, ramp-up characteristic diagrams will visualize them to support the ramp-up manager. An evaluation of the logical level realizes the estimation of the impact of in the database integrated measures and the choice of personnel structures.

Furthermore, time-variant effects that are typical for ramp-ups influence the developed model and they are adapted in the simulation's result. These effects represent the basic conditions for the production ramp-

up like learning effects in human resources and thereby change process times. As one central aspect of this model, the human resources' learning curves clearly emerge during the ramp-up phase and therefore represent a significant input variable for the ramp-up simulation.

5. SIMULATION MODEL

There are two simulation techniques predicting ramp-up target-figures, effectiveness or flow simulations and scenario techniques (Nyhuis, Heins, Großhenning, Fleischer, Lanza and Ender 2005). Specified effectiveness or flow simulations are primarily used. In particular the flow simulation is a valid method supporting the planning of complex systems (Kuhn, Reinhart and Wiendahl 1993). It can be used for the planning and also for the ramp-up and series production (Verein Deutscher Ingenieure 2000). In the VDI (German Engineer Association) guideline 3633 the use of flow simulation is described within the relation to the ramp-up and represents a basic principle regarding the standard for the analysis of ramp-up procedures, warm-up periods and transitions among defined operating conditions (Verein Deutscher Ingenieure 2000).

The integrative ramp-up simulation will be implemented by using the simulation software PlantSimulation (version 10.1). It allows a structured and comprehensible transfer of complex production systems to computer models (Tecnomatix 2008).

Below the parameters of the simulation model are described in detail. All relevant objects and influences, given a statement about the influence of certain personnel structures on the ramp-up target figures, are integrated in the simulation model. Along with control factors and planning data, the input data consisting of the technology of the machine, the ramp-up curve, the learning curve and existing resources, are incorporated into the integrative simulation model and therefore constitute its data structure.

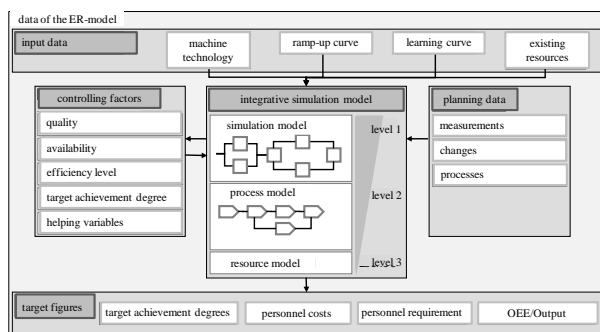


Figure 2: scheme of the ramp-up simulation

The integrative simulation model itself can be divided into three areas. Figure 2 shows the ramp-up simulation's scheme. The first area of the integrative simulation model describes the simulation model, the second one depicts the process model and the third area consists of the resource model. Data about the predicted production system including the technical structures is

stored in the simulation model and represents the improvement procedure's real integrative component where the input variables, control factors and planning data are incorporated and transformed into target figures. The ensuing process model implements the considered business processes and their impact on the technical simulation model. The output of the respective business models mostly represents manipulations of OEE-performance parameters. There is a link between the process model and the underlying resource model that allows resources to be transfer.

The flow of the simulation algorithm can be divided into the preparation of the simulation, the initialization and the simulation run. After preparing the simulation, the simulation variables are set to zero, the heuristic planning results are loaded and the input data of the simulation will be made available to the model via an open database connectivity interface. The simulated algorithmic planning run starts as soon as the simulation application is initiated.

In the end, results of the simulation will be used for an evaluation process that is going to simplify the decision making related to the optimal use of resources.

6. VERIFICATION

In order to be able to compare the results and to support a decision, two target figures will be identified, describing the system. On the one hand it involves the average negative deviation from the OEE to the optimal OEE, if the OEE-curve does not achieve the optimal OEE ($OEE_{neg.dev}$) and on the other hand it involves the personnel costs (PC). OEE_{Sim} means the simulated OEE. Two normalized target achievement degrees (TAD) are developed allowing comparison between different ramp-ups and their targets (formular 1 and 2).

$$TAD_{PC} = 1 - \frac{PC_{Sim} - PC_{min}}{PC_{max} - PC_{min}} \quad (1)$$

$$TAD_{OEE_{neg.dev}} = 1 - \frac{\overline{OEE_{neg.dev, Sim}} - \overline{OEE_{neg.dev, min}}}{\overline{OEE_{neg.dev, max}} - \overline{OEE_{neg.dev, min}}} \quad (2)$$

In order to provide evidence of the model's functionality and to optimize the forecast of the personnel requirements during ramp-up, the verification of the personnel requirement planning model is shown by an example in the engine production. This will be done to prove a realistic situation in the planning algorithms.

To verify the functionality of the ramp-up simulation, taking a look at the several ramp-up objects is necessary. Therefore, the quality of the learning curve function, the development of the employees' efficiency, the development of the OEE_{Sim} , the effects of some improvement processes, the correlation of the business process capacity utilization and the resource capacity utilization are especially regarded.

In order to verify the implementation of the learning behaviour and the increase of the efficiency,

which is thereby achieved, it is necessary to simulate a human resource with a repetitive task and to register the efficiency level of the resource as well as the operations durations. Formula 3 describes the calculation of the efficiency level of an employee j out of the functional area i . The formula shows that with an increasing number of operations done for example in the area of fault removal a_{ij} the efficiency E_{ij} of the regarded employee increases up to a certain limit. This limit is determined by the irreducibility factor M and the degression factor b (De Jong 1957). If the processes are very labour-intensive a value of $M=0,25$ and a learning rate of 70% may be recommended. According to formula 4, this results in $b=0,51$. The learning rate is a constant percentage by which the number of factor inputs will be reduced by the doubling of the cumulative outputs (Laarmann 2003).

$$E_{ij} = 100 * \frac{1}{M + \frac{1-M}{a_{ij}^b}} \quad (3)$$

$$b = -\log_2(\text{learning rate}) \quad (4)$$

Formula 5 exploits the result of E_{ij} to calculate the expected process time $t(E_{ij})$. In this context t_{100} is the process time with efficiency E_{ij} of 100.

$$t(E_{ij}) = t_{100} * \frac{100\%}{E_{ij}} \quad (5)$$

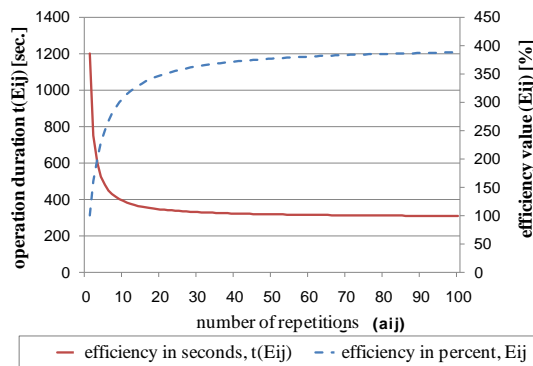


Figure 3: E_{ij} and $t(E_{ij})$ values of the ramp-up simulation

Figure 3 shows the simulated values of the operation duration and the efficiency levels of one employee. The results were calculated with $M=0,25$ which causes an efficiency limit of 400%. With an increasing number of repetitions (a_{ij}) the limit of the operation duration converges to 300 seconds. This complies 25% of the initial time for the regarded operation. These results correspond to the learning curve theory of De Jong and prove a correct implementation of the method (Rendel de Jong 1956).

An additional functionality of the ramp-up simulation is the implementation of improvement measurements. These measurements change machines or their components in their performance attributes. In order to prove this functionality, a system composed of

one machine and a set of measurements (100 single measurements) changing the quality rate is shown. First an improvement measurement with $x_{QR}=10\%$ is planned for every five days which increases the quality rate gradually. X_{QR} is the percentage improvement of the quality rate. Since day 55 there is every day a measurement like this planned to recognize the convergence against 99%. Figure 4 shows the values for the quality rate's development of one machine, calculated by the simulation application.

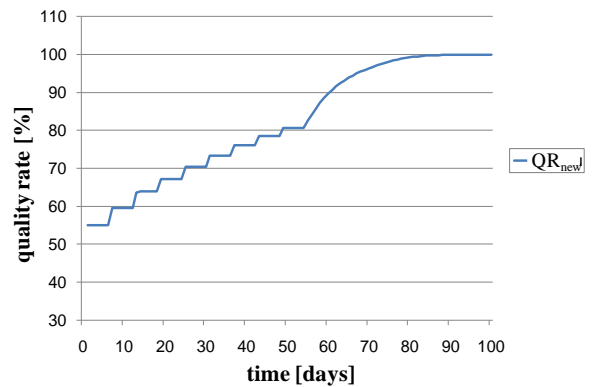


Figure 4: development of the quality rate during a simulation run

In order to verify the failure rate (λ), a failure rate of 30% and an operating time of 100 days are assumed for each machine. It is necessary to split the failure rate in a continuous and a discrete part. The irreducibility factor is fixed with $M=0,95$. For recognizing the influence of the discrete improvement measurements a measurement which should reach an improvement of $x=25\%$ is planned at time $t=10$ and $t=20$. Therefore, the failure rate gets reduced to a minimum of ϵ_{LE} , which represents the maximal level of efficiency and forms the lower bound of the failure rate. Figure 5 proves the effectiveness of the improvement measurements at time $t=10$ and $t=20$. Therefore, the functionality of the failure rate's calculation is verified.

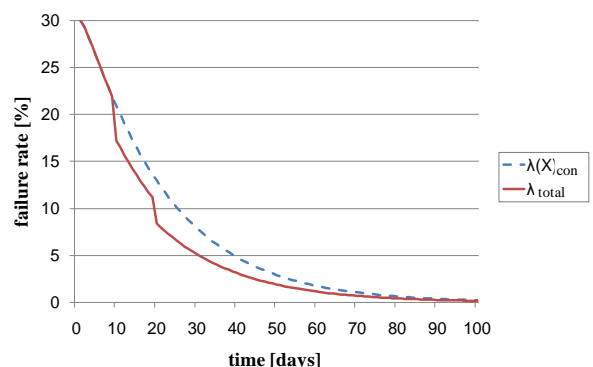


Figure 5: implementation of the failure rate

The average negative deviation of the OEE_{Sim} is used as control parameter of the ramp-up simulation. The OEE_{Sim} of the entire system is defined as the

product of the availability of the machines (A_{Sim}), the efficiency level (EL_{Sim}) and the quality rate (QR_{Sim}).

Figure 6 maps the aggregated single values of the $OEE_{Sim}(P)$ of the entire system. The aggregation is calculated with the stepwise aggregated single values in the line level, the machine level and the component level of the ramp-up simulation. Based on this, the algorithm for the personnel requirement can be used and bottleneck analysis can be executed.

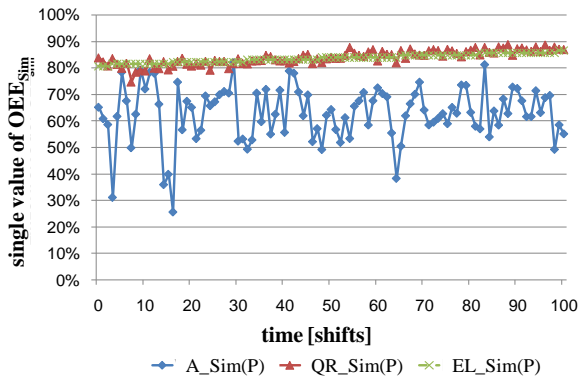


Figure 6: prognosticated $A_{Sim}(P)$, $QR_{Sim}(P)$, $EL_{Sim}(P)$

7. VALIDATION

The result of the ramp-up simulation consists of various scenarios, emerging from individual simulation experiments. These are based on different control parameters and on the heuristic personnel output configuration.

In order to validate the simulation model and to give an overview, a practical example of the personnel requirement planning is given. The example focuses on maintenance activities of a crankcase line with an aspired OEE of 70%. The actual personnel requirement is depicted during a time period so that the possibility to achieve enhanced results by using the simulation model can be demonstrated. Some improvement processes in the maintenance activities are in progress in period three (Figure 7), therefore it is necessary to plan with a larger number of employees.

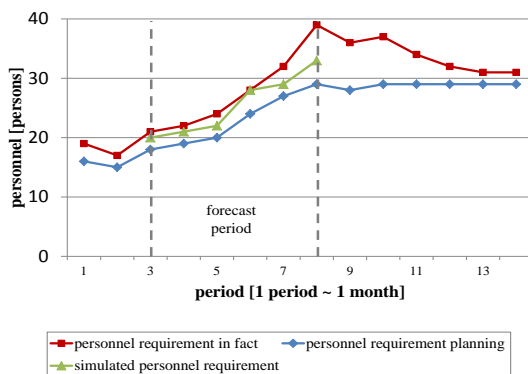


Figure 7: Comparison of the personnel requirements in fact and the simulated personnel requirements

Figure 7 visualizes the results of the personnel requirement planning calculated with conventional methods and calculated by using the simulation model. In addition, the de facto needed staff members are also marked in the same coordinate system. The figure indicates the possibility to achieve enhanced results by using the simulation model, which is presented in this paper. Nevertheless, it should be noted that the simulation model does not produce the personnel requirement as result being needed in fact. The reasons for that are some not provided processes creating the deviation between the actual personnel requirement and the personnel requirement planned by simulation. In this example a $TAD_{OEE}^{neg.dev}$ of 0.87 is realized.

Actually the personnel requirement calculated by the simulation model is indeed more accurate than the conventional personnel requirement planning.

8. CHARACTERISTIC DIAGRAMS

Concluding, the simulation results disembugue in characteristic diagrams. These diagrams support the ramp-up manager in every ramp-up phase (Figure 8) by visualizing the most important ramp-up goals and the personal requirements. The lower evaluation of the diagram shows the personnel requirement, which is necessary in order to reach the efficiency target. Due to that, the output is simulated depending on the personnel requirement. The upper evaluation of the target achievement degrees gives the planner information on how the personnel requirement affects the target achievement degrees.

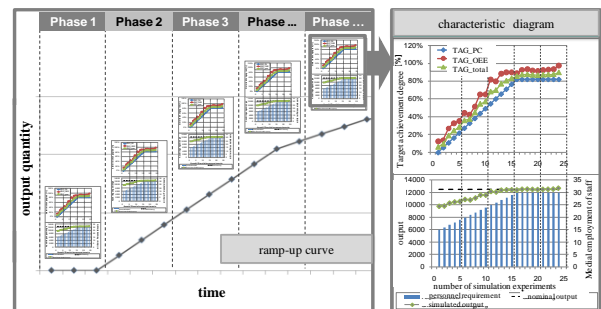


Figure 8: characteristic diagram

9. SUMMARY

The personnel requirement planning during production ramp-up plays a decisive role for the earliest possible market entry timing. Especially during the production ramp-up there is a great need regarding the research of the planning of personnel requirements. With the planning method presented in this paper and implying a simulation as main approach, it is possible to support the ramp-up manager in planning the personnel requirements economically at every stage of the production ramp-up. So it is guaranteed that the personnel requirement planning can always be displayed according to the current situation. Moreover, it can realize the economic optimum in order to reduce the costs of production. The simulation described in this

paper is specified. The use of simulation during the implementation phase allows a realization of virtual plant performance tests with a stepwise integration of order types and product versions while gradually increasing the utilization of available capacity. Furthermore, it allows the analysis of problems, their impacts and new requirements during the production ramp-up. In the end characteristic diagrams can visualize the scenarios. This approach's distinguishing element consists of the integration of time-variant factors like learning curves into the simulation model. Therefore, it is possible to get close to an optimal personnel requirement planning at every stage of the production ramp-up.

Altogether, the ramp-up simulation in the form of an improvement procedure is an excellent planning tool for production ramp-ups, especially in terms of personnel resources.

ACKNOWLEDGMENTS

We extend our sincere thanks to the Deutsche Forschungsgemeinschaft (German Research Foundation) for supporting this research project LA 2351/4-1 "Ressourcenplanung im Produktionsanlauf" ("Resource Planning during Production Ramp-Up").

REFERENCES

- Abe, E., Elzenheimer, J., Rüstig, A., 2003. Anlaufmanagement in der Serienproduktion. *ZWF Journal, Zeitschrift für wirtschaftlichen Fabrikbetrieb*, 98 Journal 4, pp 172-176.
- Bol, G., 2003. *Induktive Statistik*. 3rd edn.. Oldenbourg: Oldenbourg Verlag
- Clark, K. B., Fujimoto, T., 1991. Product Development Performance – Strategy, Organization, and Management in the World Auto Industry. 1st edn. *Harvard Business School Press*:pp97-101.
- Coordes, M., Spieckermann, S., 2001. Die Ablaufsimulation der virtuellen Prozesskette am Beispiel des neuen Audi A4. Flexibel und kostengünstig, In: 4. *Düsseldorfer Produktionstage*, Tagung; VDI-Ges. Produktionstechnik 1597. Düsseldorf: VDI-Verlag, pp 81-96.
- De Jong, R.J., 1957. The Effects of Increasing Skill on Cycle Time and Its Consequences for Time Standards. *The Official Journal of the Ergonomics Society* 42 (1957), Journal 1: pp 51-60
- Kuhn, A., Reinhart, G., Wiendahl, H-P., 1993. *Handbuch Simulationsanwendungen in Produktion und Logistik*. 1st edn. Braunschweig, Wiesbaden, Vieweg
- Kuhn, A., Wiendahl, H.P., Eversheim, W., Schuh, G., 2002. *Fast ramp-up, Schneller Produktionsanlauf von Serienprodukten – Ergebnisbericht*. Dortmund: Praxiswissen Verlag.
- Laarmann, A., 2003. *Lerneffekte in der Produktion*. Deutscher Universitätsverlag, Bochum
- Laick, T., 2003. *Hochlaufmanagement: sicherer Hochlauf durch zielorientierte Gestaltung und Lenkung des Produktionssystems*. Dissertation, Technische Universität Kaiserslautern.
- Lanza, G., 2005. *Simulationsbasierte Anlaufunterstützung auf Basis der Qualitätsfähigkeit von Produktionsprozessen*. Dissertation, Universität Karlsruhe TH.
- Nakajima, S., 1988. *Introduction to TPM*. 1st edn. Productivity Press, Inc., Cambridge Massachusetts.
- Nyhuis P., Heins M., Großhenning P., Fleischer J., Lanza G., Ender T., 2005. Simulationsunterstützte Wirkbeziehungsanalyse im Produktionsanlauf. *ZWF Zeitschrift für wirtschaftlichen Fabrikbetrieb* 100 Journal 12; pp 746-75.
- Rottinger, S., 2005. *Mehrphasige Personalentwicklungsplanung für Fertigungssysteme auf Basis des Technologiekalender-Konzeptes*. Dissertation, Universität Karlsruhe (TH).
- Schuh, G., Riedel, H., Abels, I., Desoi, J., 2002. Serienanlauf in branchenübergreifenden Netzwerken. Eine komplexe Planungs- und Kontrollaufgabe. *wt Werkstattstechnik online*, 92 Journal 11/12: pp 656-661.
- Sotskov, Yuri N., 1991. The complexity of shop-scheduling problems with two or three jobs. *European Journal of Operational Research*, 53; pp 326-336.
- Tecnomatix, 2008. *Simulation and Optimization with Plant Simulation*. Available from: <http://www.emplant.de> [Accessed 03 January 2012].
- Verein Deutscher Ingenieure (Hrsg.), 2000. VDI-Richtlinie 3633 page 1, *Simulation von Logistik-, Materialfluß- und Produktionssystemen - Grundlagen, Entwurf*. Beuth, Berlin.
- Verein Deutscher Ingenieure (Hrsg.), 2000. VDI-Richtlinie 3633 page 2, *Simulation von Logistik-, Materialfluß- und Produktionssystemen - Grundlagen, Entwurf*. Beuth, Berlin.
- Weinzierl, J., 2006. *Produktreifegrad-Management in unternehmensübergreifenden Entwicklungsnetzen – Ein ganzheitlicher Ansatz zur Entscheidungsunterstützung im strategischen Anlaufmanagement*. Dissertation, Universität Dortmund.
- Winkler, H., 2007. *Modellierung vernetzter Wirkbeziehungen im Produktionsanlauf*. Dissertation, Leibniz Universität Hannover.
- Zeugträger, K., 1998. *Anlaufmanagement für Großanlagen*. Dissertation, Universität Hannover.

STUDY ON THE DESCRIPTION METHOD OF MANUFACTURING CAPABILITY BASED ON DESCRIPTION LOGICS IN CLOUD MANUFACTURING

Yongliang Luo^(a), Lin Zhang^(a), Fei Tao^(a), Yongkui Liu^(a), Lei Ren^(a)

^(a) School of Automation Science and Electrical Engineering, Beihang University,
Beijing 100191, P. R. China

yongliang2002@gmail.com, zhanglin@buaa.edu.cn,
taofei999@gmail.com, yongkuiliu@163.com, lei_ren@126.com

ABSTRACT

Manufacturing capability (MC) sharing is one of the most important innovations in cloud manufacturing (CMfg). In order to realize the on-demand usage of MC in the CMfg, the issue of how to describe MC need to be solved first. This paper proposes a new description method of MC based on description logics (DL) oriented to CMfg. Concepts and state of the art related to MC are summarized firstly, and then the characteristics and theoretical basis of current service description language are systematically analyzed. On this basis, the description model of MC is proposed. Finally, the static and dynamic information models based on DL of MC are mainly investigated combined with practical examples.

Keywords: cloud manufacturing, manufacturing capability, description language, dynamic description logics

1. INTRODUCTION

Service, environment protection and knowledge innovation are the main factors in manufacturing competition and they are the main issued (issues) to be faced and solved for manufacturing enterprises. At the meantime, Cloud manufacturing (CMfg) as a possible solution and new manufacturing paradigm is proposed by Bohu Li and Lin Zhang(2010), it can provide theoretical and technical supports for the transformation from production-oriented manufacturing to service-oriented manufacturing. CMfg is a new service-oriented, knowledge-based, and intelligent networked manufacturing mode with high efficiency and lower consumption [Bohu Li and Lin Zhang *et al.* 2010]. In order to achieve the virtualization and servitization of manufacturing resources and manufacturing capability, CMfg is realized by combining with advanced manufacturing and information technologies organically, such as cloud computing, the internet of things, service-oriented technologies, high performance computing, information system integration, etc. CMfg can provide users with on-demand, safe and reliable application services in the whole life-cycle of products through network. It aims to achieve the agile, service-oriented, green and intelligent manufacturing, is a new phase of

networked manufacturing, as well as the materialization of service-oriented manufacturing.

At presents, CMfg is in the early stage and many related key technologies are urgent to be solved, among which manufacturing capability (MC) sharing is one of the most important ones in CMfg. Because of its complexity and less relevant studies, there is no clear definition of MC currently. So far, although the concept and connotation of MC is proposed in voluminous literature, there are no conclusive answers yet. For example, Skinner proposed the concept of MC in 1969 firstly. In his opinion, MC is a concept comprising many elements, such as cost, delivery time, quality, and the relationship between them. Richard (1973) considered that the capability includes knowledge, skills, and experience of enterprises. Khalid(2002) concluded that MC is an effective integration of related resources in the process of achieving expected target task. MC reflects the completion of manufacturing objective, and it is a performance level of the standard which is pre-set by working organization [Andreas Grobler, 2006]. Keen(2000) commented that MC is the integration of intangible and tangible resources, where the tangible resources include labor, capital, facilities and equipment, and the intangible resources include information, procedures, equipment and the organizational system. The relationship between MC and enterprise performance is primarily discussed from the perspective of achieving low operating costs and high product quality [Siri Terjesen, 2011].

Combined with above definitions about MC, according to task demands and resource characteristics of CMfg, in this paper, MC is considered as a kind of capability which can be formally represented in the manufacturing activities. MC, as an important kind of resources in CMfg system, is a manufacturing process, which reflects the capability of completing a manufacturing task or experiment supported by related manufacturing resources and knowledge. According to the concept and characteristics of MC in CMfg, MC can be divided into design capability (DC), simulation capability (SC), product capability (PC), and many other capabilities related to life-cycles of complex products. MC is closely related to manufacturing activities and manufacturing resources, and can only be

reflected in concrete activity tasks and resource elements.

In order to achieve on-demand use of MC in CMfg, the core technology about the formal description of MC needs to be solved firstly. Through the formal description of MC, it can realize not only the function sharing of resources, but also the sharing of the experience and knowledge in the manufacturing process, such as manufacturing flow, sensor data, experience of staff, and so on. The existing description languages of resources or services (such as OWL-S and WSMO) are difficult to meet the needs for the formal description of MC in CMfg because of the complexity and dynamic characteristics of MC. A new description language of MC (MCL) based on DL is presented here. The structure of the paper is structured as follows. The following section systematically analyzes and summarizes the characteristics and theoretical basis of current services description language. In section 4, description model of MCL is presented firstly, and then, the focus is shift to the static and dynamic information models based on DL of MC in combination with practical examples.

2. RELATED WORK

2.1. Description logics

Description logic (DL)[Frank Wolter *et al.* 2000, Monika, 2004] is a formal languages for knowledge representation particularly suitable for ontology. It is more expressive than propositional logic but has more efficient decision problems than first-order predicate logic. DL is used in artificial intelligence for formal reasoning on the concepts of an application domain. Importantly, it provides a logical formalism for ontology and the semantic web. A description logic (DL) model includes the following elements: concepts, roles, individuals and their relationships, where concepts are the integration of individuals, roles reflect the binary relation between different individuals.

Static field knowledge can be effectively represented and reasoned by DL, but it is difficult to satisfy the representation of the dynamic feature knowledge of service or action, while some elements such as “state” or “possible” not exist in DL. According to the above issues, some scholars extend the description logic based on action theory, dynamic logic and other related theories, and propose the dynamic description logic (DLL). DLL can not only describe static domain knowledge based on DL, but also achieve the representation and reasoning of action behavior based on the above knowledge. Basic symbols of DDL are as follows[SHEN Guohua, 2008]:

- Concept names: C_1, C_2, \dots ;
- Roles name: R_1, R_2, \dots ;
- Individual constant: a, b, c...
- Individual variable: x, y, z...

- Concept operation: \neg, \cap, \cup and quantifier: \exists, \forall ;
- Formula operation: $\neg, \wedge, \rightarrow$ and quantifier: \forall ;
- Action name: A_1, A_2, \dots ;
- Action construction: such as ; (synthesis), \cup (synchronization), * (repeat), ? (switch);
- Action variable: α, β, \dots ;
- State variable: u, v, w, ...
- State change: $u \rightarrow v$

Definition 1 (Concept) [Frank Wolter *et al.* 2000]. In DDL, related concept are defined as follows:

- (1) Atomic concept as P, all concept as T and empty concept as \perp ;
- (2) If C and D are concepts, then the following are concepts: $\neg C, C \cap D, C \cup D$;
- (3) If R is a role and C is a concept, then $\exists R.C, \forall R.C$ are concepts;
- (4) If C is a concept, α is a action, then the $[\alpha]C$ is also a concept.

Definition 2 (Action) [Frank Wolter *et al.* 2000]. A description of action like the form of expression: $A(x_1, \dots, x_n) \equiv (P_A, E_A)$, where:

- (1) A is a action name, it indicates the symbolic of action;
- (2) x_1, \dots, x_n are individual variable, indicating the operation object of action. It is also called operation variable;
- (3) P_A is a set of pre-conditions, it indicates that conditions must be satisfied before the action execution, form as:

$$P_A = \{con \mid con \in condition\};$$

- (4) E_A is a set of post-conditions, it indicates the result set after the action execution, it can be divided into two subsets: *head* and *body*, where *head* = $\{con \mid con \in condition\}$, *body* are also conditions, if each condition of *head* can be satisfied in statement u, then each condition of *body* will be satisfied in statement v.

Definition 3 (Action concept) [Frank Wolter *et al.* 2000]. Action of DDL is defined as follows:

- (1) Atomic action $A(\alpha_1, \dots, \alpha_n)$ is a action;
- (2) if α and β are action, then the following are concepts: $\alpha; \beta, \alpha \cup \beta, \alpha^*$;
- (3) if ϕ is assertion formula, then $\phi?$ is also a action.

2.2. Service description language

The mainstream description languages of service and resources in current are WSMO and OWL-S.

2.2.1. WSMO

WSMO [JIANG Zhixiong, 2008] is a conceptual model describing Semantic web services. Through its substance, it describes different aspects of web services, such as discovery, excitation, assemble and so on. Among the different aspects, WSMO focuses on solving the Web Services Interoperability problem. It mainly includes the following four elements:

(1) *Ontology* Ontology supplies the standardized definitions and descriptions of the message used in other elements, it concludes the conception, relation, function, axiom, the illustration of conception and relation, and some non-function attributes;

(2) *Service* Service describes the released Service semantic layer's functional attributes, and describe the way semantic web service communication and combination.

(3) *Objective* describes the services' objective type, describe the related users' request.

(4) *Mediator* describes the mapping relations among WSMO components' objective, and how to coordinate and interact among different WSMO elements.

WSMO is based on framework logic (F-logic), with the emphasis on describing the interoperability among the elements in service. WSMO, however, lacks the characterization of service's state and description of users' interaction. Moreover, the description of complex relationship between the elements in service is not enough either.

2.2.2. OWL-S

OWL-S [JIANG Zhixiong, 2008] is based on web ontological language (owl), which is recommended by W3C. Owl-s characterizes web service mainly in serviceprofile, processmodel and servicegrounding. Serviceprofile, which is similar to the yellow pages of service, describes the service's function and relative properties. Processmodel characters reflect service's process model, describe how a service works, and servicegrounding combines the process model, communication protocol and message format, and describes how to visit a service. The owl-s is based on description logic theory. owl-s cannot characterize the expression and ratiocination of services' dynamic natures' knowledge because description logic can only deal with the knowledge and express of service's static field, can not reflect the complex logic relationship of service and their dynamic characteristic.

In summary, ontology-based semantic web service description has been widely recognized, but there still exist the following deficiencies:

(1) It cannot describe service behavior's state transition and functional constraint information. The functional constraint information reflects only function's static information of service, ignores the description of service dynamic QoS attributes. Because

of the above mentioned drawbacks, it is hard to guarantee the comprehensive description, accurate match as well as composition of service;

(2) The description of services' ongoing interaction is insufficient. The complex service cannot be completed only through once interaction since it may need a series of interactions with requester or other service.

(3) It is lack of characterization of the relation among composition elements and services since DL could only describe the binary relation for which simply relation is expressed by tree structure. Manufacturing capability service is multi-level and multi-dimensional with the emphasis on effective integration of resources of all kinds, so how to describe inside and outside complex logical relationships of service is one of the main problems of current service describe language.

In short, this paper uses the current research achievement related to resource and service description, combines the features and requirements of manufacturing capabilities in cloud manufacturing mode, uses dynamic description logical relevant theory, studies description method mainly according to MC's static information and dynamic behavior models.

3. THE DESCRIPTION MODEL OF MCL

According to the concept and classification of MC, the description model of MC is proposed as shown in fig 3. The top-level description model of MC as follows:

$MC = (State/RelationSet, ObjectiveSet, QoSSet)$

(1) *State/relationSet* It mainly describes various complex logic relationships among elements of MC in the task execution process, and different states of MC, such as available, busy idle state, etc.

(2) *ObjectiveSet* It is the core part of MC description model, in which the task object of MC and involving such matters as resources, execution process, performance and so on are expressed.

(3) *QoSSet* It is the integration of all level services quality of MC, such as business-level QoS, service-level QoS, and so on.

Where *ObjectiveSet* can be further subdivided and abstracted as follows:

$ObjectiveSet = (InternalRelation, StaticAttribute, DynamicBehavior, ServiceQoS)$

In the above description model, *Internal Relation* is the logical relationship among inside elements of MC, it is also the subset of *State/relationSet* refer to top-level description model of MC. *StaticAttribute* mainly describes static attribute of MC including basic function information, resources description information, historical cases information and so on. *DynamicBehavior* is mainly describes the dynamic information in the execution process of MC, such as operation process, completion situation, state transformation, timing interaction, etc. *ServiceQoS* is the service-level QoS description of MC; it is the subset of *QoSSet* in the above top-level description model of MC

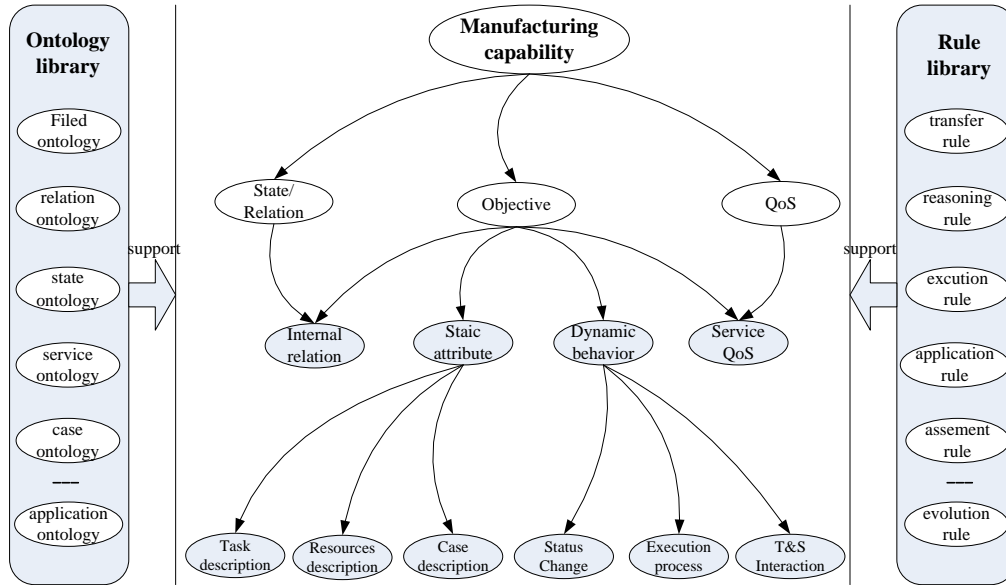


Fig. 3. The description model of MC

In addition, ontology library and rule library are built in order to provide a support for the formal description and application reasoning of MC as shown in fig 3. In which ontology library includes filed ontology, state ontology, application ontology and basic terms of MC such as concepts, roles and relations, it is the precondition for achieving semantic match of MC. Rule library mainly includes various rules related to application process of MCS, such as transfer rule, reasoning rule, execution rule, assessment rule, evolution rule, etc. It provides a basis for realizing all kinds of intelligent reasoning.

This paper mainly studies on static attributes and dynamic behavior of MC as follows.

3.1. Static attribute modeling

In this section, static attribute framework of MC based on DL is proposed by combining “from top to bottom” level description method. The top level is static attribute description model of MC, which is defined as follows:

Definition 4 (MC static description model) the static attribute description model of MC (MC_SD) can be abstractly represented by a triple as follows:

$$MC_SD = (Objective, Resources, MCase)$$

Where *Objective* is the manufacturing task, it is the basic information description set of expected target of MC. *Resources* generally are the various resources related to perform some tasks or activities. *MCase* includes relevant information related to cases of MC. All the above expression are concept of ontology, and expressed based on DL as follows:

$$MC_SD ::= (\exists hasObjective. Objective) \cap$$

$$(\exists hasResources. Resources) \cap (\exists hasMcase. Mcase)$$

Above concepts in definition 4 could be further defined by following defines:

Definition 5 (Objective) Mission objective of MC could be expressed by a triple is defined as:

$$Objective = (Basicinfo, Requirement, Goalfeature)$$

Where *Basicinfo* mainly describes the basic information of one task, such as task name, function introduction, category, transaction mode, accounting policy, etc. *Requirement* reflects the basic conditions and relevant constraints involved in the process of one task. *Goalfeature* mainly describes the feature of the expected target oriented to a task, for example, in order to product a component by a manufacturing task, which *Goalfeature* means the various information about the component including quality, performance, cost, delivery time and so on.

This model can be represented by DL such that:

$$Objective ::= (\exists hasBasicinfo. Basicinfo) \cap$$

$$(\exists hasRequirement. Requirement) \cap$$

$$(\exists hasGoalfeature. Goalfeature)$$

Definition 6 (Resources) manufacturing resources could be defined by a binary, and then expressed by DL as follows:

$$Resources = (MajorRs, AuxiliaryRs, HumanRs)$$

$$Resources ::= (\exists hasMajorRs. MajorRs) \cap$$

$$(\exists hasAuxiliaryRs. AuxiliaryRs) \cap (\exists has HumanRs. HumanRs)$$

$$MajorRs ::= (\exists MRsBasicinfo. Basicinfo) \cap$$

$$(\exists MRsFeature. Feature) \cap$$

$$(\exists MRsAwareinfo. Awareinfo)$$

$$AuxiliaryRs ::= (\exists ARsBasicinfo. Basicinfo)$$

$$HumanRs ::= (\exists HRsBasicinfo. Basicinfo) \cap$$

$$(\exists HRsSkill. K\&Skill) \cap$$

$$(\exists HRsAchievement. Achievement)$$

Where *MajorRs* is the major resources of MC, for example, the *MajorRs* of software MC is the manufacturing software, On the contrary, other resources relevant software's MC called auxiliary resources (*AuxiliaryRs*) such as computing resources. This paper mainly studies on *MajorRs*. It consists of *MRsBasicinfo*, *MRsFeature* and *MRsAwareinfo*, in which *MRsBasicinfo* describes the basic information of

major resources, for instance, equipment model, production area, buying time, etc. *MRsFeature* describes the detail parameters of resources including equipment process, outline dimension and so on. *MRsAwareinfo* includes perceptive information of equipment in execution, such as idle state, running state and so on. In addition, human resources (*HumanRs*) is defined as a special resources as distinct from *MajorRs* and *AuxiliaryRs* in this model because of knowledge and experience sharing in CMfg. It describes the information of personal and organization related to the manufacturing process, including *HRsBasicinfo* (basic information of human), *HRsSkill* (personnel composition, personnel's seniority, duty division, knowledge skill) and *HRsAchievement*(education, training, awarded, and relevant achievement).

Definition 6 (MCCase) Case of MC is represented by a triple such that:

$$MCCase=(Mcasebasicinfo, Accomplishment)$$

Where *Mcasebasicinfo* is the basic information of case, it includes user requirement, completion time and others. *Accomplishment* includes more complete information of one task. It is formulated by DL as:

$$MCCase::=(\exists hasMcasebasicinfo. Mcasebasicinfo) \cap (\exists has Accomplishment. Accomplishment)$$

3.2. Dynamic behavior modeling

Definition 7 (Constraints) In DDL various constraints like $\exists C, C(p), R(p,q), p=q$ and $p \neq q$, where $p, q \in N_i$

- As $p, q \in N_i$, each constraint has corresponding assertion formula, such that: $p=q$ and $p \neq q$ denote respectively, individual p equal q and individual p not equal q in knowledge base.
- To integer, real number, constraints can be expressed as mathematical equations and inequalities. For example, $p=q+n$, $p > q+n$, where $p, q \in N_i$ n is a constant.

Definition 8 (Action behavior model of MCS) Action behavior description models of MCS based on DDL is defined as:

$$MCS_AB(\eta_1, \eta_2, \dots, \eta_n) = (P_S, E_S)$$

Where

- *MCS_AB* is the action name of MCS, it is the action's unique identifier;
- $\eta_1, \eta_2, \dots, \eta_n$ are operation variable, are indicate the object of operation;
- P_S is a set of requirement conditions, it indicates that equirement conditions must be satisfied before the action execution, form as:
 $P_S = \{Res | Res \in Requirement\}$
- E_S is a set of result conditions, it indicates the result set is generation after the action

execution, it is the set of constraint subset: *head* and *body*, where $head = \{h | h \in Requirement\}$, $body = \{b | b \in Requirement\}$

Definition 9 (Execution process description model of MCS) If there are two processes A and B, includes four types : Sequence(;), Synchronization(\cup), Iterate(*), Switch(?), iff the follow constraints are satisfied:

- Sequence(A,B)|=A;B, satisfy
 $\{\langle u, v \rangle | u, v, w \in W, S_A[u \rightarrow v] \wedge S_B[v \rightarrow w]\}$
- Synchronization(A,B)|=A \cup B, satisfy
 $\{\langle u, v \rangle | u, v \in W, S_A[u \rightarrow v] \vee S_B[u \rightarrow v]\}$
- Iterate(A)|=A*, satisfy
 $\{\langle u, v \rangle | u, v \in W, S_A[u \rightarrow v] \vee S_A[u \rightarrow v] \vee \dots\}$
- Switch(B)|=B?, satisfy
 $\{\langle u, u \rangle | u \in W, u \models B\}$

Definition 10 (State description model of MCS) State description of MCS is composition of all assertion such as individuals, attributes and relations of each state. Let w is the set of assertion formula, define $w = \{\varphi_1, \dots, \varphi_n\}$,

and $I(w) = \{\Delta^I, C_i^{I(w)}, \dots, A_j^{I(w)}, \dots, E_k^{I(w)}\}$ is the interpretation of w , is also called model of w , abbreviated as: $I(w) = \{\Delta^I, \bullet^{I(w)}\}$. Where Δ^I is the domain of interpretation, $\bullet^{I(w)}$ is the function of interpretation. Atomic concept C_i maps a set $C_i^I \subseteq \Delta^I$, relation A_j maps a set $A_j^I \subseteq \Delta^I \times \Delta^I$, every individual maps a set $E_j^I \subseteq \Delta^I$

Definition 11 (State transformation model of MCS) Let two interpretation models of state u and state v in MCS: $I(u) = \{\Delta^I, \bullet^{I(u)}\}$, $I(v) = \{\Delta^I, \bullet^{I(v)}\}$, then let MCS $S = (P_S, E_S)$, there exists a state transformation: $u \rightarrow v$, and dynamic attribute γ_i will be changed accordingly, iff it satisfy the following conditions:

- $I(u) \models \alpha_1 \wedge \alpha_2 \wedge \dots \wedge \alpha_i \wedge \dots$, where $\alpha_i \in P_S$;
- Every ordered pair *head/body* in set E_S , satisfy:
 $I(u) \models \varphi_1 \wedge \varphi_2 \wedge \dots \wedge \varphi_i \wedge \dots \Rightarrow I(v) \models \phi_1 \wedge \phi_2 \wedge \dots \wedge \phi_i \wedge \dots$, where $\varphi_i \in head$, $\phi_i \in body$;
- There exists MCS attribute set: *Attribute* = (*Satt*, *Datt*) of S , where *Satt* is the set of static attribute, *Datt* is the set of dynamic attribute, and $\gamma_i \in Datt$, when state of MSC is changed, the γ_i will be changed accordingly.

So it expresses the state v generated from u in S , and defined as: $S[u \rightarrow v | \gamma_i]$.

4. CONCLUSIONS

Manufacturing capability sharing is a core of CMfg philosophy. Meanwhile, formal description of MC is the key technologies to achieve on-demand use. This paper studies the description method of MC based on description logics by combining the concept and characteristics of MC, and then the static information and dynamic information models based on DL of MC are mainly investigated. In the future, a prototype of MC formal description will be developed according to above proposed methods and related technologies.

ACKNOWLEDGMENTS

This paper is partly supported by the Doctoral Fund of Ministry of Education of in China (20101102110009), the National High-Tech. R&D Program (2011AA040501), China.

REFERENCES

- Skinner W, 1969. Manufacturing –missing link in corporate strategy. *Harvard business review*. 6-9, 136-145
- Richard G B, 1973. The organization of industry. *Economic Journal*. 82, 883-896
- Keen P, McDonald M, 2000. *The process edge: creating customer value and business wealth in the internet era*. McGraw-Hill. New York
- LI Bohu, ZHANG Lin, WANG Shilong, TAO Fei, et al. 2010. Cloud manufacturing: a new service-oriented manufacturing model. *Computer Integrated Manufacturing Systems*, 6(1), 1-7.
- ZHANG Lin, LUO Yongliang, TAO Fei, REN Lei, et al. 2010. Study on the key technologies for the construction of manufacturing cloud. *Computer Integrated Manufacturing Systems*, 16(11), 2510-2520
- ZHANG Lin, LUO Yongliang, FAN Wenhui, TAO Fei, REN Lei, 2011. Analyses of cloud manufacturing and related advanced manufacturing models. *Computer Integrated Manufacturing Systems*, 17(3), 0458-0468.
- Siri Terjesen, Pankaj C. Patel, Jeffrey G. Covin. 2011. Alliance diversity, environmental context and the value of manufacturing capabilities among new high technology ventures. *Journal of operations management*, 29,105-115
- Khalid Hafeez, YanBing Zhang, Naila Malak. 2002. Determining key capabilities of a firm using analytic hierarchy process. *International journal of production economics*, 76, 39-51
- Andreas Grobler. 2006. An empirical model of the relationships between manufacturing capabilities.

International journal of operations & production management, 26(5),458-485

- JIANG Zhixiong. 2008. Description of Web services based on dynamic semantic. *FUDAN university doctoral dissertation*.
- Monika Solanki, Antonio Cau, Hussein Zedan. 2004. Augmenting semantic web service descriptions with compositional specification. In *proceedings of the 13th international conference on world wide web*, ACM press,544-552
- Frank Wolter, Michael Zakharyashev. 2000. Dynamic description logics. *Advances in model logic*.
- SHEN Guohua. 2009. Research on modeling and reasoning about web services based on description logics. *Nanjing university of aeronautics and astronautics doctoral dissertation*.

AUTHORS BIOGRAPHY

Yongliang Luo received the B.S. degree and the M.S. degree in 2006 and 2009 from the Department of Computer Science at Shandong University of Science and Technology, China. He is currently working for the Ph.D. degree in Modeling simulation theory and technology at Beihang University. His research interests include service-oriented manufacturing and integrated manufacturing systems.

Lin Zhang received the B.S. degree in 1986 from the Department of Computer and System Science at Nankai University, China. He received the M.S. degree and the Ph.D. degree in 1989 and 1992 from the Department of Automation at Tsinghua University, China, where he worked as an associate professor from 1994. He served as the director of CIMS Office, National 863 Program, China Ministry of Science and Technology, from December 1997 to August 2001. From 2002 to 2005 he worked at the US Naval Postgraduate School as a senior research associate of the US National Research Council. Now he is a full professor in Beijing University of Aeronautics and Astronautics. He is an Editor of “*International Journal of Modeling, Simulation, and Scientific Computing*”, and “*Simulation in Research and Development*”. His research interests include integrated manufacturing systems, system modeling and simulation, and software engineering.

Fei Tao is currently an associate professor at Beihang University since April 2009. His research interests include service-oriented manufacturing, intelligent optimization theory and algorithm, resource service management. He is author of one monograph and over 20 journal articles of these subjects. Dr. Tao was awarded the Excellent Doctoral Dissertation of Hubei Province, China and was elected to be a research affiliate of CIRP in 2009. He is the founder and editor-in-chief of *International Journal of Service and Computing-Oriented Manufacturing (IJSCOM)*.

AN INTEGRATED BINARY-TABU SEARCH APPROACH FOR THE BUFFER ALLOCATION PROBLEM: AN INDUSTRIAL CASE STUDY

Leyla Demir^(a), Simge Yelkenci Köse^(b), Semra Tunali^(c), Deniz Türsel Eliiyi^(d)

^(a) Pamukkale University, Department of Industrial Engineering, 20070, Denizli, Turkey

^(b) Ministry of Science, Industry and Technology Directorate General for Industry, Çankaya-Ankara, Turkey

^(c) Izmir University of Economics, Department of Business Administration, Sakarya Cad. No:156, Balçova-Izmir, Turkey

^(d) Izmir University of Economics, Department of Industrial Systems Engineering, Sakarya Cad. No:156, Balçova-Izmir, Turkey

^(a)ldemir@pau.edu.tr, ^(b)simge.yelkenci@deu.edu.tr, ^(c)semra.tunali@ieu.edu.tr, ^(d)deniz.eliyi@ieu.edu.tr

ABSTRACT

In this study, an integrated binary-tabu search algorithm is proposed to solve the buffer allocation problem for a real manufacturing system producing heating exchanger in Turkey. The aim is to minimize the total buffer size in the system while improving the system performance. To achieve this objective first the production system is modeled by using simulation. After that the proposed algorithm is employed to find the optimal buffer levels for minimizing the total buffer size in the system. The experimental study shows that proposed algorithm improves the current average daily throughput rate about 31.68%.

Keywords: buffer allocation problem, simulation, tabu search, combinatorial optimization

1. INTRODUCTION

The buffer allocation problem is an NP-hard combinatorial optimization problem which involves the distribution of buffer space among the intermediate buffers of a production line. This problem arises in a wide range of manufacturing systems. The primary effect of storage buffers is to allow machines to operate nearly independently of each other. Storage buffers help reducing idle time due to starving (no input available) and blocking (no space to dispose of output). Less idle time increases average production rate of the line. However, inclusion of buffers requires additional capital investment and floor space. Buffering also increases in-process inventory. If the buffers are too large, the capital cost incurred may outweigh the benefit of increased productivity. If the buffers are too small, the machines will be underutilized or demand will not be met. Because of the importance of finding optimal buffer configuration, the buffer allocation problem is still an important optimization problem faced by manufacturing system designers.

The buffer allocation problem is solved by employing evaluative and generative methods in an iterative manner. Evaluative methods are used to

calculate the performance measures of the system, such as throughput rate and work in process levels. The decomposition method (Gershwin and Schor 2000; Helber 2001; Shi and Men 2003; Tempelmeier 2003; Shi and Gershwin 2009; Demir, Tunali and Løkketangen 2011; Demir, Tunali and Eliiyi 2012), aggregation method (Diamantidis and Papadopoulos 2004; Dolgui, Ereemeev, Kolokolov and Sigaev 2002; Dolgui, Ereemeev and Sigaev 2007; Qudeiri, Yamamoto, Ramli and Jamali 2008), generalized expansion method (Cruz, Duarte and Van Woensel 2008; Aksoy and Gupta 2010) and simulation (Lutz, Davis, and Sun 1998; Jeong and Kim 2000; Gurkan 2000, Sabuncuoglu, Erel and Kok 2002; Sabuncuoglu, Erel and Gocgun 2006; Bulgak 2006; Altiparmak, Dengiz and Bulgak 2007; Battini, Persona and Regattieri 2009; Can and Heavey 2011; Can and Heavey 2012; Amiri and Mohtashami 2011) are the most widely used methods among them. The first three methods are approximate analytical methods which are applicable under certain assumptions. To overcome these restrictive assumptions so that we could model our real system realistically simulation is used in this study. Generative methods are used for optimizing decision variables, such as buffer levels and service rate. There are various techniques used as generative methods, such as dynamic programming (Yamashita and Altiok 1998; Diamantidis and Papadopoulos 2004), gradient search method (Seong, Chang and Hong 2000; Gershwin and Schor 2000; Helber 2001), and meta-heuristics (Lutz, Davis, and Sun 1998; Spinellis and Papadopoulos 2000a; Spinellis and Papadopoulos 2000b; Spinellis, Papadopoulos and MacGregor Smith 2000; Dolgui, Ereemeev, Kolokolov and Sigaev 2002; Dolgui, Ereemeev and Sigaev 2007; Shi and Men 2003; Nourelfath, Nahas and Ait-Kadi 2005; Nahas, Ait-Kadi and Nourelfath 2009; Demir, Tunali and Løkketangen 2011; Demir, Tunali and Eliiyi 2012; Amiri and Mohtashami 2011; Can and Heavey 2011; Can and Heavey 2012).

In this study, we propose a new generative method to solve the buffer allocation problem which integrates binary search and tabu search methods. In our solution methodology, while the binary search is used as an outer control loop algorithm to minimize the total buffer size in the system tabu search is used as an inner loop algorithm to optimize the buffer levels for a given total buffer size. The proposed solution approach is employed for optimizing the buffer levels in a heating exchanger production system. The ultimate aim is to improve the average daily throughput rate in this heating exchanger system by integrating the proposed solution methodology with simulation model of the system.

The rest of this paper is organized as follows. In the next section the simulation model of the system is described in detail. The details of the proposed binary-tabu search algorithm are given in Section 3. Section 4 presents the results of computational study. Finally, concluding remarks and some future research directions are given in Section 5.

2. SIMULATION MODEL

The proposed approach is implemented to solve the buffer allocation problem in a local company operating in Izmir, Turkey. The company is produce-to-order type and produces seven types of heating exchangers. As it is seen in Figure 1, the production line is composed of pressing, forming, welding, testing, packaging and assembly stations with parallel machines. First, based on customer specifications, the steel rolls are smoothed and cut. Next, using different types of moulds, the steel rolls are processed in batches at the press station. After the press operation, each part is directed to subassembly stations where four machines operate in parallel. Then as shown in Figure 1, the parts visit the oven, welding, test and packaging stations.

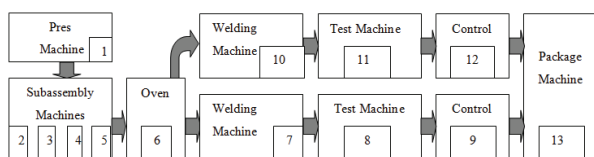


Figure 1: Production flow

The detailed simulation model of this line is developed in Arena 10.0 under the following assumptions:

- The plant operates three shifts per day including 50 and 15 minutes breaks for meal and cleaning, respectively in each shift. Each shift takes 8 hours, so the simulation model is run for 1245 minutes, corresponding to one working day.
- Raw materials are always available and there is sufficient space to store the finished products.
- The capacity to store work-in-process between the machines is limited.

- Each machine is operated by one operator, except for the press (1) and welding machine (7) (see Figure 1), which require 2 operators.
- Transporters are used for material handling between the machines in the system.
- Six different types of parts (LM1 to LM6) are pressed and then combinations of these are assembled to form seven types of heating exchangers. For example, type 1 heating exchanger is formed by an assembly of LM4 and LM5.
- Removing one type of mould from a press machine and replacing with another type requires a setup operation. To fit an appropriate distribution, the setup time records kept in the company are analyzed using Input Analyzer of ARENA 10.0 and the resulting estimates of input distributions are given in Table 1.
- Processing times are stochastic, except for the processing times on the automated press machine. Each machine is subject to random breakdown. The time-to-failure and the repair time for each machine are exponentially distributed.

Table 1: The setup times at the press machine

Parts	Setup Times (in minutes)					
	LM1	LM2	LM3	LM4	LM5	LM6
LM1	-----	U(41,47)	U(27,33)	U(32,38)	U(42,48)	U(37,43)
LM2	U(27,33)	-----	U(28,34)	U(27,33)	U(27,33)	U(42,48)
LM3	U(27,33)	U(39,45)	-----	U(32,38)	U(42,48)	U(27,33)
LM4	U(32,38)	U(35,41)	U(32,38)	-----	U(35,41)	U(35,41)
LM5	U(27,33)	U(32,38)	U(34,40)	U(27,33)	-----	U(35,41)
LM6	U(35,41)	U(27,33)	U(29,35)	U(27,33)	U(27,33)	-----

The model verification has been done by developing the model in a modular manner, using the interactive debuggers, and manually checking the results. The simulation model is validated by comparing the output of the simulation (i.e., daily throughput) with the output of the real system at 95% confidence level and the simulation model has been found to be truly representing the real system. Since the company operates on the basis of produce-to-order and starts production without any work-in-process, the warm-up period has not been considered during the experiments. Besides validating the simulation model with respect to daily throughput, we carried out further experimental studies to estimate average machine utilizations and average number in queue for each machine. As a result of these studies, it is noted that the machines 4, 5, 6 and 7 have the highest utilizations and highest number of parts waiting to be processed.

Solving this real-world buffer allocation problem involves twelve decision variables denoting the buffer sizes to allocate to each station. The objective is to determine the best buffer configuration so that the capacity of the production line can be improved with minimum total buffer size. The current average

production rate of this line is 95 heating exchangers per day and the company officials desire at least 30% improvement in the production rate. Therefore, the rate of 0.10, i.e. 125 heating exchangers per day, is defined as the desired throughput rate (f^*) of the real production system.

3. THE PROPOSED INTEGRATED BINARY-TABU SEARCH ALGORITHM

The proposed integrated binary-tabu search (B-TS) approach has two control loops, i.e., the inner loop and outer loop. While the inner loop control includes a tabu search (TS) algorithm, a binary search (BS) algorithm is employed as an outer loop. These nested loops aim at minimizing the total buffer size to achieve the desired throughput level. Figure 2 summarizes the execution mechanism of the proposed integrated B-TS approach. The outer loop, i.e. the BS algorithm, is started with a pre-specified N value, and then the maximum throughput rate that can be obtained with this N value is calculated using the TS algorithm. This throughput rate is then compared to the desired throughput rate, and new N values are suggested by the BS algorithm in an iterative manner. The procedure continues until the termination criterion of the BS algorithm is satisfied, i.e., until the desired throughput rate is achieved with the minimum total buffer size. The following sections present the details.

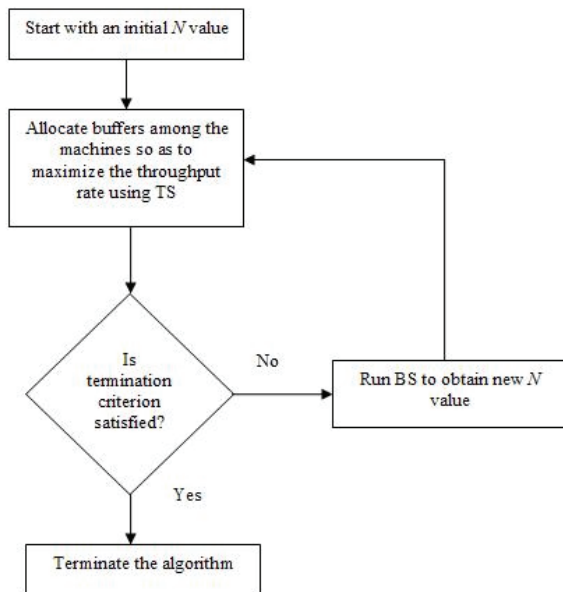


Figure 2: The framework of the integrated B-TS algorithm

3.1. Binary Search

Table 2 represents the steps of our systematic binary search. The algorithm starts by setting the upper and lower limits of total buffer size to M (a large value) and zero, respectively. The search continues between H and L until the desired throughput rate is obtained.

In this algorithm, $f(B^N)$ represents the throughput rate obtained with total buffer size N , f^* represents desired throughput level, and B^N represents buffer configuration obtained by total buffer size N .

Table 2: Pseudo code of the BS algorithm

0. (Initialization). Set $H = M$, $L = 0$.
1. Set $N = (H + L)/2$, $N^{\min} = N$.
2. Run TS algorithm for N .
3. If $f(B^N) < f^*$, set $L = N$ and $N = (H + L)/2$,
If $f(B^N) \geq f^*$, set $H = N$, $N^{\min} = N$ and $N = (H + L)/2$.
4. Until $H = L$ go to Step 2, otherwise stop.

3.2. Tabu Search

Tabu Search is a meta-heuristic method for solving combinatorial optimization problems. TS explicitly uses the history of the search, both to escape from local optima and to implement an explorative search. For more details about TS the reader can refer to Glover and Laguna (1997). The following sections explain the features of the TS algorithm adopted in this study. It should be noted that this algorithm is similar to the one in Demir, Tunali and Løkketangen (2011), except that in this study TS is integrated with BS algorithm.

3.2.1. Move representation and tabu moves

In the proposed TS algorithm, the moves are represented by $[i, j]$, where i shows the location that a given amount of buffer is added and j shows the location that the same amount of buffer is subtracted. The increment (decrement) value is set to 1. Once a move is realized, the reverse of this move is recorded as tabu. Namely, if the move $[i, j]$ produces the best solution for the current step, then the reverse move $[j, i]$ is considered as a tabu for a certain number of iterations.

3.2.2. Search space and neighborhood structure

The search space of TS is simply the space of all feasible solutions that can be visited during the search. To define the neighborhood of the current solution, there are several choices depending on the specific problem at hand. In the buffer allocation problem context, one choice could be to consider the full neighborhood of the current buffer configuration while another could be to consider only a subset of the neighborhood (Demir, Tunali and Løkketangen 2011). In this study, all feasible solutions are considered as the search space, and all neighbors of the current solution are created and evaluated.

3.2.3. Tabu tenure

The length of the tabu list, called tabu tenure (TT), is the number of iterations that tabu moves stay in the tabu list. As indicated by Glover, Taillard and Wera (1993) the size of the tabu list providing good results often grow with the size of the problem. However, no single

rule has been found to yield an effective tenure for all classes of problems. If the size of the tabu tenure is too small, preventing the cycling might not be achieved; conversely a long length may create too many restrictions. As indicated by Reeves (1996), a value of 7 for tabu tenure (TT) has often found to be sufficient to prevent cycling. Considering the problem size and after pilot experiments, TT is set to 7 throughout the algorithm.

3.2.4. Intensification

The key idea behind the concept of intensification is to implement some strategies so that the areas of the search space that seem promising can be explored more thoroughly. In general, intensification is based on a recency memory, in which one records the number of consecutive iterations that various solution components have been presented in the current solution without interruption (Demir, Tunali and Eliiyi 2012). Intensification is used in many TS implementations, but it is not always necessary. In this study, since the increment (decrement) values of the moves is set to 1 there is no need to spend time exploring in depth the portions of the search space that have already been visited, so an intensification strategy is not implemented.

3.2.5. Diversification

Diversification guides the search to unexplored regions to avoid local optimality, and it is usually based on a frequency memory where the total number of iterations of the performed moves or the visited solutions is recorded. There are two major diversification techniques known as restart diversification and continuous diversification. While the first is performed by several random restarts, the latter is integrated into the regular search process (Demir, Tunali and Eliiyi 2012). To improve the search process, the random restart diversification method is employed in the proposed TS algorithm. For the restart diversification, if the value of objective function does not change for a certain number of iterations, a random restart is applied. This value is set to 50 throughout the experiments.

3.2.6. Aspiration and termination criterion

In our TS algorithm, the tabu move is allowed if it results in a solution with an objective value better than the incumbent solution. The algorithm is terminated after a fixed number of iterations. This value is set to 1000 in our experiments.

The next section explains the implementation of the proposed solution approach in detail.

4. AN INDUSTRIAL CASE STUDY

The proposed solution methodology is employed to solve the buffer allocation problem in a heating exchanger production system explained in Section 2. The problem is mathematically formulated as follows:

Find $B = (B_1, B_2, \dots, B_{K-1})$ so as to

$$\min N = \sum_{i=1}^{K-1} B_i \quad (4)$$

subject to

$$f(B) \geq f^* \quad (5)$$

$$B_i \text{ nonnegative integers } (i = 1, 2, \dots, K-1) \quad (6)$$

$$0 \leq B_i \leq u_i \quad i = 1, 2, \dots, K-1 \quad (7)$$

where N is a fixed nonnegative integer denoting the total buffer space available in the system that has to be allocated among the $K-1$ buffer locations so as to improve the performance of the K -machine production line. In this formulation, B represents a buffer size vector, B_i is the buffer size for each location, $f(B)$ represents the throughput rate of the production line as a function of the buffer size vector, f^* is the desired throughput rate, and u_i represents the upper bounds for each buffer capacity.

Figure 3 shows the framework of the proposed solution approach explained in previous sections. In this configuration simulation model of the production system is used to obtain the average daily throughput, i.e. production rates. This throughput rate is then compared to the desired throughput rate, and a new buffer configuration is suggested by the proposed B-TS algorithm in an iterative manner. The procedure continues until the termination criterion of the algorithm is satisfied, i.e., until the desired throughput rate is achieved with minimum total buffer size.

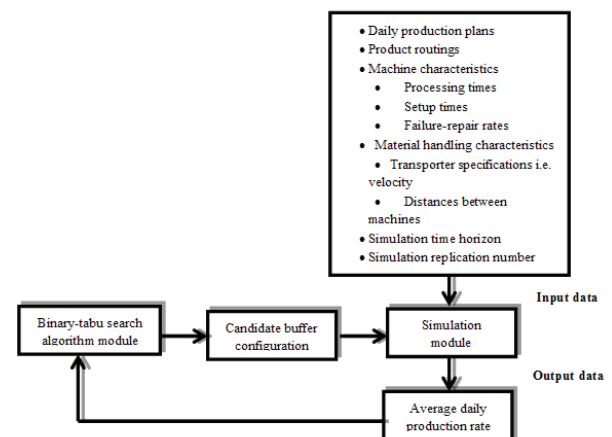


Figure 3: The framework of the proposed solution procedure for buffer allocation problem

The integrated binary-tabu search algorithm is implemented in C language. The experiments are carried out on a PC with 2 Ghz Pentium (R) 4 CPU processor, 2 GB RAM.

B-TS reaches the minimum total buffer size after 7 iterations (totally 7000 iterations as each iteration of BS algorithm involves 1000 iterations of TS algorithm). The minimum total buffer size is achieved with the buffer configuration $B = \{1, 2, 1, 1, 2, 3, 1, 3, 1, 3, 1, 1\}$. The corresponding average daily throughput rate and

the total buffer size for the proposed solution are 0.10048/minutes, 20 units, respectively. This means B-TS improves the current average daily throughput rate about 31.68 % for the system. So, it can be concluded that the proposed B-TS algorithm is very efficient to solve buffer allocation problem in a real manufacturing environment.

5. CONCLUSION

In this study, an integrated binary-tabu search algorithm is proposed to solve a real-world buffer allocation problem. This algorithm is integrated with a simulation model that captures the stochastic and dynamic nature of the production line. The simulation model is used to calculate the average daily throughput rate of the system. The experimental study shows that the proposed B-TS algorithm improves the system performance significantly.

While we solve the problem only from buffer size minimization perspective, the problem can be solved also in a multi-objective manner involving other objectives such as maximization of throughput rate, minimization of average work-in-process, and minimization of average system time. Moreover, these production oriented criteria can be integrated with some monetary criteria for profit maximization or cost minimization.

REFERENCES

- Aksoy, K.H., Gupta, S.M., 2010. Near optimal buffer allocation in remanufacturing systems with N-policy. *Computers&Industrial Engineering*, 59, 496-508
- Altiparmak, F., Dengiz, B., Bulgac, A.A., 2007. Buffer allocation and performance modeling in asynchronous assembly system operations: An artificial neural network metamodeling approach. *Applied Soft Computing*, 7, 946-956.
- Amiri, M., Mohtashami, A., 2011. Buffer allocation in unreliable production lines based on design of experiments, simulation, and genetic algorithm. *International Journal of Advanced Manufacturing*, 1-13, doi 10.1007/s00170-011-3802-8.
- Battini, D., Persona, A., Regattieri, A., 2009. Buffer size design linked to reliability performance: A simulative study. *Computers&Industrial Engineering*, 56(4), 1633-1641.
- Bulgac, A.A., 2006. Analysis and design of split and merge unpaced assembly systems by metamodeling and stochastic search. *International Journal of Production Research*, 44 (18-19), 4067-4080.
- Can, B., Heavey, C., 2011. Comparison of experimental designs for simulation-based symbolic regression of manufacturing systems. *Computers&Industrial Engineering*, 61(3), 447-462.
- Can, B., Heavey, C., 2012. A comparison of genetic programming and artificial neural networks in metamodeling of discrete-event simulation models. *Computers&Operations Research*, 39(2), 424-436.
- Cruz, F.R.B., Duarte, A.R., Van Woensel, T., 2008. Buffer allocation in general single-server queueing networks. *Computers&Operations Research*, 35(11), 3581-3598.
- Demir, L., Tunali, S., Løkketangen, A., 2011. A tabu search approach for buffer allocation in production lines with unreliable machines. *Engineering Optimization*, 43(2), 213-231.
- Demir L., Tunali, S., Eliiyi, D.T., 2012. An adaptive tabu search approach for buffer allocation problem in unreliable non-homogenous production lines. *Computers&Operations Research*, 39(7), 1477-1486.
- Diamantidis, A.C., Papadopoulos, C.T., 2004. A dynamic programming algorithm for the buffer allocation problem in homogeneous asymptotically reliable serial production lines. *Mathematical Problems in Engineering*, 3, 209-223.
- Dolgui, A., Ereemeev, A., Kolokolov, A., Sigaev, V., 2002. A genetic algorithm for the allocation of buffer storage capacities in a production line with unreliable machines. *Journal of Mathematical Modeling and Algorithms*, 1, 89-104.
- Dolgui A., Ereemeev, A., Sigaev, V., 2007. HBBA: hybrid algorithm for buffer allocation in tandem production lines. *Journal of Intelligent Manufacturing*, 18, 411-420.
- Gershwin, S.B., Schor, J.E., 2000. Efficient algorithms for buffer space allocation. *Annals of Operations Research*, 93, 117-144.
- Glover, F., Taillard, E., Werra, D., 1993. A user's guide to tabu search. *Annals of Operations Research*. 41, 3-28
- Glover, F., Laguna, M., 1997. *Tabu Search*. Dordrecht: Kluwer Academic Publishers.
- Gurkan, G., 2000. Simulation optimization of buffer allocations in production lines with unreliable machines. *Annals of Operations Research*, 93, 177-216.
- Helber, S., 2001. Cash-flow-oriented buffer allocation in stochastic flow lines. *International Journal of Production Research*, 39 (14), 3061-3083.
- Jeong, K.-C., Kim, Y.-D., 2000. Heuristics for selecting machines and determining buffer capacities in assembly systems. *Computers&Industrial Engineering*, 38, 341-360.
- Lutz, C.M., Davis, K.R., Sun, M., 1998. Determining buffer location and size in production lines using tabu search. *European Journal of Operational Research*, 106, 301-316.
- Nahas, N., Ait-Kadi, D., Nourelfath, M., 2009. Selecting machines and buffers in unreliable series-parallel production lines. *International Journal of Production Research*, 47 (14), 3741-3774.
- Nourelfath, M., Nahas, N., Ait-Kadi, D., 2005. Optimal design of series production lines with unreliable

- machines and finite buffers. *Journal of Quality in Maintenance Engineering*, 11(2), 121-138.
- Qudeiri, J. A., Yamamoto, H., Ramli, R., Jamali, A., 2008. Genetic algorithm for buffer size and work station capacity in serial-parallel production lines. *Artificial Life and Robotics*, 12, 102-106.
- Reeves, C.R., 1996. *Modern Heuristic Techniques in Modern Heuristic Search Methods*. Edited by Rayward-Smith, V.J., Osman, I.H., Reeves, C.R., Smith, G.D. England: John Wiley & Sons.
- Sabuncuoglu, I., Erel, E., Kok, A.G., 2002. Analysis of assembly systems for interdeparture time variability and throughput. *IIE Transactions*, 34, 23-40.
- Sabuncuoglu, I., Erel, E., Gocgun, Y., 2006. Analysis of serial production lines: characterization study and a new heuristic procedure for optimal buffer allocation. *International Journal of Production Research*, 44 (13), 2499-2523.
- Seong, D., Chang, Y.S., Hong, Y., 2000. An algorithm for buffer allocation with linear resource constraints in a continuous-flow unreliable production line. *Asia-Pacific Journal of Operational Research*, 17, 169-180.
- Shi, L., Men, S., 2003. Optimal buffer allocation in production lines. *IIE Transactions*, 35, 1-10.
- Shi, C., Gershwin, S.B., 2009. An efficient buffer design algorithm for production line profit maximization. *International Journal of Production Economics*, 122, 725-740.
- Spinellis, D., Papadopoulos, C.T., MacGregor Smith, J., 2000. Large Production Line Optimization Using Simulated Annealing. *International Journal of Production Research*, 38, 3, 509-541.
- Spinellis, D., Papadopoulos, C. T., 2000a. A simulated annealing approach for buffer allocation in reliable production lines. *Annals of Operations Research*, 93, 373-384.
- Spinellis, D., Papadopoulos, C.T., 2000b. Stochastic Algorithms for Buffer Allocation in Reliable Production Lines. *Mathematical Problems in Engineering*, 5, 441-458.
- Tempelmeier, H., 2003. Practical considerations in the optimization of flow production systems. *International Journal of Production Research*, 41 (1), 149-170.
- Yamashita, H., Altrok, T., 1998. Buffer capacity allocation for a desired throughput in production lines. *IIE Transactions*, 30, 883-891.

COMPREHENSIVE PROTOCOL FOR ARTIFICIAL INTELLIGENCE DEVELOPMENT

Bruce L. Toy

Lockheed Martin (Ret), Palm Harbor, FL USA

brucetoy@verizon.net

ABSTRACT

This paper presents a Functional Architecture and an Integration Protocol that support a comprehensive intelligent system. The structure is based on XML objects. Motivations drive all actions. The behavior processes use templates of stored information augmented with real-time sensor data to execute actions. Actions are controlled on independent “virtualized” segments of a processor. The brain forms predictive models of the behavior of objects it interacts with. It does this by creating simplified clones of its own behavior control structure. Secondary motivations and action preferences are linked to locations. Sensor processing and interaction with the environment is made more efficient through the creation and use of location models. A Frame of Reference defines the brain’s individuality. Training, rather than programming is the focus of development.

Keywords: AI, artificial intelligence, brain modeling, behavior modeling, cognitive process, learning

1. INTRODUCTION

This paper defines the brain in terms of a complete functional architecture and captures its essential nature, defining an approach for Artificial Intelligence implementation. There are details that help to understand complex human behavior. The focus is on the “forest” rather than the trees. Instead of analyzing things like pattern recognition algorithms (trees) the discussion looks at how to break down the forest into functional components with well defined internal interfaces. The components are described in fundamental, practical, terms with a level of detail that would support system development. There are aspects that go outside the bounds of traditional AI theory but are necessary in order to provide a complete architecture.

There have been multiple projects that seek to define a Cognitive Architecture for handling AI. Most focus on behavior modeling with some success. One good example is Soar, developed by Newell and Laird. It includes refined logical algorithms for selecting actions, but it does have a drawback. Like others, it must be managed by an external entity – human or human-produced computer program in order to be effective. A true architecture must incorporate the totality of mental functions and be independent.- living or dying on its own. Note that I am not discounting such models such as the Cognitive Architectures created to

date. Instead, I expect that this protocol could facilitate the integration of diversely developed AI elements.

1.1. Virtualization

There is an important software tool that is cited in this architecture, virtualization. (Adams and Ageson 2006) It has always been possible to set up sub-processor segments with specialized connections and functional programs. In the past this was a time-consuming task not easily automated.

Virtualization allows us to create a variable portion of a processor to be set aside for a particular task. In this protocol we call this an “action template” by which a function is activated. The template defines the way in which a processor segment is established and linked to other memory objects and input/output interfaces.

Lower animals generally have templates that exist without training. In intelligent systems there are basic defined templates but, in addition, training drives the system to build new templates of the action concepts. The application of the virtualization process will be discussed further in section 2.

1.2. Protocol Structure

The core of the protocol consists of seven layers that define the complete set of memory objects in the brain. Around this there is a wrapper consisting of a pair of functions that manage the operation and the accounting needed to control the intelligent system. The first function, the Control Program (CP), runs the operational environment and the second function, the Cognitive Structure program (CS), runs the development and administrative environment. Any computer developer will tell you that operating systems and development environments must be segregated. These two management functions are separate for similar reasons. This is one of the features that set this protocol apart from most other approaches to AI.

1.3. Protocol Definitions

The general elements in this architecture are defined as follows:

Memory concepts are groups of links in the memory that have their own identity, with three types: Object Concepts are the fundamental memory concepts that can be associated with things the system can detect or purely abstract things or ideas. Functional Concepts (also called Action Concepts or action templates) define and manage the actions your brain can execute. The functional concept is, in essence, a template for a specific activity. It is “hosted” on a virtualized segment of the processor. Motivation Concepts are the triggers

that begin all action. It is only when a sensor input triggers a motivation that any action can occur.

Location Models are structures of concepts associated with locations that the system encounters. Sometimes a location model is purely imaginary, as one created while reading a book.

Behavior Models are created by the Cognitive Structure program and are attached to all object concepts.

The Cognitive Structure (CS) program manages the memory storage through creation of links and their values (prioritization.) It establishes definitive object concepts, location models, and behavior models.

The Control Program (CP) controls the execution of actions based on link analysis. The CP makes things happen, not by commanding actions but by *allowing* a functional concept to operate as an independent action with temporary control of a portion of the brain.

The following diagram shows the complete architecture/protocol that is the basis of this paper. Each element will be discussed in detail.

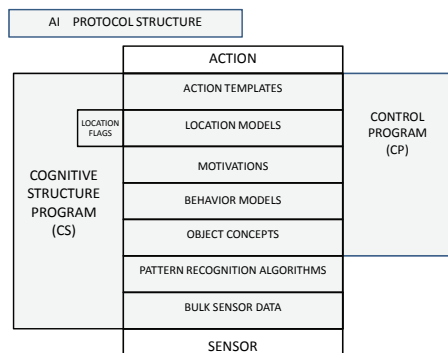


Figure 1: AI Protocol Structure

2. CONTROL PROGRAM (CP)

The Control Program (CP), one of two separate management functions, is responsible for executing actions. In order to maximize efficiency the CP has the primary role of deciding which of the available functional concepts (action templates) deserve to use a portion of the limited processor resources. It ensures that each one uses only as much of the processor as necessary and only for as long as necessary.

In this architecture, the brain is represented by a central processor that can be partitioned into independent processing units of variable size and quantity, in essence, a divisible processor.

The CP applies no logic or decision making beyond the evaluation of link prioritization – the relative strength of the link values associated with each motivation and action. These link values are managed by the CS

The control of a portion of the processor is delegated to the individual functional concept. The “permission” to use the partition of the processor is managed by the CP based on motivations and link

analysis. Any functional concept allowed to use a part of the processor will function independently until such time as its permission is withdrawn and it is disconnected.

The activation process begins when a motivation is triggered by a sensor input. The CP then reviews all active motivations to assess the priority of responding to the motivation. The nuances of this process will be enumerated as we describe the complete protocol. For now simply note that stored motivations, both positive and negative, along with the priorities assigned to their links will drive the selection of action by the CP.

If the AI structure is hosted on a reasonably powerful computing platform, one purpose of the biological CP, optimizing efficiency, is not as important. It does, however, remain as a vital element in replicating intelligence with a machine through its control of the operating environment and implementing motivations.

3. MOTIVATIONS

Some motivations are obviously inherent in the brain. Some attempts to introduce motivations focus on emotion (Minsky 2006). Such approaches have been more philosophical than practical. Biological motivations have a strong emphasis on survival, reproduction, and factors that are often not the primary interests of the AI system. We must define specific motivations for the AI and integrate them in a measurable way.

Following that, secondary motivations are one of the keys to intelligent behavior. They are generated based on experience and/or instruction and are linked to actions that result from the learned behavior. These links are given preference by link value based on instruction or experience, reinforced by training.

In addition, motivations are linked to location models, which are described later. They allow us to organize behavior patterns and link motivations and actions within specific locations.

When you go beyond the basic motivations, the use of an instructor becomes critical. Furthermore, the ability of an instructor to guide the learning process exists only to the extent that the student has an associated motivation framework. In instructional settings this takes the form of a motivation by the student to satisfy or please someone else. For an AI this motivation should focus on an educational team, to the exclusion of other individuals. Human students will have additional internal self-motivations, in varying degrees, to support the learning process. The AI should, at some stage, transition to an internal self-motivated driver to partly, or even completely, assume an independent pursuit of learning.

Secondary (learned) motivations are critical and without them it is quite possible you will not have an intelligent system. These will be discussed in more detail in the following sections.

Negative motivations (inhibitors) are needed to identify actions that produce incorrect results, waste

time, consume too much energy, or are otherwise undesirable. To achieve this we will allow the AI to contain only positive motivations with both positive and negative link values. While this probably does not mimic the biological system, which contains separate positive and negative motivations, it simplifies the design and makes the analysis task of the CP much more straightforward and less prone to errors.

It should also be noted that in some animals, but especially in humans, there are many strong motivations that appear in stages as the brain matures. The most active time for new motivations is probably the adolescent puberty stage. Also with age some motivations are reduced or disappear entirely.

This strongly suggests that for complete development of the AI we should introduce motivations in steps, indexed to achievement of learning. This would support a more passive, instructor-based system in the beginning and a transition to a more active system with added interaction with the environment, humans, and other AI systems. Maintaining control of the motivations means that we add and subtract some of them, or change priorities, throughout the life cycle of the AI.

3.1. Frame of Reference

Motivations are linked to a Frame of Reference. The AI system must have a “frame of reference”. In its most basic form this defines the biological individual but there are variations that allow the individual to identify itself with some group beyond its physical self. This may be a social group, a family, a religion, a culture, or any of a variety of groups that the individual identifies with.

The importance of the frame of reference is both subtle and powerful. It is closely tied to motivations and helps to define consciousness. In developing an AI system, the frame of reference chosen can allow the AI to evolve a distinct consciousness of its own. The consciousness can be human-like or intentionally modified to an even more complex form not yet seen in the biological realm.

The AI should have a “displaced” frame of reference, where the focus of its motivation is outside its own structure. This will allow it to better represent a particular object or entity. More importantly, however, this can be used to prevent the AI from developing an egocentric behavior pattern.

The key point to remember at this stage is that memory data is recorded based on the connections to, and the impact on, the Frame of Reference. The strength of a link will be directly proportional to that level of impact.

4. COGNITIVE INTEGRATION

One thing that makes it difficult to explain this model in one straight narrative is that there is considerable interaction between the processes. I will now describe the interrelated functions of location modeling, sensor dynamics, learning (including the memory management

of learning) and, most importantly, predictive behavior modeling. Each is dependent on the others and it is difficult to begin with any one of them because each description will not seem clear until all are integrated.

4.1. Location Modeling

Location models support a significant part of intelligent behavior and the organization the brain. Though models may contain a large number of objects the location models themselves are simple, with links to a collection of specific object concepts in memory.

One aspect of learning is building the location models of our environment. This is supported by a fundamental motivation to identify one’s location and identify objects associated with that location. With maturity we develop the location models for all the places we encounter. We can also compose models for places that are described to us.

Many children’s books focus on location modeling. They establish generic models of such places as farms, deserts, jungles, oceans, and so forth then link other object and activities to them. This activity both entertains and educates the kids,

Three specific concepts are linked with location models. First, there are secondary motivations, developed by training. These can be triggered by entering a location or, by object concepts found there. Second, and very important, are action templates tailored specifically to the location. These lead to preferred behavior patterns in specific locations. This means the CP will automatically activate the action templates for the preferred behavior functions in a given location (absent other negative motivations, of course). This will be expanded upon later. Third, there are links to behavior models of objects found in a location. This, in turn, impacts other actions we take.

It is important to note that the vast majority of the data in a location model is simply linked into it from other memory objects.

A location model can be purely abstract, or imaginary. When you read a novel you create location models of places described in the book. A good author builds these models of places and the reader can experience them through links to their own mental concepts.

The Cognitive Structure (CS) program is not only the tool that constructs the location models; it serves another function as well. It registers a “flag” to indicate all models that you are currently part of. When you change locations it changes the status flag. You will be part of several locations at one time, starting with your immediate vicinity and moving up to community, state, and so forth.

It may seem obvious to some but I should point out that any but the lowest forms of animal life will create and remember location models. A rabbit, for example, will have a complete model of its home, feeding areas, trails, water sources, and other features of its local environment. The lab rat that learns to negotiate a maze

is doing nothing more than creating a specific location model.

4.1.1. Controlling Action with Location Models

Once we have a location model in memory it serves as a linking point for action concepts.

The models affect preferred actions, or default behavior, through the attached action templates. For example, when you enter a neighbor's home your behavior will not be the same as in your own home. While the two locations are essentially similar in characteristics, the actions are driven by a largely separate set of default behaviors – all driven by learning and secondary motivations.

These memory links for action templates are structured in such a way that the CP sees a high link value when a motivation is triggered in association with a specific location model. Secondary (learned) motivations that are created in association with specific locations will produce actions in those situations and may not even be options in other locations. This occurs partly through directed training and partly through simple experience. For example, the hunger motivation produces different actions in different locations simply based on experience. Just entering a movie theater (along with specific smells) may compel many individuals to buy a large tub of popcorn, an action that they would never execute anywhere else.

This arrangement defines what could be called the “default” set of functional templates that are active in the processor at a given time. Each location model essentially guides the CP to maintain a processor segment for specific actions during normal activity in that location. Note, of course, that the location does not actually dictate action. The CP still has ultimate control and any overriding motivation and higher link values can change the priorities.

We act and react differently in different settings. This is not news to anyone but now, at least, you know how it happens.

I should also note that, in addition to location flags, the CS maintains another sort of flag for each location. It appears to identify the most recent and/or the most important action templates associated with a given location – sort of a “save game” function that allows you to pick up where you left off when you re-enter a location.

4.1.2. The Shopping Algorithm Problem

Some who study intelligent behavior point out the difficulty of creating an automation of the process of shopping in, for example, a grocery store. Perhaps the model offered here gives a methodology to address this issue.

One curious thing about location models is that you can create temporary motivations within them, either consciously or not. I would almost call them bookmarks and they can motivate an action when the location is encountered.

As for shopping, let's say that during the course of a day you note that some of your kitchen supplies are low but you are not able to go to the market until tomorrow. You create a temporary motivation to replace the ketchup. Some organized people make a list. Others make bookmark motivations in either the kitchen model or the store model. Thus, when you arrive at the store the sight of the ketchup bottles triggers the bookmark motivation to get more ketchup. This can be accomplished by either linking the motivation to the store model or by linking the kitchen model to the store model and I would expect that some individuals may do it either way.

In fact we can explain why men and women might seem to approach the task of shopping differently. Some people seem to move through a store, looking at everything, waiting for something to trigger a motivation. Others seem to have the motivation set to drive action by moving straight to the objects of interest – that is, the motivation triggers an action, as a result of entering the location, and takes the individual to a specific part of the location.

It becomes clear that the difficulty in creating a “shopping” algorithm is that the shopper needs the context provided by the location models and attached secondary motivations. In this AI structure we can implement a straightforward solution.

4.1.3. Other Links Within Locations

Other links exist that are not directly relevant to artificial intelligence but are noteworthy nonetheless. An “emotional” link is a behavior model that is attached to an object within the location that has an output (input to our system) that strongly satisfies one of our own motivations or, conversely, is a threat to our system.

Some sensor inputs will activate the imagination to visualize and experience a specific location and its links. In some people this can be very vivid. The input may be very simple. The sight of an object, the sound of the ocean, or a gunshot, as examples, can trigger strong images and reactions, almost as if one was in the specific location.

4.2. Sensor Processing

One of the more difficult problems associated with designing an AI is the handling of sensor inputs. Most of the discussion for this topic will center on visual data, but the ideas will apply to any type of sensor input for the AI system. Any AI must be compatible with the use of a variety of sensors, however not all AI systems will require the same kinds of complex sensing systems.

The processing of visual data is a highly specialized field. What I will describe here is a system for managing the data rather than the actual processing. I will only describe the framework in which the sensor data will be used and the general approach for processing. I will not attempt to duplicate or improve upon the various processing pattern recognition algorithms and analysis techniques that exist.

One of the keys to this process is the object concept we store in memory. At the core of each object is a pattern recognition algorithm that allows us to correlate the object in memory with an object in the visual field. Each pattern recognition algorithm is attached to the associated object concept. We should note at this point, though it will be discussed in more detail later, that some pattern recognition relies on simple high-level characteristics and associated location models.

You do actual pattern recognition on the small, central part of your visual field. The rest of the visual space is processed only for basic details. This includes color, intensity, texture, distance, motion, and perhaps a few others. I will refer to this broad group of processed data generally as “field data”. This data is then presented in the brain as a simple flat array with the characteristics of the pixel fields measured and shown. The objects outside the fovea are identified primarily by the determination of a specific location model (i.e. where you are) and the “field data”. This does not rise to the complexity of actual pattern recognition.

In this regard, location models are very important. The field data combined with the objects expected for that location give a presumptive identification of those objects outside the central viewing field, outside the region of pattern recognition. Pattern recognition, on the other hand, is applied to the objects you focus your attention on.

If, for example, trees are part of your location model then any objects outside the fovea that have the correct basic “field data” (color, movement, size, etc.) are identified as trees without you needing to focus on them or do any special pattern recognition. When you walk through a forest you do not need to focus your attention on an object to classify it as a tree or a bush. Note, particularly, that if there is something in that location that is similar to a bush you are not likely to notice the difference even if it is not really a bush. That is the purpose of camouflage.

What are the implications? The point is that in real-life situations, when you finally get around to doing pattern recognition you have already (1) identified your location, and (2) know the typical objects you will find there. You then apply the pattern recognition algorithms for the candidate objects that you decide to focus your interest on. This does not mean that you will not identify other “unusual” objects. It just means that you first match objects with a particular location. If there are no matches for something unusual, only then do you do a full analysis of that object.

You can even direct yourself to ignore objects that are not expected—meaning you do not apply extraneous algorithms outside a specific group of your choosing. There is a popular video on the internet that asks the viewer to watch a group of individuals wearing different colors pass large balls around. You are asked to count the number of times individuals of a specific color pass a ball. In the middle of the video a guy in a gorilla costume walks through the scene. If you are good at

focusing your attention you never even “see” the gorilla. You have specifically directed your mind to focus on specific types of pattern-recognition algorithms and process data for them only. In essence you have created, by direction, a temporary location model with a limited number of objects—and it does not include any gorillas. You can then focus all of your attention on that location model to perform an assigned task. Extraneous objects may not be “seen”.

Why did I mention this example? You must be prepared for your AI system to overlook a gorilla if you have specifically asked it to focus on other specific objects. Only then will you know you have created a truly human-like AI.

This all makes it possible to store longer-term information about visual inputs very efficiently, but it must be noted that we are storing processed data, not the complete sensor input. This makes us susceptible to inaccurate memories, based upon external suggestions or misperceptions of what we see. If we design a comparable AI we must be prepared to accept the reality that memories (not the real-time input) will contain inaccuracies, though it may be possible to minimize this by careful attention to the design of the sensor processing algorithms.

4.3. Linking Sensor Data

The XML linking structure must have two basic types of links in the memory. The first is long-term memory. These links decay over time as a normal process, but the time constant for this decay is quite long. The second is short-term links with a rapid decay time. This type of linkage is principally used with real-time sensor data. The sensor programs analyze inputs and the short-term links are created to connect the input information with the stored memory concepts.

This allows action concepts to act on the information, through their specific interaction with that long-term object concept. The need to establish other more persistent long-term links for any input data is determined by the template defined for that activity.

Perhaps more importantly, we can execute actions on objects simply because they are part of a location model. We do not actually need to focus our attention on, and do pattern recognition for, specific familiar objects that appear in a location.

Another consequence of this aspect of the model is that it enables us to better understand and define the differences between higher and lower animals. The higher animals, with greater mental capacity, will store correspondingly more details with their memory objects. The lower animals store only a few details of any given concept, using a simple set of object types. In interacting with those objects they rely on the short-term links to provide the details they need to execute functional actions. Experiments have shown that a frog, for example, responds in the same way to any small object that moves like an insect. The frogs stored memory concept appears to be based exclusively on the size and motion characteristics.

5. ABSTRACT TOOLS

We need a tool set that supports the CS and, to some extent, the CP. There is nothing particularly new or noteworthy about this set included here but it is necessary to describe it for completeness.

The four basic management tools are: **Identity**, **Linking**, **Matching** and **Difference**. This selection is supportable as a logical set of functions but its makeup may be arbitrary in some respects. There could be other breakdowns, but these four are used here both for constructing logical thought and performing other system management action of the CS.

Identity: This is a tool that creates a fundamental object concept of something you perceive. The concept is then further defined by links to characteristics.

Linking: This tool would link concepts with one another for object concepts, location models or templates.

Matching: This tool would evaluate two or more objects for similarity.

Difference: This tool would evaluate the differences found between two or more concepts by comparing them and linking them into appropriate sets.

For this AI model, these tools form the fundamental building blocks used by the CS Program. In part, this assertion is justified because any general abstract mental task can be broken down into some combination of these basic functional actions. It is also possible to see very distinct parallels between these basic functions and the corresponding first abstract abilities that appear in developing children. It is probably no coincidence that these functions (identity, linking, matching, and difference) play a fundamental role in most standardized intelligence tests.

6. DEVELOPING COMPLEX CAPABILITIES

While the CP manages actions, it is not the reasoning function. The CS manages the linking structure of the brain and provides the framework in which the actions can occur. It builds the action templates, the behavior models and the location models. These arise from sensor inputs and, more importantly, from instructive input.

The CS also has the capability to establish a temporary representative linking structure for the object concepts based on the input data itself and comparisons between concepts. Read a novel and your CS creates location models based on what the author describes. It can even proceed with analysis based upon a presumed, or temporary, set of links. This would occur, for example, when directed by a teacher to perform a new specific action.

The CS is always running in the background to create links. Beyond that, however, I must emphasize that the CS is not exactly a free-wheeling process. Like all other mental activity it must be triggered by a motivation. In that regard it is subordinate to the CP. Whether the motivation is an instructor's command or an internally-driven motivation such as boredom, it is

only by consent of the CP that the CS can perform analytic functions or "test" action templates.

6.1. Difference between CS and CP

In this model the CP controls action by activating established templates. The CS controls reasoning by a tentative or limited activation (often without connection to outputs) of a template that is in the developmental stage. The prototype templates consist of temporary action templates and location models, complete with the object and behavior model connections. The CS undertakes control of a portion of the processor for the limited execution of the template. Action can be either executed or shunted to a register of projected action as controlled by the CS. The CS then reviews actual or projected results for effect on the AI system.

In some regards we may be tempted to design a system where the CP and the CS are one and the same. You can use almost the same software to run both. However, in software terms, the CP must control the "operating environment" while the CS controls the memory structure and the "development environment". Attempts to design an AI system that combines the two functions of the CS and the CP in a single process are almost certain to fail. It is mandatory that while the actual software could overlap, the functionality must be separated in a carefully conceived architecture.

Reasoning skills of the CS depend upon access to an adequate database of information, either memory links or input data. That is, after all, the only way it can actually build a prototype template. Perhaps the preferred method would be to use an existing template and make some modifications. The acquisition of data and the training can be achieved by either external instruction or by internally controlled responses to external inputs.

In the instructional case the input and direction, especially link associations, will be explicitly provided by someone or something else, to be assimilated by your brain. Internally controlled development is driven by the whims of nature and the motivations of the individual.

I would suggest that as the biological system passes from its developing stages into a state of more routine operations, the use of this CS would be reduced to identifying familiar locations and habitual behavior patterns associated with them. The biological system will have established preferred linking structures for many input-motivation-result-action sequences and would not require the services of the CS to evaluate alternate linkages. It will have a set of location models and actions that satisfy its needs.

This will lead to a decline in the reasoning skill. The links will diminish without use and the system will function primarily in established behavior patterns. The obvious alternative is that a system motivated, either internally or externally, to continue using the CS program to develop new action concept templates will remain more capable. Thus we can understand the

importance, at least in humans, of providing new mental challenges following maturity.

6.2. Training

We can make a minor departure from the biological process that simplifies the AI learning in a structured environment where the trainer can specify exactly what the system must learn. As a programmer we can take a short cut by directing the “link values” for a concept. This would emulate a lengthy training period that produces strong links in order to reduce training time. There would still be training sessions but repetitions to produce high link values would be unnecessary (Hibbard 2004).

It may seem logical to expand this approach to the point of making “modular” action concept templates that could be separately developed and integrated into an AI as single units. I would not categorically reject this thought. However, many links in a template specifically depend on the Frame of Reference. If these are incorrectly or incompletely produced then the results could be less effective or, worse, could be destructive.

If we have a “simplified learning” mode it must be controlled by an instructor to mimic the result of repeated exercises by establishing high link values at the outset.

7. INTELLIGENCE IS PREDICTIVE – NOT REACTIVE

Now we have come to one the core principles of intelligence. This is one of the most important features of the brain’s architecture.

The intelligent brain creates a behavior model of every object in its memory data base. This model is attached to each object and provides a prediction function for that object. This is not just a passive prediction. The behavior model includes, quite importantly, the object’s responses to your actions. For every object concept there will be an associated model that predicts behavior for that object, either as an individual or general class.

You may expect this to be a complicated process and very difficult to explain; however, it is actually rather straightforward and a relatively simple process if you accept the functional model defined for the brain up to this point in this paper.

The key element is what I would call the backbone of your mental structure. That would be the motivation-action process managed by the CP. The sensor detection of an object activates a motivation and the CP assigns a responsive action.

To create each behavior model, the brain uses this self-contained function to simulate the behavior it expects from other entities.

7.1. Behavior Models

The predictive model for each object is merely a brief, simplified version of this larger AI model—in essence it is a modified copy of your own mental process. It is

created for every object and tailored to the perceived actions of that object.

The CS creates and executes a model for each object and its predicted behavior in a simple and straightforward way. It establishes a set of input, motivation, action linkages that represent the way it perceives that object to respond to its environment. Each model functions identically to your own biological mental process. The examples below will help explain that idea.

I would suggest that, for simplicity, there are three general types for the predictive model, based on specific characteristics. The processes for all three are much the same and these three model types differ only in the way we might perceive them.

7.1.1. Human-Equivalent Behavior Model

The first, and most involved, would be the Human Equivalent Model. This model is a copy of your own motivation-action concept structure. It can be applied just as it exists in your own mind but usually it is modified based upon learned data you have for the object involved. You may add a motivation, add an action, or change a priority link. Obviously we can apply it to other humans. In addition, we often extend this model to animals. In this case it is tailored to remove a portion of motivations and actions. However, children are particularly prone to use the complete model to define animal behavior.

7.1.2. Instruction Manual Behavior Model

The second type is the Instruction Manual Model. This simplified model replaces the sensor inputs with basic physical inputs, such as pushing a button, turning a knob, or manipulating some mechanical aspect of an object. This model provides defined results from the specific mechanical interactions, either by you or some other object. The obvious application of this type of model is for mechanized objects but you can apply it to a wider range of items.

7.1.3. Physics Model

The third is the Physics Model. This model generally provides action-reaction links and may be somewhat complex depending upon the types of objects being addressed. For physical objects in your environment the model will include responses to natural forces as well as your interaction with them (responses to pushing, kicking, sliding, etc.). In the physics model, motivation concepts are replaced by physical laws (e.g., an object is “motivated” to fall toward the earth because it “detects” the force of gravity); otherwise the predictive model is the same as your own mental process.

Remember, the behavior characteristics are based upon the way you interact with them as well as external forces. For example, if you push on the object, does it move? This is tied to a perception of relative mass. The Physics Model incorporates the physical characteristics of each object. That is to say, once you identify the relative mass of an object (whether by touching or by

visual clues) you can project, using a physics model, responses to physical interaction. This is one reason children are always messing with things. They are constructing their models of all of those objects around them.

As a simple example, you see someone holding an object in their hand. You can predict what will happen when they release it simply based on the model you have attached to that object. You do not need to analyze the situation; you simply run an existing model. You identify that object by sight and you have a predictive model linked to that object concept in your memory.

Let's say you perceive the object to be a rock. Your predictive model says that the object, when released will fall to the ground under the influence of gravity. Alternatively, you perceive the object to be a paper airplane. Your predictive model says that it will glide away when released. If you perceive the object to be a live bird, then it should fly away. And, finally, you may perceive the object to be a balloon with yet another prediction of what happens to it when released.

7.2. Building Models

The learning process allows you to build this predictive model of any object you encounter. For example, children learn that dogs are motivated to chase and retrieve a thrown object, a very simple template of motivation and action to create in a child's mind. That and other functions are incorporated in the concept of a dog. As the learning base is expanded the child learns that observable characteristics of the dog can be used to distinguish different behavior models for different dogs. Then, whenever you see a dog you predict its behavior based on the model. You will have sub-groups of the model based on individual types of dogs or physical appearance. The model will tell you that if you approach the dog and try to interact with it there will be an expected response. For example, growling equals aggression (triggering a danger motivation); tail wagging equals friendliness, and so forth.

Now, moving to the highest level of complexity, you will have a model of behavior for other humans. You will likely have a generic model that would be applied to any new acquaintance. This could closely match your own behavior algorithms. Then, for each individual, the model will be tailored based upon what you have observed from that individual.

You will also develop secondary models for individuals based on secondary characteristics. These you likely know as stereotypes. You meet someone in a business suit and you link them to a generic "businessman" model. You meet someone with dirty, shabby clothes and you link them to the "bum" model. When someone says: "I can't believe he just did that," it means that some behavior did not correspond to a model. As you witness a person's behavior your own CS function will refine the model.

One important offshoot of the predictive model is that we take the output of each model—the action that is expected of the object—and link that back to our own

structure of inputs and corresponding motivations. Thus when you interact with someone or something that can affect you through their action, you are then motivated to create an input to that object that produces a desired action—something that would satisfy a motivation within your own structure. This produces the results seen in many social and business interactions.

7.3. Relation to Intelligent Agents

There are many efforts to develop Intelligent Agents. These are, by definition, autonomous and self-contained intelligent units that can take action on their own and/or provide information to a higher level entity.

One of the most complete descriptions of intelligent agents is provided in Artificial Intelligence, a Modern Approach (Russell and Norvig 1995). There are a variety of types of agents described but they share some general features for using sensor data and behavior models to produce intelligent behavior.

I would suggest that, within the protocol structure offered here, the intelligent agent represents a sub-set of sensor links, behavior models, and actions. All objects are created and maintained in a single action structure (rather than linked from a reference base.) The decision rules are created for limited scenarios and updated with observed inputs. Perhaps the biggest differential, however, is that there is a single management function that executes direct control and decision authority.

That said, it should still be possible to reconcile the differences in order to incorporate intelligent agents into this type of architecture.

8. VISUAL PROCESSING AND PREDICTION

At this point the discussion concludes by returning to something that was partly covered before. Re-consider the dynamic nature of your visual input. How do you handle the constantly changing tableau of images that your system must process? This is perhaps the most difficult part of the brain function to understand. Though it is sometimes presumed, there is not a recurring analysis of a scene. A basic tenet here is that the brain works from stored memory concepts with augmented short-term data from sensors. Any object we sense around us is identified based on an array of knowledge. Furthermore, this is always a presumptive identification, though sometimes this is a near certainty.

This is where the location models and the behavior models come together for mutual support. They are linked together through the object concepts contained in a location.

Once we identify a location and associated objects, the subsequent visual processing is determined by any motivations and the predictive model we have for the associated objects. An object could be of great interest, meaning it is one whose outputs can benefit (or harm) our system. In that case the brain will perform continual updates of the predictive behavior analysis, evaluating the impact to our system. Note that this is a behavior analysis not a visual analysis. On the other hand miscellaneous objects of no direct interest are

summarily identified and receive a prediction, e.g., that picture on the wall will stay right there.

The background of the location is defined based on the location model and it is that stored memory concept we use until something changes. Until routine objects depart from the predicted behavior there is little visual processing to be done. Background objects, such as trees, are identified primarily by “field data.” That is to say we do not use explicit visual processing algorithms if they fit the background structure of our location model. Motivations can, of course, change all that. After all we could be looking for a specific kind of tree.

The impact of this analysis structure is to drastically reduce the demand for processing power because it is no longer necessary to perform the extensive scene-by-scene visual processing. Those cars passing by you on the highway are one of the best examples. You identify them summarily and use a standard memory object. You only care about them if they divert from the predicted pattern in such a way as to be a threat to you. A beginning driver, who is still in the process of completing the predictive models for all these new objects, is flooded with information. That new driver must learn to focus attention and that does not happen until a reliable set of predictive models are formed.

9. OTHER USES OF LOCATION MODELS

There is an adjunct to the use of location models that shows a possibility for understanding how we construct and use sentences to communicate with each other. If true, this would have a significant impact on other aspects of AI and communication dynamics.

Within the framework of this architecture we could reasonably believe that sentences, whether spoken or written, could communicate their thought by the creation of a temporary location model in the receiver, especially when you consider the additive nature of a conversation or string of sentences.

This process would also allow one to identify and resolve conflicts in a sentence. If, following a statement, your location model is not incomplete or has ambiguities. You would seek to resolve the ambiguity by asking for more exact information, but only if you are motivated to do so. If you have no interest in the subject then you might have no reason to seek resolution.

This use of location models also leads to an understanding of some forms of humor. When someone is telling a joke you are building a location model to match their narrative. At the conclusion of the joke, you discover that your model was not the same as the one the narrator finally revealed. At that point the intention is that you find it funny, though that is not guaranteed.

This use of location models for understanding sentence structure deserves further consideration. The concept does appear to be compatible with the architecture and supports the other aspects of interactions involving this AI protocol.

10. SUMMARY

What is shown in this paper is both a Functional Architecture and an Integration Protocol. We have defined the modular components of the system, their functions, and interfaces. This protocol will enable coordinated individual development of the fundamental components of a system that can be integrated in a dynamic environment. As long as a strict motivational structure and frame of reference are maintained the components can be remotely connected to form a single intelligence.

The greatest strength of this architecture, beyond its internal consistency, is that individual development teams could be assigned to produce defined components. As long as functional interfaces are controlled the pieces could be integrated to work as a single entity. Conversely, if one attempts to cut out portions of this architecture and splice them into other kinds of systems, the results are likely to be disappointing.

For a potential application, imagine if you will a system that would integrate large numbers of different types of sensors in such a way that many objects can be controlled or addressed by a single entity, without the need for external coordination among separate systems. This can be applied to a range of operations from business to battlefield.

REFERENCES

- Adams, Keith and Agesen, Ole (2006) A Comparison of Software and Hardware Techniques for x86 Virtualization, VMWare, ASPLOS'06 Oct 21–25
- Hibbard, B. 2004. Reinforcement learning as a Context for Integrating AI Research. Presented at the 2004 AAAI Fall Symposium on Achieving Human-Level Intelligence through Integrated Systems and Research.
- Minsky, Marvin *The Emotion Machine*. New York, NY: Simon & Schuster
- Russell, S. J. and Norvig, P (1995) *Artificial Intelligence: A Modern Approach*. New Jersey: Prentice Hall

AUTHOR'S BIOGRAPHY

The author is an engineer who has been successful in a related area of satellite system architecture and development though not directly involved in the academic AI world. **Bruce Toy** boasts a 40-year career as an engineer primarily in the development of large-scale systems and supporting infrastructure. He received a BS in Physics from UNC and an MSEE from AFIT. He is a retired USAF officer with experience in ballistic missile defense as well as satellite design and development. The AF career was followed by 20 years in private industry, primarily with Lockheed Martin, where he became a respected systems engineer and systems architect for complex integration activities. He is currently semi-retired and living in Florida.

A NEW PRACTICAL APPROACH TO ASSET LIABILITY MANAGEMENT FOR BASEL III AND SOLVENCY II

Vojo Bubevski

Bubevski Systems & Consulting™
TATA Consultancy Services™

vojo.bubevski@landg.com

ABSTRACT

A new practical approach to Asset Liability Management (ALM) is proposed, which combines Monte Carlo Simulation, Optimisation and Six Sigma Define, Measure, Analyse, Improve, Control (DMAIC) methodology. This new method determines an optimally diversified minimal variance investment portfolio, which gains a desired range of return with minimal financial risk. Simulation and optimisation are conventionally applied to find the optimal portfolio to provide the required return. In addition, the Six Sigma DMAIC methodology is used to measure and improve the portfolio management process in order to establish the optimally diversified portfolio. Applying Six Sigma DMAIC to the portfolio management process is an improvement in comparison with conventional stochastic ALM risk models. It offers financial institutions internal model options for Basel III and Solvency II, which can help them to reduce their capital requirements and Value-at-Risk (VaR) providing for higher business capabilities and increasing their competitive position, which is their ultimate objective.

Keywords: Asset Liability Management; Portfolio Optimisation – Minimal Variance; Monte Carlo Simulation; Six Sigma DMAIC; Basel III; Solvency II.

1. INTRODUCTION

Basel III is a comprehensive set of reform measures, developed by the Basel Committee on Banking Supervision, to strengthen the regulation, supervision and risk management of the banking sector. These measures aim to: i) improve the banking sector's ability to absorb shocks arising from financial and economic stress, whatever the source; ii) improve risk management and governance; and iii) strengthen banks' transparency and disclosures (Atkinson and Blundell-Wignall 2010; BCBS 2010a; BCBS 2010b; BCBS 2011; BIS 2011; Cosimano and Hakura 2011).

Solvency II is designed to introduce a harmonised insurance regulatory regime across European Union (EU) that will protect policyholders and minimise market disruption. The regulation sets stronger

requirements for capital adequacy, risk management and disclosure. Primarily this concerns the amount of capital that EU insurance companies must hold to reduce the risk of insolvency. Solvency II is an EU Directive, which needs to be approved by the European Parliament, and will be scheduled to come into effect on 1 January 2014 once it is approved (Cruz 2009; Bourdeau 2009; GDV 2005; SST 2004).

The economic capital of financial institutions is one major aspect of Basel III and Solvency II. According to a research by Mercer Oliver Wyman, the impact of the Asset Liability Management (ALM) risk, i.e. Market Risk, on the economic capital of banking and insurance companies is 64%. This is by far the largest impact compared to other quantifiable risk factors, e.g. 27% Operational Risk, 5% Credit Risk, and 4% Insurance Risk. Consequently, this paper will focus on ALM.

ALM has originated from the duration analysis proposed by Macaulay and Redington (Macaulay 1938; Redington 1952). Subsequently, ALM has evolved in a powerful and integrated tool for analysis of assets and liabilities in order to value not only the interest rate risk but the liquidity risk, solvency risk, firm strategies and asset allocation as well (Bloomsbury 2012).

The new regulation requirements introduced by Basel III and Solvency II focus on the solvency risk in order to impose a required amount of equity value on the base of the risk associated to the investments of asset portfolio. The banking and insurance industry are responding to these requirements by developing internal models based essentially on the Value-at-Risk (VaR), parametric (GARCH, EGARCH) and simulation (Monte Carlo) models, extended to Conditional Value-at-Risk (CVaR) and Copulas.

Some financial institutions extended the analysis to the cash flows by using a stress testing to generate different scenarios. In this case it is possible to analyse how the cash flows can evolve to study a strategy to hedge the risk exposure.

The financial institutions with greater equity value have the possibility to invest in riskier assets focussed on the portfolio insurance. The basic idea is to construct a Put option on the value of asset portfolio by taking a long position on the risky assets and on the default-free bonds such that their weight will be rebalanced

dynamically, which will replicate the value of a portfolio of risky assets with a protective Put option.

The frontier of Asset and Liability Management is based on stochastic optimisation and simulation models that involve an asset allocation approach by considering the liabilities side as well.

Another major aspect of Basel III and Solvency II is Financial Risk Management. Jorion, in his book for financial risk management, presented the utilisation of Monte Carlo Simulation for options' valuation and VaR calculation. He also generally elaborated on Optimal Hedging applying Optimal Hedge Ratio, i.e. the minimal variance hedge ratio. In addition, he specifically described the application of Optimal Hedging in two important cases such as Duration Hedging and Beta Hedging (Jorion 2011).

Advanced Financial Risk models involve optimisation of investment portfolios. The problem of asset allocation for portfolio optimisation was solved by Markowitz in the 1950's. Markowitz applied his mean-variance method in order to determine the minimum variance portfolio that yields a desired expected return (Markowitz 1952; Markowitz 1987).

Also, advanced Financial Risk models are stochastic and use Monte Carlo Simulation. A comprehensive elaboration on general applications of Monte Carlo Simulation in Finance was published by Glasserman (2004). Specifically, an internal Monte Carlo Simulation model for Solvency II (i.e. an ALM – Market Risk simulation model) was presented by Bourdeau (Bourdeau 2009).

Today, Six Sigma is recognized across industries as a standard means to accomplish process and quality improvements in order to meet customer requirements and achieve higher customer satisfaction. One of the principal Six Sigma methodologies is Define, Measure, Analyse, Improve, Control (DMAIC). Six Sigma applications in finance at introductory level were published by Stamatis (Stamatis 2003).

This paper presents a new practical approach to the ALM risk models for Basel III and Solvency II, i.e. the Optimisation-Simulation-DMAIC method. The new method combines Optimisation, Monte Carlo Simulation, and Six Sigma DMAIC methodology. It determines an optimally diversified minimal variance investment portfolio, which gains a desired range of return with minimal financial risk. Optimisation and Simulation are conventionally applied to find the minimal variance portfolio to provide the required return. In addition, the Six Sigma DMAIC methodology is used to measure and improve the portfolio management process in order to establish the optimally diversified portfolio.

Applying Six Sigma DMAIC to the portfolio management process is an improvement in comparison with the conventional stochastic optimisation and simulation ALM risk models. It offers financial institutions internal model options for Basel III and Solvency II, which can help them to reduce their capital requirements and VaR providing for higher business

capabilities and increasing their competitive position, which is their ultimate objective.

In order to facilitate this presentation, a very simple ALM risk model is used to demonstrate the method. Only the practical aspects of the ALM risk modelling are discussed. Microsoft™ Excel® and Palisade™ @RISK® and RISKOptimizer® were used in the demonstration experiments.

1.1. Related Work

1.1.1. ALM

Mitra and Schwaiger edited a book which brings together state-of-the-art quantitative decision models for asset and liability management in respect of pension funds, insurance companies and banks. It takes into account new regulations and industry risks, covering new accounting standards for pension funds, Solvency II implementation for insurance companies and Basel II accord for banks (Mitra and Schwaiger 2011).

In addition, Adam published a comprehensive guide to Asset and Liability Management from a quantitative perspective with economic explanations. He presented advanced ALM stochastic models for Solvency II and Basel II & III using optimisation and simulation methodologies (Adam 2007).

1.1.2. Six Sigma

Hayler and Nichols showed how financial giants such as American Express, Bank of America, and Wachovia have applied Six Sigma, Lean, and Process Management to their service-based operations by providing specific, real-world examples and offering step-by-step solutions (Hayler and Nichols 2006).

Also, Tarantino and Cernauskas provided an operational risk framework by using proven quality-control methods such as Six Sigma and Total Quality Management (TQM) in financial risk management to forestall major risk management failures (Tarantino and Cernauskas 2009).

2. ALM BY USING THE OPTIMISATION-SIMULATION-DMAIC METHOD

The following sections demonstrate the new method's procedure step-by-step for ALM Risk modelling. Actual financial market data are used in the presentation.

2.1. Problem Statement

The following is a simplified problem statement for the demonstrated ALM risk model.

Determine the optimally diversified minimum variance investment portfolio that yields a desired expected annual return to cover the liabilities. The model should allow the financial institution to reduce their capital requirements and VaR providing for higher business capabilities and increasing their competitive position. The model should help the company to achieve their ultimate objective.

2.2. Calculating Compounded Monthly Return

The monthly returns of four stocks are available for a period of seven years, i.e. 1990-1996 (Table 1). Note that the data for the period July/1990- June/1996 are not shown.

Table 1: Monthly Return (MR)

Month	Stock1	Stock2	Stock3	Stock4
Jan/1990	0.048	-0.01	-0.06	-0.01
Feb/1990	0.066	0.096	0.037	0.038
Mar/1990	0.022	0.022	0.12	0.015
Apr/1990	0.027	-0.04	-0.02	-0.04
May/1990	0.112	0.116	0.123	0.075
Jun/1990	-0.02	-0.02	-0.04	-0.01
Jul/1996	0.086	-0.07	-0.12	-0.02
Aug/1996	0.067	0.026	0.146	0.018
Sep/1996	0.089	-0.03	-0.04	0.092
Oct/1996	0.036	0.117	0.049	0.039

The Compounded Monthly Return (CMR) is calculated for each month and each stock from the given stock Monthly Return (MR) using the following formula (Table 2):

$$CMR = \ln(1 + MR)$$

Table 2: Compounded Monthly Return (CMR)

Month	CMR1	CMR2	CMR3	CMR4
Jan/1990	0.047	-0.01	-0.06	-0.01
Feb/1990	0.063	0.092	0.036	0.038
Mar/1990	0.021	0.022	0.113	0.015
Apr/1990	0.027	-0.04	-0.02	-0.04
May/1990	0.106	0.11	0.116	0.073
Jun/1990	-0.02	-0.02	-0.04	-0.01
Jul/1996	0.082	-0.07	-0.13	-0.02
Aug/1996	0.065	0.026	0.136	0.018
Sep/1996	0.085	-0.03	-0.04	0.088
Oct/1996	0.036	0.111	0.048	0.038

2.3. Fitting Distributions to Compounded Monthly Return

For the Monte Carlo method, we need the distribution of the compounded monthly return for each stock. Thus, for each stock, we determine the best fit distribution based on the Chi-Square measure. For example, the best fit distribution for the compounded monthly return of Stock 4 (i.e. CMR4) is the normal distribution, with Mean Return of 0.6% and Standard Deviation of 4.7%, presented in Figure 1.

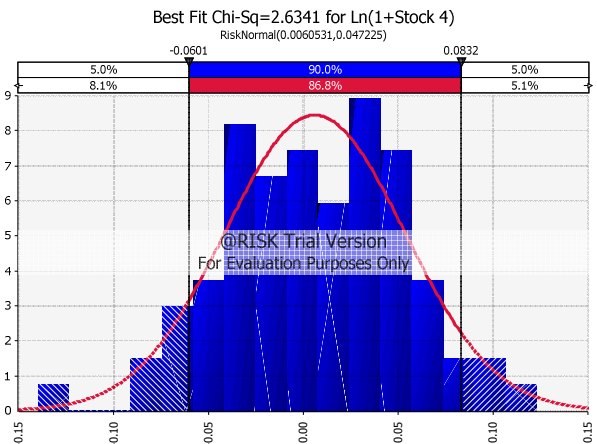


Figure 1: Stock 4 Best Fit Distribution

2.4. Finding Compounded Monthly Return Correlations

The compounded monthly returns of the stocks are correlated. We need to find the correlation to allow the Monte Carlo method to generate correlated random values for the compounded monthly returns. The correlation matrix is presented in Table 3.

Table 3: Correlation Matrix

	CMR1	CMR2	CMR3	CMR4
CRM 1	1	0.263	0.038	0.0868
CRM2	0.263	1	0.244	0.0895
CRM3	0.038	0.244	1	0.095
CRM4	0.087	0.089	0.095	1

2.5. Generating Compounded Monthly Return

The Compounded Monthly Return (CMR) is randomly generated for each stock from the best fit distribution considering the correlations. The following distribution functions of the Palisade™ @RISK® are used:

$$CMR1 = RiskLogistic(0.0091429, 0.044596)$$

$$CMR2 = RiskLognorm(1.1261, 0.077433, Shift(-1.1203))$$

$$CMR3 = RiskWeibull(6.9531, 0.46395, Shift(-0.42581))$$

$$CMR4 = RiskNormal(0.0060531, 0.047225)$$

The correlation is applied by using the “RiskCorrmat” function of the Palisade™ @RISK®.

2.6. Calculating Compounded Annual Return by Stock

The Compounded Annual Return (CAR) is calculated for each stock from the respective Compounded Monthly Return (CMR), using the following formula:

$$CAR = 12 * CMR$$

2.7. Calculating Expected Annual Mean Return on the Portfolio

The expected annual mean return on the portfolio (*EAR-Mean*) is calculated from the asset allocation weights vector (*Weights-V*) and the vector of compounded annual returns of stocks (*CAR-V*) by using the following Excel® formula:

$$EAR-Mean = SumProduct(Weights-V, CAR-V)$$

2.8. Calculating Variance, Standard Deviation and VaR of the Portfolio

The variance, standard deviation and VaR (VaR is calculated at Confidence Level of 99.95%) of the portfolio are calculated from the distribution of the expected annual mean return of the portfolio (*EAR-Mean*) by using the following Palisade™ @RISK® functions:

$$Variance = RiskVariance(EAR-Mean)$$

$$Standard-Deviation = RiskStdDev(EAR-Mean)$$

$$VaR = RiskPercentile(EAR-Mean, 0.005)$$

2.8.1. Portfolio Simulation and Optimisation

Palisade™ RISKOptimizer® is used to solve the portfolio simulation and optimisation problem. That is to find the minimal variance portfolio of investments, which yields sufficient return to cover the liabilities. Thus, the aim of the simulation and optimisation model is to minimise the variance of the portfolio subject to the following specific constraints:

- The expected portfolio return is at least 9%, which is sufficient to cover the liabilities;
- All the money is invested, i.e. 100% of the available funds is invested; and
- No short selling is allowed so all the fractions of the capital placed in each stock should be non-negative.

The model should also calculate the Standard Deviation and VaR of the portfolio.

2.8.2. Measuring Performance of the Portfolio

Palisade™ @RISK® has Six Sigma capabilities, thus it is used to simulate the optimal portfolio found above and calculate the Six Sigma metrics from the simulation distribution in order to measure the performance of the optimal portfolio. For this purpose the following Six Sigma parameters are specified:

- Lower Specified Limit (LSL) of the expected portfolio return is 5%;
- Target Value (TV) of the expected portfolio return is 9%;
- Upper Specified Limit (USL) of the expected portfolio return is 15%;

The simulation model calculates the following Six Sigma process capability metrics to measure the

performance of the investment process: i) Process Capability (*Cp*); Probability of Non-Compliance (*PNC*); and Sigma Level (σL). The following Palisade™ @RISK® functions are used:

$$Cp = RiskCp(EAR-Mean)$$

$$PNC = RiskPNC(EAR-Mean)$$

$$\sigma L = RiskSigmaLevel(EAR-Mean)$$

2.8.3. Sensitivity Analysis of the Portfolio

The next step is to calculate (quantify) the impact of the investment in every stock to the portfolio mean return, by using the sensitivity analysis features of Palisade™ @RISK®. This calculation is stochastic and it is based on the statistics of the simulation distribution.

From the calculated correlation coefficients, the stock on which the portfolio return is most dependent can be determined. In addition, the calculated regression mapped values show how the portfolio mean return is changed in terms of Standard Deviation, if the return of a particular stock is changed by one Standard Deviation.

The sensitivity analysis is used in order to determine how to improve the performance of the investment process, i.e. which stocks should be hedged to reduce the financial risk of the portfolio.

2.8.4. Simulating the Hedged Portfolio

Six Sigma Simulation is used again to simulate and measure the performance of the hedged portfolio. The Six Sigma parameters specified for this simulation are the same as in Sec. 2.8.2. Also, the model calculates the Six Sigma process capability metrics to measure the performance of the investment process as presented in Sec. 2.8.2.

2.8.5. Comparing Results and Quantifying Improvements

The final step is to compare the simulation results of the initial optimal portfolio with the hedged portfolio and quantify the improvements from three aspects, portfolio return, financial risk and investment process capability.

To quantify the improvements, the following results are compared: i) Expected Annual Return – Mean (*EAR-Mean*) for portfolio return; ii) Variance, Standard Deviation and Value-at-Risk (VaR) for financial risk; and iii) Process Capability (*Cp*), Probability of Non-Compliance (*PNC*), and Sigma Level (σL) for investment process capability.

3. RESULTS AND DISCUSSION

3.1. Portfolio Simulation and Optimisation

The optimal portfolio found by the simulation and optimisation model has the following investment fractions: 28.6% in Stock 1; 0.7% in Stock 2; 28.5% in Stock 3; and 42.2% in Stock 4. The Portfolio Return

was 9% with Variance of 22.9%, Standard Deviation of 47.8% and VaR of -19.7%.

The probability distribution of this optimal portfolio is given in Figure 2.

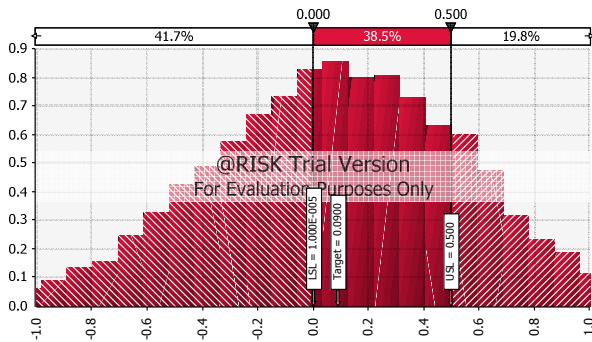


Figure 2: Portfolio Probability Distribution

The confidence levels were the following. The probability that the portfolio return will be below zero (0%), i.e. negative, is 41.7%. There is a 38.5% probability that the return will be in the range of 0%-50%, and 19.8% probability that the return will be greater than 50%.

3.2. Measuring the Portfolio Performance

The performance of the optimal portfolio found above was measured with a Six Sigma simulation model. It should be noted that the optimal portfolio found above is simulated; thus, the investment fractions for this simulation model are the same, i.e.: 28.6% in Stock 1; 0.7% in Stock 2; 28.5% in Stock 3; and 42.2% in Stock 4. The following Six Sigma parameters were specified: i) LSL = 5%; ii) TV = 9%; iii) USL = 15%.

The Portfolio Return was 9%, Variance 22.9%, Standard Deviation 47.8% and VaR -23%. These figures suggest that the financial risk for the optimal portfolio is significant.

The probability distribution of the optimal portfolio Six Sigma simulation is shown in Figure 3.

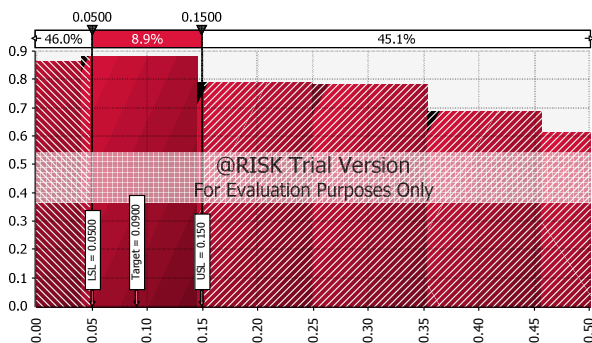


Figure 3: Portfolio Performance Distribution

The confidence levels were as follows. The probability that the portfolio return will be below 5% (i.e. below LSL) is 46%. There is an 8.9% probability that the return will be in the range of 5%-15% (i.e.

within the desired target range), and 45.1% probability that the return will be greater than 15% (i.e. above USL).

The Six Sigma metrics (i.e. the investment process capability metrics) of the optimal portfolio is shown in Table 4.

It is easy to draw the conclusion by using the Six Sigma *Probability of Non-Compliance (PNC)* metric of the process. The PNC metric determines the total probability that the portfolio return distribution will deviate from the desired specified limits. The PNC equals 0.9112, which is an extremely high probability.

Also, Cp and Sigma Level are very low, i.e. 0.0348 and 0.1115, which indicates a poor performance.

Table 4: Investment Process Six Sigma Metrics

Process	Cp	PNC	Sigma Level
Optimal Portfolio	0.0348	0.9112	0.1115

The significant financial risk and the poor performance of the optimal portfolio presented above strongly suggest that this portfolio is not acceptable. Therefore, the portfolio should be improved by hedging for example.

3.3. Sensitivity Analysis

The sensitivity analysis was used in order to determine how to improve the performance of the investment process, i.e. how to hedge the portfolio.

The correlation sensitivity graph is given in Figure 4. The graph shows that the portfolio return is most dependent on the return of Stock 4 with a correlation coefficient of 0.77. The other three stocks, i.e. Stock 3, Stock 2 and Stock 1, are less influential with correlation coefficients of 0.49, 0.46 and 0.43 respectively.

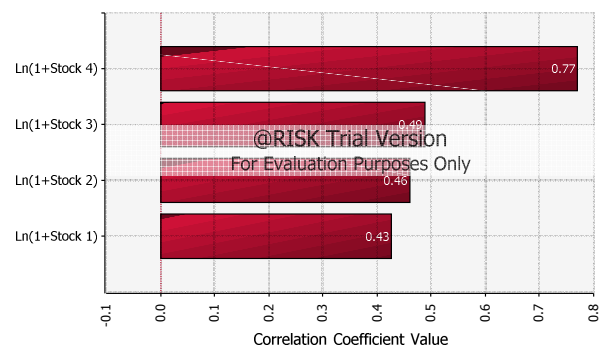


Figure 4: Correlation Sensitivity

The regression sensitivity graph is given in Figure 5. This graph shows how the portfolio mean return is changed in terms of Standard Deviation, if the return of a particular stock is changed by one Standard Deviation.

Therefore, this graph shows that if Stock 4 return is changed by one Standard Deviation, the portfolio return will be changed by 0.313 Standard Deviations (i.e. the regression mapped value is 0.313 for Stock 4). Again,

the other three stocks, i.e. Stock 3, Stock 1 and Stock 2, are less influential as their regression mapped values are 0.163, 0.141 and 0.108 respectively.

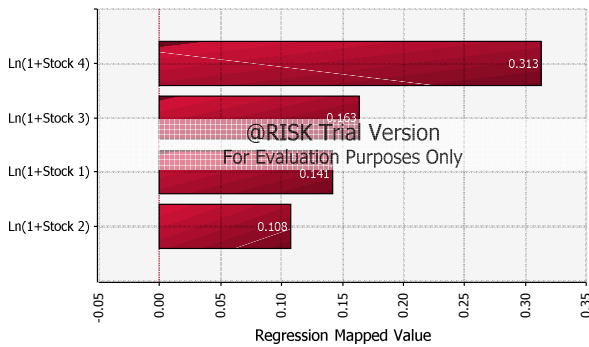


Figure 5: Regression Mapped Values Sensitivity

The conclusions of this sensitivity analysis suggested that the portfolio can be hedged for example if Stock 4 is replaced with an option of Stock 4.

3.4. Option 4 Return Data and Distribution

A part of the market data for Option 4 (i.e. an option of Stock 4) are shown in Table 5, i.e. the Monthly Return (MR) and the calculated Compounded Monthly Return (CMR) of the option. The Average CMR is 0.61% and the yearly return is 7.28%.

Table 5: Option 4 MR and CMR

Month	MR	CMR
Jan/1990	0	0
Feb/1990	0.038	0.038
Mar/1990	0.015	0.015
Apr/1990	0	0
Jul/1996	0	-0
Aug/1996	0.018	0.018
Sep/1996	0.092	0.088
Oct/1996	0.039	0.038

The best fit distribution to Option 4 CMR is shown on Figure 6.

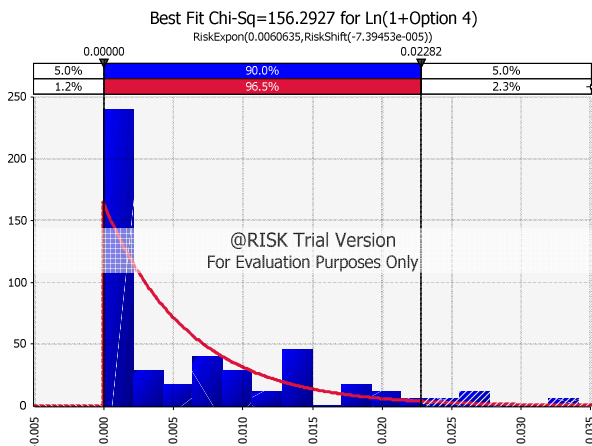


Figure 6: Option 4 Best Fit Distribution

3.5. The Hedged Portfolio Simulation

The performance of the hedged portfolio was measured with a Six Sigma simulation model. It should be noted that the Stock 4 was replaced with Option 4 (i.e. an option on Stock 4); thus, the investment fractions for this simulation model are: 28.6% in Stock 1; 0.7% in Stock 2; 28.5% in Stock 3; and 42.2% in Option 4.

The same Six Sigma parameters were specified: i) LSL = 5%; ii) TV = 9%; iii) USL = 15%.

The Portfolio Return was 9%, Variance 14.6%, Standard Deviation 38.3% and VaR -0.45%. These figures suggest that the financial risk was considerably reduced.

The probability distribution of the hedged portfolio Six Sigma simulation is shown in Figure 7. The confidence levels were as follows. The probability that the portfolio return will be below 5% (i.e. below LSL) is 44.4%. There is an 10.9% probability that the return will be in the range of 5%-15% (i.e. within the desired target range), and 44.7% probability that the return will be greater than 15% (i.e. above USL).

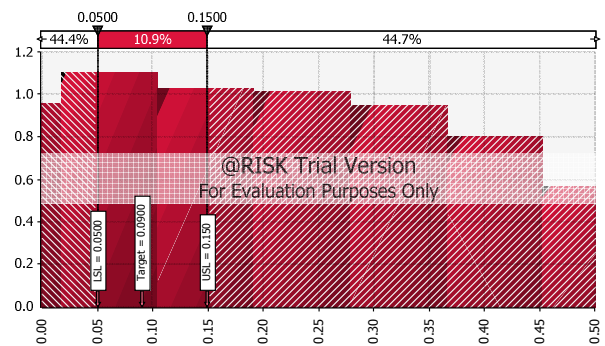


Figure 7: Hedged Portfolio Performance

The Six Sigma metrics (i.e. the investment process capability metrics) of the hedged portfolio is shown in Table 6.

Table 6: Hedged Portfolio Six Sigma Metrics

Process	Cp	PNC	Sigma Level
Hedged Portfolio	0.2176	0.5294	0.6289

Compared with the initial optimal portfolio performance, PNC was reduced from 0.9112 to 0.5294, Cp was increased from 0.0348 to 0.2176 and Sigma Level was increased from 0.1115 to 0.6289. Therefore, an important improvement was achieved with the hedged portfolio.

3.6. Sensitivity Analysis

This sensitivity analysis can be used in order to determine how to further improve the performance of the investment process, i.e. how to further hedge the portfolio. The correlation graph (Figure 8), shows that the portfolio return is most dependent on the return of

Stock 1 with a correlation coefficient of 0.72. The other two stocks and Option 4, i.e. Stock 3, Stock 2 and Option 4, are less influential with correlation coefficients of 0.67, 0.35 and 0.09 respectively.

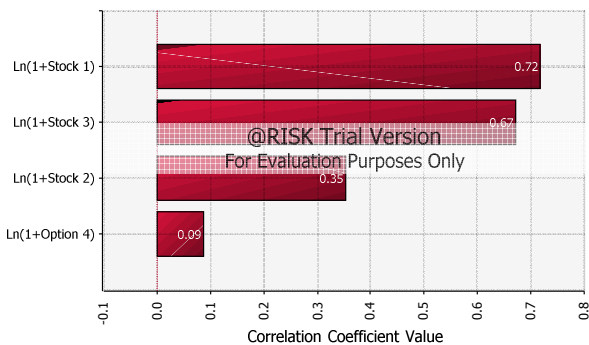


Figure 8: Hedged Portfolio Correlation Sensitivity

The regression sensitivity graph is given in Figure 9. This graph shows that if Stock 1 return is changed by one Standard Deviation, the portfolio return will be changed by 0.277 Standard Deviations (the regression mapped value is 0.277 for Stock 1). Again, the other two stocks and Option 4, i.e. Stock 3, Stock 2 and Option 4, are less influential as their regression mapped values are 0.251, 0.0065 and 0.0308 respectively.

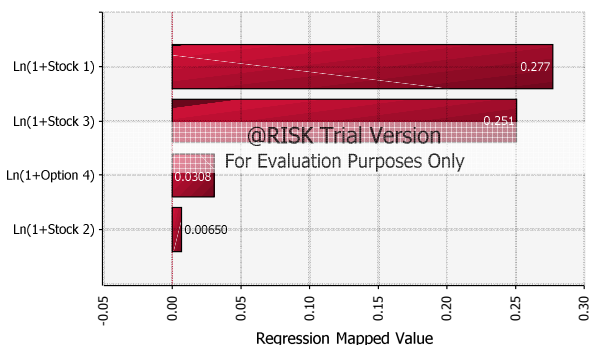


Figure 9: Hedged Portfolio Regression Mapped Values Sensitivity

The conclusions of this sensitivity analysis suggested that the hedged portfolio can be further improved (hedged) if Stock 1 is replaced with an option of Stock 1 for example.

It should be noted that this method is iterative and can be iteratively applied until an optimally diversified portfolio is established. Only the first iteration is presented in the paper.

3.7. The Method's First Iteration Results

The results of the first iteration of the method are presented and compared in this section. Table 7 shows the Mean Return, Variance, Standard Deviation and VaR of the initial optimal portfolio and the hedged optimal portfolio.

The hedged optimal portfolio was significantly better than the initial optimal portfolio. The mean return is 9% for initial and hedged portfolio but the financial

risk was considerably reduced by the hedged portfolio, i.e. i) Variance was reduced from 22.88% to 14.67%; ii) Standard Deviation was reduced from 47.84% to 38.30%; and iii) Value-at-Risk was reduced from 23.04% to only 0.45%.

Table 7: The Method's First Iteration Results

Portfolio	Mean Return	Variance	Standard Deviation	VaR
Initial	0.0900	0.2288	0.4784	-0.2304
Hedged	0.0900	0.1467	0.3830	-0.0045

The Six Sigma metrics of the first iteration is given in Table 8. The Six Sigma metrics for the hedged portfolio was also significantly improved. PNC was reduced from 0.9112 to 0.5294, Cp was increased from 0.0348 to 0.2176 and Sigma Level was increased from 0.1115 to 0.6289.

Table 8: The First Iteration Six Sigma Metrics

Process	Cp	PNC	Sigma Level
Initial Portfolio	0.0348	0.9112	0.1115
Hedged Portfolio	0.2176	0.5294	0.6289

3.8. The Optimisation-Simulation-DMAIC Method versus the Related Work

A simple comparison of the Optimisation-Simulation-DMAIC method, i.e. the new practical approach to ALM proposed in this paper, with the related work summarized in Sec. 1.1 is as follows.

3.8.1. ALM

The ALM models presented by Mitra and Schwaiger (Mitra and Schwaiger 2011) are advanced stochastic optimisation and simulation models. The ALM models published by Adam are also advanced stochastic models using optimisation and simulation (Adam 2007).

The presented Optimisation-Simulation-DMAIC model is by nature an advanced stochastic model applying optimisation and simulation, which is like the models presented in the related work. In contrast, the Optimisation-Simulation-DMAIC model uses Six Sigma DMAIC to measure and improve the portfolio management process in order to establish an optimally diversified (hedged) portfolio, which is an advantage.

3.8.2. Six Sigma

Hayler and Nichols presented applications of Six Sigma tools, e.g. Lean Six Sigma, to the financial service-based operations, which is related to the operational risk (Hayler and Nichols 2006). The work of Tarantino and Cernauskas is also related to the operational risk as they created an operational risk framework by applying Six Sigma to improve the financial risk management process from operational

point of view in general (Tarantino and Cernauskas 2009).

On the contrary, the Optimisation-Simulation-DMAIC model uses Six Sigma DMAIC in order to establish an optimally diversified (hedged) portfolio. This is a new concept as DMAIC is dynamically applied to specifically reduce the ALM Market Risk in an on-going investment portfolio management process.

4. CONCLUSION

This paper proposed a new practical and stochastic method, i.e. the Optimisation-Simulation-DMAIC method, for ALM risk modelling under Solvency II and Basel III. The method combines Optimisation, Monte Carlo Simulation and Six Sigma DMAIC methodologies in order to dynamically manage the financial ALM risk (i.e. the market risk) in an on-going investment portfolio management process. The new method applies the Markowitz's Mean-Variance and Monte Carlo Simulation methodologies in order to determine, by using stochastic calculation, the minimum variance portfolio that yields a desired expected return. In addition, the new method uses Six Sigma DMAIC to measure and improve the portfolio management process in order to establish an optimally diversified (hedged) portfolio.

Consequently, the synergy of the Optimisation, Monte Carlo Simulation and Six Sigma DMAIC methodologies, which are used by the method, provides for a significant advantage compared to the conventional ALM models.

This new Optimisation-Simulation-DMAIC method can help the financial institutions to develop or improve their Basel III and Solvency II internal risk models in order to reduce their capital requirements and VaR. Reducing the capital requirements and VaR will ultimately provide the insurance companies and banks with higher business capabilities, which will increase their competitive position on the market. Moreover, the proposed method can significantly assist the financial institutions to achieve their business objectives.

ACKNOWLEDGMENTS

I would like to thank to my daughter, Ivana Bubevska, for reviewing the paper and suggesting relevant improvements. She has also substantially helped with the editing and formatting of the paper. Her contribution has been essential for the successful publication of this work.

REFERENCES

- Adam, A., 2007. *Handbook of Asset and Liability Management: From Models to Optimal Return Strategies*, John Wiley & Sons, 26 Oct 2007.
- Atkinson P., Blundell-Wignall A. (2010). "Thinking beyond Basel III – Necessary solutions for capital and liquidity", OECD Market Trends No. 98 Volume 2010/1.

- BCBS (2010a). "Basel III: A global regulatory framework for more resilient banks and banking systems", December 2010 (rev. June 2011).
- BCBS (2010b), "Basel III: International framework for liquidity risk measurement, standard and monitoring", December 2010.
- BCBS (2011). "Revisions to the Basel II market risk framework updated as of 31 December 2010", February 2011.
- BIS (2011). "Basel III: Long-term impact on economic performance and fluctuations", Working paper No 338, February 2011.
- Bloomsbury, 2012. *Asset Liability Management for Financial Institutions: Balancing Financial Stability with Strategic Objectives*, Bloomsbury Information Ltd, 24 May 2012.
- Bourdeau, M., 2009. Market Risk Measurement Under Solvency II. In: Cruz, M., ed. *The Solvency II Handbook*, London, Risk Books – Incisive Media, 193–226.
- Cosimano Thomas F., Hakura Dalia S (2011), "Bank Behavior in Response to Basel III: A Cross-Country Analysis", IMF Working Paper WP/11/119, May 2011.
- Cruz, M., 2009. *The Solvency II Handbook*, London, Risk Books – Incisive Media.
- GDV, 2005. *Discussion Paper for a Solvency II Compatible Standard Approach*, Gesamtverband der Deutschen Versicherungswirtschaft. Available from: http://www.gdv.de/Downloads/English/Documentation_Sol_II.pdf [Accessed 20 June 2011]
- Glasserman, P., 2004. *Monte Carlo Methods in Financial Engineering*, New York, Springer Science.
- Jorion, P., 2011. *Financial Risk Manager Handbook*, New Jersey, John Wiley & Sons.
- Macaulay, F. R., 1938. "Some Theoretical Problems Suggested by the Movements of Interest Rates", National Bureau of Economic Research, New York, 1938.
- Markowitz, H.M., 1952. "Portfolio Selection", *The Journal of Finance*, Vol. 7, pp. 77-91, 1952.
- Markowitz, H.M., 1987. *Mean-Variance Analysis in Portfolio Choice and Capital Markets*, Oxford, UK, Basil Blackwell.
- Mitra, G., Schwaiger, K., 2011. *Asset and Liability Management Handbook*, Palgrave Macmillan, 29 Mar 2011.
- Redington, F. M., 1952. "Review of the Principles of Life Office Valuations", *Journal of the Institute of Actuaries*, Vol.78, part. 3, No 350, pp. 286-340, 1952.
- SST, 2004. *White Paper of the Swiss Solvency Test*, Swiss Federal Office of Private Insurance. Available from: http://www.naic.org/documents/committees_smi_int_solvency_switzerland_sst_wp.pdf [Accessed 20 June 2011]

- Stamatis, D. H., 2003. *Six Sigma for Financial Professionals*, Wiley, September 2003.
- Tarantino, A., Cernauskas, D., 2009. *Risk Management in Finance: Six Sigma and Other Next-Generation Techniques*, Wiley, May 4, 2009.
- Hayler, R., Nichols, M. D., 2006. *Six Sigma for Financial Services: How Leading Companies Are Driving Results Using Lean, Six Sigma, and Process Management*, McGraw-Hill, October 26, 2006.

AUTHORS BIOGRAPHY

Vojo Bubevski comes from Berovo, Macedonia. He graduated from the University of Zagreb, Croatia in 1977, with a degree in Electrical Engineering - Computer Science. He started his professional career in 1978 as an Analyst Programmer in Alkaloid Pharmaceuticals, Skopje, Macedonia. At Alkaloid, he worked on applying Operations Research methods to solve commercial and pharmaceutical technology problems from 1982 to 1986.

In 1987 Vojo immigrated to Australia. He worked for IBM™ Australia from 1988 to 1997. For the first five years he worked in IBM™ Australia Programming Center developing systems software. The rest of his IBM™ career was spent working in IBM™ Core Banking Solution Centre.

In 1997, he immigrated to the United Kingdom where his IT consulting career started. As an IT consultant, Vojo has worked for Lloyds TSB Bank in London, Svenska Handelsbanken in Stockholm, and Legal & General Insurance in London. In June 2008, he joined TATA Consultancy Services Ltd.

Vojo has a very strong background in Mathematics, Operations Research, Modeling and Simulation, Risk & Decision Analysis, Six Sigma and Software Engineering, and a proven track record of delivered solutions applying these methodologies in practice. He is also a specialist in Business Systems Analysis & Design (Banking & Insurance) and has delivered major business solutions across several organizations. He has received several formal awards and published a number of written works, including a couple of textbooks. Vojo has also been featured as a guest speaker at several prominent conferences internationally.

SPECTRAL APPROACH TO RELIABILITY EVALUATION OF FLOW NETWORKS

Ilya Gertsbakh^(a), Yoseph Shpungin^(b)

^(a) Department of Mathematics, Ben-Gurion University,
Beer-Sheva, Israel.

^(b) Software Engineering Department,
Shamoon College of Engineering, Beer Sheva, Israel.

^(a) elyager@bezeqint.net, ^(b) yosefs@sce.ac.il

ABSTRACT

In this paper we consider flow networks, which is an important class of networks, and which includes, for example, communication networks, transportation and supply networks, oil and power supply systems, etc. In our model, the edges are subject to failure, which may be caused by "enemy attack", earthquakes, disruption of communication channels etc. Each edge is characterized by its failure probability and flow capacity. The network reliability is defined as the probability that the flow between the source node and sink node is not less than some given threshold. Our approach to flow network reliability evaluation is based on estimating by means of an efficient Monte Carlo simulation, the network *topological invariant* called network destruction *spectrum* (D-spectrum). We consider also a design problem on flow network, namely its edge reinforcement in order to increase in an "optimal" way the network reliability.

Keywords: flow network, Monte Carlo simulation, D-spectra, network reliability design

1. INTRODUCTION

The maximum flow problem is a standard problem in operations research first solved by Ford and Fulkerson (Ford and Fulkerson 1962). They assumed that edges (and nodes) have some given nonrandom flow capacities. In stochastic flow network, it is assumed that edge (and/or node) capacities are *random*, which greatly complicates the problem and its solution.

There is a vast literature on stochastic flow networks, see (Lin 2004, 2001, Ramirez-Marquez and Coit 2005, Younes and Hassan 2011) and references there. Typically, the reliability of a stochastic flow network is measured by the probability $P(M \geq \Phi)$ that the maximal flow M which can be delivered from source s to sink t will be no less than some critical value Φ .

When network edges may be in two states (*up/down*), and $\Phi = 0$, the reliability of the network reduces to so-called s - t connectivity which, contrary to

the classical maximum flow problem, is already NP-complete since its solution is based on enumeration of all s - t paths. Quite sophisticated methods have been developed to solve this problem by applying Monte Carlo methodology, see e.g. (Elperin, Gertsbakh and Lomonosov 1991).

Further development in network reliability studies has been made by assuming that edges capacity is an integer-valued random variable (Lin 2001). The proposed solution method is based on finding all boundary points (i.e. all such path sets) which allow to deliver the minimal demand flow Φ , and on applying the inclusion-exclusion techniques to compute the desired reliability. The applicability of this method is limited to rather small networks. The work (Ramirez-Marquez and Coit 2005) deals with a similar multistate model and introduces Monte Carlo (MC) approach. The MC is based on comparing already identified elements of the set of all multistate minimal cut vectors with randomly generated system state vectors.

Also genetic algorithms have been applied for reliability evaluation of stochastic flow networks, see e.g. (Younes and Hassan 2011).

The purpose of this paper is to demonstrate how a new methodology based on so-called D-spectra and BIM-spectra can be used for analysis and design of flow network reliability.

2. BASIC NOTIONS AND DEFINITIONS

2.1. Flow Network

We define *flow network* N as a pair (V, E) , where V is a node-set and E is a set of directed edges. In our model, nodes can never fail, while edges can. If an edge fails, we say it is *down*; otherwise it is *up*. For each edge e , the probabilities $p(e)$ of being *up* and $q(e) = 1 - p(e)$ of being *down* are defined. Edges are assumed to be stochastically independent. In addition, for each edge $e=(a,b)$ directed from the node a to the node b , we define the maximal flow $c(e)$ which can be delivered from a to b along this edge.

Also let $|V| = n, |E| = m$. By state of a network we call a binary vector (x_1, x_2, \dots, x_m) , where $x_i = 1$, if an edge is *up* and $x_i = 0$, otherwise. We say that the network state is *UP* if the maximal flow from source to sink is not less than some given value Φ , and the state is *DOWN*, otherwise.

Example 1. Figure 1 below represents very simple flow network with 4 nodes and 4 edges.

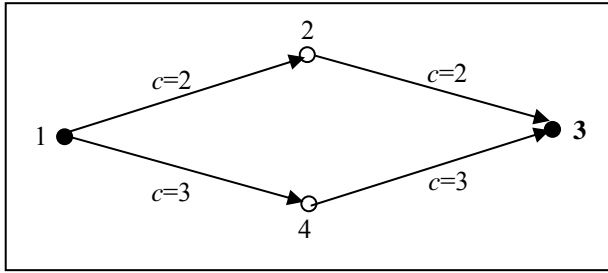


Figure 1: Flow Network with 4 Nodes and 4 Edges

It is easy to check that the maximal flow from source $s=1$ to sink $t=3$ equals 5. For example, it may be obtained by the following flows $w(i, j)$ ((i, j) is an edge defined by the nodes i and j):

$$w(1, 2) = 2, w(1, 4) = 3, w(2, 3) = 2, w(4, 3) = 3.$$

Suppose that we define the *UP* state for this network as a state with maximal flow no less than 3. Then, if for example the edge $(1,4)$ is *down*, the maximal flow equals 2, and the network is in the *DOWN* state.

2.2. D-Spectrum

Let us now introduce the so-called destruction spectrum (D-spectrum), which will play a central role in our further network flow analysis.

It is important to stress that the D-spectrum is a purely topological characteristic of the network which depends only on its structure and network *DOWN* state definition. D-spectrum is completely separated from any information regarding the real stochastic mechanism which governs system failure appearance.

Definition 1. (Gertsbakh and Shpungin 2009)

Let $\pi = (e_{i_1}, \dots, e_{i_m})$ be a permutation of network edges. Suppose that initially all edges are *up*. Start turning them from *up* to *down* by moving along π from left to right. Fix the first element e_{i_r} when the network state becomes *DOWN*. The ordinal number of this edge in the permutation is called the anchor of π and denoted $r(\pi)$.

Consider now the set of all $m!$ permutations and assign to each permutation probability $1/m!$. Define the probability of the event $A(i) = \{r(\pi) = i\}$ as

$$f_i = P(A(i)) = \frac{\text{\# of permutations with } r(\pi) = i}{m!} \quad (1)$$

Definition 2. (Gertsbakh and Shpungin 2009)

The discrete density function $\{f_i\}, i = 1, 2, \dots, m$, is called the system destruction spectrum (D-spectrum).

$F(x) = \sum_{i=1}^x f_i, x = 1, \dots, m$ is called the cumulative D-spectrum.

Example 1 (continued). Let us demonstrate the notion of D-spectrum on a network given in Figure 1. Suppose that $\Phi = 3$. The total number of permutations of 4 edges in the network is 24. Let $\pi = ((1, 2), (2, 3), (4, 3), (1, 4))$. We see that the first index such that the network state becomes *DOWN* (that is the maximal flow is less than 3) is 3. Therefore $r(\pi) = 3$ is the anchor of this permutation. After going over all permutations we arrive at the following D-spectrum of the given network:

$$f_1 = \frac{1}{2}, f_2 = \frac{1}{3}, f_3 = \frac{1}{6}.$$

The cumulative D-spectrum is

$$\text{therefore: } F(1) = \frac{1}{2}, F(2) = \frac{5}{6}, F(3) = F(4) = 1.$$

Theorem 1. (Gertsbakh and Shpungin 2009)

Suppose that all network edges have equal down probabilities, i.e. $q_i \equiv q$. Then the probability that network is in the *DOWN* state is given by the following formula:

$$P(\text{DOWN}) = \sum_{i=1}^m F(i) q^i p^{m-i} \frac{m!}{i!(m-i)!} \quad (2)$$

Rather surprising relationship (2) established in this theorem follows from the fact that the number of network failure sets $C(x)$ of size $x, x = 1, \dots, m$ can be expressed via the D-spectrum $F(x)$ by means of the following simple combinatorial relationship:

$$F(x) = \frac{C(x)}{m! / (x!(m-x)!)} \quad (3)$$

Formula (3) says that $F(x)$ is the ratio of the number of failure sets of size x among all possible sets of size x constructed from m different elements. This fact, in turn, follows from the definition of the cumulative D-spectrum $F(x)$.

It follows from (3) and independence of network edges that the probability associated with failure sets of size x equals $C(x) \cdot q^x \cdot (1-q)^{m-x}$. Now (2) follows from the fact that the network is *DOWN* if and only if it is in one of its failure states.

Example 1 (continued). Returning to our example 1, we calculate from (3) that there are $C(1)=2$ failure sets of size 1, $C(2)=5$ failure sets of size 2, $C(3)=4$ failure sets of size 3 and one failure set of size 4. For example, the failure sets of size 2 are all pairs of edges

except of the pair $((1,2), (2,3))$. We have by the theorem: $P(DOWN) = 2qp^3 + 5q^2p^2 + 4q^3p + q^4$.

Now we will introduce so-called Birnbaum Importance Measure (BIM) (Barlow and Proschan 1975) for system components. In simple words, BIM of edge j (denoted BIM_j) is the gain of network reliability obtained by replacing *down* edge j by an absolutely reliable one. Formally, BIM_j is defined as follows.

Definition 3.

$BIM_j = G(p_1, \dots, 0_j, \dots, p_m) - G(p_1, \dots, 1_j, \dots, p_m)$, where $G(p_1, \dots, 0_j, \dots, p_m)$ is the probability that the network is DOWN when edge j is down, and $G(p_1, \dots, 1_j, \dots, p_m)$ is the probability that the network is DOWN when the edge j is up.

The important role played by BIM_j follows from the fact that BIM_j equals the partial derivative of system reliability function

$R(p_1, \dots, p_m) = 1 - G(p_1, \dots, p_m)$ with respect to p_j , see (Barlow and Proschan 1975).

The knowledge of edge BIMs is the key element in finding the optimal network reinforcement strategy. The use of BIM in reliability practice was very limited since typically the system reliability function $R(p_1, \dots, p_m)$ is not available in explicit form.

It turns out that in the case of equal component reliability there is a surprising connection between the BIMs and the network D-spectrum and its modification called BIM-spectrum which allows estimating and ranking the component BIMs without knowing the analytic form of system reliability function.

Definition 4. (Gertsbakh and Shpungin 2009)

Let $N(x; 0_j)$ be the number of permutations satisfying the following two conditions:

- (i) If the first x edges in the permutation are down, then the network is DOWN;
- (ii) Edge j is among the first x elements of the permutation.

The collection

$\{z(x, j) = N(x; 0_j) \cdot x!(m-x)! / m!\}$ for a fixed j and $x = 1, 2, \dots, m$ is called the BIM $_j$ - spectrum of edge j .

The collection of all $\{z(x; j), x = 1, 2, \dots, m\}$ for $j = 1, \dots, m$ is called the network BIM-spectrum.

Let $N(x)$ be the number of permutations satisfying

- (i) only. Denote by $N(x; 1_j) = N(x) - N(x; 0_j)$.

Theorem 2. (Gertsbakh and Shpungin 2009) Let

$p_i \equiv p, q = 1 - p$. Then

$$BIM_j = \sum_{x=1}^m \frac{1}{x!(m-x)!} \cdot (N(x; 0_j)q^{x-1}(1-q)^{m-x} - N(x; 1_j)q^x(1-q)^{m-x-1}) \quad (4)$$

The hint to the proof of this theorem is the following : the first sum in (4) equals the first term

$G(p_1, \dots, 0_j, \dots, p_m)$ in the expression of BIM_j (Definition 3), and the second sum in (4) – to the second term in BIM_j in the same Definition 3.

Theorem 3. (Gertsbakh and Shpungin 2009)

If for all $1 \leq x \leq m$ the inequality $z(x, i) \geq z(x, j)$

holds then $BIM_i \geq BIM_j$, no matter what the values of q are.

Suppose that the previous condition does not take place. Then let the k be the maximal index such that $z(x, i) \neq z(x, j)$. Suppose that $z(k, i) > z(k, j)$.

Then there exists some value p_0 such that for all $p \geq p_0$ the inequality $BIM_i > BIM_j$ holds.

Example 1 (continued). Let us take the edge (1,2)

from the network in Figure 1 and compute $z_{2,(1,2)}$. It is easy to see that there are 8 permutations π such that the network is DOWN when the two first edges of π are down, and the edge (1,2) is one of them. So $z_{2,(1,2)} = 8/24$. We have for this edge the following BIM-spectrum:

$$z_{1,(1,2)} = 0, z_{2,(1,2)} = \frac{8}{24}, z_{3,(1,2)} = \frac{18}{24}, z_{4,(1,2)} = 1.$$

For edge (2,3) we have the same BIM-spectrum, and for edges (1,4) and (4,3) the BIM-spectrum is the following (x stands for the edge (1,4) or the edge (4,3)).

$$z_{1,x} = \frac{6}{24}, z_{2,x} = \frac{12}{24}, z_{3,x} = \frac{18}{24}, z_{4,x} = 1.$$

We see from this example that by Theorem 3, the BIMs of the edges (1,4) and (4,3) are greater than those of the edges (1,2) and (2,3) for all values of q .

3. MONTE CARLO FOR D-SPECTRA AND BIM-SPECTRA

Exact computation of D-spectra and BIM-spectra is an NP-hard problem. The practical way to calculate the spectra is approximating them using Monte Carlo (MC) methodology. The books (Gertsbakh and Shpungin 2009, 2011a) contain a series of efficient MC algorithms and examples of spectra calculation.

We give here a non-formal explanation of MC algorithms adopted to our purpose.

To estimate $F(x)$, simulate M random permutations $\pi = (i_1, i_2, \dots, i_m)$ of edge numbers and imitate a sequential destruction of edges by moving along a permutation from left to right and by remembering the number N_i of such permutations that the system went

DOWN on the i -th step of the destruction process. Afterwards, as an MC estimate of $F(x)$ take the ratio

$$\hat{F}(x) = (N_1 + \dots + N_x) / M.$$

Note that in order to check the state of the network on certain step of the destruction process, we use the Ford-Fulkerson algorithm (Cormen, Rivest, Leicerson, and Stein 2009) for calculating the maximal flow. If it turns out that the maximal flow is less than Φ , we say that the network is DOWN.

An important fact is that there is *no need* to check the network state on *each* step of the destruction process. The position of the anchor in a given permutation $\pi = (e_{i_1}, \dots, e_{i_m})$ can be efficiently found by applying *bisection* search algorithm, which works as follows. Erase the first $\lfloor \frac{m}{2} \rfloor$ edges of the permutation.

Check the state of the network using Ford-Fulkerson algorithm. If the network is already DOWN, the anchor

should be among the first $\lfloor \frac{m}{2} \rfloor$ positions. If the network

is UP, the anchor is among the remaining part of the permutation. Proceed in a similar way by bisecting the relevant part of the permutation until the position of the anchor is located. On the average, the number of flow checks is of magnitude $O(\log_2(m))$.

To approximate BIM-spectra, modify the above procedure and count the number of permutations $M(x; 0_j)$ equal to the number of permutations such that the system went DOWN during the first x failures and edge j was among these x components.

Example 1 (continued). Let us illustrate the D-spectrum calculation on the network in Figure 1. Take the number of permutations $M=5$. Denote the network edges: $(1,2)=1$, $(1,4)=2$, $(2,3)=3$, $(4,3)=4$. Suppose that the generated permutations are: $\pi_1 = (1, 2, 3, 4)$,

$$\pi_2 = (4, 3, 2, 1), \pi_3 = (1, 3, 2, 4), \pi_4 = (2, 1, 3, 4),$$

$$\pi_5 = (3, 1, 2, 4).$$

We see that in these five permutations the network went DOWN twice on the first step, once on the second step, and twice on the third step. So the estimators for $F(x)$ are the following:

$$\hat{F}(1) = \frac{2}{5}, \hat{F}(2) = \frac{3}{5}, \hat{F}(3) = \hat{F}(4) = 1.$$

Naturally, these values are far from the exact values (calculated above), because the number M of replications is too small.

Remark. Suppose that edge *up* probability p is not known exactly (as it usually takes place in practice) and lies in the interval $p \in [p_{\min}, p_{\max}]$. Since network reliability is a monotone function of its component reliability, we have the following bounds on $R(p)$: $R(p_{\min}) \leq R(p) \leq R(p_{\max})$. These bounds may be quite valuable in case of "fuzzy" information about the q values.

4. NUMERICAL EXAMPLES

4.1. Network Reliability as a Function of p

Let us consider the network from Figure 2. This network has 15 nodes (two of which are terminals, 1 and 2) and 35 edges.

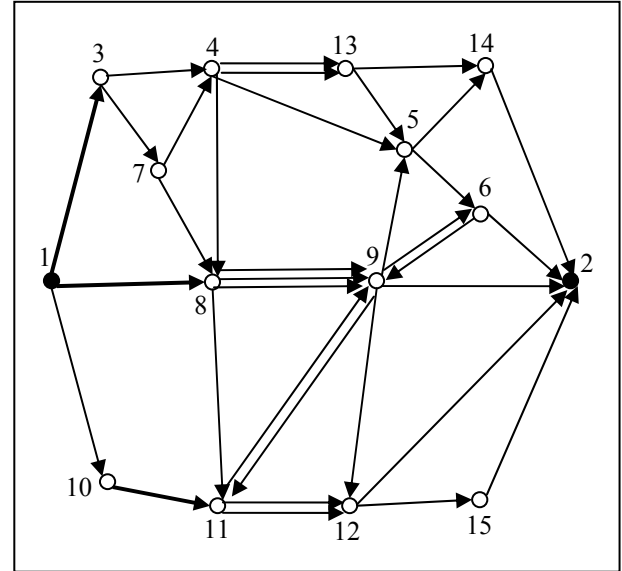


Figure 2: Flow Network with 15 Nodes and 35 Edges

The edge capacities $c(a,b)$ are given by the Table

1. In the case two nodes, say x and y are connected by some parallel edges, we denote them by $(x,y)_1$, $(x,y)_2$ and so on. We consider also edges (a,b) with flow going from a to b and in opposite direction. For example, we see in the table the edges $(4,8)$ and $(8,4)$.

The initial maximal flow for the given capacities equals 22.

Table 1: Edge Capacities

a,b	$c(a,b)$	a,b	$c(a,b)$
1,3	8	(8,9) ₃	3
1,8	9	8,11	4
1,10	8	9,5	6
3,4	6	9,6	4
3,7	6	9,2	5
4,5	6	9,11	4
4,8	6	9,12	5
(4,13) ₁	5	10,11	5
(4,13) ₂	2	11,9	4
5,6	6	(11,12) ₁	4
5,14	5	(11,12) ₂	2
6,2	6	12,2	6
6,9	3	12,15	5
7,4	5	13,14	5
7,8	4	13,5	5
8,4	4	14,2	5
(8,9) ₁	5	15,2	5
(8,9) ₂	4		

The most important characteristic of the network is its reliability $R(p) = 1 - P(\text{DOWN}; q)$ as a function of $p, p = 1 - q$. Let us demonstrate how this characteristic is computed using D-spectrum, for two values of the threshold: $\Phi = 10$ and $\Phi = 12$. Table 2 presents the edge cumulative spectra obtained by means of Monte Carlo simulation of $5 \cdot 10^4$ edge permutations. For example, the row for $x=6$ gives the probabilities 0.12924 and 0.20202 that the anchor for $\Phi = 10$ and $\Phi = 12$, respectively, is on one of the first six positions in random edge permutations.

Table 2: Edge Cumulative Spectrum

x	$F(x)$ $\Phi = 10$	$F(x)$ $\Phi = 12$	x	$F(x)$ $\Phi = 10$	$F(x)$ $\Phi = 12$
1	0	0	14	.81732	.93196
2	.00874	.01144	15	.88206	.96366
3	.02532	.0363	16	.92814	.98202
4	.05094	.0759	17	.96014	.992
5	.0851	.13134	18	.9795	.99692
6	.12924	.20202	19	.9903	.99916
7	.18566	.28702	20	.99608	.99968
8	.25376	.387	21	.9984	.99998
9	.33694	.49746	22	.99938	1
10	.43354	.61082	23	.99976	1
11	.53428	.7172	24	.9999	1
12	.63944	.81052	25	1	1
13	.735	.88198	26	1	1

With probability ≈ 0.92 the anchor is greater than 5, for $\Phi = 10$. So, with probability close to 0.92 network failure takes place after 5 edges have failed. For $\Phi = 12$, with probability close to 0.92 network failure occurs after 4 edges have failed.

Table 3 presents network UP state probabilities for various values of p . The calculations were performed using formula (2).

Table 3: $R(p)$

p	$R(p)$ $\Phi = 10$	$R(p)$ $\Phi = 12$
0.1	0	0
0.2	.000032	.000002
0.3	.001121	.000159
0.4	.0129	.0034
0.5	.0725	.0286
0.6	.2375	.1309
0.7	.5095	.3669
0.8	.7819	.6826
0.85	.8809	.8206
0.9	.9485	.9223
0.95	.9872	.9816
0.975	.9968	.9956

We see from the table that if, for example, we want to guarantee that the network is UP with

probability greater than 0.95, it is enough to demand that edges be up with $p > 0.9$, for $\Phi = 10$.

4.2. Edge Reinforcement Problem

By reinforcing an edge we mean replacing it by a more reliable one. This operation can be applied to a given number k of edges. The problem is to achieve the maximal network reliability by "the best possible" choice of the candidates for this replacement. In the case of equal edge probabilities we suggest the following method (Gertsbakh and Shpungin 2009, 2011a).

1. Estimate the BIM-spectra for all edges.
2. Range the edges by their BIM's spectra.
3. Take the first k edges with the highest BIM values and replace them by more reliable ones.

Note that this method is based on Theorem 3 from the Section 2.

Let us consider the network from Figure 2 and let $\Phi = 10$. Suppose that we can reinforce 3 edges. We skip here the intermediate results of the calculations. The final results are the following. The edges (1,3), (1,8), and (10,11) must be reinforced (they are marked bold in Figure 2). This conclusion may seem to be intuitively obvious, but for larger and more complicated networks similar conclusions are not so clear.

For illustration, the following Table 4 gives estimated values $\bar{z}(x; (a, b))$ of BIM-spectrum for one of the most important edges - (10,11), and a less important edge (13,14), for even x values.

Table 4: The BIM's Spectra

x	$\bar{z}(x; (10, 11))$	$\bar{z}(x; (13, 14))$
2	.0037	0
4	.0207	.0034
6	.0524	.0157
8	.1008	.0474
10	.1700	.1106
12	.2592	.2056
14	.3534	.3183
16	.4386	.4217
18	.5104	.5036
20	.5702	.5695
22	.6294	.6278
24	.6838	.6830
26	.7423	.7419
28	.8008	.7997
30	.8568	.8564
32	.9152	.9140
34	.9720	.9708

We see that the values of BIM-spectrum for edge (10,11) are consistently greater than those of edge (13,14). Remind that this means that (10,11) is more important than (13,14), no matter what the values of q are.

Remark. As it was noted, the BIM spectrum is a topological invariant for most reliability criteria, but in the case of flow networks the edge capacities may affect the spectrum. Nevertheless also in this case the topological features of the edge prevail on its capacity value influence.

To illustrate the remark, let us take from the network on Figure 2 two edges: (1,10) with capacity $c(1,10)=8$, and (10,11) with $c(10,11)=5$. In spite of the difference in capacities, all values of BIM-spectrum of edge (10,11) are consistently greater of those of edge (1,10).

For the second example take three parallel edges connecting nodes 8 and 9. We see from table 1 that $c((8,9)_1) > c((8,9)_2) > c((8,9)_3)$. Clearly that these three edges have the same topological features, but here the edge capacities affect the BIM-spectra, and we have $z(x, (8,9)_1) > z(x, (8,9)_2) > z(x, (8,9)_3)$.

Note that introducing parallel edges is a way of having edges with more than two states. For example, two independent edges connecting nodes 4 and 13 may be viewed as one edge with four possible capacities 0, 2, 5 and 7 with probabilities $q^2, q(1-q), q(1-q)$, and $(1-q)^2$, respectively.

5. POSSIBLE EXTENSIONS

To the best of our knowledge, there are no publications devoted to using network D-spectra technique to the study of network flow behavior in networks with unreliable edges. The model considered in this paper can be extended in several directions.

First, our method may be easily extended to the case of unreliable nodes.

Second, we can introduce several flow sources and several sinks.

Finally, introducing cost for edge reinforcement (for the purpose of increasing their reliability and/or flow capacity) will bring us to the search for the "best" predisaster design, similar to the study made by (Gertsbakh and Shpungin 2009, 2011b, Levitin, Gertsbakh, and Shpungin 2010, Peeta, Salman, Gunec, and Kannan 2010).

REFERENCES

- Barlow, R.E. and Proschan, F., 1975. *Statistical Theory of Reliability and Life Testing: Probability Models*. Holt, Rinehart and Winston, Inc.
- Cormen, T.H., Rivest, R.L., Leicerson, C.E., Stein, C., 2009. *Introduction to Algorithms*. 3rd ed. MIT Press.
- Elperin, T., Gertsbakh, I., Lomonosov, M., 1991. Estimation of network reliability using graph evolution models. *IEEE Transactions on Reliability*, 40(5), 572-581.
- Ford, L.R. and Fulkerson, D.R., 1962. *Flows in Networks*. Princeton University Press.

- Gertsbakh, I. and Shpungin, Y., 2009. *Models of Network Reliability: Analysis, Combinatorics, and Monte Carlo*. CRC Press.
- Gertsbakh, I. and Shpungin, Y., 2011a. *Network Reliability and Resilience*. Springer.
- Gertsbakh, I. and Shpungin, Y., 2011b. Predisaster Design of Transportation Network. *Transport and Telecommunication*, 12(1), 4-11.
- Levitin, G., Gertsbakh, I., and Shpungin, Y., 2010. Evaluating the damage associated with intentional network disintegration. *Reliability Engineering and System Safety*, 96(4), 433-439.
- Lin, Yi-Kuei, 2001. A simple algorithm for reliability evaluation of a stochastic-flow network with node failure. *Computers & Operations Research*, 28, 1277-1285.
- Lin, Yi-Kuei, 2004. Reliability of stochastic-flow network with unreliable branches & nodes, under budget constraints, *IEEE Transactions on Reliability*, 53(3), 381-387.
- Peeta, S., Salman, S.F., Gunec, D., and Kannan, V., 2010. Predisaster investment decisions for strengthening a highway network. *Computers and Operations Research*, 37, 1708-1719.
- Ramirez-Marquez, J.E. and Coit D.W., 2005. A Monte Carlo simulation approach for Approximating multi-state two-terminal reliability, *Reliability Engineering and System Safety*, 87, 253-264.
- Younes, A. and Hassan, M.R., 2011. A Genetic algorithm for reliability evaluation of stochastic flow network with node Failures. *International Journal of Computer Science and Security*, 4(6), 528-536.

AUTHORS BIOGRAPHY

Ilya B. Gertsbakh is Professor Emeritus in the Department of Mathematics at Ben Gurion University, Beer Sheva, Israel. He received his Ph.D. degree in applied probability and statistics from Latvian Academy of Sciences, Riga. He is author or coauthor of six books. He has published some 70 papers in international scientific journals.

Yoseph Shpungin is Head of the Software Engineering Department, at Shmoon College of Engineering, Beer Sheva, Israel. He received his Ph.D. degree in mathematics from Ben Gurion University, Beer Sheva, Israel. He is author of two books (with Ilya Gertsbakh) and many publications in international scientific journals.

ANALYSIS OF THE THREAD ASSIGNMENT BEHAVIOUR OF PARALLEL PROGRAMS ON CHIP MULTIPROCESSORS

Michael Bogner^(a), Ematinger Markus^(b), Franz Wiesinger^(c)

^(a, b, c) University of Applied Sciences Upper Austria,
Hardware/Software Design & Embedded Systems Design

^(a) michael.bogner@fh-hagenberg.at,

^(b) markus.ematinger@fh-hagenberg.at,

^(c) franz.wiesinger@fh-hagenberg.at

ABSTRACT

Nowadays, a chip multiprocessor following the x86-architecture combines at least four dedicated cores. To take benefit of this computing power, the application has to use multiple threads. To provide the parallel behavior for all processes and threads, the allocation has to change frequently. Depending on the situation, this allocation can differ and is worth to be analyzed.

The application runs a configurable amount of hard-working threads. By interfering with the core-thread-allocation several different scenarios have been tested. By recording this thread-core-allocation and the execution time, it is possible to compare the different scenarios.

The paper shows that Microsoft Windows 7 handles the thread-core-allocation in a lot of situations quite well. But the exclusion of core zero provides a performance increase. This is only useful if the number of threads is lower than the number of available processor cores. This situation also shows an additional interesting incident. Windows tries to balance the load over all processor cores very frequently.

1. INTRODUCTION

1.1. Operating System

The most actual devices use an abstraction layer between hardware and applications. This layer is called operating system (Tanenbaum, Moderne Betriebssysteme, 2003). It provides a runtime environment for the applications and handles the hardware resources like the main processor and the memory (Tanenbaum, Computerarchitektur, 2006). An operating system runs many different applications at the same time. This means that the operating system has to share the processor time between the applications. To provide a decent allocation the operating system has to switch between running application in small time slices. An application is a process. And a process can contain one or more threads. Threads and processes are basically in one of three different states. These three states are "Running", "Blocked" and "Ready". When a process or a thread gets created, it starts in the Ready state. The scheduler selects one of all available Ready

states by using a special algorithm. When the thread gets selected by the scheduler it gets switched into the Running state. At this state the thread executes his code. There are many situations, where the thread has to wait for other resources. A resource can for example be a File IO or Events. The thread gets switched to the Blocked state and has to wait until the resource is available. When the resource gets available, the thread gets switched to the Ready State. The scheduler can select this thread and continue its execution. All threads are scheduled by the operating systems scheduler. Simple applications only run their single main thread. This means if the program has to wait for a resource the whole application has to block and wait for this. The operating system runs the scheduler and switches to another application. This happens if the application runs only one thread like in Figure 1 at (a). This behavior can slow down the application. To continue the execution of the applications, the applications process has to contain multiple threads. These threads can continue the execution while another thread is blocking. This multiple threads are shown in Figure 1 at (b).

But multiple threads have also another advantage. If the machine has more the one processor core, the operating system is able to schedule multiple threads of a process to different cores. This can provide a performance increase, by executing different code on different processor cores at the same time. But this also means that the application has to hold the data of the threads consistent. In a multithreaded application many threads work together to finish faster, but depending on the application the threads are not allowed to modify the same data as another thread. This can be avoided by making the access exclusive for a single thread. This can be achieved by different synchronization mechanisms like critical sections, mutexes, semaphores, events and similar techniques. This functionality is provided by the operating systems API (application programming interface). The difference between these mechanisms is that some of them are working across the borders of a process and others work only in a single process. Depending on the operating systems, there are huge performance differences.

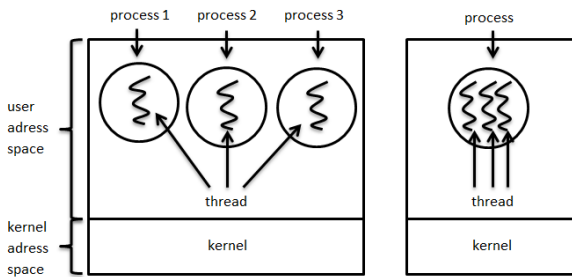


Figure 1: Threads and Process (Tanenbaum, Moderne Betriebssysteme, 2003)

1.2. Multicore processors

Before the rise of the on chip multicore processors a machine had to use multiple single core processors on a single motherboard to gain real advantage of multithreaded applications. These systems had to share the data by using special bus. It was not possible to use the on chip cache for data sharing.

Current multicore processors (David Harris, 2007) combine multiple cores in one single chip. Figure 2 shows the architecture (David A. Patterson, 2007) of an Intel Core i7 processor (Intel, 2011). The figure shows that the processor combines four dedicated processor cores on a single chip (Becchi, 2006) (Sondag, 2009). The chip uses the shared L3 cache for data sharing between the cores. The most actual multicore processors are comparable, like the AMD Phenom (AMD, 2009) and the Phenom II (AMD, 2011). Only the Intel Core 2 Quad (Intel, 2011) uses a different design, because it combines two dual core chips in one processor case. For data exchange between the two dual cores the processor has to use the main memory. Using the main memory for data exchange on a Core 2 Quad processor causes another performance loss, because the memory controller of this processor was place on a second chip on the Motherboard. This chip is called the Northbridge. For data sharing the data has to be sent from one core to the memory controller by using a bus and the same way back. This is slower than using the cache on actual quad core processors.

These multicore designs provide that the operating system is now able to run applications in parallel. It is also possible to share the data by using cache and the main memory. This data exchange is very quick. But the number of cores is not as high as the number of runnable applications. To get an increase in performance the application has to use multiple threads (Akhter S., 2006). The operating system can assign these threads to different processor cores and gain an increase in performance. Multithreaded programming does not gain performance automatically. This technique has to be used intelligent. If one thread marks the cached data of one core invalid by writing on them, this thread has to load the data from the main memory. This synchronization causes a decrease in performance. Creating threads and switching the cores decreases the performance. The threads should use the cores of a multicore processor, but should also minimize the needed overhead for synchronizations.

Depending on how these threads and processes are scheduled the performance can rise or fall. The scheduling can be restricted by setting the thread affinity. This is used to determine weak spots at Windows 7.

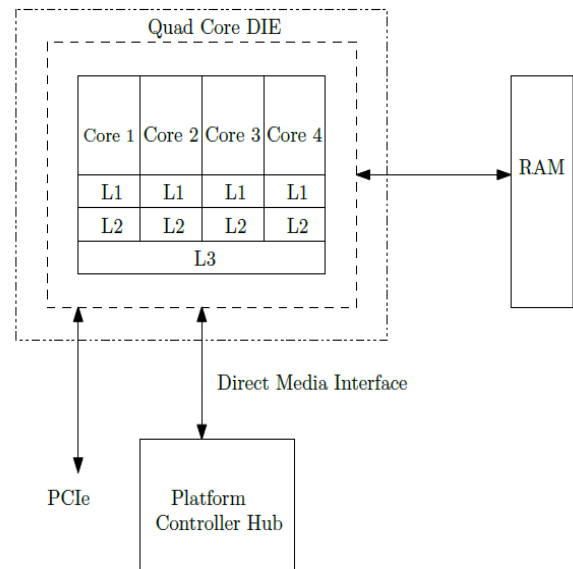


Figure 2: Intel Core i7 architecture

2. TEST

2.1. Main idea

The information that is used to find weak spots is the runtime and the thread-to-core allocation applied over the time. To get the information a test application is needed. This application is able to produce a heavy work load for every available processor core by using multiple threads. This application has to collect the thread core allocation and the runtime of each thread. The threads execute simple integer operations. After some operations the thread checks the allocation and stores the information.

Figure 3 shows the testing application. It uses the Nokia QT 4.7 Framework (Nokia, 2008-2011). On the top of the application it is possible to define the number of threads and the thread priority for the next test run. After a run has finished the logged data can be exported into a file in the well-known comma separated values (csv) format.

It also supports a simple live view of the thread-to-core allocation. But its accuracy is far away from the standalone test with the csv export, because it only samples the threads at a defined times slice. The sample rate is in the range of milliseconds. This means if the cores are faster switched, the live view will not show all cores switches.

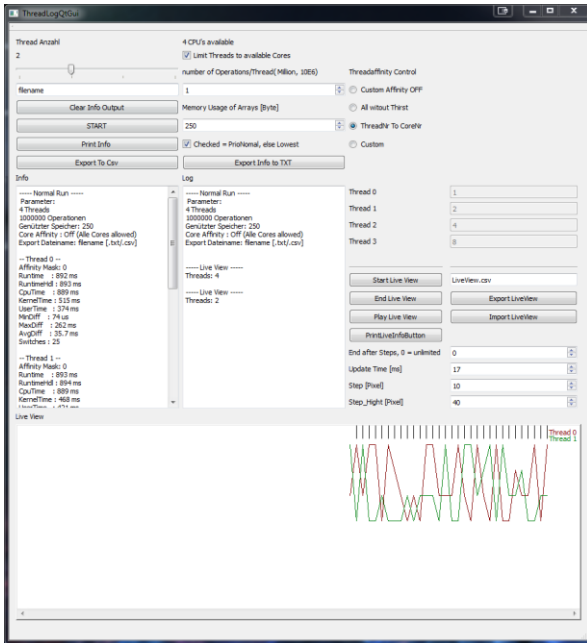


Figure 3: Screenshot of the test application

2.2. Test algorithm

To produce heavy workload a filter kernel calculates over a picture. The picture is represented by a simple two dimensional array. The array gets divided into stripes. Every thread has to calculate a single stripe of the picture. Figure 4 is showing this procedure. The integer calculation produces the work load. The size of the image is adjustable. Because of that this is not fair dividable, a small adjustment is made. Every thread has to run a fixed number of steps and calculate the filter kernel from the top left to the bottom right of their image part. If the thread reaches the end it restarts from the beginning until the number of calculate steps are reached. This provides the same workload for every thread.

To retrieve usable information at runtime it is needed to collect the thread-to-core affinity and the time. Figure 5 shows how this is done. The number of threads and the thread affinity is adjustable before the test run. To retrieve the thread-to-core affinity every thread has to retrieve the number of the core that is actually executing code. This is done by calling the Win32 API function `GetCurrentProcessorNumber`. This function returns the number of the processor core, from which core the function is called. Then the actual time is retrieved (`GetActualTime`). Therefore the Query performance counter of Windows is used (Microsoft, 2011). This counter makes it possible to retrieve the system ticks. These ticks can be converted into the time by using the Query Performance Frequency factor. This factor depends on the clock frequency of the processor. Before starting the threads a base time is stored. This time is the same for every thread. After retrieving the core number and the time, the core number is compared with the core number from the previous check (`CheckCoreChange`). If the core number is different, the core number and the time get stored. Then the

calculation continues. This procedure starts from the beginning until the needed number of calculation steps is reached. At the end all the information of all threads are collected and exported into the csv file. By using this timestamps it is possible to calculate the number of all core changes that happened while the thread was running. It is also possible to calculate the average time between the core changes.

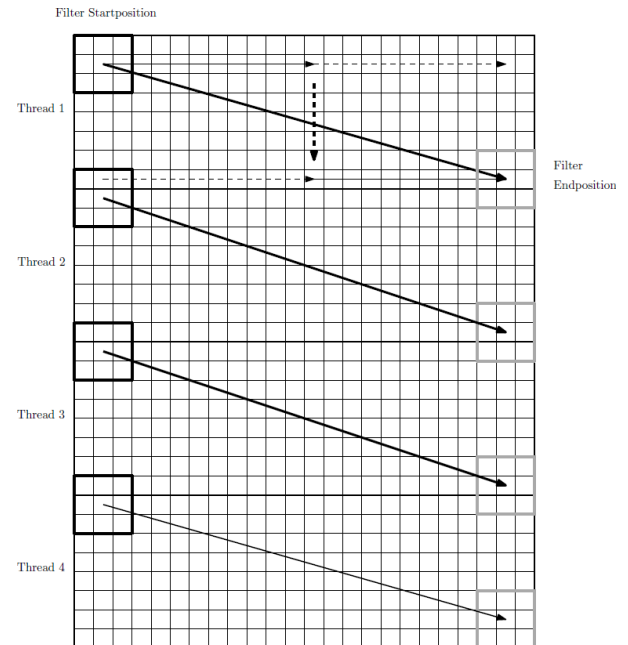


Figure 4: Picture of filterkernel

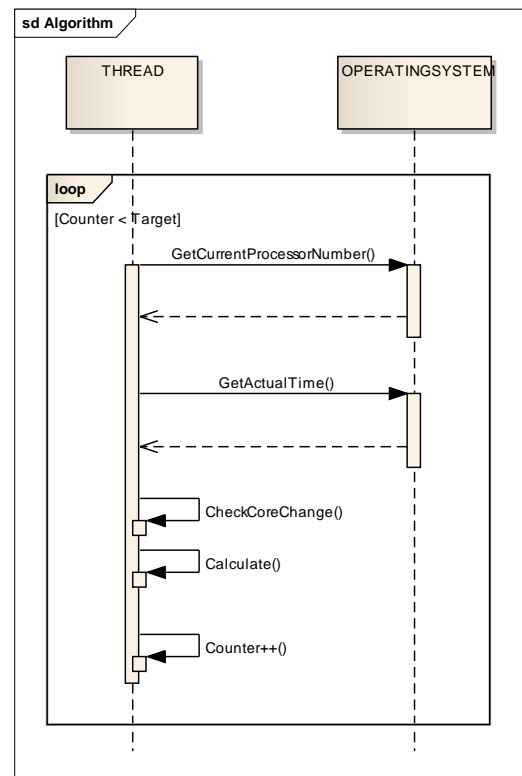


Figure 5: Algorithm of data determination

As a summary a thread retrieves the information this way:

1. Calculate the filter kernel for its position
2. Retrieve the actual core number
3. Get the actual time
4. Compare the retrieved core number (step 2) with the core number from the last check (stored in step 5)
5. Store the core number if the core number has changed
6. Continue with the calculation

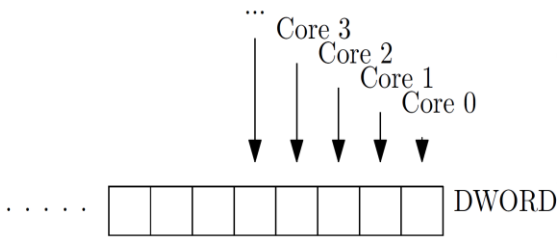


Figure 6: Thread affinity mask

Figure 6 shows the thread affinity mask. It is a DWORD which is 32 bit wide. This mask is used to set the affinity for every worker thread. This is the first thing that is done when the thread gets started. Therefore this mask is passed to the WIN32 API function `SetThreadAffinityMask`. As shown in the picture, every bit represents a processor core. Bit zero is for core zero and so on. If the bit for the core is true the thread can run on the core. If the bit is false, the core is denied. On a quad core processor only the lower four bits are important. If the mask is not set, all cores are allowed.

2.3. Test System

The main specification of the test system:

- Intel Core i7 860 quad core
 - Turbo Boost Technology disabled
 - Hyper threading disabled
- Asus P7P55D Evo mainboard
- 12 GB DDR3 Ram
- Windows 7 Professional 64 bit
- Microsoft Visual Studio 2010
 - C++
 - 32 bit Compiler

Due to better comparison between the scenarios with different number of threads the Intel Turbo Boost Technology is disabled. Otherwise a single thread test will run with higher clock rates than a test with four threads due to dynamic frequency scaling. Hyper threading is disabled, because it provides for every core one additional core. But it is wanted to compare only real quad core processors. So to disable this feature of an Intel Core i7, this is the main difference between a Core i7 and a Core i5 quad core processor, was the better choice.

2.4. Test cases

The test cases vary by the number of running threads from one up to four threads. For every different thread number the thread affinity is changed. The default thread affinity is that the operating system can execute every thread on every processor core. The second case is that every thread can only be executed on one single core. Thread zero can only run on core zero, thread one can only run on core one and so on. This will avoid that the operating system moves the threads from one core to a different core. The third main case is that every thread can be executed on every core, except core zero. This should demonstrate that core zero is preferred by the operating system. To start four threads in this situation was skipped, because there are only three runnable cores.

Furthermore there are some special cases tested. These cases are that the application starts more threads than the number of available processor cores, known as oversubscription. Other special cases are that only one or two threads are used. These threads are tested with different thread affinity. This means the thread gets bound to core zero or core three. This test should show the interference with the preferred core of the operating system.

3. RESULTS

Table 1 shows an example of the result of a single test run. It represents the average core change time for one to four threads, by using the systems default thread affinity and the exclusion of core zero. The average core change time describes the time between a thread gets pushed from one core to a different core.

Table 1: Average core change time (time in ms)

Threads	OS default	Core zero excluded
1	70.1	87.2
2	8.8	9.4
3	7.9	29.8
4	51.0	-

If the number of threads on a quad core processor is less than four and higher than one, the average core change time is below 10 ms. If the number of threads is one or equal the number of cores the average core change time is above 50 ms. This means the number of core switches with two or three threads is about 5 times higher than the number of core switches with one or four threads. If core zero is excluded, the averages core change rate of two threads is at least 3 times higher than the average core change rate of one or three threads. This behavior is shown in Figure 7. The upper screenshot of the taskmanager shows two hard working threads, where the threadaffinity is left at the default settings (all cores are allowed). The load overall load stays at 50 percent, but it is shared between all four available cores. To produced this behaviour Windows 7 has to move the threads from one core to an other core in small time

slices as shown in Table 1 at two threads. When the two threads are fixed to two cores, both cores are loaded by 100 percent and the other two cores are idle. This is shown in Figure 7 at the bottom screenshot. This scenario is comparable with a scenario where four hard working threads are executed on a quad core processor, because from the view of the process the number of threads is the same as the number of available processor cores.

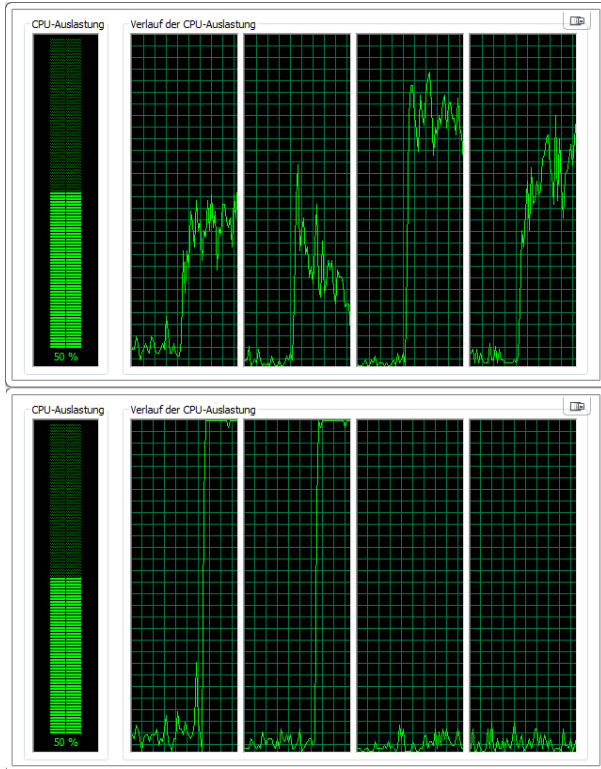


Figure 7: Comparison between default assignment and fixed assignment to core zero and core one, two threads

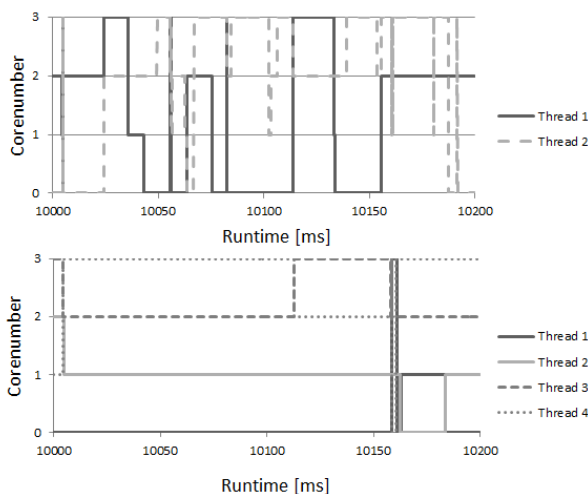


Figure 8: Core change comparison between 2 and 4 threads

Figure 8 shows a snapshot of the traced data. The time slice with 10 seconds until 10.2 seconds was randomly

chosen. The vertical axis stands for the core number where the thread was assigned. The top diagram shows the two thread situation. And the bottom diagram shows the four thread situation. It is obvious that the two threads get pushed from one core to another core much more often, than four threads. This diagram confirms the results from Table 1.

Table 2: Runtime in seconds

Threads	OS default	Core zero excluded	thread fixed to core
1	41.8	41.70	43.7
2	48.73	47.40	48.03
3	46.63	47.20	49.23
4	51.57	-	53.40

Table 2 shows the runtime in the different situations. The time is the maximum runtime of all running threads, this means this time describe the timespan between the start of all threads and the stop of all threads. The runtime of the threads don't decrease by the number of threads, because by increasing the number of threads the workload gets increased by the same factor as describe in 2.2. In every situation, except one and two threads with core zero excluded, the default affinity mask is the fastest.

The Table also shows that it is not possible to gain any performance by binding every thread to a single core. Nearly every situation provided a significantly decrease in performance.

Table 3: special cases with two threads

assignment	Runtime [s]	Difference [%]
default	48.73	0
fixed to core 0 and 1	48.03	-1.44
Core zero excluded	47.40	-2.74
Core 2 and 3	47.33	-2.87
Fixed to core 2 and 3	46.80	-3.97

Table 3 shows a special case. Therefore in every situation only two threads are started. The thread affinity mask is the only difference between the test cases. The runtime is the time when both threads have finished their work. At default the operating system is allowed to use every processor core. This time is the base for the difference compared to the other situations. At fixed to core the thread zero was bound to core zero and thread one was bound to core one. This modification provides a slight increase in performance by 1.44%. The exclusion of core zero is 2.74 percent faster than the default setting. The last two situations are, that only core two and core three are used. If the operating system is only possible to choose between core two and three the performance gain is about 2.87

% compared to the default setting. If one thread gets bound to core two and the other thread gets bound to core three, the increase in performance is about 3.97 percent. It is obvious that Windows 7 prefers core zero and that it is better to bind the threads to other cores if the number of threads is smaller than the number of available cores.

Table 4: Average and maximum runtime in seconds at oversubscription and default thread affinity

Threads	Average runtime	Maximum runtime
3	46.62	46.63
4	50.57	51.57
6	69	76.77
8	97	97.93

Table 4 shows the scenario of oversubscription. In comparison to three and four threads the oversubscription situations with six and eight threads shows interesting results. The average runtime is the average time of all threads that is needed to finish the work, while the maximum runtime is the time that is needed to finish all threads. If we take the average time it is obvious that six and eight threads are slightly faster than four threads, by including the factor that the work increases by the same factor as the number of threads. This looks like it would be really good to use oversubscription, but depending on the application it is important to take a look at the maximum runtime. When using three, four or eight threads on a quad core processor the difference between the average and the maximum runtime is very low, but with six threads the difference is much bigger. For this scenario the whole work is done after the maximum runtime. With six threads some threads would finish earlier than the others.

4. CONCLUSION

Windows 7 handles most of the situations of standard applications really well. But there are also special cases where it is possible to increase the performance by modifying the thread affinity to gain even more performance. If the processor should run only one or two threads on a quad core processor, it is possible to increase the performance by excluding core zero. For three or more threads no modification is needed.

If the number of threads is lower than the number of available processor cores Windows 7 tries to balance the work load over all processor cores. The balancing operation causes heavy core switches and challenges the cache coherence protocol of the CPU. In comparison to the situation with four threads on a quad core, the core change rate is about 5 to 10 times higher. It is possible to decrease this rate by modifying the thread affinity. Oversubscription is slightly faster than using the same number of threads than available processor cores. But if

the number of threads is no multiple of the number of cores, the runtime between the threads differs very much. Depending on the used scenario is recommended to use a number of threads that is a multiple of the number of cores.

REFERENCES

- Akhter S., R. J. (2006). *Multicore Programming: Increasing Performance through Software Multithreading*. Intel Press.
- AMD. (2009). *Key Architectural Features of AMD Phenom X4 Quad-Core Processors*. Retrieved 2011, from <http://www.amd.com/us/products/desktop/processors/phenom/Pages/AMD-phenom-processor-X4-features.aspx>
- AMD. (2011). *AMD Phenom II Key Architectural Features*. Retrieved 2011, from <http://www.amd.com/us/products/desktop/processors/phenom-ii/Pages/phenom-ii-key-architectural-features.aspx>
- Becchi, M. C. (2006). *Dynamic thread assignment on heterogeneous multiprocessor architectures*. New York: ACM.
- David A. Patterson, J. L. (2007). *Computer organization and Design*. Burlington: Morgan Kaufmann.
- David Harris, S. H. (2007). *Digital Design and Computer Architecture. From Gates to Processors*. Morgan Kaufmann.
- Intel. (2011, 5). *2nd Generation Intel Core Processor Family Desktop Datasheet, Vol. 1*. Retrieved from <http://www.intel.com/content/www/us/en/processors/core/2nd-gen-core-desktop-vol-1-datasheet.html>
- Intel. (2011, 6). *Intel Core2 Extreme Quad-Core Processor QX6000 Sequence and Intel Core2 Quad Processor Q6000 Sequence Datasheet*. Retrieved from <http://download.intel.com/design/processor/datashts/31559205.pdf>
- Microsoft. (2011). *Microsoft Developer Network*. Retrieved from <http://msdn.microsoft.com/en-us/ms348103>
- Nokia. (2008-2011). *QT 4.7 reference Documentation*. Retrieved from <http://doc.qt.nokia.com/4.7/index.html>
- Sondag, T. R. (2009). *Phase-guided thread-to-core assignment for improved utilization of performance-asymmetric multi-core processors*. Iowa: ACM.
- Tanenbaum, A. S. (2003). *Moderne Betriebssysteme*. München: Pearsons Studium.
- Tanenbaum, A. S. (2006). *Computerarchitektur*. München: Pearsons Studium.

THE STUDY OF A DETERIORATING MANUFACTURING SYSTEM USING SIMULATION AND RESPONSE METHODOLOGY

Kouedeu Annie Francie^(a), Kenne Jean-Pierre^(a), Dejax Pierre^(b), Songmene Victor^(a)

^(a)Mechanical Engineering Department, Laboratory of Integrated Production Technologies, University of Quebec, École de Technologie Supérieure, 1100, Notre Dame Street West, Montreal (Quebec), Canada, H3C 1K3

^(b)Department of Automatic Control and Industrial Engineering, Optimization of Logistic Systems, École des Mines de Nantes, La Chantrerie 4, Rue Alfred Kastler PO Box 20722 - 44307 Nantes Cedex 3 – France

^(a)Jean-Pierre.Kenne@etsmtl.ca, ^(b)pierre.dejax@mines-nantes.fr

ABSTRACT

A deteriorating production system consisting of two parallel machines with the production dependent failure rates of the machine is investigated in this paper. The machines produce one type of final products. The demand rate for the final commodity is constant and unmet demand is backlogged. The goal of the control problem is to find the production rates of both machines so as to minimize a long term average expected cost which penalizes both the presence of waiting customers and the inventory. In the proposed model, the production rate of the first machine is higher than the production rate of the second machine. The failure rate of the first machine which is the main machine depends on its production rate. The failure rate of the second machine is constant. The proposed model is based on a Markov decision process, and the stochastic dynamic programming method is used to obtain the optimality conditions. Control policy parameters are obtained by combining analytical modelling, simulation experiments and response surface methodology. Sensitivity analyses of the optimal results with respect to the system parameters are also examined to illustrate the importance and effectiveness of the proposed methodology. The usefulness of the proposed approach is outlined for more complex situations where the system must deal with non-exponential failure and multiple machines.

Keywords: production planning, stochastic dynamic programming, numerical methods, simulation

1. INTRODUCTION

Due to the constant search for increased productivity, a better service to clients, the number of scientific publications in the field of failure prone manufacturing systems has been steadily growing.

This paper investigates a stochastic deteriorating production system consisting of two parallel machines with the production rate-dependent failure rates of the machine. The stochastic nature of the system is due to machines that are subject to random breakdowns and

repairs. The machines produce one part type; whenever a breakdown occurs, a corrective maintenance is performed to restore the machines to its operational mode. Our objective is to find the production rates of the different machines so as to minimize a long term average expected cost including inventory and backlog costs. To solve the optimization problem of this paper, we propose a stochastic programming formulation of the problem and derive the optimal production policies numerically. Control policy parameters are obtained combining analytical modelling, simulation experiments and response surface methodology.

An overview of relevant literature reveals that significant contributions have been proposed based on: two parallel machines manufacturing systems (Sajadi et al. 2011), one machine with the failure rate depends on the production rate (Martinelli 2010) and a combination of the control theory and the simulation-based experimental design (Gharbi et al. 2011). This paper's main contribution lies in the study of a stochastic manufacturing system consisting of two parallel machines with the production dependent failure rates of the main machine.

A common feature of this paper is that the policies are of the hedging point type and depend on multiple thresholds. The methodology presented in this paper can be applied in the machining mechanical parts industry where there are many different parallel machines. Some of them are classical machines (constant failure rates) and the others are degraded (if they work at faster rates, they are more likely to fail).

2. STATEMENT OF THE PROBLEM

As illustrated in Figure 1, the manufacturing system studied consists of two parallel machines producing one part type denoted M_1 and M_2 . The machines are subject to random breakdowns and repairs. The repair rate is constant. The maximum production rates of machines are known and the demand for finished products is deterministic. The failure rate of M_1 which is the main machine (machine whose production rate is the highest) depends on its production rate. Then, when this machine

works at a faster rate, it is more likely to fail. In contrast, the failure rate of the second machine is constant. We assumed that M_2 can't meet the customer demand alone. The stochastic nature of the system is related to breakdowns and repairs of machines.

The state of the machines can be classified as:

- state 1 (mode 1): M_1 and M_2 are operational
- state 2: M_1 is operational and M_2 is under repair
- state 3: M_1 is under repair and M_2 is operational
- state 4: M_1 and M_2 are under repair.

We use $\xi(t)$ to denote the state of the machines with value in $B = \{1, 2, 3, 4\}$. The dynamic of the system is described by a discrete element $\xi(t)$ and a continuous element $x(t)$. The discrete element represents the status of the machines and the continuous one, the stock level. It can be positive for an inventory or negative for a backlog.

The discrete part of the system is a continuous time Markov process, with a transition rate from state α to state β denoted by $q_{\alpha\beta}^\theta$ with $\alpha, \beta \in B$. For the considered system, the corresponding 4×4 transition matrix $Q = [q_{\alpha\beta}^\theta]$ is one of an ergodic process as defined in Ross (2003).

We assume that the failure rate of the 1st machine depends on its production rate and is defined by:

$$\begin{aligned} q_{12}^{11} & \text{ if } u_1 \in (U, u_{1\max}] \\ q_{12}^{12} & \text{ if } u_1 \in [0, U] \end{aligned} \quad (1)$$

with $q_{12}^{11} \geq q_{12}^{12} \geq 0$ and $0 \leq U \leq u_{1\max}$

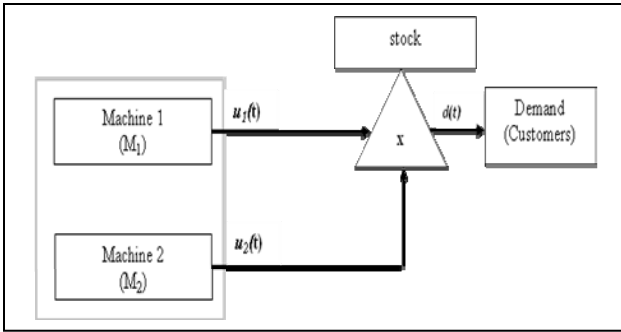


Figure 1: System under study

The transition rates verify the following conditions:

$$q_{\alpha\beta}^\theta \geq 0 \quad (\alpha \neq \beta) \quad (2)$$

$$q_{\alpha\alpha}^\theta = -\sum_{\beta \neq \alpha} q_{\alpha\beta}^\theta \quad (3)$$

The transition probabilities are given by:

$$P[\xi(t+\delta t) = \beta | \xi(t) = \alpha] = \begin{cases} q_{\alpha\beta}^\theta(\cdot) \delta t + o(\delta t) & \text{if } \alpha \neq \beta \\ 1 + q_{\alpha\alpha}^\theta(\cdot) \delta t + o(\delta t) & \text{if } \alpha = \beta \end{cases} \quad (4)$$

$$\text{with } \lim_{\delta t \rightarrow 0} \frac{o(\delta t)}{\delta t} = 0 \text{ for all } \alpha, \beta \in B.$$

Let $u_1(t)$ and $u_2(t)$ denote the production rates of M_1 and M_2 respectively, in mode α and at time t . The set of the feasible control policies $A(\alpha)$, including $u_1(\cdot)$ and $u_2(\cdot)$ depends on the stochastic process $\xi(t)$ and is given by:

$$A(\alpha) = \left\{ \begin{aligned} & (u_1(\cdot), u_2(\cdot)) \in \mathfrak{R}^2, 0 \leq u_1(\alpha, \cdot) \leq u_{1\max}, \\ & 0 \leq u_2(\alpha, \cdot) \leq u_{2\max} \end{aligned} \right\} \quad (5)$$

where $u_1(\cdot)$ and $u_2(\cdot)$ are known as control variables, and constitute the control policies of the problem under study.

The continuous part of the system dynamics is described by the following differential equation:

$$\frac{dx(t)}{dt} = u_1(t) + u_2(t) - d, \quad x(0) = x \quad (6)$$

Let $g(\cdot)$ be the cost rate defined as follows:

$$g(\alpha, x, \cdot) = c^+ x^+ + c^- x^- \quad (7)$$

The constants c^+ and c^- (\$ per parts per unit of time) are used to penalize inventory and backlog respectively, $x^+ = \max(0, x)$, $x^- = \max(-x, 0)$

The problem here is to control the production rates of the both machines. The performance criterion considered is the expected discounted cost $J(\cdot)$ given by:

$$J(\alpha, x, u_1, u_2) = E \left\{ \int_0^\infty e^{-\rho t} g(\alpha, x, \cdot) dt \right\} \quad (8)$$

$| x(0) = x, \xi(0) = \alpha$

where ρ is the discount rate. The value function of such a problem is defined as follows:

$$v(\alpha, x) = \inf_{(u_1(\cdot), u_2(\cdot)) \in A(\alpha)} J(\alpha, x, u_1, u_2) \quad \forall \alpha \in B \quad (9)$$

In Appendix A, we present the optimality conditions and the numerical methods used to solve them for the value function $v(\cdot)$ given by equation (9). The contribution of this research to the Hamilton-Jacobi-Bellman (HJB) equations is that in the modes 1 and 2 where M_1 is operational, we have four equations instead of two equations in the case of a manufacturing system without production rate dependent failure rate (see equations A.3 and A.4). The next section provides a numerical example to illustrate the structure of the control policies.

3. NUMERICAL RESULTS AND SENSITIVITY ANALYSES

3.1. Numerical results

In this section, we present a numerical example for the manufacturing system presented in Section 2. A four-state Markov process with the modes in $B = \{1, 2, 3, 4\}$ describes the system capacity. The instantaneous cost is described by equation (7).

The considered computation domain D is given by:

$$D = \{x : -20 \leq x \leq 40\} \quad (10)$$

The condition to meet the customer demands, over an infinite horizon and reach a steady state is given by:

$$\begin{cases} \pi_1 \cdot (u_{1\max} + u_{2\max}) + \pi_2 \cdot u_{1\max} + \pi_3 \cdot u_{2\max} > d \\ \pi_1 \cdot (U + u_{2\max}) + \pi_2 \cdot U + \pi_3 \cdot u_{2\max} > d \end{cases} \quad (11)$$

Table 1: Parameters of numerical example

c^+	c^-	h	U	$u_{1\max}$	$u_{2\max}$	d_1	d_2	d	q_{12}^{11}	q_{12}^{12}	q_{12}^2	q_{21}^1	q_{21}^2	ρ	q_{12}^{11}
1	100	0.5	0.70	1.2	0.65	0.5	0.5	1	0.03	0.02	0.04	0.1	0.2	0.5	0.3

Figures 2 and 3 represent the production rates at mode 1 of machines M_1 and M_2 respectively. In these figures, we can see that the thresholds z_1 and z_3 are low because both machines are operational. The results of Figure 3 suggest that as the inventory level approaches a hedging point level, it may be beneficial to decrease the production rate to gain in reliability. Figures 2 and 3 show that the production rates are set to zero for comfortable stock levels. Then, there is no need to produce parts for comfortable stock levels. From the results obtained, the computational domain of Figure 3 (M_2) is divided into three regions as in Akella and Kumar (1986) and references therein. However, the computational domain of Figure 2 is divided into four regions. This is the main contribution of this paper. The optimal production control policy consists of one of the following rules:

1. Set the production rate of M_1 to its maximal value when the current stock level is under the first threshold value ($z_1 = 0.0$);
2. Reduce the production rate of M_1 to its minimal value when the current stock level approaches the second threshold value ($z_2 = 13.0$);
3. Set the production rate of M_1 to the demand rate when the current stock level is equal to the second threshold value;
4. Set the production rate of M_1 to zero when the current stock level is larger than the second threshold value.

Where $(\pi_1, \pi_2$ and $\pi_3)$ are the limiting probability at the operational modes of the machines. Note that the limiting probabilities of modes 1, 2, 3 and 4 (i.e., π_1, π_2, π_3 and π_4), are computed as follows:

$$\pi \cdot Q(\cdot) = 0 \quad \text{and} \quad \sum_{i=1}^4 \pi_i = 1 \quad (12)$$

where $\pi = (\pi_1, \pi_2, \pi_3, \pi_4)$ and $Q(\cdot)$ is the corresponding 4×4 generator matrix. Table 1 summarizes the parameters of the numerical example for which the feasibility conditions given by equation (11) are satisfied.

The control policies obtained are the multi-hedging point policies. As shown within the numerical results and in Figure 2 and 3, the optimal production rates can be expressed as follows:

$$u_1(x, 1) = \begin{cases} u_{1\max} & \text{if } x < z_1 = 0.0 \\ U & \text{if } z_1 \leq x < z_2 = 13.0 \\ d_1 & \text{if } x = z_2 \\ 0 & \text{if } x > z_2 \end{cases} \quad (13)$$

where z_1 and z_2 are the first and second optimal threshold values of M_1 respectively.

$$u_2(x, 1) = \begin{cases} u_{2\max} & \text{if } x < z_3 = 1.5 \\ d_2 & \text{if } x = z_3 \\ 0 & \text{if } x > z_3 \end{cases} \quad (14)$$

where z_3 is the optimal threshold value of M_2 .

Unlike in Figure 2 where the tendency was to use less the maximal production rate of the first machine, Figure 4 shows that the first threshold ($z_4 = 1.0$) is higher than the case of Figure 2 because the machine works alone. However, the control policy is still a multi-hedging point policy and is defined by:

$$u_1(x, 2) = \begin{cases} u_{1\max} & \text{if } x < z_4 = 1.0 \\ U & \text{if } z_4 \leq x < z_5 = 7.5 \\ d_1 & \text{if } x = z_5 \\ 0 & \text{if } x > z_5 \end{cases} \quad (15)$$

where z_4 and z_5 are the first and second optimal threshold values of M_1 respectively.

Using the control policies given by equations (13), (14) and (15), the company will be able to take into account the availability of machines. Then, it can minimize the total cost due to failure of machines, allowing it to eventually maximize its total profit. The next section analyses the sensitivity of the policies obtained and several experimentations are conducted to ensure that the structure of the obtained policy is maintained and can be considered as a generalized policy for the general problem under study.

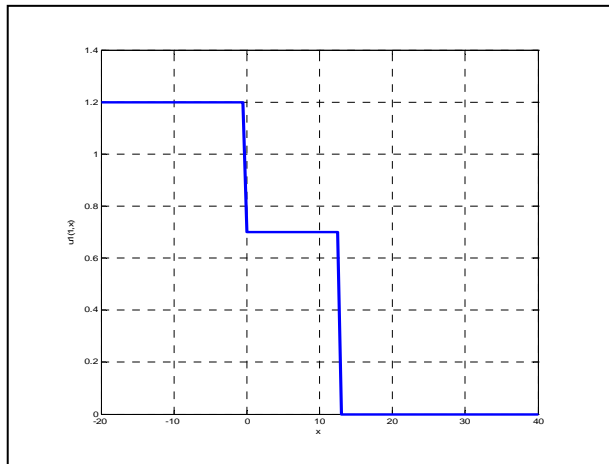


Figure 2: Production rate of M_1 at mode 1

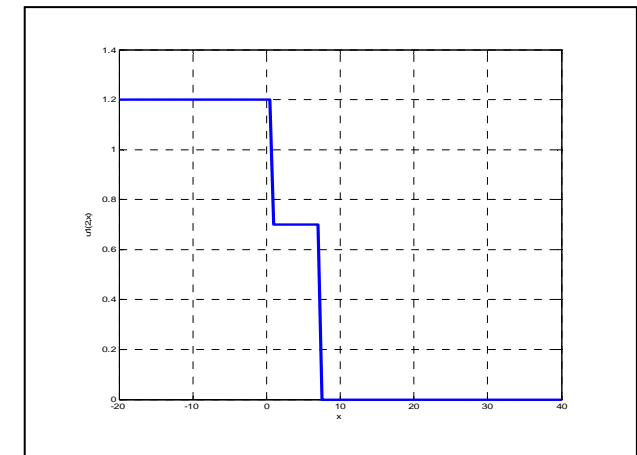


Figure 4: Production rate of M_1 at mode 2

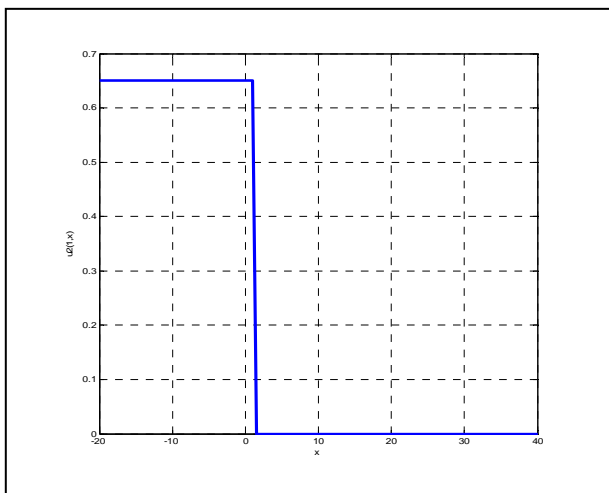


Figure 3: Production rate of M_2 at mode 1

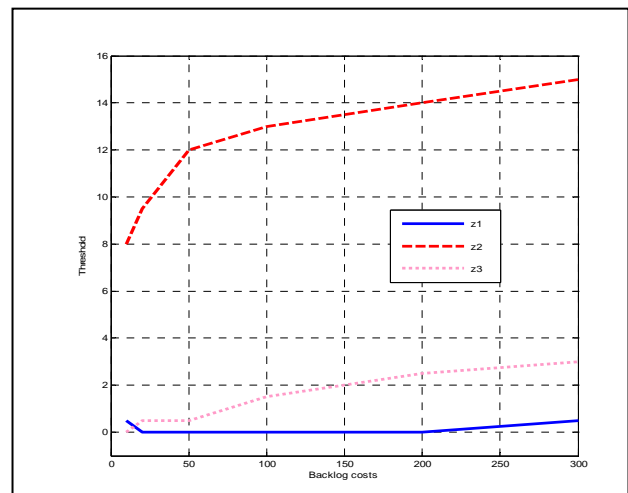


Figure 5: Threshold value at mode 1 versus backlog costs

3.2. Sensitivity analyses

A set of numerical examples are considered to measure the sensitivity of the obtained control policies and to illustrate the contribution of this paper. The sensitivity of the control policies is analyzed according to the variation of the backlog costs.

The results presented in Figures 5 and 6 show the behavior of the production rates of machines according to the variation of backlog costs. Based on these results, we can see that the value of the backlog costs is not too much impact the threshold z_1 . This is logical because at

mode 1, when both machines are operational, it was less use a first machine to its maximal production rate to take into account its reliability. The thresholds z_2 and z_3 increase in order to avoid further backlog costs. However, z_3 is far less than z_2 . Thus, it does not use the second machine a lot when both machines are producing. One prefers to use M_1 to its minimal production rate because the failure rate depends on the rate of production (for a low production rate, the probability to fail is low).

Figure 6 shows that the threshold values of M_1 at mode 2 increase as the backlog costs increase. We therefore need a lot of parts in stock to avoid further backlog costs.

Through the observations made from the sensitivity analysis, it clearly appears that the results obtained make sense and confirm and validate the proposed approach. It shows the usefulness of the proposed model given that the control policies move as predicted, from a practical view point.

4. PROPOSED SIMULATION BASED OPTIMAL APPROACH

The results from traditional methods of planning in the environment of manufacturing systems are not sufficient to reach a comfortable level of desired performances. To improve these methods, a combination of the control theory and the simulation-based experimental design, as in Gharbi et al. (2011), is used to obtain a near-optimal control policy. This could allow the possibility of developing more realistic cases. To quantify the policy, which structure is given by analytical model, simulation model are combined with experimental design and response surface methodology to estimate the optimal values of the policy's parameters. In the case of non-exponential failure distribution, the quantification parameters are also possible with the help of the simulation model, which can easily take into account the nature of any probability distributions. The incurred cost is then given by simulation model which affects the response surface model.

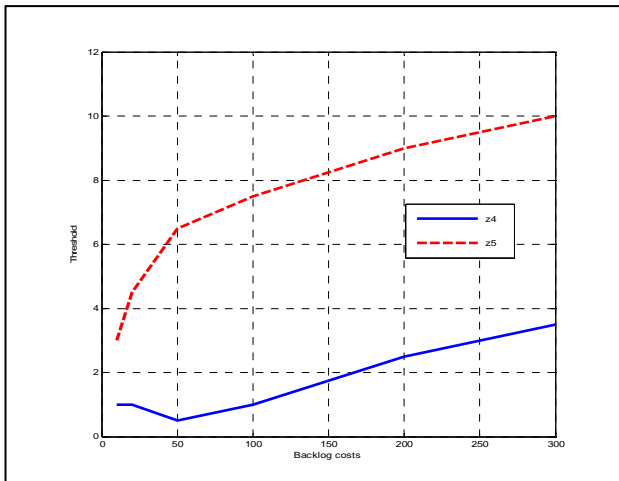


Figure 6: Threshold value at mode 2 versus backlog costs

5. SIMULATION MODEL

A discrete event simulation model that described the dynamics of the system is developed using Arena software (Arena is a powerful modeling and simulation software tool that allows the user to construct a simulation model run experiments. It generates several reports as a result of a simulation run). In order to obtain the cost of the system for a given set of input factors, the behavior of the system is simulated following the diagram shown in Figure 7 with the following block descriptions:

1. The *initialization* block sets the values of threshold (z_1, z_2 and z_3), the demand rate (d), and the machines parameters ($U, u_{1\max}, u_{2\max}, q_{12}^{11}, q_{12}^{12}, q_{12}^2, q_{21}^1$ and q_{21}^2), etc. The simulation time T_{sim} is also assigned at this step.

2. The *arrival demand* block performs the arrival of the demand for the production system at each $1/d$ unit of time. Verification is then performed on the inventory values. The inventory or the backlog level is then updated.

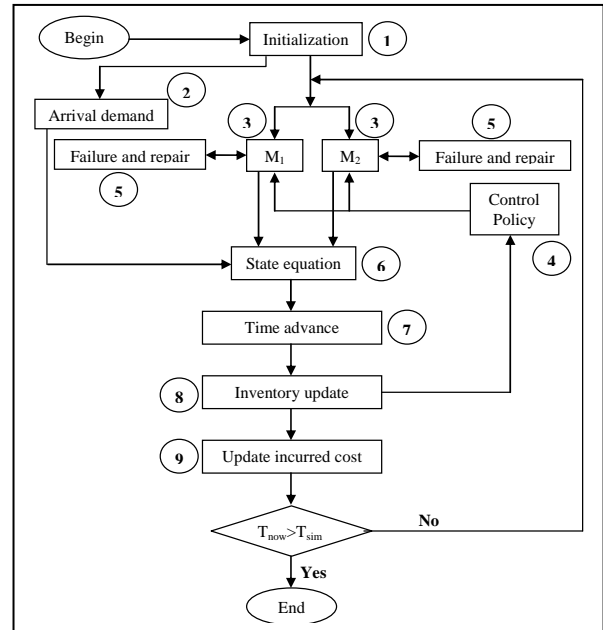


Figure 7: Diagram of simulation model

3. The M_1 and M_2 blocks represent the main machine and the second machine respectively. The machines are subject to random failures and repairs.
4. The *control policy* block is defined in Section 3 (Equations 13-15) for the system production rates. The control policy is given by the output of the inventory update block. This block permanently sends signals to verify the variation in the stock level $x(t)$.
5. The failure and repair blocks sample the times to failure ($MTBF_1$ and $MTBF_2$ of M_1 , and $MTBF_3$ of M_2) and time to repair $MTTR_1$ ($(q_{21}^1)^{-1}$) and $MTTR_2$ ($(q_{21}^2)^{-1}$) of the first machine and the second machine respectively.
6. The *state equation* is given by (5). It describes the inventory and backlog variables using the production rates set by the control policy and the variables from the failures and repairs of machines M_1 and M_2 .
7. The *time advance* block uses an algorithm provided by simulation software. It is a combination of discrete event scheduling (failures and repairs), continuous variable threshold crossing events and time step specifications.
8. The *inventory update* block updates inventories when a unit is produced or when a unit of demand for the final product occurs.

9. The *update occurred cost* block calculates the average total costs according to the levels of the inventory and backlog variables (x^+ and x^-), their corresponding costs (c^+ and c^-) and which machine is producing (M_1 and/or M_2).

The simulation runs until the current time T_{now} reaches the simulation horizon T_{sim} , which is the time needed to reach the steady state. We perform five replications of the simulation model.

6. EXPERIMENTAL DESIGN AND RESPONSE SURFACE METHODOLOGY

Given that an optimal solution of the stochastic control problem described in Section 2 exists and given the convexity property of the cost function, we define three levels for each factor to obtain a convex estimated cost function. For these reasons, a complete 3^3 experimental design and a second-order response surface model were proposed.

6.1. Numerical example

For the numerical example experiment in this section, the following values are used:

$$d = 1 \text{ units/UT}, u_{1\text{max}} = 1.2 \text{ units/UT}, U = 0.7 \text{ units/UT}, \\ u_{2\text{max}} = 0.65 \text{ units/UT}, (q_{12}^{11})^{-1} = 33 \text{ UT}, (q_{12}^{12})^{-1} = 50 \text{ UT}, \\ (q_{12}^{21})^{-1} = 25 \text{ UT}, (q_{21}^1)^{-1} = 10 \text{ UT}, (q_{21}^2)^{-1} = 5 \text{ UT}, \\ c^+ = 10 \text{ \$/unit/UT}, c^- = 100 \text{ \$/unit/UT}.$$

We also defined a new variable $a = \frac{z_1}{z_2}$ with

$0 \leq a \leq 1$ to ensure that the constraint $z_1 < z_2$ is respected. The minimum and maximum values of z_2 and z_3 were first observed using simulation experiments. The independent variable levels were then chosen as presented in Table 2.

Table 2: Level of independent variables

Factors	Low level	High level
a	0	1
z_2	0	20
z_3	0	20

We selected a 3^3 response surface design since we have three independent variables at three levels each. This design leads to the completion of 81 ($3^3 \times 3$) experimental trials. To ensure that the steady state of the cost was achieved, the simulation model was run during 25 000 months for each replication (the simulation was run for 5 replications).

6.2. Results analysis

The statistical analysis of the simulated data consists of the multi-factor analysis of variance (ANOVA). This is done using a statistical software application (STATGRAPHICS) to provide the effects of the three independent variables (z_1, z_2 and z_3) on the dependent variable (Total cost). The ANOVA table for this model is summarized in Table 3. For each main effect, interaction and quadratic effect, Table 3 includes the sum of squares, the degree of freedom (df), the mean square, an F-ratio, computed using the residual mean square, and the significance level of the P-value. The factors, the quadratics effects and the interactions were considered significant at p-values less than 5% ($p < 0.05$). The

R_{adjusted}^2 value of 0.9231 from the ANOVA table states that more than 92% of the total variability is explained by the model (Montgomery 2005).

Table 3: ANOVA table

	Sum of squares	d.f	Mean square	F-ratio	P-value
a	1117,93	1	1117,93	1,28	0,2625
z_2	504600,	1	504600,	576,09	0,0000
z_3	17077,3	1	17077,3	19,50	0,0000
aa	5586,24	1	5586,24	6,38	0,0139
az_2	1840,41	1	1840,41	2,10	0,1517
az_3	43597,4	1	43597,4	49,77	0,0000
z_2z_2	254185,	1	254185,	290,19	0,0000
z_2z_3	1592,01	1	1592,01	1,82	0,1820
z_3z_3	22071,0	1	22071,0	25,20	0,0000
Total error	60437,9	69	875,912		
Total (corr.)	912105,	80			
$R_{\text{adjusted}}^2 = 92,32\%$ ($z_1 = a * z_2$)					

The residual analysis was used to verify the adequacy of the model. A residual versus predicted value plot and normal probability plot were used to test the homogeneity of the variances and the residual normality, respectively. It can be concluded that the model is satisfactory. Due to the convexity property of the value function, the second-order response surface method was selected. The third-order interactions and all other effects were ignored. The estimated second-order model of the total cost is given by:

$$J = 5373,144 - 145,567 \cdot a - 33,4833 \cdot z_2 - 11,5967 \cdot z_3 + 70,4667 \cdot a^2 + 1,43 \cdot a \cdot z_2 + 6,96 \cdot a \cdot z_3 + 1,18833 \cdot z_2^2 - 0,0665 \cdot z_2 \cdot z_3 + 0,350167 \cdot z_3^2 \quad (16)$$

The projection of the corresponding cost response surfaces onto two-dimensional planes are presented in Figures 8(a) and 8(b). The minimum of the cost function,

$J^* = 45,03$ is located at $z_2^* = 11,31$, $a^* = 0,477$ ($z_1^* = 5,39$), $z_3^* = 10,31$. These values define the best values to be applied to the manufacturing system considered.

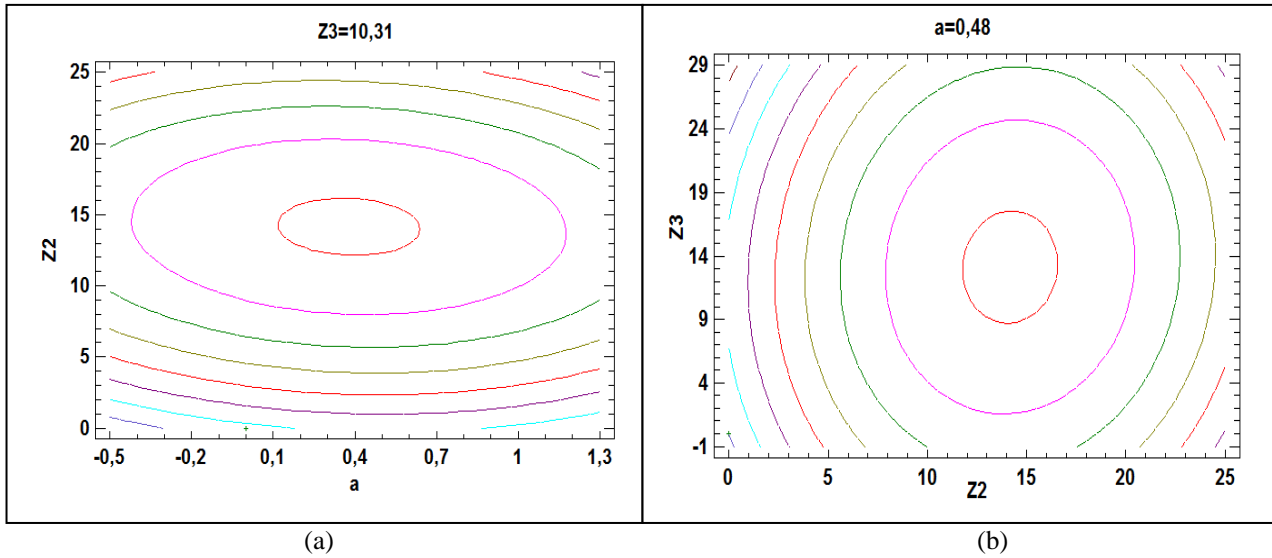


Figure 8: Contour plot of the response surface

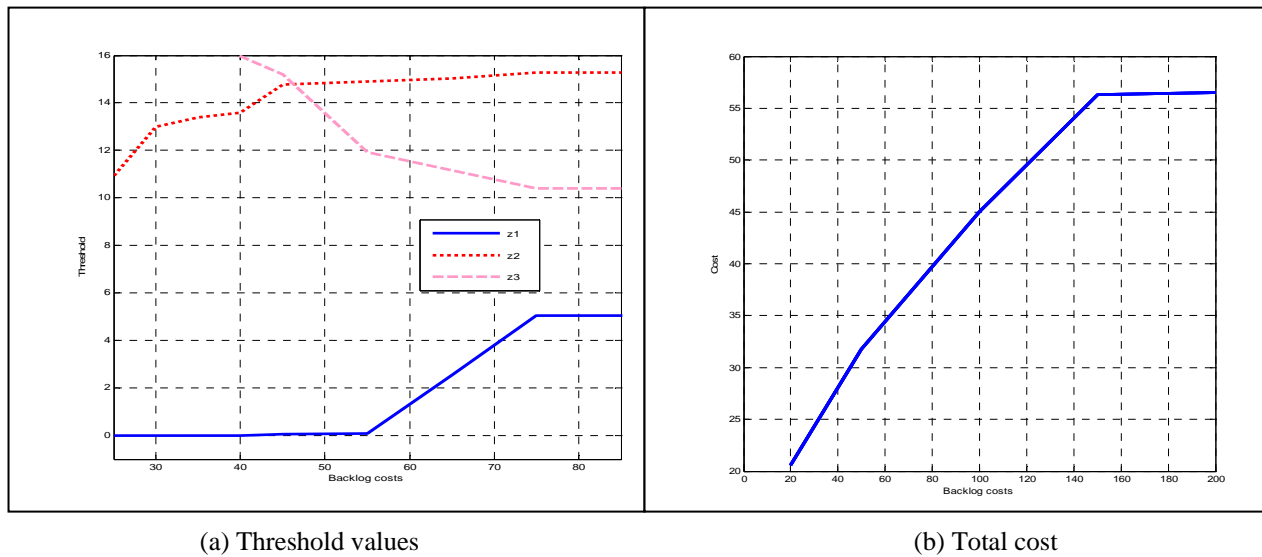


Figure 9: Trend of threshold values and total cost versus backlog costs

6.3. Sensitivity analysis

Another set of experiments is considered to measure the sensitivity of the obtained control policy with respect to backlog costs (i.e. c^-). The following variations, illustrated in Figure 9 ((a) and (b)) are explored and compared to the basic case ($c^- = 100$).

The results show that when the backlog costs decrease, the threshold levels of M_1 (z_1^* and z_2^*) decrease

in order to avoid further inventory costs, z_3^* increases. Consequently, when both machines are operational, the first machine has to work less to take into account its reliability. The overall cost decrease. Increasing c^- results in a tendency to increase the threshold values z_1^* and z_2^* in order to avoid further backlog costs. The total cost also increases and the threshold z_3^*

decreases. Thus, it does not use the second machine a lot when both machines are producing.

It clearly appears that the results obtained and discussed are coherent and confirm the numerical observation in the sense that when a cost decreases (resp. increases), the area where this costs is incurred increases (resp. decreases). But, in the case of the second machine, the chart of z_3 gives the opposite results compared with the numerical method. The simulation-based experimental design suggests using the main machine a lot when the backlog costs increase in order to avoid further backlog costs. We recall that the failure rates of the main machine depend on its production rate. Then, we have the possibility to act on its production rate.

7. CONCLUSION

Hedging point and multiple thresholds hedging point are piecewise constant control policies that can be easily implemented for planning of non-homogeneous Markov failure/repair manufacturing systems. This paper has shown that under such policies, the stock level of manufacturing systems that produce a single part-type can be obtained even when failure rates of the machine depend on the production rate of parts. From the numerical study it has been found that for two parallel machines systems, when the failure rate of the main machine depends on its production rate, the hedging point policies are optimal among feedback policies and the reliability of the machines is enhanced. This result generalizes the results of Akella and Kumar (1986) which are derived for a constant failure rate and the works of Martinelli (2010) which is derived for a single machine with production rate dependent failure rate. To optimise the production policies, an experimental approach based on design of experiments, simulation modelling and response surface methodology has been used. The usefulness of the proposed approach is outlined for more complex situations in which analytical solutions are not easy to obtain. In the future, we plan to extend the proposed model to the reverse logistics (a hybrid manufacturing and remanufacturing system) with production rate dependent failure rates of the remanufacturing machine.

APPENDIX A. OPTIMALITY CONDITIONS AND NUMERICAL APPROACH

The properties of the value function and the manner in which the Hamilton-Jacobi-Bellman (HJB) equations are obtained can be found in Martinelli (2010). He describes the optimal control policies (optimality conditions) for one-machine manufacturing system with production rate dependent failure rates. Regarding the optimality principle, we can write the HJB equations as follows:

$$\rho v(\alpha, x) = \min_{(u_1, u_2) \in A(\alpha)} \left[g(\alpha, x, u_1, u_2) + \sum_{\beta \in B} q_{\alpha\beta}^{\rho} v(\beta, x) + (u_1 + u_2 - d) \frac{\partial v(\alpha, x)}{\partial x} \right] \quad (A.1)$$

where $\frac{\partial v(\alpha, x)}{\partial x}$ is the partial derivatives of the value function $v(\alpha, x)$

The optimal control policies over $A(\alpha)$ of the right hand side of equation (A.1) are $(u_1^*(\cdot), u_2^*(\cdot))$. When the value function described by equation (9) is available, optimal control policies can be obtained as in equation (A.1).

To solve the HJB equations, the numerical method based on the Kushner (1992) approach as in Gharbi et al. (2011) and references therein is used. By approximating $v(\alpha, x)$ by a function $v^h(\alpha, x)$ and the first-order partial

derivative of the value function $\frac{\partial v(\alpha, x)}{\partial x}$ by:

$$\frac{\partial v(x, \alpha)}{\partial x} = \begin{cases} \frac{1}{h} (v^h(\alpha, x+h) - v^h(\alpha, x)) & \text{if } (u_1 + u_2 - d) > 0 \\ \frac{1}{h} (v^h(\alpha, x) - v^h(\alpha, x-h)) & \text{otherwise} \end{cases}$$

the HJB equation becomes:

$$v^h(x, \alpha) = \min_{(u_1, u_2) \in A(\alpha)} \left[\frac{g(x, \alpha, u_1, u_2) + \sum_{\beta \neq \alpha} q_{\alpha\beta}^{\rho} v^h(x, \beta) + \frac{(u_1 + u_2 - d)}{h} \left[v^h(x+h, \alpha) \text{Ind}\{u_1 + u_2 - d \geq 0\} + v^h(x-h, \alpha) \text{Ind}\{u_1 + u_2 - d < 0\} \right]}{\left(\rho + \frac{|u_1 + u_2 - d|}{h} + |q_{\alpha\alpha}^{\rho}| \right)} \right] \quad (A.2)$$

with $q_{\alpha\alpha}^{\rho} = -\sum_{\beta \neq \alpha} q_{\alpha\beta}^{\rho}$, $A^h(\alpha)$ is the numerical control grid

$$\text{and } \text{Ind}\{\Phi\} = \begin{cases} 1 & \text{if } \Phi \text{ is true} \\ 0 & \text{otherwise} \end{cases}$$

The system of equations (A.2) can be interpreted as the infinite horizon dynamic programming equation of a discrete-time, discrete-state decision process, as in Boukas and Haurie (1990). In this paper, we use the value iteration procedure to approximate the value function given by equation (A.2). Charlot et al. (2007) and references therein provide details on such methods.

The discrete dynamic programming equation (A.2) gives the following six equations:

• **state 1**

$$v^h(x,1) = \left\{ \begin{array}{l} \min_{u_2 \in [0, u_{2\max}]} \left[\frac{g(x, \alpha, u_1, u_2) + \frac{(u_1 + u_2 - d)}{h} \left[v^h(x+h,1) \text{Ind}\{u_1 + u_2 - d \geq 0\} + v^h(x-h,1) \text{Ind}\{u_1 + u_2 - d < 0\} \right] + q_{12}^2 v^h(x,2) + q_{12}^{11} v^h(x,3)}{\left(\rho + \frac{|u_1 + u_2 - d|}{h} + q_{12}^2 + q_{12}^{11} \right)} \right] \text{ if } u_1 \in (U, u_{1\max}] \\ \min_{u_2 \in [0, u_{2\max}]} \left[\frac{g(x, \alpha, u_1, u_2) + \frac{(u_1 + u_2 - d)}{h} \left[v^h(x+h,1) \text{Ind}\{u_1 + u_2 - d \geq 0\} + v^h(x-h,1) \text{Ind}\{u_1 + u_2 - d < 0\} \right] + q_{12}^2 v^h(x,2) + q_{12}^{12} v^h(x,3)}{\left(\rho + \frac{|u_1 + u_2 - d|}{h} + q_{12}^2 + q_{12}^{12} \right)} \right] \text{ if } u_1 \in [0, U] \end{array} \right.$$

(A.3)

• **state 2**

$$v^h(x,2) = \left\{ \begin{array}{l} \min \left[\frac{g(x, \alpha, u_1) + \frac{(u_1 - d)}{h} \left[v^h(x+h,2) \text{Ind}\{u_1 - d \geq 0\} + v^h(x-h,2) \text{Ind}\{u_1 - d < 0\} \right] + q_{21}^1 v^h(x,1) + q_{12}^{11} v^h(x,4)}{\left(\rho + \frac{|u_1 - d|}{h} + q_{21}^1 + q_{12}^{11} \right)} \right] \text{ if } u_1 \in (U, u_{1\max}] \\ \min \left[\frac{g(x, \alpha, u_1) + \frac{(u_1 - d)}{h} \left[v^h(x+h,2) \text{Ind}\{u_1 - d \geq 0\} + v^h(x-h,2) \text{Ind}\{u_1 - d < 0\} \right] + q_{21}^2 v^h(x,1) + q_{12}^{12} v^h(x,4)}{\left(\rho + \frac{|u_1 - d|}{h} + q_{21}^2 + q_{12}^{12} \right)} \right] \text{ if } u_1 \in [0, U] \end{array} \right.$$

(A.4)

- **state 3**

$$v^h(x,3) = \min_{u_2 \in [0, u_{2\max}]} \left[\frac{g(x, \alpha, u_2) + \frac{(u_2 - d_2)}{h} \left[v^h(x+h,3) \text{Ind}\{u_2 - d_2 \geq 0\} + v^h(x-h,3) \text{Ind}\{u_2 - d_2 < 0\} \right] + q_{21}^1 v^h(x,1) + q_{12}^2 v^h(x,4)}{\left(\rho + \frac{|u_2 - d_2|}{h} + q_{21}^1 + q_{12}^2 \right)} \right]$$

(A.5)

- **state 4**

$$v^h(x,4) = \min \left[\frac{g(x,\alpha) + q_{21}^1 v^h(x,2) + q_{21}^2 v^h(x,3) + \frac{d}{h} v^h(x-h,4)}{\left(\rho + \frac{d}{h} + q_{21}^1 + q_{21}^2 \right)} \right] \quad (\text{A.6})$$

REFERENCES

- Akella, R. and Kumar, P. R., 1986. Optimal control of production rate in a failure prone manufacturing system. *IEEE Transactions on Automatic Control* 31, 116-126.
- Boukas, E. K. and Haurie, A., 1990. Manufacturing flow control and preventing maintenance: a stochastic control approach. *IEEE Transactions on Automatic Control* 35, 1024-1031.
- Charlot, E., Kenne, J. P. et al. 2007. Optimal production, maintenance and lockout/tagout control policies in manufacturing systems. *International Journal of Production Economics* 107 (2), 435-450.
- Gharbi, A., Hajji, A. et al. 2011. Production rate control of an unreliable manufacturing cell with adjustable capacity. *International Journal of Production Research* 49 (21), 6539-6557.
- Kenné, J.-P., Dejax, P. et al. 2012. Production planning of a hybrid manufacturing-remanufacturing system under uncertainty within a closed-loop supply chain. *International Journal of Production Economics* 135 (1), 81-93.
- Kushner, H. J. a. D. J., 1992. *Numerical Methods for Stochastic Control Problems in Continuous Time*.
- Martinelli, F., 2010. Manufacturing systems with a production dependent failure rate: Structure of optimality. *IEEE Transactions on Automatic Control* 55 (10), 2401-2406.
- Montgomery, D.C., 2005. *Design and analysis of experiments*. New York: John Wiley & Sons.
- Ross, S. M., 2003. *Introduction to probabilities models*. Academic Press : 8e edition.
- Sajadi, S. M., Esfahani, M. M. S. et al. 2011. Production control in a failure-prone manufacturing network using discrete event simulation and automated response surface methodology. *International Journal of Advanced Manufacturing Technology* 53 (1-4), 35-46.

SIMULATING INNOVATION ADOPTION BEHAVIOR: LESSONS LEARNED FOR MODELERS AND PROGRAMMERS

Christian Stummer^(a), Elmar Kiesling^(b)

^(a)Department of Business Administration and Economics, Bielefeld University, Germany

^(b)Institute of Software Technology and Interactive Systems, Vienna University of Technology, Austria

^(a)christian.stummer@uni-bielefeld.de, ^(b)elmar.kiesling@tuwien.ac.at

ABSTRACT

To adopt or not to adopt an innovation is a question that is ultimately answered by individual (prospective) customers. Their behavior is of practical relevance because it drives the market success of new products or services and it also constitutes an interesting area for academic research. In the course of a research project at the University of Vienna we have developed an agent-based simulation to investigate this topic. During the initial months, we reviewed numerous tools (i.e., frameworks and modeling environments) for this purpose. In this paper we share experiences we made in this respect as well as later on when implementing the simulation tool.

Keywords: agent-based modeling, innovation adoption behavior, frameworks and modeling environments, lessons learned

1. INTRODUCTION

The prosperity and long-term survival of many firms hinge on their ability to systematically develop new products and introduce them into market successfully. Both challenges require considerable amounts of resources, which is why practitioners have a strong interest in the projection of an innovation's potential market diffusion. Agent-based simulation can capture the complex diffusion process of an innovation on the macro-level as a result of relatively simple micro-level interactions between heterogeneous individuals (who, for example, exchange information within their social network through word-of-mouth); for a recent review of agent-based diffusion models confer Kiesling et al. (2012). This notion was the starting point for a research project on quantitatively simulating and modeling the diffusion of innovations ("QuaSiMoDI"). The endeavor was financed by the Austrian Research Fund and ran from 2008 to 2011.

The simulation model that resulted from the project contributes to innovation diffusion research in that it covers all phases of the purchasing process (ranging from receiving initial information to post-purchase product experiences), takes into account initial adoption as well as repeat purchases, allows for several suppliers, accounts for temporal as well as spatial aspects, and

considers heterogeneous consumer preferences with respect to multiple product attributes.

Furthermore, emphasis has been placed on illustrating the applicability of our work by referring to a real product (i.e., a second generation biofuel that is currently under development at the Vienna University of Technology) for a particular market (i.e., Austria). Results therefore may also be useful for practitioners interested in this particular technology, because simulation experiments for several scenarios (each with its own strategy for price, communication, and roll-out) were based on real data. Also policy-makers could benefit from such simulations that enable them to assess the impact of diverse (e.g., fiscal) measures to further the diffusion of biofuels and contribute to environmental objectives. For descriptions of previous versions of the simulation confer Kiesling et al. (2009), Kiesling et al. (2010), and Günther et al. (2011).

In addition to researchers and practitioners, a third group of stakeholders may benefit from experiences gained in the QuaSiMoDI project, namely modelers and programmers who are about to embark on a similar project. It is particularly them this paper is targeted.

In the remainder we will therefore elaborate on modeling and implementation issues. First, we provide an overview of alternative frameworks that we considered as a basis for the implementation of our agent-based simulation model (Section 2). Next, we describe the platform and tools actually used (Section 3). Then, we outline the architecture of our software implementation (Section 4). Finally, we mention some general lessons learned from the research project that may be of value for modelers and programmers starting a similar endeavor (Section 5).

2. SURVEY OF AGENT-BASED SIMULATION TOOLS

In recent years, the incursion of agent-based approaches in many scientific disciplines has entailed the development of increasingly sophisticated software-platforms for agent-based modeling and simulation. Today, a modeler selecting a platform for the implementation of an agent-based model is therefore faced with an abundant range of programming languages, libraries, frameworks, and modeling environments to choose

from. In the following, we outline the basic types of available options.

2.1. Programming languages

A basic but viable approach is to implement agent-based models with “plain” general purpose programming languages rather than relying on specialized software tools. Early agent-based models were typically implemented independently following this approach (Gilbert 2002). Today, programming the whole simulation software “from scratch” still appears to be a relatively common approach, even though it leads to duplication of efforts and forces modelers working on different models to repeatedly implement the same basic functionality and algorithms. This process is error-prone, may lead to code that is not easily accessible, and impedes verification of the implementation. Object-oriented languages such as Java or C++ are typically used because core concepts like encapsulation, inheritance, and abstraction fit the agent-based modeling paradigm well. Types of agents are implemented as classes; particular agents are instances (i.e., objects) of these classes that have an internal state: agents’ interactions with one another and their environment are implemented as methods of the agent classes.

Somewhat less common approaches build agent-based simulations on top of computational mathematics systems such as Mathematica (Wolfram Inc. 2012) or Matlab (Math-Works 2012), procedural languages (e.g., StarLogo, cf. Resnick 1996), functional languages (Legéndi et al. 2009), or spreadsheet software (Macal and North 2007).

2.2. Libraries and toolkits

Specialized libraries and toolkits that provide dedicated facilities for agent-based simulation offer modelers a number of significant advantages over implementing a model from scratch. First, they provide standard mechanisms that are frequently required in agent-based modeling, such as scheduling, event handling, random number generation, network modeling, logging, visualization, and analysis. As a consequence, the resulting code can be more compact, accessible and easier to verify than custom implementations that involve large amounts of “boilerplate” code. By providing ready-made building blocks, standardized libraries can assist modelers and ideally save them time, effort, and energy.

2.3. Modeling environments

While libraries may assist modelers with only limited programming skills, they still require sufficient fluency in the underlying programming language. Modeling environments, by contrast, provide an entire graphical model building interface and allow modelers to assemble building blocks visually or with very limited syntax. They may therefore alleviate this limitation or require no programming at all. Such environments include, for example, Repast S (repast.sourceforge.net), StarLogo (education.mit.edu/starlogo), Eclipse Agent Modeling Framework (www.eclipse.org/amp), NetLogo

(ccl.northwestern.edu/netlogo), and Anylogic (www.xjtek.com/anylogic). The main disadvantage of all-encompassing modeling environments is that they may impose assumptions upon the model and limit the modeler’s ability to control detailed aspects of the simulation.

2.4. Prior Reviews

Several authors have reviewed available libraries and environments for agent-based simulation in the past. In an early survey, Gilbert (2002) provide a brief overview of the toolkits available at that time and compare the state of development of software tools for agent-based simulation to the early stages of development of statistical software. Tobias and Hofmann (2004) evaluate free Java-libraries for social agent-based simulation, comparing nineteen different characteristics across the four platforms taken into account, and conclude that the Repast environment (North, Collier, and Vos 2006) was the most advanced of the libraries at the time of the review. Railsback et al. (2006) review four main platforms (NetLogo, Mason, Repast, Swarm) and compare them by implementing a template “StupidModel” at various levels of sophistication in each of them. In total, they discuss sixteen intentionally simplified template models, and provide full specifications for all of them. Isaac (2011) refines these template models and provides implementations in Python, which the authors deem highly readable and more compact than implementations in other languages. Castle and Crooks (2006) examine eight simulation platforms, focusing particularly on evaluating geospatial capabilities. The most extensive survey to date was conducted by Nikolai and Madey (2009). The authors compare five characteristics of 53 toolkits, viz. programming language, operating system support, type of license, primary domain for which the toolkit is intended, and types of support available to the user.

We can conclude this section by asserting that several powerful tools are available to the model builder today. Table 1 summarizes the main contenders considered for the implementation of our innovation diffusion model.

3. PLATFORM AND TOOLS IN QUASIMODI

Several criteria were considered in the selection of tools for the implementation of QuaSiMoDI. First, because the simulation was deployed on a high-performance computing cluster, a platform-independent solution that could be run on various operating systems (Windows, Mac OS X, Linux) was required. Java-based frameworks offer significant advantages in this respect, because the resulting simulation program is portable and can easily be deployed on any computing platform without recompiling the code. Furthermore, the simulation returns consistent results irrespective of the underlying computing architecture, which is not guaranteed when natively compiled code is used. Moreover, almost all available Java-based frameworks can be

Table 1: Selected agent-based simulation frameworks

Framework	Website	Language(s)	License	Reviewed in
AnyLogic (Garifullin, Borshchev, and Popkov 2007)	www.xjtek.com/	UML-RT, Java	Proprietary	Castle and Crooks (2006); Nikolai and Madey (2009)
Ascape (Parker, 2001; Inchiosa, 2002)	ascape.sourceforge.net	Java	BSD	Gilbert (2002); Nikolai and Madey (2009)
MASON (Luke et al., 2004)	www.cs.gmu.edu/~eclab/projects/mason/	Java	Academic free, open source	Castle and Crooks (2006); Railsback et al. (2006); Nikolai and Madey (2009)
NetLogo (Tisue and Wilensky, 2004)	ccl.northwestern.edu/netlogo/	NetLogo language	Freeware, not open source	Castle and Crooks (2006); Railsback et al. (2006); Nikolai and Madey (2009)
RePast (v 1-3) (North, Collier, and Vos, 2006)	repast.sourceforge.net/repast_3/index.html	Java (RepastJ), Python (RepastPy), C++, .net (Repast.net)	BSD	Gilbert (2002); Tobias and Hofmann (2004); Castle and Crooks (2006); Railsback et al. (2006); Nikolai and Madey (2009)
Repast S (North et al., 2005)	repast.sourceforge.net/repast_simphony.html	Java, Groovy	BSD	Nikolai and Madey (2009)
StarLogo	education.mit.edu/starlogo	StarLogo language	Freeware, not open source	Gilbert (2002); Castle and Crooks (2006)
Swarm (Minar et al., 1996)	www.swarm.org	Objective C, Java	GPL	Gilbert (2002); Tobias and Hofmann (2004); Castle and Crooks (2006); Nikolai and Madey (2009)

easily complemented with any of the wide array of software libraries available for the Java programming language. As Java is the main programming language for many frameworks (e.g., 42% of the frameworks reviewed by Nikolai and Madey 2009), the number of available options fulfilling the first criterion is large.

Second, the continuous time approach we chose for QuaSiMoDI requires appropriate discrete event mechanisms, i.e., means for maintaining and processing a list of scheduled events. (Note that in such an approach new events can be scheduled for any future point on a continuous timeline, which is why scheduling mechanisms for events within the same “time period” as in discrete time approaches become dispensable.) Because most frameworks are based on a discrete time approach and unfold their full potential only in a discrete time setting, the number of candidate platforms was significantly reduced when this requirement was taken into account.

From the remaining options, we finally chose MASON (Luke et al. 2004), a fast discrete-event multi-agent simulation core written in Java that also provides a fast Mersenne Twister (Matsumoto and Nishimura 1998) implementation for pseudo-random number generation. MASON is open source, lightweight, and can be run without a graphical user interface or visualization on a headless server. It also provides

checkpointing capabilities and allows for simulation runs to be dynamically migrated across platforms.

The simulation was implemented in Java SE6 using several additional libraries and tools as summarized in Table 2. The list includes a number of standard tools, specialized Java libraries that provide functionality required in the simulation, and common tools for statistical analysis of results and automation of the simulation process as outlined in the following sections.

3.1. Basic Java tools

The first group of tools used in the implementation consists of Apache Maven, Apache Commons and Apache Log4j, XStream and JUnit. We used Apache Maven to manage builds and dependencies of the various Java libraries.

Verification of micro-level mechanisms is crucial in agent-based simulations, because implementation errors cannot easily be detected and traced in the simulation’s emergent macro-level output. We therefore conducted extensive unit tests of all major model components and mechanisms on the micro-level with JUnit.

The recording of detailed information results in the generation of a considerable amount of data. Therefore, a flexible logging facility that provides mechanisms to selectively activate or deactivate output at runtime and

that is executed in a separate thread that is independent of the main simulation program can provide significant performance benefits (particularly on multi-core computers). Apache Log4j fulfills these requirements and was used to produce both comma separated output for analysis and optional human readable textual log files.

Finally, we aimed for a highly generic and versatile simulation that is fully configurable at runtime. To this end, all model inputs as well as the configuration of parameters can be performed through human-readable XML files. XStream, a fast XML serializer and deserializer, was used to read these XML files and import parameters into the simulation.

Table 2: Platform, libraries, and tools used

Component	Website	Purpose
Java SE6	java.sun.com	Implementation of the simulation
MASON	www.cs.gmu.edu/~eclab/projects/mason	Agent-based simulation core
Apache Maven	maven.apache.org	Build management
jUnit	www.junit.org/	Unit and integration testing
CERN Colt library	acs.lbl.gov/software/colt	Probability distributions, statistics
JUNG	jung.sourceforge.net	social network generation and visualization
GeoTools GIS toolkit	geotools.codehaus.org	Geospatial model, shapefile reading, distance calculations
Apache Commons, Log4j	www.apache.org	Utility classes, logging of output and simulation results
XStream	xstream.codehaus.org	XML deserialization for parameter and configuration files
Perl	www.perl.org	Automation of parameter sweeps and analysis process
Gnu R	www.r-project.org	Analysis of results; graphs

3.2. Specialized libraries

A number of specialized libraries were required to implement various aspects of the model. First, the

model incorporates probability distributions in many places. The CERN Colt library (more precisely, functionality provided in the `cern.jet` package) was therefore a valuable resource that allowed for a very generic implementation without “hardcoding” any distributions into the code. The resulting simulation tool allows modelers to select from various types of distributions for specific simulation scenarios at runtime through configuration of XML parameter files.

Next, the Java Universal Network/Graph Framework (JUNG) was used for visualizing, reading, writing, and analyzing the social networks. This library also provides implementations of some of the generative network algorithms.

Finally, we used GeoTools GIS toolkit to implement the geospatial model and read population density data in ESRI shapefile format.

3.3. Tools for analysis and automation

Gnu R was used extensively to analyze and plot data. Bash and Perl scripts came into play for automating the simulation process, the discretization of data, and the analysis as well as plotting of results.

4. IMPLEMENTATION

Major design objectives for the implementation of the simulation included (i) reproducible results, (ii) provision of a flexible parameterization mechanism, (iii) no “hardcoding” of parameter values in the program code, and (iv) scalability and support for parallelization.

The first objective was achieved by initializing the random number generators in the simulation with random seeds from a configuration file. Integration tests were performed regularly during the implementation process to ensure that simulation runs with the same parameter sets and seeds always yield identical results.

The second and third objectives were achieved by means of a convenient parameterization mechanism based on a number of separate XML files, each of which configures particular aspects of the model. Major advantages of this method are that the parameter files are human-readable, can be easily edited, and that they can be validated against XML Schemas (XSD). The partitioning into separate files allows for their reuse in multiple scenarios and avoids redundancy. In order to simulate the diffusion of an innovation at varying price levels, for example, the same set of parameter files can be used for all price levels, with the sole exception of the pricing policy file. A single line that points to the pricing policy to use in the simulation has to be edited in a configuration file that binds the parameter set together (`run.xml`). The left-hand side of Figure 1 illustrates the configuration files and their relations.

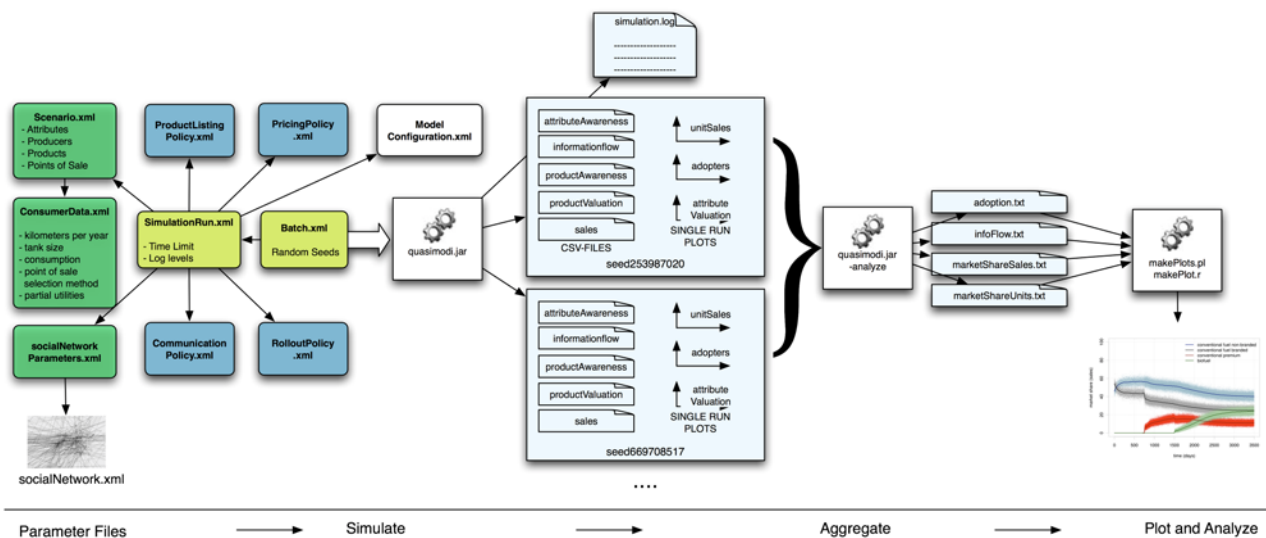


Figure 1: Architecture and simulation workflow

The fourth objective was achieved by dividing the steps in the simulation process into distinct program modules. Rather than optimizing for parallelization within individual replications (i.e., use of multiple processing cores to process events in a simulation run), we designed the simulation tool in a way that a set of runs with varying random seeds can be performed in parallel on multiple cores or computing nodes and results can then easily be collected, aggregated, and analyzed in a separate step. In particular, the following four distinct steps are performed for each simulation scenario, as illustrated in Figure 1: (i) Modeling of the scenario to simulate in a number of configuration files, (ii) simulation of the scenario for the number of replications specified, (iii) discretization and aggregation of results of individual simulation runs, and (iv) plotting and analysis of results.

5. GENERAL LESSONS LEARNED

General lessons learned in the course of the QuaSiMoDI project that go beyond the selection of suitable frameworks and modeling environments can be roughly divided in four groups. Firstly, there is a need for a sound empirical foundation; “just” setting up an agent-based model and to implement the corresponding simulation tool is no longer sufficient in order to make some valuable contribution to the field. Instead it is essential (and strongly demanded by many reviewers) to mirror micro-level factors and processes from real markets. In the QuaSiMoDI application case we therefore organized a focus group for criteria identification, performed a conjoint analysis for consumers’ preference elicitation, and did additional empirical social research with a standardized questionnaire in order to secure additional information on the structure of the underlying social network and the communication behavior of (potential) customers. All in all, these activities have cost several months of work (and also financial resources for the market research institution that

provided us access to their representative panel), but, in retrospective, it was worth the effort.

Secondly, it turned out that both the structure of the social (communication) network and corresponding parameters (e.g., concerning communication frequency) have considerable impact on simulation results. This raises a number of promising topics for further research, e.g., investigating stylized social network characteristics that are prevalent in different types of (consumer) markets. Unless sufficient evidence is available in literature, we strongly recommend placing particular emphasis on empirical data acquisition in this respect.

Validation of simulation results forms a third challenge that has to be mastered. For QuaSiMoDI we performed (i) a conceptual validation for which, as an example, we grounded our innovation decision-process on Roger’s (1962) well-established framework, (ii) an internal validation with extensive unit and integration testing, (iii) a micro-level external validation for calibration (e.g., with a check for implausible values or inconsistent preference values from the conjoint analysis) as well as for verification (e.g., whether the micro-level output concerning choice of gas station is consistent with reported behavior or whether agents’ communication behavior reflects assumptions), (iv) a macro-level external validation for which we performed a face validation with experts and also compared simulation results with data for market diffusion of premium (fossil) fuels from Germany, and (v) a cross-model validation for which we replicated stylized facts formalized in the model by Bass (1969).

Finally, it was essential to gather a team of experts with complementary competences. For the QuaSiMoDI project they came from the fields of innovation management, marketing, organization studies, sociology, operations research, and IT. On a personal note, working in such an interdisciplinary team made “tons of fun” (as a former colleague from the University of Texas would have phrased it) and certainly has been among the most appealing aspects in pursuing this endeavor.

ACKNOWLEDGMENTS

In the course of the QuaSiMoDI project we obviously did not just review platforms and implement the simulation tool, but also perform many more tasks (such as properly modeling the purchase decision or information transfer, setting up the social network, or testing the tool with data from a real-world application). This has been joint work together with several others, most prominently with Markus Günther, Rudolf Vetschera, and Lea Wakolbinger who have considerably contributed to the QuaSiMoDI research endeavor for which we are just grateful. Finally, we thank the Austrian Science Fund (FWF) for financial support by grant No. P20136-G14.

REFERENCES

- Bass, F., 1969. A new product growth model for consumer durables. *Management Science*, 15 (5), 215-227.
- Castle, C.J., Crooks, A.T., 2006. *Principles and concepts of agent-based modelling for developing geospatial simulations*. Working paper 110. Centre for Advanced Spatial Analysis, University College London.
- Garifullin, M., Borshchev, A., Popkov, T., 2007. Using AnyLogic and agent-based approach to model consumer market. *Proceedings of the 6th EUROSIM Congress on Modelling and Simulation*, pp. 1-5. Sept. 9-13, Ljubljana (Slovenia).
- Gilbert, N., 2002. Platforms and methods for agent-based modeling. *Proceedings of the National Academy of Sciences*, 99, 7197-7198.
- Günther, M., Stummer, C., Wakolbinger, L.M., Wildpaner, M., 2011. An agent-based simulation approach for the new product diffusion of a novel biomass fuel. *Journal of the Operational Research Society*, 62 (1), 12-20.
- Inchiosa, M.E., 2002. Overcoming design and development challenges in agent-based modeling using ASCAPE. *Proceedings of the National Academy of Sciences*, 99 (90003), 7304-7308.
- Isaac, A.G., 2011. The ABM template models: a reformulation with reference implementations. *Journal of Artificial Societies and Social Simulation*, 14 (2), 5.
- Kiesling, E., Günther, M., Stummer, C., Wakolbinger, L.M. (2012) Agent-based simulation of innovation diffusion: A review. *Central European Journal of Operations Research*, 20 (2), 183-230.
- Kiesling, E., Günther, M., Stummer, C., Wakolbinger, L.M., 2009. An agent-based simulation model for the market diffusion of a second generation biofuel. In: M.D. Rossetti M.D., R.R. Hill, B. Johansson, A. Dunkin, R.G. Ingalls R.G., eds. *Proceedings of the Winter Simulation Conference (WSC 2009)*, pp. 1474-1481. Dec. 13-16, Austin (Texas, USA).
- Kiesling, E., Günther, M., Stummer, C., Vetschera, R., Wakolbinger, L.M., 2010. A spatial simulation model for the diffusion of a novel biofuel on the Austrian market. In: A. Bargiela, S.A. Ali, D. Crowley, E.J.H. Kerckhoffs, eds. *Proceedings of the 24th European Conference on Modelling and Simulation (ECMS 2010)*, pp. 41-49. June 1-4, Kuala Lumpur (Malaysia).
- Legéndi, R., Gulyás, L., Bocsi, R., Máhr, T., 2009. Modeling autonomous adaptive agents with functional language for simulations. In: L. Seabra Lopes, N. Lau, P. Mariano, L.M. Rocha, eds. *Progress in Artificial Intelligence, Lecture Notes in Computer Science 5816*. Berlin: Springer, 449-460.
- Luke, S., Cioffi-Revilla, C., Panait, L., Sullivan, K., 2004. MASON: a new multi-agent simulation toolkit. *Proceedings of the 2004 SwarmFest Workshop*, pp. 1-8. May 9-11, Ann Arbor (Michigan, USA).
- Macal, C., North, M., 2007. Agent-based modeling and simulation: desktop ABMS. In: S.G. Henderson, B. Biller, M.-H. Hsieh, J. Shortle, J.D. Tew, R.R. Barton, eds. *Proceedings of the Winter Simulation Conference (WSC 2007)*, pp. 95-106. Dec. 9-12, Washington D.C. (USA).
- MathWorks, 2012. Matlab. Available from: <http://www.mathworks.com> [accessed 5 July 2012].
- Matsumoto, M., Nishimura, T., 1998. Mersenne twister: a 623-dimensionally equidistributed uniform pseudorandom number generator. *ACM Transactions on Modeling and Computer Simulation*, 8 (1), 3-30.
- Minar, N., Burkhart, R., Langton, C., Askenazi, M., 1996. *The Swarm simulation system: a toolkit for building multi-agent simulations*. Working paper 96-06-042. Santa Fe Institute, Santa Fe.
- Nikolai, C., Madey, G., 2009. Tools of the trade: a survey of various agent based modeling platforms. *Journal of Artificial Societies and Social Simulation*, 12 (2), 2.
- North, M.J., Collier, N.T., Vos, J.R., 2006. Experiences creating three implementations of the Repast agent modeling toolkit. *ACM Transactions on Modeling and Computer Simulation*, 16 (1), 11-25.
- North, M.J., Howe, T.R., Collier, N.T., Vos, J.R., 2005. The Repast Symphony runtime system. In: C.M. Macal, M.J. North, and D. Sallach, eds. *Proceedings of the Agent 2005 Conference on Generative Social Processes, Models, and Mechanisms*, pp. 151-158. Oct. 13-15, Argonne (Illinois, USA).
- Parker, M.T., 2001. What is Ascape and why should you care? *Journal of Artificial Societies and Social Simulation*, 4 (1), 5.
- Railsback, S.F., Lytinen, S.L., Jackson, S.K., 2006. Agent-based simulation platforms: review and development recommendations. *Simulation*, 82 (9), 609-623.
- Resnick, M., 1996. StarLogo: an environment for decentralized modeling and decentralized thinking. In: *Conference companion on Human factors in computing systems: common ground*. New York, NY: ACM Press, 11-12.
- Rogers, E.M., 1962. *Diffusion of innovations*. New York, NY: The Free Press.

- Tisue, S., Wilensky, U., 2004. NetLogo: a simple environment for modeling complexity. *Proceedings of the International Conference on Complex Systems (ICCS 2004)*, pp. 1-10. May 16-21, Boston (Massachusetts, USA).
- Tobias, R., Hofmann, C., 2004. Evaluation of free Java-libraries for social-scientific agent based simulation. *Journal of Artificial Societies and Social Simulation*, 7 (1), 6.
- Wolfram Inc., 2012. Mathematica. Available from: <http://www.wolfram.com> [accessed 5 July 2012].

AUTHORS' BIOGRAPHY

Christian Stummer currently holds the Chair of Innovation and Technology Management at the Department of Business Administration and Economics at Bielefeld University, Germany. Before, he has served as an associate professor at the University of Vienna, Austria, as the head of a research group at the Electronic Commerce Competence Center (EC3) at Vienna, and as a visiting professor at the University of Texas at San Antonio, United States. His research interests focus on (quantitative) modeling and providing proper decision support particularly so with respect to new product diffusion and project portfolio selection. Prof. Stummer has published two books, more than thirty papers in reviewed journals, and numerous other works. He is a member of several societies such as INFORMS, the German Operations Research Society, or the MCDM Society, acts as a reviewer for many journals, and recently has become member of the editorial board of the EURO Journal on Decision Processes.

Elmar Kiesling is a postdoctoral researcher at the Institute of Software Technology and Interactive Systems at Vienna University of Technology, Austria. He holds a master's degree in international business administration and a PhD in management, both from the University of Vienna. His research interests include agent-based modeling and simulation, multi-criteria decision analysis and decision support systems, visualization of multivariate data, and information security management.

THE HIGH SPEED TRAIN INTERIOR NOISE REDUCTION USING MULTI-CHANNEL ANC SYSTEM

Young Min Kim^(a), Jong Il Bae^(b), Kwon Soon Lee^(c)

^(a)Dong-A University, Busan, Korea

^(b)Pukyong National University, Busan, Korea

^(c) Dong-A University, Busan, Korea

^(a)kdudals119@naver.com, ^(b)jibae@pknu.ac.kr, ^(c)kslee@dau.ac.kr

ABSTRACT

In this paper, the high speed train interior noise reduction performance of the multi-channel ANC system was evaluated. A 1x2x2 multi-channel ANC algorithm was used for this purpose because high speed train interior noise has various noise sources. Experiments were carried out at two positions in floor, using pure-tone noise, to find the optimal positions of the control speakers and error microphones. At the selected optimal position, an ANC system performance evaluation experiment was carried out at variable heights, using high speed train interior noise. As a experiment result, the active noise control system shown good performance in the near position and high position from primary noise.

Keywords: Active noise control, multi-channel FXLMS, Noise canceling

1. INTRODUCTION

In terms of speed and reliability, the high speed train technology can reach the levels of the corresponding technologies in advanced countries, but interior noise reduction technological development is more needed.

In high speed train, passive interior-noise control system was applied to meet the interior-noise legal standards by structural design of the vehicle, but the passenger's demand for a pleasant environment has not still satisfied.

In addition, the use of the passive noise control method for interior-noise reduction increases the vehicle's weight and the fuel consumption. Therefore, active noise control research is needed [1].

In this paper, the experiment of the ANC system performance evaluate has been performed using pure-tone noise and high speed train interior noise, according to the positions and heights of the control speakers and error microphones.

2. MULTI-CHANNEL ANC SYSTEM

2.1. The multi-channel FXLMS algorithm[2-4]

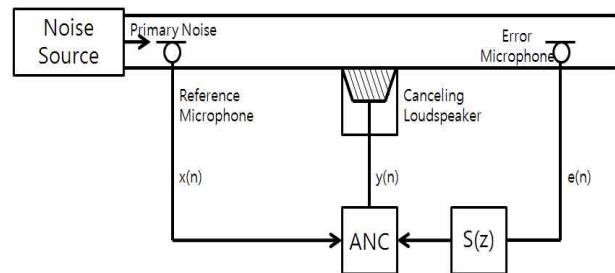


Figure 1: ANC system in duct

In the active noise control system, as shown in Fig. 1, noise signal $x(n)$ dose not correspond to control signal $y(n)$ due to the additional path transfer function $S(z)$ existing between error signal $e(n)$ and control signal $y(n)$. Thus, it will result in system instability. The FIR filter can solve this problem by updating a weight vector after the estimation of the secondary path to $\hat{S}(z)$. This method is called the FXLMS ANC system. Fig. 2 shows the structure of the FXLMS ANC system.

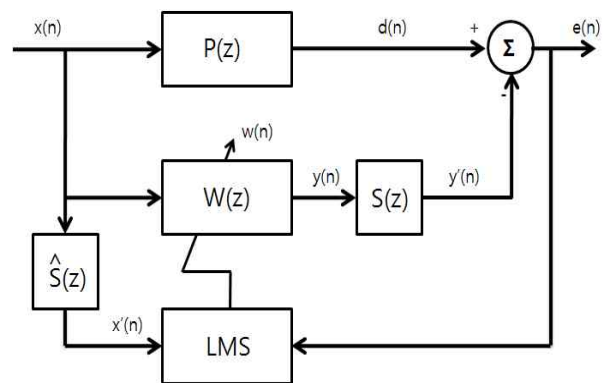


Figure 2: Block diagram of the FXLMS algorithm

Because the high speed train has a variety noise sources, the multi-channel ANC system should be applied to it instead of the existing single-channel ANC system.

The multi-channel (1x2x2, one noise source speaker, two control speakers, two error microphones) FXLMS algorithm was used for the reduction of the interior noise of a high-speed train. It has two primary transfer

functions, four secondary path transfer functions, and four estimated secondary path transfer functions.

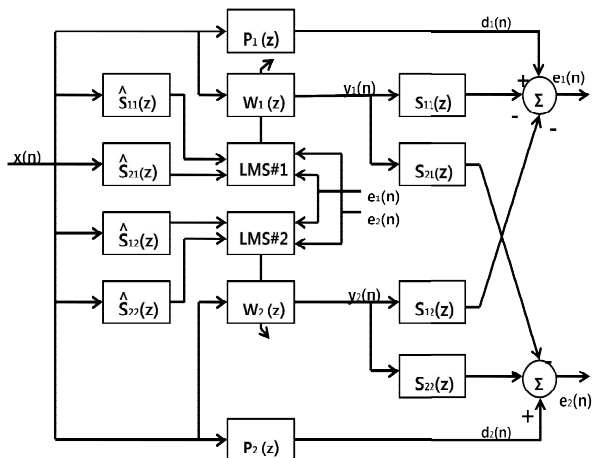


Figure 3: The Multi-channel FXLMS algorithm

Fig. 3 is block diagram of the multi-channel FXLMS. Here, $x(n)$ is the input signal, $y_1(n), y_2(n)$ are output signals, $d_1(n), d_2(n)$ are reference signals, $e_1(n), e_2(n)$ are error signals, $P_1(z), P_2(z)$ are primary transfer functions, $S_{11}(z) \sim S_{22}(z)$ are secondary path transfer functions, $\hat{S}_{11}(z) \sim \hat{S}_{22}(z)$ are estimated secondary path transfer functions, and $W_1(z), W_2(z)$ are adaptive filters.

3. SIMULATION

In this paper, the simulation were performed for high speed train interior noise reduction using open-space noises and tunnel noises. The simulation were performed in two positions. Two positions are shown in Fig. 4. The control speakers were located at the center. The distance between the control speakers and the error microphones is 75cm, and the control speakers height is 50cm.

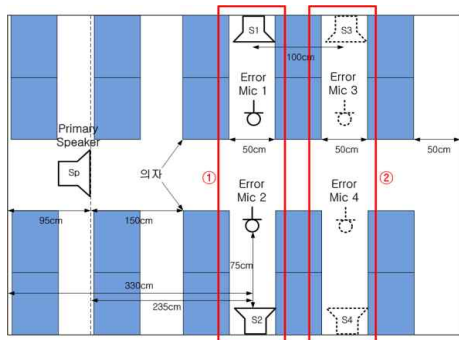
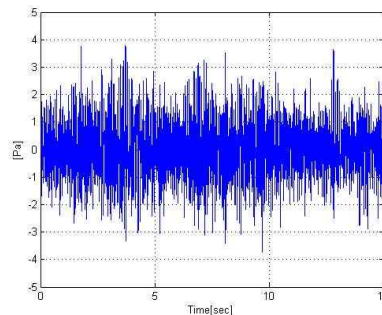


Figure 4: The ANC system position in the test-bed

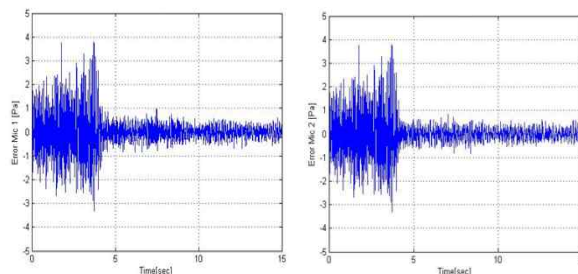
The simulation were performed to compare the performance of the ANC algorithm in positions ① and ② using 2 noises(The open space – window, aisle; and the tunnel – window, aisle; speed is 200~250km/h).

3.1. The simulation of open-space noise

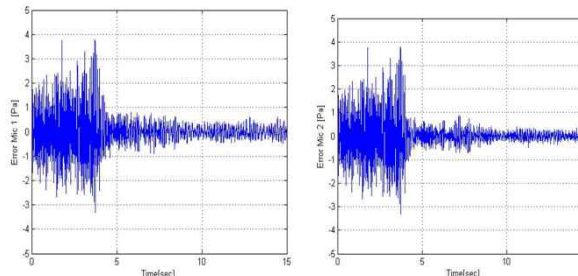
In the simulation, all the conditions are same, as follows. The step size : 0.0005, filter order : 256.



(a) The interior noise of high speed train in the open-space section



(b) The error mic 1 and 2 in position ①

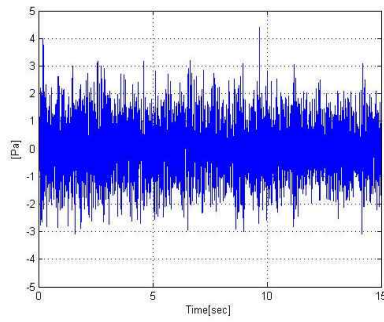


(c) The error mic 1 and 2 in position ②

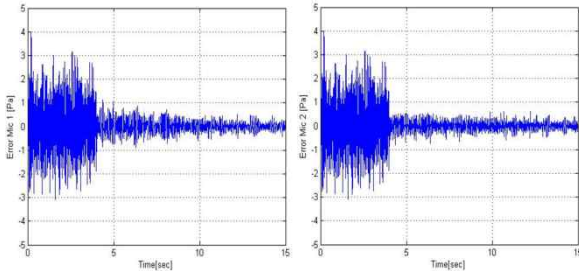
Figure 5: The simulation results of open-space window noise

In the simulation results, position ① was reduced by 43.3dB on average, and position ② was reduced by 36.6dB on average.

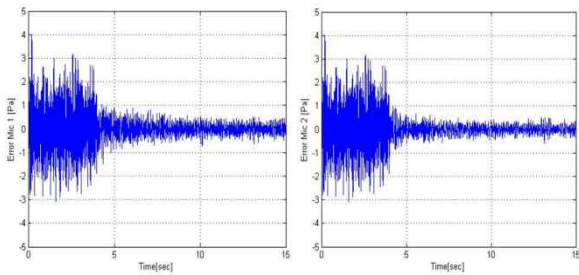
3.2. The simulation of tunnel noise



(a) The interior noise of high speed train in the tunnel section



(b) The error mic 1 and 2 in position ①



(c) The error mic 1 and 2 in position ②

Figure 6: The simulation results of tunnel window noise

In the simulation results, position ① was reduced by 38.3dB on average, and position ② was reduced by 32.1dB on average.

4. PERFORMANCE EVALUATION OF ANC SYSTEM

To evaluate the performance of the ANC algorithm, the following test bed experiment was performed. First, a pure-tone experiment was performed to find the optimal position of the control speakers and error microphones. In the pure-tone experiment, a good reduction effect position was selected, and the performance of the ANC algorithm was evaluated using the high speed train interior noise. The test bed's size was downscaled (length - 573cm, width - 290cm, height - 246cm) as compared with the actual size (length - 1870cm, width - 290cm, height - 348 cm), but the other parameters were similar.

4.1. Pure-tone experiment

The pure-tone experiment was performed to compare the performance of the ANC algorithm in positions ① and ② using 120, 280, and 360Hz pure-tones.

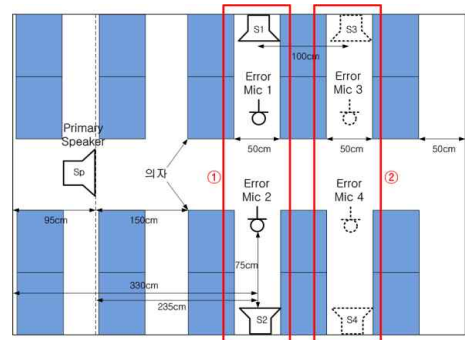
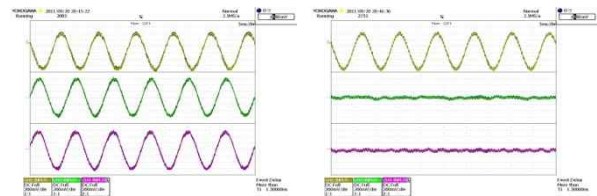


Figure 7: The ANC system position in the test-bed for pure-tone

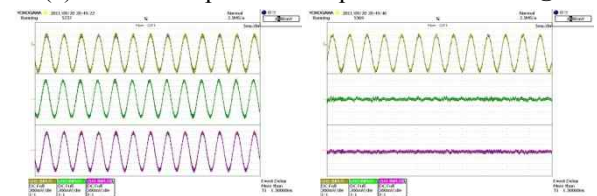
The control speakers were located at the center. The distance between the control speakers and the error microphones is 75cm, and the control speakers height is 50cm.



(before ANC)

(after ANC)

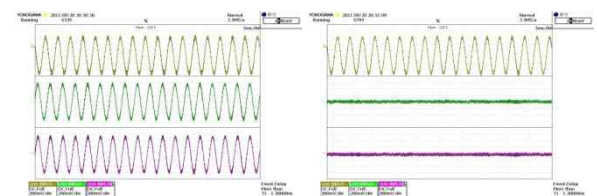
(a) The 120Hz pure-tone experiment result in ①



(before ANC)

(after ANC)

(b) The 280Hz pure-tone experiment result in ①



(before ANC)

(after ANC)

(c) The 360Hz pure-tone experiment result in ①

Figure 8: The experiment results using pure-tone noise

In the experiment results, position ① was reduced by 6.5dB on average, and position ② was reduced by

3.6dB on average. The reduction effect was more effective at position ① near the noise source.

4.2. High speed train interior-noise experiment

The high speed train experiment was performed in position ①, which shown a good result in the previous experiment. Each noise was divided as follows: open space - window, aisle; and tunnel - window, aisle. Fig. 9 is ANC system in the test-bed.



Figure 9: The ANC system in the test-bed at the 50cm height

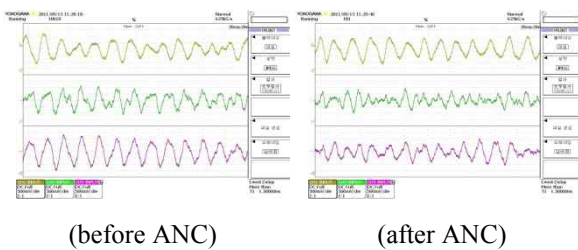


Figure 10: The open-space window noise experiment result with 50cm

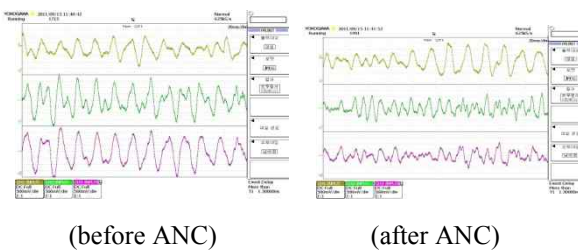


Figure 11: The tunnel window noise experiment result with 50cm

In the experiment results at the 50cm height, the open-space-window noise was reduced by 6dB on average, and the open-space-aisle noise was reduced by 5.8dB on average. On the other hand, the tunnel-window noise was reduced by 4.7dB on average, and the tunnel-aisle noise was reduced by 4.8dB on average.

In the graph, the first wave is the noise source signal, the second is the waveform of error microphone 1, and the third is the waveform of error microphone 2.

Fig. 12 shows that the speakers and microphones heights were changed to 80cm. To evaluate the

performance of the ANC algorithm depending on the height change, the speakers and microphones were placed at a height of 80cm. Like the previous experiment, the high speed train experiment was performed using open-space and tunnel noises.



Figure 12: The ANC system in the test-bed at the 80cm height

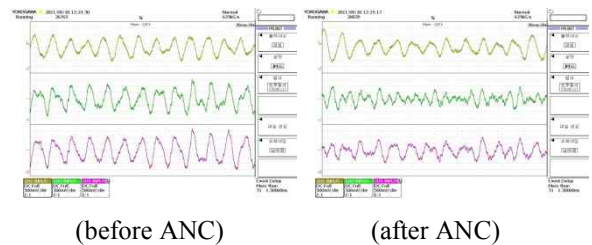


Figure 13: The open-space window noise experiment result with 80cm

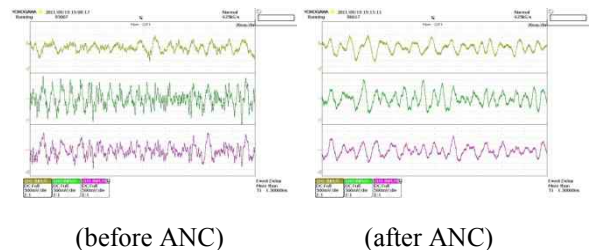


Figure 14: The tunnel window noise experiment result with 80cm

In the experiment results at the 80cm height, the open-space-window noise was reduced by 7.1dB on average, and the open-space-aisle noise was reduced by 5.8dB on average. On the other hand, the tunnel-window noise was reduced by 8.3dB on average, and the tunnel-aisle noise was reduced by 7.5dB on average.



Figure 15: The ANC system in the test-bed at the 110cm height

In the experiment results at the 110cm height, the open-space-window noise was reduced by 10.6dB on average, and the open-space-aisle noise was reduced by 10.1dB on average. On the other hand, the tunnel-window noise was reduced by 11.4dB on average, and the tunnel-aisle noise was reduced by 10.8dB on average.

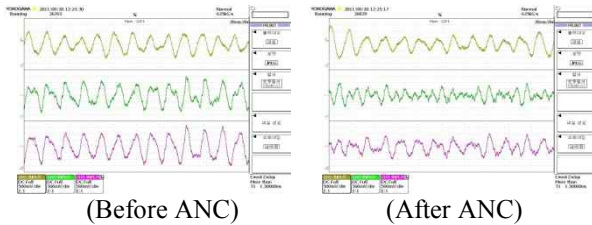


Figure 16: Open-space window noise experiment result with 110cm height

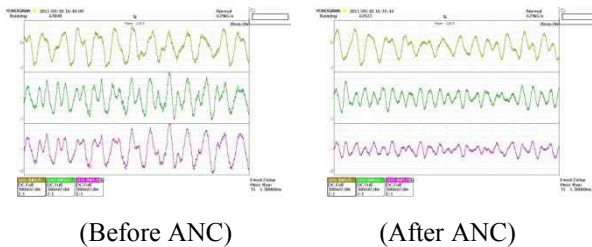


Figure 17: Tunnel window noise experiment result with 110cm height

5. CONCLUSION

In this study, simulations and ANC system performance evaluation experiments were carried out at various positions and heights, using pure-tone noise and high speed train interior noise. The results were as follows:

First, the result of simulation using multi-channel FXLMS algorithm show average reduction index by 39.9dB in the open-space section, and show average reduction index by 35.2dB in the tunnel section. Therefore, applying the active noise control in the tunnel section was more effective than open-space section.

Second, for the pure-tone noise experiment at various positions, at a location near the noise source, the noise was reduced by 6.5dB on average, and at a location far from the noise source, the noise was reduced by 3.6dB

on average. In this experiment, better results were shown at the location near the noise source.

Third, the high speed train noise experiment was performed at the position where the position was selected in the previous experiment. The results of the experiment at the 50cm height are as follows: the open-space noise was reduced by 5.9dB on average, and the tunnel noise was reduced by 4.8dB on average.

Fourth, the results of the high speed train noise experiment at the 80cm height are as follows: the open-space noise was reduced by 6.5dB on average, and the tunnel noise was reduced by 7.9dB on average.

Fifth, the results of the high speed train noise experiment at the 110cm height are as follows: the open-space noise was reduced by 10.4dB on average, and the tunnel noise was reduced by 11.1dB on average.

Finally, As simulations and experiment results, the active noise control system shown good performance in the near position and high position from primary noise.

In the future, more experiments are needed at various locations to find the optimal positions of the control speakers and error microphones. There is a plan to expand the multi-channel system into a 2x2x2 or 2x2x4 system.

Table 1: The result of experiment(Error Mic 1)

Section	Noise position	The height of ANC system	Before ANC [dB]	After ANC [dB]	Reduction [dB]
Open-space	Window	50cm	99.8~103.1	94.8~97.2	5.5
		80cm	99.5~103.4	93.7~96.7	6.3
		110cm	98.5~102.6	90.1~92.9	9.1
	Aisle	50cm	95.6~98.7	89.4~93.5	5.7
		80cm	92.8~99.3	89.7~93.2	4.6
		110cm	95.9~99.4	86.9~90.4	9.0
Tunnel	Window	50cm	101.7~103.3	96.8~99.4	4.4
		80cm	101.8~103.9	94.2~95.9	7.8
		110cm	100.5~103.4	89.5~91.2	11.6
	Aisle	50cm	102.0~103.8	98.4~99.2	4.1
		80cm	102.1~104.0	95.9~96.8	6.7
		110cm	99.8~104.2	90.5~93.4	10.1

ACKNOWLEDGMENTS

This work was supported by the Korea Research Foundation Grant funded by Korean Government(MOEHRD) (KRF-2012-0055-핵 09B1409)

REFERENCES

- Dae Yoon Rye, Sung Ik Han, Sae Han Kim and Kwon Soon Lee, "Development of the Recurrent Neural Network for Active Noise Reduction of a Railway Vehicle," KIEE, Vol. 41, Pp. 2004-2005, July 2010.
- Dong Jun Ahn, 1997, "Design of Adaptive Filters for Active Noise Control," Doctoral dissertation, University of Dan Kook.
- Sung Dae Seo, 2007, "Active Noise Control Using Stabilized Adaptive Filters," Doctoral dissertation, University of Dan Kook.
- Sen M. Kuo, Dennis R. Morgan, 1996, "Active Noise Control System, Algorithms and DSP Implementations" New York, John Wiley & Sons.
- S. J. Elliot and P. A. Nelson, "Active Noise Control," IEEE sign, Process Mag., Vol. 10, Pp. 12-35, 1993.
- S. M. Kou and D. R. Morgan, "Active Noise Control: a Tutorial Review," IEEE proc, 87, Pp. 973-993, 1999.
- Hyun Cheol Cho, Kwon Soon Lee and Hyun Do Nam, "A Neural Multiple LMS based ANC System for Reducing Acoustic Noise of High-speed Trains," KIEE, Vol. 58P, No. 4, Pp. 385-390, 2009.
- Sung Dae Seo, 2007. "Active Noise Control Using Stabilized Adaptive Filters," Doctoral dissertation, University of Dan Kook.
- Jae Chul Kim and Chan Woo Lee, "Analysis of Interior Noise of KTX in Tunnel with Concreted Track," KSNVE, Vol. 17, No. 11, Pp. 1037-1042, 2007.

MULTI-ACTORS DISTRIBUTED CONTROL SYSTEMS: REINFORCEMENT SIGNAL BY SHANNON'S ENTROPY

Youcef Zennir⁽¹⁾, Denis Pomorski⁽²⁾

⁽¹⁾Laboratoire d'automatique de Skikda, 26 route el-hadaik, 21000 Skikda, Algérie

⁽²⁾Laboratoire L.A.G.I.S, Polytech'Lille, Bâtiment D, 59655 Villeneuve d'Ascq, France

⁽¹⁾youcefzennir@yahoo.com ⁽²⁾denis.pomorski@univ-lille1.fr

ABSTRACT

This paper presents a multi-actors distributed control systems in an unknown environment. These actors are reactive entities able to react to the stimuli coming from the environment and to choose between several actions. In order to improve their behaviour (i.e. in order to choose the good action) in the course of time, the multi-actors system must be able to use reinforcement learning. This signal of reinforcement is, until now, a signal whose values are previously defined. We propose to raise this technique by using the Shannon's entropy to measure the coherence of the action choice using the transformation of the reinforcement signal table. This stage, of local training will allow the improvement of the control of the global system and coordination between the various actors. The results of the simulation show that the actor can learn to control its trajectory efficiently.

KeyWords: Reinforcement learning, distributed control, Q-learning, multi-actors systems.

1. INTRODUCTION

The multi-actors systems in which actors must learn together how to achieve a common task, this constitutes a very active field of research (Claus 1998), (Littman 2001), (Hu 1998). A difficulty in such systems is of knowing how to coordinate the actors effectively so that they gain ones from the others without harming any of them. The reactive actors considered in this article react to receive stimuli of the environment.

These actors can be observed but, contrary to the cognitive actors, they cannot communicate. As an example of a distributed control system we consider a robot model with several sensors (actors) moving in an unknown environment. The planning of coordination and communication between the actors is not effective. It is then interesting to resort to training, such as the reinforcement learning which is based on a process test/error to acquire the desired behaviour. The object of this work is to study and develop a method of learning for multi-actors systems with the use of the theories of data fusion (Shannon's entropy) to measure the

coherence of the choice of the action by the transformation of the reinforcement signal table.

2. REINFORCEMENT LERANING

Reinforcement learning, is one of the most active research areas in artificial intelligence, it is a computational approach for learning whereby an agent tries to maximize the total amount of reward it does receive when interacting with a complex, and uncertain environment.

In the standard reinforcement learning model an agent interacts with its environment (Sutton 1998). This interaction takes the form of the agent sensing the environment based on this sensory input, this enable choosing an action to perform in the environment. The action changes the environment in some manner and this change is communicated to the agent through a scalar reinforcement signal.

There are three fundamental parts of a reinforcement learning problem: the environment, the reinforcement function, and the value function.

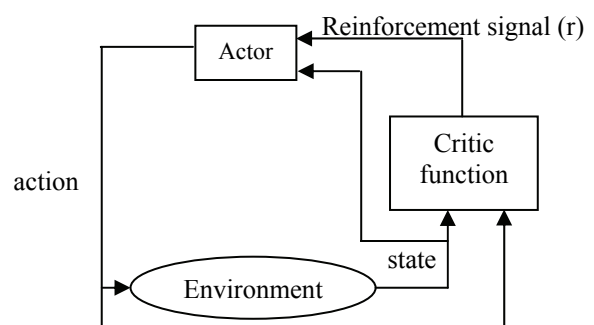


Figure 1: The actor-environment interaction in reinforcement learning.

Q-learning (Zennir 2004) is a recent form of Reinforcement Learning algorithm that does not need a model of its environment and can be used online. Therefore, it is very suited for repeated games against an unknown opponent. Q-learning algorithms works by estimating the values of state-action pairs $Q(s,a)$.

The value $Q(s,a)$ is defined to be the expected discounted sum of the future payoffs obtained by taking action "a" from state "s" and following an optimal policy thereafter. Once these values have been learned, the optimal action from any state is the one with the highest Q-value. Its simplest form, *1-step Q-learning* is defined by

$$Q(s,a) \leftarrow Q(s,a) + \alpha [r + \gamma \cdot \max_{a'} Q(s',a') - Q(s,a)] \quad (1)$$

- α : learning rate, γ : discount factor.

In this case, the learned action-value function, Q , directly approximates Q^* , the optimal action-value function, is independent of the policy being followed. This dramatically simplifies the analysis of the algorithm and enabled early convergence proofs. The policy still has an effect in that it determines which state-action pairs are visited and updated. However, all what is required to correct the convergence is that all pairs continue to be updated.

As we have discussed before, this is a minimum requirement in the sense that any guaranteed method must fulfil this requirement to find optimal behaviour in the general case. Under this assumption and based on the usual stochastic approximation conditions on the step-size sequence, Q has been shown to converge with probability one to Q .

The Q-learning algorithm is shown in procedural form in Figure 2.

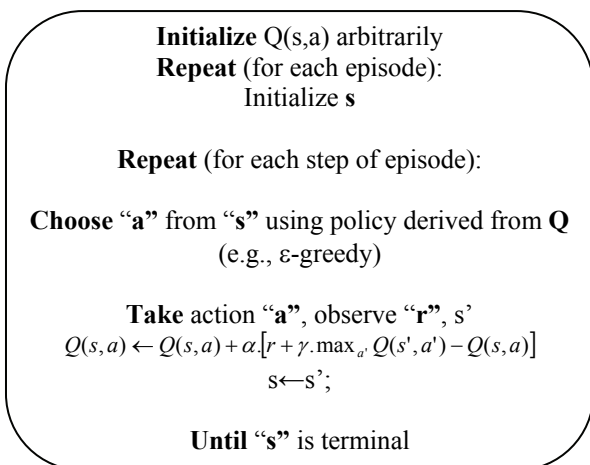


Figure 2: Q-learning algorithm.

Shortly, we have:

- ϵ : Probability to use a random action instead of the optimal policy.

It was proven, for example in (Jaakkola 1994), that if spaces of states and actions S and A are finished, if α_t is such as:

$$\sum_t \alpha_t = \infty \quad \text{and} \quad \sum_t \alpha_t^2 \leq \infty \quad (2)$$

This algorithm is for one actor, but where more than one actor work in the same space we have other algorithms adapted for this new context.

3. REINFORCEMENT LEARNING IN A MULTI-ACTORS CONTEXT

Let us consider a system made up of N actors A_i ($i=1... N$) whose interaction with the environment is defined by:

- A space actions $\alpha_i = \{a_{i1}... , a_{ij}... , a_{iN_i}\}$ for each actor A_i ($i=1... N$), with $N_i = \text{card}(a_i)$;
- A space states $S = \{s_1, ... , s_i, ... , s_M\}$;

At the times "t", each actor carries out an action which is clean on the basis of state preceding "s_t" of the environment. These joint actions ($a_1... a_i... , a_N$) (with $a_i \in \alpha_i$) cause a transition towards the state "s'" (the apostrophe meaning the moment "t+1"). According to architecture used, one critic's function allows to reward the actors. Among architectures of training by reinforcement the most used, we distinguish centralized, distributed and multi-actors architecture.

With a centralized approach of the reinforcement learning, state information are collected only in one decision centres, which updates the utility values and decides actions for each actor. By indicating $|A|$ the number of achievable actions by each actor (the number is identical for all the actors without loss of generalization), and $|S|$ the number of states attainable by the system, the table of $Q(s, a)$ in memory is of size $|S| * |A|^N$.

A same reinforcement signal is allotted to all the actors whatever the contribution of each one of those to the success or the failure of the common task. The expected advantages of this centralized approach are:

- A global vision of the system, allowing examining the all situations accessible by the actions from the actors.
- The possible problems of coordination between actors are solved on a single level of decision.

This approach presents the following inconvenient:

- The total system is sensitive to the failure of the single decision centres.
- The number of pair state/action (s, a) grows exponentially with the number of actors.
- Beneficial actions on the global system can be penalizing for an actor, because it is not held account of the local constraints.

3.1. Distributed architecture

With a distributed architecture (Zennir 2003) the actors do not receive necessarily the same information of state or the same signal reinforcement, and perform their own training. By supposing that N actors share the same information of state, the number of $Q(s, a)$ to update is $N * |S| * |A|$. The expected advantages of this distributed approach are:

- A greater flexibility (facilitated adaptation to the unforeseen modifications of the environment).
- A greater reliability (the individual error is tolerated).
- A greater robustness (the capacity of resolution results from the collective and not from an individual).
- Each actor can take into account local constraints.
- The number of pair state/action (s, a) grows proportionally with the number of actors.

In the distributed reinforcement learning approach, the strategies which can follow the actors implied in the same task can be individual or collective. According to an individual strategy each actor carries out his learning by ignoring the other actors. That amounts of learning by applying the algorithms acts as if each actor were alone.

The environment of the actor is then non stationary but during the learning, a "a" share carried out since the same state "s" always does not lead to the same state "s" because the state reached depends on the actions of the other actors.

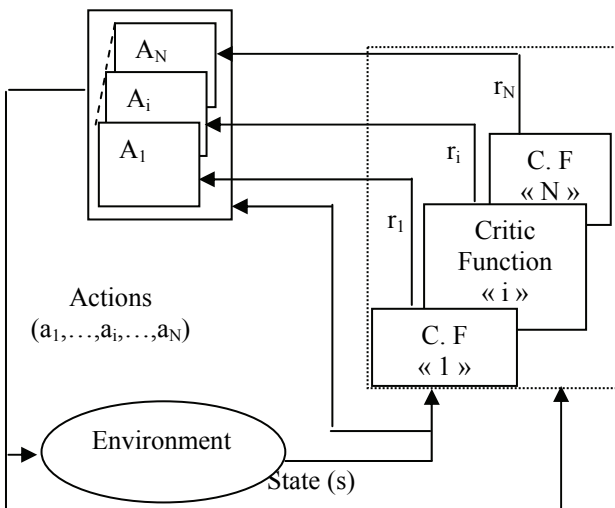


Figure 3: Distributed approach of reinforcement learning: one reinforcement signal « r_i » for each actor.

But this architecture presents the following difficulties: Within the context of a collective task the consequences of the action of an actor depend on the actions of the other actors.

- When they are defined, the local goals pursued by each actor must be compatible with the global objective.
- Mechanisms of co-operation among which, synchronization, collaboration, coordination can be necessary.

3.2. Multi-Actors architecture

Learning behaviours in a multiagent environment is crucial for developing and adapting multiactor systems. Reinforcement learning techniques have addressed this problem for a single actor acting in a stationary environment, which is modelled as a Markov decision process. But, multi-actors environments are inherently non-stationary since the other actors are free to change their behaviour as they also learn and adapt. Hu (Hu 1998), (Zennir 2004) extended the Q-multi-actor algorithm to general-sum games.

The extension requires that each agent maintain values for all the other actors. Also, the linear programming solution used to find the equilibrium of zero-sum games is replaced with the quadratic programming solution for finding an equilibrium in general-sum games.

The game must have a unique equilibrium, which is not always true of general-sum stochastic games. This is necessary since the algorithm strives for the opponent-independence property of Q-multi-actors, which allows the algorithm to converge almost regardless of the other agent's actions. With multiple equilibrium it is important for all the actors to play the same equilibrium in order to have its reinforcing properties. So, learning independently is not possible. It is supposed that at the time to act some actors do not know a priori the actions which are selected by the other actors but within the same given group, each one of them knows a posteriori executed action by the other members of the group.

Within the context of a collective vision, we consider an algorithm in which it is possible to the actors of a group to hold account of the actions selected by the other members. The principle is described in the following example: considering three actors 'i', 'j', 'k' laying out each one of two possible actions noted 0 and 1. For each state s , the actors maintain four Q-value tables corresponding to the four possibilities of action of the two other actors (Figure 5).

Each actor chooses the action leading to a hope of maximum gain i.e. that which, for a given state "s", corresponds to the line comprising the largest value of gains (gain 7 in Figure 5), even if the other actors choose or not the actions corresponding to the column comprising this value. However, at the reception of the reinforcement signal, the actor updates the value also corresponding to the choice of action of the other actors.

Thus in the example of Figure 3, if the actor 'j' executes action 0 and the actor 'k' action 1, it is the Q = - 4 value intersection between the line $a_j = 1$ and the column $a_j = 0, a_k = 1$ which is modified.

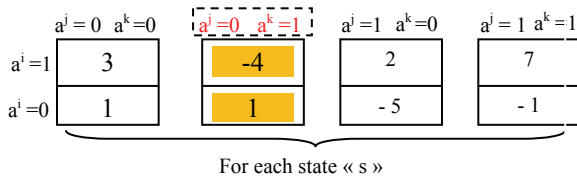


Figure 4: Q-Value for actor 'i' in state 's', with 3 actors 'i', 'j', 'k' and 2 actions.

The value of Q, which is updated at each iteration, is that which corresponds to the actions really executed. According to this approach, for each member 'i' of a given group of K actors, the Q-learning algorithm becomes:

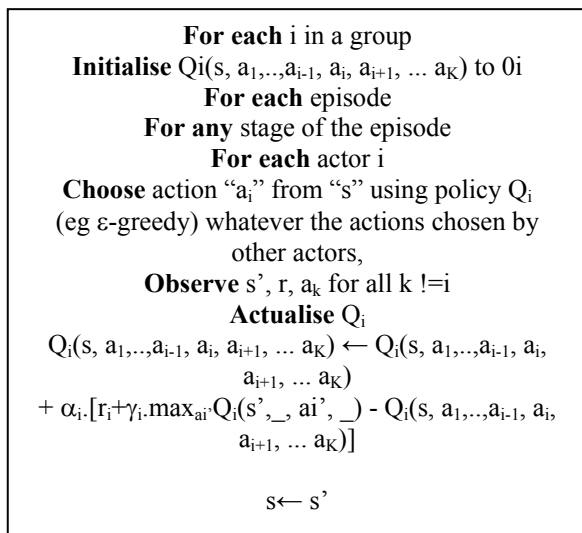


Figure 5: Q-multi-actors Algorithm's.

4. REINFORCEMENT'S SIGNAL USED IN LITERATURE

The signal of reinforcement is determined by the critical function, based on rules. The choice of the rules of delivery of this signal largely conditions the success of the learning and the final behaviour of the actor (Touze 1993). To be convinced some, let us evoke some examples:

- To make move a robot towards a goal, one can at every moment give a reward which is inversely proportional to his distance with the goal or which is a function of the final result.
- To build an actor which the goal is to leave a labyrinth, one can give a null reward most of the time, and "+1" as soon as the actor reaches the exit (Kaelbling 1996).

To prevent such an actor does not knock himself against the walls; one can sanction it each time that it

touches a wall by allotting to him a penalty (Buffet 2003). In general the choice of these rules is based on the intuition. The signal of reinforcement is a discrete signal, limited, composed of two or three values to the maximum.

5. VALIDATION OF ACTOR CHOICES

Knowing the state "s" in which the environment is, the actor must make a decision as for the action which it must take. With an aim of identifying this action, and especially of knowing if it is single or not, we can use the resulting tools from the information's theory. The variable which one seeks to explain is thus the action "a_i", knowing the state "s". Thus, knowing that the environment is in the state "s_i", several cases of figures can occur:

- The actor A_i will be able to make a decision have single if there is only one signal of positive reinforcement for $S=s_i$.
- In the contrary case, the signal of reinforcement will not make it possible to the actor to make a no ambiguous decision.

We can thus propose to use the reinforcement transformation table in the following way

$$p_{j/k} = \frac{r_{kj}}{\sum_{j=1}^{N_i} \text{sign}(r_{kj}) \text{ avec } r_{kj} > 0} \text{ if } P_{kj} > 0 \quad (3)$$

$$p_{j/k} = 0 \text{ else}$$

We can thus draw up the following table:

	a_i						
S	α_1	α_2	..	α_j	...	α_{N_i}	
s_1				.			
s_2				.			
...				.			
s_k	$P_{j/k}$	
....							
s_m							

Figure 6: Coherence table $[P_{j/k}]$

where : $P_{j/k} := \{p_{j/k}; k \in K, j \in J\}$,
 $K = \{1, 2, \dots, m\}$;
 $m = \text{card } S$;
 $J = \{1, 2, \dots, N_i\}$;
 $N_i = \text{card } a_i$

$P_{j/k}$ can be seen as a measurement of choice coherence's of the action J knowing that the environment is in the state s_k .

The coherence of the decision-makings of the actor "a_i" is thus maximum if there is only one "1" per line of the preceding table. In the opposite case, the data are incoherent. We can quantify this inconsistency by used concepts resulting from the information's theory: indeed, the intensity of connection between two variables "S" and "a_i" can be moderate by means of the conditional entropy (Pomorski 1991):

$$H(a_i/S) = H(S, a_i) - H(S) \\ = - \sum_{k,j} p_{kj} \cdot \log p_{j/k} \quad \text{with } p_{kj} = \sum_k p_{j/k} \quad (4)$$

Based on $H(Y/X)$ and $H(Y/S)$, two indices of "modelisability" are used:

$$m(a_i/S) = 1 - \frac{H(a_i/S)}{H(a_i)} \quad (5)$$

Moderate of a_i par S. It is a measure of the inconsistency of the action's sensors A_i.

$$q(Y/S) = \frac{H(Y) - H(Y/S)}{H(Y) - H(Y/X)} \quad (6)$$

Moderate the quality of the model, more easy $Y = \tilde{f}(S)$ compared to the quality of the $Y = f(X)$ model.

6. SIMULATION

We considered two actors removing themes selves in an unknown environment and obstacles are placed in different positions. The objective of each actor is to find as quickly as possible the goal supposed to be in a fixed position. The research of the goal is based on a reinforcement learning process of the Q-learning type. In this application, we study the application of the two approach of reinforcement learning (distributed and multi-actors architecture) with the use of the Shannon's entropy for measurement of reinforcement signal and to study the choice of the actions and coordination between the actors.

Simulation with distributed architecture, each actor has a process of training based on Q-learning.

Each actor has a function Q-value (s, a) represented by a table of dimension 400 lines (a number of the states) and 4 columns (a number of possible actions for each actor).

We applied ε-greedy strategy for the exploration of the actions. Figure 7 represents the training of the actor "i" with a distributed architecture.

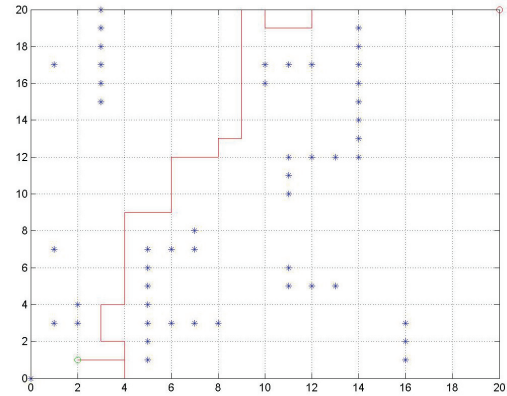


Figure 7: Trajectory of the actor « i ». *Certitude « i » = 0.1094, $\gamma=0.9$, $\alpha=0.1$, $\varepsilon=0.1$.*

In figure.6, we noticed that more than 1000 iterations, the actor "i" arrives to find the goal more than 960 times in the phase of training and 1000 times in the test. We noticed that the time of training (the iteration count to find the goal) is smaller when "ε" is closer to 1.

For the simulation with multi-actors architecture, each actor has a process of training based on Q-learning. The choice of the action for an actor independent of the action is chosen by the other actor, but the update function $Q(s, a_j)$ of an actor to take into accounts the action chosen by the other actor.

Each actor (i and j) has a critical function. We applied ε-greedy strategy for the exploration of the actions. We have test with two actors. The following figures show the results obtained.

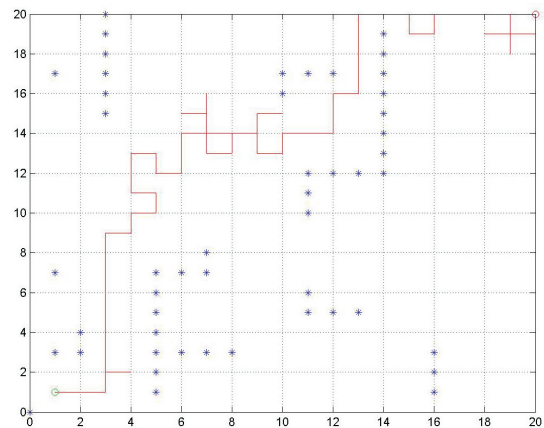


Figure 8: Trajectory of the actor « j ». *Certitude « j » = 0.2004, $\gamma=0.5$, $\alpha=0.1$, $\varepsilon=0.5$.*

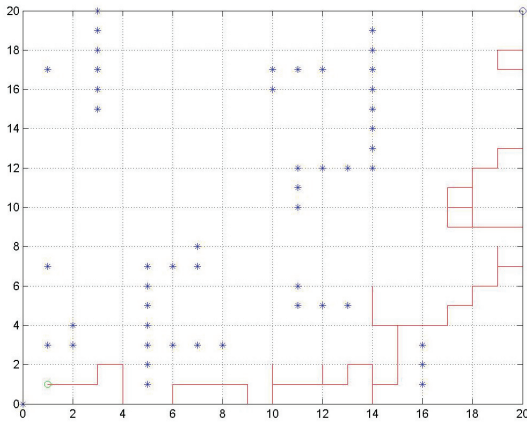


Figure 9: Trajectory of the actor « i ». $Certitude = 0.1565$, $\gamma=0.9$, $\alpha=0.1$, $\varepsilon=0.5$.

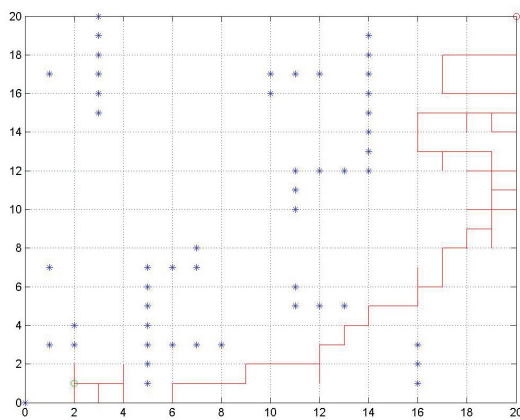


Figure 10: Trajectory of the actor « j ». $Certitude « j » = 0.1402$, $\gamma=0.9$, $\alpha=0.1$, $\varepsilon=0.1$.

We have noticed that with the Q-multi-actors approach, the number of times that the actors "i" and "j" have to find the goal is larger than in the distributed architecture. We also noticed that the certainty for the actor "I" or "J" are larger compared to the two preceding architecture. The multi-actors approach with a strategy of communities gives the best results.

7. CONCLUSION

We have presented in this paper some problems of distributed control system in a multi-actors system. Then we gave a short definition of the reinforcement learning with its principle and various architectures for the improvement of actors' behaviours. In the third part we have been dealing with Shannon's entropy which we have used to treat the coordination and the training of the actors and the measurement of the coherence choices of the action for the transformation of the reinforcement signal table.

The results show that the main advantage of distributed is the reduction in communication costs. The Q-learning distributed and Q-multi-actors algorithms which we have presented in this paper with Shannon's entropy technique for reinforcement signal calculated

show that with a given actor, the training is faster and that the Shannon's entropy shows well that the actor did not manage to learn and to coordinate with the other actors and it shows that there is coherence in the choice of the actions.

Finally, generally the number of equation to solve simultaneously increases very quickly with the number of actors. Our future work is as follows:

We study the application of these learning's architecture on a great number of actors to treat the complexity of coordination and to deal with the problems of training time. We will study too with multi-actors architecture the problems of interaction, communication and the co-operation between the various actors.

REFERENCES

- Claus C., and Boutillier C., 1998. *The Dynamics of Reinforcement Learning in Cooperative Multiagent Systems*. AAAI, pp.746-752.
- Littman M. L., 2001. *Value-function reinforcement learning in Markov games*. Journal of cognitive Systems Research 2, Elsevier, pp. 55-66.
- Hu.J., Wellman M.P.,1998. *Multiagent Reinforcement Learning: Theoretical Framework and an Algorithm*. 15th International Conference on Machine Learning, in Madison, Wisconsin, USA, pp. 242-250.
- Sutton R.S., and Barto A.G., 1998. *Reinforcement Learning*, Mit press, Cambridge, Bradford book, 322p., ISBN 0-262-19398-1.
- Jaakkola J., Jordan M.I., and Singh S.P., 1994. *Reinforcement learning algorithm for partially observable markov decision problems*", In G.Tesauro, Eds, advances in neural information processing systems, vol. 7, pp.345-352.
- Touzet C., 1993. *Apprentissage par renforcement neuronal d'un comportement d'obstacles pour le mini-robot Khepera*. Second European congress on systems sciences, Prague, pp.5-8.
- Buffet O., Dutech A., and Charpillet F., 2003. *Apprentissage par renforcement pour la conception de systèmes multi-Agents réactifs*". In Journées Francophones sur les Systèmes Multi-Agents, Hammamet, Tunis, pp.219-231.
- Pomorski D., Staroswiecki M., Barboucha M., 1990. *Modelling complex systems via the analysis of qualitative data*. MIM-s2, Bruxelles, p6.
- Zennir Y., and Couturier P., 2004. *Control of the trajectory of a hexapod robot based on distributed Q-learning*. IEEE International Symposium on Industrial Electronics, Ajaccio, France, pp.277-282.
- Zennir Y., Couturier P., and Bétemps M., 2003. *Distributed reinforcement learning of a six-legged robot to walk*. IEEE 4th International conference on control and automation, Control chapter, Singapore, Montreal section, Montréal, Canada, pp.896-900.

SIMULATION OF GRASS PHENOPHASES IN INNER MONGOLIA, CHINA

Yurong Wei 1^{(a)(b)}, Xuebiao Pan 2^(c), Yanfang Cao3^(d), He Zhou4^{(a)*}

^(a) Institute of Grassland Science China Agriculture University, Beijing 100094, China

^(b) The Ecological and Agricultural Meteorological Centre, Meteorological Bureau of Inner Mongolia, Huhhot, Inner Mongolia 010051, China

^(c) Institute of Resources and Environment, China Agriculture University, Beijing 100094, China

^(d) The Meteorological Information Centre of Inner Mongolia, Meteorological Bureau of Inner Mongolia, Huhhot 010051, China

^(a) zhouhe@cau.edu.cn, ^(b) yuerong_w@126.com, ^(c) panxb@cau.edu.cn, ^(d) nmcaoyanfang@126.com

ABSTRACT

Improved understanding of grass developmental responses to environmental conditions can lead to more reliable predictions of herbage production, and may help in the design of plants that are better matched to their environment. There are modules in most crop growth models to simulate plant phenological development but not to model grass development on natural grassland. An algorithm to quantify the relationship between phenology and environmental factors including temperature, photoperiod and soil moisture was proposed in this paper. A dataset of phenological observation for four natural perennial grass species: *Allium anisopodium*, *Stipa baicalensis*, *Cleistogenes squarrosa* and *Artemisia frigida* from 1995 to 2007 was used to validate the model. The results showed that the model could simulate phenology of the species with acceptable accuracy.

Keywords: simulation, grassland, grass development, phenology

1. INTRODUCTION

The observation of the timing of plant emergence and flowering is a long-standing feature of human societies because plant phenology is a comprehensive reflection of climatological and ecological systems and the indicators of climate change (Leith, 1974; Fang and Yu, 2002; Fitter and Fitter, 2002; Dose and Menzel, 2004). Recently there has been a resurgence of interest in plant phenology because of climate change. Global climate change has increased the length of the growing season in temperate regions by as much as 12–18 d over the last two decades of last century (Zhou et al., 2001). This includes an earlier onset of the growing season (Menzel et al., 2006), as well as an extension of the growing season in the autumn.

Developmental processes are recognised either via changes in the number (not the size) of plant organs, or via the time taken for particular morphological events such as flowering. Thus, plant development may be measured via the number of leaves formed and, as leaves die, plant senescence and the onset of dormancy. Important stages can also be defined that enable

estimates of the speed of plant development to be made (Porter et al., 1987). Plant development is heavily dependent on both high and low temperatures for the control of the rate of development and the switch from the vegetative to the reproductive state. The rate of development is affected by temperature in the ways: (1) a period of low temperature early in development hastens progress towards flowering in many temperate plant species and cultivars - this is low-temperature vernalisation; (2) besides vernalisation, progress towards flowering is normally hastened by a temperature increase between a base value and an optimum. Responses across this suboptimal range of temperatures can be modified by photoperiod or vernalisation; and (3) above the optimum temperature further warming causes the developmental rate to decelerate. Although temperature is major dominant element on controlling plant development, there are other environmental factors playing a role in it, e.g. photoperiod and the status of soil moisture in the root zone.



Figure 1: Location of Xilingol Steppe in Inner Mongolia, China

There are modules in most crop growth models to simulate plant phenological development but not to model grass development on natural grassland. The objective of the paper is to describe the algorithm to quantify the relationship between grass phenological development and environmental factors including temperature, photoperiod and soil moisture. A dataset of phenological observation for four natural perennial grass species in Xilingol steppe of Inner Mongolia, China was used to validate the model. The Xilingol

steppe located at the latitude of 43°57'N, the longitude of 116°04'E and the altitude of 989.5m above the sea level(Figure 1).

2. MATERIALS AND METHODS

2.1. Climate Change Background

Xilingol steppe not only provides a natural biological defence for northern china, but also is the most important animal husbandry productive place. Xilingol grassland was degenerate since 1980. The serious problem was that the degenerate speed is not being slowly, but accelerated. Some researcher reported that it was caused by over graze in grassland (Qing-feng,L et al, 2002), but others reported that it was caused by climate change (Yang, H et al, 2009).

Dominated by a continental climate, Xilingol grassland has a windy spring and winter, with frequent droughts in spring and summer, sometimes even a long drought period lasting from spring until autumn. The consequence of this is that the ecosystems in the region are fragile and sensitive to a changing climate. As global temperature changes, annual mean temperature in Xilingol also has the tendency to rise (Table 1 and Figure 1). The annual precipitation has the tendency to decrease (Figure 2), and the sunshine hours has also decrease (Figure 3).

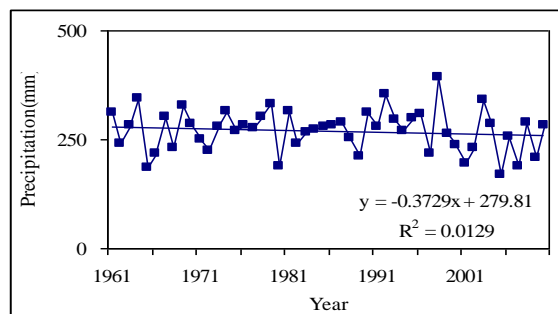


Figure 3: Annual Precipitation Tendency in Xilingol Grassland

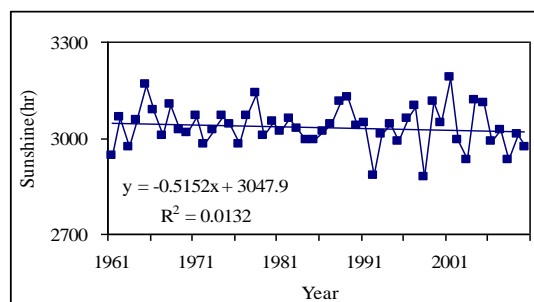


Figure 4: Annual Sunshine Hours Tendency in Xilingol Grassland

Table 1: Annual Climate Change Tendency in Xilingol Grassland

Years	Temp* °C/10a	Tmax °C/10a	Tmin °C/10a	Prec mm/10a	Suns hr/10a
1961-1990	.24	.03	.54	-.13	5.22
1971-2000	.54	.42	.68	7.52	-5.22
1981-2010	.66	.68	.60	-14.13	-6.89

Temp: annual mean temperature

Tmax: annual mean maximum temperature

Tmin: annual mean minimum temperature

Prec: annual precipitation

Suns: annual sunshine hour

Table 2: Climate Change Tendency from Different Season in Xilingol Grassland

season	Years	Temp* °C/10a	Tmax °C/10a	Tmin °C/10a	Prec mm/10a	Sunl hr/10a
Spring	1961-1990	0.2	-0.1	0.5	-1.3	4.4
	1971-2000	0.6	0.5	0.7	3.2	-2.9
	1981-2010	0.5	0.4	0.5	6.7	-18.6
1961-2010		0.4	0.2	0.6	2.4	-6.9
Summer	1961-1990	0.0	-0.1	0.3	-2.2	4.3
	1971-2000	0.4	0.3	0.6	7.5	-5.6
	1981-2010	0.8	0.8	0.6	-19.4	10.3
1961-2010		0.4	0.3	0.5	-6.4	3.5
Autumn	1961-1990	0.3	0.0	0.7	1.7	-2.1
	1971-2000	0.5	0.4	0.6	-4.3	2.4
	1981-2010	0.8	0.8	0.6	-0.6	2.8
1961-2010		0.5	0.4	0.6	-0.4	-1.1
Winter	1961-1990	0.1	0.0	0.3	1.1	7.4
	1971-2000	0.9	0.8	1.1	0.7	0.5
	1981-2010	0.8	0.9	0.8	-1.0	1.2
1961-2010		0.5	0.4	0.6	0.5	3.1
Growing Season	1961-1990	0.0	-0.3	0.4	-2.7	9.5
	1971-2000	0.5	0.3	0.6	7.3	-7.0
	1981-2010	0.7	0.6	0.6	-14.1	-2.5
1961-2010		0.4	0.2	0.5	-4.8	-0.5

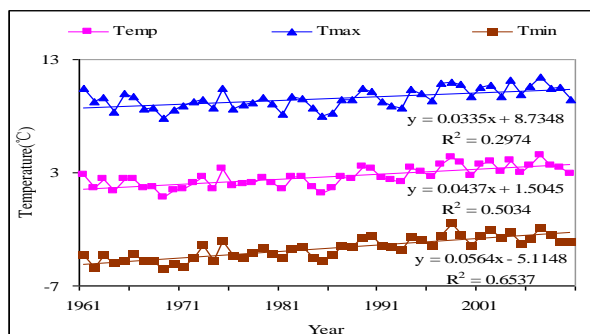


Figure 2: Annual Mean Temperature Tendency in Xilingol Grassland

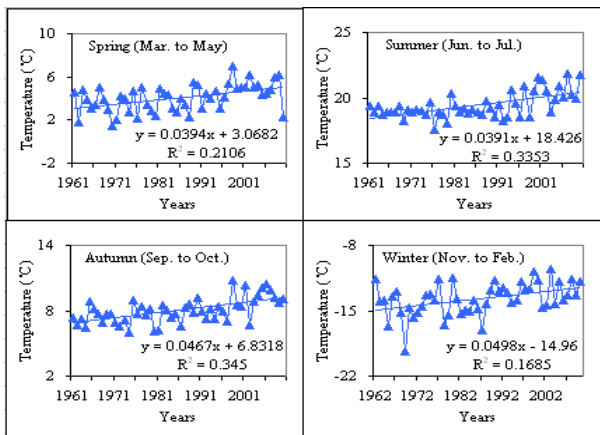


Figure 5: The Seasonal Temperature Change Tendency in Xilingol Grassland

The climate change is different in each season. In the periods of temperature increase, whether it were annual, winter or spring temperatures, mean minimum temperatures increased more than mean temperatures, with the exception of summer and autumn for the later observational period. The spring and winter temperatures (minimum as well average) of 1971 - 2000 increased much faster than those during the baseline period of 1961 to 1990. From the 1981-2010, the summer and autumn temperature increased much faster than those period 1961 to 1990 and 1971 to 2000 (Table 2). Season climate change tendency can be see in figure 4 and figure 5.

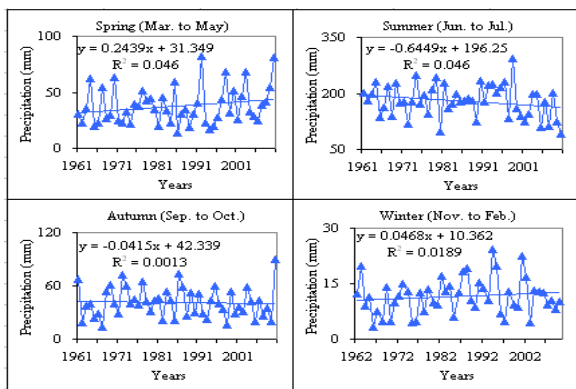


Figure 6: The Seasonal Precipitation Change Tendency in Xilingol Grassland

The spring precipitation tendency is increase and the summer precipitation tendency is decrease. Autumn and winter has no more change.

2.2. Phenological Observation

Phenology of plants is a comprehensive reflection of seasonal climatological and cyclic ecological conditions and may be used as an indicator of climate change (Lieth, 1984; Fang & Yu, 2002; Dose and Menzel, 2004; Li, et al., 2005). The phenological studies based on the

European Monitoring Network showed that phenology in spring advanced significantly and events in autumn were extended. The International Phenological Garden (IPG) data gathered from 1959-1993 in European countries revealed that the growing season has extended by 10.8 days since the 1960s while the beginning of spring phenology advanced by 6 days (Roetzer et al., 2000; Estrella and Sparks, 2007).

Similar results were observed from the China Phenology Observing Network. It showed that spring phenology advanced and autumn phenology was delayed in North and Northeast China (Fang and Yu, 2002; Zheng, Ge and Zhao, 2003; Tao, Masyuki, Yokozawa and Xu, 2006; Yurong, W, et al, 2010).

But for natural perennial grass species the result is different from woody and herb plants. All four grass species spring phenology was delayed. Three of four grass species flowering phenology was advanced, and half grass species withered phenology was advanced.

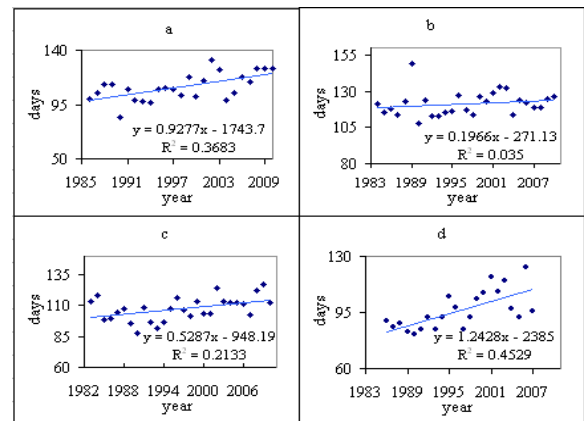


Figure 7: Four Grass Species Regrowth Phenology in Xilingol Grassland (a. *Allium anisopodium* b. *Cleistogenes squarrosa* c. *Stipa baicalensis* d. *Artemisia frigida*)

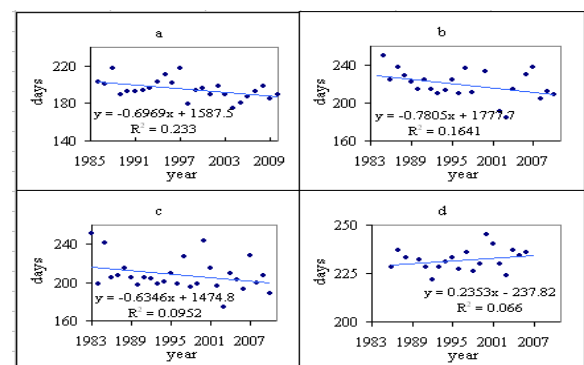


Figure 8: Four Grass Species Flowering Phenology in Xilingol Grassland (a. *Allium anisopodium* b. *Cleistogenes squarrosa* c. *Stipa baicalensis* d. *Artemisia frigida*)

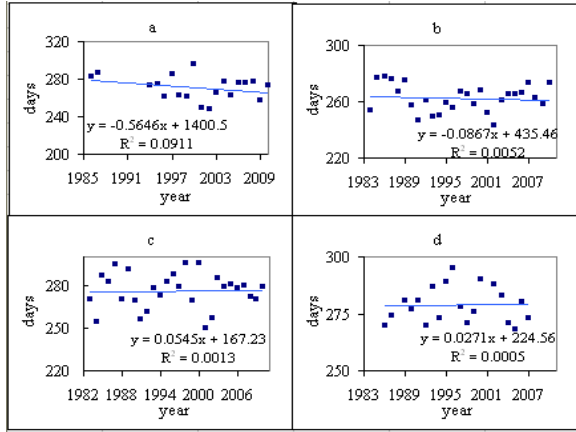


Figure 9: Four Grass Species Withered Phenology in Xilingol Grassland (a. *Allium anisopodium* b. *Cleistogenes squarrosa* c. *Stipa baicalensis* d. *Artemisia frigida*)

2.3. Model development

Plant development is estimated based on its requirement for heat, expressed in degree.days, and threshold temperatures during different stages. It is divided into three periods for perennial grasses: regrowth - flowering, flowering - withered and withered - regrowth (dormancy). The development index is expressed as:

$$Development\ index = \sum \frac{T_{add}}{ADD} \quad (1)$$

where ADD is an required accumulated degree-days for a given period and T_{add} is accumulated temperature from the beginning of a given period to the current time of simulation when it is still within the period.

$$T_{add,i} = \begin{cases} T_{a,i} \times [1 - e^{-kp \times (Dayl_i - photop)}] & (T_{a,i} \geq T_c) \\ 0 & \end{cases} \quad (2)$$

where $T_{a,i}$ is air temperature on the i day, $Dayl_i$ is day length (hr) on the i day, T_c is threshold temperature for a given development stage below which there is no temperature accumulated. kp is a photo-period response control parameter, and $photop$ is critical photo-period during vegetative stage (hr). For long-day plants, it is zero when day-length on the day is shorter than pp_c .

The sigmoid function described by Streck et al. (2003) was chosen to be implemented in order to avoid introducing more parameters into the model:

$$f(VD) = \frac{VD^5}{22.5^5 + VD^5} \quad (3)$$

where VD is cumulated vernalisation days since emergence of an over-winter plant. Because of the nature of the sigmoid curve, the function approaches to its maximum value only as VD approaches ∞ . It would be possible for plant to have an indefinite period for the process. For simplification, it is assumed the

vernalisation process finishes when the function is greater than 0.95.

One VD is attained when the plant is exposed to the optimum temperature for a period of one day. As temperature departs from the optimum, only a fraction of one VD is accumulated by the plant at a given calendar day:

$$VD = \sum_{i=0}^n f_{VD,i} \quad (4)$$

and

$$f_{VD,i} = \begin{cases} 0.0 & (T_i \leq T_{vmin} \text{ or } T_i \geq T_{vmax}) \\ \frac{T_i - T_{vmin}}{T_{vopt} - T_{vmin}} & (T_{vmin} < T_i \leq T_{vopt}) \\ \frac{T_{vmax} - T_i}{T_{vmax} - T_{vopt}} & (T_{vopt} < T_i < T_{vmax}) \end{cases} \quad (5)$$

where T_i is daily average temperature at the given day i , and T_{vmin} , T_{vopt} and T_{vmax} are minimum, optimum and maximum temperatures that control the response function to air temperature, respectively.

In order to consider the effect of soil water on plant development, a reduction on daily accumulated temperature was made during vegetative and reproductive stages. When the ratio of actual evapotranspiration rate to potential evapotranspiration rate is less than a user-defined critical ratio value, 30% and 40% of accumulated temperature on that day was reduced during the period of regrowth - flowering and that of flowering - defoliation, respectively.

2.4. Observational data

Phenological data came from the Livestock Meteorological Experimental Station of Xilingol League, Inner Mongolia, located at the latitude of 43°57'N, the longitude of 116°04'E and the altitude of 989.5m above the sea level(Fig.1).

There are two native level livestock meteorological experimental stations in China. Xilingol station is one of them. Except routine weather observation items, the station have other four kind of observation work. One is natural phenology work, which include woody, herb plant and migratory bird phenology. Second is grass growth and developmental, include phenology and biomass. The third is soil moisture. And the last one is livestock gain weight.

Woody plants:*Populus tomentosa*, *Salix babylonica* L. and *Ulmus pumila* L. Herb plants:*Taraxacum mongolicum*, *Plantago asiatica* and *Iris ensata*. Migratory birds:*Anser fabalis serratirostris* and *Hirundo rustica gutturalis Scopoli*.

More than seven grass species are observed phenology and height(Table 1).

Table 1: Observation Grass Species in Xilingol

Chinese name	Latin Name	Data length	Validate Species
Xiyecong	<i>Allium tenuissimum</i>	1986-2010	
Chaoyinzicao	<i>Cleistogenes squarrosa</i>	1984-2010	*
Mudifu	<i>Kochia prostrata</i>	2002-2010	
Aicong	<i>Allium anisopodium</i>	1986-2010	*
Keshizhenmao	<i>Stipa krylovii</i>	1983-2010	*
Lenghao	<i>Artemisia frigida</i>	1986-2007	*
Yangcao	<i>Leymus chinensis</i>	1983-2010	

The plot is fixed. Effect on climate change or weather conditions some grass species can not be observed in some years. For example, Due to succession drought *Leymus chinensis* can not be monitor in some years. Sometime it can be monitor the regrowth, but can not be see the flowering. Although it is key constructive species in Xilingol steppe. Therefore, the follow four grass species are choose to validate model. There are *Allium anisopodium*, *Stipa baicalensis*, *Cleistogenes squarrosa* and *Artemisia frigida*

The most three important phenophases of regrowth, flowering and withering of dominated recorded was used from 1995 to 2007.

Weather data are required to simulate phenological development of the species. As the temporal iteration step is daily-time-step-based, daily maximum and minimum air temperatures, wind speed and precipitation (for water cycle) are essential in the weather dataset. Both daily solar radiation above the canopy and net radiation are estimated from other relevant weather elements.

3. RESULTS AND DISCUSSION

Table 1: Comparison Between Simulated (Sim.) and Observed (Obs.) Flowering Dates of Six Perennial Grass Species (The Numbers Within the Table are Days Since the Beginning of a Year. ‘-’ Indicates no Data Available)

Year	<i>Allium Anisopodium</i>		<i>Cleistogenes Squarrosa</i>		<i>Stipa Baicalensis</i>		<i>Artemisia Frigida</i>	
	Sim.	Obs.	Sim.	Obs.	Sim.	Obs.	Sim.	Obs.
1995	197	-	223	228	229	234	232	236
1996	193	-	219	225	218	235	218	233
1997	194	-	224	-	233	-	237	241
1998	187	187	211	218	207	218	207	232
1999	197	203	224	-	228	235	226	238
2000	188	-	225	240	227	-	231	260
2001	190	207	228	-	222	-	239	-
2002	203	-	233	203	243	-	230	232
2003	202	197	232	193	220	196	228	235
2004	189	186	222	223	227	230	224	246
2005	196	193	228	-	234	-	251	245
2006	197	187	224	230	232	230	262	236
2007	194	193	224	238	230	251	236	236

Simulation results for the dates of flowering and defoliation for those species were compared with

observed dates (Table 1 and 2), which showed that the model could simulate the occurrence of phenophases with acceptable accuracy. Apparently there are discrepancies between simulated and observed dates. There may be several reasons contributed to the discrepancies. Firstly the model is a simplified assumption to mimic the dynamics of phenology on which many physiological and chemical processes control. It is necessary to improve the functionality of the model, especially the effect of soil water on them. And secondly actual phenophase could last several days even longer which inevitably causes the errors of observation. Among the species, the estimation for *Artemisia frigida* has the largest discrepancy compared with observed dates in individual years, which it is worth investigating it further.

Table 2: Comparison between simulated (sim.) and observed (obs.) withering dates of six perennial grass species (the numbers within the table are days since the beginning of a year. ‘-’ indicates no data available)

Year	<i>Allium Anisopodium</i>		<i>Cleistogenes Squarrosa</i>		<i>Stipa Baicalensis</i>		<i>Artemisia Frigida</i>	
	Sim.	Obs.	Sim.	Obs.	Sim.	Obs.	Sim.	Obs.
1995	246	248	252	250	262	255	283	289
1996	244	252	247	244	250	250	256	295
1997	238	-	252	-	272	-	301	278
1998	238	234	238	244	237	239	244	271
1999	240	237	251	-	255	257	259	276
2000	222	-	253	252	258	-	272	290
2001	233	241	254	-	245	-	269	-
2002	250	-	259	228	271	-	259	288
2003	255	240	267	220	250	243	272	283
2004	238	243	255	252	259	260	270	271
2005	234	246	253	-	256	-	294	268
2006	241	243	250	253	261	261	314	280
2007	239	-	250	-	254	270	268	273

ACKNOWLEDGMENTS

The research is funded by 2007BACO3A02-3 and GYHY200706024 of the Ministry of Sciences and Technology, China.

REFERENCES

Evans, W.A., 1994. Approaches to intelligent information retrieval. *Information Processing and Management*, 7 (2), 147–168.

Dose, V., and Menzel, A., 2004. Approaches to intelligent information retrieval. *Global Change Biology*, 10:259-272.

Fang, X., and W. Yu. 2002. Progress in the studies on the phenological responding to global warming. *Advance in Earth Sciences*, 17:714-719.

Fitter, A.H., and R.S.R. Fitter. 2002. Rapid changes in flowering time in British plants. *Sciences* 296:1689-1691.

Leith, H. 1974. Phenology and seasonality modeling. *Springer-Verlag, New York*.

Menzel, A., T.H. Sparks, N. Estrella, et al. 2006. European phenological response to climate

- change matches the warming pattern. *Global Change Biology* 12:1969-1976.
- Porter, J.R., E.J.M. Kirby, W. Day, et al. 1987. An analysis of morphological stages in Avalon winter wheat crops with different sowing dates and at ten sites in England and Scotland. *Journal of Agricultural Science* 109:107-121.
- Streck, N.A., A. Weiss, and P.S. Baenziger. 2003. A generalized vernalization response function for winter wheat. *Agron. J.* 95:155-159.
- Weir, A.H., P.L. Bragg, J.R. Porter, and J.H. Rayner. 1984. A winter wheat crop simulation model without water or nutrient limitations. *J. Agr. Sci.* 102:371-382.
- Zhou, L.M., C.J. Tucker, R.K. Jaufmann, D. Slayback, N.V. Shabanov, and R.B. Myneni. 2001. Variations in northern vegetation activity inferred from satellite data of vegetation index during 1981 to 1999. *Journal of Geophysical Research Atmospheres*. 106:20069-20083.
- Dose, V. and Menzel, A. 2004. Bayesian analysis of climate change impacts in phenology. *Global Change Biology*, 10, 259-272.
- Tao, F., Masayuki, Yokozawa and Xu, Y. 2006. Climate changes and trends in phenology and yields of field crops in China 1981–2000. *Agricultural and Forest Meteorology*, 138, 82–92.
- Zheng, J., Ge, Q. and Zhao, H. 2003. Changes of plant phenological period and its response to climate change for the last 40 years in China. *Chinese Journal of Agrometeorology*. 24, 28-33. (In Chinese)
- Qingfeng, L., Fusheng, L. and Lan, W. 2002. A primary analysis on climatic change and grassland degradation in Inner Mongolia. *Agricultural Research in the Arid Areas*. 20, 98-102. (In Chinese)
- Yang, H., Yongfei, B., Yonghong, L. and Xingguo, H. 2009. Response of Plant Species Composition and Community Structure to Long-Term Grazing In Typical Steppe of Inner Mongolia. *Chinese Journal of Plant Ecology*. 33, 499-507. (In Chinese)
- Yurong, W., Yanfang C., Xuebiao P. and Ruiqing G. 2010. The Impact of Climate Change on Phenology of Woody Plants in Inner Mongolia, China. *Proceedings of 2010 Climate Change and Ecosystem Response Conference*, 147-152. July, 2010. Inner Mongolia, China.

AUTHORS BIOGRAPHY

Yurong Wei, research fields is grassland ecology and climate change. As an visiting scholar had been in Hohenheimer University, Stuttgart, Germany and Oregon University, Oregon, USA.

Some projects have been done, there were “Research on the climate fluctuation impact on the grassland ecological recovery period”. “Developing the monitor and assessment technology to ecological system of farming-pastoral ecotone in Northern China”. “Climate change impact and adaptation key technology in steppe grassland” etc.

CAPABILITY OF TODAY'S PROGRAM VERIFICATION: A PRACTICAL APPROACH FOR BETTER QUALITY AND RELIABILITY IN INDUSTRIAL APPLICATIONS

Michael Bogner^(a), Johannes Schiller^(b), Franz Wiesinger^(c)

^(a, b, c)University of Applied Sciences Upper Austria – Embedded Systems Design,
Softwarepark 11, A-4232 Hagenberg, AUSTRIA

^(a) michael.bogner@fh-hagenberg.at, ^(b) johannes.schiller@fh-hagenberg.at, ^(c) franz.wiesinger@fh-hagenberg.at

ABSTRACT

Software programs are an essential part of our everyday's life. Starting with large software programs on the PC, via complex control systems for the industrial area, to safety-critical software solutions for the automotive and aerospace industry; software is almost everywhere. Especially nowadays a high degree of reliability and security is essential. But due to the constantly growing size and complexity of such software programs the verification effort is increasing too. For this reasons, beneath dynamic testing and manual reviews, automatic verification methods became more and more popular. This paper deals with the expected benefits and the effectiveness of static code analysis and especially shows the limitations of this technique. Empirical tests have been developed and various code analysis tools employed. The paper discusses the obtained results. It becomes apparent that current code analysis tools can already find a variety of potential errors and weaknesses while critical cases are still undetected.

Keywords: static code analysis, software, testing, verification, Goanna Studio, PC-lint, Yasca, C++

1. INTRODUCTION

Current software programs become more complex from year to year. The test and verification effort for these software programs is constantly increasing and it becomes increasingly intricate to maintain these systems properly. Therefore, automatic static code verification became more and more popular in the last few years. Beneath dynamic testing methods and manual code reviews, static code analysis is another instrument to ensure the safety and reliability of future software programs. Even before the actual execution of the software program, the program code is checked against weaknesses and errors by a strict set of rules.

Therefore static code analysis can already be used in early stages of development to detect critical errors in software programs and eliminate them. This paper provides a brief introduction to the topic of static code analysis and shows the current state of the art respectively the power of technology in this area.

Static code analysis is a method for quality assurance of software programs. The underlying program code is statically checked for weaknesses and errors. At automatic static code analysis the analysis of

the program code is performed using special software programs. To analyze the program code as effective as possible, these code analysis tools use a large number of different kinds of analysis methods and software metrics. The respective program code must neither be complete nor executable (Hoffmann 2008, Liggesmeyer 2009).

Static code analysis can be used everywhere where software is developed. Especially for large software projects or for safety critical applications the use of static code analysis is recommended. Some programming conventions, like MISRA-C++ (MISRA 2008) or the UK Defence Standard 00-55 (German 2003), explicitly stipulate the use of static code analysis for safety-critical software. At the same time static code analysis cannot replace ordinary, dynamic testing methods.

The aim of this study was to determine the practical benefits of static code analysis and the current state of the art in this area. Therefore it was attempted to use real life examples and analysis tools which are preferably different.

2. RELATED WORK

Static code analysis has become increasingly important in the last years. For this reason there are many works which deal with the investigation of static code analysis (Muchnick 1981, Hoffmann 2008, Liggesmeyer 2009) and other with the evaluation and comparison of static analysis tools (Emanuelsson 2008, Hofer 2010, Almoosawi 2006). Many works in this field are more specialized in the theoretical operating principles (Fehnker 2007, Miller 2007) or concentrate on a very specific area of computer programming (Cong 2009, Cooper 2002).

3. VERIFICATION METHODOLOGIES

In the context of software development, verification means to ensure that a given program code or algorithm meets its formal specification. In the case of static code analysis, the instruction set and the syntax of the programming language form the formal specification.

Static code analysis tools use a variety of different methods to verify the correctness of the respective program code. For example dataflow- and controlflow-analyses are used. Some tools, like Goanna Studio transform the respective program code into a finite state machine and use model checking techniques for the

evaluation. Beneath these hard criteria the tools often use software metrics to determine the quality of the respective program code. Therefore the program code will be converted into different quantifiable values. Among the most popular metrics are Halstead-, McCabe-, component- and structural metrics (Hoffmann 2008, Liggesmeyer 2009, Fehnker 2006, Fehnker 2007).

Static code analysis can not give any information about the functional correctness of a program code. Even if static code analysis couldn't find any errors or flaws in the program, there is no guarantee that the examined program delivers the correct result.

4. USED SOFTWARE SOLUTIONS

To determine the current state of the art of static code analysis, three different code analysis tools have been evaluated. To get a broad overview of the subject it was attempted to choose software solutions that are as different as possible.

The choice fell on the following software solutions: Goanna Studio, PC-lint and Yasca.

4.1. Goanna Studio

Goanna Studio is a C++ code analysis tool by the company Red Lizard Software. It follows the approach to use model checking for searching the program code quickly and effectively. Model checking is an automated process to analyze transition systems. Therefore, the C++ code needs to be converted into a context-free grammar. After that it will be analyzed through the model checker. Especially in large projects this can lead to performance advantages. Another advantage of this method is the simple and fast expandability of the analyzing-rules (Huuk et al. 2008, Fehnker et al. 2007, Red Lizard Software 2012)

Goanna Studio was used in the version 2.4.1 (trial version).

4.2. PC-lint

PC-lint is a C / C++ code analysis tool by the company Gimpel Software. It is one of the well-established code analysis tools on the market. It is a pure console application. This has affects on the clarity and usability of the tool. However there are some plug-ins available which can add GUI elements to PC-lint. This is advisable especially for large projects. One of the biggest advantages of PC-lint is that it supports a variety of different Compilers and programming conventions (Gimpel Software 2012).

PC-lint was used in the version 9.00.

4.3. Yasca

In addition to these two commercial solutions the open source solution Yasca was added to the evaluation. It is under the GNU General Public License and may therefore be used free of charge. Yasca is a simple code analysis tool which offers far away as much setting opportunities as the other two solutions. Thereby it combines several different code analysis tools like

CppCheck, RATS, etc. in it. These analysis tools can be added to Yasca via plug-ins. It is also possible to add your own rules (Scovetta 2012, Cppcheck 2011, Fortify Software 2012).

Yasca was used in the version 2.21.

5. THE TEST CODE

The selected software solutions were evaluated using an extensive test code. This test code covers the major areas of the programming language and includes a broad range of errors typically found in industrial applications. By combining on the one hand, frequently occurring errors with on the other hand more complex errors, the suitability for daily use of static code analysis should be covered and the limits of the current technology demonstrated.

5.1. The programming language

C++ was selected as programming language for the test code. C++ is a very well known and widely used programming language. Beneath C and Assembler, C++ plays more and more a role in safety-critical areas, such as Embedded Systems. Especially in these areas a high degree of safety and reliability is essential. Through the use of so-called programming conventions, such as MISRA-C++, the programming language can gain additional security. However the programming language is therefore somewhat limited in their functionality. PC-Lint is the only one of the three software solution that supports the programming convention MISRA-C++.

5.2. Structure of the test code

The test code was structured in several projects. Each of them concentrates on a specific area of the programming language. To analyze the performance of the different code analysis tools, it was attempted to build as much errors as possible into the individual projects. A large part of these errors are typical errors from the daily practice. To verify the limitations of static code analysis these errors were supplemented by some more specific and complicated errors. Additionally in some cases deliberately messy code was used, to simulate real conditions and make it more difficult for the evaluated analysis tools.

The following sections of the programming language are covered by the test code:

- Bounds Checking
- Division by Zero
- Memory Leaks
- Over- / Underflows
- Out-of-Scope Errors
- Problems with Classes
- Problems with Threads: Deadlock
- Problems with Threads: Race Condition

5.3. Examples

Below are a few examples of errors which are included in the test code. The errors in the test code are on the one hand self-designed. On the other hand a large

In Listing 2 the programmer intended to create an integer array *pa* with the size of *n* (10). However a small error crept in. Instead of square brackets the programmer used round brackets. Therefore, instead of creating an array with the size of 10, an integer value with the initial value of 10 will be created. As a consequence, each access, except of the first one, results in a violation of the memory area representing a serious error. Furthermore the allocated memory for the integer value *pa* will be freed with the keyword *delete []* instead of *delete*, which normally will not lead to any serious problems. Anyhow there is no guarantee that it would cause unwanted side effects on some systems.

5.3.3. Example 3

Listing 3: Program code of Example 3.

```

1 class Number{
2 public:
3     Number(int val = 0):Num(val){}
4     ~Number(){}
5
6     int getNum(){
7         return Num;
8     }
9 private:
10    int Num;
11 };
12
13 int main(){
14     Number *n1 = new Number(5);
15     Number *n2 = new Number();
16     //...
17     n2 = n1;
18     //...
19     delete n1; n1=0;
20     //...
21     delete n2; n2=0;
22     return 0;
23 }

```

Listing 3 shows a good example how the default Copy Constructor respectively Assignment Operator can lead to problems. The class *Number* has a member variable *Num*. In the *main* statement two instances of the class *Number* were dynamically created, *n1* and *n2*. The programmer wants to assign the value of *n1* to *n2* and uses the Assignment Operator. However, instead of copying the value of *n1* to *n2*, the memory address will be copied. Therefore after this assignment both pointer point to the same memory address. In most of the cases this is not intended and can lead to unwanted behaviour. In this case the memory would be freed twice, which can lead to security flaws and crashes.

5.4. Test Criteria

For reasons of clarity and comprehensibility only faults with a security level of *error* or *warning* were considered in the evaluation. The code analysis tool Yasca finds on its own admission only errors which would not be found by a conventional compiler. The code analysis tool Goanna Studio is integrated in the IDE of the MS Visual Studio and shares therefore the

same error-window with the compiler. For this reason, errors which were already found by the compiler are not included in the evaluation of Yasca and Goanna Studio. To have a comparable basis, MS Visual Studio 2008 (SP1) was used as compiler for all test cases. All test cases could be compiled without any errors.

6. RESULTS OF THE EVALUATION

This Chapter provides a compact overview of the various kinds of errors found by the individual code analysis tools. Therefore all found errors of a section are compared with the expected errors for the same section. In some cases additional errors were found by the analysing tools. This additional errors were also added to the evaluation and it was determined whether these errors refer to real problems (true positive) or not (false positive). No code analysis tool can find all faults without generating some false positives. An analysis tool can only be called “safe” if it really displays all found errors and warnings. Although this increases the number of false positives, but therefore the number of false negatives is as low as possible (Emanuelsson 2008).

6.1. Overview Goanna Studio

Table 1 shows an overview of the errors found by the code analysis tool Goanna Studio. Goanna Studio found 42 of 84 errors expected and therefore achieved a success rate of 50%. Furthermore it found six additional errors. These errors are indicators for unnecessary functions or assignments. Five of these additional errors are real errors (true positives) and one is a false report (false positive). This results in one false positive of 48 errors found (ca. 2%).

Table 1: Overview of errors found by Goanna Studio.

Results Goanna Studio				
Section	Expected errors	Errors found	Additional errors found	Errors not found
Bounds Checking	15	7	0	8
Division by Zero	4	4	1	0
Memory Leaks	16	7	1	9
Over- / Underflows	6	3	0	3
Out-of-Scope	6	5	1	1
Classes	29	14	0	15
Deadlock	6	2	3	4
Race Condition	2	0	0	2
Summary	84	42	6	42

6.2. Overview PC-lint

Table 2 shows an overview of the errors found by the code analysis tool PC-lint. PC-lint found 54 of 85 errors expected and therefore achieved a success rate of 63,6%. Furthermore it found 42 additional errors. These

are, however, 30 times the warning 586. This warning refers to an unauthorized function of the MISRA programming convention. This is mainly to functions which are used for dynamic memory management, as new, delete, etc. Admittedly these functions are in violation of the MISRA guidelines, but cause no direct errors. For this reason, these errors not considered for the calculation of the false positives. Therefore there are six correct errors (true positives) of a total of twelve additional errors found. This results in six false positives of 96 errors found (ca. 6,25%).

Table 2: Overview of errors found by PC-lint.

Results PC-lint				
Section	Expected errors	Errors found	Additional errors found	Errors not found
Bounds Checking	15	10	7	5
Division by Zero	4	2	0	2
Memory Leaks	16	13	15	3
Over- / Underflows	6	4	0	2
Out-of-Scope	6	6	0	0
Classes	30	14	16	16
Deadlock	6	3	1	3
Race Condition	2	2	3	0
Summary	85	54	42	31

6.3. Overview Yasca

Table 3 shows an overview of the errors found by the code analysis tool Yasca. Yasca found 18 of 78 errors expected and therefore achieved a success rate of 23,1%. Furthermore it found seven additional errors. These are, however, rather indications than real error messages. Therefore a further classification in false respectively true positives is unnecessary.

Table 3: Overview of errors found by Yasca.

Results PC-lint				
Section	Expected errors	Errors found	Additional errors found	Errors not found
Bounds Checking	13	5	1	8
Division by Zero	3	0	0	3
Memory Leaks	16	9	0	7
Over- / Underflows	5	1	1	4
Out-of-Scope	4	2	1	2
Classes	29	1	0	28
Deadlock	6	0	4	6
Race Condition	2	0	0	2
Summary	78	18	7	60

6.4. Summary

On average, the three evaluated code analysis tools found approximately 46% of all in the test code contained errors. It is striking that there are sometimes significant differences between the various code analysis tools. For example, the open source tool Yasca finds with about 23% by far the fewest errors. The two commercial software solutions find however at least 50% of all included errors. The evaluated code analysis tools differ not only in the number of detected errors, but also by the errors found themselves. Each of the evaluated code analysis tools found at least one error, which none of the other two solutions could find. Therefore it can be found about 75% of all in the test code included errors by sequential execution of all three analysis tools (Figure 5). In consequence it is advisable to use several different analysis tools for the analysis of safety-critical systems.

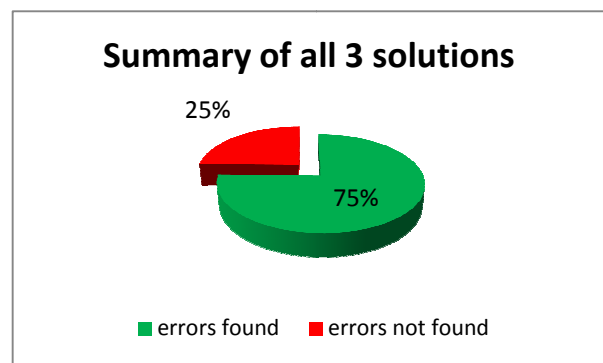


Figure 5: Summary of all 3 solutions.

Furthermore, the evaluation has shown that for small projects, the false positive rate is already well below 10%. However for large projects this value can be in some cases significantly higher. This is largely because of the increased complexity and the resulting dependencies in large projects. For this reason the subsequent evaluation of large projects can be extremely time-consuming. In such projects it is therefore advisable to use static code analysis already at the beginning of the project.

7. CONCLUSION

The evaluation of the three software solutions has shown that static code analysis is already capable to find a variety of potential errors and weaknesses within software programs. It is noticed here that certain error classes can be found very well, while others can barely be detected or can't be detected at all. For example memory leaks and out-of-bounds errors can be recognized very reliable, while errors relating to threads remain in general unrecognized. Also the context in which an error occurs plays an important role, whether this error can be found by static code analysis or not. The program code that needs to be analyzed doesn't have to be completed; neither does it to be executable. For this reason static code analysis can be used in software projects very early. Consequently, potential

errors and weaknesses can be identified and corrected as soon as possible. This can save time and money. At the same time the number of new errors can be reduced to a minimum and therefore the analysis can be kept manageable. This approach is advisable, especially for large projects.

Furthermore, it is advisable to invest enough time for the configuration of the code analysis tools and for the selection of the right programming conventions in such projects. The selection of the highest security level is in many software projects unnecessary and only leads to increased effort. The same applies to programming conventions such as MISRA-C++. In safety-critical software such conventions are essential, but in normal projects a subset of these rules is often more than sufficient.

Static code analysis can not replace dynamic testing. While dynamic testing methods are especially checking the correct function of the program code, static code analysis mainly ensures the correct and safe use of the respective programming language.

All in all, static code analysis is a simple and fast way to improve the quality of software programs without stealing too much of the developers time. Static code analysis can not replace traditional testing methods, but it provides a solid addition to these, which can already be used in very early stages of a software project. In addition static code analysis can find kinds of errors, which can't be found by other testing methods, like e.g. dead code.

Static code analysis offers a cheap and easy method to increase the security and reliability of software programs and should therefore be used in software development as common as conventional testing methods like dynamic testing or code reviews.

REFERENCES

- The Motor Industry Software Reliability Association, 2008. *Guidelines for the Use of the C++ Language in Critical Systems*.
- Emanuelsson, P. and Nilsson, U., 2008. *A Comparative Study of Industrial Static Analysis Tools*. Techn. Ber., Linköping University: Dep. of Computer and Information Science.
- Hoffmann, D. W., 2008. *Software-Qualität*. Heidelberg: Springer-Verlag.
- Liggesmeyer, P., 2009. *Software-Qualität: Testen, Analysieren und Verifizieren von Software*. Heidelberg: Spektrum-Verlag.
- Breymann, U., 2005. *C++ - Einführung und professionelle Programmierung*. München: Carl Hanser Verlag.
- Dewhurst, S., 2002. *C++ Gotchas: Avoiding Common Problems in Coding and Design*. Boston: Addison-Wesley.
- Intel Corporation, 2010. *About Static Security Analysis Error Detection*. Available from: <http://software.intel.com> [accessed 10 April 2012].
- Wolf, J., 2009. *C++ von A bis Z*. Bonn: Galileo Computing.
- Klein, T., 2003. *Buffer Overflows und Format-String-Schwachstellen*. Heidelberg: Dpunkt-Verlag.
- German, A., 2003. *Software Static Code Analysis Lessons Learnt*. Techn. Ber., QinetiQ Ltd.
- Fehnker et al., 2007. Model Checking Software at Compile Time. *Proceedings of the First Joint IEEE/IFIP Symposium on Theoretical Aspects of Software Engineering*. pp. 45-56. Washington, D.C. (USA)
- Huuk et al., 2008. Goanna: Syntactic Software Model Checking. *Proceedings of the 6th International Symposium on Automated Technology for Verification and Analysis*. pp. 216-221. Heidelberg: Springer-Verlag.
- Red Lizard Software, 2012. *Goanna Studio*. Available from: <http://redlizards.com/index.php> [accessed 10 April 2012].
- Gimpel Software, 2012. PC-lint. Available from: <http://www.gimpel.com/html/index.htm> [accessed 10 April 2012].
- Scovetta, M. V., 2012. *Yasca*. Available from: <http://www.scovetta.com/yasca.html>. <http://www.scovetta.com/yasca.html>. [accessed 10 April 2012].
- Cppcheck, 2012. *A tool for static C/C++ code analysis*. Available from: <http://sourceforge.net/apps/mediawiki/cppcheck/index.php>. [accessed 10 April 2012].
- Fortify Software, 2012. *RATS - Rough Auditing Tool for Security*. Available from: <https://www.fortify.com/ssa-elements/threat-intelligence/rats.html>. [accessed 10 April 2012].
- Fehnker et al., 2006. *Goanna - A Static Model Checker*. Available from: http://www.ssrn.nicta.com.au/publications/papers/Fehnker_HJLR_06.pdf [accessed 5 July 2012]
- Hofer, T., 2010. *Evaluating Static Source Code Analysis Tools*. Available from: <http://infoscience.epfl.ch/record/153107/files/ESS-CAT-report.pdf> [accessed 10 April 2012].
- Almossawi et al., 2006. *Analysis Tool Evaluation: Coverity Prevent*. Carnegie Mellon University, Pittsburgh, PA, USA.
- Muchnick, S and Jones, N., 1981. *Program Flow Analysis: Theory and Applications*. Prentice-Hall, Inc., Englewood Cliffs, New Jersey.
- Cong et al., 2009. *Evaluation of Static Analysis Techniques for Fixed-Point Precision Optimization*. *Proceedings of the 2009 17th IEEE Symposium on Field Programmable Custom Computing Machines*. Pp. 231-234. Washington, D.C. (USA).
- Cooper, K. and Xu Li, 2002, *An Efficient Static Analysis Algorithm to Detect Redundant Memory Operations*. Dep. of Computer Science Rice University Houston, Texas, USA.
- Miller, D., 2007, *A Proof-Theoretic Approach to the Static Analysis of Logic Programs*. Dep. of Computer Science Rice University Houston, Texas, USA.

THE CLOUD MANUFACTURING SERVICES PLATFORM STRUCTURE AND KEY TECHNOLOGIES RESEARCH IN THE MOULD INDUSTRY

Songxin Shi ^(a), Youmin Rong ^(b), Guojun Zhang ^(c), Shi Wang ^(d)

^(a)School of Mechanical Science and Engineering, Huazhong University of Science and Technology, Wuhan 430074, China

^(b)School of Mechanical Science and Engineering, Huazhong University of Science and Technology, Wuhan 430074, China

^(c) School of Mechanical Science and Engineering, Huazhong University of Science and Technology, Wuhan 430074, China

^(d) DG-HUST Manufacturing Engineering Institute, Dongguan 523808, China

^(a) shisongxin@qq.com, ^(b) rong_youmin@126.com, ^(c) zgj@mail.hust.edu.cn, ^(d) 8668816@qq.com

ABSTRACT

The phenomenon of uneven distribution of manufacturing resource and capacity is more serious in mould industry, but the approach of existing manufacturing models is difficult to strike a balance in terms of stability, quality and credit of services. On the basis of the analysis of the problems of mould industry, this paper proposes the mould cloud-manufacturing platform supporting industrial clusters cooperation; then analyzes the content of the platform in which the service of platform focused on the full life cycle platform of the product and the upstream and downstream of industrial chain. The system structure of the platform and key technologies are studied. This research will play an exemplary role for application of cloud manufacturing in other industries.

Keywords: industrial clusters, mould, cloud-manufacturing platform, system structure

1. INTRODUCTION

Mold is the basic process and equipment of the modern manufacturing industry. About 60 to 80 percent of parts that are employed in automobiles, home appliances, electronics, communication, instruments and aerospace mainly depend on the mold to manufacturing. At present, mould industry characteristics in China mainly present as follows:

1. Most mold enterprises are small or medium. The fund which enterprise offered is on a smaller scale, and the industry owns high concentration accompanied with regional characteristics.
2. The apparent demands of product individuality lead enterprise production management to be very complex. What's more, product design ability and relevant performance have important significance to the enterprise development.
3. Manufacturing equipment resources, mainly in the numerical control equipment, are not balance.

4. The driving type production comes true through small batch production facing to resources; business process is complicated; the collaboration of resources is also strong.
5. The requirement of intermediate and high-end production is strong, but in short supply.

In China, the above shortages always lead the mold industry to the following main problems: most enterprises owing low proportion of technical personnel, absention of independent research and development capacity, lacking of sophisticated testing equipment, lowing level of enterprise management, and being short of modern methods and means in product development, and so forth .

Facing the mold production shortages and existing problems, mould industry urgently need to use the advanced manufacturing model and related technologies, to integrate all available resources, so as to realize the mold production flexibly and agilely through effective manufacturing resources sharing and cooperative management, in response to the changes in demand of the customer and the market.

China's manufacturing industry informatization has done a lot of exploration and practice in manufacturing mode, such as the network manufacturing ^[1], the Application Service Provider (ASP) ^[2], and manufacturing grid ^[3], and it has promoted the development of small and medium-sized enterprises. However, it is difficult to establish the public platform for industrial cluster cooperation to offer an agile, high quality, low price and integrated service, for the problem of the service and operation mode, the personalized service support, operation mechanism and so on.

Reference the thought of cloud computing "on-demand service", the cloud manufacturing is a new manufacturing mode combined with all kinds of advanced technologies. Academician Bohu Li ^[4~6], professor Haicheng Yang ^[7], and professor Xinjian Gu

[8] etc have made full discussion on the concept of the cloud manufacturing, and point out that the cloud manufacturing is a new mode and new technology owning characteristics, such as facing to service, high efficiency, low energy consumption, and agile manufacturing. Cloud manufacturing emphasizes the use of information technology to integrate all kinds of manufacturing resources, and through virtualization technology to provide users with standardization service. Users can acquire all kinds of services through the cloud-manufacturing platform. At the same time, these services have a quantity of features, such as real-time utilization, paying according to the demand, safety, reliability, high quality and low-cost. In conclusion, cloud manufacturing process to the concept of manufacturing as service which is different from the traditional WEB mode (software as a service).

On the basis of the characteristics of mold industry, we build the mould cloud-manufacturing platform which can support the collaboration of industry clusters. We firstly put forward the construction content of the platform; then study the system structure of the platform; lastly discuss the key technology in the platform construction and operation process. The platform will contribute to promoting the sharing level of ability and region internal manufacturing resources, improving the overall industry utilization rate of resources and capacity, and promoting mold industrial upgrading.

2. THE PLATFORM CONTENT RESEARCH

The cloud-manufacturing platform is a trading platform between manufacturing resources and manufacturing ability, and mould enterprises can trade equipment, technology, human resources and management on the platform, so the service content of the platform is mould product life cycle, service object is mold industry chain upstream and downstream. At the same time, the relationship between the platform and the enterprise is loose coupling, therefore the service provided through the platform need to be integrated and to achieve more grain size and multi-scale control. In the product life cycle service, the platform can provide six big tool set, namely product design, performance analysis, process simulation, precision processing, quality inspection, and production management. Therefore, the six tool set basically covers the whole process of mould manufacturing. In the aspect of upstream and downstream industry chain, the platform provides support for coordination and cooperation among mould equipment manufacturing, mould, home appliances, automobile, electronics, hardware, and other enterprises. The whole platform is divided into three levels, including cloud platform, cloud services and cloud application. Moreover, its specific content is as shown in figure 1.

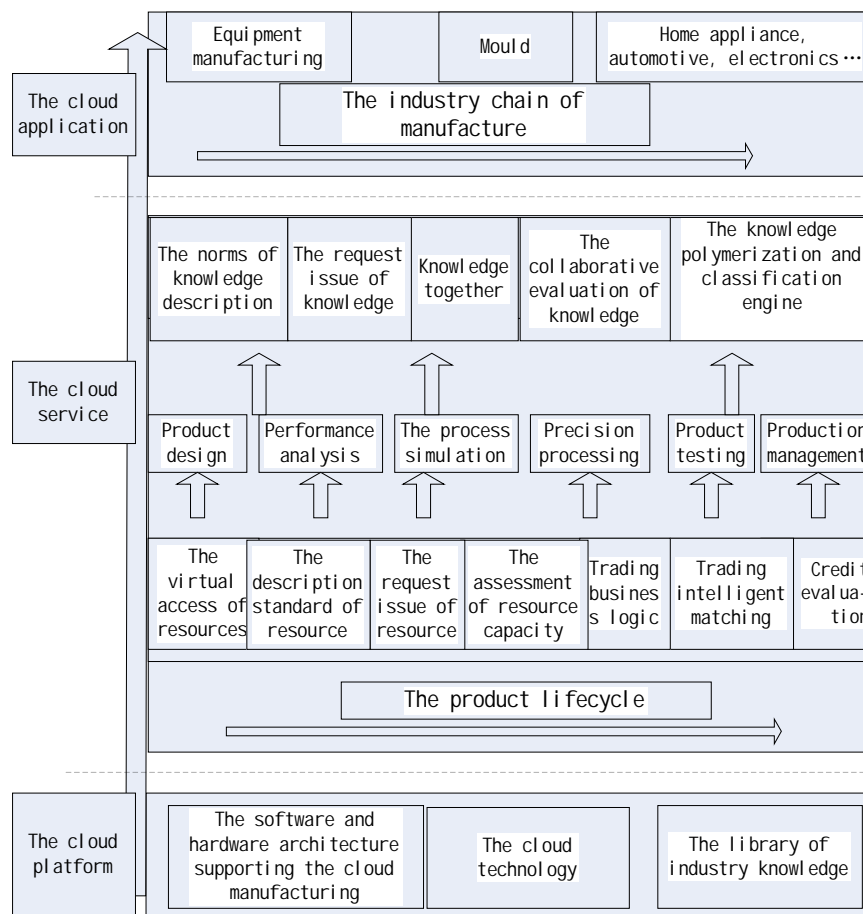


Fig 1: The Content of Mould Cloud-manufacturing platform

Cloud platform is the infrastructure of the whole platform, builds the structure system of the software and hardware to support the cloud manufacturing, researches various technologies of clouds by soft and hard resources, and arranges related knowledge base about the mould industry. Cloud services is the middleware layer of whole platform, and it will make service resources virtual, integrate various service tools, and offer multi-granularity and multi-scale service interface for the upper. The cloud application is the presentation layer of the whole platform, calls all kinds of the tools set according to the demands of users, directly provides service for the upstream and the downstream mold firms.

3. THE RESEARCH OF PLATFORM SYSTEM ARCHITECTURE

Professor Chao Yin expounded a general cloud manufacturing service platform in literature [9] orienting to small and medium-sized enterprises, which includes fundamental support layer, integrated operation environment, platform tools layer, the manufacturing resource layer, platform service building layer, service component layer, business model layer, trading layer and user layer. In this paper, we build the cloud-manufacturing platform used in the mould industry which can stand by the industry clusters writing according to the characteristics of mould industry and the feasibility of the technology, just as shown in fig2.

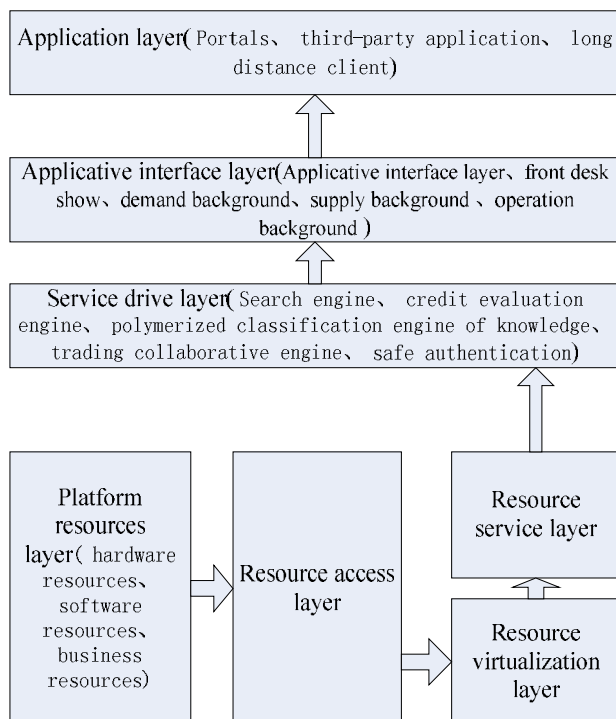


Fig 2: The Cloud Manufacturing Platform System Architecture

On basis of the source, platform services resources can be classified to the operator's own resources and private resources which can be moved to cloud-manufacturing platform through the lease. From the

nature, platform services resources also can be divided into hardware resources, software resources and industry knowledge base. Therefore, it is possible to solve heterogeneous structure of resource description by building platform resources and resource access layer to standardize the source and classify of the resources.

The resource platform needs to realize functions, mainly including multiple conditions retrieval, trading, monitoring and evaluation, etc. Thus, constructing virtual layer abstracts physical resources, features descriptors can be built to match with all kinds of resources, and resource virtualization layer also needs to construct related grain size parameters to provide interfaces for controlling after instantiation of resources.

The platform is wide range of resources, which are different among different resources. Constructing resources services layer can classify and integrate virtual resources, and provide unified descriptors of service interface to outside in order to afford integrated service conveniently. Resource service layer establishes relevant scale parameters supplying interface for scale control of the service.

The platform service drive layer that includes search engine, credit evaluation engine, polymerized classification engine of knowledge, trading collaborative engine, safe authentication with trading caused and so on is the control layer of the whole platform. And it formulates the basic operation rules of the working platform, monitors all information imported to the platform, analyzes semantics intelligently, submits to the relevant engine, and exports result to the specific page.

The applicative interface layer of the platform utilizes the function provided by the service drive layer to create the basic function and service module. The object of service includes four major categories (platform operators, platform providers, operator resources platform demanders, professional software and hardware resources development team). The four levels of service respectively are the front desk show, the demand background, the supply and demand background and operation background. In a word, the applicative interface layer constructs the application of the whole cloud manufacturing services system.

The application layer provides support for trading and using of the whole cloud-manufacturing. Web portal offers the foundation of the multilateral trade, remote client to control the cloud manufacturing resources (mainly for the soft resources, including local application, online application, cloud computing platform application and SAAS application) and third party applications to afford expansion ability of the cloud-manufacturing platform, such as the third party pay and CA certificate, etc.

4. THE KEY TECHNOLOGY RESEARCH OF THE PLATFORM

Professor Lin Zhang [10] discusses the key technology research of generally manufacturing service platform. In addition, this paper will continue to research the key

technology of this cloud-manufacturing platform in the process of creating and running combined with the characteristics of the mold industry. The key technology mainly consists of the platform service model, resources ability access, resources intelligent search, credit evaluation, service life cycle management.

4.1. The research of platform service pattern

To ensure the normal operation of the platform, the platform will use the cloud service mode of the four winds cooperation which includes service platform operators, the manufacturing capacity providers, the demand side of manufacturing services and developers of service tools, and its can make full use of the professionally technical resources, the market demand of resources and software development resources, its as shown in figure 3.

4.2. The platform resources access research

The cloud manufacturing services platform provides services including hard resources (processing, testing, designing equipment instrument), industry resources (designing model, analyzing data, etc) and software resources (designing, analyzing software and all kinds of application management system).Therefore, in platform

resources and access of services, we first need to analyze the characteristics of the resources and services, extract the characteristic parameters of each type resources, and establish appropriate and convenient assessment, so as to the access and application of resources and services. The access process is as shown in figure 4.

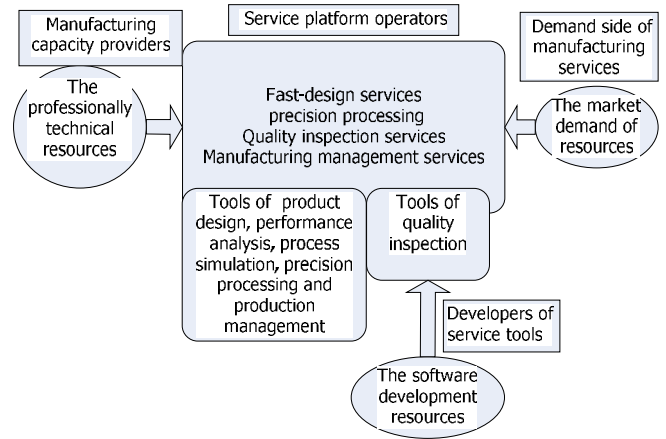


Fig 3: Platform Service Mode

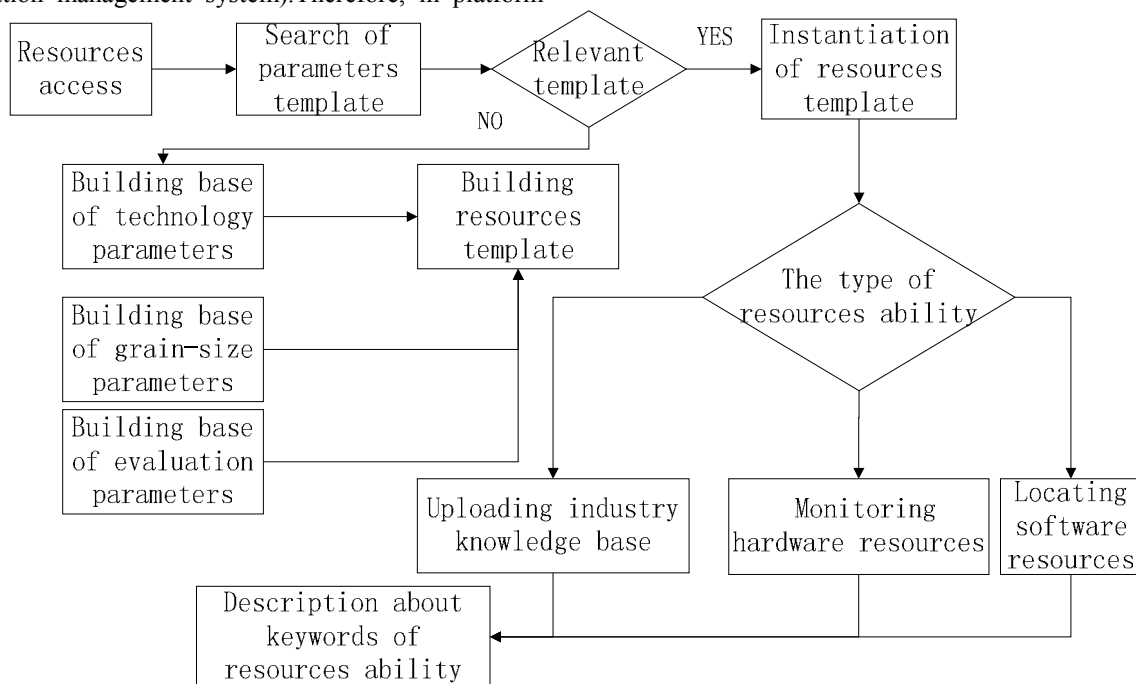


Fig 4: The Platform Resources Access

4.3. The intelligent search research of platform resources

It is necessary to establish engine system in the light of mould manufacturing resources and standard search of manufacturing ability. And then, this engine system can be used to search related products, services and industry knowledge. Combining mould manufacturing products with service classification standards, the engine system realizes precise search of knowledge, the manufacturing

resources and the ability of manufacturing. Platform will establish the standardization of the industry, the unified technology parameters database, establishing a uniform product manufacturing base, the service base, the enterprise library, can realize the configuration of the parameters template, realize manufacturing capability/service ability trading standardization. On this basis, the platform makes business cooperation between the demand side and service provider true. Platform

resources construction of intelligent search engine is as shown in figure 5.

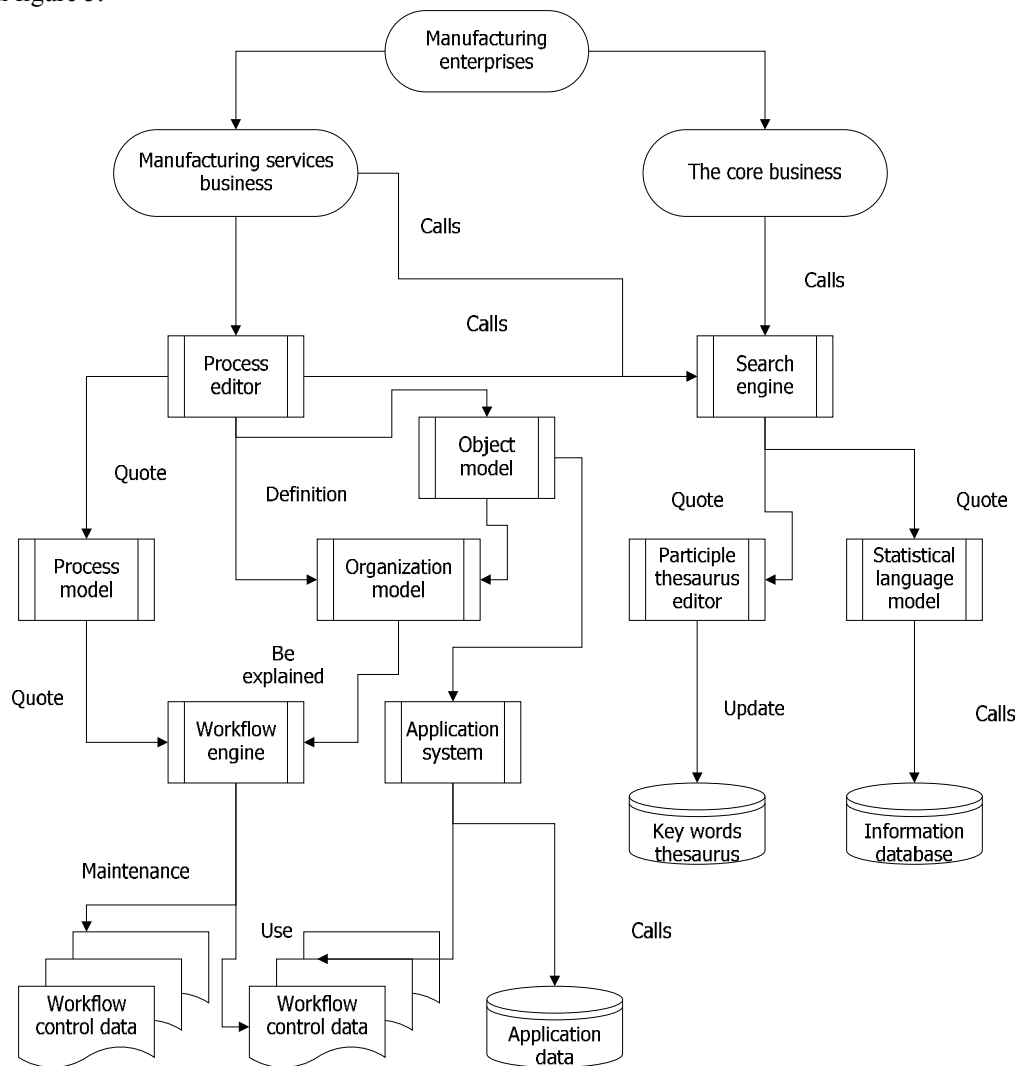


Fig 5: The Model of Intelligent Search of Platform Resources

4.4. The credit evaluation research of the platform

Because the cloud-manufacturing platform owns itself characteristics, such as trading platform remote, virtual, information asymmetry and silver goods delivery lag, it is destined to be the business model accompanied with the high efficiency and high risk. As a result, the control risking is the foundation of successful operation. Platform will build validation, evaluation, evaluation, classification, audit, supervision mechanism on the business. Operators of the cloud-manufacturing platform, as an third independent and authority institutions in credit evaluation, the authentication and management, establish seamless linking relationships with internal credit management institution or related departments. The trust of system,

enterprise relationship and mutual combination are considered as a core engine for them to realize trade of the cloud manufacturing. The platform can monitor the whole tracking management of the cloud platform and the credit of related enterprises. Namely, the cloud services will offer the services of monitoring, evaluation and after-sales service system. In addition, the management agency that has no relationship with the related enterprises described on above carries out this two-interconnected mechanism of the credit management, so as to establish support system of network services for all the service objects. The credit evaluation system of platform is as shown in figure 6.

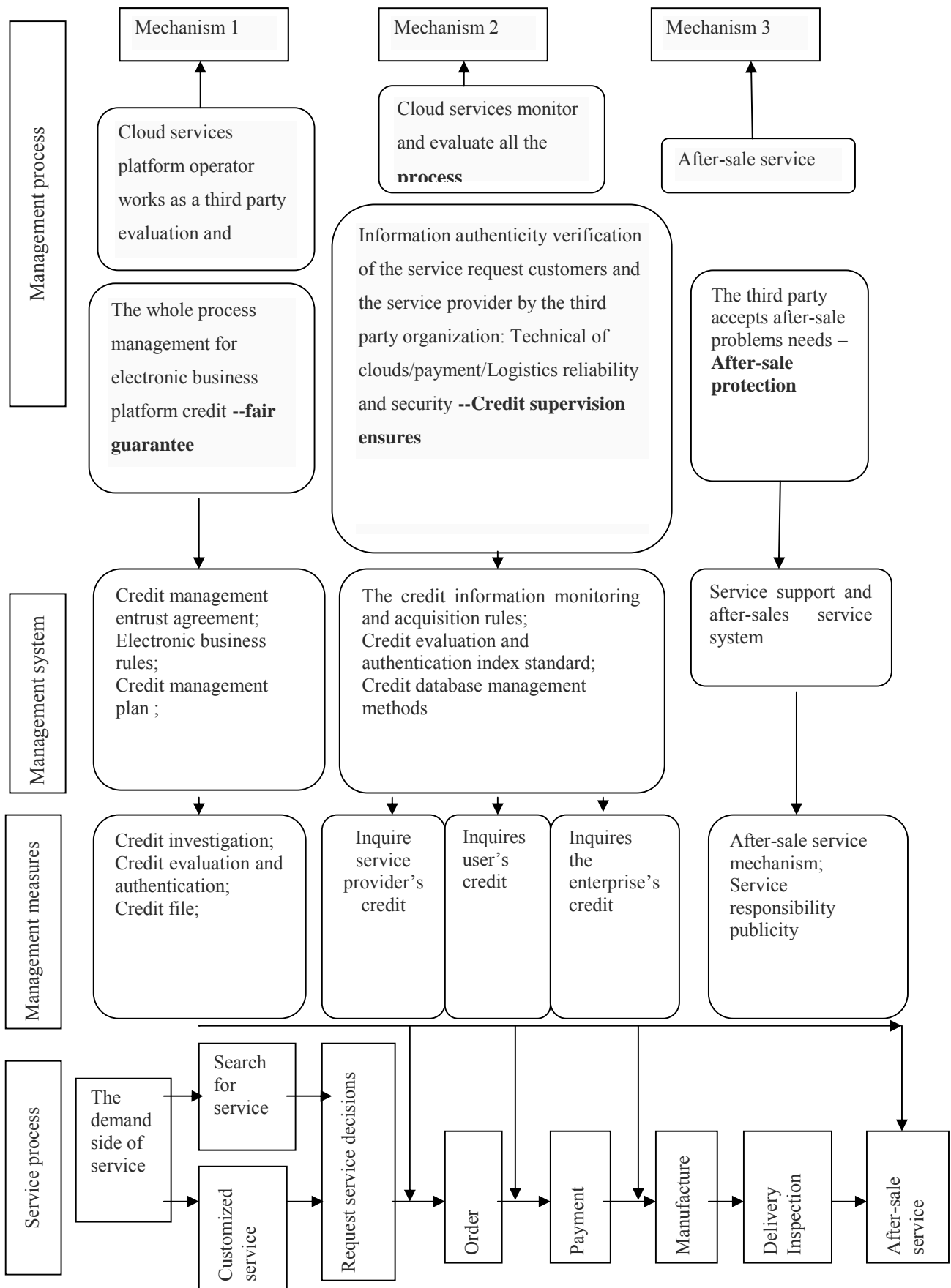


Fig 6: The Credit Evaluation System of Platform

4.5. The research of life cycle management about the platform service

To improve the service level of the platform, and promote enterprise adhesion of the platform, the service afforded

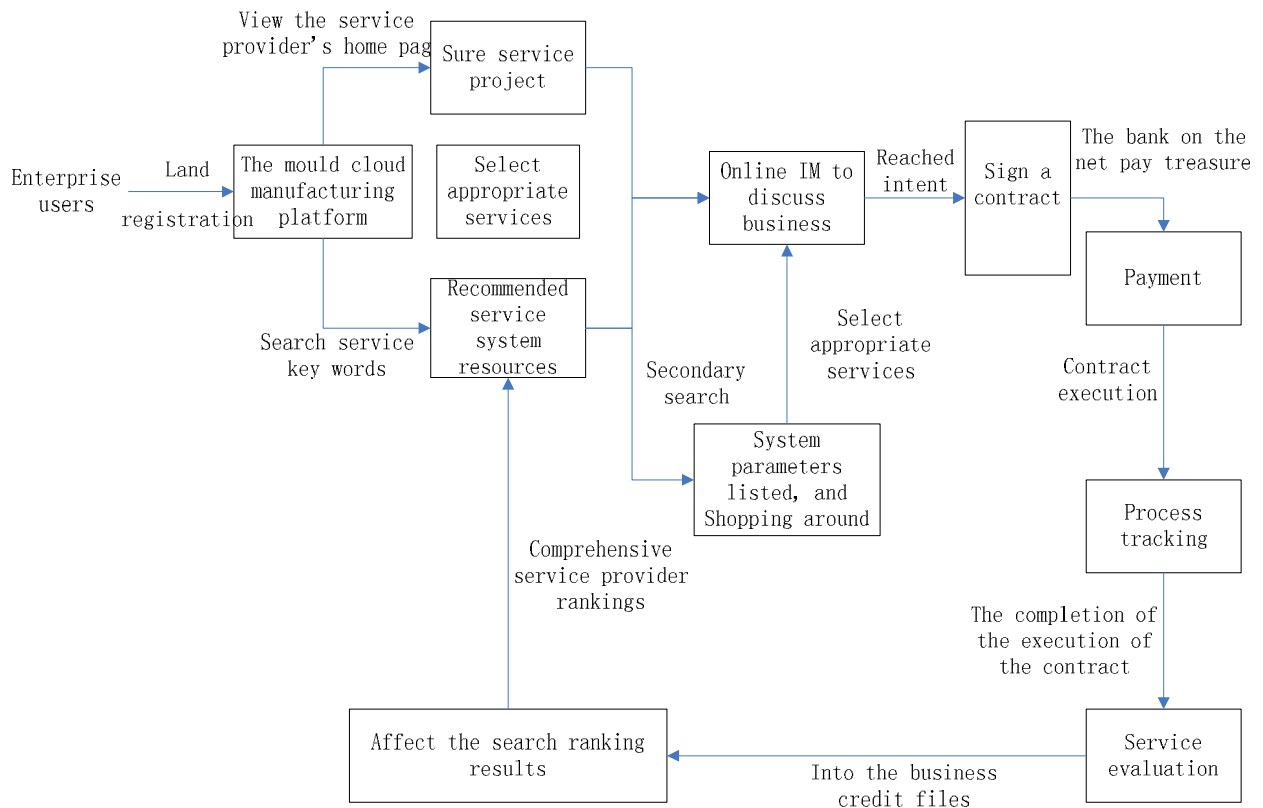


Fig 7: The Life Cycle Management of the Manufacture Service

5. THE LAST WORD

Some cities of China, such as Beijing, Jiangsu, Zhejiang and Guangdong provinces, have already set up a batch of special industrial cluster towns, and been existed a kind internal relationship of competition and development, but existing manufacturing mode is hard to develop information service platform for industrial clusters of collaboration. In this paper, according to the characteristics of the mould manufacturing industry, the cloud-manufacturing platform in the mould industry is put forward to support industrial cluster cooperation, and we analyze content needed to build and research the system structure and key technologies of the platform. The establishment of platform will contribute to integrating regional internal resources and ability, improving the competition ability of the industry, and promoting the development of the manufacturing industry to a higher level. However, it is for a long time to create relate database used to been search.

ACKNOWLEDGMENTS

I would like to express my gratitude to all those who have helped me writing this thesis.

First and foremost, my deepest gratitude goes primarily to the National Natural Science Foundation of

by the platform is the life cycle of manufacture with the universal technology of human computer interaction, and the life cycle of manufacture is shown in figure 7 below.

China. The support from them gives me opportunity to research the cloud manufacturing services platform in the mould industry, and the project number is No. 50905065.

Secondly, I would like to express my heartfelt gratitude to my tutor, Professor Guojun Zhang and Dr.Songxin Shi. I offer sincere thanks to them for the encouragement and support they have shown me, all of which have been of inestimable worth to the completion of my thesis.

The last but not least, my thanks would go to my beloved family for their loving consideration and great confidence. I also owe my sincere gratitude to my friends, such as Xuming Wang, Ying Liu, Wen Du and so forth, who give me their help and time in listening to me and helping me work out my problems during the difficult course of the research.

REFERENCES

- GU Xin-jian, CHE Ji-xi, JI Yang-jian, et al, 2010. Group Technology in Cloud Manufacturing[J]. *THE GROUP TECHNOLOGY AND PRODUCTION MODERNIZATION*, 27(3):1-4.
- LIU Fei, LEI Qi, SONG Yu-chuan, 2003. Connotation, state-of-the-art and research tendency of networked manufacturing[J]. *CHINESE JOURNAL OF MECHANICAL ENGINEERING*, 39(8):1-6.

- LI Bo-hu, ZHANG Li, WANG Shi-long, et al, 2010. Cloud manufacturing: a new service-oriented networked manufacturing model[J]. *COMPUTER INTERGATED MANUFACTURING SYSTEMS*, 16(1):1-7.
- LI Bo-hu, ZHANG Lin, CHAI Xu-dong, 2010. Introduction to Cloud Manufacturing[J]. *ZTE COMMUNICATIONS*, 16(4):5-8.
- LI Bo-hu, ZHANG Lin, REN Lei, et al,2011. Further discussion on cloud manufacturing[J]. *COMPUTER INTERGATED MANUFACTURING SYSTEMS*, 17(3): 449-457.
- WALSH K.R., 2003. Analyzing the application ASP concept: technologies, economies, and strategies [J].*Communications of the ACM*, 46(8):103-107.
- YANG Hai-cheng,2010. Cloud manufacturing is a manufacturing service[J]. *MANUFACTURING INFORMATION ENGINEERING OF CHINA*, 6:22-23.
- YAN Bo, HUANG Bi-qing, ZHENG Li, et al,2004. Research on grid and its application in manufacturing industry. *COMPUTER INTERGATED MANUFACTURING SYSTEMS*, 10(9): 1021-1030.
- YIN Chao, HUANG Bi-qing,LIU Fei, et al,2011. Common key technology system of cloud manufacturing service platform for small and medium enterprises[J]. *COMPUTER INTERGATED MANUFACTURING SYSTEMS*, 17(3):495-503.

- ZHANG Lin, LUO Yong-liang, TAO Fei, et al,2010. Study on the Key Technologies for the Construction of Manufacturing Cloud[J]. *COMPUTER INTERGATED MANUFACTURING SYSTEMS*, 16(11):2510-2520.

AUTHORS BIOGRAPHY

Youmin Rong, master graduate student of School of Mechanical Science and Engineering, School of Mechanical Science and Engineering, Huazhong University of Science and Technology, and his major is Mechanical engineering, and his E-mail address is rong_youmin@126.com.

Guojun Zhang, Doctoral tutor of School of Mechanical Science and Engineering, and his research direction manufacturing system simulation and integration, and his E-mail address is zgj@mail.hust.edu.cn.

Songxin Shi, lecturer of School of Mechanical Science and Engineering, Huazhong University of Science and Technology, and his resarch direction is manufacturing system simulation and integration, and his E-mail address is shisongxin@qq.com.

Shi Wang, staff of DG-HUST Manufacturing Engineering Institute, and his resarch direction mainly is manufacturing industry information and internet of thing, and his E-mail address is 8668816@qq.com.

MONTE CARLO RAY-TRACING APPROACH TO EFFECTIVELY DESIGN THE ELLIPSOIDAL REFLECTOR OF SOLAR SIMULATORS

Marco Bortolini^(a), Mauro Gamberi^(b), Alessandro Graziani^(c), Riccardo Accorsi^(d), Emilio Ferrari^(e)

^{(a),(c),(d),(e)}Department DIEM – Industrial Mechanical Plants, University of Bologna,
Viale Risorgimento 2, 40138 Bologna, Italy

^(b)Department of Management and Engineering, University of Padova,
Stradella San Nicola 3, 36100 Vicenza, Italy

^(a)marco.bortolini3@unibo.it, ^(b)mauro.gamberi@unipd.it, ^(c)alessandro.graziani6@unibo.it,
^(d)riccardo.accorsi2@unibo.it, ^(e)emilio.ferrari@unibo.it

ABSTRACT

Solar simulators are widely adopted devices to artificially reproduce the emission spectrum of the Sun. Their use, in lab tests and analyses, allows to study the effect of solar radiation on both materials and components. This paper focuses on the effective design of the ellipsoidal reflector for concentrating solar simulators. A Monte Carlo ray-tracing approach is proposed to study the reflector geometric configuration maximizing the target incident radiation and optimizing the radiative incident flux distribution. Developed ray-tracing model includes the main physical and optic phenomena affecting light rays from the source to the target area, e.g. absorption, deviation, reflection, distortion, etc. Proposed model is integrated to a Monte Carlo simulation to properly design the ellipsoidal mirror reflector of a small scale solar simulator based on an OSRAM XBO® 3000W/HTC OFR Xenon short arc lamp as light emitting source. Several scenarios are tested and the main obtained evidences are summarized.

Keywords: solar simulator, ray-tracing, Monte Carlo simulation, reflector surface design

1. INTRODUCTION

Solar simulators provide a luminous flux approximating natural sunlight spectrum. Their basic structure includes a metal support frame, a light source, e.g. high flux arc lamp with power supplier and igniter, and a reflective surface to properly orient the emitted rays lighting the target area. The reflector shape allows the system to generate a concentrated or non-concentrated light beam through an ellipsoidal or parabolic reflector. Figure 1 shows an example of concentrating solar simulator structure, highlighting the main functional modules.

The relevance of such systems, in lab tests and analyses, is frequently discussed by the recent literature presenting several applications for a wide set of research fields. Petrash et al. (2007) both review the topic and describe a 11,000 suns high-flux solar simulator. Domínguez et al. (2008), Domínguez et al. (2009), Pravettoni et al. (2010), Rehn and Hartwig (2010), Hussain et al. (2011) and Meng et al. (2011a)

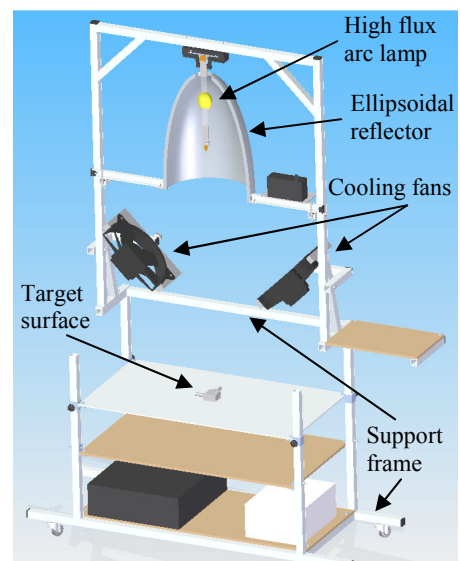


Figure 1: Single Lamp Solar Simulator, Main Functional Modules

present different studies about the design and development of high flux solar simulators applied to both concentrating and non-concentrating photovoltaic systems. Amoh (2004) and Meng et al. (2011b) describe the design of solar simulators to test multi-junction solar cells for terrestrial and space applications. Kreuger et al. (2011) develop a 45 kW solar simulator for high-temperature solar thermal and thermo-chemical researches, while Codd et al. (2010) present a low cost high flux simulator to study the optical melting and light absorption behavior of molten salts. All these contributions focus on the relevance of the proper design of the system to achieve high performances in both flux intensity and uniformity on the target area. Mirror reflective surface represents a crucial component to gain these purposes. An accurate shape design and simulation of the physical and optic properties is essential to the simulator construction (Johnston 1995).

Ray-tracing algorithms combined to Monte Carlo analyses are recognized as effective approaches to test the performances of different configurations of the

reflective surface (Petrasch et al. 2007, Chen et al. 2010, Ota and Nishioka 2010, Cooper and Steinfeld 2011).

This paper presents an effective Monte Carlo ray-tracing approach to properly design the ellipsoidal reflector of concentrating solar simulators. Developed approach is applied to study the optimal shape of the ellipsoidal reflector for a small scale solar simulator based on a OSRAM XBO® 3000W/HTC OFR Xenon short arc lamp (<http://www.osram.com>). A description of the implemented approach is provided giving full details about the steps of the ray-tracing algorithm together with the simulated scenarios. Finally, the main obtained evidences are discussed.

The reminder of this paper is organized as follows: Section 2 describes the steps of the implemented ray-tracing model, Section 3 presents the Monte Carlo analysis to design the ellipsoidal reflector of solar simulators and introduces the developed case study. In Section 4, the case study results are discussed while Section 5 concludes this paper with suggestions for further research.

2. REFLECTOR OPTICAL DESIGN THROUGH RAY-TRACING APPROACH

In geometrical optics, the foci of an ellipsoid of revolution are conjugate points (Petrasch et al. 2007). If no distortion effects occur, each ray emitted by a punctiform source located in one of the foci passes through the other after a single specular reflection (Figure 2).

According to this principle, concentrating solar simulators are designed. The light source, reproducing Sun emission spectrum, and the target area, e.g. the studied material or component, are located at the foci of an ellipsoidal mirror reflective surface.

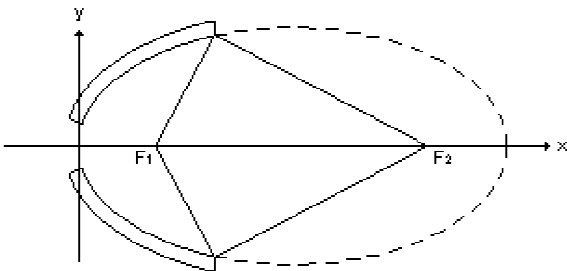


Figure 2: Geometrical Optic of Ellipsoid of Revolution

Considering experimental contexts, the following main conditions and phenomena contribute to reduce the global system radiation transfer efficiency, expressed as the ratio between the light flux that reaches the target and the global emitted flux.

- Finite area of the emitting light source.
- Absorption phenomena due to the presence of light source quartz bulb, source electrodes and reflective surface.

- Deviation and distortion phenomena due to the specular dispersion errors of the reflective surface.
- Losses due to rays falling out of the reflector shape.

These conditions affect all the operative contexts and can not be neglected in the solar simulator design. Their impact in reducing the system performances is strongly correlated to the features of the emitting source, the target shape and, particularly, to the reflector shape and characteristics.

Proposed ray-tracing approach analytically studies the ray trajectories, predicting the global transfer performances, given a configuration of the source, reflector and target surface. Figure 3 summarizes the step sequence of the proposed approach highlighting the stages where losses in transfer efficiency occur.

According to the major literature (Petrasch et al. 2007, Dominguez et al. 2008, Kreuger et al. 2011) the light source is assumed to emit isotropic radiation uniformly from its surface. Consequently, the emission point, P_0 , is randomly located on the whole source surface. Incident ray direction, \mathbf{v} , is defined following Lambert's cosine law distribution, as expressed in Eq. (1) (Steinfeld 1991)

$$\mathbf{v} \times \mathbf{n} = \cos(\sin^{-1}\sqrt{U}) = \sqrt{1-U} \quad (1)$$

where \mathbf{n} is the normal direction to the emitting surface, in P_0 , and U a random number drawn from a [0,1] uniform distribution. Proper quartz bulb and electrodes absorption phenomena are considered by introducing two coefficients, i.e. bulb and electrodes absorption coefficients, that reduce the emitted radiation and decrease the system transfer efficiency, i.e. losses at the light source stage.

For each emitted ray, the point of intersection with the ellipsoidal surface, P_1 , is computed. If P_1 falls out of the surface shape or in the hole necessary to install the light source, the ray is lost and the process finishes. Otherwise, two possibilities occur. Generally, the mirror reflects the ray but, in few cases, an absorption phenomenon occurs and the ray is not reflected at all. In this circumstance, modeled considering a proper absorption coefficient, the process ends, i.e. losses at the reflector stage.

Considering the reflected rays, their direction, \mathbf{r} , needs to be estimated. Distortion effects, caused by the specular dispersion errors of the reflective surface, affect \mathbf{r} vector. As widely discussed by Cooper and Steinfeld (2011), geometric surface errors modify the normal vector, \mathbf{k} , to the ellipsoid surface. The authors identify two angular components of the dispersion error, i.e. the azimuthal angular component, θ_{err} , and the circumferential component, φ_{err} . By applying the, so called, Rayleigh method they outline proper expressions to estimate these angular errors.

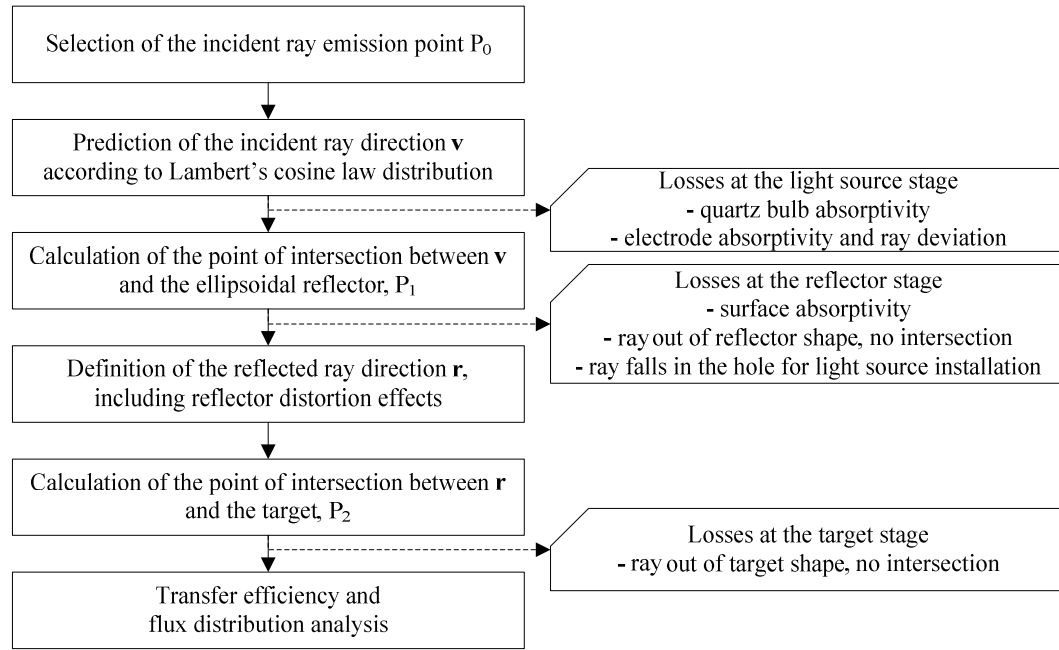


Figure 3: Steps and Losses of the Proposed Ray-Tracing Approach

$$\theta_{err} = \sqrt{2} \cdot \sigma_{err} \cdot \sqrt{-\ln U} \quad (2)$$

$$\varphi_{err} = 2\pi U \quad (3)$$

where σ_{err} is the standard deviation of the dispersion azimuthal angular error distribution, including all distortion effects, and U a random number drawn from a $[0,1]$ uniform distribution.

As a consequence, to estimate the direction of \mathbf{k} , in the point of intersection P_1 , the theoretic normal vector \mathbf{k}' needs to be twofold rotated with rotation angles equal to θ_{err} and, then, φ_{err} . θ_{err} rotation is around a vector orthogonal to the plane where the major ellipse lies while the second rotation is around \mathbf{k}' .

The normal direction to the reflective surface, in P_1 , allows to calculate the reflected ray direction, \mathbf{r} , according to Eq. (4) (Steinfeld 1991).

$$\mathbf{r} = \mathbf{v} - 2 \cdot (\mathbf{k} \times \mathbf{v}) \times \mathbf{k} \quad (4)$$

The intersection between \mathbf{r} and the plane where the target lies allows to calculate the coordinates of the common point P_2 . If P_2 is inside the target area the ray correctly hits the target, otherwise the ray is lost and the transfer efficiency decreases, i.e. losses at the target stage. This study does not consider multiple reflection phenomena.

Finally, the distance and mutual position between P_2 and the ellipsoid focus point allows to study the radiative incident flux distribution on the target area.

3. MONTE CARLO SIMULATION

Several geometric and optic parameters affect the global transfer efficiency of solar simulator systems. A list of them, classified according to the physical component they belong to, is provided in follows.

Parameters of the light source (generally an high flux arc lamp):

- Shape and dimensions.
- Emission light spectrum.
- Emission surface shape and dimensions, e.g. sphere, cylinder, etc.
- Emission direction distribution.
- Absorption coefficients of quartz bulb and electrodes (if present).
- Interference angle of electrodes (if present).

Parameters of the ellipsoidal reflector:

- Reflector shape, identified by the two ellipsoid semi-axes or by the major semi-axis and the truncation diameter.
- Reflector length, i.e. the distance between the vertex, on the major axis, and the longitudinal truncation section.
- Absorption coefficient.
- Standard deviation of the dispersion azimuthal angular error distribution, previously called σ_{err} .

Parameters of the target surface:

- Shape, e.g. circular, squared, rectangular.
- Dimensions.
- Relative position toward the ellipsoid.

For a given a set of such parameters, the geometric and optical features of the solar simulator are univocally identified and the ray-tracing approach, described in previous Section 2, can be applied, cyclically, to study the system performances, simulating a large number of emitted light rays. Furthermore, varying one or several of these parameters, through a *what-if analysis*, the best configuration of the whole system can be pointed out.

The authors developed a customized *MatLab*® interface to speed the simulation process, calculate and represent the system transmission performances.

3.1. Case study. Design of a small scale solar simulator

The following case study provides an empirical application of the described ray-tracing approach and Monte Carlo design simulation strategy.

A small scale solar simulator is investigated. The overall structure of the plant is represented in previous Figure 1 and the main functional modules are shortly introduced in Section 1. In this context, the effective design of the ellipsoidal reflector is analyzed. Both the emitting source and target area features are assumed constant, while several configurations of the reflector shape, corresponding to different sets of parameters, are tested and performances compared.

The considered emitting source is an OSRAM XBO® 3000W/HTC OFR Xenon short arc lamp (<http://www.osram.com>) with a luminous flux of 130000 lumen and an average luminance of 85000 cd/cm². Other relevant data about the shape of the considered high flux lamp are summarized in Table 1 and shown in Figure 4.

Table 1: Key Features of the Emitting Source Shape. Refer to Figure 4 for Notations

Light Source Parameters		
Lamp length (overall)	l_1	398mm
Lamp length	l_2	350mm
Lamp cathode length	a	165mm
Electrode gap (cold)	eo	6mm
Bulb diameter	d	60mm
Electrode interference angles	ϑ_1	30°
	ϑ_2	20°

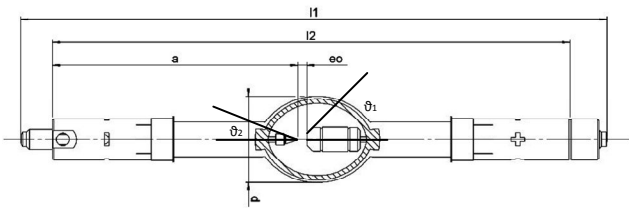


Figure 4: High Flux Emitting Source, Structure and Notations

The target surface is squared, side length of 50 mm, and it lies on a plane located on one of the two foci of the ellipsoidal reflector, orthogonal to the ellipsoid major axis.

Considering the ellipsoidal mirror reflector, the next Table 2 and related Figure 5 summarize all the tested scenarios, providing the adopted ranges of variation and the considered incremental steps for the four following parameters defining the reflector shape and optic features:

- Ellipsoid major semi-axis length, A

- Ellipsoid truncation section diameter, TD
- Standard deviation of the dispersion azimuthal angular error distribution, σ_{err}
- Reflector length, i.e. the distance between the vertex, on the major axis, and the longitudinal truncation section, L

Table 2: Tested Configurations for the Ellipsoidal Reflector. Refer to Figure 5 for Notations

Reflector Parameters [mm]			
	Min	Max	Step
A	200	1000	100
TD	100	$2A$	50
σ_{err}	0.005	0.01	0.005
L	$A - \sqrt{A^2 - TD^2}/4$	A	50

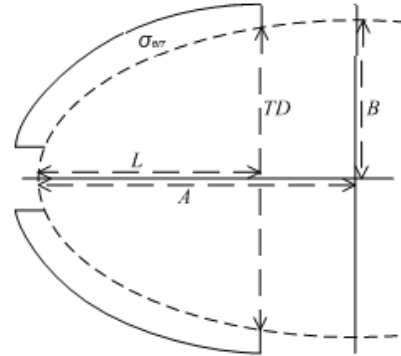


Figure 5: Ellipsoidal Reflector, Shape and Notations

The minor semi-axis of the ellipsoid, called B in Figure 5, can be analytically calculated as

$$B = \frac{A \cdot TD}{2\sqrt{L(2A-L)}} \quad (5)$$

and it is not a free parameter to define the ellipsoid shape.

Furthermore, a constant mirror absorption coefficient of 4% is considered in the analysis.

3840 scenarios appear and need to be simulated, i.e. *what-if analysis*. For each scenario, $N = 5 \times 10^5$ emitted rays are traced and results collected.

4. CASE STUDY RESULTS AND DISCUSSION

The following data are collected in all tested scenarios.

- N_A , number of rays absorbed by the light source (quartz bulb and electrodes).
- N_H , number of rays lost due to the presence of the hole used to install the light source.
- N_L , number of rays falling out of the reflector shape.
- N_R , number of rays absorbed by the mirror reflector.
- N_T , number of reflected rays hitting the target.
- N_O , number of reflected rays that do not hit the target.

These data allow to measure the role played by the ellipsoidal reflector shape on the global optic performances.

Furthermore, the following key indices are calculated to highlight the impact of the reflector features on the solar simulator transfer efficiency.

- Losses due to the reflector shape, i.e. ellipsoid shape, hole and truncation diameters.

$$\xi_1 = \frac{N_H + N_L}{N - N_A} \quad (6)$$

- Losses due to the optic and distortion effects caused by the reflector surface errors.

$$\xi_2 = \frac{N_R + N_O}{N - N_A - N_H - N_L} \quad (7)$$

- Global reflector transfer efficiency.

$$\eta = (1 - \xi_1) \cdot (1 - \xi_2) = \frac{N_T}{N - N_A} \quad (8)$$

- Statistical distribution of the reflected rays on the target surface, i.e. the mean distance M_D and standard deviation σ_D of the point of intersection between the rays and the target, P_2 , and the ellipsoid focus point.

Table 3 shows an example of the obtained results presenting the twenty best and worst scenarios. In addition to previous notations, ε indicates the ellipsoidal reflector eccentricity, defined as

$$\varepsilon = \sqrt{1 - B^2/A^2} \quad (9)$$

and included in the [0,1] range.

Figure 6 shows a radiative flux map for the best scenario. The squared dashed line identifies the target area whereas all dots inside the square are the rays that

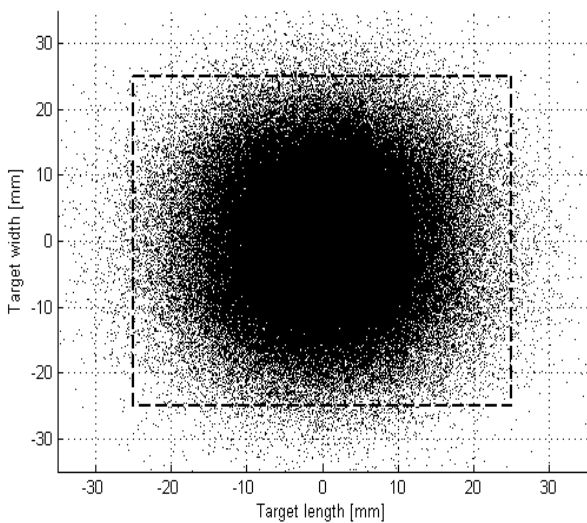


Figure 6: Radiative Flux Map for the Best Scenario.

correctly hit the target, while the other dots are the rays causing the losses at the target stage (see Figure 3).

Values of the global transfer efficiency vary from 92.407% of the best scenario to 1.072% of the worst case. Consequently, a first relevant outcome of the analysis is the heavily influence, for solar simulator performances, of the reflector design. Considering the best scenarios of Table 3, the ξ_1 and ξ_2 loss indices have values lower than 9% while the large amount of the rays are concentrated close to the target, i.e. mean distance between rays and the ellipsoid focus point, M_D , close to 10 mm and standard deviation, σ_D , included between [5,13] mm. On the contrary, the main cause for the performance decrease are the losses due to the reflector shape. With reference to the worst scenarios of Table 3, high values of ξ_1 , greater than 93%, are always experienced while ξ_2 does not present a regular trend. The main reason for these losses is the critic length of the reflector, i.e. the parameter L . All worst scenarios have very small values for this parameter, e.g. 50 or 100 mm, so that a great number of the emitted rays are lost because they do not hit the mirror reflector. The very high value of the number of rays falling out of the reflector shape, N_L , included between the 80% and 86%, clearly highlights the main cause for the global transfer efficiency decrease.

The standard deviation of the dispersion azimuthal angular error distribution, previously identified as σ_{err} , represents another relevant parameter affecting the global performances of the system. As expected, low values of σ_{err} correspond to high global transfer efficiency values. However, to reduce the standard deviation error an increase of the reflector production costs is necessary because of the major accuracy required during reflector manufacturing and mirror surface treatments. The graph in Figure 7 correlates the reflector length to the global transfer efficiency for the two simulated values of σ_{err} , i.e. 0.005 mm and 0.01 mm. The obtained values are listed in Table 4.

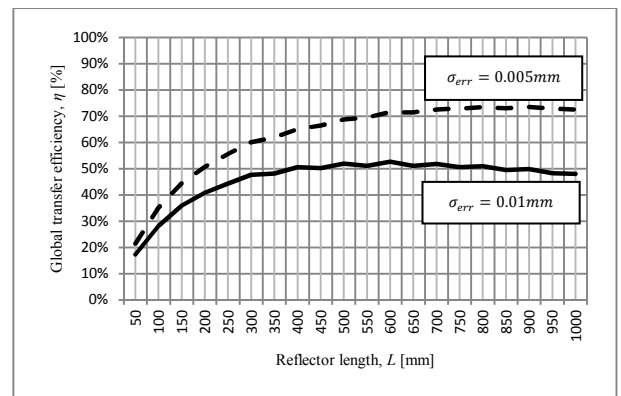


Figure 7: Correlation between the Reflector Length and Global Transfer Efficiency for the Two Values of σ_{err} .

Results, for the tested two values of the standard deviation of the dispersion azimuthal angular error distribution, present similarities in the waveforms. Low values of the reflector length are associated to very poor

Table 3: What-if Analysis Results. Twenty Best and Worst Scenarios.

Rank	A	TD	σ_{err}	L	B	ϵ	N_A	%	N_H	%	N_L	%	N_R	%	N_T	%	N_o	%	ξ_1	ξ_2	η	M_D	σ_D
1	600	650	0.005	600	325	0.841	65506	13.10%	5585	1.12%	6771	1.35%	16942	3.39%	401501	80.30%	3695	0.74%	2.844%	4.889%	92.407%	8.284	6.387
2	700	700	0.005	700	350	0.866	65865	13.17%	6287	1.26%	719	0.14%	16935	3.39%	399723	79.94%	10471	2.09%	1.614%	6.416%	92.073%	9.867	7.265
3	700	750	0.005	700	375	0.844	65477	13.10%	2107	0.42%	5849	1.17%	17211	3.44%	399732	79.95%	9624	1.92%	1.831%	6.291%	91.993%	9.622	7.147
4	600	600	0.005	600	300	0.866	65943	13.19%	13355	2.67%	702	0.14%	16782	3.36%	399052	79.81%	4166	0.83%	3.239%	4.988%	91.935%	8.521	6.205
5	600	700	0.005	600	350	0.812	65936	13.19%	1491	0.30%	13675	2.74%	16838	3.37%	398989	79.80%	3071	0.61%	3.494%	4.753%	91.919%	8.077	7.453
6	500	550	0.005	500	275	0.835	65626	13.13%	12034	2.41%	7907	1.58%	16699	3.34%	396935	79.39%	799	0.16%	4.591%	4.222%	91.381%	6.918	5.108
7	500	600	0.005	500	300	0.800	65623	13.12%	4064	0.81%	16235	3.25%	16688	3.34%	396752	79.35%	638	0.13%	4.673%	4.184%	91.338%	6.705	5.281
8	700	800	0.005	700	400	0.821	65424	13.08%	499	0.10%	11629	2.33%	17004	3.40%	396659	79.33%	8785	1.76%	2.791%	6.105%	91.275%	9.462	7.226
9	600	650	0.005	550	326	0.839	65174	13.03%	5308	1.06%	13451	2.69%	16698	3.34%	395752	79.15%	3617	0.72%	4.314%	4.883%	91.014%	8.298	6.631
10	700	700	0.005	650	351	0.865	65824	13.16%	6088	1.22%	5619	1.12%	16789	3.36%	395000	79.00%	10680	2.14%	2.696%	6.502%	90.977%	9.868	7.868
11	700	750	0.005	650	376	0.844	65819	13.16%	1925	0.39%	11180	2.24%	16775	3.36%	394742	78.95%	9559	1.91%	3.018%	6.254%	90.916%	9.661	12.983
12	600	600	0.005	550	301	0.865	65393	13.08%	13003	2.60%	6290	1.26%	16493	3.30%	394753	78.95%	4068	0.81%	4.439%	4.951%	90.830%	8.508	6.197
13	800	800	0.005	800	400	0.866	65306	13.06%	2336	0.47%	744	0.15%	17232	3.45%	394171	78.83%	20211	4.04%	0.709%	8.675%	90.678%	11.228	8.321
14	600	750	0.005	600	375	0.781	65675	13.14%	286	0.06%	21051	4.21%	16654	3.33%	393652	78.73%	2682	0.54%	4.913%	4.682%	90.635%	7.923	10.472
15	800	850	0.005	800	425	0.847	65715	13.14%	659	0.13%	5146	1.03%	17002	3.40%	392510	78.50%	18968	3.79%	1.337%	8.395%	90.381%	11.004	8.655
16	600	700	0.005	550	351	0.811	65720	13.14%	1407	0.28%	21106	4.22%	16375	3.28%	392244	78.45%	3148	0.63%	5.184%	4.741%	90.321%	8.074	6.300
17	700	850	0.005	700	425	0.795	65720	13.14%	211	0.04%	17598	3.52%	16642	3.33%	392119	78.42%	7710	1.54%	4.101%	5.847%	90.292%	9.232	10.141
18	700	650	0.005	650	326	0.885	65836	13.17%	13360	2.67%	584	0.12%	16704	3.34%	391884	78.38%	11632	2.33%	3.212%	6.743%	90.262%	10.109	7.391
19	700	650	0.005	700	325	0.886	65749	13.15%	13333	2.67%	512	0.10%	16895	3.38%	391933	78.39%	11578	2.32%	3.188%	6.773%	90.255%	10.112	7.375
20	500	500	0.005	500	250	0.866	65597	13.12%	24369	4.87%	722	0.14%	16449	3.29%	391887	78.38%	976	0.20%	5.776%	4.257%	90.213%	7.188	6.463
3821	600	450	0.005	50	563	0.346	65447	13.09%	35	0.01%	409130	81.83%	1016	0.20%	24347	4.87%	25	0.01%	94.158%	4.100%	5.603%	53.826	4427
3822	600	450	0.01	50	563	0.346	65927	13.19%	23	0.00%	408554	81.71%	1053	0.21%	22152	4.43%	2291	0.46%	94.126%	13.116%	5.103%	128.611	23924
3823	1000	850	0.005	100	975	0.222	65157	13.03%	11	0.00%	411962	82.39%	897	0.18%	21344	4.27%	629	0.13%	94.741%	6.672%	4.908%	92.488	5811
3824	800	500	0.005	50	718	0.440	65429	13.09%	22	0.00%	412160	82.43%	911	0.18%	21118	4.22%	360	0.07%	94.848%	5.677%	4.860%	43.496	2531
3825	900	800	0.01	100	873	0.243	65717	13.14%	11	0.00%	406282	81.26%	1085	0.22%	20798	4.16%	6107	1.22%	93.555%	25.695%	4.789%	383.653	150438
3826	1000	1050	0.01	150	997	0.082	66030	13.21%	8	0.00%	406182	81.24%	1177	0.24%	20351	4.07%	6252	1.25%	93.599%	26.742%	4.689%	199.142	7646
3827	900	500	0.01	50	761	0.535	65500	13.10%	23	0.00%	407282	81.46%	1145	0.23%	17951	3.59%	8099	1.62%	93.741%	33.992%	4.131%	58.225	2676
3828	1000	500	0.01	50	801	0.599	65804	13.16%	12	0.00%	403926	80.79%	1218	0.24%	17887	3.58%	11153	2.23%	93.031%	40.885%	4.120%	28.040	65
3829	800	500	0.01	50	718	0.440	65880	13.18%	27	0.01%	411665	82.33%	937	0.19%	16543	3.31%	4948	0.99%	94.834%	26.240%	3.811%	75.963	5461
3830	1000	550	0.005	50	881	0.474	66168	13.23%	12	0.00%	415741	83.15%	730	0.15%	16257	3.25%	1092	0.22%	95.833%	10.078%	3.747%	53.311	5468
3831	1000	850	0.01	100	975	0.222	65330	13.07%	12	0.002%	412098	82.42%	871	0.17%	15910	3.18%	5779	1.16%	94.810%	29.477%	3.660%	256.684	37704
3832	700	500	0.005	50	674	0.272	65630	13.13%	19	0.004%	419413	83.88%	589	0.12%	14309	2.86%	40	0.01%	96.561%	4.211%	3.294%	71.500	12637
3833	900	550	0.005	50	837	0.368	65986	13.20%	18	0.004%	420144	84.03%	543	0.11%	12947	2.59%	362	0.07%	96.808%	6.533%	2.983%	55.009	2629
3834	700	500	0.01	50	674	0.272	65828	13.17%	14	0.003%	418994	83.80%	585	0.12%	12729	2.55%	1850	0.37%	96.507%	16.058%	2.932%	100.957	3266
3835	1000	550	0.01	50	881	0.474	65808	13.16%	16	0.003%	416421	83.28%	687	0.14%	11242	2.25%	5826	1.17%	95.911%	36.683%	2.589%	91.629	6668
3836	900	550	0.01	50	837	0.368	65775	13.16%	16	0.003%	420351	84.07%	558	0.11%	9775	1.96%	3525	0.71%	96.809%	29.463%	2.251%	135.650	13985
3837	1000	600	0.005	50	961	0.277	65848	13.17%	8	0.002%	427627	85.53%	269	0.05%	6052	1.21%	196	0.04%	98.499%	7.135%	1.394%	101.737	18564
3838	800	550	0.005	50	790	0.156	65524	13.10%	11	0.002%	428332	85.67%	236	0.05%	5867	1.17%	30	0.01%	98.588%	4.337%	1.350%	87.917	8513
3839	800	550	0.01	50	790	0.156	65207	13.04%	7	0.001%	428814	85.76%	251	0.05%	4882	0.98%	839	0.17%	98.626%	18.252%	1.123%	195.014	16000
3840	800	550	0.005	50	790	0.156	65586	13.12%	11	0.002%	427651	85.53%	296	0.06%	4658	0.93%	1798	0.36%	98.446%	31.013%	1.072%	226.342	40309

Table 4: Dependence of η from L and σ_{err} .

L [mm]	η [%]		
	$\sigma_{err} = 0.005\text{mm}$	$\sigma_{err} = 0.01\text{mm}$	Gap
50	21.468%	17.227%	4.241%
100	35.103%	28.149%	6.954%
150	44.465%	35.948%	8.517%
200	50.718%	40.766%	9.952%
250	55.610%	44.188%	11.423%
300	60.049%	47.626%	12.423%
350	61.918%	48.110%	13.808%
400	65.090%	50.614%	14.476%
450	66.357%	50.201%	16.156%
500	68.722%	51.918%	16.804%
550	69.477%	51.042%	18.435%
600	71.596%	52.595%	19.002%
650	71.427%	50.988%	20.440%
700	72.510%	51.780%	20.730%
750	72.834%	50.592%	22.241%
800	73.403%	50.979%	22.425%
850	72.976%	49.454%	23.521%
900	73.467%	49.773%	23.694%
950	72.867%	48.299%	24.569%
1000	72.506%	48.039%	24.466%

performances, i.e. $\eta < 30\%$. Optimal conditions are, respectively, for reflector length of 800 mm and $\sigma_{err} = 0.005$ mm and of 600 mm for $\sigma_{err} = 0.01$ mm. A significant performance increase occurs for values of L included in [50,450] mm range, while for higher values of the reflector length, i.e. $L > 500$ mm, the global transfer efficiency presents comparable values.

Finally, considering the gap between the performances in the trends identified by the two values of σ_{err} , an increase, from 4.241% to 24.466%, occurs. High values of σ_{err} have a crucial impact on the global transfer efficiency in presence of high values of L . Long reflectors force the emitted rays to cover long trajectories from the source to the mirror and, then, from the mirror to the target. An error, caused by anomalies in the mirror surface, generates an angular deviation of the ray path. This deviation is amplified by the distance between the mirror and the target. Consequently, if L increases the standard deviation of the dispersion azimuthal angular error distribution must have low values not to significantly reduce the values of η .

Another relevant parameter for the effective mirror reflector design is the ellipsoid eccentricity, ε , defined in previous Eq. (9) and included in the [0,1] range. It identifies the mutual position of the vertices and the foci. If ε is equal to 0 the ellipsoid is a sphere, i.e. $A = B$, values of ε between 0 and 1 are for eccentric geometries where $B < A$. If $\varepsilon = 1$ the ellipsoid

degenerates into a plane and the foci lay upon the vertices on the major axis.

Developed *what-if analysis* highlights a range of optimal values for the ellipsoid eccentricity, to maximize the global transfer efficiency, included between 0.75 and 0.9, as represented in Figure 8, correlating the ellipsoidal mirror eccentricity to the values of η . Each dot represents one of the 3840 simulated scenario.

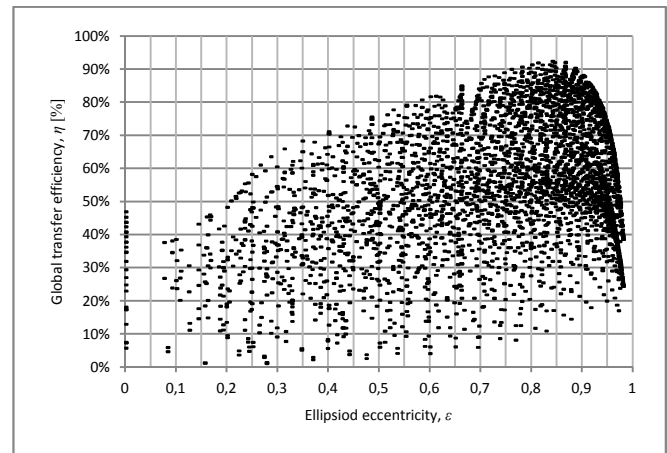


Figure 8: Correlation between the Ellipsoid Eccentricity and Global Transfer Efficiency.

This outcome may be in contrast to the major literature (Steinfeld and Fletcher (1988), Steinfeld (1991)) suggesting low values of ε to maximize the reflector global transfer efficiency. On the contrary, in the proposed analysis values of eccentricity close to zero generate the worst performances. A reasonable explanation for this evidence lies in the adopted reflector modeling approach. Literature ray-tracing models and related results approximate the reflector with an ellipsoid of revolution neglecting both the truncation section, i.e. the parameter previously called TD , and the hole necessary to install the light source. The proposed ray-tracing approach includes these two elements in the analytical model to provide a realistic and accurate description of the physical system.

The presence of these elements significantly modifies the geometric and optic features of the solar simulator introducing the so-called losses at the reflector stage (see Figure 3) that significantly contribute to the global transfer efficiency decrease, especially for the scenarios where L and ε assume low values (see Table 3). In fact, if ε is low the foci are located far from the vertices on the ellipsoid major axis and close to the geometrical center, i.e. the point of intersection of the two axes. In this circumstance, the light source, located on one ellipsoid focus point, juts out from the reflector profile so that a large number of the emitted rays do not hit the reflector surface. The lower the reflector length, the higher these losses occur.

On the contrary, in eccentric reflectors the light source is close to the ellipsoid major axis vertex and a lower number of rays are lost. However, very high

values of ε , i.e. $\varepsilon > 0.9$, cause an increase of the losses at the reflector stage and a decrease of η . This is due to the presence of the hole for the light source installation. A focus point located close to the reflector vertex, i.e. eccentric reflector, increases the value of N_H , i.e. the number of rays lost due to the presence of the hole used to install the light source, so that, also in this case, the global transfer efficiency decreases. As introduced, optimal values for the reflector eccentricity are in the [0.75,0.9] range.

5. CONCLUSIONS AND FURTHER RESEARCH

This paper presents a Monte Carlo ray-tracing approach facing the effective design of solar simulators. Developed model reproduces the trajectories of light rays considering the main physical and optic phenomena that occur from the source to the target area. Ellipsoidal geometries are focused. In particular, the solar simulator reflector is a truncated ellipsoid of revolution with the light source located on one focus and the target area on the other. Proposed ray-tracing approach includes the main losses at the source, reflector and target stages and affecting the global system transfer efficiency.

The ray-tracing approach is integrated to a Monte Carlo *what-if* analysis to simulate the performances of several reflector geometries. A case study, based on an OSRAM XBO® 3000W/HTC OFR Xenon short arc lamp, is described simulating 3840 scenarios and varying four major parameters, i.e. the ellipsoid major axis, the truncation diameter, the reflector length and the standard deviation of the azimuthal angular error distribution affecting the quality and reflectivity of the mirror surface. For each scenario, data about losses and the number of rays on target are collected and summarized in the three key indices proposed in Eq. (6) to (9) together with a statistic analysis of the distribution of rays on target.

The main outcomes highlight the relevance of the proper design of the reflector shape to obtain high values of the global transfer efficiency. The gap between the best and worst scenarios is higher than 90%. Furthermore, correlations between the four considered parameters is highlighted. As example, high values of the reflector length, in presence of high values of the standard deviation of the azimuthal angular error distribution, amplify the global transfer efficiency decrease, while, low values of the ellipsoid eccentricity, relating the major axis length to the truncation diameter, cause an increase of the lost rays.

The obtained parameters, for the best of the simulated scenarios, are of 600 mm for both the ellipsoid major semi-axis and reflector length, 325 mm for minor semi-axis and σ_{err} equals to 0.005 mm. For this scenario, the global transfer efficiency is 92.407% while the distribution of rays on the target area has a mean distance from the focus point of 8.284 mm and a standard error of 6.387 mm.

Further research mainly deals with a validation of the case study results through the development of the

solar simulator and a trial campaign. To this purpose, the authors already purchased the ellipsoidal reflector and they are now developing the overall structure of the solar simulator to collect experimental data to be compared to the Monte Carlo simulation evidences.

REFERENCES

- Amoh, H., 2004. Design for multi-solar simulator. *Proceedings of SPIE – The International Society for Optical Engineering*, 5520. pp. 192-199. August 4-6, Denver (Colorado, USA).
- Chen, C.F., Lin, C.H., Jan, H.T., 2010. A solar concentrator with two reflection mirrors designed by using a ray tracing method. *Optik*, 121, 1042–1051.
- Codd, D.S., Carlson, A., Rees, J., Slocum, A.H., 2010. A low cost high flux solar simulator. *Solar Energy*, 84, 2202–2212.
- Cooper, T., Steinfeld, A., 2011. Derivation of the angular dispersion error distribution of mirror surfaces for Monte Carlo ray-tracing applications. *Journal of Solar Energy Engineering*, 133 (4), 44501 1-4.
- Domínguez, C., Antón, I., Sala, G., 2008. Solar simulator for concentrator photovoltaic systems. *Optics express*, 16 (19), 14894–14901.
- Domínguez, C., Askins, S., Antón, I., Sala, G., 2009. Characterization of five CPV module technologies with the Helios 3198 solar simulator. *IEEE*, 1004–1008.
- Hussain, F., Othman, M.Y.H., Yatim, B., Ruslan, H., Sopian, K., 2011. Fabrication and irradiance mapping of low cost solar simulator for indoor testing of solar collector. *Journal of Solar Energy Engineering*, 133 (4), 44502 1–4.
- Johnston, G., 1995. On the analysis of surface error distributions on concentrated solar collectors. *Transactions of the ASME*, 117, 294–296.
- Kruger, K.R., Davidson, J.H., Lipiński, W., 2011. Design of a new 45 kWe high-flux solar simulator for high-temperature solar thermal and thermochemical research. *Journal of Solar Energy Engineering*, 133 (4), 11013 1–8.
- Meng, Q., Wang, Y., Zhang, L., 2011a. Irradiance characteristics and optimization design of a large-scale solar simulator. *Solar Energy*, 85, 1758–1767.
- Meng, Q., Wang, Y., 2011b. Testing and design of a low-cost large scale solar simulator. *Proceedings of SPIE – The International Society for Optical Engineering*, 8128, August 22-23, San Diego (California, USA).
- Osram, *Technical information No. 5264*. Available from: <http://www.osram.com> [accessed May 2012].
- Ota, Y., Nishioka, K., 2010. 3-dimensional simulator for concentrator photovoltaic modules using ray-trace and circuit simulator. *Proceedings of the 35th IEEE Photovoltaic Specialists Conference*,

- PVSC 2010*, pp. 3065-3068, June 20-25, Honolulu (Hawaii, USA)
- Petrash, J., Coray, P., Meier, M., Brack, M., Häberling, P., Willemin, D., Steinfeld, A., 2007. A novel 50 kW 11.000 suns high-flux solar simulator based on an array of xenon arc lamps. *Journal of Solar Energy Engineering*, 129, 405–411.
- Pravettoni, M., Galleano, R., Dunlop, E.D., Kenny, R.P., 2010. Characterization of a pulsed solar simulator for concentrator photovoltaic cell calibration. *Measurement Science and Technology*, 21, 1–8.
- Renh, H., Hartwig, U., 2010. A solar simulator design for concentrating photovoltaics. *Proceedings of SPIE – The International Society for Optical Engineering*, 7785, August 1-4, San Diego (California, USA).
- Steinfeld, A., 1991. Exchange factor between two spheres placed at the foci of a specularly reflecting ellipsoidal cavity. *International Communications in Heat and Mass Transfer*, 18, 19–26.
- Steinfeld, A., Fletcher, E.A., 1988. Solar energy absorption efficiency of an ellipsoidal receiver-reactor with specularly reflecting walls. *Energy*, 13 (8), 609–614.

DEVELOPMENT AND EVALUATION OF VISUALIZATION SYSTEM OF GLOBAL CONTAINER FLOW FOR INTERNATIONAL MANUFACTURERS

Hisashi Takizawa^(a), Hiromichi Akimoto^(b), Kenji Tanaka^(c), Jing Zhang^(c)

^(a)Ministry of Land, Infrastructure, Transport and Tourism, Japan (At the time of study, The University of Tokyo)

^(b)Korea Advanced Institute of Science and Technology

^(c)The University of Tokyo

^(a)hisashi.takizawa.info@gmail.com, ^(b)akimoto@kaist.ac.kr,
^(c)kenji_tanaka@sys.t.u-tokyo.ac.jp, ^(c)chou@sys.t.u-tokyo.ac.jp,

ABSTRACT

Because of the increase of the number of world-wide manufacturers especially those have their factories in Asia and major markets in Europe and the US, the lead time of transportation in manufacturers' supply chain is increasing. However, for shippers, status information of their container cargos and container ships are limited. It prevents the shippers from optimizing their logistics operation. Accordingly, the authors have developed a global logistics simulation of containers based on multi-agent method. The developed visualization system enables international manufacturers to support logistics management and comprehend container transportation. The simulation result shows that the proposed system can reduce shippers' logistics cost by 17%.

Keywords: logistics simulation, visualization, supply chain, multi-agent simulation, container flow

1. INTRODUCTION

Since 1990, many of Japanese world-wide manufacturers have been developing their production sites in Asia. Therefore, the importance of supply chain management, which can administrate whole procurement process of product from factories to consumers, has also been increasing because lead time between factories and consumers in distant major markets has been increasing. Hence, the use of information management system, such as Enterprise Resource Planning system, is expanding.

However, since the development of factories in Asia attributes to long lead time between production and consumption places, demand fluctuation in distant market causes opportunity losses and dead stocks. This problem is caused by unshared information among many agents of global supply chain although they already implemented information technology in their other part of supply chain. Particularly, ocean shipment makes it difficult for manufacturers to catch instantaneous information of product because they receive information indirectly from shipping line and third party logistics companies, whereas ocean shipment lacks punctuality more than other transportation due to

the delay by marine condition and offshore queue. This fact made manufacturers outsource transportation to third party logistics. As a result, information of time loss and time fluctuation is less transparent, which is unacceptable to factories and vendors.

To deal with this problem, radio-frequency identification device (RFID) has been introduced in order to capture real time information of cargo and incorporate them in production and transportation plan. In fact, there are movements for visualization of cargo in many parts of the world. In Japan, Ministry of Economy, Trade and Industry conducted an experiment of visualizing the transportation between Japan and the Netherlands. However, it has not achieved real-time visualization of cargo information. Therefore, it is necessary to develop a visualization system which enables the shippers to share cargo information with logistics companies, support their decision making of logistics simultaneously and to evaluate the effectiveness of the system.

Existing researches for these problems include Supply Chain Management (SCM). Since Oliver and Webber (1982) discussed SCM in 1982, many researchers have studied production and distribution for SCM, such as bullwhip effect and optimum inventory policy (Lee et al. 1997). As a recent study, Venu Nagali (2008) indicated that quantification of demand and price risk enabled Hewlett-Packard to reduce 300 million dollars manufacturing cost by proposing three different scenarios of risk and contracting suppliers with the proposition. Although transportation lead time is assumed to be fixed in these researches, Chandra Charu(2008) indicated that optimum stock volume and procurement volume depend on lead time. Thus, we should consider variable lead time in order to implement optimum supply chain.

On the other hand, some researchers had succeeded in the reduction of transportation cost by optimizing route and fleet of shippers' firm. As an example of the study of transportation network, Sato and Miyata (2006), Sato et al. (2007) and Kimura et al. (2008) modeled dynamic simulation of transportation and selection of lowest total cost route. However, these studies focused on only transportation of whole logistics.

Although there are researches of applying RFID, most of them are focused on only direct effect, such as reduction of labor cost, labor hours, and mistakes by labor (Wang and Lin 2007, Chow and Choy 2007). There are not so many researches which showed effect of RFID on whole logistics. A particular example which is focused on the effect of RFID on whole logistics is by Bill C. Hardgrave (2008) It reduced the risk of stock shortage by implementing RFID in Wal-mart as an experiment. Also, Young (2009) demonstrated that introducing RFID make it possible for manufacturers, distribution centers and retailers to reduce average stocks when they can share visible information of inventory. However, those researches didn't include visibility of cargo during transportation.

As it can be seen in the above researches, approaches to manufacturing and retailing, and to transporting are separated and they didn't implement dynamic system which supports both shippers and shipping firms by integrating information. Thus, it is necessary to develop a system which integrates information of both shipper and shipping firms and visualizes them dynamically for global manufacturers.

In this paper, we will accomplish modeling of global production, transportation and consumption, and visualizing comprehensive container flow which can support management of logistics using actual operation data of a company. In the system, we consider the stock in transportation as well as the stock at the manufacturer and retailer because most of the lead time involved in logistics is marine transportation. The supposed users of the system are shipping firms and shippers.

In this study, we use actual data of a Japanese international electric manufacturer. The company has several product models, which are manufactured in three Asian areas, and shipped to vendors in North America, Europe, Japan, and other Asian countries.

In order to accomplish the above objective, we will construct a multi-agent and time-discrete simulation modeling manufacturing, transportation, and vendors described in the 2nd chapter, implement visualization of shipper's dynamic logistics, the results of which are given in the 3rd chapter, and evaluate validness of the simulation in the 4th chapter.

2. MODELLING OF SIMULATION

2.1. Overview of Simulation

Since there are many agents in global transportations, we model each agent in the simulation. We also implement time scale in the simulation in order to model the dynamic and complex activities in container flow as in Figure 1. By utilizing the simulation of container transportation network by Takizawa (2010), we implement the multi-agent and time-discrete simulation which models international logistics.

We divided the simulation into 4 subsystems; Database, Operation, Management, and Viewer. Database subsystem holds the whole static and dynamic data of the system. Operation subsystem consists of

players of global logistics, such as ports, vendors, and container ships and they have their own elements and functions. Management subsystem makes decision, such as demand forecasting and transportation schedule planning. Viewer subsystem is independent from other parts and it visualizes whole flow of container and analyzes the time variation of stock. In this system, the simulator notifies each subsystem of updating their status each time step. After updating all subsystems, Simulator increments time step. With synchronizing all subsystems, Simulator repeats this loop until the end of simulation.

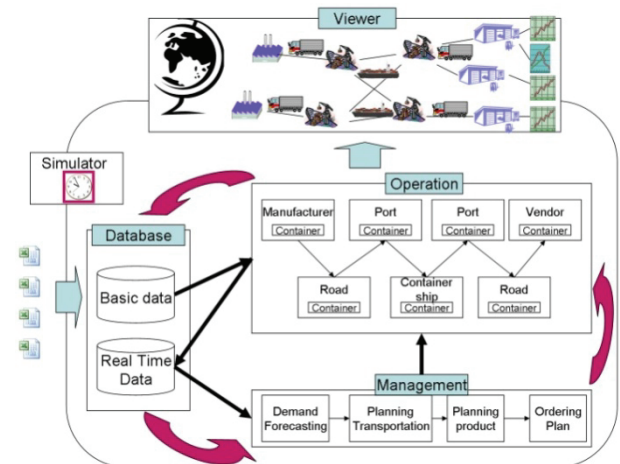


Figure 1: Schematic Diagram of Simulation

2.2. Database subsystem

Database integrates and controls all information of production, transportation, and sales. One type of data is static data which is necessary to build up elements of Operation. The other type of data is dynamic data which writes and reads all agents in simulation. Our simulation saves latest information in Database, updates predictions of logistics and inventory and then supports management of logistics.

Static data includes data of area, factory, vendor, port, container ship, road transportation and demand. Dynamic data includes estimated container route schedule, actual container route schedule, sales forecasting and actual sales.

2.3. Operation subsystem

Operation models company's logistics in the real world. However, it is necessary to discrete each composing elements and model them in order to simulate non-linear event, like logistics. Elements of logistics are cargo, container, container ship, road transportation, factory, vendor, and port, and the simulator includes them. We will construct the simulator by Java, one of the object-oriented languages, and define the above model of elements as Class, which packages both attributes and operations.

Cargo class models a group of products in the real world, thus, it has only attributes, no operations. Attributes are composed of a name of products, density, and the number of products.

Container class is a unit of cargo when cargo can be transported on network, and has only attributes. Attributes are composed of a container ID, product list, maximum volume, current volume, estimated container route schedule, and actual container route schedule.

Containership class models a link whose concept is travelling around nodes in transportation network with discrete schedule. The attributes are composed of a name of a container ship, schedule list including time and place of both departure and arrival, and velocity. Operations are composed of updating schedule and updating global position.

Road class is a concept of a link which connects two nodes and provides continuous transportation. The difference of road transportation and container ship is whether their schedule is discrete or successive and the schedule is independent or not from clients. Attributes are composed of velocity, positions of origin and destination, and a container list. Operations are composed of updating the global position. In this simulation, we assume road transportation as trucks.

Factory class is a node which manufacture product based on plan. Attributes are composed of the global position and manufacturing plan. Operations are composed of producing, packaging product into containers, and loading containers on a link.

Vendor class is a node which sells products and consumes them in later based on daily demand. Attributes are composed of the global position and a demand list. Operations are composed of consuming products and loading containers on a link.

Port class is a node which is on the way of transportation and also handles containers. Attributes are composed of the global position and hold a container list. Operations are composed of loading and unloading container.

In order to initialize Operation subsystem, Management subsystem creates every element when the simulation starts. After simulation started, each element acts independently and represents complex container flow for the following.

1. Each factory produces a product in each time step and packages it into a container.
2. Road transportation delivers the container to a port.
3. The port loads the container on a container ship when it stopped the port.
4. After the container ship reached the destination port, the destination port unloads the container and delivers it to the vendor, the destination, by road transportation.
5. Upon arriving at the vendor, the container is unpacked and consumed on the time of demand. Products will disappear from the simulation when they are consumed.

2.4. Management subsystem

Management subsystem models a scheme that shippers make a decision of future logistics based on the past

records and simultaneously order plans to Operation subsystem. Thus, it has 4 functions; prediction of demand, planning of transportation, planning of production, and ordering plans.

In this study, we assume that the prediction of demand is accurate. When we have to consider the limited accuracy of prediction in the future study, we will apply non-linear sales forecasting which predicts future demands based on the past records in the simulation as indicated by Tanaka (2010).

Planning of transportation has three steps. Firstly, we detect practical transportation in order to limit the number of searching results of schedule. Since calculating every available schedule consumes much time and thus is unrealistic, we exclude the schedule which transit via hub ports. Secondly, we create possible schedule by selecting several transportations between origin and destination, then calculate lead time and fee of transportation. Thirdly, we examine each schedule by the sum of fee and multiplication of lead time and time value. The optimum schedule is defined as minimum sum of the above.

In this study, planning of production is assumed to be deadline list of daily production which is calculated by planning of transportation and based on delivery date.

Ordering plans is a function which submits all the results of the decisions by Management subsystem to Operations subsystem.

3. VISUALIZATION OF INTERNATIONAL CONTAINER FLOW

3.1. Visualization for supporting global manufacturing companies

Visualization which enables us to comprehend whole stock in a supply chain instantaneously can assess accurate stock and accomplish avoiding dead stocks and opportunity loss, and securing the most effective transportation route.

In this system, we implemented the following visualization methods developed by Nomura (2008) and Chou (2008).

3.1.1. Time series analysis

Figure 2 is an example of time series analysis of stock, arrival and sales of a certain product at a certain vendor. The upper graph is the time history of stocks in the inventory, and the lower graph is that of accumulated stocks. The red vertical line indicates current time and the right part of the line indicates the predicted future behavior. It is possible because we can visualize the future state by sharing information of containers in transportation and of prediction at the vendor. In addition, the accumulated curve enables us to assess the characteristic of a demand trend for each product model easily after the sales started. This information is useful for sales forecasting. As a result, this analysis may help us to avoid ordering ineffectual production plan because

managers of manufacturers are able to see future stock and characteristics of selling.

3.1.2. Shipping lead time analysis

Figure 3 is an example which visualized stock in transportation with the same route. Colors show the time of places where containers have stayed, such as factory, port, and ocean. The horizontal line is ordered by the manufacturing time of each container. This analysis may help planning of production and transportation by assessing the dead stock based on manufacturing time and assessing characteristic of lead time each year.

3.1.3. Tracing analysis

Figure 4 shows an example of tracing analysis of a product for a vendor in order to assess stock in transportation based on their time of manufacturing. Each graph shows the progress of stock of the place, in order of process of logistics. Each layer is colorized by the week when they were produced. Therefore, when we find overstocking, it is easy to detect when the excessive group was produced and which part of logistics caused the problems. In general, the fast decrease of the thickness in a layer indicates fast turnover rate of the product. On the contrary, if a certain layer keeps its thickness longer time, we can easily assess whether the problem came from transportation, like emergent air transport, or came from the wrong production plan in the factory.

3.2. Visualization of container flow on globe

In the previous section, we visualized progress of stock at each place from upper stream to lower stream of the supply chain. In this section, we will visualize both a position and volume of cargo in transportation.

Figure 5 is an example of visualizing all of 1049 container ships, and volume of products in logistics on a plain map. This allows assessing the whole container ship and products on the earth instantaneously.

However, visualization on a plain map is not always informative for global manufacturers and marine transporters because long distance ocean routes are distorted and containers and ships look congested on the plain map. To solve this problem, we visualized on the globe as in Figure 6. The state of the simulation is displayed on Google Earth simultaneously. On the globe, ship routes are displayed correctly and more information are intuitively comprehensible. In fact, both of Figure 5 and Figure 6 are animation and displayed simultaneously during simulation.

Unfortunately we cannot demonstrate yet, we can propose several solutions which is beneficial both for manufacturers and shipping firms. For instance, implementing several global manufacturers makes it possible for both manufacturers and shipping firms to optimize fleet schedule based on future gross transportation. If one manufacturer has enough containers to charter container ships, marine

transporters can optimize lead time and the number of ships based on the trend of products and time-value.

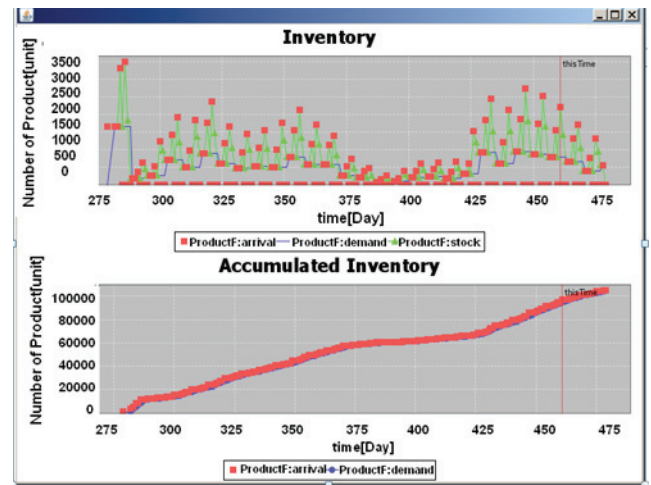


Figure 2 : Time Series Analysis of Stock (An Example of the Vendor in North America)

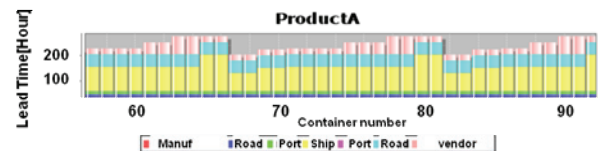


Figure 3 : Analysis of Shipping Lead Time of Each Container (An example of the Electronics Product)

4. EVALUTATION OF SIMULATION

4.1. Premises of evaluation

To verify the system, we evaluate our simulation by examining the Japanese electric company's actual logistics data. In the actual data, they have lots of dead stocks and inappropriate transportation schedule.

According to our assumptions for this evaluation, our simulation implemented prediction of demand in Management subsystem. Moreover, one effect of visualization, transparency of information by sharing logistics data with factories, transporters, and vendors, is quantitatively assessable. However the other effect of visualization, optical comprehension, is qualitative. Thus, we evaluate the former effect of visualization, sharing information and optimizing network.

Shipper's loss of each product is defined as sum of transportation fee C and multiplication of lead time T_i and time value V . Therefore, shipper's loss of actual data L_{actual} is defined as equation 1, and shipper's loss of simulation L_{sim} is defined as equation 2. In this case, the interval of simulation t_{end} is 2 years and C is either ocean tariff or air tariff. In actual data, the number of production and sales is different because demand prediction is not accurate and there are many dead stocks. On the other hand, the number of production and sales is same in simulation because we assumed demand prediction is accurate. Therefore, we must adjust the difference of number in order to major the

effect of planning transportation by visualization. V is decreasing 0.37[USD/Day], according to Sato (2006). The areas of vendors we have examined are Asia, Europe, and North America.

$$L_{\text{actual}} = \left\{ \sum_{t=1}^{t_{\text{end}}} (V \cdot T_t + C) N_{\text{actual}_t} \right\} \frac{\sum_{t=1}^{t_{\text{end}}} N_{\text{sim}_t}}{\sum_{t=1}^{t_{\text{end}}} N_{\text{actual}_t}} \quad (1)$$

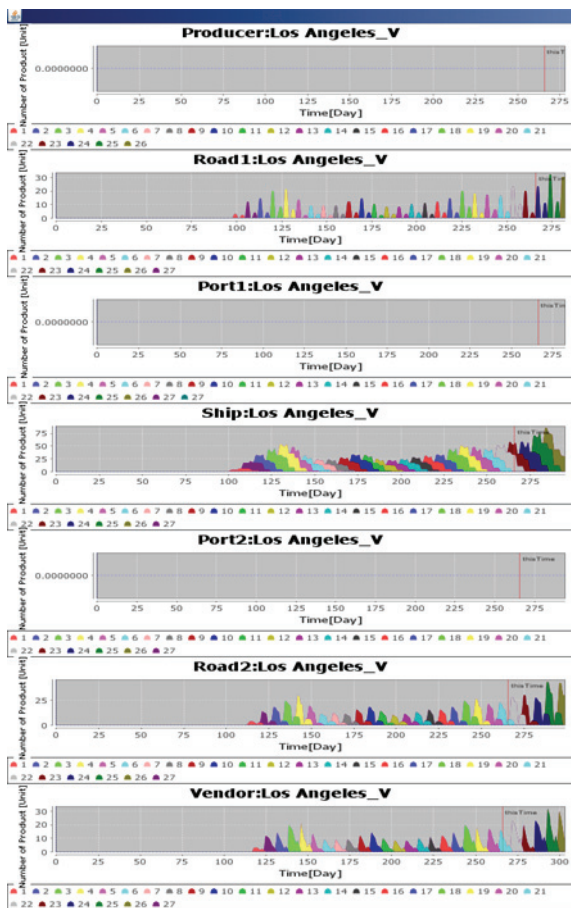


Figure 4 : Tracing Analysis of Shipping Stock (An Example of the Electronics Product; China to North America)

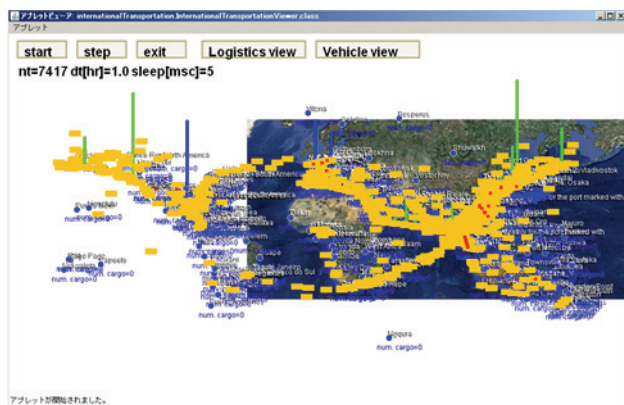


Figure 5 : Visualization of International Logistics on Plane Panel

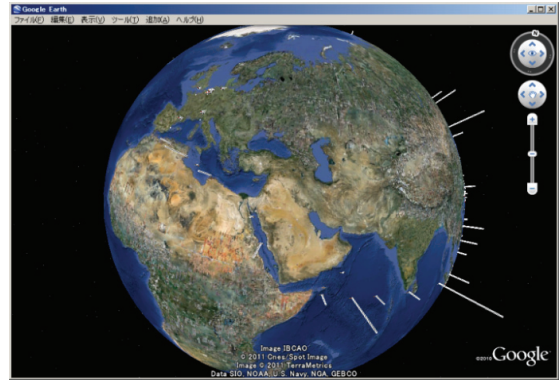


Figure 6: Visualization of International Logistics on Google Earth

$$L_{\text{sim}} = \left\{ \sum_{t=1}^{t_{\text{end}}} (V \cdot T_t + C) N_{\text{sim}_t} \right\} \quad (2)$$

4.2. Result of evaluation

The result based on equation 1 and 2 is shown in Figure 7. While Asian sales areas has improved only by 8%, North American sales area has improved by 16%, and European sales area has improved by 20%. Converting to the amount of money, reduction of shipper's loss in Asian area was 2.7 million USD, reduction of shipper's loss in North America was 22 million USD, and reduction of shipper's loss in Europe was 14.5 million USD. The reason why European logistics improved most is that they have longest distance between factories in Asia and vendors in Europe. Thus, the optimization of transportation was effective in long distance logistics because high air tariff was replaced with cheap ocean tariff and ocean lead time become shorter. In total, shipper's loss was decreased by 16% and 39.3 million USD.

Summing up, we demonstrated the validity of the visualization of simulation by reducing shipper's loss, which is achieved by optimized transportation planning through transparent information between factories, transportations, and vendors.

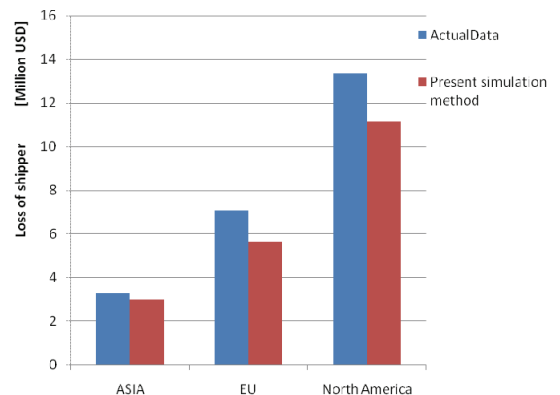


Figure 7: Difference of Shipper's Loss of Cost and Time-value for Each Sales Area

5. CONCLUSION

We developed and visualized the system which models global logistics and supports management for manufacturers. Evaluation of simulation by actual data leads us to conclude that visualization of logistics makes it possible to reduce manufacturers' loss.

ACKNOWLEDGMENTS

This study was conducted in the University of Tokyo in 2011. The present affiliation of the first author, Ministry of Land, Infrastructure, Transportation and Tourism, Japan, is not responsible for the contents of this article.

REFERENCES

- Chandra, C., Grabis, J., 2008. Inventory management with variable lead-time dependent procurement cost. *Omega*, 36, 877 – 887.
- Chow, H.K.H, Choy, K.L., Lee, W.B., 2007. A dynamic logistics process knowledge-based system – An RFID multi-agent approach. *Knowledge-Based Systems*, 20 (4), 357-372.
- Hardgrave, B.C, Langford, S., Waller, M., Miller, R., 2008. Measuring the Impact of RFID on Out of Stocks at Wal-Mart. *MIS Quarterly Executive*, 7 (4), 181-192.
- Kimura, T., Akimoto, H., Miyata, H. 2008. A design method of the container transportation network between Japan and China. *Conference proceedings, the Japan Society of Naval Architects and Ocean Engineers*, 439-442. May, Nagasaki (Japan).
- Lee, M.Y., Cheng, F., Leung, Y.T., 2009. A quantitative view on how RFID can improve inventory management in a supply chain. *International Journal of Logistics Research and Applications*, 12 (1), 23–43.
- Lee, H.L., Padmanabhan, P., Whang, S., 1997. Information distortion in a supply chain: The bullwhip effect. *Management Sci.* 43, 546-558.
- Nomura, Y., 2008. *Guro-bal seizougyou no keiei shien shisutemu no kenkyu*[Simulation-Based Business Administration for Global Industrial Companies] . Thesis (Master). The University of Tokyo.
- Oliver, R.K., Webber, M.D., Supply Chain Management: Logistics Catches Up with Strategy, 1982.
- Sato, S., Akimoto, H., Miyata, H., Sato, Y., 2007. Route selection system of the sea-land combined container transport between Japan and China. *Conference proceedings, the Japan Society of Naval Architects and Ocean Engineers*. 487-490, May, Tokyo (Japan).
- Sato, Y., Miyata, H., 2006. Discrete type simulation of sea transportation between Japan and China, *Proceedings of Japan Society of Naval Architects and Ocean Engineers*, pp. 17-18, Tokyo(Japan).
- Takizawa, H., Takechi, S., Akimoto, H., 2010. Selection and evaluation of network and hub ports for international container transportation around Japan, *Journal of the Japan Society of Naval Architects and Ocean Engineers*. 11, 173-179.
- Tanaka, K., 2010. A sales forecasting model for new-released and nonlinear sales trend products. *Expert Systems with Applications*. 37, 7387–7393.
- Nagali, V., Hwang, J., Sanghera, D., Gaskins, M., Pridgen, M., Thurston, T., Mackenroth, P., Branvold, D., Scholler, P., Shoemaker, G., 2008. Procurement Risk Management (PRM) at Hewlett-Packard Company. *Interfaces*.38 (1), 51-65.
- Wang, L.C., Lin, Y.C., Lin, P.H., 2007. Dynamic mobile RFID-based supply chain control and management system in construction. *Advanced Engineering Informatics*. 21, 377-390.
- Zhang, J., 2008. *Guro-baru kigyou keiei shien system* [System for global industrial administration]. Japan: Zichosya.

AUTHORS BIOGRAPHY

Hisashi Takizawa: Received master's degree from the Graduate School of Engineering, the University of Tokyo in 2011. His research fields are in logistics and multi-agent simulation. Currently he is working in the Maritime Bureau of Ministry of Land, Infrastructure, Transport and Tourism, Japan.

Hiromichi Akimoto: Graduated from the PhD course at the University of Tokyo in 1996. After working at Tottori University and University of Tokyo, Japan, he has been a Visiting Foreign Professor in the Division of Ocean Systems Engineering, KAIST, Republic of Korea, from Oct. 2011. His research fields are in computational fluid dynamics, logistics, renewable energy and high-speed ships.

Kenji Tanaka: After working at McKinsey & Company and Nihon Sangyo Partners, he acquired PhD in Engineering at the University of Tokyo in 2009. His research fields are social diffusion models of rechargeable battery re-use services, sales projection with production and distribution efficiency, and competitiveness assessments of retailers' distribution.

Jing Zhang: Acquired PhD from the University of Tokyo. Currently researching Social logistics and Global Company Management systems.

AEMOS: AN AGENT-BASED ELECTRONIC MARKET SIMULATOR WITH ONTOLOGY-SERVICES AND SOCIAL NETWORK SUPPORT

Maria João Viamonte^(a), Virgínia Nascimento^(a), Nuno Silva^(a), Paulo Maio^(a)

^(a) GECAD – Knowledge Engineering and Decision Support Research Center, Institute Of Engineering – Polytechnic of Porto (ISE/IPP), Dr. António Bernardino de Almeida 431, Porto, Portugal

{mjv, vlrn, nps, pam}@isep.ipp.pt

ABSTRACT

In E-commerce environments software agents are used in automated negotiations. When agents communicate they do not necessarily use the same vocabulary or ontology. However, if they want to interact successfully they must find correspondences between the terms used in their ontologies. This paper proposes to enhance agent-based electronic markets with a set of ontology-services to facilitate communication between agents. However, humans tend to be reluctant to accept other's conceptualizations/ontologies. For that they must be convinced that a good deal can be achieved. In this context, the application and exploitation of trust relationships captured by social networks can result in the establishment of more accurate trust relationships between businesses and customers, as well as the improvement of the negotiation efficiency.

Keywords: agent based simulation, electronic markets, ontology mapping negotiation, social network analysis

1. INTRODUCTION

In an efficient agent-mediated electronic market, where all the partners, both sending and receiving messages have to lead to acceptable and meaningful agreements, it is necessary to have common standards, like an interaction protocol to achieve deals, a language for describing the messages' content and ontologies for describing the domain's knowledge (Hepp, 2008) (Fensel, et al., 2001) (Obrst, et al., 2003).

The need for these standards emerges due to the nature of the goods/services traded in business transactions. The goods/services are described through multiple attributes (e.g. price, features and quality), which imply that negotiation processes and final agreements between sellers and buyers must be enhanced with the capability to both understand the terms and conditions of the transaction (e.g. vocabulary semantics, currencies to denote different prices, different units to represent measures or mutual dependencies of products).

In order to provide an answer for this need we developed the AEMOS system - Agent-Based Electronic Market with Ontology-Service System, a multi-agent market simulator with ontology services.

The AEMOS system is an innovative project (PTDC/EIA-EIA/104752/2008) supported by the Portuguese Agency for Scientific Research (FCT).

The system proposes an ontology-based information integration approach, exploiting the ontology mapping paradigm, by aligning consumer needs and the market capacities, in a semi-automatic mode, improved by the application and exploitation of the trust relationships captured by the social networks.

In this paper we give a brief introduction to the AEMOS system model (Section 2) detailing the Ontology Services component (Section 3). We then present the social network component (Section 4) illustrating how agents exploit social network information in combination with the meta information captured during the agent's business interactions.

2. AEMOS SYSTEM

AEMOS includes a complex simulation infrastructure; able to cope with the diverse time scales of the supported negotiation mechanisms and with several players competing and cooperating with each other. In each situation, agents dynamically adapt their strategies, according to the present context and using the dynamically updated detained knowledge (Viamonte, et al., 2006).

AEMOS is flexible; the user completely defines the model he or she wants to simulate, including the number of agents, each agent's type, ontologies and strategies. This infrastructure is detailed in (Viamonte, et al., 2011).

2.1. Multi-Agent Model

The model includes several types of agents divided into two main groups namely, external agents and internal agents. The external agents are agents whose behavior is intended to be simulated and studied. The main types of external agents are: Buyers (B) who are agents representing consumers; and Sellers (S) who are agents representing suppliers.

The internal agents are the ones who support the communication and negotiation between external agents. The main internal agents are: the Market Facilitator (MF) that is responsible for the information integration process in the message exchange between

external agents. It is an intermediate agent during the negotiation process that ensures, or tries to ensure that both parties are able to understand each other; the Ontology Mapping Intermediary (OM-i) that is responsible for the ontology mappings' management and for the ontology's instances translation process. This agent is able to propose ontology mappings and to translate ontology's instances when requested; and the Social Network Intermediary (SN-i) that is the agent responsible for the discovery of agents' trust (or proximity) relations captured through social network analysis techniques applied on the market information. This agent is able to support the OM-i agents on their tasks and to advise external agents about proposed ontology mappings or negotiating partners.

In other to participate in the market, an external agent must register first, indicating the ontologies it uses and, optionally, its personal data and preferences.

2.2. The Negotiation Model

The negotiation protocol used in AEMOS is bilateral contracting where B agents are looking for S agents that can provide them with the desired products at the best conditions.

Negotiation starts when a B agent sends a request for proposal (RFP). In response, a S agent analyses its own capabilities, current availability, and past experiences and formulates a proposal (PP). On the basis of the bilateral agreements made among market players and lessons learned from previous bid rounds, both agents revise their strategies for the next negotiation round and update their individual knowledge module.

The negotiation protocol has three main actors: B agents, S agents and MF agent. Both agents, B and S may seek advice with a SN-i agent in order to decide about the acceptance/formulation of a proposal.

When a deal is closed, the B agent is expected to perform the payment, and the S agent the delivery, according to the CBB model (Runyon & Stewart, 1987). Then, when the transaction is completed, both agents are invited to evaluate the whole process (i.e. rate the negotiation partner and, if it's the case, the used ontology mappings).

If some agent frequently fails to close a deal or perform the payment or delivery, the negotiating partner can express its dissatisfaction with the agent, sending a declaration of depreciation with the agent's behavior to the MF agent. On the other hand, if an agent has a history of satisfactory interactions with another agent, it can express its satisfaction by sending a declaration of appreciation with the agent's behavior to the MF agent.

3. THE ONTOLOGY-SERVICES COMPONENT

To provide a transparent semantic interoperability between all e-commerce actors, AEMOS has an ontology-services infrastructure whose system architecture recognizes three new types of actors: the Ontology Matching Service (OM-s) agent that is able to specify an alignment between two ontologies based on

some ontology matching algorithm. There are several OM-s on the marketplace, each one providing the same service but based on distinct matching approaches (Euzenat & Shvaiko, 2007); the Ontology Matching Information Transformation (OM-t) agent that is responsible for transforming any information represented according to one ontology (i.e. source ontology) to information represented according to a target ontology, using an already specified alignment between those two ontologies; and the Ontology Matching Repository (OM-r) agent that registers the agreed ontology alignments specified between agents' ontologies. These alignments are applied to enable further agents' interactions.

These actors deploy a set of relationship types whose goal is to automate and improve the quality of the results achieved in the e-commerce transactions.

3.1. The Integration Protocol

Considering the previous descriptions, a more complete and complex protocol is now detailed, including the OM-i and SN-i agents in the system, Figure 1.

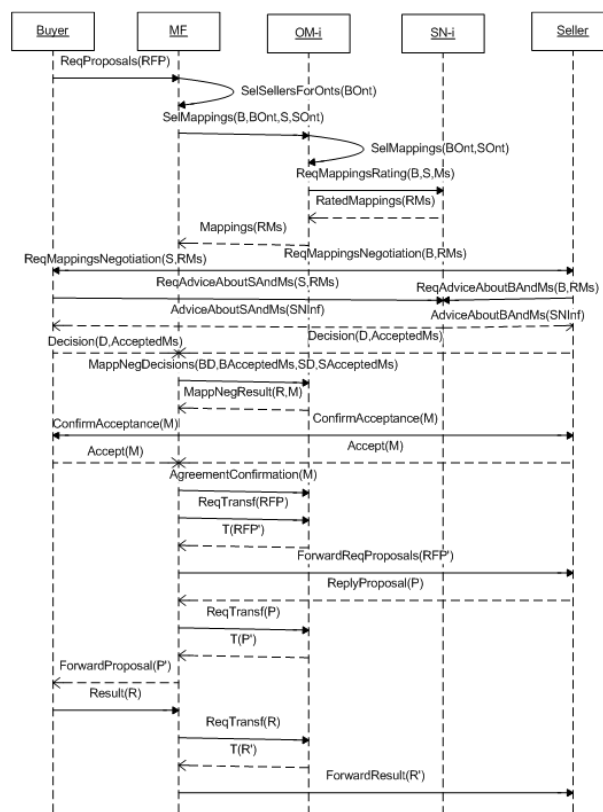


Figure 1: The Integration Protocol

The integration starts when a B agent sends a request for proposal message to the MF agent. In response, the MF tries to find possible S agents for the request by selecting the ones using the same ontology as the B agent or an ontology with known correspondences.

When B and S use different ontologies the OM-i starts the ontology mapping specification process, with the support of other entities, including matching agents,

ontology mapping repositories and SN-i. SN-i is responsible for retrieving the relevant information from ontology mapping repositories and social networks. Past similar ontology mapping experiences undertaken by agents with trust relationships with B and S will be used by SN-i to compile the social network repository information. Because the request for this information is the exclusive responsibility of OM-i, both B and S are advised to perform a similar verification (eventually using other SN-i) once the ontology mappings are submitted for negotiation.

At the ontology mapping negotiation, both B and S decide about their interest in negotiating with the proposed partner and the ontology mappings that are preferred. The decisions are sent to the OM-i who will check for a possible agreement. If an agreement is found both B and S are required to confirm their acceptance.

Despite the fact that Figure 1 represents only the acceptance scenario, a rejection scenario is also possible, in which case no further interaction will occur between B and S. In case the mapping is accepted, MF resumes the protocol by requesting to OM-i the RFP data transformation. Using the ontology mapping document, RFP data represented according to B's ontology is transformed into data represented according to S's ontology. The transformed data (RFP') is forwarded to S, which will process it and will reply to MF. MF will then request the transformation of the proposal data (P) and will forward the transformed proposal (P') to B. B processes it and will accept or formulate a counterproposal (CP). As illustrated, once a mutually acceptable ontology mapping is established between B's ontology and S's ontology, all messages exchanged between B and S through MF are forwarded to OM-i for transformation.

Notice that Figure 1 represents one single S agent in the system, but in fact multiple S agents capable of replying to the request may exist in the marketplace. In such case, the system would replicate the previous protocol for as many capable S agents.

4. THE SOCIAL NETWORK COMPONENT

During the simulation, information about the market, its participants and their interactions is collected and maintained. This information is then provided to SN-i agents who apply social network analysis techniques (Wasserman & Faust, 1994) in order to capture proximity relations between agents. This knowledge allows the improvement of the market's functioning by supporting agents on their decisions.

4.1. Relationship Graph Building

A SN-i agent starts by building the agent's relationship graph by comparing each agent to all others, determining the existence and intensity of relations between pairs of agents. For each pair of agents, the SN-i evaluates:

- The similarity between their attributes (normally, personal data or preferences provided during the registration phase);
- The similarity of their actions (rating ontology mappings, rating other agents, declarations about other agents);
- The existence of appreciation relations between them (relation that exists when one of the agents declared appreciation or depreciation with the other's behavior).

The intensity of the relationship between the pair of agents results from the weighted average of the values obtained for each of these evaluations.

4.1.1. Agents' Attributes Similarity Evaluation

To evaluate the similarity of attributes, the SN-i extracts properties of the information provided by both agents during their registration on the market, normally personal data and preferences. There are different types of properties that can be characterized by the type of value, namely discrete (e.g. marital status) or continuous (e.g. age), and the number of times they can be declared by an agent, namely functional (only one, e.g. marital status) or non-functional (e.g. trusted community).

The value of similarity for a continuous property can be obtained by (Wu, et al., 2007):

$$contPropEval(a, b, p) = 1 - \frac{|p(a) - p(b)|}{\max(p) - \min(p)} \quad (1)$$

Where a and b are the analyzed agents, p is the evaluated property, $p(a)$ and $p(b)$ are the values of the property p for agents a and b respectively, $\max(p)$ is the maximum limit for property p and $\min(p)$ is the minimum limit. Following the same conventions, now with $p(a)$ and $p(b)$ representing the set of values of the property p for agents a and b respectively, the similarity value of a discrete functional property is given by (Luz, 2010):

$$discFuncPropEval(a, b, p) = \begin{cases} 1: |p(a) \cap p(b)| > 0 \\ 0: otherwise \end{cases} \quad (2)$$

The similarity value of a non-functional discrete property is given by (Luz, 2010):

$$discNonFuncPropEval(a, b, p) = \frac{|p(a) \cap p(b)|}{|p(a) \cup p(b)|} \quad (3)$$

SN-i will compare each property that is declared for both agents. The result of this evaluation is obtained by averaging all calculated values.

4.1.2. Agents' Actions Similarity Evaluation

For the evaluation of similarity of agents' actions, the SN-i considers the following actions: (i) rating an ontology mapping; (ii) rating an agent; and (iii) declaring appreciation/depreciation with an agent's

behavior. SN-i starts by checking if both agents performed the same type of action over the same market's element (ontology mapping or agent), and if so, checks if they performed it in a similar way (e.g. if both agents gave a positive rating to a determined agent).

For this evaluation it is applied a similar approach to the one used for non-functional discrete properties, considering as a property an action performed over some market's element. SN-i will calculate the similarity of each action performed over the same element and then the final value of this evaluation is obtained by averaging all calculated values.

4.1.3. Agents' Appreciation Relations

The appreciation relations correspond to the declaration of appreciation or depreciation with an agent's behavior. The agent includes a value in this declarations that determines if it's a declaration of appreciation (positive value), or depreciation (negative value), and its intensity (e.g. a high negative value represents a high level of dissatisfaction). The result of the evaluation of appreciation/depreciation relations corresponds to the average of the values attributed in the declarations. If no relation exists the value is zero.

4.1.4. Resultant Relationship Graph

SN-i obtains a value for each of the three evaluations mentioned above (Sections 4.1.1, 4.1.2 and 4.1.3), and the relationship intensity value corresponds to the weighted sum of these values.

After repeating the process for all pairs of agents a relationship graph is obtained, where each node represents an agent and each edge represents a relation between two agents. The resultant graph is directed, weighted and signed, meaning that each relation is directed (not bidirectional), has an intensity value associated which might be positive or negative.

The graph is updated when new information is provided and is consulted when necessary.

4.2. SN-i Functionalities

As illustrated in Figure 1, an SN-i agent may receive two types of requests:

- Request to evaluate a set of ontology mappings for a pair of agents: in Figure 1, request $ReqMappingsRating(B,S,Ms)$, where Ms corresponds to the list of ontology mappings to evaluate for a given pair of agents, namely B and S agents;
- Request to advise an external agent about the use of an ontology mapping and/or the negotiation with a proposed partner: in Figure 1, requests $ReqAdviceAboutSAndMs(S,RMs)$ and $ReqAdviceAboutBAndMs(B,RMs)$, where RMs is the list of ontology mappings to evaluate for the agent that performed the request, and S and B correspond to the agents that should be evaluated.

In order to fulfill these requests, the SN-i should be able to:

- Determine the confidence value of the proposed ontology mapping for an agent, or pair of agents;
- Determine the level of trust that an agent should have with the proposed negotiating agent.

4.2.1. The Confidence Value of an Ontology Mapping for an Agent

The confidence value of an ontology mapping (M) for an agent a is obtained considering the (i) evaluation of the ontology mapping information taking into account the agent's preferences ($mapInfoEval(a,M)$), (ii) the ratings of the ontology mapping given by agents that have a relationship with the analyzed agent ($relAgtsRateEval(a,M)$) and (iii) the rating given by the agent itself ($rate(a,M)$):

$$mappingTrustValue(a,M) = \alpha.mapInfoEval(a,M) + \beta.relAgtsRateEval(a,M) + \gamma.rate(a,M) \quad (4)$$

where α , β and γ are the weights attributed to each evaluation.

For the evaluation of the ontology mapping information a simple approach is followed:

$$mapInfoEval(a,M) = \delta.mapMetricsEval(M) + \epsilon.prevPerformanceEval(M) + \zeta.relEntitiesEval(a,M) + \eta.valuedPropEval(a,M) \quad (5)$$

where δ , ϵ , ζ and η are the weights attributed to each evaluation, and:

- The ontology mapping metrics, i.e. $mapMetricsEval(M)$, is given by the percentage of covered concepts and properties of the agent's ontology, and the average percentage of properties mapped by concept:

$$mapMetricsEval(M) = mappedConceptsPercent(M) + mappedPropertiesPercent(M) + avgMapPropByConceptPercent(M) \quad (6)$$

- The previous performances of the ontology mapping, i.e. $prevPerformanceEval(M)$. In this case some historic information about the prior usage of the ontology mapping, namely the average loss of information during the transformation process ($avgLossInfo(M)$), can be considered:

$$\begin{aligned} prevPerformanceEval(M) = \\ 1 - avgLossInfo(M) \end{aligned} \quad (7)$$

- The ontology mapping related entities (i.e. the communities responsible for its creation and maintenance) comparing with the ones the agent trust. $relEntitiesEval(a,M)$ is given by the sum of the weight attributed by the agent to the trusted entities that are related to the mapping ($CE(a,M)$, meaning common entity between a and M). This value is then divided by the sum of the weights of all entities that the agent trusts (TE). If no weight is attributed it is considered to be 1:

$$relEntitiesEval(a,M) = \frac{\sum weight(a,CE(a,M))}{\sum weight(a,TE)} \quad (8)$$

- The ontology's concepts or properties covered by the mapping, comparing with the ones valued by the agent, i.e. $valuedPropEval(a,M)$. It is given by the sum of the weights attributed by the agent to the properties/concepts that are both valued by the agent and covered by the mapping ($CP(a,M)$), divided by the sum of the weight of all properties/concepts valued by the agent (VCP):

$$valuedPropEval(a,M) = \frac{\sum weight(a,CP(a,M))}{\sum weight(a,VCP)} \quad (9)$$

To evaluate the ratings given by related agents, the SN-i consults the relationship graph, selecting the agents with closest relations (i.e., relations with higher positive value) with the analyzed agent who rated the ontology mapping. The SN-i can continue searching the graph for related agents until the obtained information is considered sufficient. The value of the analysis is given by the average of the ratings ($rate$) made by the related agents (RA), weighted by the intensity of its relation to the agent ($relVal$).

$$relAgtRateEval(a,M) = \frac{\sum_{b \in RA} relVal(a,b).rate(b,M)}{\sum_{b \in RA} relVal(a,b)} \quad (10)$$

By considering the information about the ontology mapping, and not only the evaluations made by the related agents, the cold start problem (a typical problem of collaborative recommendation systems that rises when an item, here an ontology mapping, has no previous evaluations) does not occur. The historic information about ontology mapping's performance, namely average loss of information during the transformation process, enables a fair comparison between those ontology mappings that contemplate only a relatively small part of an ontology (that in the current context is usually the only part that is relevant) with those who have a higher coverage but the same relevant parts.

4.2.2. The Confidence Value of an Ontology Mapping for a Pair of Agents

When SN-i receives a request to evaluate a set of ontology mappings for a pair of agents, the process described above (Section 4.2.1) is repeated for each mapping for each of the two agents, i.e., for a pair of agents, namely agent a and agent b , SN-i calculates the confidence value of each mapping M for agent a ($mappingTrustValue(a,M)$) and for agent b ($mappingTrustValue(b,M)$), and the confidence value of the mapping M is obtained by averaging the calculated values:

$$\begin{aligned} mappingTrustValue(a,b,M) = \\ (mappingTrustValue(a,M) + \\ mappingTrustValue(b,M)) / 2 \end{aligned} \quad (11)$$

4.2.3. The Level of Trust an Agent Should Have with another Agent

The level of trust that an agent should have with another (confidence value of the relation) is determined in a similar way to the previously described for the ontology mapping. In this case the SN-i considers the ratings that the agents closest to the one that performed the request gave to the agent that is being analyzed ($relAgtAgtEval$) and the one given by the agent itself ($rate$). It also considers the existence and intensity of a relation between the requester and the analyzed agents ($relVal$). The metric can be represented as:

$$\begin{aligned} agentTrustValue(a,b) = \\ \lambda.relVal(a,b) + \\ \mu.relAgtAgtEval(a,b) + \\ \sigma.rate(a,b) \end{aligned} \quad (12)$$

where a is the agent that performed the request, b is the agent being analyzed, and λ , μ and σ are the weights attributed to each component. The evaluation of the related agents' ratings of agent b can be obtained by:

$$relAgtAgtEval(a,b) = \frac{\sum_{c \in RA} relVal(a,c).rate(c,b)}{\sum_{c \in RA} relVal(a,c)} \quad (13)$$

When an agent seeks advice about another, some information like (i) the tendency of the agent's ratings (i.e. if the rates given by other agents are stable, increasing or decreasing), (ii) the agent's prestige (obtained through the analysis of its positive relations), and (iii) the agent's global and local satisfaction (obtained through the analysis of the transactions' negotiation both with the requester agent and with all agents) can be very important, and should be provided as additional information about the agent.

Some evaluations (represented by equations 4, 5 and 12) have weights associated to each component that allows differentiating its relevance to the final value. These weights are defined by the user at the simulation configuration.

5. CONCLUSIONS

New generation of e-commerce applications allows e-commerce actors (represented by software agents) to adopt different ontologies to describe their universe of discourse, their needs and their capabilities, raising an heterogeneity problem that is seen as a corner stone for interoperability, namely for communication. Therefore, to achieve a consistent and compatible communication, agents need to reconcile their vocabularies, through an ontology matching process, resulting in the alignment of their ontologies. While in several domains of application the alignment specification can be done in design-time, e-commerce scenarios require that alignment specification is done in run-time since e-commerce actors have no prior knowledge of the other actors with whom they will interact.

AEMOS relies on the conviction that the marketplace must provide a technological framework promoting and enabling the semantic integration between parties through the use of ontology matching. Yet, it is our conviction that the marketplace must encourage agents to play an important role in the required matching process. Even though, that cannot be a mandatory issue and therefore the marketplace must be equipped to deal with agents having different ontology matching capabilities. It is envisaged that by taking part in the matching process agents may become more confident in the underlying communication process and in face of that consider the e-commerce exchanged data (e.g. RFP and PP) more reliable (safe) and consequently become more proactive in the marketplace.

ACKNOWLEDGMENTS

This work is supported by FEDER Funds through the “Programa Operacional Factores de Competitividade - COMPETE” program and by National Funds through FCT “Fundação para a Ciência e Tecnologia” under the projects: FCOMP-01-0124-FEDER-PEst-OE/EEI/UI0760/2011; PTDC/EIA-EIA/104752/2008.

REFERENCES

- Euzenat, J., & Shvaiko, P. (2007). *Ontology matching*. Springer.
- Fensel, D., Ding, Y., Omelayenko, B., Schulten, E., Botquin, G., Brown, M., et al. (2001). Product Data Integration in B2B E-Commerce. In *IEEE Intelligent Systems* 16 (pp. 54-59).
- Hepp, M. (2008). *GoodRelations: An Ontology for Describing Products and Services Offers on the Web*. In Proc. Of the 16th International Conference on Knowledge Engineering and Knowledge Management (EKAW2008) (Vol. 5268, pp. 332-347). Springer LNCS.
- Luz, N. (2010). *Semantic Social Network Analysis*. MSc Thesis, Instituto Superior de Engenharia do Instituto Politécnico do Porto, Dep. Of Computer Science Engineering, Porto, Portugal.
- Obrst, L., Liu, H., & Wray, R. (September de 2003). *Ontologies for Corporate Web Applications*. *AI Magazine*, 24(3), pp. 49-62.
- Runyon, K., & Stewart, D. (1987). *Consumer Behavior* (3rd ed.). Merrill Publishing Company.
- Viamonte, M. J., Ramos, C., Rodrigues, F., & Cardoso, J. C. (2006). ISEM: A Multi-Agent Simulator For Testing Agent Market Strategies. In *IEEE Transactions on Systems, Man and Cybernetics – Part C: Special Issue on Game-theoretic Analysis and Stochastic Simulation of Negotiation Agents* (Vol. 36(1), pp. 107-113).
- Viamonte, M. J., Silva, N., & Maio, P. (2011). *Agent-Based Simulation of Electronic Marketplaces With Ontology-Services*. In *The 23rd European Modeling & Simulation Symposium (Simulation in Industry)*. Rome, Italy.
- Wasserman, S., & Faust, K. (1994). *Social Network Analysis: Methods and Applications* (1st ed.). Cambridge University Press.
- Wu, B., Pei, X., Tan, J., & Wang, Y. (2007). *Resume Mining of Communities in Social Network*. In *Seventh IEEE International Conference on Data Mining Workshops (ICDMW 2007)* (pp. 435-440). Omaha, NE, USA.

AUTHORS BIOGRAPHY

Maria João Viamonte is a professor and researcher in the Knowledge Engineering and Decision Support Research Center (GECAD) of the School of Engineering at the Polytechnic Institute of Porto. Her research areas include multi-agent systems, simulation, agent mediated electronic commerce and decision support systems. Viamonte has a PhD in electrical engineering from the University of Trás-os-Montes and Alto Douro. Contact her at mjv@isep.ipp.pt

Virgínia Nascimento is a graduate student in the Knowledge Engineering and Decision Support Research Center (GECAD) of the School of Engineering at the Polytechnic Institute of Porto. Her research areas include multi-agent simulation, agent mediated electronic commerce and decision support systems, learning techniques. Contact her at vlrn@isep.ipp.pt

Nuno Silva is a professor and researcher in the Knowledge Engineering and Decision Support Research Center (GECAD) of the School of Engineering at the Polytechnic Institute of Porto. His research areas include Information Integration, Knowledge Engineering and the Semantic Web. Silva has a PhD in electrical engineering from the University of Trás-os-Montes and Alto Douro, Portugal. Contact him at nps@isep.ipp.pt

Paulo Maio is a professor and researcher in the Knowledge Engineering and Decision Support Research Center (GECAD) of the School of Engineering at the Polytechnic Institute of Porto. His research areas include ontology matching problem applied to multi-agent systems promoting agents' interoperability. He is also a PhD student at the University of Trás-os-Montes and Alto Douro. Contact him at pam@isep.ipp.pt

A DECISION SUPPORT SYSTEM FOR INTERMODAL TRANSPORTATION NETWORKS MANAGEMENT

Maria Pia Fanti^(a), Giorgio Iacobellis^(b), George Georgoulas^(c), Chrysostomos Stylios^(d), Walter Ukovich^(e),

^(a)Dept. of Electrical and Electronic Engineering - Polytechnic of Bari

^(b,d)Dept. of Informatics and Telecommunications Technology, Technological Educational Institute of Epirus

^(c)Teorema Engineering S.r.l., Area Science Park Basovizza, Trieste, Italy

^(e)Dept. of Engineering and Architecture- University of Trieste

^(a)fanti@deemail.poliba.it, ^(b)iacobellis@deemail.poliba.it, ^(c)georgoul@teleinfom.teiep.gr, ^(d)stylios@teiep.gr,
^(e)ukovich@units.it,

ABSTRACT

This paper specifies a Decision Support System (DSS) devoted to manage Intermodal Transportation Networks (ITN). With the aim to support decision makers in the management of the complex processes in the ITN, we describe the architecture of a DSS and its main components. In order to obtain a generic DSS, we employ the Unified Modeling Language (UML) to describe the components and the architecture of the DSS and we apply the solutions based on Service Oriented Architecture, the simulation drivers and window services.

Keywords: Decision Support System, Intermodal Transport Network, Unified Modeling Language, Simulation.

1. INTRODUCTION

An Intermodal Transportation Network (ITN) is defined as a logistically linked system integrating different transportation modes (rail, ocean vessel, truck etc.) to move freight or people from one place to another in a timely manner (Boschian et al. 2011; Crainic and Kim 2007; Macharis and Bontekoning 2004). There is a great availability of various alternative means and routes and so the complexity of ITN is continuously increased. On the other hand the availability of the new Information and Communication Technologies (ICT) that could be used to support the Decision Makers (DM) and the huge amount of acquired information, require the development of new models and methods for decision support (Coronado et al. 2009, Giannopoulos 2004). It is widely accepted that ITN decision making is a very complex process, due to the dynamical and large-scale nature of the intermodal transportation chain, the hierarchical structure of decisions, as well as the randomness of various inputs and operations. Researchers have followed similar approaches from other application areas (e.g., production processes), and they have identified different hierarchical/functional levels for transportation systems (Dotoli et al. 2009, Caris, Macharis, and Janssens 2008). More precisely the

levels are the following: a) the strategic level, related to the long-term definition of the transportation network, to the selection of the different transportation modes and to the evaluation of the feasible flows (capacities of the nodes and of the arcs); b) the tactical level, related (on a middle-short term) to the management of logistic flows connected to the information flow and to the transportation network that is topologically and dimensionally defined at the higher (strategic) level; c) the operational level, including real-time decisional processes that concern the resource assignment, the vehicle routing definition, and so on. In particular, assuming a real time availability of the information regarding the conditions of the network (like unexpected requests of transportation, variations in the availability of the transportation system, road conditions and traffic flows), operational decisions should be taken in a dynamic context.

Since intermodal transportation is more data-intensive than conventional transportation means, the modern ICT tools help to produce, manipulate, store, communicate, and/or disseminate information and provide useful information about the state of the system in real time and therefore manage and change on-line paths, vehicle flows, orders and deliveries. Dotoli et al. (2009) proposed an integrated system that is based on a reference model and a simulation module to support the decision making process. The integrated system tracks the state changes from the real ITN and evaluates performance indices typical of the tactical and real time management, such as utilization, traffic indices and delivery delays (Viswanadham, 1999).

This paper takes into account the integrated system proposed in (Dotoli et al. 2009), and it specifies a Decision Support System (DSS) devoted to manage ITNs for taking tactical decisions, i.e., in an off-line mode, and operational decisions, i.e., in real time. Indeed, due to the complexity of the system, the DM needs support during the decision making process. There are proposed typical methodologies for decision making, which depend on the type of ITN problems that are addressed. Moreover, suitable optimization

algorithms can be used for the definition of new long term policies, and employ the treatment of massive volumes of data to address multicriteria problems. In any case, the utilization of computer-based approaches to support the decision making procedures is a necessity. Different type of computer-based systems have been developed that are used widely according to the activity and the type of problem that they support.

This paper proposes a generic DSS that is devoted to manage complex ITN systems, based on the Unified Modeling Language (UML) (Miles and Hamilton 2006), a visual modeling language that is suitable to describe and specify software engineering. Moreover, we specify the components and the architecture of the DSS and the corresponding software tools. In addition, all solutions included in the proposed DSS are based on a Service Oriented Architecture (SOA) approach that guarantees the interoperability of the simulation and optimization drivers.

2. THE DSS STRUCTURE

In this section, we describe the main components of the proposed DSS.

Usually DSSs are categorized on the basis of different characteristics of the systems, e.g. whether they are for personal or group oriented decision making (Gorry and Scott Morton 1971; Keen and Scott Morton 1978; Delen et al. 2010; Power 2002). Based on the type of the application, DSSs are divided in desktop and web based applications. Despite the different categories of DSS, all of them share common characteristics; i.e., a typical DSS should include four main components: the data component, the model component, the decision component, and the interface component. Here, a UML class diagram is used to describe the main structure of the DSS. In particular, UML has standard notation and syntax and is composed of thirteen main types of diagrams, each one serving a different purpose and describing the system from different points of view. We consider two views of the DSS: *the structural view* is described by the package and class diagrams that illustrate the different types of objects which the system consists of and their relationships; *the behavioral view* is described by activities diagrams that describe the rules that the system follows to operate in a complete and correct manner, to avoid misunderstanding on both the user side and the developer side.

2.1. The DSS Components

Figure 1 shows the UML class diagram of the proposed DSS architecture. More precisely, each class is represented by a rectangular box divided into compartments. The first compartment holds the class name, the second holds attributes and the last holds operations. More precisely, attributes are qualities and named property values that describe the characteristics of a class. In addition, operations are features that specify the class behavior. Moreover, classes can exhibit relationships that are represented by different graphic connections: association (solid line),

aggregation (solid line with a clear diamond at one end), composition (solid line with a filled diamond at one end), inheritance or generalization (solid line with a clear triangle at one end), realization (dashed line with a clear triangle at one end) and dependency (dashed line with an arrow at one end). By class diagrams each component can be modeled as a different class illustrating the different types of objects that the system can have and their relationships.

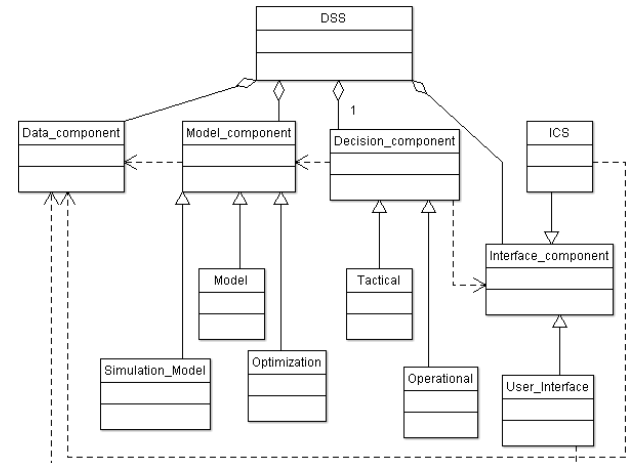


Figure 1: The DSS Structure

In the following we briefly specify the DSS components shown in Fig. 1.

Data component. This module is a database that can be denoted as internal and external data base. The data are internal if they come from organization's internal procedures and sources such as products and services prices, recourse and budget allocation data, payroll cost, cost-per-product etc. Moreover, external data are related to the competition market share, government regulations etc. and may come from various resources such as market research firm, government agencies, etc. In some cases the DSS can have its own database or it may use other organizational databases that can be connected directly with them.

Model component. This component mainly includes a simulation model, a mathematical model, and a set of optimization algorithms suitable to analyze effects of choices on the system performances. The models describe the operations at different management levels and the type of functions varies with the operation that they support.

Interface component. This module is the part of the DSS that is responsible of the communication and interaction of the system with the DM. Such a component is very important because regardless of the quality and quantity of the available data; the accuracy of the model is based on this interface. Indeed, this component includes an Information Communication System (ICS) that is able to interact with the real system and maintains the consistency between the stored data and the real system.

Decision component. This component consists of two second level classes: the operational decision class

and the tactical decision class. Moreover, such classes include the performance indices that have to be considered in order to take the decisions. In addition, in relation with the performance indices and the object of the decisions, the DSS has to collect the decision rules and the optimization procedures that are used by the model and the simulation component.

3. THE DSS ARCHITECTURE

This section describes in detail the DSS components presented in Section 2. Moreover, Fig. 2 shows the architecture of the realized system by enlightening the connections among the modules.

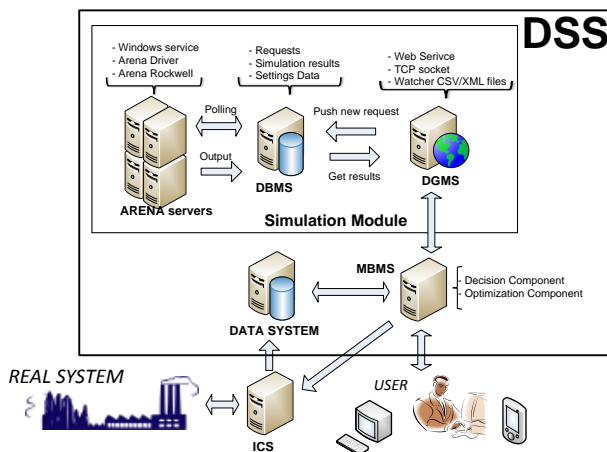


Figure 2: The DSS architecture.

3.1. The Data Component

We distinguish three different kinds of data. The first data are managed by the Data Base Management System (DBMS) that stores the internal data used by the decision and the simulation components. More precisely, the DBMS stores the requests of a new simulation with its input data, the data related to internal variables of the simulation model, and the outputs produced by simulations. Furthermore, the DBMS contains the queue of the requests to be sent to the simulation server, the state of each request and the results of the simulation. Moreover, it stores the description of all the simulation models that are available for the simulation runs.

The second and third kind of data are stored in the Data System: the internal data and the external data. The internal data represent all data necessary to describe the internal procedures, e.g. the time required for each activity, the number of available resources, the capacity of parking areas and safety levels, etc. On the other hand, the external data are information coming in real time from the system: the current number of vehicles, the information about the conditions of the roads, the accidents, the road maintenance works, the weather conditions, etc.

3.2. The Model Component

The model component is the core of the DSS: it consists of the simulation model and the optimization component.

3.2.1. The simulation model

The simulation model mimics the system, applies the optimization strategies proposed by the optimization module and provides the performance measures.

In the proposed solution, the simulation model is implemented by the Arena servers. In particular, each Arena server consists of the following main elements:

- **The ARENA software.** In such a server the simulation models are implemented and executed in the Arena Rockwell environment (Kelton 2009).
- **The Windows service.** The service is automatically started, it monitors the DBMS, as soon as a new simulation request is loaded, the service executes the simulation by the arena driver and loads results on the DB.
- **ARENA driver.** This component is the driver that connects the system to the software ARENA: it is in charge of starting and stopping simulations.

By the proposed architectural solution, we can provide a set of Arena servers and each server is independent from the others. Then, the number of operative Arena servers can dynamically change on the basis of the computational effort that is required in real time. Moreover, such an approach allows a parallel execution of the simulation requests by reducing the total execution time.

3.2.2. The Optimization Component

The second basic module of the model component is the optimization module (see Fig. 1) that combines a variant of Particle Swarm Optimization (PSO) (Kennedy 1995) with an Optimal Computing Budget Allocation (OCBA) scheme (Chen 2000). In particular, the original PSO algorithm was introduced in 1995 by Eberhart and Kennedy (Kennedy 1995). Its main concept includes a population, called a swarm, of potential solutions of the problem at hand, called the particles, probing the search space. The particles iteratively move in the search space with an adaptable velocity, retaining in a memory the best positions they have ever visited, i.e., the positions with the lowest function values (considering only minimization problems). The exploration capability of PSO is promoted by information exchange among particles. More specifically, each particle is assigned to a neighborhood. In the global PSO variant, also known as *gbest*, the neighborhood of each particle is the whole swarm and the overall best position is the main information provider for all particles. On the other hand, in the local PSO variant, also known as *lbest*, the neighborhoods are strictly smaller, usually consisting of a few particles. In such cases, each particle may have its own leader that influences its velocity update. In real

life problems we usually accept good enough solutions instead of the globally optimal solution. Therefore, in case of “noisy” functions, “following” the “best” particle becomes a bit involved since the actual value of a particle is obscured by noise and repeated function evaluations are required in order to more accurately estimate the true value. Especially in situations where a function evaluation is a costly process, a compromise should be reached between the need for an accurate estimate of the true value and the need to have as few as possible unnecessary function evaluations.

The OCBA was proposed by Chen (2000) as a procedure to optimally allocate a predefined number of trials/replications in order to maximize the probability of selecting the best system/design: allocate replications not only based on the variance of the different designs but also taking into account the respective means. More specifically, the noisier the simulation output (larger variance), the more replications are allocated while more replications are also given to the design that its mean is closer to that of the best design.

The global version of the PSO uses the mean values for each performance measure that are evaluated by a low number of replications. Then using the OCBA procedure more replications are allocated in order to increase the probability of correctly identifying the best particle, whose value is used to guide the search of the swarm.

3.3. Interface Component

In the presented architecture we implement two interfaces: the first interface connects the simulation module with the Model Base Management Server (MBMS) by means of the Dialog Generation/Management Server (DGMS) module; the second one connects the DSS and the real system through the MBMS.

In particular, the ICS module (see figure 2) represents the information system of the whole infrastructure and is the interface between the real system and the information system. It updates the system status stored in the Data System in real time.

The DGMS allows the communication between the decision component and the simulation component. It receives requests from the decision component such as running a new simulation or retrieving the results of a finished simulation. All requests coming from the MBMS are loaded into the DBMS by the DGMS. In order to guarantee the modularity of the architecture and the possibility to execute the DSS components under different platforms, we implement the following three different ways to communicate with the DGMS:

- **Web Service (WS).** The WS can trigger a new simulation, provides information about the state of the request and gives the simulation results. A web service is a process running on a server and allowing a client to execute a process on the server. This kind of application communicates by the Simple Object Access Protocol (SOAP).

- **TCP Socket.** This application is a process running on the server that creates a listener on a preconfigured communication gate. The MBMS sends messages to DGMS by the TCP channel. These messages are strings codified by a prefixed communication protocol. By this application the MBMS can request a new simulation or access to stored data.
- **File Watcher.** This process monitors the files on a shared folder. As soon as a new file is loaded by an FTP client, it analyses the contents of the file and executes the corresponding operations. When a simulation goes to an end, the file watcher creates a report file in the same folder so that all data are available to the client.

Furthermore, the MBMS shows data to the DM: if the current performance of the system is not satisfactory, then the DM can decide to evaluate the impact of some decision using a “what if” approach. The MBMS allows the DM to run a simulation directly without the decision module control. This proposed solution is very useful for the DM and contributes to generalize all the features offered by the DSS.

3.4. The Decision Component

The MBMS server implements the decision component. In particular, it monitors the system state stored in the Data System component and decides if it is necessary to run a new simulation or not. Indeed, if the performances of the system decrease, then the decision component starts the optimization and the decision procedure. Figure 3 shows the used decision approach that is based on the optimization module and the validation by the simulation. More precisely, the optimization algorithms propose some solutions that are sent to the simulation module. The ICS provides the current state of the system by returning the values of the variables that cannot be determined by the DSS. Then the DSS invokes the simulation module: the simulation starts and applies the proposed management strategies. The obtained performance indices allow evaluating the impact of the proposed solution on the system. Then a new set of candidate variables are passed to the simulation model and the process continues till the algorithm leads to a satisfactory decision described by a set of candidate variables. In this model, the candidate variables are the controllable inputs that may change in the tactical or operational decision making process.

In the proposed DSS, the hybrid optimization module (PSO+OCBA) is connected by a web service to the simulation module. The optimization module sends inputs and the number of replications for each candidate solution/design and it records the outputs, again through the web service.

The average values of the outputs are sent to the OCBA procedure that decides if a number of extra replications are required. The average outputs are used to guide the PSO procedure: the process is repeated till a good number of available replications is obtained.

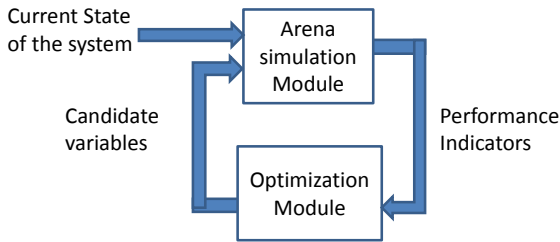


Figure 3: The Decision approach

On the basis of the current state of the system and the design variables, the DSS can be used to take decision both at the tactical and operational levels. In particular, at the tactical level the input variables are generated stochastically, while at the operational level the inputs come from the ICT tools of the real systems.

4. THE PILOT CASE

The proposed DSS has been realized to manage at tactical level an ITN composed of the port of Trieste (Italy), the dry port of Ferneti, and the railway station of the Roll on-Roll off freight trains. Mainly, the DSS deals with the decisions about the import and export flow of goods and the containers management and transportation. The DSS is designed in the framework of the SAIL Project, sponsored by the European Commission under the 7th Framework Program, Specific Program PEOPLE - Marie Curie Actions.

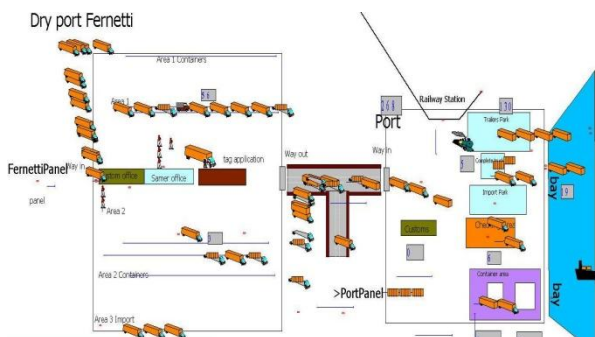


Figure 4: ARENA MODEL

In order to specify the simulation model in Boschian et al. (2011), the authors identified the main events occurring in a transportation system and described the main classes of the system: the port area, the inland port area, the road connection system and the rail network system. Furthermore, some interviews are previously performed to the actors involved in the process and the necessary data and the relations are collected. The involved resources and their availability are identified and the following performance indices are considered:

- throughput, i.e., the number of units boarded in a time units;
- average lead time, i.e., the time elapsed from the arrival of a new units till its system output;
- the average resources utilization;

- the average queue lengths of the users that have to acquire resources.

Figure 4 shows a sketch of the simulation model realized in the ARENA environment. The DSS allows us to identify all the weakness and the bottlenecks of the system. Moreover, some optimization strategies are proposed and analyzed at tactical level.

5. CONCLUSIONS

This paper specifies a Decision Support System devoted to manage Intermodal Transportation Networks and to take tactical and operational decisions. We describe the DSS architecture and, in particular, the decision process that is based on two main modules: the optimization and the simulation module. Moreover, we show how the DSS is designed by applying SOA and web server approaches. Hence, the obtained DSS can be realized in a distributed framework in order to face the system complexity.

Future work will describe in more detail the decision procedures of the DSS.

ACKNOWLEDGMENT

This work is supported by the E.U FP7-PEOPLE-IAPP-2009, Grant Agreement No 251589, Acronym: SAIL.

REFERENCES

- Boschian, V., Dotoli, M., Fanti, M.P., Iacobellis, G. and Ukovich, W., 2011. A metamodeling approach to the management of intermodal transportation networks. *IEEE Transactions on Automation Science and Engineering*, vol. 8: pp. 457-469.
- Caris, A., Macharis, C., and Janssens, G.K., 2008. Planning Problems in Intermodal Freight Transport: Accomplishments and Prospects. *Transportation and Planning Technology*, vol. 31: pp. 277-302.
- Chen, C.H., Lin, J., Yücesan, E. and Chick, S.E., 2000. Simulation Budget Allocation for Further Enhancing the Efficiency of Ordinal Optimization. *Journal of Discrete Event Dynamic Systems: Theory and Applications*, Vol. 10: pp. 251-270.
- Coronado, A.E., Coronado, E., and Lalwani, C.S., 2009. Wireless Vehicular Networks to Support Road Haulage and Port Operations in a Multimodal Logistics Environment. *Proceedings of IEEE/INFORMS International Conference on Service Operations, Logistics and Informatics*, pp. 62-67, July 22-24, Chicago (IL, USA).
- Crainic, T.G. and Kim, K.M., 2007. Intermodal transportation. In: C. Barnhart and G. Laporte, ed. *(Transportation) Handbooks in Operations Research and Management Science*, vol. 12. Amsterdam: North-Holland/Elsevier, 467-537.
- Delen, D., Sharda, R., and Turban, E., 2010. *Decision Support and Business Intelligence Systems. 9th Edition*. New Jersey, USA: Prentice Hall.
- Dotoli, M., Fanti, M.P., Iacobellis, G., and Mangini, A.M., 2009. A First Order Hybrid Petri Net Model

for Supply Chain Management. *IEEE Transactions on Automation Science and Engineering*, vol. 6: pp. 744-758.

- Giannopoulos, G.A., 2004. The Application of Information and Communication Technologies in Transport. *European Journal of Operational Research*, vol. 152: pp. 302-320.
- Gorry, A.G. and Scott Morton, M.S., 1971. A framework for management information systems. *Sloan Management Review*, vol. 13: pp. 55-70.
- Keen, P.G.W. and Scott Morton, M.S., 1978. *Decision support systems: An organisational perspective*. Reading, MA: Addison-Wesley.
- Kelton, W.D., Sadowski, R.P., and Swets, N.B., 2009. *Simulation with Arena. 5th Edition*. Boston (MA): McGraw-Hill.
- Kennedy, J. and Eberhart, R.C., 1995. Particle swarm optimization. *IEEE International Conference on Neural Networks*, pp. 1942-1948, Perth (Australia).
- Macharis, C. and Bontekoning, Y.M., 2004. Opportunities for OR in Intermodal Freight Transport Research: a Review. *European Journal of Operational Research*, vol. 153: pp. 400-416.
- Miles, R. and Hamilton, K., 2006. *Learning UML 2.0*. Sebastopol, CA (USA): O'Reilly Media.
- Power, D., 2002. *Decision Support Systems: concepts and resources*. Westport, USA: Quorum Books.
- SAIL project. Available from: <http://www.teorema.net/it/UM/ReD/HarborLogistics/SAIL.aspx>
- Viswanadham, N., 1999. *Analysis of manufacturing enterprises: An approach to leveraging value delivery processes for competitive advantage*. Boston: Kluwer Academic.

AUTHORS BIOGRAPHY

Maria Pia Fanti received the Laurea degree in electronic engineering from the University of Pisa, Italy in 1983. Since 1983 she has been with the Department of Electrical and Electronic Engineering of the Polytechnic of Bari (Italy), where she was Assistant Professor from 1990 till 1998 and associate professor till April 2012. Now she is full professor of Control Systems in the same department. Her research interests include discrete event systems, Petri nets, modeling and control of automated manufacturing systems, supply chains, transportation systems, health care systems. She has published around 160+ papers and one textbook on these topics.

Giorgio Iacobellis received the Laurea degree in Electronic Engineering in 2004 from Polytechnic of Bari and the Ph.D. degree in Computer Science Engineering in 2009 from the same University. From February 2005 to February 2006, he was a research fellow and from December 2010 to November 2011 he was post-doc at Polytechnic of Bari. He currently works as an Experienced Researcher for the SAIL Project. His research interests include modeling, simulation, and

control of discrete event systems, Petri nets, supply chains and urban traffic networks, distribution and internal logistics, management of hazardous materials, management of drug distribution systems and healthcare systems.

George Georgoulas received his diploma and PhD degrees from the Department of Electrical and Computer Engineering of the University of Patras in 1999 and 2006, respectively. He has worked as a postdoctorate fellow in the Intelligent Control Systems Laboratory at The Georgia Institute of Technology, USA, from 2006 till 2008. He currently works as an Experienced Researcher for the SAIL Marie Curie Project. He has published over 70 journal and conference papers, book chapter and technical reports. His main scientific interests include: Computational Intelligence Techniques, Evolutionary methods, Global optimization methods and Decision Support Systems.

Chrysostomos D. Stylios is an Assistant Professor at Dep. of Informatics and Telecommunications Technology, Technological Educational Institute of Epirus; he is a senior researcher at Telematics Center Department of Computer Technology Institute & Press. He was a visitor assistant professor at Computer Science Dep., of University of Ioannina. He received his Ph.D from the Department of Electrical & Computer Engineering University of Patras in 1999. He received the diploma in Electrical & Computer Engineering from the Aristotle University of Thessaloniki in 1992. He has published over 100 journal and conference papers, book chapter and technical reports. His main scientific interests include: Fuzzy Cognitive Maps, Soft Computing techniques, Computational Intelligence Techniques, Evolutionary methods, Neural Networks, Support Vector Machines, Knowledge Hierarchical Systems and intelligent data fusion and Decision Support Systems for Medical application.

Walter Ukovich was Assistant Professor of Electrical Engineering at the Engineering Faculty of the University of Trieste, Italy, from 1970 to 1985, and Associate Professor of Operations Research at the same University from 1985 to 1999. He is now full professor of Operations Research at the same University. Prof. Ukovich was from 2008 till 2011 director of the Department of Electrical Engineering, Electronics and Computer Science and was responsible for the curriculum in Management Engineering. He has been a member of the Evaluation Boards of the National Research Council, the Universities of Trieste, the Polytechnic of Turin, and the University Institute of Architecture of Venice. His main research interests are in Optimization, Logistics, Production Planning and Control and Health Management Systems and he is the author of over one hundred scientific papers.

ELECTRIC FIELD AND STRAIN EFFECTS ON SURFACE ROUGHNESS INDUCED SPIN RELAXATION IN SILICON FIELD-EFFECT TRANSISTORS

Dmitri Osintsev^(a,b), Oskar Baumgartner^(a), Zlatan Stanojevic^(a), Viktor Sverdlov^(a), and Siegfried Selberherr^(a)

^(a)Institute for Microelectronics, TU Wien, Gußhausstraße 27-29, A-1040 Wien, Austria

^(b)Volgograd State Technical University, Lenin Avenue 28, 400131 Volgograd, Russia

Email: {Osintsev|Baumgartner|Stanojevic|Sverdlov|Selberherr}@iue.tuwien.ac.at

ABSTRACT

Spintronics attracts at present much interest because of the potential to build novel spin-based devices which are superior to nowadays charge-based devices. Utilizing spin properties of electrons opens great opportunities to reduce device power consumption in future electronic circuits. Silicon, the main element of microelectronics, is also promising for spin-driven applications. Understanding the details of the spin propagation in silicon structures is a key for novel spin-based applications. We investigate the surface roughness induced spin relaxation in a silicon-on-insulator-based spin field-effect transistors for various parameters including the potential barrier at the interfaces, the film thickness, and shear strain. Shear strain dramatically influences the spin opening a new opportunity to boost spin lifetime in a silicon spin field-effect transistor.

Keywords: spin relaxation, $\mathbf{k}\cdot\mathbf{p}$ model, shear strain, surface roughness, spin MOSFET

1. INTRODUCTION

Since modern microelectronic devices are near to their fundamental scaling limits, a further boost of their performance could be eventually provided by changing their operational principles. Promising results have been already obtained by utilizing the spin properties of electrons. In order to achieve significant advantages by utilizing spin, materials possessing a long spin life-time and low relaxation rate must be used.

Silicon is the primary material for microelectronics. The long spin life time in silicon is a consequence of the weak spin-orbit interaction and the spatial inversion symmetry of the lattice (Li and Appelbaum 2011, Li and Dery 2011). In addition, silicon is composed of nuclei with predominantly zero magnetic moment. A long spin transfer distance of conduction electrons has already been demonstrated experimentally (Huang, Monsma, Appelbaum 2007). Spin propagation at such distances combined with a possibility of injecting spin at room (Dash, Sharma, Patel, de Jong, Jansen 2009) or even elevated (Li, Van't Erve, Jonker 2011) temperature in silicon makes the

fabrication of spin-based switching devices quite plausible in the upcoming future. However, the relatively large spin relaxation experimentally observed in electrically-gated lateral-channel silicon structures (Li and Appelbaum 2011) might become an obstacle in realizing spin driven devices (Li and Dery 2011), and a deeper understanding of the fundamental spin relaxation mechanisms in silicon is urgently needed (Song and Dery 2012).

In this work we investigate the influence of the intrinsic spin-orbit interaction on the subband structure, subband wave functions, and spin relaxation matrix elements due to the surface roughness scattering in thin silicon films. Following Li and Dery (Li and Dery 2011), a $\mathbf{k}\cdot\mathbf{p}$ approach (Bir and Pikus 1974, Sverdlov 2011) suitable to describe the electron subband structure in the presence of strain is generalized to include the spin degree of freedom.

In contrast to Li and Dery (Li and Dery 2011), our effective 4x4 Hamiltonian considers only relevant [001] oriented valleys with spin included, which produce the low-energy unprimed subband ladder. Within this model the unprimed subbands in the unstrained (001) film are degenerate without spin-orbit effects included. An accurate inclusion of the spin-orbit interaction results in a large mixing between the spin-up and spin-down states, resulting in spin hot spots along the [100] and [010] axes characterized by strong spin relaxation due to the spin-orbit coupling. These hot spots should be contrasted with the spin hot spots appearing in the bulk system (Cheng, Wu, Fabian 2010, Li and Dery 2011). Their origin lies in the unprimed subband degeneracy in a confined electron system which effectively projects the bulk spin hot spots at the edge of the Brillouin zone to the center of the 2D Brillouin zone.

Shear strain lifts the degeneracy between the unprimed subbands (Sverdlov 2011). The energy splitting between the otherwise equivalent subbands removes the origin of the spin hot spots in a confined silicon system, which should substantially improve the spin lifetime in gated silicon systems.

2. METHOD

We solve numerically the Hamiltonian

$$H = \begin{bmatrix} H_1 & H_3 \\ H_3^\dagger & H_2 \end{bmatrix} \quad (1)$$

with H_1 , H_2 , and H_3 defined as

$$H_j = \left[\frac{k_z^2}{2m_t} + \frac{(-1)^j k_0 k_z}{m_l} + \frac{k_x^2 + k_y^2}{2m_t} + U(z) \right] I, \quad (2)$$

$$H_3 = \begin{bmatrix} D\varepsilon_{xy} - \frac{k_x k_y}{M} & (k_y - k_x i)\Delta_{SO} \\ (-k_y - k_x i)\Delta_{SO} & D\varepsilon_{xy} - \frac{k_x k_y}{M} \end{bmatrix}. \quad (3)$$

Here $j = 1, 2$, I is the identity 2×2 matrix, m_t and m_l are the transversal and the longitudinal silicon effective masses, $k_0 = 0.15 \times 2\pi/a$ is the position of the valley minimum relative to the X point in unstrained silicon, ε_{xy} denotes the shear strain component, $M^{-1} \approx m_t^{-1} - m_0^{-1}$, and $D = 14\text{eV}$ is the shear strain deformation potential. The spin-orbit term $\tau_y \otimes (k_x \sigma_x - k_y \sigma_y)$ with

$$\Delta_{SO} = 2 \left| \sum \frac{\langle X_1 | p_j | n \rangle \langle n | [\nabla V \times p]_j | X_2 \rangle}{E_n - E_X} \right|, \quad (4)$$

couple states with the opposite spin projections from the opposite valleys. σ_x and σ_y are the spin Pauli matrices and τ_y is the y -Pauli matrix in the valley degree of freedom. In the Hamiltonian (1) $U(z)$ is the confinement potential, and the value $\Delta_{SO} = 1.27\text{meVnm}$ computed by the empirical pseudopotential method (Figure 1) is close to the one reported by Li and Dery (Li and Dery 2011).

3. RESULTS AND DISCUSSION

3.1. Valley splitting calculations

First we investigate the dependence of the valley splitting on the value of the potential barrier at the interfaces. The numerical results are obtained for the wave vector $k \parallel [110]$ with the values $k_x = 0.1\text{nm}^{-1}$ and $k_y = 0.1\text{nm}^{-1}$. Figure 2 shows the splitting for different values of the quantum well width. The valley splitting theory in SiGe/Si/SiGe quantum wells (Friesen, Chutia, Tahan, Coppersmith 2007) predicts that in the case of a symmetric square well without an electric field the valley splitting is inversely proportional to the conduction band offset ΔE_c at the interface.

However Figure 2 demonstrates clearly that the dependence is more complicated. For the quantum well of 1.36nm width the splitting first increases but later saturates. For the quantum well of 3.3nm width a significant reduction of the valley splitting around the conduction band offset value 1.5eV is observed. A further increase of the conduction band offset leads to an increase of the subband splitting value. For the quantum well of 3.3nm thickness the valley splitting saturates at about 0.17meV.

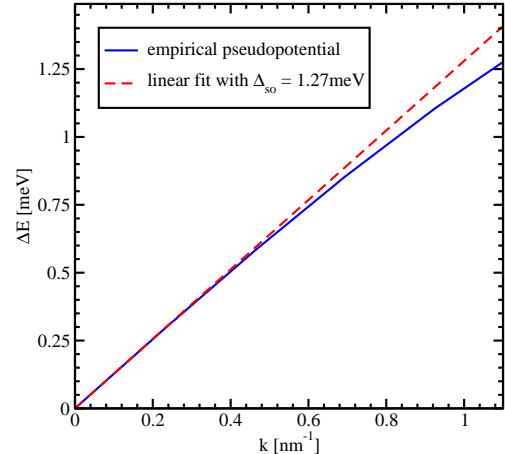


Figure 1: Empirical pseudopotential calculations of the spin-orbit interaction strength by evaluating the gap opening at the X -point between X_1 and X_2 for finite k_x

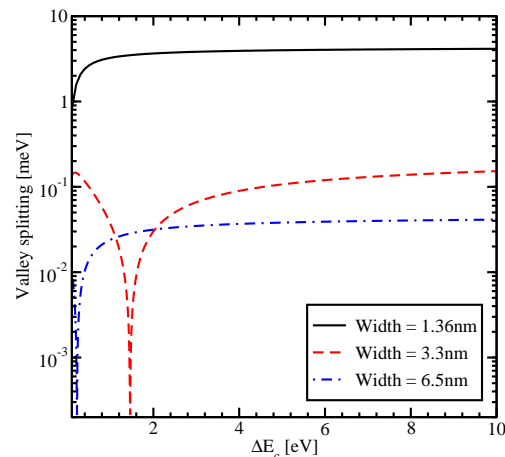


Figure 2: Splitting between the lowest unprimed electron subbands as a function of the conduction band offset at the interface for different thicknesses of the unstrained silicon film without electric field

For the quantum well of 6.5nm width a significant reduction of the valley splitting is observed for a conduction band offset value 0.2eV. The subband splitting saturates at a value 0.04meV. Although for the values of the conduction band offset smaller than 4eV the valley splitting depends on ΔE_c , for larger values of the conduction band offset it saturates indicating that the strength of the orbit-valley interaction at the interface is proportional to ΔE_c (Friesen, Chutia, Tahan, Coppersmith 2007).

The valley splitting as a function of the conduction band offset for the film of 3.3nm thickness without the electric field is shown in Figure 3. Without shear strain the valley splitting is significantly reduced around the conduction band offset value of 1.5eV. For the shear strain value of 0.25% and 0.5% the sharp reduction of the conduction subbands splitting shifts to a smaller value of ΔE_c However the region of significant

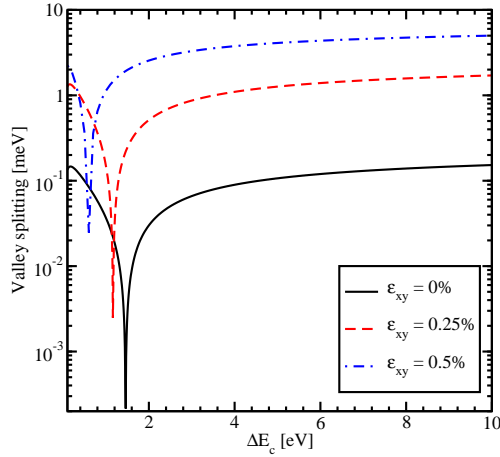


Figure 3: Valley splitting as a function of the conduction band offset for the film thickness 3.3nm without electric field

reduction is preserved even for the large shear strain value of 0.5%. The value of the valley splitting at saturation for large shear strain is considerably enhanced as compared to the unstrained case.

The influence of the effective electric field on the region of sharp splitting reduction is demonstrated in Figure 4. With the electric field applied the reduction in the region of interest around the conduction band offset value 1.5eV becomes smoother. However, for values of the conduction band offset smaller than 1.5eV the reduction of the valley splitting is still observed. For the values larger than 1.5eV the subband splitting slightly increases and then saturates. For the electric field value of 0.05MV/cm the saturation value of the valley splitting is almost equal to the saturated valley splitting value without electric field. For the stronger electric field of 0.5MV/cm the valley splitting reduction vanishes completely and the splitting becomes almost independent of the conduction band offset.

According to Friesen *et al.* (Friesen, Chutia, Tahan, Coppersmith 2007) the barrier height ΔE_c does not directly enter the expression of the valley splitting for a perfectly smooth interface in the presence of the electric field. The result shown in Figure 4 for the large electric field value is in a good agreement with the theory.

The splitting of the lowest unprimed electron subbands as a function of the silicon film thickness for several values of the conduction band offset at the interfaces is shown in Figure 5. The valley splitting oscillates with the film thickness increased. According to the theory (Sverdlov, Baumgartner, Windbacher, and Selberherr 2009), we generalize the equation for the valley splitting in an infinite potential square well including the spin-orbit coupling as

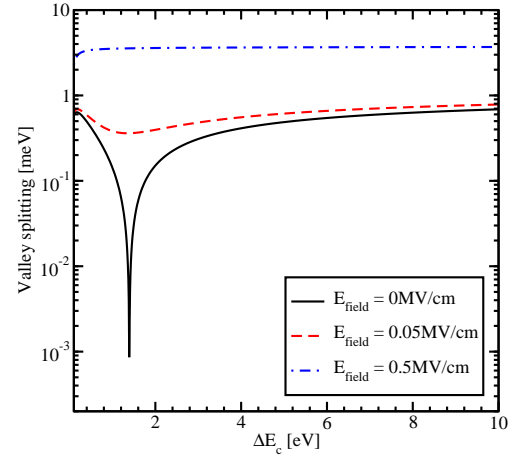


Figure 4: Dependence of the valley splitting on the conduction band offset at the interface for different values of the electric field, the shear strain value is 0.125%, and the quantum well width is 3.3nm

$$\Delta E_n = \frac{2y_n^2 B}{k_0 t \sqrt{(1-y_n^2 - \eta^2)(1-y_n^2)}} \left| \sin \left(\sqrt{\frac{1-y_n^2 - \eta^2}{1-y_n^2}} k_0 t \right) \right|, \quad (5)$$

with y_n , η , and B defined as

$$y_n = \frac{\pi n}{k_0 t}, \quad (6)$$

$$\eta = \frac{m_l B}{\hbar^2 k_0^2}, \quad (7)$$

$$B = \sqrt{\Delta_{so}^2 (k_x^2 + k_y^2) + \left(D \epsilon_{xy} - \frac{\hbar^2 k_x k_y}{M} \right)^2}. \quad (8)$$

Here t is the film thickness. As it was shown earlier the conduction band value of 4eV provides a subband splitting value close to the saturated one. Because Equation 5 is written for an infinite potential square well, a slight discrepancy is observed between the theoretical curve and the numerically curve calculated for the conduction band offset value 4eV in Figure 5. A large value of the conduction band offset shows better agreement between the theory and numerically obtained results.

The valley splitting as a function of the quantum well width for different values of the effective electric field is shown in Figure 6. Without electric field the valley splitting oscillates as shown in Figure 5. With electric field the oscillations are not observed in thicker films. According to Friesen *et al.* (Friesen, Chutia, Tahan, Coppersmith 2007) the condition for the independence of the valley splitting from the quantum well width is

$$L^3 > \frac{2\pi^2 \hbar^2}{m_l e E_{field}}. \quad (9)$$

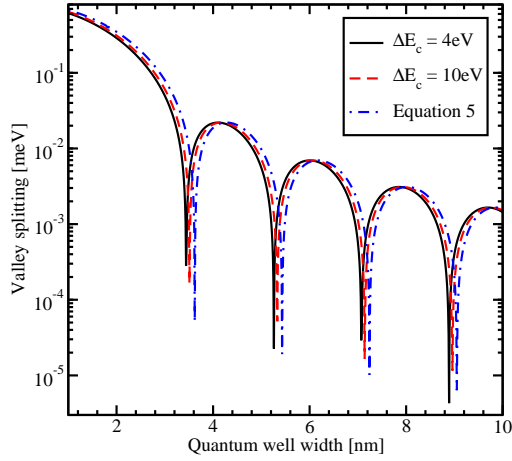


Figure 5: Splitting of the lowest unprimed electron subbands as a function of the silicon film thickness for several values of the band offset at the interface, the shear strain value is 0.05%, $k_x = 0.1\text{nm}^{-1}$, $k_y = 0.2\text{nm}^{-1}$

For thinner structures, the quantization is caused by the second barrier of the quantum well. The shape of the oscillations is therefore similar to that in the absence of an electric field. For the electric field of 0.05MV/cm the quantum well width should be larger than 6.9nm in order to observe the valley splitting independent on the quantum well width. This value is in good agreement with the simulation results shown in Figure 6.

We now discuss the effect of shear strain on the conduction band splitting and spin relaxation due to scattering induced by the surface roughness. The surface roughness scattering matrix elements are taken to be proportional to the square of the subband function derivatives at the interface (Fischetti, Ren, Solomon, Yang, and Rim 2003). A (001) oriented silicon film of 4nm thickness is considered, the incident wave $\mathbf{k}||[510]$, the values $k_x = 0.5\text{nm}^{-1}$, $k_y = 0.1\text{nm}^{-1}$, the scattered wave $\mathbf{k}'||[\bar{5}\bar{1}0]$, the values $k'_x = -0.5\text{nm}^{-1}$, $k'_y = -0.1\text{nm}^{-1}$, the spin is injected along $[110]$ direction.

Figure 7 shows the dependence of the valley splitting on strain. Without electric field the valley splitting reduces significantly around the strain values 0.116% and 0.931% as shown in Figure 7. With electric field applied the minimum around the strain value 0.931% becomes smoother, however, for the strain value around 0.116% the sharp reduction of the valley splitting is preserved. For large electric field the valley splitting reduction around the value 0.931% vanishes completely. For the strain value 0.116% the sharp reduction of the valley splitting is still preserved at a minimum value, which is determined by the spin-orbit interaction term, only slightly affected by the electric field. As follows from Equation 5 the splitting between the subbands depends on $D\varepsilon_{xy} - \frac{\hbar^2 k_x k_y}{M}$, and the degeneracy between the unprimed subbands is increased, when this term is nonzero.

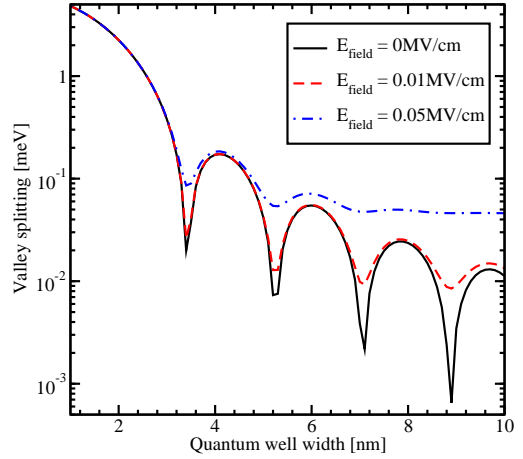


Figure 6: Splitting of the lowest unprimed electron subbands as a function of the film thickness for different values of the effective electric field, the shear strain value is 0%, the conduction band offset is 4eV, $k_x = 0.1\text{nm}^{-1}$, $k_y = 0.1\text{nm}^{-1}$

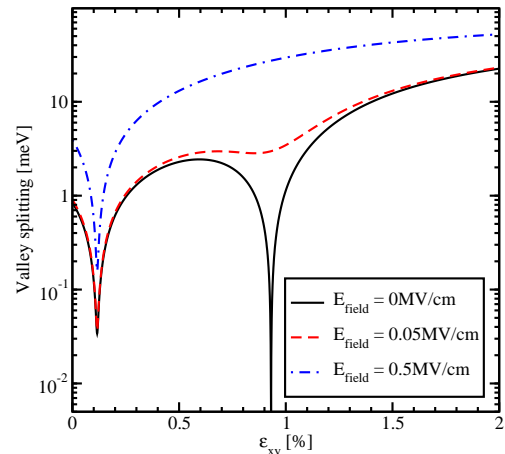


Figure 7: Splitting of the lowest conduction subbands as a function of shear strain for different values of the electric field, the quantum well thickness is 4nm, the conduction band offset is 4eV, $k_x = 0.5\text{nm}^{-1}$, $k_y = 0.1\text{nm}^{-1}$

For $k_x = 0.5\text{nm}^{-1}$, $k_y = 0.1\text{nm}^{-1}$ the strain value 0.116% causes this term to vanish and minimizes the valley splitting, in good agreement with the first sharp valley splitting reduction in Figure 7. The valley splitting is also proportional to $\left| \sin \left(\sqrt{\frac{1-y_n^2-\eta^2}{1-y_n^2}} k_0 t \right) \right|$. The second minimum in the valley splitting around the strain value 0.931% in Figure 7 is because of the zero value of the $\left| \sin \left(\sqrt{\frac{1-y_n^2-\eta^2}{1-y_n^2}} k_0 t \right) \right|$ term. The effective electric field alters the confinement in the well and is therefore able to completely wash out the minimum in valley splitting due to the sine term. However, in agreement with (5), it can only slightly affect the minimum due to the shear strain dependent contribution, in agreement with Figure 7.

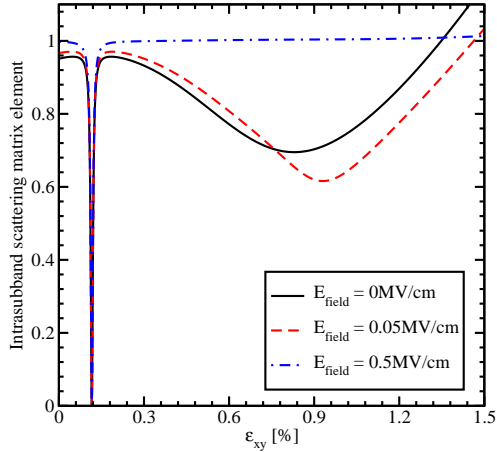


Figure 8: Intrasubband scattering matrix elements normalized by their values for zero strain as a function of shear strain for different electric field values

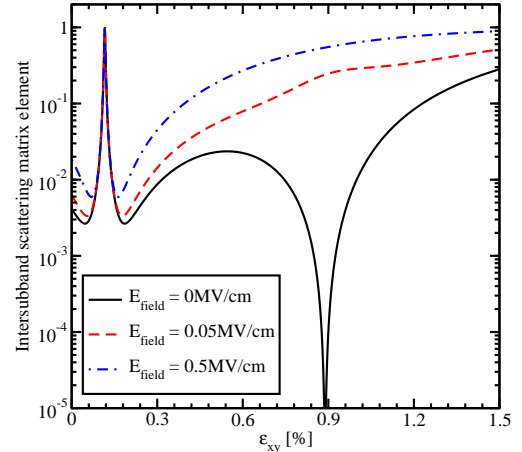


Figure 9: Intersubband scattering matrix elements normalized to the value of the intravalley scattering at zero strain as a function of strain for different electric field values

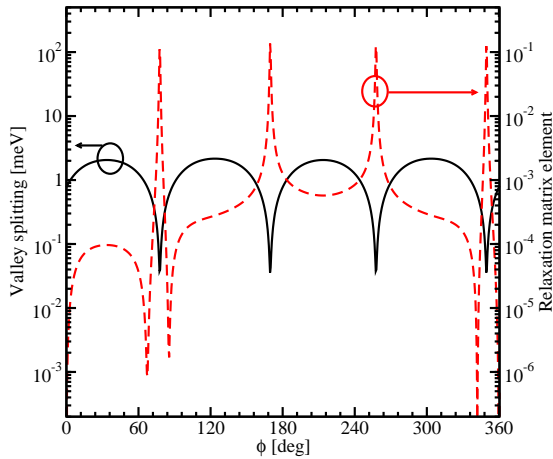


Figure 10: Dependence of the normalized spin relaxation matrix elements and valley splitting on the angle between the incident and scattered waves for the quantum well thickness is 4nm, the conduction band offset is 4eV, $k_x = 0.5\text{nm}^{-1}$, $k_y = 0.1\text{nm}^{-1}$, $E_{\text{field}} = 0\text{MV/cm}$, $\varepsilon_{xy} = 0.01\%$

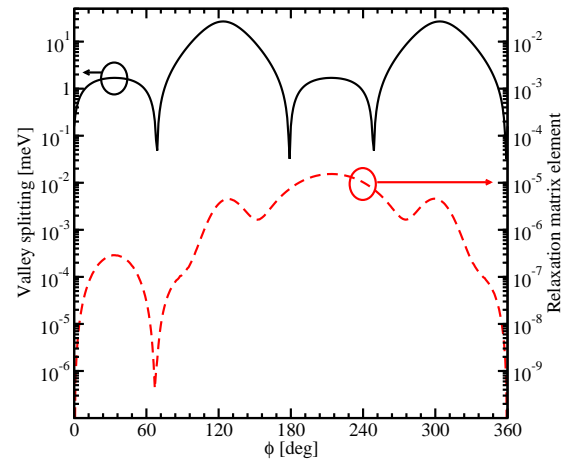


Figure 11: Dependence of the normalized spin relaxation matrix elements and valley splitting on the angle between the incident and scattered waves for the quantum well thickness is 4nm, the conduction band offset is 4eV, $k_x = 0.5\text{nm}^{-1}$, $k_y = 0.1\text{nm}^{-1}$, $E_{\text{field}} = 0\text{MV/cm}$, $\varepsilon_{xy} = 0.92\%$

3.2. Scattering and relaxation matrix elements calculations

The surface roughness at the two interfaces is assumed to be equal and statistically independent. It is described by a mean and a correlation length (Fischetti, Ren, Solomon, Yang, and Rim 2003). Figure 8 and Figure 9 show the dependences on strain and electric field of the matrix elements for the intra-subband and inter-subband scattering. The intra-subband scattering matrix elements have two decreasing regions shown in Figure 8. These regions are in good agreement with the valley splitting minima in Figure 7. For higher fields the second decreasing region around the shear strain value of 0.9% vanishes. For the electric field of 0.5MV/cm the intra-subband matrix elements are sharply reduced only for the shear strain value of 0.116%. At the same time, the inter-subband matrix elements show a sharp increase around the shear strain value of 0.116%.

The electric field does not affect much the valley splitting provided by the zero value of the term $D\varepsilon_{xy} - \frac{\hbar^2 k_x k_y}{M}$, and the sharp increase in the inter-subband matrix elements is observed at higher fields.

At the same time the electric field washes out and a sharp minimum around the shear strain value of 0.9% in Figure 9 occurs. With the electric field increased the confinement pushes the carriers closer to the interface which results in both inter- and intra-subband scattering matrix elements increased.

Figure 10 and Figure 11 show the sum of the inter- and intra-subband spin relaxation matrix elements (normalized to the intravalley scattering at zero strain) on the angle between the incident and scattered wave vectors simultaneously with the valley splitting calculated for the scattered wave. As shown in Figure 10, for small strain the sharp increases of the

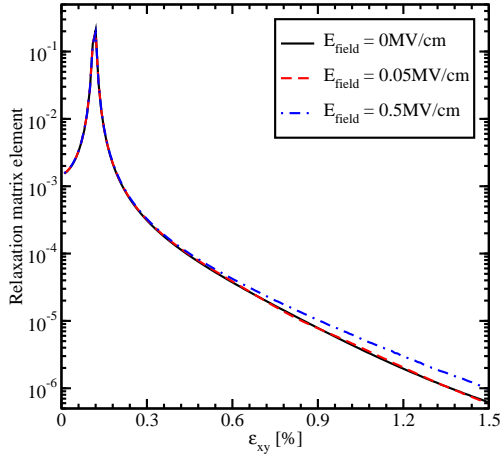


Figure 12: Spin relaxation matrix elements normalized to intravalley scattering at zero strain dependence on shear strain for several values of the electric field, $k_x = 0.5\text{nm}^{-1}$, $k_y = 0.1\text{nm}^{-1}$

relaxation matrix elements are correlated with the minima in the valley splitting, which occur for the values of the angle determined by zeroes of the $D\varepsilon_{xy} - \frac{\hbar^2 k'_x k'_y}{M}$ term. This is the condition of the formation of the so called spin hot spots characterized by spin mixing. In contrast to Figure 10, the valley splitting reduction due to the $\left| \sin \left(\sqrt{\frac{1-\gamma_n^2 - \eta^2}{1-\gamma_n^2}} k_0 t \right) \right|$ term shown in Figure 11 does not lead to sharp increases in the spin relaxation matrix elements on the angle between the incident and scattered waves.

The dependence of the spin relaxation matrix elements shear strain for several values of the electric field is shown in Figure 12.

The spin relaxation matrix elements increase until the strain value 0.116%, the point determined by the spin hot spot condition. Applying strain larger than 0.116% suppresses spin relaxation significantly, for all values of the electric field. In contrary to the scattering matrix elements (Figure 8 and Figure 9), the relaxation matrix elements demonstrate a sharp feature only for the shear strain value of 0.116% at zero electric field. Large electric field leads to an increase of the relaxation matrix elements due to the additional field-induced confinement resulting in higher values of the surface roughness induced spin relaxation matrix elements.

3.3. Overlap calculations

In the presence of strain and confinement the four-fold degeneracy of the n -th subband is partly lifted by forming an $n+$ and $n-$ subset (the valley splitting), however, the degeneracy of the eigenstates with the opposite spin projections $n \pm \uparrow$ and $n \pm \downarrow$ within each subset is preserved.

The degenerate states are chosen to satisfy

$$\langle \uparrow n \pm | f | n \pm \downarrow \rangle = 0, \quad (10)$$

with the operator f defined as

$$f = \cos \theta \sigma_z + \sin \theta (\cos \varphi \sigma_x + \sin \varphi \sigma_y), \quad (11)$$

where θ is the polar and φ is the azimuth angle defining the orientation of the injected spin. However, the expectation value of the operator f computed between the spin up and down wave functions from the different subsets is nonzero, when the effective magnetic field direction due to the spin-orbit interaction is different from the injected spin quantization axis:

$$\bar{f} = \langle \uparrow n \pm | f | \bar{\uparrow} n \downarrow \rangle \neq 0. \quad (12)$$

Figure 13, Figure 14, and Figure 15 show the dependence of \bar{f} on the orientation of the injected spin for $k_x = 0.1\text{nm}^{-1}$, $k_y = 0.1\text{nm}^{-1}$ for different values of shear strain. The absolute value of the overlap \bar{f} characterizes the strength of the spin up/down states mixing caused by the spin-orbit interaction. The spin mixing significantly decreases with shear strain increased in the whole range of spin orientations. This result explains the spin relaxation reduction with shear strain.

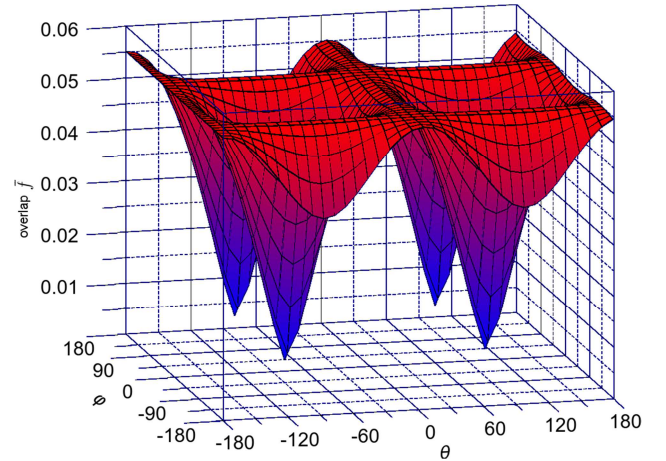


Figure 13: Dependence of the overlap of wave functions between two lowest conduction subbands on the spin injection direction for $k_x = 0.1\text{nm}^{-1}$, $k_y = 0.1\text{nm}^{-1}$, the shear strain value is 0%

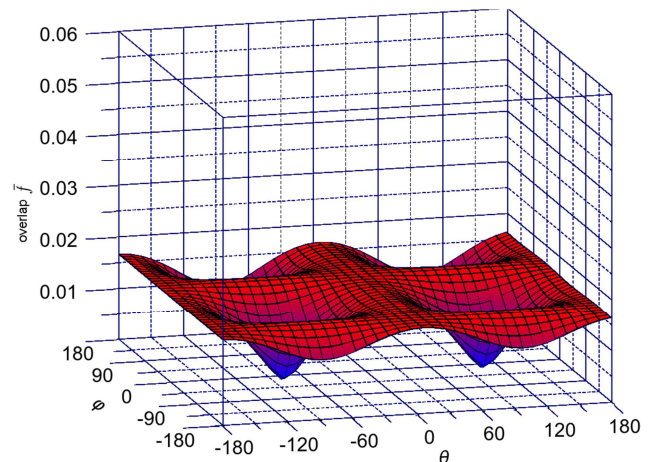


Figure 14: Dependence of the overlap of wave functions between two lowest conduction subbands on the spin injection direction for $k_x = 0.1\text{nm}^{-1}$, $k_y = 0.1\text{nm}^{-1}$, the shear strain value is 0.1%

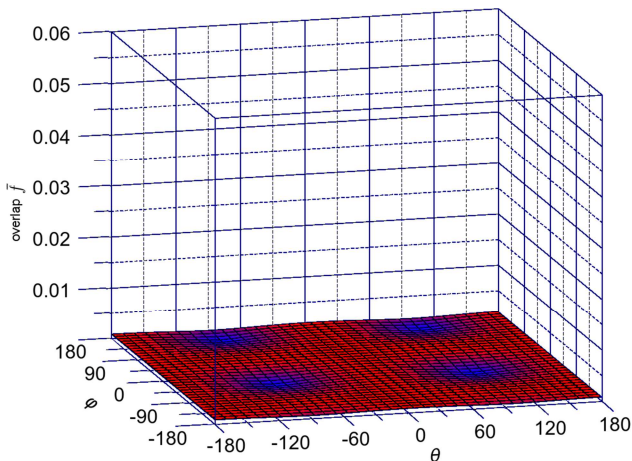


Figure 15: Dependence of the overlap of wave functions between two lowest conduction subbands on the spin injection direction for $k_x = 0.1\text{nm}^{-1}$, $k_y = 0.1\text{nm}^{-1}$, the shear strain value is 1%

4. CONCLUSION

We have investigated the lowest unprimed electron subband splitting in a thin film of a SOI-based silicon spin field-effect transistors in a wide range of parameters, including the conduction band offset at the interfaces, the width of the film, the effective electric field, and the shear strain value. We have included the spin-orbit interaction effects into the effective low-energy $\mathbf{k}\cdot\mathbf{p}$ Hamiltonian to investigate the valley splitting, scattering, and spin relaxation induced by the surface roughness. We have demonstrated that the valley splitting minima due to zero values of the sin-like term can be removed by the electric field, but the minimum due to a vanishing $D\varepsilon_{xy} - \frac{\hbar^2 k_x k_y}{M}$ term is preserved even for large electric fields. We have shown that, due to the inter-subband splitting increase, the matrix elements for spin relaxation decrease rapidly with shear strain. Thus, shear strain used to enhance electron mobility can also be used to boost spin lifetime.

ACKNOWLEDGMENT

This work is supported by the European Research Council through the grant #247056 MOSILSPIN

REFERENCES

- Bir, G.L., Pikus, G.E., 1974. *Symmetry and strain-induced effects in semiconductors*. New York/Toronto: J. Wiley & Sons.
- Cheng, J.L., Wu, M.W., Fabian, J., 2010. Theory of the spin relaxation of conduction electrons in silicon. *Physical Review Letter*, 104, 016601.
- Dash, S.P., Sharma, S., Patel, R.S., de Jong, M.P., Jansen, R., 2009. Electrical creation of spin polarization in silicon at room temperature. *Nature*, 462, 491–494.
- Fischetti, M.V., Ren, Z., Solomon, P.M., Yang, M., and Rim, K. 2003. Six-band $\mathbf{k}\cdot\mathbf{p}$ calculation of the hole mobility in silicon inversion layers: Dependence on surface orientation, strain, and silicon thickness. *Journal of Applied Physics*, 94, 1079.
- Friesen, M., Chutia, S., Tahan, C., Coppersmith, S.N. 2007. Valley splitting theory of SiGe/Si/SiGe quantum wells. *Physical Review B*, 75, 115318.
- Huang, B., Monsma, D.J., Appelbaum, I., 2007. Coherent spin transport through a 350 Micron thick silicon wafer. *Physical Review Letters*, 99, 177209.
- Li, C.H., Van't Erve, O.M.J., Jonker, B.T., 2011. Electrical injection and detection of spin accumulation in silicon at 500 K with magnetic metal/silicon dioxide contacts. *Nature Communications*, 2, 245.
- Li, J., Appelbaum, I., 2011. Modeling spin transport in electrostatically-gated lateral-channel silicon devices: Role of interfacial spin relaxation. *Physical Review B*, 84, 165318.
- Li, P., Dery, H., 2011. Spin-orbit symmetries of conduction electrons in silicon. *Physical Review Letters*, 107, 107203.
- Song, Y., Dery, H., 2012. Analysis of phonon-induced spin relaxation processes in silicon. *arXiv:1201.6660v1 [cond-mat.mtrl-sci]*. Available from: <http://arxiv.org/pdf/1201.6660v1> [April 2012].
- Sverdlov, V., 2011. *Strain-induced effects in advanced MOSFETs*. Wien - New York. Springer.
- Sverdlov, V., Baumgartner, O., Windbacher, T., and Selberherr, S. 2009. Modeling of modern MOSFETs with strain. *Journal of Computational Electronics*, 8, 3–4.

DETECTING THIN BONES AND MODELING COD SKELETON

T. Helgason^(a,b), R.A. Gudmundsdottir^(b), K.L. Valtysdottir^(c), K. Andersen^(c)

^(a)Research- and development department, Landspítali-University Hospital, Iceland

^(b)Biomedical Engineering Department, Reykjavik University, Iceland

^(c)Marel ehf, Gardabaer

^(a)thordur@landspitali.is

ABSTRACT

Fish bones in fillets can be serious problem both to the consumer and to the processing company. Filets with bones are likely to reduce the consumption especially in traditionally weak fish consumption areas. Fish bones can be dangerous leading to wounds in the human digestion tract. Fish, such as cod, have fine structured skeleton and the bone density is lower than that of man. Five cods were scanned with a normal hospital computer tomography (CT) scanner. Their skeletons were segmented out of the data set and a model reconstructed. The model is evaluated by visual inspection and compared to the cod to see what is missing from the skeleton. The density of the bones and otoliths is measured. The results show an almost complete skeleton with thin bones compared to the pixel size of image and with bones that are considerably lower in density than trabecular human bones.

Keywords: Modelling, Cod, Bone detection, Computer tomography

1. INTRODUCTION

Detection of cod bones is of interest in the food processing industry. At the moment bone detection is done by humans that visually look into the fish filet in front of an illuminated desk. The file lies on a transparent plastic plate with a light source underneath the plate. Light penetrates through the plastic and the fish filet and this way the observing human can detect bones or other obstacles inside the filet. If a bone is detected the part of the file is cut away. Disadvantage of this method is that it is not reliable, not every bone is detected. Another disadvantage is that humans are different in detecting the bones making varying outcome of the fish processing. Thirdly, as pointed out by Mery and collaborators 2011, every product needs to be fully reliable to ensure consumer safety but humans tend to get tired and that calls for redundant checks which in turn both slow down the processing time and increase costs. Slower processing time also reduces the quality of the fish.

These circumstances call for a reliable and cost effective way to detect bones in fish filets. Several

methods have been discussed in the literature. Many of them are discussed in Mery and collaborators 2011. Also some of us have worked on the issue, see Andersen 2003. Most of these works have in common that they process two dimensional images of the filet. Either light or X-ray images are used. Then several different image processing approaches are used to detect bones. Still, automatic detection of fish bones is extremely difficult, particularly regarding the smallest bones. Also Mery and collaborators 2011 come to this conclusion.

Accurate three dimensional (3D) information about the cod skeleton can help in the development of automated bone detection methods. Pre-information can help localizing where to expect bones. Filleting and other fish processing machines can build upon that. Using X-ray computer tomography imaging (CT) the cod skeleton can be reconstructed in three dimensions to a certain degree. Some bones might be missing from the images due to extremely small thickness or their low density, i.e. low X-ray attenuation.

In this work a common medical computer tomography is evaluated for detecting bones in fish. A 3D model is made of the cod's skeleton and inspected upon missing bones or bones reduced in size. The hypothesis is that thin bones and of low density might be missing or not modelled in full size. Results are promising for further research in this application.

2. MATERIAL AND METHODS

Two cods were scanned in a normal hospital CT scanner. They were scanned in one scan, meaning that the scanning parameters are the same for both cods. The CT data was then processed to segment the cod's skeleton from the rest of the tissue.

2.1. Material

The two cods are 63 cm and 62 cm long respectively. They were caught at the coast of Iceland and time from catch to scan is counted in hours but not exactly known. They had been processed in a normal way, the fish was gilled, the trunk cut open and the interstitials taken away. They had been kept cold with ice from the moment of catch to scan but not frozen. No salt was

used. They are very similar in size, one is though a little bit longer and with bigger circumference.

2.2. CT scan

The CT scanner used is a Philips Brilliance 64 designed for human clinical use. The lowest available X-ray tube voltage of 80 KV was used corresponding to soft tissue examination. A spiral CT was made with slice thickness of 0.67 mm, a distance of 0.33mm from centre of one slice to the centre of the next slice, i.e. in the z direction along the scan axis. This means that the slices are redundant; each slice covers half of the same volume as the next slice before covers. So there is a 50% redundancy. To cover the total length of the cods body, 63cm and 62 cm respectively, 1909 slices were needed. The image matrix of each slice has 512 x 512 pixels covering an area (field of view) of 344 mm both in x and y direction. So the size of each voxel is 0.672 x 0.672 x 0.670 mm. The total amount of data for both cods is therefore 512 x 512 x 1909 that is in total 500 Mega voxels. Each voxel is digitized with 12 bit or 1,5 byte so the total amount of data is 1,5 x 500 giving 750 Mbyte of data for the whole scan of the two cods. The data set of the cod's contains three dimensional information of tissue density, and therefore also of the skeleton, of the whole cod. Since each tissue type has a different density the different tissues can be analyzed with this data, so the skeleton and bones can be differentiated from the tissue.

2.3. Bone segmentation

Specialized software (Mimics) designed for analysis of human CT images is used for analysis of the cod's tissue. Each CT slice is a two dimensional (2D) image of a cross-section though the cods body. Each 2D image is composed of picture elements, in short pixels, and is referred to as voxels, volume elements, in a 3D image. Each of them is characterized by its Hounsfield value, HU. The staple of these cross-section images along the longitudinal axis of the cod make up the 3D description of its whole body. By sorting out the voxels having their HU values in certain interval special tissue type can be separated from the rest of the body, i.e. segmented. The group of voxels segmented makes out a geometrical model of the corresponding tissue.

The X-ray attenuation property is specific for each tissue type. The following formula describes the attenuation of an X-ray passing through a material of length x:

$$I = I_0 e^{-\mu x} \quad (1)$$

where I_0 is the intensity of the incoming X-ray and I the intensity of the X-ray after being attenuated in the material it was passing. μ is called attenuation coefficient and is a property of the material. Hounsfield units (HU) are calculated from the formula:

$$HU = 1000 \cdot \frac{\mu_{\text{voxel}} - \mu_{\text{water}}}{\mu_{\text{water}}} \quad (2)$$

This way each voxel in the 3D data set gets its specific HU value characterising the X-ray attenuation properties of the material in that specific point of space. This value is relative to water. The HU for water is zero. Tissue that has higher density and therefore attenuates X-rays more than water have positive HU. This is the case f.ex. for muscles and bone. Tissue that has lower density and therefore attenuates X-rays less than water have negative HU. This is the case f.ex. for fat and lungs in human. Now the process of segmentation can be described by the following somewhat simplified steps:

1. First a so called mask is created by using thresholds. It is composed by all the voxels that have HU value in a defined interval. We use HU in the interval from 226 up to 3071
2. Next a function called region growing is used. By starting at a voxel within the skeleton it finds all voxels that are connected to the starting voxel. This is done for all disconnected parts of the skeleton.
3. Step three is done manually. Voxels which were left out are added manually to the mask. It is also possible to perform this step after step four.
4. The fourth step is so called erode region growing. There can be voxels included in the model that do not belong to the anatomical structure of interest. To eliminate these they are separated from the model with at least one voxel layer and erased. Then normal region growing is performed again and a new mask is created.
5. The fifth step is to do dilate region growing if too many voxels have been erased from the structure. This gives a desired structure of the fish.
6. Step six is used when certain regions of interest are analyzed. The model is then divided into smaller parts by the help of Boolean operations.

In this work the result of the segmentation process described above is a 3D model of the cod skeleton including the fins and the otoliths. After segmentation the tissue analysis is made on the basis of Hounsfield (HU) values and pixel distribution. Volume, density, distribution can be measured and evaluated.

Further description of our segmentation methods and tissue analysis methods can be found in Helgason 2011, Gargiulo 2012 and Johannesdottir 2006.

2.4. Tissue analysis and evaluation

Bone density measurements were done for the following parts of the skeleton: all bones, tail, head, body without head, operculum bone, mid section and the otoliths. For this the skeleton model was divided into these parts and a special mask made for each. In that form the HU values of the voxels belonging to each part can be processed and used in calculations. The average bone density in each part was calculated according to the following equation:

$$\overline{HU} = \frac{1}{n} \sum_{i=1}^n HU_i \quad (3)$$

Where n is the number of voxels inside the corresponding part of the cods skeleton, that is belonging to a model of that part. Many of the fish bones are considerably thinner than the dimensions of the voxels which are 0,672 x 0,672 x 0,67 mm. This means that beside the bone itself other tissue types influence the HU value for the particular voxel. Mostly that is soft tissue that lowers the HU value. And since all voxels that have lower HU than 226 are excluded from the skeleton model it is to be expected that particularly thin bones are not a part of the skeleton model. This can be the case even though the thin bone has high density. This leads to the assumption that the average HU numbers calculated according to equation 3 from the voxels in the different parts of the skeleton are not necessarily accurate. They can be both higher and lower.

The cod skeleton model is inspected visually on the computer screen and compared to a normal cod skeleton. Missing elements are registered. These can be whole bones or a part of a bone. Another effect is that bones of sub-voxel size lying close together are seen as one plane and not as individual bones. This is the result of the limited resolution of the CT device.

3. RESULTS

The results are shown in table 1 and in figures 1- 5. Table 1 gives an overview of average bone density in several parts of the cod's skeleton. Figure 1 and 2 show the skeleton of the cod's head. Figure 3 gives the model of the whole skeleton of both cod's. This shows in particular the possibilities to find single bones. Figure 4 shows the operculum bones and figure 5 the otoliths.

3.1. Cod bone density

Table 1 gives an overview of density in some parts of the cod's skeleton. The values are calculated with equation 3 for the whole skeleton and six different parts of the skeleton. The two examples of cod show no substantial difference in bone density. Though cod 2 has higher values in all parts except in the operculum bone. The tail bones have the lowest density. The mid

section, where the most valuable parts of the fish are, has a HU of 750 as does the head. Interesting is the considerable higher density of the otoliths, which brings up a question about the purpose of this.

The bone density values from all skeleton parts show that they are good X-ray attenuators and hence suggest that X-rays are suitable for their detection and CT devices are applicable for that purpose.

Table 1: Average density values of cod bones at various locations in the skeleton. There is no considerable difference between the two cod's.

	Cod 1	Cod 2
All bones	769.0 HU	787.2 HU
Tail	511.7 HU	554.6 HU
Head	750.5 HU	771.9 HU
Body (no head)	721.5 HU	737.5 HU
Operculum bone (Fig. 4)	901.4 HU	879.3 HU
Mid section	752.2 HU	754.3 HU
Otolith (Fig. 5)	2928.9 HU	2935.0 HU

3.2. Bone model

Figure 1 and figure 2 display the same model of the cods head. Figure 1 shows the head model from the right side and figure 2 shows the same head model from the front. As can be seen these figures the skeleton of the cod head is almost complete. Some missing elements are very thin or of low density. At other places bones even of sub-voxel dimensions are detected as such but are displayed at the least as a whole voxel giving the flash perception of a thicker or more massive bone. This is only of concern for small structures.

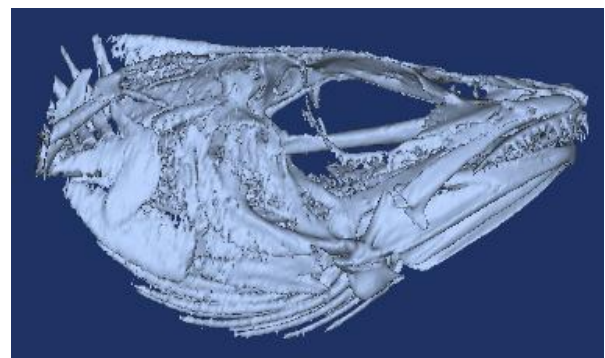


Figure 1: Cod head skeleton model seen from the right side. The model is reconstructed from CT data. Some structures have dimensions smaller than the voxel size and are not imaged in full extent.

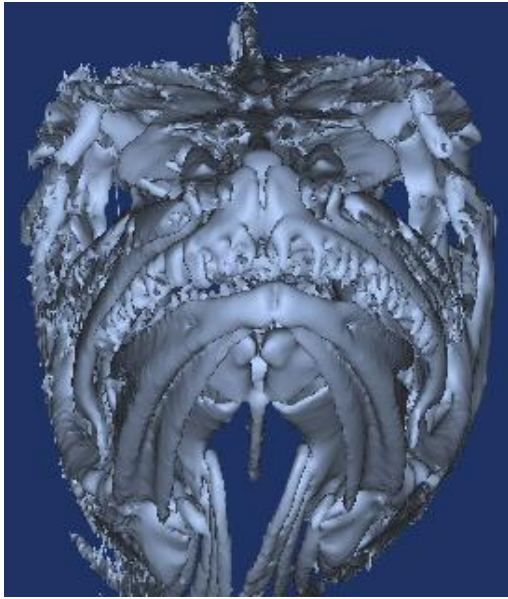


Figure 2: The same model as in figure 1 but rotated 90 degrees, that is the cods head skeleton seen from the front.

Figure 3 shows the two skeleton models, one from each cod. Let us recall that the models are made from 1909 CT slices, each 0,67 mm thick and 0,33mm apart. That results in a clear model displaying also thin bones in diameter smaller than the voxels. But it also clearly displays the drawbacks of the applied CT scanner. From investigating figure 3 following observations can be made:

- Bones that are in diameter smaller than the voxels are, in some cases, still imaged as bones, are therefore part of the model
- Bones with higher density than the lower threshold of 226 HU are not in the model if they have small diameter and contribute not enough to the voxel to raise its HU value

above the threshold. Especially bones that have a smaller diameter distally are shown shorter than they are in reality since the density values for the distal voxels are beneath the lower threshold. This can be seen in the tail and in the side fins in figure 3.

- Thin bones that lie close to each other are modelled as one piece or one plane. This can be seen in the tail and very clearly in the side fins in figure 3. In the side fins the bones are arranged as rays from a light source. The distance between the increases going from proximal to distal. Proximal they are modelled as one piece but distal they are modelled as separated bones. In between there is an area where they are in one piece but the formation of bones can be seen.
- Comparing the models of the two tails of the cod's in figure 3 it can be observed that the lower part of the lower cod has bones that are modelled as single bones all the way up to the spine. As a contrast to that in the upper part of the same tail the bones fusion in one solid body. That is also the case in the tail of the upper cod.

The results show a complete model of the two cod skeletons. Missing parts, as described above, give a somewhat false perception of the anatomy of the skeleton. Some bones in the model are too short and some are too thick and still others have fusion in one piece. This does not disturb the human eye so much since it can build on previous experience on how skeletons like this are built. But it is a problem for automated vision.

Figure 4 shows models of the operculum bone in the two cod's. This is the bone with the highest density in the cod's body.

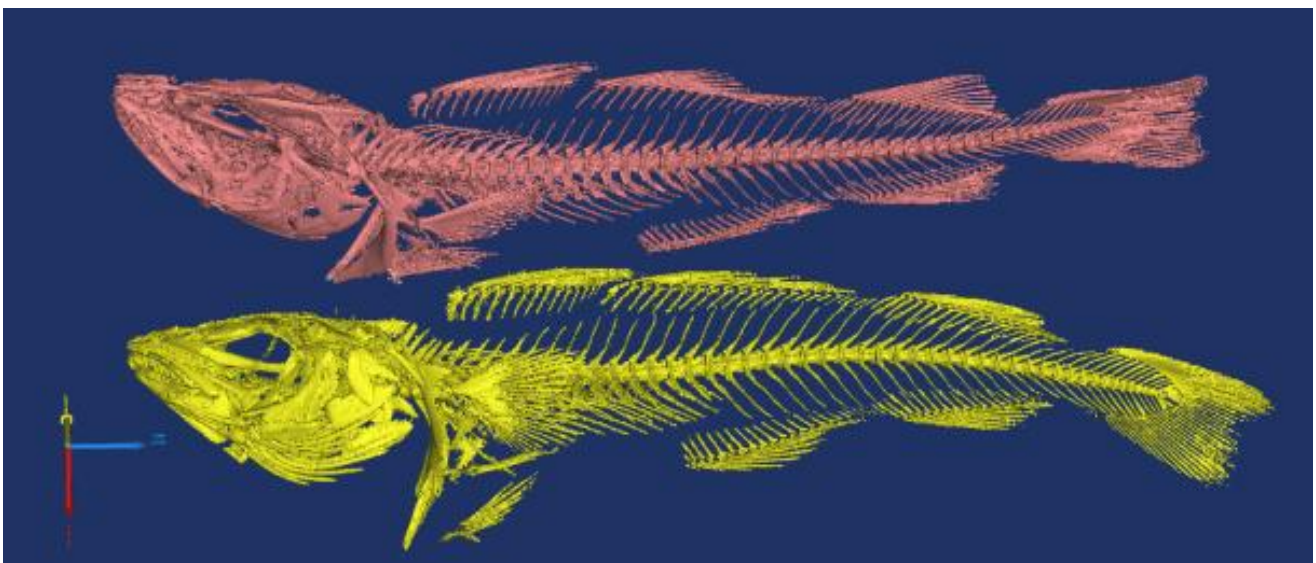


Figure 3: Two cod skeletons. The models are a result from 1909 CT slices 0,67 mm thick and 0,33 mm apart. The whole skeleton can be seen, although some bones are not in their full length, others appear more voluminous than they are in reality and some are not distinguishable from each other and form a solid body



Figure 4: Operculum bone model from the two cod's under inspection in this work. They are the most dense bones in the fish, meaning that they have the highest HU values on average.

3.3. Otoliths

The otoliths models are shown in figure 5. The otoliths give important information on the cod and can be analyzed to some extent in these images. They are the objects in the cod's body with the highest density and are considerably denser with more than 2900 HU where as the next one, the operculum bone, has 900 HU.

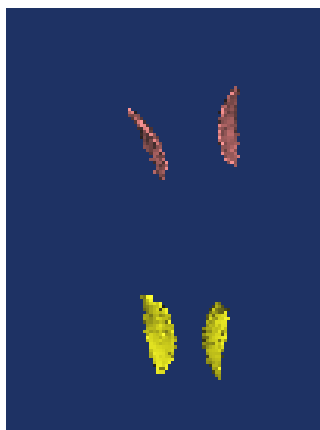


Figure 5: Shows the otoliths, i.e. most dense part of the cod placed inside the cod head.

DISCUSSION AND CONCLUSION

Detection of thin bones of low density can be done and they can be modelled in a cod skeleton. This information can be of use in detecting single thin bones. However if the bones are tight together they are not detected as single bones but rather like a merged single piece or plane. Reconstructing the fish skeleton from CT data can be done to a certain degree. Missing parts due to small thickness or low density, could in a normal case, be predicted using anatomical knowledge of the species being investigated. Another way to increase the accuracy of the cod's skeleton model would be to use a CT device with higher spatial resolution. At the same

time the field of view can easily be smaller. These two goals go together well. They can be reached simply by diminishing the diameter of the gantry's aperture having the scanned object further away from the CT sensors and nearer to the X-ray tube. This gives enlarged projections of the subject onto the sensors.

Automated processing of fish requires exact and reliable work but at the same time devices that are not too expensive and with low running cost. Medical CT devices have in recent years become considerably more cost effective. This is also the case for micro CT devices for research purposes. This gives the hope that CT technology can be made cost effective for food processing. Further research is, however, necessary to pinpoint the requirements of a CT for fish processing.

ACKNOWLEDGMENTS

This work has been supported in part by the Icelandic RANNIS Technology Development Fund.

REFERENCES

- Andersen, K, 2003. X-ray techniques for quality assessment. In: Luten, J.B., Oehlenschläger, J., Olafsdottir, G, eds. *Quality of Fish from Catch to Consumers*. Wageningen Academic Publishers, 283-286.
- Gargiulo, P, Carraro, U, Mandl, T, Kern, H, Zampieri, S, Mayr, W, Helgason, T, 2012. Anthropometry of Human Muscle Using Segmentation Techniques and 3D Modelling: Applications to Lower Motor Neuron Denervated Muscle in Spinal Cord Injury. In: Preedy, V.R., ed. *Handbook of Anthropometry. Physical Measures of Human Form in Health and Disease*. US:Springer, 323-354
- Helgason, T, Gargiulo, P, Knútsdóttir, S, Gudmundsdottir, V, Kern, H, Carraro, U, Ingvarsson, P, Yngvason, S, 2011. "Monitoring Muscle Growth and Tissue Changes Induced by Electrical Stimulation of Denervated Degenerated Muscles with CT and Stereolithographic 3D Modelling." In: Narayan, R, Calvert, P, eds. *Computer Aided Biomanufacturing*. Weinheim Germany, Wiley-VCH, 130-146
- Johannesdottir, F, 2006. *Bone: use it or lose it*. MS thesis. University of Iceland
- Mery, D, Lillo, I, Loebel, H, Riffo, V, Soto, A, Cipriano, A, Miguel, J, Aguilera, M, 2011. Automated fish bone detection using X-ray imaging. *Journal of Food Engineering*. 105 (2011): 485-492

AUTHORS BIOGRAPHY

Thordur Helgason made his BS degree in electrical engineering from University of Iceland in 1982, a Dipl.-Ing. degree in Biomedical engineering from University of Karlsruhe in W-Germany 1985 and a Dr.-Ing. Degree from the same school 1990. Since then Helgason has been working in Landspítali the University hospital in Iceland in the field of medical engineering. Dr Helgason has been teaching in the faculty of medicine and faculty of engineering at the University of Iceland. Since 2005 he is a lecturer at the University of Reykjavík and is currently an associate professor at that university. Research interests of Dr. Helgason are in the field of Neural engineering, rehabilitation and modelling. Dr. Helgason is the president of the Icelandic Society of Medical Engineering and Medical Physics.

Rannveig Ása Guðmundsdóttir made her BS in Biomedical engineering in University of Reykjavík 2011. Rannveig Ása worked at Landspítali-University Hospital Department for Research and development 2011 to 2012. Her work was on modelling muscles of a spinal cord injured patients and on modelling of fish bone. She is currently a MS student at Chalmers University of Technology in Gothenburg, Sweden.

Kristín Líf Valtýsdóttir finished her B.Sc. degree in industrial engineering in 2009, and M.Sc. in mechanical engineering in 2011, both from University of Iceland. The main focus of her M.Sc. work was on cooling and processing techniques in the fish industry. She received a scholarship for the master's thesis and worked as well as a research scientist at Matis – Icelandic Food and Biotech R&D. Since early 2012 she has been working as a project manager at the fish industry centre at Marel, a developer of food processing equipment and systems.

Kristinn Andersen received his B.S. degree in electrical engineering from University of Iceland in 1982. He carried out research work at Vanderbilt University, USA, worked on research projects with NASA on arc welding and robotics, and received his Ph.D. degree from Vanderbilt University in 1993. Dr. Andersen has since been with Marel, a developer of food processing equipment and systems. His work includes the development of computer vision technology for on-line inspection, weighing technology and he initiated and supervised the company's development of X-ray technology for product inspection. Presently he is a senior RTD manager at Marel, responsible for collaborative projects on new technologies.

ANALYSIS OF AGENTS' BEHAVIOR IN MULTIAGENT SYSTEM

Kateřina Slaninová^(a), Jan Martinovič^(a), Pavla Dráždilová^(a), Dominik Vymětal^(b), Roman Šperka^(b)

^(a)VSB - Technical University of Ostrava
Faculty of Electrical Engineering and Computer Science
Czech Republic

^(b)Silesian University in Opava
School of Business Administration in Karviná
Czech Republic

^(a)katerina.slavinova@vsb.cz, jan.martinovic@vsb.cz, pavla.drazdilova@vsb.cz,
^(b)vymetal@opf.slu.cz, sperka@opf.slu.cz

ABSTRACT

Multi-agent systems are commonly used for simulation purposes. The authors focused on agent-based technology in the business process simulation, especially on the analysis of the agent-based simulation outputs in order to facilitate the verification of the used methodology. The paper deals with an analysis of agents' behavior in multi-agent model of business processes. The main goal of the paper is to find, how selected methods can influence finding of behavioral patterns of selected agents in the system and how the amount of extracted sequences can be reduced. Extraction of behavioral patterns was performed by process mining and pattern mining methods with the focus on the sequences. The authors present the comparison of selected methods for the definition of agents' behavior with the focus to selected characteristics of observed methods. Behavioral patterns and relations between them create complex networks; thus, the extraction of behavioral patterns is optimized by spectral graph partitioning. Moreover, the visualization of groups of agents with similar behavior is presented.

Keywords: system modeling, multi-agent systems, behavioral patterns, process mining

1. INTRODUCTION

The overall idea of proposed methodology is to simulate real business processes and to provide predictive results concerning the management impact. This should lead to improved and effective business process realization. The paper deals with the analysis and visualization of agents' behavior to facilitate the verification of the simulation model and to effectively observe the reaction of the model in relation to the initialization of its input attributes, or in relation to the influence of the model environment.

The presented approach deals with a lot of influences that are not able to be captured by using any business process model (e.g. the effects of the

collaboration of business process participants or their communication, experience level, cultural or social factors). The statistical method has only limited capabilities of visual presentation while running the simulation. Finally, an observer does not actually see the participants of business process dealing with each other.

Agent-based simulations dealing with a company simulation can bring several crucial advantages (De Snoo 2005), (Jennings et al. 2000). They can overcome some of the problems identified above. It is possible to involve unpredictable disturbance of the environment into the simulation with the agents. All of the mentioned issues are the characteristics of a multi-agent system (MAS).

This paper is structured as follows. Section 2 briefly informs about the multi-agent framework developed. Section 3 contains the description of the proposed method used for the analysis of the agents' behavior in the multi-agent system, and finally, the experiments with real data collection from multi-agent system are presented in Section 4.

2. AGENT-BASED SIMULATION MODELING

The authors deal with the agent-based simulation model, which is described in (Macal and North 2005), with the focus to Business Process Management (BPM) (Yan et al. 2001). Usual business process simulation approaches are based on the statistical calculation, as can be seen for example in (Scheer and Nuttgen 2000, Islamov and Rolkov 2010). But only several problems can be identified while using the statistical methods. The model uses the advantages of the agent technology (communication, cooperation, social behavior), to describe some of the core business processes of a typical business company. The authors developed a business process simulation framework (Vymetal et al. 2012) in order to simulate the real behavior of the company on the market. JADE (Bellifermine 2010) platform was used for the implementation, which

provides running and simulation environment allowing for the distribution with thousands of software agents.

The core of this paper is the analysis of agent-based simulation outputs. To ensure the outputs, above mentioned framework was used to trigger simulation experiments. The simulation framework covers business processes supporting the selling of goods by company sales representatives to the customers. It consists of the following types of agents: sales representative agents (representing sellers), customer agents, an informative agent (provides information about company market share, and company volume), and manager agent (manages the communication between seller and customer). All the agent types are developed according to the multi-agent approach. The interaction between agents is based on the FIPA contract-net protocol; see Figure 1 (FIPA 2002).

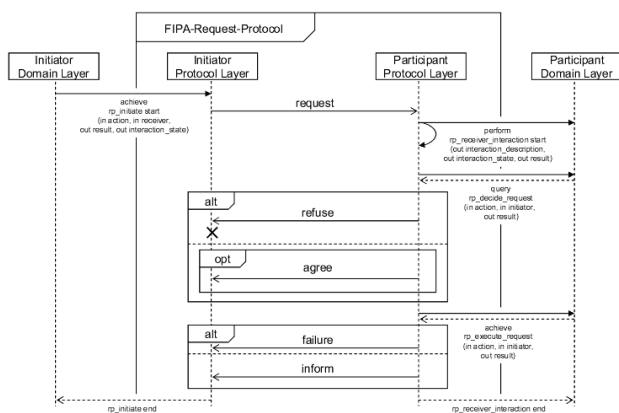


Figure 1: FIPA Contract-Net Protocol

The number of customer agents is significantly higher than the number of sales representative agents in the model because the reality on the market is the same. The behavior of agents is influenced by two randomly generated parameters using the normal distribution (amount of requested goods and a sellers' ability to sell the goods). In the lack of real information about the business company, there is possibility to randomly generate different parameters (e.g. company market share for the product, market volume for the product in local currency, or quality parameter of the seller). The influence of randomly generated parameters on the simulation outputs while using different types of distributions was presented in (Vymetal et al. 2012). The simulation uses random values instead of real data.

The overall workflow of the system proposed can be described as follows (see Figure 2).

The customer agents randomly generate the requests to buy some random pieces of goods. The sales representative agents react to these requests according to their own internal decision functions and follow the contracting with the customers. A production function is used to define the value of the negotiated price. The purpose of the manager agent is to manage the requests exchange. The contracting results into the sales events. More indicators of sale success like revenue, amount of sold goods, incomes, and costs are analyzed as well.

Each action running in the simulation framework was recorded in the log file. The log file serves as a dataset for further analysis described in Section 4.

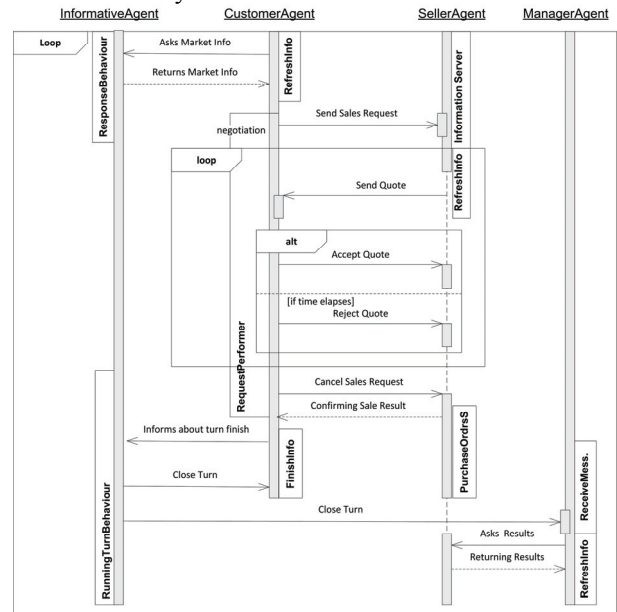


Figure 2: Workflow of Proposed System

3. ANALYSIS OF AGENTS' BEHAVIOR

The verification of the business process model is based on the analysis of recorded outputs. The approach described in this paper is focused on the analysis of agents' behavior in the model, which is recorded in a log. The log is a simple text file, where each row represents one event. The main structure, which is valid for all agents, consists of TimeStamp (date and time when the event was performed), AgentID (each agent has its unique ID), AgentClassName, TypeOfAction, ActionAttribute.

Definition of the agent behavior was performed using the methods of process mining (Aalst 2011; Aalst et al. 2004). Then, the agents' behavior in the model can be described by a set of event sequences. The paper is oriented to comparison of methods used for finding behavioral patterns of the agents and to their description on the basis of similarity of extracted sequences.

Behavioral patterns were extracted by the methods used for the sequence comparison; their description was provided using methods of text processing. Two basic groups of algorithms for the comparison of two or more categorical sequences are generally known. The first group divides the algorithms by the fact, whether the sequences consist of ordered or unordered elements. The second group of algorithms focuses on the comparison of the sequences with the different lengths and with the possible error or distortion.

The agent behavior in the business process simulation can be described by a set of event sequences. A *sequence* is an ordered list of elements (in this approach events), denoted $s = (e_1, e_2, \dots, e_m)$. Given two sequences $s = (e_1, e_2, \dots, e_m)$ and $u = (f_1, f_2, \dots, f_l)$. Sequence s is called a subsequence of u , denoted as

$s \subseteq u$, if there exist integers $1 \leq j_1 < j_2 < \dots < j_m \leq l$ such that $e_1 = f_{j_1}, e_2 = f_{j_2}, \dots, e_m = f_{j_m}$. Sequence u is than a super sequence of s .

3.1. Comparison of Sequences

For easier description of the agents' behavior, behavioral patterns were extracted with the focus to the similarity between the sequences.

The basic approach to the comparison of two sequences, where the order of elements is important, is The longest common substring (LCS) method (Gusfield 1997), see example in Table 1. As obvious from the name of the method, the main principle of the method is to find the length of the common longest substring. Given the two sequences $s = (e_1, e_2, \dots, e_m)$ and $u = (f_1, f_2, \dots, f_l)$, we can find such subsequence $v = (g_1, g_2, \dots, g_p)$, where $g_k = e_{(i+k-1)} = f_{(j+k-1)}$ for all $k = 1, \dots, p$ and $p \leq m, l$.

The LCS method respects the order of elements in the sequence. However, the main disadvantage of this method is that it can find only the identical subsequences, where no extra element is presented in the sequence. For some domains, typically where a large amount of different sequences exists, this fact gives too strict limitation. As a solution of this problem can be considered The longest common subsequence method (LCSS), described for example in (Hirschberg 1977), see example in Table 1. Contrary to LCS method, this LCSS method allows (or ignores) the inserted extra elements in the sequence, and therefore, it is immune to slight distortions.

	1.	2.	3.
Sequence s	EABCF	EAEBCE	ABBCC
Sequence u	ZABCT	FABCF	EABCE
LCS	ABC	BC	AB
LCSS	ABC	ABC	ABC
T-WLCS	ABC	ABC	ABBCC

Table 1: Results of Algorithms for Subsequence Detection

Whether the similarity of compared sequences is defined as a function using a length of common subsequence, one characteristic of this method can be found. The length of the common subsequence is not immune to the recurrence of the identical elements, which can occur only in one of the compared sequences. We can find such situations, for example due to inappropriate sampling or due to any kind of distortion.

In some applications, it is suitable (or sometimes even required) to eliminate such type of distortions and to work with them like with the equivalent elements. The solution is in another method, The time-warped longest common subsequence (T-WLCS) (Guo, A. and Siegelmann, H. 2004), see example in Table 1. The method combines the advantages of LCSS method with dynamic time warping (Müller, M. 2007). Dynamic time warping is used for finding the optimal

visualization of elements in two sequences to match them as much as possible. This method is immune to minor distortions and to time non-linearity. It is able to compare sequences, which are for standard metrics evidently not comparable.

The method emphasizes recurrence of elements in one of the compared sequences. Due to this fact, the length of the common subsequence can be longer than the shorter length of the compared sequences. In the experiments described in the paper, the authors compare the impact of LCS, LCSS and T-WLCS methods to finding the behavioral patterns and to construct the agents' profiles based on their behavior in multi-agent system.

3.2. From Log to Agents' Network

As the first step of the approach, a set of agent profiles was generated. In the agent profile, each agent has assigned its set of sequences performed by it. The sequences were extracted using similar principle as extraction of traces in business process analysis (Aalst 2011). However, in our approach, the trace is defined in relation to one agent, not to one case. Given a set of agents $A = \{A_1, A_2, \dots, A_n\}$, where each agent is described by its set of sequences representing the agents' behavior during the business process simulation in the MAS. Thus, we have for all A_i a set $S_i = \{s_{1i}, s_{2i}, \dots, s_{mi}\}$. Set of all possible sequences, which can occur in the log is given by $S = \cup S_i$ for all $i = 1, 2, \dots, n$.

Afterwards, finding the behavior patterns of agents was performed. Since obtained sequences are often similar with inconsiderable differences, the next three steps of proposed approach are oriented to finding behavioral patterns, which can better describe the agents' behavior during the simulation. Finding of behavioral patterns is based on a weight of the sequence relation. In the paper the results for three methods: LCS, LCSS, and T-WLCS are compared.

A weighted graph $G = (V, E, W)$ describing relations between the sequences was constructed, where the nodes represent sequences ($V = S$) and edges are evaluated by the weight of the relation between two sequences (depending on the selected method), and which is higher than selected threshold ($w_{ij} > \theta$).

The obtained graph is then divided into clusters with the similar sequences using spectral clustering, improved by our proposed Left-Right Oscillate algorithm. For more details, see our previous work (Martinovic et al. 2012). Thus, set of sequences S is divided into clusters C_j , where $S = \cup C_j$ and $j = 1, \dots, c$, which is count of the clusters.

Afterwards, selected clusters are described by its representatives, called behavioral patterns. The main principle is that each representative is the most similar to the other sequences in the cluster. Finding a representative sequence of a cluster C_j is based on

finding a sequence with the maximal sum of relation weights (depending to the selected method) to the other sequences s_k within the cluster C_j .

For each agent A_j its own reduced profile P_j is then created, which determines the agent using behavioral patterns. The reduced agent profile is a binary vector of a dimension c (count of clusters), which gives information about characteristic behavioral patterns of the given agent.

A weighted graph describing the relations between agents was generated at the last step. The nodes of the graph represent the agents identified by its unique ID, vertices represent the relations between the agents. The relation between agents was defined by the similarity of their behavior using cosine measure.

4. EXPERIMENTS ON SIMULATION MODEL

In the experiments, the log file generated by MAS for the simulation of one year with 52 turns (one turn is equivalent to one week) was used. The log file contained 557760 records of agents' activities. Four types of agents: ManagerAgent, InformativeAgent, CustomerAgent and SellerAgent were defined in the simulation model. The basic description of the log file is presented in Table 2.

Agent Class	Records	AgentInstances
ManagerAgent	54	1
InformativeAgent	107	1
CustomerAgent	406 482	498
SellerAgent	151 098	51
Sum	557 760	552

Table 2: Log File Description

4.1. Sequence Extraction

The records from the log file were used for the extraction of sequences. As mentioned in Section 3.2, the methodology of Aalst was used, modified to our approach based on the multi-agent system requirements. During the extraction, each sequence was related to one agent; its start and end points were detected by the start and the end of one turn. For described data collection, we have obtained set S consisted of 1974 sequences, and 24 types of different sequences used in the simulation. We assume more diverse output in future experiments, due to planned simulations with more variable initialization of input parameters of agents.

4.2. Finding of Behavioral Patterns

This phase of the experiments was oriented to an exploration, how the different methods for measurement of relation weight between two sequences can influence the finding of the behavioral patterns. The following methods have been tested: LCS, LCSS and T-WLCS. All the methods can find the longest common subsequence α of compared sequences β_x and β_y , where $\alpha \subseteq \beta_x \wedge \alpha \subseteq \beta_y$, where $\beta_x \in S$ and $\beta_y \in S$.

For description of used methods, see Section 2. The relation weight R_w was counted by Equation 2.

$$R_w(\beta_x, \beta_y) = \frac{(l(\alpha) * h)^2}{l(\beta_x) * l(\beta_y)}, \quad (1)$$

where $l(\alpha)$ is a length of the longest common subsequence α for sequences β_x and β_y ; $l(\beta_x)$ and $l(\beta_y)$ are analogically lengths of the compared sequences β_x and β_y , and

$$h = \frac{\text{Min}(l(\beta_x), l(\beta_y))}{\text{Max}(l(\beta_x), l(\beta_y))} \quad (2)$$

Table 3, Table 4 and Table 5 describe obtained components with similar sequences for each method and for different threshold θ (level of relation weight R_w).

θ	Components (Size)	Isolated Nodes
0.9	1 (2)	22
0.8	2 (2,2)	20
0.7	3 (2,2,2)	18
0.6	4 (2,2,2,2)	16
0.5	4 (4,4,2,2)	12
0.4	5 (6,6,2,2,2)	6
0.3	3 (11,7,2)	4
0.2	3 (11,8,2)	3
0.1	3 (11,8,2)	3

Table 3: Components of Sequences, LCS

θ	Components (Size)	Isolated Nodes
0.9	1 (2)	22
0.8	2 (2,2)	20
0.7	3 (4,2,2)	16
0.6	4 (5,2,2,2)	13
0.5	3 (9,4,2)	9
0.4	4 (9,6,2,2)	5
0.3	3 (11,7,2)	4
0.2	3 (11,8,2)	3
0.1	3 (11,8,2)	3

Table 4: Components of Sequences, LCSS

θ	Components (Size)	Isolated Nodes
0.9	2 (7,2)	15
0.8	3 (7,3,2)	12
0.7	3 (8,7,2)	7
0.6	3 (9,8,2)	5
0.5	2 (11,8)	5
0.4	3 (11,8,2)	3
0.3	3 (11,8,2)	3
0.2	3 (11,8,2)	3
0.1	3 (11,8,2)	3

Table 5: Components of Sequences, T-WLCS

As we can see from Table 3 and Table 4, we have obtained for level $\theta=0.2$ the same 3 components of similar sequences for both methods LCS and LCSS, while for method T-WLCS the same 3 components have

agent system have the appropriate behavior like has been programmed.

The agents' behavior was described using the behavioral patterns, obtained via sequential pattern mining methods and methods for the determination of relations between the sequences. Concretely, LCS, LCSS, and T-WLCS methods were compared in the experiments to discover, how the selected method can influence the finding of the agents with the similar behavior.

The detailed description of the outputs obtained using each method was presented in Section 4.2. From the obtained outputs we can see, that each method has its specific approach to the determination of the relations between the sequences. Due to this fact we can say, that each method can be used for different type of data collection. Moreover, the selection of the method depends on what process with selected behavioral patterns we intend to do.

In the cases, where we need more detailed division of sequence clusters to find more accurate behavioral patterns like in this data collection from the multi-agent system, LCS method is the most suitable. In other cases, where we have large data collections with various types of sequences (typical domains are analysis of users' behavior on the web, or analysis of business processes), method T-WLCS is better to use. This method is immune to minor distortions and to time non-linearity, and emphasizes the recurrence of the elements in one of the compared sequences. Finally, LCSS method generates the outputs more similar to LCS method, but more compact.

Visualized groups of agents with similar behavior during the simulation, extracted using LCS method is presented in Figure 5

As presented in the described experiments, LCS method is the most suitable for the presented data collection. However, we assume more diverse output in future experiments with proposed simulation model, due to planned simulations with more variable initialization of input parameters of agents. Therefore, T-WLCS or LCSS method will be more suitable in the future experiments with MAS.

ACKNOWLEDGMENT

This work was supported by SGS, VSB – Technical University of Ostrava, Czech Republic, under the grant No. SP2012/151 Large graph analysis and processing.

REFERENCES

- Aalst, van der W. M. P., 2011. *Process Mining: Discovery, Conformance and Enhancement of Business Processes*. Heidelberg: Springer.
- Aalst, van der W. M. P., Reijers, H. A., and Song, M., 2005. Discovering social networks from event logs. *Computer Supported Cooperative Work*, 14(6): 549–593.
- Bellifemine, F., Caire, G. and Trucco, T., 2010. *Jade Programmer's Guide. Java Agent Development Framework*. Available from: http://jade.tilab.com/doc/programmers_guide.pdf. [Accessed 16 January 2012].
- De Snoo, D., 2005. *Modelling planning processes with TALMOD*. Master's thesis, University of Groningen
- FIPA 2002. FIPA Contract Net Interaction Protocol Specification. Available from: http://jadex.informatik.uni-hamburg.de/docs/jadex-0.96x/userguide/predef_cap.html [Accessed 12 July 2012].
- Guo, A. and Siegelmann H., 2004. *Time-Warped Longest Common Subsequence Algorithm for Music Retrieval*. Universitat Pompeu Fabra.
- Gusfield, D., 1997. *Algorithms on Strings, Trees and Sequences: computer Science and Computational Biology*. Cambridge University Press.
- Hirschberg, D.S., 1977. Algorithms for the Longest Common Subsequence Problem. In *J. ACM*, 24(4), 664-675.
- Jennings, N.R., Faratin, P., Norman, T.J., O'Brien, P. and Odgers, B., 2000. *Autonomous agents for business process management*. *Int. Journal of Applied Artificial Intelligence* 14, pp. 145–189
- Islamov, R. and Olkov, A., 2010. The Use of Analytical-Statistical Simulation Approach in Operational Risk Analysis. In: *Enterprise Risk Management Symposium*. Society of Actuaries.
- Macal, C.M. and North, J.N., 2005. Tutorial on Agent-based Modeling and Simulation. In *Proceedings: 2005 Winter Simulation Conference*.
- Martinovic, J., Drazdilova, P., Slaninova, K, Kocyan, T., and Snasel, V., 2012. Left-Right Oscillate Algorithm for Community Detection used in E-learning system. In *IEEE Proceedings: 11th International conference Computer Information Systems and Industrial Management Applications, CISIM '12*. IEEE Computer Society. In print.
- Müller, M., 2007. *Information Retrieval for Music and Motion*. Springer.
- Scheer, A.W. and Nuttgens, M., 2000. ARIS architecture and reference models for business process management. In *Business Process Management, LNCS*. 1806: pp. 376–389.
- Vymetal, D., Spisak, M. and Sperka, R., 2012. An Influence of Random Number Generation Function to Multiagent Systems. In *Proceedings: LNAI 7327: Agent and Multi-Agent Systems: Technology and Applications*. KES AMSTA 2012. Berlin Heidelberg: Springer-Verlag, Germany. pp.340-349. ISSN 0302-9743. ISBN 978-3-642-30946-5. DOI 10.1007/978-3-642-30946-5. Available from: <http://www.springerlink.com/content/g71k68505h76x1wx/>.
- Yan, Y., Maamar, Z. and Shen, W., 2001. *Integration of Workflow and Agent Technology for Business Process Management*.

AUTHORS BIOGRAPHY

K. Slaninová is a PhD student at VŠB – Technical University in Ostrava, Faculty of Electrical Engineering, and an assistant professor at the Silesian University in Opava, School of Business Administration in Karviná, Department of informatics.

J. Martinovič is an associate professor at VŠB – Technical University in Ostrava, Faculty of Electrical Engineering.

P. Dráždilová is an assistant professor and PhD student at VŠB – Technical University in Ostrava, Faculty of Electrical Engineering.

D. Vymětal is a vice dean at the Silesian University in Opava, School of Business Administration in Karviná, and a head of department of informatics.

R. Šperka is an assistant professor and PhD candidate at the Silesian University in Opava, School of Business Administration in Karviná, Department of informatics.

USING GRAPHIC PROCESSORS FOR HIGHSPEED SIMULATIONS AND OTHER HIGH PERFORMANCE COMPUTATIONS

Thomas Wiedemann ^(a)

^(a) University of Applied Science Dresden

^(a) wiedem@informatik.htw-dresden.de

ABSTRACT

Current hardware development is characterized by an increasing number of multi-core processors. The performance advantages of dual and quad core processors have already been applied in high-speed calculations of video streams and other multimedia tasks. New options arise from the increasing power of new graphic processors. They include up to 1600 shading processors, which can also be used for universal computations at present. The paper discusses possible applications of graphic processors in simulation and other areas of high computation needs, like FEM or flow-analysis. The implementation of parallel threads on more than one core requires substantial changes in the software structure, which are only possible inside the source code. The paper also introduces feasible architectures and compares the CUDA and OpenCL approach.

Keywords: Grid computing, CUDA, OpenCL

1. INTRODUCTION

Since 2005, we have observed a quiet revolution in hardware development – the performance of graphic processor units (GPU) has been developing at a speed leading to a ten times higher performance against standard central processors (CPU) (see Fig. 1/from (Kirk and Hwu 2010)). But the development of CPU's has been slowing down since 2003 due to energy consumption and heat-dissipation issues limiting a further increase of clock frequency. As demonstrated in Fig. 1, the performance of actual graphical processing units (GPU's) achieves 1000 GFlops, a value lying in the range of older super computers. It is quite sure, that this revolution will continue also in the next years as a result of a very strong competition between the two major players – AMD and NVIDIA.

As a matter of fact, simulation science has already searched for the highest feasible performance (Wiedemann 2000). Otherwise, there exist completely new hardware architectures and requirements (see 2.2). The implementation of parallel threads on a large number of cores leads to substantial changes in the software structure. Changes like these are only feasible inside the source code and cannot be executed with COTS-simulation systems.

As a conclusion, we may expect a new era of high performance software development. This paper introduces not only options and constraints of the new hardware, but also the changes in the simulation software resulting from

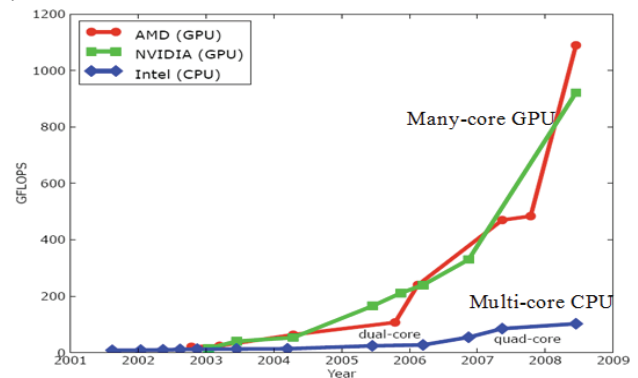


Figure 1: Performance chart ((Kirk and Hwu 2010))

The new hardware architecture of modern GPU's was primarily designed for high-end 3D-computer games. In these games, the high quantity of processors is used for parallel computing of high-quality images with fine-grained textures and sophisticated rendering algorithms. The first versions of such GPU's were tailored to special purposes and could not carry out universal computations (Kirk and Hwu 2010). The current versions are now capable of calculating common types of algorithms with double precision.

Resulting from the orientation on graphic algorithms, the hardware also follows a special architecture. First the host system and the graphic processor have separate memory and control areas. Programs for the graphic processor must be compiled in a special way and transferred to the graphic subsystem. The memory bandwidth of the GPU is up to ten-fold higher than the standard RAM memory of the host.

The GPU processor is divided into a number (16...128) of computing blocks, whereby each block consists of a grid of streaming core processors (cores). The number of cores inside a block is not fixed, but can be defined dynamically by the control program. High-end GPU processors, like the ATI Radeon™ HD 5870, are equipped with up to 1600 streaming cores.

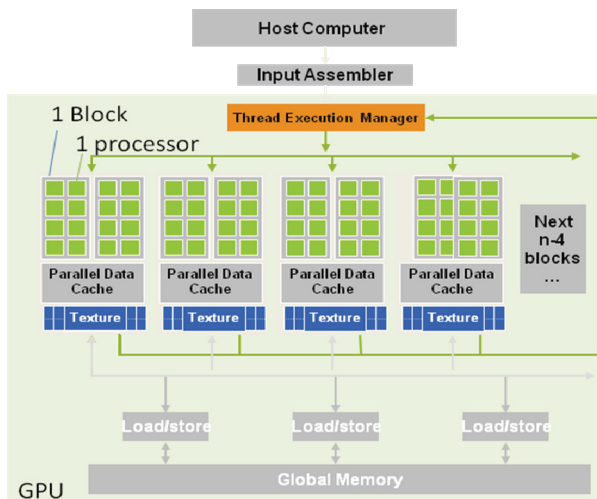


Figure 2: GPU architecture ((Kirk and Hwu 2010))

Memory organization is a significant limiting fact. The fastest memory is the shared memory inside the blocks. Only cores inside a block are able to communicate upon shared memory and to synchronize their work. Synchronization of cores between different blocks is slow and poorly supported! These aspects should be considered, when simulation scenarios are evaluated. A second, much more critical constraint is the single program multiple-data (SPMD) programming model of GPU's. This means, that inside a block, only one program is executed over different areas of data. If a program like this includes a branch, then the alternative else-branch is performed after executing the then-branch, which slows down execution at all. For graphical applications with large data streams, like encoding of videos or rendering complex 3D scenes, this model is suitably adapted, since it reduces the necessary ratio of logics inside the small processors.

If a complex program is executed, this programming model must be considered carefully! An approach is demonstrated on the following pages.

2. GPU'S IN UNIVERSAL COMPUTATIONS

2.1. General discussion of multi core applications

The main algorithms and mathematical foundations of simulation systems are well defined and efficient (Heusmann and Wiedewitsch 1995). Although the software tools for continuous (CS) and discrete simulation (DS) are very different, there exist two general options for using parallel computing environments.

First, the model itself is divided in smaller sub-models and each sub-model is computed on one core. This Parallel Simulation approach has been known for about 25 years (Perumalla 2006). As a result of the necessary communication between the sub-models, this approach is very complex.

During the last decade the possible speedup degraded. The main reason is the nearly constant

communication speed and increasing computation performance. The communication speed of standard parallel computers is limited by the simple phenomenon of distance between the computing cores. Let us assume a distance of 30 cm, only, than it takes the signal at light speed about 1ns ($t=s/v=0.3m/3*10^8 m/s$), lying in the range of 3 periods of a 3 GHz processor. Additional delays occur by the electronics' latencies themselves. In summary, the resulting speedup of parallel computation can decrease (fall down?) to 2 or even below 1 on multi-core machines, when the models are not suitably distributed on the cores. However, the new hardware architecture of GPU's may improve this situation again: First, by smaller distances of the core inside the chip die (<2mm) and second, by optimized synchronization hardware inside the same chip.

The second approach uses each core for computing exactly one simulation model, which is also known as Hyper Computing (Perumalla 2006). The larger number of cores is used for calculating the models n-time, e.g. by applying different random number seeds. Speeding up of such computations is nearly equal to the number of the cores and could be guaranteed in practice.

From a practice point of view, the Hyper computing approach is very interesting and to be used easily, if we leave the single simulation view and look on the whole simulation process. Nearly all larger simulation studies must consider random numbers inside the model or different input data scenarios. For statistical correctness, over 20 or more simulation runs must be executed for getting significant results. If there are different input data sets – Ndatasets, this number can be multiplied by the number of simulation runs Nruns, since all runs are independent one from each other and can be computed simultaneously. As a conclusion, running Ndatasets * Nruns, we obtain Ndatasets statistical significant results over all data input sets.

If there are no different input scenarios, than Ndatasets runs could be used for making a sensitive test, which provides significant information about the quality of simulation variables used.

2.2. Performance considerations in Hyper Computing

Against the background of the new GPU architecture, it makes sense to subdivide calculations into two different classes. Typical graphical computations are also subdivided into different computation classes, like transforming, rendering and shading of 3D objects with textures. The resulting GPU architecture (see Figures 2 and 1.2) provides an adequate support to different computing groups.

Let us assume that the simulation models only differ in their specific random numbers, whereas input data and computation are always the same. This is true for a large number of continuous simulations, but only a small number of discrete event simulations.

Concludingly, a set of N_{datasets} can be computed with N_{runs} each, whereby each block of N_{runs} computes one significant result for one of the datasets.

Since the maximum number of $N_{\text{datasets}} * N_{\text{runs}}$ is 512, a definition of $N_{\text{run}}=32$ runs and $N_{\text{datasets}}=16$ data sets is a good practical combination.

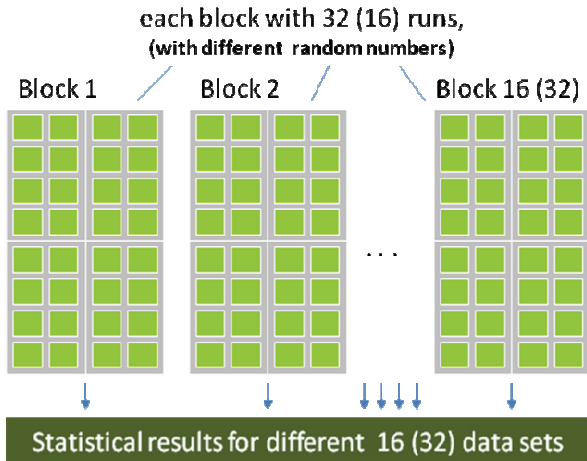


Figure 2: Hyper computing scenarios

If such a combination of variance and sensitive computation is realized, than the possible speedup can be the number of parallel running cores, in this case up to 512! This speedup does not depend on special methods of disaggregation of complex simulation models. The method can be adapted easily to new hardware characteristics, e.g. if the limit of 512 computing units in a block is extended (up to 1024 or more?) in the next years.

2.3. Typical scenarios for independent and equal simulation runs in a Hyper Computing context

In the field of **continuous simulation**, all formulae must be equal and only differ in the vector index of the input data and the index of the random number generator:

$$dv/dt = f(a(idx), vstart(idx), rand(idx))$$

The value of the idx -variable is equal to the $blockidx$ -value of the core inside the block. The $blockidx$ is automatically determined by the host program at the start of the parallel runs and counts all the used cores from 1 to N .

In the example, each run may have different values for acceleration a , the initial speed $vstart$ and the random values of the motion, like wind or engine characteristics. Like mentioned before in chapter 2.2, additional cores can be used for calculating sensitive tests or different data input sets.

A similar formula *may* be used for **Monte-Carlo-simulations (MC)** (e.g. for determining Π) :

```
for (int i=1; i<= experiments; i++)
{ x = rand1(blockidx); y = rand2(blockidx);
  r_testPI = x * x + y * y;
  if ( fabs(r_testPI) < Radius) hit++;
} PI = hit / experiments * 4; // get PI by MC
```

The $rand1()$ and $rand2()$ are typical random number generators, where the seed and current value are stored in a vector, referenced by the $blockidx$ -value again. For both applications, speedup may grow up to the number of cores used in parallel.

2.4. Parallel execution in discrete simulation

Application of GPU's in the discrete event simulation is much more difficult. In general, the objects are very different in their characteristics, and thus code execution is not equal, which, in turn, slows down execution speed in the context of the single program multiple-data (SPMD) programming model.

One special option is possible, if the simulation model consists of objects with nearly identical characteristics and an equal schedule sequence (e.g. each minute a customer is served or nothing is done)! Such a code for one object of some hundreds of objects could be described by the following expression:

```
while ( running )
{ if ( mynext_time > simtime)
  // do nothing
  else { /* do actions */
    p= getnextproduct(blockidx);
    optime = workon_product(p);
    mynext_time = simtime +optime;
  } _syncthread(); // wait for the other ...
}
```

In any case, the two branch sections *then {}* and *else {}* are executed in sequence and not in parallel, but the first section does nothing and the loss of speed is minimal. The functions $getnextproduct()$ and $workonproduct()$ should execute the same code, only depending from the $blockidx$ -value of the core, which corresponds to the number of the machine in the simulation model.

Of course, this approach is limited by the restrictions of the single program multiple-data (SPMD) programming model. Much more complex discrete simulation models must be executed on different cores in result of their heterogeneous code, but the number of such cores is not so high. Future work on the hardware will give new opportunities also for discrete simulation in this area.

2.5. Using GPU's for high-performance applications

All the discussed scenarios for the different simulation methods are valid also for other computations in the CAD/CAM area. Like in simulation, the GPU can be used in two different modes:

- If the data or computation model is distributed in space and the computation algorithms are the same with different parameters, the GPU cores can run in parallel over a distributed model.
- If the data or model is not distributed, the cores could be used for equal runs with changing experiment parameters. For example, a complex CAD or CAM calculation could be done for different levels of external temperature or mechanical stress.

Mixed modes of the two options are also possible!

2.6. Optimization with GPU's

A third level of parallelization is possible by using optimization techniques. The approach from chapter 1.3-1.5 can be extended by using the results of the basic runs in an optimization method with independent points, like the Monte-Carlo optimization method or genetic algorithms.

On the GPU stream cores, a method like this would be distributed in the following way:

- One single optimization point is calculated by 16 or 32 cores inside one block.
- 32 or 16 blocks are used for getting the points for 32 or 16 individuals in the search space.
- One additional block works as an optimization control block and collects all the points and calculates the next generation of individuals.

If there are more blocks available, the whole optimization run can be started for a second or third time with different starting values for using all computing cores.

Let us assume that there are 32 runs executed for each of the 16 individuals. With this assumption, we provide the maximum number of 512 cores on a computing unit. But if there are 1600 cores in a high performance GPU like the ATI HD 5870, we can perform three runs of these optimizations, providing a total speedup of 1500.

2.7. Conclusion

Consequently, it is easier and much more flexible to use a Hyper computing approach. The major limiting factor is the single program multiple-data (SPMD) programming model inside the blocks, which defines some constraints on the bandwidth of code.

3. PREREQUISITES AND FUTURE DEVELOPMENT

The GPU hardware is supported by special API's and C-style programming libraries. Both companies, AMD and Nvidia, provide special software drivers and programming environments (Nvidia 2012) (OpenCL 2012) (OpenAcc 2012).

3.1. CUDA, OpenCL and OpenAcc

In 1999, Nvidia invented the GPU-multicore architecture and supported/ supports the hardware with its proprietary CUDA technology (Nvidia 2012). AMD and its subdivision ATI assist the own hardware and also the Nvidia hardware with the open and non-proprietary OpenCL technology (OpenCL 2012). A third option is available since 2012 – the OpenAcc-interface (OpenAcc 2012).

Until summer 2012, the final result of this competition has still been open:

- Nvidia's CUDA is more efficient and easier to use on the Nvidia GPU's.

- The OpenCL is much more flexible, but requires more development efforts. OpenCL can be executed also on multi-core CPU's.
- OpenAcc is only an extension of C-compilers and tries to generate automatic code for the GPU from standard C-code. The performance will be lower in most cases, but the ease of use will be higher compared to CUDA and OpenCL.

From the author's point of view, the final result will mainly depend on the OpenCL and OpenAcc development.

3.2. New hardware opportunities

New hardware from Nvidia, based on the next-generation CUDA architecture codenamed "Fermi" brings the performance of a small supercomputing cluster to the desktop. Compared to a Cray-I from 1980 with 150 MFlops and a price of about 8 Mio \$ one card now offers 480 GFlops for a price of a desktop PC. Up to 4 cards can be combined in a PC, which offers a peak performance of nearly 2 Terraflops. The future development of the hardware will continue and the results will be very interesting for all areas of high speed computing !

3.3. Final summary

The new GPU architectures are very promising for applications with a high demand of computation for a low price. Practical results are feasible and will show speedup's of some hundreds at a very interesting price, compared with traditional parallel computers.

REFERENCES

- Kirk D., Hwu W. 2010. Programming Massively Parallel Processors: A Hands-On Approach
- Heusmann J., Wiedewitsch J. 1995. "Future Directions of Modeling and Simulation in the Department of Defense", Proc. of the SCSC'95, Ottawa, Canada
- Wiedemann, T., 2000. VisualSLX – an open user shell for high-performance modeling and simulation, *Proceedings of the 2000 Winter Simulation Conference*, Orlando Florida
- Perumalla K., 2006 "Parallel and Distributed Simulation: Traditional Techniques and Recent Advances". *Proceedings of the 2006 Winter Simulation Conference*
- Nvidia 2012. available from developer.nvidia.com/ [Accessed 15.7.12]
- OpenCL 2012 available from www.khronos.org/opencl/ [Accessed 15.7.12]
- OpenAcc 2012 available from www.openacc.org/ [Accessed 15.7.12]

PROJECT MANAGEMENT GAMES USING HIGH LEVEL ARCHITECTURE

Ronald Ekyalimpa^(a), Simaan Abourizk^(b), Yasser Mohamed^(c), Farzaneh Saba^(d)

^(a) PhD Candidate, Dept. of Civil and Environmental Engineering,
Univ. of Alberta, Edmonton, Alberta, Canada T6G 2G7.

^(b) Professor, Dept. of Civil and Environmental Engineering, Univ. of
Alberta, Edmonton, Alberta, Canada T6G 2G7.

^(c) Professor, Dept. of Civil and Environmental Engineering, Univ. of
Alberta, Edmonton, Alberta, Canada T6G 2G7.

^(d) PhD Graduate, Dept. of Civil and Environmental Engineering,
Univ. of Alberta, Edmonton, Alberta, Canada T6G 2G7.

^(a)rekyalimpa@ualberta.ca, ^(b)abourizk@ualberta.ca, ^(c)yaly@ualberta.ca, ^(d)fsaba@ualberta.ca

ABSTRACT

Numerous simulation games have been developed since the 60's by researchers within the construction domain. These games were developed for a specific purpose and possess a unique implementation strategy and structure. This paper summarizes some of these games and further discusses a subset of them, particularly those developed within the CONstruction SYNthetic Environment (COSYE). A prototype for a game development framework was proposed based on review of these games. It is proposed to implement this prototype within a distributed simulation environment to ensure consistency, interoperability, and reusability of the components and the game as a whole. COSYE is chosen to provide such an environment because it has the necessary ingredients for developing and maintaining such a prototype. The paper further discusses some concepts of distributed simulation, the features that exist within the COSYE framework, and the standards on which the COSYE framework operates i.e. High Level Architecture (HLA).

Keywords: Simulation games, prototype, COSYE, HLA

1. INTRODUCTION

The pace of the construction industry has traditionally been driven by the needs of its clients and national and global economies in general. This makes it a highly dynamic industry. Lately, projects within this industry have significantly evolved with respect to complexity and size. They are generally larger and more complex, demanding more refined competencies, with respect to cost and time efficiency, safety and quality from the people executing them. As a result, average recent university graduates generally find it challenging to match this required skill set, especially if they are a product of a program that utilizes traditional methods of classroom instruction. Moreover, the industry is highly competitive at an individual and company level.

An effective way of resolving such issues is to use methods complementary to traditional ones. Examples of these methods include site visits, the use of simulation games, the use of case studies and guest lectures from experts in the industry. Simulation games have a lot of potential to develop the desired competencies amongst students because they create a virtual construction site environment with which the students interact as though they were on a real job site. Also, the implementation of these games does not demand significant logistical requirements compared to the other methods, and yet, the players experience sufficient training time and the desired benefits are realized. Therefore, the use of simulation games in construction education needs to be given more emphasis and the tools required to support their use must be up-to-date and easy-to-use.

This paper reviews the structure and development of past simulation games with the objective of deriving common features among them from which a generic game development prototype can be proposed. It is envisaged that this prototype will simplify the development process of future games. Although the prototype can be applied in any suitable environment while developing a game, the authors base their discussion in this paper on an environment that supports the development and execution of distributed simulation systems, COSYE, developed at the University of Alberta by the second and third authors of this paper.

2. CONSTRUCTION MANAGEMENT GAMES

A review of the various simulation-based games that have been implemented in the past within the construction domain reveals a significant degree of diversity with respect to their structure, internal processing algorithms and overall purpose. Nonetheless, they can be placed within two broad categories: process centric games and non-process centric games.

Process centric games are those that model site-level operations using typical process interaction

modeling approaches. They involve a lot of resource manipulations and event scheduling (which replicate the complex logical sequence of project activity execution). The purpose of such games is to teach students how to allocate resources as construction progresses, and how to deal with other uncertain events that are typical of construction projects such as labor strikes, equipment failures, bad weather and other unforeseen poor site conditions. These games develop student skill and knowledge regarding how to effectively keep projects in control amidst such unfavorable circumstances. Examples of games that have been developed in this category include: a foundation excavation game (Au and Parti 1969), CONSTRUCTO (Halpin 1976), a road construction game (Harris et al. 1977), the muck game (Al-Jibouri and Mawdesley 2001) and a tunneling game (Ekyalimpa et al. 2011). CONSTRUCTO was developed by Halpin in 1976 to teach students how to deal with unforeseen site conditions such as labor shortages and unfavorable weather conditions while executing a construction project. It was also aimed at teaching students how to manage resources on their projects from a constrained global resource pool. The foundation game developed by Au and Parti in 1969 was focused on teaching students how to deal with the dynamics and uncertainties associated with building foundation excavation and construction. The muck game was introduced by Al-Jibouri in 2001 and its main purpose was to teach students the concepts involved in earth-moving operations.

The non-process centric games focus their efforts on teaching students the different concepts of bidding strategies, cost estimation, scheduling and dispute resolution. Examples of games within this category include Construction management game (Au and Parti 1969), SUPERBID (AbouRizk 1993), STRATEGY (McCabe et al. 2000), equipment replacement game (Nasser 2002), virtual construction negotiation (Yaouyenyong et al. 2005), Easy Plan (Hegazy 2006), and MERIT (Wall and Ahmed 2006). Different versions of superbid have been developed since the release of the original version by AbouRizk. These have adapted different implementation approaches and have had some additions made to them, such as the virtual player implemented in a version of superbid within COSYE by AbouRizk et al (2010). Details of this version of the game, along with other games implemented within COSYE, will be discussed in this paper.

In their paper, AbouRizk et al (2010) pointed out that with the advances in computing technologies, most of the games discussed above have been rendered obsolete as they can no longer be implemented on today's computers. This could be attributed to the static nature of the methodologies that were used to implement these games. Nonetheless, there are a number of insights to be gained from reviewing the different implementation strategies used for developing the games. These approaches can be summarized as those that were: (1) operated on standalone computers, (2) implemented in a database-server environment, (3)

developed in a web-based environment and (4) implemented in a distributed simulation environment like COSYE. For a game setting, a file server, web-based server and distributed simulation approaches offer more implementation flexibility and are acceptable. This issue will be further discussed in the conceptual framework for game development.

3. DISTRIBUTED SIMULATION USING COSYE AND THE HLA

COSYE is an application programming interface which supports the development of large-scale distributed synthetic simulation environments. It is based on the High Level Architecture (IEEE 1516) standard for developing large-scale models (AbouRizk and Hague 2009) and facilitates the creation of separate simulation components (also known as federates) and their integration into a single simulation system (known as a federation) during execution.

The HLA standards are guidelines prescribed by the Institute of Electronic and Electrical Engineers (IEEE) to ensure that distributed simulation systems are developed in an interoperable, reusable and consistent manner. The HLA standard is comprised of three components, namely: the rules, the Object Model Template (OMT) and the Interface specifications.

A typical distributed simulation system will be represented by one federation and a number of federates. A federation can be defined as a virtual space/environment which represents a distributed simulation system. It has different components (federates) that are responsible for its simulation behavior. A federate on the other hand is a piece of software with the capability of participating in a federation execution. Figure 1.0 shows a schematic layout of a distributed simulation system with the different components. Some of these components will be explained in detail. The COSYE framework provides the services required to create federates and integrates them into an executable federation. COSYE has different components which facilitate developers to achieve this. They include: a Run Time Infrastructure (RTI), an OMT editor, a federate host, and a federate form.

3.1. The Run-Time Infrastructure (RTI)

The RTI is software that hosts the virtual distributed simulation environment referred to as a federation. It also manages communications between the different components (federates) within this virtual environment, along with other features such as the object instances and messages within the environment. COSYE has its own RTI which has the ability to support multiple instances of federations. Communication exchanges between the components are not direct, but rather, to the RTI, which delivers these messages in the right order and right time. A message thread sent from the source to a receipt is referred to as a *call* while a response to such messages is referred to as a *callback*.

The exchange of messages between the RTI and federate is accomplished in the HLA and COSYE through the *federateambassador* and *RTIambassador*, which reside within each federate (as shown in Figure 1.0). A federate ambassador and RTI ambassador are classes defined within the *Cosye.Hla.Rti* library. These classes have methods which permit federate developers to make calls and receive call-backs. In COSYE, a federate ambassador is created within a federate by generating a new instance of the federate ambassador class as in any object-oriented programming development (using the *new* keyword). The RTI ambassador, on the other hand, is created when the federate successfully connects to the RTI server. This is accomplished by invoking the connect method of the federate ambassador which takes the location of the RTI (i.e. its URL) as a string parameter. If the call is successful, the method returns a reference to an object of type RTI ambassador that is stored for later use; otherwise an appropriate exception is thrown.

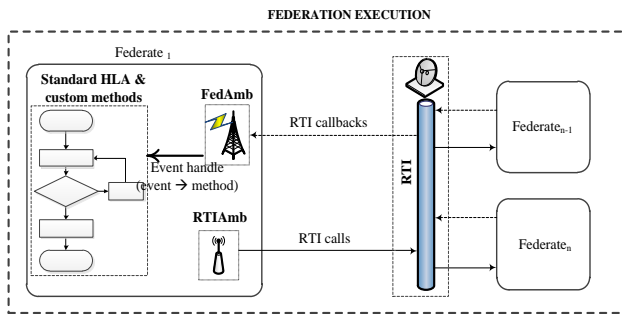


Figure 1: Conceptual Model of a Typical Federation Execution in COSYE

All this is done before the federate joins any federation. Once these exist within the federate, it can send a message requesting to create a federation, join it, execute, resign and destroy the federation. Most communications from the RTI are received by the federate ambassador which in turn translates them into respective methods in which user defined code/algorithms are implemented. It is within these methods that a developer defines the overall behavior of the federate. The RTI ambassador has methods that facilitate a federate to send information/requests to the RTI.

3.2. The COSYE OMT Editor and the Federate Object Model (FOM)

The HLA standard stipulates that an OMT is comprised of a Federate Object Model (FOM) and a Simulation Object Model (SOM). The FOM documents the object model for the federation while the SOM documents a federate's object model. The COSYE framework provides an OMT editor as a plugin within visual studio. This is added to visual studio after referencing the *Cosye.Hla.OMT* library within visual studio. The OMT editor allows developers to visually create and edit their FOMs or SOMs with ease. Figure 2.0 shows a screen shot of an FOM developed in visual studio.

The FOM is a document that specifies all the objects that will participate in a given federation execution. It represents a structured way for developers to specify the objects and interactions that exist within the federation. This is achieved through the use of the concept of a class in the Dot Net sense. The HLA provides for two types of classes; those that represent *object classes*, and those that represent *interaction classes*. Objects represent instances which persist in the simulation while interactions represent messages and do not persist during simulation execution.

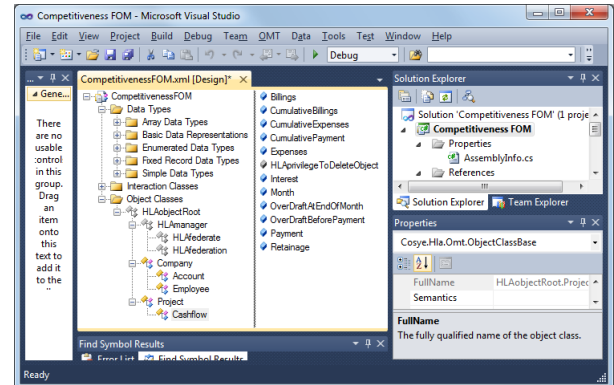


Figure 2: Screen Shot of the COSYE OMT Editor in Visual Studio

The FOM is structured in such a way that allows for the definition and storage of these classes and their associated fields. For the object classes, the FOM documents the name of the class and its attributes. The FOM includes specifications of the interaction class name and its parameters. However, lacking within the FOM are the methods for these classes. In the FOM, the developer can also specify the data type of the attributes and parameters, permission to publish or subscribe to them and the nature of delivery of messages about these attributes during the simulation. Every federation must have one FOM that is documented according to the Object Model Template (OMT), as stipulated in the first rule within the HLA standards (Kuhl et al. 2000).

3.3. The COSYE Federate Form, Federate Host and Test Federate

The federate form is a component that exists within COSYE in the *Cosye.Hla.Framework* namespace. It can be added to a visual studio development project as an inherited form. A sample of a federate windows form within visual studio is displayed in Figure 3.

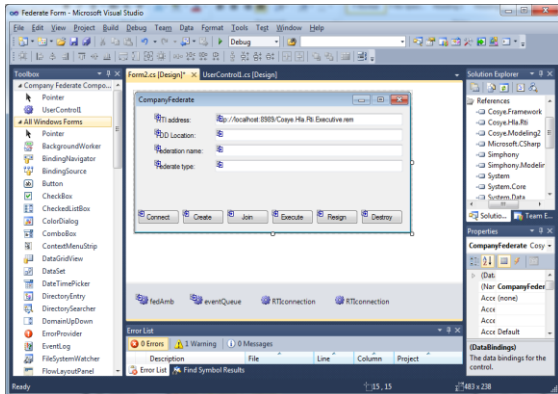


Figure 3: COSYE Federate Form in Visual Studio

This form can be used to develop a federate quickly without the need of several lines of code to implement its participation within a federation execution.

The federate host is a component that can be found within the *Cosye.Hla.Framework* name space in COSYE. This component serves as a container in which different federates participating in a federation execution are put together to provide a simple user interface. Figure 4 shows a screen shot of a sample federate host in COSYE.

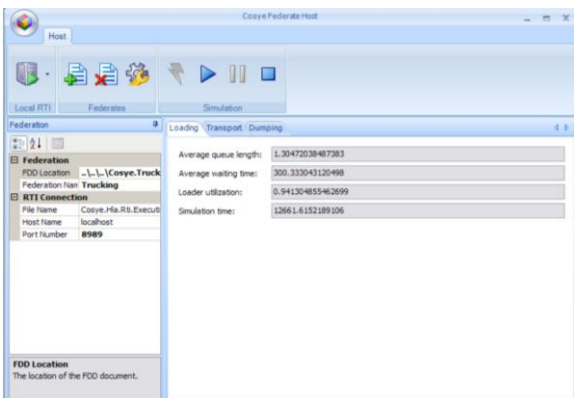


Figure 4: Federate Host (Adapted from AbouRizk 2011)

The federate host can also be used as an interface for (1) starting and shutting down the RTI (2) inputting specifications required for connecting to the RTI (i.e. the RTI host name, the port number and the name of the RTI) and (3) receiving inputs for creation of a federation (i.e. the federation name and the FOM location). The user can add or remove federates from the federate host using the respective buttons. The federation can also be created, executed and terminated within this interface.

The test federate is another component within COSYE that is used by both inexperienced and experienced developers. The former use it as a tool that facilitates the fast and easy creation, execution and destruction of a federation in COSYE. It helps them appreciate the manner in which COSYE manages the various services that the HLA provides for, such as management of: a federation, time, objects, ownership and declaration. The latter users apply it for verifying

their federation development process. The test federate can also be used for verifying the behavior of the RTI. Figure 5 is a screen shot of a sample test federate within COSYE.

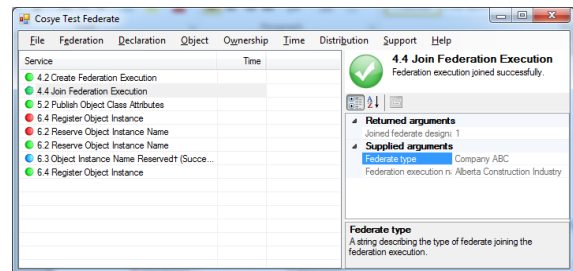


Figure 5: The Test Federate Interface in COSYE

The test federate traces a log of all the calls and callbacks made within the federation execution, along with the exceptions thrown.

4. A REVIEW OF SIMULATION GAMES DEVELOPED IN COSYE

Three games that were previously developed within COSYE are reviewed within this section with the objective of establishing features that are common to them. These features are then used as a basis for proposing the generic game development prototype for the construction domain.

4.1. The Crane Lift Planning Game

A “Mobile crane lift planning game” is the first of the three COSYE games to be discussed in this paper. The objective of this game is to teach students the concepts, knowledge and skills necessary to analyze and plan heavy lift operations on a congested site using mobile cranes.

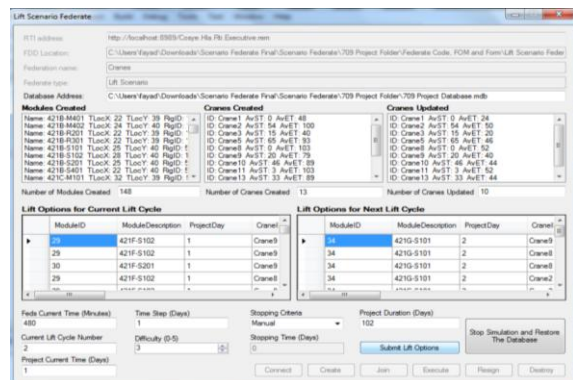


Figure 6: Scenario Set-up Federate in the Crane Lift Planning Game (Adapted from Ekyalimpa and Fayyad 2010)

The game comprised of three core federates, namely: a scenario-setup federate (developed by Ekyalimpa and Fayyad 2010), a player federate (developed by Jangmi et al. 2010) and an operations simulator (developed by Gonzales et al. 2010). Figures 6 and 7 show screen shots of interfaces for the scenario-setup federate and the player federate.

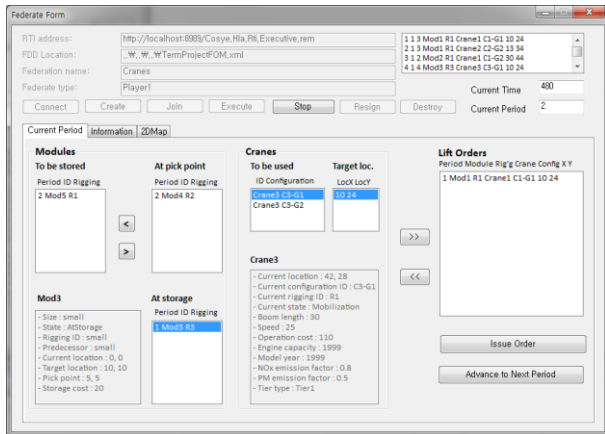


Figure 7: Player Federate in the Crane Lift Planning Game (Adapted from Jangmi et al. 2010)

In this game, an industrial construction site is assumed in which modules have to be lifted into place using mobile cranes. Modules arrive from a hypothetical assembly yard and would either be temporarily put aside while waiting to be lifted into position, or they would be offloaded into storage in case the predecessor modules have not yet been installed. This is because not all the modules arrive to site in the order in which they are to be erected on site. A finite number of mobile cranes with specified lift capacities were to be assigned to lift modules the designed location. In some cases, a mobile crane would have to be moved from one location to another in order to complete a lift. Once a lift plan has been generated (speculating the modules to be lifted, the cranes to lift them and the positions in which the lifts should be executed), this information is passed on to an operations simulator that executes the plan within a simulation environment. From the simulation, we get an indication of the time taken to complete the entire operation, including vital statistics such as the utilization of the crane resources and the time consumed before modules are erected (waiting time). This is done in cycles (module arrivals lift plan generation and lift plan execution).

This game was developed as a term project in an advanced simulation course that makes use of the COSYE environment for simulation implementations. The game is comprised of five components (federates), namely: administrator, player, operations, visualization and emissions. The visualization and emissions federates are not discussed in this paper. A conceptual model for the game implementation (federation) is shown in Figure 8.

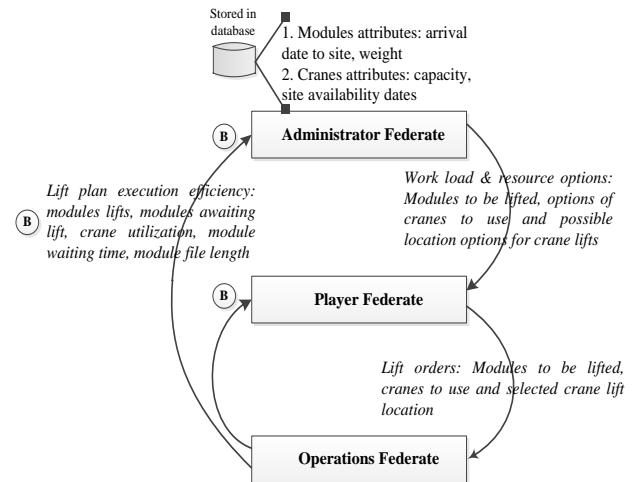


Figure 8: Interaction between Federates in the Crane Lift Planning Game

4.2. The Bidding Game (with a Virtual Player)

Different versions of the bidding game have been developed since the release of the original version, SUPERBID, by AbouRizk in 1993. However, the version discussed in this section is that developed within the COSYE framework by AbouRizk et al (2010). The primary purpose of the bidding game was to teach students bidding strategies. This version of the game comprised of six federates (shown in Figure 9). At the beginning of the game, a federation is created by the administrator federate, into which it subsequently joins. If there is a need for a virtual player, the administrator federate starts up and enables an instance of it to join the federation. Player federates then join the federation with each player representing a unique general contractor. As each player federate joins the execution, an instance of each is created. A bank account is created for each player with an initial amount of money in it, which is randomly sampled from a statistical distribution. The market federate joins the federation execution creating an instance of a market in which projects and sub-contractors will exist for the general contractor to pick from as the game advances. The player makes a decision regarding which projects to bid on, secures a bond for the bid of interest, selects subcontractors, and then submits its bid, which includes their profit margin. As the game advances, the project is awarded to the contractor that submitted the lowest bid. The winning contractor is the one who creates the most value (has the most money in their account) at the end of the game. The performance of the player in each period is dependent on the quality of the subcontractors that the contractor chooses to use, their past experience in building similar projects and the location of these projects relative to the contractor's location.

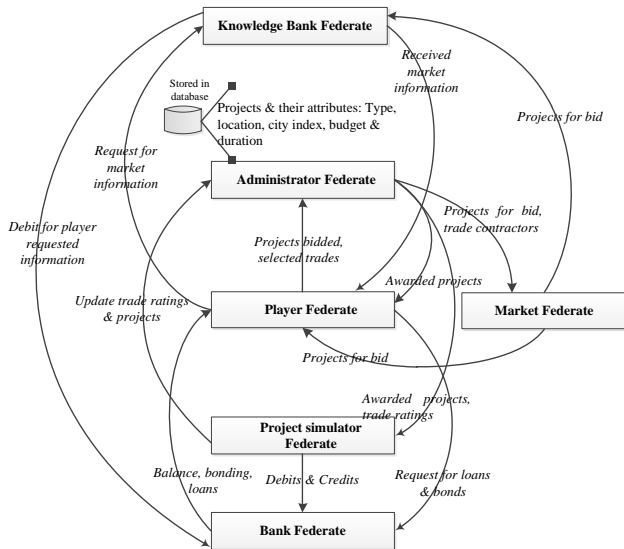


Figure 9: Interaction between Federates in the Bidding Game

4.3. The Tunneling Game

The tunneling game was built off of an existing tunneling federation. This federation was initially developed to support the planning and analysis of a tunnel to be built, or one already in construction. Incorporating gaming features into the federation was possible because the HLA and COSYE developments facilitate extensibility while maintaining their interoperability and reusability characteristics. One component (federate) was developed from scratch to host a number of gaming facilities, namely: the user interface, the reporting facilities and the scenario generator. Figure 10 presents a screen shot of this federate.

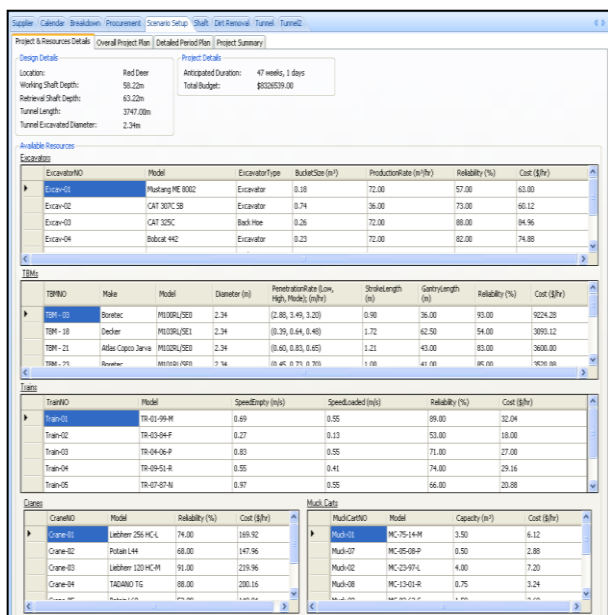


Figure 10: User Interface of the Tunneling Game (Adapted from Ekyalimpa et al. 2010)

Making use of the existing federate simulating an actual tunnel construction, the game created an instance of a tunnel which the students would be expected to construct. Attributes of the tunnel as such the length, depth, soil conditions, diameter, budget and schedule, would all be made available to the player. The tunnel instances are created from an access database that contains a list of different tunnel scenarios. This database also contains a list of different resources that would be required to execute the project. In this game, resource options would be made available to the players, such as different sizes of muck carts and different quality of TBMs (with respect to excavation rate and failure rate). Each of these would have a different cost associated with them. At the beginning of the game, players would be expected to develop a plan in which they decide the rate at which they would like to perform the work (meters advanced/day) and the resources they would like to assign to achieve that work (size and number of muck carts, type of TBM and number of crew members). For each play period, the simulator would take this plan as its input and generate results (money spent, actual time taken and liner distance advanced) at the end of the period which would be available for the player to review. If the player were not content with their performance in the last period, they could change their plan in order to improve. At the end of the game session, players would be ranked based on their performance using earned value methodology. This game teaches students how to plan for the construction operations, especially within the domain of tunneling. A concept design for this game is presented in Figure 11.

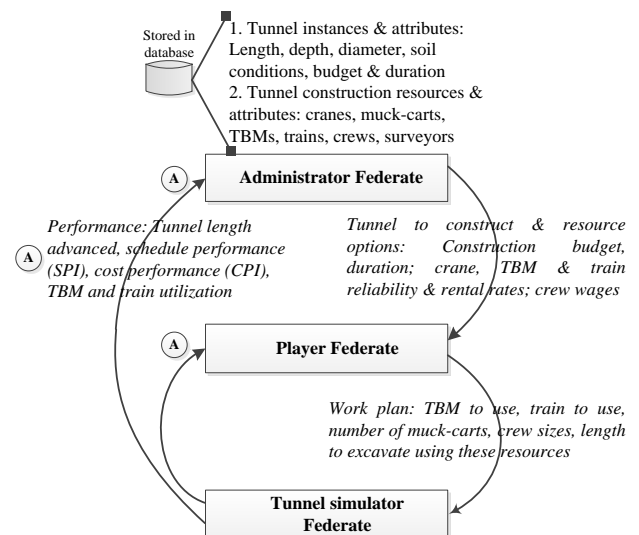


Figure 11: Interaction between Federates in the Tunneling Game

5. A PROTOTYPE FOR GAME DEVELOPEMENT

Based on the review of the games developed in COSYE, a prototype for game creation was proposed which is intended to simplify the development process. The prototype was summarized from a perspective of

component software and then from an object model perspective. These are discussed in the following sub-sections.

Given that there is a diverse range of environments in which construction management games have been implemented in the past, it should be mentioned that the generic game development prototype can also be used in any of these i.e. in a database-server setting or a web-based environment. However, for the sake of discussion in this paper, a distributed simulation environment like COSYE is proposed for use.

5.1. Software Structure of the Prototype

The structure of the prototype represents the software pieces that need to be created to obtain a fully functional game. They include: an administrator, a process simulator, player and virtual player (shown in Figure 12). This section discusses the features expected in each piece, including their anticipated simulation behavior.

The game administrator is a component which will always exist within any simulation-based game because it controls the creation and destruction of the game. Besides this, the administrator regulates a number of features during the game session such as:

- Managing the creation of possible game scenarios to be simulated.
- Managing time (the length of time between decision windows and the length of decision window).
- Varying the difficulty level of the game.
- Tracking the performance of each player.
- Enabling or disabling the virtual player from participating in the simulation.

In order to accomplish its time management responsibilities, this federate needs to be implemented as a time-stepped simulation. It also needs to be linked to a storage medium, like a database, from which it reads all the possible scenarios to be populated in the game. The administrator of the game, who in most cases will be a tutor of the instructed course, will require an interface for this federate which displays reports of player performance and other occurrences in the game during execution. This federate should have a criterion for rating the performances of each player. To guarantee that this federation will destroy the federation, it should be the last federate to achieve the “ReadyToTerminate” synchronization point, usually after a pre-determined criteria is achieved.

The game simulator represents a component that uses the inputs from the player to processes the work that needs to be done. It generates performance measures based on the actual progress made in executing this work. It is also responsible for modeling the uncertainty that surrounds the execution of this work. In order to do this, the simulator federate needs to be implemented using a time management scheme.

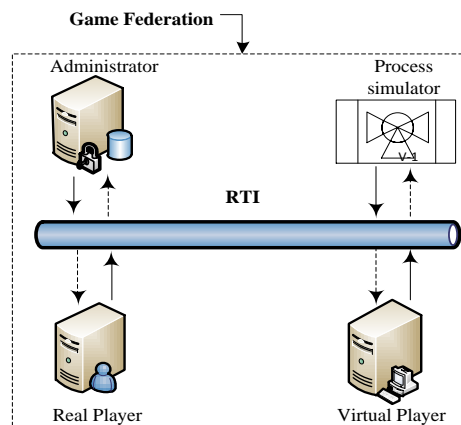


Figure 12: Conceptual Model for the Game Development Prototype

This federate may be designed as a next-event simulation or a time-stepped simulation depending on how the processing of the operation is implemented. It is mandatory for all simulator federated implemented as next-event simulation to make use of a discrete event simulation engine in its implementation. This is not the case with a time stepped simulation.

Regardless of the implementation approach used, simulator federates go through two cyclic windows during the game execution, namely, a simulation window and a decision window. The simulation window represents the phase in which the computation of algorithms is done to give rise to results which are then published. The simulator federate should be designed so that this simulation window occurs during the time granting state of the federate. The decision window, on the other hand, should be implemented in the time advancing state. This is shown in the protocol diagram in Figure 13. Federates involved in time management can have two possible states during federation execution, a time advancing state and a time granting state. A federate enters a time advancing state as soon as a call is made to the RTI to advance its time. In COSYE, this may be through a *NextMessageRequest* or a *TimeAdvanceRequest*. A federate enters a time granting state when it receives a time advance grant from the RTI.

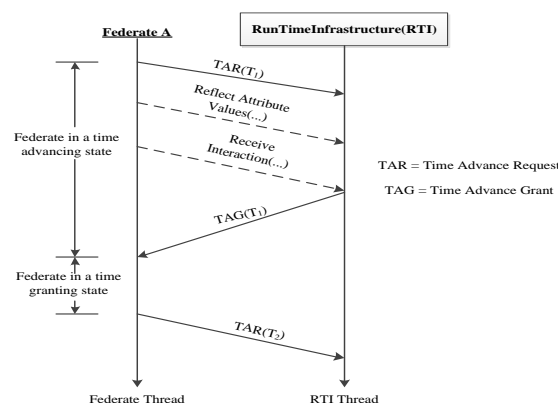


Figure 13: Schematic of a Protocol Diagram showing the States in time-stepped federate

For event-driven federates, the simulation window involves invoking the *DiscreteEventSimulationEngine.Simulate* (theGrantedTime) and *RTIAmb.NextMessageRequest* (*DiscreteEventSimulationEngine.TimeNext*) methods sequentially. These two methods are implemented within the time advance grant call-back of the simulator federate (when the federate is in a time granting state). This represents the processing of simulation events (algorithms) which were scheduled within the *ReflectAttributeValues* and *ReceiveInteraction* call-back methods of this federate during its time advancing state. The decision window represents a phase when the simulation engine is not doing anything. During this window, results are viewed in the player federate. Also, choices submitted by each player are received by the simulator federate, which translates them into corresponding simulation events that are scheduled to take place at the appropriate time.

In time-stepped federates, the simulation window is also within the time granting state of the federate. Simulation algorithms are processed within the time advance grant call-back method. The last statement within this method is a request for time advancement which changes the state of the federate into a time advancing state. During the time advancing state, the *ReflectAttributeValues* and *ReceiveInteraction* call-back methods of this federate are invoked as messages arrive at the federate.

In case a process discrete event simulation model (such as a Symphony special purpose template model) already exists for the domain being modeled, this model can be federated so that it participates within the respective game federations as an event-driven simulator component. This concept was successfully applied in the development of the tunneling game.

The player component is the portion of the game which participants directly interact with. The most important aspect of the player is its interface design. This should be made so that it is easy for the player to: (1) view the different game options available for upcoming play periods, (2) make a choice and submit it and (3) view their cumulative performance results from previous play periods. The game should have the capability of creating a unique instance of the federate for each participant in the game, with the exception of the virtual player which should be created by the administrator.

A virtual player is an optional, although very useful component, which is included in a game execution in situations where players engaged within a game session are generally inexperienced. The virtual player represents an experienced participant from whom the other players can learn as a result of the challenges that it poses.

5.2. Generic Federation Object Model for the Game Prototype

One other aspect investigated when comparing the three simulation games developed in COSYE was the federation object model. These were compared to establish the existence or non-existence of common features amongst them. It was established that there were some aspects of commonality amongst them which formed a basis for the standard federation object model for future game development efforts. Table 1 summarizes the object classes and parameter classes that should be present within an FOM of a game to be developed within COSYE. The associated attributes and parameters to these classes are also detailed.

Table 1: Specifications of an FOM for the Game Development Prototype

Class Type	Proposed Class Name	Attribute/Parameter
Object class	Player	Name, performance parameters, performance rating
	Scenario - projects	TBD
	Scenario - resources	TBD
Interaction class	Simulation window	Session number, time span
	Decision window	Window number, time span
	Game play options	TBD
	Player decisions	TBD
	Play period performance	TBD

Details of the data types and send order (time stamped or receive order) are left to the developer to determine. For some of the classes, attributes or parameters are highly dependent on the nature of the game being developed, and hence, are left at the discretion of the developer to determine. These have been tagged as "TBD."

6. CONCLUSIONS

The idea of using construction management simulation games as a teaching aide in construction education is relevant, especially in today's industry where there are growing expectations for construction graduates to perform well on the job, particularly in the early years of their careers. Simulation games adequately resolve the challenges that such expectations pose by serving as tools that are used to develop the skills, knowledge and experience (while still in school) required to deal with the problems that graduates face. The advances in computer technologies provide an opportunity to extend the process of developing more relevant and exciting games to effectively achieve this goal. A conceptual model that structures, guides and simplifies such developments has been presented in this paper.

The COSYE framework is proposed as an appropriate environment in which such a prototype can be effectively implemented, although other

environments, such as file server or web server systems can be used with a few modifications. The main features within COSYE that are required for developing a game federation have also been discussed.

REFERENCES

- AbouRizk, S., 2010. Enhancing the competitiveness of the construction industry in Alberta. *IRC Renewal Application, Term 4*.
- AbouRizk, S. and Hague, S., 2009. An overview of the COSYE environment for construction simulation. *Proceedings of the 2009 Winter Simulation Conference*, pp. 2624-2634. December 13-16, Austin (Texas, USA).
- AbouRizk, S. M., 1993. Stochastic simulation of construction bidding and project management. *Microcomputers in Civil Engineering*, 8 (2), 343-353.
- Al-Jibouri, S. and Mawdesley, M., 2001. Design and experience with a computer game for teaching construction project planning control. *Engineering Construction and Architectural Management*, 8 (5), 418-427.
- Au, T., Bostleman, R., and Parti, E., 1969. Construction management game – deterministic model. *Journal of Construction Division*, 95 (CO1), 25-38.
- Au, T., and Parti, E. W., 1969. Project planning game for foundation excavation. *Journal of the Construction Division*, 95 (CO1), 11-21.
- Ekyalimpa, R., Al-Jibouri, S., Yasser, M., and AbouRizk, S., 2011. Design of a tunnel simulation game for teaching project control in construction. *Proceedings of Construction Research Congress Conference*, pp. 2118-2128, June 14-17, Ottawa (Ontario, Canada).
- Ekyalimpa, R., and Fayyad, S., 2010. Administrator federate module in the Crane Lift Planning Game, internal report for Advanced Simulation course (Advanced topics in Construction Engineering and Management), University of Alberta.
- Gonzalez, C., Hu, D., and Mogadam, M., 2010. Operations federate module in the Crane Lift Planning Game, internal report for Advanced Simulation course (Advanced topics in Construction Engineering and Management), University of Alberta.
- Halpin, D., 1976. CONSTRUCTO – an interactive gaming environment. *Journal of the Construction Division*, 102 (CO1), 145-156.
- Harris, F. C., and Evans, J. B., 1977. Road construction – simulation game for site managers. *Journal of the Construction Division*, 103 (CO3), 405-414.
- Hegazy, T., 2006. Easy plan: computer game for simplified project management training. *Proceedings of the first International Construction Specialty Conference (CSCE)*, n.p. May 23-26, Calgary, (Alberta, Canada).
- Jangmi, H., Zhang, H., and Farzaneh, S., 2010. Player federate module in the Crane Lift Planning Game, internal report for Advanced Simulation course (Advanced topics in Construction Engineering and Management), University of Alberta.
- Kuhl, F., Weatherly, R., and Dahmann, J., 2000. *Creating computer simulation systems: an introduction to the high level architecture*. Prentice-Hall International PTR, One Lake Street, Upper Saddle River, NJ 07458.
- McCabe, B., Ching, K. S., and Rodriguez, S., 2000. STRATEGY: a construction simulation environment. *Proceedings of Construction Congress*, pp. 115-120. Orlando (Florida, USA).
- Nassar, K., 2002. Simulation gaming in construction: ER - the equipment replacement game. *Journal of Construction Education*, 7 (1), 16-30.
- Scott, D. and Cullingford, G., 1973. Scheduling game for construction industry. *Journal of the American Society of Civil Engineers*, 99 (CO1), 81-92.
- Yaoyuenyong, C., Hadikusumo, B. H. W., Ogunlana, S. O., and Siengthai, S., 2005. Virtual construction negotiation game – an interactive learning tool for project management negotiation skill training. *International Journal of Business and Management Education*, 13 (2), 21-36.

RONALD EKYALIMPA

Ronald is a Ph.D. student at the Hole School of Construction Engineering in the Department of Civil and Environmental Engineering at the University of Alberta. His research focus is in the area of construction simulation.

SIMAAN M. ABOURIZK

Simaan holds an NSERC Senior Industrial Research Chair in Construction Engineering and Management at the Department of Civil and Environmental Engineering, University of Alberta, where he is a Professor in the Hole School of Construction Engineering. He received the ASCE Peurifoy Construction Research Award in 2008.

YASSER MOHAMED

Yasser is an Associate Professor in Construction Engineering and Management in the Department of Civil and Environmental Engineering, at the University of Alberta. His research focuses on simulation modelling of construction processes to support project planning and control.

FARZANEH SABA

Farzaneh graduated with her Ph.D. from the Hole School of Construction Engineering in the Department of Civil and Environmental Engineering at the University of Alberta. She now works for AECOM as a Structural Engineer.

PERFORMANCE OF EARLIEST COMPLETION STRATEGY IN ORDER SORTATION SYSTEMS

Fahrettin Eldemir ^(a), Elif Karakaya ^(b)

^(a)Fatih University- Department of Industrial Engineering

^(b)Technische Universität Dortmund- Chair of Factory Organization

^(a) feldemir@fatih.edu.tr, ^(b) karakaya@lfo.tu-dortmund.de

ABSTRACT

The Order Accumulation and Sortation Systems (OASS) are becoming more important as distribution centers try to gain competitive advantages. There are certain key parameters that affect the performance of Sortation Systems. The effect of these parameters can be measured by how they are affecting throughput or average sortation time. The time required to sort mixed items depends on the sortation strategy employed in the system. A new strategy called Earliest Completion Rule has been introduced. In this study, an analytical model for calculation of average sorting time of a newly introduced sortation strategy has been developed. It has been observed that the new strategy decreases the sortation time significantly. While available analytical models assume that all orders are at the same size (quantity), in this study this assumption is relaxed. Both analytical models and simulations are employed to compare sortation strategies for different order combinations and for various design choices. AutoMod Software is used as the simulation tool.

Keywords: logistics, sortation strategies, material handling, simulation

1. INTRODUCTION

In today's competitive world, it is desirable that a distribution center runs at its optimal settings to gain a competitive advantage. More efficient distribution centers are needed to respond to increasing competition and to an increased emphasis placed on time-based service. In distribution centers, long lists of orders are put together in an intensive way. Each customer order can include various items in different quantities. In classical order picking procedure, each order is collected by an assigned picker and the products in this list might be stored at different storage addresses. Therefore, pickers may end up travelling to far distances in a warehouse in order to complete the list and searching the items all over the warehouse. This situation often causes unnecessary transportation costs and ineffective worker utilizations. To overcome shortages mentioned above, the zone picking method is widely used in warehouses. In this picking method, the

items from different orders are arranged over again (batch orders) and the same product types be collected by the same workers. With this method, order pickers are assigned to a specific zone. In this way, unproductive travel time will disappear. However, although this situation saves time and speed, the items of accumulated orders are completely mixed because the items collected by different pickers arrive of the packing are at different times. While waiting for the other items from the same order they are accumulated in a place. There is no doubt that these products (items) have to be sorted according to the product type and quantity before shipping. At this point, sortation systems (these are often automated systems) are used.

The optimal condition for a given system studied would be one in which the rate of sortation (i.e., throughput rate) is maximized, thus minimizing the wave sortation time without increasing the capital and operating costs. There is a trade-off between the rate and cost. Using more resources such as labor and machines can increase the rate of sortation; however, the cost of sortation thus increases. This research focuses on maximizing the throughput rate of a given system and assumes that the other variables, such as cost and operating design parameters, are held within satisfactory limits.

There are different sortation strategies available: namely, Fixed Priority Rule, Next Available Rule, and Earliest Completion Rule. Some analytical models for these sortation strategies have been developed in earlier studies. However, the sortation models are limited to one induction lane and one sortation lane.

2. LITERATURE REVIEW

Up to this point, only a few studies have dealt with Accumulation and Sortation Order System (OASS). The first example of related to sortation strategies is developed by Bozer et al. (1988). The Fixed Priority Rule (FPR) is for lane assignment by simulating different waves of orders. Johnson (1998) developed a dynamic sortation strategy which is called Next Available Rule (NAR) and compared it with "FPR". Eldemir (2006) developed an alternative sortation strategy called Earliest Completion Rule (ECR) by using order statistics.

Closed-loop simple conveyor design researches contain a different numbers of induction lane and sortation lanes. Especially the first studies are hypothesized one induction and one sortation lane. However, later on, due to increase of orders and product variability, the conveyor design converted into many induction and sortation lanes. The following, table summarizes the literature on closed-loop conveyor system analysis according to the number of its induction and sortation lanes.

Table 1: Literature Review about Conveyor Design

Sortation Literature Summary					
Citation	Method	Problem Setting			
		One Ind.	Many Ind.	One Sort	Many Sort.
Bozer and Sharp (1985)	Simulation	√		√	
Bozer et al (1998)	Simulation	√			√
Johnson and Lofgren(1994)	Simulation	√			√
Johnson (1998)	Analytical	√			√
Meller (1997)	Analytical	√			√
Schmidt and Jackman(2000)	Analytical	√		√	
Johnson and Meller(2002)	Analytical		√		√
Russell and Meller(2003)	Descriptive		√		√
Bozer (2004)	Analytical		√		√
Eldemir (2006)	Analytical	√		√	

3. SORTATION SYSTEM DESIGN

3.1. One-One Model

In One-One Model (Figure 1), one induction lane and one sortation lane are available. Induction lane is sometimes called as “accumulation lane”, as well. When the literature is evaluated thoroughly, it can be observed that this model is the first applied model to the re-circulating conveyor. For instance, Bozer and Sharp (1985) have carried out this model in order to develop sortation strategies.

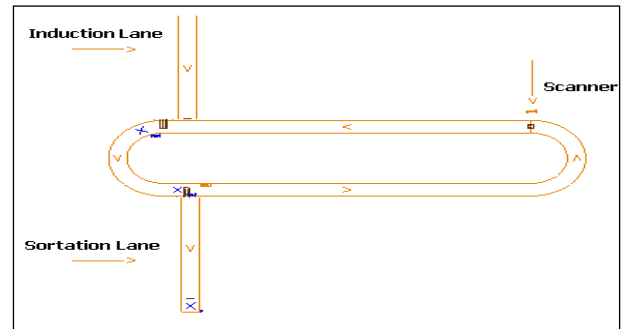


Figure 1: One - One Model Conveyor Design

3.2. One-Many Model

The One - Many Model (Figure 2) differs from the previous model since it has more than one sortation lane. When compared with others, this model is the frequently applied. For instance, Johnson and Lofgren (1994), Johnson (1998), Meller (1997) have used this model in their studies.

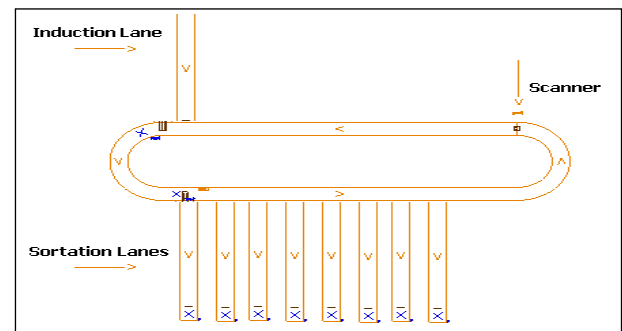


Figure 2: One - Many Model Conveyor Design

4. SORTATION STRATEGIES

Sortation strategies can be classified into two families, fixed priority rules (FPR) and dynamic assignment rules. In fixed priority rules, the orders are prioritized before sortation based on a certain rule. Dynamic assignment rules are assignment strategies that consider the item locations on the conveyor. The most common examples of this family are the next available rule (NAR) and the earliest completion rule (ECR). All parameters are determined below:

Table 2 : Notation

y	Number of items within an order
m	Number of orders within a wave
l	Length of closed-loop conveyor
v	Speed of conveyor
t	Time for an item to circulate around main sortation line
n	Number of accumulation lanes
i	Item index within an order
j	Order index within a wave
q	Number of orders sorted thus far

4.1. Fixed Priority Rule (FPR)

Sortation time evaluation by using Fixed Priority Rule is exemplified underneath. The number of accumulation lanes is accepted as one and the number of items within the order is constant.

The length of the track (closed-loop conveyor) is:

$$T = \frac{L}{v} \quad (1)$$

Assuming that the location of item i in the order j is uniformly distributed onto the conveyor, items will keep their positions on the conveyor throughout the sorting process, because the closed-loop conveyors speed is constant. Thus sorting time is found by subtraction of the last item from the first item.

The probability distribution function for the uniform distribution will be:

$$f_{l_{j1}}(l) = \left(\frac{y}{T}\right) \left(1 - \frac{l}{T}\right)^{y-1} \quad 0 \leq l \leq T \quad (2)$$

The expected time for the first item to arrive to the sortation lane will be:

$$E(l_{j1}) = \frac{T}{y+1} \quad (3)$$

In the same way, the probability distribution function of the last order statistic will be:

$$f_{l_{j[y]}}(l) = \left(\frac{y}{T}\right) \left(\frac{l}{T}\right)^{y-1} \quad 0 \leq l \leq T \quad (4)$$

The expected location of the last item will be:

$$E(l_{j[y]}) = \left(\frac{y \cdot T}{y+1}\right) \quad (5)$$

Thus, the expected time difference between the last item and first item will be:

$$E_{TS} = \frac{T(y-1)}{y+1} \quad (6)$$

Under FPR, the orders are ranked at the beginning of the sortation process. Two fixed priority rules which are commonly used in industry: namely “the smallest order first” and “the largest order first”. The expected dispersion is the same for all orders since the location of the items in each order is independent from the other items of the other orders. For this reason, the index of $[j]$ is eliminated from the expression (5). The expected

gap between order $[j]$ and following order $[j]$ is the expected difference between the position of the first box in the order $[j]$ and the last box in the previous order $[j]$.

$$E_{TG} = E(l_{j1} - l_{[j-1][y]}) = \left(\frac{T}{y+1}\right) \quad (7)$$

Under FPR, the sorting time for all orders within the specific wave will be the sum of all gaps and spreads as follows:

$$T_{FPR} = \frac{m \cdot T \cdot y}{y+1} \quad (8)$$

4.2. Next Available Rule (NAR)

In the Next Available Rule, once sortation of an order is finished, the next order is selected dynamically. Sortation lane selects the first item (box) that arrives and the items belong to same order as the next for the sortation process. Those boxes will be sent to shipping next. The expected sorting time for each of them depends on the number of orders which left to be sorted.

In this Next Available Rule, the expected sorting time for each order is depends on the number of orders which left to be sorted. Assuming that the locations of the items (l) in the remaining orders are independent and uniformly distributed, and q the number of orders sorted. Then the following formulation shows the probability distribution function of the first box:

$$f_{l_{j1}}(l) = \left(\frac{y(m-q)}{T}\right) \left(1 - \frac{l}{T}\right)^{y(m-q)-1} \quad 0 \leq l \leq T \quad (9)$$

The expected value of the gap between the last item of order $[q]$ and the next order is given below:

$$E_{TG}(q) = \frac{T}{y(m-q)+1} \quad (10)$$

The expected location of the last item of the order $[q+1]$ is thus derived:

$$E(l_{[q+1][y]}) = T \left(1 - \frac{m-q}{y(m-q)+1}\right) \quad (11)$$

Additionally, the expected time difference between the last item and first item will be:

$$E_{TS} = T \left(1 - \frac{m-q+1}{y(m-q)+1}\right) \quad (12)$$

Under NAR, the sorting time for all orders within the specific wave will be as follows:

$$T_{NAR} = T \cdot \sum_{q=0}^{m-1} \left(1 - \frac{m-q}{y(m-q)+1} \right) \quad (13)$$

4.3. Earliest Completion Rule (ECR)

In the dynamic assignment category, another sortation strategy model is the Earliest Completion Rule (ECR). When sortation of an order is finished, the next order is determined based on the location of the last items. The order with the last item being closest to the accumulation lane is selected as the next order to be sorted. Like NAR, the sortation time will depend on the number of orders which are going around on the main sortation lane. Assuming that all items are randomly and uniformly distributed on the closed-loop conveyor and the item locations are independent of each other, from order statistics, the probability density function of the last item of an order (f_{l_y}) will be the following:

$$f_{l_y}(l) = \left(\frac{y}{T} \right) \left(\frac{l}{T} \right)^{y-1} \quad 0 \leq l \leq T \quad (14)$$

The cumulative distribution of l_y will be:

$$F_{l_y}(l) = \left(\frac{l}{T} \right)^y \quad 0 \leq l \leq T \quad (15)$$

The decision time comes for the next order; there are $m-q$ orders which are waiting to be sorted. Therefore, there will be $m-q$ last cartons which are distributed on the closed-loop conveyor with probability density function given by (14). Among these last cartons, the one with lowest l value located closest distance to the accumulation lane will be selected. The probability density function of this smallest l value can be attained by using the first order statistics.

$$\begin{aligned} f_{l_y^{\min}}(l) &= (m-q) \cdot [1 - F_{l_y}]^{m-q-1} \cdot f_{l_y} \\ &= (m-q) \cdot \frac{y}{T} \cdot \left[1 - \left(\frac{l}{T} \right)^y \right]^{m-q-1} \cdot l^{(y-1)} \\ &0 \leq l \leq T \end{aligned} \quad (16)$$

The expected order sorting time $[q+1]$ can be found from the following statement:

$$E(l_{[q+1][y]}) = \frac{y(m-q)}{T^{y(m-q)}} \cdot \int_{l=0}^T [l^y \cdot (T^y - l^y)^{m-q-1}] dl \quad (17)$$

In Earliest Completion Rule, the total wave sortation time is given:

$$T_{ECR} = \sum_{q=0}^{m-1} \left(\frac{y(m-q)}{T^{y(m-q)}} \cdot \int_{l=0}^T [l^y \cdot (T^y - l^y)^{m-q-1}] dl \right) \quad (18)$$

5. EXPERIMENTATION

5.1 One-One Model

5.1.1 Analytical Model

An empirical method is used to compare ECR, FPR and NAR. In developing the analytical models, several assumptions are made to facilitate the analysis. To illustrate the expressions for the three sorting strategies, the time to traverse the re-circulating conveyor is $T = 100$ seconds, and there are $m = 10$ orders in each wave with $y = 5$ boxes per order. For analytical model experimentations, MAPPLE software is used.

Table 3: Sorting Times for Numerical Examples

Sorting Sequence (Order number)	Order Sorting time (seconds)		
	FPR	NAR	ECR
1	83,33	80,39	57,26
2	83,33	80,43	58,40
3	83,33	80,49	59,70
4	83,33	80,56	61,19
5	83,33	80,65	62,94
6	83,33	80,77	65,04
7	83,33	80,95	67,64
8	83,33	81,25	71,02
9	83,33	81,82	75,76
10	83,33	83,33	83,33
Total	833,30	810,64	662,29

5.1.2 Simulation Model

A simulation method is used as well in order to compare ECR, FPR and NAR. Several assumptions are made to facilitate the simulation analysis. To illustrate the expressions for the three sorting strategies, the time to traverse the re-circulating conveyor is $T = 222, 8$ seconds, and there are $m = 10$ orders in each wave with $y = 5$ boxes per order. A hundred repetitions are done for each simulation experiment. Then, the mean value of these repetitions is taken.

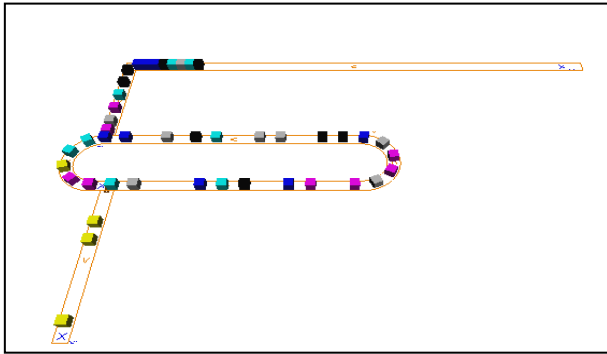


Figure 3: One-One Design Model Simulation Figure

For simulation model experimentations, AUTOMOD software is used. Figure 3 is the figure of the AutoMod software for One-One Design Model.

Table 4: Sorting Time Comparison for One-One Model by Using Simulation Model

Model	FPR	NAR	ECR
One-One Model	2.248,78	2.179,25	1.841,70

5.1.3 Simulation Model versus Analytic Model

Simulation model and Analytical model outputs according to different scenarios are illustrated in the following Table 5.

Table 5 : Sorting Time Comparison for One-One Model Both Simulation and Analytical Models

Orders/ Wave	Items/ Orders	Wave Sorting Time (seconds)			Wave Sorting Time (seconds)		
		<i>Analytical Model</i>			<i>Simulation Model</i>		
		FPR	NAR	ECR	FPR	NAR	ECR
24	1	2676	214	214	2915	442	442
12	2	1784	1478	992	2033	1724	1484
8	3	1338	1246	974	1574	1507	1268
6	4	1070	1033	878	1298	1279	1120
4	6	765	754	695	1003	991	920
3	8	595	591	563	823	829	792
2	12	412	411	403	640	643	634
1	24	214	214	214	442	442	442

As Table 5 demonstrates, the Simulation Model's results are higher than the Analytical Models in every case. The reason for this is that in the simulation model, there are some additionally spent times. The following figure points out spending time locations on the simulation system.

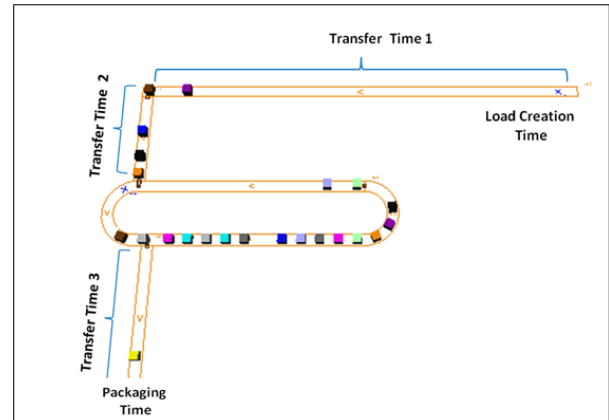


Figure 4: Extra Times Spending for Simulation

Table 6 shows averages of extra time for each spending point, which are shown in the previous figure. Besides, if subtraction is taken from simulation model to analytical model, the average difference is approximately 239 seconds. Also, the sum of the extra spending time is 234.86 second. Thus, we can say that these two numbers are too close to each other.

Table 6: Sort of Spending Time for Simulation

Spending Time	Duration
Transfer Time 1	49,5
Transfer Time 2	29,76
Transfer Time 3	35,2
Load Creation time	69,7
Packaging Time	50,7
Total Time	234,86

5.2 One-Many Model

5.2.1 Simulation Model

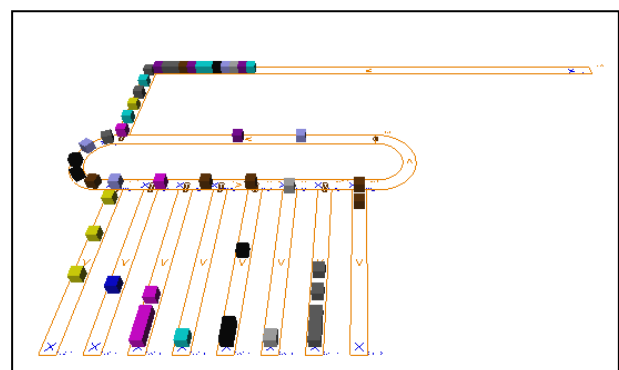


Figure 5: One - Many Design Model Simulation Figure

As can be seen clearly, the best One-Many Model is ECR model. Since the lowest value emphasizing the average of the total sorting time is given by ECR model.

Table 7 : Sorting Time Comparison for One - Many Model by Using Simulation Model

Model	FPR	NAR	ECR
One-Many Model	690,61	678,72	651,21

5.3 Random and Equal Number of Items in the Order

Earlier studies assumed that the number of items in an order is the same. For example, in Johnson's article (1998) an accepted item number is $y=5$ for any event. In practice, it is known that it cannot be provided for every wave. The number of items varies from one order to another.

Table 8 : Sorting Time Comparison of Sorting Strategies According to Number of y

	Number of y	FPR	NAR	ECR
One-One Model	Random	2142,65	2.116,97	1.818,30
	Equal	2248,78	2.179,25	1.841,70
One-Many Model	Random	668,95	650,04	636,46
	Equal	690,61	678,72	651,21

As illustrated by the figures above, random item size provides more time saving than equal item size also this does not reflect reality.

5.4 Number of Orders versus Number of Items

Different numbers of items and order combinations are designed in order to comprehend the sortation strategies behavior for various situations. After preparing 8 combinations, for example, 24-1 means that there are 24 different orders within a wave and all orders have only one item. Table 9 represents the strategies' results:

Table 9: Total Sortation Time for Different Sortation Lanes in One - One Model

Orders/ Wave	Items/ Orders	Wave Sorting Time (seconds)		
		FPR	NAR	ECR
24	1	2.915,41	441,8	441,8
12	2	2.032,74	1.723,56	1.484,25
8	3	1.574,19	1.506,52	1.268,18
6	4	1.297,91	1.279,31	1.119,80
4	6	1.003,05	990,58	919,74
3	8	822,74	828,92	792,45
2	12	639,51	642,73	634,12
1	24	441,8	441,8	441,8

As can be seen in Figure 6, great savings can be accomplished in total sortation time for every experiment by using ECR.

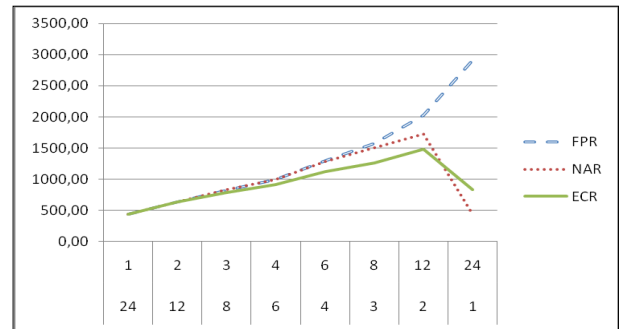


Figure 6: Total Sortation Time for Different Sortation Lanes in One - One Model

5.5 Effect of the Distance between Sortation Lanes

The following section will discuss whether distance between sortation lower is significant or not. In order to understand the effect, different model configurations are redesigned. The following two figures are about One-One Model. In the first figure, the sortation lane is located close to the induction lane to avoid a waste of time to reach the sortation lane. In the second one, the sortation lane is placed at the furthest point from the induction lane.

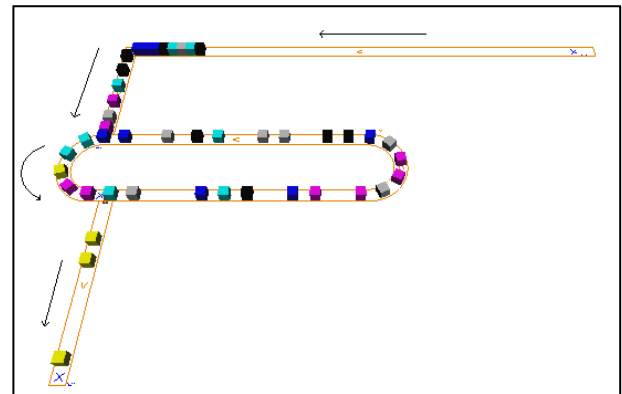


Figure 7: Close Sortation Lane for One - One Model

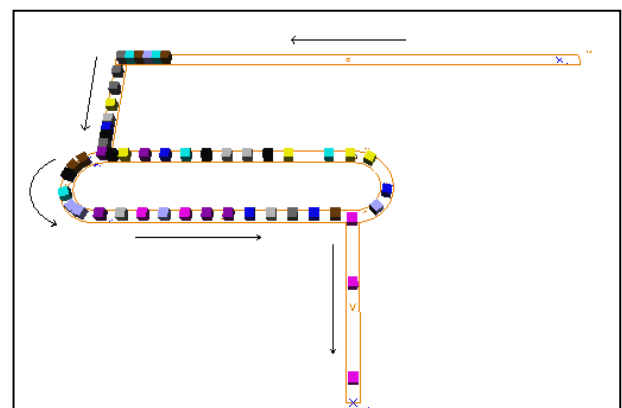


Figure 8: Remote Sortation Lane for One-One Model

Two designs are compared by sending the same number of orders and items. The results are shown in Table 10.

Table 10 : Different Distances between Sortation Lanes for One-One Model

Position of Sortation Lane	FPR	NAR	ECR
Close	2.248,78	2.179,26	1.841,71
Remote	2.248,03	2.179,14	1.841,61

As it can be understood from both tables and Figure 9, there is no significant difference in total sortation time between “Close” and “Remote” design. Thus the effect of the distance between sortation lanes in One-One Model is unimportant.

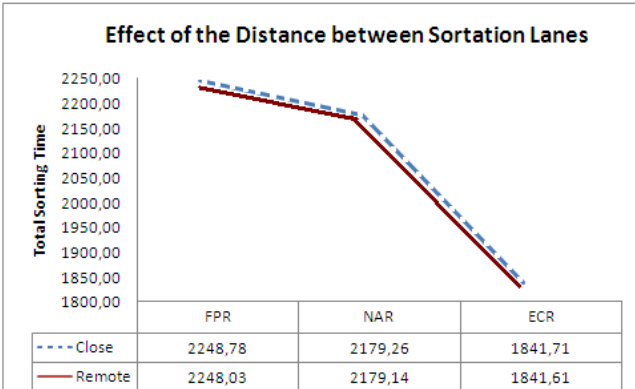


Figure 9: Effect of Distance between Sortation Lanes

The same analysis is repeated in One-Many Model. Differently from the previous figure in this figure, there are two sortation lanes. The following section will discuss whether, in this case, the distance between lane is significant or not. In order to understand the effect, two model configurations are redesigned. In the first figure, lanes are close to each other, whereas in the second figure they are located at the biggest possible distance.

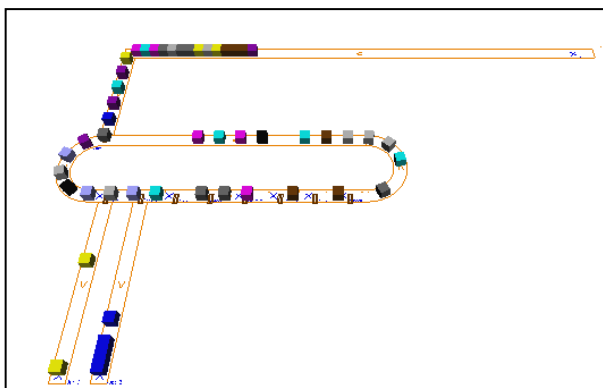


Figure 10: Close Sortation Lane for One - Many Model

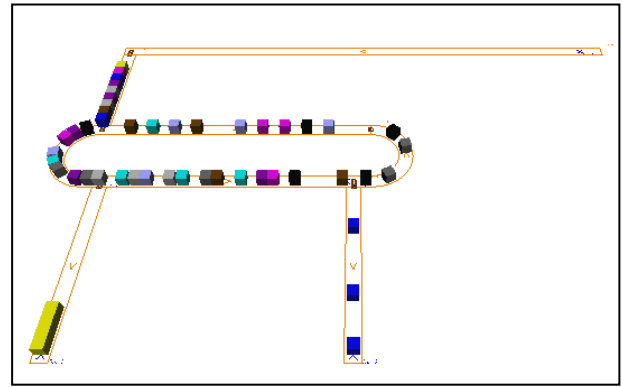


Figure 11: Remote Sortation Lane One - Many Model

The two designs are compared by sending the same number of orders and items. Results are shown in Table 11.

Table 11: Different Distance between Sortation Lanes for One - Many Model

Position of Sortation Lane	FPR	NAR	ECR
Close	1320,20	1502,12	1177,70
Remote	1375,42	1553,47	1261,14

As can be seen from in both Table 11 and Figure 12 the close sortation lane gives the best results. In fact, the difference between the two designs is not extremely big, but not insignificant either.

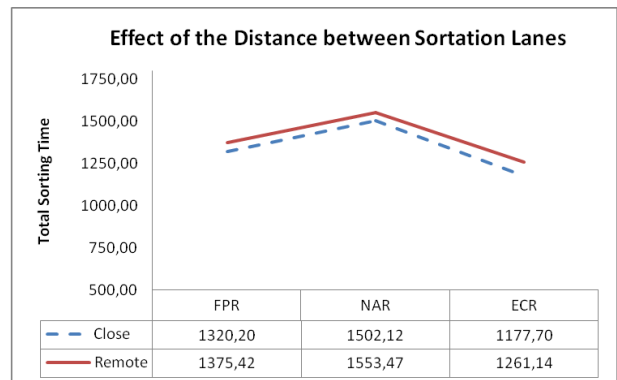


Figure 12: Effect of Distance between Sortation Lanes for One - Many Model

5.6 One –One Model versus One-Many Model

In the under mentioned situations, 12 orders that have just 2 items are sent to One - One Model, while doubled orders, in other words 24 orders that have 2 items are sent to One - Many Model which has two sortation lanes. Before the sortation, our estimation is that both outputs should be close to each other. Because the second one has double performance if it is compare to first one so twice as many order can be sorted in the same time.

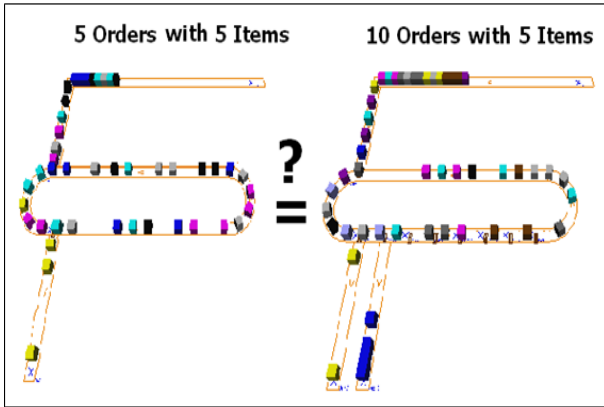


Figure 13: One – One Model versus One - Many Model

In this experimentation, number of orders $m = 10$ and number of items $y = 5$ are taken. Then, the number of orders is reduced by half. The results of this set of experiments are listed in Table 12.

Table 12: One - One Model versus One - Many Model

Model	Order	Item	FPR	NAR	ECR
One-One Model	10	5	1320,20	1502,12	1177,70
One-Model Model	5	5	1174,40	1147,94	1036,34

Distinctively, One-One Model for all strategy has less sortation time than One-Many Model. Thus, the doubling order size takes much more time even if one sortation lane to added.

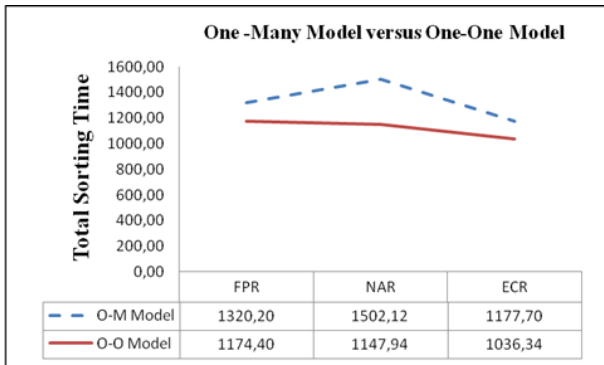


Figure 14: Effect of Distance between Sortation Lanes

6. CONCLUSION

In the course of this article, available sortation strategies have been compared and a set of modeling approaches in simulation and in analytical has been developed for the design and analysis of conveyor sortation systems. Consequently, the following conclusions can be drawn:

Based on simulation models, FPR, NAR and ECR sortation strategies have been compared. Overall outputs are represented as follows in Figure 15.

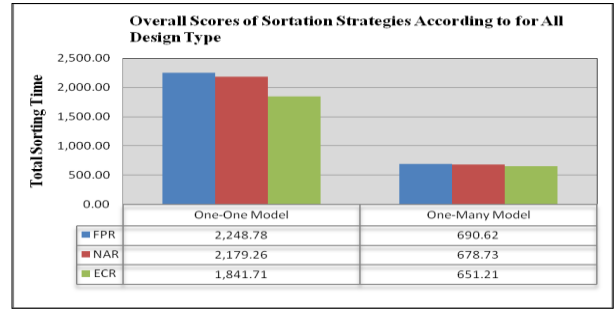


Figure 15: Effect of Distance between Sortation Lanes

Simulation models are developed for all designs, therefore, the results of simulation models are compared with analytical models and, this way, the simulation has been proved

Different scenarios are simulated by varying design and operational parameters. In contrast to the conclusions drawn by earlier studies in the field, random item size in an order supports better results. Besides, it is more appropriate for a real case.

The impact of distance between sortation lanes has been examined by designing model configurations. For One-One Model, there is no significant effect, whereas in One-Many Model the effects of distance cannot be ignored.

Design parameters and operational parameters have been compared. This study has demonstrated that adding extra sortation lane is insufficient to sort a doubled number of orders.

Future research can be pursued in the following directions:

- Analytical models for One - Many Model is required. In this research, analytical model is applied to only One - One Model. Thus, for other models, an analytical model should be developed in order to make comparisons with the result of the simulation model.
- Order configurations can be varied. For instance, 120-1 order combination is worth examining in order to clearly contemplate the behavior of sortation strategies.
- Other operational parameters such as conveyor speed, order assignment to specific lane before sorting and wave algorithm need to be conducted to see their effects.
- Other design parameters such as type of conveyor (circular and non-circular) and length of circulation conveyor must be analyzed.
- This research aimed to provide a case study. The design parameters of this study can be applied to a real case.

REFERENCES

- Bozer, Y.A., Hsieh, Y. J. 2004. Expected waiting times at loading stations in discrete-space closed-loop conveyors. *European Journal of Operational Research*, vol. 155(2), p. 516-532
- Bozer, Y.A., Quiroz, M. Sharp, G.P. 1988. An evaluation of alternate control strategies and design issues for automated order accumulation and sortation system. *Material Flow*, vol. 4, p. 265-282
- Demongodin, I., Prunet, F. 1993. Simulation modeling for accumulation conveyors in transient behavior. *COMPEURO 93*, Paris, France, p. 29-37
- Dotoli M., Iacobellis, G., Stecco, G. and Ukovich W. 2009. Performance Analysis and Management of an Automated Distribution Center, *IEEE Industrial Electronics IECON '09*, Porto, Portugal p 4371-4376
- Dotoli M., Iacobellis, G, Stecco, G., Ukovich W., 2009. Performance Analysis and Management of an Automated Distribution Center, IEEE
- Gagliardi, J, Angel R, Renault, J. 2010. A simulation modeling framework of multiple-Aisles Automated Storage and Retrieval System, *CIRRELT* vol. 57
- Eldemir, F. and Malmborg, C.J. 2006. Earliest Completion Rule: An Alternative Order Sortation Strategy. *Progress in Material Handling Research*, 2006, 1, p. 147-155
- Harit, S., Taylor G.D. 1995. Framework for the Design and Analysis of Large Scale Material Handling Systems. *Winter Simulation Conference*, Arlington, VA, USA, p. 889-894.
- Jayaraman, A., R. Narayanaswamy, et al. 1997. A sortation system model. *Winter Simulation Conference*, Atlanta, GA, USA, p. 866-871
- Jing, G., Kelton, W. D., Arantes, J.C. 1998. Modeling a Controlled Conveyor Network with Merging Configuration, *Proceeding of the Winter Simulation Conference*, Washington, DC, USA, p. 1041-1048
- Johnson, M. E., 1998. The impact of Sorting Strategies on Automated Sortation System Performance *IIE Transactions*, vol. 30(1), p. 67-77
- Johnson, M. E., Russell, M. 2002. Performance analysis of split-case sorting systems. *Manufacturing & Service Operations Management*, vol. 4(4), p. 258-274
- Johnson, M. E., Lofgren, T. 1994. *Model Decomposition speeds distribution center design Interfaces*, vol. 24(5), p. 95-106
- Koster, R., Le-Duc, T. and Roodbergen, K.J. 2007. Design and control of warehouse order picking: A literature review. *European Journal of Operational Research* vol.182, p. 481-501
- Le-Duc, T. and de Koster, R. 2005. Determining Number of Zones in a Pick-and-pack Order picking System. *ERIM Report Series Research in Management*, Rotterdam
- Maxwell, W. and Wilson, R., 1981. Deterministic models of accumulation conveyor dynamics, *International Journal of Production Research*, vol. 19(6), p. 645-655
- Meller, R. D. 1997. Optimal order-to-lane assignments in an order accumulation/sortation system. *IIE Transactions* 29, p.293-301
- Roodbergen, K.J. and Vis, I.F.A. 2009. A survey of literature on automated storage and retrieval system *European Journal of Operational Research*, Vol.194, p. 343-362
- Russell, M. L. and Meller, R. D. 2003. Cost and throughput modeling of manual and automated order fulfillment systems. *IIE Transactions*, vol.35, p. 589-603
- Schmidt, L. C. and Jackman, J., 2000. Modeling recirculating conveyors with blocking, *European Journal of Operational Research*, vol. 124, p. 422-436
- Sonderman, D. 1982. An analytic model for recirculating conveyors with stochastic inputs and outputs. *Internal Journal of Production Research*, vol. 20, p. 591-605

AUTHORS BIOGRAPHIES

Fahrettin Eldemir works as Assistant Professor at the Fatih University. He received his Ph.D. in Industrial Engineering from the Rensselaer Polytechnic Institute and his MS in Industrial Engineer from the Rensselaer Polytechnic Institute. His email address is <feldemir@fatih.edu.tr >

Elif Karakaya is a Ph.D. student in Chair of Factory Organization at the Technique University Dortmund. She received her M.S. in Industrial Engineering from the Fatih University, and her B.S. in Industrial and Computer Engineering from the Kltr University. Her email address is <karakaya@ifo.tu-dortmund.de>

RECONFIGURABLE AND LAYOUT-AWARE STORAGE SYSTEM FOR NETWORK-BASED SIMULATION MODELS IN THE SIMULATOR D³FACT

Hendrik Renken^(a), Felix A. Eichert^(b), Markus Monhof^(c)

^{(a)(b)(c)}Business Computing, especially CIM
Heinz Nixdorf Institute
University of Paderborn
Fürstenallee 11
33102 Paderborn, Germany

^(a)funsheep@mail.upb.de, ^(b)eichert@mail.upb.de, ^(c)monhof@mail.upb.de

ABSTRACT

Current simulation software typically provides limited types of storage components. But for accurate simulation results, warehouse operations have to be modeled close to reality. The static design of storage components found in current simulation software complicates the process of modeling. Especially the paths for workers or forklifts through a warehouse have to be defined manually. Furthermore, when the user makes changes to the warehouse layout he also has to adjust the paths. This process is cumbersome, time consuming and error prone. In this article we describe a warehouse system that can be customized to fit a diverse variety of storage types. Our implementation drives an automated mechanism, re-calculating paths when changes to the layout are made. Besides that, different storage types can be combined into one warehouse and the whole system may be reconfigured at runtime. At last we show the integration of the presented concepts into our research platform d³fact.

Keywords: material flow systems, d³fact, simulation, warehousing

1. INTRODUCTION

Simulating a system to understand its behavior for certain inputs is a well-established scientific method and is broadly used in research as well as in the industry. Today's enterprise simulation software uses network-based modeling to implement processes occurring in a company. Examples are production systems, warehousing systems or inter-company logistics. For these areas simulation software typically offers a wide range of building blocks where each contains a specific function or behavior. The combination of those blocks allows easy modeling even of complex scenarios. One part of a company that needs specific and detailed treatment is the storage area, because the question "Where to store this specific part?" can get quite complex and hard to answer. Some software packages therefore offer special products to answer just this one question (Incontrol Simulation

Software 2012). Thus modeling a plausible, complex and customizable storage is an important task. Our approach of a generic warehouse component allows us to define arbitrary warehouse layouts. This includes the combination of different storage types, e.g. block or rack storages. Furthermore, the storages can be located throughout the whole model.

When modeling a warehouse the definition of the drivable paths of the operating units (OU), e.g. forklifts or workers, consumes a major part of the deployed time. Especially, these paths have to be adjusted by the modeler every time the layout of the warehouse changes. In this paper we describe a solution that automatically adapts to layout changes and to reconfigured warehouse components at runtime. In our approach we integrate our generic warehouse component into a system for automated motion path finding (Fischer et al. 2010). This ensures that the OUs can be used throughout the model to transport goods. Due to the proposed design it makes no difference whether the goods are transported between machines, storages or, machines and storages.

In this paper we present our concept of a generic warehouse implementation with integration to a generic transportation service utilizing OUs like forklifts or workers. Furthermore we briefly lay out the implementation into our simulator d³fact.

2. CONCEPTS

In the following we will briefly describe the scenario used throughout this paper and the ideas behind our concept. To illustrate one possible application of the described components we use the multi-floor building example, which was introduced in Fischer et al. (2010).

The building is a factory laid out on three floors with production areas on the top floor, a storage area on the middle floor and a distribution center at its base (see Figure 1). Forklifts or workers either transport the production work pieces. Therefore ramps and stairs connect the different floors. The factory produces wheel caps. Plastic pellets are pressed into unfinished components. These components are then further

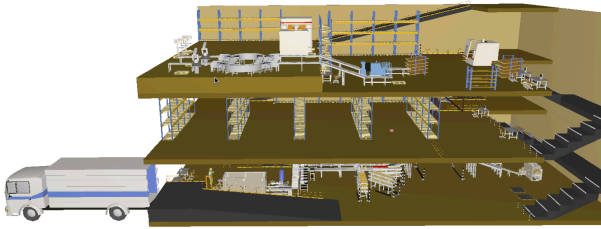


Figure 1: The Scenario: A Multi-Floor Factory Building.

processed into two different finished products. Customers can order the unfinished components (for individual processing) and of course the finished products. The model supports orders in large quantities as well as rush orders in small quantities. Products can be stored in large quantities on the middle floor. The lower floor is used as a packaging and shipping area. Forklifts transport large quantities of orders, while the workers can retrieve small quantities for rush orders or when parts are found to be missing during prepackaging. To model these dynamics the workers must have access to every storage area in the model, even the interim storages.

We can now use our warehouse component and its adaptive logistics to model the (interim) storage on the different floors. On each floor, storage racks are located. In the front of most of the machines block storages for interim storage can be found. Since we are not modeling the different storages as different warehouses in terms of our warehouse component, we can access every stored work piece from everywhere at any time. Using our warehouse component we can even easily add, move or remove storage racks at runtime without caring about the motion paths of the forklifts or workers. These paths are adapted to the new layout during the simulation. Furthermore, changes made to the set of storage components are also directly adapted. This enables rapid prototyping of new ideas and easy optimization of storage layouts, even throughout the whole factory.

The warehouse component is based on the concept of separation of the storage of actual goods from the logistic operations, which are executed on the storage. Figure 2 shows the basic structure that results from this separation. There are two main components that make up a warehouse: The *Storage* and the *Logistic Component*. The first one holds the goods in a specific storage structure, e.g. in a block storage or rack storage. The latter handles the input and output operations of the warehouse by executing appropriate storage/ retrieval operations. These operations can involve OUs moving the goods. The paths taken by the OUs to process the operation must be set manually in current simulation software. Because the manual approach takes a lot of time, we propose the usage of an automatic motion planning system.

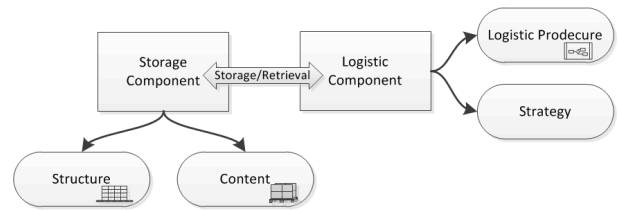


Figure 2: This Figure shows the Main Structure of the Warehouse Component in d³fact.

3. RELATED WORK

While there are many applications of warehouse simulations the number of related works, addressing generic and easy-to-use modeling approaches for warehouse simulations, are very scarce.

Muller (1989) identifies components that need special attention when building an automated warehouse system. He describes three modeling approaches and notes that the modeling complexity differs for different objectives and uses. Unlike us he does not outline a generic component, which lowers the modeling time, but gives general advices what to consider when modeling a warehouse for different types of simulation results. He identifies, among others, the warehouse layout and control logic, which we call strategy, as important components to consider when modeling a warehouse.

Gunal et al. (1993) provides a simulation model for *Automated Storage and Retrieval Systems* (AS/RS) and gives conclusions about the general use of them. The authors found that most of their code they had written to simulate a particular warehouse could be reused for similar scenarios. Since they are focusing on AS/RS they do not provide a solution to change the layout of the warehouse. So their generalization is limited to characteristics of AS/RS like for example the number of aisles or the number of pick-and-drop stations.

Takakuwa (1996) is also focuses on AS/RS and utilizes a component (building block) approach. He presents predefined AS/RS and *Automated Guided Vehicles* (AGVs) components that can be combined to serve different applications. Due to the focus on AS/RS systems with AGVs the presented components for the warehouse are not as highly customizable as ours. The only layout, which is supported, is the aisle based rack layout of AS/RS, which is one building block for which some parameters could be set. So the approach of splitting a warehouse in different components is done in that way that AGVs and conveyors are part of warehouses. In our simulator there also exists components for AGVs and conveyors, but we do not limit their application to warehousing scenarios.

In contrast to that the problem of automated path finding in geometrical space is well researched. Motion planning in general is e.g. discussed in (Canny 1988) and (Brady 1982). de Berg et al. (2008) describes motion planning based on trapezoidal space partition, obstacle enlargement to support OUs with a size and how to support OUs with rotation. Latombe (1991) also addresses motion planning in general but furthermore,

he discusses several problems in depth, one has to deal with when creating a motion planning system. This includes e.g. how to manage obstacles, multiple moving objects and kinematic constraints. The system (Fischer et al. 2010) utilized in this paper uses an octree as a structure to partition the geometric space. It is based on a two dimensional approach by Chen et al. (1997). Also there are methods, which especially can be used in warehouses. Klaas et al. (2011) describe a knowledge-based approach on automated way finding for AGVs in dynamic warehouse environments (He also utilizes the method presented by Fischer et al. (2010)). A real-time motion planning method for highly dynamic environment with multiple participants is given in Vannoy and Xiao (2008).

4. THE WAREHOUSE COMPONENT

As stated before, the warehouse component is based on the concept of separating the storage of the actual goods from the logistic operations, which are executed on the storage (cp. Figure 2).

4.1. The Storage Component

The *Storage Component* defines the storage's structure. One part of the structure is the position of the goods. This way, the *Storage Component* can determine the position of each good in space and the distance between them. This is needed, to compute the time needed to access a good and to properly visualize the storage.

The other part describes through specific rules which positions and therefore which goods are accessible. In the following we explain the rule system on the example of a block storage. However, it is easy to model a specific, e.g. custom storage type, by just replacing the rules. The block storage depicted in Figure 3 has a total space for eight goods, where goods occupy four spaces. Now the aforementioned access rules for block storages define the space *B1* as inaccessible, because *B2* is occupied. One has to remove the good from *B2* to access *B1*. Also it is physically not possible to store a good in *A2* without an occupied *A1* space. Therefore, *A2* is also inaccessible.

To implement a new storage type, the structure and access rules have to be defined and stored goods of to be mapped to certain positions. This makes it very easy to customize a warehouse for a specific scenario.

We further separated the goods from the actual space they are stored in (cp. Figure 2). This design enables the interchangeability of the storage types. The storage type can be modified by simply replacing a structure by another one and then remapping the stored goods to the new structure. Because the set of stored goods is not affected, this can be done even at runtime. The user now can start a simulation and change the parameters of the warehouse - including the storage type - while the simulation continues. This is a big advantage for rapid prototyping. Even while a simulation is running, a user can play around with the storage type and test the performance of each getting a direct feedback.

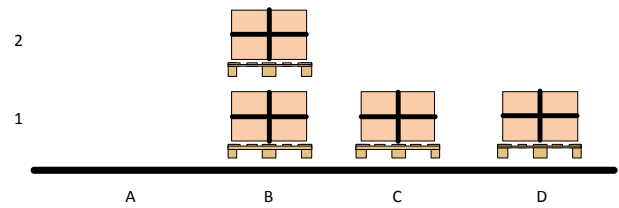


Figure 3: This is a Basic Representation of a Block Storage. There are Eight Spaces in this Storage. In Four of Them Goods are Stored.

4.2. The Logistics Component

Until now, we only discussed the static structure of our warehouse. In this section we will explain how the goods are transferred in and out of the *Storage Component*. The *Logistics Component* represents an interface to a storage and executes the input and output operations on the storage component.

The component itself is an abstract state machine and represents the generic input/output operation and the current state of such an operation. In our implementation an operation can be in the three states *Idle*, *Searching* and *Delivering*. A separate *Logistics Procedure* contains the logic how a particular good is stored or retrieved. The supervising component uses the procedure to compute the time needed for a particular operation. Such a procedure can e.g. implement the usage of OUs like forklifts or workers, represent a harbor crane, or an AS/RS. More abstract the procedure can even be directly related to the storage type and allow the implementation of physical processes like gravity for chute based storage types.

In our scenario of the multi-floor factory the racks on the second floor are embedded into the usual material flow using procedures that utilize forklifts to transport the goods. However, the interim storages in the top floor at the machines are embedded into the material flow using simple procedures with a static timed delay. Furthermore, to let workers from the lower floor also “see” and access these storages for rush orders, the interim storages have a second logistics component with a procedure utilizing the workers. In Section “MODEL-WIDE MOTION PLANNING INTEGRATION” we will cover the implementation of this system into a model wide transportation system in detail.

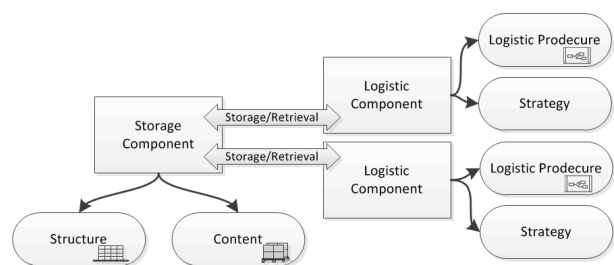


Figure 4: Several Logistics Access One Storage. Each Logistic has its own Production Definitions and Strategy.

This design of the logistics component has several advantages. Due to the decoupling of the logistics from the storage, it is easy to change the properties, like the storage capacity or type - especially at runtime. Furthermore, several logistic components can serve one storage component at the same time as you can see in Figure 4. In that figure you can see an example of two *Logistic Components* accessing one storage object. This enables, e.g. the modeling of several harbor cranes unloading a container ship or several forklifts serving one storage object at the same time.

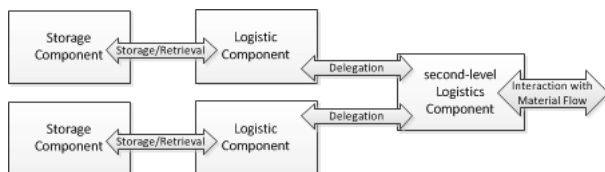


Figure 5: A *Second-Level Logistics Component* Delegates Operations to Two First-Level Components.

To allow the combination of all kinds of storage types into one “logical” warehouse we use *second-level Logistics Components*. These components aggregate several first-level components and the storage structures they are attached to as it can be seen in Figure 5. If an input/output-operation has to be executed the second-level component delegates the operation to the appropriate first-level component. This allows the integration of the first-level components into the material flow as usual and furthermore provides the same interface for the overall warehouse. Depending on the logistics component responsible for the current operation, the state of the second-level component is adapted. This ensures parallel operations for the different first-level components but also sequential operations on a particular logistics component. Depending on the state of the first-level components one could also choose different strategies, although we didn’t explore this further. Besides the structural planning, the warehouse strategy usually is the focus of optimization in real life. Since changes made to the strategy usually do not result in expensive investments, it is a usual practice to optimize this part first. A strategy in the warehouse component determines a free storage space for a good to be stored in the component. Due to the volatility of the strategy, it is a separate component in the *Logistic Component*. This allows the strategy to be exchanged with customized implementations for static models and during runtime. It is even possible to have the strategy exchanged automatically, e.g. triggered by events generated from the simulation.

5. LAYOUT-ADAPTIVE WAREHOUSE LOGISTICS

Utilizing an automated motion planning system to access a storage object allows the implementation of layout-adaptive warehouse logistics. Up to this point, we assumed that the storage structure of a warehouse is static. The layout of a warehouse component was

interchangeable, but the layouts themselves are static. This circumstance prevents the optimization of some important aspects of warehouses and their layouts, especially during a simulation run. A modeler might want to try different values for the gap between racks in a storage object to optimize space utilization and access by forklifts. Goetschalckx and Ratliff (1991) explain an approach to calculate optimal lane depths in block storage systems and compare their results to traditional concepts where all lanes have the same depths. With our system, a simulation-based comparison could be easily done with several different lane configurations.

The current, static implementation results in a try-and-error approach, which makes the optimization of a warehouse layout slow and cumbersome. One reason for this is, that by changing certain values of a warehouse, many other values have to be changed as well. For example, when using OUs to access a warehouse the *Logistic Procedures* need to know the exact positions of the goods to calculate the time needed to move. When the position of a storage object is changed or the layout of the scene changes, the motion paths to the storage spaces can get compromised. In current implementation the modeler has to manually adapt the paths, which is a complex and cumbersome task.

With the integration of an automated motion planning system, we enable the modeler to freely reposition storage structures. This enables him to easily test different settings. Furthermore, due to the proposed separation of the different components, changing the location of a storage object does not affect the stored goods or current operation. This means, the modeler can adjust the layout during a simulation run, getting direct feedback. How we integrated the motion planning into a model-wide transportation system is explained in the next section.

6. MODEL-WIDE MOTION PLANNING INTEGRATION

An important factor for simulation analysis is realistic motion paths through a defined factory layout. Typically, these paths have to be modeled manually, which is a cumbersome, time consuming and error prone task. Besides that, these paths have to be manually maintained when changing the layout.

To solve this problem Fischer et al. (2010) present a motion planning framework for automatic route calculation in three-dimensional environments. The framework is capable of automatic analysis of a given factory layout and of computation of motion paths for moving objects like fork lifts or workers (cp. Figure 6). At first the scene is divided into small cubes, called voxel. These voxel then are analyzed for a driving surface for a specific moving object, taking into account the size and the supported slope.

A problem arises from the usage of these moving objects with a warehouse like the one from our scenario (cp. Figure 1). Because the racks are located throughout the factory, transportation tasks vary with the location

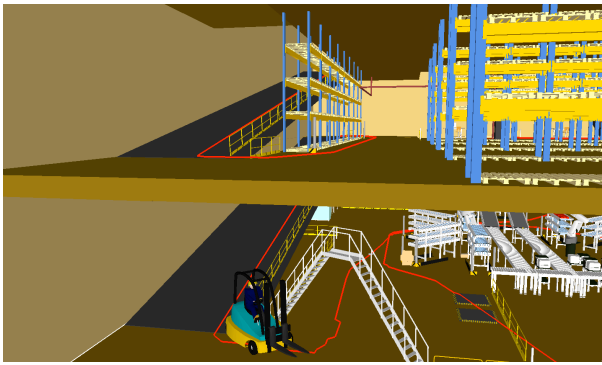


Figure 6: Motion Planning in a Production Plant Modeled in d³fact.

of the object carrying out the task. Taking these variations into account are very important for the overall performance of such a simulation model.

To solve this problem we use a supervisor that schedules transportation tasks to minimize the overall processing time. The system is implemented in a very generic way so that we can use it to carry out transportations from a machine to particular storage space or even to drive housekeeping processes. The supervisor is a core component of the model-wide transportation system. It collects transportation jobs and schedules them to the operation units. A job always contains a start and an end position. Based on these positions a pick-up and a drop-off time can be estimated. These are updated whenever the scheduled plan changes due to new or updated jobs. As stated earlier, the *Logistics Procedures* are the interfaces between the warehouse logistics and the transportation system. While the logistics component itself is integrated into the material flow. Consider, that one of the machines on the top floor of our example finishes a product. Now a worker has to transport the product to a rack. The logistics component, connected to the machine, receives the information about the finished product. It asks the procedure, how long does it take to transport the item. The procedure itself issues a new job with the start position being the machine and the drop-off position being the rack to the transportation system. To control which OU processes which job, only certain OUs capable of handling the issued jobs are linked to the *Logistics Procedure*. The transportation system then integrates the job into its plan, considering the different available OUs and their positions. The procedure then notifies its parent of the estimated completion time, which changes its state from *Idle* to *Delivering*. When the job is finished the component returns into the *Idle* state.

7. IMPLEMENTATION INTO D³FACT

In our discrete event simulation software d³fact (Renken et al. 2011) we use a concept called *composition and aggregation* to remove the need for a static type hierarchy in our component definitions. While static inheritance type hierarchies are simple to understand since it is natural for us humans to arrange

objects taxonomically (Sommerville 2004, Shaw and Garlan 1996), they can become hard to maintain because of the limited possibilities for enhancement. With the two patterns *composition* and *aggregation* a type hierarchy can be simplified or completely removed (Gregory 2009, Deacon 2005). The benefit of this concept is exposed when it is used to combine entirely different subsystems into one object. In d³fact an object is represented by a dynamic set of “properties”. While there are very different approaches to identify a set of properties, we use a generic container concept to sustain the object-oriented approach common in current simulation model architectures. The container type provides methods to manage its properties (add, delete, get by key, etc.).

Simple properties like numerical values or strings are passive, meaning they do not react to state changes and also do not cause them. These properties are aggregated (the weak ownership): The container object owns them but they are not bound to the life cycle of the container object. The “logic” instead, is an active property, because it does react to state changes. E.g. when an event is caught, the “logic” initiates the processing of the event as a perception. Composition strongly binds a property to a container, which means the property is bound to the container’s life cycle and also receives a reference to it. Through this reference the property can access the container, the simulation core, the model and other objects within the model.

We are able to attach so called “listeners” to various objects and also properties. Through these properties, objects are able to get notified when various events or changes happen in the simulated system, for example when other properties are changed. The listener concept allows for handling dynamics in the system, as well as implementing measuring figures such as throughput of a simulation model.

The components presented in are implemented using this object-oriented approach. The *Storage Component* and the *Logistic Component* each are implemented as logic properties combinable in a container object. For commencing operations on the storage, the *Logistic Component* has a reference to the *Storage Component*. While the basic operations are composed into these containers, the specific behavior of the storage and the logistic is each implemented into a separate property. These are used by the logic properties to process events that are triggered by other parts of the scene.

8. CONCLUSION

We presented a generic and flexible warehouse implementation. The presented concept allows the modeling of different types of storages with minimum effort. The components can be combined to form bigger, logical warehouses. This allows the usage of model spanning processes like the fork lifts and workers retrieving goods from our example. Through the separation of the goods and the storage structure we are even able to reconfigure the components at runtime,

enabling rapid prototyping. In combination with a motion planning component, it is possible to change the layout of the warehouse without caring about the motion paths for the operating units.

REFERENCES

- Brady, M., 1982. Robot motion: Planning and control. The MIT Press.
- Canny, J., 1988. The complexity of robot motion planning. The MIT Press.
- Chen, D.Z. and Szczerba, R.J. and Uhan, J., 1997. A framed-quadtree approach for determining Euclidean shortest paths in a 2-D environment. *IEEE Trans. Robotics Automat.* 13(5):. 668 – 681.
- de Berg, M. and van Kreveld, M. and Cheong, O. and Overmars, M., 2008. *Computational Geometry: Algorithms and Applications*. Springer-Verlag Berlin Heidelberg.
- Deacon, J., 2005. Object-Oriented Analysis and Design. ADDISON-WESLEY.
- Fischer, M. and Renken, H. and Laroque, C. and Schaumann, G. and Dangelmaier, W., 2010. Automated 3D-Motion Planning for Ramps and Stairs in Intra-Logistics Material Flow Simulations. *Proceedings of the 2010 Winter Simulation Conference (WSC 2010)*. IEEE, Omnipress, 1648 – 1660.
- Goetschalckx, M. and Ratliff, H., 1991. Optimal lane depths for single and multiple products in block stacking storage systems. *IIE TRANSACTIONS*, 23, no. 3, 245–258.
- Gregory, J., 2009. Game engine architecture. A K Peters, first ed.
- Gunal, A. and Grajo, E. and Blanck, D., 1993. Generalization of an AS/RS model in SIMAN/CIMENA. *Proceedings of the 25th conference on Winter simulation*. ACM, 857–865.
- Incontrol Simulation Software, 2012. *Enterprise Dynamics Products*. Available from: <http://www.incontrolsim.com/en/products.html> [April, 2012].
- Klaas, A. and Laroque, C. and Dangelmaier, W. and Fischer, M., 2011. Simulation aided, knowledge based routing for AGVs in a distribution warehouse. *Proceedings of the 2011 Winter Simulation Conference*. IEEE, 1668– 1679.
- Latombe, J.C., 1991. Robot motion planning. Springer.
- Muller, D., 1989. AS/RS and warehouse modeling. *Proceedings of the 21st conference on Winter simulation*. ACM, 802–810.
- Renken, H. and Fischer, M. and Laroque, C., 2011. An Easy Extendable Modeling Framework for Discrete Event Simulation Models and their Visualization. *Proceedings of The 25th European Simulation and Modelling Conference - ESM'2011*.
- Shaw, M. and Garlan, D., 1996. Software Architecture: Perspectives on an Emerging Discipline. Prentice Hall.
- Sommerville, I., 2004. Software Engineering. Addison Wesley, seventh ed.
- Takakuwa, S., 1996. Efficient module-based modeling for a large-scale AS/RS-AGV system. *Proceedings of the 28th conference on Winter simulation*. IEEE Computer Society, 1141–1148.
- Vannoy, J. and Xiao, J., 2008. Real-time adaptive motion planning (ramp) of mobile manipulators in dynamic environments with unforeseen changes. *Robotics*, IEEE Transactions on, 24, no. 5, 1199–1212.

AUTHORS BIOGRAPHY

Hendrik Renken studied computer science at the University of Paderborn, Germany. Since late 2007 he is a research assistant at the Heinz Nixdorf Institute. His research interests are multi-domain simulation engines and in particular material flow simulation models.

Felix A. Eichert studies business computing at the University of Paderborn, Germany. Since early 2008 he is a student assistant at the Heinz Nixdorf Institute. In his bachelor thesis, he designed the warehouse component described in this paper.

Markus Monhof studies business computing at the University of Paderborn, Germany. Since mid 2011 he is a student assistant at the Heinz Nixdorf Institute. He helps to extend the simulator d³fact to new problem domains.

TOWARDS THE IMPLEMENTATION OF A HANDBALL PLAYER AGENT FRAMEWORK

João Jacob[†], Rosaldo J. F. Rossetti[‡], António Coelho[†], Rui Rodrigues

[†] INESC TEC – INESC Technology and Science

[‡] Artificial Intelligence and Computer Science Laboratory (LIACC)

Department of Informatics Engineering (DEI)

Faculty of Engineering, University of Porto (FEUP)

Rua Dr. Roberto Frias S/N, 4200-465, Porto – PORTUGAL

{joao.jacob, rossetti, acoelho, rui.rodrigues}@fe.up.pt

ABSTRACT

Sports simulation can help to assess the performance of strategies and players in a sand-boxed environment. Ultimately it can lead to improved real-life performance of actual teams if it is able to provide useful information to the team coach or manager. Many tools are now available for many different sports, most notably Soccer Server Simulator, a soccer simulator, that has already attracted many researchers from the artificial intelligence community into developing intelligent agents (soccer players) for them to form teams to play against each other in simulated matches. This paper presents a methodology for developing agents for testing and further developing the Handball Sport Simulator, which is based on the Soccer Server Simulator. The main contribution of this work is to provide a basic, expandable, agent architecture, specifically capable of playing at a Handball Sport Simulator server, while at the same time testing what features and sport's rules of the Handball Sport Simulator have been implemented correctly.

Keywords: workstation design, work measurement, ergonomics, decision support system

1. INTRODUCTION

Agent-based models as means of portraying complex environments such as sport games are not new. These simulators consist of several agents cooperating and competing towards common or opposite goals. Information exchange, coordinating tasks or competing for resources are appropriate scenarios to be modeled through the multi-agent metaphor. This is also verifiable in real-life situations, thus making agents a valuable addition for simulators that attempt to simulate those scenarios, being sports simulators very complete, as cooperation and coordination are needed as well as the competition for a goal.

Several of these simulators exist, for many sports. One of the most widely known is the Soccer Server Simulator, which even has its own category in the RoboCup competition (Chen 2002). The goal of this simulator is to be a tool useful for the development and testing of artificial intelligence techniques, as it serves as a test-bed for teams of agents to compete with the same resources, implying that one team can only defeat another if it is tactically superior. As this simulator is

agent based (each agent represents one player in a game), it allows for everyone interested in developing an agent to do so in any programming language, provided that it respects the client-server protocol that the Soccer Server Simulator requires.

However, there are still other sports that lack the availability of an easy-to-use agent-based simulator. In order to bridge this gap, a Handball Server Simulator (Santiago 2011) was recently developed, being based on the Soccer Server Simulator's core engine. This allowed the Handball Server Simulator to retain most of the added value of the original Soccer Server Simulator, such as the ease of use and the ease of developing agents for it. However, being such a new simulator, there are currently no agents developed specifically for it, and as such, it is difficult to assert if the simulator is missing features (such as game rules) or if those already present were incorrectly implemented.

The purpose of this work is to provide a framework for the development of simple cooperative handball agents capable of testing the implemented features of the handball server. It is not the focus of this work the development of a highly robust and competitive handball agent. The agent can be later improved upon, as it is further tested with the simulator, while the simulator is also updated taking these tests into consideration.

The remaining part of this paper is organized as follows; the Methodology section, describes the designed model, how it was implemented and the limitation of certain approaches. The Results section provides some results of the testing of the prototype agent in the Handball Server Simulator, and finally the Conclusions section, summarizes the achieved goals and criticizing the obtained results whereas also providing some future goals for the rest of this project.

2. RELATED WORK

Multi agent simulation is a technique used for simulation in several scenarios with different purposes (Murakami 2003). One possible scenario for multi agent simulation to be used is team sports. The most notable simulator would be the Soccer Server Simulator that is used in the RoboCup competition (Chen 2002). There are practically no multi-agent sports simulators similar to the Soccer Server Simulator for other sports. In order to fill this gap the Handball Server Simulator was

developed (Santiago 2011). It provides a solution for simulating handball matches in a similar way to that of the Soccer Server Simulator.

Although there are no other agents developed for the Handball Server Simulator, since the basis of the simulator is the Soccer Server Simulator, it is possible to adapt existing ones. Considering that most of the principles used in the development and testing of agents for the Soccer Server Simulator also apply for the Handball counterpart, an existing soccer agent can be adapted easily with minor changes in the client-server protocol and expected changes in its behavior, as it will now be playing handball and should perform accordingly. Having this in mind we opted to adapt an existing agent architecture, designed for the Soccer Server Simulator, into a Handball Server Simulator player.

Zang and associates discuss on of how agent architectures can be developed specifically for the usage in the Robocup soccer simulator (Zhang 2000). They explain how agents interact with the simulation environment, capturing information from it, building representations of that information, deliberating and acting based on those representation and the information exchanged among them. They also provide an overview of the architecture of some teams which take part in that competition. The CMUnited-99 (Reis 2001) (a former champion of the competition) was identified as having a behavior-based architecture, a common architecture for agents, as they take actions depending on the actual world state. Other architectures were identified, such as the layered architecture. This architecture is similar to that of the architecture used in this work, where there is a clear separation between layers of basic abilities or actions, client-server commands, interpretation of received information and higher level abilities, such as spatial reasoning and ponderation. This architecture can be found in teams such as RobologKoblenz99, among others (Certo 2007).

Candea and associates noted the importance of coordination in multi-agent simulations such as the Robo Cup simulator (Candea 2001). They mention how communication based coordination can help improve team performance and self-organization in a more reliable way. Other forms of coordination, as well an autonomous coordination or heterogeneous agents' coordination are referred. However, communication based coordination as a means of distributed coordination was found to be the preferred approach in their work, as it eases the burden of coordination (agents do not have to rely on "coach" like tactics) and ensures homogeneity. The issues identified, such as the dynamic assignment of roles and team strategies are important ones. These issues and the importance of roles in this context have also been identified elsewhere (Åberg 1998).

Positioning the agents of a team correctly is also an issue, since the environment they are at is very dynamic. Akiyama proposed a solution for finding suitable positions for each agent, based on the status of

the environment (Akiyama 2008). The method requires training data to be collected and has several advantages such as being fast, scalable, accurate and reproducible. A similar approach was that of Reis and his associates, that based the positioning and coordination of a team on predefined tactics and formations (Reis 2001). This allowed the team to dynamically change the gameplay, position and roles of its players in different situations of the game. They considered a "High level decision module" that was responsible for outputting adequate actions taking into account formations, roles, state of the world and the game's situation. The adaptability of this solution provided very positive results with the FC Portugal team (using this approach) winning most matches against several of the RoboCup teams.

Genetic algorithms have also been used for the training and performance evaluation of RoboCup simulator teams (Aronsson 2003). However, they are hindered by the usual limitation of this type of algorithms, such as overfitting, limited search space, expensive computation and premature convergence. Even so, it was proven that it is possible for software robots to learn the rules of simulated soccer.

3. METHODOLOGIC APPROACH

The aim of this work is to provide a framework for the creation of handball player agents for the Handball Server Simulator while also testing it via the agents developed with said framework.

3.1. Specifications of a Handball Player Agent

Although there are some similarities between the Soccer Server and the Handball Server, as they both simulate a team sport, played with a ball, two opposite goals on a rectangular field, since the rules for each sport are different, there has to be differences between them.

As such, it is expected that a player agent developed for the Handball Server Simulator will differ from one aimed at the Soccer Server Simulator. Similar to a soccer player agent, however, a handball player agent will attempt to accomplish its goals while ensuring that the game's rules are respected. In light of this, it is possible to adapt a soccer player agent's code into a handball one as they differ (in terms of their own logic) in rules to respect (which influences their available actions).

3.2. Handball Server Simulator communication protocol

The Handball Server Simulator, like the Soccer Server counterpart is part of a client-server architecture consisting of a game (the server) that is disputed by two teams, formed by several players (the clients). The server will provide information regarding the game's state to all of the agents so that the agents may deliberate upon it and act by sending to the server individual actions. Each agent receives both common (such as the game's score or what the other players are saying) and unique information (such as what is in its

field of view) from the server. Thanks to this approach, both servers allow for clients to be implemented in diverse ways, as long as they respect the server's protocol.

Prior to designing and developing the agent's behaviors it was deemed necessary the creation of an architecture for its basic modules. Since the Handball Server Simulator was based on the protocol of the Soccer Server Simulator, searching for a released simple Soccer Server Simulator agent's code that could serve as a basis for this work. From that basic code, we could change the needed protocol parts and agent behaviors.

Since the communication between the Handball Server Simulator and the clients (agents) is made via sockets (UDP/IP), these clients may be implemented in any language and run on any device as long as they comply with the server's protocol.

Determining what the protocol was, relied on consulting the Soccer Server Simulator's protocol (Chen 2002) as well as the source code for the Handball Server Simulator. The handball simulator has many common aspects with the Soccer Server Simulator's protocol as it can be seen in the table 1 and table 2.

Table 1: Comparison between Soccer Server Protocol and Handball Protocol (Client to Server)

Soccer Server	Handball Server	Behaviour
Init	Init	Registers the player in the server
Kick	Throw	Allows a ball that is in possession by the player to be kicked or thrown with varying force and angle
-	Step	The agent takes one step with the ball in its hand without releasing it (moving without dribbling)
Catch	Catch	The agent catches a ball that is in his range of action
Change_View	Change_View	Allows the agent to change its viewing angle. A wider angle allows for more information to be seen and a narrower one for the information seen to be of higher quality
Say	Say	The agent can share information with all agents present in the field
Move	Move	Places the agent instantly at a given position of the field (only available when the game hasn't started)
Sense_Body	Sense_Body	Asks for a sense_body command to be sent back from the server

Turn	Turn	Allows the agent to rotate its whole body a variable number of degrees
Turn_Neck	Turn_Neck	Allows the agent to only turn his head a variable number of degrees while keeping the rest of the body in the same orientation
Dash	Dash	The agent is capable of running at a certain direction and intensity

Table 2: Comparison between Soccer Server Protocol and Handball Protocol (Server to Client)

Soccer Server	Handball Server	Behaviour
Hear	Hear	Agent is capable of receiving all messages that were transmitted to the server using the Say command from any agent
See	See	Agent captures visual information relative to his position and orientation, as the presence of other players, the ball, goals or game lines
Sense_Body	Sense_Body	Provides some information of the current situation of the agent such as current speed and stamina

As the above two tables show, there is not much difference from the handball server to the soccer server in terms of protocol. The two major differences are the Step command, that does not exist in the Soccer Server and the Throw command that behaves exactly like the Kick counterpart in the Soccer Server. The Step command is, as the name suggests, a step to be performed with the ball in hand (assuring that the ball is not lost, unlike dribbling with the ball in the Soccer Server). However, as the rules of Handball imply, only 3 steps may be taken with the ball in possession.

4. A FRAMEWORK TO DEVELOP HANDBALL PLAYER AGENTS

Since the goal of this work was to create a basis for the development of Handball Server Simulator agents, there was no need to choose a Soccer Server Simulator agent with complex behavior code. As such, the chosen base code was of the krislet-0.2 (Langner,2011) agent as it was a simple soccer agent that was already capable of processing many soccer server commands, being some of those commands also present in the handball server.

This agent was chosen instead of other candidates (such as Agent2D) as it contained nearly no logic for soccer or other sport-related notions, such as strategy. Since the focus of this work is mainly to create agents that test what features the handball server has working,

a complex agent isn't needed. The portion of code that was responsible for the agent's connection to the server was mostly left unaltered as the Handball Server Simulator's protocol is similar to the Soccer Server Simulator's in that aspect, and only values such as the port of the running server and team names were changed. Other elements, concerning the client-server protocol, that were present in the original agent's code were replaced or omitted in the final code.

Besides the client-server protocol, the original architecture of the agent was mostly left intact. However, there were some changes worth noticing.

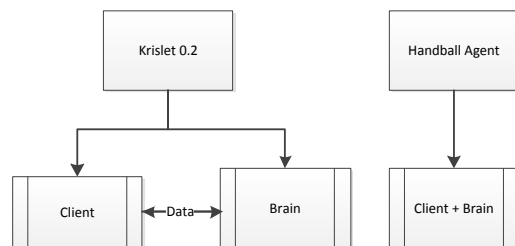


Figure 1: Diagram representing original architecture (left) versus the final architecture (right)

As it can be seen in figure 1, above, the original architecture was multi-threaded. This feature served the purpose of running the "Brain" thread (responsible for the decision making process) concomitantly with the "Client" thread (responsible for the client-server communication and parsing of the data), allowing for the agent to never miss a server communication, even while performing the needed calculations prior to sending a command to the server. Although, in theory, this can be considered a useful feature there were some issues to be addressed:

Synchronism: If the "Brain" thread was processing a received command, the "Client" thread should not update that received command in the event of receiving a server communication, as it might lead to mixing old information with new one. This means that new information is stored in a stack and the Brain will access the next item in that stack whenever it is done processing the current one. This can lead to the client's notion of the game's current state to be severely out of synchronization with the server's.

Wasted cycles: If the "Brain" thread finishes computing a command and has not received a new command to process, it will continuously verify if there are new requests to process. Even though the authors of the original code included a *sleep* call to help reduce the number of wasted cycles, this means that there is a possibility that the server and client are not synchronized, as the server may send new information to the client while the "Brain" thread is sleeping, wasting several milliseconds in this state.

All these issues pointed that a multi-threaded agent was difficult to synchronize and as such would not add any value to the solution, as it led mostly to wasted processing cycles. There is no gain in using separate threads for the retrieval and sending of commands and

the processing of said commands if these tasks are to be executed sequentially. So, the architecture was changed to a single threaded one. This was done easily, and meant only changing the "Brain" thread's infinite cycle to a simple function that would be called each time whenever the "Client" thread would receive the server's commands. Part of the "Brain's" thread was left intact, the part that dealt with initializations and preprocessing, as we felt it would not interfere with synchronization issues when the agent started processing game instructions.

Table 3: Comparison between the original code's protocol and the final code's protocol

Original Code Protocol	Final Code Protocol
Init	Init (altered to include default values)
Shoot	Throw (operates the same way as shoot)
Say (unused in Brain class)	Say (altered to be used with objects of the Message class)
Dash	Dash
Turn	Turn
Catch(unused in Brain class)	Catch
Move	Move
See	See
Sense_Body(unused in Brain class)	Sense_Body
Hear(unused in Brain class)	Hear

As the above table 3 depicts, the original code's protocol did implement many commands (the Client class had each command implemented individually as a function). However, many of these commands were not used for the original agent behavior.

Most notably, the original soccer agent's code did not make use of the "say" command for inter-agent communication. This is a much needed feature for developing a cooperative team of agents for any team sport. In order to fill this blank, a "Message" class was created that allows the agent to send and receive coordination-specific content.

Instantiating a handball player and results
After designing the final architecture of the agent, it was necessary to develop a prototype handball agent. This agent should make use of all the previous mentioned features of the developed architecture. The developed agent implements a simple behavior, as depicted in figure 2.

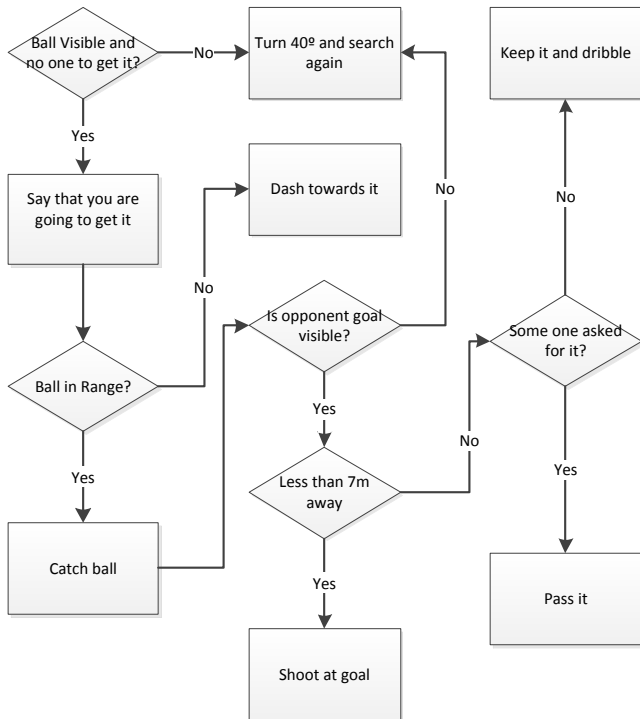


Figure 2: Agent Behavior

With this behavior, the commands present in table 2 were tested. Note that inter-agent communication and coordination was also tested and allowed for simple teamwork to be achieved. The untested commands were inherited directly from the Soccer Server Simulator’s core engine and, as such, did not need any testing in order to validate them.

Table 4: Test coverage of client-server commands

Handball Server	Testing Status
Init	Tested
Throw	Tested
Step	Tested
Catch	Tested
Change_View	Untested
Say	Tested
Sense_Body	Tested
Turn	Tested
Turn_Neck	Tested
Dash	Tested
Score	Untested

And the following simulator objects were identified and used correctly by the handball agent.

Table 5: Simulator object identified and use in the agent’s behavior

Object retrieved by “see”	Presence in agent behavior
Ball	Present

Flag	Present
Player	Present
Goal	Present
Line	Present

Finally, we were able to validate the following rules of the sport[10] in the Handball Server Simulator. This validation was made by checking the messages that were sent and received by the agent and the server, and by the game’s referee. Additionally, most of these could be seen via the server’s graphical viewer.

Table 6: Handball rules verification by the agent when connected to a server

Handball Testing Status	Server Status	Handball Server Testing Status
Do not block or kick ball using feet		Server doesn’t verify
Do not hold ball for more than three seconds		Tested
Do not bounce the ball, catch the ball and bounce it again		Server doesn’t verify
Take no more than three steps with the ball caught		Tested
Do not enter goal area		Tested
Do not touch the ball lying inside the goal area		Server doesn’t verify
Do not charge the opponents or run into a defending player		Untested
Do not engage in passive play		Server doesn’t verify
Do not steal the ball from the hands of an opponent		Untested
Do not push or hold attacking player’s body		Untested
Stay at least 3 meters away from the attacking player when restarting the game		Server doesn’t verify
Goalkeeper cannot take the ball outside the area		Tested
Goalkeeper cannot take the ball inside the area		Tested

As table 6 suggests, some defensive features were untested, as the focus of the agent’s behavior is mainly an offensive one. These untested features have to be validated by a human, (passive play, charging, pushing or holding adversaries) much like how “fouls” are handled by humans in the soccer server (Chen 2002). Other rules were not verified by the handball server,

meaning that although the agent was tested in a scenario where that rule would be infringed, the handball server did not punish the team for doing so.

5. CONCLUSIONS AND FUTURE WORK

The current work served both the purpose of creating a foundation for the development of future handball server simulator agent behaviors and of exposing the limitations of the server that result in an unrealistic representation of the sport. Although nearly all issues are due to the fact that the server has its roots in the Soccer Server Simulator, these issues were less relevant there. These issues revolve around the fact that the simulator is a 2D simulator and the players' physiognomy has been simplified. This means that at this time the server is incapable of determining if:

- The ball has been blocked or kicked using the feet
- The player is "in the air" when inside the goal area
- There was physical contact, such as a collision between opposing players
- The dribble was valid
- The defending player is closer than 3 meters to the attacking player when the game is being restarted

The Handball Server Simulator is also missing the implementation of some other handball rules, but that does not have to do with the simulators limitations. In fact, even in real life some rules are difficult to apply; for instance, the "passive play" rule is triggered if the players in possession of the ball aren't focused on attacking, solely preoccupied in maintaining the ball possession, a free throw is awarded to the opposing team.

The presented agent behavior server the purpose of proving that, currently, developing and testing handball agents is somewhat limited, as some rules of a handball game go unverified by the server. Furthermore these issues, if left unattended, can also lead to agents using strategies that would be rendered unusable in real life (such as long distance shots at the goal or passive play). Even so, these issues are acceptable due to the simulator being in its early days of development and having inherited some of these limitations from the Soccer Server Simulator. Hopefully, these foundations for the development of handball agents can help perfect the simulator, as it tested most of the rules and features already present in the Simulator.

We have presented the foundations of a handball agent, and also developed and tested a cooperative sample agent. Although the agent itself is still lacking some features, such as the capability of determining his position or the position of fellow and opposing players, these features can be easily added, thanks to the division of the "client" communication with the server and the "brain" component of the agent, responsible for the behavior and decision making of the agent. In fact, any further alteration to the agent is expected to be made only on the "Brain" component.

The next step for this project is to further develop the handball agent framework in parallel with the Handball Server Simulator. The development of a complete, cooperative and intelligent handball team of agents is the ultimate goal to be achieved. However, for that to happen, the Handball Server Simulator must see further development as well, to become more complete. Furthermore, testing new server features and developing more complex handball agent behavior will be needed and as such, the proposed handball agent framework will serve as a base for these future steps in this project.

REFERENCES

- Åberg, H. (1998). *Agent Roles in RoboCup Teams*. Science And Technology , (February), 1-24.
- Candea, C. (2001). *Coordination in multi-agent RoboCup teams*. Robotics and Autonomous Systems, 36(2-3), 67-86. doi:10.1016/S0921-8890(01)00137-3
- Chen, M., Foroughi, E., Heintz, F., Huang, Z., Kapetanakis, S., Kostiadis, K., Kummeneje, J., et al. (2002). *RoboCup Soccer Server*.
- H. Akiyama(2008), *Multi-agent positioning mechanism in the dynamic environment*, RoboCup 2007: Robot Soccer World Cup XI, pp. 377-384, 2008.
- International Handball Federation, *Rules of the Game* , July 2010
- J. Aronsson (2003), *Genetic Programming of Multi-agent Systems in the RoboCup Domain*, M.Sc thesis, Lund Institute of Technology, 2003.
- J. Certo, N. Lau, L.P. Reis (2007), *A generic multi-robot coordination strategic layer*, First International Conference on Robot Communication and Coordination. Athens, Greece, 2007.
- L. Reis and N. Lau (2001), *Situation based strategic positioning for coordinating a team of homogeneous agents*, Balancing Reactivity and Social Deliberation in Multi-Agent Systems, From RoboCup to Real-World Applications, 2001.
- Langner, K., *Krislet* 0.2 (<http://www.ida.liu.se/~frehe/RoboCup/Libs/Sources/> Last accessed on September 3 , 2011).
- Santiago, C. B., & Reis, L. P. (2011). *Foundations for Creating a Handball Sport Simulator*. Information Systems and Technologies CISTI, 2011
- Y. Murakami, T. Ishida, T. Kawasoe, and R. Hishiyama (2003), *Scenario description for multi-agent simulation*, Proceedings of the AAMAS '03, pp. 369-376, 2003.
- Y. Zhang (2005), *Multi-agent systems: the Tao of Soccer* , Tutorial presented at SFU Survey, March 8th 2005.
- Zhang, B., Chen, X., Liu, G., & Cai, Q. (2000). *Agent architecture: a survey on RoboCup-99 simulator teams*. Proceedings of the 3rd World Congress on Intelligent Control and Automation (Cat. No.00EX393),1, 194-198. Ieee. doi:10.1109/WCICA.2000.859946Y.

MODELLING THE EFFECT OF SUGAR REFINERY POLLUTION IN A RURAL AREA IN CENTRAL MEXICO

Wellens A.^(a), González J.^(b), Torres-Jardón R.^(c), Barrera H.^(d)

^(a, b)Facultad de Ingeniería, Universidad Nacional Autónoma de México

^(c, d)Centro de Ciencias de la Atmósfera, Universidad Nacional Autónoma de México

^(a)wann@unam.mx, ^(b)julioadolfogonzalez@hotmail.com, ^(c)rtorres@atmosfera.unam.mx,
^(d)hbarrera@atmosfera.unam.mx

ABSTRACT

Mathematical models for atmospheric dispersion are being used in a wide variety of industrial applications. One of the most used Gaussian models is AERMOD, recommended by the US EPA to determine air pollution dispersion in urban and rural areas. AERMOD is used to determine the expected impact on air quality due to the operation of a sugar refinery located in a rural village in central Mexico. Air pollutant emission due to fuel oil and bagasse combustion during the refining process is considered as well as pre-harvest sugarcane burning.

Keywords: air pollution, dispersion modeling, AERMOD, sugarcane processing, pre-harvest burning

1. INTRODUCTION

A high percentage of the sugar supply is obtained from sugar cane (*Saccharum officinarum*), which is one of the most extensively cultivated grasses in tropical and subtropical regions in the globe. Brazil is the major producer of sugar cane in the world, being Mexico the second most important producer in Latin America (CVCA 2010).

An efficient crop can produce from 100 to 150 tons of sugar cane per hectare per year, having an efficiency of 12 to 13% for the extraction of sugar. In the extraction process, the sugar cane is grounded and squeezed to obtain the juice, generating bagasse as the principal sub-product. Bagasse consists basically of cellulose fibers, lignin and pentosan and has an elevated percentage of humidity (50%), sugar (about 2% on average) and strange materials (0.5% on average). Depending on different factors, such as ripeness, percentage of strange material, extraction type, *etc.*, up to 15-25% of the grounded sugar cane corresponds to bagasse. This material has been used traditionally as an energy source for the production process in sugar mills, due to their calorific power, converting these facilities in self-sufficient for power generation and thus *green*. As the production process in a sugar mill includes internal combustion, typically air pollutants as particulate matter, NO_x and SO₂ are emitted to the atmosphere.

The AERMOD dispersion model (US-EPA 2012) was used to estimate the effect of sugar cane processing in central Mexico; this model is a regulatory steady-state plume modeling system provided by the US-EPA that includes a wide range of options for modeling air quality impacts of pollution sources, making it a popular choice among the modeling community for a variety of applications.

AERMOD, as any other mathematical dispersion model, provides only an estimate of the atmospheric concentration of environmental pollutants, and its results depend on the quality of the corresponding input data, and the methodology used for its determination.

2. CASE STUDY

2.1. Study Area

Sugar cane was introduced in Mexico during the sixteenth century; sugar industry infrastructure has been developed since then. In the southern region of central Mexico, sugar production and commercialization has been one of the principal subsistence means since 1690. Different ancient haciendas are now industrialized sugar refineries. The process includes boilers which are operated under three different conditions: fuel oil only, bagasse only and mixed fuel (fuel oil and bagasse) feeding, so typical combustion pollutants such as fly ash, smoke and flue gases are expected to be emitted into the air in the region.

A typical sugar mill located in central Mexico at about 910 meters above sea level which has been working since approximately 75 years, is used to demonstrate the usefulness of the AERMOD. This sugar refinery is active during the sugar cane harvest time, which lasts 180 days (November – May). In this *zafra* period, the refinery works 24 hours a day and processes a daily average of 7 tons of sugar cane. Until two years ago, the plant was working with old processing units and 5 chimneys – including the original concrete chimney that has been in use since the mill started operations - using bunker oil fuel mixed with or without bagasse. Simple dust separators were used for controlling fly ash. However, as a response to claims of the surrounding local population, the process

was improved, more efficient dust control equipment was installed and fossil fuel use was reduced, using at present mainly biomass fuel (bagasse). The original concrete chimney was closed in May 2011 after the zafra period; it was replaced by a new chimney that started operations on December 6th, 2012. Nevertheless, although process conditions were considerably improved, the local population still claims that the sugar refinery is the most important source of pollution in the area.

Another issue of importance is that usually the sugar cane is burned in the field previous to harvesting, in order to increase the efficiency of the refining process. The refinery can also process the so-called green or not burned sugar cane, which however lowers process efficiency as the direct harvesting generates a higher proportion of impurities as roots and leaves in the raw material.

The raw sugar cane is supplied by 11 thousand hectares of cane plantations, owned by local peasants and distributed in different rather small and often irregular parcels located at distances up to 50 km from the refinery. According to its ripeness, approximately 7 tons of sugar cane needed daily are selected from day to day. Generally, different parcels provide the daily need of raw sugar cane, so up to 12 different burning sites may be expected. The pre-harvest burning takes place during approximately one hour in the morning. As the harvesting season (November-May) coincides with the dry season and thus worst conditions for air pollutant dispersion, it is likely that this burning will have a negative impact on the air quality in the surroundings of the sugar cane parcels, emitting fly ash and smoke that are very visible to the local population.

Figure 1 presents a general view of the studied sugar refinery; a difference in strength of emitted air pollutants is clearly visible in the photo; this is due to the specific operating conditions of each processing unit, as for example the used fuel type or effectiveness of the emission control systems.

Figure 2 shows a map of the study area, indicating the distribution of the sugar cane plantations near the mill.



Figure 1. Studied Sugar Refinery

2.2. Aim of the Study

The general aim of the study is to determine the influence area for the dispersion of air pollutants emitted by a typical sugar refinery in a rural area in central Mexico, based on present operating conditions and the use of the Gaussian dispersion model AERMOD.



Figure 2. Map of the Sugar Factory and Surrounding Sugar Cane Plantations. The Shaded Area Marks the Property Limits of the Mill

Specific aims are:

- Estimate the surrounding air quality by means of mathematical dispersion modeling.
- Determine whether or not the observed air pollution in the area can be assumed to come from the refinery.
- Determine if recent changes in the process have resulted in improvements on local air quality.
- Estimate the importance of the on-site sugar cane burning during the harvesting period.

3. METHODS

The AERMOD model was used to compare the contribution of the sugar refinery before and after the process improvements. Also the influence of sugar cane burning during the sugar cane harvest period on the particle concentrations was studied. The simulated pollutants are particulate matter ($\leq 80 \mu\text{m}$ in aerodynamic diameter), NO_x and SO_2 . AERMOD is a steady-state plume model that assumes that concentrations at all distances during a modeled hour are governed by the temporally averaged meteorology of the hour. In the stable boundary layer (SBL), it assumes the concentration distribution to be Gaussian in both the vertical and horizontal. In the convective boundary layer (CBL), the horizontal distribution is also assumed to be Gaussian, but the vertical distribution is described with a bi-Gaussian probability density function. In addition, in the CBL, AERMOD treats "plume lofting," whereby a portion of plume mass, released from a buoyant source, rises to and remains near the top of the boundary layer before becoming

mixed into the CBL. AERMOD requires only a single surface measurement of wind speed (measured between 7 z_o and 100m (where z_o is the surface roughness height), wind direction and ambient temperature. The general concentration equation used by AERMOD is:

$$C\{x, y, z\} = \frac{Q}{\bar{u}} p_y\{y; x\} p_z\{z; x\} \quad (1)$$

where Q is the source emission rate, \bar{u} is the effective wind speed, and p_y and p_z are probability density functions which describe the lateral and vertical concentration distributions, respectively.

3.1. Topography

AERMOD can run on flat terrain or considering the topographic elevations of the receptors and sources considered in the model; this information can be extracted from a digital elevation model (DEM), available from USGS topographic data. The sugar refinery is located in a flat area; however, east of the study region an area of rough topography can be observed (figure 3), so AERMOD was run in the complex orography mode. To introduce the topographic information, the digital elevation model corresponding to the region surrounding the sugar cane production facility was downloaded from the www.webgis.com site. This file was converted to the required AERMAP format and included in the modeling project.

Figure 3 represents the topography of the study area in three dimensions.

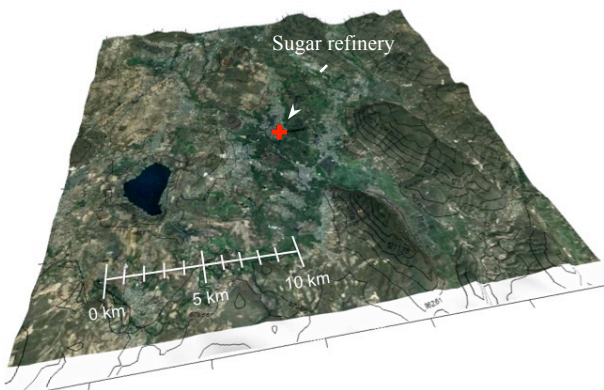


Figure 3. Digital Elevation Model for the Sugar Production Facility Surroundings (Vertical Exaggeration = 3x)

3.2. Meteorology

Meteorological information provided by the Forestry, Farm and Livestock National Research Institute (INIFAP), was analyzed for the year 2011, and statistical wind information for May 2011 was used to set a downwind air quality monitoring campaign for the most important ambient air pollutants and meteorological parameters during the last two weeks of the 2012 *zafra* and harvesting period.

Meteorological information of the study zone required by AERMOD includes: station number and location, year, Julian day, hour, temperature, wind

speed and direction, precipitation, humidity, station pressure and cloudiness. The standard meteorological files are converted to “.sfc” and “.pfl” files, respectively for surface and upper air meteorological information. Cloudiness is not routinely measured in meteorological stations in Mexico, so it is assumed to be zero. For modeling effects, only events were considered where precipitation was zero, because particle transport reduces when precipitation exists.

To generate the required “.sfc” y “.pfl” files, typical albedo, Bowen ratio y roughness length values are needed; these values were chosen according to the land use in the area, corresponding to respectively cultivated land from North to ESE directions and urban land use for the rest (see figure 4). Table 1 indicates the resulting land use parameters used in the AERMOD runs.

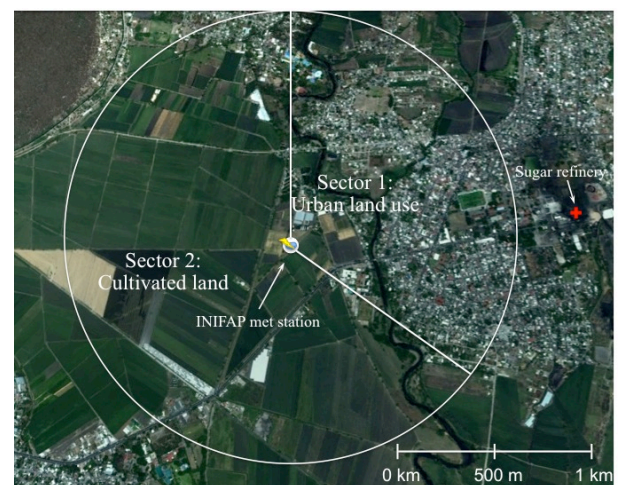


Figure 4. Land Use Sectors Specified in the Model

Table 1. Used Land Use Parameters

Sector	Albedo	Bowen ratio	Surface roughness length
1	0.28	0.75	0.0725
2	0.2075	1.625	1

3.3. On-site Monitoring

Preliminary AERMOD modeling was performed to be able to locate a temporary ambient air monitoring station in a specific site at the end of the harvesting period, in order to detect possible air pollutants transport from the refinery plant.

During May-June 2011, wind was coming prevalently from ESE-E and WSW-SW directions. According to this information, the 2012 monitoring site was set within the INIFAP research site, located at about 1.5 km from the refinery in WSW direction. Therefore, both the pollutant concentrations due to the dispersion of the sugar mill emissions when the wind was blowing towards the INIFAP and the background concentrations registered when wind was blowing in the opposite direction could be observed. The monitoring station was an AIRPOINTER (figure 5), which is a compact multi gas air quality monitoring system

capable of continuously measuring CO, NO/NO₂/NO_x, O₃, SO₂, and PM_{2.5}, and has meteorological sensors for wind speed, wind direction, ambient temperature, relative humidity, ambient atmospheric pressure, and precipitation.

An additional portable *DAVIS* meteorological station was set at the top of an elevated water tank (45 m) near the boiler stacks of the sugar refinery in order to check the representativeness of wind profile predictions of the model (figure 6).



Figure 5. Air Pointer Monitoring Station Installed in the INAFAP



Figure 6. Installation of a *DAVIS* Meteorological Station in the Sugar Refinery

3.4. Sugar cane burning

Sugar cane plantations in a 2 km radio area surrounding the plant were referenced geographically to be able to model the effect of daily sugar cane burning on air

quality. Only the nearest plantations were considered, as parcels at further distances are not likely to affect air quality in the village.

A daily processing rate of 7 tons of sugar cane corresponds to about 69.1 hectares/day; among the parcels dedicated to sugar cane harvesting in the 2 km radius around the facility, a random area of 69.1 hectares was selected. Emission factors for pre-harvest sugar cane burning (US-EPA 2005; Ribeiro 2008; Hall *et al.* 2012) were used to estimate particulate and NO_x emissions generated by the burning and the affectation was determined by means of the AERMOD model. Used emission pre-harvest burning emission factors are specified in table 2.

Table 2. Emission Factors for Pre-Harvest Burning

Pollutant	Emission factor (g/s m ²)
PST	0.0092273
NO _x	0.0006944

3.5. Plant Emissions

Data of the emissions strength and physical characteristics of the 5 boiler stacks were provided by the staff of the sugar refinery. The physical characteristics of the sources are presented in table 3, while tables 4 and 5 indicate the emission strength before and after the change to the use of bagasse as a fuel. Note that emission source 1 corresponds to the concrete chimney that stopped working in May 2011; chimney 1b is the new chimney.

Table 3. Physical Source Characteristics

Characteristics	Emission sources					
	1	1b	2	3	4	5
Height (m)	30	30	30	36	30	36
Diameter (m)	0.6	2.3	1.62	1.6	1.6	1.6
Exit velocity (m/s)	5.94	18.5	9.16	9.16	8.20	9.14
Exit temperature (K)	399	458	433	494	427	458

Table 4. Average Source Emissions 2009-2011

Pollutant	Emission sources				
	1	2	3	4	5
SO ₂ (g/s)	7.2	22.34	26.42	19.33	20.25
NO _x (g/s)	0.46	4.91	2.35	3.37	3.47
PST (g/s)	0.05	0.64	0.51	0.62	0.47

Table 5. Source Emissions 2012

Pollutant	Emission sources				
	1b	2	3	4	5
SO ₂ (g/s)	91.75	NA	21.94	19.64	21.89
NO _x (g/s)	18.26	NA	4.31	3.84	4.41
PST (g/s)	23.17	NA	4.84	1.94	1.93

Tables 4 and 5 indicate that SO₂ concentration has stayed the same after the process improvements, while NO_x and PST concentrations have increased considerably. This is because bagasse has a lower calorific capacity, so more fuel is needed when using bagasse than when using fossil fuels.

3.6. AERMOD Implementation

To implement AERMOD, the following activities were performed:

- Obtaining of the DEM of the study region
- Mounting of the regional topography in the terrain preprocessor for its posterior use in the AERMOD dispersion model
- Obtaining of Google Earth maps for the study area and their geographical referencing
- Adaptation of the 2011 meteorological information with the meteorological preprocessor AERMET and introduction of the resulting data in AERMOD
- Specification of the modeling region and receptor grid
- Compilation of the physical characteristics and emissions values for the emission sources
- Physical determination of the geographical references of the emission sources and inclusion of the geo referenced elements in the dispersion model.

4. RESULTS

4.1. Meteorology

The wind speed in the area is quite low, presenting average wind speeds of 2.1 m/s, 42% of calms and over 80% of winds below 4 m/s. Predominant wind directions are from southeast in winter, and from southwest in summer, being the wind speed lower in winter. Figure 7 presents the wind rose for 2011.

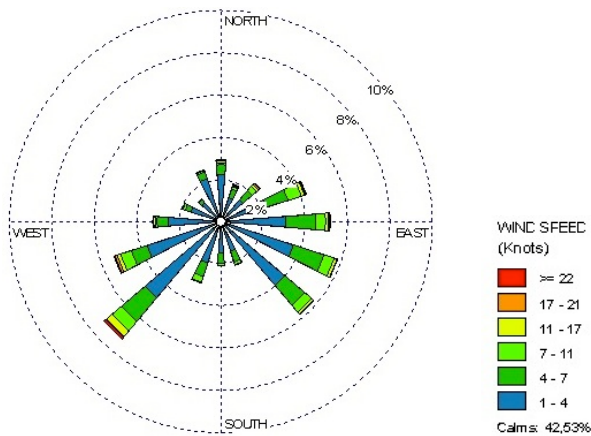


Figure 7. Wind rose in the study area, 2011

4.2. Particulate Matter Concentration

The 24-hour average PST concentration was estimated with AERMOD using the meteorological information for the 2011 *zafra* period. Operating conditions before and after the process improvements were modeled, using the land use parameters specified in table 1. Figures 8 and 9 respectively present the modeling results for the maximum 24-hour PST concentrations found during the *zafra* period, before and after the partial substitution of fossil fuel by bagasse.

Figures 8 and 9 indicate that maximum 24-hour PST concentrations were found to be respectively 6

$\mu\text{g}/\text{m}^3$ when only fossil fuel is used and $39 \mu\text{g}/\text{m}^3$ when approximately half of the fossil fuel is substituted by bagasse. The increase of maximum PST concentrations is due to the lower calorific capacity of bagasse, so more bagasse than fossil fuel is needed for the sugar refining process. Still, the present fuel configuration generates local PST pollution far below the $210 \mu\text{g}/\text{m}^3$ specified as the maximum concentration in the Mexican norm NOM-025-SSA1-1993.

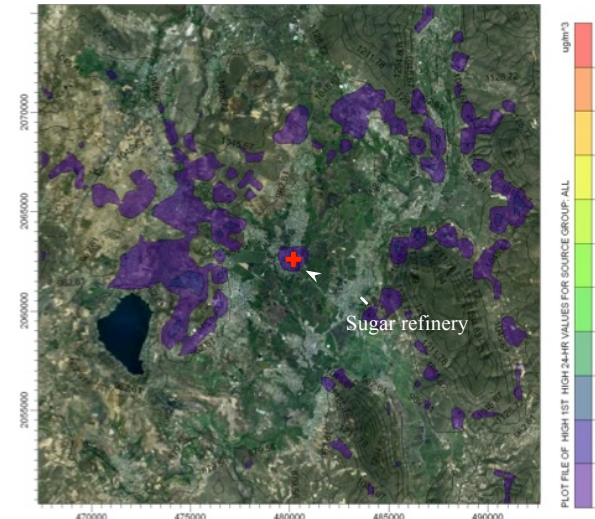


Figure 8. Maximum 24-hour PST Concentrations due to Sugar Refinery Operations, using Fossil Fuels. Ene-May 2011

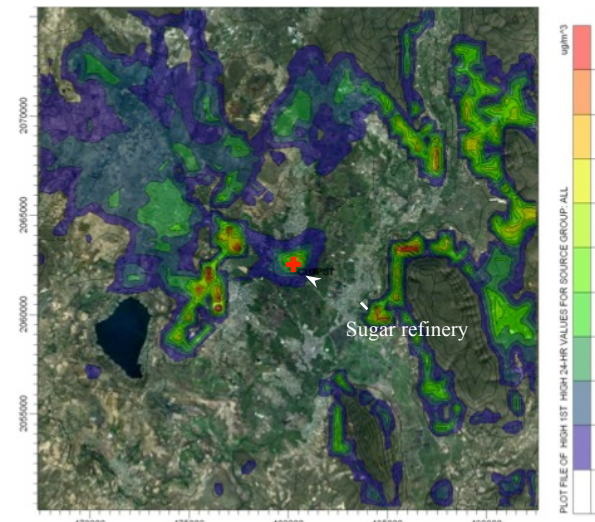


Figure 9. Maximum 24-hour PST Concentrations due to Sugar Refinery Operations, using Bagasse and Fossil Fuels. Ene-May 2011

4.3. Influence of the Pre-Harvest Burning

To analyze the influence of pre-harvest burning on the air quality in the region, 6 parcels with an approximate total surface of 7000 ha in the neighborhood of the mill were randomly selected, simulating the selection of daily sugar cane crops according to their maturity; the emission factors from table 2 were used.

Figure 10 presents the result of the corresponding AERMOD modeling for PST concentration; the sugar cane parcels are indicated in red. It indicates that pre-harvest burning in the fields near the refinery, although this last for only about an hour each morning, is generating huge hourly PST concentrations in nearby houses. Hourly concentrations over $175\ 000\ \mu\text{g}/\text{m}^3$ are found, corresponding to 24-hour concentrations of $730\ \mu\text{g}/\text{m}^3$, and thus to 3.5 times the national standard of $210\ \mu\text{g}/\text{m}^3$. Big sugar cane parcels will cause more harm than smaller parcels, as the PST emissions are spread; up to 2 km from the burning front concentration values over the 24-hour standard can be expected. For NO_x , a similar conclusion can be drawn, although NO_x concentrations are lower than PST concentrations.

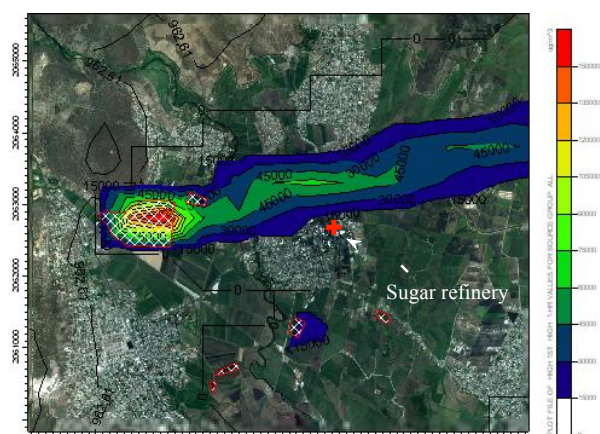


Figure 10. Influence of pre-harvest burning on particulate matter concentration, hypothetical run for December 3, 2011

It is important to note that 90% of pre-harvest burning PST corresponds to small particles ($< 0.5\ \mu\text{m}$), which are dangerous to human health, as stated for example by Ribiero (2008).

5. CONCLUSIONS

AERMOD modeling indicates that pre-harvest burning of sugar cane presents local PST concentrations over 3.5 the national standard; this phenomenon is a lot more important than PST pollution originated in the refining process.

Although the use of bagasse in the extraction process is more sustainable than the use of fossil fuels, its use increments the PST concentrations expected in the surroundings of the sugar mill by approximately 6. However, none of the used fuel combinations generate PST concentrations that violate the national standard.

Future work includes comparison of AERMOD results with ambient air concentrations recorded in the Air Pointer monitoring station during the 2012 *zafra* period.

ACKNOWLEDGEMENTS

The authors wish to thank Dr. Alma Delia Baez-Gonzalez from INIFAP for the meteorological information provided for this study.

REFERENCES

- CVCA, 2010. *Monografía de la caña de azúcar*, Comisión Veracruzana de Comercialización Agropecuaria, Gobierno de Veracruz.
- Hall, D., Wu, Ch., Hsu, Y., Stormer, J., Engling, G., Capeto, K., Wang, J., Brown, S., Li, H., Yu, K., 2012. PAHs, carbonyls, VOCs and PM_{2.5} emission factors for pre-harvest burning of Florida sugarcane, *Atmospheric Environment* 55, 164-172.
- Ribeiro, H., 2008. Sugar cane burning in Brazil: respiratory health effects, *Revista de Saúde Pública* 42 (2), 2-6.
- US-EPA, 1995. *AP-42 Compilation of Air Pollutant Emission Factors, vol. 1. Open Burning (Chapter 2.5)*, fifth edition. Available from: <http://www.epa.gov/ttn/chief/ap42/ch02/final/c02s05.pdf> [accessed 15 June 2012]
- US-EPA, 2012. *Support Center for Regulatory Air Models*, Technology Transfer Network. <http://www.epa.gov/scram001/> [accessed 25 July 2012]

AUTHORS BIOGRAPHY

Ann Wellens is a chemical engineer with postgraduate studies in Industrial Administration (KUL, Belgium) and a master degree in Environmental Engineering (UNAM, Mexico). At the moment she is a full-time lecturer in the Systems Department of the Industrial and Mechanical Engineering Division of the National Autonomous University of Mexico (UNAM). She has been working in air pollution issues for the last 15 years, dictating courses, collaborating in research projects and participating in conferences related with mathematical modeling of air pollution dispersion and statistics.

Julio González obtained his bachelor degree in Industrial Engineering (Acapulco, México).

Ricardo Torres-Jardón is a senior research assistant in the Center for Atmospheric Sciences, UNAM, in Mexico City. He has a B.S. in chemical engineering and a M.S. in environmental engineering both from UNAM and a Ph.D. in environmental engineering from the University of Cincinnati. He has more than 30 years of experience working on air pollution and atmospheric chemistry monitoring research in Mexico.

Hugo Barrera is a PhD student in the Earth Sciences Graduate Program, National Autonomous University of Mexico in Mexico City. He received a B.S. in environmental engineering sciences from the National Polytechnic Institute (IPN) and a M.S. in earth sciences from UNAM. His experience includes a tenure as a chemist at the Centro Nacional de Investigación y Capacitación Ambiental, National Institute of Ecology (INE, SEMARNAT) and a research stay at the Molina Center for Energy and the Environment in San Diego among others. He has participated in several research projects on air pollution monitoring.

ENRICHING A DEVS META-MODEL WITH OCL CONSTRAINTS

Stéphane GARREDU^(a), Evelyne VITTORI^(b), Jean-François SANTUCCI^(c), Dominique URBANI^(d)

^(a) ^(b) ^(c) ^(d) University of Corsica, UMR-CNRS 6134

^(a)garredu@univ-corse.fr, ^(b)vittori@univ-corse.fr, ^(c)santucci@univ-corse.fr, ^(d)durbani@laposte.net

ABSTRACT

The purpose of this paper is to show how the platform-independent meta-model for DEVS formalism we have been working on can be enriched with Object Constraint Language (OCL) constraints. OCL is a declarative language (without any side effect) and allows us to control both the class attributes and the relationships between classes, in order to facilitate the modeling process and even the code generation towards a DEVS framework. To do so, we chose to follow a MDE, and in particular MDA approach, because OCL 2.0 is now aligned with UML 2.0 and MOF 2.0, which parts of MDA. The implementation of our meta-model with its OCL refinements has been done within Eclipse Modeling Framework (in which OCL 2.0 has been fully implemented) and its meta-meta-formalism Ecore.

Keywords: DEVS, modeling, MDE, MDA, EMF, Ecore, OCL, meta-modeling, PIM

1. INTRODUCTION

Since 20 years, with the great improvements in computers science, the interest for modeling and simulation has been evolving increasingly. Among the several formalisms dedicated to modeling and simulation of discrete-event systems, DEVS formalism appears to be the most famous one because of its ability to represent various systems (with its several extensions) and to simulate them. The interoperability of DEVS models is reduced because of the existing DEVS simulators.

The approach our team has been working on aims to ease the modeling process, increase the interoperability of DEVS models and improve code-writing process (using automated code generation). From our point of view, it can be done if we use some specific features of Model Driven Engineering (MDE) methodology and if we apply them to the world of modeling and simulation. The main advantage of MDE is that it is composed of a useful set of standards, and their purpose is to improve the reusability of the models and the code generation process.

An important part of our approach is to allow the description of DEVS models in a unified way: it implies that such a description has to be achieved without considering the platform in which the models will be simulated. To stick to this philosophy, each DEVS model should conform to the same pattern. This pattern

should provide all the necessary DEVS concepts in order to create DEVS models in a unified way: such a pattern is called a meta-model (it is fully detailed in a paper “in press”). It describes the syntax and the semantics of a formalism.

A meta-model has to be described with a meta-formalism such as XML, or one of the concrete implementations of the well-known OMG Meta Object Facility (MOF). The one we used is the Eclipse Modeling Framework (EMF) Ecore, and can graphically be represented with UML class diagrams : we use them in this paper to present the main meta-classes of our DEVS meta-model.

The usual meta- formalisms are not refined enough to provide all the relevant aspects of a specification. They usually are cannot fully specify a modeling formalism, and they are often extended with the ability to express constraints. Even if those constraints can often be expressed with natural language, it is very hard to implement. Constraints must be expressed in a formal way. Object Constraint Language (OCL) provides such an ability. It is used to describe constraints on UML models as well as on MOF-typed meta-models, that is the reason why we said it was aligned with UML 2.0 and MOF 2.0.

We will use this language to define some important constraints on our DEVS meta-model : as a consequence, the number of meaningful models will be limited, but they will be more accurate. The purpose of this paper is to show how the needed constraints on our DEVS meta-model (and in a general way, on other meta-models) can be identified and implemented. Of course, those steps can be applied to any other kind of meta-models.

This paper is organized as follows: the first part is the background section, it focuses on the essential concepts of DEVS formalism and software engineering (MDE, and in particular UML and MDA, OCL). We conclude it by a presentation of our approach dedicated to the improvement of DEVS models interoperability and object-oriented code generation towards DEVS simulators.

The second part, which can be seen as a specific background, sums-up the most important features of the meta-model we defined for DEVS formalism : we give an overview of the meta-class hierarchy, then we focus on (using package diagrams associated to class-diagrams) the *DEVSExpression* and *DEVSRule*

concepts, and we describe how we chose to represent the couplings between models. We conclude by a discussion, which highlights some conditions, in the formal definition of DEVS formalism, which are not expressed yet in our meta-model. This will introduce the third part, dedicated to the OCL constraints we put on the meta-classes which belong to *DEVSExpression*, *DEVSRule* and *Coupling* packages. After that, we give an example of a model which could have been validated without our constraints but which is now not meaningful anymore. We finally conclude this paper by giving an outline of it, and we say a few words about our future work.

2. BACKGROUND

All caps, bold, flush left. Use Times New Roman Font and 10 points in size. Start the text on the next line. Please use the “HEADING 1” style.

The headings for the Abstract, Acknowledgements, Appendix, References and Authors Biographies sections are not numbered. Please use “HEADING” style. Insert one blank line before each heading.

Do not include any kind of page numbers, headers or footers. Final page numbers will be inserted by the publisher.

2.1. DEVS

DEVS formalism, introduced in the 70’s by Pr. B.P. Zeigler (Zeigler 1989) (Zeigler et al. 2000) is based on discrete events, and it provides a framework with mathematical concepts based on the sets theory and systems theory concepts to describe the structure and the behavior of a system.

Almost any system can be modeled with DEVS formalism, if it has finites states and finite transitions between its states, in a finite time interval, and interacts with its environment through events sent and received on its communication ports. A DEVS model represents, as other kinds of models do, a simplified version of reality. DEVS formalism is modular and hierarchical; it allows the definition of 2 kinds of models: atomic models and coupled models. DEVS makes an explicit separation between a model and its simulator: the latter is “automatically” built from the former. It has been formally proved that the entity “simulator” is able to execute correctly the behaviour described by the entity “model”. It has also been formally proved that DEVS is closed under composition, which means that a coupled model (composed of several models) can be seen as a unique atomic model.

As there exist many DEVS-oriented simulators and frameworks (DEVS Standardization Group 2012) the interoperability of DEVS models is reduced.

2.1.1. DEVS Atomic Models

The tiniest element in DEVS formalism is the atomic model. It is specified as follows.

$$AM = \langle X, Y, S, ta, \delta_{int}, \delta_{ext}, \lambda \rangle, \text{ where :}$$

- $X = \{(p,v)|p \in InputPorts, v \in X_p\}$ is the input

events set, through which external events are received; *InputPorts* is the set of input ports and X_p is the set of possible values for those input ports

- $Y = \{(p,v)|p \in OutputPorts, v \in Y_p\}$ is the output

events set, through which external events are sent; *OutputPorts* is the set of output ports and X_p is the set of possible values for those output ports

- S is the states set of the system;

- $ta: S \rightarrow R_0^+ \cup +\infty$ is the time advance function

(or lifespan of a state);

- $\delta_{int}: S \rightarrow S$ is the internal transition function;

- $\delta_{ext}: Q \times X \rightarrow S$ with $Q = \{(s,e)|s \in S,$

$e \in [0, ta(s)]\}$ is the external transition function;

- $\lambda: S \rightarrow Y$, with $Y = \{(p,v)|p \in OutputPorts,$

$v \in Y_p\}$ is the output function;

The simplest transition is called the internal transition : at a given moment, a system is in a state

$s \in S$. Unless an external event occurs on an input port,

the system remains in the s state for a duration defined by $ta(s)$. When $ta(s)$ expires, the model sends the value

defined by $\lambda(s)$ on an output port $y \in Y$, and then it

changes to a new state defined by $\delta_{int}(s)$. Such a transition, which occurs because of the expiration of $ta(s)$, is an internal transition.

The other transition type is called the external transition, because it is triggered by an external event. In this case, it is the $\delta_{ext}(s,e,x)$ function which defines which state is the next one (s is the current state, e is the

elapsed time since the last transition, and $x \in X$ is the event received).

In both cases, the system is now in a new state s' for a new duration $d' = ta(s')$ and the algorithm restarts.

2.1.2. DEVS Coupled Models

A coupled model is composed of at least one submodel (atomic or coupled). A coupled model can be seen as a parent-model which describes a hierarchy (i.e. a list of sub-models, the links between itself and the submodels it is composed of, and the links between the submodels themselves). A coupled model is formally defined by

$$MC = \langle X, Y, D, \{Md | d \in D\}, EIC, EOC, IC, \text{select} \rangle, \text{ where :}$$

- $X = \{(p,v) | p \in \text{InputPorts}, v \in X_p\}$ is the input events set, through which external events are received; InputPorts is the set of input ports and X_p is the set of possible values for those input ports
- $Y = \{(p,v) | p \in \text{OutputPorts}, v \in Y_p\}$ is the output events set, through which external events are sent; OutputPorts is the set of output ports and X_p is the set of possible values for those output ports
- D is the set of component names, $d \in D$
- Md is a DEVS model (either atomic or coupled)
- EIC is the set of external input couplings; an external input coupling is a link between the input port of the current coupled model and the input port of any of its submodels

- EOC is the set of external output couplings; an external output coupling is a link between the output port of the current coupled model and the output port of any of its submodels
- IC is the set of internal couplings; an internal coupling is a link which involves the output port of a submodel and the input port of another submodel
- select is the tiebreaker function

Figure 1 is an example of a coupled model containing two submodels: an atomic model and a coupled model, which contains itself two atomic models. The coupling functions (EOC, EIC, IC) are indicated and the ports are represented by black diamonds. For instance, Coupled 2 has two input ports, and one output port. Atomic 3, contained by coupled 2, has one input port, and one output port.

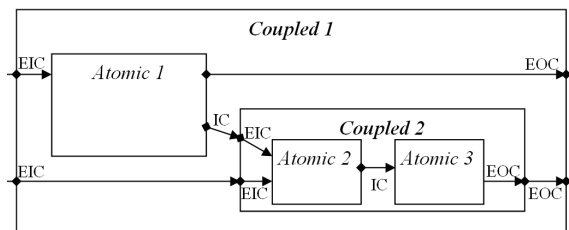


Figure 1: A DEVS coupled model

2.2. DEVS Software engineering and meta-modeling

2.2.1. UML

Unified Modeling Language (UML) is a graphical set of modeling formalisms: it provides a toolkit which enables one to model the structural aspects of a system as well as its behavior (Booch et al. 1998).

UML is owned by the Object Management Group, and its current version is UML 2.4.1 (OMG 2011). Its main advantage is that it is considered as a standard formalism by a large worldwide community of users. We use in this paper UML class and package diagrams to represent the meta-classes of our DEVS meta-model.

2.2.2. UML and meta-levels

A UML model, for instance a UML class diagram (that we will use later to describe our meta-model) is an abstraction of a system from the real world located at the lowest abstraction level: M0. Such an abstraction takes place at a higher level: M1. It is defined by its meta-model at, once more, a higher level: M2. This meta-model describes, using a language or formalism, the elements that can be used to design the model and their relationships with each other. Such a description is defined at a higher level by Meta Object Facility (MOF), a language used to describe other languages. This level is M3. MOF is defined on itself, i.e. it is described in MOF terms. Hence, there is no level higher than M3 (Figure 2).

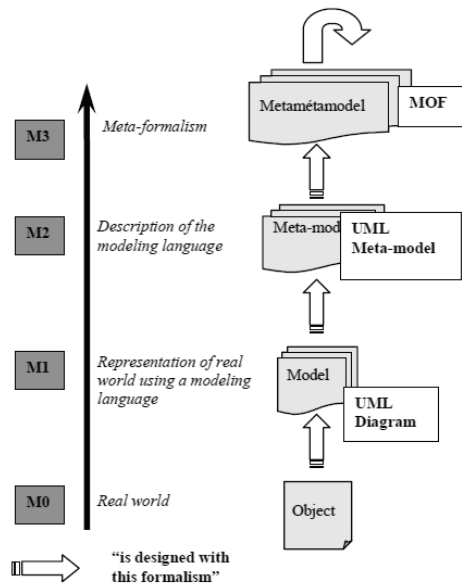


Figure 2: UML and the “meta” levels

2.2.3. MDE, MDA and EMF

Model Driven Engineering is a software development methodology which focuses on creating and exploiting domain models. MDE is a generic approach, and its most famous implementation is Model Driven Architecture, owned by the OMG.

We can also quote the Eclipse ecosystem of programming and modelling tools (Eclipse 2012). EMF (EMF 2012) is a particular part of Eclipse which contains and implements a set of MDA standards: in fact, MDA and EMF are very close one to each other, the latter uses and implements the concepts inherited from the former, and we use both of them in our approach. MDA (Model Driven Architecture) (OMG, 2001) is a software design approach initiated by the OMG in 2001 to introduce a new way of development based upon models rather than code. With MDA approach, everything is a model, even the transformations between models are considered as models.

MDA defines a set of guidelines for defining models at different abstraction levels, starting from Computational Independent Models (CIMs) to platform independent models (PIMs), then from PIMs to platform specific models (PSMs) which are tied to a particular technology (i.e. platform). The translation from one PIM to one or several PSMs is to be performed automatically by using transformation tools. MDA also enables transforming a PSM into source code. The advantage of such an approach is the great reusability of models. OMG provides a set of standards dedicated to this approach. Although UML was at the beginning the basis of the OMG works on MDA, it is now Meta-Object Facility which appears to be the most basic standard.

According to this standard, each formalism involved in a MDA process at any level (PIM, PSM) is

to be specified by a meta-model expressed in terms of MOF elements. As MOF was not given a concrete syntax, our meta-model was implemented using EMF. The MOF equivalent in EMF is Ecore. Ecore can be seen as an implementation of MOF, in the same way that EMF uses the MDA concepts.

2.2.4. OCL

Object Constraint Language (OMG 2006) is a formal and strongly typed modeling language proposed by the OMG in order to specify unambiguous constraints on UML 2.0 models, and even MOF 2.0 meta-models (i.e. fully aligned with MOF and MDA).

As it is a pure specification language OCL enables us to write expressions without side effects. When an OCL expression is evaluated, it simply returns a value. It cannot change anything in the model, nor in the meta-model. Moreover, it is not possible to write program logic or flow control in OCL. It is not possible to invoke processes or activate non-query operations within OCL. Because OCL is a modeling language in the first place, OCL expressions are not by definition directly executable.

In this paper, we will use OCL to specify *invariants* on our meta-classes and their relationships (i.e. conditions that have to be fulfilled by any instances of the meta-classes) so that the instances of the meta-model must conform to those conditions.

2.3. Our Approach

The DEVS meta-model we designed is located at the M2 level and uses the concepts given by the highest level (M3). The meta-meta-formalism we used is EMF Ecore.

Some theoretical aspects of our approach are presented in a more detailed way in (Garredu et al. 2011). Figure 3 shows a larger view of our philosophy : the DEVS meta-model enables to specify platform-independent models (DEVS PIMs) which are in fact instances of this meta-model. Thanks to transformation rules, those models can be used for an automated object-oriented code generation towards a DEVS simulator. But the other huge advantage of following a MDE approach is that the DEVS meta-model can be seen as a single entry-point for other DEVS-like (i.e. based on states, transitions and events) formalisms: also using transformation rules at the M3 level, it is possible to specify mappings from any DEVS-Like formalism towards our DEVS meta-model. In other words, any model written in a DEVS-like formalism can be transformed in a DEVS model. Then, as a normal DEVS model, it can be used, as we said before, to generate object-oriented code.

3. MAIN ELEMENTS OF OUR DEVS METAMODEL

3.1.1. Overview of the hierarchy

The most important package of our meta-model is the *DEVSMODEL* package (Figure 4). It shows that a DEVS

model can be either atomic or coupled. If it is coupled, it must contain at least a submodel.

Types are defined differently following the object-oriented languages. So, our meta-model must be able to handle types, in a generic way. We chose to represent only 4 basic types, but this can be easily extended. The package representing types is given by Figure 5.

Every DEVS model has at least an output port and can have an input port. Every port must be given a name and a type, and can be either an input port or an output port (Figure 6).

We introduced with this meta-model an important basic concept which is common to many elements of this meta-model: the *DEVSExpression*.

3.1.2. DEVSExpression package

In a formal point of view, a DEVS atomic model is composed of a finite set of its possible states S linked by deterministic transitions. Those states are distinct values; it implies that the fact of changing a state may lead to the creation of another state.

This is not a problem for the systems of which the states are known (and can be enumerated) but it becomes one when we have to deal with states which

take their values in infinite sets, for instance $[0;1] \in R$.

To solve this problem, we chose to represent a state by instance, the simplest one is given by the *ta* function; it describes the fact of returning a value after evaluating a state.

what we call a *state variable*. It takes a new value when the state changes (i.e. each new state change will lead to a change of the value of the state variable). Therefore, only a state variable is used to represent a collection of states which belong to the “same kind”. A state variable must be named, and must be typed. It can also be affected a literal value.

We chose to describe state variables and types, and they can be included in a larger set which is called *DEVSExpression*.

It is one of the basis of our meta-model. As a *StateVar* is a *DEVSExpression*, a *LitteralBasicValue* (see Figure 9) is also *DEVSExpression* but a simpler one: in fact the simplest one because it is composed of a unique typed value. We built this package (see Figure 7) in a modular way, in order to facilitate its modification by enriching it with other sub-classes. *DEVSComplex* can be a starting point to do so.

3.2. Rule package

In spite of the differences between the DEVS functions, we can notice that every function can describe a test, an action on a variable, a message. Those descriptions follow a sort of pattern which is often the same: a set of enumerations. We call those enumerations *DEVS Rules*.

The purpose of a rule is to represent a set of operations on specific elements. To be more accurate, these are not exactly operations but descriptions. For

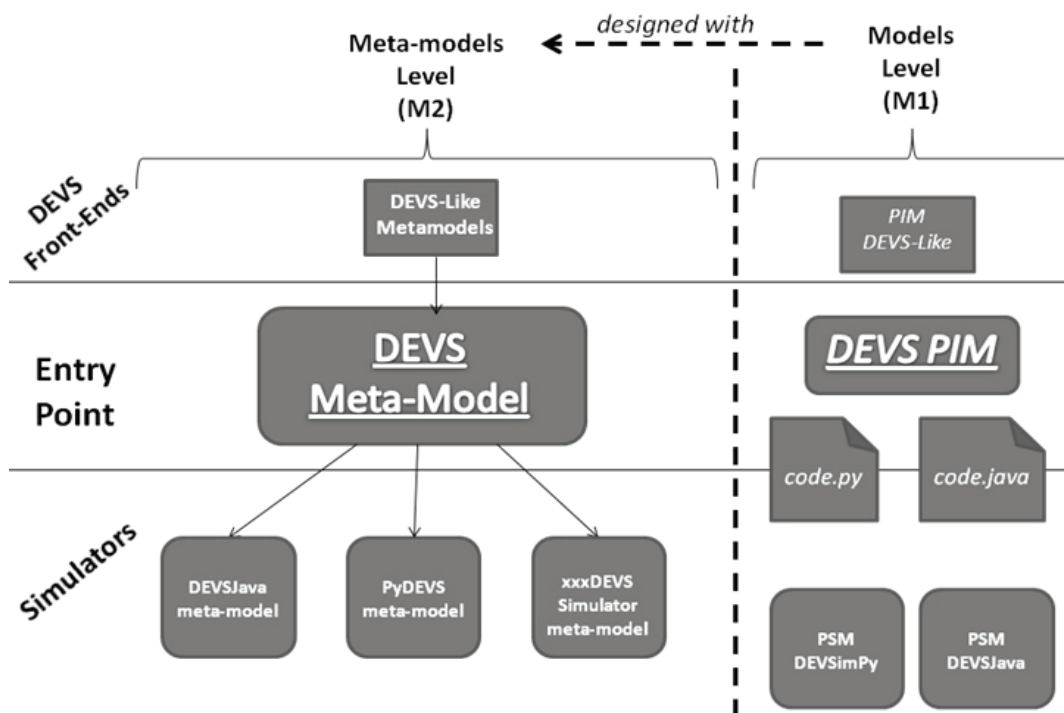


Figure 3: The DEVS meta-model used as a single entry-point towards DEVS simulators

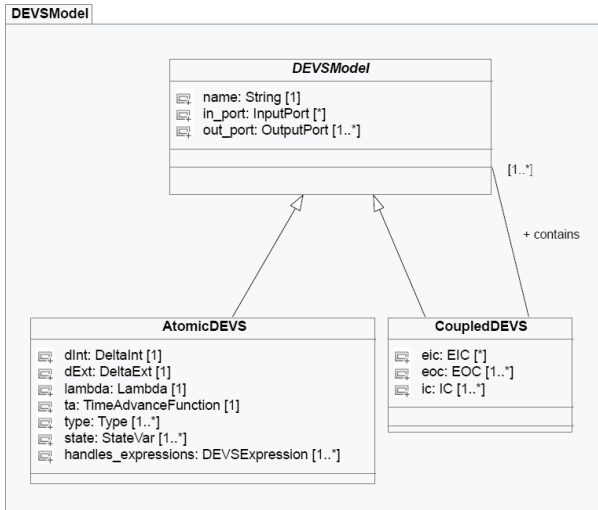


Figure 4: The *DEVSMODEL* package

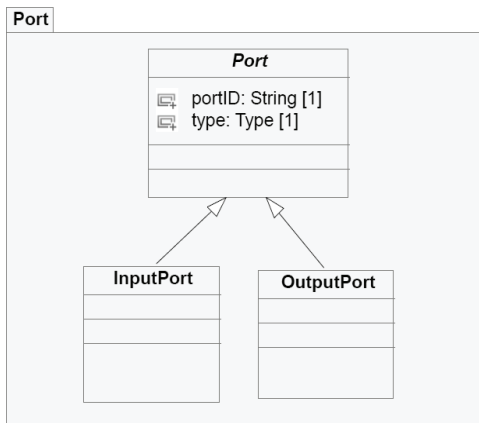


Figure 5: The *Port* package

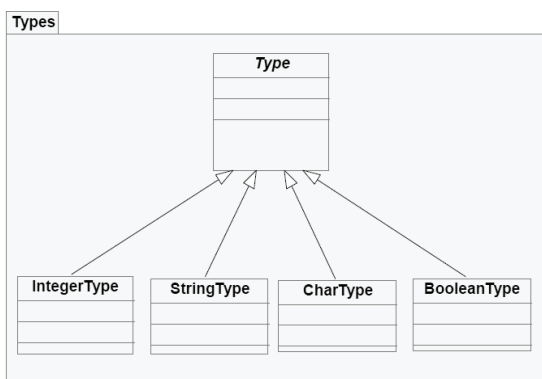


Figure 6: The *Types* package

The purpose of a rule is to represent a set of operations on specific elements. To be more accurate, these are not exactly operations but descriptions. For instance, the simplest one is given by the *ta* function; it describes the fact of returning a value after evaluating a state. A rule is always composed of a *condition* and an *action*. Figure 8 shows the organization of the *Rule* package, it uses the two next packages : see Figures 9 and 10. Those figures represent the *Conditions* and *Actions* used in the Rules. A *condition* (see Figure 9) is described by a test: a left member, a comparator, and a right member. It can be a test on an input port (in the case of an external transition function) or on a state variable (in every DEVSMODEL atomic function, there is a test on a state variable). An *action* is the description of an action: an output action (on a port), or a state change action (in the case of a transition function). Figure 10 shows the *Action* package.

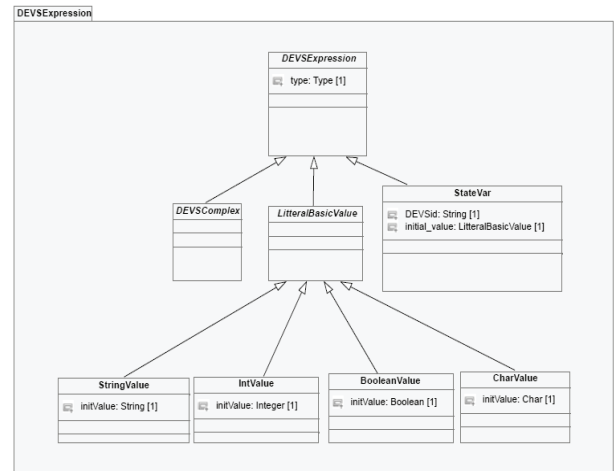


Figure 7: The *DEVSEXPRESSION* package

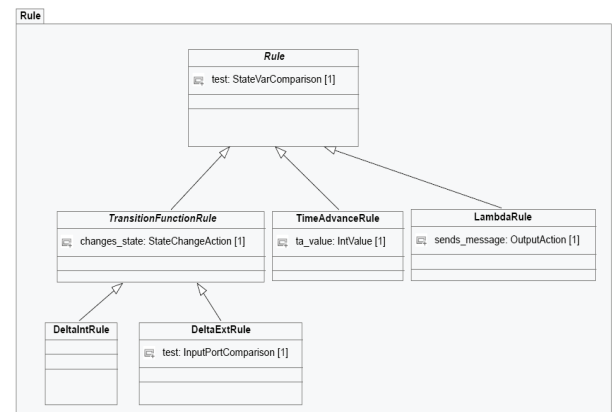


Figure 8: The *Rule* package

3.3. Rule package

In spite of the differences between the DEVSMODEL functions, we can notice that every function can describe a test, an action on a variable, a message. Those descriptions follow a sort of pattern which is often the same: a set of enumerations. We call those enumerations *DEVSMODEL Rules*.

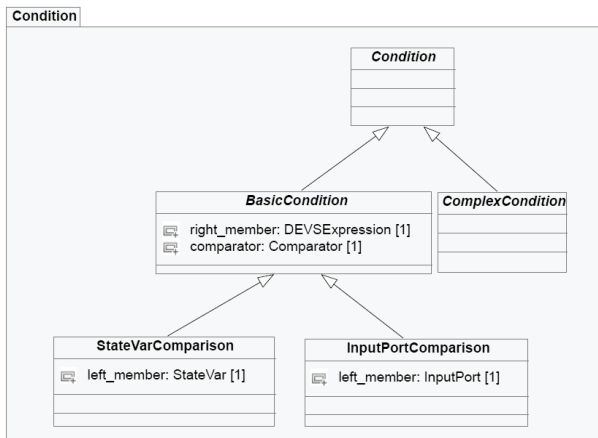


Figure 9: The *Condition* package

3.4. Coupling Package

The meta-class which describes the coupling functions (in the coupled models) is given by Figure 11. As usual, there is an abstract class (*Coupling*) from which inherit 3 sub-classes: EIC, EOC, IC.

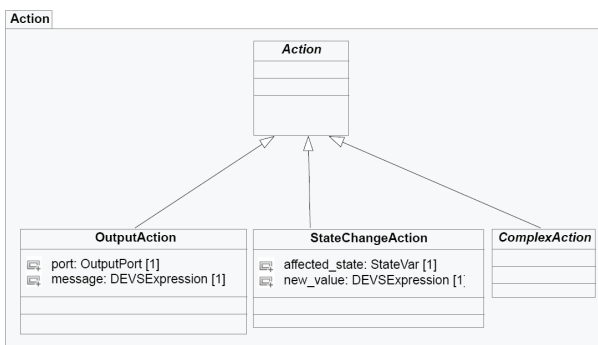


Figure 10: The *Action* package

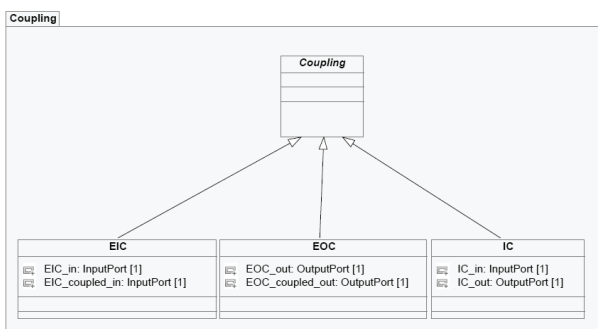


Figure 11: The *Coupling* package

3.5. Discussion

The DEVS meta-model we show here is accurate enough to specify several DEVS models. Though, the modeler must take care of several parameters while he designs a system. If we look at the DEVS formal definition, we can see that : an IC function involves an input port and an output port, an EIC function involves two input ports, and an EOC function involves two output ports. That is transcribed in the that a previous figure representing the coupling functions. But, how can we specify that, for instance, an IC function must use

the ports of two sub-models of the current coupled model?

Reasoning in the same way, how can be sure that the initial value of a *StateVar* and its type belong to the same type? How can we verify that a *StringValue* has the correct corresponding type (*StringType*)?

All those questions have the same process: a comparison between the formal definition of DEVS and our meta-model, or a reasoning on what makes a model be meaningful or not (a non-meaningful model always leads to “modeling mistakes”).

The next part is dedicated of all the refinements we can apply to our meta-model in order to make it be far more accurate than before.

4. ADDING OCL CONSTRAINTS TO OUR METAMODEL

In this part we use the EMF OCL 3.1.0 language to describe the constraints on our meta-model. The constraints were directly implemented in the EMF framework, and (added to the corresponding meta-classes).

4.1. DEVSExpression Constraints

4.1.1. StateVar Constraints

As we have seen before, we must verify that a *StateVar* which is given a String type cannot contain a reference to a value from another type. This can easily be done :

```

invariant StateVarTypeConstraint:
self.type = self.initial_value.type;
  
```

A *StateVar* must also be identified: its attribute DEVSid must not be empty, so we write :

```

invariant idNotEmpty:
self.DEVSid.size()>0;
  
```

4.1.2. LitteralBasicValue Constraints

As a child of *DEVSExpression*, a *LitteralBasicValue* can be a type which is different from the value it carries. We must prevent that. Every new *LitteralBasicValue* must have the same type than the type of the value it carries. Moreover, a *StringValue* must not be empty :

- *IntValue* must be typed with *IntegerType*

```

invariant intIsInt:
self.type.oclType().name = 'IntegerType';
  
```
- *CharValue* must be typed with *CharType*

```

invariant charIsChar:
self.is.type.oclType().name = 'CharType';
  
```
- *BooleanValue* must be typed with *BooleanType*

```

invariant boolIsBool:
self.type.oclType().name = 'BooleanType';
  
```
- *StringValue* must be typed with *StringType* and not empty

```

invariant stringIsString:
self.type.oclType().name =
'StringType';
invariant nameNotEmpty:
self.str_val.size()>0

```

4.2. DEVSRules Constraints

In every comparison, we must verify that the type of the left member (a *Port*, a *StateVar*...) belongs to the same type as the element it is compared to:

- In the *StateVarComparison* meta-class :

```

invariant svcTypeConstraint:
self.left_member.type=self.right_member.type;

```

- In the *InputPortComparison* meta-class :

```

invariant ipcTypeConstraint:
self.left_member.type=self.right_member.type;

```

In the same way, we must verify that the types match in an *Action*. In the case of an *OutputAction*, we must verify that the output port given as a parameter belongs to the current atomic model :

- For a *StateChangeAction* :

```

invariant stateChangeTypeConstraint:
self.affected_state.type=self.new_value.type;

```

- For an *OutputAction* :

```

invariant outputActionTypeConstraint:
self.port.type=self.message.type;

invariant portBelongsToCurrentAtomic:
self.port.oclContainer()=self.oclContainer();

```

4.3. Coupling Constraints

Here we present 3 groups containing 3 constraints each. Those constraints are very important because they prevent hazardous couplings between ports. The last

constraint of each group verifies that two ports have the same type.

- EIC must have a reference to an input port from the current coupled model and a reference to the input port of a submodel

$(Md|d \in D)$

```

invariant EICcurrentModelInputPort :
self.oclContainer()=self.EIC_coupled_in.oclContainer();

```

```

invariant EICsubmodelInputPort :
self.oclContainer()=self.EIC_in.oclContainer().oclContainer();

```

```

invariant EICtypes:
self.EIC_coupled_in.type =
self.EIC_in.type;

```

- It is the same thing for EOC, but with output ports :

```

invariant EOCcurrentModelOutputPort :
self.oclContainer()=self.EOC_coupled_out.oclContainer();

```

```

invariant EOCsubmodelOutputPort :
self.oclContainer()=self.EOC_out.oclContainer().oclContainer();

```

```

invariant EOCTypes:
self.EOC_coupled_out.type=self.EOC_output.type;

```

- IC must link the input and output ports of two submodels :

```

invariant ICsubmodelInputPort :
self.oclContainer()=self.IC_in.oclContainer().oclContainer();

```

```

invariant ICsubmodelOutputPort :

```

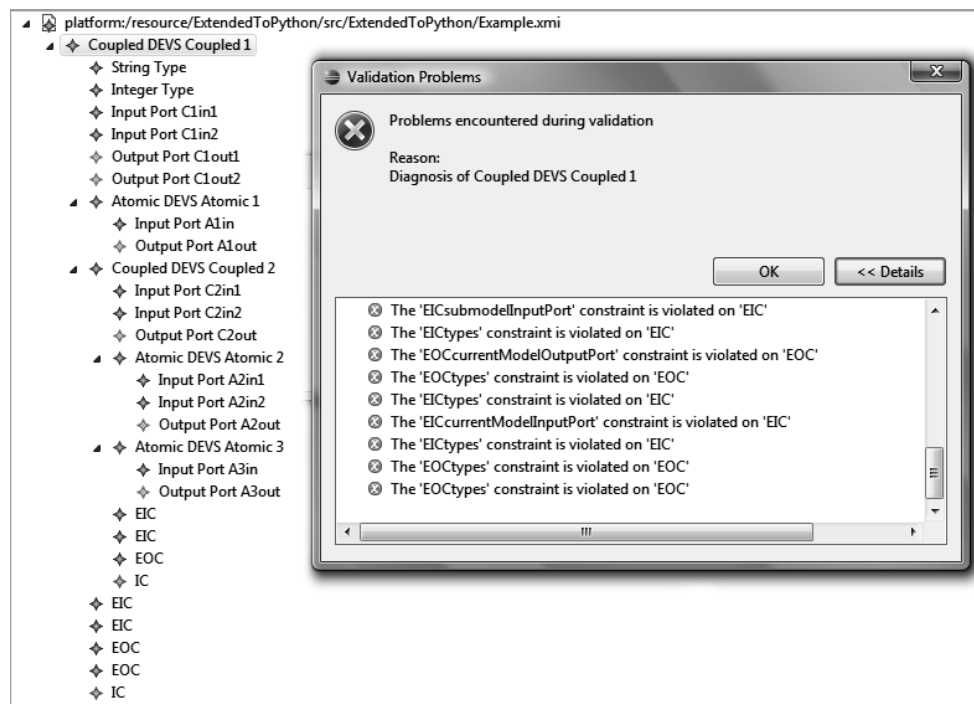


Figure 12: Testing OCL constraints with Eclipse Modeling Framework and our DEVS meta-model

```
self.oclContainer()=
self.IC_out.oclContainer().oclContain
er();

invariant ICtypes:
self.IC_out.is_typed=self.IC_out.is_t
yped;
```

5. EXAMPLE

We chose to re-create the hierarchy of Figure 1 in this example in order to test the class invariant constraints we put on the meta-classes of *Coupling* package. We tried to make voluntary mistakes in the definition of the coupling functions and tried to validate our model instance. The errors raised by EMF are shown in the following screenshot (Figure 12). The other kind of constraints we put on other classes are fully functional too.

6. CONCLUSION

In this paper, we have presented the main meta-classes of our meta-model for DEVS then we have shown how they could be enriched and refined with OCL constraints. Without those constraints, even if the instantiated models would have been “correct” in terms of our meta-model, from a DEVS point of view they would not. OCL can be seen as a super-layer which cannot work the fundamental layer created by the meta-model. This super-layer depicts more precisely the meta-attributes and the meta-relationships between the meta-classes. Using those two layers was possible because of the tight links which exist between OCL and

MOF : those links exist in EMF too between Ecore and EMF OCL.

In a near future, we plan to describe how OCL can be used as a super-layer for Model To Model transformations. This is another side of OCL usage: instead of being used to describe class invariants, it is used this time to create queries and navigate in the links between the instances of a meta-model.

REFERENCES

- G. Booch, J. Rumbaugh, and I. Jacobson. 1998. “The unified Modeling Language User Guide”. Addison-lesley.
- DEVS Standardization Group, Carleton University Website, 2012
<http://cell-devs.sce.carleton.ca/devsgroup/?q=node/8>
- Eclipse 2012 <http://www.eclipse.org/>
- EMF 2012 <http://www.eclipse.org/modeling/emf/>
- S. Garredu, E. Vittori, J.-F. Santucci, D. Urbani, “A methodology to specify DEVS domain specific profiles and create profile-based models”, IEEE-IRI 2011, 3-5 Aug. 2011, Las Vegas, NV, USA, pp. 353 - 359
- OMG 2001. Model Driven Architecture homepage <http://www.omg.org/mda/>
- OMG 2006. Object Management Group website, OCL section, <http://www.omg.org/spec/OCL/2.0/>
- OMG 2011. Unified Modeling Language: Superstructure and infrastructure, version 2.4.1, August 2011
<http://www.omg.org/spec/UML/2.4.1/>

- Zeigler B.P., 1989. "*DEVS Representation of Dynamical System*", in Proceedings of the IEEE, Vol.77, pp. 72-80
- Zeigler, B. P., H. Praehofer, and T.Kim. 2000. Theory of Modeling and simulation. 2nd ed. Academic Press

SIMULATION OPTIMISATION AND MONITORING IN TACTICAL AND OPERATIONAL PLANNING OF DELIVERIES

Galina Merkurjeva^(a), Vitaly Bolshakov^(b)

^(a)^(b)Riga Technical University, Kalku Street 1, LV-1658, Riga, Latvia

^(a)Galina.Merkurjeva@rtu.lv, ^(b)Vitalijs.Bolsakovs@rtu.lv

ABSTRACT

Data mining, simulation, heuristic optimisation and monitoring techniques are applied to improve complex planning decisions at tactical and operational levels. The paper presents an integrated approach to product delivery planning and scheduling built on integration of these technologies. A business case in tactical and operational planning of deliveries is given in the paper. Cluster analysis of dynamic demand is described. The region clustering of customers is performed through multi-objective optimisation. Vehicle scheduling is introduced and performed for the routed solution.

Keywords: clustering, simulation, metaheuristics, optimisation, tactical planning, vehicle routing, scheduling

1. INTRODUCTION

To ensure the competitiveness, a modern business management requires application of a number of methods in the field of information technologies and operations research. To get the best solution of the problem, these methods must be highly integrated to complement each other.

In the paper, a business case for a logistics department of a distribution centre (DC) for a retail store network is discussed. Four core technologies, such as data mining, computer simulation, optimization and monitoring, applied for an integrated planning and control of deliveries are discussed (see Fig. 1).

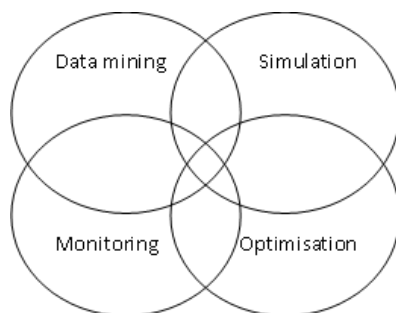


Figure 1: Technologies Integration

Here, data mining techniques are used to perform a cluster analysis in order to define natural grouping of input data, e.g., geographical locations of customers and

their demand data in order to define various types of tactical delivery plans. Simulation provides evaluating of specific operational decisions in advance, e.g., while comparing vehicle routes and schedules. Simulation enhanced with metaheuristic optimization allows searching for the optimal solutions at an operational planning level. In particular, an integrated use of data mining, simulation and metaheuristic optimization techniques are described in Merkurjeva et al. 2011. Here, the scheme of integrated planning and control of deliveries is extended by including monitoring tasks.

Despite the fact that the main field of monitoring application is maintenance of already existing business processes, the monitoring may be also applied at the different stages of the business planning process.

2. MONITORING IN SIMULATION OPTIMISATION

Applications of monitoring at tactical and operational planning levels are illustrated in Figure 2. Here, a simulation model is interpreted as a representation of a real system, which input data is based on the data obtained from the real system.

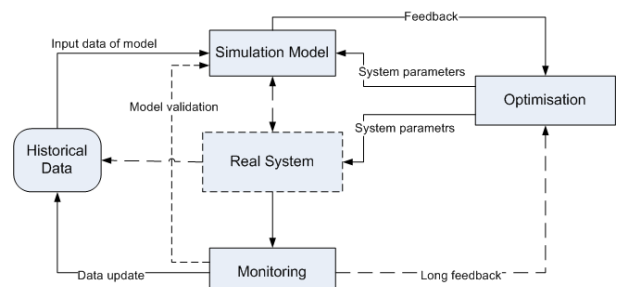


Figure 2: Role of Monitoring

Monitoring can be used already during the modeling phase or even before a simulation model is developed, in order to create a set of historical data. In the delivery planning problem, these data could be observations of customer demand, or data received from vehicles tracking in order to define more realistic simulation model for vehicle routing and scheduling tasks.

If a simulation model is already built and verified, monitoring is a key technique for its complete

validation. In this case, monitoring data provides a good basis for the black-box validation and especially for the solution validation of the model. Here, solution validation means determining that the results obtained from the model of the proposed solution are sufficiently accurate for the purpose at hand (Robinson 2004). Continuous collection of observation data via monitoring provides adjustments for the existing model, and makes it adaptive for the changing and developing environment.

Within the optimisation stage of an integrated planning approach, a simulation model provides a feedback link to a parametric optimisation tool in order to test the proposed parameters of the investigated system (Fig. 2). Also, due to a relatively short-time response of the model, the meta-heuristic optimisation tool is effectively exploring system behaviour on the model. It is also worth considering that if the best found decision is applied for the real system, due to different simplifications and aggregations in a simulation model the behaviour of the system with this proposed solution may differ from expected.

Moreover, real-time monitoring in integrated planning and control is used in practice. Modern advantages in information and communication technologies allow managing a vehicle fleet in real-time. Vehicle tracking with GPS, information on the route and customer requirements can be applied for the rerouting and rescheduling of vehicles.

3. BUSINESS CASE

In real-life applications the delivery planning and scheduling problem has different stochastic performance criteria and conditions. Optimisation of transportation schedules itself is computationally time-consuming task which is based on the data from tactical planning of weekly deliveries. This research focuses on the methodology that will allow reducing the affect of the demand variation on the product delivery planning and scheduling, and avoid numerous time-consuming planning adjustments and high computational costs.

In the distribution centres, this problem is related to deliveries of various types of goods to a net of stores, in predefined time windows, taking into account transportation costs and product demand variability. The problem has also a high number of decision variables, which complicates the problem solution process. Heuristic methods and commercial software that are usually applied could lead to non-effective solutions, high computational costs and high time consumption.

In practice, product demand from stores is variable and not deterministic. As a result, the product delivery tactical plan that is further used for vehicle routing and scheduling has to be adjusted to real demand data, and product delivery re-planning supervised by a planner is often required. This task is time-consuming and requires specific knowledge and experience of planning staff in this domain. Moreover, in practice a cluster analysis of the product demand data and potential

tactical plans is not performed. But the most suitable delivery plan could be defined as a result of such an analysis that would ensure high quality solutions to schedule an optimisation problem and reduce computational costs of the problem solution.

The paper presents an integrated approach to product delivery planning and scheduling built on a cluster analysis, simulation optimisation and monitoring techniques.

4. INPUT DATA CLUSTERING

First, a cluster analysis is applied to process input data and select an effective product delivery tactical plan for the upcoming week. Then, it is used to group customers into groups, based on their geographical location and average weekly demand.

4.1. Cluster Analysis of Dynamic Demand Data

Here, a cluster analysis (Seber 1984) is aimed (Merkuryeva, Bolshakov, Kornevs 2011): 1) to find a number of typical dynamic demand patterns and corresponding clusters of planning weeks; and 2) to construct a classification model that for any week allows determining an appropriate demand pattern, allocating a specific week to one of previously defined clusters and determining the correspondent product delivery plan. In the business case, the historical data on daily number of delivered products for 52 weeks are used and specified by weekly demand time-series each representing a sequence of points – daily numbers of product deliveries for a specific week.

The K-means clustering algorithm (MacQueen 1967) is used. It aims to divide n observations into a user-specified number k of clusters, in which each observation belongs to a cluster with the nearest mean representing a cluster centroid. The result is a set of clusters that are as compact and well-separated as possible. An appropriate number of k clusters, or typical demand patterns is defined by using silhouette plots (Kaufman and Rousseeuw 1990). Higher mean values of silhouettes show better clustering results that determine better clusters giving the best choice for a number of clusters. In this method, a numerical measure of how close each point is to other points in its own cluster compared to points in the neighbouring cluster is defined as follows:

$$s_i = \frac{b_i - a_i}{\min(a_i, b_i)}, \quad (1)$$

where s_i is a silhouette value for point i , a_i is an average dissimilarity of point i with the other points in its cluster, and b_i is the lowest average dissimilarity between point i and other points in another cluster.

K-means clustering experiments have been performed for the number of clusters from 2 to 8. Then for each clustering experiment, silhouette plots have been built, and mean values of silhouettes per cluster have been calculated. Analysis of silhouettes mean

values leads to the conclusion that the best cluster separation could be done at $k=4$ with a silhouette mean value equal to 0.558. Clusters 1 to 3 seem to be appropriately clustered. Dynamic patterns received for clusters from 1 to 3 are presented in Fig. 3.

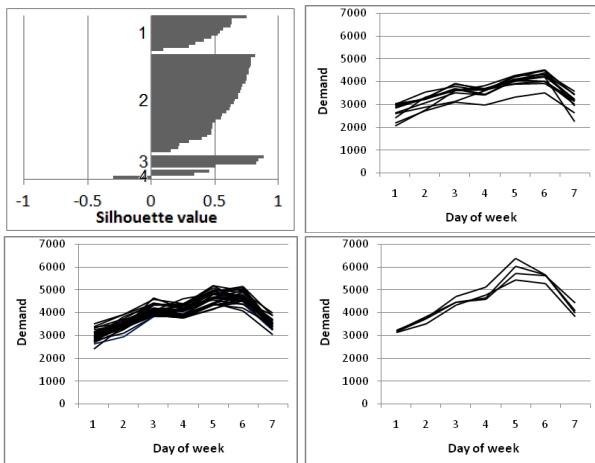


Figure 3: Silhouette Plot for the Number of Clusters $k=4$ and Demands Patterns with a Mean Value Greater than 0.5 (Merkuryeva et al. 2011)

A classification model (Merkuryeva, Bolshakov, Kornevs 2011) that assigns an appropriate demand cluster is presented by an NBTree, which induces a hybrid of decision-tree and Naive-Bayes classifiers. This algorithm is similar to classical recursive partitioning schemes, except that leaf nodes created are Naive-Bayes categorizers instead of nodes predicting a single class (Seber 1984). For a specific week, an NBTree allows identifying an appropriate cluster and then choosing weekly tactical delivery base plan corresponding to this cluster. Then, selected weekly delivery plan is used for optimisation of parameters of vehicle schedules.

4.2. Region Clustering Through Multi-Objective Optimisation

In practice, weekly delivery planning is done based on data about store allocations to geographical regions. In the business case, all stores are grouped into 12 regions. However, this grouping has been made manually and seems not to be effective. Additionally, rearranging of regions is required when a new store is opened. Also, it is desirable to get regions with a uniform total weekly demand.

Here, the region clustering task is formalised as a multi-objective optimisation problem. Input data contains the number of stores n , the number of regions k , two geographical coordinates x_i and y_i for each store i , $i = 1, \dots, n$ defined in the Cartesian coordinate system and the total weekly demand d_i for each store i .

Decision variables are defined that for each store i assign a region (or cluster), i.e.

$$a_i \in \{1, 2, \dots, k\}; i = 1 \dots n. \quad (2)$$

Two objective functions are introduced in the problem. The first one determines how good generated regions from the geographical location point of view are, while the second objective function defines if the total demand is equally distributed among these regions. Both objective functions are minimized as follows:

$$f_1 = \sum_{j=1}^k \sum_{i \in A_j} r(i, j) \rightarrow \min, \quad (3)$$

$$f_2 = \sum_{j=1}^k \left| \sum_{i \in A_j} d_i - \frac{\sum_{i=1}^n d_i}{k} \right| \rightarrow \min, \quad (4)$$

where f_1 defines the sum of distances $r(i, j)$ between centroids i of the regions and stores j assigned to them, and f_2 is the sum of variances of the total demand for each region and the average demand per region. No additional constraints are defined in the optimisation problem.

To solve the problem, a multi objective optimisation Nondominated Sorting Genetic Algorithm II (NSGA-II) (Deb 2002) implemented in HeuristicLab optimisation framework (Wagner 2009) is applied. The optimization problem itself is implemented as a multi-objective optimisation problem plug-in of HeuristicLab with integer encoding of solutions and their evaluation by two mathematical functions (3) and (4).

In experiments with NSGA-II, the following operators were applied: a discrete crossover operator for integer vectors (Gwiazda 2006); an uniform one position manipulator (mutation operator) (Michalewicz 1999); and a crowded tournament selector (Deb 2002). A termination criterion is defined by a number of generations, i.e. 10000 generations in this case.

Selected solution in the middle of the Pareto front (see Fig. 4) obtained with the NSGA-II algorithm has compact clusters or regions. Moreover, these results show that only two regions demands are much lower than others. Further leveraging of the region demand could make worse the geographical location of regions with higher priority.

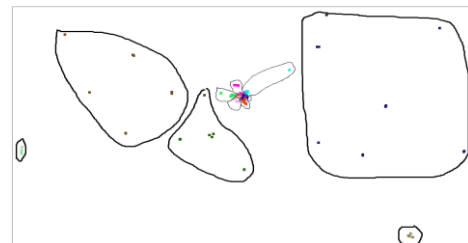


Figure 4: Solution in the Middle of the Pareto Front

5. VEHICLE ROUTING AND SCHEDULING

Within the proposed integrated delivery planning and scheduling approach, vehicle routing and scheduling tasks are solved at the operational planning level. Data from a delivery tactical plan, which description is out of the paper scope, are transferred. For each planning day,

vehicle routes and schedules are defined to minimize their transportation costs.

5.1. Vehicle Routing with Time Windows

Classical statement of the vehicle routing problem with time windows (VRPTW) is applied (Cordeau et al. 2001). Input data includes a set of customers, and data about their geographical locations and demand. Each customer has to be served by one vehicle and only once within a planning horizon. For each customer time window when it has to be served is defined. Vehicles routes start and end in DC. Shortest routes for a fleet of homogenous vehicles with limited capacity have to be found.

To solve the problem, a coarse-grained island genetic algorithm with offspring selection (IOSGA) (Affenzeller et al. 2009) was applied. IOSGA parameters are defined as follows: a proportional selector; 5 islands; 200 individuals in population; ring mutation each 20 generations with 15% rate; random individuals are replaced with best from the neighbouring island. Maximal selection pressure was set to 200, and mutation was applied with 5% rate. Mutation operators provided in HeuristicLab framework were involved.

A set of optimisation experiments were performed in order to define which of crossover operators provides most relevant results (see Fig. 5). These results were obtained with GVR crossover (Pereira et al. 2002) and with edge recombination (ERX) and maximal preservative (MPX) crossovers for solutions encoded in Alba encoding (Alba and Doronso 2004). Application of the ERX crossover provided the best results in terms of the total distance and preserved the defined number of available vehicles. However, the results obtained for Alba encoded solutions were worse in terms of the capacity constraints violation. In turn, application of GVR crossover although provides solutions with an overflow of number of vehicles, nevertheless the capacity constraints are satisfied in most cases.

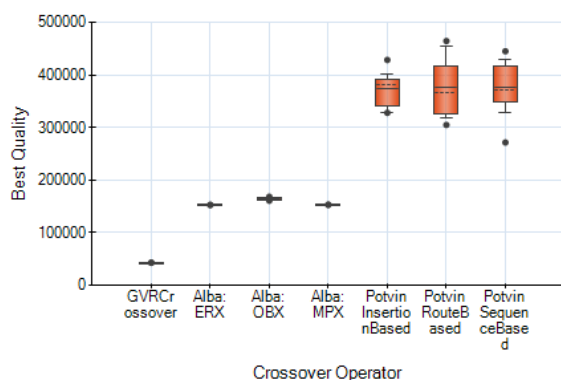


Figure 5: Performance of Crossover Operators in VRP

Finally, a crossover operator which works with an unlimited number of vehicles, but provides best results in terms of keeping routes not overloaded such as GVR crossover was selected. To minimize a number of

required vehicles later, the vehicle scheduling problem is introduced in the next paragraph.

5.2. Vehicle Scheduling for the Routed Solution

While solving the classical VRPTW it is assumed that any vehicle may perform only one route in the planning horizon. Each route starts and ends in the depot of the distribution centre, and defines the sequence of the customers served.

In the business case, all routes are shortened by the capacity of vehicles. Both routing and scheduling tasks are performed each day, and planning horizon is defined by 24h. This leads to ineffective solutions, where each vehicle generally performs only one short task of a few hours long and most of the day this vehicle is idle.

This problem can be formulated as Vehicle Scheduling Problem with Time Windows (VSPTW) and solved with methods and tools developed in (Merkuryeva and Bolshakov 2012). Here, the routes correspond to the trips in the VSPTW task and are assumed to be independent from vehicles; and vehicles may perform any fair number of routes during the day.

As far as the final solution of the VRPTW task is feasible for the capacity and time window constraints, it could be optimised by combining and compacting routes to increase vehicle utilization. As a result, during the day each vehicle can perform a sequence of the predetermined routes. Application of the vehicle scheduling for the solution of vehicle routing problem allows reducing a number of required vehicles.

Here, the problem statement described in (Merkuryeva and Bolshakov 2012) has been modified. Routing was performed for each group of delivered goods. Furthermore, for all customers time windows and service times were introduced, which made the problem definition more flexible. Input data used in the vehicle routing task is transferred to the vehicle scheduling one. The vehicle loading time is replaced by a service time in DC.

Let note that for the unification with a VRPTW, a sequence of stores in trips in a new statement was defined as route. Correspondingly, moving times in a trip were interpreted as transportation times in a route. Finally, a vehicle capacity is not involved in the problem, as in the VRP all vehicles have same capacity, and no route of feasible VRP solution will exceed this value.

5.3. Route Scheduling

To implement a solution for vehicle scheduling problem, a problem plug-in in HeuristicLab optimisation framework was developed. Input data are defined as follows:

- Ready time for each customer, in minutes;
- Due time for each customer;
- Service time for each customer;
- List of routes (obtained in VRP solution);
- List of route transportation times, which includes times for vehicles to move between

sequential points of routes (obtained in VRP solution);

- Estimated number of vehicles.

Solution fitness evaluator in the plug-in simulates a schedule of a solution candidate and identifies time windows mismatches, evaluates idle times and the total usage time for each vehicle. Two types of soft constraints are introduced:

1. Number of times when a vehicle arrives to a customer after due time defined by N_{ad} ;
2. Number of vehicles with working hours more than 24 h defined by N_{ot} .

Fitness function f summarizes vehicle idle times, when a vehicle waits to fit the time window, and a number of constraint violations are multiplied by penalty values:

$$f = \sum_{i \in V} t_i + k_{ad} N_{ad} + k_{ot} N_{ot} \rightarrow \min, \quad (5)$$

where t_i is the total idle time of vehicle I ; V defines a set of available vehicles; k_{ad} and k_{ot} are the penalty coefficients for late arrivals and overtimes, correspondingly, and k_{ad} , k_{ot} are assumed to be significantly greater than 1.

A chromosome for solution candidates is encoded as the permutation which consists of integer values. Integers that are larger than the number of routes encode gaps in the chromosome, where for a vehicle a new sequence of routes starts. Other integers define corresponding routes in sequences. The encoding used is similar to one described in Alba and Dorronsoro (2004) for a vehicle routing problem. Application of permutation based encoding allows easy usage of different recombination and mutation operators.

For the schedule optimisation purpose, an Evolution Strategies algorithm implemented in HeuristicLab (Wagner 2009) is applied.

5.4. Experimental Results

Various series of optimisation experiments were performed to determine a suitable algorithm for the VSPTW. Following algorithms were examined: evolution strategies (ES), genetic algorithm (GA), island genetic algorithm with 5 islands (IGA) and offspring selection genetic algorithm (OSGA) (Affenzeller et al. 2009). Maximal preservative crossover and insertion manipulator were defined as genetic operators for all algorithms. To determine a suitable algorithm, numbers of solution evaluations performed to obtain candidate solutions of the equal fitness were compared on hard instances, with a low number of vehicles and short time windows. Results of optimisation experiments for a single instance are shown in Figure 6.

The results of comparisons show that same instance is solved with ES and OSGA in shortest time, while GA without modifications demonstrated the worst results. This behaviour of optimisation algorithms can be explained with potentially small effectiveness of the

crossover operator against a mutation operator. The evolution strategy was chosen as most suitable as it has ability to provide globally optimal results of VSP with fewer evaluations.

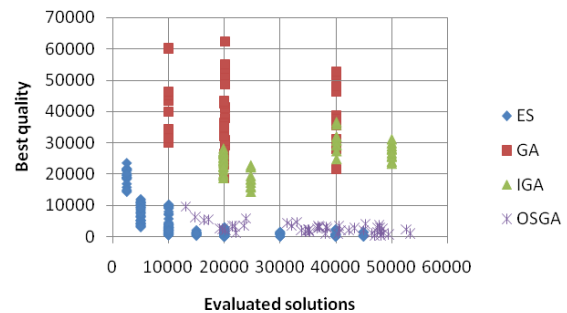


Figure 6: Productivity of Different Optimisation Algorithms for VSPTW

Following, a sample experiment based on one day plan and specific demand data for 53 stores is described. Time windows for most stores are defined from 6:00 a.m. to 9:00 p.m. Some stores can be served in any time.

Application of IOSGA for VRP has given 34 routes in the best found solution (see Figure 7). Most of the vehicles in the solution have very short routes due to a small vehicle capacity. But, due to long time windows of customers it is possible to combine these routes.

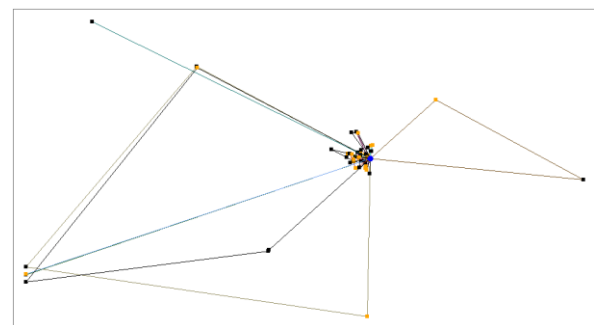


Figure 7: VRP Solution of the Case Instance

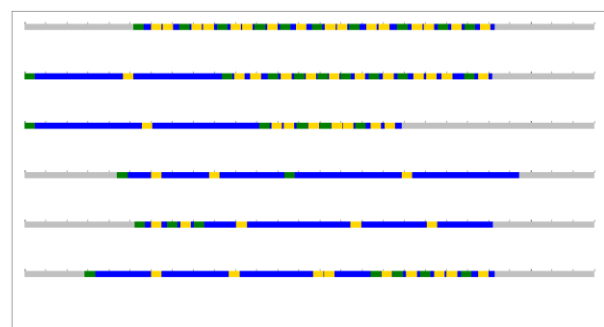


Figure 8: VSP Solution of the Case Instance

Finally, evolution strategies (100+20) were applied for the data obtained in VRP. A number of available vehicles in input data were varied. As a result, it was concluded that the problem instance had globally optimal solutions with all constraints satisfied if at least

6 vehicles are available. The correspondent Gantt chart is shown in the Figure 8. Green lines in the figure correspond to the loading times in DC and define beginning of routes from the VRP solution, blue ones to transportation times, and yellow lines define unloading times at stores.

Similar experimental results were obtained also for another problem instances. Better vehicle utilization was achieved for the instances with larger time windows.

5.5. Monitoring

Here, monitoring provides a long feedback link to an optimization tool at the operational and tactical levels of planning (Fig. 2). After the best solution found in the optimisation is applied in a real life, a new state of the system observed in monitoring is used to adjust parameters of the simulation model. In turn, an adjusted model is applied in further simulation optimisation experiments. And, despite the increasing a time factor, a simulation optimiser is applied to find benefits of a real-life system, and more realistic solutions will be received.

6. CONCLUSIONS

Combination of data mining, simulation, optimisation and monitoring techniques provides the powerful integrated planning approach that ensures effective decisions on various stages and levels of the delivery planning process. A cluster analysis of the input data reasonably reduces the dimensions of the tactical planning tasks and complexity of planning tasks at the operational level. The proposed vehicle scheduling method that complements vehicle routing ensures effective route and schedule solutions for a short-term delivery planning. This method can be applied for vehicle routing and scheduling tasks, where routes are very short in comparison with a planning horizon.

ACKNOWLEDGMENTS

This work has been supported by the European Social Fund within the project “Support for the implementation of doctoral studies at Riga Technical University” and by the program “Estonia-Latvia-Russia cross border cooperation Programme within European Neighborhood and Partnership instrument 2007-2013”, project 2.1/ELRI-184/2011/14 “Integrated Intelligent Platform for Monitoring the Cross-Border Natural-Technological Systems”.

Authors are grateful to the developers of the HeuristicLab environment for the possibility of using it in the research, and to personally Prof. M. Affenzeller, researchers E. Pitzer and S. Vonolfen for their support in the development and implementation of vehicle routing and scheduling tasks.

REFERENCES

Affenzeller, M., Winkler, S., Wagner, S., Beham, A., 2009. *Genetic Algorithms and Genetic*

Programming: Modern Concepts and Practical Applications. Chapman & Hall/CRC.

Alba, E., Dorronsoro, B., 2004. Solving the vehicle routing problem by using cellular genetic algorithms. *Proceedings of EvoCOP 2004*, pp. 11–20. April 5-7, Coimbra, Portugal.

Deb, K., Pratap, A., Agarwal, S., Meyarivan, T., 2002. A Fast and Elitist Multiobjective Genetic Algorithm: NSGA-II. *IEEE Transactions on Evolutionary Computation*, 6(2), pp. 182-197.

Cordeau, F., Desaulniers, G., Desrosiers, J., Solomon, M.M., Soumis, F., 2001. VRP with Time Windows. In: Toth P., Vigo D., eds. *The vehicle routing problem*. Philadelphia, PA, USA: Society for Industrial and Applied Mathematics, pp. 157–193.

Gwiazda, T.D., 2006. *Genetic algorithms reference Vol. I. Crossover for single-objective numerical optimization problems*. TOMASZGWIAZDA E-BOOKS.

Kaufman, L., Rousseeuw, P.J., 1990. *Finding Groups in Data: An Introduction to Cluster Analysis*. Hoboken, NJ: John Wiley & Sons, Inc.

MacQueen, J. B., 1967. Some Methods for Classification and Analysis of MultiVariate Observations. *Proc. of the 5th Berkeley Symposium on Math. Statistics and Probability*, Vol. 1, pp. 281–297.

Merkuryeva, G., Bolshakov, V., 2012. Simulation-based Fitness Landscape Analysis and Optimisation for Vehicle Scheduling Problem. In: Moreno D.R., et al., eds. *Computer Aided Systems Theory – EUROCAST 2011, Part I, LNCS 6927*, pp. 280–286.

Merkuryeva, G., Bolshakov, V., Kornevs, M., 2011. An Integrated Approach to Product Delivery Planning and Scheduling. *Scientific Journal of Riga Technical University*, 5 (49), pp. 97–103.

Michalewicz, Z., 1999. *Genetic Algorithms + Data Structures = Evolution Programs. Third, Revised and Extended Edition*. Springer-Verlag Berlin Heidelberg.

Pereira, F.B., Tavares, J., Machado, P., Costa E., 2002. GVR: A New Genetic Representation for the Vehicle Routing Problem. *Proceedings of the 13th Irish International Conference on Artificial Intelligence and Cognitive Science (AICS '02)*, pp. 95–102. September 12-13, Limerick, Ireland.

Robinson, S., 2004. *Simulation. The Practice of Model Development and Use*. John Wiley & Sons, Ltd.

Seber, G.A.F., 1984. *Multivariate Observations*. Hoboken, NJ: John Wiley & Sons, Inc.

Wagner, S., 2009. *Heuristic Optimization Software Systems - Modeling of Heuristic Optimization Algorithms in the HeuristicLab Software Environment*. PhD Thesis. Institute for Formal Models and Verification, Johannes Kepler University Linz, Austria.

UNSUPERVISED LEARNING APPROACH TO FEATURE SELECTION IN BIOLOGICAL DATA ANALYSIS

Witold Jacak^a, Karin Proell^b

^a Department of Software Engineering

Upper Austria University of Applied Sciences Hagenberg, Austria

^b Department of Medical Informatics and Bioinformatics

Upper Austria University of Applied Sciences Hagenberg, Austria

ABSTRACT

In this paper we present a novel method for scoring function specification and feature selection by combining unsupervised learning with supervised cross validation. Unsupervised clustering methods (k-means, one dimensional Kohonen SOM, fuzzy c-means) are used to perform a clustering of object-data for a chosen subset of input features and given number of clusters. The resulting object clusters are compared with the predefined original object classes and a matching factor (score) is calculated. This score is used as criterion function for heuristic sequential feature selection and novel cross selection algorithm.

Keywords: Index Terms— classification, clustering, feature selection, k-mean, fuzzy c-mean, Kohonen SOM, MLP

1. INTRODUCTION

Classification of biological data means to develop a model that will divide biological observations into a set of predetermined classes N . Typically a biological data set is composed of many variables (features) that represent measures of biological attributes in biological experiments. A common aspect of biological data is its high dimensionality that means the data dimension is high, but the sample size is relatively small. This phenomenon is called high dimensionality-small sample problem (Kwak et al. 2002, Maiorana et al. 2008, Zhang et al. 2000). The smaller the sample, the less accurate are the results of classification and the amount of error increases.

Traditional statistical classification procedures such as discriminant analysis are built on the Bayesian decision theory (Kwak et al. 2002, Raghavendra et al. 2010, Silva et al. 2012). In these procedures, a probability model must be assumed in order to calculate the posterior probability upon which the classification decision is performed. One major limitation of the statistical models is that they work well only when the underlying assumptions are satisfied. Users must have a good knowledge of both data properties and model capabilities before the models can be successfully applied (Kohavi et al. 1997, Törmä et al. 1996). The recent research activities in classification problem have established that neural networks are a promising alternative to various conventional classification methods (Chen et al. 2006, Maiorana et al. 2008, Su et al. 2000, Raghavendra et al. 2010, Zhang et al. 2000, Ye et al. 2002). Neural networks are data driven self-adaptive systems in a way that they can adjust themselves to the data without any explicit

specification of a functional or distributional form for the underlying model. Neural networks are able to estimate the posterior probabilities, which provide the basis for establishing classification rules and performing statistical analysis (Zhang et al. 2000, Ye et al. 2002). The effectiveness of neural network classification has been tested empirically, and depends on the quality of input data.

There are many reasons to perform feature selection before developing the classification model. Feature selection problems are found in all supervised and unsupervised neural network learning tasks including classification, regression, time-series prediction, and clustering (Lee et al. 2004, Maiorana et al. 2008, Raghavendra et al. 2010, Törmä et al. 1996).

Using all features to create the model does not necessarily give the best performance (peaking phenomenon) (Maiorana et al. 2008, Pal et al. 2002). A model with less features (variables) is faster to construct and easier to interpret, especially in biological data mining where a domain expert should interpret and validate such a model. Using classical supervised clustering and classification methods could lead especially in case of small sample sets, to a faster overfitting of a model during the training phase and to worse prediction performance. Previously performed feature selection could avoid overfitting and improve the model performance in prediction.

Generally, the feature selection problem deals with choosing those input variables from the measurement space (all input variable) that are most predictive for a given target and constitute the feature space. The main objective of this process is to retain the optimum number of input variables necessary for the target recognition and to reduce the dimensionality of the measurement space so that an effective and easily computable model can be created for efficient data classification. Appropriate feature (input variable) selection can enhance the effectiveness of an inference model.

Feature selection methods can be grouped in four categories (Kwak et al. 2002, Maiorana et al. 2008, Zhang et al. 2000).

1) Filter techniques select the features by looking only at the intrinsic property of input data and ignore feature dependencies. These techniques are independent of the classification model (Kwak et al. 2002).

2) Wrapper methods use the hypothesis model for search of a feature subset. Hypothesis models are usually

constructed in a supervised way during the training phase (e.g. Bayes model or multi-layer perceptron neural network MLP) but they increase the risk of overfitting especially in case of small sample sizes (Kohavi et al. 1997).

3) Embedded techniques in which the search for an optimal subset of features is built into classifier construction (Kohavi et al. 1997, Su et al. 2000, Thangavel et al. 2006).

4) Feature selection after classification uses discriminant analysis to find sensitive variables (Kwak et al. 2002, Pal et al. 2002).

These techniques can be used by exhaustive search or heuristic search. The exhaustive search method tries to find the best subset among 2^m candidate subsets, where m is the total number of features. Such a search could be very time consuming and practically unacceptable; even for a medium-sized feature set. Heuristic search methods, which use a learning approach, reduce computational complexity (Kwak et al. 2002). There are two kinds of learning methods, supervised learning and unsupervised learning. In case of supervised learning the incorporation of prior knowledge about membership of classes into the training data is the key element to substantially improve classification performance. But full knowledge increases the risk of overfitting during the training phase of the model and as a consequence prediction performance for novel data decreases. On the other hand unsupervised learning ignores interaction with the classifier model (Faro et al. 2005, Maiorana et al. 2008, Törmä et al. 1996, Ye et al. 2002).

In this paper we present a novel method for scoring function specification and feature selection by combining unsupervised learning with supervised cross validation. A one dimensional Kohonen SOM (Self-Organizing Map) is used to perform a clustering of objects-data for a chosen subset of input features and given number of clusters. The resulting object clusters are compared with the predefined original object classes and a matching factor (score) is calculated. This score is used as criterion function for heuristic sequential feature selection. Additionally, the significance of an individual feature for recognition of original classes or composed groups of original classes is calculated based on this matching factor. The results are compared and aggregated with the result of sequential feature selection to find the final sensitive feature space. Sequential feature selection searches for a subset of the features in the full model with comparative predictive power. The final result is a reduced model with only few of the original features. In the next step these features are used to build and train the MLP network model for object classification.

2. UNSUPERVISED NEURAL NETWORKS BASED MATCHING FACTOR

The four different clustering methods are used to perform clustering for given number of cluster based on object-data for chosen input features subset. Those obtained clusters

are finally compared and validated with the predefined original classes and matching factors (scores) are calculated. The system for classifying object-data model consists of four procedures working in parallel: k-mean clustering, fuzzy c-mean clustering, one dimensional Kohonen SOM neural network and hierarchical clustering. Usually the output neurons of SOM are arranged in a bi-dimensional array, but we use an implementation of the network where the output neurons are arranged along a single layer (SL configuration). In the SL configuration the classes are given by the output neurons. In this case there is no topological similarity between output neurons since adjacent output neurons do not represent necessarily similar classes.

The resulting clusters are compared to one another and to the predefined target classes by using the matching factor p . A final score takes into account only the results of the independent clustering procedures with pairwise high matching factors and a high matching factor between its cluster and the original target classes. The final score is calculated as the mean value of the matching factors of these clusters. The system for calculating the matching factor is presented in Fig. 1.

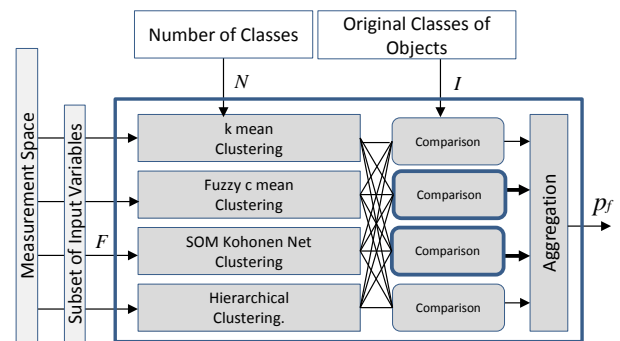


Fig. 1 Calculation of global matching score

Let $I = \{1, \dots, N\}$ be a set of indexes of target classes L and $J = \{1, \dots, N\}$ be a set of indexes of cluster set K generated from pure input data of objects with unsupervised learning using for example SOM-SL neural network. Let $L_i \in L$ be a subset of objects belonging to original class $i \in I$ and $K_j \in K$ is a subset of objects belonging to cluster $j \in J$ created by the SOM-SL network. For each $i \in I$ and $j \in J$ we define the Jaccard matching coefficient c_{ij} as follows

$$c_{ij} = \frac{|L_i \cap K_j|}{|L_i \cup K_j|} \quad (1)$$

We use this coefficient to define the global matching factor p_f between the generated cluster and the original target classes in an iterative manner. For $n=1, \dots, N$ we calculate

$$p_{ij}^n = \begin{cases} c_{ij} & \text{if } c_{ij} = \max\{c_{ik} | l \in I_{n-1}, k \in J_{n-1}\} \text{ and} \\ & s_i = \sum(c_{ik} | k \in J_{n-1}) = \min \text{ and} \\ & s_j = \sum(c_{ij} | l \in I_{n-1}) = \min \end{cases} \quad (2)$$

where $I_0=I$, $J_0=J$, and $J_n=J_{n-1} - \{j\}$, $I_n=I_{n-1} - \{i\}$. Calculation stops when J_n and I_n are empty sets.

It is easy to observe that the $N \times N$ sized matrix $P = [p_{ij}]$ has only N elements greater zero and represent the best allotment of the generated clusters to the original classes. The global matching factor p_f can be defined as mean value of non-zero elements of P :

$$p_f = \text{avg}(p_{ij}) \quad \text{where } p_{ij} > 0 \quad (3)$$

The matching factor describes the score of recognizing the original target classes by unsupervised clustering which is simply based on input data without prior knowledge of classes. This factor uses posterior knowledge to calculate the score for validating the chosen set of individual features or group feature groups. The choice of features should maximize the matching factor.

3. FEATURE SELECTION SYSTEM

The matching factor p_f is used as score for finding the sensitive group of input features. The feature selection system contains two modules: one module for sequential feature selection techniques with matching factor as quality criterion function, and one module for searching individual sensitive features, which discriminate the chosen group of composed subset of original predefine classes. The system is presented on Fig.2.

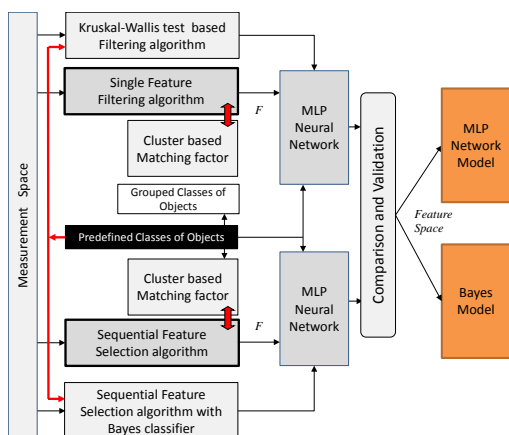


Fig. 2 Mixed feature selection system based on unsupervised learning

3.1. Features cross selection method

The subset of original classes $\{L_i, L_k, \dots, L_m\} \subset L$ is grouped together into one new class $LC_i = \cup \{L_i, L_k, \dots, L_m\}$, which contains all objects data from its components. The new classes set LC cover a set of original classes, i.e.

$$\cup LC_i = \cup L$$

The new set of target classes determines the new number of classes. This number $|LC|$ is used for unsupervised clustering the previously grouped input data with clustering procedures and next to calculate the matching factor between generated clusters and the new classes set. In this way we can search for significant features, which discriminate the subsets of original classes. Usually the grouping of original classes into larger new classes is not accidental and is performed based on domain specific

knowledge concerning properties of objects being classified.

For each group of target classes and also for original classes it is possible to test the significance of every single variable due to its predictivity of the target classes. After the calculation of the matching factor individually for each variable, only variables with matching factor greater than a given threshold-value are chosen from all m variables as candidates for feature space.

Let LC^k ($k = 1, \dots, M$) denote the k -th experiment with chosen subsets of original target classes then $F^k \subset \{1, \dots, m\}$ is the set of selected sensitive features for the best recognition of the new composed classes in this experiment. When the chosen new larger classes sets LC^k meet the condition

$$\cap LC^k = L \quad (4)$$

then the selected sensitive features for recognition of the full original target could be defined as

$$F = \cup F^k \quad (5)$$

Such selected features are compared to feature sets found by the forward/backward sequential selection procedure. Both candidates of sensitive feature sets are used to train a multi-layer perceptron neural network (MLP) to build the model and to evaluate the performance of target recognition and prediction.

4. EXPERIMENTS AND RESULTS

In this study, the aim is to test the quality of a feature selection method based on a combination of unsupervised learning and posterior validation in comparison to standard statistic algorithms. A collection of biological data for 288 objects is used in experiment. The objects belong to four predefined classes (target classes) $L = \{A, B, C, D\}$. Each object is described with 89 input measurement variables (parameters). The measurement space - full feature set - is therefore $F = (f_1, \dots, f_{89})$.

The task is to find a subset of input variables $F_i \subset F$ with a minimal number of sensitive features, which recognize the four target classes without loss of classification quality. This subset will be used to develop a model for object classification. Additionally the feature sets, which recognize two subsets of the original target classes were identified. In the first the classes A, B and C, D are combined together i.e. $LC^1 = \{\{A \cup B\}, \{C \cup D\}\}$ and in the second the classes A, C and B, D i.e. $LC^2 = \{\{A \cup C\}, \{B \cup D\}\}$. Since $LC^1 \cap LC^2 = L$, the union of sensible features for recognition of LC^1 and LC^2 could be used as a discriminant feature set for the whole target classes set L .

For all groups of target classes we calculate the matching factor p_f individually for each input variable and compare it to statistical significance of Kruskal-Wallis one-way analysis of variance test results. We consider a threshold equal to 80% of maximal value of p_f to filter the first candidate set of significant features. The matching factor for single variable, the inverse of the p-value of Kruskal-Wallis test and filtered set of features for recognition of four original classes is presented in Fig.3.

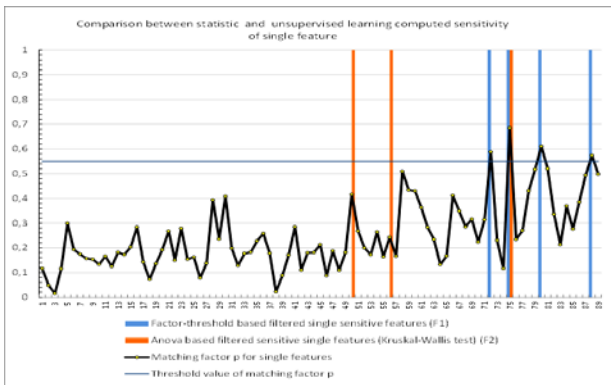
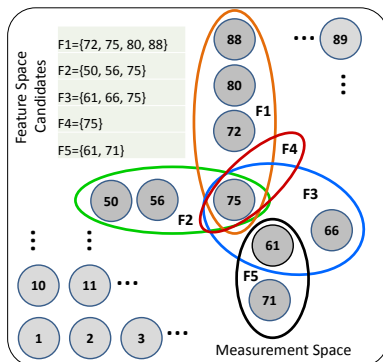


Fig. 3 The matching factor for single variable and filtered set of features for recognition of four original classes

The whole collection of data was used as input features for a forward sequential feature selection with the SOM matching factor p_f as performance criterion and additionally we performed a second sequential feature selection with a Bayes classifier as performance function. The selected features in both approaches are presented in Fig. 4.

Both methods applied for previously described classes LC^1 and LC^2 found only one single sensitive feature in each of both cases, $\{f_{61}\}$ and $\{f_{71}\}$ respectively (see Fig.4.). The union of these is used as the new features subset of candidates for feature space. The results of the applied feature selection techniques are presented in Fig.4.



Method	Selected Features	Prediction performance
Factor-threshold based filtered single sensitive features (F1)	F1={72, 75, 80, 88}	87,8%
Anova based filtered sensitive single features (Kruskal-Wallis test) (F2)	F2={50, 56, 75}	78,3%
Sequential feature selection with matching factor p as performance function (F3)	F3={61, 66, 75}	95,7%
Sequential feature selection with Bayes classifier as performance function (F4)	F4={75}	73,9%
Features selected as union of discriminants of subsets of target classes (F5)	F5={61, 71}	99,2%

Fig.4. Features selected with different algorithms for recognition of 4 original object classes

After the feature selection phase a multi-layer perceptron network is used to classify the training and validation dataset in the reduced feature space. The classification results are compared with the classes indicated in the original dataset.

The results of feature selection were validated with a two-layer perceptron network (MLP) with four neurons in the hidden layer. The data set was divided into training set - 70 % of samples and test set -30% of samples. The correct classification rate to original class in percent is presented in

Fig. 5.

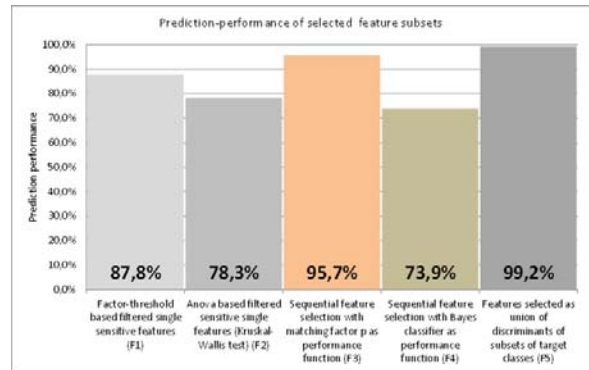


Fig.5. Comparison of classification-performance of selected features subsets

The feature spaces found using the combined unsupervised clustering and the posterior validation for matching factor calculation show a better classification rate for predefined original classes as features selected with classical statistic methods (Fig. 5). It demonstrates the feasibility and effectiveness of the proposed novel method for score calculation, which is independent of the classification model.

5. CONCLUSION

In this paper a feature selection method independent of the underlying classification model and based on clustering algorithms of the Kohonen SOM family, k-mean, fuzzy c-mean with posterior validation has been proposed. The analysis was performed on biological data. The presented method can be classified as a heuristic method, which obtains an effective feature reduction with almost the same correct classification rate. Heuristics is designed on an unsupervised learning approach. The optimal number of feature space dimensions is therefore difficult to determine. Future works are to extend the analysis to datasets with different number of samples and to further investigate the distance measures to assess the impact on classification performance.

REFERENCES

- Chen Y., Abraham A., Yang B., "Feature selection and classification using flexible neural tree", Neurocomputing, Vol. 70, 2006
- Faro G., Giordano D., Maiorana F., "Discovering complex regularities by adaptive Self Organizing classification," Proceedings of WASSET, Vol. 4, 2005:
- Kohavi R., John G. H., "Wrappers for feature subset selection," Artificial Intelligence, vol. 97, no. 1-2, 1997
- Kwak N., Choi C., "Input Feature Selection for Classification Problems", IEEE Transactions on Neural Networks, Vol. 13, No. 1, 2002
- Lee K., Booth D., State K., Alam P., "Backpropagation and Kohonen Self-Organizing Feature Map in Bankruptcy Prediction" in Neural Networks in Business Forecasting, edited by G. Peter Zhang, , Idea Group Inc., 2004

- Maiorana F., “*Feature Selection with Kohonen Self Organizing Classification Algorithm*”, World Academy of Science, Engineering and Technology, Proceedings of WASET, Vol. 45, 2008
- Su Mu-Chun, Chang Hsiao-Te, “*Fast Self-Organizing Feature Map Algorithm*”, IEEE Transactions on Neural Networks, Vol. 11, no. 3, 2000
- Pal S. K., De R. K., Basak J., “*Unsupervised Feature Evaluation: A Neuro-Fuzzy Approach*”, IEEE Transactions on Neural Networks, Vol. 11, No. 2, 2000
- Raghavendra B. K., Simha J. B., “*Evaluation of Feature Selection Methods for Predictive Modeling Using Neural Networks in Credits Scoring*”, Int. J. Advanced Networking and Applications, Vol-02, Issue: 03, 2010
- Silva B., Marques N., “*Feature clustering with self-organizing maps and an application to financial time-series for portfolio selection*”, Proceedings of Intern. Conf. of Neural Computation, ICNC, 2010
- Thangavel K., Shen Qiang, Pethalakshmi A., “*Application of Clustering for Feature Selection Based on Rough Set Theory Approach*”, AIML Journal, Volume (6), Issue (1), January, 2006
- Törmä M., “*Self-organizing neural networks in feature extraction*”, Intern. Arch. of Photogrammetry and Remote Sensing, Vol. XXXI, Part 2, 1996
- Zhang G. P., “*Neural Networks for Classification: A Survey*”, IEEE Transactions on Systems, Man, And Cybernetics—Part C: Applications And Reviews, Vol. 30, No. 4, 2000
- Ye H., Liu H., “*A SOM-based method for feature selection*”, Proceedings of the 9th International Conference on Neural Information Processing (ICONIP’02), Vol. 3, 2002

IMPROVED LINEARITY CMOS MULTIFUNCTIONAL STRUCTURE USING COMPUTATIONAL CIRCUITS

Cosmin Popa

University Politehnica of Bucharest,
Faculty of Electronics, Telecommunications and Information Technology, Romania

cosmin_popa@yahoo.com

ABSTRACT

Original low-power low-voltage multifunctional structure with improved performances will be presented, allowing to implement (with minor changes in the design) two important functions: signal gain with theoretical null distortions and simulation of a perfect linear resistor with positive equivalent resistance. The great advantages of the increased modularity and controllability and of the reduced design costs associated represent an immediate consequence of the multiple functions realized by the proposed structures. The linearity is strongly increased by implementing original techniques, while the silicon occupied area per function is reduced as a result of the proposed multifunctionality. The structures are implemented in $0.35\mu\text{m}$ CMOS technology and are supplied at $\pm 3V$. The circuits present a very good linearity (in the worst case, $THD < 0.4\%$), correlated with an extended range of the input voltage (at least $\pm 0.5V$). The tuning range of the active resistors is about hundreds $k\Omega - M\Omega$.

Keywords: Linearity, multifunctionality, computational circuits, VLSI design

1. INTRODUCTION

An important goal in VLSI designs is represented by the possibility of a multiple use for the same cell, the increased modularity that could be achieved being reflected in an important reduction of the design costs per implemented function.

The differential amplifier is an important stage of a large area of applications, including high-performances analog/mixed ICs, such as operational amplifiers, voltage comparators, voltage regulators, video amplifiers, modulators and demodulators or A/D and D/A converters. The linearity of the circuit is relatively poor because of the fundamental nonlinear characteristic of MOS transistors, resulting the possibility of achieving a relatively good linearity only for a restricted input voltage range (the amplitude of the input voltage for the classic differential amplifier using MOS transistors in saturation have to be below a few hundreds of mV). In conclusion, it results the necessity of implementing a linearization technique for decreasing the superior-order nonlinearities of the MOS differential stage and for increasing the available range for the input voltage amplitudes. It exists in literature many

circuit techniques used to improve the MOS differential amplifier linearity. It was presented in [1], [2] a third and fifth-order harmonics cancellation with good results and a relatively simple circuit implementation.

A constant-sum of the gate-source voltages circuit connection was described in [3] and it allows an important reduction of the total harmonic distortions coefficient of the circuit. In [4], it was presented and implemented in CMOS technology a simple technique based on square-root circuits for improving the CMOS differential stage linearity, which compensates the quadratic characteristic of the MOS transistor in saturation.

CMOS active resistors are very important blocks in VLSI analog designs, mainly used for replacing the large value passive resistors, with the great advantage of a much smaller area occupied on silicon. Their utilisation domains includes amplitude control in low distortion oscillators, voltage controlled amplifiers and active RC filters. These important applications for programmable floating resistors have motivated a significant research effort for linearising their current-voltage characteristic. The first generation of MOS active resistors [5], [6] used MOS transistors working in the linear region. The main disadvantage is that the realized active resistor is inherently nonlinear and the distortion components were complex functions on MOS technological parameters. A better design of CMOS active resistors is based on MOS transistors working in saturation. Because of the quadratic characteristic of the MOS transistor, some linearization techniques [7], [8] were developed in order to minimize the nonlinear terms from the current-voltage characteristic of the active resistor. An important class of these circuits, referring to the active resistors with controllable negative equivalent resistance, covers a specific area of VLSI designs, finding very large domains of applications such as the canceling of an operational amplifier load or the design of Deboo integrators with improved performances.

The original idea proposed in this paper is to use a linear CMOS differential amplifier for obtaining (with minor changes in the design) two important functions:

- The signal gain with theoretical null distortions;
- Simulation (in a first-order analysis) of a perfect linear resistor using exclusively MOS active devices, having the advantages of a very good controllability of the equivalent resistance and of an important reduction of the silicon occupied

area, especially for large value of the simulated resistance;

2. THEORETICAL ANALYSIS

2.1. Analysis of the classical MOS differential amplifier

The analysis of the large signal operation for the classical MOS differential structure (Fig. 1) can quantitatively evaluate the circuit's nonlinearity, being possible to determine the weight of each superior-order distortion introduced by the structure nonlinearity.

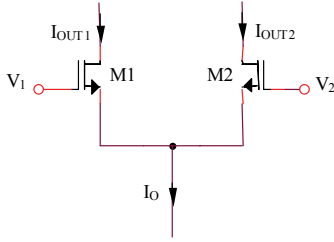


Figure 1: Classical MOS differential structure

The output currents of the classical differential amplifier can be expressed as a function of the differential input voltage as follows:

$$(I_{OUT1})_{1,2} = \frac{I_O}{2} \pm \frac{I_O}{2} \sqrt{\frac{KV^2}{I_O} - \frac{K^2V^4}{4I_O^2}} \quad (1)$$

so:

$$I_{OUT1} = \frac{I_O}{2} + \frac{I_O}{2} \sqrt{\frac{KV^2}{I_O} - \frac{K^2V^4}{4I_O^2}} \quad (2)$$

$$I_{OUT2} = \frac{I_O}{2} - \frac{I_O}{2} \sqrt{\frac{KV^2}{I_O} - \frac{K^2V^4}{4I_O^2}} \quad (3)$$

The differential output current will be:

$$I_{OUT2} - I_{OUT1} = -\frac{V}{2} \sqrt{4KI_O - K^2V^2} \quad (4)$$

The $(I_{OUT2} - I_{OUT1})(V)$ function is strongly nonlinear, the quantitative evaluation of the nonlinearity being possible using the Taylor series expansion. The Taylor series expansion of the transfer function (4) can be written as follows:

$$(I_{OUT2} - I_{OUT1})(V) = -K^{1/2}I_O^{1/2}V + \frac{K^{3/2}}{8I_O^{1/2}}V^3 + \frac{K^{5/2}}{128I_O^{3/2}}V^5 + \dots \quad (5)$$

or:

$$(I_{OUT2} - I_{OUT1})(V) = a_1V + a_3V^3 + a_5V^5 + \dots \quad (6)$$

a_k being constant coefficients with respect to V differential input voltage. So, as a result of squaring characteristics of MOS transistors biased in saturation, the classical MOS differential amplifier behavior is extremely nonlinear. The first term from (6) is linearly dependent on the input voltage, while the following two terms model the third-order and fifth-order nonlinearities of the differential structure. In conclusion, it is obviously the necessity of implementing a linearization technique for improving the performances of the classical MOS differential stage (good linearity for a relatively extended range for the amplitudes of the input voltage).

2.2. Improved linearity MOS differential structure

An improved linearity MOS differential structure is proposed in Fig. 2. "SQ" block represents a squaring circuit, having the original implementation presented in Fig. 4.

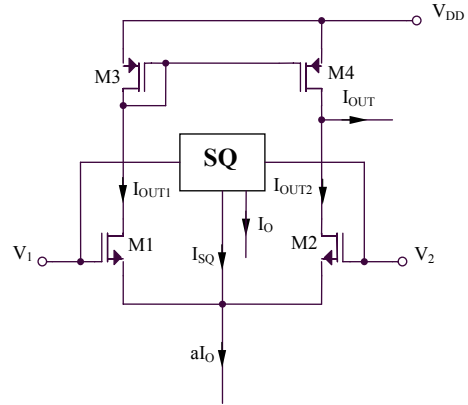


Figure 2: Improved linearity MOS differential structure

The differential output current for this circuit has the following expression:

$$I_{OUT} = (V_1 - V_2) \sqrt{K(aI_O - I_{SQ}) - \frac{K^2}{4}(V_1 - V_2)^2} \quad (7)$$

In order to obtain a linear behavior of the proposed differential structure, the I_{SQ} output current of the squaring circuit "SQ" must be the sum of a constant term and a term proportional with the square of the differential input voltage:

$$I_{SQ} = bI_O - \frac{K}{4}(V_1 - V_2)^2, \quad (8)$$

b being a positive constant, depending on the particular implementation of the squaring circuit. Replacing (8) in (7), it results:

$$I_{OUT} = \sqrt{(a-b)KI_O}(V_1 - V_2) = G_m(V_1 - V_2) \quad (9)$$

$G_m = \sqrt{(a-b)KI_O}$ being the circuit equivalent transconductance.

2.3. Implementation of the squaring circuit "SQ"

The proposed method for designing the required voltage squaring circuit is based on a differential amplifier (Fig. 3), having a controllable asymmetry between the geometries of its composing transistors. This difference between the aspect ratios of MOS transistors will introduce in the output currents of the differential amplifier a term proportional with the square of the differential input voltage.

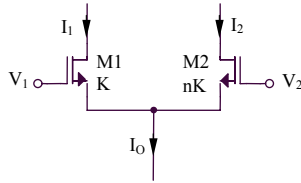


Figure 3: Asymmetrical differential structure

The differential input voltage, V , can be expressed as follows:

$$V = V_{GS1} - V_{GS2} = \sqrt{\frac{2I_1}{K}} - \sqrt{\frac{2(I_O - I_1)}{nK}}, \quad (10)$$

resulting:

$$\frac{K}{2}V^2 = I_1 + \frac{I_O - I_1}{n} - 2\sqrt{\frac{I_1(I_O - I_1)}{n}}. \quad (11)$$

The expression of I_1 current can be obtained solving the following second-order equation, derived from (11):

$$I_1^2 \left[\left(\frac{n-1}{n} \right)^2 + \frac{4}{n} \right] + \left(\frac{I_O - KV^2}{n} \right)^2 + I_1 \left[2\frac{n-1}{n} \left(\frac{I_O - KV^2}{n} \right) - \frac{4I_O}{n} \right] = 0 \quad (12)$$

So:

$$I_1 = \frac{I_O}{n+1} + \frac{n(n-1)}{2(n+1)^2}KV^2 + \frac{nV}{(n+1)^2} \sqrt{2KI_O(n+1) - K^2nV^2} \quad (13)$$

and:

$$I_2 = I_O - I_1 = \frac{nI_O}{n+1} - \frac{n(n-1)}{2(n+1)^2}KV^2 - \frac{nV}{(n+1)^2} \sqrt{2KI_O(n+1) - K^2nV^2} \quad (14)$$

The complete realization of a voltage squaring circuit, based on the previous proposed method, uses a cross-coupling of two differential amplifiers having controllable asymmetries between their geometries, M1-M2 and M3-M4 (Fig. 4).

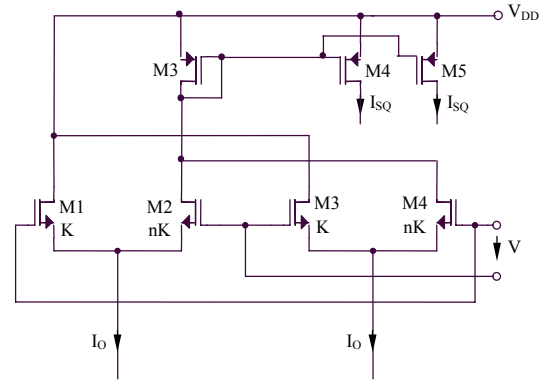


Figure 4: Squaring circuit

Using (13) and (14), it results:

$$I_{SQ} = I_{D2} + I_{D4} = \frac{nI_O}{n+1} - \frac{n(n-1)}{2(n+1)^2}KV^2 - \frac{nV}{(n+1)^2} \sqrt{2KI_O(n+1) - K^2nV^2} + \frac{nI_O}{n+1} - \frac{n(n-1)}{2(n+1)^2}KV^2 + \frac{nV}{(n+1)^2} \sqrt{2KI_O(n+1) - K^2nV^2} = \frac{2nI_O}{n+1} - \frac{n(n-1)}{(n+1)^2}KV^2 \quad (15)$$

2.4. Positive resistance active resistor circuit

The proposed active resistor circuit with positive equivalent resistance is presented in Fig. 5.

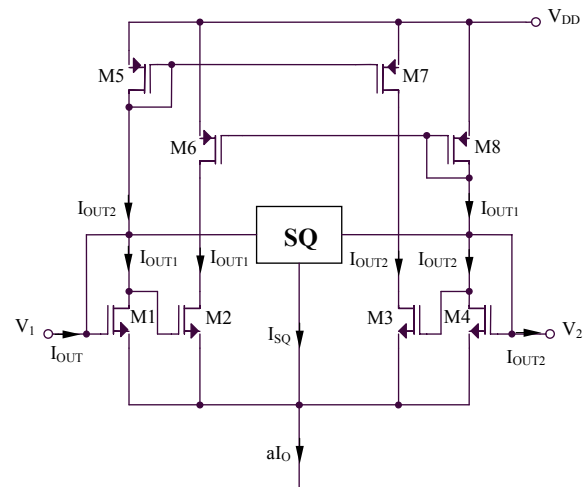


Figure 5: Positive resistance active resistor circuit

The current passing between the input pins V_1 and V_2 , $I_{OUT} = I_{OUT1} - I_{OUT2}$ has the following expression:

$$I_{OUT} = (V_1 - V_2) \sqrt{K \frac{aI_O - I_{SQ}}{2} - \frac{K^2}{4} (V_1 - V_2)^2}, \quad (16)$$

because each differential amplifier M1-M4 and M2-M3 is biased at a current equal with $I_{OUT1} + I_{OUT2} = (aI_O - I_{SQ})/2$. Using the expression (15) of I_{SQ} current, it results:

$$I_{OUT} = (V_1 - V_2) \sqrt{\frac{KI_O}{2} \left(a - \frac{2n}{n+1} \right) + \frac{K^2 (V_1 - V_2)^2}{2} \left[\frac{n(n-1)}{(n+1)^2} - \frac{1}{2} \right]}. \quad (17)$$

The conditions for obtaining a linear behavior of the circuit can be written as $\frac{n(n-1)}{(n+1)^2} = \frac{1}{2}$,

resulting $n_{1,2} = 2 \pm \sqrt{5}$ and:

$$I_{OUT} = (V_1 - V_2) \sqrt{\frac{KI_O}{2} \left(a - 2 \frac{2 \pm \sqrt{5}}{3 \pm \sqrt{5}} \right)}. \quad (18)$$

The equivalent resistance of the circuit presented in Fig. 5 will be:

$$R_{ECH} = \frac{V_1 - V_2}{I_{OUT}} = \left[\frac{KI_O}{2} \left(a - 2 \frac{2 \pm \sqrt{5}}{3 \pm \sqrt{5}} \right) \right]^{-1/2}. \quad (19)$$

3. SIMULATED RESULTS

The SPICE simulation $I_{OUT1,2}(V)$ based on $0.35 \mu m$ CMOS technology parameters for the original differential amplifier from Fig. 2 (representing the core of the multifunctional structure) is presented in Fig. 6, showing a very small linearity error. The supply voltage corresponds to low-power requirements, $V_{DD} = 3 V$.

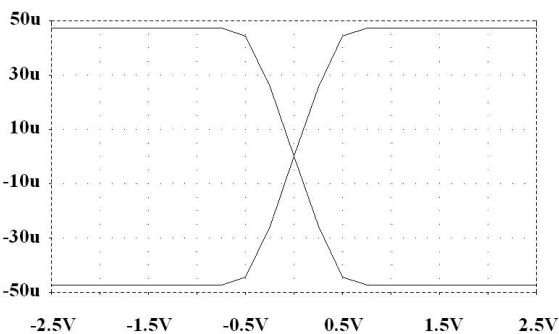


Figure 6: Simulation of the transfer characteristic for the original differential structure

4. CONCLUSIONS

An original low-power low-voltage multifunctional structure with improved performances was presented, allowing to implement (with minor changes in the design) two important functions: signal gain with theoretical null distortions and simulation of a perfect linear resistor with positive equivalent resistance. The great advantages of the increased modularity and controllability and of the reduced design costs associated represent an immediate consequence of the multiple functions realized by the proposed structures. The linearity is strongly increased by implementing original techniques, while the silicon occupied area per function is reduced as a result of the proposed multifunctionality. The structures are implemented in $0.35 \mu m$ CMOS technology and are supplied at $\pm 3V$. The circuits present a very good linearity (in the worst case, $THD < 0.4\%$), correlated with an extended range of the input voltage (at least $\pm 0.5V$). The tuning range of the active resistors is about hundreds $k\Omega - M\Omega$.

REFERENCES

- [1] Grasso, A.D., Pennisi, S., „High-Performance CMOS Pseudo-Differential Amplifier”, Circuits and Systems, 2005. ISCAS 2005. IEEE International Symposium on, 23-26 May 2005, pp. 1569 - 1572 Vol. 2.
- [2] Jongchan Kang, Kyungho Lee, Jehyung Yoon, Yisun Chung, Sungbo Hwang, Bumman Kim, „Differential CMOS Linear Power Amplifier with 2nd Harmonic Termination at Common Source Node”, Radio Frequency integrated Circuits (RFIC) Symposium, 2005. Digest of Papers. 2005 IEEE, 12-14 June 2005, pp. 443-446.
- [3] Jongchan Kang, Jehyung Yoon, Kyoungjoon Min, Daekyu Yu, Joongjin Nam, Youngoo Yang, Bumman Kim, „A Highly Linear and Efficient Differential CMOS Power Amplifier with Harmonic Control”, Solid-State Circuits, IEEE Journal of, Volume 41, Issue 6, June 2006, pp. 1314-1322.
- [4] Mohieldin, A.N., Sanchez-Sinencio, E., Silva-Martinez, J., „A Fully Balanced Pseudo-Differential OTA with Common-Mode Feedforward and Inherent Common-Mode Feedback Detector”, Solid-State Circuits, IEEE Journal of, Volume 38, Issue 4, April 2003, pp. 663-668.
- [5] Z. Wang, “Current-controlled Linear MOS Earthed and Floating Resistors and Application,” *IEEE Proceedings on Circuits, Devices and Systems*, 1990, pp. 479-481.
- [6] L. Sellami, “Linear Bilateral CMOS Resistor for Neural-type Circuits,” *Proceedings of the 40th Midwest Symposium on Circuits and Systems*, vol. 2, 1997, pp. 1330-1333.
- [7] C. Muniz-Montero, R. Gonzalez-Carvajal, A. Diaz-Sanchez, J.M. Rocha, “Low Frequency, Current Mode Programmable KHN Filters Using Large-Valued Active Resistors”, Circuits and Systems, 2007. ISCAS 2007. IEEE International Symposium on, 27-30 May 2007, pp. 3868 – 3871
- [8] T. Sanchez-Rodriguez, C. Lujan-Martinez, R. Carvajal, J. Ramirez-Angulo, A. Lopez-Martin, “CMOS Linear Programmable Transconductor Suitable for Adjustable Gm-C Filters”, *Electronics Letters*, Volume 44, Issue 8, April 10 2008 Pp. 505 – 506

THE IMPACTS OF DATA INACCURACY ON RETAILER'S PERISHABLE INVENTORY

Mert Bal^(a), Alp Ustundag^(b)

^(a) Yildiz Technical University, Mathematical Engineering Dept., Istanbul, Turkey

^(b) Istanbul Technical University, Industrial Engineering Dept., Istanbul, Turkey

^(a) mert.bal@gmail.com, ^(b) ustundaga@itu.edu.tr

ABSTRACT

Since perishable products such as fresh produce, dairy and meat have a finite usable lifetime and constitute more than a third of the worldwide sales at grocery retailers, controlling the inventories of these products is increasingly important. Without alignment of physical inventory and information system inventory, inventory information becomes inaccurate due to product spoilage and the retailer cannot take efficient inventory decisions. The purpose of this research is to investigate how the data inaccuracy affects the retailer's inventory performance for different levels of product lifetime, uncertainty of demand and lead time. Using a simulation model, the lost sales, product spoilage, average inventory and order quantities are calculated to investigate the retailer's performance over a 365 day period and ANOVA analysis is performed to examine the results.

Keywords: Perishable, Product lifetime, Inventory, Simulation, Data inaccuracy.

1. INTRODUCTION

Perishable products such as fresh produce, dairy and meat constitute more than a third of the worldwide sales at grocery retailers (Broekmeulen and Donselaar, 2009). The life of perishable product is a function of the product's characteristics and the environment in which the product is stored. An efficient cold chain is very essential to ensure that the product remains fresh for the expected duration. Beside the safety, timely production and delivery of perishable goods are very important. The rapid and continuous decaying characteristic of perishables makes the suppliers postpone the time to produce and deliver the product as fast as possible. However, a lot of perishable items exceed the expiration date in retailer's inventory. If the retailer doesn't track the items in real time, inventory data will become inaccurate. Therefore, inventory decisions will be taken with inaccurate data and the lost sales will increase.

According to Kendall and Lee (1980), the critical objectives of perishable product inventory management are (i) satisfying demand by carrying sufficient inventories (ii) holding down inventory carrying costs (iii) keeping the amount of product spoilage (outdating)

at an acceptable level, and (iv) maintaining quality by using the product while it is still fresh, and (v) keeping the cost rotation low.

Efficient inventory management is very critical for the retailer to increase the profitability. However, due to the discrepancy between physical inventory and information system inventory, the retailer cannot take efficient inventory decisions.

This study focuses on data inaccuracy of the retailer's perishable inventory and investigates the impacts of this inaccuracy on retailer's perishable inventory for different levels of product lifetime, demand and lead time uncertainty. Using a simulation model, the lost sales, product spoilage, average inventory and order quantities are calculated to investigate the retailer's performance.

This paper starts with the review of the relevant literature. Section 3 and 4 describe the simulation model and the experimental design respectively. Section 5 analyzes and evaluates the simulations results. Finally, Section 6 presents the conclusions and outlines further research.

2. LITERATURE REVIEW

Most of the existing inventory models in the literature assume that items can be stored indefinitely to meet the future demands. However, certain types of commodities deteriorate in the course of time and hence are unstable. Inventory problems for deteriorating items have been studied extensively by many researchers from time to time. There are several literature reviews on perishable inventory system (Nahmias, 1982; Raafat, 1991; Goyal and Giri, 2001). Most publications focus on pricing and lot sizing models (Ferguson et al., 2007; Li et al., 2007; Dye, 2007; Teng et al., 2007; Elmaghraby and Keskinocak, 2003; Chu et al., 1998), or with 2 echelon systems (Wee et al., 2007, Zaroni and Zavanella, 2007; Ferguson and Ketzenberg, 2006; Sarker et al. 2000).

Research in this area started with the work of Within (1957) who considered fashion goods deteriorating at the end of prescribed storage period. One of the focuses of the research on perishable products is interaction and coordination in supply chains (Song et al., 2005). For example, Goyal and Gunasekaran (1995) developed an

integrated production- inventory-marketing model for determining the economic production quantity and economic order quantity for raw materials in a multi-stage production system. Yan and Cheng (1998) studied a production-inventory model for perishable products, where they assumed that the production, demand and deterioration rate are all time-dependent. They gave the conditions for a feasible point to be optimal. Arcelus et al. (2003) modeled a profit maximizing retail promotion strategy for a retailer confronted with a vendor's trade promotion offer of credit and/or price discount on the purchase of regular or perishable products. Kanchanasuntorn and Techanitisawad (2006) investigated the effect of product deterioration and retailers' stockout policies on system total cost, net profit, service level, and average inventory level in a two-echelon inventory-distribution system, and developed an approximate inventory model to evaluate system performance. Li, Cheng and Wang (2007) developed economic-order-quantity model (EOQ)-based models with perishable items to evaluate the impact of a form postponement strategy on the retailer in a supply chain.

Owing to the fact that this study investigates the impact of data inaccuracy on perishable inventory, it will be meaningful to mention about the past studies about inventory inaccuracy. Several researchers focusing on inventory management have dealt with the effect of inventory errors on supply chain performance, and investigated the effect on performance factors of decreasing inventory inaccuracy. In this context, Delanuay et al. (2007) classified the errors causing inventory discrepancies in supply chains and defined four types of errors. The first is permanent shrinkage in the physical stock due to theft, obsolescence, or breakage. The second is misplacement, which is temporary shrinkage in the physical stock that can be replaced after every counting or after every period. The others are the randomness of the supplier yield and the transaction type. The random yield of the supplier is a permanent loss or surplus in the physical inventory due to supplier errors, and transaction type errors affect the information system differently than the first three errors, which modify the physical inventory.

Most studies in this area have used the simulation method to measure the effects of inventory inaccuracy on supply chain performance. Kang and Gerschwin (2005) used simulations to emphasize the problem of shrinkage in physical inventory that may increase lost sales because of items being unexpectedly out of stock. They found that with an error rate of theft as small as 1% of the average demand, the disturbance led to 17% of demand lost. Fleisch and Tellkamp (2005) examined the relationship between inventory inaccuracy and performance in a retail supply chain, considering more error types than the previous study. They simulated a three echelon supply chain with one product in which end-customer demand is exchanged between the echelons, and studied how incorrect deliveries, misplacement, theft, and unsaleable goods affect

inventory inaccuracy, the out-of-stock level, and the costs related to inventory inaccuracy. The results of the study showed that inaccuracies caused by theft appear to have the biggest impact on supply chain performance compared to inaccuracies caused by unsaleable goods or low process quality. Lee et al. (2004) used simulations to study the effects of inventory accuracy on inventory reduction and level improvement in a three echelon supply chain considering the (s,S) policy decisions, unlike other studies. They found that using automatic identification technology, average inventory held decreased by 16%, and total back orders decreased by 22% when the (s,S) policy decisions are made with accurate inventory information. Rekik et al. (2008) optimized an inventory management model by considering a single period Newsvendor problem with inaccuracies in the inventory. They compared three approaches. In the first approach, the retailer is unaware of errors in the store. In the second approach, the retailer is aware of the errors and optimizes its operations by taking this issue into account. The third approach deals with the case where the retailer deploys an advanced automatic identification technology to eliminate errors. They concluded that getting information on misplacement errors and taking them into account when optimizing the ordering decision can lead to important savings and does not necessitate the deployment of a particular system, the retailer can benefit from this improvement by adjusting his ordering quantity

There are many papers addressing the perishable inventory systems. To the best of our knowledge, there exists no paper studying the impacts of data inaccuracy on perishable inventory of which product lifetime is finite. In this paper, we will investigate the impacts of data inaccuracy on retailer's perishable inventory for different levels of product lifetime, demand and lead time uncertainty to fill this gap in the literature. Using a simulation model, the lost sales, product spoilage, average inventory and order quantities are calculated to investigate the retailer's performance.

3. SIMULATION MODEL

In our simulation model, we worked on a two-echelon supply chain which is composed of a retailer and manufacturer. Depending on customer demand, the retailer places orders with the manufacturer. The manufacturer delivers the product with fixed product lifetime (t) as soon as possible and doesn't hold any inventory. The Economic Order Quantity (EOQ) method is used as the inventory model at the retailer (Eq 1). The inventory replenishment point (s) is determined depending on the average lead time (L') and average demand (D') (Eq 2). Products at the retailer are placed on the shelves based on FIFO principle.

$$EOQ = \sqrt{(2 * D' * c_{order}) / c_{inventory}} \quad (1)$$

$$s = L' * D' \quad (2)$$

In our simulation model, the retailer fulfills the end customer demand daily basis and counts the inventory for different periods (p). It is expected that a gap will occur between physical and system inventory since the retailer is unaware of the outdated products (Y) until next counting date.

Daily closing system inventory (I) is calculated by adding the difference between the daily opening system inventory and customer demand (D) to daily incoming items (Q) from the manufacturer (Eq. 3). Physical inventory is calculated in the same way, considering the quantity of outdated products (Eq. 4). As orders are placed depending on the system inventory level, lost sales occur depending on the physical inventory level. At the end of a period (p), inventory is counted and the data are corrected; thus, the system and physical inventories become equivalent (Fleisch and Tellkamp, 2005):

$$I_i^{system} = I_{i-1} - D_i + Q_i \quad (3)$$

$$I_i^{physical} = I_{i-1} - D_i + Q_i - Y_i \quad (4)$$

The model calculates daily lost sales (LS), outdated products (PS) and inventory level (I) for different values of the input variables which are inventory counting period (p), product lifetime (t), standard deviation of lead time (sl) and demand (sd). At the end of the each 365 days (a year), total lost sales (TLS) as a percentage of total customer demand, total quantity of outdated products (TPS), yearly average inventory (AI) and total order quantity (NQ) are reported annually. The process flow of the simulation model is illustrated in Fig. 1.

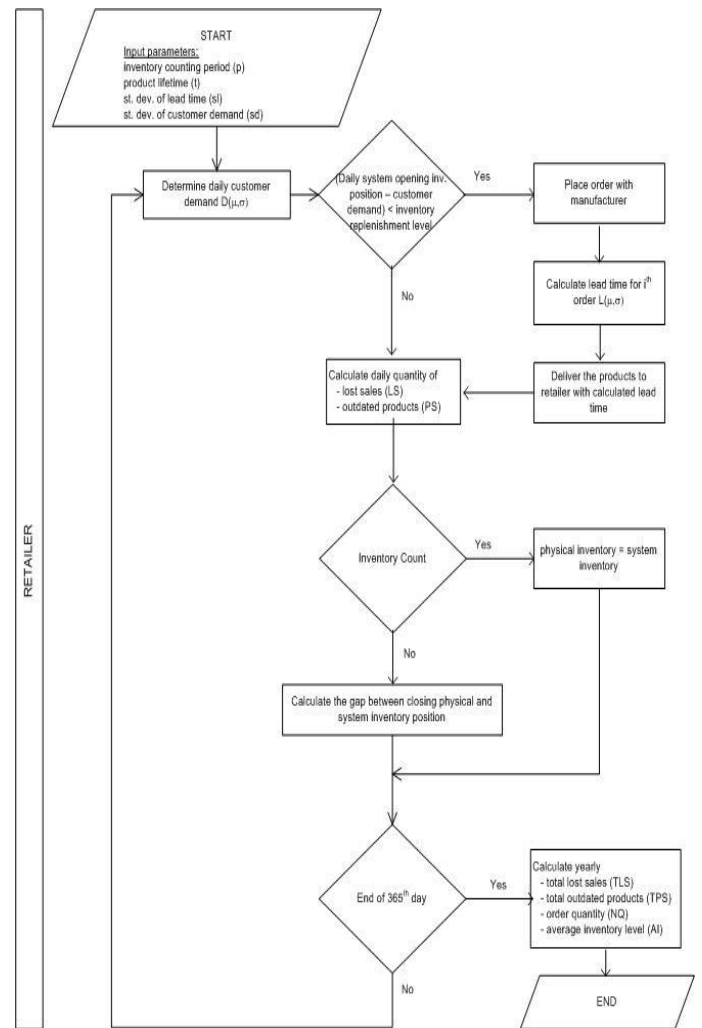


Figure 1. Simulation model process flow

4. EXPERIMENTAL DESIGN

In this study, the experiments are conducted for the products having very short shelf lives. And in order to investigate different levels of inventory inaccuracy, the simulation is run for the cases of that the inventory is counted each day, once a week and once every two weeks (p). The longer the period of inventory counting, the higher the data inaccuracy occurs in system inventory. The demand and lead time uncertainty (sd,sl) are determined as 25%, 50% and 75%. The aim of this study is to show how different levels of data inaccuracy affect the inventory performance of the retailer under uncertainty of the demand and lead time. Additionally, it is also investigated how data inaccuracy affect the inventory performance when the products have different levels of lifetime. In this model, end-customer demand is independently and identically normally distributed, with a daily average (D') of 500 items. The average lead time of the orders (L'), order cost (c_{order}) and inventory holding cost ($c_{inventory}$) are chosen to be 2 days, \$20 and \$0.0014 respectively. Using the simulation model, the lost sales, outdated products, average inventory and order quantities are calculated on

yearly basis to investigate the retailer's performance. Different levels of the independent variables of inventory counting period (p), product lifetime (t), standard deviation of lead time (sl) and demand (sd) are given in Table 1.

Table 1. Levels of independent variables

Independent variables	Levels
Inventory counting period (days)	1 -7-14
Product lifetime (days)	8-9-10
Demand uncertainty (st, %)	25-50-75
Lead time uncertainty (sl, %)	25-50-75

5. EVALUATION OF THE SIMULATION RESULTS

The simulations to examine the impacts of data inaccuracy on retailer's perishable inventory are carried out using the commercial software Crystal Ball Version 7.2.1. The independent factors of inventory counting period, product lifetime, standard deviation of lead time and demand were used in 81 (3x3x3x3) combinations. Additionally, the simulations are run 100 times for each combination to minimize the possible errors arising from the random variables. In the simulation model, the lost sales, product spoilage, average inventory and order quantities are calculated to investigate the retailer's performance over a 365 day period. ANOVA analysis is performed to examine the results of the simulation model using SPSS.

The rising level of inventory counting period increases the data inaccuracy (Fleisch and Tellkamp, 2005). According to the results of a Tukey test of ANOVA post-hoc analysis shown in Table 2, the rising level of data inaccuracy increases the discrepancy between system and physical inventory and thus the lost sales. Since the level of retailer's physical inventory is lower than the level of the system inventory, the retailer fulfills the customer demand at a lower rate. Additionally the rising data inaccuracy decreases the yearly number of orders placed by the retailer and average inventory level. And the decreasing level of average inventory decreases the yearly quantity of product spoilage.

Table 2. ANOVA Tukey Test for inventory counting period for the retailer

Dependent Variable	(I) Inventory Counting Period	(J) Inventory Counting Period	Mean Difference (I-J)	Std. Error	Sig.
Lost Sales	1	7	-1,0%	0,1%	5,1E-09
		14	-3,4%	0,1%	5,1E-09
	7	1	1,0%	0,1%	5,1E-09
		14	-3,5%	0,1%	5,1E-09
	14	1	5,4%	0,1%	5,1E-09
		7	3,5%	0,1%	5,1E-09
Product Spoilage	1	7	6683	300	5,1E-09
		14	9839	300	5,1E-09
	7	1	-6683	300	5,1E-09
		14	3157	300	5,1E-09
	14	1	-9839	300	5,1E-09
		7	-3157	300	5,1E-09
Average Inventory	1	7	107	5	5,1E-09
		14	200	5	5,1E-09
	7	1	-107	5	5,1E-09
		14	93	5	5,1E-09
	14	1	-200	5	5,1E-09
		7	-93	5	5,1E-09
Number of Orders	1	7	3	0	5,1E-09
		14	5	0	5,1E-09
	7	1	-3	0	5,1E-09
		14	2	0	5,1E-09
	14	1	-5	0	5,1E-09
		7	-2	0	5,1E-09

When we investigate the impact of data inaccuracy for different levels of product lifetime, we notice that the rising level of data inaccuracy increases the lost sales. And the increase rate in lost sales becomes higher for perishables with lower product lifetime, as the trend lines show (Fig 2). However, the rising value of data inaccuracy decreases the number of orders and consequently the yearly average inventory so decreases. And the decreasing yearly average inventory reduces the quantity of product spoilage. Figure 2 also indicates that the perishables with higher product lifetime have higher inventory level and consequently less lost sales

and product spoilage.

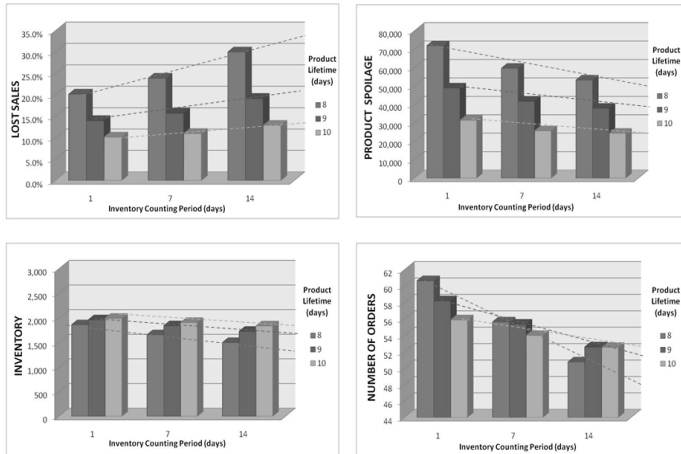


Figure 2. The impact of data inaccuracy for different values of product lifetime

As seen in Figure 3, high level of demand uncertainty increases the number of orders and thus the level of inventory. Therefore high level of demand uncertainty decreases the lost sales but increases the quantity of product spoilage due to higher inventory levels. In our model, when the demand uncertainty exceeds the level of 50%, the number of orders and the average inventory level become much more higher, and therefore the product spoilage increases to higher value. As shown in Figure 3, the rising level of data inaccuracy increases the lost sales and decreases the level of product spoilage. Additionally, with increasing data inaccuracy, the increase rate in lost sales and decrease rate in product spoilage become greater with higher demand uncertainty, as the trend lines show.

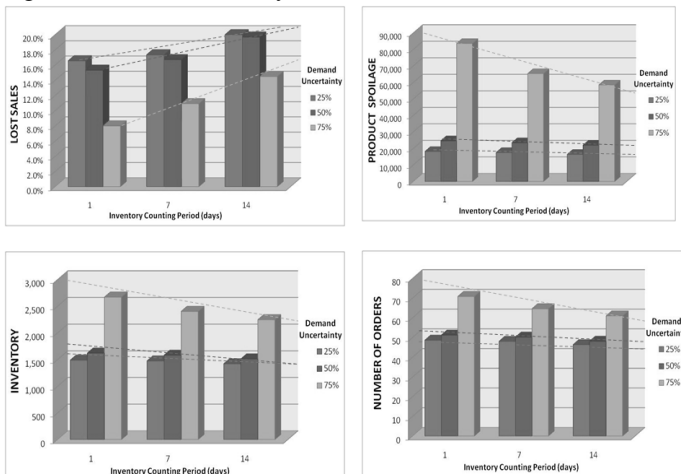


Figure 3. The impact of data inaccuracy for different values of demand uncertainty

As seen in Figure 4, high level of lead time uncertainty increases the quantity of product spoilage. However it decreases the number of orders and thus the level of inventory. Therefore the lost sales are greater in higher level of lead time uncertainty. As shown in Figure 4, the rising level of data inaccuracy increases the lost sales and decreases the level of product

spoilage. And Figure 4 also indicates that the increase rates in lost sales become slightly greater with increasing lead time uncertainty, as the trend lines show.

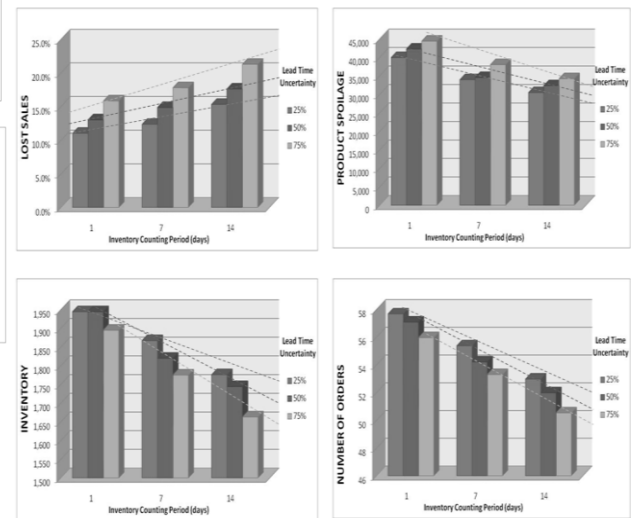


Figure 4. The impact of data inaccuracy for different values of lead time uncertainty

In summary, the results of the simulation study show that the inventory inaccuracy is much more critical for perishables with lower product lifetime under higher demand and lead time uncertainty. Selling perishables with lower product lifetime, the retailer has higher lost sales and product spoilage. The lower the product lifetime, the greater the impact of data inaccuracy is on retailer's inventory performance. Under higher demand uncertainty, the lost sales become lower but the product spoilage higher. And the data inaccuracy affects the retailer's inventory performance much more with increasing demand uncertainty. Under higher lead time uncertainty, the retailer becomes higher lost sales and product spoilage. And the increasing data inaccuracy affects the inventory performance much more with increasing lead time uncertainty.

6. CONCLUSION

Perish ability of either raw materials or finished products is a major problem for companies. Due to the limited product lifetime, an ineffective inventory management at each stage in the supply chain from production to consumers can lead to high system costs including ordering costs, shortage costs, inventory handling costs, and outdated costs. Without alignment of physical inventory and information system inventory, inventory information becomes inaccurate due to product spoilage and the supply chain performance decreases. However, the power of information technology can be harnessed to help supply chain members increase their operation performance (Yu et al., 2001). Advanced Auto-ID technologies can be used to decrease the data inaccuracy across the supply chain.

The purpose of this research is to contribute to the literature on perishable inventory systems by investigating how the data inaccuracy affects the retailer's inventory performance for different levels of product lifetime, demand and lead time uncertainty.

Using a simulation model, the lost sales, product spoilage, average inventory and order quantities are calculated to investigate the retailer's performance. It is shown here that the impact of data inaccuracy on retailer's inventory performance becomes greater with lower product lifetime. And the data inaccuracy affects the retailer's inventory performance much higher with increasing demand and lead time uncertainty.

In conclusion, the results show that decreasing data inaccuracy is much more important for perishables with lower product lifetime under higher demand and lead time uncertainty to increase the inventory performance. In a future study, the impact of data inaccuracy on perishable inventory systems will be investigated on a three echelon supply chain.

REFERENCES

- Arcelus, F.J., Shah, N.H. Srinivasan, G., 2003. Retailer's pricing, credit and inventory policies for deteriorating items in response to temporary price/credit incentives, *International Journal of Production Economics*, Vol. 81–82 (11), 153–162.
- Broekmeulen, R.A.C.M. Donselaar, K.H., 2009. A heuristic to manage perishable inventory with batch ordering, positive lead-times, and time-varying demand, *Computers and Operations Research*, Vol. 36 (11), 3013-3018.
- Chu, P., Chung, K.J., Lan, S.P., 1998. Economic order quantity of deteriorating items under permissible delay in payments, *Computers & Operations Research*, Vol. 25 (10), 817–824.
- Delanuay, C., Sahin, E. and Dallery Y., 2007, A literature review on investigations dealing with inventory management with data inaccuracies, *Proceedings of the 1st RFID Eurasia Conference* pp. 20-26, Istanbul, (Istanbul, Turkey).
- Dye, C. Y., 2007. Joint pricing and ordering policy for a deteriorating inventory with partial backlogging, *Omega*, Vol. 35 (2), 184–189.
- Elmaghraby, W., Keskinocak, P., 2003. Dynamic pricing in the presence of inventory considerations: research overview, current practices, and future directions, *Management Science*, Vol. 49 (10), 1287–1309.
- Ferguson, M., Ketzenberg, M.E., 2006. Information sharing to improve retail product freshness of perishables, *Production and Operations Management*, Vol. 15 (1), 57–73.
- Ferguson, M., Jayaraman, V. Souza, G.C., 2007. Note: an application of the EOQ model with nonlinear holding cost to inventory management of perishables, *European Journal of Operational Research*, Vol. 180 (1), 485–90.
- Fleisch, E., Tellkamp C., 2005. Inventory inaccuracy and supply chain performance: a simulation study of a retail supply chain, *International Journal of Production Economics*, Vol.95, 373-385.
- Goyal, S.K., Gunasekaran, A., 1995. An integrated production inventory- marketing model for deteriorating items, *Computers & Industrial Engineering*, Vol. 28 (4), 755–762.
- Goyal, S.K., Giri, B.C., 2001. Recent trends in modeling of deteriorating inventory, *European Journal of Operational Research*, Vol. 134, 1–16.
- Kanchanasuntorn, K., Techanitisawad, A., 2006. An approximate periodic model for fixed-life perishable products in a two-echelon inventory-distribution system, *International Journal of Production Economics*, Vol. 100 (1), 101–115.
- Kang, Y., Gershwin, S., 2005. Information inaccuracy in inventory systems: stock loss and stockout, *IIE Transactions*, Vol. 37, 843-859.
- Kendall, K.E., Lee, S.M., 1980. Improving perishable inventory management using goal programming, *Journal of Operations Management*, Vol. 1 (2), 77-84.
- Lee, Y.M., Cheng, F., Leung, Y.T., 2004, Exploring the impact of RFID on supply chain dynamics, *Proceedings of the 36th conference on Winter simulation* pp. 1145-1152. (Washington, D.C, USA).
- Li, J., Cheng, T.C. and Wang, S., 2007. Analysis of postponement strategy for perishable items by EOQ-based models, *International Journal of Production Economics*, Vol. 107 (1), 31–38.
- Li, J., Wang, S.Y., Cheng, T.C.E., 2008. Analysis of postponement strategy by EPQ-based models with planned backorders, *Omega*, Vol. 36 (5), 777-788.
- Nahmias S., 1982. Perishable inventory theory: a review, *Operations Research*, Vol. 30, 680–708.
- Raafat, F., 1991. Survey of literature on continuously deteriorating inventory models, *Journal of the Operational Research Society*, Vol. 42, 27–37.
- Rekik, Y., Sahin, E., Dallery, Y., 2008. Analysis of the impact of the RFID technology on reducing product misplacement errors at retail stores, *International Journal of Production Economics*, Vol. 112, 264-278.
- Sarker, B.R., Jamal, A.M.M., Wang, S. 2000. Supply chain models for perishable products under inflation and permissible delay in payment, *Computers & Operations Research*, Vol. 27(1), 59–75.
- Song, X.P., Cai, X.Q., Chen, J., 2005, Studies on interaction and coordination in supply chains with perishable products: A review, Chan, C.K., Lee, H.W.J. (Eds.), *Successful Strategies in Supply Chain Management*. Idea Group Publishing, Hershey, PA, USA, pp. 222–248.
- Teng, J.T., Ouyang L.Y., Chen, L.H., 2007. A comparison between two pricing and lot-sizing models with partial back logging and deteriorated

- items, *International Journal of Production Economics*, Vol. 105 (1), 190–203.
- Wee, H.M., Jong, J.F., Jiang, J.C., 2007. A note on a single-vendor and multiple-buyers production-inventory policy for a deteriorating item, *European Journal of Operational Research*, Vol. 180 (3), 1130–1134.
- Whitin, T.M., 1957, *Theory of Inventory Management*, Princeton University Press, Princeton, NJ.
- Yan, H., Cheng, T.C.E., 1998. Optimal production stopping and restarting times for an EOQ model with deteriorating items, *Journal of Operational Research Society*, Vol. 49,1288–1295.
- Yu, Z., Yan, H., Cheng T.C.E., 2001. Benefit of information sharing with supply chain partnerships, *Industrial Management & Data Systems*, Vol. 101 (3), 114-119.
- Zanoni, S., Zavanella, L., 2007. Single-vendor single-buyer with integrated transport- inventory system: models and heuristics in the case of perishable goods, *Computers &Industrial Engineering*, Vol. 52 (1), 107–123.

AUTHORS BIOGRAPHY

Mert Bal

Dr. Mert Bal is a research assistant at the Mathematical Engineering Department of Yildiz Technical University. He received his B.Sc., M.Sc. and PhD degrees from Mathematical Engineering Department of Yildiz Technical University 1999, 2001 and 2008, respectively. His areas of interest include: machine learning, uncertainty reasoning, artificial intelligence, soft computing, rough set theory, formal concept analysis, decision support systems, and simulation.

Alp Üstündağ

Assoc. Prof. Dr. Alp Üstündağ is a lecturer at Industrial Engineering Department in Istanbul Technical University and also the head of RFID Research and Test Lab in the same university. He has also worked in IT and finance industry from 2000 to 2004. His current research interests include RFID, supply chain and logistics management, risk management, IT/IS systems, soft computing. He has published many papers in international journals and presented various studies at national and international conferences and seminars. He has conducted a lot of research and consulting projects in reengineering, logistics management and supply chain management.

SIMULATION FOR ASSESSING SECURITY-BASED POLICIES IN IMPORT/EXPORT OPERATIONS

Pasquale Legato^(a) and Rina Mary Mazza^(b)

^{(a), (b)}Department of Electronics, Computer and System Sciences (DEIS)
University of Calabria
Via P. Bucci 42C
87036 Rende (CS), Italy

^(a)legato@deis.unical.it, ^(b)rmazza@deis.unical.it,

ABSTRACT

In today's business environment, manufacturing and distribution companies have elevated their concern for security. They are working hard to ferret out risks and inefficiencies that may occur as their products and services move along the supply chain network. In this study we consider security issues from the stand point of a shipping agency providing import/export services. The objective of our study consists in the evaluation of security-based operating procedures and modalities that can lead to significant reductions in the controls that occur within the company activity due to both inside and third-party formalities (e.g. controls performed by the local Customs Office). The costs and benefits related to the adoption of new security-based policies and practices are estimated via discrete-event simulation. In the output analysis of multiple simulation replications, significant computational savings are achieved by introducing a fixed-point procedure to generate confidence intervals for the security-based performance measures of interest.

Keywords: logistics, security, discrete-event simulation, output analysis

1. INTRODUCTION

It is common knowledge that, ever since the September 11 attacks on the World Trade Center, governments, most branches of industry and citizens alike have drastically elevated their concern for safety and security. Although both deal with preventing negative events and conditions, these terms are normally regarded as representing distinct properties: safety deals with non intentional (accidental) negatives, whereas security deals with intentional (malicious) one (Gkonis and Psaraftis 2010). Methodologically speaking, this difference is significant enough to require an approach that spans across the increasingly specialized sub-disciplines of law, commerce and science.

These words ring especially true in the supply chain arena as many companies are working hard to ferret out risks, inefficiencies and, thus, costs of both safety and security efforts. In particular, the

globalization of most industries has sparked heightened awareness of the various risks and vulnerabilities that products are exposed to as they move along the supply chain continuum from design and sourcing to manufacture, transportation, distribution and final sale to the consumer. Supply networks are long and complex. Many entities, including outsourcers and subcontractors located world-wide, handle the product as it moves across geographical and national borders, thereby creating many physical and temporal threats that pose a risk to product safety and security (Maruchecka et al. 2011).

Research theories and methodologies, as well as regulations and standards have addressed these problems to provide fresh insights and innovative solutions. Here we consider security issues from the stand point of a shipping agency providing import/export services. The objective of our study consists in the evaluation of security-based operating procedures and modalities that, in terms of performance, can lead to a 30% reduction in the controls that occur within the company activity due to both inside and third-party formalities, such as the controls performed by the local Customs Office. The costs and benefits related to the adoption of new security-based policies and practices will be evaluated via simulation. The paper is organized as follows. In the Problem Description paragraph, the security problem at hand is described by considering both internal and external influences ranging from technical solutions to national and international initiatives. Special attention is then given to the company's so-called import process, the most important for growth and exposure to security threats. In the Simulation paragraph, the convenience of using a fixed-point procedure against a two-stage procedure when generating interval estimates during the output analysis of the simulation study is examined. In the Numerical Experiments paragraph, *as is* simulations and *to be* scenario analyses are presented to assess and compare the before and after status of the company's security orientation. Finally, conclusions are drawn in the last section.

2. PROBLEM DESCRIPTION

A shipping agency providing import/export services is called to interact with carriers, customs, harbor offices, warehouses, forwarding agents, stevedores, border controls, port authorities, terminals and any other sorts of bodies and organizations belonging to the so-called port community. The information flows generated by the interactions among the above actors of the container supply chain are certainly a major concern when taking into account security issues for a company whose main activities are based on information processing, rather than physical transformations and/or transfer operations. In this sense, we follow a two-stage approach to model and analyze the security problem within the container supply chain from the standpoint of the shipping agency. In the first stage, recognition and formalization activities of the logistic processes in the container supply chain are carried out in order to: *i*) represent rules and operation modalities used by actors when dealing with containers; *ii*) define interactions and information exchanges; *iii*) build a formal model with the objective of reorganizing the logistic processes in the container supply chain and evaluating performance measures in terms of specific security issues. In the second stage, the overall system developed in the first stage (i.e. control and communication procedures among the actors, data exchange and decision control along the container supply) is tailored to the shipping company under analysis and assessed via simulation.

In this section, we first provide some general background on security matters by considering both internal and external influences ranging from technical solutions to international initiatives. We then focus on the representation and discussion of the shipping company's major service: the import process, the most important for growth, third-party interaction and exposure to security threats. The objective of adopting security-based policies consists in pursuing a 30% decrease in the number of controls performed by the company and the local Customs Office when carrying out activities related to the import process.

2.1. Background Information

Technology can certainly aid any company in its struggle to improve security in the management of container import/export flows. Driven by the increasing importance of pervasive computing, information technology (IT) can especially provide support via comprehensive and flexible hardware and software applications. To fix ideas, one may choose from a variety of solutions among which, but not limited to:

- electronic seals;
- biometric technologies;
- closed circuit TV systems;
- RFIDs, radio frequency identification;
- other systems (acoustic, gamma-ray, x-ray, radiation detection, vapor/trace detection);
- GPSs, global positioning systems;
- A-GPSs, assisted global positioning systems;

- extended tracking technologies.

Whatever the solution implemented, the real challenge consists in keeping data and information exchange along the supply chain fast, lean and secure. From a quantitative perspective, the size and awareness of the problem runs back in time and can be summarized by the following figures (Infotransport 1994):

- 70% of the documents pertaining to transport is automatically generated, printed and sent on paper and then manually reintroduced into other computer-based processing systems;
- error rates in documentation reach 50%;
- the cost for providing paper document management in container transport operations lies between 7% and 10% of the value of the product itself.

Therefore, it is quite clear how an accurate and computer-based data and document processing can cut the general costs and time loss in logistics.

As a result, the competitiveness of the overall (Italian) transport system can benefit from the introduction of these IT solutions. However, even greater benefits can be achieved when similar solutions are implemented with respect to the initiatives that customs and governments from countries worldwide are promoting. Examples are the SAFE framework of standards, the ISO standards, the Transported Asset Protection Association (TAPA), the International Ship and Port Facilities Security Code (ISPS), the Customs-Trade Partnership Against Terrorism (C-TPAT), the Container Security Initiative (CSI), the Operation Safe Commerce (OSC), the Secure Freight Initiative (SFI), and the Bioterrorism Act.

In particular, for the purposes of our study, we consider the ISO/PAS 28000 specification for security management systems for the supply chain. ISO/PAS 28000 specifies the requirements for a security management system, including those aspects critical to security assurance of the supply chain: financing, manufacturing, information management and the facilities for packing, storing and transferring goods between modes of transport and locations, as well as personnel training and emergency procedures in case "security events" happen to occur.

A schema for designing a system compliant with the ISO/PAS 28000 standard must include:

- security planning and management;
- risk planning and management;
- a formal and shared description of the activities and processes carried-out by the organization, including the definition of the instructions and procedures set by the organization for security management (e.g. operational controls, emergency management, security programs and objectives, monitoring and measurements);

- management of preventive and corrective actions;
- (ongoing) review of activities and continuous improvement.

When adopting a management model compliant with the ISO/PAS 28000 standard, a risk analysis should be performed to identify the risks that can compromise container security. Rather than discussing how the risk analysis is carried out (Haimes 1998), here we report on the critical issues that have been brought about in the shipping company’s activity. First of all, although the organization is aware of the need of tools for security monitoring, it normally exploits time-proven company practices and simply focuses on the recruitment of qualified personnel. Second, synergies seem possible between security and pre-existing systems compliant with quality standards and/or to-be systems for the automatic management of the company document workflow. Last, but not least, although interest for security is manifest, there is little knowledge allowing the implementation of a “formal” security system based on rigorous tools and methodologies.

This stated, in the following, special attention is given to the shipping company’s so-called import process, the most important for growth, third-party interaction and exposure to security threats.

2.2. The Import Process

The import process plays a leading role in the shipping company’s business. It features both company and third-party control policies (i.e. Customs) that affect the overall complexity of the process. The actors involved include: *i*) customers meant as final addressees of the imported goods or their intermediaries (i.e. subjects demanding a service); *ii*) the shipping company as shipper and representative of the customer by carrying out on his/her behalf all the necessary formalities related to the import of the goods (i.e. subjects offering a service); *iii*) Customs, the authority that is responsible for collecting and safeguarding customs duties and provides clearance for the goods that enter (exit) the Nation’s territory and whose controls are an integrated part of the import service; *iv*) the container terminal, the concessionaire of the area in which container handling and interchange of goods in cargo units, as well as inspection activities in cooperation with the Customs Office are carried out. A flowchart (see Figure 1) and a step-by-step description of the import process follows.

A customer applies for a request to import goods and the shipping company issues a so-called *bill of lading* (in the following bill). As required by the company procedure, the bill is first assigned an “open” position. It is then (eventually) processed according to two main sub-processes: the *forwarding* option and/or the *verification of sanitary formalities* option. The former is a marketing-like process intended to extend the transportation service beyond the terminal and way on to the final destination indicated by the addressee. The latter is a process referring to the fito-sanitary and

veterinary controls of the goods required at border crossings.

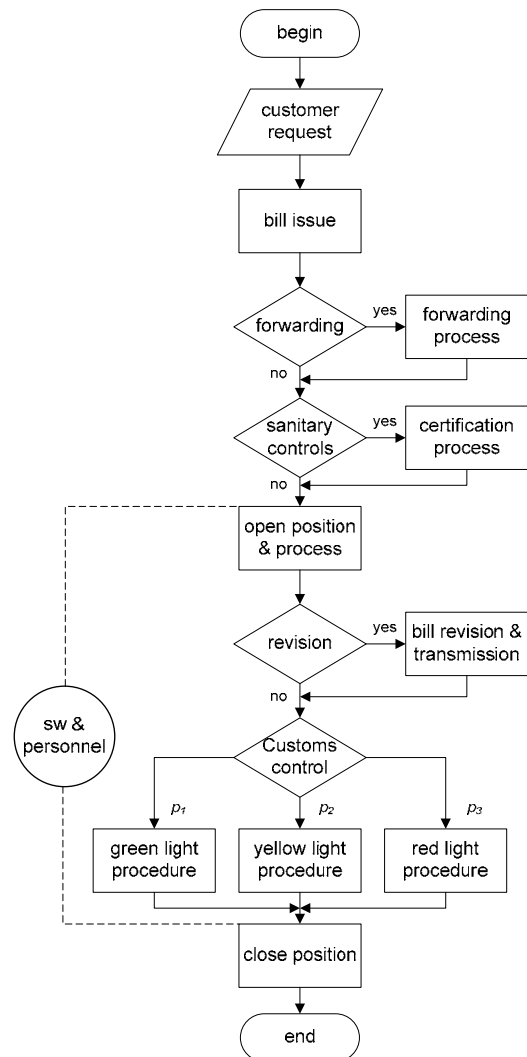


Figure 1: The Model of the Import Process

The opening and processing of the bills requires both active resources, such as qualified company personnel, and passive resources, such as software systems that provide for the electronic management of the bills.

Table 1: Skills of Company Personnel

Skills				
Unit	Import	Export	Transits	Marketing
1	✓	✓	✓	
2	✓	✓	✓	
3	✓	✓	✓	
4	✓	✓	✓	
5	✓	✓	✓	
6		✓	✓	
7		✓	✓	
8		✓	✓	
9				✓
10				✓

For each unit belonging to the first category of resources, the number of employees and types of skills of each employee must be specified. As shown by Table 1, in the shipping company under analysis, both *single-skilled* and *multi-skilled* personnel are available.

Once the resources for bill processing have been assigned (i.e. management software and technical personnel, but also marketing personnel if the bill undergoes the forwarding option), the classification of the goods and the customs declaration must be fulfilled. The effort required in this part of the customer service, depends on both the number of containers and the number of customs codes that need to be considered in each bill. Observe that custom codes may be updated by the competent authorities during the actual bill processing. As a result, some fields of the bills may require a revision (nearly 6% of the times). Bill revision is also necessary every time a misinterpretation of customer information leads company personnel to commit an incorrect completion of customs documentation (11% of the times). According to the historical data of the company under examination, inaccuracies refer to:

- number of packages (42%);
- package weight (4%);
- country of origin (41%);
- value of goods (12%);
- addressee/shipper (1%).

Whatever be the cause, the technical staff must perform a sort of re-processing of the bill in order to carry out the corrections required. After the revision process is completed, a communication pertaining to the revised bill is sent to the Customs Office for approval. Bill processing may be considered closed only after receiving an acknowledgement to the above procedure.

As for inspection activities performed by the Customs Office, in a broader sense the representation of this control is placed in relation to the outcome returned from the Customs IT system. This outcome, in turn, can be classified as:

- green light or AC - Automated Control ($p_1 \approx 31\%$ of the cases) in which no further forms of control are carried out by the Customs officers assigned to the inspection activity;
- yellow light or DC - Document Control ($p_2 \approx 36\%$ of the cases) in which the related documentation is considered respondent to the Customs declaration or the eventual differences are of limited significance and, thus, considered immediately remediable;
- red light ($p_3 \approx 33\%$ of the cases) in which an SC - Scanner Control is performed or a GV - Goods Visit operation is carried out, meaning a real physical control of the goods inside of the container. In both cases (SC and GV), a request must be sent to the terminal to apply for control services. These occur in

cooperation with the local Customs Office in order to guarantee the presence of the Customs officer delegated to hold the hearing on the terminal premises. The terminal provides for container transfer in the inspection area and, concomitantly, prearranges all that is necessary to carry out the inspection (e.g. container opening, handling of containerized goods, etc.).

Given the complexity and stochastic nature of many of the features in the above model, simulation has been chosen to evaluate the adoption of new security-based policies and practices within the import process.

3. SIMULATION

The design and implementation of the “import process simulator” has been carried-out in compliance with the conventional steps used to guide a thorough and sound simulation study (Banks et al. 2001). Rather than providing a general description of these steps, here we focus on the output analysis of simulation. In particular, we present and discuss the convenience of using a fixed-point procedure against the classic two-stage procedure (see from page 511 on in Law and Kelton 2000) in order to limit the standard error when generating interval estimates for the security-based performance indices examined in the Numerical Results paragraph.

Let X be the normal random variable representing the performance index of interest and $\mu \doteq E(X)$ the mean value that we want to estimate by an interval of random width, centered on the sample mean $\bar{X}(n)$. Using standard notations for Student-t quantiles, confidence level and sample variance, the interval estimator at the $1 - \alpha$ level of confidence is:

$$\bar{X}(n) \pm t_{n-1; 1-\alpha/2} \frac{S(n)}{\sqrt{n}} \quad (1)$$

In our case, the n parameter corresponds to the number of simulation replications to be set by the modeler before actually performing the simulation study. Hence, we want to determine the value of n that allows the modeler to keep the half-width of interval (1) within a predefined limit. The resulting fixed-point procedure provides an estimate of μ that satisfies the so-called relative error criterion (Nakayama 2002). In this respect, observe that

$$\left| \bar{X}(n) - \mu \right| = \left| t_{n-1; 1-\alpha/2} \frac{S(n)}{\sqrt{n}} \right| < \varepsilon |\mu| \quad (2)$$

where $\varepsilon > 0$ stands for the target relative error. Thus, a fixed-point procedure may be set as soon as the dependence of both ε and the standard deviation from n is highlighted as follows:

$$\left| \frac{t_{n-1;1-\alpha/2} S(n)}{\bar{X}(n) \sqrt{n}} \right| = \varepsilon(n) \quad (3)$$

where the sample mean is used instead of μ . The fixed-point schema is illustrated in Table 2.

Table 2: The Fixed-Point Procedure

1	set $k = 0$, read n_k and ε_{target}
2	compute $\varepsilon(n_k)$
3	$\bar{X}(n_k), S^2(n_k)$
4	$\varepsilon(n_k) = \frac{t_{n-1;1-\alpha/2} * S(n_k)}{\sqrt{n_k} * \bar{X}(n_k)}$
5	if $\varepsilon(n_k) > \varepsilon_{target}$ Compute
6	$n_{k+1} = \left\lceil \frac{t_{n-1;1-\alpha/2} * S^2(n_k)}{\varepsilon_{target}^2 * \bar{X}^2(n_k)} \right\rceil$
7	$k = k + 1$ and go to Step 2
8	else STOP.
9	return $\left[\bar{X}(n_k) \pm t_{n-1;1-\alpha/2} \frac{S(n_k)}{\sqrt{n_k}} \right]$

To fix ideas, if the target average waiting time of a bill before actual processing is meant to be within 5% of the real value with probability $1 - \alpha$, then ε is set equal to 0.05.

The above scheme is able to account for the changes in mean and variance estimation and, thus, it allows to dynamically adjust the number of runs required to generate the confidence interval within the predefined error. Practically speaking, this can enable significant savings from a computational point of view which, in simulation, always represents a major issue.

4. NUMERICAL EXPERIMENTS

The purpose of the simulation experiments is to compare the “as is” organization of the import process with its “to be” organization based on policies compliant with security assurance. As a result, the company management should be able to choose the operating procedures and “optimal” security-oriented modalities for the import process that, in terms of performances, can lead to a 30% reduction of the controls sampled out on the shipping company’s workflow within the related container supply chain network.

The experiments are carried out under Rockwell’s Arena simulation package (version 11) and run on a personal computer equipped with an Intel® Core™2 Duo 1.58 Ghz processor and 2.93 gigabytes of RAM. The models in Arena include VBA (Visual Basic® for Applications) blocks that allow to insert user-defined code. In this study, these blocks are used to interact with worksheets under Microsoft® Excel 2002 in order to record the output data produced by the simulator and generate 95% intervals estimates according to the fixed-

point procedure previously described in the Simulation paragraph.

4.1. As Is Simulation Model

In order to reproduce the import process as it is currently run by the company, the experiments use data from the first semester of 2009. This data is represented by means of synthetic estimators, once lag-correlation type mathematical procedures based on the mutual distance between data have been used to support the prerequisite of independence. Different types of distribution forms are then identified as “candidate” representations of the data models. Finally, the goodness of these distribution functions is verified by employing frequency histograms, p-p plots and the proper goodness-of-fit tests in which a comparison occurs between the empirical distribution forms and the theoretical distribution forms.

For illustrative purposes, some modeling examples of the bill processing times are given in Tables 3 and 4 and Figures 2 and 3. Obviously, to complete this part of the study, the previous steps are applied to obtain models for all the input data required by the import process (i.e. bill issuing, forwarding, certifications, software updates, bill revisions and green light, yellow light and red light responses)

Table 3: Data for Bill Processing

Semester I 2009	
number of observations	644
min observation	23
max observation	65
mean	24.45
median	23
variance	13.43
lexis ratio	0.15
skewness	6.62
data independence	yes

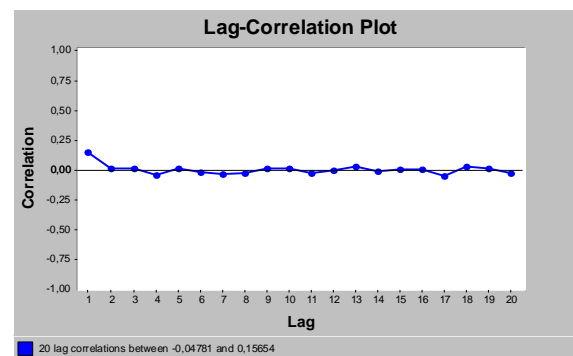


Figure 2: Verification of Absence of Correlation among Bill Processing Times

Table 4: Input Models for Bill Processing Times

Semester I 2009		
Model	Score	Location, Scale, Shape
Weibull	85.71	22.96, 0.46, 0.42
Gamma	79.76	22.96, 5.09, 0.29
Log-Logistic	77.38	0.00, 23.75, 22.53

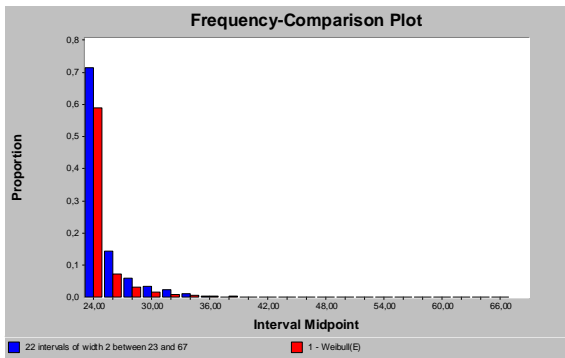


Figure 3: Histogram for Bill Processing Times

Thanks to the validation of the “as is” model (Sargent 2007), it is possible to assess whether or not the operating model is an accurate representation of the real system and, thus, continue with the experiments for the “to be” model. As for this matter, the simulator returns performance measures based on both intermediate and final check points (e.g. monthly and semiannual). This output is then compared with the real performance measures recorded by the company for the period of interest. These include, but are not limited to, the average number of *i*) bills completed, *ii*) forwarding operations, *iii*) sanitary verifications, *iv*) outcome of the inspections carried out by the Customs Office classified according to one of the three categories previously defined (i.e. green light, yellow light and red light), as shown in Table 5.

Table 5: Validation on a Selection of Average Monthly Results

Index	Results	
	Real Data	Simulator
N° of bills completed	107.33	[106.25 - 109.11]
N° of forwardings	35.83	[35.03 - 36.10]
N° of certifications	24.67	[24.55 - 25.43]
N° of green lights	33	[32.80 - 34.08]
N° of yellow lights	38.83	[38.43 - 39.35]
N° of red lights	35.5	[34.76 - 35.94]

The above results appear to be satisfactory. Therefore, the simulator can be used to perform the what-if analyses planned to evaluate future key security-based company policies.

4.2. To Be Simulation Model

The objective of achieving a 30% reduction of the controls sampled out on the import process calls for the evaluation of alternative organizations for the corresponding document workflow. In particular, as pointed out in §2, for this purpose the current and, most of all, the future company security-oriented policies rely on monitoring activities whose effectiveness mainly depends on the recruitment and training of company personnel. To realize the importance of this matter, one may consider the correlation between the presence of qualified personnel and the correct use of the software

that supports the company workflow. As a matter of fact, this business function will be considered as one of the key elements on which what-if analyses will be performed to estimate the effect of the controls carried out by the local Customs Office on the different scenarios under examination.

From a general point of view, the Customs Office (or, more precisely, the Customs of the European Union) has set the objective of finding an equilibrium point between the speed of exchanges and the effectiveness of controls based on anti-illicit trafficking, fraud and counterfeiting actions. The related control systems use modern technologies for an automatic risk management based on a constant analysis of the traffic flows. The corresponding control policies involve a subjective risk assessment of every operation in order to favor “reliable” economic operators (i.e. “white lists” vs “black lists”).

According to the data collected from the customs declaration, an IT process is used to verify the documentation related to the aforesaid declaration. Practically, the reliability of an operator is estimated through a series of prefixed parameters on which the Customs Office performs its own controls. In particular, the so-called “risk profiles” are closely correlated to the combination of the following elements of the Customs declaration:

- origin and destination of goods;
- addressee of goods;
- sender of goods;
- type and characteristics of goods.

This stated, here we will consider parameters on which the company can act with some degrees of freedom: the number of errors in the customs declaration and, as a consequence, the number and types of revisions required. In brief, the higher the result of n° of revisions/total n° of bills, the lower the reliability of the operator and, thus, the higher the number of the controls. The logical nexus between these two factors leads to test a series of hypothesis that, if verified, draw a corollary that supports the decrease in Customs controls. The latter is the overall goal of the simulation study.

In the case study under examination, out of the 644 bills processed in the first semester of 2009, the company recorded:

- 30% of inspections;
- 11% of revisions, followed by inspections in 33% of the cases;
- 33% of demands for certifications, followed by inspections in 33% of the cases.

According to what was previously stated on the reliability of the operator, one may assume that a decrease in the number of (bill) revisions is followed by a decrease in the number of inspections as well. In particular, the decrease could be pursued by *i*) training

the technical personnel with the objective of reducing the number of errors in the documentation or *ii*) planning the update operations of the company software with the objective of drastically reducing the number of revisions. Since the effect of neither of the above actions is known *a priori*, the “to be” simulation model consists in a sensitivity analysis based on total error reduction (i.e. 100%) or partial error reduction (i.e. 50%, 25% and 10%) and, thus, the estimation of the consequences of these reductions in terms of company or Customs controls.

In hypothesis n°1 based on personnel training, each simulated scenario returns estimates for the average reduction in the number of bills to undergo a revision process each month. The total number of hours during which the above bills are held in detention by Customs waiting for approval is estimated as well. Observe from Table 6 how both of these factors affect controls and the productivity of the related company departments which is slowed down by Customs detentions. It is quite clear that a reduction in bill revisions from [11,60 - 12,16] to [5.71 - 5,98], on one side, results in a reduction of company controls and, on the other, it additionally cuts the 33% of revised bills followed by Customs controls. Therefore, this “medium” scenario (i.e. 50% option in Table 6) has a significant impact on the company’s operating efficiency and is coherent with the objectives of the simulation study.

Table 6: Results from What-if Analysis based on Security-driven Training Activities

Training	Monthly Analysis	
	N° of revisions	Customs Detention (h)
Pre-training	[11.60 - 12.16]	[46.88 - 49.08]
10%	[10.30 - 10.79]	[42.48 - 44.11]
25%	[8.60 - 9.07]	[35.40 - 37.05]
50%	[5.71 - 5.98]	[23.41 - 24.56]
100%	0	0

Figure 4 illustrates the trend in the reduction of the total number of hours (per month) of bill detention by Customs, according to more frequent and regular percentage variations.

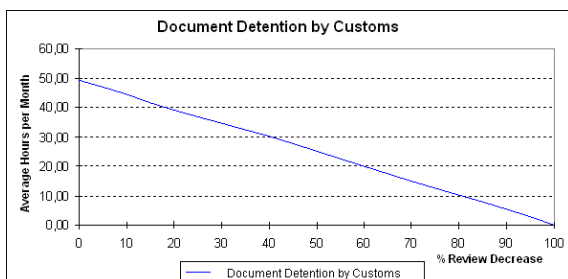


Figure 4: Trend of Document Detention by Customs based on Security-driven Training Activities

In hypothesis n°2 based on planning software update operations, one must consider the following factors. Update operations can be necessary due to software bugs, a phenomenon which is normally

negligible, or variations in the data used for calculations in Customs charges. In the latter case, the software devoted to such purpose features a heavy use of third-party archives that, in turn, require continuous updates (e.g. the archives containing customs duties, currency change, variations of agreements between countries, etc.). As a result, errors can be forced from delays in updates which, due to organizational deficiencies, are often left to the good will of a single company operator who may not have the skill to perform such update.

The related what-if analysis is carried out by estimating the average number of revised bills (per month), along with the time required to carry out the software updates and subsequent bill revisions. By analogy with the first what-if hypothesis, Customs inspections follow the software updates, therefore, further reductions are brought about in both company and Customs controls. In this sense, for each scenario Table 7 records the average number of bill revisions related to software updates, as well as the total time effort that, in turn, holds back the productivity of the corresponding company department.

Table 7: Results from What-if Analysis based on Security-driven SW Maintenance

Maintenance	Monthly Analysis	
	N° of Revisions	Time Effort (h)
Pre-maintenance	[6.21 - 6.69]	[1.57 - 1.73]
10%	[5.26 - 6.29]	[1.08 - 1.84]
25%	[4.15 - 5.72]	[0.65 - 1.55]
50%	[2.71 - 3.73]	[0.29 - 0.97]
100%	0	0

Figure 5 illustrates the trend in the reduction of the total number of hours required to perform software updates and the revision of those bills for which processing activities were interrupted due to the software update.

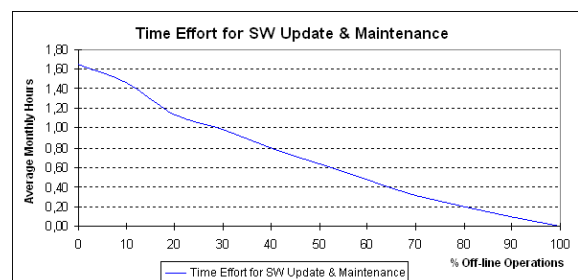


Figure 5: Trend of Time Effort for Security-driven SW Update and Maintenance

The present simulation study is completed with some key considerations on the estimates reported in Tables 6 and 7. These 95% confidence intervals have been generated according to our fixed-point procedure for keeping the error (1) within a predefined limit (2), rather than a classic two-stage procedure. Since the proposed scheme accounts for the changes in the mean and variance estimation, it allows to dynamically adjust the number of runs required to generate the confidence intervals within the predefined error.

Table 8: Fixed-point versus 2-stage Procedure for Error Control in Confidence Intervals

Scenario	Performance	$\Delta\%$
1	N° of Revisions	37.50%
	Customs Detention	47.37%
2	N° of Revisions	47.37%
	Customs Detention	44.44%
3	N° of Revisions	16.67%
	Customs Detention	9.09%

In terms of (average) computational savings ($\Delta\%$ is the n° of runs saved in percentage), Table 8 shows how the fixed-point procedure outperforms the 2-stage procedure in error control during the generation of interval estimates for the security-based performance measures across the three scenarios under analysis.

5. CONCLUSIONS

Security-based procedures compliant with the ISO/PAS 28000 standard have been tested via simulation with respect to the import process of a shipping company. The what-if approach adopted to evaluate the impact of the above procedures has returned promising estimates as far as reducing the number of bills to be revised by the company is concerned. These (interval) estimates have been obtained with a reduced computational effort, by using a fixed-point procedure to determine the number of simulation replications which ensure a standard error below a target value. Besides the general objectives of the study, an additional research opportunity has risen from a methodological point of view: the quest for advanced techniques of *importance sampling* that allow to properly analyze scenarios by means of simulation when an insufficient quantity/quality of data is available.

ACKNOWLEDGMENTS

This work has been partially supported by the Italian Ministry for Education, University and Research (MIUR) under the e-Log Project, grant n° DM28145.

REFERENCES

- Banks, J., Carson, J.S., Nelson, B.L., and Nicol, D.M., 2000. *Discrete-Event System Simulation*. 3rd ed. Upper Saddle River, New Jersey: Prentice-Hall, Inc.
- Gkonis, K.G. and Psaraftis, H.N., 2010. Container transportation as an interdependent security problem. *Journal of Transportation Security* 3:197–211.
- Haimes, Y., 1998. *Risk Modeling, Assessment and Management*, New York: John Wiley.
- Infotransport, 1994. *Stato dell'arte dell'informatica nei trasporti*. Infotransport 22/04/94.
- Law, A.M. and Kelton, W.D., 2000. *Simulation Modeling and Analysis*. Third Edition. McGraw-Hill: New York.

Maruchecka, A., Greisb, N., Menac, C., and Caid L., 2011. Product safety and security in the global supply chain: Issues, challenges and research opportunities. *Journal of Operations Management* 29:707–720.

Nakayama, M.K., 2002. Simulation Output Analysis. *Proceedings of the 2002 Winter Simulation Conference*, 23-34, San Diego, CA, USA.

Sargent, R.G., 2007. Verification and Validation of Simulation Models. *Proceedings of the 2007 Winter Simulation Conference*, 124-137, Washington, DC, USA.

AUTHORS BIOGRAPHY

Pasquale Legato is an Associate Professor of Operations Research at the Faculty of Engineering - University of Calabria, Rende (CS, Italy), where he teaches courses on simulation for system performance evaluation. He has published on queuing network models for job shop and logistic systems, as well as on integer programming models. He has been involved in several national and international applied research projects and is serving as a reviewer for many international journals. His current research activities focus on the development and analysis of queuing network models for logistic systems, discrete-event simulation and the integration of simulation output analysis techniques with combinatorial optimization algorithms for real-life applications in Transportation and Logistics. His home-page is www.deis.unical.it/legato.

Rina Mary Mazza received her Laurea degree in Management Engineering and obtained a Ph.D. degree in Operations Research at the University of Calabria, Rende (CS, Italy). She is currently head of the “Research Projects Office” at the Department of Electronics, Computer and System Sciences (DEIS) of the above University. She has a seven-year working experience on Knowledge Management and Quality Assurance in Research Centers. She is also a consultant for operations modeling and simulation in terminal containers. Her current research interests include discrete-event simulation and optimum-seeking by simulation in complex logistic systems. Her e-mail address is rmazza@deis.unical.it.

TRAFFIC LIGHT SIMULATION WITH TIME-VARYING TRAFFIC DISTRIBUTION AT JUNCTIONS

Carmine De Nicola^(a), Rosanna Manzo^(b), Vincenzo Moccia^(c), Vincenza Tufano^(d)

^{(a), (b), (c), (d)} Department of Electronic and Computer Engineering,
University of Salerno, Via Ponte Don Melillo, 84084, Fisciano (SA), Italy

^(a)denicola@diima.unisa.it, ^(b)rmanzo@unisa.it, ^(c)moccia@diima.unisa.it, ^(d)tufano@diima.unisa.it

ABSTRACT

The aim of this paper is to simulate the effect of traffic lights and time-varying flows distribution at junctions of urban traffic networks. We consider a macroscopic model for road networks based on conservation law, describing the motion of cars as a continuous flow. At junctions some Riemann solvers to find a unique solution to Riemann problems are introduced.

In particular we propose a micro-algorithm to define a Riemann solver in situations in which a road in some time-instant is empty and the corresponding problem can be under-determined. Then, we discuss the correct use of Riemann solvers to capture the presence of traffic lights and time-varying behavior of drivers at junctions. Simulation results for a 2×2 junction and a comparison among the effects of changing traffic lights cycles in a network are shown.

Keywords: fluid-dynamic model for traffic networks, conservation law, Riemann solvers, traffic lights simulation.

1. INTRODUCTION

To study car traffic phenomena, researchers from various areas proposed a lot of models, among which fluid-dynamic ones. The latter treat traffic from a macroscopic point of view: the evolution of macroscopic variables, such as density and average velocity of cars, is considered.

The basic fluid-dynamic model is due to Lighthill, Whitham and Richards (LWR model) (Lighthill and Whitham, 1955; Richards 1956), according to which the motion of cars along a road can be modeled by a conservation law, regarding the density of cars as the main quantity to be looked at. To overcome the limitations of the LWR model, other alternatives were searched for, such as second and third order models (Helbing 2001; Colombo 2002; Bellomo and Coscia 2005). Recently, the LWR model was extended to networks (Coclite, Garavello and Piccoli 2005; Garavello and Piccoli 2006).

Since traffic networks consist of a finite set of roads meeting at some junctions, the dynamics at junctions is captured solving Riemann problems which are Cauchy problems with constant initial data on each

road. In order to solve uniquely Riemann problems some assumptions are made:

- the incoming traffic distributes to outgoing ones according to fixed (statistical) coefficients;
- drivers behave to maximize the through flux.

More precisely, if the number of incoming roads is greater than that of outgoing ones, some right of way parameters have to be added.

Once the solution to a Riemann problem is provided, piecewise constant approximations via a wave front tracking algorithm can be constructed (Bressan 2000; Garavello and Piccoli 2006).

In this paper starting from Coclite, Garavello, Piccoli model, we describe the evolution of vehicles flows respecting traffic lights cycles and defining time-varying distribution at junctions in order to take account the dynamic behavior of drivers. Then we introduce a micro-algorithm and a Riemann solver to cover these typical situations. Numerical schemes such as the Godunov method, based on exact solutions to Riemann problems (Godlewski and Raviart 1991; Godunov 1959) are used to solve numerically the conservation law along roads.

The paper is organized as follows. A model for traffic networks is introduced in Section 2. Section 3 is devoted to the definition of Riemann solvers at junctions. In particular the micro-algorithm and Riemann solvers for traffic lights and time-varying distribution coefficients are described. Numerical methods are presented in Section 4. Some simulation results for a typical scenario of a simple 2×2 junction (two incoming roads and two outgoing ones) are shown in order to test and verify the adopted approach in Section 5. The section ends with a comparison between different configurations of two traffic lights in a network with three junctions.

2. MODELING CAR TRAFFIC NETWORKS

A road network is schematized by the couple (I, J) , where $I = \{I_i : i = 1, \dots, N\}$ represents the set of roads, while J is the collection of junctions connecting roads. Fixed a junction $J \in J$, we denote by $Inc(J)$ and $Out(J)$, respectively, the set of all incoming roads,

numbered from 1 to n , and the set of all outgoing ones, numbered from $n+1$ to $n+m$ (see Figure 1).

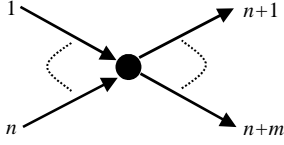


Figure 1: example of a $n \times m$ junction.

Each road is represented by an interval $I_i = [a_i, b_i] \subseteq \mathfrak{R}$.

According to the LWR model, we describe the evolution of cars density along each road by

$$\partial_t \rho_i + \partial_x f(\rho_i) = 0, \quad (1)$$

where $\rho_i = \rho_i(t, x) \in [0, \rho_{\max}]$ is the cars density on road I_i , ρ_{\max} is the maximal density, $f(\rho) = \rho v(\rho)$ is the flux, and $v(\rho)$ is the average velocity.

On the flux f we assume that

(F) $f: [0, 1] \rightarrow \mathfrak{R}$ is smooth, strictly concave, $f(0) = f(1) = 0$. Therefore there exists a unique strict maximum $\sigma \in]0, 1[$.

The dynamics at each junction $J \in J$ is determined by solving a Riemann Problem (RP), which is a Cauchy problem with constant initial data on each incident road. The solution is formed either by continuous waves, called *rarefactions*, or by traveling discontinuities, called *shocks*. In order to find a unique solution some Riemann Solvers (RS) are defined, based on rights of way and traffic distribution parameters.

Definition 1. A Riemann Solver for the junction J is a map $RS: [0, 1]^n \times [0, 1]^m \rightarrow [0, 1]^n \times [0, 1]^m$ that associates to Riemann data $\rho_0 = (\rho_{1,0}, \dots, \rho_{n+m,0})$ at J a vector $\hat{\rho} = (\hat{\rho}_1, \dots, \hat{\rho}_{n+m})$ so that the solution on an incoming road I_i , $i = 1, \dots, n$, is given by the wave $(\rho_{i,0}, \hat{\rho}_i)$ and on an outgoing road I_j , $j = n+1, \dots, n+m$, is given by the wave $(\hat{\rho}_j, \rho_{j,0})$. We require the consistency condition

$$(CC) RS(RS(\rho_0)) = RS(\rho_0).$$

In particular, for a $n \times m$ junction, RSs are based on the following rules:

(A) drivers distribute at a junction according to some traffic distribution coefficients which represent the preferences of drivers from the incoming roads to outgoing ones and they are collected in the matrix:

$$A = \{\alpha_{ji}\}_{j=n+1, \dots, n+m, i=1, \dots, n} \in \mathfrak{R}^{m \times n} \quad (2)$$

such that $0 < \alpha_{ji} < 1$, $\sum_{j=n+1}^{n+m} \alpha_{ji} = 1$, where α_{ji} is the percentage of drivers who, arriving from the i th incoming road, take the j th outgoing road.

(B) Respecting (A) rule, drivers behave so as to maximize the flux through the junction $J \in J$.

(C) If $n > m$, it is assumed that not all cars can enter the outgoing roads and let Q be the amount that can do it. Then $p_i Q$ cars come from the i th road to the generic j th one, with $i = 1, \dots, n$ and $j = n+1, \dots, n+m$, and p_i can be thought as a right of way parameter.

3. RIEMANN PROBLEMS AT JUNCTIONS

Let J be a $n \times m$ junction. The density functions on incoming and outgoing roads are denoted as $(t, x) \in \mathfrak{R}^+ \times I_i \rightarrow \rho_i(t, x) \in [0, \rho_{\max}]$, $i = 1, \dots, n$ and $(t, x) \in \mathfrak{R}^+ \times I_j \rightarrow \rho_j(t, x) \in [0, \rho_{\max}]$, $j = n+1, \dots, n+m$. We observe that the waves generated on incoming roads must have negative velocity, while the outgoing ones positive velocity. For this reason, some bounds on possible states reached by a solution to an RP at J exist. Precisely, if we set $\gamma_i = f(\rho_i)$, we have:

Proposition 2. Let $(\rho_{1,0}, \dots, \rho_{n+m,0})$ be the initial densities of an RP at J . The maximal fluxes γ_i^{\max} , $i = 1, \dots, n$ and γ_j^{\max} , $j = n+1, \dots, n+m$, that can be obtained on incoming roads and outgoing ones, respectively, are the following:

$$\gamma_i^{\max} = \begin{cases} f(\rho_{i,0}) & \text{if } \rho_{i,0} \in [0, \sigma], \\ f(\sigma) & \text{if } \rho_{i,0} \in]\sigma, \rho_{\max}], \end{cases} \quad i = 1, \dots, n, \quad (3)$$

$$\gamma_j^{\max} = \begin{cases} f(\sigma) & \text{if } \rho_{j,0} \in [0, \sigma], \\ f(\rho_{j,0}) & \text{if } \rho_{j,0} \in]\sigma, \rho_{\max}], \end{cases} \quad j = n+1, \dots, n+m. \quad (4)$$

Theorem 3. Let J be a $n \times m$ junction. For every initial data $(\rho_{1,0}, \dots, \rho_{n+m,0})$, there exists an unique admissible weak solution $\rho = (\rho_1, \dots, \rho_{n+m})$ to (1) at J , respecting rules (A), (B) and (C), such that

$$\rho_1(0, \cdot) \equiv \rho_{1,0}, \dots, \rho_{n+m}(0, \cdot) \equiv \rho_{n+m,0}. \quad (5)$$

Moreover, there exists a unique vector $(\hat{\rho}_1, \dots, \hat{\rho}_{n+m})$ such that

$$\hat{\rho}_i \in \begin{cases} \{\rho_{i,0}\} \cup]\tau(\rho_{i,0}), \rho_{\max}] & \text{if } 0 \leq \rho_{i,0} \leq \sigma, \\ [\sigma, \rho_{\max}] & \text{if } \sigma \leq \rho_{i,0} \leq \rho_{\max}, \end{cases} \quad (6)$$

with $i = 1, \dots, n$, and

$$\hat{\rho}_j \in \begin{cases} [0, \sigma] & \text{if } 0 \leq \rho_{j,0} \leq \sigma, \\ \{\rho_{j,0}\} \cup [0, \tau(\rho_{j,0})[& \text{if } \sigma \leq \rho_{j,0} \leq \rho_{\max}, \end{cases} \quad (7)$$

with $j = n+1, \dots, n+m$, where $\tau: [0, 1] \rightarrow [0, 1]$ is the map such that $f(\tau(\rho)) = f(\rho)$ for every $\rho \in [0, 1]$ and $\tau(\rho) \neq \rho$ for every $\rho \in [0, 1] \setminus \{\sigma\}$.

In order to show the construction of the RS satisfying rules (A) and (B) we recall the following simple cases:

Case 1 - 2×1 junction;

Case 2 - 1×2 junction.

Case 1. We consider the junction in Figure 2 with two incoming roads, 1 and 2, and one outgoing road 3.

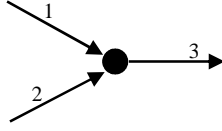


Figure 2: a 2×1 junction.

Fix a right of way parameter $p \in]0, 1[$ describing the percentage of cars crossing the junction. The solution is built as follows. To maximize the through traffic, according to rule (B), we set

$$\hat{\gamma}_3 = \min \left\{ \hat{\gamma}_1^{\max} + \hat{\gamma}_2^{\max}, \hat{\gamma}_3^{\max} \right\}, \quad (8)$$

where $\hat{\gamma}_i^{\max}$, $i=1,2$ and $\hat{\gamma}_3^{\max}$ are respectively given by relations (3) and (4). Observe that A is given by the column vector $(1,1)$. Considering the space (γ_1, γ_2) and the lines

$$\gamma_2 = \frac{1-p}{p} \gamma_1, \quad (9)$$

$$\gamma_2 + \gamma_1 = \hat{\gamma}_3, \quad (10)$$

we indicate with P the intersection point between lines (9) and (10). Therefore the final fluxes must belong to the admissible region

$$\Omega = \left\{ (\gamma_1, \gamma_2) : 0 \leq \gamma_1 + \gamma_2 \leq \hat{\gamma}_3, 0 \leq \gamma_i \leq \gamma_i^{\max}, i=1,2 \right\}. \quad (11)$$

We distinguish two different cases:

1. P belongs to Ω .
2. P does not belong to Ω .

In the first case (Figure 3) we set $(\hat{\gamma}_1, \hat{\gamma}_2) = P$, while in the second case (Figure 4) we set $(\hat{\gamma}_1, \hat{\gamma}_2) = Q$, where Q is given by the intersection $\Omega \cap \{(\gamma_1, \gamma_2) : \gamma_1 + \gamma_2 = \hat{\gamma}_3\}$. Once determined $\hat{\gamma}_1, \hat{\gamma}_2, \hat{\gamma}_3$ we are able to compute in a unique way $\hat{\rho}_1, \hat{\rho}_2, \hat{\rho}_3$ applying Theorem 3.

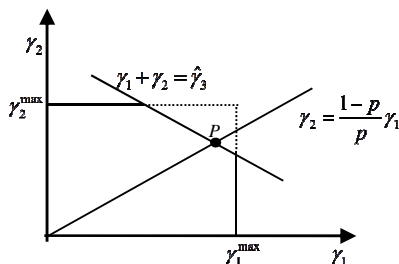


Figure 3: P belongs to Ω .

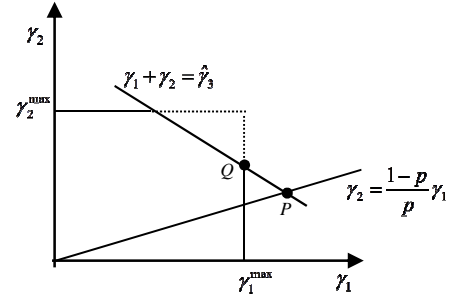


Figure 4: P does not belong to Ω .

Case 2. Deal with the junction in Figure 5 characterized by one incoming road 1 and two outgoing roads, 2 and 3.

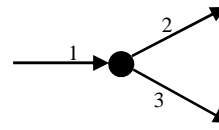


Figure 5: a 1×2 junction.

The rules (A) and (B) are only used. The distribution matrix is given by

$$A = \begin{pmatrix} \alpha \\ 1-\alpha \end{pmatrix}, \quad (12)$$

where $\alpha \in]0, 1[$ and $(1-\alpha)$ indicate the percentage of cars which, from road 1, goes to roads 2 and 3, respectively. Due to rule (B), the solution to RP is

$$\hat{\gamma} = (\hat{\gamma}_1, \hat{\gamma}_2, \hat{\gamma}_3) = (\hat{\gamma}_1, \alpha \hat{\gamma}_1, (1-\alpha) \hat{\gamma}_1), \quad (13)$$

where $\hat{\gamma}_1 = \min \left\{ \hat{\gamma}_1^{\max}, \frac{\hat{\gamma}_2^{\max}}{\alpha}, \frac{\hat{\gamma}_3^{\max}}{1-\alpha} \right\}$. Finally, we

determine $\hat{\rho}_1, \hat{\rho}_2, \hat{\rho}_3$ by Theorem 3.

3.1. RS for generalized junctions

Now we focus on some particular cases for a $n \times m$ junction with $n > m$. Starting from the discussion done in subsection 2.1, Case 1, we are able to define a RS, through the archetype of a linear programming (LP) problem. Without loss of generality we can analyze the sub-case of a $n \times 1$ junction as shown in Figure 6.

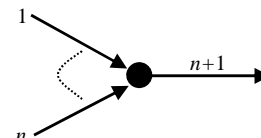


Figure 6: $n \times 1$ junction.

For each incoming road we fix a right of way parameter $p_i \in]0, 1[$, $i = 1, \dots, n$, such that $\sum_{i=1}^n p_i = 1$.

According to rule (B), we set

$$\hat{\gamma}_{n+1} = \max\{\gamma_1 + \dots + \gamma_n, \gamma_{n+1}\}, \quad (14)$$

or we can say that the objective function of this problem is $\max(\gamma_1 + \dots + \gamma_n)$. The admissible region is given by the set

$$\Omega = \left\{ (\gamma_1, \dots, \gamma_n) : \sum_{i=1}^n \gamma_i \leq \hat{\gamma}_{n+1}, 0 \leq \gamma_i \leq \gamma_i^{\max}, \forall i \right\}. \quad (15)$$

Considering the n -dimensional space $(\gamma_1, \dots, \gamma_n)$ we can determine the unique solution as the intersection of

$$\gamma_i = \frac{p_i}{p_1} \gamma_1, \forall i = 2, \dots, n, \quad (16)$$

$$\sum_{i=1}^n \gamma_i \leq \hat{\gamma}_{n+1}. \quad (17)$$

We remark that, since no graphical method can be applied, the solution point P is obtained using the simplex method to solve the LP problem defined in (15), (16), (17) with objective function in (14).

Then if P belongs to Ω , we set $(\hat{\gamma}_1, \hat{\gamma}_2, \dots, \hat{\gamma}_n) = P$, otherwise, $\hat{\gamma}_1 = \gamma_1^{\max}$, and we run the simplex method adding this constraint to the LP problem.

Observe that if at some time instant $\gamma_1 = 0$, the solution is given by $(\hat{\gamma}_1, \hat{\gamma}_2, \dots, \hat{\gamma}_n) = (0, 0, \dots, 0)$. Since this is not acceptable (the through traffic flow is different from zero), in order to determine the correct solution the following micro-algorithm, consisting of three steps, is implemented:

1. Search the incoming road with minimum traffic right of way parameter, except that with zero density.
2. Set the priority constraints, as in (16), referred to the choice at step one.
3. Solve the corresponding LP problem.

Let us discuss the case of an $1 \times m$ junction, as in Figure 7, in which the distribution matrix is the following

$$A = \begin{pmatrix} \alpha_1 \\ \vdots \\ \alpha_m \end{pmatrix}, \quad (18)$$

with $\alpha_i \in [0, 1]$, $i = 1, \dots, m$, and $\sum_{i=1}^m \alpha_i = 1$.

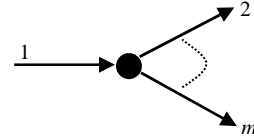


Figure 7: an $1 \times m$ junction.

In this case the flux vector of solution to the RP is

$$\hat{\gamma} = (\hat{\gamma}_1, \alpha_2 \hat{\gamma}_1, \dots, \alpha_m \hat{\gamma}_1), \quad (19)$$

where

$$\hat{\gamma}_1 = \min \left(\gamma_1^{\max}, \frac{\gamma_2^{\max}}{\alpha_2}, \dots, \frac{\gamma_m^{\max}}{\alpha_m} \right). \quad (20)$$

Now, we are able to describe the LP problem for a $n \times m$ junction assuming $n > m$. In order to satisfy the rules (A), (B) and (C), we get the following LP problem:

$$\max \sum_{i=1}^n \gamma_i, \quad (21)$$

$$0 \leq \sum_{i=1}^n \alpha_{1,i} \gamma_i \leq \gamma_1^{\max}, \quad (22)$$

$$\vdots$$

$$0 \leq \sum_{i=1}^n \alpha_{m,i} \gamma_i \leq \gamma_m^{\max},$$

$$\gamma_i = \frac{q_i}{q_1} \gamma_1, \forall i = 2, \dots, n, \quad (23)$$

$$0 \leq \gamma_i \leq \gamma_i^{\max}, \forall i = 2, \dots, n, \quad (24)$$

which can be solved using the simplex method. Then the outgoing fluxes are given by

$$(\hat{\gamma}_{n+1}, \dots, \hat{\gamma}_{n+m}) = \left(\sum_{i=1}^n \alpha_{1,i} \hat{\gamma}_i, \dots, \sum_{i=1}^n \alpha_{m,i} \hat{\gamma}_i \right). \quad (25)$$

3.2. RS for time dependent traffic

The real dynamic behavior of drivers at junctions is captured considering time dependent distribution coefficients, which means that, for instance, during a time period of the day, the traffic flows towards some specific direction, while in the successive period towards another one. Then, the matrix A is time dependent. Moreover we include a traffic light on the incoming side of a junction of type 2×2 (Figure 8), where 1, 2 are the incoming roads and 3, 4 are the outgoing ones.

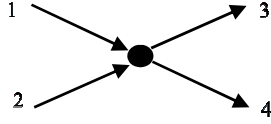


Figure 8: 2×2 junction.

Assume the distribution coefficients are two piecewise constant functions

$$\alpha(t) = \begin{cases} \eta_1 & 0 \leq t < \tau, \\ \eta_2 & \tau \leq t \leq T, \end{cases} \quad (26)$$

$$\beta(t) = \begin{cases} \eta_2 & 0 \leq t < \tau, \\ \eta_1 & \tau \leq t \leq T, \end{cases}$$

with $0 < \alpha(t) < 1, 0 < \beta(t) < 1$ and $\alpha(t) \neq \beta(t)$, for each $t \geq 0$. We define two piecewise constant maps as $\chi_1 = \chi_1(t)$, $\chi_2 = \chi_2(t)$, with $\chi_1(t) + \chi_2(t) = 1$ and $\chi_i(t) \in \{0, 1\}$, $i = 1, 2$, for each $t \geq 0$, which represent traffic lights. The values 0 and 1 correspond, respectively, to red and green lights. The matrix A is given by

$$A = \begin{pmatrix} \chi_1(t)\alpha(t) & \chi_2(t)\beta(t) \\ \chi_1(t)(1-\alpha(t)) & \chi_2(t)(1-\beta(t)) \end{pmatrix}. \quad (27)$$

First, let $\chi_i(t) = 1, i = 1, 2$ (no traffic lights) and fix $t < \tau$; to find the solution $(\hat{\gamma}_1, \hat{\gamma}_2)$ at junction we solve the following LP problem:

$$\begin{aligned} & \max \gamma_1 + \gamma_2, \\ & \eta_1 \gamma_1 + \eta_1 \gamma_2 \leq \gamma_3^{\max}, \\ & (1-\eta_1)\gamma_1 + (1-\eta_2)\gamma_2 \leq \gamma_4^{\max}, \\ & 0 \leq \gamma_1 \leq \gamma_1^{\max}, \\ & 0 \leq \gamma_2 \leq \gamma_2^{\max}. \end{aligned} \quad (28)$$

Clearly, for a time-instant belonging to the interval $[\tau, T]$, the LP problem will be defined taking account the different values of distribution coefficients, as in (26).

Now, if we suppose that, for some $t < \tau$, $\chi_1(t) = 1$ and $\chi_2(t) = 0$, i.e. for road 1 the green light is set, while for road 2 red light, the traffic flows from road 1 to roads 3 and 4. In this case the LP problem can be reduced to

$$\begin{aligned} & \max \gamma_1, \\ & \eta_1 \gamma_1 \leq \gamma_3^{\max}, \\ & (1-\eta_1)\gamma_1 \leq \gamma_4^{\max}, \\ & 0 \leq \gamma_1 \leq \gamma_1^{\max}. \end{aligned} \quad (29)$$

4. NUMERICAL METHOD

The space (t, x) is discretized via a numerical grid in $\mathfrak{R}^N \times (0, T)$ using the following notations:

- Δx is the space grid size;
- Δt is the time grid size;
- $(x_m, t_n) = (m\Delta x, n\Delta t)$ for $n \in \mathcal{N}$ and $m \in \mathcal{Z}$ are the grid points.

The values of the velocity v and the density ρ , on the grid are denoted, respectively, by $v_m^n = v(x_m, t_n)$ and $\rho_m^n = \rho(x_m, t_n)$.

In order to find a numerical solution for the conservation law along roads, the Godunov scheme is used. The initial datum ρ_0 is approximated by

$$v_m^0 = \frac{1}{\Delta x} \int_{x_m - \frac{1}{2}\Delta x}^{x_m + \frac{1}{2}\Delta x} \rho_0(x) dx. \quad (30)$$

The Godunov scheme is based on exact solutions v^Δ to RP at points $(m - \frac{1}{2})\Delta x$, $m \in \mathcal{Z}$ and on the projection of the solution

$$v_m^{n+1} = \frac{1}{\Delta x} \int_{x_m - \frac{1}{2}\Delta x}^{x_m + \frac{1}{2}\Delta x} v^\Delta(t_{n+1}, x) dx. \quad (31)$$

This procedure can be repeated inductively on every t_n . Under the CFL (Courant-Friedrichs-Lewy) condition

$$\Delta t \sup_{m,n} \left\{ \sup_{\rho \in I(\rho_m^n, \rho_{m+1}^n)} |f'(\rho)| \right\} \leq \Delta x, \quad (32)$$

the waves, generated by different RP, do not interact. We can use the Gauss-Green formula to compute v^{n+1} .

The flux in $x = x_m - \frac{1}{2}\Delta x$ for $t \in (t_n, t_{n+1})$ is given by

$$f \left(\rho \left(t, x_m - \frac{1}{2}\Delta x \right) \right) = f \left(W_R \left(0; v_{m-1}^n, v_m^n \right) \right), \quad \text{where}$$

$W_R \left(\frac{x}{t}; v_-, v_+ \right)$ is the self-similar solution between v_-

and v_+ . Similarly for the point $x = x_m + \frac{1}{2}\Delta x$:

$$f\left(\rho\left(t, x_m + \frac{1}{2}\Delta x\right)\right) = f\left(W_R(0; v_m^n, v_{m+1}^n)\right). \text{ As the flux is time invariant and continuous, we can put it out of the integral and, setting } g^G(\rho, v) = f\left(W_R(0; \rho, v)\right) \text{ under the condition (35), the scheme can be written as:}$$

$$v_m^{n+1} = v_m^n - \frac{\Delta t}{\Delta x} \left(g^G(v_m^n, v_{m+1}^n) - g^G(v_{m-1}^n, v_m^n) \right). \quad (33)$$

In general the numerical flux of Godunov is

$$g^G(\rho, w) = \begin{cases} \min_{z \in [\rho, w]} f(z), & \text{if } \rho \leq w, \\ \max_{z \in [w, \rho]} f(z), & \text{if } w \leq \rho. \end{cases} \quad (34)$$

4.1. Boundary condition

Fix a condition at the incoming boundary (incoming flow) $x = 0$: $u(0, t) = \rho_1(t)$, $t > 0$, and study equation only for $x > 0$. Inserting a ghost cell, we define the numerical condition as

$$v_0^{n+1} = v_0^n - \frac{\Delta t}{\Delta x} \left(g^G(v_0^n, v_1^n) - g^G(\rho_1^n, v_0^n) \right), \quad (35)$$

where $\rho_1^n = \frac{1}{\Delta t} \int_{t_n}^{t_{n+1}} \rho_1(t) dt$ takes the place of v_{-1}^n .

Analogously, the outgoing boundary is defined as follows. Let $x < L = x_N$, then we have

$$v_N^{n+1} = v_N^n - \frac{\Delta t}{\Delta x} \left(g^G(v_N^n, \rho_2^n) - g^G(v_{N-1}^n, v_N^n) \right), \quad (36)$$

where $\rho_2^n = \frac{1}{\Delta t} \int_{t_n}^{t_{n+1}} \rho_2(t) dt$ takes the place of v_{N+1}^n that is a ghost cell value.

4.2. Condition at junctions

For roads connected to a junction at the right endpoint we set

$$v_N^{n+1} = v_N^n - \frac{\Delta t}{\Delta x} \left(\hat{\gamma}_i - g^G(v_{N-1}^n, v_N^n) \right), \quad (37)$$

while for roads connected to a junction at the left endpoint we have

$$v_0^{n+1} = v_0^n - \frac{\Delta t}{\Delta x} \left(g^G(v_0^n, v_1^n) - \hat{\gamma}_j \right), \quad (38)$$

where $\hat{\gamma}_i, \hat{\gamma}_j$ are the flux solutions.

5. SIMULATION RESULTS

In what follows we choose a flux function $f(\rho) = \rho(1-\rho)$ which admits a unique maximum $\sigma = \frac{1}{2}$.

5.1. Simple Junction Scenario

Now we focus on a typical scenario of a 2×2 junction with a traffic light, where 1,2 are the incoming roads and 3,4 are the outgoing ones, as shown in Figure 8.

Consider the length of each road as normalized, a simulation time interval $[0, T]$ with $T = 10$ (which represents a time horizon of observation) and a numerical grid with $\Delta x = 0.12$ and $\Delta t = CFL \times \Delta x = 0.108$ where $CFL = 0.9$. The number of discrete time instants is given by the ratio $\frac{T}{\Delta t} = 93$

and accordingly the time variable t is referred to these instants. Further we assume the following data:

$$\begin{aligned} \rho_{1,0} = \rho_{2,0} = \rho_{3,0} = \rho_{4,0} &= 0, \\ \rho_{1,b} = \rho_{2,b} = \rho_{3,b} = \rho_{4,b} &= 0.3, \end{aligned}$$

where for $i = 1, 2, 3, 4$, $\rho_{i,0}$ is the initial density data, $\rho_{i,b}$ is the boundary density data.

From (3) and (4) we get that the maximal fluxes γ_i^{\max} are the following:

$$\gamma_1^{\max} = \gamma_2^{\max} = \gamma_3^{\max} = \gamma_4^{\max} = 0.5.$$

The traffic light is modeled by two functions, one for each incoming road, $\chi_1(t)$ and $\chi_2(t)$:

$$\chi_1(t) = \begin{cases} 1 & 0 \leq t < 20, \\ 0 & 20 \leq t < 40, \\ 1 & 40 \leq t < 60, \\ 0 & t \geq 60, \end{cases}$$

$$\chi_2(t) = \begin{cases} 0 & 0 \leq t < 20, \\ 1 & 20 \leq t < 40, \\ 0 & 40 \leq t < 60, \\ 1 & t \geq 60. \end{cases}$$

Finally, for the distribution coefficient α we consider two different cases:

- α constant;
- $\alpha = \alpha(t)$, i.e. time varying.

5.1.1. Case of constant distribution

The distribution matrix is given by

$$A = \begin{pmatrix} \alpha \\ 1 - \alpha \end{pmatrix} = \begin{pmatrix} 0.5 \\ 0.5 \end{pmatrix},$$

which means that the same quantity of cars is distributed on outgoing roads.

The evolution of traffic density on each road is shown in the following figures.

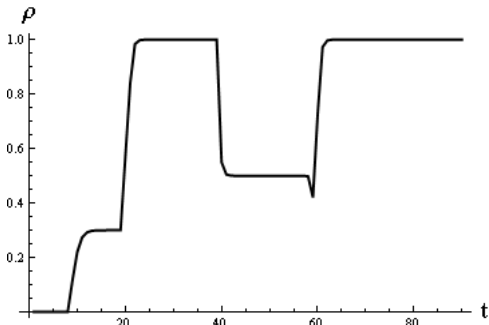


Figure 9: density on road 1 .

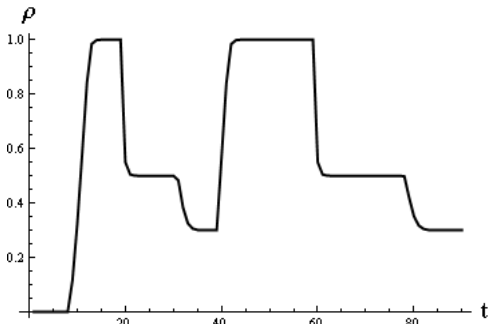


Figure 10: density on road 2 .

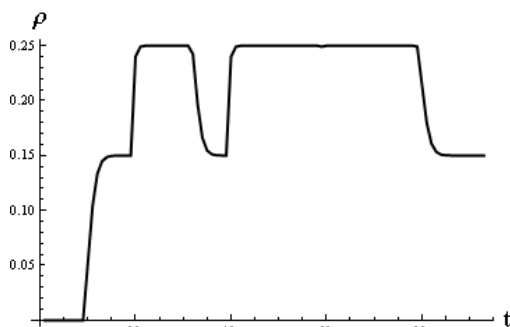


Figure 11: density on roads 3,4 .

As we can see from Figures 9 e 10, in the first time interval $[0,20[$, when the traffic light is green on incoming road 1, ρ_1 increases until the value 0.3, i.e. it reaches the boundary condition, while ρ_2 tends to the value 1, which means that the road 2 is saturated and, consequently, congests. Then, in the successive interval $[20,40[$, when the traffic light is green on road 2, ρ_2 decreases in such way that the road decongests until it reaches the value of density $\sigma = 0.5$, i.e. when the flux attains the maximum. Observe that this behavior is periodic since we choose the same alternate traffic light cycles.

For the outgoing roads (Figure 11), considering the same distribution coefficients, we see that in $[0,20[$ $\rho_3 = \rho_4 = 0.15$ as we expect; in fact from the only incoming road, i.e. road 1, the incoming density is 0.3. Then, in $[20,40[$, since the incoming density from road

2 is equal to 1 but $\gamma_2^{\max} = 0.5$, the corresponding incoming density is $\sigma = 0.5$, so that $\rho_3 = \rho_4 = 0.25$.

5.1.2. Case of time-varying distribution

The distribution matrix is given by

$$A = \begin{pmatrix} \alpha(t) \\ 1 - \alpha(t) \end{pmatrix}$$

where $\alpha(t) = -\frac{0.4}{80}t + 0.7$.

Here the evolution of traffic density on the incoming roads is the same of the previous case with constant α , while on the outgoing roads it is shown in the following figures.

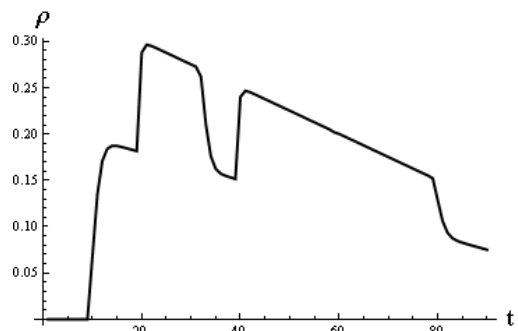


Figure 12: density on road ρ_3 .

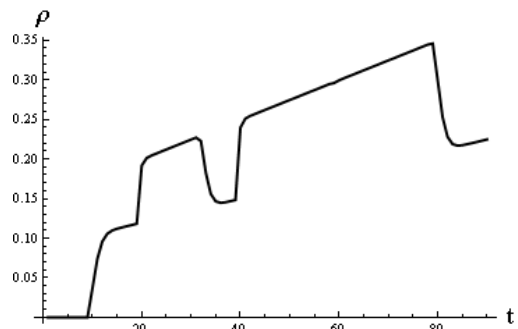


Figure 13: density on road ρ_4 .

We can observe that the effect of time-varying distribution consists in a modulation of the whole outgoing traffic. In general, the behavior of the drivers is captured more realistically finding the right dynamic modeling of distribution coefficients.

5.2. Network Scenario

In this section, we study a network scenario with three different junctions:

- $J_1 - 2 \times 1$,
- $J_2 - 2 \times 2$ with distribution coefficients $\alpha_4 = 0.5$ and $\alpha_6 = 0.5$,
- $J_3 - 3 \times 1$ with priority parameters $p_6 = 0.5$, $p_7 = 0.2$ and $p_8 = 0.5$,

linked as in Figure 14.

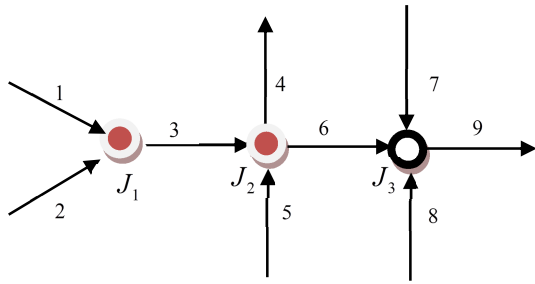


Figure 14: a network with three junctions.

On each road, we set $\rho_{i,0} = 0$, and boundary condition $\rho_b = 0.3$. In accordance to CFL condition we set $\Delta x = 0.0123$.

Now, the goal is to compare the effects due to changes of traffic light cycles on the evolution of fluxes outgoing from the network such as to choose the better strategy able to minimize congestion phenomena.

First, we assume in J_1 and J_2 two traffic lights having the green-red cycles as in Table 1.

Table 1: green-red cycles for J_1 and J_2 .

Time instants	J_1		J_2	
	Road 1	Road 2	Road 3	Road 5
0 - 99	Green	Red	Green	Red
100 - 199	Red	Green	Red	Green
200 - 299	Green	Red	Green	Red
300 - 399	Red	Green	Red	Green
400 - 499	Green	Red	Green	Red
500 - 599	Red	Green	Red	Green
600 - 699	Green	Red	Green	Red
700 - 799	Red	Green	Red	Green
800 - 903	Green	Red	Green	Red

Focusing on the network outgoing roads, i.e. roads 4 and 7, the simulation results of the density evolution are shown, respectively, in Figures 15 and 16.

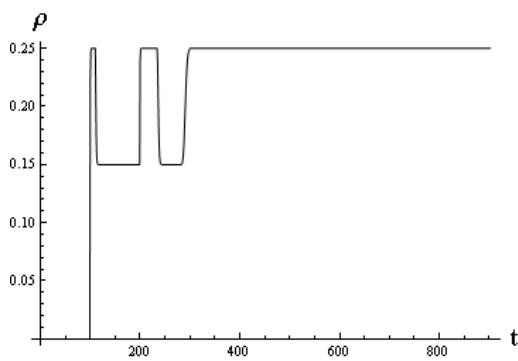


Figure 15: density on road 4.

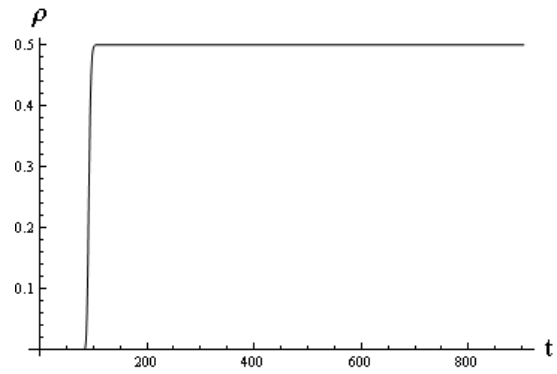


Figure 16: density on road 9.

Now, we change the traffic light cycles as shown in Table 2 and Table 3, setting different time instants.

Table 2: green-red cycles for J_1 .

Time instants	J_1	
	Road 1	Road 2
0 - 99	Green	Red
100 - 199	Red	Green
200 - 299	Green	Red
300 - 399	Red	Green
400 - 499	Green	Red
500 - 599	Red	Green
600 - 699	Green	Red
700 - 799	Red	Green
800 - 903	Green	Red

Table 3: green-red cycles for J_2 .

Time instants	J_2	
	Road 3	Road 5
0 - 49	Green	Red
50 - 149	Red	Green
150 - 249	Green	Red
250 - 349	Red	Green
350 - 449	Green	Red
450 - 549	Red	Green
550 - 649	Green	Red
650 - 749	Red	Green
750 - 849	Green	Red

In this case the density evolution on roads 4 and 7 is represented in Figures 18 and 19.

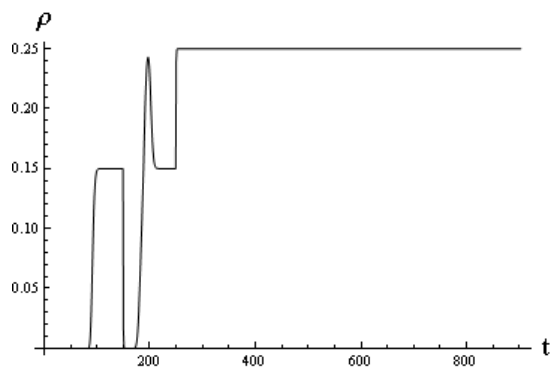


Figure 18: density on road 4.

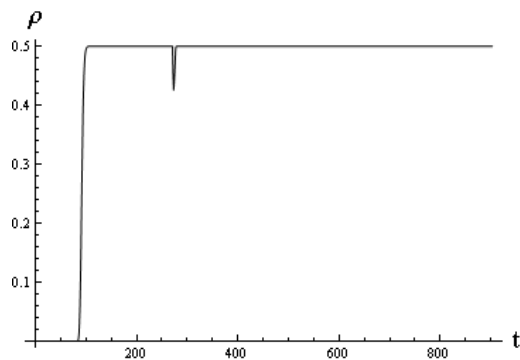


Figure 19: density on road 9.

Notice that, in the second configuration case of traffic lights, the outgoing fluxes are greater than the first case.

Finally, we conclude that, choosing a right policy for the management of fluxes at a junction, playing on distribution coefficients and traffic lights cycles, it is possible to improve traffic conditions and minimize congestion effects.

REFERENCES

- Bellomo, N., Coscia, V., 2005. First order models and closure of the mass conservation equation in the mathematical theory of vehicular traffic flow. *C. R. Mec.* 333, pp. 843-851.
- Bressan, A., 2000. *Hyperbolic Systems of Conservation Laws – The One Dimensional Cauchy Problem.* Oxford Univ. Press.
- Coclite, G., Garavello, M., Piccoli, B., 2005. Traffic flow on road networks. *SIAM Journal on Mathematical Analysis*, vol. 36, no. 6, pp. 1862-1886.
- Colombo, R.M., 2002. Hyperbolic phase transitions in traffic flow, *SIAM J. Appl. Math.*, vol. 63, no. 2, pp. 708-721.
- Garavello, M., Piccoli, B., 2006. *Traffic flow on Networks.* Applied Math. Series, American Institute of Mathematical Sciences, vol. 1.
- Godlewski, E., Raviart, P.A., 1991. Hyperbolic systems of conservation laws, *Mathematics and Applications*, 3-4, Ellipses, Paris.
- Godunov, S.K., 1959. A finite difference method for the numerical computation of discontinuous solutions

of the equations of fluid dynamics, *Matematicheskii Sbornik*, vol. 47, pp. 271-290.

Helbing, D., 2001. Traffic and related self-driven many particle systems. *Reviews of Modern Physics*, vol. 73, pp. 1067-1141.

Lighthill, M.J., Whitham, G.B., 1955. On kinetic waves. II. Theory of traffic flows on long crowded roads. *Proc. Roy. Soc. London Ser. A*, vol. 229, pp. 317-345.

Richards, P.I., 1956. Shock waves on the highway. *Oper. Res.*, vol. 4, pp. 42-51.

AUTHORS BIOGRAPHY

CARMINE DE NICOLA was born in Salerno, Italy, in 1972. He graduated in Electronic Engineering in 2002 with a dissertation on simulations of processor IAPX 86. He obtained PhD in Mathematics in 2011 at the University of Salerno. He actually is a researcher assistant in Operations Research at the Department of Electronic and Computer Engineering of the University of Salerno. His scientific interests are about fluid – dynamic models for the analysis of traffic flows on road and supply chains networks and queueing systems and networks.

His e-mail address is denicola@diima.unisa.it.

ROSANNA MANZO graduated cum laude in Mathematics in 1996 and obtained PhD in Information Engineering in 2007 at the University of Salerno. She is a researcher in Mathematical Analysis at the Department of Electronic and Computer Engineering of the University of Salerno. Her research areas include fluid – dynamic models for traffic flows on road, telecommunication and supply networks, optimal control and queueing theory. She is author of about 50 papers appeared on international journals and many publications on proceedings.

Her e-mail address is rmanzo@unisa.it.

VINCENZO MOCCIA was born in Cercola (NA), Italy, in 1984. He graduated cum laude in Computer Science in 2009 at the University of Salerno. He is currently a PhD student in Applied Mathematics at the University of Salerno. His research interests include models for optimal scheduling in airport context and fluid-dynamic models for simulation of road traffic networks.

His e-mail address is moccia@diima.unisa.it.

VINCENZA TUFANO was born in Napoli, Italy, in 1983. She graduated cum laude in Computer Science at the University of Salerno. She is actually a PhD student in Applied Mathematics at the University of Salerno. Her research interests include image partitioning, video segmentation procedure and fluid-dynamic models for traffic flows on road networks.

Her e-mail address is tufano@diima.unisa.it.

VARIABLE INTERACTION NETWORKS IN MEDICAL DATA

Stephan M. Winkler ^(a), Michael Affenzeller ^(b), Gabriel Kronberger ^(c),
Michael Kommenda ^(d), Stefan Wagner ^(e), Witold Jacak ^(f), Herbert Stekel ^(g)

^(a-f) University of Applied Sciences Upper Austria
Heuristic and Evolutionary Algorithms Laboratory
Softwarepark 11, 4232 Hagenberg, Austria

^(a, b, f) University of Applied Sciences Upper Austria
Bioinformatics Research Group
Softwarepark 11, 4232 Hagenberg, Austria

^(g) General Hospital Linz
Central Laboratory
Krankenhausstraße 9, 4021 Linz, Austria

^(a) stephan.winkler@fh-hagenberg.at, ^(b) michael.affenzeller@fh-hagenberg.at, ^(c) gabriel.kronberger@fh-hagenberg.at,
^(d) michael.kommenda@fh-hagenberg.at, ^(e) stefan.wagner@fh-hagenberg.at,
^(f) witold.jacak@fh-hagenberg.at, ^(g) herbert.stekel@akh.linz.at

ABSTRACT

In this paper we describe the identification of variable interaction networks in a medical data set. The main goal is to generate mathematical models for standard blood parameters as well as tumor markers using other available parameters in this data set. For each variable we identify those variables that are most relevant for modeling it; relevance of a variable can in this context be defined via the frequency of its occurrence in models identified by evolutionary machine learning methods or via the decrease in modeling quality after removing it from the data set.

Several data based modeling approaches implemented in HeuristicLab have been applied for identifying estimators for selected tumor markers and cancer diagnoses: Linear regression and support vector machines (optimized using evolutionary algorithms) as well as genetic programming.

Keywords: medical data analysis, data mining, evolutionary algorithms, variable interaction networks

1. INTRODUCTION, RESEARCH GOALS

In this paper we present research results achieved within the Josef Ressel Centre for Heuristic Optimization *Heureka!*: Data of thousands of patients of the General Hospital (AKH) Linz, Austria, have been analyzed in order to identify mathematical models for cancer diagnoses. We have used a medical database compiled at the central laboratory of AKH in the years 2005 – 2008: A series of routinely measured blood values of thousands of patients are available as well as several tumor markers (TMs, substances found in humans that can be used as indicators for certain types of cancer). Not all values are measured for all patients; especially tumor marker values are determined and documented

mainly if there are indications for the presence of cancer. The results of empirical research work done on the data based identification of estimation models for standard blood parameters as well as tumor markers are presented in this paper: The main goal is to generate mathematical models for standard blood parameters as well as tumor markers using other available parameters in this data set. For each variable we identify those variables that are most relevant for modeling it; relevance of a variable can in this context be defined via the frequency of its occurrence in models identified by evolutionary machine learning methods or via the decrease in modeling quality after removing it from the data set.

2. VARIABLE INTERACTION NETWORKS

2.1. General Approach

The main goal in the identification of variable interaction networks is to determine in how far variables interact which other variables in the given data set. We identify these interactions by modeling all given variables and determining the importance / relevance of all potential input variables; influences above some pre-defined threshold are considered relevant and are shown in respective graphical representation of this interaction network. An exemplary interaction network is shown in Figure 1.

In (Winkler et al. 2006), for example, variable selection results were shown partially resembling interaction networks; in (Kronberger 2011) the author showed variable interaction networks for a blast furnace process, an industrial chemical process, and macro-economic data dependencies using symbolic regression based on genetic programming.

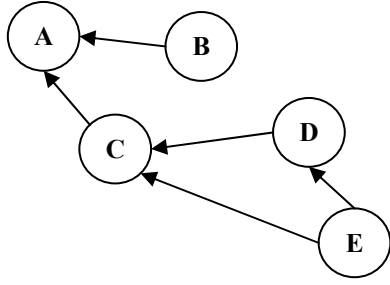


Figure 1: An exemplary variables interaction network. Variable A is influenced by variables B and C, while C is influenced by D and E (which also influences D).

2.2. Calculation of the Impact (Relevance) of Variables

In the present research work we estimate the relevance of the available variables (i.e., standard blood parameters and virtual tumor markers) with respect to models. There are several methods for calculating the relevance of variables (see for example (Winkler 2009) and (Affenzeller et al. 2009)); the following approaches are used in the context of this research work:

2.2.1. Frequency Based Relevance of Variables:

The relevance of a variable (at index i) with respect to a given model m can either be defined as the number of references in this model (calculated using function $freq_1$) to this variable, or simply as 1 if there is a reference to this variable and 0 if not ($freq_2$).

$$freq_1(i, m) = |\{v: v \in m.variables \ \& \ v.VarIndex = i\}| \quad (1)$$

$$freq_2(i, m) = \begin{cases} 1: & \exists v : (v \in m.variables \ \& \ v.VarIndex = i) \\ 0: & otherwise \end{cases} \quad (2)$$

2.2.2. Impact Based Relevance of Variables - Impact of Variables with Respect to Models

The estimation of a variable's impact on the evaluation of a model is done by temporarily replacing the values of exactly this variable and evaluating the model using the resulting manipulated data base. We here use replacement methods using averaging, constants, linear regression and additive Gaussian noise; a given variable (at index i) is replaced without changing any other part of the data basis. We transfer the original data basis $Data$ consisting of N variables with n samples each to a manipulated data basis $Data_i(r)$ with manipulated variable number i using a replacement function r as

$$\forall (i \in [1; N]): Data_{i(r)} = [Data_1, Data_2, \dots, r(Data_i), Data_{i+1}, \dots, Data_N] \quad (3)$$

The replacement functions used replace a particular variable using a given constant value (r_{const}), its mean value (r_{mean}), its linear trend (r_{linreg}), or the addition of Gaussian noise (r_{agn}). Now it is possible to calculate the variable's impact with respect to the model

m by evaluating the model on the manipulated data set $Data_i$ and measuring the resulting difference between the original output values and those calculated on the manipulated data.

This measurement can be done on the basis of the mean squared difference function $impact_{msd}$, e.g.:

$$impact_{msd}(i, m, r) = \frac{1}{n} \sum_{j=1}^n ([eval(m, Data)]_j - [eval(m, Data_i(r))]_j)^2 \quad (4)$$

2.2.3. Impact Based Relevance of Variables - Impact of Variables with Respect to Algorithm Performance:

After identifying the models that are used most frequently and seem to be most important for the models created by the identification algorithms, we estimate the importance of variables (or groups of variables) by removing them from the list of available input and repeating the modeling process. Thus, again we use $Data_i(r)$ for calculating the relevance of variable i and define the relevance of variable i with respect to a modeling method m , a replacement method r and a fitness function f as

$$impact_{alg}(i, m, r, f) = \frac{f(eval(m, Data))}{f(eval(m, Data_i(r)))} \quad (5)$$

3. MACHINE LEARNING METHODS APPLIED

In this section we describe the modeling methods applied for identifying estimation models for tumor markers and cancer diagnoses: On the one hand we apply hybrid modeling using machine learning algorithms and evolutionary algorithms for parameter optimization and feature selection (as described in Section 2.1), on the other hand we use genetic programming (as described in Section 2.2). In (Winkler et al. 2011), for example, these methods have also been described in detail.

3.1. Hybrid Modeling Using Machine Learning Algorithms and Evolutionary Algorithms for Parameter Optimization and Features Selection

Feature selection is often considered an essential step in data based modeling; it is used to reduce the dimensionality of the datasets and often conducts to better analyses. Given a set of n features $F = \{f_1, f_2, \dots, f_n\}$, our goal here is to find a subset of F , F' , that is on the one hand as small as possible and on the other hand allows modeling methods to identify models that estimate given target values as well as possible. Additionally, each data based modeling method (except plain linear regression) has several parameters that have to be set before starting the modeling process.

The fitness of feature selection F' and training parameters with respect to the chosen modeling method is calculated in the following way: We use a machine learning algorithm m (with parameters p) for estimating predicted target values $est(F', m, p)$ and compare those to the original target values $orig$; the coefficient of determination R^2 function is used for calculating the

quality of the estimated values. Additionally, we also calculate the ratio of selected features $|F'|/|F|$. Finally, using a weighting factor α , we calculate the fitness of the set of features F' using m and p by comparing the estimated values to the originally given target values:

$$fitness(F', m, p) = \alpha \cdot |F'|/|F| + (1 - \alpha) \cdot (1 - R^2(est(F', m, p), orig)). \quad (5)$$

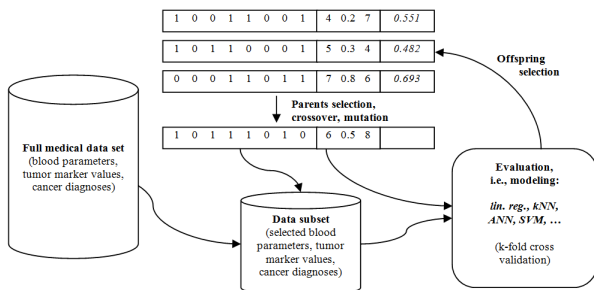


Figure 2: A hybrid evolutionary algorithm for feature selection and parameter optimization in data based modeling. Machine learning algorithms are applied for evaluating feature sets.

In (Alba et al. 2007), for example, the use of evolutionary algorithms for feature selection optimization is discussed in detail in the context of gene selection in cancer classification. We have now used evolutionary algorithms for finding optimal feature sets as well as optimal modeling parameters for models for tumor diagnosis; this approach is schematically shown in Figure 2: A solution candidate is here represented as $[s_1 \dots p_{1 \dots q}]$ where s_i is a bit denoting whether feature F_i is selected or not and p_j is the value for parameter j of the chosen modeling method m . This rather simple definition of solution candidates enables the use of standard concepts for genetic operators for crossover and mutation of bit vectors and real valued vectors: We use uniform, single point, and 2-point crossover operators for binary vectors and bit flip mutation that flips each of the given bits with a given probability. Explanations of these operators can for example be found in (Holland 1975) and (Eiben 2003).

We have used strict offspring selection (Affenzeller et al. 2009): Individuals are accepted to become members of the next generation if they are evaluated better than both parents.

In (Winkler et al. 2011) we have documented classification accuracies for tumor diagnoses using this approach for optimizing feature set and modeling parameters.

The following machine learning algorithms have been applied for identifying estimators for selected tumor markers and cancer diagnoses: Linear regression and support vector machines.

3.2. Genetic Programming

As an alternative to the approach described in the previous sections we have also applied a classification algorithm based on genetic programming (GP, Koza (1992)) using a structure identification framework

described in Winkler (2008) and Affenzeller et al. (2009).

We have used the following parameter settings for our GP test series: The mutation rate was set to 15%, gender specific parents selection (Wagner 2005) (combining random and roulette selection) was applied as well as strict offspring selection (Affenzeller et al. 2009) (OS, with success ratio as well as comparison factor set to 1.0). The functions set described in (Winkler 2008) (including arithmetic as well as logical functions) was used for building composite function expressions.

In addition to splitting the given data into training and test data, the GP based training algorithm used in our research project has been designed in such a way that a part of the given training data is not used for training models and serves as validation set; in the end, when it comes to returning classifiers, the algorithm returns those models that perform best on validation data.

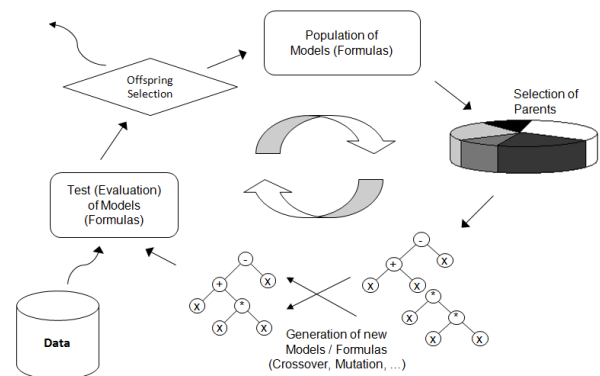


Figure 3: Genetic programming including offspring selection.

4. DATA BASE

The blood data measured at the AKH in the years 2005-2008 have been compiled in a database storing each set of measurements (belonging to one patient): Each sample in this database contains a unique ID number of the respective patient, the date of the measurement series, the ID number of the measurement, standard blood parameters, tumor marker values, and cancer diagnosis information. Patients' personal data were at no time available for the authors except for the head of the laboratory.

In total, information about 20,819 patients is stored in 48,580 samples. Please note that of course not all values are available in all samples; there are many missing values simply because not all blood values are measured during each examination. Further details about the data set and necessary data preprocessing steps can for example be found in Winkler et al. (2010) and Winkler et al. (2011), e.g.

Standard blood parameters include for example the patients' sex and age, information about the amount of cholesterol and iron found in the blood, the amount of hemoglobin, and the amount of red and white blood

cells; in total, 29 routinely available patient parameters are available.

Literature discussing tumor markers, their identification, their use, and the application of data mining methods for describing the relationship between markers and the diagnosis of certain cancer types can be found for example in Koepke (1992) (where an overview of clinical laboratory tests is given and different kinds of such test application scenarios as well as the reason of their production are described) and Yonemori (2006).

As described in Winkler et al. (2010) and Winkler et al. (2011), information about the following tumor markers is stored in the AKH database: AFP, CA 125, CA 15-3, CA 19-9, CEA, CYFRA, fPSA, NSE, PSA, S-100, SCC, and TPS.

5. CASE STUDY RESEARCH RESULTS: FEATURES RELEVANT FOR PREDICTING BREAST CANCER DIAGNOSIS AND THE CORRESPONDING VARIABLES INTERACTION NETWORK

5.1. Data Preprocessing

From the data base mentioned in the previous section we have selected a subset of samples containing standard blood data, tumor markers, and the information whether the corresponding patient was diagnosed with breast cancer or not. All samples represent female patients; we have selected samples that contain at least 80% valid values and replaced all missing values by the median of the respective variable.

Furthermore, variables containing less than 80% valid values were removed. Finally, the samples were filtered in such a way that 50% of the remaining samples represent patients with breast cancer and 50% patients without a positive breast cancer diagnosis. This leads to a data set consisting of 636 samples; Table 1 summarizes all relevant key parameters of the so compiled data base.

Table 1: Data base used for breast cancer diagnosis variables interaction network case study

Number of samples	636
Number of samples in	
class 0 (no breast cancer diagnosed)	318
class 1 (breast cancer diagnosed)	318
Number of available variables (features)	30
standard values	26
tumor markers (AFP, C125, C153, PSA)	4

5.2. Modeling Results, Variable Impacts and Variable Interaction Network

5.2.1. Impact of Variables on Breast Cancer Diagnosis

For estimating breast cancer diagnoses we have used the data set described in 5.1 and applied tree based genetic programming using the HeuristicLab 3.3.6 framework

(Wagner (2009), <http://dev.heuristiclab.com>); the most important GP settings are summarized in Table 2.

GP was used for learning models for the breast cancer diagnosis using all available variables; subsequently, following the strategy described in Section 2.2.3 all features were (one by one) removed from the data basis and the resulting classification accuracy compared to the accuracy achieved using all variables. Figure 4 visualizes the most important results of these tests showing the average test accuracies of five repetitions with five-fold cross-validation: Using all variables 75.47% of the given samples are correctly classified, after removing for example C125 the accuracy drops to 69.81%, and after removing C153 even to 60.85%. All not displayed features do not seem to have a relevant impact as their removal did not lead to a decrease of the classification accuracy below 75%.

Table 2: GP parameters

Population size	1000
Size limits	
maximum tree height	8
maximum tree size	100
Mutation rate	15%
Offspring selection	strict
max. selection pressure	100
Function basis	Arithmetic and logic functions

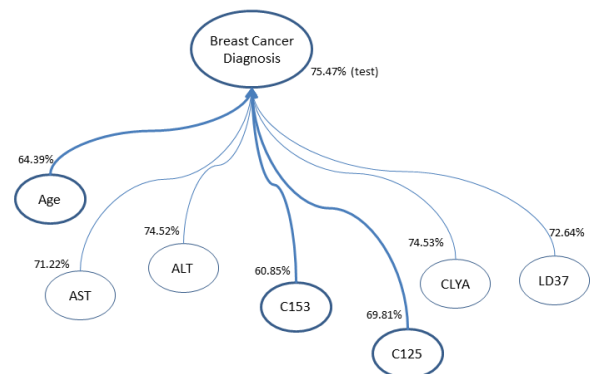


Figure 4: Classification accuracies for breast cancer diagnoses

5.2.2. Medical Variables Interaction Network

Following the modeling of breast cancer diagnoses, all variables in the data set have been modeled using the hybrid approach described in Section 3.1: A genetic algorithm with strict offspring selection was used for optimizing feature selections and algorithm parameters for linear regression and support vector machines that are used for modeling each available variable. Table 3 summarizes all relevant parameters for this modeling approach.

Again, five repetitions were executed (applying five-fold cross-validation) for each modeling scenario. All variables that were eventually selected by the evolutionary process (either for linear regression modeling or support machines) were collected; from this information we have developed a variables

interaction network that represents all relevant relationships among variables. Figure 5 represents the so composed network showing relevant impacts for variables that can be modeled with test prediction squared correlation coefficient (R^2) greater than 0.4

Table 3: GA + linReg / SVM parameters

Population size	10
Mutation rates	
feature selection flip	30%
algorithm parameter mutation	30%
Offspring selection	strict
max. selection pressure	100
Initial variable selection probability	30%

6. CONCLUSION

In this paper we have discussed a data-based approach for calculating the importance of medical variables for estimating cancer diagnoses using machine learning; furthermore, this modeling based impact analysis has also been used for constructing variable interaction networks describing the relationship among medical features.

As we have seen in the empirical section of this paper, there are several features that are of significant importance for the success of estimating breast cancer diagnoses; not surprisingly, the most important ones are tumor markers. The subsequently generated interaction

network shows the most important relationships among the analyzed medical variables.

ACKNOWLEDGMENTS

The work described in this chapter was done within the Josef Ressel-Centre *Heureka!* for Heuristic Optimization sponsored by the Austrian Research Promotion Agency (FFG).

REFERENCES

- Affenzeller, M., Winkler, S., Wagner, S., A. Beham, 2009. *Genetic Algorithms and Genetic Programming - Modern Concepts and Practical Applications*. Chapman & Hall/CRC. ISBN 978-1584886297. 2009.
- Alba, E., García-Nieto, J., Jourdan, L., Talbi, E.-G., 2005. Gene selection in cancer classification using PSO/SVM and GA/SVM hybrid algorithms. *IEEE Congress on Evolutionary Computation 2007*, pp. 284 – 290.
- Eiben, A.E. and Smith, J.E. 2003. Introduction to Evolutionary Computation. *Natural Computing Series*, Springer-Verlag Berlin Heidelberg.
- Holland, J. H., 1975. *Adaption in Natural and Artificial Systems*. University of Michigan Press.
- Kronberger, G., 2011. *Symbolic Regression for Knowledge Discovery*. Schriften der Johannes Kepler Universität Linz, Universitätsverlag Rudolf Trauner.
- Koepke, J. A., 1992. Molecular marker test

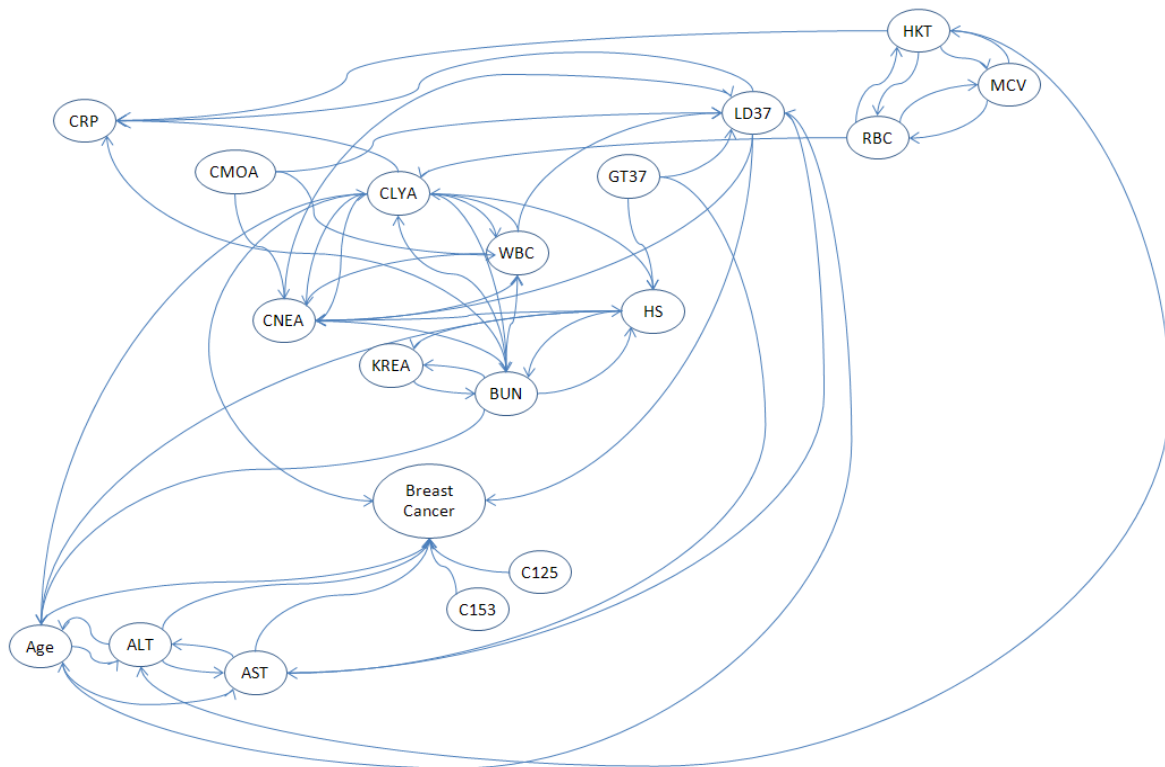


Figure 5: Interaction network of medical variables

standardization. *Cancer*, 69, pp. 1578–1581.

Wagner, S., 2009. *Heuristic Optimization Software Systems - Modeling of Heuristic Optimization Algorithms in the HeuristicLab Software Environment*. PhD Thesis, Institute for Formal Models and Verification, Johannes Kepler University Linz, Austria.

Winkler, S. M., Efendic, H., del Re, L., 2006. Quality Pre-Assesment in Steel Industry Using Data Based Estimators. In S. Cierpisz, K. Miskiewicz, A. Heyduk (ed.), *Proceedings of the IFAC Workshop MMM'2006 on Automation in Mining, Mineral and Metal Industry*, pp. 185-190. International Federation for Automatic Control.

Winkler, S., Affenzeller, M., Jacak, W., Stekel, H., 2010. Classification of Tumor Marker Values Using Heuristic Data Mining Methods. *Proceedings of Genetic and Evolutionary Computation Conference 2010, Workshop on Medical Applications of Genetic and Evolutionary Computation*, pp. 1915–1922.

Winkler, S., Affenzeller, M., Jacak, W., Stekel, H., 2011. Identification of Cancer Diagnosis Estimation Models Using Evolutionary Algorithms – A Case Study for Breast Cancer, Melanoma, and Cancer in the Respiratory System. *Proceedings of Genetic and Evolutionary Computation Conference 2011, Workshop on Medical Applications of Genetic and Evolutionary Computation*.

Winkler, S., 2009. *Evolutionary System Identification - Modern Concepts and Practical Applications*. Schriften der Johannes Kepler Universität Linz, Reihe C: Technik und Naturwissenschaften. Universitätsverlag Rudolf Trauner. ISBN 978-3-85499-569-2.

Yonemori, K., Ando, M., Taro, T. S., Katsumata, N., Matsumoto, K., Yamanaka, Y., Kouno, T., Shimizu, C., Fujiwara, Y., 2006. Tumor-marker analysis and verification of prognostic models in patients with cancer of unknown primary, receiving platinum-based combination chemotherapy. *Journal of Cancer Research and Clinical Oncology*, 132(10), pp. 635–642.

AUTHORS BIOGRAPHIES



STEPHAN M. WINKLER received his PhD in engineering sciences in 2008 from Johannes Kepler University (JKU) Linz, Austria. His research interests include genetic programming, nonlinear model identification and machine learning. Since

2009, Dr. Winkler is professor at the Department for Medical and Bioinformatics at the University of Applied Sciences (UAS) Upper Austria at Hagenberg Campus; since 2010, Dr. Winkler is head of the Bioinformatics Research Group at UAS, Hagenberg.



MICHAEL AFFENZELLER has published several papers, journal articles and books dealing with theoretical and practical aspects of evolutionary computation, genetic algorithms, and meta-heuristics in general. In 2001 he received his PhD in engineering sciences and in 2004 he received his habilitation in applied systems engineering, both from the Johannes Kepler University of Linz, Austria. Michael Affenzeller is professor at UAS and head of the Josef Ressel Center *Heureka!* at Hagenberg.



GABRIEL KRONBERGER received his PhD in engineering sciences in 2010 from JKU Linz, Austria, and is a research associate at the UAS Research Center Hagenberg. His research interests include genetic programming, machine learning, and data mining and knowledge discovery.



MICHAEL KOMMENDA finished his studies in bioinformatics at Upper Austria University of Applied Sciences in 2007. Currently he is a research associate at the UAS Research Center Hagenberg working on data-based modeling algorithms for complex systems within *Heureka!*.



STEFAN WAGNER received his PhD in engineering sciences in 2009 from JKU Linz, Austria; he is professor at the Upper Austrian University of Applied Sciences (Campus Hagenberg). Dr. Wagner's research interests include evolutionary computation and heuristic optimization, theory and application of genetic algorithms, and software development.



WITOLD JACAK received his PhD in electric engineering in 1977 from the Technical University Wroclaw, Poland, where he was appointed Professor for Intelligent Systems in 1990. Since 1994 Prof. Jacak is head of the Department for Software Engineering at the Upper Austrian University of Applied Sciences (Campus Hagenberg).



HERBERT STEKEL received his MD from the University of Vienna in 1985. Since 1997 Dr. Stekel is chief physician at the General Hospital Linz, Austria, where Dr. Stekel serves as head of the central laboratory.

IDENTIFICATION OF PATTERNS IN MICROSCOPY IMAGES OF BIOLOGICAL SAMPLES USING EVOLUTION STRATEGIES

Daniela M. Borgmann ^(a), Julian Weghuber ^(b), Susanne Schaller ^(c),
Jaroslaw Jacak ^(d), Stephan M. Winkler ^(e)

^(a, c, e) University of Applied Sciences Upper Austria
Bioinformatics Research Group
Softwarepark 11, 4232 Hagenberg, Austria

^(b) University of Applied Sciences Upper Austria
Department of Bio- and Environmental Technology
Stelzhamerstraße 23, 4600 Wels, Austria

^(d) Johannes Kepler University Linz
Institute of Applied Physics
Altenbergerstraße 69, 4040 Linz, Austria

^(a) daniela.borgmann@students.fh-hagenberg.at, ^(b) julian.weghuber@fh-wels.at,
^(c) susanne.schaller@fh-hagenberg.at, ^(d) jaroslaw.jacak@jku.at, ^(e) stephan.winkler@fh-hagenberg.at

ABSTRACT

In this paper we describe an algorithm based on evolutionary algorithms for determining patterns in images of biological samples (especially living cells) generated using the micro-patterning assay approach. In order to identify these patterns it is necessary to identify symmetric grids in nanoscale microscopy images.

The algorithm presented in this paper is based on evolution strategies (ES): After downsampling the image using a correlation based approach for estimating the optimal downsampling rate, initial grids are constructed which are repeatedly evaluated and mutated for creating new candidates from which the best ones are promoted to the next generation. In the experimental section of this paper we analyse the performance of several ES strategies for identifying optimal grids in several images of biological samples.

Keywords: bioinformatics, evolution strategy, μ -patterning assay

1. INTRODUCTION: USING THE μ -PATTERNING ASSAY FOR THE DETECTION OF PROTEIN-PROTEIN-INTERACTIONS IN LIVING CELLS

The cellular membrane of biological cells is an important integral part of cellular interaction processes. The membrane itself represents a physical barrier between intracellular and extracellular spaces and hereby generates a tiny reaction volume – the biological cell. In order to guarantee the proper function of a cell, interactions between the extracellular environment and the intracellular space are necessary.

In many cases interactions take place with the help of proteins (receptors), which can be found integrated or on the surface of cell membranes. The communication between these receptors is regulated by so-called messenger-substances; for example the binding of insulin to the insulin receptor activates this receptor, which leads to decreased blood sugar levels. Another example can be found in the context of cell-growth: Binding of epidermal growth factor (EGF) to the EGF-receptor (EGFR) can stimulate cell proliferation.

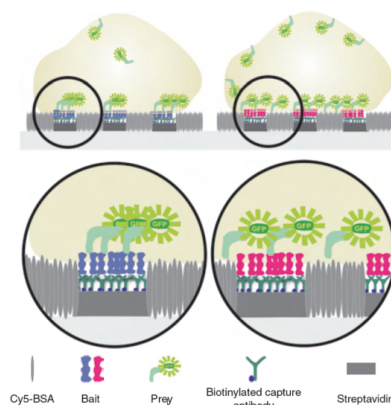


Figure 1: Basic principle of μ -patterning assay

A faulty regulation or an incorrect transmission of EGF can thus lead to cancer.

Protein-protein interactions, especially in cell membranes, represent a key element for many cellular processes. Nowadays, the number of available methods for the detection and quantification of protein-protein interactions in living cells is limited. Some of them entail serious drawbacks like insufficient sensitivity or a high number of false-positive or false-negative results.

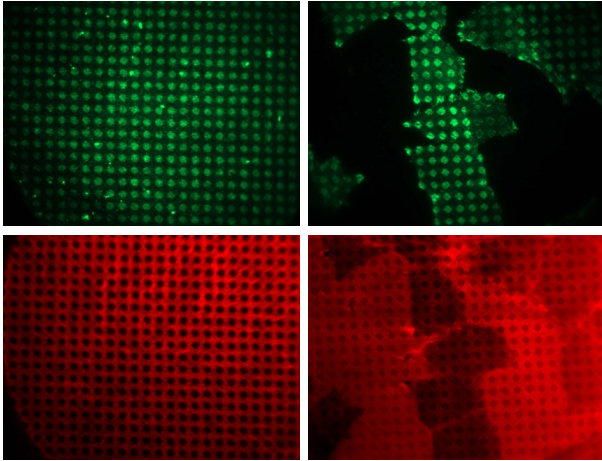


Figure 2: Left column: fluorescently labelled bait antibody control, right column: bait-prey redistribution in living cells on μ -biochips; top: green channel images (interaction detection channel), bottom: red channel images (BSA-Cy5 grid)

A very sensitive method to detect protein-protein interactions in living cells is called micro-patterning assay ((Schwarzenbacher et al., 2008) and (Weghuber et al., 2010a) and (Weghuber et al., 2010b)). Figure 1 illustrates the basic principle of this technique: In order to identify and quantify interactions between a fluorophore-labelled protein (prey) and a membrane protein (bait) *in vivo*, a specific ligand to the exoplasmic domain of the bait is arranged in micropatterns on a glass surface. The intermediate gaps are passivated with BSA. When cells expressing the bait are plated on such surfaces, the bait follows the antibody patterns. To address bait-prey interactions, the lateral distribution of fluorescently tagged prey is analysed and compared with the antibody/BSA micropatterns. Interaction leads to pronounced co-patterning, whereas no interaction yields homogeneous prey-distribution. To detect the interactions a TIRF-based fluorescent microscopy imaging system is best suited, since it allows a strong background reduction from peripheral cell volume.

In order to benefit from the advantages of the μ -patterning technique, appropriate software is needed. Currently this is not the case. During the analyses of bait-prey protein interactions a large amount of data is collected, which has to be analysed. This analysing process cannot be carried out with the possibilities provided in an acceptable time. Thus, new algorithmic solutions are necessary.

2. RESEARCH GOAL: OPTIMIZATION OF GRIDS FOR DETECTING PATTERNS IN BIOLOGICAL IMAGES

The goal of the research work presented in this paper is to develop an algorithm that is able to automatically identify grid structures in images of biological samples labelled by μ -patterning.

The main idea is the analysis of two different kinds of images which represent in combination one biological sample:

- Green light intensity images represent fluorescently labelled protein spots, known as patterns, which are to be analysed.
- Red light intensity images represent the lattices which were used to produce the micro patterned glass plate.

Real world examples for input data analysed in this research work can be seen in Figure 2.

Within these images the patterns have to be separated from areas that represent the lattices. Thus, what is needed is a method that is able to identify symmetric grids within the red channel images and uses these grids to identify pattern areas in the corresponding green channel images.

3. DATA PREPROCESSING

3.1. Correlation Based Optimal Downsampling

In order to decrease the runtime consumption of further image analysis steps (including the identification of grid structures), the analyzed red channel images are downsampled (Lin and Dong 2006) using a correlation threshold θ :

Starting with downsampling rate (*dsr*) 2, the *dsr* is constantly increased until the correlation (Rodgers and Nicewander 1988) of the downsampled image and the original image becomes less than θ .

3.2. Transformation of Greyscale to Binary Images

In order to distinguish pattern areas from lattice, pixels below a pre-defined greyscale intensity level are transformed to white representing grid pixels, others to black ones. Additionally, pixels with intensity above a pre-defined threshold are also transformed to black. This leads to binary images as the one exemplarily shown in Figure 3.

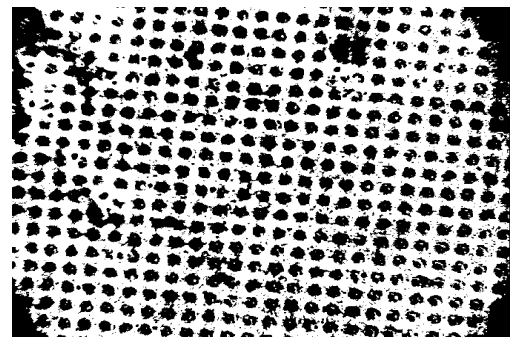


Figure 3: Binary representation of a red channel image

4. IDENTIFICATION OF GRID STRUCTURES IN IMAGES OF BIOLOGICAL SAMPLES BASED ON EVOLUTION STRATEGIES

In this section we describe an approach for identifying grid structures in images using evolution strategies: First, an initial grid is identified, which is repeatedly evaluated and mutated for creating new candidates from which the best ones are promoted to the next generation.

4.1. Evolution Strategies

Evolution strategies (ESs), beside GAs the second major representative of evolutionary computation, were developed since the 1960s, primarily by a German research community around Rechenberg and Schwefel at the Technical University of Berlin, and have been extensively studied in Europe (see for example (Rechenberg 1973) and (Schwefel 1994)).

As it is an evolutionary algorithm, the optimization process based on ES is executed by applying operators in a loop, i.e., main operations are applied on the solution candidates repeatedly until a given termination criterion is met. Similar to GAs, an ES works with a population of individuals; each individual is characterized by its parameter vector which is used to calculate the individual's fitness value. In every step of the algorithm's execution (that is, in each generation), the old population is replaced by a new one. Still, there are differences between GAs and ESs, especially in the form of their genotypes, the calculation of the fitness values and the operators (mutation, recombination and selection):

- ESs most frequently use real-coding of design parameters, they model the organic evolution at the level of individual's phenotypes; the representation used is a fixed-length real-valued vector, each position in the vector corresponds to a feature of the individual.
- Whereas GAs use mutation only for avoiding stagnation, mutation is the main reproduction operator in evolution strategies: Each component of the parameter vector is mutated individually in each generation. Small mutations are more likely than big ones, the standard mutation distribution being the Gaussian mutation ($N(0, \sigma)$).
- In addition to mutation, recombination can be used to create a new individual (a "child") out of two "parents", too. Recombining two ES solution candidates means calculating the geometric average of the parents' parameter vectors.
- In contrast to nature and GAs, the selection of ESs works in a totally deterministic way: In each generation only the best individuals survive.

Examples for mutation and recombination in the context of ESs are shown in Figure 4:

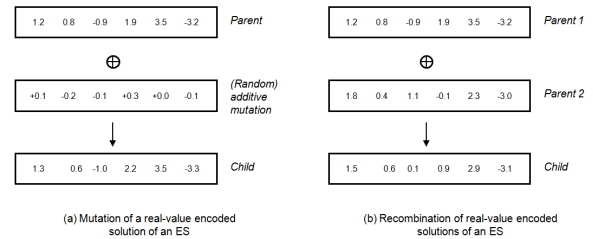


Figure 4: Exemplary solution candidates and the effect of genetic operations in ES

In each generation of an ES algorithm, λ children are produced by μ parent individuals; by selection, the best children are chosen and become the parents of the next generation. Typically, parent selection in ES is performed uniformly randomly, with no regard to fitness; survival in ESs simply saves the μ best individuals, which is only based on the relative ordering of fitness values.

Basically, there are two selection strategies for ESs:

- The (μ, λ) -strategy: μ parents produce λ children; the best μ children are selected and form the next generation's parents.
- The $(\mu + \lambda)$ -strategy: If this selection model, also called the "plus-selection", is applied, μ parents produce λ offspring; parents and children together form a pool of potential new parents, and the best μ individuals are selected from this pool to become the next generation's parents.

The main procedure steps of the execution of ES is summarized and graphically shown in Figure 5.

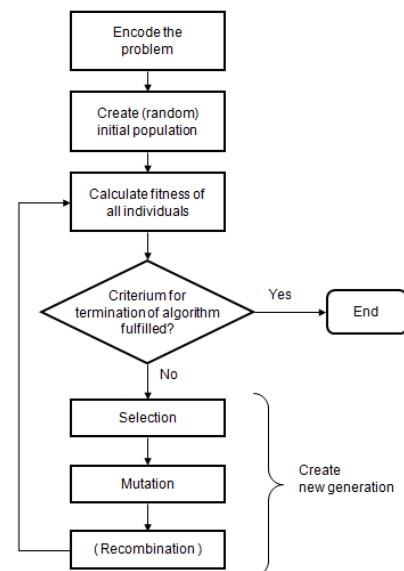


Figure 5: Workflow of the standard evolution strategy (ES) algorithm

Rechenberg proposed a heuristic for the adaptation of the mutation variance, the so-called 1/5 success rule (which was originally proposed for the special case of a

(1+1) ES; similar rules have also been stated for other ES-variants): The quotient of the number of the successful mutants (those that improve the population's quality) to all mutants should be about 1/5. If this quotient is greater than 1/5, then the mutation variance should be increased; if the quotient is less than 1/5 (which means that less than 20% of the mutations produce better mutants), the mutation variance should be reduced.

Additionally, this ES workflow is extended as proposed by Schwefel (Schwefel 1994) so that there is an individual mutation strategy parameter for each parameter of the solution candidate. Thus, the mutation strength of each feature is also optimized during the evolutionary process.

4.2. Solution Candidates Representing Grids

A solution candidate is represented as a composition of four parameters and its quality measure. As shown in Figure 6, the four parameters are:

- The grid's *deflection*, the inclination of the grid referring to the image orientation,
- the grid's *width*, i.e., the distance between two gridlines,
- the *horizontal offset* of a reference vertical grid line,
- the *vertical offset* of a reference horizontal grid line.

4.3. Evaluation of Grid Solution Candidates

In order to obtain a robust and reproducible comparison between various grid solution candidates an evaluation function has been defined; this evaluation function calculates the quality of a solution candidate comparing the binary image, retrieved from the input grid image, with the solution candidate itself.

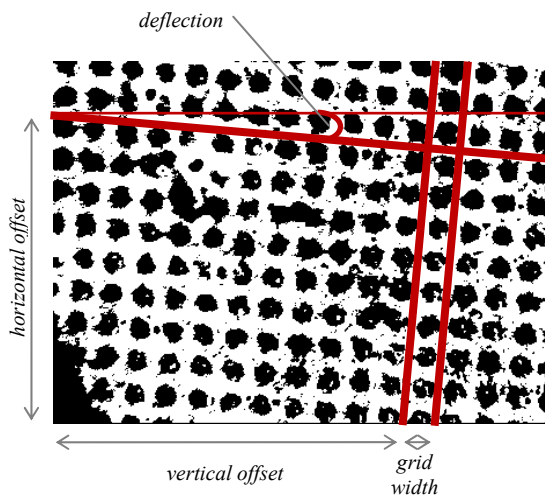


Figure 6: Parameters of a grid candidate

4.3.1. Computation of the Whole “Expected” Grid Defined by a Grid Solution Candidate

As a solution candidate is only represented by four parameters, it is clearly necessary to expand the solution candidate of the size of the initial image and thus retrieve the whole grid defined by this parameter combination.

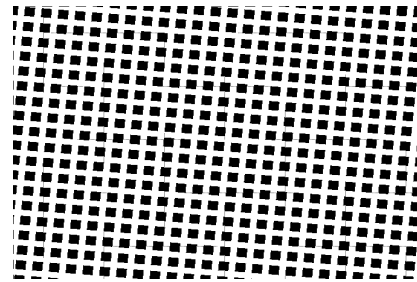


Figure 7: Exemplary expected grid

This clamping process is done by calculating all gridlines appearing in the initial image and furthermore ($gridwidth * gridwidthTolerance$) additional lines on the left and the right side of the original line. These additional lines are calculated to be aware of inaccuracies in the original grid picture and therefore to avoid faulty calculations of intensity and contrast values in the analyses steps later on.

The result of a fully clamped expected grid can be seen in Figure 7. The result is a binary image with white-coloured grid lines and black-coloured patterns.

4.3.2. Comparison with Initial Binary Image

The actual quality of a solution candidate (*grid*) is computed by the comparison of each pixel of the expected grid image ($expected(grid)$) with the corresponding pixel of the binary representation of the original image (*binary*). The number of positive comparisons is summed up over all pixels p and divided by the total number of pixels N . The retrieved value is within the range $[0, 1]$.

$$N(binary) = |\{p | p \in binary\}| \quad (1)$$

$$P(grid, binary) = |\{expected(grid)[p] = binary[p]\}| \quad (2)$$

$$quality(grid, binary) = \frac{|P(grid, binary)|}{|N(binary)|} \quad (3)$$

4.4. Identification of Initial Solution Candidates

In order to start the identification of grid structures we determine initial solution candidates which are calculated from the binary image. The first step is to define three gridlines (two vertical and one horizontal) in order to be able to complete the grid definition. A gridline itself is composed of an offset-value, which determines the position within the image, and its

deflection. A gridline can be evaluated by calculating the percentage of white pixel-values compared to the binary image (as defined in Equation 5).

- First, starting from some area A within the image (e.g., the right upper quarter of the image), all possible vertical gridlines in this are evaluated:

$$\forall (x \in x_A, deflection \in [-0.2; +0.2]):$$

$$l = verticalGridline(x, deflection);$$

$$quality(l) = eval(l, binaryImage) \quad (4)$$

$$eval(gridline, binaryImage) = \frac{|\{p | p \in gridline \wedge binaryImage[p] = white\}|}{|\{p \in gridline\}|} \quad (5)$$

The best gridline with offset x and deflection $def(l_{opt}(x_{opt}, def_{opt}))$ so found in A is the starting point for the construction a complete grid definition.

- Second, the best next parallel gridline l_{opt2} to l_{opt} is computed by iteratively decreasing (or increasing) x (starting at x_{opt}) and evaluating the so created lines with the same deflection def_{opt} until the next local optimum in the set of possible vertical gridlines is found.
- Finally, all horizontal gridlines in A with deflection $-def_{opt}$ are calculated:

$$\forall (y \in y_A):$$

$$l = horizontalGridline(y, -def_{opt});$$

$$quality(l) = eval(l, binaryImage) \quad (6)$$

The best of these is selected as l_{opt3} .

These three lines (l_{opt} , l_{opt2} , and l_{opt3}) define an initial grid candidate identified in the area A .

This initial grid construction heuristic is performed five times in different starting areas of the given image; the best so found solution candidate is subsequently optimized by the ES algorithm.

5. EXPERIMENTAL RESULTS

In order to demonstrate ability of the here presented approach to identify optimal grids in biological microscopy images, 8 exemplary samples have been selected. These samples represent microscopy images of living cells and their size is 1344 by 1024 pixels.

In the following tables we summarize the qualities achieved for these samples for downsampling tolerances 0.8 and 0.9 as well as varying ES parameter settings (plus selection as well as mutation strategy adaptation as described previously were applied in all tests). In Figure 8 we show the average improvements achieved by one specific ES configuration for the given samples (w.r.t. the initial qualities); examples of grid structures

found for one of the chosen microscopy images are shown in Figure 9.

Image Sample	Quality		Improvement [%]
	initial	optimized	
1	0.749	0.788	5.213%
2	0.726	0.822	13.335%
3	0.701	0.778	11.110%
4	0.605	0.804	32.738%
5	0.651	0.767	17.779%
6	0.584	0.733	25.424%
7	0.696	0.699	0.459%
8	0.548	0.570	3.978%
Mean Improvement [%]			13.754%

Table 1: Results achieved with downsampling tolerance 0.8, $\mu = 5$, $\lambda = 10$, and 100 ES iterations

Image Sample	Quality		Improvement [%]
	initial	optimized	
1	0.682	0.770	12.964%
2	0.709	0.803	13.208%
3	0.649	0.776	19.599%
4	0.572	0.808	41.124%
5	0.543	0.719	32.484%
6	0.525	0.619	17.813%
7	0.561	0.661	17.781%
8	0.594	0.643	8.263%
Mean Improvement [%]			20.404%

Table 2: Results achieved with downsampling tolerance 0.9, $\mu = 5$, $\lambda = 10$, and 100 ES iterations

Image Sample	Quality		Improvement [%]
	initial	optimized	
1	0.749	0.786	4.968%
2	0.726	0.816	12.424%
3	0.701	0.774	10.523%
4	0.605	0.801	32.232%
5	0.651	0.763	17.202%
6	0.584	0.729	24.867%
7	0.696	0.698	0.418%
8	0.548	0.562	2.593%
Mean Improvement [%]			13.154%

Table 3: Results achieved with downsampling tolerance 0.8, $\mu = 5$, $\lambda = 10$, and 40 ES iterations

Image Sample	Quality		Improvement [%]
	initial	optimized	
1	0.682	0.769	12.825%
2	0.709	0.800	12.784%
3	0.649	0.775	19.446%
4	0.572	0.804	40.435%
5	0.543	0.717	32.145%
6	0.525	0.619	17.818%
7	0.561	0.661	17.697%
8	0.594	0.642	8.065%
Mean Improvement [%]			20.152%

Table 4: Results achieved with downsampling tolerance 0.9, $\mu = 5$, $\lambda = 10$, and 40 ES iterations

Image Sample	Quality		Improvement [%]
	initial	optimized	
1	0.749	0.788	5.174%
2	0.726	0.822	13.278%
3	0.701	0.778	11.042%
4	0.605	0.802	32.543%
5	0.651	0.763	17.231%
6	0.584	0.732	25.402%
7	0.696	0.698	0.406%
8	0.548	0.565	3.031%
Mean Improvement [%]			13.513%

Table 5: Results achieved with downsampling tolerance 0.8, $\mu = 3$, $\lambda = 15$, and 40 ES iterations

Image Sample	Quality		Improvement
	initial	optimized	
1	0.682	0.769	12.820%
2	0.709	0.784	10.491%
3	0.649	0.776	19.607%
4	0.572	0.807	41.078%
5	0.543	0.758	39.594%
6	0.525	0.684	30.274%
7	0.561	0.661	17.731%
8	0.594	0.641	8.018%
Mean Improvement			22.452%

Table 6: Results achieved with downsampling tolerance 0.9, $\mu = 3$, $\lambda = 15$, and 40 ES iterations

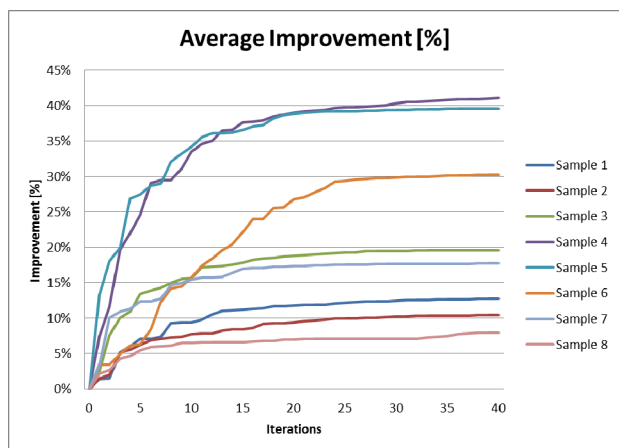


Figure 8: Average improvement during the evolutionary process for the 8 given samples (compared to the initial solution candidate) achieved with $\mu = 3$, $\lambda = 15$, and downsampling tolerance 0.9.

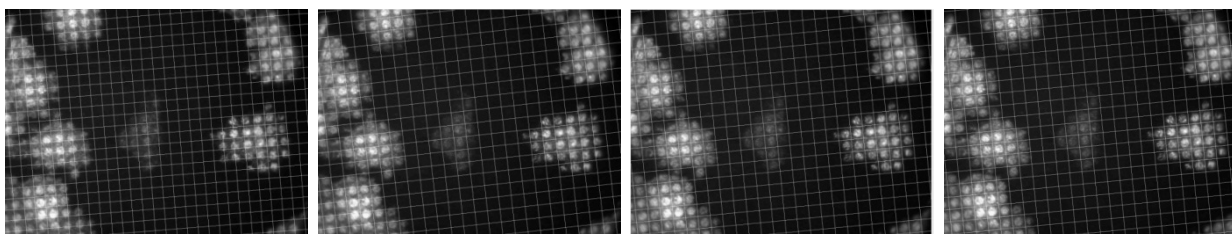


Figure 9: Grid improvement during the ES process ($\mu = 5$, $\lambda = 10$, downsampling tolerance 0.9; first image: initial solution (quality 0.55), second image after 10 iterations (quality 0.62), third after 20 iterations (quality 0.71), fourth after 40 iterations (final grid quality: 0.72)

6. CONCLUSION

In this paper we have described an evolutionary process with an initial construction heuristic that is able to automatically identify grids in microscopy images of biological samples. In future work this approach shall be included in a fully automated bioinformatical image analysis framework that is designed for biomedical research.

ACKNOWLEDGMENTS

The work described in this paper was done within the research project μ Prot/DETECTOR sponsored by Basic Research Program of the University of Applied Sciences Upper Austria.

REFERENCES

- Lin, W., Dong, L., 2006. Adaptive Downsampling to Improve Image Compression at Low Bit Rates. *IEEE Trans. Image Processing* 15:2513-2521.
- Rechenberg, I., 1973. *Evolutionsstrategie*. Friedrich Frommann Verlag.
- Rodgers, J. L., Nicewander, W. A. 1988. Thirteen ways to look at the correlation coefficient. *The American Statistician* 42:59-66.
- Schwarzenbacher, M., Kaltenbrunner, M., Brameshuber, M., Hesch, C., Paster, W., Weghuber, J., Heise, B., Sonnleitner, A., Stockinger, H., Schütz, G. J., 2008. Micropatterning for quantitative analyses of protein-protein interactions in living cells. *Nature methods* 5:1053-1060.
- Schwefel, H.-P., 1994. *Numerische Optimierung von Computer-Modellen mittels der Evolutionsstrategie*. Basel: Birkhäuser Verlag.
- Weghuber, J., Sunzenauer, S., Plochberger, B., Brameshuber, M., Haselgrübler, T., Schütz, F. J., 2010. Temporal resolution of protein-protein interactions in the live-cell plasma membrane. *Analytical and Bioanalytical Electrochemistry* 397: 3339-3347.
- Weghuber, J., Brameshuber, M., Sunzenauer, S., Lehner, M., Paar, C., Haselgrübler, T., Schwarzenbacher, M., Kaltenbrunner, M., Hesch, C., Paster, W., Heise, B., Sonnleitner, A., Stockinger, H., Schütz, G.J., 2010. Detection of protein-protein interactions in the live cell plasma membrane by quantifying prey redistribution upon bait micro patterning. *Methods in Enzymology*, 472: 133-151.

AGENT-MONITORED ANTICIPATORY MULTISIMULATION: A SYSTEMS ENGINEERING APPROACH FOR THREAT-MANAGEMENT TRAINING

Tuncer I. Ören^(a), Levent Yilmaz^(b)

^(a)University of Ottawa, School of Electrical Eng. and Computer Science, Ottawa, Ontario, K1N 6N5 Canada

^(b)Auburn University, Computer Science and Software Engineering, Auburn, AL 36849, USA

^(a)oren@eecs.uOttawa.ca, ^(b)yilmaz@auburn.edu

ABSTRACT

Agent-monitored multisimulation provides a powerful paradigm to conceive and perform experimentations not possible by traditional simulation techniques. Multisimulation was developed for simulation-based conflict management and training purposes. Anticipatory behavior has several advantages over reactive behavior. Monitoring multisimulation studies by agents bring additional benefits. First, overviews of several types of threats and the relevance and importance of anticipation are given. Then, the possibilities offered by multisimulation and agent-monitored anticipatory multisimulation are presented. Afterwards, the appropriateness of agent-monitored anticipatory multisimulation is shown for several types of synchronous or asynchronous threat management and training.

Keywords: Agent-monitored anticipatory multisimulation, predictive display, types of threats, simulation-based threat-management training

1. INTRODUCTION

Emerging threats find those individuals, groups, or nations that cannot anticipate and counteract them on time. Merely reacting to events is not sufficient. As shown by Galvani (1737-1798) and Volta (1745-1827), even a dead frog can react. Intelligent entities (humans or advanced software agents) can do better than simply reacting. What is important is the ability to anticipate possible threat(s) and take precautions before it is too late. We realize that an appropriate methodology needs to be developed to help decision makers and concerned individuals to get worthwhile experience (or training) to realize the consequences of and to manage several types of possible threats which may occur synchronously or asynchronously.

Four pillars of our methodology are: (1) behaviorally anticipatory systems, (2) multisimulation (to allow experimentation with several aspects of reality at the same time), (3) agent-monitored simulation to benefit from capabilities of software agents, and (4) systems engineering (to benefit from systems approach and systems engineering to explore solutions for complex social issues).

Agent-monitored multisimulation provides a powerful paradigm to conceive and perform experimentations not possible by traditional simulation techniques.

Multisimulation was developed for simulation-based conflict management and training purposes (Yilmaz and Ören 2004; Yilmaz et al. 2006). Anticipatory behavior has several advantages over reactive behavior. Monitoring multisimulation studies by agents bring additional benefits.

The article is organized as follows: Background information about threats and multisimulation are given in sections 2 and 3. Behaviorally anticipatory systems are presented in section 4. Agent-monitored anticipatory multisimulation and simulation-based threat-management training are presented in sections 5 and 6. Section 7 consists of the highlights of a case study. Finally, section 8 covers our conclusion and reports our on-going work on multisimulation.

2. THREATS

A "threat" is an indication of something impending and usually undesirable or unpleasant. It may be: (1) an expression of an intention to inflict evil, injury, or damage on another usually as retribution or punishment for something done or left undone; (2) an expression of an intention to inflict loss or harm on another by illegal means and especially by means involving coercion or duress; or (3) something that by its very nature or relation to another threatens the welfare of the latter. (Merriam-Webster).

Threats can be targeted to individuals, groups, or nations, as well as to environment. A large variety of threats exist. They can be external (exogenous) or internal (endogenous) and they can be subtle or overt. For example, terrorism (which can be exogenous or endogenous) is unfortunately a well known threat. Sometimes, neglect may induce a chain of events which may end up by becoming a threat. In a country, for example, unchecked power of a leader may foster a potential dictator which may then become a threat to the regime of the country and to its citizens. The declining quality of drinking water may become a business opportunity to offer bottled water which may end up by being an environmental threat due to the thrown away empty bottles.

We are well aware of the limits of: (1) rational thinking (Damassio 1994), (2) dysrationalia –which is defined as the inability to think and behave rationally despite adequate intelligence– (Stanovitch 2009), and even (3) the "upside of irrationality" (Ariely 2010).

However, we also observe that most types of threats are results of some chains of events. Our thesis is that, as intelligent people, if we are better educated or at least trained to acquire experience in anticipating results of chains of events, we may take precautionary measures on time to avoid unnecessary disasters. For example, denying fundamental rights to a minority (ethnic, religious, or else) in a society would entail reaction and may become a source of serious threat. In another area, it should be possible to monitor, fiscal responsibility of bankers who offer credits to individuals beyond their means, before their practice become a national disaster. Similarly, fiscal responsibility of countries should be possible to be monitored before the chain of events end up by becoming national, regional disasters and threatening world economy.

3. ANTICIPATORY MULTISIMULATION

Multisimulation allows simulation of several aspects of reality at the same time. In its simplest form, while a simulation run is progressing, if a significant development occurs, then in the simulation study a branching can occur. In this case, while the main simulation study continues, a second simulation starts to explore the new development. For example, while simulating functioning of a city, if there is a threat such as an explosion somewhere in the city, an additional simulation of this threat may start. While these two simulations are running, if there is yet another significant event, a third simulation may start. Even if the threats occur in different parts of the city, each threat would require some resources and may have implications for the others, such as need for resources from a common pool; hence they may have some relations. Therefore, multisimulation can provide realistic and valuable experience for decision makers.

In general, when a branching occurs in a simulation study, the old and new simulation runs may use the same or different models –with same or different parameters– under same or different scenarios.

An interesting generalization of the multisimulation concept is its application to thought experiments. In this case, at a given situation, the implications of several alternative scenarios can be explored.

3.1 Multisimulation within a taxonomy of simulation

To appreciate the position of multisimulation with respect to some other types of simulation, Table 1a and 1b outline a taxonomy of simulation based on the characteristics of model behavior generation. (There are many other types of simulation based on other criteria. See for example Ören (2011, 2012). Table 1a is based on hardware used in the simulation, as well as time and purpose of using simulation.

Table 1b is based on the process of generation of model behavior. Gaming simulation or serious (simulation) games are intermittent simulations; i.e., at certain interaction times, simulation is interrupted, some information is made available to players (or decision makers). Based on the available information, the players

make decisions, i.e., change values of controllable variables and/or parameters, and if feasible, models. Then simulation resumes.

Table 1a. Taxonomy of Simulation Based on Characteristics of Model Behavior Generation

► **Category** • Criteria: *Type of simulation*

<p>► Hardware use</p> <ul style="list-style-type: none"> • <u>Hardware is used</u>: <i>Simulator (man-in-the-loop-simulation)</i> • <u>Hardware is not used</u>: <i>Simulation</i> <p>► Time</p> <ul style="list-style-type: none"> • <u>Real-time</u>: <i>Real-time simulation</i> • <u>Compressed time</u>: <i>Compressed-time simulation</i> • <u>Expanded time</u>: <i>Expanded-time simulation</i> <p>► Purpose</p> <ul style="list-style-type: none"> • <u>Value-free decision</u>: <i>Value-free simulation</i> • <u>Descriptive decision</u>: <i>Descriptive simulation</i> • <u>Explanatory decision</u>: <i>Explanatory simulation</i> • <u>Predictive decision</u>: <i>Predictive simulation</i> • <u>Normative decision</u>: <i>Normative simulation</i> • <u>Evaluation</u>: <i>Evaluative simulation</i> • <u>Prescription</u>: <i>Prescriptive simulation</i>

Table 1b. Taxonomy of Simulation Based on Process of Model Behavior Generation

► **Category** • **Criteria** (•• Subcriteria):

Type of simulation (Subtype of simulation)

<p>► Process of generation of model behavior</p> <ul style="list-style-type: none"> • Continuous: <i>Simulation run, (Single-run simulation study)</i> • Intermittent: <ul style="list-style-type: none"> •• <u>Multiple runs</u>: <i>[Multiple-run] simulation study, Antithetic run, Regenerative simulation, Sensitivity simulation</i> •• <u>Nested simulation</u>: <i>Optimizing simulation: (Simulation within optimization, Optimization within simulation)</i> <i>Expert system (ES) & Simulation: (Simulation within ES, ES within simulation)</i> •• <u>Interaction among decision makers (players)</u>: <i>Gaming simulation, Game-theoretic simulation, Serious games</i> <u>If competition</u>: <i>Zero-sum games (Wargaming, Business gaming)</i> <u>If cooperation</u>: <i>Non-zero-sum games (Peace games)</i> <u>If coopetition</u>: <i>Cooperative simulation within competitors</i> •• <u>Interaction between behavior generation and the real system</u>: <i>Stand-alone simulation, Integrated simulation</i> •• <u>Multiple simulations</u>: <i>(with or without interaction of simulation and real system) (with or without interaction among decision makers (players): Multisimulation</i>
--

So far as interaction between simulation and the real system is concerned, there are two cases: In *stand-*

alone simulation, simulation is independent of the operation of the real system, as it is the case in most simulation studies. In *integrated simulation*, the operations of real system and simulation are either synchronous or interwoven. Integrated simulation is used to monitor the operation of a real system or to enrich its operation.

In the case of multisimulation, at the branching points, decisions can be made as it is the case in serious simulation games, or there can be interaction with real system as it is the case in integrated simulation (Yilmaz et al. 2007).

Anticipatory multisimulation is multisimulation of anticipatory systems. The power of anticipatory multisimulation can be used as predictive displays of the consequences of several alternative scenarios at critical decision points. Hence, the potential undesirable (including catastrophic) states can be displayed, therefore can be avoided, before they happen.

4. SYSTEMS ENGINEERING

4.1 What is System Engineering?

A system is a construct or collection of different elements related in a way that allows the achievement of a common objective (Thayer 2005). The elements of the system include hardware, software, people, facilities, policies, and other factors coordinated to achieve system objectives.

System engineering (SE) involves the application of engineering and management practices to transform the user needs into a system specification and realization that most efficiently meets the need. SE entails the technical management functions that controls and coordinates the overall system development activities. As such, it revolves around a generic problem solving process that gradually evolves specifications toward a realization of the requirements that satisfy objectives set forth at the beginning of a project.

4.2 The Functions of System Engineering

System Engineering involves:

- *System conception* that deals with the process of involving users in conceiving an application and identifying tentative requirements.
- *Problem specification*, which identified and formulates the needs and constraints imposed by the problem domain. Domain analysis constitutes the fundamental component of problem specification. Application analysis entails the description of the parts of the system that are visible to the user.
- *Solution analysis*, which determines the set of possible ways to satisfy requirements, overviews the solutions, and selects an optimal strategy.
- *Process planning* that identifies the tasks, their scheduling and interdependencies, estimates the size and cost of the project, and determines the required effort to complete the project.

- *Process control and product evaluation* that determines the strategies to control and measure the progress and evaluates the product via testing, inspection, and analysis.

In (Yilmaz and Ören 2009; Ören and Yilmaz 2009; Ören and Yilmaz 2012), we elaborated on how M&S and SE can support each other. Here, we discuss the role of M&S in systems, why M&S requires SE, and why Simulation Systems Engineering (SSE) is necessary. Simulation is becoming a dominant technology in many systems engineering applications. In defense-related training systems, simulations are being embedded to create virtual scenarios. Symbiotic simulation systems have been proposed as a way of solving this problem by having the simulation and the physical system interact in a mutually beneficial manner.

4.3 Why does M&S Require SE?

As discussed above, M&S systems are becoming more and more complex and they are being embedded with other system in a system of systems context to serve larger objectives. In developing such simulations the solution space must be defined before assigning functionality to various components. The SE perspective provides an opportunity to specify the solution for the acquirer prior to allocation of functionality onto hardware, software, and simulation systems.

4.4 Why is SSE Necessary?

M&S development costs are rising partly due to increased complexity. Craftsmanship approach to M&S in the small does not scale to M&S in the large. Consequently, such complex and extremely large simulation systems require technical system management and SE oversight. Unless such oversight is present, the following problems are likely to emerge.

- Simulation system becomes unmanageable.
- Costs are overrun and deadlines can be missed.
- Greater risk exposure arises.
- Requirements may not be met.
- The simulation fails to satisfy its objectives.
- Maintenance costs increase.

5. BEHAVIORALLY ANTICIPATORY SYSTEMS

An anticipatory system is a system whose next state depends on its current state as well as the current perceptions of its future state(s) (Ören and Yilmaz 2004). That is, a behaviorally anticipatory system incorporates perceptions of future states into decision-making to improve its effectiveness in developing actions that lead to situations with high utility and payoffs. That is, in a threat scenario, having an anticipatory perception in terms of predictive models of opponents and/or the threat environment is expected to improve decision-making. Specifically, in evolving threat situations, predefined course of actions and strategies may be obsolete, and reactive strategies that cannot properly

anticipate effects fail to reliably respond to emerging activity in a timely manner. Also, reactive behavior is severely inertial for tasks where multiple goals need to be pursued. Therefore, purposive reliable course of actions should not simply be reactive to situation, but also consider anticipations of the effects expected.

The role of anticipation in threat-management training can be conceptualized in terms of the elements of anticipatory behavioral control, shown in Figure 1.

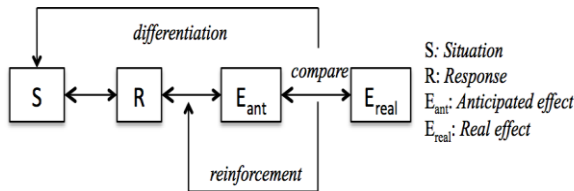


Figure 1: Anticipatory Behavioral Control

According to theory of anticipatory behavioral control, (1) behavioral act or response (R) is accompanied with an anticipation of its effects, (2) anticipated (simulated) and real effects are compared, (3) the credit assigned between response and anticipation is strengthened when the anticipations are accurate and weakened otherwise, (4) finally, $R - E_{ant}$ relations are differentiated by behavior relevant situational stimuli.

Based on these characteristics, a behaviorally anticipatory threat-management and training system needs to incorporate interpretation facilities as a precursor to (1) comprehend and draw accurate inferences about the evolving and volatile threat environment, (2) have context-sensitive pragmatism by considering the likely effects of course of actions, and (3) have situational definition as a direct input to action recommendation. Drawing inferences about the world requires presence of predictive models for the generation and understanding of effects. In principle, a behaviorally anticipatory system is a system containing predictive model of itself and/or of its environment, which allows it to change at an instant in accord with the model's predictions pertaining to a later instant. This ability can also be used to compensate for the absence of or fuzziness in information and data available during training. Anticipation and anticipatory learning during a threat-management training scenario can involve generation of a multitude of dynamic models of course of actions in a given practical situation and the resolution, through a reward or punishment mechanism, of their threat in an action.

Figure 2 illustrates components of a hypothetical anticipatory learning framework in threat-management training. The training system is coupled with a multisimulation system to explore expected effects of identified plausible course of actions. Due to uncertainty, models executed by the multisimulation system can examine the effects of strategies in multiple possible environments. As the user gains better insight about the threat and develops more accurate predictive threat models, the system can shift from exploratory analysis to exploitation of increasingly accurate environmental models to discern effective strategies under the given

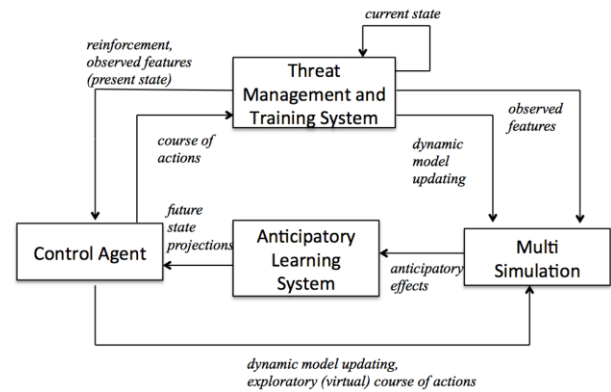


Figure 2: Anticipatory Learning in Threat Management

environment. In this context, multisimulation can be construed as generator of futures. Situation-Response (S-R) training systems are slow since they are able to propagate reward only one step at a time and only in direct interaction with the environment. An anticipatory learning/training system will be able to form explicit environmental models and use them to propagate reward faster. The control/interface agent (or trainee) uses the future state projections generated by the learning system. On the other hand, before acting on the actual training scenario, the user can continue to experiment in the virtual environment via further experimentation using the multisimulation engine. As the threat environment and the scenario unfold in real-time, the models executed by the multisimulation system need to be in synch with the emerging behavior in the threat scenario. This requires proper dynamic model and parameter updating mechanisms.

6. AGENT-MONITORED ANTICIPATORY MULTISIMULATION FOR THREAT-MANAGEMENT TRAINING

Multisimulation with multimodels, multispect models or multistage models needs mechanisms to decide when and under what conditions to replace existing models with a successor or alternative. The control agent, shown in Figure 2, monitors the multisimulation subsystem through the anticipatory learning component. The control agent partly enables branching into contingency plans and behavioral rules in response to scenario or phase change during experimentation. Graphs of model families may facilitate derivation of feasible sequence of models that can be invoked or staged. More specifically, a graph of model families can be used to specify alternative staging decisions. Each node in the graph depicts a model, whereas edges denote transition or switching from one model to another.

Model recommendation in multisimulation can simply be considered as the exploration of the model staging space that can be computed by reachability analysis of the graph. There are two modes for the usage: (1) Offline enumeration of paths using the graph and performing a staged simulation of each model in sequence one after the other, unless a model staging operation becomes infeasible due to conflict between the

transition condition and the precondition of the successor model and (2) run-time generation of potential feasible paths as the simulation unfolds. In both cases, a control agent plays a key role to qualify a successor model. The first case requires derivation of sequence of models using a traversal algorithm. The edges relate families of models. Therefore, the actual concrete models, the preconditions of which satisfy the transition condition need to be qualified, since transition to some of these model components may be infeasible due to conflict between a candidate model and inferred situation.

Candidate models and associated simulations can be maintained by the control agent using focus points. A focus point manages branch points in the simulation frame stack. Suppose that a goal instance (i.e., stage transition condition) is at the top of the stack. If only a single model qualifies for exploration, then it is pushed onto the stack. Yet, if more than one model matches the condition, a simulation focus point is generated to manage newly created simulation branching (discontinuity) points, each one of which have their own contexts.

When a path is exhausted, the closest focus point selects the next available model to instantiate the simulation frame or return to the context that generated the focus point. As threat management scenarios are explored, a network of focus points is generated. Determining which focus point should be active at any given time is the responsibility of the control agent. When more than one model is qualified, then the agent needs to decide which one to instantiate. Control rules can inform its decision. Three steps involve in deploying a new simulation frame in such cases: matching, activation, and preference. The matching step should both syntactically and semantically satisfy the request. The activation step involves running a dynamic set of rules that further test the applicability of models with respect to contextual constraints. Finally, the preference steps involve running a different set of rules to impose an activation ordering among the active frames.

7. HIGHLIGHTS OF A CASE STUDY

7.1 Advance Warning Systems and Protection for Sustaining Humanitarian Operations

In humanitarian operations, carrying supplies and food aid to those in need is increasingly becoming a challenging task. Supply convoys are routinely disrupted to undermine international conflict resolution efforts.

Consider the problem of escorting a convoy along an unknown territory. Smaller convoys use high-speed as a means of defense while larger convoys are restricted to lower speeds and must make numerous stops to maintain formation and navigate through cities. A cyber-physical escort system using UAVs could enhance the safety of the convoy. Among the goals of such a Cyber-Physical System (CPS) of UAVs is to cooperatively follow friendly convoy vehicles along both known and unknown routes and provide situational awareness information to determine whether road

ahead/behind and sides are clear. As a team of UAVs conduct cooperative search, tracking, and acquisition, collision avoidance becomes critical, as any scenario that considers dynamic updating of paths requires deconfliction of flight plans of cooperating vehicles. This scenario gets complicated further due to failure of UAVs to anticipate ground vehicles' turn direction, lack of maneuvering agility, difficulty in managing multiple simultaneous views of targets, and mechanical limits of the sensor's gimbal system. Also, radar and optical sensors will have limitations in terms of range, resolution, sensitivity in low light/obscured conditions, and motion stability. These limitations bring with them uncertainties in target detection, identification, and tracking. Furthermore, a cooperative UAV team should be able to track an unfriendly moving target when requested, while also accounting for obstructions to viewing and terrain changes. As a result, robust strategies are needed to cope with uncertainty as well as ambiguity (lack of clarity). In such evolving situations, predefined control strategies may be obsolete and reactive control methods that cannot properly anticipate effects fail to reliably respond to emerging activity in a timely manner. Also, reactive control systems are severely inertial for tasks where multiple goals need to be pursued. Therefore, purposive reliable behavior should not simply be reactive to situation, but also consider anticipations of the effects expected.

7.2 Application of Anticipatory Multisimulation

A multisimulation system coupled with a convoy escort system can leverage real-time observations using an input exploration component responsible for conducting input analysis and selecting appropriate distributions for the environmental models. At this stage, dynamic model updating to attain consistency between the cyber (simulation) and physical components is critical. Samples from these distributions can then be integrated with controller parameters to form one model ensemble for each Agent-based Simulation Process (ASP) in a multisimulation. Ideally, each ASP can be mapped to one or more CPU cores. If the simulation population is large or if hardware resources are limited, multiple ASPs can run on a single core. Outputs from the ASPs may take the form of fitness and robustness measure of the individual simulations averaged across all of the replications. While robust strategies generated by symbiotic adaptive multisimulation can be used by the agent controller to update the coordination behavior of physical and/or simulated UAVs, anticipatory learning could improve over time both the self-simulation and the physical system by rewarding effective control strategies.

8. CONCLUSION

Chains of some events may end up by becoming major threats to individuals, groups, or nations. Proper education and training of individuals may help them to realize the importance of anticipatory consideration and evaluation of alternatives and to take precautions to avoid—at least certain types of—disasters. A systems engineering approach, coupled with multisimulation methodology

would even allow them to acquire necessary experience by allowing simulation of several aspects of reality at the same time.

Our research will continue (1) refining the methodology, including cognitive simulation such as understanding and misunderstanding in human behavior simulation and (2) in developing examples.

REFERENCES

- Ariely, D., 2010. *The Upside of Irrationality*. Harper-Collins Publishers, New York, NY.
- Damassio, A.R., 1994. *Descartes' Error: Emotion, Reason, and the Human Brain*, Putnam Publishing, Merriam-Webster-threat. *Webster's Third New International Dictionary, Unabridged*. Merriam-Webster, 2002. <http://unabridged.merriam-webster.com> (13 May 2012).
- Ören, T.I., 2011. A Critical Review of Definitions and About 400 Types of Modeling and Simulation. *SCS M&S Magazine*, 2:3 (July), pp. 142-151.
- Ören, T.I., 2012 (Invited Keynote Paper.) The Richness of Modeling and Simulation and its Body of Knowledge. Proceedings of SIMULTECH 2012, 2nd International Conference on Simulation and Modeling Methodologies, Technologies and Applications. Rome, Italy, July 28-31, 2012.
- Ören, T.I. and Yilmaz, L., 2004. Behavioral Anticipation in Agent Simulation, Proceedings of WSC 2004 - Winter Simulation Conference, Washington, D.C., December 5-8, 2004, pp. 801-806.
- Ören, T.I. and Yilmaz, L., 2009. On the Synergy of Simulation and Agents: An Innovation Paradigm Perspective. Special Issue on Agent-Directed Simulation. *The International Journal of Intelligent Control and Systems (IJICS)*, Vol. 14, Nb. 1, March 2009, 4-19.
- Ören, T.I. and Yilmaz, L., 2012. Synergies of simulation, agents, and systems engineering. *Expert Systems with Applications* 39:1 (January 2012), pp. 81-88.
- Stanovitch, K.E., 2009. Rational and Irrational Thought: The Thinking That IQ Tests Miss. *Scientific American Mind*, Nov.
- Thayer, H. R., 2005. "Software System Engineering: A Tutorial," In *Software Engineering Volume 1: The Development Process* (Third Edition). Pp. 31-46. Wiley Inter-Science.
- Yilmaz, L., Lim, A., Bowen, S., and Ören, T.I., 2007. [Requirements and Design Principles for Multisimulation with Multiresolution, Multistage Multimodels](#) Proceedings of the 2007 Winter Simulation Conference, pp. 823-832, December 9-12, Washington, D.C..
- Yilmaz, L. and Ören, T.I., 2004. Towards Simulation-based, Problem-solving [Environments for Conflict Management in Computational Social Science](#), Proceedings of Agent 2003 - The Agent 2003 Conference on Challenges in Social Simulation, Chicago, Illinois, October, 2-4, 2003, pp. 25-37.
- Yilmaz L. and Ören, T.I. (Eds.), 2009. *Agent-Directed Simulation and Systems Engineering*, Wiley Series in Systems Engineering and Management. ISBN: 978-3-527-40781-1. Wiley-Berlin, Germany.
- Yilmaz, L., Ören, T.I., and Ghasem-Aghaee, N., 2006. Simulation-Based Problem Solving Environments for Conflict Studies: Toward Exploratory Multisimulation with Dynamic Simulation Updating. *Simulation, and Gaming Journal*. vol. 37, issue 4, pp. 534-556. DOI (Digital Object Identifier): 10.1177/1046878106292537.

AUTHORS BIOGRAPHY

Dr. **Tuncer ÖREN** is a professor emeritus of computer science at the University of Ottawa, Canada. His **research interests** include: (1) advanced modeling and simulation methodologies such as multimodeling and multisimulation; (2) agent-directed simulation; (3) agents for cognitive and emotive simulations especially for threat-management training including representations of human personality, emotions, emotional intelligence, understanding and misunderstanding; (4) reliability, quality assurance, failure avoidance, and ethics; as well as (5) body of knowledge and (6) terminology of simulation. He has over 450 [publications](#), has contributed to over 400 [conferences](#) and seminars held in over 30 countries and has delivered almost 200 invited talks. Dr. Ören has been **recognized**, by IBM Canada, as a pioneer of computing in Canada. He received Information Age Award from the Turkish Ministry of Culture, and was inducted to SCS Modeling and Simulation Hall of Fame (Lifetime Achievement Award).

Dr. **Levent YILMAZ** is Associate Professor of Computer Science and Software Engineering and holds a joint appointment with the Industrial and Systems Engineering department at Auburn University. He received M.S. and Ph.D. degrees from Virginia Polytechnic Institute and State University (Virginia Tech). His research interest are in Modeling & Simulation, Agent-directed Simulation, and Complex Adaptive Systems with a focus in advancing the theory and methodology of modeling and simulation and developing computational models of socio-technical, cognitive, and cultural systems with applications to science of science and innovation policy. He is an elected member of the Board of Directors of the Society for Modeling and Simulation International and is currently serving as the Editor-in-Chief of *Simulation: Transactions of the Society for Modeling & Simulation International*. Dr. Yilmaz also serves as editorial board member and Associate Editor for the *Simulation & Gaming, International Journal of Simulation and Process Modeling*, and *International Journal of Engineering Education*. He is member of ACM, IEEE Computer Society, Society for Modeling and Simulation International (SCS), and Upsilon Pi Epsilon.

MOTIVATION PROBLEMS IN THE PROCESS OF MASS REDUCTION THROUGH MODELLING AND SIMULATION

Maja Atanasijević-Kunc^(a), Tina Sentočnik^(b), Simon Tomažič^(c), Jože Drinovec^(d)

^(a) University of Ljubljana, Faculty of Electrical Engineering, Slovenia

^(b) Medico dr. Sentočnik, d.o.o., Ljubljana, Slovenia

^(c) University of Ljubljana, Faculty of Electrical Engineering, Slovenia

^(d) University of Maribor, Faculty for Medicine, Slovenia

^(a) maja.atanasijevic@fe.uni-lj.si, ^(b) medico.center@siol.net, ^(c) simontomaz@gmail.com, ^(d) joze.drinovec@lj-kabel.net

ABSTRACT

An important observation is the fact that overweight and obesity (obesity being in 1997 by World Health Organization recognised as a chronic disease which has to be healed) have reached epidemic extensions and represent an important social and economic burden for the countries as well as for many individuals. They also represent a risk factor for developing several chronic diseases and consequently serious health complications. In the paper a description organization is presented enabling the coexistence of different models indicating several problem levels and so giving the estimation of overweight and obese population, connections with other diseases or risk factors and estimation of economic burden as well as the possible consequences of healing interventions. Special attention is devoted to the efficacy of open and close – loop weight control at the level of individual patient and the potential consequences to the observed population.

Keywords: obesity, motivation problems, modelling, control design

1. INTRODUCTION AND MOTIVATION

Unhealthy life style very frequently consists of inactivity, stress, improper and/or too rich or abundant food resulting in a number of problems among which the first one is usually overweight.

A simple index of weight-for-height (known as body mass index - BMI) is commonly used in classifying overweight and obesity in adult population. It is defined as the weight in kilograms divided by the square of the height in meters (kg/m^2). It provides rough but very useful measure of overweight and obesity as is the same for both sexes and for all ages of adults (WHO 2011). It is important to mention that now-days physicians pay attention also to waist circumference but this parameter was not taken into account during this study because of the lack of statistical data.

Regarding WHO (WHO 2011) overweight is defined as a BMI equal to or more than 25, and obesity as a BMI equal to or more than 30. Children were defined as overweight or obese using the 85th and 95th percentiles of the reference curves. WHO's latest

estimations indicate that globally in 2008 approximately 1.5 billion adults (age 20+) were overweight (WHO 2011).

It is important to point out that overweight and obesity are not the problem only by itself (lower immune system, more difficult movement, not very high self-esteem, social isolation, ...), but they lead also to serious health consequences. Risk increases progressively as BMI increases. Raised body mass index is a major risk factor for chronic diseases such as diabetes type 2 (MMWR 2004; Daousi et al. 2006; Atanasijević-Kunc et al. 2008b; Atanasijević-Kunc and Drinovec 2011), hyper- and dislipidemia and hypertension (Atanasijević-Kunc et al. 2008b), but can evolve also to serious cardiovascular disease (Atanasijević-Kunc et al. 2008b; 2011), musculoskeletal disorders (Corbeil et al. 2001), and some cancers (WHO 2011; Atanasijević-Kunc et al. 2008a).

These conditions have also a significant social consequences and economic impact on the health care systems (Atanasijević-Kunc et al. 2012).

Obesity was in 1997 by World Health Organization recognized as a chronic disease. It is very difficult to be treated successfully in spite of the fact that the main energy equilibrium laws are known in great details (Hall 2010; Navarro-Barrientosa et al. 2011).

The goals of the paper are:

- to review in short some of the modelling approaches when analysing the problems connected with overweight and obesity,
- to present the modelling structure which enables the coexistence of different models which can share the simulation results to present different view-points of the problem,
- and to introduce the description of motivation problems which can help in understanding of patient's behaviour through the process of mass reduction.

2. MODELLING OBESITY

As has been indicated in the previous section, obesity is a multi-dimensional problem. It is dangerous and as such important for each individual patient. It has to be treated. It represents an important risk factor for a great

number of other diseases. Because of epidemic extensions this chronic disease has become also an economic burden which can't be neglected.

All these important facts have stimulated the development of models and concepts concerning the problems with increased body mass. They all contribute to better problem understanding, enable problem analysis and represent a step toward a reduction of this burden. Models can be, similar to other modelling problems from the field of medicine, pharmacy and life sciences (Hoppensteadt and Peskin 2002; Stahl 2008; Atanasijević-Kunc et al. 2008a; Belič 2009; Arnold 2010; Atanasijević-Kunc and Drinovec, 2011), divided regarding very different criteria. Some of them are:

- **the level of problem observation**
some of the models describe the problems from the perspective of the whole observed population or specific group of patients (Santonja et al. 2010; Kovács et al 2011; Atanasijević-Kunc et al. 2012), even more frequent are presentations at the level of individual patient (Abdel-Hamid 2002; Hall 2010; Navarro-Barrientosa 2011), sometimes changed mechanical properties are observed (Corbeil et al. 2001), but the problems can be described also at the level of chemical reactions (Abdel-Hamid 2002);
- **connections with other diseases, risk factors or processes**
are also frequently indicated (Navarro-Barrientosa 2011; Atanasijević-Kunc et al. 2012), while in some cases authors focus only to overweight and obesity control (Hall 2010);
- **treatment, treatment policy, treatment efficacy, economic burden of treatment, economic efficacy**
here again the processes can be observed from the view-point of each individual, while sometimes also wider situation is taken into account, like health - care system or even global social and economic environment (Atanasijević-Kunc et al. 2012);
- **psychological and behavioural problem interpretations**
are reaching more and more attention as treatment efficacy is still essentially under desired level (Navarro-Barrientosa 2011);
- **static or dynamic, problem description**
when static descriptions are used statistical properties are frequently presented for problem interpretation (Landi, et al. 2010), while dynamical models (Abdel-Hamid 2002; Hall 2010; Navarro-Barrientosa 2011) enable also the observation of different transient responses; in such cases time is frequently used as independent variable, but sometimes also patients' age is chosen to be independent variable in problem description (Atanasijević-Kunc et al. 2012);
- **continuous or discrete problem description**

- **open and/or closed – loop problem interpretation**

where also dynamic changes of closed – loop operation can be of great interest (Kovács et al. 2011);

- **other possible criteria**

which can be taken into account are qualitative models, agent based models, expert system, ...;

Regarding the diversity of used modelling approaches and corresponding goals it seems interesting to develop the structure with which it would be possible to illustrate the burden of epidemic extensions of obesity at the level of observed population and corresponding economic consequences and main relations with risk factors, other diseases and processes. In addition it is important to enable the study of problem minimization and its efficacy.

The proposed structure is presented in Fig. 1. It consists of different levels which indicate problem observation from the population perspective. Here only main direct flows are indicated while in some situations also feedback loops can be expected.

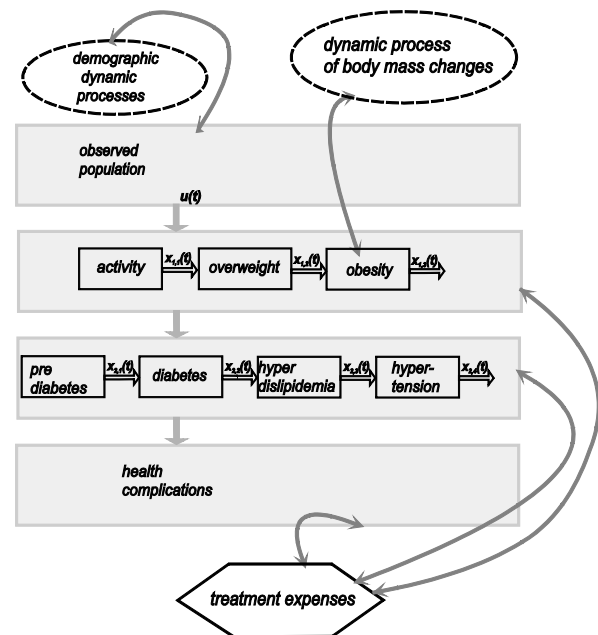


Figure 1: Diseases development in the population

In addition also some other important dynamical processes or modelling results of complementary models can be combined with the results of the main structure.

Resembling modelling structures (like in Santonja 2010) usually describe the whole population separated into compartments, taking into account the incidence or prevalence of developing diseases or disease stages (like: normal, overweight, obese, extreme obese). Each compartment is represented as homogeneous entity where age of the patients from the observed group or compartment is not of prime importance. These groups

are observed through time (months or years) regarding body mass changes.

We have decided to observe the indicated groups of patients in such a way that also age of patients can be interpreted as an independent variable. The reason for this decision is the fact that development of chronic diseases depends strongly also on patients' age.

At the first level of the proposed structure the whole observed population is taken into account. The input signal to the second level is a unity step indicating the observation start time that is at birth. At the next level the processes which are defining life style are taken into account. Among them is, as an exception, also obesity as one of the earliest chronic diseases. In the third level the most frequent chronic diseases are indicated, starting with the pre-diabetes, which can sometimes be regarded as a curable disease. At the fourth level serious health complications are taken into account. Each of indicated diseases is described with the prevalence response regarding patients' age through the whole life time. Each of presented blocks in Fig. 1 is described with dynamic model which transforms input signals to outputs, calculating patients' prevalence distributions of indicated disease. They were identified using available statistical data for each disease and for diseases' combinations.

This representation can therefore be understood as an extension of decision tree formalism (Atanasijević-Kunc and Drinovec, 2011) which is frequently used in pharmacoeconomical studies (Arnold, 2010; Stahl, 2008). In contrast to classical decision tree (which is a static problem description) proposed representation comprises, as mentioned, also a time component.

Another advantage of this structure is that it indicates some of process properties and gives the possibility of simple results combination with demographic data to evaluate the number of observed people or patients as will be illustrated in the next section. This information can further be combined with treatment expenses and so also economic burden can be estimated.

Treatment interventions in overweight and obese patients usually start with the observation of energy imbalance. In spite of the fact that rather good model predictions for body mass reduction are available (Abdel-Hamid 2002; Hall 2010; Navarro-Barrientosa 2011) the prevalence of overweight and obesity is very high. The question is why, because the great majority of these patients would like to lose few kilograms. A very simple answer (which needs additional study) is that also in the cases where the way of problem solution is completely clear it is not simple to be realized. Some interesting facts which prove this situation are the following.

A great effort invested in losing weight is often ineffective, sometimes even harmful (Abdel-Hamid 2002). After years of little change, sales of diet pills and supplements have more than quadrupled since 1996, but the prevalence and incidence of obesity is still increasing. Products like:

- slimming soaps that slough off fat in the shower,
- miracle pills that get rid of excess pounds without dieting or exercise,
- plastic earplugs that curb the appetite,
- and even a glittering ring called Fat-Be-Gone that when slipped on a finger trims hips, buttocks and thighs

are of great interest?!?

Among US adults participating in programs for losing or maintaining weight, only 17.5% were following recommended guidelines for reducing calories and increasing physical activity (Navarro-Barrientosa et al. 2011).

Obviously very strong processes are influencing patient's behaviour during mass reduction treatment. One of our goals is to present through modelling and simulation at least some of them. This can help in understanding and designing efficient mass reduction programs.

3. SIMULATION RESULTS

3.1. Social burden at the population level

To illustrate the burden of obesity and some of related processes at the population level let's choose to observe Austria as an example of developed EU country. Social burden is indicated through the number of obese patients.

In Fig. 2 the number of people regarding their age (Statistik Austria 2012) is illustrated together with developed model predictions for the next 50 years. Model is using average statistical data regarding fertility, mortality and migrations from 2006 to 2010. Fertility was calculated regarding the number of people in the age window from 18 to 45. It was estimated that each year 2.32% newborns are expected regarding the mentioned group of people. In 2010 the largest group of people was old approximately 45 years while in 2060 the maximum can be expected around the 70s. The population is becoming older also in this country. The number of newborns is expected to decrease for 30% through the next 50 years resulting in reduction of the whole population for 13%.

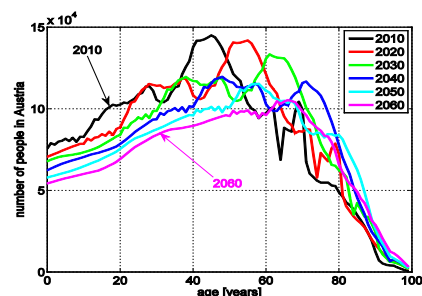


Figure 2: Population prediction from 2010 to 2060 in Austria

As indicated in Fig. 1 an important risk factor for developing obesity represents inactivity (Brock et al 2009). To the group of active people are most often

classified those, who are active 30 minutes or more on at least five days a week (BHFSW 2012a). Usually activity in men and women slightly differ, but the average prevalence model response is illustrated in Fig. 3 (Atanasijević-Kunc et al. 2012).

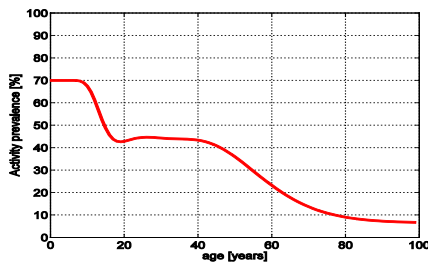


Figure 3: Prevalence of activity

Combination of this result with the number of people in Austria (Fig. 2) enables the calculation of the number of active people (see Fig. 4).

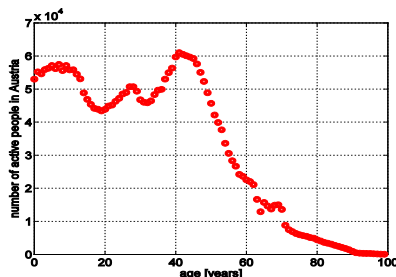


Figure 4: Number of active people in Austria (3 200 000 or 38%)

The prevalence of obesity differs from country to country and is also different regarding men and women (Berghöfer et al. 2008). Obesity is developed from those who are overweight. The ratio between both groups changes slightly with patients' age but was estimated in average to be: overweight/obese = 1.3, and therefore for both group of patients only one model was developed (BHFSW 2012b; Atanasijević-Kunc et al. 2012). Model responses describing average prevalence are illustrated in Fig. 5 and in Fig. 6 where also those who are active and those who are not can be observed.

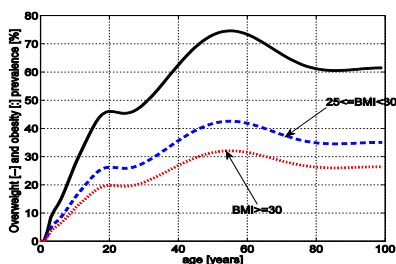


Figure 5: Prevalence of overweight and obese population and the sum of both groups

Combination of these results with population number show that in Austria over 4.4 million people

have BMI greater than 25, or with other words 55% are overweight or obese.

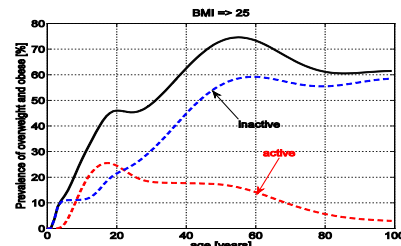


Figure 6: Prevalence of overweight and obese active and inactive population

Both, inactivity and obesity are very important regarding the development of diabetes type 2 (D2) (Valensi et al. 2005). It was discovered that most adults (up to 90%) with diagnosed diabetes were overweight or obese (MMWR, 2004), 52% were obese, and 8.1% had morbid obesity (Daousi 2006).

Before D2 is fully developed patients have a pre-diabetes which in general significantly differs from D2 regarding the fact that when strict life change is adopted taking into account corresponding diet and activity, sometimes complemented by corresponding drug treatment, patients can return to normal condition. Sometimes this transition is (for example due to a long lasting pre-diabetes) not possible, but in such situations D2 development is in most cases significantly postponed. Pre-diabetes is not a true disease but can be interpreted as a serious risk factor for developing D2 and cardiovascular diseases. Over 30% of people with pre-diabetes develop D2 within five years (Valensi et al. 2005). The average conversion rate was estimated at 5.8% per year with wide variations which depend on differences in age, BMI, ethnicity, etc.. It is very important to accent that several well-designed randomized controlled trials (Valensi et al. 2005) have been reported that categorically confirm the benefits of interventions in the pre-diabetes. Standardized diet with reduced food intake, increased physical activity and sometimes also additional drug treatment can reduce the incidence of D2 for almost 60% (in mentioned studies from 25% to 58%). But, it is important to point out that the intensive lifestyle modification was nearly twice as effective in preventing D2. It is therefore evident that an active management of pre-diabetes can be very effective in preventing the progression of diabetes.

Model responses presenting average prevalence distribution of pre-D2 and D2 are illustrated in Fig. 7, while in Fig. 8 number of D2 patients are shown and among them also those who have BMI>25. In Austria 31% of population are pre-D2 patients, while 7.8% have D2.

3.2. Economic burden

Practically all who have unhealthy body mass (BMI>25) would like to lose their weight. At least 40 % from the age window of 18 to 60 are experimenting with the drugs which are available without the medical

prescription. 30% of people from the same age window are using drugs, prescribed by physician (20%-sibutramin; 80%- orlistat). 80% of patients with BMI>40 need also anti-depressive treatment (fluoxetine). In addition the expenses are needed for these patients due to examination and laboratory.

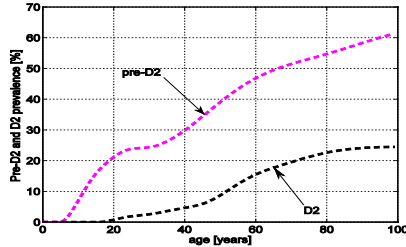


Figure 7: Prevalence of pre-D2 and D2

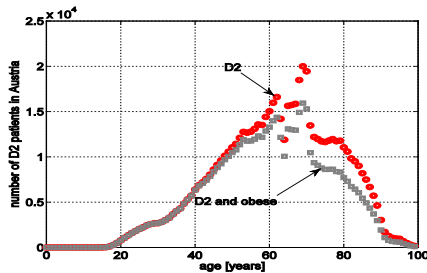


Figure 8: Number of patients with D2 in Austria

It was estimated (Atanasijević-Kunc et al. 2012) that in Austria around €30 per patient is spend each year for direct treatment expenses, while approximately the same amount is needed also for the indirect expenses. Regarding a population of one million people this represents an economic burden of over €36 million each year.

When observing Fig. 9, where the number of D2 patients is illustrated for 2010 and prediction for 2060, it can be expected that the burden of obesity will become even more concerning, as the ratio between working and retired people is decreasing, while at the same time the number of D2 patients is increasing.

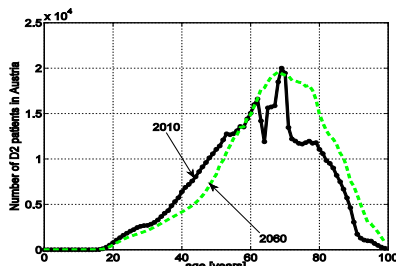


Figure 9: Number of patients with D2 in Austria in 2010 and in 2060

From this it is clear that decrease of obese and overweight population would represent an essential increase of life quality for many individuals. In addition it would save a lot of money needed for drugs, medical services and interventions. Straightforward problem solution is therefore body mass reduction.

3.3. Dynamical process of body mass reduction

For quantification of the problem solution several mathematical models are available. In this case we have used the three - compartment model (Chow and Hall 2008; Navarro-Barrientosa et al. 2011) for an average person. Model enables to differ among fat-free body mass (ffm) and fat mass (fm), where ffm is represented as a sum of lean mass (lm) and extra cellular fluid (ecf). Equation for daily energy balance is:

$$EB(t) = EI(t) - EE(t) \quad (1)$$

where $EI(t)$ represents daily energy intake and $EE(t)$ daily energy expenditure. Energy intake depends on food and its caloric value:

$$EI(t) = k_1 ci(t) + k_2 fi(t) + k_3 pi(t) \quad (2)$$

$ci(t)$ indicating carbohydrate intake, $fi(t)$ fat intake and $pi(t)$ protein intake, and constants k_i are: $k_1=4kcal/gram$, $k_2=9kcal/gram$, $k_3=4 kcal/gram$. It is recommended that protein intake represents 20-30%, fat intake 15-20% and carbohydrate intake 55-60% daily intake of the food. Daily energy expenditure is calculated as follows:

$$EE(t) = tef(t) + PA(t) + rmr(t) \quad (3)$$

where $tef(t)$ is thermic effect of feeding which usually ranges from 7 to 15% of the total energy intake (11% in our case), $PA(t)$ represents energy spent on physical activity and $rmr(t)$ is the so called resting metabolic rate. It refers to the energy needed to maintain basic physiological processes. It represents a substantial percentage (45-70%) of energy expenditure for the typical individual. The daily energy balance $EB(t)$ is partitioned into one of three compartments:

$$\frac{dfm(t)}{dt} = \frac{(1-p(t))EB(t)}{\rho_{fm}} \quad (4)$$

$$\frac{dlm(t)}{dt} = \frac{p(t)EB(t)}{\rho_{lm}} \quad (5)$$

$$\frac{decf(t)}{dt} = \frac{\rho_w}{K} \left(B - \xi_{Na} (ecf(t) - ecf_{init}) - \xi_{Cl} \left(1 - \frac{ci}{ci_b} \right) \right) \quad (6)$$

where $\rho_{lm} = \rho_{fm} = 1800 kcal/kg$, B is the change of sodium in mg/d, ci_b is the baseline carbohydrate intake, $K=3.22mg/ml$, $\xi_{Na}=3 mg/ml/d$, $\xi_{Cl}=4000 mg/d$, $\rho_w=1kg/l$.

$$p(t) = \frac{C}{C + fm(t)}, \quad C = 10.4 \frac{\rho_{lm}}{\rho_{fm}} \quad (7)$$

Daily energy expenditure can be expressed explicitly as:

$$EE(t) = \beta EI(t) + \delta BM(t) + D + \gamma_{lm} lm(t) + \gamma_{fm} fm(t) + \eta_{fm} \frac{dfm(t)}{dt} + \eta_{lm} \frac{dlm(t)}{dt} \quad (8)$$

where $\beta=0.24$ (coefficient of thermic effect of feeding), δ is physical activity coefficient, $\gamma_{lm}=22 kcal/kg/d$, $\gamma_{fm}=3.2 kcal/kg/d$, $\eta_{lm}=320 kcal/kg$, $\eta_{fm}=180 kcal/kg$, while constant D accounts for initial conditions.

In our case an average person (between men and women) was taken into account. From his-hers average height (1.72m regarding 11 European countries) and average BMI=32 also the average mass of this person was estimated to be 94.6688kg. Regarding medical recommendations such person should lose around 30kg to satisfy BMI=22 in the middle of desired BMI interval. The initial fat mass was estimated from the regression equations (Jackson 2002): $fm(0)=34.7$ kg.

Simulation result is illustrated in Fig. 10, where the vertical lines indicate the years of observation while the horizontal lines indicate desired range of BMI. Through the first year energy balance is in equilibrium and body mass is not changing. After the first year physical activity is increased for 210 kcal per day what can be realized with 45 minutes of walk. Such increased energy expenditure results after two years in desired BMI. If this person is able to continue with such life modification he-she reaches recommended steady state.

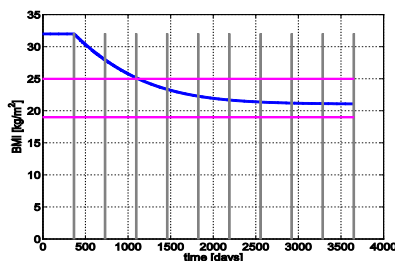


Figure 10: Lowering BMI in average obese person with increased activity (45 minutes of walk)

Let's take into account the following assumptions. 80% of obese and inactive people age 20 and older are motivated to undertake the presented regime of increased activity. With this they are immediately transferred into the group of active population, where they remain. After two years of activity they are also transferred out from overweight and obese population and they remain in the group of people with healthy body mass (Figs. 11 and 12).

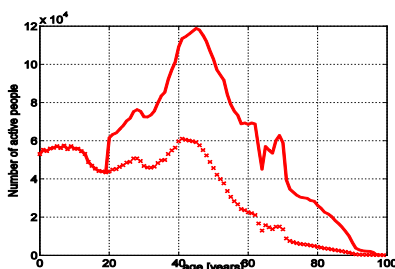


Figure 11: Increase of the number of active patients with BMI>25

The reduction of obese population would of course first decrease direct expenses due to obesity and later on also indirect expenses because of reduced number of the patients with D2 and other diseases. Expected decrease of D2-patients through longer transient is illustrated in Fig. 13.

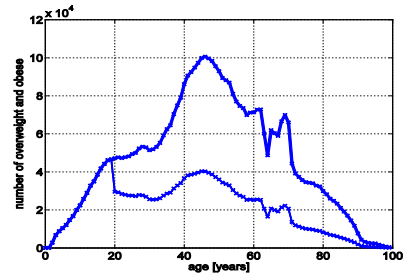


Figure 12: Decrease of the number of patients with BMI>25

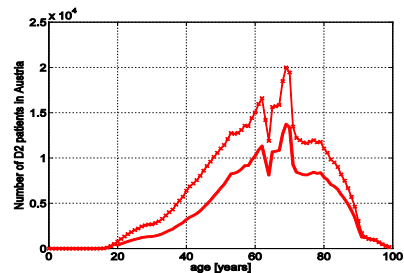


Figure 13: Decrease of D2 patients

3.4. Treatment efficacy analysis

In spite of the fact that treatment could, at least theoretically, be realized in most cases without any expenses (as proved with simulation experiment), mainly with increased activity (or/and moderate decrease of food energy intake) which is anyway recommended for the healthy life style, the result is far from ideal and is actually expected to become even worse (WHO 2011). The problem is obviously far more complicated and is in practice a very demanding one even in the situations when experts are involved to help in corresponding treatment.

First attempts of deeper problem understanding and treatment were realized by psychiatrists Bruch (1948) and Stunkard (1959). They have realized that around 98% of patients regain undesired body mass. Now-days the efforts are directed mainly in problem prevention and in implementation of programs which would enable efficient and long – term treatment (O'Rahilly and Farooqi 2008; Karasu and Karasu 2010; Hall and Jordan 2008; Sentočnik, 2012).

It is important to take into account, that reasons for obesity are numerous and patients represent very inhomogeneous group. Patients with higher BMI are more difficult to be treated successfully.

Mass reduction usually starts with self – treatment experiments, next stage is performed regarding the advices of family doctor, sometimes also personal trainers are engaged. If the results are not satisfying more intensive programs are available at basic health – care system. Treatment is intensified and personalized at sanatoriums where specialists with the help of multidisciplinary team perform integral treatment. Final stage, that is surgical help, is usually suggested when other possibilities proved to be insufficient.

Successfulness of mass reduction is very often evaluated regarding long – term weight stabilization and

the reduction of risk factors of chronic diseases (Sentočnik 2012). In successful patients the need for drug treatment is frequently omitted.

3.4.1. Open – loop treatment approach

As already mentioned the treatment efficacy in obese patients is in general not very high and the main reasons are different problems which influence patients' behaviour in such a way that they are unable to follow the recommended guidelines for reducing calories and/or increasing physical activity.

It seems therefore very important to complement energy equilibrium description with the model of behavioural interventions which would indicate the most important treatment interventions. Navarro-Barrientosa et al. (2011) suggested the usage of the so called theory of planned behaviour, which was extended to dynamic interpretation with interesting analogy in hydraulic system interpretation. It is however not very clear how to influence directly the parameters like attitude, subjective norm and intention to reach desired level of behaviour.

Regarding the results of long research work in sanatorium Medico dr. Sentočnik one of the most important and transparent factor influencing the patient's behaviour habits is the frequency of realized treatments. Patients are usually invited (after starting detailed examination and developed plan of interventions) to come regularly each week to the sanatorium where the prescribed corresponding treatment is performed (including physical activity, psychological treatment, ...). It is very important that the patient realizes these treatments regularly. If treatments are postponed or omitted the efficacy of treatment is always essentially decreased.

We have decided to describe this observation through the level of motivation which has the range from 0 to 100%. If the patient is 100% motivated, he/she completely realizes the prescribed intervention, when motivation is 0% this means his-hers eating/activity pattern remains the same as before the treatment. The level of motivation is influencing prescribed activity and energy intake. It can be expected that during one year of regular treatment motivation becomes strong enough so that patient is able to master new habits by him(her)self. The idea is illustrated in Figs. 14 to 18.

For this experiment previously mentioned three – compartment model of average obese person was used. In Fig. 14 motivation is illustrated. Each time when he/she realizes weekly treatment, motivation is increased to 100%. Between these weekly treatments motivation is decreasing, but with the increased number of visits the lowering is less intensive.

In Fig. 15 energy intake is presented. It was taken into account that the patient should decrease the energy intake to 1900 kcal per day, which represents the day reduction of 560 kcal which is in harmony with medical directions for the obese persons. In Fig. 15 energy intake is oscillating as a result of motivation influence.

Energy expenditure (Fig. 17) is decreasing because of mass reduction, which is illustrated in Fig. 18. When the desired body mass is reached energy intake can be increased to the value of new energy equilibrium.

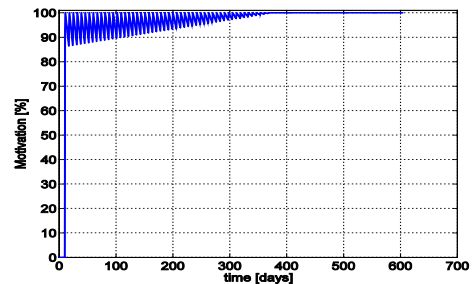


Figure 14: Motivation in patient with regular treatment

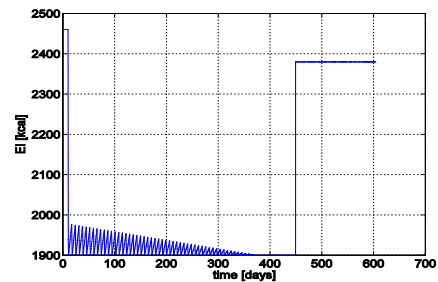


Figure 15: Energy intake in patient with regular treatment

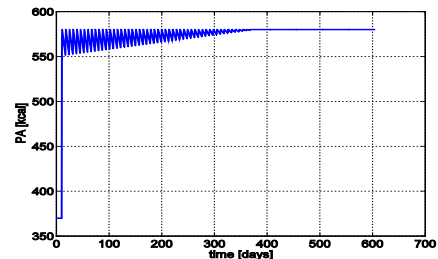


Figure 16: Physical activity in patient with regular treatment

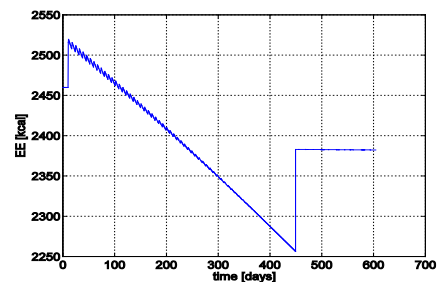


Figure 17: Energy expenditure in patient with regular treatment

The second experiment illustrates the situation where the patient is realizing the treatments regularly for two month. Then he/she feels he has become strong enough to finish the treatment by him(her)self. But in this case it can be expected that motivation starts to drop and reaches the starting position in next two months (Fig. 19). This further influences energy intake

(Fig. 20), physical activity (Fig. 21), and energy expenditure (Fig. 21).

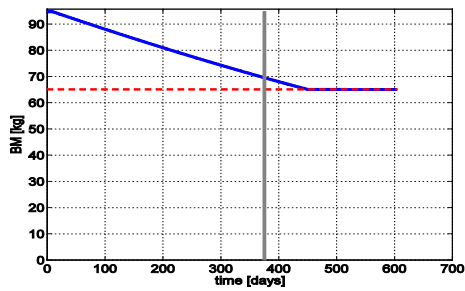


Figure 18: Body mass in patient with regular treatment

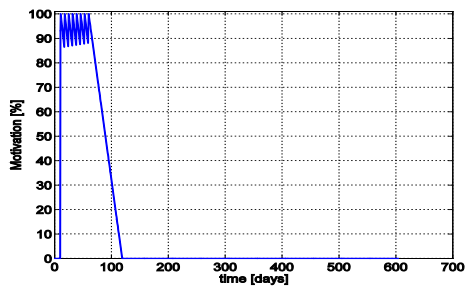


Figure 19: Motivation in patient with unregular treatment

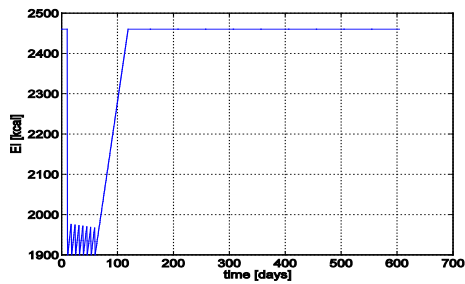


Figure 20: Energy intake in patient with unregular treatment

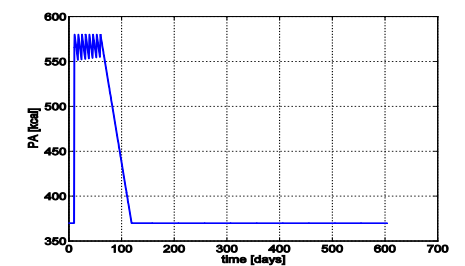


Figure 21: Physical activity in patient with unregular treatment

Body mass of the patient is in this case far from desired value (Fig. 23).

As interventions are in this case pre-defined and remain unchanged during treatment regarding body mass, this treatment can be interpreted as open loop.

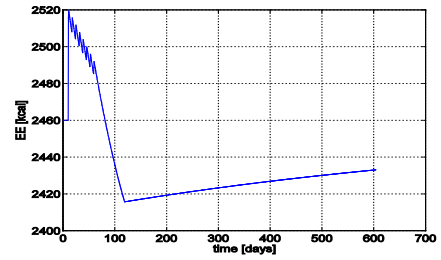


Figure 22: Energy expenditure in patient with unregular treatment

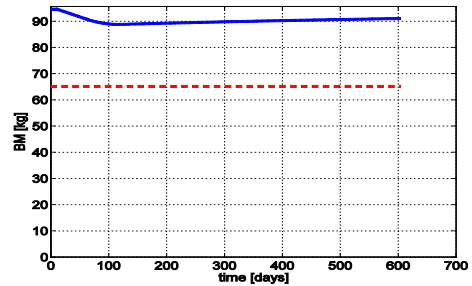


Figure 23: Body mass in patient with unregular treatment

3.4.2. Closed – loop treatment approach

Medical specialists usually carefully supervise patient's progress and health status and can of course react if the process of mass reduction is not satisfactory. This situation is illustrated in Figs. 24 to 28.

In Fig. 24 desired (reference) and actual body mass reduction is illustrated for the situation when the patient regularly realizes prescribed weekly treatments.

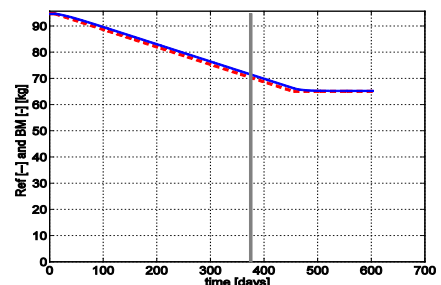


Figure 24: Reference body mass and body mass (solid line) in patient with regular closed-loop treatment

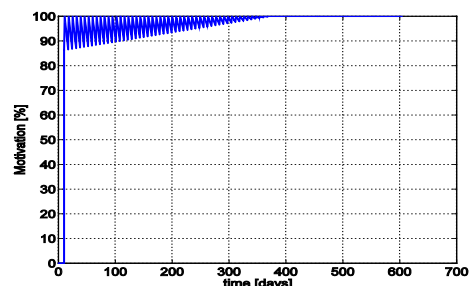


Figure 25: Motivation in patient with regular closed-loop treatment

Motivation is as a consequence high enough and also energy intake (Fig. 26), physical activity (Fig. 27),

and energy expenditure (Fig. 27) are correspondingly maintained using proportional controller.

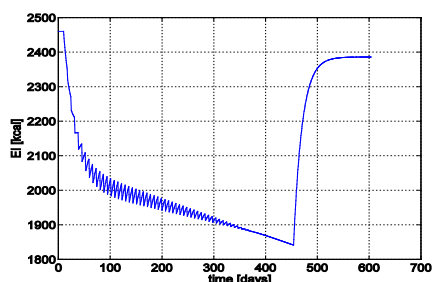


Figure 26: Energy intake in patient with regular closed-loop treatment

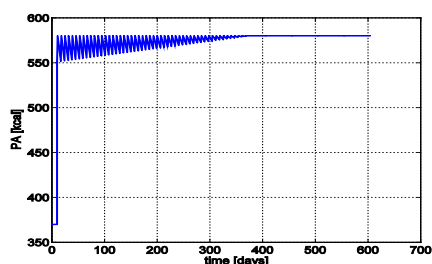


Figure 27: Physical activity in patient with regular closed-loop treatment

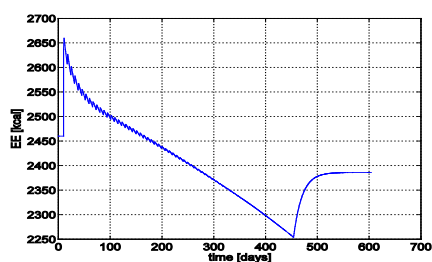


Figure 28: Energy expenditure in patient with regular closed-loop treatment

In the case when the patient stops with regular treatment, feedback loop is disconnected and control action is disabled. The result becomes in this case very similar to those indicated in Figs. 19 to 23.

It is important to mention that the presented model is still far from the final version and is in this case illustrated only for an average person.

In the future further tuning will be performed taking into account also the matching with the real patient data. It can be expected that also control law needs further development where also the behavior of medical specialists can play an important role.

4. CONCLUSIONS

In the paper a description organization is presented enabling the coexistence of different models indicating different problems connected with overweight and obesity. When observing an European country, like for example Austria, it can be expected that around 55% of population has BMI>25 or higher as recommended. In the population of one million people for these patients each year around € 360 million is needed. It can be

expected that this burden will increase in the future because of population ageing.

For efficient treatment long – term weight stabilization should be achieved which demands also long – life change of life style for all overweight and obese patients. This is a tremendous practical problem. In the paper the steps through modelling results are indicated which base also on a very long research in sanatorium Medico dr. Sentočnik.

The model needs further improvement and that will be our future research goal.

REFERENCES

- Abdel-Hamid, T.K., 2002. Modeling the dynamics of human energy regulation and its implications for obesity treatment, *System Dynamics Review*, 18 (4), 431–471.
- Arnold, R.J.G. (Editor), 2010. *Pharmacoeconomics, From Theory to Practice*, CRC Press, Taylor & Francis Group, Drug Discovery Series/13, Boca Raton.
- Atanasijević-Kunc, M., Drinovec, J., Mrhar, A., 2008a. Usage of Modelling and Simulation in Medicine and Pharmacy. *Journal of Slovene Medical Society*, 77 (1), 57–71.
- Atanasijević-Kunc, M.; Drinovec, J.; Ručigaj, S., Mrhar, A., 2008b. Modelling of the risk factors and chronic diseases that influence the development of serious health complications. *Journal of Slovene Medical Society*, 77, (8), 487–498.
- Atanasijević-Kunc, M., Drinovec, J., Ručigaj, S., Mrhar, A., 2008c. Modeling the influence of risk factors and chronic diseases on the development of strokes and peripheral arterial-vascular disease. *Simulation Modelling Practice and Theory*, 16 (8), 998–1013.
- Atanasijević-Kunc, M., Drinovec, J., Ručigaj, S., Mrhar, A., 2011. Simulation analysis of coronary heart disease, congestive heart failure and end-stage renal disease economic burden. *Mathematics and Computers in Simulation*, <http://dx.doi.org/10.1016/j.matcom.2010.10.024>.
- Atanasijević-Kunc, M., Drinovec, J., 2011. *Burden of diabetes type 2 through modelling and simulation. Topics in the prevention, treatment and complications of type 2 diabetes*. Zimering, M. B. (Ed.). Rijeka, InTech, cop., 3–28.
- Atanasijević-Kunc, M., Drinovec, J., Sentočnik, T., 2012. Burdens of obesity: multi-model description. *Full paper preprint volume of the 7th Vienna Conference on Mathematical Modelling, MATHMOD*, Vienna University of Technology, Austria.
- Belič, A., 2009. Modelling in systems biology, neurology and pharmacy. *Mathematical and Computer Modelling of Dynamical Systems*, 15 (6), 479–491.
- Belič, A., Ačimovič, J., Naik, A., Goličnik, M., 2012. Analysis of the steady-state relations and control-

- algorithm characterisation in a mathematical model of cholesterol biosynthesis. *Simulation modelling practice and theory*, doi: 10.1016/j.simpat.2011.12.010.
- Berghöfer, A., Pischon, T., Reinhold, T., 2008. Obesity prevalence from a European perspective: a systematic review, *BMC Public Health*, 8:200 doi:10.1186/1471-2458-8-200
- BHFSW 2012a. British Heart Foundation Statistics Website, Age differences and physical activity, <http://www.heartstats.org/atozpage.asp?id=4955>.
- BHFSW 2012b. British Heart Foundation Statistics Website, Trends in the prevalence of overweight and obesity, <http://www.heartstats.org/datapage.asp?id=1011>.
- Brock, D.W., Thomas, O., Cowan, C.D., Allison, D.B., Gaesser, G.A., Hunter, G.R., 2009. Association Between Insufficiently Physically Active and the Prevalence of Obesity in the United States, *Journal of physical activity & health*, 6 (1), 1–5.
- Bruch, H., 1948. Psychological aspects of obesity, *Bulletin of N.Y. Academy of Medicine*, 1948; 24: 73-86.
- Chow, C.C., Hall, K.D., 2008. The dynamics of human body weight change, *PLoS Computational Biology*, 4 (3), 1–13.
- Corbeil, P., Simoneau, M., Rancourt, D., Tremblay, A., Teasdale, N., 2001. Increased Risk for Falling Associated with Obesity: Mathematical Modeling of Postural Control, *IEEE Transactions on neural systems and rehabilitation engineering*, 9 (2), 126–136.
- Daousi, C., Casson, I.F., Gill, G.V., MacFarlane, I.A., Wilding, J.P.H., Pinkney, J.H., 2006. Prevalence of obesity in type 2 diabetes in secondary care: association with cardiovascular risk factors, *Postgraduate Medical Journal*, 82, pp. 280–284 doi:10.1136/pmj.2005.039032.
- Hall, K., Jordan, P., 2008. Modeling weight-loss maintenance to help prevent body weight regain, *American Journal of Clinical Nutrition*, 88, 1495–1503.
- Hall, K., 2010. Mechanisms of Metabolic Fuel Selection Modeling Human Metabolism and Body-Weight Change, *IEEE engineering in medicine and biology magazine*, 36–41.
- Hoppensteadt, F.C., Peskin, C.S., 2002. *Modeling and Simulation in Medicine and the Life Sciences*, Springer-Verlag, New York.
- Jackson, A.S., Stanforth, P.R., Gagnon, J., Rankinen, T., Leon, A., and et al., 2002. The effect of sex, age and race on estimating percentage body fat from body mass index: The heritage family study, *International Journal of Obesity Related Metabolic Disorders*, 26, 789–796.
- Kovács, L., Szalay, P., Ferenci, T., Drexler, D.A., Sápi, J., Harmati, I., Benyó, Z., 2011. Modeling and optimal control strategies of diseases with high public health impact, *Proceedings of 15th International Conference on Intelligent Engineering Systems*, pp. 23-28, June 23–25, Poprad, Slovakia.
- Karasu, S.R., Karasu, T.B., 2010. *The Gravity of Weight, A Clinical Guide to Weight Loss and Maintenance*, American Psychiatric Publishing, Washington DC.
- Landi, A., Piaggi, P., Lippi, C., Santini, F., Pinchera, A., 2010. Statistical Toolbox in Medicine for Predicting Effects of Therapies in Obesity, *Proceedings of IEEE Workshop on Health Care Management (WHCM)*, 18 – 20 February.
- MMWR, 2004. Prevalence of Overweight and Obesity Among Adults with Diagnosed Diabetes - United States, 1988-1994 and 1999—2002. Morbidity and Mortality Weekly Report (MMWR), 53(45); pp. 1066-1068, Centers for Disease Control and Prevention (CDC), <http://www.cdc.gov/mmwr/preview/mmwrhtml/m5345a2.htm>.
- Navarro-Barrientosa, J.E., Riveraa, D.E., and Linda M. Collins, L.M., 2011. A dynamical model for describing behavioural interventions for weight loss and body composition change, *Mathematical and Computer Modelling of Dynamical Systems*, 17 (2), 183–203.
- O’Rahilly, S., Farooqi, I.S., 2008. Human Obesity: A heritable Neurobehavioral Disorder that is highly Sensitive to Environmental Conditions, *Diabetes*, 97, 2905-2910.
- Santonja, F.J., Villanueva, R.J., Jodar, L., Gonzalez-Parra, G., 2010. Mathematical modelling of social obesity epidemic in the region of Valencia, Spain, *Mathematical and Computer Modelling of Dynamical Systems*, 16 (1), 23-34.
- Sentočnik, T., 2012. *Eating disorders*, Psychiatric Clinic, Ljubljana, 81-98, in Slovene language.
- Stahl, J.E., 2008. Modelling Methods for Pharmacoeconomics and Health Technology Assessment, An Overview and Guide, *Pharmacoeconomics*, 26 (2), 131–148.
- Statistik Austria 2012. <http://www.statistik.at/>
- Stunkard, A.J., 1959. Eating patterns and obesity. *Psychiatric Q*, 33:284-292.
- Valensi, P., Schwarz, P., Hall, M., Felton, A. M., Maldonato, A., Mathieu, C., 2005. Pre-diabetes essential action: a European perspective, *Diabetes & Metabolism*, 31 (6), 606-620.
- WHO - World health organization, 2011. *Obesity and overweight*, Fact sheet No. 311, <http://www.who.int/mediacentre/factsheets/fs311/en/>.

RESEARCH ON SIMPLIFIED MODELLING STRATEGY FOR VIRTUAL COMMISSIONING

Peter Hoffmann ^(a), Reimar Schumann ^(b), Talal M.A. Maksoud ^(c) and Giuliano C. Premier ^(d)

^{(a),(b)} University of Applied Sciences and Arts Hannover, 30459 Hannover, Germany
^{(c),(d)} University of Glamorgan, Pontypridd, Wales, UK, CF37 1DL

^(a) peter.hoffmann@fh-hannover.de, ^(b) reimar.schumann@fh-hannover.de, ^(c) tmaksoud@glam.ac.uk,
^(d) gcpremier@glam.ac.uk

ABSTRACT

Virtual commissioning (VC) of manufacturing systems has been a research topic for more than a decade, but there are still problems in accomplishing a VC; especially in respect to the effort needed to build a simulation model. To date the design of simulation models requires a considerable effort from skilled experts in each enterprise which seeks to use VC. Small and medium-sized enterprises (SME) usually do not have those experts. This fact and the significant effort typically make VC unattractive to SMEs. To overcome this problem it is necessary to provide sufficiently detailed simulation models of manufacturing systems, in a more cost effective and accessible way. This paper proposes changes in the way simulation models are generated and presents new concepts for simplified and systematic design of manufacturing system models for VC based on standardised recipes formalising design of mechatronic component models from CAD data.

Keywords: CAD, manufacturing systems, simulation model building, virtual commissioning

1. INTRODUCTION

Nowadays in a global competition, manufacturing systems must enable cost effective and flexible production. The industrial environment is characterised by shortening of product life-cycles, increasing number of product variants and a requirement for rapid time-to-market, which leads to a progressively tightening timeframe for manufacturing system engineering and the need for better planning quality at the same time.

Manufacturing systems are composed of many off-the-shelf parts and some purpose-built parts or sub-systems, like storage, magazines, conveyors, handling and transportation systems, machining and assembling tools, robots, control and HMI systems. After the product and plant planning phase the following engineering of manufacturing systems includes the mostly sequentially executed phases: mechanical engineering, electrical engineering and automation engineering with programming of robots, PLCs and HMI (Fig. 1).

Hitherto, after completing engineering, procurement and assembly, the real commissioning is finally done, and the traditional way of testing using the real plant and the real control system is still common. Design problems and programming errors in significant quantities remain undetected before the first system start-up. As a consequence of this procedure time and money consuming corrective measures become necessary. Because of time pressure and the risk of damages only rudimental failure scenarios are tested at this stage and unidentified errors result in additional time delays and increased costs during the early production phases.

One way of overcoming this dilemma could be virtual commissioning conducted between completed engineering and assembly of production facilities. The intention of VC is to test manufacturing systems and associated control programs through simulation conducted before the real systems are realised.

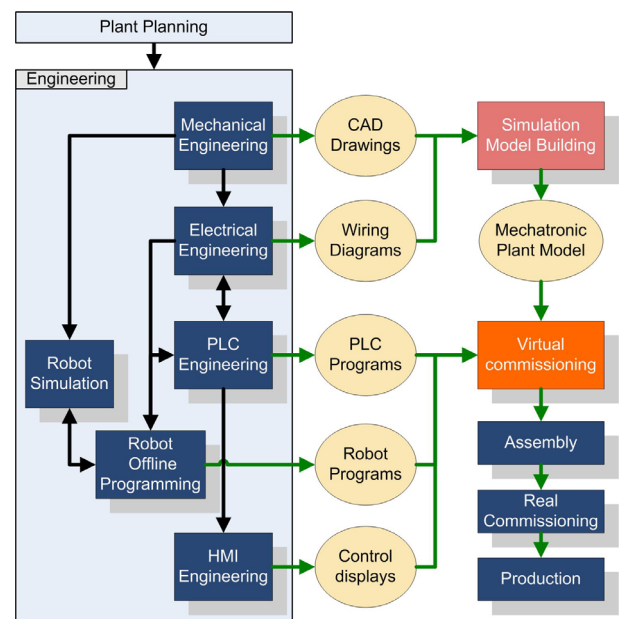


Figure 1: Engineering work-flow with VC

Conducting a VC requires a virtual manufacturing system. For this purpose a simulation model building

process combining data from different engineering tools is necessary. Currently this modelling is typically done using simulation tools promoted for VC.

An important goal of VC is the early validation of PLC code in conjunction with associated mechanical and electrical design, in order to reduce the considerable time delays during commissioning (Zäh & Wunsch 2005). Delays which are caused by the error-prone control code design. This and other advantages such as reduced real commissioning time and higher quality planning are meanwhile reported by many researchers, as reviewed in e.g. (Hoffmann et al. 2010, Jain et al. 2010). Many authors report the beneficial effects of VC (Zäh et al. 2006, Reinhart & Wunsch 2007, Rossmann et al. 2007) but indicated also the great effort needed for simulation model building (Park et al. 2006, Botaschanjan et al. 2009, Zäh et al. 2006, Neugebauer & Schob 2011). The review in (Hoffmann et al. 2010) showed a need for changes in the way simulation models are generated in order to reduce the effort as well as skills needed to build a virtual manufacturing system for VC.

2. DISTINCTION BETWEEN SIMULATION AND VIRTUAL COMMISSIONING

In spite of the mechatronic configuration of modern manufacturing systems, the development process is still focused on mechanical engineering and consequentially the simulation has concentrated primarily on design and mechanical engineering; where fit and specified behaviour of mechanical plant components must be ensured.

Simulation may be conducted by starting with plant design and material flow simulation, then continuing through all engineering phases to the realisation of a virtual manufacturing system with generic or approximate and parsimonious models. Sometimes the term VC is also used for these types of simulations, but a realistic VC is not possible until detailed engineering design has been completed and the real components have been identified.

For the sake of this discussion, the authors understand VC to be the simulation of comprehensively specified manufacturing systems using virtual simulation models and the original and unmodified control programs intended for deployment on the real system – as opposed to design verification by simulation in early engineering phases.

2.1. Separate simulation of mechanics and control – How both should work

To achieve a separate verification of mechanical design, a 3D simulation which is independent of the real control programs is sufficient to test the expected and specified mechanical behaviour (i.e. with no interaction with simulated or real controller).

In separately verifying control programs, a simple simulation at I/O level is often done (without interaction with realistically simulated mechanical elements, which would reflect the specified static and dynamic

behaviour of the manufacturing system e.g. with timing functions).

Such separate simulations are able to detect on one side mechanical resp. geometrical planning errors and on the other side deviations from the nominal behaviour instigated by control functions within the simulation tool.

2.2. Integrated simulation of mechanics and control – How the system will work

If the impact of control programs on the 3D mechanical behaviour of the manufacturing system is to be tested in detail and in an integrated manner, modelling and simulation of the complete functional chains is necessary. These chains would link control programs through sensors, actuators and drives onto the mechanical movements, and would include both, simulation of mechanical behaviour and of control programs. To achieve this, it is necessary to build a comprehensive mechatronic plant model (Fig.1), which should have its conceptual origin already modelled in CAD.

Such a VC is able to detect simultaneously errors in mechanical design, electrical design and control software. Typical errors have previously been identified (Neugebauer & Schob 2011). In contrast to real-world commissioning, testing of failure scenarios without endangering people or the risk of damages, is possible (Rossmann & Heinze 2010).

A VC requires a coupling between controller and the 3D plant simulation tool. This is possible through the following two configurations:

- HIL (hardware in the loop) using simulated plant and real PLC which is often realised using OPC (OLE for Process Control). The use of OPC together with simulation tools is critically analyzed in (Carlsson et al. 2012). A few tools support direct coupling via fieldbus or fieldbus emulation. Even the coupling of real robot controllers is possible within special configurations.

For the HIL configuration, the real PLC is required in advance, but VC is realisable before building the plant.

- SIL (software in the loop) using simulated plant and simulated PLCs. This is possible for different virtual robot controllers and is provided by several simulation tools. In addition to robot controllers, the plant simulation tool CIROS© (RIF 2012) provides the internal simulation of a Siemens S7 PLC or coupling to S7-PLCSIM via OPC.

The SIL configuration allows a complete VC without any hardware of the manufacturing system.

3. APPLICATION OF VC IN LARGE COMPANIES OR SME

3.1. Virtual Commissioning in large companies

In the context of the “Digital Factory” it is in principle possible to use the complex off-the-shelf factory planning suites of tools from the market-leading vendors (Delmia®, Siemens®) for a VC. These suites of tools support all phases of factory planning, but they usually require high investment costs, a high-level of training, high deployment penetration (whole departments), in-house secondment of consultants from the vendors for the implementation of custom-built functions and the laborious building of model libraries designed to the user’s specifications. Therefore, only large companies (e.g. in the automotive industry) selectively choose to conduct a VC using such suites of tools. Nevertheless the simulation models of complex manufacturing systems for VC are often not available in sufficient time to be justified for this purpose.

3.2. Virtual Commissioning in SME

The possibility and the advantages of VC are generally not well known in SMEs neither are the tools for VC, apart from perhaps, as part of the “Digital Factory” solutions. Consequently, there is only limited use of these solutions by SMEs, because they generally do not have the resources to start solving their problems with such “Digital Factory” suites of tools. (Drath et al. 2008b, Westkämper et al. 2003).

The start-up costs (licences, training etc.) are very high. These suites of tools are often too complex for SME to reasonably assimilate, and the change needed, from their previous practice using simpler and independent tools to these suites of tools would not generally be plausible. There is a lack of ‘easy to use’ engineering and simulation environments which could assist engineers in SMEs to set up and conduct VC. The time pressure during projects prohibits the simultaneous introduction of new methods and tools and would, in conjunction with the lack of skilled experts, inhibit uptake and the prerequisite building of simulation model libraries. If the number of newly built production lines is too small, there would be no return on investment in the training of personal and the modelling efforts for one project. Also, if the next project is dissimilar to the first, the modelling would often require again high efforts, as it will not allow the reuse of the already built library models. As a result of these facts,

the level of use of VC in SMEs is rare (Stern et al. 2010).

4. BUILDING SIMULATION MODELS FOR VC

Today, more than a dozen commercial simulation tools like ABB RobotStudio®, CIROS®, Delmia Automation®, InVision®, KUKASim® and VisualComponents® (3D-Create...), to name but a few, are available and applicable to VC.

In the context of this paper, the 3D plant simulation system CIROS® (RIF 2012) was chosen as an example. It was originally developed as robot simulation tool COSIMIR® at the University of Dortmund and allows HIL and SIL simulation as described in section 2.2. In addition, CIROS® provides features such as sensor and actuator simulation, collision detection, transport simulation for carrier based systems or AGVs, and also provides an XML model interface. Unfortunately, all such simulation tools require very difficult and time-consuming simulation model building.

The simulation model building procedure can be divided into two different modelling tasks:

1. (Low-level) component modelling
If not all required component models are available in the library of the simulation tool, (which is in general the case when starting with VC) remarkable efforts become necessary to build additional models from available CAD data.
2. (High-level) plant modelling
With CIROS® (and other comparable tools) the simulation model for the plant can be composed from component models using the simulation editor and provided that all required component models are already contained in the component model library.

By the means of high-level plant modelling it is relatively easy to set up a mechatronic plant model for VC, but even if this modelling of the virtual plant may be partially based on the plant CAD data provided by the plant designers: Especially the exact placement and the interconnection of the components is attendant on additional effort.

During the mechanical engineering of manufacturing systems CAD data of many off-the-shelf

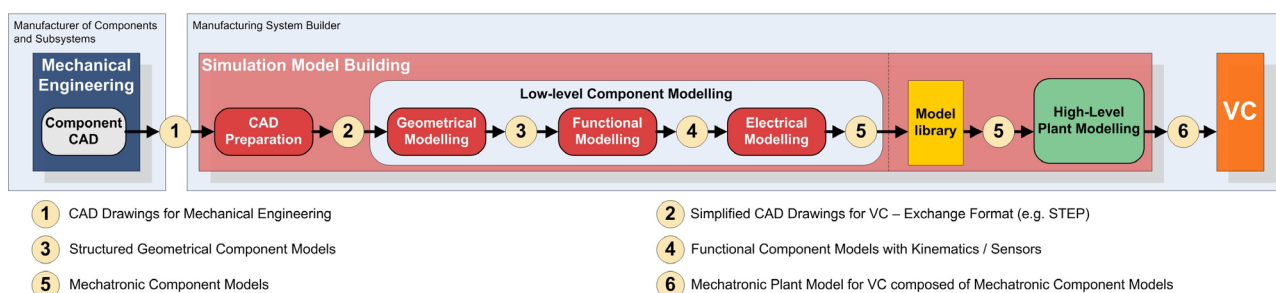


Figure 2: Workflow from CAD Drawings to Mechatronic Plant Model

components or subsystems (supplied by manufacturers) and of some purpose-built designs (in-house work) are composed to a 3D CAD plant model.

The primary source for the component models should be the manufacturer of components and subsystems. However, nowadays the component manufacturers provide 3D CAD data of the components (at best). This means that for all components not available in the component model library of the simulation tool a CAD preparation and low-level component modelling procedure (Fig. 2) must be carried out by the user which complicates the simulation model building for VC considerably and requires specific modelling expertise.

In this paper the low-level modelling procedure of components is critically reviewed and alternative approaches are proposed. The starting point is the 3D CAD model data for the components available either from the component manufacturers or the plant designers. In both cases (plant and component modelling) the 3D CAD model data must be pre-processed and transferred from the CAD system to the simulation system to allow efficient simulation of the geometry and the identification of model structures.

4.1. CAD Data Transfer

The CAD data transfer from CAD tools to simulation tools has other requirements than the data exchange between different CAD/CAM tools used in manufacturing engineering. Not necessary for VC are e.g. detail data like finish specification or tolerances, material data in contrast may make sense, e.g. for the simulation of an inductive sensor.

A big problem exists to date at the interface between the different CAD tools and simulation tools for VC (Fig. 2, ②). Even if functionally structured CAD models are available, the data interfaces allow in general only partial transfer (without kinematics) of this structure information.

In order to transfer kinematics additionally to geometry it is possible to use API (Application Programming Interface) functions for access to internal data of the CAD tool. Such a solution was demonstrated by (Neugebauer & Schob 2011). The disadvantage of this approach is the necessary programming and software maintenance of each combination of CAD tool and simulation tool.

From the authors point of view it is more promising to further develop suitable CAD exchange formats. There are a lot of established exchange formats with special advantages available (Friedewald et al. 2011, Fröhlich 2011), but none has established for exchange of kinematics.

In principle suitable formats for the exchange of geometry and kinematics are STEP (STandard for the EXchange of Product model data) and the Automation Markup Language - AutomationML (Drath et al. 2008a).

STEP supports kinematics since 1996 with its application protocol AP214, Part105 (Haenisch et al.

1996), but to date there is no industrial implementation in a tool. First approaches are presented by (Hedlind et al. 2011, Li et al. 2011).

AutomationML is a neutral, intermediate data format based on XML for automation data storage and exchange including component model data, not limited to geometry and kinematics.

The intention of AutomationML is the reduction of engineering efforts and quality improvement by interconnecting heterogeneous tools, which may become especially valuable when setting up VC with different tools and exchange of model data using AutomationML.

AutomationML combines several already existing standards respectively data formats.

- CAEX (IEC 62424) is used as top level format for the description of the topology and hierarchical structure of objects used in the manufacturing system (including necessary properties and relations between objects).
- COLLADA for describing the 3D geometry with mechanical interconnections and dependencies. The possibility of exchanging kinematics between different tools (e.g. 3D CAD and simulation tools for VC) is an important advantage compared to the exchange formats like STEP used today, where only exchange of geometry is implemented in tools.
- PLCOpen XML is used for the description of overall behaviour (including electrical and control information like I/O relations). Regarding the term “behaviour” it has to be distinguished between the internal behaviour of physical objects and the description of PLC code for controlling physical objects.

A first implementation of COLLADA import with kinematics into a simulation tool (ABB RobotStudio©) is presented in (Kuhlenkötter et al. 2010).

4.2. CAD Preparation

3D CAD data are the basis for the building of the simulation models, and CAD preparation is the first step for the design of mechatronic component models and thus important for VC. The 3D CAD data delivered from the manufacturers of components and subsystems or generated during plant design are not in general directly suitable for use in a VC simulation because most CAD models are geometrically too complex. This is why, a thorough model analysis and simplification of the CAD model data is usually necessary especially to reduce calculations. The goal is to reduce the number of details (geometrical elements) resulting in a reduced number of facets in the simulation model.

For example, the CAD data of aluminium profiles, used for many constructions within manufacturing systems (Fig. 6), must definitely not be used for simulation without simplification. Their complex

structures (Fig. 3) could extremely increase number of facets and extend calculation time.

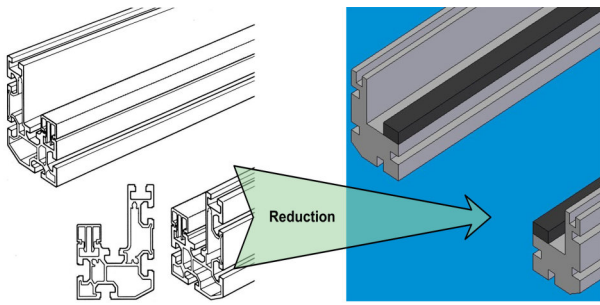


Figure 3: Example for simplified CAD from Bosch CTS© transport system

The complexity of CAD data is not the sole problem; the inner structure of a CAD models has often to be changed as well (to e.g. reduce calculation loading in the simulation and for better model handling inside simulation tools).

As consequence, the preparation of 3D CAD data for simulation has two requirements:

1. The CAD data complexity must be reduced to make real-time 3D rendering and visualisation possible. Even if the simulation tool is able to calculate independently the 3D visualisation, the visualisation should not differ that much. Deviation would hinder the human visual analysis of the operations in the virtual manufacturing system. This ability is simulation tool dependent; e.g. CIROS© provides configurable visualisation rates.
2. The model structure should consider actuating elements and sensors. The dependencies of objects moving together/separately or being stationary, and which geometrical objects are sensors, are all relevant and important.

A small example is shown in Fig. 4. The model structure has to consider a moving object (stopper) and two sensors.

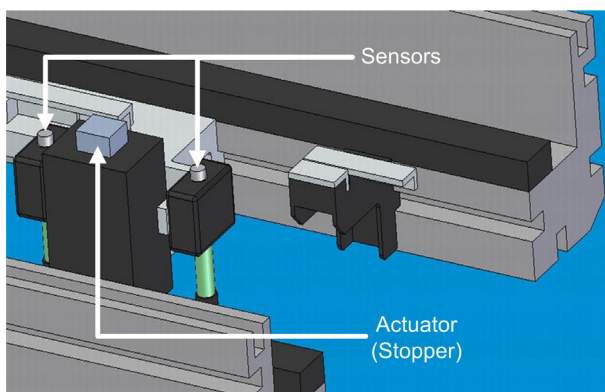


Figure 4: Stopper unit with sensors from Bosch CTS© transport system

If the CAD data provided are not appropriately structured especially with separation of moving parts, the data is not directly usable for the following low-level component modelling, nor is it possible to base a simulation on such model. In worst case, a CAD redesign may become necessary to provide in the geometry data the inner structures required for simulation.

In principle the preparation of CAD data can be done inside the simulation tool (see section 5.1, Fig. 5), which is often the case today, but then dispensable data has to be deleted and the model has to be restructured there with cumbersome detail work.

More efficient and overall faster would it be to prepare the 3D CAD data already inside CAD or simplification respectively conversion tools. In comparison with these tools the relevant simplification capabilities of simulation tools are limited and less controllable and the restructuring work is affiliated with more effort.

Modern CAD tools already provide several automated simplification features with adjustable filters to remove irrelevant geometrical features and irrelevant geometrical objects. If this functionality is not sufficient, it is possible to use specialised simplification respectively conversion tools such as: CADdoctor© (Elysium 2012), CADfix© (ITI-Transcendata 2012) or PolyTrans©/Nugraf© (Okino 2012).

Regarding the requirements mentioned above, the workflow for CAD model preparation for VC should comprise the following steps.

4.3. Simplification

Simplification can be done by removing features and removing parts.

- Feature Suppression: Removal of geometrical features irrelevant for simulation such as:
 - Holes, bosses, pockets, breakthroughs (not round), labels
 - Fillets, chamfers, roundings
 - Ribs, steps, slots
- Object Filtering: Removal of irrelevant geometrical objects like such as:
 - Hidden invisible parts
 - Small or other selected parts

The waiving of elaborate textures, respectively the definition as separate objects which can be deleted easily, is reasonable to allow further shortening of calculation time.

4.4. Component Structuring

Adjusting the CAD model inner structure is the crucial factor for CAD preparation. The model has necessarily to be separated to:

- static units
- moving units
- sensors

Up to now the building of assemblies in mechanical engineering is not done considering the functional interaction of parts, but rather aspects like common manufacturing are respected. Sometimes, that will lead to assemblies wherein static parts are mixed with moving parts. This was reported e.g. in (Hollander & Sappei 2011).

Assemblies created in mechanical engineering are often static, or all parts of an assembly move together. Converting such assemblies to single parts makes sense to minimise the calculation needs of simulation.

While working with CIROS© this practise has also proven advantageous for better handling of models during functional component modelling, because much less objects appear in the model editor.

Sensors have to be separate parts, regardless of belonging to a static unit or a moving unit.

The result of this preparation procedure will be a simplified component CAD model structured according to mechatronic considerations suitable for low-level component modelling.

After revising the CAD model, in respect to the feature objects and the structure to be adopted, conversion from exact model in a meshed surface model must then be done.

4.5. Tessellation/Meshing

The original CAD model is tessellated into a mesh of polygons, often done by triangulation to build a triangular mesh. Generally, it is essential to reduce the quantity of polygons for simulation purposes. Mesh simplification is a separate area of research for a long time and extensive studying originated a lot of techniques and algorithm. Basically, they can be divided into two groups (Kwak et al. 2010):

- Iterative coarsening of the complete mesh by removing polygons until a specified goal (e.g. number of polygons) is achieved
- Iterative refinement of a newly generated mesh (based on an initial approximation) by inserting polygons

The research in (Kuhlenkötter et al. 2010) shows the influence of quantity of facets and type of mesh (polygonal/triangular) on calculation time using ABB RobotStudio© as example. Unsurprisingly, the import duration and calculation time for collision detection ascends with quantity of facets, but the conducted experiments with a COLLADA importer offer big differences between polygonal meshes and triangular meshes. Ascending polygon quantity shows steeply rising import duration shortly exceeding one hour and leading to problems of insufficient RAM. In contrast, importing triangular meshes shows a gently inclined curve. Simulation tools for VC make use of collision detection between geometrical objects, and here as well triangular meshes show the advantage of significant shorter calculation time.

These findings allow the assumption to preferably use triangular meshed models for VC, and to limit the quantity of triangles as much as reasonable. Especially geometrical objects to be checked against each other with collision detection should contain as few triangles as possible.

CAD data providing different LOD (levels of detail) would be beneficial for simulation purpose. CIROS© for example supports different, changeable LOD.

5. RECIPES FOR LOW-LEVEL MODELLING

5.1. Conventional Low-Level Component Modelling from CAD Data (at the example CIROS©)

The starting point for this procedure is the 3D CAD model data for the components available either from the component manufacturers or the plant designers.

Building a low-level mechatronic component model in the conventional way means to describe the whole functional chain of the model, and can be divided into three stages: geometrical, functional and electrical modelling. The carrying out of this non-trivial procedure requires considerable modelling expertise and effort. Especially SMEs usually do not have the needed modelling experts.

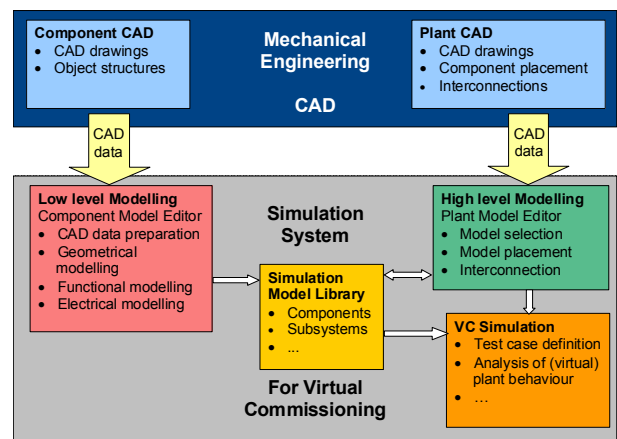


Figure 5: Simulation model generation: conventional recipe

5.1.1. Geometrical Modelling

Building mechatronic simulation models starts with the import and preparation of CAD drawings. For this purpose CIROS© currently provides import filters for STEP (AP203/214), STL, VRML and IGES. Simplification of exceedingly complex geometric data and restructuring would become necessary, if this had not been done in an external CAD preparation. CIROS© provides merging, aligning and optimisation of CAD data.

Adjusting the inner structure of these models considering static parts, actuating elements and sensors is the crucial step in creating the model. As mentioned above, the import of standard CAD data supplied from hardware vendors or in-house mechanical engineering often results in an unstructured or unsuitably structured

geometrical model. Having created appropriately structured geometrical models, these must be equipped with functions (functional modelling) and electrical inputs and outputs (electrical modelling).

5.1.2. Functional Modelling

As indicated in section 4.1 today it is not or only partially possible to transfer the inner structure of the 3D CAD model from the CAD to the simulation system, so it is necessary to manually equip the geometrical models with kinematics and when indicated with sensor functions.

CIROS© provides for this purpose several actuator functions such as translation, rotation, gripping and different types of sensor functions e.g. ultrasonic, optical, capacitive, inductive or light barrier. It is necessary to manually allocate actuator and sensor functions to the respective parts of the geometrical models. This results in the definition of integrated functional models such as push cylinder, rotational cylinder, turntable, sensor, gripper and so on. These models need parameterisation e.g. stroke and speed of cylinders or timing, measurement range, switch distance and hysteresis of sensors.

5.1.3. Electrical Modelling

For the final electrical modelling, it is necessary to manually assign electrical inputs and outputs to sensors and actuators in the functional models. CIROS© allows interactive, graphical editing of these connections. Later these I/Os will be linked to I/Os of control programs thus creating complete mechatronic simulation models.

5.2. Alternative Low-Level Component Modelling

To reduce the modelling effort for the user the following alternative approaches may be taken.

5.2.1. Component simulation model to be provided by manufacturer

For electrical CAE systems the component simulation models are generally provided by the component manufacturers. So in the long term a similar approach should be taken also for the components of manufacturing systems, i.e. the simulation models should be provided by the component manufacturers. This means that the manufacturers (and not the users) will have to handle the low-level modelling of their components. The motivation to undertake this effort can only be provided by the users, especially by the big users of simulation tools which may define the provision of simulation models as a general delivery condition in their commercial terms.

5.2.2. Low-level modelling during CAD design

The component designers have a clear view of the functional structure of the component. Today, however, only part of this general functional view is implemented in CAD models which represent predominantly CAD drawings perhaps with some limited object specifications. This means that the additional functional knowledge of the designer must be documented

separately or transferred from the designer to later users individually.

This is why the authors propose that:

- In future versions of CAD systems the functional and structure information of components must become an integral part of CAD design.
- The education of future designers should consider the structural organisation and inclusion of functional information (as required among others for the simulation models) in the CAD data. This should result in CAD model data with sufficient functional and structure to feed also simulation systems directly.
- In addition the CAD data interfaces must be empowered to transfer not only geometrical but also functional information (kinematics).

6. RECIPES FOR HIGH-LEVEL PLANT MODELLING

6.1. Conventional Recipe for High-Level Plant Modelling

The engineering of manufacturing plants is in general documented using CAD systems showing the placement of components in 3D and the interconnections of them. Simulation systems like CIROS© allow the aggregation and simulation of virtual manufacturing systems based on components in their internal library containing several mechatronic components or subsystems (for CIROS© e.g. from Festo© FMS such as conveyor systems (Fig. 6), assembly stations, handling stations and stocks, even robot models from different vendors (ABB©, FANUC©, KUKA©, Mitsubishi© etc.) have already been included. A similarly concept uses e.g. ABB RobotStudio© with so called “Smart Components”, but regarding robots it is limited to the use of ABB© products.

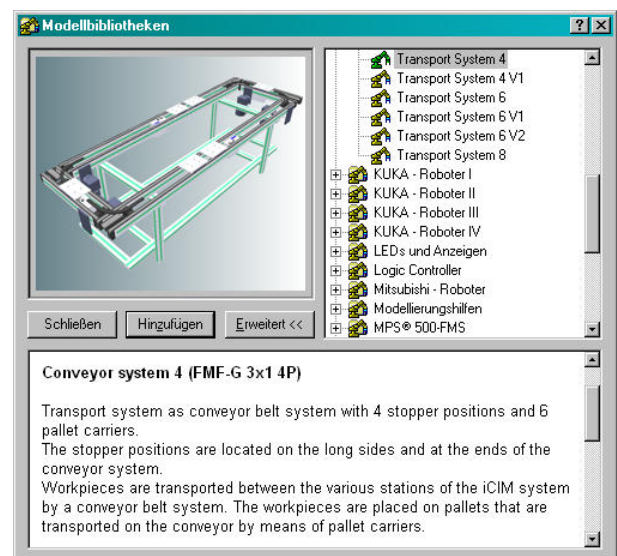


Figure 6: Example subsystem from CIROS© model library

These library models already contain the functional interaction of mechanical behaviours for actuators and sensors. If it is possible to compose the mechatronic plant model from such mechatronic components – high-level plant modelling - it is relatively easy to set up and conduct VC, because it will only require little additional effort when composing the plant model within the 3D editor and configuring I/O connections.

However, nowadays the geometrical information for the placement of the components and for their connections must be manually transferred from the CAD drawings provided by plant engineering.

6.2. Improved Recipe for High-Level Plant Modelling

In order to simplify high-level plant modelling for simulation the placement and interconnection information should be collected comprehensively already during CAD and transferred automatically to the simulation system such that the placement and interconnection of the components in the simulation model is done automatically (Fig. 7). This can be accomplished either by using improved data interfaces or by integration of CAD and simulation tool.

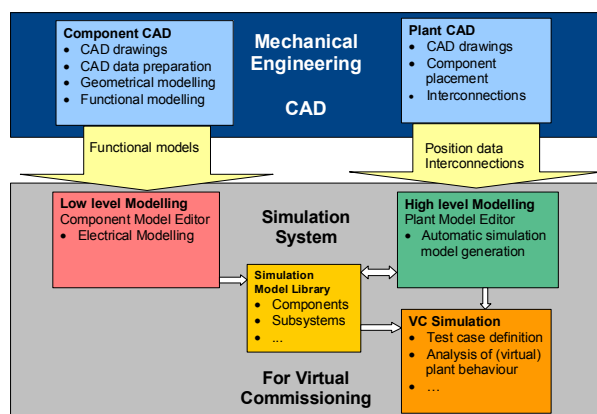


Figure 7: Simulation model generation: alternative recipe

The proposed approach of providing mechatronic models by the manufacturers of components or subsystems is supported by AutomationML.

7. SUMMARY AND FUTURE PROSPECTS

Currently, the simulation model building is carried out manually by the users of VC. It is not entirely possible until the engineering of manufacturing system is completely finished and all components are accurately specified. The necessary and laborious preparation of CAD models and low-level component modelling tends to result in serious time pressures. This may reach the point where delayed completion of the mechatronic plant models might result in their delivery after the real-world manufacturing system has been built.

An important first step towards simulation model building to be a task for control system engineers and commissioning engineers from SMEs would be the unimpeded transfer of CAD data to component

modelling. The data flow should facilitate and be directly applicable to low-level component modelling suitable for VC. Therefore, it is required that designers in CAD departments in components and subsystems manufacturing enterprises and designers from enterprises engineering, building and/or commissioning manufacturing systems consider the supply of such data. The supply of appropriate CAD data would greatly reduce the laborious CAD preparation always repeated at every use to a one-time activity. The low-level component modelling which remains necessary nowadays would be better facilitated and simplified. To achieve this goal there is a need for information to be gathered from designers creating CAD models, persuasion the manufacturers of components and subsystems to provide additional CAD data is recommended to facilitate component models for VC. In order to advance thinking in mechatronic units, CAD education in universities should address model transfer, reduction and reuse for low-level component modelling.

The future goal should be the availability of complete mechatronic models (like the models available today at end of low-level component modelling) provided by the manufacturers of components and subsystems. Already today the manufacturers should change over to provide 3D CAD data suitable for VC; this would be a good basis for future building of mechatronic models. Besides an appropriate exchange format like AutomationML, joint efforts for standardisation (e.g. model content) will be necessary for this purpose.

REFERENCES

- Botaschanjan, J., Hummel, B., Hensel, T. and Lindworsky, A., 2009. Integrated behavior models for factory automation systems, *Emerging Technologies & Factory Automation, 2009. ETFA 2009. IEEE Conference on*, pp. 1-8.
- Carlsson, H., Svensson, B., Danielsson, F. and Lennartson, B., 2012. Methods for Reliable Simulation-Based PLC Code Verification, *Industrial Informatics, IEEE Transactions on*, 8, 2, pp. 267-278.
- Drath, R., Lüder, A., Peschke, J. and Hundt, L., 2008a. AutomationML - the glue for seamless automation engineering, *IEEE International Conference on Emerging Technologies and Factory Automation, ETFA 2008*, 15-18 Sept. 2008, Hamburg, pp. 616-623.
- Drath, R., Weber, P. and Mauser, N., 2008b. An evolutionary approach for the industrial introduction of virtual commissioning, *Emerging Technologies and Factory Automation, 2008. ETFA 2008. IEEE International Conference on*, Hamburg, pp. 5-8.
- Elysium, 2012. *Interactive geometry verification and healing for multi-CAD data exchange, geometry simplification for CAE, plus tools for*

- Rapid Prototyping and Reverse Engineering*, Available from: <http://www.elysiuminc.com/Products/caddocto r.asp> [accessed July 10th, 2012]
- Friedewald, A., Lödding, H., Lukas, U. F. V., Mesing, B., Roth, M., Schleusener, S. and Titov, F., 2011. *Benchmark neutraler Formate für den prozessübergreifenden Datenaustausch im Schiffbau*, Fraunhofer IGD.
- Fröhlich, A., 2011. *3D-Formate im Engineering-Umfeld – ein Vergleich*, Whitepaper, Darmstadt, PROSTEP AG.
- Haenisch, J., Kroszynski, U., Ludwig, A. and Sørensen, T., 1996. *Specification of a STEP Based Reference Model for Exchange of Robotics Models : Geometry, Kinematics, Dynamics, Control, and Robotics Specific Data*.
- Hedlind, M., Klein, L., Li, Y. and Kjellberg, T., 2011. Kinematic structure representation of products and manufacturing resources, *Proceedings of the 7th CIRP-Sponsored International Conference on Digital Enterprise Technology*, Athens, Greece.
- Hoffmann, P., Schumann, R., Maksoud, T. M. A. and Premier, G. C., 2010. Virtual Commissioning of Manufacturing Systems - A Review and new Approaches for Simplification, *Proceedings of the 24th European Conference on Modelling and Simulation*, June 1st - 4th, 2010, Kuala Lumpur, Malaysia, pp. 175-181.
- Hollander, A. and Sappei, S., 2011. *Virtual preparation of Tetra Pak Filling Machine*, Göteborg, Sweden, CHALMERS UNIVERSITY OF TECHNOLOGY, Master Thesis
- Iti-Transcendata, 2012. *Solutions for CAD/CAM/CAE/PLM interoperability*, Available from: <http://www.transcendata.com/products/cadfix/index.htm> [accessed July 11th, 2012]
- Jain, A., Vera, D. A. and Harrison, R., 2010. Virtual Commissioning of Modular Automation Systems, *10th IFAC Workshop on Intelligent Manufacturing Systems (2010)*, July 1st - 2nd, 2010, Lisbon, Portugal.
- Kuhlenkötter, B., Schyja, A., Hypki, A. and Miegel, V., 2010. Robot Workcell Simulation with AutomationML Support - An Element of the CAx-Tool Chain in Industrial Automation, *Robotics (ISR), 2010 41st International Symposium on and 2010 6th German Conference on Robotics (ROBOTIK)*, 7-9 June 2010, Munich, Germany, pp. 1076-1082.
- Kwak, J.-G., Park, S. and Chang, M., 2010. Geometric data simplification for a virtual factory, *The International Journal of Advanced Manufacturing Technology*, 50, 1, pp. 409-418.
- Li, Y., Hedlind, M. and Kjellberg, T., 2011. Implementation of kinematic mechanism data exchange based on STEP, *Proceedings of the 7th CIRP-Sponsored International Conference on Digital Enterprise Technology*, Athens, Greece, pp. 152-159.
- Neugebauer, R. and Schob, U., 2011. Reducing the model generation effort for the virtual commissioning of control programs, *Production Engineering*, 5, 5, pp. 539-547.
- Okino, 2012. *Okino PolyTrans and NuGraf, Professional 3D Translation/Translator and Conversion/Converter Software for CAD, NURBS, Skinning, DCC and Animation*, Available from: <http://www.okino.com/default.htm> [accessed February 29th, 2012]
- Park, C. M., Bajimaya, S. M., Park, S. C., Wang, G. N., Kwak, J. G., Han, K. H. and Chang, M., 2006. Development of Virtual Simulator for Visual Validation of PLC Program, *International Conference on Computational Intelligence for Modelling Control and Automation, and International Conference on Intelligent Agents, Web Technologies and Internet Commerce (CIMCA-IAWTIC'06)*.
- Reinhart, G. and Wünsch, G., 2007. Economic application of virtual commissioning to mechatronic production systems, *Production Engineering*, 1, 4, pp. 371-379.
- Rif, 2012. *CIROS Engineering*, Available from: <http://www.ciros-engineering.com/en/home/> [accessed May 11th, 2012]
- Rossmann, J. and Heinze, F., 2010. Modeling and simulation of malfunctions in automation systems, *Emerging Technologies and Factory Automation (ETFA), 2010 IEEE Conference on*, 13-16 Sept. 2010, pp. 1-8.
- Rossmann, J., Stern, O. and Wischnewski, R., 2007. Eine Systematik mit einem darauf abgestimmten Softwarewerkzeug zur durchgängigen Virtuellen Inbetriebnahme von Fertigungsanlagen von der Planung über die Simulation zum Betrieb, *GMA-Kongress 2007*, 12th and 13th June 2007, Baden-Baden, VDI-Berichte 1980, pp. 707-716.
- Stern, O., Hoffmann, P. and Schumann, R., 2010. KMU und VIBN in der Fertigungstechnik, *Meeting of VDI/VDE-GMA FA 6.11 CACE*, Dec. 1st, 2010, Ladenburg.
- Westkämper, E., Bierschenk, S. and Kuhlmann, S., 2003. Digitale Fabrik – nur was für die Großen?, *wt Werkstattstechnik online*, 93, 1/2, pp. 22-26.
- Zäh, M. F. and Wünsch, G., 2005. Schnelle Inbetriebnahme von Produktionssystemen, *wt Werkstattstechnik online*, 95, 9, pp. 699-704.
- Zäh, M. F., Wünsch, G., Hensel, T. and Lindworsky, A., 2006. Nutzen der virtuellen Inbetriebnahme: Ein experiment - Use of virtual commissioning: An experiment, *ZWF Zeitschrift fuer Wirtschaftlichen Fabrikbetrieb*, 101, 10, pp. 595-599.

AUTHORS BIOGRAPHY

Peter Hoffmann studied computer engineering at the University of Applied Sciences and Arts Hannover and obtained his Dipl.-Ing. degree in 2000 and is now working as research staff member at the automation engineering lab at the same university. In addition he is currently a PhD student at the Faculty of Advanced Technology at the University of Glamorgan. His main research interest is in the field of control design for manufacturing systems and more specifically he is interested in verification and validation of PLC programs

Reimar Schumann received the PhD degree in Automatic Control from the Technical University Darmstadt in 1982. During his industrial career he was responsible for the design and development of a third generation digital process control system. Since 1989 he is teaching process control at the University of Applied Sciences and Arts Hannover. His current research interest is focussed on process and production control and system design.

Talal M. A. Maksoud is a Reader in the University of Glamorgan. He has over 30 years experience in research. He has published over 75 papers in Journals and international conferences. He has published several best papers in the field of advanced grinding technology. His main interests are in Grinding technology, heat transfer analyses, computational fluid dynamics, Aerodynamics, and Artificial Intelligence use in Manufacturing. Dr Maksoud has supervised over dozen PhD's as well as MPhil's. He has acted as external and internal examiner for several PhD's. He is a recognised referee for several peer reviewed academic Journals.

Giuliano C. Premier is a Professor in the University of Glamorgan and senior member of the Sustainable Environment Research Center (SERC). His research activities cover modelling, control, instrumentation, renewable energy systems, biological wastewater treatment. His Ph.D. concerned the modelling and control of anaerobic digestion (AD) processes. His research also includes industrial computer aided control system design (through a longstanding collaboration with the University of Applied Sciences, Hannover). He has and continues to contribute to collaborative projects with universities and industrial partners.

OPTIMAL AMBULANCE LOCATION, AT UNIVERSITY OF MEXICO, EMPLOYING SIMULATION

Jose A. Vindel ^(a)

^(a)Engineering Faculty, University of Mexico

alexandervindel@comunidad.unam.mx

ABSTRACT

This study was undertaken to make more efficient the ambulance service at the University of Mexico in terms of response time and their location through a simulation model, programmed in SIMIO, which represents the real system and allowed us to propose a strategic location of these ambulances, provided by a location model.

Keywords: ambulance location, simulation, location model.

1. INTRODUCTION

The University of Mexico provides the population located on its main campus with various services, including libraries, general store, medical service, sports and recreation, to name a few. On the other hand, the medical service also counts with an emergency center, which provides ambulance service, being responsible of addressing any circumstances required. The service covers an approximate area of 3.5 square miles, as shown in Figure 1, with a daily population greater than 258.617 people, according to table 1. Considering the above, the response time plays an important role to provide care and protect human life, stating the reason of this research, proposing a strategic location of the ambulances, improving the response time, and bringing this service at the time when it is required.

Table 1. Population Statistics from the main campus

Year	Undergraduate Student	Graduate Student	Professorate
2008	167,891	22,527	43,151
2009	172,444	23,875	43,252
2010	179,052	25,036	44,348
2011	180,763	25,167	44,869
2012	187,195	26,169	45,253

This paper presents a combination of tools: discrete event simulation and integer programming. Discrete event simulation was used because of its power to simulate complex and detailed systems. (Perez Cardona Gomez Olarte, Escudero, 2008).

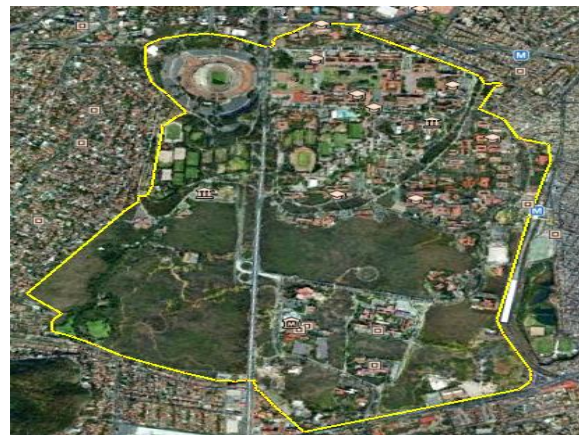


Figure 1. Aerial View of main campus

The following sections give a brief description of the simulation model and its methodology; as well as the location model, and the conclusions achieved.

2. SIMULATION MODEL

This section gives a brief description of the model building, along with the methodology used, and the results obtained.

2.1 Methodology

The methodology (Flores, Cortez, 2006) conducted for this article was as shown in Figure 2.

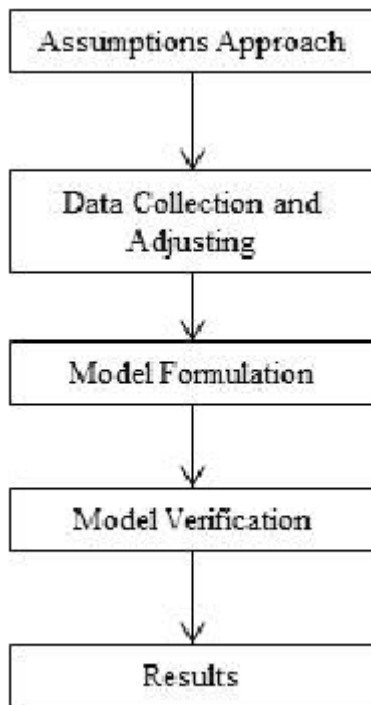


Figure 2. Methodology Followed

2.2 Assumptions Approach

Several assumptions were raised for this project, such as:

- Free circuit traffic.
- Constant ambulance speed of 60 km / h.
- Students, workers, and externals are the only affected population.
- Events occur only on the main buildings of each of the faculties.

It was proposed to work with an ambulances location zoning by considering the proximity areas between faculties, as shown in Table 2.

Table 2. Suggested Zones

Zone	School	School	School
1	Law	Economics	
2	Medicine	Dentistry	
3	Engineering	Languages	Architecture
4	Philosophy	Central Library	
5	Political Sciences		
6	Sciences		
7	Accounting		
8	Psychology		
9	Chemistry		
10	Social Labor		
11	Veterinary	Animal Husbandry	
12	Engineering Annex		

2.3 Data Collection and Adjusting

The data was extracted from the formats conducted by emergency medical technicians at the University of Mexico, considering information from 2008 to 2011, including all the days of the week. The collected data specified place, day of week of the event, and person served; information concentrated in Table 3 and Table 4.

Table 3. Total number of events per day and zone

Weekday	1	2	3	4	5	6	7
	Zone						
1	44	55	48	49	69	15	8
2	52	44	49	51	51	15	10
3	37	52	37	47	34	9	7
4	31	39	30	43	38	15	11
5	16	23	8	19	27	10	3
6	35	43	62	49	39	9	2
7	29	29	34	37	34	9	3
8	12	10	17	14	14	2	1
9	18	23	24	29	32	4	2
10	4	7	11	11	10	0	1
11	10	22	19	12	11	4	3
12	11	11	18	12	10	3	0

Table 4. Total number of people served per zone

Person served	Student	Employee	Other
Zone			
1	194	56	38
2	130	72	70
3	121	60	42
4	112	49	46
5	67	18	21
6	154	67	18
7	136	25	14
8	45	17	10
9	83	30	19
10	29	6	9
11	37	21	23
12	41	16	8

These data was fitted using EasyFit software, which allows the adjustment of probability distributions, providing the necessary parameters to consider in the simulation model presented in Table 5.

Table 5. Adjusting parameters

	Geometric	Neg. Binomial	
	p	n	p
Zone 1	.02373	4	.10046
Zone 2	.02509	6	.13608
Zone 3	.03043	4	.12167
Zone 4	.03271	8	.23007
Zone 5	.06195	4	.23935
Zone 6	.02846	3	.08644
Zone 7	.03846	4	.16234
Zone 8	.09091	4	.30435
Zone 9	.05036	3	.16003
Zone 10	.13725	3	.33478
Zone 11	.07955	4	.27207
Zone 12	.09722	4	.030172

According to the tests of fit goodness (Anderson-Darling and Kolmogorov-Smirnov) that offer the same program; the shaded values for each zone were taken into account. Furthermore, it was estimated the percentage of persons requiring such services as shown in Table 6. These values allow the estimation of the service demands.

Table 6. Percentage of type of people served per zone

Zone	%Student	%Employee	%Other
1	67%	19%	14%
2	48%	26%	26%
3	54%	27%	19%
4	54%	24%	22%
5	63%	17%	20%
6	64%	28%	8%
7	78%	14%	8%
8	61%	24%	15%
9	63%	23%	14%
10	66%	14%	20%
11	46%	26%	28%
12	63%	25%	12%

2.4 Model Formulation

Once analyzed the data, the simulation model was built in SIMIO; this software allows you to build and run dynamic 3D models of a variety of systems, such as manufacturing, supply chains, emergency departments, airports and service systems. This software uses a modeling approach by objects, where the models are constructed by combining objects representing physical components of the system. Simian model may represent the real system (SIMIOA LLC, 2010), this allows a more simple interaction between the shaper and the system to model, in addition to its visual appeal, as shown in Figure 3.



Figure 3. Simulation model in SIMIO

This model was built taking each zone as an entities generator source, which represent the events that require the attention of the ambulances.

2.5 Model Verification

The model was verified by checking the nonexistence of no logical error when running the simulation; at the time the data was also analyzed by reviewing the results obtained were consistent with the real system.

2.6 Simulation Results

In this model each zone events were estimated considering the semester from August 2012 to December of that year, the model was run with ten replicas, figures 4-6.

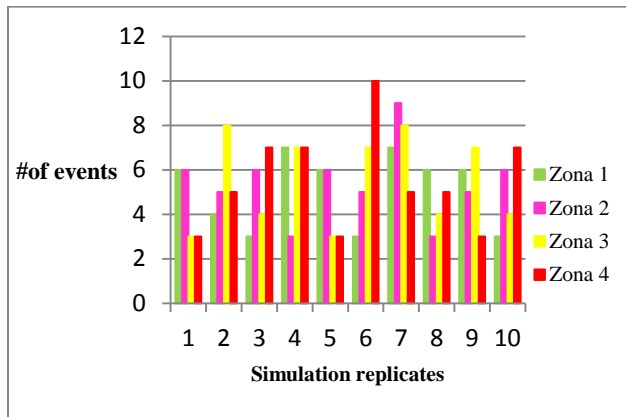


Figure 4. Number of Events per zone (1-4)

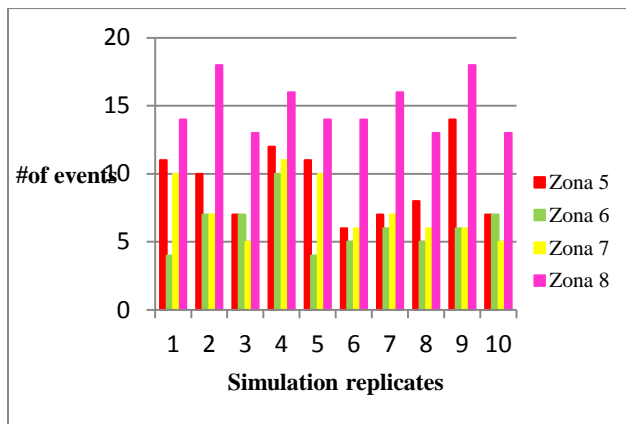


Figure 5. Number of Events per zone (5-8)

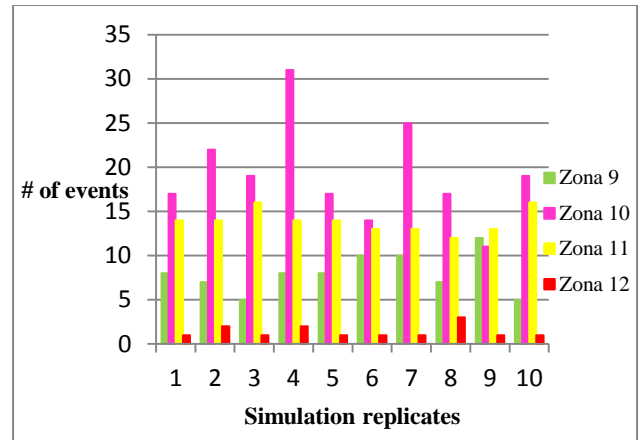


Figure 6. Number of Events per zone (9-12)

The model also provided results which show the time of transport along the simulation, as Figure 7 demonstrates.

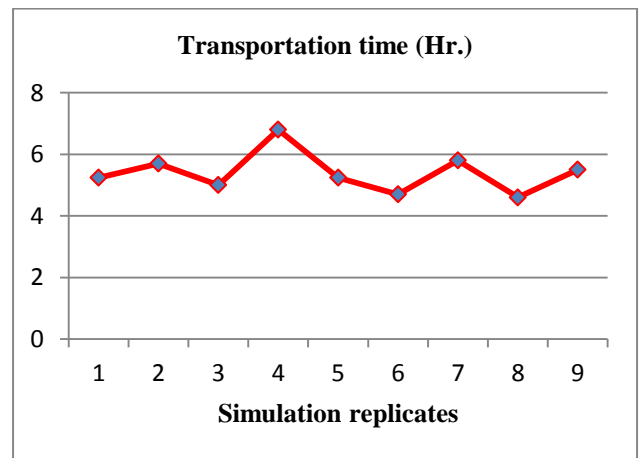


Figure 7. Transportation time

From the same model, the amount of people requiring the ambulance services was obtained, as seen in Figure 8.

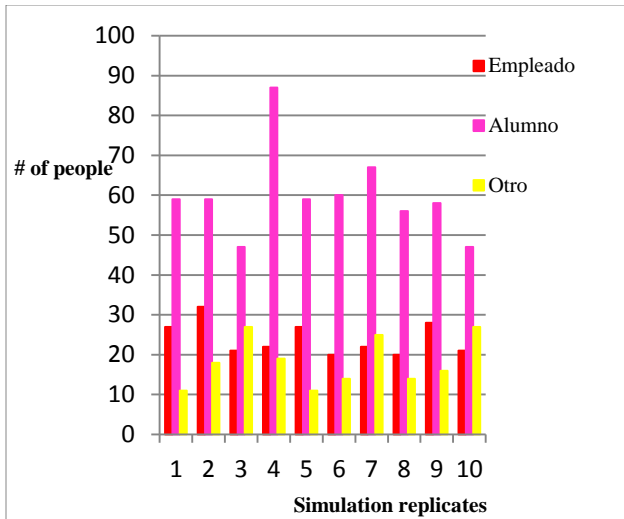


Figure 8. Number of people served

3. LOCATION MODEL

The MCLP model (Maximal Covering Location Problem), proposed by Church and ReVelle (1974), is an alternative to address and consider the deficiencies of the model SCLM (Set Covering Location Model), maximizing the population coverage restricted to the number of ambulances available, making the best use of the available resources.

One of the problems associated with the fixed coverage model is that the number of facilities (resources) needed to meet the demands of each node is likely to exceed the existent amount. The model even treats the nodes identically, which means that it is equally important to cover a demand node requiring 10 visits, to one that generates 100 per year (Daskin, 1995). These two concerns are considered to determine the number of facilities (resources) to be located and maximize the number of covered claims, this is exactly what the maximum coverage model aims; in order to formulate this model the follow definitions are used:

$$\max: \sum_i h_i Z_i \quad (1)$$

$$Z_i \leq \sum X_j \forall i \quad (2)$$

$$\sum_j X_j \leq P \quad (3)$$

From equation (1) h_i denotes the demand of node i , Z_i is a binary variable which equals 1 if the node is covered, 0 otherwise; of equation (2) X_j is also a binary variable which will value 1 if the ambulance is located at the site j , 0 otherwise; of equation (3) P value represents the total number of ambulances to locate.

The result gave the following table showing the ambulance and the zone where it was located, Table 7.

Table 7. Relationship between ambulance and zone covered

Ambulance	Zone
1	8
2	5
3	3
4	12

4. RESULTS

The solution of the location model is implemented in the simulation model to evaluate the results, showing a decrease on the transport time and therefore the response time, as shown in Figure 9.

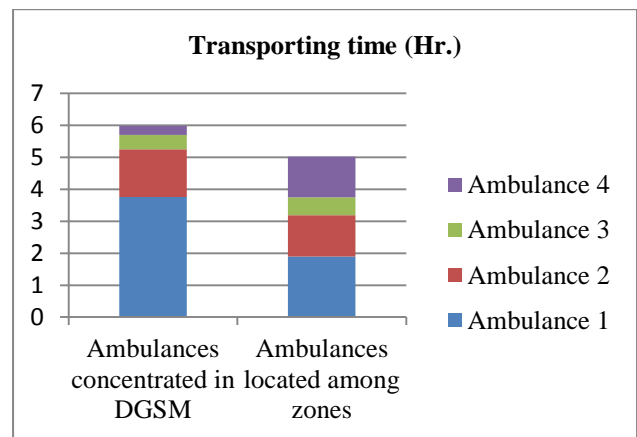


Figure 9. Graphical comparison between the original system and the proposed model

As noted in the chart above (Figure 9), there is a decrease of 16.1%, and a better distribution of labor between ambulances, generating savings in terms of maintenance and fuel, among others. Appreciating an even more efficient service.

5. CONCLUSIONS

The discrete event simulation is a useful tool for analyzing the system in question and it is possible to develop models able to represent satisfactorily all the phenomenon included on the system's activities. These models made possible the diverse scenarios experimentation with a statistically acceptable reliability, evaluating escenarios with an increased demand and others to reduce the response time; therefore, the combined use of optimization techniques, such as zoning

and simulation, improves the system's optimal values search; allowing the simulation and analysis of a large number of alternatives.

ACKNOWLEDGMENTS

We thank the Direction of Medical Services at the University of Mexico, especially to Fernando Roldan Espinoza who provided access to the records used for data extraction and his wife Esther Perez Segura who provided the initial contact with the agency. Likewise, we thank Dr. Idalia Flores de la Mota for his objective oversight during the project.

REFERENCES

Church, R L., Reville, C. 1974. The maximal covering location problem. *Papers of the Regional Science Association*, 32, 101 – 118.

Daskin S. Mark. "Network and Discrete Location. Models, Algorithms, and Applications". Ed. Wiley, 1995. pp. 92 - 95.

Flores, I., Cortés, M. 2006. *Simulation Notes*. Mexico, National Autonomus University of Mexico.

SIMIO LLC. 2010. *Introduction to SIMIO*.

Pérez, K, Cardona, L, Gómez, S, Olarte, T, Escudero, P. 2008. Simulation and Optimization in a Health Center in Medellín, Colombia. *Proceedings of the Winter Simulation Conference*. 1362 – 1367, December 7-10, InterContinental Hotel, Miami, Florida, USA.

AUTHOR'S BIOGRAPHY

Jose Alexander Vindel studied Industrial Engineering at University of the Valley of Mexico (UVM), he's currently studying a Masters in Operations Research, and his lines of interest are logistics and simulation.

SIMULATION OF THE OPERATION OF A METRO STATION

Jorge Andrés García^(a), Idalia Flores^(b)

^(a) Facultad de Ingeniería, UNAM

^(b) Facultad de Ingeniería, UNAM

^(a) artaban@comunidad.unam.mx, ^(b) idalia@unam.mx

ABSTRACT

This document presents a simulation study carried out in a metro station in Mexico City, which was made in order to determine whether the station has sufficient capacity to meet passengers demand in hours of maximal influx (6 to 9 am) and to evaluate some scenarios of interest. The document begins by presenting an introduction to the metro station, then defines specifically the problem and presents the methodology followed; it presents the simulation model built in SIMIO and then shows the results. Finally, we give some conclusions about the operation of the station.

Keywords: metro simulation, simio, collective transport system, metro station.

1. INTRODUCTION

The **Constitucion de 1917** station is one of the main stations of the Collective Transport System (CTS) of Mexico City, in an average weekday, it receives an influx of over 110,000 passengers and about 18% of them access the station in the morning, from 6 to 9 am. In the next table, it is shown the busiest stations on an average weekday in 2011:

Table 1: Average Weekday Influx in the Busiest Stations

No.	Station	Line	Influx
1	Cuatro Caminos	2	130,511
2	Indios verdes	3	128,417
3	Constitución de 1917	8	111,188
4	Pantitlán	9	106,643
5	Pantitlán	A	101,723

The station is located on Ermita Avenue, almost at the cross with Periferico Avenue. It is classified as a surface terminal that belongs to the Line 8 of the CTS, which does not link with any other line of the transport system. To the north of the station there are 2 bridges that serve as access and exit. To the south there is a bridge that

serves only as entry and another that serves only as exit. In this direction, there is a Bus Terminal that has more than 21 routes, which connects to the south, central, north and east of the city.

The Station is a multimodal transfer center that connects the south-eastern region of Mexico City.

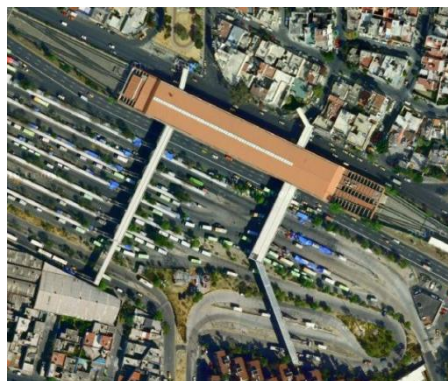


Figure 1: Aerial view of Constitucion de 1917 station

The Station has 2 ticket offices for selling tickets, each of them located at the longitudinal ends of the station.

It was decided to make the study because the Constitucion of 1917 station is one of the busiest terminals and the highest passenger flow occurs from 6 to 9 am on a weekday.

It is common at that time, that the lines to buy tickets exceed the capacity of the available space and invade other areas. For example the Northeast access stairs and the south corridor exit.

The station also presents saturation on the platform, to a point that it is not possible to access it, jeopardizing the safety of passengers.

Different factors has been widely studied in metro stations. There are some studies related to the behavior of passengers during boarding and alighting trains (Zhang et al., 2006), or the impact that the size of the access gates has on the flow of passengers (Hoogendoorn and Daamen, 2004).

Other studies are focus on specific factors such as pedestrian flow (Cheung and Lam, 1997), route selection (Cheung and Lam, 1998) or speed-flow relationships (Daly et al., 1991). In this case, we decided to focus on the relationships between passengers, ticket offices and the platform.

The present study aims to determine whether the station has, at this time, sufficient capacity to meet passengers demand and to evaluate some scenarios of interest such as including ticket machines, or the possible impact that the decrease of passengers will have due to the opening of a new metro line.



Figure 2: Pictures of Constitucion de 1917 station

2. PROBLEM DEFINITION

The following research questions are formulated to serve as a guide during the study:

- Is there sufficient capacity at the ticket office to deal the passengers demand?
- What is the average time that a person should expect to wait from the moment he reaches the station until he leaves on a train?
- Is there enough capacity on the facilities or are they overwhelmed by the number of passengers?

The scope of the investigation is limited to the Constitucion de 1917 station, which belongs to the Line 8 of the CTS; we study the influx of passengers on weekdays and from 6 to 9 am, which are the maximal influx hours.

We only consider the people who arrive to the station *from outside of the system*, and we do not consider the passengers that come from the previous station because they are a low number at that hour.

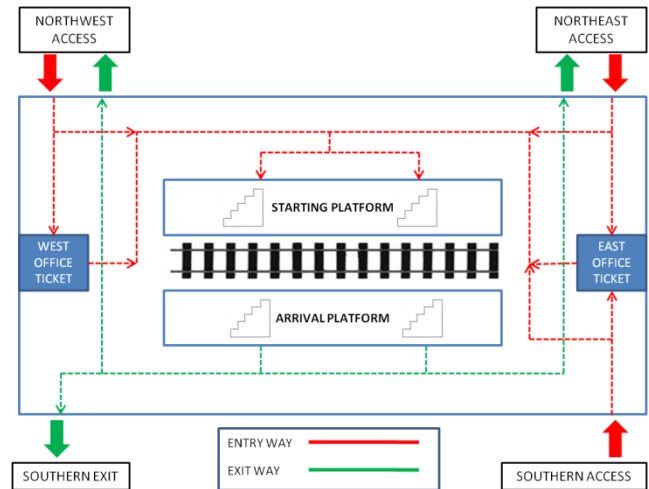


Figure 3: Diagram of the System

The objective is to obtain descriptive measures of the performance of Constitucion de 1917 station, throughout a simulation study that models waiting times at ticket offices and on the platform, determine whether it has sufficient capacity and to evaluate some scenarios of interest.

3. METHODOLOGY

The order in which the research was made followed the next methodology (Flores, 2006):

3.1. Problem definition

Here we determined the general objective and also the specifics ones of the research, the scope, and resources needed to carry it out.

3.2. System conceptualization

Once the research problem had been defined, we determined *which aspects or factors are the most relevant* and have the greatest explanatory behavior of the phenomenon, to decide whether to include them in the model and with what level of detail.

3.3. Data collecting

Once the system conceptualization was completed, we determined the information we had available, if it was reliable and what other information was needed to be collected according to the requirements of the model.

3.4. Model formulation

SIMIO software was selected to carry out the simulation due to their robustness and ease of use. We constructed a

model that incorporates the relevant aspects defined above.

3.5. Verification and validation of the model

Some tests were performed to find and correct logic errors in the model and other tests were made to ensure that the model results maintain a correspondence with the real system, so the model could adequately predict actual system behavior within the defined framework.

3.6. Design of experiments

In this part we defined scenarios of interest and they were expressed in terms of the parameters that will experience change.

3.7. Data analysis

Here we compile the obtained results and some conclusions were drawn about the current operation of the system.

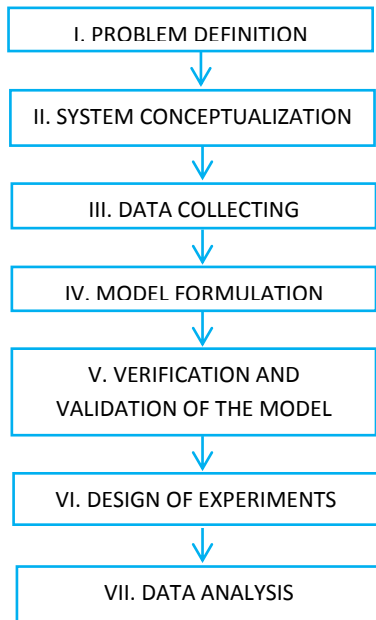


Figure 4: Methodology Followed

4. SIMULATION MODEL

4.1. System conceptualization

On the definition of the objective of this study, we determined the elements that are relevant for modeling the system. In the following diagram it can be seen that the system has three entries, corresponding to the doors: *Northwest*, *Northeast* and *Southern Access*.

There are two ticket offices which are independent one from another, so a passenger that is at any of the ticket offices can't reach the other from there because there is a physical barrier.

Finally we have the *platform*, which is the space where passengers wait for the train to arrive.

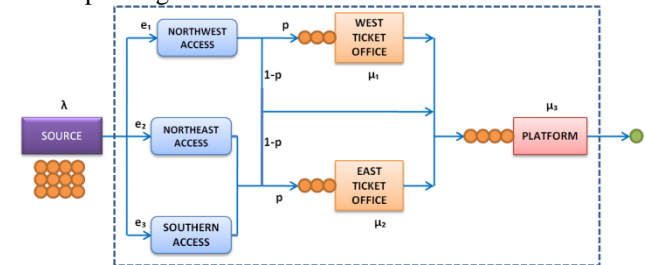


Figure 5: Diagram of the Process

4.2. Data collecting

Most of the information related to the operation of the station was obtained from the website of the CTS where they provide many useful data. However, it was necessary to take field samples to determine: the proportion of arrival of passengers associated with the access doors, the service times of the ticket offices and the departure times of the trains.

It should be mentioned that the collection of data also served to validate some of the data provided by CTS in its page. The data collection was taken on these days: Monday, Wednesday, and Friday; from 06:00 to 09:00.

4.3. Model formulation

The model was built as a system with one source that generates entities, any of them can enter to the station by one of the three accesses and follows a path that divides into two at each ticket office. There, for every entity, is a probability p to buy a ticket (therefore the entity goes into the waiting line) and a probability $1-p$ to go straight to the platform, where the entity waits until a train arrives.

As mentioned above the software selected to carry out the simulation was SIMIO. We used the following objects:

4.3.1. Entities

We used two types of entities. The first type is the *passengers* and four types of passengers were created, each with a different movement speed to represent the passengers that walk at different speed. The other type of entities is the *trains* which are generated at the station.

4.3.2. Sources

We used two sources. The first one generates the passenger entities according to an exponential distribution. During the time considered in this investigation, the arrivals of passengers change throughout the time, so it was decided to change the parameter of arrivals in a stepwise way.

The parameter starts with a fixed value and then starts to increase until a maximum, after it reaches it, the parameter decreases. The following table shows the parameter values associated to time:

Table 2. Arrival Rate of Passengers per Hour

No	Time	λ	Classification
1	6:00-6:30	3,889.64	Minimal
2	6:30-7:00	5,834.46	Regular
3	7:00-7:30	9,724.10	Maximal
4	7:30-8:00	9,724.10	Máximal
5	8:00-8:30	5,834.46	Regular
6	8:30-9:00	3,889.64	Minimal

The second source generates the train entities that were properly adjusted to a triangular probability distribution.

4.3.3. Servers

There are two *servers*, which correspond to the ticket offices; each one on either side of the station. As mentioned before there is no path that connects them, so they are considered independent. Each ticket office can have up to two people at service and they have a single queue which follows a FIFO (First In First Out) discipline. The distribution of time between services was adjusted to a triangular probability distribution.

4.3.4. Combiner

A *combiner* was used to represent the platform where the passengers wait until a train arrives. This object was chosen because the arrival of a train can be modeled as an event where **one** train is combined with n number of passengers, where n is the minimal between the maximal train's capacity and the number of passengers waiting in the platform at that moment:

$$n = \min\{\text{train's capacity}, \text{passengers waiting}\} \quad (1)$$

4.3.5. Sink

A *sink* is an object that destroys the entities; in this case we only used one sink to destroy both types of entities.

4.3.6. Paths and Nodes

The *paths* were used to determine the trajectory of the entities within the system and the *nodes* to represent the points where the entities select one of many paths. For example, the path that comes from the passengers source has a node which represents the decision of selecting one of the three possible entries; each one goes to a different door (northwest, northeast and south). The probability of selecting one of them is e_i such that:

$$e_1 + e_2 + e_3 = 1 \quad (2)$$

It is noteworthy that the model dimensions are scaled with the actual facility, and with the use of the *path* object (that takes some time to be traveled by an entity depending on the distance it has), the model better reflects the movement of passengers within the station.

Below there are some images of the simulation model:



Figure 6: East Ticket Office



Figure 7: West Ticket Office



Figure 8: Platform

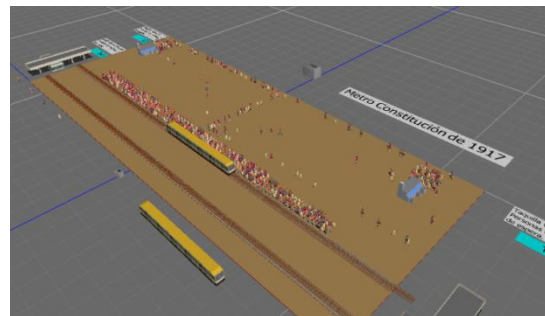


Figure 9: Simulation with SIMIO

4.4. Verification and validation of the model

To validate the model we used the following techniques:

4.4.1. Comparison with the real system

We ran a simulation using the parameter of maximal influx and we compared the number of people waiting in the queue on both ticket offices and on the platform; the results obtained were similar to the amount of passengers in the real system.

4.4.2. Behavior in extreme cases

We ran a simulation with significant delays on train departures and a large agglomeration of passengers was produced on the platform to the point of saturating it. This has happened on rare occasions in the real system, with similar results.

In another test we significantly decreased the influx of passengers to the station and we noticed that there were no queues on both servers (ticket offices) as well as on the platform. That situation is common to see in the real system at times when the influx of passengers is low.

5. DESIGN OF EXPERIMENTS

5.1. Scenario A. Current conditions

We ran a simulation of the system under the conditions in which it works currently considering that each ticket office is working with two servers, and the arrivals of the trains change with the time as shown in the table 2.

The purpose is to know the measurements of the system's performance during normal conditions at peak traffic hours.

5.2. Scenario B. Two servers remain closed

In this scenario we simulated the event in which one of the servers on the east side and another on the west side ticket office, are disabled to operate, either because of absenteeism of the workers or not having the necessary equipment or any other case.

The purpose is to determine the impact to the system when the ticket offices have only one server during peak traffic hours.

5.3. Scenario C. Ticket vending machines

We simulated the event that there are installed two ticket vending machines, one on each side of the station next to the ticket offices. We assume that the speed of service of the machines is equal to the time of service of the server in the ticket office.

The purpose is to determine the possible reduction of waiting time at the ticket offices that these ticket vending machines can provide.

5.4. Scenario D. A decrease on the influx

We simulated the scenario that the influx of passengers to the station decreases by 10% due to implementation of

Line 12 of the CTS, so the amount of people from the south-east region of the city would be reduced.

The purpose is to assess the potential impact on the station due to the expected reduction of passenger influx.

5.5. Scenario E. Constant departure time

We wanted to know the impact on waiting times and number of people on the platform when the time between arrivals of the trains is constant, taking as the constant parameter the *mode* of the triangular distribution.

The purpose is to evaluate the change in the average waiting time and average number of passengers waiting on the platform when the arrivals between trains remain constant.

In this table there is a summary of the information about the scenarios considered above:

Table 3. Summary Table of Scenarios.

Scenario	Description
A	The simulation is run with current operation conditions.
B	One of the servers at each ticket office is disabled.
C	One ticket vending machine is installed at each side of the station.
D	There is a decrease of 10% on the arrival of passengers.
E	The time between the arrivals of the trains is constant.

6. RESULTS

The experiment consisted of running the simulation over the period considered (three hours), changing the parameter of arrivals according to the above table. There were 10 replicates of each experiment. This was repeated for each scenario considered.

Scenario A represents the measure of comparison with the rest. The results are shown below:

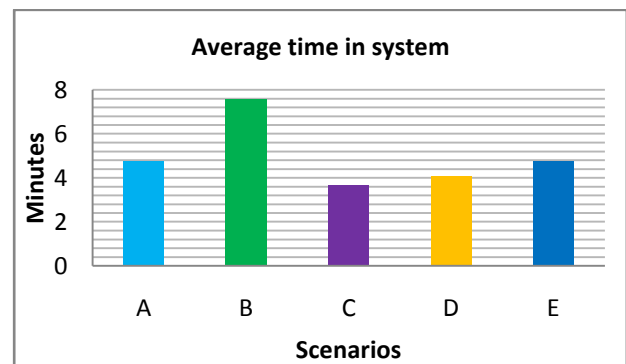


Figure 10: Average Time in System

The average time in the system is **5.2 minutes** under normal conditions. We can see that when there is only one

server on each side (scenario B), the time increases by almost 60%. In addition, if ticket vending machines are set up (scenario C) the average time in the system would be reduced by 25%.

The scenario D which considers a 10% decrease in the influx of passengers, has an impact of about 15% less on average time in system, a total of **4.1 minutes**.

Finally, if the arrivals of the trains have a constant time, it would not significantly affect the average time in system (Scenario E), which is **4.75 minutes**.

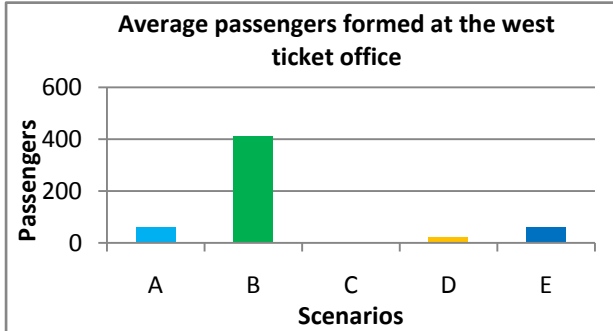


Figure 11: Average Passengers Formed at the West Ticket Office

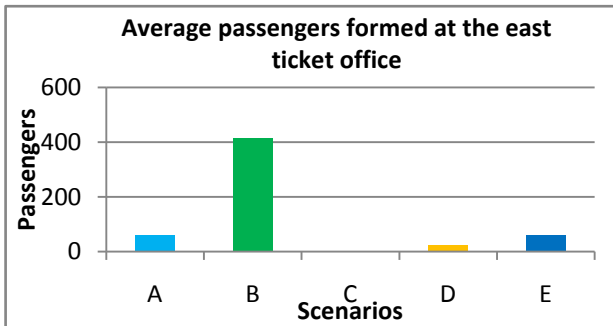


Figure 12: Average Passengers Formed at the East Ticket Office

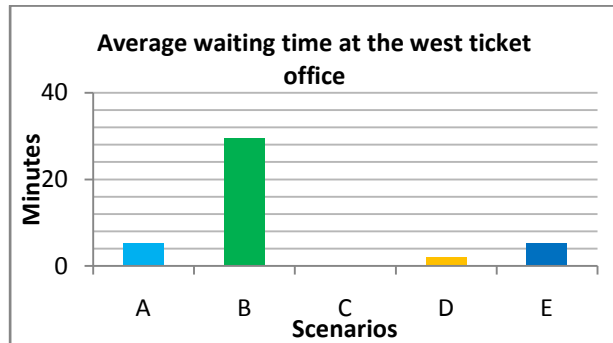


Figure 13: Average Waiting Time at the West Ticket Office

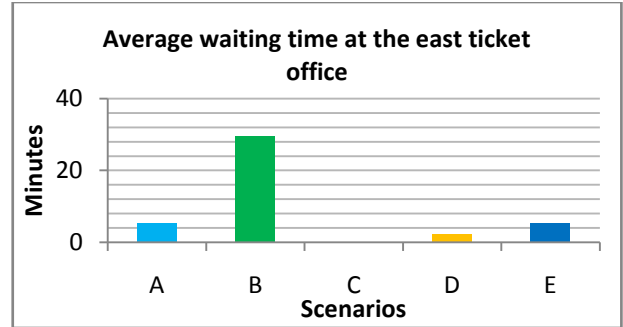


Figure 14: Average Waiting Time at the East Ticket Office

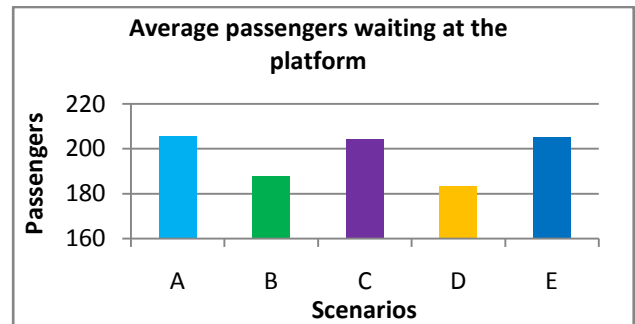


Figure 15: Average Passengers Waiting at the Platform

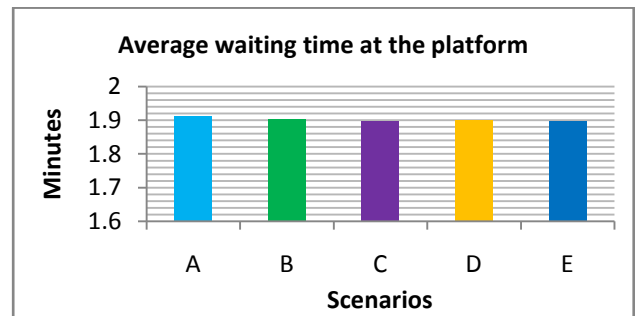


Figure 16: Average Waiting Time at the Platform

On the platform there were **205.6 passengers** and **1.91 minutes** on average waiting time for the A scenario. For B scenario, these values decreased slightly to **187.6 passengers** and **1.9 minutes**. This may be because of the lower capacity of the servers which implies that a greater amount of passengers are stopped in them. For the C scenario, there were **204.4 passengers** and **1.89 minutes** and it does not represent a significant change. In the D scenario there were **183.5 passengers** and **1.89 minutes**. For the E scenario there were **205.2 passengers** and **1.89 minutes**, a little variation compared to scenario A.

7. CONCLUSIONS

This study has been useful in understanding the impact of some operational policies on the service to passengers. It

has also allowed a better understanding of the behavior of passenger arrivals.

With the results obtained it is possible to perform a cost-benefit analysis to evaluate the installation of ticket vending machines. Simulation has been a useful tool in studying stochastic systems.

There is sufficient capacity to meet the passengers demand in peak traffic hours. In the case of the ticket offices, while both work with two servers (cashiers), the number of passengers that are lined up to buy tickets is kept under control, but if any of them works with less servers then the number of people increases significantly, leading to a potentially hazardous situation. For the platform there is a similar case. The crowding of passengers that is produced there is generated because of the preference to travel sitting rather than standing, so the passengers remain in the platform until they can get a seat on a train. This situation increases the number of passengers waiting in the platform.

The servers at the ticket offices have a major impact on the total time in the system. Although approximately 80% of the passengers do not buy a ticket at the considered hours, the largest time that is spent in the system take place at the ticket offices, where the wait in the queue is more than double than the wait on the platform. If one of the servers could not be open in any of the ticket offices, it would generate an increase of seven times in passengers waiting, and five times in waiting times, which is a significant impact. On the other hand, the use of ticket vending machines greatly reduces important queue length and waiting times, in such a way that could be a viable option to improve the overall performance of the station.

If the time between arrivals of the trains is constant, this would not imply a reduction on the number of passengers that are waiting on the platform. According to the data obtained, the decrease of passengers at the platform is minimal, indicating that the current operating times are satisfactory.

A decrease in the influx flow is equivalent to the installation of ticket vending machines. We can observe a similar behavior in the system's variables when we increase the capacity of the servers and when we decrease the influx of the passengers; except in the average number of passengers waiting on the platform, where the C scenario is higher than the D in approximately 20 people. Therefore, it would not be advisable to install ticket vending machines if a decrease of passengers influx is expected.

REFERENCES

Cheung, C.Y., Lam, W.H.K., 1997. A study of the bi-directional pedestrian flow characteristics in the

Hong Kong mass transit railway stations. *Journal of Transportation Engineering*, 1607-1619.

Cheung, C.Y., Lam, W.H.K., 1998. Pedestrian route choices between escalator and stairway in MTR stations. *Journal of Transportation Engineering*, Vol. 124, No. 3, pp. 277-285.

Coss Bu, Raúl. 2009. *Simulación. Un enfoque práctico*. 2da. Edición, México. Limusa

Daly, P.N., McGrath, F., Annesley T.J., 1991 Pedestrian speed/flow relationships for underground stations. *Traffic Engineering and Control*, London, Vol. 32, Issue 2, pp. 75-78.

Dirección General del STC, *Evaluación externa 2010 del diseño e implementación de la política de Transporte Colectivo de Pasajeros en el Distrito Federal*. México

Flores de la Mota, Idalia and Elizondo Cortés Mayra, 2006. *Apuntes de simulación*. México, UNAM.

Gutiérrez González, Eduardo. 2011. *Fundamentos de la teoría de las probabilidades para ingeniería y ciencias*. 2da edición. México. Libudi

Gutiérrez González, Eduardo. 2007. *Tablas y fórmulas estadísticas* 1ra ed, México. Nauka Educación.

Hoogendoorn, S.P., Daamen, W., 2004. Design assessment of Lisbon transfer stations using microscopic pedestrian simulation. *Computers in Railways IX*. pp. 135-147, 2004, Dresden, Germany.

Qi, Zhang et al. 2006. Modeling and simulation of passenger alighting and boarding movement in Beijing metro stations. *Transportation Research Part C*, Vol. 16, 635-649.

Ríos Insúa, David et. al. 2009. *Simulación. Métodos y aplicaciones*. 2da edición, México. Alfa Omega.

AUTHOR'S BIOGRAPHY

Jorge Andres Garcia studied Industrial Management at the Unidad Profesional Interdisciplinaria de Ingeniería y Ciencias Sociales y Administrativas (UPIICSA). He is currently studying a Master in Operations Research. His line of research is Optimization in Production Planning.

Idalia Flores de la Mota studied mathematics at the Sciences Faculty of the UNAM, then a Master and a Ph.D. in Operations Research at the Engineering Faculty. She has taught at various universities and has participated in national and international conferences. Her lines of research are Simulation and Optimization of the Supply Chain.

AUTOMATED VERIFICATION OF CARDIOVASCULAR MODELS WITH CONTINUOUS INTEGRATION TOOLS

M. Bachler^(a), B. Hametner^(b), C. Mayer^(c), J. Kropf^(d), M. Gira^(e), S. Wassertheurer^(f)

^{(a) - (f)}AIT Austrian Institute of Technology GmbH, Health & Environment Department, Biomedical Systems
^{(a) - (b)}Vienna University of Technology, Institute for Analysis and Scientific Computing

^(a)martin.bachler@student.tuwien.ac.at, ^(b)bernhard.hametner@ait.ac.at, ^(c)christopher.mayer@ait.ac.at,
^(d)johannes.kropf@ait.ac.at, ^(e)matthias.gira@ait.ac.at, ^(f)siegfried.wassertheurer@ait.ac.at

ABSTRACT

Models in general, but especially in medicine, need extensive testing and verification to ensure that they do not contain errors and produce correct results. Traditionally, this happens after completing the development. In this work an approach to automated and continuous testing, verification and documentation based on a continuous integration tool is presented. This practice has several advantages in comparison to the traditional way of verification. As the model is verified after every single change that is made to it, one benefit is the earlier and more precise tracing of errors. Another advantage is the aggregation of code generation, software building, testing, verifying and documentation in one tool to ensure maximum automation and to reduce expenditure of time. Furthermore, due to the integration of central versioning systems, it makes working in development teams easier. In this work, the development processes of two cardiovascular models are incorporated into a continuous integration system.

Keywords: continuous integration, cardiovascular model, model verification, development tools

1. INTRODUCTION

In contrast to model checking, which ensures the formal validity of a software system, model verification tests the correctness of the results derived from a given model. In medicine, the verification of physiologic models can be done, for example, by comparing these results with real world measurements.

This verification process traditionally starts after the development of the model is completed and executable software has been build, whereas the building process itself is usually carried out manually and step by step. Finally, documentation of model and verification is produced by hand. All these steps have to be carried out each time the model is changed.

Figure 1 shows a diagram of this typical development approach, e.g. as described by Bachler et al. (2011).

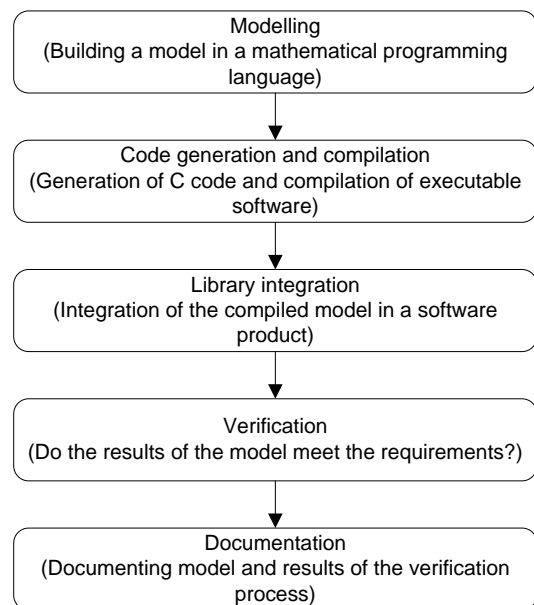


Figure 1: Typical Development Process of a Software Product based on a Model

Among others, one big disadvantage of this approach is the late verification of the model. Finding an error in the fourth step (verification) of the process usually forces the developer to go back to step two (code generation and compilation) or even step one (modelling), depending on the mistake.

Another drawback can be found in environments where the model is subject to continual changes. Usually, several changes are made to the model before the building process is started again. Therefore it is not easy to track back errors found during the verification and relate them to a specific change.

Although these issues are addressed by best practice paradigms such as “test early, test often” they tend to reoccur in many different software development processes, not only in model based algorithm development. Following these fundamental practices seems to be harder than one would expect. The automation of the entire building process can help to enhance the frequency of testing and verification (Duvall, Matyas, and Glover 2007).

In this work the automation of the development processes of two software products containing cardiovascular models using the continuous integration tool and open source software Jenkins in the version 1.473 is described.

2. METHODS AND MATERIALS

In the first part of this chapter, two concrete software products containing cardiovascular models are presented. Their development processes, which were transferred into a continuous integration system, will be described. One of the models is dealing with the calculation of certain parameters using pulse wave analysis, the other is used for the detection of features in electrocardiography.

The second part deals with continuous integration tools in general and the software tool Jenkins in particular.

2.1. Pulse Wave Analysis

Pulse wave analysis (PWA) in general deals with the determination of several cardiovascular parameters calculated from the pulse wave travelling through human arteries. The AIT Austrian Institute of Technology GmbH developed a non-invasive and easy to use method based on recordings of the pulse wave by means of an occlusive blood pressure cuff (Wassertheurer, Mayer, and Breitenacker 2008; Wassertheurer et al. 2010; Hametner 2011; Hametner et al. 2012; Weber et al. 2011; Wassertheurer, Hametner, and Weber 2011; Nunan et al. 2012).

Certain software algorithms for the calculation of parameters for the aortic blood pressure, arterial stiffness and wave reflection are part of this method. As this system is subject to ongoing research, the underlying models are changed continually. Furthermore, several developers are involved in the modelling and building process. Hence, these models and algorithms are perfect candidates to be incorporated in a continuous integration system.

The model based algorithms used for the pulse wave analysis are developed in the mathematical programming language MathWorks MATLAB® in the version R2007b and converted to C code using Embedded MATLAB®. This C code is compiled into dynamic link libraries using standard C compilers and integrated in a software product written in the programming language Java. The original development process followed the steps shown in Figure 1.

The whole development process is summarised in Figure 2. In the original setting, the transition from MATLAB® code to the DLL was semi-automatic using shell-scripts. The integration of the DLL in the Java-Environment, software tests and verification as well as the documentation was done manually.

2.2. Electrocardiography

Electrocardiography (ECG) is the measurement of the electric activity of the cardiac muscle. It is a non-invasive, painless technique and is widely used in the

assessment of heart failures. The tracing of one heartbeat consists of a P wave representing the atrial depolarization, a QRS complex showing the ventricular depolarization and a T wave at the ventricular repolarisation.

The software algorithm is able to detect beginning, peak and end of the QRS complex, the P and the T wave of each heartbeat automatically and in real time (Bachler et al. 2011).

The results of this algorithm are verified by comparing them to annotations made by medical experts with data from different ECG databases (Goldberger et al. 2000).

Like the algorithms for pulse wave analysis, this software is written in MATLAB®, converted to C code, compiled to a dynamic link library and integrated in a software product written in Java (shown in Figure 2). Again, the transition from MATLAB® code to the DLL is semi-automatic, whereas integration, verification and documentation are done by hand. Therefore several build steps from the pulse wave analysis algorithm can be reused.

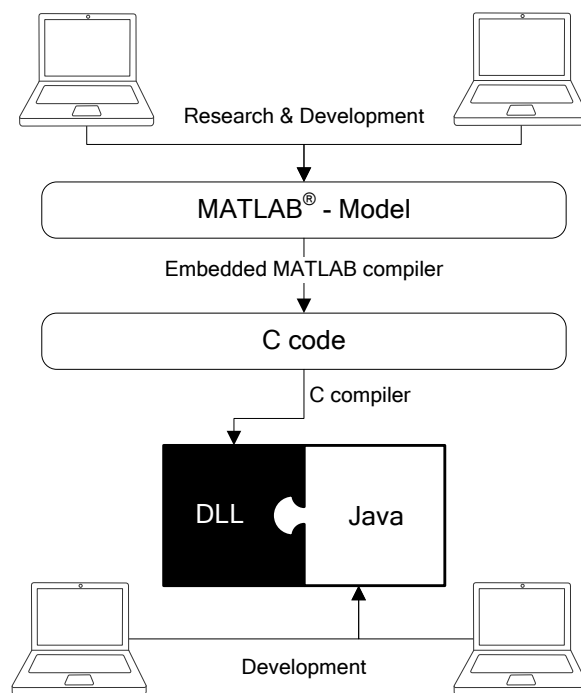


Figure 2: Development of different parts of the software system for Pulse Wave Analysis and ECG Analysis

2.3. Continuous Integration

Continuous integration helps implementing “best practices” in software development by automating the whole building process (code generation, compilation, testing and verification) and the documentation thereof (Duvall, Matyas, and Glover 2007).

Focused mainly on the principles of centralisation, “test early, test often”, automation of build and documentation, and feedback, a continuous integration system usually features (as shown in Figure 3):

- A version control repository,
- A continuous integration server,
- Build scripts, and
- A feedback mechanism.

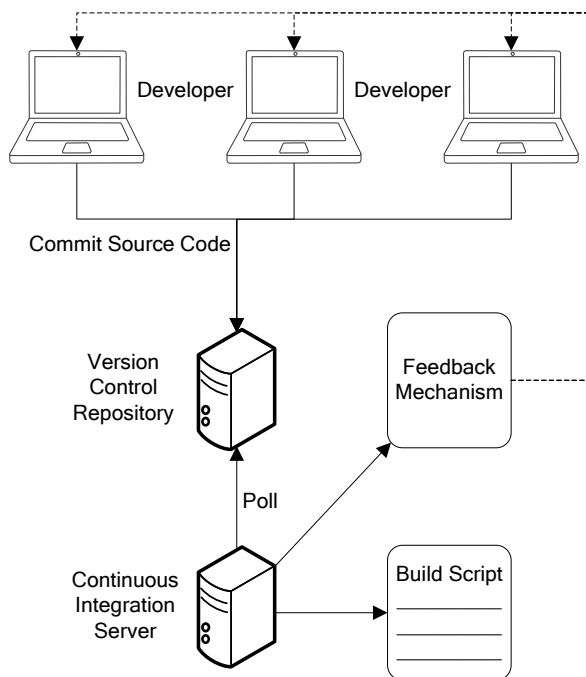


Figure 3: Basic Components of a Continuous Integration System (Duvall, Matyas, and Glover 2007)

2.3.1. Centralisation

In research and development teams, usually a file server is utilized as central data storage accessible to all team members. Typically a version control system such as Concurrent Versions System (CVS) or Apache Subversion (SVN) is used to keep track of all changes made to the files.

Continuous integration systems support the practice of using central versioning systems and integrate them seamlessly without any change necessary. A central continuous integration server frequently checks for changes in the source code stored in the version control system. If a change is detected, the building process is carried out according to some predefined build scripts.

2.3.2. Test Early, Test Often

Testing is part of the building process. Automated software tests (including the verification of the results obtained using the model) are executed each time after the software was compiled. As the building process is started after each change in the source code that is submitted to the version control system, the only thing developers need to do is to commit their code every time they add or change something. As a consequence, every single change leads to a full test and verification of the whole system and therefore also the model. This narrows down bug tracking to where did the error occur (i.e. in which development step) and when did it occur

(i.e. after which change in the model), therefore making errors a lot easier to resolve (Duvall, Matyas, and Glover 2007).

2.3.3. Automation of Build and Documentation

With tools such as GNU Make (originating from UNIX systems and mainly used for the C programming language), Apache Ant and Apache Maven (primarily for development in Java), build automation tools are already widely used. But instead of running these tools on the machines of developers (which probably prevents them from doing something else in the meantime), they are incorporated in the continuous integration system and executed on a dedicated continuous integration server.

Therefore, existing build scripts can be reused easily in a continuous integration system. Furthermore, different sorts of scripts can be combined to create a fully automated build environment.

In addition to the compilation process and automated testing, sophisticated scripts allow the automated verification of the results of the model based algorithms described above and the automated generation of verification reports.

2.3.4. Feedback

As building, testing and documentation is completely taken over and automated by the continuous integration system, there has to be a mechanism to inform the developer of success or errors in the build. Usually, the continuous integration server is configured to send an e-mail to either a predefined address (probably the coordinator of the team) or to the developer that initiated the building process by committing code changes.

If errors occur during the building process, the feedback contains detailed descriptions of them to allow fast and easy debugging. Otherwise, build artifacts are generated. These usually consist of executable software or compiled libraries, test results and verification reports.

2.4. The Continuous Integration tool Jenkins

Jenkins is an extendable, web based continuous integration tool written in Java and published under the open source MIT license. It supports several build tools such as Apache Ant, different versioning systems such as Apache Subversion and automatic software testing tools. It is a fork (spin-off) from the continuous integration system Hudson supported by Oracle (Wiest 2010).

Originally, it was designed for Java projects only, but with the capability of using plugins its features can be extended far beyond this limited purpose (Wiest 2010).

Projects can be created and managed via a web interface using an ordinary browser. Therefore, every developer can access the same configuration data, adapt them or check the status of a certain project (Wiest 2010).

Jenkins is not limited to one central continuous integration server but can incorporate several distinctive nodes running different operating systems. This feature is especially essential if the source code has to be compiled for different platforms such as Linux, Mac OS X or Microsoft Windows, but can also help distributing the work load to several building machines (Wiest 2010).

2.5. Using Jenkins for the Development of the Algorithms based on Cardiovascular Models

As described earlier in this section, some parts of the development process were already automated using shell scripts. Also the version control system Apache Subversion in the version 1.6 was already in use. So, when implementing Jenkins with the projects for pulse wave analysis and ECG analysis, the main work was the combination of all single steps into one completely automated process. The biggest challenge was the creation of automated verification reports. In contrast to standard software tests, which primarily give a yes/no-answer to the question of the absence of runtime-bugs, verification has to quantify the difference between the results obtained using the model and a reference. Therefore, the report of the verification process cannot be simply the output of a standard software test but has to include extensive statistical analyses of the results.

2.5.1. Assessment of the Initial Situation

To create an overview of the steps necessary for porting the whole development process to Jenkins, an assessment of the initial situation has to be performed:

1. Modelling: The models used in pulse wave analysis and ECG analysis are written in the programming language MATLAB[®]. As this is the creative part of the development process done by researchers and developers, it is not possible to automate this task.
2. Code generation: Using scripts written in MATLAB[®], models and algorithms from step 1 are converted to code in the C programming language.
3. Code compilation: In this step, dynamic libraries are created for Linux, Mac OS X and Microsoft Windows. Therefore, three building machines with different operating systems are in use. Shell scripts for these compilation processes already exist, but they have to be executed on each machine manually.
4. Library integration: The three libraries built in step 3 are integrated in a Java project, which again is build using a shell script on one of the machines mentioned in the step above.
5. Verification: The verification consists basically of three parts: verifying the MATLAB[®] model itself, verifying the libraries integrated in the Java project and running automated software tests. For the first part, a MATLAB[®] script is used to compare the results derived using the

models with a reference and to quantify the differences. The libraries are verified manually on their respective operating system (Linux, Mac OS X and Microsoft Windows) by executing the Java software, loading the reference data, performing the calculations and exporting the results. These results are then compared and quantified using a MATLAB[®] script. The automated software tests are executed using a shell script and the testing framework TestNG (Beust and Suleiman 2007).

6. Documentation: The documentation of the results of the verification is done manually by summarising all results generated in step 5 and describing the changes since the last version of the software.

2.5.2. Adaption to a Fully Automated Continuous Integration

Several steps were taken to adapt the existing development procedures and to integrate them in Jenkins:

1. Jenkins was configured to access the version control repository and to frequently check for modifications of the model. If a modification is detected, it will perform a clean check-out of the source code and start the whole building process.
2. To automatically run MATLAB[®] scripts, MATLAB[®] was installed on the same machine as Jenkins. These scripts can be executed by Jenkins through a shell script which starts MATLAB[®] without user interface and runs the MATLAB[®] script. These scripts are used for code generation and verification.
3. To compile the C source code for different operating systems, three machines were set up to run Jenkins: one Linux, one Mac OS X and one Microsoft Windows machine. Also, three Jenkins projects were created, one for each platform. Each was configured to be built only on one designated machine using the appropriate shell scripts. The scripts could be reused without modification (Berg 2012).
4. The verification of the libraries was automated by transferring the evaluation of the reference data to the automated TestNG tests. Instead of loading the reference data and exporting the results manually, these steps have been added to the already existing TestNG tests. These tests are executed by Jenkins automatically after compilation is finished.
5. To automate the documentation of the verification as far as possible, the MATLAB[®] script quantifying the differences between model, libraries and reference was adapted to write these results into a file. A source file in the document markup language LaTeX was

prepared to automatically read and summarise these results. The LaTeX typesetting system is executed by Jenkins after all other development steps have been finished successfully to produce a PDF document containing all results of the verification process. This document also features the possibility of adding text to allow a manual description of the results. Therefore, the repetitive part of the generation of the documentation was automated using Jenkins. The creative part, which includes a detailed description of the changes in the model as well as an interpretation and discussion of the results of the verification, is still left to researchers and developers.

3. RESULTS

Figures 4 and 5 present a qualitative comparison of the workflow before and after the introduction of the continuous integration system to the development process of the software products containing the cardiovascular models.

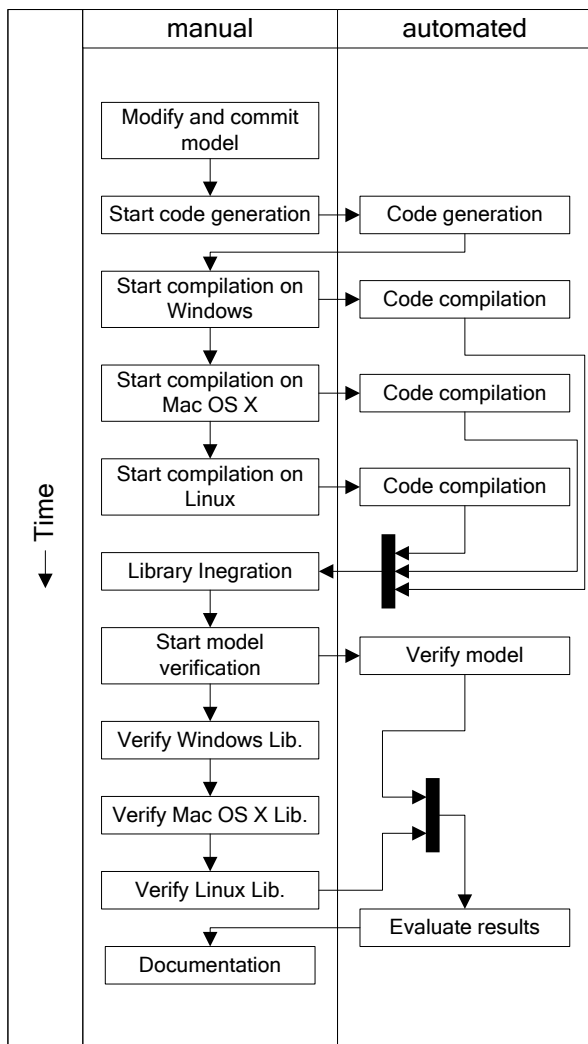


Figure 4: Manual and Automated Tasks in the Development Process without Continuous Integration

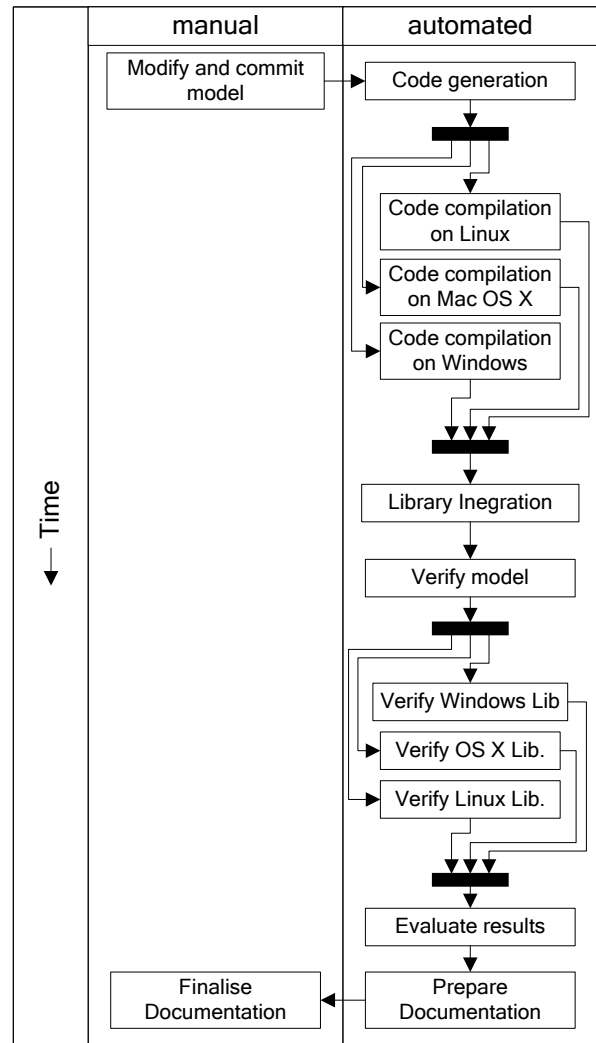


Figure 5: Manual and Automated Tasks in the Development Process with Continuous Integration

Table 1 gives an overview of the time spent by a single developer on different sorts of tasks, assuming that there are no errors in the model (please note that the given time spans are rough estimates and that the true values depend heavily on the amount of reference data used for verification and the time spent on the creative part of the documentation).

Table 1: Comparison of Time Spent by a single Developer on Different sorts of Tasks with and without a Continuous Integration System (CI)

Time spent by developer	Without CI	With CI
Overall	60 min	15 min
On repetitive tasks	45 min	0 min
On creative tasks	15 min	15 min

3.1. Discussion

The heavy overhead of repetitive tasks burdening the developer in a development process without a continuous integration system (see Table 1) usually lowers the frequency of code compilation, code testing

and model verification. Therefore, usually several changes are made to the model and only verified once. Assuming that one of these changes leads to an error during the verification process, it is hard to determine the source of the error as there are multiple possibilities. Shifting this overhead to the continuous integration system and triggering the whole build-and-verify-process after every single change that is made to the model leads to a higher frequency of builds and therefore a higher frequency of verifications. Errors are detected immediately and can be resolved in less time.

4. CONCLUSION

Using the continuous integration tool Jenkins and several of its extensions, the development, verification, and documentation processes of software systems containing cardiovascular models were automated. The developer is relieved of repetitive tasks and the frequency of model verifications during the development is raised. Lowering the expenditure of time of the building process due to automation and the time needed for the fixing of bugs because of earlier and more accurate error reports lead to a speed up of the release of new versions of the software.

REFERENCES

- Bachler, M., Mayer, C., Hametner, B., and Wassertheurer, S., 2011. Automatic detection of QRS complex, P and T wave in the electrocardiogram. *Abstractband / 21. Symposium Simulationstechnik: ASIM 2011*, 37. September 7-9, 2011, Winterthur, Switzerland.
- Berg, A., 2012. *Jenkins Continuous Integration Cookbook*. Birmingham:Packt Publishing Ltd.
- Beust, C., and Suleiman, H., 2007. *Next generation java™ testing: testing and advanced concepts*. Boston:Addison-Wesley Professional.
- Duvall P. M., Matyas S., Glover A., 2007. *Continuous Integration: Improving Software Quality and Reducing Risk*. Boston:Addison-Wesley Professional
- Goldberger, A. L. et al., 2000. PhysioBank, PhysioToolkit, and PhysioNet: Components of a New Research Resource for Complex Physiologic Signals. *Circulation* 101:e215-e220.
- Hametner, B., 2011. *Arterial Pulse Wave Analysis: Impact of Models for Impedance and Wave Reflection*. Doctoral thesis. Vienna University of Technology.
- Hametner B., Weber T., Mayer C., Kropf J., Wassertheurer S., 2012. Effects of Different Blood Flow Models on the Determination of Arterial Characteristic Impedance. *Preprints MATHMOD 2012 Vienna – Abstract Volume*. 2012:262.
- Nunan, D., Wassertheurer, S., Lasserson, D., Hametner, B., Fleming, S., Ward, A., and Heneghan, C., 2012. Assessment of central haemodynamics from a brachial cuff in a community setting. *BMC Cardiovascular Disorders* 12:48.
- Wassertheurer S., Mayer C., Breitenecker F., 2008. Modeling arterial and left ventricular coupling for non-invasive measurements. *Simulation Modelling Practice and Theory* 16:988-997.
- Wassertheurer S., Kropf J., van der Giet M., Baulmann J., Ammer M., Hametner B., Mayer C., Eber B., Magometschnigg D., 2010. A new oscillometric method for pulse wave analysis: comparison with a common tonometric method. *Journal of Human Hypertension* 24:498-504.
- Wassertheurer S., Hametner B., and Weber T., 2011. Model based estimation of aortic pulse wave velocity. *Artery Research* 5:162.
- Weber, T., Wassertheurer, S., Rammer, M., Maurer, E., Hametner, B., Mayer, C.C., Kropf, J., and Eber, B., 2011. Validation of a brachial cuff-based method for estimating central systolic blood pressure. *Hypertension* 58:825-832.
- Wiest, S., 2010. *Continuous Integration mit Hudson/Jenkins: Grundlagen und Praxiswissen für Einsteiger und Umsteiger*. Heidelberg:dpunkt Verlag.

OPTIMIZING VENTRICULAR WORK: A MATTER OF CONSTRAINTS

Bernhard Hametner^{(a),(b)}, Stephanie Parragh^(b), Christopher Mayer^(a),
Johannes Kropp^(a), Siegfried Wassertheurer^{(a),(b)}

^(a)AIT Austrian Institute of Technology GmbH, Vienna, Austria

^(b)Vienna University of Technology, Austria

bernhard.hametner@ait.ac.at, stephanie.parragh@tuwien.ac.at, christopher.mayer@ait.ac.at,
johannes.kropp@ait.ac.at, siegfried.wassertheurer@ait.ac.at

ABSTRACT

The analysis of aortic blood pressure and flow represent an important tool to predict cardiovascular risk. A Windkessel model relating pressure and flow, together with an optimal performance criterion of left-ventricular work, is used to generate the aortic flow pattern for a given central pressure curve. For the corresponding optimization problem, different physiologically relevant constraints are specified, but due to the limited number of degrees of freedom not all of them can be included at once. The optimization problem is solved with every possible combination of constraints and the resulting flow and pressure curves are analyzed. These waveforms show that the choice of constraints strongly affects the accuracy of the generated curves. Constraining aortic flow during diastole appears to be the best choice, but a physiologically shaped flow and pressure pattern cannot be achieved simultaneously with the applied objective function and constraints.

Keywords: pulse wave analysis, blood flow model, cardiovascular system, aortic pressure waveform

1. INTRODUCTION

The circulation of blood in the human cardiovascular system is determined by pressure and flow. Both state variables depend on the mechanisms of the heart and the properties of the vessels. Therefore they can be used to characterize the status of the cardiovascular system of a specific person, and several methods and parameters have been developed for this purpose, which are often subsumed as pulse wave analysis (PWA).

Beside systolic and diastolic blood pressure levels obtained from brachial pressure readings, also parameters reflecting arterial stiffness and wave reflection in the aorta are supposed to yield important information about cardiovascular risk. Their computation is based on analysis of central arterial waveforms of pressure and/or flow and thus require measurements thereof (Chirinos and Segers 2010b, Laurent et al. 2006, Mitchell 2009). See Fig. 1 for a stylized example of aortic pressure and flow waveforms.

Arterial pressure can be measured rather easily by

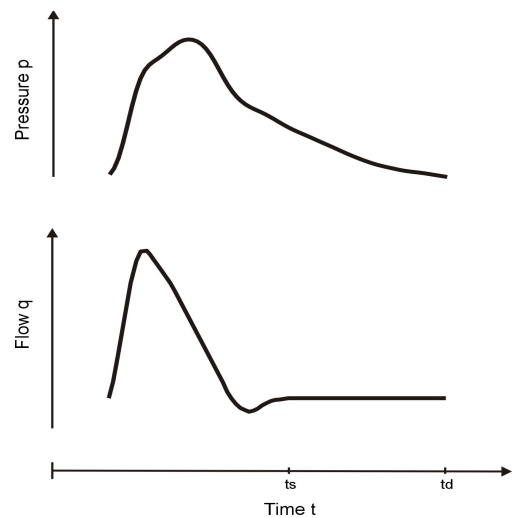


Figure 1: Exemplary waveforms of aortic blood pressure (upper panel) and flow (lower panel)

non-invasive oscillometric or tonometric techniques on peripheral sites, and validated transfer functions provide an aortic pressure curve (Karamanoglu et al. 1993, Wassertheurer et al. 2010b, Weber et al. 2011). A non-invasive measurement of aortic flow on the other hand is more cumbersome and consequently not convenient for clinical applications (Chirinos and Segers 2010a).

Different models for generating blood flow patterns based solely on information from pressure readings have been developed to overcome this limitation. One approach is to replace the unknown flow wave by an estimate, e.g. a triangular approximation, generated with the help of parameters derived from the (known) aortic pressure wave.

Westerhof et al. (2006) studied the accuracy of a triangular waveform to determine parameters of wave reflection in the aorta by the means of wave separation analysis. They achieved results close to those obtained with measured flows, whereas Kips et al. (2009) found substantial differences in a similar study. They again tested a triangular approximation of the blood flow for the application in pulse wave separation, but in contrast to the other study, they used a pressure waveform derived from non-invasively measured data to base their

approximation on. They outlined this fact as their main limitation and as a probable explanation for the differing results. Therefore, since non-invasive techniques are preferable for clinical application, this method might be disadvantageous. Along with the triangular waveform, they also examined the qualities of a newly proposed estimate with a more physiological form, which is obtained by averaging the normalized measured flow waves of various patients. Even though thereby the same waveform (except for an individualized timing) is used for every patient, the results were improved in comparison to the triangular form. Yet for the reflection parameters determined with the use of this curve, the deviations from measured values were still considerable.

Another approach is to use a Windkessel equation to establish a functional relation between pressure and flow. The assumption that the heart works in an optimal manner, i.e. that the power dissipation is minimized under given constraints, enables the computation of an aortic root flow and the corresponding pressure contour (Pfeiffer and Kenner 1978; Yamashiro, Daubenspeck, and Bennett 1979). Subsequently, the parameters of the Windkessel model can be identified by fitting the calculated to the measured pressure wave to finally obtain the left ventricular ejection pattern (Estelberger 1977).

One advantage of this method is that the flow curve is modeled with physiological significant parameters (Westerhof et al. 2009). Hence establishing the model itself already yields information about the arterial system without further analysis. Its main drawback is that the number of constraints that should be taken into account exceeds the degrees of freedom in the optimization problem. Therefore certain constraints have to be omitted.

A specific choice of constraints to generate a flow curve is currently used in the ARCSolver algorithms for PWA (Hametner 2011b, Mayer 2007, Wassertheurer et al. 2010a). Cardiac output determined in this way, i.e. by using the modeled aortic root flow, showed a good correlation with the one obtained from invasively measured data (Wassertheurer et al. 2008). Furthermore this model is part of algorithms that provide accurate and clinically relevant estimates of wave reflection parameters which are capable of predicting cardiovascular risk. (Hametner et al. 2011a, Hametner et al. 2012, Weber et al. 2012). This indicates that even without including all constraints a reliable description of the hemodynamics in the arterial system can be achieved with this method.

The aim of this study is to solve the optimization problem with different combinations of constraints and characterize the resulting pressure and flow curves, which should bring further insights in the dynamical behavior of the underlying model.

2. METHODS

To generate a central flow curve, first of all pressure and flow are related over a Windkessel equation. Then

the considered constraints are formulated and subsequently the resulting optimization problem is solved by the means of calculus of variations.

2.1. Windkessel Models

Windkessel models describe a dynamic relation between pressure and flow in the arterial system. The pressure is thereby assumed to be the same all over the arterial tree, because the whole system is modeled as one compartment, which makes spatial distributions impossible. The idea is based on the comparison of the volume elasticity of the large arteries with the air chambers in old-fashioned fire-engine pumps. During systole, the blood is ejected from the left ventricle with high pressure whereby the elastic arteries close to the heart expand. After closing of the valves, the pressure drops and thus the arteries relax again. By doing so, the contained blood is discharged, providing a continued blood flow during diastole (Westerhof et al. 2009).

In 1899 Otto Frank formulated the mathematical equations to relate pressure and flow in terms of a compliant and a resistant element (Hametner 2011b). The arterial compliance C_a is defined as the change in blood volume V caused by a change in blood pressure p

$$C_a = \frac{dV}{dp} \quad (1)$$

and thus gives a measure of the elasticity of the arteries, i.e. their capacity to store blood. It is assumed to be constant.

The peripheral resistance R_p characterizes the power dissipation in the area of the arterioles and capillaries and describes the proportionality between mean blood pressure \bar{P} and mean peripheral blood flow \bar{X} :

$$R_p = \frac{\bar{P}}{\bar{X}} \quad (2)$$

As mass has to be conserved, the change in blood volume over time corresponds to the difference of inflow and outflow, see Eq. 3.

$$\frac{dV}{dt} = q(t) - x(t) \quad (3)$$

Thereby q denotes the aortic root flow, i.e. the blood ejected from the left ventricle. Combining Eqs. (1) to (3) yields the model equations of the two-element Windkessel:

$$\begin{aligned} q(t) &= C_a R_p \dot{x}(t) + x(t) \\ p(t) &= R_p x(t) \end{aligned} \quad (4)$$

During diastole, when the aortic valve is closed and thus q equals zero, the system becomes a linear homogeneous differential equation in x with the following solution (t_d denotes the length of a heartbeat):

$$x_d(t) = x_{t_d} e^{\frac{t_d-t}{R_p C_a}}, \quad x_{t_d} = x(t_d) \quad (5)$$

Hence the model predicts an exponential decay for the diastolic peripheral flow and consequently the blood pressure with time constant $R_p C_a$, which coincides approximately with the physiological form. But with the development of improved measurement methods enabling recording of the aortic root flow, the shortcomings of the model during systole became clear (Westerhof et al. 2009).

Therefore a third element was added to improve the predicted behavior during left ventricular contraction. The resulting three-element Windkessel consists, like Frank's model, of the arterial compliance C_a , the peripheral resistance R_p , plus an additional resistor R_c (Estelberger 1977).

The characteristic resistance R_c includes the power dissipation in the area of the large arteries due to the viscoelastic properties of blood and vessel walls. It affects the aortic root flow q and thus only the behavior of the model during systole. Figure 2 shows an electrical analog of the three-element Windkessel used in this study.

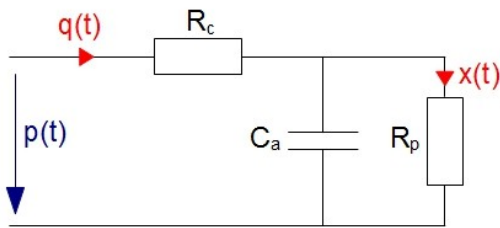


Figure 2: Electrical analog of the three-element arterial Windkessel model

Application of Ohm's law as well as Kirchhoff's circuit laws yields a differential system for pressure and flow, that constitute the model equations:

$$\begin{aligned} q(t) &= R_p C_a \dot{x}(t) + x(t) \\ p(t) &= R_c q(t) + R_p x(t) \end{aligned} \quad (6)$$

Even though the model still has its weaknesses at capturing high frequency details, the overall predicted waveform of the aortic pressure p is close to the physiological one for a given root flow q (Westerhof et al. 2009).

2.2. Optimization of Left Ventricular Work

The Windkessel model characterizes an open dynamical system that takes the flow q as input and returns the pressure p as output. Hence the established relation is unidirectional, i.e. blood pressure depends on blood flow (and the properties of the system), but not vice versa. Therefore, in order to generate an aortic root flow (the input) from a given pressure curve (the output) a feedback mechanism has to be included to couple flow with pressure (the input with the output) (Estelberger

1977). This is done by assuming that the work of the heart is subject to an optimization principle, i.e. that it works with minimal effort to provide a certain outflow.

This approach is based on the hypothesis, that biological systems have evolved to operate on minimal energy requirements. For the major breathing pattern characteristics in man this was found to be true, as the concept of minimal power dissipation made their explanation possible. Since the energy expenditure of the heart exceeds that of breathing, it seems convincing that similar regulation mechanisms also occur in the heart (Hämäläinen and Hämäläinen 1985; Yamashiro, Daubenspeck, and Bennett 1979).

The ventricular work over one heartbeat can be calculated as (t_s denotes the ejection time):

$$W = \int_0^{t_s} p(t) q(t) dt \quad (7)$$

Optimal performance of the heart is achieved when the cardiac output required by the body is produced with the lowest energy consumption possible, i.e. with the least work done by the left ventricle. Thus an optimal flow should minimize the integral in Eq. 7 under the constraint that a specific stroke volume V_s

$$V_s = \int_0^{t_s} q(t) dt \quad (8)$$

has to be reached. By introducing a Lagrange multiplier μ , this problem can be formulated as:

$$\int_0^{t_s} p(t) q(t) + \mu q(t) dt \rightarrow \min \quad (9)$$

With the use of the Windkessel model (see Eq. 6), Eq. 9 can be expressed in terms of the peripheral flow x together with its derivative. Thereby an isoperimetric problem is obtained, which is solved by calculus of variations, resulting in a second order differential equation for x with the following general solution (λ denotes the eigenvalue of the differential equation):

$$x(t) = Ae^{\lambda t} + Be^{-\lambda t} + C \quad (10)$$

Thus additional constraints are needed to determine the three unknowns (A, B, C).

Beside V_s , another obvious constraint is the periodicity of the peripheral flow over one cardiac cycle:

$$x(0) = x(t_d) = x_0, \quad (11)$$

or equivalently (see Eq. 5):

$$x(0) = x_0, \quad x(t_s) = x_0 e^{\frac{t_d-t_s}{R_p C_a}} \quad (12)$$

Furthermore the aortic flow should be zero at the beginning of the heartbeat and during diastole when the cardiac valve is closed:

$$q(0)=q(t_s)=0 \quad (13)$$

Altogether five constraints have been formulated (Eq. 8 and Eqs. 11-13) but the general solution of the optimization problem has only three degrees of freedom. Therefore only three conditions can be chosen to solve the problem exactly.

To analyze the behavior of the formulated model, the problem is implemented in Matlab (MathWorks, Natick, MA, USA) and all possible combinations of constraints are studied. The parameters in the Windkessel equation as well as ejection time, heart rate and stroke volume are fixed within the physiological range, see table 1 (Estelberger 1977).

Table 1: Parameter values

NAME	NOTATION	VALUE	UNIT
stroke volume	V_s	71	ml
peripheral resistance	R_p	0.82	mmHg·ml ⁻¹ ·s
characteristic resistance	R_c	0.015	mmHg·ml ⁻¹ ·s
arterial compliance	C_a	1	ml·mmHg ⁻¹
length of cardiac cycle	t_d	0.664	s
ejection time	t_s	0.26	s

3. RESULTS

There are ten possible combinations of the five constraints described above.

Inclusion of both boundary conditions for the aortic flow, i.e. $q(0)=q(t_s)=0$, gives a concave aortic flow and a decreasing peripheral flow x and pressure p . The quantitative outcome differs strongly depending on the third constraint.

When solely the initial value of q is taken into account, the aortic flow is increasing and peripheral flow x as well as pressure p become convex during systole. Quantitatively, the results are very similar in all three cases.

Considering the boundary condition $q(t_s)=0$ for the aortic flow without constraining $q(0)$, the results show the same qualitative and quantitative behavior for all choices of the two other constraints: a decreasing aortic flow q , a concave peripheral flow x as well as a concave pressure p .

The last possible combination excludes the boundary conditions for q , thus the stroke volume V_s and the periodicity of the peripheral flow, $x(0) = x(t_d) = x_0$, are considered as constraints. With the fixed parametrization this results qualitatively and quantitatively in almost exactly the same pressure and flow as in the previous case. But depending on the initial value of the peripheral flow x_0 , q can vary from decreasing to increasing, x and p from concave to

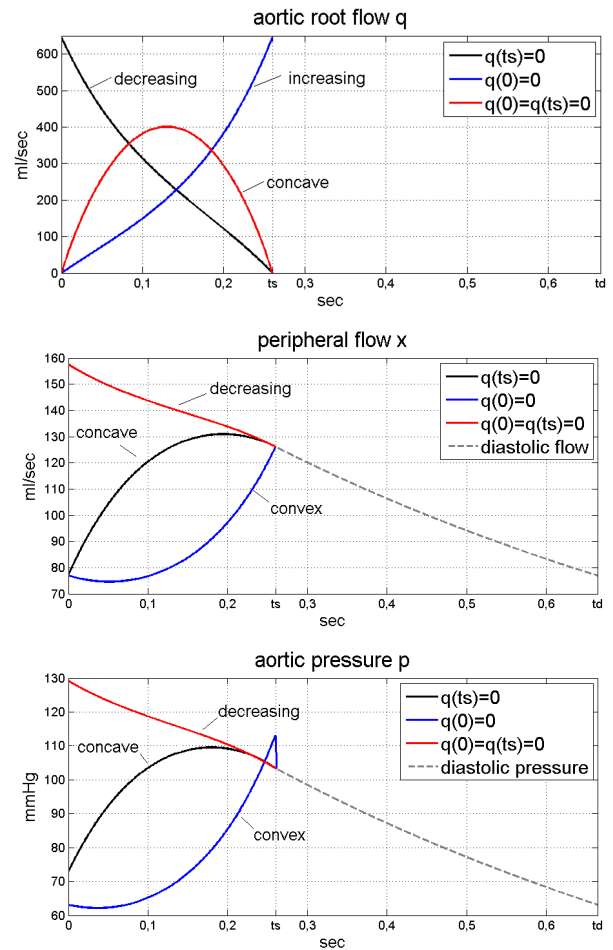


Figure 3: Examples of aortic root flow (upper panel), peripheral flow (middle panel) and aortic pressure (lower panel) for the three different types of qualitative behavior

convex, whereas for the other combinations of constraints no change in the qualitative behavior occurs.

All qualitative shapes are shown in Fig. 3 for central and peripheral flow as well as pressure.

4. DISCUSSION

The results clearly show that the choice of constraints strongly affects pressure and flow when optimizing left ventricular work. In total, three types of qualitative behavior can be distinguished, which will be discussed separately.

A first type of qualitative behavior occurs when the aortic flow is supposed to be zero at the beginning and the end of systole, i.e. $q(0)=q(t_s)=0$. This type is characterized by a concave aortic flow and a decreasing aortic pressure. Even though the shape of q seems reasonable, that of p is inaccurate, since firstly, it is not periodic and secondly, it implies that the increase in volume during blood ejection causes a decrease in pressure. Furthermore the quantitative outcomes are not in a physiological range. The combination including the stroke volume as third constraint, i.e. the constraints described in Eqs. 8 and 13, might seem to be a natural choice for generating an ejection pattern, as all

constraints including q are considered. But for this combination, the predicted pressure reaches values of more than 800 mmHg, which is a multiple of the normal maximum. The other two possible choices for the third condition required are to restrain initial systolic or end diastolic peripheral flow. In the first case, pressure as well as stroke volume are greatly underestimated (the computed stroke volume is 5.3 ml, the maximal pressure 63 mmHg). In the second case, although pressure varies in a more realistic range, the predicted stroke volume is still far too low (10.85 ml).

In conclusion, these combinations of constraints show weaknesses in both the qualitative and the quantitative results.

Another type of behavior can be observed when the constraint $q(0)=0$ is used without $q(t_s)=0$. In this case, the results show an increasing aortic flow and a convex systolic pressure. Again, the qualitative agreement of both pressure and flow with observed patterns is poor. The peak pressure as well as the maximal flow are not reached until the end of systole, which differs substantially from the physiological form. Especially with regards to the identification of system parameters by fitting of the modeled to the measured pressure wave, this could create difficulties. Therefore, also this second type does not provide appropriate waveforms for further analysis.

Finally, a decreasing aortic flow and a concave pressure characterize the third class of results. This situation arises from the specification of q being zero after the valves have closed, i.e. $q(t_s)=0$. With the chosen parametrization, the results are almost exactly the same for all three possible combinations of constraints. Therefore, when V_s remains unconstrained (this would correspond to the case, where the periodicity of the peripheral flow x is in focus), the obtained patterns can be used for stroke volume determination (Estelberger 1977). For the parameter values specified in Table 1, the area enclosed by the modeled aortic flow gives 70.9674 ml compared with the demanded 71 ml. On the other hand, also the periodicity of x can be achieved without including it explicitly.

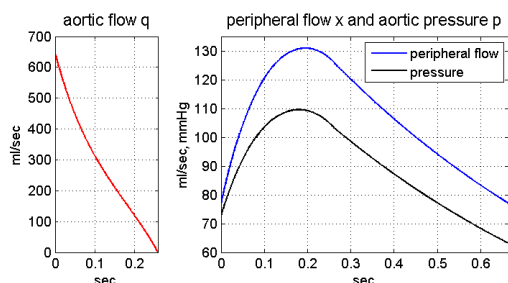


Figure 4: Pressure and flow shapes from an optimization with $q(t_s)=0$

Figure 4 depicts a set of computed curves representative for all three combinations with $q(t_s)=0$. Although the aortic flow wave is physiologically

incorrect, as it shows an infinite slope at the beginning of blood ejection, the pressure curve is in qualitative accordance with human measurements. Waveforms of this type are also used in the ARCSolver. There, a combination of constraints including the stroke volume in addition to $q(t_s)=0$ is used.

With the chosen parametrization, also the results obtained by leaving the aortic flow unconstrained belong to this type. For these patterns, the major shape predictions were shown to be consistent with measured ones in a dog, both for varying cardiac output and heart rate (Yamashiro, Daubenspeck, and Bennett 1979). Yet, in this case, flow as well as pressure react sensitively on changes in x_0 , see Fig. 5. An increase of 5 ml/sec (6.5%) already results in a completely different shape of the curves. For practical applications, this might be disadvantageous as x_0 is determined by the diastolic aortic blood pressure obtained from measurements and/or further computations thereof.

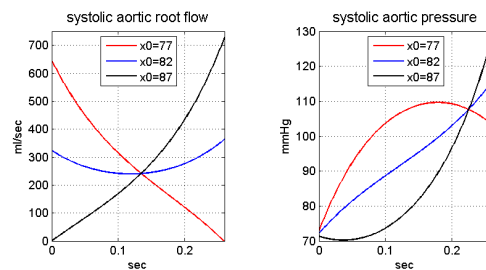


Figure 5: Results for aortic flow q (left) and pressure p (right) with an unconstrained aortic flow for different values of x_0

In summary, the variants based on a combination of constraints including $q(t_s)$ but not $q(0)$ provide the best results with regards to both the quantitative and qualitative behavior. Furthermore it can be seen that the condition $q(0)=0$, which is needed for a physiological shape of the aortic flow, causes a qualitative deterioration of the results whenever included.

4.1. Conclusions and Perspectives

The analysis of different combinations of constraints revealed that a physiological waveform of both pressure and flow cannot be achieved simultaneously with the presented method and the corresponding choices for the objective function and constraints.

Comparing the combinations of constraints which lead to the same type of behavior indicates that the boundary conditions of the aortic flow q are the key determinants for the shape of the curves. Except for the case where no boundary value of q is taken into account, the qualitative behavior is fully determined by whether $q(0)$ or $q(t_s)$ or both are set to zero. The choice of additional constraints as well as initial-systolic or end-diastolic peripheral blood flow x_0 thereby only influence the quantitative outcome. This does not apply when the boundaries of q are not constrained. In this case, the qualitative properties of pressure and flow are indeed

affected by changes in x_0 and thus by the diastolic pressure.

A description of the system that is closest to reality is achieved when the aortic root flow is decreasing. To improve the shape of the ejection pattern, the outflow has to be forced to start at zero, but by doing so the existing benefits of the current solution should not be lost. The aim of future work will be to extend the method in a way that allows the inclusion of additional conditions, in particular the zero initial aortic flow. This could be done by modifying the performance criterion or by using more than three constraints and searching for approximate solutions for such an overdetermined problem.

REFERENCES

- Chirinos, J.A. and Segers, P., 2010a. Noninvasive Evaluation of Left Ventricular Afterload Part 1: Pressure and Flow Measurements and Basic Principles of Wave Conduction and Reflection. *Hypertension* 56(4):555-562.
- Chirinos, J.A. and Segers, P., 2010b. Noninvasive Evaluation of Left Ventricular Afterload Part 2: Arterial Pressure-Flow and Pressure-Volume Relations in Humans. *Hypertension* 56(4):563-570.
- Estelberger, W., 1977. Eine neue nichtinvasive Pulskontur-Schlagvolumenbestimmungsmethode aufgrund eines Optimierungsmodells der Herzarbeit. *Biomedizinische Technik* 22:211-217.
- Hämäläinen, R.P. and Hämäläinen, J.J., 1985. On the Minimum Work Criterion in Optimal Control Models of Left-Ventricular Ejection. *IEEE Transactions on Biomedical Engineering* 32(11):951-956.
- Hametner B., Wassertheurer, S., Weber, T. and Breitenecker, F., 2011a. Non-invasive determination of pulse wave intensity using a dynamic blood flow model. *Abstract Booklet Einsteins in the City*, BE.6. April 14-15, New York City (New York, US).
- Hametner, B., 2011b. *Arterial Pulse Wave Analysis: Impact of Models for Impedance and Wave Reflection*. Thesis (PhD). Vienna University of Technology.
- Hametner, B., Weber, T., Mayer, C., Kropf, J. and Wassertheurer, S., 2012. Effects of Different Blood Flow Models on the Determination of Arterial Characteristic Impedance. *IFAC-PapersOnLine*, in press.
- Karamanoglu, M., O'Rourke, M.F., Avolio, A.P. and Kelly, R.P., 1993. An analysis of the relationship between central aortic and peripheral upper limb pressure waves in man. *European Heart Journal* 14(2):160-167.
- Kips, J.G., Rietzschel, E.R., De Buyzere, M.L., Westerhof, B.E., Gillebert, T.C., Van Bortel, L.M. and Segers, P., 2009. Evaluation of Noninvasive Methods to Assess Wave Reflection and Pulse Transit Time From the Pressure Waveform Alone. *Hypertension* 53(2):142-149.
- Laurent, S., Cockcroft, J., Van Bortel, L., Boutouyrie, P., Giannattasio, C., Hayoz, D., Pannier, B., Vlachopoulos, C., Wilkinson, I. and Struijker-Boudier, H., 2006. Expert consensus document on arterial stiffness: methodological issues and clinical applications. *European Heart Journal* 27(21): 2588-2605.
- Mayer, C., 2007. *Pulse contour analysis model for non-invasive determination of hemodynamical parameters*. Thesis (PhD). Vienna University of Technology.
- Mitchell, G., 2009. Arterial Stiffness and Wave Reflection: Biomarkers of Cardiovascular Risk. *Artery Research* 3(2):56-64.
- Pfeiffer, K.P. and Kenner, T., 1978. Untersuchungen zur Frage der optimalen Abstimmung zwischen Arteriensystem und Herzstätigkeit. *Biomedizinische Technik* 23(s1):276-277.
- Wassertheurer, S., Hametner, B., Kropf, J., Mayer, C., Eber, B. and Weber, T., 2010a. Novel non-invasive method to assess wave reflection from the pressure waveform alone. *Artery Research* 4(4):145.
- Wassertheurer, S., Kropf, J., Weber, T., van der Giet, M., Baulmann, J., Ammer, M., Hametner, B., Mayer, C., Eber, B. and Magometchnigg, D., 2010b. A new oscillometric method for pulse wave analysis: comparison with a common tonometric method. *Journal of Human Hypertension* 24(8):498-504.
- Wassertheurer, S., Mayer, C., Breitenecker, F., 2008. Modeling arterial and left ventricular coupling for non-invasive measurements. *Simulation Modelling Practice and Theory* 16:988-997.
- Weber, T., Wassertheurer S., Rammer, M., Maurer, E., Hametner, B., Mayer, C., Kropf, J. and Eber, B., 2011. Validation of a Brachial Cuff-Based Method for Estimating Central Systolic Blood Pressure. *Hypertension* 58:825-832.
- Weber, T., Wassertheurer, S., Rammer, M., Haiden, A., Hametner, B. and Eber, B., 2012. Wave Reflections, Assessed With a Novel Method for Pulse Wave Separation, Are Associated With End-Organ Damage and Clinical Outcomes. *Hypertension* (published online ahead of print, may 14).
- Westerhof, B.E., Guelen, I., Westerhof, N., Karamaker, J.M. and Avolio, A., 2006. Quantification of wave reflection in the human aorta from pressure alone: A proof of principle. *Hypertension* 48(4):595-601.
- Westerhof, N., Lankhaar, J.W. and Westerhof, B.E., 2009. The arterial Windkessel. *Medical and Biological Engineering and Computing* 47(2):131-141.
- Yamashiro, S.M., Daubenspeck, J.A. and Bennett, F.M., 1979. Optimal regulation of left ventricular ejection pattern. *Applied Mathematics and Computation* 5(1):41-54.

OPTIMAL CONTROL STRATEGIES FOR LOW FUEL CONSUMPTION IN A GDI ENGINE UNDER SINGLE AND MULTIPLE INJECTION

M. Costa^(a), L. Allocca^(b), P. Sementa^(c)

^{(a), (b), (c)}CNR – Istituto Motori, Viale Marconi, 8 – 80125, Naples, ITALY

^(a)m.costa@im.cnr.it, ^(b)l.allocca@im.cnr.it, ^(c)p.sementa@im.cnr.it

ABSTRACT

The optimization of the mixture formation process in a GDI (gasoline direct injection) engine equipped with a high-pressure seven-hole injector is pursued by coupling a 3D model of the in-cylinder processes with an optimization tool. The 3D model of the in-cylinder processes is developed on the ground of experimental data. Injection strategies, as preliminary experimentally characterized on a Bosch tube, are considered as occurring or in a single event or in multiple events. The advantages of splitting injection into four parts are discussed. Optimal injection strategies and time of spark advance are chosen in order to reduce the gasoline consumption, hence to increase the engine energy efficiency. The effects of the mixture formation process on the formation of the main pollutants are also discussed.

Keywords: multidimensional engine modeling, gasoline direct injection, optimization, multiple injections

1. INTRODUCTION

The preferred route towards the reduction of both the fuel consumption and the exhaust noxious emissions in internal combustion engines remains the control of the mixture formation and combustion processes taking place within the combustion chamber, a complicated task, affected by many variables. In the recent years, the high cost and time needed to achieve optimisation through engine bench testing alone has drawn interest of developers towards the use of Computational Fluid Dynamics (CFD) analyses. Nowadays, the link between the need to reduce greenhouse gas emissions and the use of advanced engine simulation is so well assessed, that also the coupling between traditional 3D engine simulation tools with algorithms able to explore the model constants space in an automatic way, as genetic or robust search methods, is being considered. During each iteration, the decision variables are manipulated using various operators (selection, combination, crossover or mutation) to create new design populations, i.e. new sets of decision variables. Optimization algorithms, on the other hand, may be used to drive the choice of a design solution, or configuration, between various alternatives, hence in a role that is more congenial and traditional [Thévenin and Janiga, 2008]. Examples of application of genetic

algorithms to the design of diesel engines are found in the paper by Wickman *et al.* [Wickman, Senecal, Reitz, 2001] and de Risi *et al.* [De Risi, Donateo, Laforgia, 2003.]. A more recent application by Dempsey and Reitz [Dempsey, Reitz, 2011] explores the possibility of reducing the pollutant emissions in a reactivity controlled engine, fed with both diesel and gasoline.

Present work is aimed at discussing the assessment of a procedure for the fuel consumption reduction of a GDI engine, based on the optimal synchronization of the injection event within the working cycle.

GDI is nowadays one of the most pursued solutions to improve the performances of spark ignition (SI) engines from both an energetic and an environmental point of view. This is mainly due to the possibility to precisely control and adapt the fuel amount and injection timing to the specific load and speed operating condition. Achievement of optimal charge conditions over the whole working map is affected by many parameters, whose effects are complex and overlapped. This is the reason why injection modulation and splitting are being considered also in SI engines, in analogy with compression ignition ones.

Multiple injection strategies are already employed in present GDI engines under special operating regimes, as for mixture formation at engine cold start, to increase the temperature for the converter light-off, to achieve a smooth idle and to reduce the engine tendency to knock [Kuwahara, Ueda, Ando, 1998]. In the future, these strategies may be used also to control the combustion process and/or to prevent misfiring or high emission levels.

The interactions of multiple injection events between themselves and with the surrounding air motion surely needs further investigation. The synchronization of each single injection event within the working cycle, in fact, must be optimized having in mind a certain objective of power output or pollutants emissions, and accounting for the complex mutual effects of the spray liquid droplets motion and the surrounding air flow. Especially when injection is realised during the intake stroke, the air flow assumes a configuration that strongly depends on the instantaneous valve position and on the pressure difference between the intake ducts and the cylinder. Macroscopic vortexes form under the intake valves

having a diameter comparable with the valve diameter. The position of the vortex axes is not fixed but moves as they get open or closed. This determines effects on the spray entering the combustion chamber of an entity that depends on the particular instant of time being considered for injection.

The effects of single or multiple injection strategies on the performance of a single cylinder 4-valve, 4-stroke GDI engine are here numerically analyzed. A 3D engine model, developed by Montanaro *et al.* [Montanaro, Sorge, Catapano, Vaglieco, 2012], is employed to the scope. The runs of the 3D model are driven by the Simplex algorithm to search for the injection strategy and spark advance that reveal optimal for the combustion development. After the optimal injection pressure is identified, the gasoline supply is considered as subdivided into four successive events, each delivering a same mass of gasoline. The optimization algorithm is again used to automatically manage the 3D engine model under multiple injections, hence, it is used to explore the actual advantages of modulating the mixture formation for low consumption and reduced pollutants.

2. THE 3D ENGINE MODEL

The 3D engine model employed within the present study is developed in the context of the software AVL Fire™. Details of the model assessment are given in the paper by Montanaro *et al.* [Montanaro, Sorge, Catapano, Vaglieco, 2012], where specifications of the engine under study and of the considered seven-hole injector are also given. The approach followed for the simulation of the spray dynamics within the engine cylinder is the classical coupling between the Eulerian description of the gaseous phase and the Lagrangian description of the liquid phase. The train of droplets entering the computational domain in correspondence of the injector holes exit section suffers various concurring effects as it travels, as break-up, evaporation,

coalescence. The droplets break-up phenomenon is simulated according to the sub-model of Huh-Gosman, whose constant determining the break-up time, C_1 , is to be properly adjusted. The initial size of droplets at the nozzle exit section, is considered as not constant, but variable according to a probabilistic log-normal distribution, whose variance, σ , is another parameter to be properly tuned. A preliminary experimental characterization of the employed seven-hole injector, here not described for the sake of brevity, served to the spray sub-model validation, hence to the C_1 and σ definition, according to an automatic procedure assessed by Costa *et al.* [Costa, Sorge, Allocca, 2012].

3. OPTIMIZATION OF THE INJECTION STRATEGY

As previously said, present work aims at investigating the injection strategy realising the mixture whose characteristics are optimal for power generation in a high performance GDI engine. Two analyses are effected, one for single injection, by changing injection pressure (p_{inj}) and start of injection (SOI), one for injection split into four equal parts, by changing the start of the first injection event (SOI_1) and the dwell time between each event and the next. The dwell time is assumed constant between the first and the second, the second and the third, the third and the fourth injection event. In all the situations, the Simplex algorithm is used to search for the inputs maximizing the indicated mean effective pressure (IMEP) in the closed valve period of the engine working cycle. The injected gasoline mass is considered constant, namely equal to 20.16 mg/cycle, in order to realize a lean stratified combustion (air to fuel ratio, A/F, equal to 16.9) at the engine speed of 1500 rpm. Another design variable of the optimization problem is identified in the time of spark ignition (start of spark - SOS), since it obviously strongly affects the combustion development.

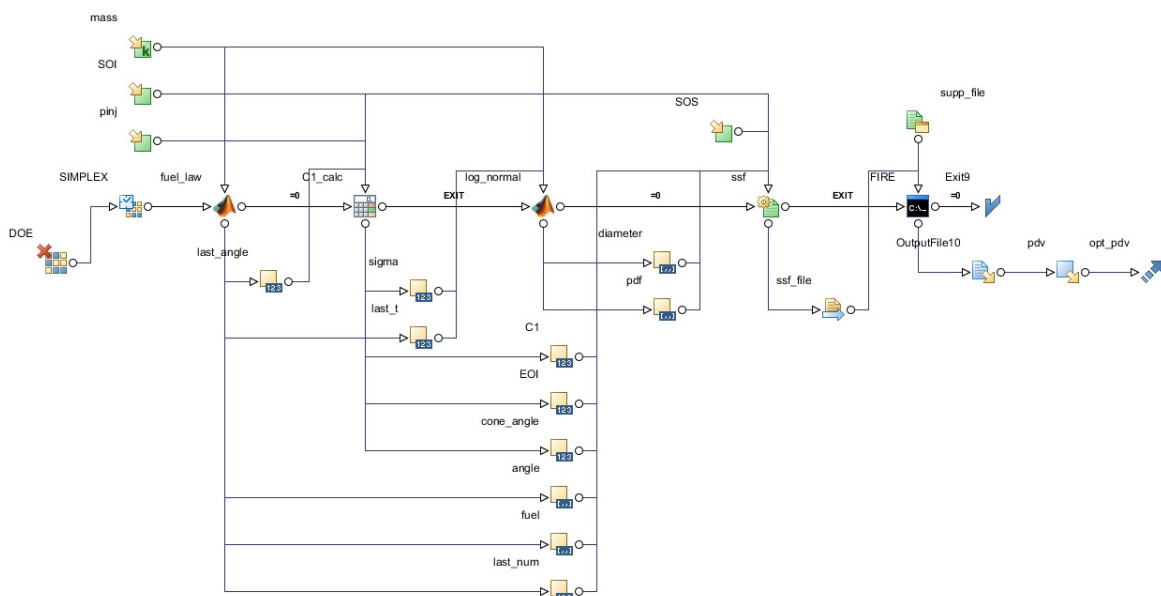


Figure 1: Flow chart of the optimization problem for the single injection case.

The choice of the range of variation of the samples, as well as the step between successive samples, that obviously influences the efficiency and speed of the optimization procedure, is properly made starting from a certain initial point.

3.1. Optimization in the single injection case

The scheme of the optimization problem solved in the case of single injection is reported in Figure 1. The input variables defining the injection strategy and the SOS are visible. The definition of the injection strategy, accounting for an injection pressure variation in the range 5 to 15 MPa, needs a discussion.

The injector under study, as previously said, was experimentally characterized by injecting gasoline, according to some engine strategies, in an optically accessible vessel for the measure of the single jet cone angle and penetration length. The instantaneous mass flow rate was also measured in a Bosch tube [Bosch, 1966, Wallace, 2002]. Measured cone angles and mass flow rates, indeed, are input variables of the spray sub-model included in the 3D engine model. The experimental availability of these variables, however, is limited to a few values of the injection pressure. Therefore, a scaling is included within the project of Figure 1 in order to account for the variation of this quantity at constant injected mass. Figure 2 shows the mass flow rate measured at the injection pressure of 6 and 10 MPa, together with the profiles relevant to the injection pressures of 5 and 15 MPa, derived by scaling the experimental data on the ground of a coefficient proportional to the square root of the difference between injection and environment pressure. On the other hand, the employed spray sub-model also needs the specification of the initial droplets size, namely the definition of the value of the variance of a log-normal distribution whose expected value is evaluated according to the following formula:

$$D_{th} = C_d \left(\frac{2\pi\tau_f}{\rho_g u_{rel}^2} \right) \lambda^* \quad (1)$$

being τ_f the gasoline surface tension, ρ_g the surrounding gas density, u_{rel} the relative velocity between the fuel and the gas, C_d a constant of the order of the unity (indeed taken equal to the unity), and the parameter λ^* deriving from the hydrodynamic stability analysis and indicating the dimensionless wavelength of the more unstable perturbation to the liquid-gas interface at the injector exit section. Therefore, an interpolation of the optimal values of the C_1 and σ constants found according to the procedure defined in [Costa, Sorge, Allocca, 2012] is used, as shown in Figure 3. With interpolated data, all the needed distributions of initial droplets size can be defined. As an example, Figure 4 represents four distributions for different injection pressures. The reliability and portability of the spray sub-model as this variable is

changed, indeed, was proven by authors also with reference to other injectors.

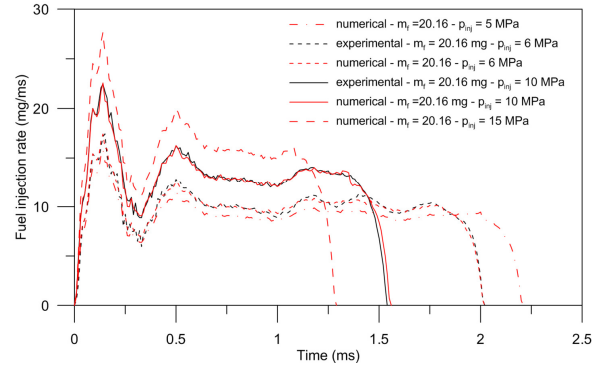


Figure 2: Mass flow rates: measurements and numerical scaling, at 6 and 10 MPa.

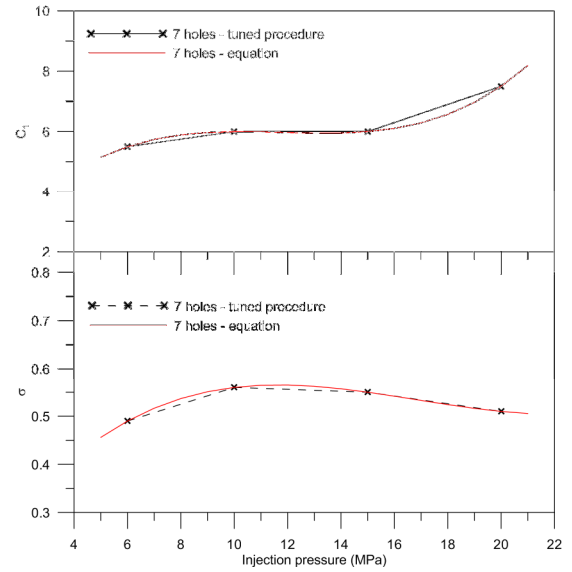


Figure 3: Interpolation of the optimal values of the constant C_1 (top) and the variance (bottom).

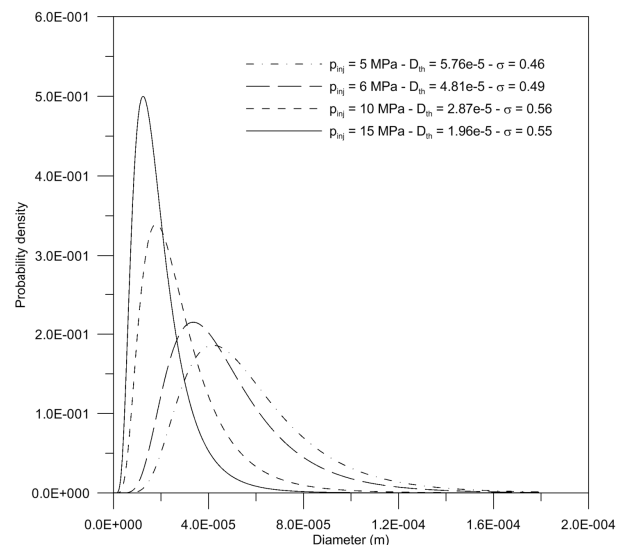


Figure 4: Initial size of droplets at $p_{inj} = 5, 6, 10, 15$ MPa.

Results of the optimization analysis relevant to the single injection case are reported in Figures 5 and 6, where the IMEP of each computed cycle in the closed valve period, made dimensionless with respect to the value relevant to the starting point cycle ($IMEP_{ref}$), is represented in a bubble plot in the p_{inj} -SOI and the p_{inj} -SOS planes. The triple of values of p_{inj} , SOI and SOS maximizing the engine performance is just the one assumed as reference (starting point), namely $p_{inj}=6$ MPa, $SOI=650^\circ$ (58° after inlet valves closing, IVC) and $SOS=707^\circ$ (13° before the top dead center, BTDC).

The effect of the injection strategy on the main pollutants is clarified by Figures 7 and 8. Figure 7 is a bubble plot in the p_{inj} -SOI plane, where the bubble size is proportional to the ratio between the NO amount at the exhaust valves opening (EVO) of each computed cycle and the one assumed as reference case (NO_{ref}), also at EVO. Figure 8 is a bubble plot representing the ratio between the unburned equivalence ratio (UER) at EVO (proportional to the unburned hydrocarbons amount) and the one of the reference case.

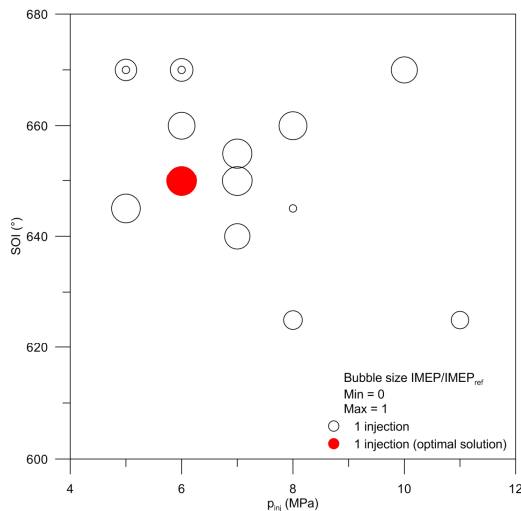


Figure 5: IMEP: bubble plot of the single injection optimization in the p_{inj} - SOI plane.

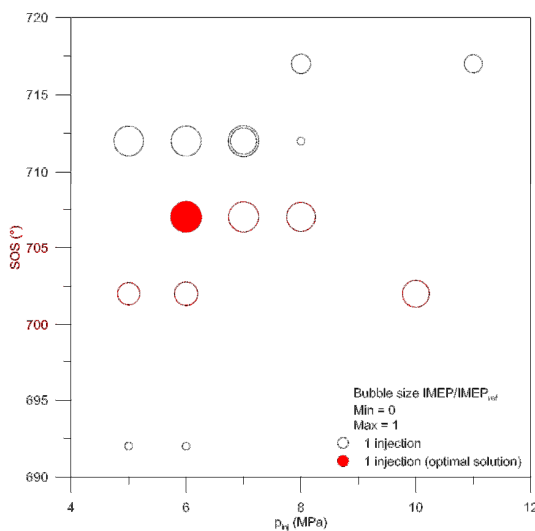


Figure 6: IMEP: bubble plot of the single injection optimization in the p_{inj} - SOS plane.

The optimal solution is characterized by a quite high value of the NO amount at the exhaust, while the unburned hydrocarbons are really low.

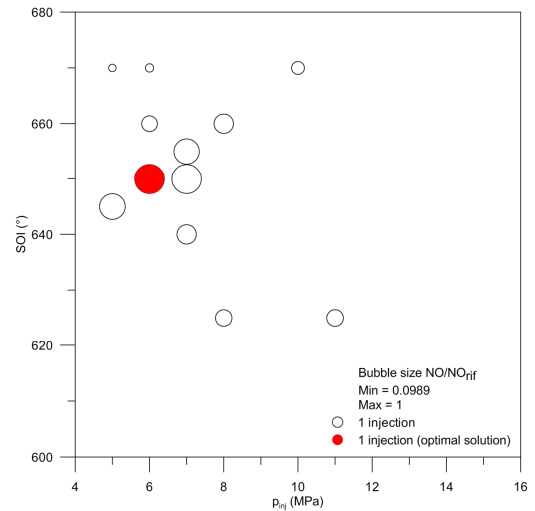


Figure 7: NO: bubble plot of the single injection optimization in the p_{inj} - SOI plane.

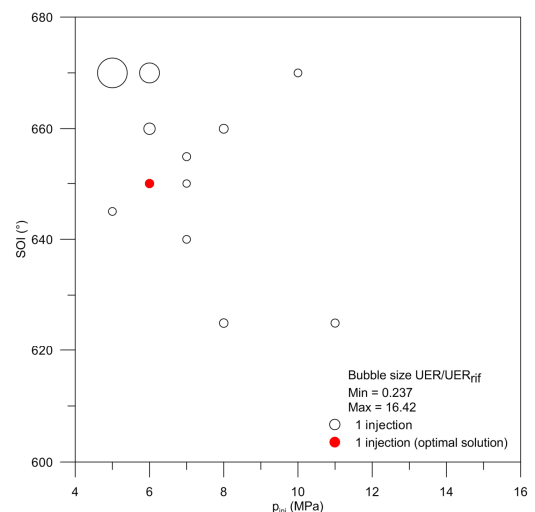


Figure 8: Unburned equivalence ratio: bubble plot of the single injection optimization in the p_{inj} - SOI plane.

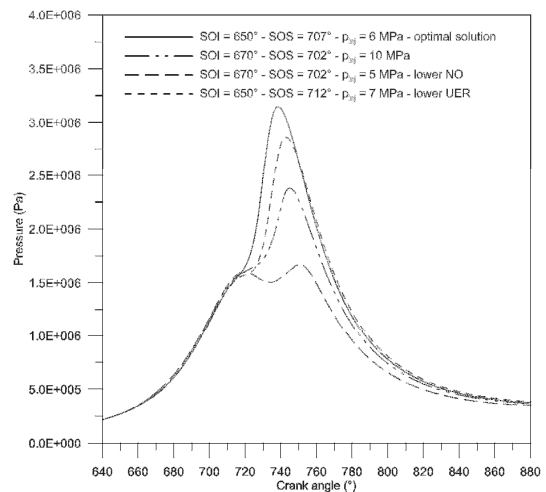


Figure 9: Computed in-cylinder pressure for four different injection strategies.

The dramatic effect of the chosen variables on the in-cylinder pressure at moderate-load is visualized in Figure 9, where four different in-cylinder pressure cycles are plotted. It is evident that the optimal solution has a cycle area greater than the other ones. The cycles relevant to the lower NO case and the lower unburned hydrocarbon case are also reported. These two are really characterized by a low power output, especially the one relevant to the lower NO value.

3.2. Optimization in the multiple injection case

The afore described analysis leads to individuate the optimal injection pressure at 6 MPa. Keeping this variable as fixed, a further analysis is here discussed, where injection is considered as split into four parts. Figure 10 represents the comparison between the single injection case and two different quadruple injections, each characterized by a certain value of the constant dwell time between successive events (kept constant). Each of the four injections is assumed to deliver the same fuel quantity, hence 5.04 mg, for a total of 20.16 mg/cycle.

The optimization analysis is performed by changing the SOI of the first injection event, SOI_1 , the dwell time between successive events, and the time of SOS. Figures 11 represents the IMEP of each computed cycle in the closed valve period, made dimensionless with respect to the value relevant to the reference single injection cycle ($IMEP_{ref}$) (same as for single injection) in the SOI_1 -SOS plane. The optimal quadruple strategy is characterized by $SOI_1=625^\circ$ (25° before the SOI found as optimal in the single injection case) $Dwell=7^\circ$, $SOS=692^\circ$ (28° BTDC). The optimal solution for the quadruple injection case comes out being better than the optimal solution for single injection. As shown in Table 1, that is a summary of the results of the single case and quadruple case optimization processes, a gain equal to the 8.9% in the IMEP is evident for injection split into four parts. Figure 12 and Figure 13 shows, respectively, the bubble plots relevant to the NO and unburned equivalence ratio, always made dimensionless with respect to the relevant quantities of the reference single injection case.

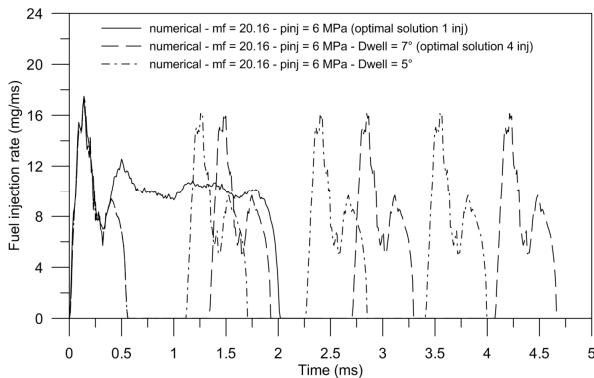


Figure 10: Mass flow rates for single and quadruple injections at 6 MPa at constant total mass.

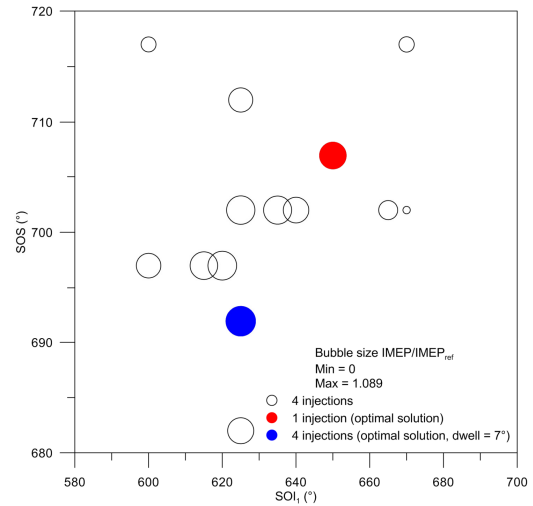


Figure 11: IMEP: bubble plot of the quadruple injection optimization in the $SOI_1 - SOS$ plane.

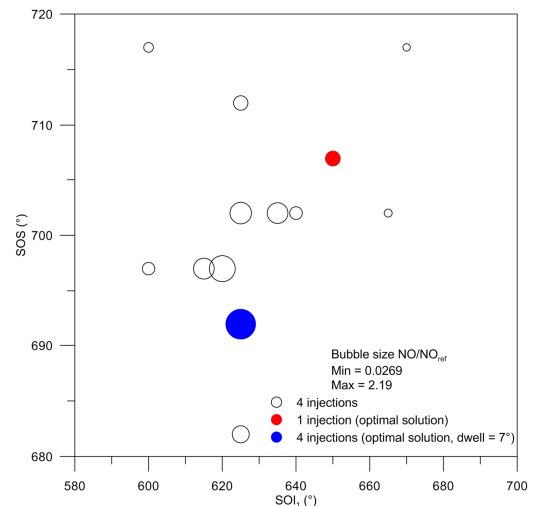


Figure 12: NO: bubble plot of the quadruple injection optimization in the $SOI_1 - SOS$ plane.

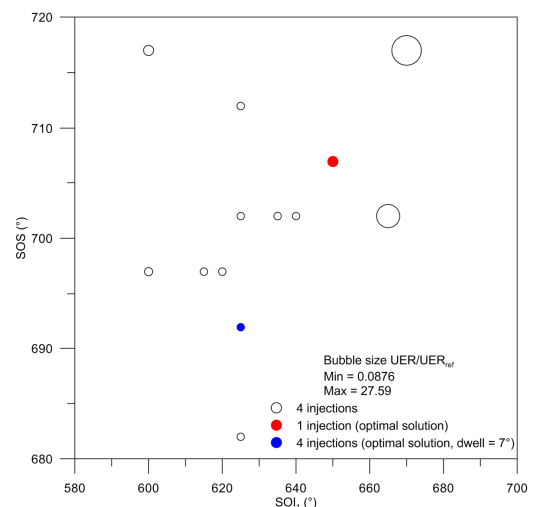


Figure 13: Unburned equivalence ratio: bubble plot of the quadruple injection optimization in the $SOI_1 - SOS$ plane.

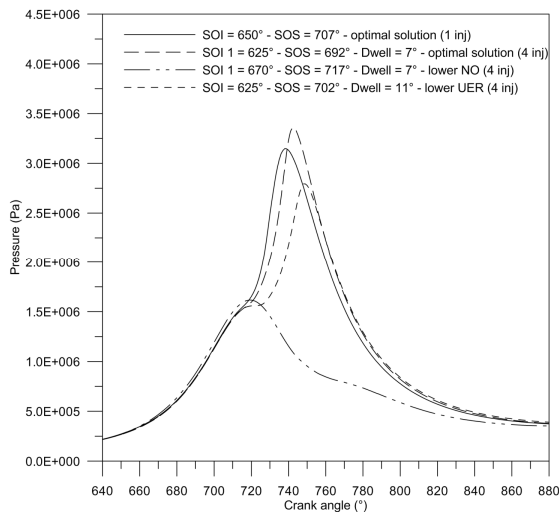


Figure 14: Computed in-cylinder pressure for optimal single and optimal quadruple injections. Lower NO and UER cases for quadruple injection are also represented.

Optimal	IMEP/IMEP _{ref}	NO/NO _{ref}	UER/UER _{ref}
1 injection	1	1	1
4 injections	1.089	2.19	0.0977

Table I. Summary of the optimization results

The NO amount, indeed, suffers a bad effect from the injection splitting, whereas an improvement in the burning of hydrocarbons is evident. Refer to Table 1 to quantify these aspects.

Figure 14, finally shows the comparison between the pressure cycles relevant to the optimal single and the optimal quadruple injection. The gain in the pressure cycle area, that obviously reflects in a gain of about the 9% in the gasoline consumption in the considered lean mixture case, is well visible. Two other pressure cycles are reported: the one relevant to the lower NO amount for four injection ($NO/NO_{ref}=0.0269$), and the one relevant to the lower unburned hydrocarbons at the exhaust ($UER/UER_{ref}=0.0876$), that however is meaningless due to the low power output.

4. CONCLUSIONS

Results of optimization analyses devoted to increase the energy efficiency of a GDI engine under overall lean stratified charge conditions (at moderate speed, moderate load) are discussed.

The study is performed through numerical simulation, by employing a 3D engine model assessed on the ground of experimental data. Under both single and quadruple injections, the 3D engine model is automatically driven by an optimization algorithm that searches for the maximum pressure cycle area (in the pressure volume plane), at constant injected mass of gasoline.

Under single injections the value of injection pressure is varied between 5 and 15 MPa, while the start of injection is changed in the range 600° - 670° (intake valves close at 592° , TDC is at 720°). A third variable is

considered, namely the time of spark advance, changed in the 682° - 717° range. The value of injection pressure found as optimal is $p_{inj}=6\text{MPa}$, the $SOI=650^{\circ}$ (injection all realized during compression), $SOS=707^{\circ}$. The point found as optimal, with respect to the others, is also characterized by a low value of unburned hydrocarbons at the exhaust, but a quite high value of NO. However, this may be considered as a secondary problem due to the possibility to resort to after-treatment systems of this kind of pollutant.

The optimization analysis relevant to the four injection case leads to the interesting result of a further gain in the energy efficiency achievable through splitting injection. This can be quantified as equal to about the 9%, with a positive effect also on the unburned hydrocarbons.

The procedure developed by authors for the optimization of the engine performance has a broad range of applicability. It is here considered to increase the energy efficiency of a lean stratified combustions in a high performance GDI engine.

REFERENCES

- Thévenin, D., Janiga, G. (eds.), 2008. *Optimization and Computational Fluid Dynamics*, Springer-Verlag, Berlin Heidelberg.
- Wickman, D.D., Senecal, P.K., Reitz, R.D., 2001. Diesel engine combustion chamber geometry optimization using genetic algorithms and multi-dimensional spray and combustion modeling, SAE Paper 2001-01-0547.
- De Risi, A., Donato, T., Laforgia, D., 2003. Optimization of the combustion chamber of direct injection diesel engines. SAE Paper 2003-01-1064.
- Dempsey, A.B., Reitz, R.D., 2011. Computational optimization of reactivity controlled compression ignition in a heavy-duty engine with ultra low compression ratio, SAE Paper 2011-24-0015.
- Kuwahara, K., Ueda, K., Ando, H., 1998. Mixing Control Strategy for Engine Performance Improvement in a Gasoline Direct Injection Engine. SAE Paper 980158.
- Montanaro, A., Sorge, U., Catapano, F., Vaglieco, B.M., 2012. Multidimensional modelling of the in-cylinder processes in a GDI Engine, 24th European Modeling & Simulation Symposium (EMSS 2012), Wien. Paper 77.
- Costa, M., Sorge, U., Allocca, L., 2012. CFD optimization for GDI spray model tuning and enhancement of engine performance, *Advances in Engineering Software*, 49: 43-53.
- Bosch, W., 1966. The Fuel Rate Indicator: A New Measuring Instrument For Display of the Characteristics of Individual Injection, SAE Paper 6607496.
- Wallace, I., 2002. *Injection Rate Gauge: Pass Off Information and User Instructions - Fuel & Engine Management Systems*, Graz.

PRODUCTION SCHEDULING ON MULTIPLE LINES WITH SHARED RESOURCES

Francesco Costantino^(a), Giulio Di Gravio^(a), Fabio Nonino^(b), Matteo Cappannoli^(a), Tommaso Silvestri^(a)

^(a) Department of Mechanical and Aerospace Engineering
^(b) Department of Computer, Control, and Management Engineering
University of Rome "La Sapienza"

francesco.costantino@uniroma1.it

Keywords: production scheduling, mixed-model assembly, multiple lines, shared resources.

ABSTRACT

In the research area of scheduling, many simulation models were developed to test solutions, generally established by optimization algorithms or heuristics. In the paper presented is a simulation model for scheduling problems of orders in the case of a multiple production lines with shared resources. The studied problem deals with the management of a specific number of work teams available for many operations, with skills to consider in the assignment of the workloads.

Moreover, the simulation model needs to consider the work teams' efficiency that depends on the season and on the production level. These characteristics are managed by software to test alternative solutions for the scheduling of the multi-product productions, where the lot size and the due dates change order by order.

To verify the simulation model, it was tested to a real case of a motorcycle production plant, where different scheduling rules were considered and assessed measuring the performances and their effect on a specific objective function based on lateness.

1. INTRODUCTION AND BACKGROUND

Manufacturers nowadays often face the challenge of providing a rich product variety as lower cost as possible. This typically requires the implementation of cost efficient, flexible production systems on multiple lines, since by using single model assembly lines, manufacturing companies were able to efficiently produce big quantities of a product, that nowadays are rarely required.

Thus, production processes in a wide range of industries rely on modern mixed-model assembly systems, which allow an efficient manufacture of various models of a common base product on a flexible production system. However, the observed diversity of mixed-model lines makes the planning of sequence essential for exploiting the benefits of this production organization.

This scheduling problem is often called mixed-model assembly line scheduling (Leu *et al.*, 1996) and can be also referred to the permutation flowshop scheduling

problem. In such a production system, the managers want to sequence the different products, thus obtaining a high service level (product mix) without delays in products delivery while respecting the constraints of capacity.

The variability on the final product involves production variables to be considered, as human resources flexibility, production line capabilities to work on specific products, set-up times depending on the adopted scheduling, therefore the production sequence of the products becomes important as a central issue. Hence, after an assembly line has been balanced (work has been spread out over the line stations), the order in which units have to be introduced into the assembly line must be considered by taking into account certain criteria.

To sequence mixed-models in assembly lines some criteria have been considered in the literature (Scholl, 1999), two main sequencing objectives are the constant rate of part usage (Monden, 1983; Miltenburg, 1989; Bautista *et al.*, 1996), and the leveling of work load (Yano and Bolat, 1989; Xiaobo and Ohno, 2000). More than one criterion has also been considered simultaneously (Aigbedo and Monden, 1997; Kotani *et al.*, 2004).

In addition to the long- to mid-term assembly line balancing problem (see Baybars, 1986; Scholl and Becker, 2006; Becker and Scholl, 2006; Boysen *et al.*, 2006), mixed-model assembly lines give rise to a short-term sequencing problem, which has to decide on the production sequence of a given number of model copies within the planning horizon, like a day or a week.

With this background, the paper presents a simulation model for the analysis of the short term scheduling in a mixed-model lines production.

In the simulation two general objectives are targeted:

- *Workload related objectives.* The manufacture of varying models typically leads to move human resources (operators) on different machines or lines. The flexibility asks for continuous changes but those can bring to decrease in the workload times and in delay on productions.
- *Just-in-Time objectives.* Since the flexibility is a target this cannot be paid with excessive lateness on due date, back orders or high level

of stocks of finished products and consequent immobilization losses and risks. With this in mind every scheduling has to be assessed in its capacity to be just-in-time with the established due date.

2. CASE STUDY DESCRIPTION

The case study regards an Italian motorcycle company, where different products are realized on multiple production lines and where a significant issue is the typical mixed-model scheduling problem.

The productive capacity of the studied plant is around 1800 units per day in high season, using eleven assembly lines: the first four are devoted to motorcycles, while the remaining seven are for scooters. The Company has decided to adopt a "multi-model" lines strategy, assigning a limited number of models in each line, thus ensuring short set-up times, thanks to the affinity of the models worked on the same line.

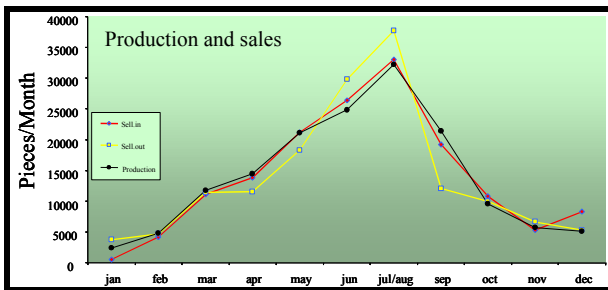


Figure 2: Seasonality in motorcycles' production

The criticality of the situation is however reflected in the low season, e.g. in winter and autumn seasons (Figure 2), when the market demand is low, the number of active production lines decreases, the workteams are halved and, therefore, forced to move between the lines, from a minimum of two to a maximum of three, following a chessboard logic. An example of this situation is shown in Figure 3, where the team X moves periodically between the lines I and J, where different models are assembled.

The main aim is, in fact, to propose and compare different short-term (weekly and daily) production plans, built around the availability of effective human resources, in order to identify the most effective solutions in terms of time and cost.

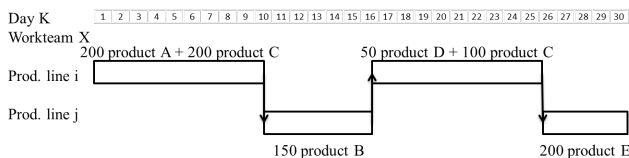


Figure 3: Example of chessboard between two lines

2.1. Objective

The minimization of time and costs is carried out considering a target function (T.F.), expressed by a weighted sum where the weights are provided in collaboration with the company's planner:

$$T.F. = \alpha_i \cdot \sum CB_i + \beta_i \cdot \sum SU_i + \gamma_i \cdot \sum T_i \quad (1)$$

Where:

CB_i = time lost in the chessboard for the i -th batch;

SU_i = time spent in the set-up of the line for the i -th batch;

T_i = advance or delay of the i -th batch compared to the due dates;

$\alpha_i, \beta_i, \gamma_i$ = related weights.

Through the use of quantitative indicators can be determined the quality of a scheduled plan, using an evaluator module capable of expressing a "vote" for the scheduled plan, using a series of cost's indicators, expressed in the target function:

- Costs for the Set-up of the lines;
- Costs of chessboard between the lines;
- Costs of delay or advance compared with the date agreed for the delivery.

The data input for the evaluator module are:

- **Lots** ordered according to a specific scheduling to test;
- **Status Team**: last line the team has worked on;
- **Status Line**: last worked model (line and model have the same index i since each one is related to the other);
- **Release dates**: the date of actual start of production;
- **Due dates**: the date agreed for delivery;
- **Cycle Time** to assemble the models, with differences from model to model.

2.2. Complexity of the problem

The complexity of the problem is linked with the orders that day by day are added to the production plan and have to be scheduled with the lowest impact on costs and service levels.

Therefore it becomes necessary a proper management of the available resources, through the study of the chessboard and scheduling problems.

The way the workteam has to shift between the lines depends on the two ways the line can be left:

- Leaving the line "full" after it stopped will leave semi-assembled models on the line: this method is useful when it is expected that the team will be back soon on that line and the same model;
- Leaving the line "empty" the workteam finishes to assemble all the provided models: this is worth it when it is expected that in a few days the team will assemble a different model on that line.

Considering the real configuration of the line and the convenience in not immobilizing items upon them, the most appropriate solution, among the two above, is the second one: moving the team to a blank line to another,

with loss of time due to the shifting of the team that are still small. In this situation the operators, as they move, can begin assembling the new model, but the faster line must be adapt to the slower one, so the loss of time will depend on the speed of both lines (Figure 4).

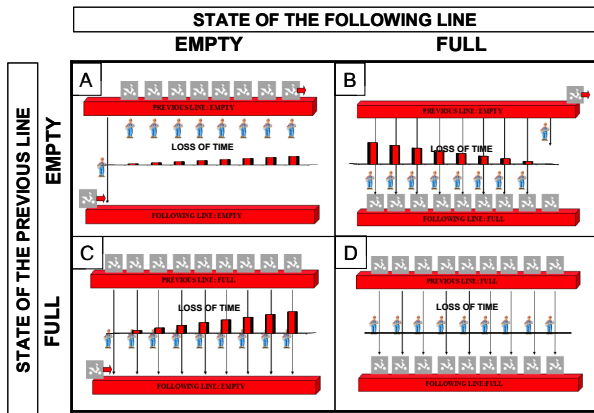


Figure 4: Time lost in the four shifting choices

The time lost in the empty-empty chessboard configuration is:

$$\text{LOST TIME} = TC_{\text{reached}} \times (N_{\text{reached}} - 1) / 2$$

In the evaluation of the time lost in chessboard are considered:

- CT = cycle time;
- ΔTC = difference, positive, between the cycle times of the two lines;
- N = number of operators on the line.

As regards the calculation of the time lost for the set-up, it's possible to proceed as follows: if the line of the batch i is the same of the batch i-1, the time spent for the set-up is calculated according to two based situations: if the model is the same, the time lost in the set-up of the line is zero, otherwise the set-up time of the line is equal to a motorcycle and two clamps free, i.e. at the time of execution of a task multiplied by three.

Figure 5 summarizes the loss of time, when the lot changes, due to the two issues of setup and chessboard:

	Time losses	
	Fixed	Variable (depending on models production times)
Chessboard	Time needed for the team shifting	Shifting strategy between lines (empty-empty, full-full, ...)
Job changes on the same line	Time needed for the movement of two free clamps	Adaptation to the slowest present model

Figure 5: Loss of time when the lot changes

2.3. Simulation approach

To study better the complexities discussed so far, the choice was to model and develop a methodology to

handle the incoming data of the different scheduling tested, to process the results, and analyze them in relation with the targets of the company, or in relation to the results obtained with other scheduling.

This approach has been applied to the problem called Permutation flow shop sequencing problem which consists in having to process (in the same order) on M machines, N job, which identify, in the case of the production lines, with different batches. The input data are the main orders MPS, which correspond to the batches to be produced, planned in the medium term.

The case study has in fact provided the information to realize a simulation model, tested with a four month production plan on two assembly lines, which are handled, in low season, by one workteam. The model has been developed through the use of SIMUL8 simulation software and the Microsoft EXCEL program.

3. MODEL DESCRIPTION

The simulation model was built by a combination of an object oriented software (SIMUL8) and MS Excel. The integration was obtained by using the specific simulation language called Visual Logic, which allows the full customization of the simulation objects and the communication with other software.

The construction of the graphical structure of the model and of its functional characteristics was based on input data supplied by the company; input data and constraints of the real production are transmitted on the simulator through the interface with the MS Excel file or Visual Logic on the Simulator.

The information on the Orders provided directly by the company are:

- Work calendar of the workteam;
- Quantity of the lot;
- Delivery date of the order;
- Line which the model will be worked on;
- Total processing time of a job (in relation to different models);
- Efficiency of the workteam (98%).

The model can simulate in a few moments the real operating conditions established in advance; dynamically simulate different types of scheduling, by changing from time to time the sequence of orders received as a function of the variables mentioned above, obtaining results that are transcribed in the MS Excel sheet of process and analysis of results. The outputs of the simulation are of two types: those related to the whole system performance (i.e. percentage of use of the machines of the two lines and of the resources) and those related to the minutes of start and end of production, crossing times of the batches, delays or advance on delivery dates, and time lost in the chessboard and set-up. Specifically, the results are: delay / advance max, average delay / advance, number of orders late / early, total days of delay / advance, average flowtime, makespan, total time lost in the chessboard, total time lost for the set-up, target

function.

These results refer to the use of the simulation model to see and measure the effects of scheduling heuristically planned through different combinations of the input data, related to the orders. The scheduling rules and heuristics used with the simulation model were based on the real options for the easy scheduler available in the enterprise plus the use of a genetic algorithm, implemented by the authors but not yet optimized for the specific case study. The basic rules, the results of are showed later, process orders with one of the sequent logic:

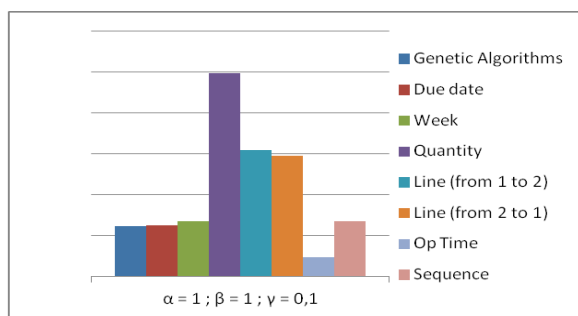
- start from the first to be satisfied (*due dates*);
- before the more little lots (*quantity*);
- just schedule depending on the arriving order (*week*);
- gather together the orders of a specific line reducing the chessboard (*line*);
- sequence by the operation time for one product (*op time*);
- choose just to balance the load of the lines in a specific time window (*sequence*).

Through the use of the MS Excel macro functions, it was possible to record several scheduling, and selecting and testing them quickly and easily.

4. RESULTS

The results of analysis and comparison of different scheduling tested are facilitated by the use of histograms that allow a more immediate graphical display of the results and can lead the company to strategic considerations. The histograms show all the heuristic scheduling tested, each one is related to his respective value of a specific performance parameter. The performance parameters considered are presented.

4.1. Target function

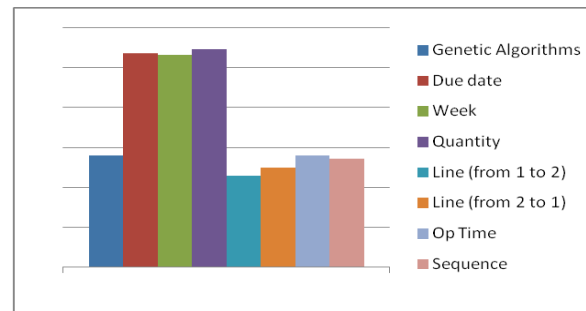


$$T.F. = \alpha_i \cdot \sum CB_i + \beta_i \cdot \sum SU_i + \gamma_i \cdot \sum T_i$$

related weights: α_i ; β_i ; $\gamma_i = 1; 1; 0,1$

The Scheduling that minimizes the target function is the one that better meets the needs of the company since it takes into account more variables of interest established by the company itself and how these variables affect in terms of cost and time.

4.2. Flowtime



This parameter indicates how much time is elapsed, on average, from the moment a job enters the production to the time is completed:

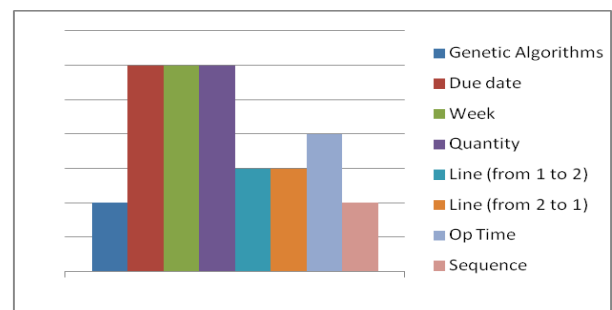
$$F_{med} = \frac{\sum_{j=1}^N F_j}{N}$$

Where:

N: jobs total number

To minimize this delay means increasing the number of operations the company performs in the range of time considered because it leads to an increase in remaining production capacity. This principle however must be used only in case of real need (speed of response to the customer), as if the volumes of requests remain constant, the saturation level of the machines would be decreased,

4.3. Makespan



This parameter is similar to the completion time of the last job being processed, i.e. the extent of time necessary to complete all tasks.

Similarly to the case of the minimization of flowtime, a solution which minimizes the makespan should be adopted in all those cases where it is desired to increase the residual capacity of the existing resources with the aim of increasing the production volumes. The evaluation in this case is on a parameter that does not aggregate average values (such as the flowtime average) but retains the total impact

$$MAK = \max(C_j) - \min(I_j)$$

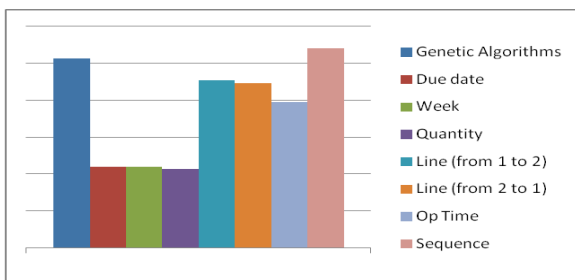
Where:

C_j : Job j production completion date;

I_j : Job j production starting date.

The makespan depends on the scheduling since a bad operative planning may repeatedly cause the occurrence of the phenomenon of "bottlenecks". that is the slowing down of a faster lot that enters in the production line after a slower lot, with the line that takes the rate of production of the slower lot and the value of the makespan which therefore increases.

4.4. Average saturation coefficient of the system



This parameter indicates how long, compared to the makespan, the M machines at issue were engaged in the processing of different orders:

$$S_{med} = \frac{\sum_{i=1}^M \sum_{j=1}^N t_{i,j}}{MAK}$$

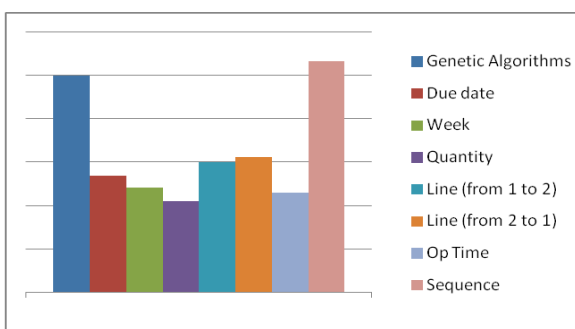
Where:

$t_{i,j}$: Job j production time on the machine i.

The situations which is convenient to use this policy are when every start and stop of the machine brings inefficiencies and significant periods of not added value, or when it is particularly expensive the purchase and maintenance of the resources.

In the case study considered the choice of the scheduling affects for only a few percentage points on the saturation of the system that is relatively low (with a range that varies from 42% to 45%) because of the choice made by the company to maintain operational policy of mixed-model lines, even in low season. The main advantage of this choice is the ease of configuration of the line and of its arrest, with expense, however, in the saturation of the lines themselves.

4.5. Average coefficient of human resources



This parameter indicates the percentage of time the operator is engaged in manufacturing, and large inefficiencies of this type can not be accepted by the company since brings clearly a loss of competitiveness.

5. CONCLUSION AND FUTURE RESEARCH

Simulation study showed that the scheduling process in the mixed-model production strongly effects global performances of just-in-time and workloads.

The develop tools are robust in its application and can be a decision support tool to assess specific scheduling solutions, taking into account multiple production parameters, from the production times, to the operators efficiency.

The natural development of the model allows not only to investigate the effects of variability on the production times and of other characteristics. Moreover a link to optimization algorithms can be introduced to fast assess available solutions and see their global effects.

REFERENCES

- Aigbedo, H., Monden, Y., 1997. A parametric procedure for multicriterion sequence scheduling for just-in-time mixedmodel assembly lines. *International Journal of Production Research* 35, 2543–2564.
- Allahverdi, A., Ng, C.T., Cheng, T.C.E., Kovalyov, M.Y., 2008. A survey of scheduling problems with setup times or costs. *European Journal of Operational Research*, 187 (3), 985–1032.
- Bautista, J., Companys, R., Corominas, A., 1996. Heuristics and exact algorithms for solving the Monden problem. *European Journal of Operational Research* 88, 101–113.
- Baker, K.R., Bertrand, J.W.M., 1982. A dynamic priority rule for scheduling against due-dates. *Journal of Operations Management*, 3 (1), 37–42.
- Bautista, J., Cano, J., 2008. Minimizing work overload in mixed-model assembly lines. *International Journal of Production Economics*, 112, 177–191.
- Baybars, I., 1986. A survey of exact algorithms for the simple assembly line balancing problem. *Management Science* 32, 909–932.
- Boysen, N., Fliedner, M., 2006. Comments on “Solving real car sequencing problems with ant colony optimization. *European Journal of Operational Research* 182, 466–468.
- Boysen, N., Fliedner, M., Scholl, A., 2009. Sequencing mixed-model assembly lines: Survey, classification and model critique. *European Journal of Operational Research*, 192, 349–373.
- Boysen, N., Fliedner, M., Scholl, A., 2009. The product rate variation problem and its relevance in real world mixed-model assembly lines. *European Journal of Operational Research*, 197, 818-824.
- Daniels R.L. and Mazzola J.B., 1994. Flow Shop Scheduling with Resource Flexibility. *Operations Research*, 42 (3), 504-522.
- Hall, R.W., 1991. *Queuing Methods for Services and Manufacturing*, Prentice-Hall, Englewood Cliffs, NJ.

- Li, Z., Ierapertitou, M., 2008. Process scheduling uncertainty: review and challenges. *Computers & Chemical Engineering* 32 (4–5), 715–727.
- Kotani, S., Ito, T., Ohno, K., 2004. Sequencing problem for a mixed-model assembly line in the Toyota production system. *International Journal of Production Research* 42, 4955–4974.
- Miltenburg, J., 1989. Level schedules for mixed-model assembly lines in just-in-time productions systems. *Management Science* 35, 192–207.
- Monden, Y., 1983. *Toyota Production System*. Industrial Engineering and Management Press, Institute of Industrial Engineers, Atlanta, GA.
- Scholl, A., Becker, C., 2006. State-of-the-art exact and heuristic solution procedures for simple assembly line balancing. *European Journal of Operations Research* 168, 666–693.
- Parthanadee P., Buddhakulsomsiri J., 2010. Simulation modeling and analysis for production scheduling using real-time dispatching rules: A case study in canned fruit industry, *Computers and Electronics in Agriculture*, 70, 245–255.
- Ponnambalam, S.G., Aravindan, P., Chandrasekaran S. 2001. Constructive and improvement flowshop scheduling heuristics: an extensive evaluation. *Production Planning and Control*, 12 (4), 335-344.
- Portmann M.C., 1997. Scheduling Methodology: Optimisation and Compu-search Approaches I, *The Planning and Scheduling of Production System: Methodologies and Applications*, ed. Artiba A., Elmaghraby S. E. Chapman & Hall, 271-300.
- Rajendran, C., Holthaus, O., 1999. A comparative study of dispatching rules in dynamic flowshops and jobshops. *European Journal of Operational Research* 116 (1), 156–170.
- Ruiz, R. and Maroto, C., 2005. A comprehensive review and evaluation of permutation flowshop heuristics. *European journal of operational research*, 165, 479-494.
- Xiaobo, Z., Ohno, K., 1997. Algorithms for sequencing mixed models on an assembly line in a sit production system. *Computers and Industrial Engineering* 32, 47–56.
- Yano, C.A., Bolat, A., 1989. Survey, development and applications of algorithms for sequencing paced assembly lines. *Journal of Manufacturing and Operations Management* 2, 172–198.

ENHANCED CONFIDENCE INTERPRETATIONS OF GP BASED ENSEMBLE MODELING RESULTS

Michael Affenzeller^(a), Stephan M. Winkler^(b), Stefan Forstenlechner^(c), Gabriel Kronberger^(d),
Michael Kommenda^(e), Stefan Wagner^(f), Herbert Stekel^(g)

^(a-f) University of Applied Sciences Upper Austria
Heuristic and Evolutionary Algorithms Laboratory
Softwarepark 11, 4232 Hagenberg, Austria

^(a,b) University of Applied Sciences Upper Austria
Bioinformatics Research Group
Softwarepark 11, 4232 Hagenberg, Austria

^(g) General Hospital Linz
Central Laboratory
Krankenhausstraße 9, 4021 Linz, Austria

^(a) michael.affenzeller@fh-hagenberg.at, ^(b) stephan.winkler@fh-hagenberg.at, ^(c) stefan.forstenlechner@fh-hagenberg.at
^(d) gabriel.kronberger@fh-hagenberg.at, ^(e) michael.kommenda@fh-hagenberg.at, ^(f) stefan.wagner@fh-hagenberg.at,
^(g) herbert.stekel@akh.linz.at

ABSTRACT

In this paper we describe the integration of ensemble modeling into genetic programming based classification and discuss concepts how to use genetic programming specific features for achieving new confidence indicators that estimate the trustworthiness of predictions. These new concepts are tested on a real world dataset from the field of medical diagnosis for cancer prediction where the trustworthiness of modeling results is of highest importance.

Keywords: data mining, genetic programming, ensemble modeling, medical data analysis

1. INTRODUCTION, RESEARCH GOALS

Genetic Programming (GP) plays an outstanding role among the data-mining techniques from the field of machine learning and computational intelligence: Due to its model representation, GP is able to produce human interpretable models without any assumptions about the nature of the analyzed relationships. Furthermore, GP-based data analysis has been shown to have good generalization; GP is also able to simultaneously evolve the structure and the parameters of a model with implicit feature selection. Due to the combination of these aspects GP is considered a very powerful and also robust method for various data analysis tasks.

Apart from these general aspects of genetic programming based modeling, the hybridization of symbolic regression and ensemble modeling is still rarely considered. A good overview article about genetic programming and ensemble modeling has been

presented by Keijzer and Babovic (Keijzer, Babovic 2000).

In this paper we introduce new methods for the generation and interpretation of model ensembles consisting of symbolic regression / classification models; concretely, we introduce new confidence measures for assessing the trustworthiness of genetic programming ensemble models. Furthermore, we discuss and interpret symbolic classification ensemble modeling results achieved for medical data mining tasks.

The experimental part of the paper discusses the value of trust of correct classifications opposed to the value of trust of incorrect classifications, and analyzes if the confidence of the correctly classified instances is significantly higher than that of the incorrectly classified samples.

2. THEORETICAL FOUNDATIONS

2.1. Genetic Programming Based Symbolic Classification

Symbolic classification with genetic programming uses the general concept of a genetic algorithm in order to search the space of hypotheses which are represented as mathematical formulae in structure tree representation. We have also applied a classification algorithm based on genetic programming (GP, Koza (1992)) using a structure identification framework described in Winkler (2008) and Affenzeller et al. (2009).

We have used genetic programming with gender specific parents selection (Wagner 2005) (combining random and roulette selection) as well as strict offspring

selection (Affenzeller et al. 2009) (OS, with success ratio as well as comparison factor set to 1.0) as this variant has proven to be especially suited for symbolic classification. The function set described in (Winkler 2008) (including arithmetic as well as logical ones) was used for building composite function expressions.

In addition to splitting the given data into training and test data, the GP based training algorithm used in our research project has been designed in such a way that a part of the given training data is not used for training models and serves as validation set; in the end, when it comes to returning classifiers, the algorithm returns those models that perform best on validation data.

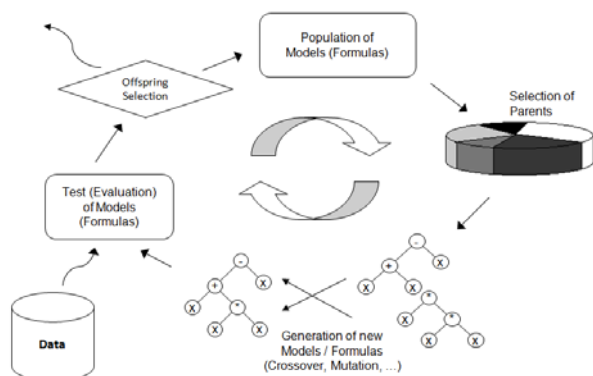


Figure 1: Genetic programming including offspring selection.

The used fitness function is the mean squared error of the training samples using a threshold value that gives optimal accuracy on the training data set. The distance between a certain prediction and the threshold will be used in our ensemble interpretation to achieve additional estimates about the trustworthiness of the ensemble prediction.

2.2. Ensemble Modeling

Ensemble modeling techniques may be used as an extension to various regression and classification techniques. Supported by the increasing availability of hardware resources and parallel computing infrastructures, the general concept of ensemble modeling is used in order to increase the reliability and robustness of predictive models.

The general idea is to apply not only a single hypothesis for predictive modeling but a large number of stochastically independent models. The result of an ensemble predictor is typically given by the average or mean value of the ensemble results for regression modeling or by some kind of majority voting for classification tasks. The reliability of an ensemble prediction may be indicated by the variance of the ensemble results for regression or by the clearness of the majority voting in classification applications (Keijzer, Babovic 2000).

Basically the idea of ensemble modeling can be coupled with any stochastic hypothesis search technique. A well-known example is given by the concept of random forests (Breiman, 2001) where ensemble modeling is integrated into the general concept of tree learning strategies.

In this paper we discuss the integration of ensemble modeling into the concept of genetic programming based symbolic classification under the special focus of developing and analyzing extended confidence estimates of the ensemble modeling results.

3. NEW CONFIDENCE MEASURES OF SYMBOLIC CLASSIFICATION ENSEMBLE MODELS

The idea is to combine the degree of majority of a majority voting with the average clearness of the ensemble predictors for a certain sample.

On the one hand, a certain prediction will be considered the more reliable the clearer the result of the majority voting is. If we evaluate, for example, 99 ensemble models we will have more trust in a 91 to 8 majority than in a 50 to 49 majority. This kind of interpretation may be applied to any ensemble model as it does not use genetic programming specific aspects.

Assuming a two-class classification problem the corresponding first confidence measure cm_1 is defined as

$$cm_1 := 2 \left(\frac{|votes(winning\ class)|}{|votes|} - 0,5 \right) \in [0, 1]$$

The fraction of votes for the winner class in relation to the total number of ensemble votes ($(|votes(winning\ class)|)/(|votes|)$) will range between 0.5 and 1 for the majority vote. In order to normalize this confidence measure between 0 and 1 we have adapted the formula accordingly.

On the other hand we will discuss a second indicator of trustfulness which is unique to genetic programming which optimizes the mean squared error of residuals in the training data set. Supposing a two-class classification problem with the classes 0 and 1 we will rather trust an ensemble predictor where most of the prognoses are clustered around 0 compared to a predictor where the ensemble results will be around 0.45. The according second confidence measure cm_2 is therefore designed to consider both, the majority of the voting as well as the uniqueness of the certain ensemble predictors for a certain sample. Concretely cm_2 is defined as

$$cm_2 = \min \left(\frac{\Delta(m(t), m(e))}{\Delta(m(t), class)}, 1 \right) \in [0, 1] \quad (3)$$

where Δ denotes the difference between the mean value of the ensemble thresholds and the median or mean value of the ensemble predictions in the nominator of the formula. In the denominator of the formula the distance Δ between the median or mean value of the thresholds and the class value predicted by the ensemble is represented (which is basically the range for the predictors). The confidence cm_2 will therefore on the

one hand be rather low ($cm_2 \approx 0$) if the majority of ensemble predictors are near the threshold; on the other hand, if the majority of ensemble votes is around the actual class this confidence will rather high ($cm_2 \approx 1$). By considering some kind of average value (median or mean), confidence measure cm_2 is expected to implicitly consider both, the majority of the voting result and the uniqueness of the single ensemble predictors.

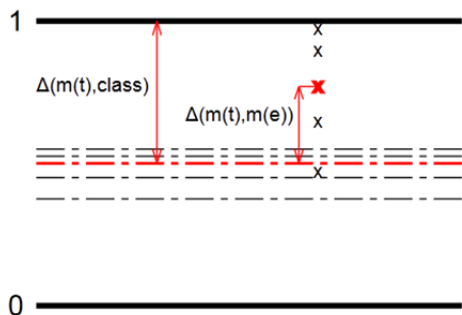


Figure 1: Illustration of different GP ensemble estimators and their corresponding thresholds.

As illustrated in Fig. 1 for the second confidence measure cm_2 the difference between the mean ensemble predictor $m(e)$ to the mean threshold $m(t)$ is considered with respect to the difference between the mean threshold $m(t)$ and the corresponding class.

The effectiveness of the both confidence measures cm_1 and cm_2 will be analyzed by discussing the average confidence of correct predictions compared to the average confidence of incorrect predictions. Of course, confidence is expected to be higher for correct predictions and the delta between confidence in correct predictions and incorrect predictions may be used in order to interpret the suitability of the concrete confidence measure for a certain application. Due to its usage of additional information cm_2 is expected to be more suited than cm_1 in general for binary classification problems.

4. THE MEDICAL DATASET

In this section we describe results achieved within the Josef Ressel Centre for Heuristic Optimization *Heureka!*: Data of thousands of patients of the General Hospital (AKH) Linz, Austria, have been preprocessed and analyzed in order to identify mathematical models for cancer diagnoses. We have used a medical database compiled at the central laboratory of AKH in the years 2005 – 2008: 28 routinely measured blood values of thousands of patients are available as well as several tumor markers (TMs, substances found in humans that can be used as indicators for certain types of cancer). Not all values are measured for all patients, especially tumor marker values are determined and documented only if there are indications for the presence of cancer. The results of empirical research work done on the data based identification of estimation models for standard blood parameters as well as tumor markers. The main

goal is to generate mathematical models for cancer prediction based on blood parameters.

The blood data measured at the AKH in the years 2005-2008 have been compiled in a database storing each set of measurements (belonging to one patient): Each sample in this database contains an unique ID number of the respective patient, the date of the measurement series, the ID number of the measurement, standard blood parameters, tumor marker values, and cancer diagnosis information. Patients' personal data were at no time available for the authors except for the head of the laboratory.

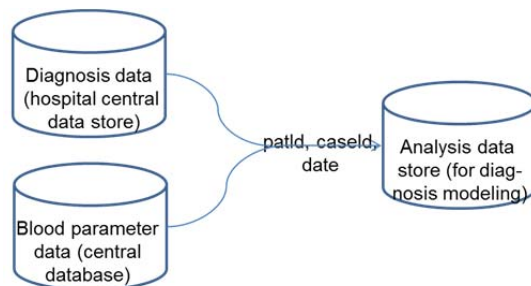


Figure 2: Integration of the relevant data from different hospital databases

In total, information about 20,819 patients is stored in 48,580 samples. Please note that of course not all values are available in all samples; there are many missing values simply because not all blood values are measured during each examination. Further details about the data set and necessary data preprocessing steps can for example be found in Winkler et al. (2010) and Winkler et al. (2011), e.g.

Standard blood parameters include for example the patients' sex and age, information about the amount of cholesterol and iron found in the blood, the amount of hemoglobin, and the amount of red and white blood cells; in total, 29 routinely available patient parameters are available.

An important aspect in the data preprocessing stage was to identification of relevant blood parameters for a positive cancer diagnosis. In order to identify characteristic blood parameters for a positive cancer prediction we have collected those blood parameters which have been measured in a time window of two weeks before the first cancer diagnosis based in ICD 10 classification of diseases. Blood parameters taken earlier may not be characteristic as the patient may still have been healthy at that time and measurements taken after the diagnoses may be diluted due to medical treatment. The blood parameters for the class of healthy persons have been taken only from patients with no positive cancer diagnosis in their case history.

patient	date	[..blood parameters..]	diagnosis
1001	01.01.2004	[...]	-
1001	01.01.2005	[...]	-
1001	01.01.2006	[...]	-
1001	29.05.2007	[...]	-
1001	01.06.2007	[...]	-
1001	02.06.2007	[...]	-
1001	15.06.2007	[...]	C61
1001	02.07.2007	[...]	C61
1001	15.07.2007	[...]	C61
1001	02.09.2007	[...]	C61
1001	01.01.2008	[...]	C61
1001	05.02.2008	[...]	-
1001	01.03.2008	[...]	-
1001	17.03.2008	[...]	-
1001	01.01.2009	[...]	-

healthy (assumption) [rows 1-3]
relevant measurements [rows 4-6]
maybe misleading due to therapy [rows 7-9]
healthy (assumption) [rows 10-12]

Figure 3: Identification of appropriate periods of relevant measurements for cancer diagnosis

5. GENETIC PROGRAMMING

For generating the ensemble models we have used gender specific strict offspring selection genetic programming which is available in the HeuristicLab 3.3.6 framework <http://dev.heuristiclab.com>.

We have used the following parameter settings for our GP test series: The mutation rate was set to 20%, gender specific parents selection (Wagner 2005) (combining random and roulette selection) was applied as well as strict offspring selection (Affenzeller et al. 2009) (OS, with success ratio as well as comparison factor set to 1.0). The functions set described in (Winkler 2008) (including arithmetic as well as logical ones) has been used for building composite function expressions.

In addition to splitting the given data into training and test data, the GP based training algorithm used in our research project has been designed in such a way that a part of the given training data is not used for training models and serves as validation set; in the end, when it comes to returning classifiers, the algorithm returns those models that perform best on validation data.

6. RESULTS

For the results presented in this section a set of GP-based models of different model sizes have been generated for the prediction of breast cancer based solely on blood parameters and also based on blood parameters together with its corresponding tumor markers (C125, C15-3, CEA). The main GP parameters have been adjusted according to the settings shown in Table 1.

Algorithm	Offspring Selection Genetic Programming
Runs	100 per tree size (with three different tree sizes)
TreeCreator	Probabilistic Tree Creator
Symbols	+, -, *, /, sin, cos, tan, exp, log, IfThenElse, <, >, and, or, not
Fitness function	MSE (mean squared error)
Selector	GenderSpecific (Random, Proportional)
Mutator	ChangeNodeTypeManipulation, FullTreeShaker,

	OnePointTreeShaker, ReplaceBranchManipulation
Crossover	SubtreeCrossover
Elites	1
Population Size	700
Mutation Rate	20%
Maximal Generations	1000
Maximal Selection Pressure	100
Cross Validation Folds	5
Tree size (Length/Depth)	20/7, 35/8, 50/10

Table 1: Algorithmic settings

Overall 300 (100 per tree size) independent runs have been performed for predicting breast cancer and the 75 best models concerning their training quality have been used for ensemble modeling as well as for standard evaluations as shown in Table 2. Table 2 shows the average training and test qualities of the best 75 training models (the same ones which are used also for the ensemble models and confidence analyses). Moreover the training and test accuracies of the overall best training model are shown in Table 2.

Tables 3 and 4 show the results in ensemble interpretation for modeling breast cancer with standard blood parameters alone (Table 3) as well as together with tumor markers as additional input features. Together with the accuracies the confidence measures described in section 3 are shown for the correctly as well as for the incorrectly classified instances.

There are several conclusions that can be drawn from the following result tables:

- The results – especially the test results – of the ensemble predictions (Tables 3 and 4) are better than the results achieved with conventional GP models.
- The confidence in the predictions measured by the two confidence measures cm_1 and cm_2 is significantly higher for the correctly classified instances than in those of the incorrectly classified instances. The delta is even higher if tumor markers can be used for the models.
- The distribution of the two confidence values for the correctly and incorrectly classified instances with cm_1 (left boxplots) and cm_2 (right boxplots) indicate high potential for future research based on these confidence measures: By introducing a confidence threshold below which the results are categorized as untrustworthy, the trusted results are expected to have significantly higher quality.
- Contrary to the theoretical considerations of Section 3 the statistical properties of the more complex cm_2 do not seem to lead to more

significant differentiation between the correctly and incorrectly classified instances.

	Avg. training accuracy of 100 best models	Avg. test accuracy of 100 best models	Training accuracy of best model	Test accuracy of best training model
Breast with TM	83.17%	77.89%	84.74%	79.33%
Breast without TM	76.79%	72.61%	78.15%	73.08%

Table 2: Results with standard GP-based predictive modeling (without ensemble modeling)

	Majority Vote	Average Threshold
Accuracy training	78.47%	78.47%
Accuracy test	76.49%	76.49%
Average Confidence Correct Classified	$cm_1 = 0.8202$	$cm_2 = 0.4835$
Average Confidence Incorrect Classified	$cm_1 = 0.5543$	$cm_2 = 0.2525$
Confidence Delta	0.2659	0.2310

Table 3: Breast cancer without tumor marker

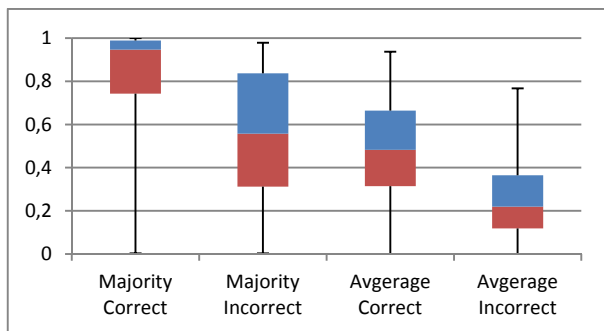


Figure 4: Boxplot breast cancer without tumor marker

	Majority Vote	Average Threshold
Accuracy training	84.99%	84.99%
Accuracy test	81.44%	81.44%
Average Confidence Correctly Classified	$cm_1 = 0.8500$	$cm_2 = 0.6182$
Average Confidence Incorrectly Classified	$cm_1 = 0.4806$	$cm_2 = 0.2449$
Confidence Delta	0.3694	0.3733

Table 4: Breast cancer with tumor marker

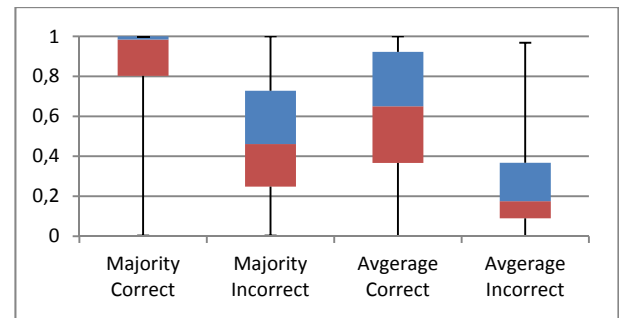


Figure 5: Boxplot breast cancer with tumor marker

7. CONCLUSION

In this paper two confidence measures have been discussed for predictive models generated by GP-based ensemble modeling. The results for a breast cancer data set have shown that the confidence for the correctly classified instances is significantly higher than the confidence for incorrectly classified instances which is considered as the main result of this contribution and which opens new areas of application especially for predictive modeling in the medical field where the confidence in a prediction is very important.

Obvious aspects for future investigations in this field are analyses for further cancer types as well as the introduction of a new class for the uncertain prediction (below a certain confidence threshold) and corresponding analyses of the statistical properties of the so achieved predictions.

ACKNOWLEDGMENTS

The work described in this chapter was done within the Josef Ressel-Centre *Heureka!* for Heuristic Optimization sponsored by the Austrian Research Promotion Agency (FFG).

REFERENCES

- Affenzeller, M., Winkler, S., Wagner, S., A. Beham, 2009. *Genetic Algorithms and Genetic Programming - Modern Concepts and Practical Applications*. Chapman & Hall/CRC. ISBN 978-1584886297. 2009.
- Breiman, L. 2001. Random Forests. *Machine Learning* 45, pp. 5 – 32.
- Keijzer, M., Babovic, V., 2000. Genetic Programming, Ensemble Methods and the Bias/Variance Tradeoff – Introductory Investigations. *Lecture Notes in Computer Science, 2000, Volume 1802/2000*, pp. 76-90.
- Wagner, S., 2009. *Heuristic Optimization Software Systems - Modeling of Heuristic Optimization Algorithms in the HeuristicLab Software Environment*. PhD Thesis, Institute for Formal Models and Verification, Johannes Kepler University Linz, Austria.
- Winkler, S., Affenzeller, M., Jacak, W., Stekel, H., 2010. Classification of Tumor Marker Values Using Heuristic Data Mining Methods. *Proceedings of Genetic and Evolutionary Computation Conference 2010, Workshop on*

Medical Applications of Genetic and Evolutionary Computation, pp. 1915–1922.

Winkler, S., Affenzeller, M., Jacak, W., Stekel, H., 2011. Identification of Cancer Diagnosis Estimation Models Using Evolutionary Algorithms – A Case Study for Breast Cancer, Melanoma, and Cancer in the Respiratory System. *Proceedings of Genetic and Evolutionary Computation Conference 2011, Workshop on Medical Applications of Genetic and Evolutionary Computation*.

AUTHORS BIOGRAPHIES



MICHAEL AFFENZELLER has published several papers, journal articles and books dealing with theoretical and practical aspects of evolutionary computation, genetic algorithms, and meta-heuristics in general. In 2001 he received his PhD in engineering sciences and in 2004 he received his habilitation in applied systems engineering, both from the Johannes Kepler University of Linz, Austria. Michael Affenzeller is professor at UAS, Campus Hagenberg, and head of the Josef Ressel Center *Heureka!* at Hagenberg.



STEPHAN M. WINKLER received his PhD in engineering sciences in 2008 from Johannes Kepler University (JKU) Linz, Austria. His research interests include genetic programming, nonlinear model identification and machine learning. Since 2009, Dr. Winkler is professor at the Department for Medical and Bioinformatics at the University of Applied Sciences (UAS) Upper Austria at Hagenberg Campus; since 2010, Dr. Winkler is head of the Bioinformatics Research Group at UAS, Hagenberg.



Stefan Forstenlechner received his BSc in software engineering in 2011 from the Upper Austria University of Applied Sciences, Campus Hagenberg. He is currently pursuing studies for his master's degree and working at UAS Research Center Hagenberg within *Heureka!*.



GABRIEL KRONBERGER received his PhD in engineering sciences in 2010 from JKU Linz, Austria, and is a research associate at the UAS Research Center Hagenberg. His research interests include genetic programming, machine learning, and data mining and knowledge discovery.



MICHAEL KOMMENDA finished his studies in bioinformatics at Upper Austria University of Applied Sciences in 2007. Currently he is a research associate at the UAS Research Center Hagenberg working on data-based modeling

algorithms for complex systems within *Heureka!*.



STEFAN WAGNER received his PhD in engineering sciences in 2009 from JKU Linz, Austria; he is professor at the Upper Austrian University of Applied Sciences (Campus Hagenberg). Dr. Wagner's research interests include evolutionary computation and heuristic optimization, theory and application of genetic algorithms, and software development.



WITOLD JACAK received his PhD in electric engineering in 1977 from the Technical University Wroclaw, Poland, where he was appointed Professor for Intelligent Systems in 1990. Since 1994 Prof. Jacak is head of the Department for Software Engineering at the Upper Austrian University of Applied Sciences (Campus Hagenberg) where he currently also serves as Dean of the School of Informatics, Communications and Media.



HERBERT STEKEL received his MD from the University of Vienna in 1985. Since 1997 Dr. Stekel is chief physician at the General Hospital Linz, Austria, where Dr. Stekel serves as head of the central laboratory.

MULTIDIMENSIONAL MODELLING OF THE IN-CYLINDER PROCESSES IN A GDI ENGINE

A. Montanaro^(a), U. Sorge^(b), F. Catapano^(c), B.M. Vaglieco^(d)

^{(a), (d)}CNR – Istituto Motori, Viale Marconi, 8 – 80125, Naples, ITALY

^{(b), (c)}DIME – University of Naples, Via Claudio, 21 – 80125, Naples, ITALY

^(a)a.montanaro@im.cnr.it, ^(b)u.sorge@im.cnr.it, ^(c)f.catapano@im.cnr.it, ^(d)b.m.vaglieco@im.cnr.it

ABSTRACT

The study is focused on the assessment of a 3D numerical model able to simulate the in-cylinder processes characterizing the operation of GDI (gasoline direct injection) engine equipped with a high-pressure injector system. The engine is experimentally characterized at the test bench. One of the 4 cylinders is modified to allow two optical accesses that leave unvaried the combustion chamber configuration and allows capturing images of the mixture formation and combustion processes. A sub-model of high portability allows simulating the spray dynamics, whose validation is made on the ground of experimental data collected with the injector mounted in a confined vessel. A preliminary study of the spray-wall impingement is also carried out, that allows better predicting the gasoline deposition and splashing phenomena.

Keywords: multidimensional engine modeling, gasoline direct injection, spray-wall impingement

1. INTRODUCTION

A way to significantly improve the energetic efficiency of internal combustion engines without making a major shift away from conventional technologies is well recognized in the use of direct injection (DI). In spark ignition (SI) engines, in particular, gasoline direct injection (GDI) is today considered indispensable to decrease fuel consumption, hence CO₂ emissions, as coupled with downsizing and turbo-charging. Thanks to the more precise control of the injection timings feasible through DI, well known limits of the port fuel injection (PFI) engines in the combustion control and fuel supply response are overwhelmed. The GDI technology, indeed, especially with the employment of new generation high-pressure injectors in the multi-hole configuration, has the great advantages of improving the mixture formation process, with a positive effect on combustion stability and pollutant emissions formation. Knock tendency is also favorably affected due to the decrease of the charge temperature consequent the in-cylinder gasoline evaporation [Alkidas, 2008]. Nevertheless, the complexity of modern engines makes for assuring optimal mixture conditions at all the engine loads and speeds to be a really difficult task. Exploiting

the capability of numerical techniques to achieve a complete control of the mixture formation process over the whole engine working map, to increase fuel economy, improve combustion stability, and reduce engine-out emissions is surely an issue of great importance in the automotive field.

Present work is aimed at developing a 3D engine model of the in-cylinder processes occurring in a modern GDI engine. The engine model assessment is supported by three experimental campaigns. The employed seven-hole injector is first preliminary experimentally characterized in a confined vessel and on a Bosch tube to tune the 3D sub-model for the spray dynamics. Experiments relevant to collect data for the validation of the sub-model for the spray-wall impingement are also carried out by making for the spray to orthogonally hit a flat plate, possibly heated at some given temperatures. Finally the engine is characterized to collect in-cylinder pressure data and images of the spray development. The engine, in fact, exhibits optical accesses enabling to explore an area including the spark and the gasoline spray. After a short description of the sub-models assessment, main results of the 3D engine simulation are presented, with reference to an overall lean, medium-speed medium-load operating condition.

2. EXPERIMENTAL APPARATUS

2.1. Spray Characterization

The GDI injector considered in the present work is a mini-sac seven-hole Bosch HDEV 5.1 with solenoid actuation. The injector holes diameter is equal to 0.179 mm. The static flow rate is of 13.7 g/s at the injection pressure of 10 MPa. Figure 1 represents a sketch of the spray footprint, drawn on a plane orthogonal to the injector axis, placed at a distance of 30 mm from the holes.

Commercial gasoline ($\rho = 740 \text{ kg/m}^3$) is used within all the experimental campaign, as delivered by a hydro-pneumatic injection system without rotating organs. The injector system is managed by a programmable electronic control unit (PECU). This is an open system able to reproduce the injector energizing currents for the desired strategy in terms of number of injection pulses, durations, rise and dwell times. The

PECU reproduces as an output a TTL signal, related to the injection event, used to synchronize also the consecutive images management and acquisitions. The PECU, in fact, also control the synchronized image acquisition set-up.

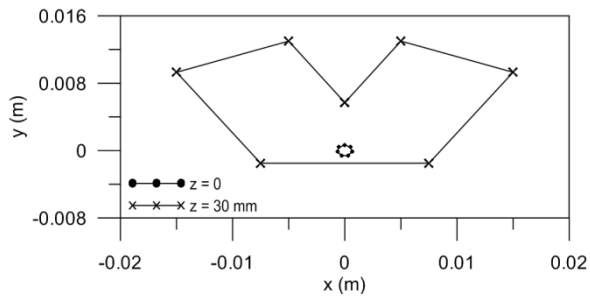


Figure 1: Holes position and spray footprint on a plane placed at 30 mm from the holes.

Three types of analysis are conducted: a) instantaneous mass flow rates are measured by means of an AVL Meter operating on the Bosch principle [Bosch, 1996; Wallace, 2002]; b) the single jet penetration length and cone angle of a freely developing spray are obtained by image processing techniques; c) the spray impingement on an orthogonal wall, possibly heated by image processing is used to characterize.

The instantaneous mass flow rate measured by the AVL fuel rate meter is integrated to gain the total injected mass and to verify its accordance with the measured one by means of a precision balance.

Images of the spray are collected by injecting the spray in an optically-accessible vessel containing nitrogen at controlled conditions of temperature and pressure. The injector command is generated by the PECU. A synchronized pulse starts both the flash enlightening and shutter of a high-resolution CCD camera (1376x1040 pixels, 12 bit resolution, 0.5 μ s shutter time). Images of the spray are collected at different instants from the start of injection (SOI) with a 50 mm lens obtaining a spatial resolution 0.103 mm/pixel (while for impinging test at 0.0658 mm/pixel). An overview of the experimental scheme for the image acquisition is reported in [Alfuso., Allocca, Greco, Montanaro, Valentino, 2008]. The captured images are processed off-line by means of a proper software, able to extract the parameters characterizing the spray dynamics, namely penetration length and cone angle of one of the seven jets compounding the spray. The images processing analysis is carried out in different steps: image acquisition and background subtraction, filtering, fuel spray edges determination and tip penetration measurements. Background subtraction and median filter procedures are adopted during the image acquisition to remove impulse noise and stray light, so to maintain sharp the spray edge. This is determined by selecting an intensity threshold level for separating the fuel region from the background ambient gas. The experiments devoted to determine the spray atomization characteristics in the case of impingent on an orthogonal wall are carried at different

injection pressures (p_{inj}), wall distance (h) and wall temperature (T_{wall}). Two of the considered conditions are reported in Table 1.

p_{inj} (MPa)	5.5	5.5
T_{wall} (K)	300	473.15
h (mm)	20	20

Table I: Experimental conditions for impinging sprays.

2.2. Optical Engine

The experimental apparatus for the characterisation of the engine performance includes the following modules: the spark ignition engine, an electrical dynamometer, the fuel injection line, the data acquisition and control units, as well as the emission measurement system. The electrical dynamometer allows the engine operation under both motored and firing conditions.

The engine under study is a SI DI, inline 4-cylinder, 4-stroke, displacement of 1750 cm^3 , turbocharged, high performance engine. It has a wall guided injection system with a seven-hole injector located between the intake valves and oriented at 70° with respect to the cylinder axis. The engine is equipped with a variable valve timing (VVT) system in order to optimize intake and exhaust valve lift for each regime of operation. The engine is not equipped with after-treatment devices. Further details of the engine are reported in Table II.

Unitary displacement [cm^3]	435.5
Bore [mm]	83
Stroke [mm]	80.5
Turbine	Exh. gas turbocharger
Max. boost pressure [bar]	2.5
Valve timing	Intake and exhaust VVT
Compression ratio	9.5:1
Max. power [kW]	147.1 @ 5000 rpm
Max. torque [Nm]	320.4 @ 1400 rpm

Table II. Engine specifications

Optical measurements are carried out through an optical access on the engine head, as reported in Figure 2. A custom protective case for an endoscopic probe, equipped with an optical sapphire window (5 mm in diameter), is installed in the engine head in the 4th cylinder. This system enables exploring an area including the spark and the fuel injection using an endoscope with a viewing angle of 70°. The field of view turns out to be centered in the combustion chamber and perpendicular to the plane of tumble motion.

Imaging measurements from ultraviolet (UV) to visible are performed by means of the optical experimental set-up shown in Figure 2. In particular, the endoscopic probe is coupled to a high spatial and temporal resolution intensified charge coupled device (ICCD) camera. It has a 78 mm focal length, f/3.8 UV Nikon objective, and an array size of 512x512 pixels and 16-bit dynamic range digitization at 100 kHz. The

optical assessment allows a spatial resolution approximately 0.19 mm/pixel, and a spectral range from UV (180 nm) until visible (700 nm). The intensifier-gate duration is equal to 1° crank angle (CA) for all investigated conditions. The dwell time between two consecutive images is set at 1° CA. A post-processing of the optical data is applied to obtain geometrical information from each image, such as the flame front area and the radius [Sementa, Vaglieco, Catapano, 2012]. Moreover, a quartz pressure transducer is installed into the spark plug in order to measure the combustion pressure. The in-cylinder pressure and the related parameters as the coefficient of variance (COV) of the IMEP, and the rate of chemical energy release are evaluated on an individual cycle basis averaged over 500 cycles [Heywood, 1988; Zhao, Ladommatos, 2001].

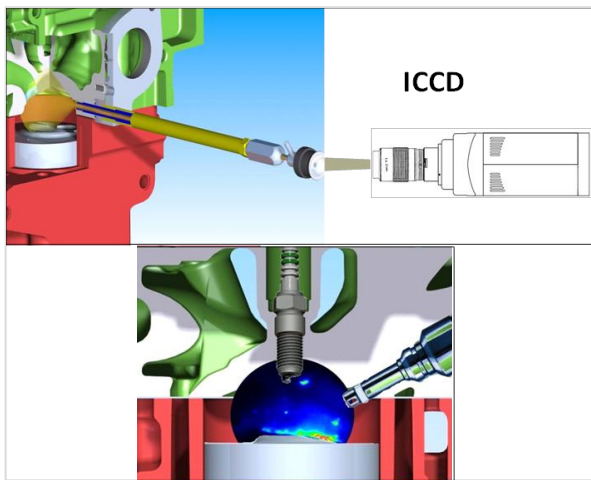


Figure 2: Sketch of the experimental setup for optical investigation and detail of the combustion chamber

The engine test discussed in the following of the paper is that relevant to an engine speed of 1500 rpm, a medium load (injected gasoline $m_f = 20.16$ mg/cycle, air to fuel ratio $A/F = 16.9$), injection pressure of 6 MPa, start of spark (SOS) set at 13° before the top dead center (BTDC) and start of injection (SOI) at 70° BTDC.

3. NUMERICAL SIMULATION

The here discussed 3D engine model is developed within the software AVL Fire™. The preliminary phase of the model set-up consisted in the assessment and validation of the sub-models for the spray dynamics and of the spray wall impingement, made by reproducing the experimental tests described in section 2.1. These aspects, indeed are believed of great importance to well reproduce the mixture formation process in a GDI engine.

The approach followed for the description of the two-phase turbulent flow is the classical coupling between the Eulerian description of the gaseous phase and the Lagrangian description of liquid phase. The coupling between the two phases is made through source terms representing the exchange of mass, momentum and energy in the balance equations.

3.1. The sub-models for the spray dynamics and the wall impingement

The spray is assumed as a train of droplets entering the computational domain at the initial time and with a given distribution of diameters. The effects of turbulent dispersion, coalescence, evaporation, wall interaction and break-up of droplets are treated with proper sub-models. In particular, the effect of the turbulent dispersion is treated following the sub-model by O'Rourke [O'Rourke, Bracco., 1980], coalescence with the sub-model by Nordin [Nordin, 2001], evaporation with the sub-model by Dukowicz [Dukowicz, 1979]. The model used to reproduce the wall interaction is the one proposed by Kuhke [AVL Fire™ User Guide, 2011].

Details of the validation phase of the sub-model reproducing the dynamics of a freely developing non evaporating spray are given in the paper by Costa *et al.* [Costa, Sorge, Allocca, 2012]. Some results are here reported.

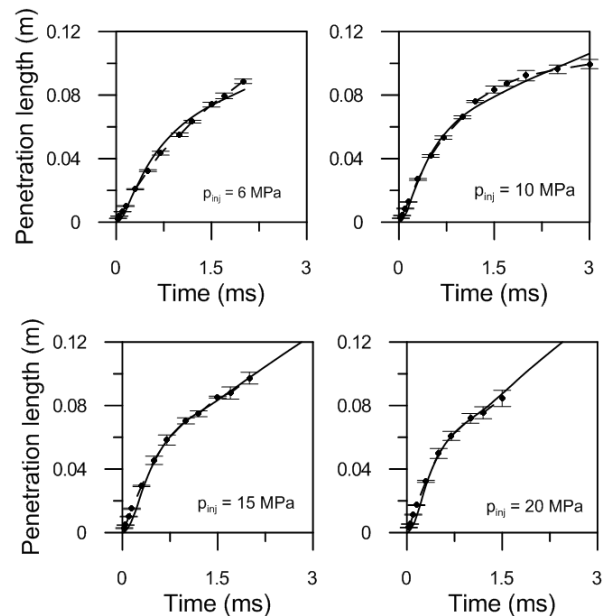


Figure 3: Numerical (continuous line) and experimental (dashed line with dots) penetration lengths of the GDI spray in confined vessel at various pressures. Error bars are also represented.

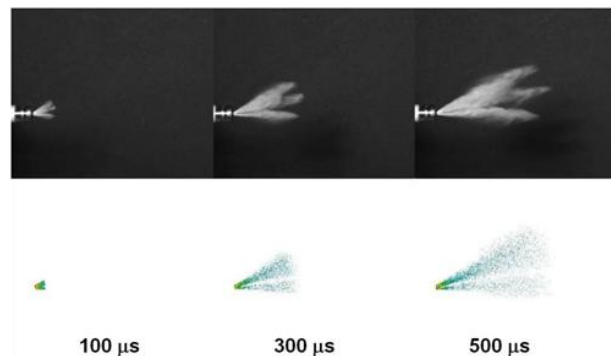


Figure 4: Experimental collected (top) and numerical computed (bottom) images of the spray at the injection pressure of 15 MPa

Figure 3 is the comparison between the numerical (average over the seven jets) and the experimentally measured penetration lengths (one of the seven jets) for four different injection pressures. The agreement between the sub-model results and the experiments is really good. The spray structure is also quite well reproduced, as shown in Figure 4, that shows experimental and numerical images of the spray at various instants of time from the SOI at $p_{inj}=15$ MPa.

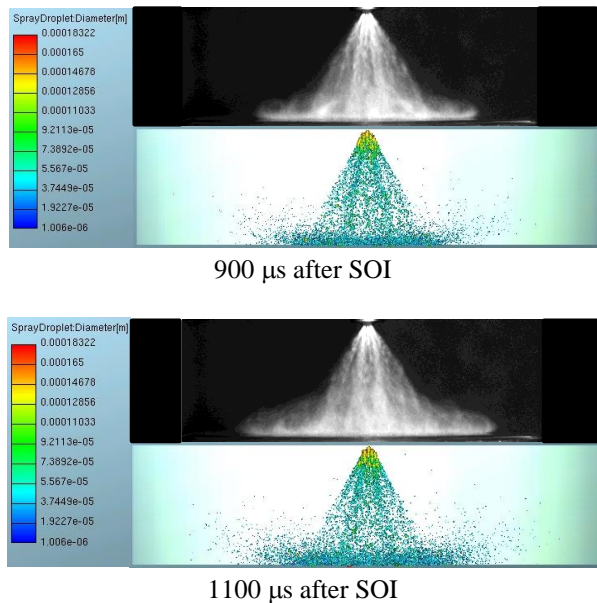


Figure 5: Comparison between experimental (top) and numerical (bottom) images of impinging sprays for $p_{inj}=5.5$ MPa, $T_{wall}=300$ K at two instants of time.

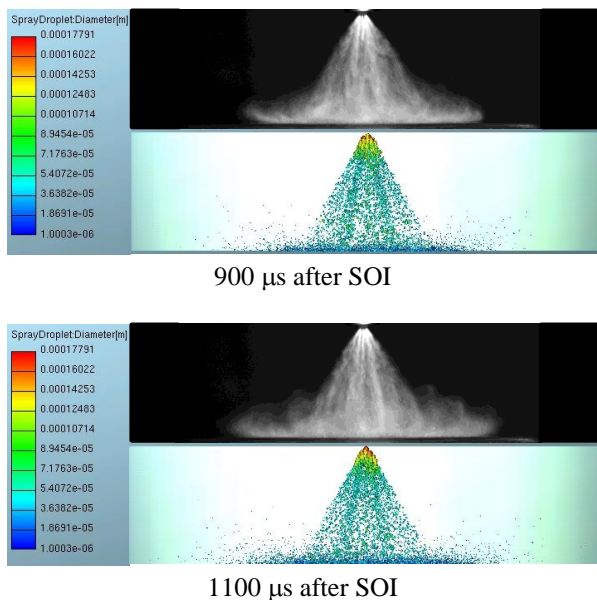


Figure 6: Comparison between experimental (top) and numerical (bottom) images of impinging sprays for $p_{inj}=5.5$ MPa, $T_{wall}=473$ K at two instants of time.

The impingement of a spray on a wall gives rise to the deposition of a liquid film and to a secondary atomization of the impacting droplets. The process is

strongly affected by the conditions of pressure, velocity and temperature of the surrounding gas and by the value of the wall temperature. The tuning of the impingement sub-model is here carried out at different injection pressures, initially for $T_{wall}=300$ K, than by considering impingement on a warm wall ($T_{wall}=473$ K).

The spray structure of the wall impingement process is shown in Figure 5. The comparison between the experimental measurement s and the numerically computed spray is made at 900 μ s and 1100 μ s after the SOI, for $T_{wall}=300$ K, $p_{inj}=5.5$ MPa, $h=20$ mm. The comparison relevant to $T_{wall}=473$ K, are reported in Figure 6, again at 900 and 1100 μ s after SOI. The numerical computation well describes the shape and the impingement of the spray, for both the examined cases.

3.2. The 3D Engine Model

The discretization of the computational domain is made through a home-made procedure, instead than resorting just to the pre-processing software included in the AVL Fire™ graphical user interface (GUI), namely the fame engine plus (FEP) module.

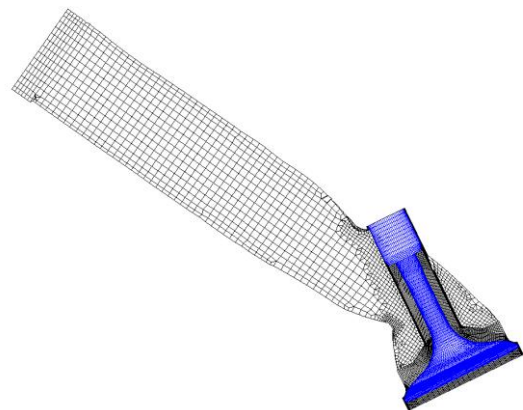


Figure 7: Computational grid relevant to the intake duct.

The search for a compromise solution between accuracy of results and low calculation time, indeed, needs a "customized" methodology for the grid design, able to allow easy changes as a consequence of possible variations of the valve lift profile. The computational domain made of the cylinder and the intake and exhaust ducts is subdivided into different sub-domains, some of which are discretized through the FEP module, while others are discretized "manually", to only generate hexahedral cells. Figure 7, as an example, shows the volume surrounding the intake valve and the intake duct. The cells are all hexahedral around the valve, as obtained by rotation of a regular 2D properly designed grid. Finally, Table III is indicative of the employed cell numbers. It is to be pointed out that different ranges are considered, namely different intervals of crank angles are taken, with domain activated or deactivated depending on the particular stroke being considered (in the closed valves period, say, the computational domain is made of just the combustion chamber - the intake duct is activated and really attached to the combustion chamber only when intake valves starts being opened).

Also, data reported in Table III are mean ones, namely indicative numbers typical of the grid size used in a certain range. In the Fire code, in fact, a “rezone” is necessary to avoid excessive cells distortion, hence the grids are substituted by other ones when the cell quality gets worst.

Range	Cells number
Exhaust Stroke	390000
Intake Stroke	331000
Closed Valve Period	185000

Table III: Employed grid resolution.

The charge turbulent motion within the computational domain is modeled through the $k-\zeta-f$ model, the combustion process according to the ECFM 3Z model [Colin, Benkenida, Angelberger, 2003]. NO formation follows the extended mechanism formulated by Zeldovich. A semi-empirical model for soot formation is also considered. Boundary conditions for the 3D model are derived from experimental measurement in the intake and exhaust ducts. Initial conditions are set according to the experimental data. The computation is initiated at the crank angle of top dead center (TDC), some degrees before the intake valves opening (IVO).

The whole engine cycle is simulated. A preliminary validation phase, here not reported for the sake of brevity regarded the computation of a motored pressure cycle, the check about the repeatability of results obtained over more than one computational cycle (necessary due to the kind of imposed initial conditions) and a check about the grid invariance of the obtained results. The comparison between the experimentally measured and the numerically computed pressure cycle in the medium-speed, medium-load lean condition is reported in Figure 8. Both the intake stroke and the compression stroke are quite well reproduced. The combustion phase is also in good agreement.

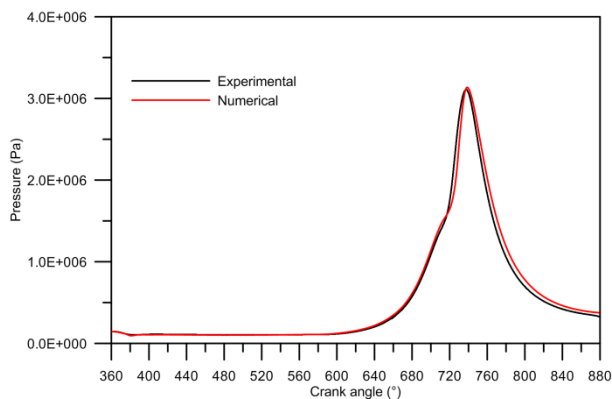
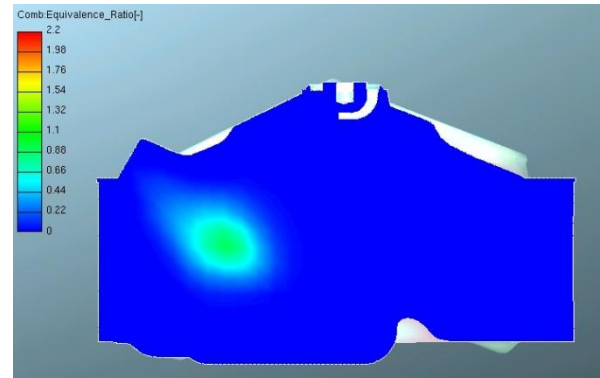
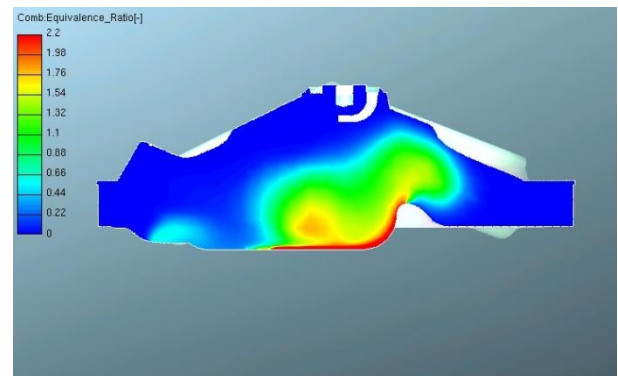


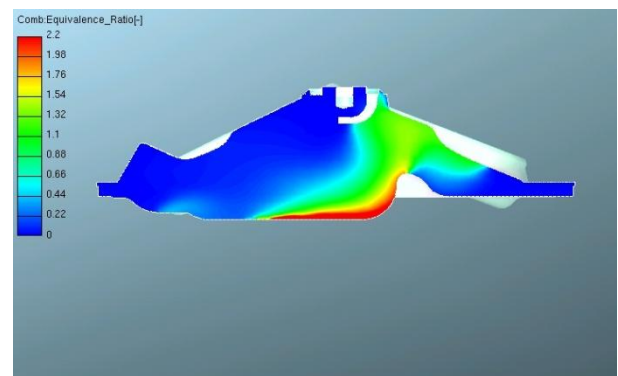
Figure 8: Comparison between the experimental collected and numerically computed pressure cycles.



6° after SOI.



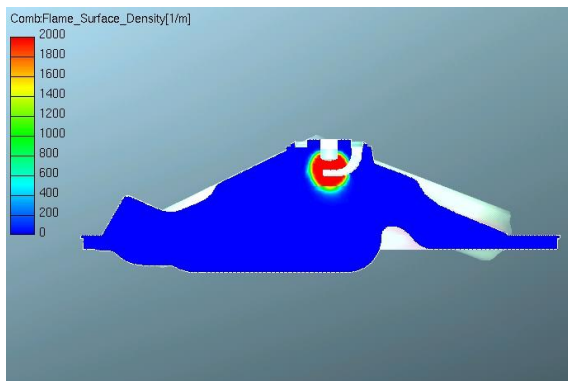
40° after SOI.



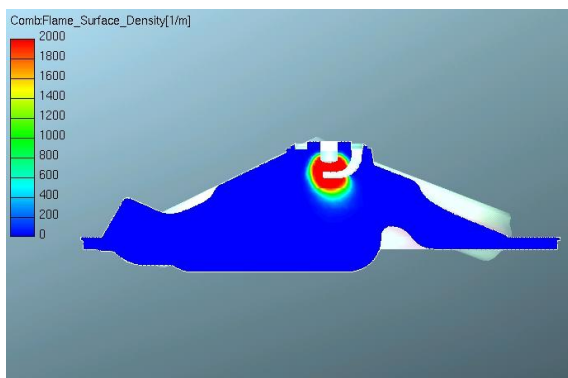
SOS

Figure 9: Numerical equivalence ratio distribution on a plane passing through the spark plug at various crank angles after SOI.

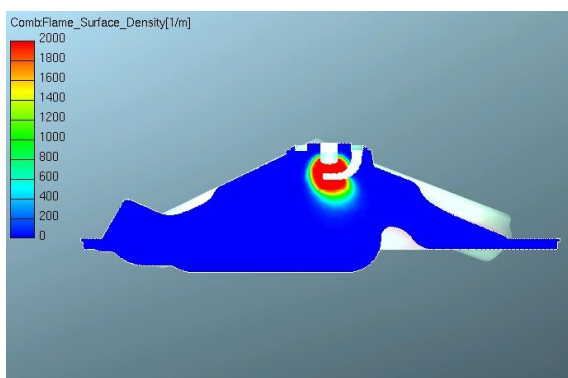
The reliability of the assessed model in reproducing the in-cylinder processes is good. Detailed information concerning the mixture formation and combustion evolution, therefore, can be derived by drawing relevant variables distributions on some internal planes. Figure 9, as an example, shows the distribution of the mixture equivalence ratio (local air to fuel ratio over stoichiometric air to fuel ratio) on a plane passing through the spark plug at three different instants of time, namely 6° after SOI, 40° after SOI and at the time of spark ignition (SOS).



SOS.



2° after SOS (TDC).



3° after SOS.

Figure 10: Flame surface density distribution on a plane passing through the spark plug at various crank angles after SOS.

The flame front evolution after SOS is instead shown in Figure 10.

4. CONCLUSIONS

Experiments performed to characterize the dynamics of a freely evolving spray issuing from a seven-hole injector and its impingement on a cold or heated wall are used to tune proper sub-models to be included in a 3D engine model. This last is assessed to reproduce the in-cylinder phenomena of a high performance GDI engine, also experimentally characterized at the test bench. The presented model is suitable of being included within a multi-objective optimization tool to optimize the engine performance,

by changing input parameter as injection strategy or time of spark ignition.

REFERENCES

- Alkidas, A.C., 2007, Combustion Advancements in Gasoline Engines, *Energy Conversion and Management* 48; 2751-2761.
- Bosch, W., 1966, The fuel rate indicator: a new measuring instrument for display of the characteristics of individual injection, SAE Paper 6607496.
- Wallace, I., 2002, Injection Rate Gauge: Pass Off Information and User Instruction, *Fuel & Engine Management System*, Graz.
- Alfuso, S., Allocca, L., Greco, M., Montanaro, A., Valentino, G., 2008, Time and Space Characterization of Multi-hole GDI Sprays for IC Engines by Images Processing and PDA Techniques, ILASS08-071.
- Sementa, P., Vaglieco, B.M., Catapano, F., 2012, Thermodynamic and optical characterizations of a high performance GDI engine operating in homogeneous and stratified charge mixture conditions fueled with gasoline and bio-ethanol, *Fuel*, 96, 204 – 219.
- Heywood, J.B., 1988, *Internal Combustion Engine Fundamentals*, New York: McGraw-Hill.
- Zhao, H., Ladommatos, N., 2001, *Engine Combustion Instrumentation and Diagnostics*. SAE Int., Inc.
- O'Rourke, P.J., Bracco, F.V., 1980, Modeling of Drop Interactions in Thick Sprays and a Comparison with Experiments, *Institution of Mechanical Engineers (IMECHE)*, London.
- Nordin, W.H., 2001, *Complex Modeling of Diesel Spray Combustion*, Thesis (PhD), Chalmers University of Technology.
- Dukowicz, J.K., 1979, Quasi-steady droplet change in the presence of convection, informal report Los Alamos Scientific Laboratory, *Los Alamos Report LA7997-MS*.
- AVL Fire™ v2011 User Guide – Lagrangian - Multiphase.
- Costa, M., Sorge U., Allocca L., 2012, CFD Optimization for GDI Spray Model Tuning and Enhancement of Engine Performance, *Advances in Engineering Software*, 49, 43 – 53.
- Colin, O., Benkenida, A., Angelberger, C., 2003, 3D Modeling of Mixing, Ignition and Combustion Phenomena in Highly Stratified Gasoline Engines, *Oil & Gas Science and Technology – Rev. IFP Energies Nouvelles*, 58 47-62.

AUTOMOTIVE PROCESSES SIMULATED BY AN ODE-PDE MODEL

Nicola Pasquino^(a), Luigi Rarità^(b)

^(a)Department of Industrial Engineering,
University of Salerno, Via Ponte Don Melillo, 84084, Fisciano (SA), Italy
^(b)Centre of Research for Pure and Applied Mathematics,
c/o Department of Electronic and Computer Engineering,
University of Salerno, Via Ponte Don Melillo, 84084, Fisciano (SA), Italy

^(a)nipasquino@unisa.it, ^(b)lrarita@unisa.it

ABSTRACT

This paper presents some simulation results for a supply chain, that describes the different construction phases of car engines. In particular, the supply chain is modeled using differential equations: the load evolution is given, inside each arc, by a conservation law with constant processing rate; the dynamics at a node is solved considering ordinary differential equations for queues, that model the exceeding parts. For simulations, some numerical schemes based on Upwind and explicit Euler methods are proposed and compared with alternative approaches, which use different time and space meshes and data structures. This last alternative allows to obtain high computational gains, with consequent advantages in terms of industrial processes simulations.

Keywords: conservation laws, supply chains, fast numerical methods, simulation.

1. INTRODUCTION

The automotive industry designs, develops and sells motor vehicles, and is one of the most important economic sector in the world. In reality, when we refer to “Automotive”, we indicate a very general area, involving all logistic and industrial operations connected to vehicles. A particular care is devoted to the study of all automotive processes, especially in terms of quality control and supply chain management, hence obtaining optimal performances either in terms of goodness of products or production times. To achieve this aim, it is fundamental to use models able to capture all dynamics connected to production processes.

The aim of this paper is to study a model for supply chains and to present a possible application within the automotive sector: the assembling of car engines. Supply chains have been modeled using various mathematical approaches. Some models are discrete and based on considerations of individual parts, while others are continuous (see Armbruster et al. 2006a, Armbruster et al. 2006b, Armbruster et al 2004, Daganzo 2003), and based on partial differential equations. Probably, the first paper, that relies on continuous equations, was

Armbruster et al. 2006a, where authors, using a limit procedure on the number of parts and suppliers, have obtained a conservation law (see Bressan 2000), whose flux involves either the parts density or the maximal productive capacity. But other continuous models for supply chains have been introduced (see Bretti et al. 2007, D’Apice et al. 2006, Göttlich et al. 2005, Göttlich et al. 2006) due to the difficulty of finding solution for the general equation proposed in Armbruster et al. 2006a. Also extensions on networks have been made (D’Apice et al. 2009, Helbing et al. 2004, Helbing et al. 2005).

In this paper, we examine the model proposed in Göttlich et al. 2005, obtained by considering suppliers on which the processing rate is constant and having queues in front of each supplier. The outcome is an ordinary differential equation (ODE) – partial differential equation (PDE) model (ordinary differential equations for queues, and conservation laws for density of parts), for which existence and uniqueness of the solution has been proved in Herty et al. 2007.

Two numerical schemes are analyzed: the explicit Euler one for the ODE and the Upwind method for the PDE. For details, see also Cutolo et al. 2011. Notice that the ODE – PDE model guarantees positivity of queue buffer occupancies (and densities), while this is not granted for the Upwind-Euler scheme. Thus first we consider fluxes corrections to avoid this drawback. The choice of time and space meshes can be uniform over suppliers only in case of rational ratios among lengths. Hence, we study different discretizations of the Upwind-Euler to deal with the general case and also to reduce computational complexity (the convergence of the scheme is completely proved in Cutolo et al. 2011). With this aim, we further study the use of logic pointers to update the computed density values on arcs.

Finally, simulations are made. It is proven that: the correction for guaranteeing the positivity of solutions is necessary to avoid high numerical errors; Upwind – Euler methods and their variants have almost the same characteristics either in terms of numerical approximations or computational times; the use of logic pointers to update density values allows to obtain the

same approximations of the classical Upwind – Euler methods and to reduce CPU times of almost 90%. Using the proposed numerical approaches, simulative results are obtained for a supply chain modeling the assembling phases of car engines. In particular, following the real industrial processes, a function, which is first increasing, then constant and finally decreasing, is chosen as input profile. The obtained results show that arcs starts to be full in a short time, unlike queues, which increase and decrease slowly. A way to accelerate the system dynamics is to change the constant level of injection. Although this can be useful to avoid queues in some parts of the supply chains, the problem of accelerating industrial processes is not completely solved. A possible solution is to change the input profile, with the aim of not compromising the overall performances of the system in terms of quantity of processed engines.

The outline of the paper is the following. Section 2 deals with the mathematical model for supply chains. Section 3 presents the numerical methods for the proposed model: classical Upwind and explicit Euler schemes are shortly described, with corrections to maintain positivity of solutions; then, considering different choices of space and time meshes, some variants of the basic methods are proposed. Some techniques for the reduction of the computational complexity are addressed in Section 4. Finally, Section 5 reports the simulation results: first, CPU times and numerical errors for the described numerical approaches are examined; then, the case study of car engines construction is shown.

2. A MODEL FOR SUPPLY CHAINS

In this section, we describe an ODE – PDE model for supply chains (Göttlich et al. 2005, Göttlich et al. 2006, Herty et al. 2007) where, beside the conservation laws formulation suggested in Armbruster et al. 2006, the transition of parts among suppliers is described by time – dependent queues.

A supply chain is a directed graph consisting of arcs $\mathcal{J} = \{1, \dots, N\}$ and vertices $\mathcal{V} = \{1, \dots, N-1\}$. Each arc $j \in \mathcal{J}$, parameterized by an interval $[a_j, b_j]$, models a supplier. Each vertex is connected to one incoming arc and one outgoing arc and arcs are assumed to be consecutively labelled, i.e. arc j is connected to arc $j+1$ and $b_j = a_{j+1}$ (see Figure 1). For the first and the last arc, we either set $a_1 = -\infty$ and $b_N = +\infty$, respectively, or provide boundary data for the inflow and outflow.

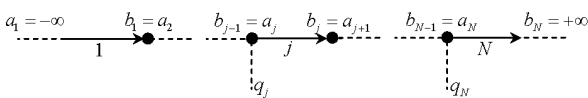


Figure 1: A generic supply chain

Each supplier j has a queue in front of itself, i.e. at $x = a_j$, and is characterized by a maximum processing capacity $\mu_j > 0$, length $L_j > 0$ and a processing time $T_j > 0$. The rate $v_j := L_j/T_j$ represents the processing velocity. Indicating by $\rho_j^{t,x} := \rho_j(t, x)$ the density of parts in the supplier j at point x and time t , the evolution of parts is described by the conservation law:

$$\partial_t \rho_j^{t,x} + \partial_x f_j(\rho_j^{t,x}) = 0, \quad \forall x \in [a_j, b_j], \quad t > 0, \quad (1)$$

where the flux function $f_j(\rho_j^{t,x}) : [0, +\infty[\rightarrow [0, \mu_j]$ is given by:

$$f_j(\rho_j^{t,x}) = \min\{\mu_j, v_j \rho_j^{t,x}\}. \quad (2)$$

The interpretation of equation (1) is the following: parts are processed with velocity v_j but with a maximal flux μ_j .

Each queue buffer occupancy is a time dependent function $t \rightarrow q_j(t)$. If the capacity of the supplier $j-1$ and the demand of the supplier j are not equal, the queue increases or decreases its buffer. More precisely, we have, $\forall j = 2, \dots, N$:

$$\frac{d}{dt} q_j(t) = \varphi_{j-1}^b - \varphi_j^a, \quad q_j(0) = q_{j,0} \geq 0, \quad (3)$$

where $\varphi_{j-1}^b := f_{j-1}(\rho_{j-1}^{t, b_{j-1}})$ is given by the evolution on supplier $j-1$, and the flux on the outgoing arc j , $\varphi_j^a := f_j(\rho_{j-1}^{t, a_j})$, is defined as:

$$\varphi_j^a = \begin{cases} \min\{\varphi_{j-1}^b, \mu_j\}, & q_j(t) = 0, \\ \mu_j, & q_j(t) > 0. \end{cases} \quad (4)$$

Notice that the flux φ_j^a depends on the capacity of the queue: if the queue buffer is empty, the inflow to supplier j is equal to the outflow from supplier $j-1$; otherwise the inflow is maximal. Hence, when $q_j(t) > 0$, the processing occurs at the maximal possible rate, μ_j , so to empty the queue as fast as possible.

Finally, the complete system of equations is given by:

$$\begin{aligned} \partial_t \rho_j^{t,x} + \partial_x f_j(\rho_j^{t,x}) &= 0, \quad \forall x \in [a_j, b_j], \quad t > 0, \quad j \in \mathcal{J}, \\ \rho_j^{0,x} &= \rho_{j,0}(x) \geq 0, \end{aligned} \quad (5)$$

$$\frac{d}{dt}q_j(t) = \begin{cases} \varphi_{j-1}^b - \min\{\varphi_{j-1}^b, \mu_j\}, & q_j(t) = 0, \\ \varphi_{j-1}^b - \mu_j, & q_j(t) > 0, \end{cases} \quad (6)$$

$$q_j(0) = q_{j,0} \geq 0, j \in \mathcal{J} \setminus \{1\}.$$

Moreover, the following holds:

Lemma 2-1

Consider a supply chain evolution $\rho_j^{t,x}$, $q_j(t)$, i.e. a solution to (5) – (6). Then, for every $t \geq 0$ and x , it holds $\rho_j^{t,x} \geq 0$, $j \in \mathcal{J}$; $q_j(t) \geq 0$, $j \in \mathcal{J} \setminus \{1\}$.

For the proof, see Cutolo et al. 2011.

3. NUMERICAL METHODS

Numerical results for solving the dynamics on a supply chain are obtained finding, for each arc j , suitable approximations either for the density $\rho_j^{t,x}$ or the queue buffer occupancy $q_j(t)$. In particular, we need a PDE numerical method and an ODE one: we choose the Upwind scheme for (5) and the explicit Euler scheme for (6).

A suitable theoretical approach for the convergence analysis is in Cutolo et al. 2011.

3.1. Classical schemes (Ordinary Methods, OMs)

First, we report the classical Upwind and explicit Euler schemes for the discretization of (5) and (6). From now on, we call such numerical approximation types “Ordinary Methods” (OMs).

For each arc $j \in \mathcal{J}$, define a numerical grid in $[0, L_j] \times [0, T]$ using the following notations:

- $\Delta x_j = \frac{L_j}{N_j}$ is the space grid mesh, where N_j is the number of segments into which we divide the j -th supplier;
- $\Delta t_j = \frac{T}{\eta_j}$ is the time grid mesh, where η_j denotes the number of segments into which $[0, T]$ is divided;
- for $i = 0, \dots, N_j$, $n = 0, \dots, \eta_j$, grid points are $(x_i, t^n)_j = (i\Delta x_j, n\Delta t_j)$;
- ${}^j\rho_i^n$ is the value taken by the approximated density at the point $(x_i, t^n)_j$;
- q_j^n is the value taken by the approximate queue buffer occupancy at time t^n .

We get that the Upwind method reads as:

$${}^j\rho_i^{n+1} = {}^j\rho_i^n - \frac{\Delta t}{\Delta x} v_j ({}^j\rho_i^n - {}^j\rho_{i-1}^n), \quad (7)$$

$$j \in \mathcal{J}, i = 0, \dots, N_j, n = 0, \dots, \eta_j,$$

where the CFL condition (Leveque, 2002) is given by:

$$\Delta t \leq \frac{\Delta x}{\max_j v_j}. \quad (8)$$

The explicit Euler method is given by:

$$q_j^{n+1} = q_j^n + \Delta t (f_{j-1, out}^n - f_{j, inc}^n), \quad (9)$$

$$j \in \mathcal{J} \setminus \{1\}, n = 0, \dots, \eta_j,$$

where $f_{j-1, out}^n = f_{j-1}^{(j-1)} \rho_{N_{j-1}}^n$ and

$$f_{j, inc}^n = \begin{cases} \min\{f_{j-1, out}^n, \mu_j\}, & q_j^n(t) = 0, \\ \mu_j, & q_j^n(t) > 0. \end{cases} \quad (10)$$

Boundary data are treated using ghost cells and the expression of inflows given by (10). Assuming that $L_j, j \in \mathcal{J}$, have rational ratios, it is possible to choose a space grid mesh Δx and a common time grid mesh Δt .

Notice that (9) does not necessarily maintain the positivity properties of the true solutions given by Lemma 2-1. In order to accomplish positivity of queue buffer occupancies, the following modification for $f_{j, inc}^n$ is needed (see Cutolo et al. 2011 for details):

$$f_{j, inc}^n = \frac{q_j^n \mu_j + \Delta t (\mu_j - f_{j-1, out}^n) f_{j-1, out}^n - q_j^n f_{j-1, out}^n}{(\mu_j - f_{j-1, out}^n) \Delta t}. \quad (11)$$

The correction (11) on the boundary incoming data for the supplier j influences the approximation of $\rho_j^{t,x}$, with consequent effects on the dynamics for following suppliers and queues.

3.2. Use of different grid meshes

Now, we discuss the assumption of choosing different space and/or time grid meshes. This is necessary in the general case in which lengths $L_j, j \in \mathcal{J}$, have not rational ratios, but it can also be useful for reducing the computational complexity, as we will see.

3.2.1. Different space meshes (Different Spatial Step Method, DSSM)

For each supplier $j \in \mathcal{J}$, the numerical grid in $[0, L_j] \times [0, T]$ is defined choosing a fixed time grid mesh Δt ; then, different space grid meshes are necessary. Setting $\Delta x_j := v_j \Delta t$, grid points are $(x_i, t^n)_j = (i\Delta x_j, n\Delta t)$, $i = 0, \dots, N_j, n = 0, \dots, \eta_j$.

The Upwind scheme for the parts density of arc j now reads:

$${}^j \rho_i^{n+1} = {}^j \rho_i^n - \frac{\Delta t}{\Delta x_j} v_j \left({}^j \rho_i^n - {}^j \rho_{i-1}^n \right),$$

$$j \in \mathcal{J}, i = 0, \dots, N_j, n = 0, \dots, \eta_j.$$

The CFL condition is automatically satisfied since:

$$\Delta t = \min \left\{ \frac{\Delta x_j}{v_j} : j \in \mathcal{J} \right\}. \quad (13)$$

For queues we refer again to equation (9). In case of negative values of queues, (11) still holds.

In what follows, we define ‘‘Different Spatial Step Method’’ (DSSM) the procedure for finding the numerical solutions of (5) and (6) using: Upwind scheme for densities, equation (12), with different CFL conditions (13); Euler scheme for queues, equation (9).

3.2.2. Different time meshes (Different Temporal Steps Method, DTSM)

We now consider the case of different temporal meshes (and same space meshes). Fix two consecutive arcs $j-1$ and j . Then, two different numerical grids are defined, whose points are, respectively:

$$\left(x_k, t^{n_{j-1}} \right)_{j-1} = \left(k \Delta x, n_{j-1} \Delta t_{j-1} \right),$$

$$k = 0, \dots, N_{j-1}, n_{j-1} = 0, \dots, \eta_{j-1},$$

$$\left({}^j x_k, t^{n_j} \right) = \left(k \Delta x, n_j \Delta t_j \right),$$

$$k = 0, \dots, N_j, n_j = 0, \dots, \eta_j.$$

For the queue buffer occupancy, the explicit Euler is given by:

$$q_j^{n_j+1} = q_j^{n_j} + \Delta t_j \left(f_{j-1, out}^{n_j} - f_{j, inc}^{n_j} \right), \quad (16)$$

where $f_{j, inc}^{n_j}$ is computed as in (10), while $f_{j-1, out}^{n_j}$ must be suitably computed. If $\Delta t_{j-1} < \Delta t_j$, we define $m(n_j)$ and $M(n_j)$ as:

$$m(n_j) := \sup \{ m : m \Delta t_{j-1} \leq n_j \Delta t_j \}; \quad (17)$$

$$M(n_j) := \inf \{ M : M \Delta t_{j-1} \geq (n_j + 1) \Delta t_j \}, \quad (18)$$

and set

$$f_{j-1, out}^{n_j} = \sum_{l=1}^{M(n_j) - m(n_j) - 1} \Delta t_{j-1} f_{j-1} \left({}^{j-1} \rho_{N_{j-1}}^{m(n_j)+l} \right) +$$

$$+ \left[\left(m(n_j) + 1 \right) \Delta t_{j-1} - n_j \Delta t_j \right] f_{j-1} \left({}^{j-1} \rho_{N_{j-1}}^{m(n_j)} \right) +$$

$$+ \left[\left(n_j + 1 \right) \Delta t_j - \left(M(n_j) - 1 \right) \Delta t_{j-1} \right] f_{j-1} \left({}^{j-1} \rho_{N_{j-1}}^{M(n_j)-1} \right). \quad (19)$$

Notice that, in the particular case $\Delta t_j = \gamma \Delta t_{j-1}$, $\gamma \in \mathbb{N} \setminus \{1\}$, we simply have:

$$f_{j-1, out}^{n_j} = \sum_{l=1}^{M(n_j) - m(n_j) - 1} \Delta t_{j-1} f_{j-1} \left({}^{j-1} \rho_{N_{j-1}}^{m(n_j)+l} \right) =$$

$$= \sum_{l=1}^{\gamma} \Delta t_{j-1} f_{j-1} \left({}^{j-1} \rho_{N_{j-1}}^{\gamma n_j + l} \right). \quad (20)$$

If, on the contrary, $\Delta t_{j-1} > \Delta t_j$, we set:

$$f_{j-1, out}^{n_j} = f_{j-1}^{\left\lfloor \frac{n_j \Delta t_j}{\Delta t_{j-1}} \right\rfloor}, \quad (21)$$

where $\lfloor \cdot \rfloor$ indicates the floor function. The CFL condition now reads:

$$\Delta t_j \leq \frac{\Delta x}{v_j}, \quad j = 1, \dots, N. \quad (22)$$

In case of negative values of queues, fluxes corrections have to be considered. The modifications w.r.t. Section 3.1 can be easily computed and are omitted for sake of space.

In what follows, we indicate by ‘‘Different Temporal Step Method’’ (DTSM) the procedure for computing the numerical solutions of (5) and (6) using: Upwind scheme for densities, equation (7); Euler scheme for queues, equation (16).

4. IMPROVEMENTS OF CPU TIMES

Beside numerical methods for solving equations (5) and (6), some alternative computational ways are considered for the simulation of large networks. Such approaches are essentially based on OMs; hence, their numerical precision (in terms of approximations) is the same of OMs.

4.1. Use of a Logic Pointer (Logic Pointer method, LPm)

Consider the Upwind method (7). If space and time grid sizes are set following the relation $\Delta t_j = v_j \Delta x_j$, then

${}^j \rho_{i+1}^{n+1} = {}^j \rho_i^n$, namely: the density values at time $n+1$ are obtained by those at time n by shifting of one position in the space grid. The computational

complexity can be highly reduced by using a logic pointer, that allows to avoid the data shift in the vector of densities.

Such strategy is explained as follows: consider a supplier of length L , divided into n segments. At $t=0$, we suppose that the supplier is empty. At $t=1$, the density value V_1 on the first segment is computed and the pointer is set to position 1. At $t=2$, densities should be shifted while the new density value for the first segment, V_2 , is computed. The physical shift inside the vector is not considered and the pointer is updated to the second position corresponding to V_2 , discarding the previous value and considering cyclic order in the vector. This operation is repeated until a time $t=n$, see Figure 2, where the dashed arrow indicates the density on the first segment of the arc. Notice that at $t=n+1$ the new density is placed in the first segment and the pointer is set back to position 1, and so on.

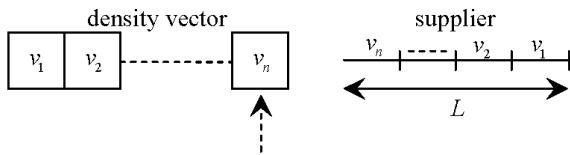


Figure 2: situation at $t = n$

Operations and computational costs for OMs and LPm (Logic Pointer method) are examined in the following tables, where # denotes the cardinality.

Table 1: computational costs for OMs

Operations	Computational costs
Densities	$\sim \sum_j \# \frac{L_j}{\Delta x_j}$
Boundary data	$\sim \# \mathcal{J} \times \frac{T}{\Delta t_j}$

Table 2: computational costs for LPm

Operations	Computational costs
Densities	$\sim \# \mathcal{J}$
Logic pointers	$\sim \# \mathcal{J}$
Boundary data	$\sim \# \mathcal{J} \times \frac{T}{\Delta t_j}$

Notice that the update of densities for each supplier depends on space grid size for OMs. Such dependence vanishes using the LP approach, while the cost of logic pointer update is fixed. Therefore, we get a substantial reduction of computational costs.

4.2. Different indices numeration (DIN)

For a supply chain, each supplier is identified by an index, that belongs to a concatenated list. We get that a sequential research, which implies a computational time directly proportional to the number N of suppliers, is

required. The computational complexity is $O(N)$ in the worst case, namely when the last arc of the list must be found.

In order to decrease the computational complexity, a vector, “SC”, whose i -th element identifies the i -th arc by a pointer, is used. Hence, the generic arc i is found by a direct access to the i -th position of the vector SC, namely we refer to $SC[i]$. In this case, the numerical complexity of the research operation is always $O(1)$, and it is independent from N .

We indicate this technique by “DIN” (Different Indices Numeration).

5. SIMULATIONS

In this section, we present some simulation results to foresee the behaviour of queues and parts densities on supply chains. In particular, after examining some cases to study the effects due to negative queues, goodness of approximations and CPU times for different numerical approaches, we focus on a supply chain to simulate a typical process of the Automotive Sector.

5.1. Test 1 – effects due to negative queues

In this first analysis we focus on the importance of flux corrections in case of oscillating queue buffer occupancies.

Consider a supply chain with $N = 4$ suppliers and the following parameters: $L_j = T_j = 1$, $j = 1, \dots, 4$; $\mu_1 = 50$, $\mu_2 = 15$, $\mu_3 = 12$, $\mu_4 = 6$. The initial conditions are: $\rho_j^{0,x} = 0$, $j = 1, \dots, 4$, $q_j(0) = 0$, $j = 2, 3, 4$. A total simulation time $T = 400$ is considered and for the first arc the inflow profile is given by $f_1(t) = 9 \left(1 + \sin \frac{3\pi t}{50} \right)$. Figure 3 presents the evolutions of uncorrected and corrected queue buffer occupancies $q_2(t)$, simulated by OMs with $\Delta x = \Delta t = 0.2$. It is evident that meaningful numerical errors exist if flux corrections are not used.

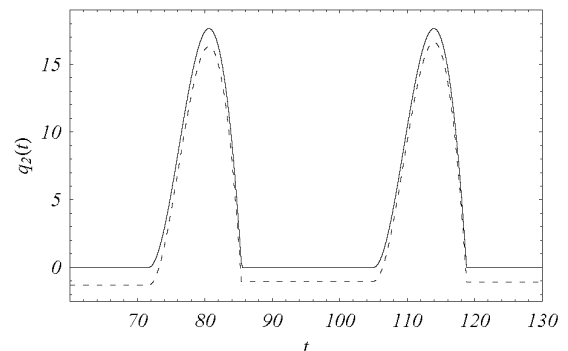


Figure 3: Evolution of q_2 : behaviour with flux correction (continuous line) and without flux correction (dashed line)

At time $t \approx 80.5$, the relative difference among peaks of corrected and uncorrected queue buffer occupancies is

about 8%. In particular, we have an overestimation of the peak in absence of numerical correction. Such erroneous approximation of $q_2(t)$ has a cascade effect, influencing the evolution of parts density for the supplier 2, but then also queues $q_3(t)$, $q_4(t)$, $\rho_3(t,x)$ and $\rho_4(t,x)$. This phenomenon is clearly shown in Figure 4, where $\rho_3(359,x)$ is represented with and without correction: the evolution of $\rho_3(359,x)$ is completely different from the one computed in absence of corrections.

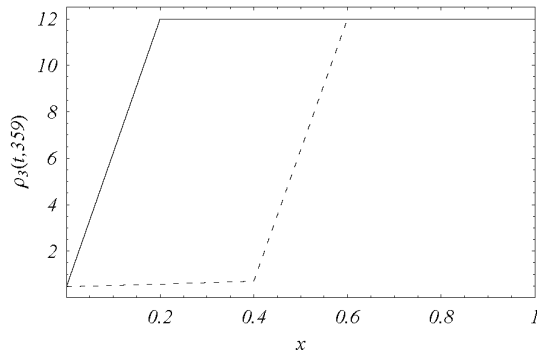


Figure 4: density on arc 3 at $t = 359$ with flux correction (continuous line) and without flux correction (dashed line)

At $x = 0.2$, the relative error in $\rho_3(359,x)$ is about 95%, which is evidently unacceptable. We conclude that corrections due to negative queues are necessary in order to achieve adequate numerical results.

5.2. Test 2 – OMs versus alternative numerical schemes

We consider a supply chain with $N = 5$ suppliers. Maximal fluxes, processing times and lengths of each supplier are reported in Table 3.

Table 3: parameters of the supply chain

Supplier	μ_j	T_j	L_j
1	10	1	1
2	8	1	0.4
3	6	3	1.2
4	4	1	0.4
5	3	1	0.4

We assume that all arcs and queues are empty at $t = 0$. The total simulation time is $T = 300$. The inflow for the first supplier is given by:

$$f_1(t) = \begin{cases} 9t/25, & 0 \leq t \leq 50, \\ 36 - 9t/25, & 50 < t \leq 100, \\ 0, & 100 < t \leq T. \end{cases} \quad (23)$$

In Figure 5, we present the simulation results for queue buffer occupancies, obtained by OMs with

$\Delta x = 0.0125$, $\Delta t = 0.5\Delta x$. In this particular case, queues are never zero as $\mu_2 > \mu_3 > \mu_4 > \mu_5$. Moreover, although processing velocities $v_j, j = 2, 3, 4, 5$, are the same, q_4 is higher than other ones.

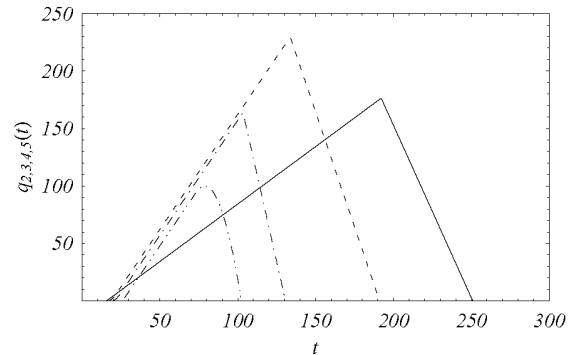


Figure 5: behaviour of queues using OMs; $q_2(t)$, dot dot dashed line; $q_3(t)$, dot dashed line; $q_4(t)$, dashed line; $q_5(t)$, continuous line

We then run the same test for DSSM and DTSM, choosing, respectively, $\Delta t = 0.0125$ and $\Delta x = 0.0125$. Other parameters for such methods are the same used for the analysis by OMs. In Figure 6, the behaviour of the queue buffer occupancy $q_2(t)$ is depicted. Notice that different numerical approximations give rise to very similar results.

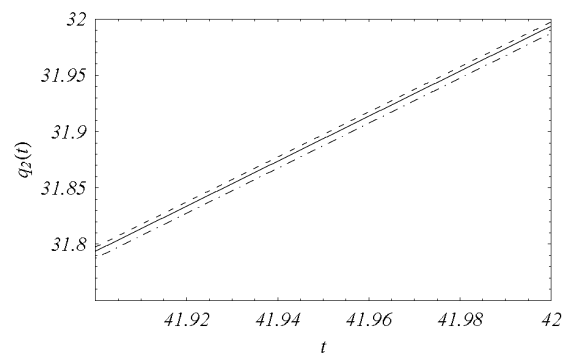


Figure 6: numerical approximation of $q_2(t)$ using different methods: OMs (continuous line); DSSM (dot dashed line); DTSM (dashed line)

Further comments on CPU times (measured in seconds and computed by a Pentium 4, CPU 2 GHz, RAM 2 Gb) and convergence errors (see Cutolo et al. 2011) is made to compare methods. The following tables report the obtained results.

Table 4: CPU times and errors for OMs

Δx	CPU	errors
0.00625	1.203	0.15253
0.0125	0.531	0.207522
0.025	0.218	1.04845

Table 5: CPU times and errors for DSSM

Δt	CPU	errors
0.00625	1.218	0.18187
0.0125	0.468	0.27742
0.025	0.296	0.89847

Table 6: CPU times and errors for DTSM

Δx	CPU	errors
0.00625	1.323	0.19152
0.0125	0.513	0.23211
0.025	0.252	0.97051

From the obtained results, we conclude that the considered methods have almost the same characteristics, as for goodness of approximation versus CPU times and errors.

Using OMs for simulations, we compare the CPU performances with the alternative approaches described in Section 4. Consider a sequential supply chain with five suppliers for which $L_j = T_j = 1, j = 1, \dots, 5$. We first use OMs with different $\Delta x = \Delta t$; empty queues and arcs as initial condition; inflow profile for the first supplier as in (23); total simulation time $T = 300$. CPU times (measured in seconds and computed by a Pentium 4, CPU 2 GHz, RAM 2 Gb) are then compared with the ones obtained by LPm and DIN. The results are in the following table (notice that we indicate by LD the combined usage of LPm and DIN).

Table 7: CPU times versus Numerical Approaches (NA)

NA	$\Delta x = 0.00625$	$\Delta x = 0.0125$	$\Delta x = 0.025$
OMs	0.953	0.406	0.265
LPm	0.281	0.234	0.219
LD	0.266	0.234	0.203

Notice that using LPm and DIN allows to obtain a concrete reduction of CPU times. Such effect is more evident when the number of arcs of the supply chain is very large, as shown from the following simulation case.

Consider a supply chain with $N = 50$ arcs, and the following characteristics: $L_i = T_i = 1, i = 1, \dots, 50$; $\mu_1 = 100$; $\mu_i = 5, i = 2, \dots, 50$. For OMs we choose different $\Delta x = \Delta t$; empty queues and arcs as initial condition; inflow profile for the first supplier as in (23); total simulation time $T = 150$. CPU times (measured in seconds and computed by a Pentium 4, CPU 2 GHz, RAM 2 Gb) are then compared with the ones obtained by LPm and DIN. Table 8 shows the results.

Table 8: CPU times versus Numerical Approaches (NA)

NA	$\Delta x = 0.00625$	$\Delta x = 0.0125$	$\Delta x = 0.025$
OMs	54.75	1.921	0.859
LPm	1.688	0.984	0.531
LD	0.546	0.25	0.265

Notice the CPU times for OMs and LD: there is a reduction of more than 90% in the worst case ($\Delta x = 0.00625$).

We conclude that, especially for large networks, fast approximations can be obtained using LD. The numerical precision is the same of OMs.

5.3. Test 3 – Simulation of a process for assembling car engines

We present some simulation results of a supply chain, that assembles car engines. For a generic engine, the most important components are: a set of cylinders (typically, they can be four, six or eight) that contain pistons; a crankshaft, that determines the piston's up and down motion inside the engine; a connecting rod, that connects pistons to the crankshaft; a sump, that surround the crankshaft.

For assembling car engines with eight cylinders, we refer to a supply chain with twenty arcs and nineteen nodes, represented in Figure 7. Notice that, as reported in Göttlich et al. 2006, each arc can represent either a conveyor belt or a given machine.

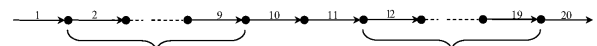


Figure 7: supply chain with twenty arcs and nineteen nodes

In this particular case, each arc has a precise role inside the process: arcs 1 and 20 are assumed to be conveyor belts, while the other ones are seen as machines. Arc 1 transports engines skeletons; arcs 2 – 9 are useful to insert pistons and cylinders (each arc inserts one cylinder and the relative pistons inside the primitive engines); the aim of arc 10 is to insert the crankshafts inside engine skeletons; arc 11 creates connections between sumps and crankshafts; arcs 12 – 19 join together crankshafts and pistons; finally, arc 20 transports the assembled engines to a test box. Notice that the queues in front of each arc $j, j = 2, \dots, 20$, represent the quantity of engines (or better of semi-finished product) that is not immediately processed or directed to the test box.

We simulate the supply chain of Figure 7 using OMs with $\Delta t = \Delta x = 0.02$ and assuming:

- total simulation time: $T = 3000$;
- $L_i = T_i = 1, i = 1, \dots, 20$;
- $\mu_1 = 500$; $\mu_{20} = 15$;
- $\mu_j = 34 - 2j, j = 2, \dots, 13$;
- $\mu_j = 21 - j, j = 14, \dots, 19$.

Finally, as input profile, we get:

$$f(t) = \begin{cases} t, & 0 \leq t \leq k, \\ k, & k < t \leq 150 - k, \\ 150 - t, & 150 - k < t \leq 150, \\ 0, & 150 < t < T. \end{cases} \quad (24)$$

where $k \in [0, 50]$. Considering (24), we represent the situation in which engine skeletons are injected inside the system following, first, a linear increasing profile (hard injection); then, a constant one; finally, a decreasing one (light injection). Choosing opportunely k , it is possible to control the injection times for the three different work conditions.

We show some results for $k = 50$. In Figures 8 – 10, queues are represented. Notice that, for the chosen values of $\mu_j, j = 1, \dots, 20$, there is a queue for each arc with the exception of arc 20, for which $q_{20}(t) = 0 \forall t \in [0, T]$ as $\mu_{19} < \mu_{20}$. Moreover, $q_2(t)$ is smoother than other queues because arc 2 receives directly goods from arc 1, whose dynamics obeys the input profile (24). Slopes of queues $q_j(t), j = 3, \dots, 13$, are different from the ones of $q_j(t), j = 14, \dots, 19$, as we have two distinct sets of parameters $\mu_j, j = 1, \dots, 20$. Moreover, although the input profile is zero $\forall t \geq 150$, queues dynamics is very slow. This is confirmed by $q_{19}(t)$, that vanishes at $t \approx 2500 \gg 150$.

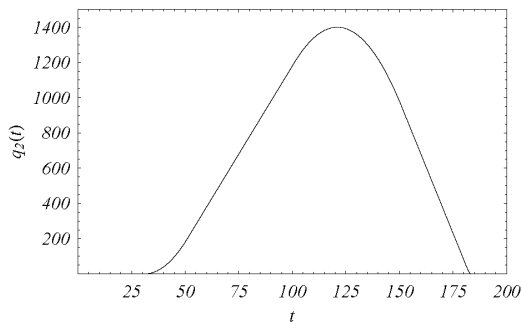


Figure 8: behaviour of $q_2(t)$

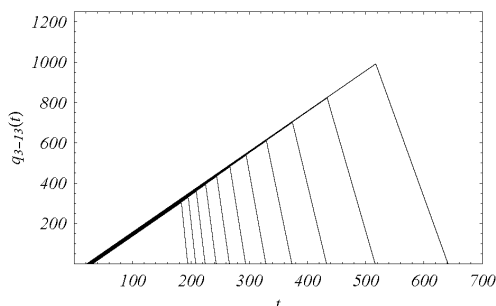


Figure 9: dynamics of queues $q_j(t), j = 3, \dots, 13$; $q_3(t)$ is the first on the left; $q_4(t)$ is the second on the left, and so on

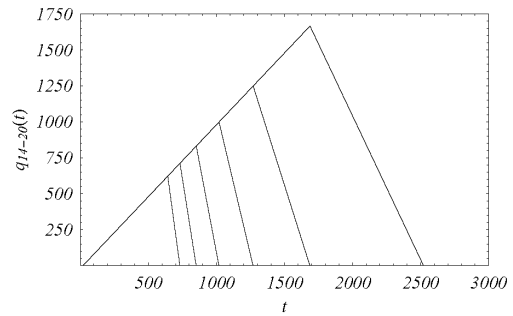


Figure 10: queues $q_j(t), j = 14, \dots, 20$; $q_{14}(t)$ is the first on the left; $q_{15}(t)$ is the second on the left, and so on

In Figure 11, the density of arc 2 for various time instants is reported. Unlike the behaviour of queues, arcs become full in a short time, namely arc 2 at $t = 30$ already reaches the maximal density value (coincident with μ_2 as $v_2 = 1$).

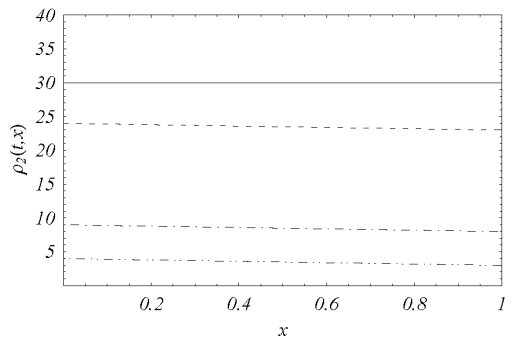


Figure 11: density $\rho_2(t, x)$ for different time instants; $t = 5$ (dot dot dashed line); $t = 10$ (dot dashed line); $t = 25$ (dashed line); $t = 30$ (continuous line)

The presence of queues is due either to the values of $\mu_j, j = 1, \dots, 20$, or the level k in (24). For example, if $k \leq \mu_2 = 30$, $q_2(t) = 0 \forall t \in [0, T]$. In general, for assigned $\mu_j, j = 1, \dots, 20$, the level k determines the queues evolution, namely: the input profile guides dynamics of the whole supply chain, when it is not possible to redesign the system, in terms of maximum processing capacities, lengths and processing times.

In Figure 12, we represent the cost functional:

$$J(k) = \frac{\sum_{j=2}^{20} \int_0^T q_j(t) dt}{19}, \quad (25)$$

which measures the average area described by queues of the examined supply chain versus the injection level k .

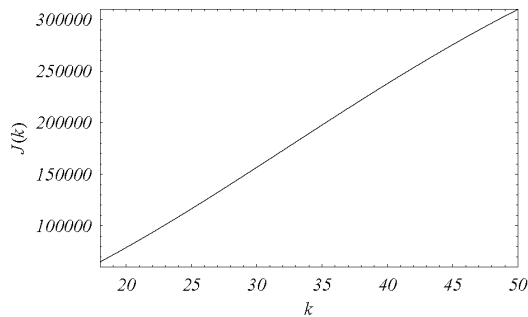


Figure 12: behaviour of $J(k)$

We notice that $J(k)$ is almost linear with k , indicating that, although in some cases queues are not formed for all suppliers ($k \leq 30$), there is always a sort of proportionality in overall queues contributions for various injection levels. A simple way to erase queues is to change the input profile, but this means to redesign the overall system.

A further remark can be done on CPU times (measured in seconds and computed by a Pentium 4, CPU 2 GHz, RAM 2 Gb). In Table 8, some results, obtained using OMs and LD, are compared for two different values of k . Notice that CPU times are similar for the same used numerical approach although, for $k = 20$, the system is characterized by $q_j(t) = 0, j = 2, \dots, 7 \forall t \in [0, T]$. Finally, we conclude that, also for this particular case of simulation, the reduction of times in using LD is high.

Table 8: CPU times

k	OMs	LD
50	5.968	1.610
20	5.937	1.515

6. CONCLUSIONS

In this paper, starting from the model proposed in Göttlich et al. 2005, flows on a supply chain, modelling the car engines construction, have been studied.

A numerical analysis of the model has proved that it is possible to obtain high computation gains and numerical precision of the classical numerical schemes.

Using fast methods, the simulation has showed that, choosing opportunely the constant injection level of the input profile, it is possible to modulate queues but not to erase them completely. Future studies aim to foresee which is the optimal input flow, that allows to obtain high performances either in terms of queues reduction or computational gains.

REFERENCES

Armbruster, D., Degond, P., Ringhofer, C., 2006. A model for the dynamics of large queueing networks and supply chains, *SIAM Journal on Applied Mathematics*, 66 (3), pp. 896-920.
 Armbruster, D., Degond, P., Ringhofer, C., 2006. Kinetic and fluid models for supply chains

supporting policy attributes, *Transportation Theory Statist. Phys.*

Armbruster, D., Marthaler, D., Ringhofer, C., 2004. Kinetic and fluid model hierarchies for supply chains, *SIAM J. on Multiscale Modeling*, 2 (1), pp. 43-61.
 Bressan, A., 2000. Hyperbolic Systems of Conservation Laws - The One - dimensional Cauchy Problem, Oxford University Press.
 Bretti, G., D'Apice, C., Manzo, R., Piccoli, B., 2007. A continuum - discrete model for supply chains dynamics, *Networks and Heterogeneous Media (NHM)*, 2 (4), pp. 661-694.
 Cutolo, A., Piccoli, B., Rarità, L., 2011. An Upwind - Euler scheme for an ODE - PDE model of supply chains, *SIAM Journal on Computing*, 33 (4), pp. 1669-1688.
 Daganzo, C., 2003. A Theory of Supply Chains, Springer Verlag, New York, Berlin, Heidelberg.
 D'Apice, C., Manzo, R., 2006. A fluid dynamic model for supply chains, *Networks and Heterogeneous Media (NHM)*, 1 (3), pp. 379-398.
 D'Apice, C., Manzo, R., Piccoli, B., 2009. Modelling supply networks with partial differential equations, *Quarterly of Applied Mathematics*, 67 (3), pp. 419-440.
 Helbing, D., Lammer, S., Seidel, P., Seba, T., Platkowski, T., 2004. Physics, stability and dynamics of supply networks, *Physical Review E* 70, 066116.
 Helbing, D., Lammer, S., 2005. Supply and production networks: from the bullwhip effect to business cycles, in D. Armbruster, A. S. Mikhailov, and K. Kaneko (eds.) *Networks of Interacting Machines: Production Organization in Complex Industrial Systems and Biological Cells*, World Scientific, Singapore, pp. 33-66.
 Godunov, S. K., 1959. A finite difference method for the numerical computation of discontinuous solutions of the equations of fluid dynamics, *Mat. Sb.* 47, pp. 271-290.
 Göttlich, S., Herty, M., Klar, A., 2005. Network models for supply chains, *Communication in Mathematical Sciences*, 3 (4), pp. 545-559.
 Göttlich, S., Herty, M., Klar, A., 2006. Modelling and optimization of Supply Chains on Complex Networks, *Communication in Mathematical Sciences*, 4 (2), pp. 315-330.
 Leveque, R. J., 2002. Finite Volume Methods for Hyperbolic Problems, Cambridge University Press, Cambridge, 2002.
 Herty, M., Klar, A., Piccoli, B., 2007. Existence of solutions for supply chain models based on partial differential equations, *SIAM J. Math. An.*, 39 (1), pp. 160-173.

AUTHORS BIOGRAPHY

NICOLA PASQUINO was born in Napoli, Italy, in 1974. He graduated cum laude in Mechanical

Engineering in 2001, with a thesis on supply chains modeling and optimization using fuzzy logic. He obtained PhD in Material and Production Engineering at the University of Naples discussing a thesis about supply chains management. He is actually an assistant professor at the University of Salerno. His scientific interests are about models for productive processes, with particular emphasis on supply chains management and quality control.

His e-mail address is nipasquino@unisa.it.

LUIGI RARITÀ was born in Salerno, Italy, in 1981. He graduated cum laude in Electronic Engineering in 2004, with a thesis on mathematical models for telecommunication networks, in particular tandem queueing networks with negative customers and blocking. He obtained PhD in Information Engineering in 2008 at the University of Salerno discussing a thesis about control problems for flows on networks. He is actually a research assistant at the University of Salerno. His scientific interests are about numerical schemes and optimization techniques for fluid – dynamic models, queueing theory, and knowledge models for the Cultural Heritage area.

His e-mail address is lrarita@unisa.it.

EVOLUTION TRACKING IN GENETIC PROGRAMMING

Bogdan Burlacu^(a), Michael Affenzeller^(b), Michael Kommenda^(c), Stephan M. Winkler^(d), Gabriel Kronberger^(e)

^(a-e)University of Applied Sciences Upper Austria
Heuristic and Evolutionary Algorithms Laboratory
Softwarepark 11, 4232 Hagenberg, Austria

^(a)bogdan.burlacu@fh-hagenberg.at, ^(b)michael.affenzeller@fh-hagenberg.at, ^(c)michael.kommenda@fh-hagenberg.at,
^(d)stephan.winkler@fh-hagenberg.at, ^(e)gabriel.kronberger@fh-hagenberg.at

ABSTRACT

Much effort has been put into understanding the artificial evolutionary dynamics within genetic programming (GP). However, the details are yet unclear so far, as to which elements make GP so powerful. This paper presents an attempt to study the evolution of a population of computer programs using HeuristicLab. A newly developed methodology for recording heredity information, based on a general conceptual framework of evolution, is employed for the analysis of algorithm behavior on a symbolic regression benchmark problem. In our example, we find the complex interplay between selection and crossover to be the cause for size increase in the population, as the average amount of genetic information transmitted from parents to offspring remains constant and independent of run constraints (i.e., tree size and depth limits). Empirical results reveal many interesting details and confirm the validity and generality of our approach, as a tool for understanding the complex aspects of GP.

Keywords: genetic programming, tree fragments, evolutionary dynamics, schema theory, population diversity, bloat, introns

1. INTRODUCTION

A difficult task in genetic programming is to explain the evolutionary behavior of highly polymorphic, dynamic populations of computer programs. Evolution within GP is characterized by complex genotype-phenotype relations that make it difficult for researchers to identify the influential factors of emergent behavior and the underlying mechanisms behind phenomena such as loss of diversity, overfitting, bloat and introns.

Although these phenomena have been correlated by scientists with different algorithmic components (run constraints, genetic operators, function and terminal set), the main reason a causal relationship could not be derived from the work is two-fold.

On the one hand, on the theoretical level, problems arise from the inherent complexity of the Genotype-Phenotype map, which is a mathematical function to describe the relationships between genotype and

phenotype. Phenotypic innovation is the result of genetic modification mediated by the GP-map (Stadler and Stephens 2003, Stadler 2006). The notion of phenotypic neighborhood induced by the GP-map may differ fundamentally from any notion of “nearness” among phenotypes based solely on the comparison of their morphological features (Fontana and Schuster 1998). Therefore, stronger metrics and measurements are required for describing fitness landscape topologies in the presence of many-to-one relationships, i.e., sets of genotypes folding into essentially the same (at least on the semantic level) phenotypic structure. Difficulties in fulfilling this particular requirement make it unclear how to determine the role of selection, crossover and mutation in genetic programming.

On the other hand, the presence of representational bias (how genotypes are represented) or procedural bias (determined by genetic operators and fitness function) in the algorithm, varying across different problem domains, and the delicate balance between performance (training accuracy) and robustness (test accuracy) makes it unclear which innovations or algorithmic improvements are related to the underlying dynamics and which ones exploit particularities of a specific class of problems. Understanding the relationship between bias and generalization ability of genetic programming is crucial in designing algorithms with good generalization capabilities (Kushchu 2002).

In this paper, we focus on the study of genetic algorithms under the framework of neo-Darwinian evolution. The suggested approach, based on the tracking of all genetic information that flows through the evolutionary graph, constitutes the first step in an attempt to analyze and explain the influence and interplay of genetic operators.

The paper is organized as follows: Section 2 provides a brief overview of the essential biological concepts of evolution at the base of this approach. A brief summary of other research in this area is described in Section 3. In Section 4, the implementation of the HeuristicLab tracking plugin is detailed. Section 5 discusses some preliminary results concerning the distribution of tree and fragment lengths sampled by crossover, and Section 6 is devoted to conclusions.

2. CONCEPTS OF ARTIFICIAL EVOLUTION

Evolution is the result of selection acting upon the genetic variation within a population. In other words, it requires variation in phenotype, differential reproduction on the basis of phenotype, and heredity of the traits associated with differential reproduction. Some traits associated with better fitness survive and propagate further while others – and their corresponding genes – become extinct in the population.

In genetic programming, operators such as crossover and mutation act on genotypes, while fitness-based selection acts on phenotypes. In this context, we take genes to be minimal fragments consisting of symbols (primitives) and terminals.

The ability of the genetic operators to produce useful variation (i.e., new compositions of symbols, variables and constants) plays a crucial role in algorithm performance; this requirement, however, is not sufficient to guarantee algorithm convergence, as there are cases when a relevant gene becomes extinct before getting the chance to become useful. Moreover, the closure property of the GP function set makes it possible, in theory, for genetic operators to produce variation *ad infinitum*. In practice, this possibility is limited by size and depth constraints, but this does not prevent the occurrence of bloat (i.e., gradual increase in tree size), or the appearance of introns (“intra-genic region” – segments of non-viable, inefficient or neutral code), as an effect of selection pressure. One of the key challenges in GP is to eliminate introns and bloat while at the same time maintaining just enough diversity in the population so that the search can succeed.

3. RELATED WORK

This section provides a summary of existing research on the topic of evolutionary dynamics, or, more generally, on how information from successive generations (genealogical information or otherwise significant indicators like size, fitness) can guide the search process or explain, predict or improve various aspects of artificial evolution.

Burke et al. (2003) improve population diversity by taking into account lineage information in the selection phase. A genetic lineage is defined as the connection from the root parent to those individuals which were created, via crossover, from that individual. Lineage selection is implemented as an additional step to bias selection towards different lineages from the initial population. In effect, the selected parents are the results of tournament selection across lineages, so that the selection pressure is reduced from the *fittest* individuals to the *fit and diverse* (Burke et al. 2003). In terms of evolutionary dynamics, the authors conclude that adding diversity can worsen fitness on some problems that clearly benefit from elitism in a hill-climbing environment, but may avoid local optima, when deception is embedded into the problem.

In a subsequent paper, Gustafson et al. (2005) focus on the analysis of survival rates, mating success and dissimilarity between offspring and parents. They

reach the conclusion that similar parents (with the same fitness) are unlikely to produce better offspring and they introduce a simple rule to prevent mating between solutions with the same fitness. Their work supports the idea that GP search may be improved by producing more differently fit solutions.

Another work by Smart et al. (2007) suggests a methodology for investigating the building blocks hypothesis in GP, by aggregating statistical information of fragments and fragment schemas. A fragment is defined as a connected set of nodes from the program tree. A fragment schema is defined as the set of all programs containing a specified fragment at some point in the program tree. In their paper, Smart et al. use the concept of *maximal fragment*, defined as the largest fragment contained in all subtrees from some subset of the population. The set of maximal fragments can be analyzed in various ways to identify properties of the set of all fragments (Smart et al. 2007). The analysis relies on a subtree-mining algorithm called TRIPS (TRee mIning algorithm using Prüfer Sequences) capable of finding frequent subtrees (fragments) from a forest of tree structures. The TRIPS algorithm is explained in detail in Tatikonda et al. (2006).

Finally, in a series of papers, Poli et al. detail the correlation between the mean program size at generation 0, the average arity of the primitive set and the internal node distributions of mixed arity trees. They develop a size evolution equation which is an exact formalization of average program size dynamics. It is shown that under standard subtree-swapping crossover (uniform selection of crossover points), the population converges to a limiting tree length distribution that will exponentially sample smaller programs (Poli and McPhee 2008, Dignum and Poli 2008). For this reason, crossover depth and size limits are found to actually have a positive effect towards bloat, as small trees are more likely to be sampled, but are less likely to generate new programs. In Poli and McPhee (2008), an effective method for dynamically setting the parsimony coefficient, and thus controlling the average program length in the population, is derived from the size evolution equation.

The work of Poli et al. is especially important as it lays the foundations for a mathematical model of evolutionary search. It also emphasizes the important role of the interplay between selection and crossover, which determines GP behavior.

4. TRACKING OF EVOLUTION DATA

This section outlines our proposed methodology for the study of evolutionary dynamics within GP, with a focus on genetic operator behavior and fragment statistics. In the context of this paper, a fragment denotes a subtree (usually swapped by crossover) that is part of a bigger rooted tree (the individual).

4.1. Analysis of Inheritance Information

The tracking functionality was implemented in HeuristicLab, a framework for heuristic and

evolutionary algorithms developed at the Heuristic and Evolutionary Algorithms Laboratory (HEAL) of the Upper Austria University of Applied Science (<http://dev.heuristiclab.com>). Inheritance information is recorded in the form of an evolutionary graph, in which nodes represent individuals and arcs represent heredity relationships between them. It is clear that the graph itself consists of the union set of all lineages in the population. This representation was chosen for its potential to provide additional insight into the process of evolution by investigating the changes in the topological and algebraic properties of the graph.

Figure 1 shows an example of an individual (marked with a rectangle), its genealogy and its tree structure, in which the genetic information it received from the parent is highlighted. The interface facilitates the investigation of lineages, heredity and how the genetic material is assembled from lower building blocks during evolution.

4.2. Tree and Fragment Similarity

In addition to tracking fragments transmitted via genetic recombination, it is also possible for arbitrary tree fragments to be matched against the population of individuals. This powerful tool can be used to investigate the distribution of certain fragments or schemas within the population.

Fragment matching is done according to three sets of rules. The terminology used below refers to *Symbols* which represent functions or operators, *Variables* which represent elements from the data set, and *Constants* which are random numbers supplied as inputs to the functions alongside the variables.

- S₁ „Exact”: the entire fragment must be matched one-for-one: symbol names and arities must be the same, as well as variable names and weights, or constant values
- S₂ “High”: exact matching of symbols, partial matching of leaf nodes – they are required to be of the same type (Variables or Constants)
- S₃ “Relaxed”: exact matching for symbols, leaf nodes are considered wildcards

It is clear that for sets S₁, S₂, S₃ of matched fragments given by the three similarity rules defined above, S₁ ⊆ S₂ ⊆ S₃. Moreover, fragments contained in

S₂ and S₃ are isologous (i.e., having a similar structure but containing different leafs). Isologous tree fragments can be considered elements of a set S of phenotypic instances of a gene G, in which case G can also be viewed as a schema. This provides a way to identify useful genes or schemas in the population.

Figure 2 shows an example of fragment matching. The tree fragment highlighted on the right was matched against multiple individuals in the population. The black nodes represent “exact” matches, the dark gray ones represent “high” matches, while the normal gray ones represent “relaxed” matches.

5. EMPIRICAL CASE STUDY

The study of tree fragments was done on a symbolic regression problem (*Poly-10*) where the target function is the 10-variable cubic polynomial:

$$f(x) = x_1 x_2 + x_3 x_4 + x_5 x_6 + x_7 x_8 x_9 + x_3 x_6 x_{10}$$

Population size	500
Generations	200
Selector	Tournament (size=3)
Crossover	Size-fair crossover (p=0.9)
Mutation	Multi-mutation operator (p=0.15)

Table 1: Genetic Algorithm Settings

In a first phase, our run analysis focused on the distribution of parent, children and fragment lengths across generations. For the Poly-10 problem, a maximum tree size of 100 nodes was used.

Empirical data from a standard GP run shows that, with the size-fair crossover, which only performs a swap if the size and depth limits are respected, the children length is not very different from the length of the parent, and is, on average, smaller (Figure 3).

This result is somewhat surprising as it contrasts to the overall behavior of all the trees in the population (including those that did not reproduce) which is characterized by a gradual increase in length throughout evolution. The apparent contradiction can be explained by the interplay between crossover, which drives the size distribution of children towards smaller lengths, and selection, which tends to reduce diversity, thus promoting uniformity in the population at the expense of smaller, less fit programs.

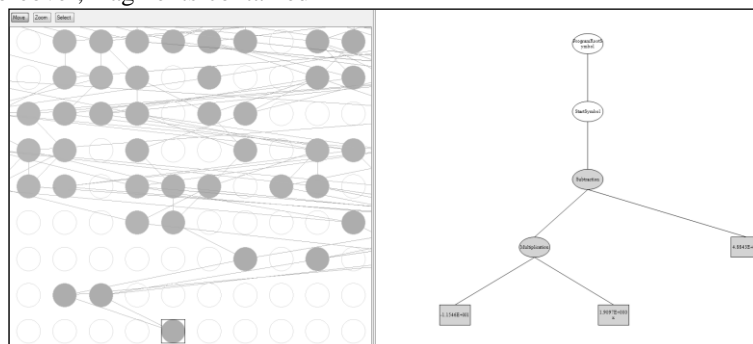


Figure 1: On the left, an individual (marked with a rectangle) and its genealogy. On the right, the tree structure of the individual. The highlighted nodes belong to the fragment that was received via crossover.

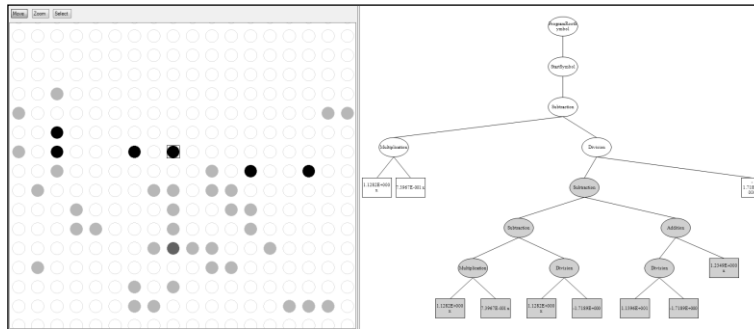


Figure 2: Example of fragment matching according to the three similarity criteria: black – “exact”, dark gray – “high” and gray – “relaxed”. The matched fragment is highlighted in the right-hand side.

To verify this, we propose a similarity measure based not on whole tree comparison, but on comparison between tree fragments that get transmitted via crossover. The similarity value is obtained by dividing the total number of identical fragments in the population (matched by the “exact” similarity measure) by the number of similarity groups they form.

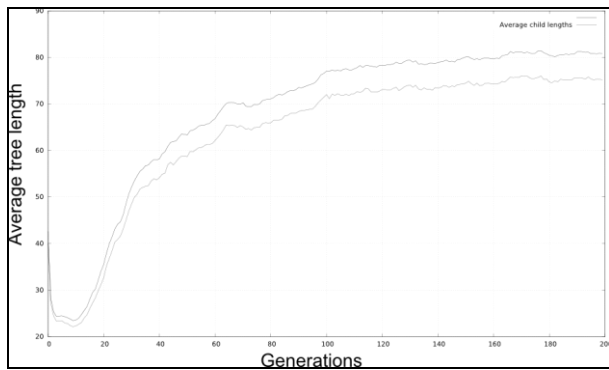


Figure 3: Average parent and child lengths over 200 generations (10-run average)

The evolution of fragment similarity is shown in Figure 4, and is measured in average number of similar fragments per generation. The probability of a fragment occurring multiple times in the population is a product between the probability its containing individual gets selected multiple times and the probability that the fragment itself is sampled by crossover more than once. Therefore, it is reasonable to assume that even a small increase in the average number of identical fragments (i.e., similarity in the genetic material which gets passed to the offspring) can in fact mean a big decrease in population diversity.

Another interesting result is that the average size of the crossover fragments tends to remain constant throughout the run. The only factor influencing average fragment size seems to be the average arity of the available functions. Figure 4 shows an increase in average fragment length in the beginning of the run (first 20 generations), followed by a decrease and stabilization at a fragment size value of approximately 4.6 nodes. This can be explained by the fact that, after the initial exploratory phase of the algorithm, when many different points in the solution space are sampled, the search becomes gradually more local and the

accepted changes become those that have a small positive effect and do not affect the overall structure of the tree.

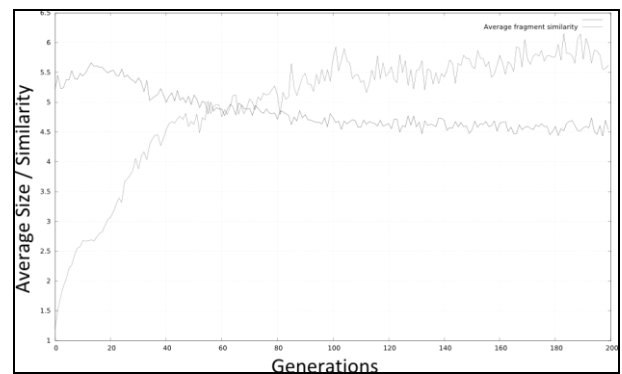


Figure 4: Fragment similarity increasing from 1 to 5.5, fragment length stabilizing at ~4.6 nodes

The correlation between fragment size and search locality becomes more obvious if we look at the Offspring Selection Genetic Algorithm (Affenzeller et al. 2009). We outline the main idea of the algorithm here: in OSGA the selection mechanism is extended to include an “offspring selection” step after the parents are selected via the usual means (i.e., proportional, roulette or tournament selection). In this extra step, the fitness value of the offspring is compared with the fitness values of its parents (either the worst or best parent, or an average between the two). Only the offspring that are able to outperform their parents (denoted as “successful” offspring) are accepted as candidates for the further evolutionary process, according to a predefined *success ratio* which gives the percentage of the population that is expected to surpass their parents’ fitness. The rest of the population is filled with random individuals chosen from the pool of individuals that were also created by crossover but did not reach the success criterion. This strategy guarantees that evolution is resumed mainly with crossover results that were able to mix the properties of their parents in an advantageous way. The value of selection pressure is given by the quotient of new individuals that had to be created until the success ratio was reached, and the number of individuals in the population (Affenzeller et al. 2009).

Consequently, in OSGA, because of the dynamic selection pressure, the shift from global to local search is more pronounced and the correlation with average fragment size is easier to observe. Similar to successful/unsuccessful individuals, we define a successful fragment as a fragment contained in an individual that was selected for reproduction. The OSGA algorithm run settings are shown in Table 2.

Population size	500
Generations	1000
Maximum tree depth	10
Maximum tree length	100
Selector	Proportional
Crossover	Size-fair crossover
Mutation rate	20 %
Comparison factor	1
Success ratio	1

Table 2: OSGA Algorithm Settings

Note that even though the algorithm is allowed to run for 1000 generations, the termination criteria will be reached before that, when the selection pressure exceeds a predefined threshold (when no more successful individuals can be produced).

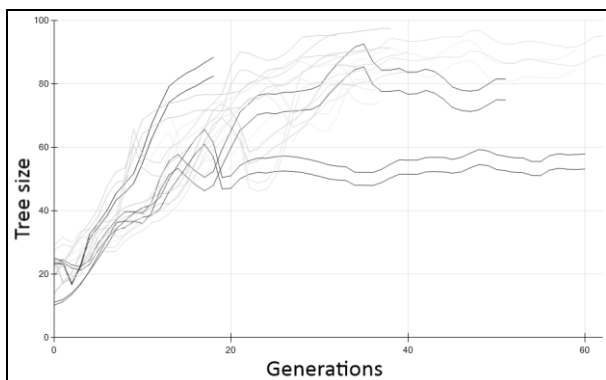


Figure 3: OSGA – average parent/child lengths, 10 runs

Figure 3 shows the evolution of parent/child average length for 10 OSGA runs. The average child length is always lower than the average parent length. Different runs have different lengths depending on when the stop criterion is reached

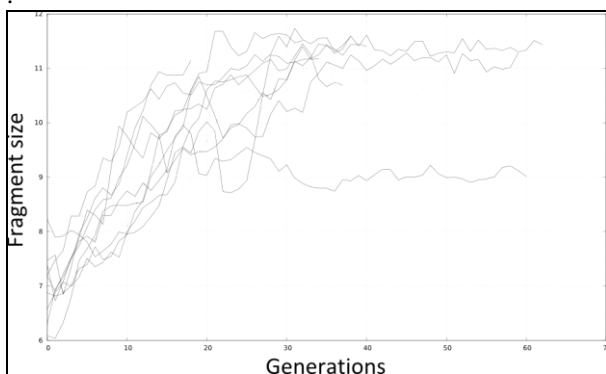


Figure 4: OSGA – average fragment sizes, 10 runs

In OSGA, the selection pressure increases as it becomes harder to produce successful offspring. This translates into an overall increase in fragment size as the algorithm spends more effort trying to find new and better programs. However, while the average fragment size increases (Figure 4), the average size of successful fragments gradually becomes smaller, as the search converges (Figure 5). This proves that a selection pressure steering mechanism is an effective guide for the evolutionary search. In contrast with the standard GA, the OSGA behavior illustrates more clearly what happens when the search converges. The accepted modifications gradually become smaller until no better children can be obtained from the available genetic material.

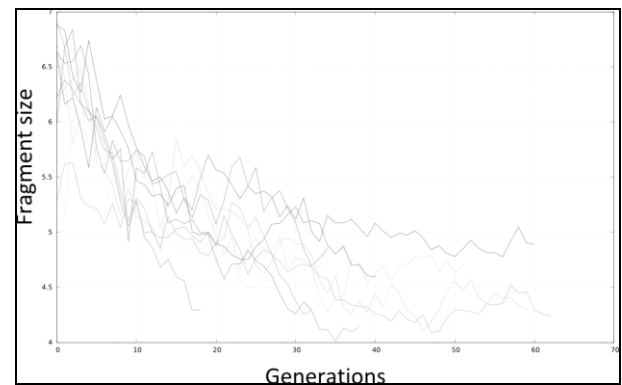


Figure 5: OSGA – average size of successful fragments, 10 runs

6. DISCUSSION AND CONCLUSIONS

In this paper, we described a powerful and general methodology for analyzing the evolutionary dynamics in genetic programming. The approach integrates the basic principles of evolution with a set of novel techniques for the tracking and analysis of inheritance and hereditary information.

Preliminary results are promising as they bring insights into the behavior of genetic operators and their combined effects. In our test case, we explain the increase in the average size of individuals as the result of the complex interplay between crossover and selection.

The fragment statistics acquired during the run provide an additional insight into the behavior and dynamics of the evolutionary run. The increase in fragment similarity shows how genetic diversity is lost as the search progresses. The results show that average fragment length stabilizes and remains constant, and that although the overall tendency of the GA population is to increase in size, the children produced by crossover are on average smaller than their parents. Using the notion of “successful” fragments, we provided an image and explanation of GP convergent behavior.

Future research will provide more details regarding the extent to which each genetic operator influences the overall behavior of the algorithm. Detailed lineage analysis in terms of fragments and fitness similarities can reveal more about the characteristics of the

underlying genotype-phenotype mappings. Concerning the evolutionary graph, we plan to see if the underlying topology can substantially affect the results of the evolutionary process.

Overall, the work described in this paper opens a breadth of new possibilities for the study and understanding of genetic programming and artificial evolution.

REFERENCES

- Affenzeller, M., Winkler, S., Wagner, S., Beham, A., 2009. *Genetic Algorithms and Genetic Programming: Modern Concepts and Practical Applications*. Chapman & Hall/CRC ©2009.
- Burke, E., Gustafson, S., Kendall, G. and Krasnogor, N., 2003. Is Increased Diversity in Genetic Programming Beneficial? An Analysis of Lineage Selection. *Evolutionary Computation*, 8-12 Dec 2003, Vol. 2, pp. 1398-1405.
- Dignum, S. and Poli, R., 2008. Crossover, Sampling, Bloat and the Harmful Effects of Size Limits. *EuroGP'08 Proceedings of the 11th European conference on Genetic programming*, pp 158-169. March 26-28, 2008. Naples, Italy.
- Fontana, W. and Schuster, P., 1998. Continuity in evolution: On the nature of transitions. *Science*, 29 May 1998, Vol. 280, no. 5368, pp. 1451-1455.
- Gustafson, S., Burke, E.K. and Krasnogor, N., 2005. On Improving Genetic Programming for Symbolic Regression. *Proceedings of the 2005 IEEE Congress on Evolutionary Computation*, CEC 2005, 2-5 Sep 2005, Vol. 1, pp. 912-919.
- Kushchu, I., 2002. Genetic Programming and Evolutionary Generalisation. *IEEE Transactions on Evolutionary Computation*, Vol. 6, No. 5, October 2002.
- McPhee, N., Ohs, B. and Hutchison, T., 2008. Semantic building blocks in genetic programming. *EuroGP'08 Proceedings of the 11th European conference on Genetic programming*, pp 135-145. March 26-28, 2008. Naples, Italy.
- Poli, R., McPhee, N.F., 2008. Covariant Parsimony Pressure for Genetic Programming. Technical Report, CES-479, Department of Computing and Electronic Systems, University of Essex, UK, 2008.
- Smart, W., Andrae, P. and Zhang, M., 2007. Empirical Analysis of GP Tree-Fragments. *EuroGP'07 Proceedings of the 10th European conference on Genetic programming*, pp. 55-67. April 11-13, 2007, Valencia, Spain.
- Tatikonda, S., Parthasarathy, S. and Kurc, T., 2006. TRIPS and TIDES: new algorithms for tree mining. *CIKM '06 Proceedings of the 15th ACM international conference on Information and knowledge management*, pp. 55-67. 2006. New York, NY, USA.

AUTHORS BIOGRAPHIES



BOGDAN BURLACU received his MsC in computer science and systems engineering in 2009 from the “Gheorghe Asachi” Technical University in Iasi, Romania. Currently he is a research associate in the Heuristic and Evolutionary Algorithms Laboratory in Hagenberg, under the supervision of Michael Affenzeller.



MICHAEL AFFENZELLER has published several papers, journal articles and books dealing with theoretical and practical aspects of evolutionary computation, genetic algorithms, and meta-heuristics in general. In 2001 he received his PhD in engineering sciences and in 2004 he received his habilitation in applied systems engineering, both from the Johannes Kepler University of Linz, Austria. Michael Affenzeller is professor at UAS, Campus Hagenberg, and head of the Josef Ressel Center *Heureka!* at Hagenberg.



MICHAEL KOMMENDA finished his studies in bioinformatics at Upper Austria University of Applied Sciences in 2007. Currently he is a research associate at the UAS Research Center Hagenberg working on data-based modeling algorithms for complex systems within *Heureka!*.



STEPHAN M. WINKLER received his PhD in engineering sciences in 2008 from Johannes Kepler University (JKU) Linz, Austria. His research interests include genetic programming, nonlinear model identification and machine learning. Since 2009, Dr. Winkler is professor at the Department for Medical and Bioinformatics at the University of Applied Sciences (UAS) Upper Austria at Hagenberg Campus; since 2010, Dr. Winkler is head of the Bioinformatics Research Group at UAS, Hagenberg.



GABRIEL KRONBERGER received his PhD in engineering sciences in 2010 from JKU Linz, Austria, and is a professor at the UAS Research Center Hagenberg. His research interests include genetic programming, machine learning, and data mining and knowledge discovery.

ON THE ANALYSIS, CLASSIFICATION AND PREDICTION OF METAHEURISTIC ALGORITHM BEHAVIOR FOR COMBINATORIAL OPTIMIZATION PROBLEMS

Andreas Scheibenpflug^(a), Stefan Wagner^(b), Erik Pitzer^(c), Bogdan Burlacu^(d), Michael Affenzeller^(e)

^(a-e) Heuristic and Evolutionary Algorithms Laboratory (HEAL)
University of Applied Sciences Upper Austria
Softwarepark 11, 4232 Hagenberg, Austria

^(a) ascheibe@heuristiclab.com, ^(b) swagner@heuristiclab.com, ^(c) epitzer@heuristiclab.com, ^(d) bburlacu@heuristiclab.com,
^(e) maffenze@heuristiclab.com

ABSTRACT

Metaheuristics are successfully applied in many different application domains as they provide a reasonable tradeoff between computation time and achievable solution quality. However, choosing an appropriate algorithm for a certain problem is not trivial, as problem characteristics can change remarkably for different instances and the performance of a metaheuristic may vary considerably for different parameter settings. Therefore it always takes qualified algorithm experts to select and tune a metaheuristic algorithm for a specific application. This process of algorithm selection and parameter tuning is frequently done manually and intuitively and requires a large number of empirical tests.

In this contribution the authors propose several measurement values to characterize the search behavior of different metaheuristics for solving combinatorial optimization problems. Based on these measurements algorithms can be classified and models can be learnt to predict the algorithms behavior for new parameter settings. This helps to understand the interdependencies and impacts of parameters, to identify promising parameter values, to formalize the parameter tuning process, and to reduce the number of required test cases.

Keywords: Metaheuristics, Parameter Tuning, Algorithm Behavior Analysis, Performance Prediction

1. MOTIVATION

In the last decades researchers have created a wide range of metaheuristics. There are various forms from trajectory-based metaheuristics (e.g. Simulated Annealing (Kirkpatrick, Gelatt, and Vecchi 1983), Tabu Search (Glover 1989)) to population-based metaheuristics (e.g. Evolutionary Algorithms (Holland 1975), Scatter Search (Laguna and Marti 2002), Particle Swarm Optimization (Kennedy and Eberhart 1995)) or hybrid metaheuristics (Talbi 2002). The evolution of so many different metaheuristic optimization algorithms results from the fact that no single method can outperform all others for all possible problems. As postulated in the No Free Lunch Theorem (Wolpert and Macready 1997), such a general-purpose and universal

optimization strategy is impossible. One strategy can always outperform another, if it is more specialized to the structure of the tackled problem instance. Consequently it always takes qualified algorithm experts to select and tune a metaheuristic algorithm for a concrete application.

Choosing an appropriate method for a certain problem is not an easy task, as problem characteristics may change for different instances and the performance of a metaheuristic may vary considerably with different parameter settings. Therefore the choice of a well-suited method and according parameter values (parameter tuning) is a crucial aspect when applying metaheuristics (Smit and Eiben 2009).

Because parameter tuning is a time consuming task that needs to be performed by a human expert, various attempts have been made to improve and automate this process. Hyperheuristics (Özcan, Bilgin and Korkmaz 2008) try to combine multiple simpler heuristics in a single algorithm that is able to solve a class of problems. Parameterless algorithms (Nadi and Khader 2011) try to reduce or eliminate the parameters of a metaheuristic which would make parameter tuning obsolete. Similarly to parameterless algorithms, metaheuristics utilizing parameter control (Eiben, Michalewicz, Schoenauer, and Smith 1999) need less parameter configuration but still exhibit parameters, which are automatically tuned during the execution of the algorithm. Meta-optimization (Smit and Eiben 2009) is another approach where the problem of finding good parameters is seen again as an optimization problem and can therefore be optimized by a metaheuristic. Even though meta-optimization optimizes the parameters of metaheuristics, the meta-level algorithm still has to be parameterized by a human expert.

These methods often lead to robust results for different problems, although it is difficult to achieve the same quality level as with manually tuned parameter settings which are adapted to the characteristics of a specific problem. Therefore, manual parameter tuning is still essential, if the solution quality of an algorithm should be maximized.

The process of parameter tuning can be interpreted as a search process itself. When performed by a human expert it is often done intuitively by observing the runtime and quality characteristics of an algorithm. On the contrary, when applying a parameter grid search parameter values are sampled in a fixed pattern which is usually only suitable for a small amount of value combinations. Meta-optimization approaches try to apply some intelligent search procedure for navigating through the parameter space and identifying good settings, although this approach is not practically usable in many cases due to the enormous computational effort.

In this contribution the authors propose measurement values which describe the search behavior of an algorithm for making parameter tuning more systematic and comparable. The remainder of this paper is organized as follows: Section 2 describes the proposed behavioral measures. Section 3 describes use cases for the proposed measures and details on the advantages of retrieving additional information about the search process. Section 4 describes the work the authors plan to conduct in the future.

2. BEHAVIORAL MEASURES

In this section various measures are described which can be used to analyze the behavior of population-based or trajectory-based metaheuristics when solving combinatorial optimization problems:

Solution Similarity:

A problem with population-based metaheuristics is often that populations tend to converge to a solution candidate too quickly and diversity is lost within the population. The solution similarity gives a crucial hint on why a metaheuristic is not able to achieve the desired performance. Similarity can be calculated by comparing each individual to each other and averaging these values for each generation.

Similarity can also be expressed using allele frequency analysis (Wagner 2004) which investigates the alleles of a population. For example unique alleles are the amount of distinct alleles contained in a population. Therefore this measure may also be used to get a deeper insight into the diversity of the population and can offer a reason why a metaheuristic is not able to generate better offspring.

Spread of Solutions:

While some algorithms such as local search only cover little parts of the solution space more intensively, other algorithms that are intentionally built with diversification in mind are able to cover broader parts of the solution space. This measurement therefore captures how wide spread the solutions are in the solution space over the complete run of the algorithm.

Amount of Improvement:

Metaheuristics can have difficulties in improving the quality of solution candidates. The reason for this is that

an operator might not be able to generate new solutions with a better quality than the original solution. The Offspring Selection Genetic Algorithm (Affenzeller, Winkler, Wagner and Beham 2009) for example uses a *comparison factor* to define the percentage by which the quality of the generated offspring has to succeed the worse parent. Similar the improvement ratio defines the percentage by which the quality of the offspring increases or decreases compared to the worse parent.

This measure offers information about the performance of an operator. In the parameter tuning process operators are often measured by the quality of the best found solution. This measure therefore gives a more detailed view into the performance and behavior of a single operator without being influenced by other parameters.

In the case of a genetic algorithm for example, this measure can show how well the crossover and mutation operators work. Therefore it can also be used to analyze how well the mutation and crossover operators work together and how much of an improvement each operator contributes to the overall improvement of the solution candidate.

Step Size of Moves:

If a metaheuristic only provides one type of solution generation method (meaning no distinction between an intensification and a diversification step), this measurement tracks the average size of the jump an algorithm makes from one solution candidate to the next.

Convergence Speed:

As already mentioned a problem of metaheuristics is often that they converge too quickly to a certain solution candidate and are then not able to generate improved solutions. The convergence speed therefore measures how long it takes until individuals have reached a certain similarity and the population is converged. This measure observes the solution similarities over time and shows therefore how quickly an algorithm converges.

Success Ratio:

Convergence can also be seen as the problem that a metaheuristic is not able to generate offspring that succeeds the quality of the parents. Even if the algorithm and used operators are able to generate better offspring there might still be individuals that do not succeed their parents. The Offspring Selection Genetic Algorithm takes this fact into account by adding a parameter *success ratio* which defines the amount of better offspring that has to be generated for the next generation. Similar to this concept the ratio of solutions which are better than the parents to the amount of worse children are captured. This measure shows how difficult it is for the algorithm to generate new and successful offspring.

Coverage of the Solution Space:

This measure captures how much of the solution space is covered by an algorithm. Often metaheuristics allow duplicate solutions in their population while others intentionally prohibit such a state. This measure therefore shows the ratio of overall distinct solutions to the number of overall solutions generated during the algorithm execution.

Intensification/Diversification Ratio:

Metaheuristics often provide special mechanisms for intensification and diversification. For example Scatter Search uses an explicit diversification step (the population rebuild method) when no better individuals can be found. It additionally uses an improvement method which is applied after the solution recombination method to further improve the generated solutions (intensification). Similarly, simulated annealing generally tries to find better solutions, but also incorporates worse solution candidates with a certain probability. The intensification/diversification ratio therefore provides information about the amount of usage of these two methods.

Intensification/Diversification Frequency:

Metaheuristics often apply intensification or diversification operations periodically or based on a certain scheme. This measurement value captures the frequency between intensification and diversification operations.

Diversification Intensity:

When metaheuristics include explicit diversification mechanisms, they usually incorporate new and diverse solutions into the search process or accept worse quality solutions. The diversification intensity measures to which degree diverse candidates are accepted.

3. USE CASES AND ADVANTAGES OF BEHAVIORAL MEASURES

In this section use cases for the proposed measurement values are described. The goal of having behavioral measurements for algorithms is to use them as a basis for further algorithm analyses and prediction.

Behavioral algorithm measures make algorithms comparable to each other. At the moment algorithms are mostly compared by their achieved quality and the number of evaluated solutions. We argue that comparisons solely based on the quality are not enough as they only give information about the performance but not the reason for it. Furthermore, these measures give hints about potentially successful parameter settings. If an algorithm performs poorly, these measurements can explain the reason for this particular behavior. Using the quality as a measure alone could lead to the wrong impression that an algorithm is not suited for a certain problem. But behavioral measures can give a reason why this is the case and help to find parameter configurations that work better. An example for such a case is e.g. a genetic algorithm that has a bad quality as

well as a high convergence speed and a low coverage of solution space. A researcher could therefore infer from these results that a higher population size or mutation rate could lead to a better quality instead of discarding the algorithm because of the initial poor results.

Behavioral measures could also be used by algorithms to predict potentially good parameter settings. Such algorithms could use this information to pursue a more informed search process by repeating the execution, analyzing the calculated behavioral measures and then infer new and better parameter settings. These algorithms would work much more like a human expert doing parameter tuning who learns from his mistakes and tries to improve on them.

These algorithms need to be able to generate new parameter configurations based on the calculated behavioral measures. This could be realized by defining a rule set for behavioral measures. Therefore algorithms could react if a behavioral measure has a certain value which indicates that a parameter should be adjusted in the next run as it would potentially lead to better results. A disadvantage of the rule set approach is that it is difficult to capture all states of different measures as well as the right parameter settings to counter potential bad behavior.

Another possibility to infer new parameter configurations is to use supervised learning methods to create models for predicting algorithm performance for new parameter settings. Having a large data set, parameter settings based on the behavioral measures can be learned. This allows sampling new parameter configurations and discarding those where the model predicts a bad performance.

Additionally, fitness landscape analysis (FLA) (Pitzer and Affenzeller 2012) can be used to improve the parameter prediction. FLA offers metrics for problem instances that describe certain characteristics of the problem. This information could be used as well together with algorithm behavioral measures to choose parameter configurations more systematically.

The above described rule set for parameter generation can also be used in a similar way as algorithms using parameter control. While the before described parameter tuning algorithms work on a data set of results generated by executing standard metaheuristics, these new parameter control algorithms would tune and adapt their parameters based on a defined rule set at runtime.

4. CONCLUSION AND FUTURE WORK

Algorithm behavior analysis represents a profound basis for further algorithm analysis. Besides giving researchers a tool for getting a better insight into the inner dynamics of algorithms and help to understand the interdependencies and impacts of parameter settings, these measures can be used to predict potentially good parameter settings based on either rule sets or supervised learning methods. Furthermore, the prediction models can be used to determine promising parameter settings and to steer parameter tuning into the

right direction which reduces the amount of required test cases. Additionally algorithms that use behavioral measures for online parameter tuning could be realized using a rule set for parameter control which would allow these algorithms to follow a more systematic search process.

In the future the authors will implement the proposed measurements. There is a proper need of detailed information about the inner workings of the search process to be able to choose parameter settings more systematic instead of intuition. Another future task is the development of the proposed parameter tuning and parameter control algorithms which utilize the behavioral measures.

Additionally, these measures should also be integrated into the optimization knowledge base. The Optimization Knowledge Base (OKB) (Scheibenpflug, Wagner, Pitzer and Affenzeller 2012) is an open database for storing information about algorithms, problems and the results collected from executing algorithms. It gives researchers a tool for gaining a better understanding of the behavior of algorithms by providing a huge data set of already generated results for different algorithms on various problems as well as meta-information for problems. While the OKB can be used to support parameter tuning and algorithms by providing a memory, it can also serve as a platform for researchers to publish their results and make their contributions more transparent. Besides storing the results of metaheuristic runs, the optimization knowledge base also stores information about problems which is generated by fitness landscape analyses.

The OKB therefore already gives researchers a huge source of information that can be used to partially explain the behavior of metaheuristics. The results together with the parameter settings saved in the OKB show which settings in combination with which algorithms works well on specific problems. The values collected from fitness landscape analyses can be used to get a feeling for the problem at hand and may also be used to explain the behavior of algorithms or parameter settings. A feature the optimization knowledge base is missing is support for algorithm behavior measures. These measures could be used to explain the behavior of algorithms and why certain algorithms exhibiting a certain behavior work well on certain problems having certain problem characteristics.

Furthermore, the information can be used by applications that automatically optimize new and unknown problems. If a new problem is to be optimized, the fitness landscape analysis can be used to calculate the similarities from the new problem to all known problems. Then the results for the similar problems can be gathered and the parameter settings of the best runs can be used for optimizing the new problem.

We argue that this method, as described until now, needs more information about the algorithms besides the best achieved quality. If the OKB contains algorithm behavior measures, parameter tuning

algorithms could use the information contained in the OKB together with the algorithm behavioral measures for supervised learning methods to create models to predict algorithm performance for new parameter settings. This allows sampling new parameter configurations and discarding those where the model predicts a bad performance. This would drastically minimize the run time and lead to a much more deliberate search process.

ACKNOWLEDGMENTS

The work described in this paper was done within the Josef Ressel-Centre HEUREKA! for Heuristic Optimization sponsored by the Austrian Research Promotion Agency (FFG).

REFERENCES

- Wolpert, D. H., Macready, W. G., 1997. No Free Lunch Theorems for Optimization. *IEEE Transactions on Evolutionary Computation*, 1 (1), 67–82.
- Talbi, E.-G., 2002. A taxonomy of hybrid metaheuristics. *Journal of Heuristics*, 8(5), 541-564.
- Smit, S.K., Eiben, A.E, 2009. Comparing parameter tuning methods for evolutionary algorithms. *IEEE Congress on Evolutionary Computation*, 399-406.
- Kirkpatrick, S., Gelatt, C. D., Vecchi, M. P., 1983. Optimization by Simulated Annealing. *Science*, 220, 671-680.
- Glover, F., 1989. Tabu Search - Part I. *Inform Journal on Computing*, 1 (3), 190-206.
- Holland, J. H., 1975. Adaptation in natural and artificial systems. *University of Michigan Press*.
- Laguna, M., Marti, R., 2002. Scatter Search: Methodology and Implementations in C. *Kluwer Academic Publishers*.
- Kennedy, J., Eberhart, R., 1995. Particle swarm optimization. *Proceedings of the IEEE Conference on Neural Networks*, 4, 1942 -1948.
- Özcan, E., Bilgin, B., Korkmaz, E.E., 2008. A comprehensive analysis of hyper-heuristics. *Intelligent Data Analysis*, 12 (1), 3–23.
- Nadi, F., Khader, A. T., 2011. A parameter-less genetic algorithm with customized crossover and mutation operators. *Proceedings of the 13th annual conference on Genetic and evolutionary computation*, 901-908.
- Eiben, A. E., Michalewicz, Z., Schoenauer, M., Smith, J., 1999. Parameter control in evolutionary algorithms. *IEEE Transactions on Evolutionary Computation*, 3, 124-141.
- Mercer, R., Sampson, J., 1978. Adaptive search using a reproductive metaplan. *Kybernetes*, 7, 215-228.
- Affenzeller, M., Winkler, S., Wagner, S., Beham, A., 2009. *Genetic Algorithms and Genetic Programming*. Chapman & Hall/CRC.
- Scheibenpflug, A., Wagner, S., Pitzer, E., Affenzeller, M., 2012. Optimization Knowledge Base: An Open Database for Algorithm and Problem Characteristics and Optimization Results,

Proceedings of the Genetic and Evolutionary Computation Conference (GECCO).

Pitzer, E., Affenzeller, M., 2012. A comprehensive survey on fitness landscape analysis, *Recent Advances in Intelligent Engineering Systems*, 378, 161-191.

Wagner, S., 2004. *Looking Inside Genetic Algorithms*. Universitätsverlag Rudolf Trauner.

Smit, S. K., Eiben A. E., 2009. Comparing parameter tuning methods for evolutionary algorithms. *IEEE Congress on Evolutionary Computation*, 399-406.

received his PhD in engineering sciences and in 2004 he received his habilitation in applied systems engineering, both from the Johannes Kepler University of Linz, Austria. Michael Affenzeller is professor at UAS, Campus Hagenberg, and head of the Josef Ressel Centre *Heureka!* at Hagenberg.

AUTHORS BIOGRAPHIES



ANDREAS SCHEIBENPFLUG

received his MSc in software engineering in 2009 from the University of Applied Sciences Upper Austria. He is currently research assistant at the Heuristic and Evolutionary Algorithms Laboratory at the

University of Applied Sciences Upper Austria.



STEFAN WAGNER received his PhD in

engineering sciences in 2009 from JKU Linz, Austria; he is professor at the Upper Austrian University of Applied Sciences (Campus Hagenberg). Dr. Wagner's

research interests include evolutionary computation and heuristic optimization, theory and application of genetic algorithms, and software development.



ERIK PITZER received his diploma in

software engineering in 2004 at the Upper Austria University of Applied Sciences. Since 2004 he has been working as a research associate at the Research Center Hagenberg of the Upper Austria

University of Applied Sciences and at the Decision Systems Group of Harvard Medical School in Boston. Erik Pitzer is currently working on his PhD thesis in the field of fitness landscape analysis for the design and analysis of meta-heuristic algorithms.



BOGDAN BURLACU received his MSc

in computer science and systems engineering in 2009 from the "Gheorghe Asachi" Technical University in Iasi, Romania. Currently he is a research associate in the Heuristic and

Evolutionary Algorithms Laboratory in Hagenberg, under the supervision of Michael Affenzeller.



MICHAEL AFFENZELLER has

published several papers, journal articles and books dealing with theoretical and practical aspects of evolutionary computation, genetic algorithms, and meta-heuristics in general. In 2001 he

CLOUD MANUFACTURING PLATFORM ARCHITECTURE

Lei Ren^{(a) (b)}

^(a) School of Automation Science and Electrical Engineering, Beihang University, Beijing 100191, China;

^(b) Engineering Research Center of Complex Product Advanced Manufacturing System, Ministry of Education, Beijing 100191, China

leo.renlei@gmail.com

ABSTRACT

With a new trend of service orientation, high efficiency and low consumption, and knowledge innovation in global manufacturing, networked manufacturing is facing great challenges. Cloud Manufacturing, as a new service-oriented agile manufacturing paradigm over networks, deriving from the idea of Cloud Computing, can provide on-demand collaborative services supporting whole life circle manufacturing applications by sharing virtualized manufacturing resources via cloud networks. The achievement of this promising paradigm depends on powerful Cloud Manufacturing platform which meets the requirements of both resource providers and consumers. This paper presents a design of Cloud Manufacturing platform architecture which includes resource perception layer, virtual resource layer, middleware layer, application supporting layer, and user interface layer. The design can give comprehensive support to achieve the goal of Cloud Manufacturing. We also discuss the key technologies in Cloud Manufacturing platform, which presents a map for future research of this new area.

Keywords: cloud manufacturing, cloud computing, cloud simulation, cloud manufacturing platform, networked manufacturing

1. INTRODUCTION

The evolution of contemporary manufacturing has adapted itself to the development of economy globalization that gives rise to the requirements of quick response to global market. Current manufacturing is no longer limited to traditional production and fabrication, but a life-circle management of product covering analysis, design, simulation, experiment, fabrication, business management, after-sale service, etc. The competition in global manufacturing calls for dynamic alliance of manufacturing companies distributed in geographically different locations all over the world, resulting in virtual manufacturing organizations across Internet and intranet. The combination of manufacturing with information technology, such as distributed manufacturing networks and computer supported

collaborative work, has proven a powerful means to support effective global manufacturing management of whole life circle of product (Zhan *et al.* 2003). In recent years, network manufacturing technology based on distributed computing, such as Application Service Provider (ASP) (Flammia 2001), Manufacturing Grid (Fan *et al.* 2004), etc., has become one of the essential advanced techniques to support the collaboration of distributed manufacturing companies over networks. For example, Manufacturing Grid can integrate and schedule manufacturing resources dispersed in networks such as material, device, information, business process, human, etc. to support complex collaborative manufacturing tasks.

However, current available network manufacturing technologies are facing new challenges. From a perspective of business mode, current solutions do not provide incentives for manufacturing service providers in ASP or Grid because of the absence of pricing and accounting mechanism according to QoS evaluation and actual usage of resources. Thus, it is difficult to promote the market-oriented network manufacturing for both manufacturing service providers and consumers at market equilibrium.

Other than the problem of business mode, there are still technical roadblocks as well. One is that the encapsulated manufacturing services based on service-oriented architecture (SOA) mainly offer support for the soft-resources such as CAD/CAE software. The current SOA-based manufacturing techniques (Sun *et al.* 2008) cannot penetrate through the underlying infrastructure especially for the hard-resources such as critical fabricating devices in production chain. Therefore, the partial SOA solution cannot achieve efficient integration of manufacturing resources.

Additionally, as the green manufacturing (Gomes *et al.* 2004) is getting increasingly important for energy saving, manufacturing applications make an urgent demand for high efficient and low consumption of resources management especially in the large-scale and complex manufacturing domains. Complex manufacturing applications often need to perform collaborative computing tasks and deal with a vast amount of data, which calls for dynamical aggregation

of distributed resources at the peak computing point. While current network manufacturing techniques always cannot meet the need of resources for peak computing, the average utilization of resources is much low because a majority of common manufacturing tasks only consume a few resources.

Moreover, a large number of knowledge accumulated in manufacturing domains has gained little effective utilization in current network integration solutions. The knowledge covers a wide range of domain-specific ontology, expert experience, simulation models, etc., which can supply semantic support for manufacturing service management and business process optimization to achieve intelligent manufacturing. Yet, current network manufacturing techniques cannot make full use of knowledge to implement intelligent integration and management of manufacturing resources.

Cloud Computing (Armbrust *et al.* 2009) provides a new business paradigm for service-oriented distributed computing, which together with techniques of virtualization (Lei *et al.* 2012), Internet of Things (IoT) (Wolf 2009), Semantic Web (Acuna and Marcos 2006), and High Performance Computing (HPC) (Benioff and Lazowska 2005) appears to be promising solutions to tackle the problems above.

To address these concerns, Cloud Manufacturing (Zhang *et al.* 2012) provided a new model of service-oriented distributed manufacturing based on the idea of Cloud Computing. Cloud Manufacturing provided a promising business mode for both manufacturing service providers and consumers by the way of on-demand sharing and provision of distributed resources. Besides, Cloud Manufacturing leverages IoT and virtualization techniques to ensure that both soft-resources and hard-resources could be plugged in and virtualized into services. Also, virtualization and HPC give a support for high efficient utilization of virtualized resources. Further, Cloud Manufacturing focuses more on knowledge-based semantic integration to achieve intelligent manufacturing.

The achievement of this new paradigm depends on powerful Cloud Manufacturing platform which meets the requirements of both resource providers and consumers. This paper presents a design of Cloud Manufacturing platform architecture comprising resource perception layer, virtual resource layer, middleware layer, application supporting layer, and user interface layer. The design can give comprehensive support to achieve the goal of Cloud Manufacturing. We also discuss the key technologies in Cloud Manufacturing platform, which presents a map for future research of this new area.

2. RELATED WORK

Network manufacturing technology put emphasis on information integration, process integration, and enterprise integration to establish resources sharing environment across Internet and intranet. ASP, SOA-based manufacturing and

Manufacturing Grid are among most popular ones. ASP presented an information system outsourcing paradigm in that application service providers, as vendor, could supply services for users through networks. SOA-based manufacturing typically used web services as a unified standard to implement integration of distributed and heterogeneous manufacturing resources. Manufacturing applications (mainly refer to software) are encapsulated into loosely coupled, interoperable, and protocol-independent services based on WSDL, SOAP and UDDI. Manufacturing Grid defines a set of standard protocols and middleware to provide interoperable services built on different manufacturing nodes, which can concurrently support access to different resource types such as computing, storage, software, etc, which thus can disassemble large-scale and complex tasks into networked and loosely coupled nodes acting in concert to complete parallel computing processes (Fan *et al.* 2004). In contrast to Cloud Manufacturing, current available solutions for network manufacturing introduced above do not build a successful business operation paradigm that support effective pricing and accounting mechanism, and they cannot attain high utilization of manufacturing resources by taking advantage of virtualization and knowledge-based intelligent management.

There are a variety of different definitions for Cloud Computing. For example, it refers to a large-scale distributed computing paradigm that is driven by economies of scale, in which a pool of abstracted, virtualized, dynamically-scalable, managed computing power, storage, platforms, and services are delivered on demand to external customers over the Internet (Foster *et al.* 2008). Cloud Computing is considered as a new business paradigm describing supplement, consumption and delivery model for IT services by Utility Computing (Mladen 2008) based on the Internet. The typical examples of public Utility Computing include Google AppEngine, Amazon Web Services, Microsoft Azure, IBM Blue Cloud, Salesforce. So far, Cloud Computing is regarded as the sum of IaaS (Infrastructure as a Service), PaaS (Platform as a Service), and SaaS (Software as a Service) (Buyya *et al.* 2009). Cloud Computing providers can deliver on-demand services covering IT infrastructure, platform, and software via virtualization and service encapsulation technology. Thus, it can meet the needs of ever-rising scale of computing and storage of consumers and lead to decrease in IT investment cost at the same time. Cloud Computing introduces a promising business model and technical approach to the problems network manufacturing facing. For example, virtualization technology can support deep encapsulation of a logic entity of IT infrastructure (e.g., CPU, memory, disk, and I/O) and software into a pool of virtual machines, thus it can achieve high efficient and low consumption of resources. While current virtualization technology in Cloud Computing can build virtualized entities for soft-resources in network manufacturing, it cannot solve the encapsulation of

hard-resources (e.g., lathe and fabricating equipment) problems that is essential to efficient manufacturing collaboration. Also, manufacturing need more support of knowledge including product design models, expert experience, production process logic, collaboration rules, etc. which is not emphasized in Cloud Computing.

Along with the advance in Cloud Computing, the Internet of Things (IoT) has become a promising technology that provides possibility to interconnect all physical things via wireless sensors, RFID, embedded technology, etc. besides the IT infrastructure over the Internet. So, IoT can offer an approach that ensures the hard-resources plugged into Cloud Manufacturing and then virtualized to services.

Semantic Web gives a standard formal model describing knowledge by ontology such as OWL and provides support for semantic service computing such as OWL-S (Martin, *et al.* 2007), which can thus be adopted to manufacturing knowledge modeling and intelligent service management.

Under the pushing of large-scale and complex manufacturing applications such as Boeing787 aircraft, High Performance Computing (HPC) will offer powerful support for massively scalable data processing and parallel computing to achieve high efficient collaborative manufacturing through the whole life-cycle of product in Cloud Manufacturing.

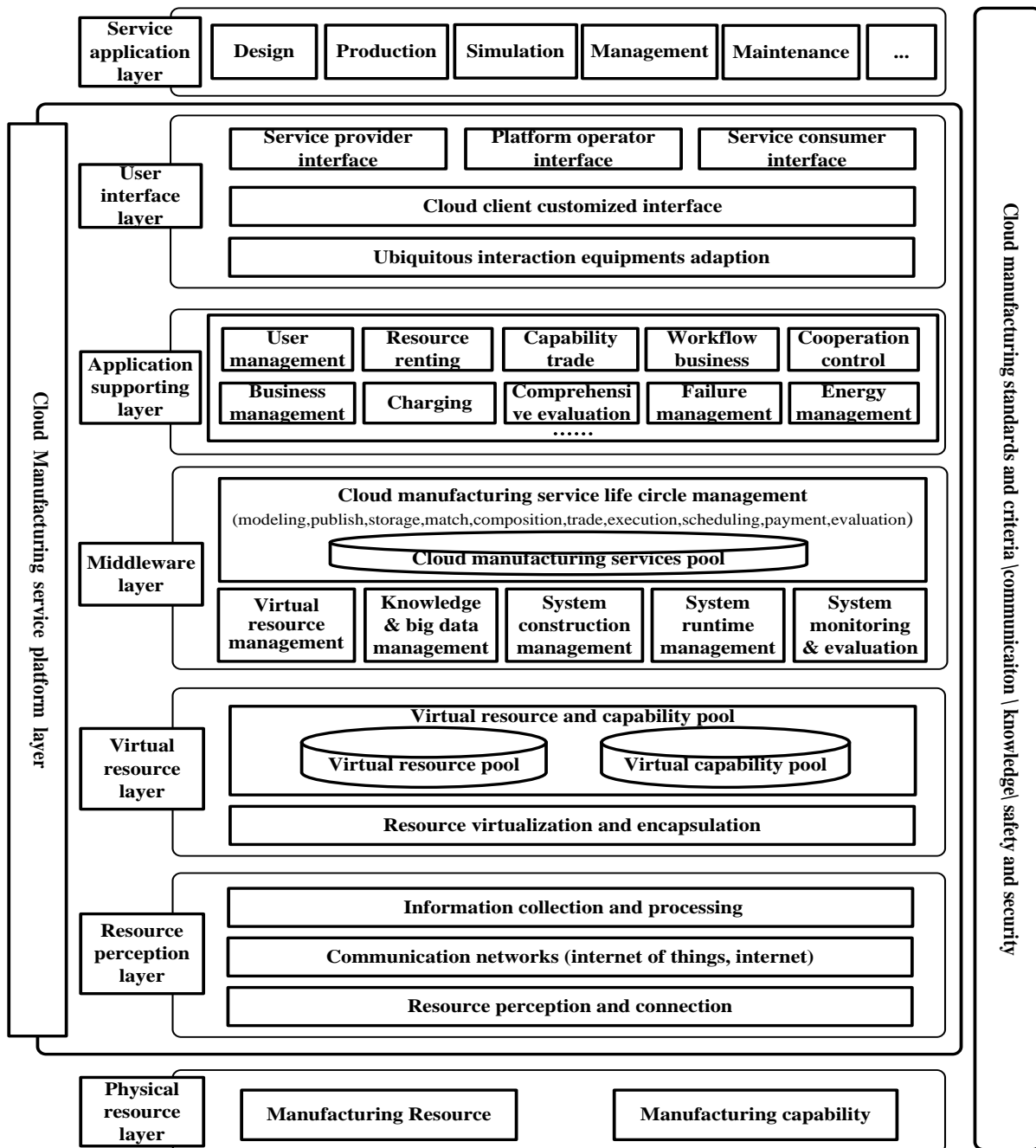


Figure 1: Cloud Manufacturing platform architecture

3. CLOUD MANUFACTURING PLATFORM

Figure 1 shows the layered architecture of Cloud Manufacturing platform. It consists of five layers: *resource perception layer*, *virtual resource layer*, *middleware layer*, *application supporting layer*, and *user interface layer*. Cloud Manufacturing platform can integrate a broad range of manufacturing resources as Figure 1 illustrates, and provide support for whole life circle manufacturing applications.

3.1. Physical Resource Layer

The *Physical Resource Layer* includes *manufacturing resource and capability*. This is an abstraction of a variety of manufacturing units distributed in geographically different places.

Manufacturing resource comprise a variety of underlying resources including three classes: hard-resource, soft-resource, and IT infrastructure. Hard-resources refer to manufacturing equipments such as fabricating device, milling machine, etc., which should be first plugged into cloud networks by means of wireless sensors or IoT so as to build up cloud terminals that could be accessed and controlled. Soft-resources involve all kinds of CAD/CAE/CAX software, simulation tools, model/algorithm repository, and domain knowledge. Some special software, such as Matlab, Adams, Easy5, Protel, and CodeV, is essential to domain-specific applications. Moreover, manufacturing applications always need domain knowledge to support product life-circle management. A great number of legacy models or algorithms for mechanism, control, dynamics, thermodynamics, and so on are indispensable to knowledge-based manufacturing. Besides hard-resource and soft-resource especially for manufacturing, physical resources also comprise IT infrastructure such as computing cluster, storage center, network device, and other IT hardware.

Here manufacturing resource differs from manufacturing capability in that the former is used to describe “what I have” while the latter indicates “What I can do”. So the capability should be described with more semantics than typical resource. In fact, it is the manufacturing capability trade that the providers and consumers are dealing with. Indeed, manufacturing capability roots in manufacturing resource merged together with human intelligence and knowledge to supply design capability, production capability, experiment capability, simulation capability, and management capability that are inevitable to life circle manufacturing.

3.2. Resource Perception Layer

The *Resource Perception Layer* is responsible for making the manufacturing resources and capability plugged into manufacturing clouds. The terminals are connected into clouds over comprehensive networks such as IoT, internet, and mobile networks. The so called plug-in needs special intermediate hardware devices which provide adaptive interfaces for diverse manufacturing machines connected in. Meanwhile, a wide variety of sensors play an important role to

transform passive machines into intelligent active ones. For example, pressure sensors and temperature sensors can be used to perceive the real-time states of chemical plant installations and the perception information makes it possible for remote controller in clouds to give an alarm and do better scheduling. RFID and other wireless sensors give support for tracing materials in logistics.

Another indispensable function in this layer is information collection and processing because there should be enormous data generating constantly by sensors. The mass data need de-noising to generate clean data, and the trimmed data need to do further organization and classification to provide valuable information desired by applications.

3.3. Virtual Resource Layer

Virtual resource in Cloud Manufacturing differs from Cloud Computing in that it extend the definition to a large degree. Virtualization in Cloud Manufacturing refers to transforming physical manufacturing resources and capability into logic and abstract ones with standard interfaces to handle inputs and outputs. This layer is responsible for this transformation. Then the virtual ones decouple themselves from the physical ones. As a result, there would be a large number of virtual units that make the management of manufacturing resources and capability more flexible.

In addition, in this layer there are two types of pools where the virtual units are assembled. One is virtual resource pool and the other is virtual capability. The pools seem like UDDI in SOA architecture. This layer provides needed basic functions for management of virtual units pool such as encapsulation, registration, query, update, etc. Moreover, this layer supports intelligent and optimal composition of virtual units for complex requirements single virtual unit cannot meet, such as a product design request that need diverse resources across multiple organizations.

3.4. Middleware Layer

Middleware Layer packaged commonly used functions in clouds into different modules that provide standard interfaces used by *Application Supporting Layer*. This layer comprises six types of middleware to realize virtual resource management, knowledge & big data management, system construction management, system runtime management, system monitoring & evaluation, and cloud manufacturing service life circle management, respectively.

The virtual resource management middleware is responsible for management of virtual resource and capability pools. The knowledge & big data management middleware acts as the provider of multi-domain knowledge to give intelligent support for both life circle of manufacturing applications and life circle of cloud services. Moreover, this middleware provides support for parallel storage and high performance processing of the big data generated by clouds. Most of the big data are semi-structured and unstructured, and

cannot be organized, stored, and analyzed efficiently by means of traditional relational database management systems. The system runtime management middleware masters the customized runtime system. It need manage coordination among cloud services, involving workflow control, resource allocation, time and space synchronization. In addition, it handles runtime fault tolerance and implement live migration of tasks, e.g., finding substitute resources and then copy task contexts to new physical manufacturing nodes. System monitoring & evaluation middleware acquires customized system parameters and provides various qualitative and quantitative models for evaluation of performance, QoS, and etc. Cloud service management middleware offers support for management of the whole life circle of cloud services, and the functions including service modeling, publishing, storage, matching, composition, trade, execution, scheduling, payment, and evaluation.

3.5. Application Supporting Layer

The *Application Supporting Layer*, on basis on the middleware interfaces, encapsulates the functions frequently used by manufacturing applications into service components.

The user management component is used to manage user personal information, accounts and roles. The resource renting component helps resource requesters to find needed resources and rent them. The capability trade component acts as the intermediary agent between capability providers and consumers. The workflow business component is used to manage complex service composition. The cooperation control component is responsible for management of collaborative and interactive services. The business management component serves as a business manager to handle business affairs such as contracts. The charging component is used to compute the fees according to rates of resources and capability. The comprehensive evaluation component provides both interfaces for end-users to score and APIs for automatic evaluation by the platform. The failure management component is to deal with runtime faults to keep systems reliable. The energy management component aims at realize optimized utilization of energy.

3.6. User Interface Layer

The *User Interface Layer* play an indispensable role for end-users in Cloud Manufacturing systems. End-users have different roles in manufacturing applications and they also have diverse requirements concerning how to access mysterious clouds. It is the issue of ubiquitous usability (Jacob *et al.* 2008). This layer provides support for divers interaction terminal equipments such as PC, pad computer, smart phone, and PDA, so end-users may use cloud services without limitations of time and space.

Moreover, this layer offers cloud client customization for different end-users keep their individual interfaces, and the interfaces can be changed flexibly. To facilitate the three main roles of end-users,

this layer provides three types of portals for service providers, platform operators, and service consumers.

4. SUMMARY

As a new promising research area, Cloud Manufacturing is facing great challenges. Design issues of Cloud Manufacturing platform play a significant role since it occupies an indispensable intermediate position between service providers and requesters. This paper presents a design of Cloud Manufacturing platform architecture and discusses the key technologies in each layer. This architecture includes resource perception layer, virtual resource layer, middleware layer, application supporting layer, and user interface layer. The design can support comprehensive connection and perception of hard-resource and soft-resource, and the registered resources in clouds are described with semantics to support knowledge-based match between supply and demand. In addition, the networked resources can be virtualized into logic ones for flexible composition and decomposition according to needs, as well as published as standard services for effective cooperation across different enterprises over heterogeneous environments. Moreover, it can provide on-demand collaborative services to establish customized networked systems according to consumer's requirements supporting whole life circle manufacturing applications by sharing virtualized manufacturing resources via networks in clouds. Therefore, the design can provide a solution to give comprehensive support to achieve the goal of Cloud Manufacturing.

Future work is to establish a Cloud Manufacturing application example for large-scale and complex product such as aircraft to evaluate the architecture.

ACKNOWLEDGMENTS

The research is supported by the NSFC (National Science Foundation of China) Projects (No. 61103096) in China, the National High-Tech Research and Development Plan of China under Grant No. 2011AA040501, and the Fundamental Research Funds for the Central Universities in China.

REFERENCES

- Zhan H. F., Lee W. B., Cheung C. F., Kwok S. K., and Gu X. J., 2003. A web-based collaborative product design platform for dispersed network manufacturing, *Journal of Materials Processing Technology*, 138, 600–604.
- Flammia G., 2001. Application service providers: challenges and opportunities, *IEEE Intelligent Systems and Their Applications*, 16(1), 22–23.
- Fan Y., Zhao D., Zhang L., Huang S., and Liu B., 2004. Manufacturing grid: needs, concept, and architecture. *Lecture Notes in Computer Science*, 3032, 653–656.
- Sun H., Yu T., Liu L., and He Y., 2008. Service-oriented manufacturing grid system, *Computer Integrated Manufacturing Systems*, 14(1), 56–63.
- Gomes C. F., Yasin M. M., and Lisboa J. V., 2004. A literature review of manufacturing performance measures and measurement in an organizational context: a

- framework and direction for future research, *Journal of Manufacturing Technology Management*, 15(6), 511–530.
- Armbrust M., Fox A., Griffith R., Joseph A. D., Katz R. H., and etc., 2009. Above the clouds: A Berkeley view of Cloud computing, *Technical report UCB/EECS-2009-28, Electrical Engineering and Computer Sciences*, University of California at Berkeley, Berkeley, USA.
- Lei, R., Lin Z., Fei T., Xiaolong, Z., Yongliang, L., and Yabin, Z., 2012. A methodology toward virtualization-based high performance simulation platform supporting multidisciplinary design of complex products. *Enterprise Information Systems*, 6(3), 267-290.
- Wolf W., 2009. Cyber physical systems, *Computer*, 42(3), 88–89.
- Acuna C. and Marcos E., 2006. Modeling semantic web services: A case study, *Proceedings of the 6th International Conference on Web Engineering (ICWE)*, ACM Press, , pp. 32–39.
- Benioff M.R. and Lazowska E.D., 2005. Computational Science: Ensuring America's Competitiveness, President's Information Technology Advisory Committee (PITAC).
- Zhang L., etc. Cloud Manufacturing: a new manufacturing paradigm. *Enterprise Information System*(accepted). 2012.
- Foster I., Zhao Y., Raicu I., and Lu S., 2008. Cloud Computing and Grid Computing 360-degree compared, in *Grid Computing Environments Workshop*, pp. 1–10.
- Mladen A. V., 2008. Cloud Computing – Issues, Research and Implementations, *Journal of Computing and Information Technology*, 16(4), 235–246.
- Buyya, R., Yeo C.S., Venugopal S., Broberg J., and Brandic I., 2009. Cloud computing and emerging IT platforms: Vision, hype, and reality for delivering computing as the 5th utility. *Future Generation Computer Systems*, 25 (6), 599-616.
- Martin D., Burstein M., Mcdermott D., and Mcilraith S., 2007. Bringing semantics to web services with owl-s, *World Wide Web*, Springer-Verlag.
- Jacob R., Girouard A., Hirshfield L., and etc., 2008. Reality-based interaction: a framework for post-WIMP interfaces, *Proceedings ACM 26th SIGCHI conference on human factors in computing systems*, pp. 201–210.

AUTHORS BIOGRAPHY

Lei Ren, Ph.D. Dr. Lei Ren received Ph.D. degree in 2009 at the Institute of Software, Chinese Academy of Sciences, China. From 2009 to 2010 he worked at the Engineering Research Center of Complex Product Advanced Manufacturing System , Ministry of Education of China. He is currently a researcher at the School of Automation Science and Electrical Engineering, BeiHang University. He is also a senior researcher at the Engineering Research Center of Complex Product Advanced Manufacturing System, Ministry of Education of China now. He is a member of SCS and SISO. His research interests include high performance simulation platform, integrated manufacturing systems, Cloud Simulation, Cloud Manufacturing and Cloud Computing.

SYMBOLIC REGRESSION USING TABU SEARCH IN A NEIGHBORHOOD OF SEMANTICALLY SIMILAR SOLUTIONS

Gabriel Kronberger^(a), Andreas Beham^(b)

^(a,b) University of Applied Sciences Upper Austria, School of Informatics, Communications and Media

^(a)gabriel.kronberger@fh-hagenberg.at, ^(b)andreas.beham@fh-hagenberg.at

ABSTRACT

In this paper we describe for the first time a tabu search algorithm for symbolic regression. The novel contribution presented in this work is the idea to use a metric for semantic similarity to generate moves in such a way that branches are only replaced with semantically similar branches. In symbolic regression separate parts of the solution are linked strongly; often a small random change of one part might disrupt a link and thus, can completely change the semantics of the solution. We hypothesize that by introducing the semantic similarity constraint, the fitness landscape for tabu search becomes smoother as each move can only change the fitness of the solution slightly. However, empirical evaluation on a set of simple benchmark instances shows that the approach described in this paper does not perform as well as genetic programming with offspring selection and there is no big difference between random and semantic move generation.

Keywords: symbolic regression, tabu search, genetic programming, semantic similarity

1. INTRODUCTION

Symbolic regression is a data-modeling approach for regression analysis where the structure of the model is not specified explicitly but must be discovered automatically. Thus, it can also be used in situations where no or only limited information about the modeled system is available and it would be hard to specify a fitting model structure manually. Symbolic regression has first been described in the context of genetic programming (Koza 1992) and has since become a popular benchmark task for genetic programming. However, symbolic regression has also been used successfully to solve real-world problems occurring for instance in industry, medicine and finance.

Tabu search is a trajectory-based meta-heuristic for solving difficult, usually combinatorial, optimization problems (Glover 1999). To avoid getting stuck in local optima, it uses the concept of short-term and long-term memory to achieve a good balance between diversification and intensification stages of the search process.

In this contribution we present a new approach for symbolic regression which is based on tabu search

instead of an evolutionary algorithm. We describe the motivation for the algorithm and also discuss details of the implementation and necessary parameters. Additionally, we also describe the difficulties we had when transforming the initial concept into a working implementation and highlight the problems of finding good parameter values for the algorithm. An empirical evaluation of the proposed approach on a set of symbolic regression benchmark instances is also given to facilitate comparison with a genetic programming approach. The main contribution of this article is the description of a neighborhood function which produces semantically similar neighbors to improve the smoothness of the tabu search trajectory and a new semantic aspiration criterion for tabu search.

2. MOTIVATION

Symbolic regression based on genetic programming is an idea that is already more than 20 years old. However, there are still several open topics that are actively researched. These open topics are probably one of the reasons that symbolic regression still has not matured to a technology that can be used easily and routinely in practical applications. The list of open topics includes performance, overfitting, extrapolation capabilities, model complexity, and a workable theory for evolutionary operators, to name some examples. The recently proposed fast function extraction (FFX) (McConaghy 2011) side steps some of the above mentioned issues and demonstrates that symbolic regression does not necessarily have to be solved with an evolutionary algorithm. Instead it uses an approach based on regularization and coordinate descent (Hastie 2009) to search for parsimonious models by combining only relevant features from a large set of features including the original variables and (non-linear) transformations of the original variables. The advantage of this approach is its efficiency and, thus, can also be applied to large datasets and in a semi-automatic matter. Additionally, it is not necessary to tune a large number of parameters. McConaghy argues that because of these advantages it is much closer to a usable technology than genetic programming. A drawback is that the space of model structures considered by FFX is smaller than the space typically considered by GP, which also includes deeply nested functions.

FFX is a new algorithmic approach to symbolic regression that is not rooted in the evolutionary computation framework and, thus, can be advantageous in comparison to traditional GP approaches. It certainly allows a new perspective and can lead to better insights into the characteristics of the problem domain. This last aspect in particular has motivated us to look at yet another different approach based on tabu search which manipulates an initial solution using iterative moves to improve the solution step by step.

An important issue for trajectory-based algorithms is the design of a move operator for generating potential alterations of the solution that allow to efficiently walk towards a local optimum in the fitness landscape. For this it is necessary to understand the potential effects of solution alterations regarding the semantics of the whole solution. The mapping of syntactic and semantic similarity of GP solutions is generally rather chaotic and not well understood. One major issue is that disconnected parts of the solution can be strongly linked, and thus, the alteration of one branch can have a big effect on the global semantics of the whole solution even for small local alterations. Getting a better understanding of the semantic consequences of evolutionary operators is still an open research topic and recently a number of operators which try to include semantic information into the evolutionary process have been described (Nguyen 2010, Nguyen 2011, Krawiec 2011, Krawiec 2012). This has lead us to consider a semantically constrained move operator which should lead to a smoother fitness landscape.

In the following we first describe the general algorithm conceptually and then discuss the necessary details for the implementation of the algorithm. The aim is to find an efficient algorithm that is able to find accurate solutions also for hard problem instances. The main hypothesis is that tabu search using semantically similar moves improves the search, so that solutions for hard problems can be found. We do not yet discuss the generalization capabilities and parsimony of solutions in this paper.

3. PREVIOUS WORK

Variants of tabu programming that are similar to the approach discussed in this contribution have been described previously (Abdel-Rahman 2011, Balicki 2007, Balicki 2009). However, these variants use a different way to generate moves and in particular do not use a neighborhood function that leads to semantically similar neighbors and a smoother search trajectory. This extension which can be implemented rather easily for symbolic regression is described in this contribution for the first time.

4. CONCEPTUAL DESCRIPTION

Solutions are represented as symbolic expression trees in the same way as in tree-based GP. The internal nodes of the tree contain symbols of operators and functions and the leaf nodes contain input variables. The set of symbols for functions and variables is a parameter of

the algorithm. Figure 1 shows an exemplary symbolic regression model.

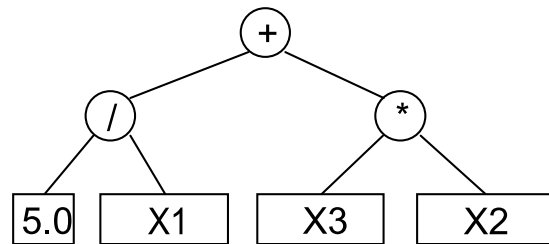


Figure 1: Example of a Symbolic Regression Model.

The proposed approach is based on the standard formulation of tabu search (Glover 1999). We use only a single tabu list for short-term memory and allow aspiration of moves. Initially a random solution is generated as a starting point. This solution is iteratively manipulated by applying the best move from a set of possible moves after checking a tabu criterion. In one move a branch of the tree is removed and replaced by a valid branch from a pool of branches. The pool of branches for replacement is filled with small random branches in the initialization step of the algorithm. We chose to use a pool of pre-generated branches to prevent continuously generating and evaluating random branches in the main loop of the algorithm. The main loop involves: generating moves, checking the tabu list, applying the best move, and updating the tabu list.

Two different modes are possible for move generation, random mode and semantic mode. In random mode, a number of cut points in the current solution are selected randomly and for each cut point a random replacement branch is selected randomly from the pool. In semantic mode, the cut points in the current solution are also selected randomly, however, then for each cut-point the semantically most similar branches from the replacement pool are selected. The semantic similarity of a branch in the current solution and a branch from the pool is determined by the squared Pearson's correlation coefficient of the output of the branch and the replacement branch. Branches with a large R^2 have a similar output as the original branch that is to be replaced and, thus, should only have a small effect on the overall quality of the model. By iteratively replacing branches with semantically similar branches the algorithm can walk on a smooth trajectory to more accurate solutions. To facilitate exploration of worse solutions the algorithm uses the tabu-list to guide search to different regions of the hypotheses space.

When a move is applied the exact point where the root of the new branch has been inserted is added to the tabu list and is thus locked and must not be changed for some time. Several aspiration criteria are used to allow certain moves that would otherwise be tabu for instance if a new best-of-run solution would be found.

A maximal size and depth limit is used to prevent uncontrolled growth of the solution.

5. DETAILED DESCRIPTION

5.1. Parameters

Based on the conceptual description of the algorithm a number of parameters can be derived. The most important parameters are the number k of randomly selected cut-points M and the number n of replacement branches for each cut-point. The total number of moves $|N|$ generated in each iteration results as the product of these two parameters. A parameter for the maximal number of iterations is necessary to stop the algorithm. The size of the tabu list determines how long a manipulated point in the tree is protected against manipulations. The size of the solution is limited by two parameters for the maximal solution length and solution depth. Additionally, the two additional parameters limit the length and depth of the replacement branches in the pool and another parameter is necessary for the size p of the pool F .

5.2. Algorithm Description

1. Create an initial solution (tree) randomly.
2. Create a vector of p branches $F = (f_1, \dots, f_p)$ with a maximal length of f_{max_length} and a maximal depth of f_{max_depth} .
3. Evaluate all branches to create a vector of outputs $O = (o_1, \dots, o_p)$ for each of the p fragments.
4. Create a set of k cut-points $M = \{m_1, \dots, m_k\}$ randomly, where a manipulation point is a node (internal or external) of the solution candidate.
5. Initialize the set of moves $N = \{\}$.
6. If mode is semantic then continue at 7. else continue at 8.
7. For each manipulation point (semantic):
 - (a) Calculate the output out_m of the branch.
 - (b) Calculate the R^2 value of the output out_m of the branch and all outputs of the fragments O .
 - (c) Select n fragments with the highest R^2 value (< 1) and create n moves from the solution candidate replacing the branch at the manipulation point with each of the selected fragments and add the new moves to N .
 - (d) Goto 9.
8. For each manipulation point (random):
 - (a) Select n fragments from the pool F randomly and create n moves from the solution candidate replacing the branch at the manipulation point with each of the selected fragments and add the new moves to N .
9. Remove all moves from N which do not fulfill the aspiration criterion and would manipulate a node which is in the tabu-list. If all moves are tabu then keep one randomly chosen move.
10. Evaluate the fitness of all moves by temporarily applying each move and evaluating the accuracy of the resulting model.

11. Select the move that leads to the best accuracy (might be smaller than the accuracy of the current solution candidate).
12. Apply the move to the solution candidate to produce the current solution of the next iteration and add the manipulated point to the tabu-list.
13. Update the best-of-run solution if the current solution candidate has a better accuracy.
14. If the stopping criterion is true then stop and return the best-of-run solution, otherwise go to step 4.

In the move generation steps the maximal depth and length of the tree is restricted by generating only moves that produce trees smaller than the given limits. In semantic mode the most similar branches are selected, however, perfectly similar replacement branches ($R^2=1$) are not considered because such a move would have no effect on the output of the solution.

When a move is applied to the solution the existing branch is not simple replaced with the branch from the pool, but instead a swap operation is performed. The existing branch is added to the pool instead of the just inserted branch.

5.3. Tabu Criterion

Moves that would manipulate a node that has recently been replaced in another move are tabu. The length of the tabu list determines how long a manipulated node is locked. For comparing two moves we calculate the path to the manipulated node starting from the root node. This path can be represented as a list of integers where each element is the index of the sub-tree that leads to the manipulated node. For instance in Figure 2 the path [1,0] leads to the red node which is a new node that has been inserted in a previous move. The path must match exactly with the path of a previous move to make a move tabu, i.e. changing a sub-branch below a previously inserted branch is allowed.

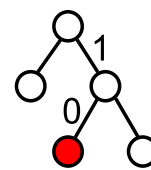


Figure 2: Example for a Path to a Manipulated Position in the Tree.

5.4. Aspiration

Several aspiration criteria are used to allow moves that would otherwise be tabu. The first aspiration criterion allows moves which would lead to a new best-of-run quality.

The second aspiration criterion is necessary to allow moves that manipulate a path that has recently been manipulated in an earlier move, when a more recent move replaced a larger branch containing the previously inserted branch. Figure 3 shows the solution

and the tabu manipulation points for three consecutive moves. First the single red node is replaced and the point is locked. In the second move the first move is undone because the whole right branch is replaced. As stated above only the manipulated point is set to tabu. The newly added nodes below the manipulation points can be changed immediately in consecutive moves. In particular the point replaced in the first move which is still in the tabu list can be manipulated again. This is accomplished through the aspiration criterion. In the third step the whole left branch is replaced. Now both, the direct left and right children of the root node are locked. All other nodes might be manipulated in consecutive moves.

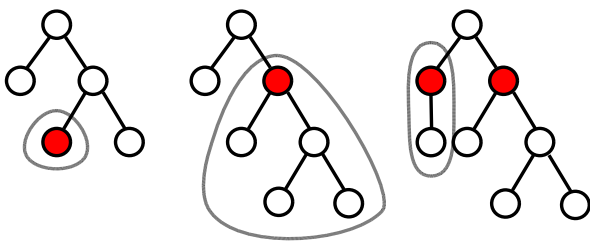


Figure 3: Aspiration Criterion for Moves That Are Undone with a Later Move.

The third aspiration criterion incorporates semantic information. The underlying idea is that moves should be aspired when the solution is changed in the same location, but in such a way that the solution is less similar to a previous solution than the current solution (i.e. semantically walking backwards). In particular, it is allowed to make moves that lead to a new solution when it is less similar to a previous solution than the current solution, even when the manipulation point would be tabu. Figure 4 shows the relevant similarities for two visited solutions (with branches A and B) and a potential new solution with a branch C , where A , B and C are all on the same location of the solution. First the semantic similarity of the two branches of the previous move ($R^2(A,B)$) is determined. If the semantic similarity of the original branch and the replacement branch of the current move ($R^2(A,C)$) is smaller than $R^2(A,B)$ the move is allowed. A move that would insert a branch C that is again more similar to the original branch A is not allowed.

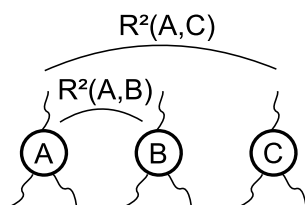


Figure 4: The semantic aspiration criterion allows tabu moves (C) if the result is less similar to the original (A) than the previously inserted branch (B).

5.5. Application of Moves

Because semantic similarity of branches is determined using the squared correlation coefficient which is invariant to changes in scale and location it is necessary to linearly scale a branch before inserting it into the solution. This has the negative effect that four additional tree nodes are necessary for each inserted branch (two constants and an addition and multiplication operator). Especially, the constant nodes are problematic because the correlation is zero for all possible replacements. This has the effect that constant nodes are replaced with a random branch from the pool which is then scaled in such a way to produce a constant output (multiplication with zero). In order to prevent such manipulations we check this special case and replace constant nodes only with unscaled branches. This is a rather uncomfortable workaround and should be addressed in a better way future work. An alternative would be to use the mean of squared errors as the metric for semantic similarity, but then the pool size should be much larger to increase the likelihood to find similar replacement branches.

Another important aspect of move application is that the replaced branch in the solution is added to the pool of replacement branches. This is necessary to prevent losing already well fitted branches because of a bad random manipulation. If the replaced branch is instead added to the pool, this branch can later be reused in a different, or even the same position in the solution.

5.6. Model Size Limits

Interestingly, without limiting the size of the model we also observed a steady growth of the model in initial experiments. This growth resulted from the fact that small fragments were replaced by on average larger fragments. Inserting a new branch instead of a terminal node leads to a set of new docking points which are definitely not in the tabu list and the algorithm can then easily find another move leading to a minor quality improvement replacing one of the newly introduced terminal nodes.

To prevent this growth of solutions we introduced limits for the maximal tree size and depth that are checked when generating possible moves.

6. DISCUSSION

A major issue in the configuration of the algorithm proved to be finding good parameter values for the number of cut-points and the number of replacement branch for each cut-point. If the number of cut-points is small then it is very likely that a move replaces a branch near the root of the solution which leads to a deleterious move that destroys the already well fitted solution frequently. On the other hand if the number of cut-points is large then it is very easy to find a move that has only a minor positive or negative effect on the solution fitness by replacing a node deep down in the tree with a similar node. This leads to the unwanted behavior where tabu search plateaus on a sub-optimal

solution without any significant changes until a deleterious manipulation occurs.

Initial experiments showed that the performance of the algorithm depends very strongly on the balance of these two parameter values; however, we have not yet executed experiments to determine good general parameters and instead rely on a reasonable default setting.

Another difficulty for the algorithm are constants in the solution and in the branches in the replacement pool. As constants have zero correlation with all possible outputs, the semantic similarity of all branches to constants is very low. This makes it necessary to handle constants specifically in the algorithm. In the experiments we have not allowed constants in the initial branches in the replacement pool; however, through the linear scaling of branches constants are automatically introduced into the solution over the run. We leave the analysis of the effects of constants and the development of a better way of handling constants for future work.

One advantage of trajectory-based algorithms is that changes to solutions can often be calculated incrementally. For symbolic regression solutions this is principally also possible because only the parents of the newly inserted branch have to be re-evaluated. The outputs of all other branches can be cached as they are not affected by the insertion of a new branch. This would also be possible for sub-tree crossover in genetic programming; however, because tabu search only uses a single solution at any time instead of a whole population, caching becomes feasible.

The calculation of semantic similarity leads to a rather large overhead as for each move the output of the original branch has to be compared to the output of all fragments in the pool and thus the asymptotic runtime complexity is $O(kp)$. Additionally, the calculation of the squared Pearson's correlation coefficient grows linearly with the number of observations.

7. EMPIRICAL EVALUATION

For the empirical evaluation of the proposed approach we used two sets of relatively easy benchmark instances defined by Keijzer and Nguyen as described in (McDermott et al., 2012). We compared three different algorithms: symbolic regression based on genetic programming and the proposed approach using semantic move generation and random move generation. The parameter settings for genetic programming and tabu search are shown in Table 1 and Table 2. Because the benchmark instances are relatively easy we used only a small number of iterations for tabu search and the number of evaluated solutions for GP was set in such a way to allow the at least the same number of evaluated solutions as for tabu search.

Table 1: Genetic Programming Parameter Settings

Parameter	Value
Population size	100
Offspring selection	Success ratio = 1 Comparison factor = 1

Parent selection	Gender-specific (random/proportional)
Max. evaluated solutions	50,000
Max. selection pressure	100
Tree creation	PTC2
Size limits	Length=80, Depth = 12
Function set	+,*,%, variables (no random constants)

Table 2: Tabu Search Parameter Settings

Parameter	Value
Iterations	1,000
Number of cut-points (k)	1
Number of fragments (n)	100
Size limits	Length=80, Depth = 12
Fragment size limits	Length=8, Depth=4
Pool size ($ F $)	1,000
Function set	+,*,%, variables (no random constants)

We executed ten independent repetitions for each algorithm configuration and benchmark instance.

8. RESULTS

The results of the empirical evaluation on the simple benchmark problems are shown in Table 3. It can be clearly seen that the genetic programming configuration works best for almost all instances and finds the solution for about half of the instances. There is no clear difference between tabu search with random move generation in comparison to tabu search with semantic move generation. In both tabu search configurations the semantic aspiration criterion has been used.

Table 3: Result Comparison

Instance	OSGP	TS random	TS semantic
Keijzer-1	0.9552	0.7141	0.7594
Keijzer-4	0.1612	0.0678	0.1183
Keijzer-5	1.0000	0.9931	0.9966
Keijzer-6	1.0000	0.4901	0.5911
Keijzer-7	0.9999	0.2867	0.1849
Keijzer-8	0.9732	0.9726	0.9789
Keijzer-10	0.9990	0.9768	0.9784
Keijzer-11	0.9787	0.9581	0.9435
Keijzer-12	0.9995	0.9692	0.9534
Keijzer-13	0.8976	0.7491	0.6763
Keijzer-14	0.9793	0.8000	0.8206
Keijzer-15	0.9771	0.9449	0.9397
Nguyen-1	1.0000	0.9879	0.9975
Nguyen-2	1.0000	0.9504	0.9929
Nguyen-3	1.0000	0.9903	0.9963
Nguyen-4	1.0000	0.9909	0.9925

Nguyen-5	1.0000	0.9726	0.9598
Nguyen-6	1.0000	0.9780	0.9522
Nguyen-7	1.0000	0.9863	0.9717
Nguyen-8	0.9999	0.9877	0.9602
Nguyen-9	0.9993	0.9961	0.9962
Nguyen-10	0.9998	0.9960	0.9962

9. DISCUSSION OF RESULTS

The result of the algorithm comparison is rather devastating and clearly indicates that the described approach for tabu search based symbolic regression is still rather immature, as it fails to find good solutions even for easy benchmark instances. Detailed analysis of the results for the Keijzer-6 and Keijzer-7 instances where TS performed a lot worse than GP showed that in these runs a scaling problem occurred. The algorithm found almost correct solutions, but they were at the bottom of a deep tree where the upper layers scaled and re-scaled the output multiple times. This has led to numeric instabilities which then reduced the accuracy of the solutions.

Generally the solutions generated by TS often contained deeply nested structures with many fragments introduced by the linear scaling of replacement branches. In particular, solutions often contained many constants. This issue should be analyzed in more detail in future work as constants are particular bad for the semantic move generation as mentioned above.

Another aspect that should be researched in more detail is the issue that replacing a branch near the root leads to a complete disruption of the solution while replacing branches deep down in the tree often have only a minor effect on the solution output. This is a direct consequence of the tree-based representation and makes design of useful move operators very difficult. Future work should consider different move operators than just simply replacing branches as discussed in this contribution.

Finally it could be helpful to add a form of diversification strategy for instance through long-term memory. In this paper we only used a tabu-list for short term memory to facilitate exploration of the fitness landscape in addition to the local improvement of the semantic move operator.

ACKNOWLEDGMENTS

The work described in this chapter was done within the Josef Ressel-Centre Heureka! for Heuristic Optimization sponsored by the Austrian Research Promotion Agency (FFG).

REFERENCES

Abdel-Rahman H., Emad Mabrouk, Masao Fukushima, 2011, Tabu Programming: a New Problem Solver through Adaptive Memory Programming over Tree Data Structures, *International Journal of Information Technology and Decision Making* 10(2):373 – 406.

Balicki, J., 2009, Some numerical experiments on multi-criterion tabu programming for finding Pareto-optimal solutions, *WSEAS Transactions on Systems* 8(1):241 – 250.

Balicki, J., 2007, Hierarchical Tabu Programming for Finding the Underwater Vehicle Trajectory, *International Journal of Computer Science and Network Security* 8(11):32 – 37.

Glover, F., Laguna, M., 1999, *Tabu Search*, Kluwer Academic Publishers.

Hastie, T., Tibshirani, R., Friedman, J., 2009, *The Elements of Statistical Learning*, Springer.

Krawiec, K., 2011, Learnable Embeddings of Program Spaces, *Proceedings of the 14th European Conference on Genetic Programming*, LNCS (6621) 166 – 177, Springer Verlag.

Krawiec, K., 2012, Medial Crossovers for Genetic Programming, *Proceedings of the 15th European Conference on Genetic Programming*, LNCS (7244) 61 – 72, Springer Verlag.

Koza, J., 1992, *Genetic Programming: On the Programming of Computers by Means of Natural Selection*, MIT Press

McConaghy, T., 2011, Fast, Scalable, Deterministic Symbolic Regression Technology, *Genetic Programming Theory and Practice IX*, Springer

McDermott, J., White, D.R., Luke, S., Manzoni, L., Castelli, M., Vanneschi, L., Jaskowski, W., Krawiec, K., Harper, R., De Jong, K., O'Reilly, U.-M., Genetic Programming Needs Better Benchmarks, *Proceedings of GECCO'2012*, July 7-11, 2012, Philadelphia, Pennsylvania, pp. 791 – 798, ACM.

Nguyen, Q.U., Nguyen, X.H., O'Neill, M., 2011, Examining the landscape of semantic similarity based mutation, *Proceedings of the 13th annual conference on genetic and evolutionary computation (GECCO'11)*, ACM, 12-16 July 2011, pp. 1363 – 1370.

Nguyen, Q.U., Nguyen, T.H., Nguyen, X.H., O'Neill, M., 2010, Improving the Generalisation Ability of Genetic Programming with Semantic Similarity based Crossover, *Proceedings of the 13th European Conference on Genetic Programming (EuroGP2010)*, LNCS (6021) 184 – 195, Springer

CUSTOMIZING CODE OF DEVS MODELS ACCORDING TO USER REQUIREMENTS USING LSIS_DME

M. HAMRI and R. MESSOUCI
LSIS UMR 7296- Aix-Marseille Université
Domaine universitaire de Saint Jérôme
Avenue Escadrille Normandie Niemen
13397 MARSEILLE Cedex 20
amine.hamri@lsis.org, rabah.messouci@lsis.org

Keywords: DEVS, design of atomic models, DEVS queuing system

Abstract

In this paper, we discuss two ways to code DEVS atomic models the first one is based on the switch-case statement in which no phase is described for the atomic model to simulate. The second one is based DEVS-phase design pattern in which we objectify phases and transitions. These ways of coding are integrated into the LSIS_DME tool to generate a complete compilable code of the DEVS-phase model and a partial code (template) that the user should complete in case of a DEVS atomic model without phases.

1. INTRODUCTION

In last decade, many DEVS tools have been developed to provide frameworks to model and simulate DEVS models. ADEVs (ADEVs, 2006), the oldest one, is a toolkit that suggests to the user to design DEVS models in object paradigm. DEVsJAVA (DEVsJAVA, 2012) provides a friendly-user framework to the user to make graphical DEVS coupled models and at his charge to design atomic models by coding them. Other frameworks avoid the user a coding step and propose to make both atomic and coupled models in graphical way. A process insures the transformation of graphical models into interpretable ones for the simulation process. By analyzing DEVS frameworks of the literature, we identify two categories:

- 1) DEVS frameworks in which the design of atomic models is let to the user. Often he should extend an abstract class or implement an interface to define the corresponding DEVS atomic model, and
- 2) DEVS frameworks in which a standard design of atomic models is defined to allow graphical or XML description. However, we remark that there is no framework allowing different designs of atomic models in unique one. In our approach, we propose to catch different designs of atomic models inside a unified framework and provide to the user the more adequate design to the current atomic model to code. The paper is organized as follows: Section 2 gives a recall

on DEVS concepts and discusses the current LSIS_DME approach. Section 3 proposes two ways of software designs to help the user in coding atomic models. Section 4 integrates the discussed designs in LSIS_DME to make variable the process of code automatic generation. An example of a queuing system is shown and discussed in Section 5. Finally, we conclude on the proposed and future works.

2. RECALLS

2.1. DEVS Formalisms

A DEVS model (Zeigler et al., 2000) consists of DEVS coupled and atomic models. An atomic model is structured as follows:

$Atomic = (X, Y, S, \delta_{int}, \delta_{ext}, D)$ where
 X, Y : sets of input and output ports respectively.
 S : set of state variables
 $\delta_{int} : S \rightarrow S$, the internal transition function. It defines the set of autonomous transitions.
 $\delta_{ext} : Q \times X \rightarrow S$ such $Q = \{(s, e) | s \in S, 0 \leq e \leq D(s)\}$, the external transition function. It defines according to the occurring event x and the elapsed time e on the current state s which transition to fire.
 $D : S \rightarrow \mathbb{R}^+$, for each state the function D defines the max duration in which the model still to fire an autonomous transition.

However, based on the encapsulation of atomic models, coupled ones are made. This construction is in respect with the following structure:

$Coupled = (X, Y, D, M_{d \in D}, IC, EIC, EOC, select)$
 X, Y : are sets of input and output ports respectively
 D : names of component and M_d : model of D component
 IC, EIC and EOC : sets of internal, external input and external output couplings respectively.
 $Select$: function priority between components.

2.2. LSIS_DME tool

LSIS_DME tool (Hamri and Zacharewich, 2007) is a full environment allowing DEVS and GDEVs modeling and simulation. The user defines DEVS and GDEVs in graphical way using a bottom-up approach. Firstly, he starts with modeling

atomic models, and then he stores them in his library who may share it with other users for further reuse. Secondly, he reuses these basic models (both atomic and coupled models) by drag and drop to build new coupled models. Also, these new models are stored in a library for further reuse again. The storage format of any DEVS, LSIS_DME distinguishes atomic models from coupled ones. Once, the user stores an atomic model, the tool transforms this graphical description into a Java code to express the pure DEVS (or GDEVS) behavior and a formatted file that contains structural and graphical data of the concerned model. Still the coupled model is transformed into a formatted structure according to definition of DEVS coupled formalism.

To summarize, we recall the LSIS_DME approach shown on figure below. Firstly, the user describes an atomic or coupled model by drag and drop necessary elements (state, transition or basic model). Then, he checks the current model using DEVS-Compiler to avoid logical errors (determinism, ambiguity, completeness and port coupling) before launching simulation. Once, the user saves its model he can start simulation. Then an output simulation report is given to the user to analyze the corresponding behavior.

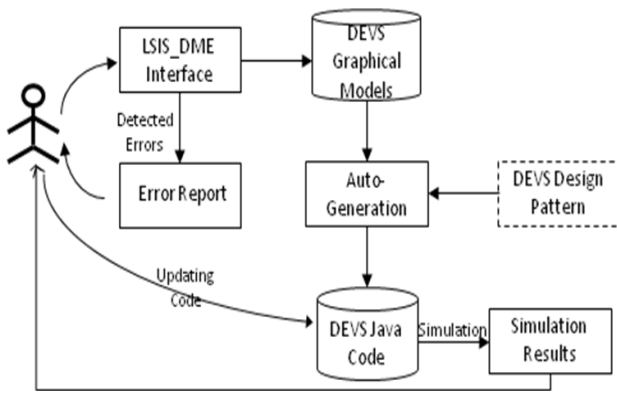


Figure 1. LSIS_DME approach

LSIS_DME allows modeling only DEVS-phase atomic models i.e. DEVS models in which the behavior is specified using phases (Praehofer and Pree, 1993). Sometimes, the user may use an infinite state machine to describe a DEVS atomic model, due to the fact he employs state variables with infinite domain. However (Honig and Seck, 2012) propose an approach based on DEVS-phase modeling called PhiDEVS. So we can imagine that any DEVS or GDEVS atomic model could be reduced to a DEVS-phase model. In addition, almost DEVS models seen in the literature are phase-based models and at least they are based on two phases: active and passive (Zeigler et al., 2000). Consequently, the DEVS-phase design stills valid to implement any DEVS models, by adopting specific design for LSIS_DME simulator. However to get an architecture to take into account different designs of atomic

models, we update the communication between the simulation process and model to simulate.

In the next section, we discuss how LSIS_DME user may choose between a DEVS-phase design and an ad-hoc design based on the switch-case statement.

3. A SOFTWARE DESIGN APPROACH TO MODEL AND SIMULATE DEVS ATOMIC COMPONENT

The abstract simulator of DEVS consists of a process that manages messages to send out or to receive from an atomic model. At design level, (Zeigler et al., 2000) define an interface to make interaction between the simulator and the atomic model to simulate. In fact, this is a contract between the user who will design the atomic model and should implement this interface. Next, the simulator acts on the model to simulate through the implemented methods to create DEVS behaviors. This strategy is employed in DEVJSJAVA.

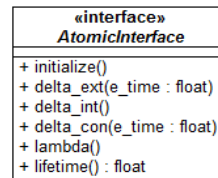


Figure 2. DEVS interface of atomic models

In LSIS_DME, we reuse this advanced design to make a structured communication between each atomic model to simulate and the simulator. In fact using such an interface, we give to the user a great freedom to design its atomic models and we guaranty interoperability between them. However two constraints are necessary to correctly build atomic models: i) the atomic model should hold a reference on the current state of the model; and ii) the DEVS atomic model should implement all methods of DEVS interface. In the following, we discuss two possible designs of DEVS atomic models.

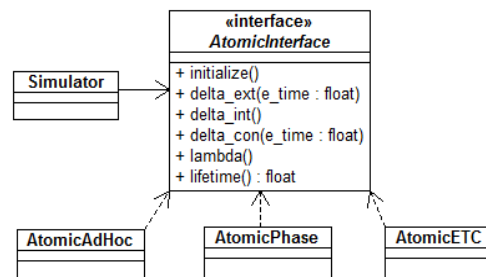


Figure 3. Communication between LSIS_DME simulator and different designs of atomic models

This architecture that distinguishes the interface of the model

to simulate from the model itself provides the possibility to integrate atomic models with new designs.

3.1. Ad-hoc design of DEVS atomic models

The ad-hoc design of DEVS atomic models consists on implementing the DEVS interface to define a DEVS component. The user may define infinite or enumerated state variables. Then based on these variables, the user defines the evolution of the model from a state to another through the methods `delta_ext()` and `delta_int()`. This design is useful to implement models like DEVS SISO models in which only an input and an output ports, both expressed with real (Zeigler and Sargoughian, 2005).

```

public void initialize(){
    phase = "passive";
    sigma = INFINITY;
    store = 0;
    response_time = 10;
    super.initialize();
}
public void Deltext(double e,double input){
    Continue(e);
    if (phaseIs("passive")){
        if (input != 0) // 0 is query
            store = input;
        else holdIn("respond", response_time);
    }
}
public void deltint( ){
    passivate();
}
public double Out( ){
    if (phaseIs("respond")) return store;
    else return 0;
}
}

```

Figure 4. DEVS behavior of a ramp

However, designing complex behavior of atomic models with different phases and ports, still difficult due to the fact the user will employ the switch-case or if-else statement to implement such a behavior. In this case, the code is less structured, less readable and hard to maintain. In fact, once the user makes changes on the model, he should reflect them on the code. Unfortunately, this will take much time due to inflexibility of such a code.

3.2. DEVS-Phase pattern to design atomic models

To remind to the ad-hoc design of atomic models, we propose the DEVS-phase design pattern. In this pattern we objectify phases and transitions to make the code of atomic models object-oriented. We recall briefly this design pattern according to the following structure:

Name: DEVS-Phase design pattern

Context: this pattern is useful to design DEVS behaviors expressed with phases to obtain a corresponding object-oriented code.

Solution: the AtomicPhase class holds a reference on the current phase of the model. It also holds the input and output ports vectors and concrete phase and transition classes inside vectors. This class has the responsibility to make

state changes according to the received event via the method `delta_ext()` or `delta_int()`. It identifies the concrete `ExtTransition` or `IntTransition` object to fire. These transition classes hold a reference on their future phase and the simulator will act the state change by updating the current phase reference.

In addition, this pattern encapsulates through transition classes the following methods:

- i) `action()`: this abstract method computes the new values of state variables outside the phase variable, and
- ii) `performOutput()`: this abstract method identify the output and computes the output event to send out of the internal transition to fire.
- iii) `guard()`: a Boolean method that decides whether or not the transition may be fired.

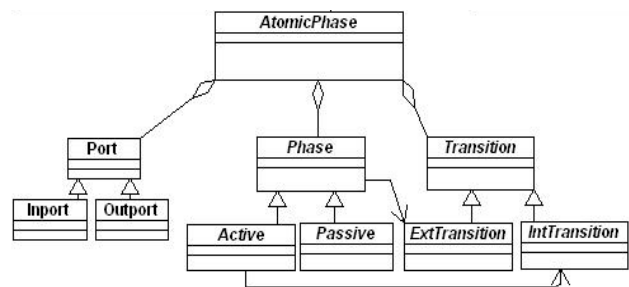


Figure 5. Class diagram of the DEVS-phase pattern

- Advantages: +) well-structured code
 +) easy code to maintain
 +) flexible structure to add new DEVS behaviors at run-time (adding new phases and transitions, or modifying the target of a transition, etc.).

- Lacks: -) skills on object programming are necessary to manipulate directly the code of this design pattern.
 -) no mechanism to check if the updated model at run-time stills correct.

4. CODE AUTOMATIC GENERATION FROM DEVS ATOMIC MODELS

The field of code automatic generation is promoted by Model Driven Architecture. It consists on transforming a model expressed with some language into a different language or a programming language. The benefits of such an approach are: i) avoiding coding errors and speeding-up the implementation process; and ii) providing a direct mapping from the atomic models to designed ones.

The DEVS standardization group recognizes that automatic code generation is in progress for DEVS field and should be more developed to get significant advances. In fact the current works are focused on transforming DEVS atomic and coupled models written in Java and C++ into DEVS XML files (and vice-versa) through the DEVXML language. The main advantage of this language is to allow interoperability

between various models.

Obviously, we integrate code automatic generation in LSIS_DME approach by proposing to the user to choose which kind of generated code is useful for him. According to the atomic model type (SISO or phase-based model) the user may customize the generated code through the tool.

4.1. Partial code automatic generation from Ad-hoc models

Such models are not phase-based models. Consequently, the DEVS-phase pattern is not applied. However we make only automatic the generation of the model interface; that means the port sets and domain of each port in addition to the DEVS methods are generated automatically. Then the user completes the body of each DEVS method to implement the expected behavior and to define the set of state variables.

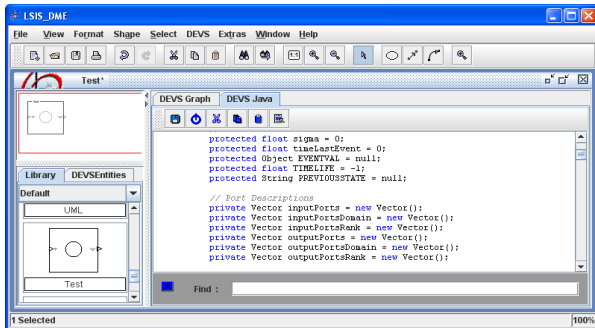


Figure 6. DEVS template of an atomic model generated from LSIS_DME tool

Unfortunately, the consistence of the code is not insured and the user should take care to avoid undesired scenarios.

4.2. Code automatic generation from DEVS-phase based models

Once a DEVS-phase based model description is established by the user, the tool generates a Java code from the graphical. The code is object-oriented and its architecture is designed according to the DEVS-phase pattern.

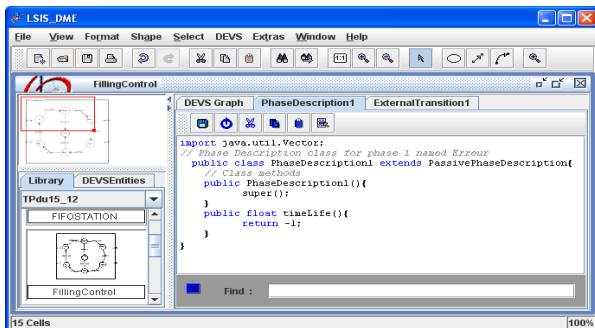


Figure 7. A phase class generated with LSIS_DME

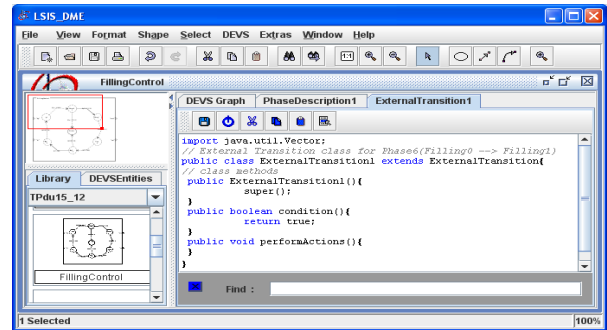


Figure 8. An external transition class generated with LSIS_DME

The generated code is open to hand-modification. The user may introduce pieces of code that are not supported by the graphical description due to grammar syntax limitation of LSIS_DME.

5. QUEUING SYSTEM

5.1. Example

Let us consider a queuing system consisting of one queue and one resource. Jobs arrive at any time, they are served according to their arrival date i.e. first in queue first out. To note that jobs arrive with a Poisson distribution ($\lambda = 1$). In addition, jobs occupy the resource for some units of time (u.t). The inter-departures from the resource are exponentially distributed ($\mu = 2$). With this analytical model, we compute mathematically some indicators like average waiting time using the following equation:

$$\text{Average waiting time} = (\mu - \lambda) / \mu(\mu - \lambda) = 0.5 \text{ u.t}$$

The simulation that we propose to simulate such a system is well-known in the literature of DEVS. Three DEVS components are necessary: Generator, Queue and Resource.

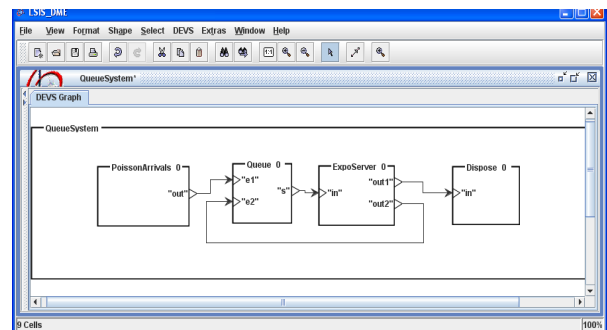


Figure 9. DEVS coupled model of queuing system

The generator, as the name indicates, generates jobs with a Poisson distribution. In addition it computes the number of generated jobs. Each job remains in the queue until the resource is released. The queue model consists of two phases "active" and "passive". In passive phase, the length of the

queue is zero (there is no job waiting) and the resource is free. Once a new job arrives, it is immediately sent out to the resource and the queue model changes phase from passive to active. To note that the generator is a DEVS ad-hoc design, the other models Queue, Resource and Dispose follow a DEVS-phase design.

5.2. Simulation results

The table 1 shows simulation results of the model of the queuing system example.

Based on the table 1, the average waiting time (AWT) is compared to that provided by the model M/M/1. This comparison shows that the waiting time of the simulation result converges to the result of mathematical one when simulation duration (the replication length) increases. So we can suppose that the model is valid.

Table 1. Simulation results

Replication	Average Waiting Time (u.t)		
	Simulation duration (u.t)		
	10 ⁴	10 ⁵	10 ⁶
1	0,7210	0,7205	0,5572
2	0,7211	0,7204	0,5572
3	0,7213	0,7206	0,5572
4	0,7214	0,7206	0,5573
5	0,7215	0,7207	0,5573
6	0,7215	0,7211	0,5573
7	0,7220	0,7211	0,5573
8	0,7217	0,7211	0,5573
9	0,7216	0,7213	0,5575
10	0,7216	0,7215	0,5579
Average waiting time of replications (u.t)	0,7215	0,7209	0,5573

Complex scenarios may be defined through the simulation model of queuing system like the resource fails, customizing the service time of jobs, etc. for which it is difficult to define a mathematical model.

6. CONCLUSION

This paper proposes different forms of DEVS atomic designs. The most used one consists on using a DEVS behavior using the switch-case statement. However, this design suffers from the following lacks: the corresponding code is difficult to read and not well-structured. In addition it is difficult (in some cases impossible) to make further modifications or extensions. From that, we propose an alternative way to design atomic models based on DEVS-phase pattern. These two designs are integrated into a unique framework that supports new designs of atomic models. Consequently DEVS models implemented differently are simulated by the same simulator.

In the near future, we will develop experimental studies to compare the proposed designs and to show which one may be useful according to the user requirements. In other works, we will define software metrics to evaluate indicators like time execution, heap memory size, etc. to help user to choose which design is more suitable to implement his atomic models.

7. REFERENCES

- ADEVs, 2006 software site: <http://sourceforge.net/projects/adevs>. Last accessed March 2012.
- DEVsJAVA, 2012. ACIMS software site: <http://www.acims.arizona.edu/SOFTWARE/software.html> Last accessed March 2012.
- Hamri, M. and G. Zacharewicz. 2007 LSIS-DME: An environment for modeling and simulation of DEVS specifications. in: AIS-CMS International modeling and simulation multicongress, Buenos Aires - Argentina, February 8-10 2007, pp. 55-60, ISBN 978-2-9520712-6-0. Honig and M. Seck, 2012. PHI-DEVs: Phase Based Discrete Event Modeling. Symposium on Theory of Modeling Simulation - DEVS Integrative MS Symposium (DEVs). SpringSimâ12, Florida-USA March 26-29 2012.
- Praehofer H. and D. Pree Visual Modeling Modeling of DEVS-based Multi-Formalism Systems based on Higraphs Proceedings of the 1993 Winter G. W. Evans, M. Mollaghasemi, Simulation Conference pp 595 â 603.
- Zeigler, B., H. Praehofer and T. G. Kim. 2000. Theory of modeling and simulation. Second edition Academic Press.
- Zeigler B and H. Sarjoughian, 2005. Introduction to DEVS Modeling and Simulation with JAVA: Developing Component-Based Simulation Models. <http://www.acims.arizona.edu/PUBLICATIONS/publications.shtml>. Last accessed March 2012.

SIMULATION OF HYDROCARBON SALES SERVICES OF THE NATIONAL UNIVERSITY OF MEXICO FOR THE SCENARIO ANALISYS THAT IMPROVE RETURN ON EQUITY

Israel Andrade Canales ^(a), Citlalli Dorantes Bolaños ^(b)

^(a) National University of Mexico

^(b) National University of Mexico

^(a) iandradec@unam.mx, ^(b) buris_100@comunidad.unam.mx

ABSTRACT

The National University of Mexico (UNAM) has different types of services that support the daily activities of campus, such as pre-hospital service, transport, commercial services, security, sports, cultural activities, etc. Some of these services provide sufficient funds to the University, in particular, the sale of hydrocarbons, which is not restricted to the university vehicle fleet but also offered to individuals, has a significant potential return on equity. Therefore, we examined the operation of this service to determine whether it is fully exploited. As a result of this analysis, we showed that gains not differ much from the costs because not all resources are utilized.

This paper shows a case study which analyzes the sale hydrocarbon service, using simulation techniques, to find plausible scenarios that would improve the economic benefit, by leveraging the space and resources available without investing in infrastructure.

Keywords: simulation, scenarios, servers, returns on equity, leaking profits.

1. INTRODUCTION

The system is simulated in the present work is the gas station located between University Avenue and one of the main entrances to University (Figure 1). It is owned by the UNAM, and according to the General Direction of General Services (DGSG) in 2004 attended around 774,000 users, recording a sale of 15' 465,000 liters of fuel. It has annual income about 117 million Mexican pesos (approximately 9 MM\$), and approximate cost of 112 million Mexican pesos (8.6 MM\$), accounting for a net gain of 5 million (0.4 MM\$).

There are 3 turns: morning (11 dispatchers), Evening (10 dispatchers) and Special (7 dispatchers). Its organizational structure is as follows:

1. Responsible of the gas station
2. Manager
3. Supervisor
4. Dispatchers



Figure 1: System's satellital photo

2. CONSIDERATIONS

We consider some characteristics of the gas station obtained through observation of their behavior, among which are the following.

The station has 10 fully operable fuel pumps, which can only be accessed by University Avenue. Because of this, it is common to first fill the pumps closest to the main street and cars rarely go to the furthest. This is due to lack of personnel to properly distribute the formation of drivers.

Another feature of the system is that, for the location and size of the gas station, at most may have 3 cars in line, which occurs in the first bombs of service. This causes the saturation of the first bombs and drivers decide to continue their way.

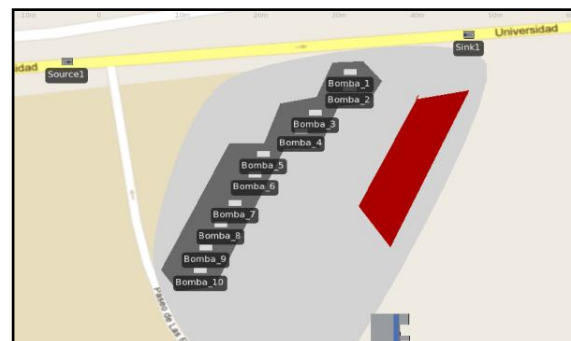


Figure 2: Model's aerial photo

3. PROBLEMATIC

The station has an infrastructure which generates costs such as maintenance and the costs of personnel working. On the other hand, we have observed that the times in which the gas station has increased demand, and thus has the major earnings, are: from 8:00 to 9:00 and from 15:00 to 16:00.

During these times the 10 pumps are available, so there are 10 dispatchers working, however, the furthest servers are idle because there is not an allocation policy and then, the demand in these pumps is not high, creating the idle staff. This causes unnecessary personnel costs. Therefore, we want to understand the behavior of the system with a smaller number of available servers from 15:00 to 16:00 hours.

4. OBJECTIVE

We want to make a simulation study for hydrocarbon sales in a gas station between the hours of 3:00 pm to 4:00 pm in order to understand the functioning of the system and thus raise some scenarios for decision making regarding the number of servers. The simulation study allows us to know some indicators such as:

- Vehicles served.
- Vehicles unattended.
- Average time of service.
- Average time in the system.
- Actual capacity of the system.
- Policies to improve performance.

Some questions we want answered are:

- Is it possible to improve the system? Under which circumstances?
- Does the system performance is adequate?

4.1. Specific Objectives

Simulate the behavior of the real system through different scenarios, then analyze the system to propose an allocation policy and compare this results. Finally estimate the full capacity of the system in the proposed schedule. The gap of the real system and the full capacity scenario would indicate what would be the return on equity or the loss of gains.

5. METHODOLOGY

Discrete-event simulation modeling is an accepted method for predicting the performance of complex systems like hydrocarbon sale services.

However, we have to follow an adequate methodology to gain useful understanding of the likely performance of the real system and then predict the system's behavior in some scenarios. This is where the design of simulation experiments plays an important role (Barton 2010).

In this paper, these experiments allow us to calculate the probably return equity can be gained. Next diagram shows the methodology followed for the simulation of the system.

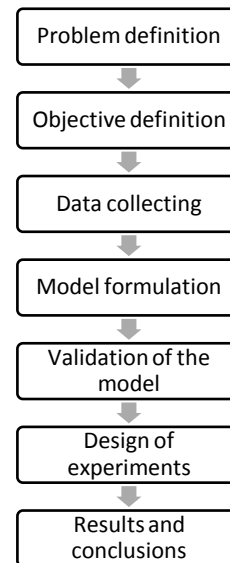


Figure 3: Methodology

6. SIMULATION

Following the methodology described above we break down each phase.

6.1. Data Collecting

It was necessary to identify the following variables in order to build the model, taking into account ten servers:

- Arrival time of vehicles.
- Service time.
- Queues
- Leisure time.

Table 1: Data collected

Data from one server chosen at random	
Nº. vehicles	24
Arrival time (<i>minutes</i>)	2.45
Service time (<i>minutes</i>)	1.92
Queues	0.1
Leisure time (<i>minutes</i>)	0.5

We note that in the last three pumps (located at the bottom of the gas station), leisure time dispatchers was up to 15 minutes on average. The data collected, taking into account the 10 pumps are summarized in Table 2.

Table 2: Data collected

Data from 10 servers	
Nº. vehicles	203
Arrival time (<i>minutes</i>)	16
Service time (<i>minutes</i>)	1.92
Queues	2.3
Leisure time (<i>minutes</i>)	10

This sample data help us to identify our simulation input model using to accept or reject each of the distribution families in a list of well-known alternatives.

We used EasyFit® Software to fit a distribution function to data collected, obtaining the following distributions:

1. For the arrival time of vehicles, we obtained an exponential distribution (Figure 4) with parameter:

$$\lambda = 16 \text{ seconds}$$

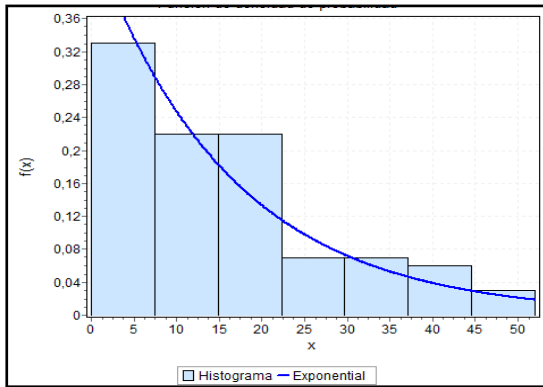


Figure 4: Distribution for arrival time of vehicles

2. For the service time, we obtained an uniform distribution (Figure 4) with parameters:

$$a = 0.94, b = 2.90 \text{ minutes}$$

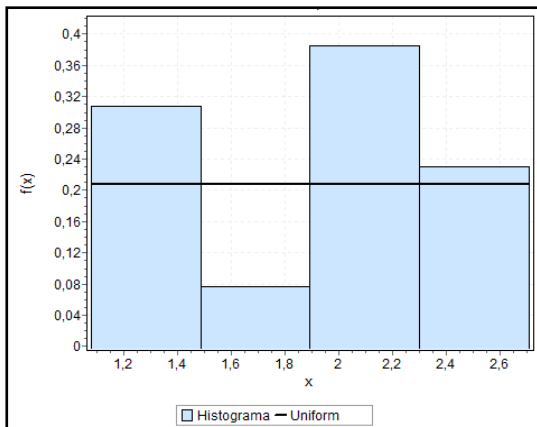


Figure 5: Distribution for the service time

6.2. Model formulation

Using previous distributions we determinate the number of distinct model settings to be run, and the specific values of each one. These include:

- Scenario I: This model is the common scenario in which the system operates.
- Scenario II: This model represents the real capacity of the system and it operates with an allocation policy. We have called it: "Ideal System".
- Scenario III: In this model, we incorporate changes in the input process because we are

not only interested in getting a good model for an input process, but also in seeing how the system will react to changes in that input (Biller 2002). For this scenario we change the parameters of the distribution for know the full capacity of the real system.

After this, we used Simio Simulation Software® to build the three different scenarios.

6.3. Scenario I

From 3:00 pm to 4:00 pm the gas station has available 10 bombs (servers), however the last two usually are empty, so we built a scenario with 8 pumps available to verify that the model behaves as close to reality.

We consider that the first 6 pumps can generate queues of at most 3 cars, because if it exceed this number is blocked University Avenue.

For the two remaining bombs, the queues can be of at most 2 cars, as the queues that are generated in the first 6 bombs do not allow larger queues on the servers 7 and 8 (the last 2 bombs).

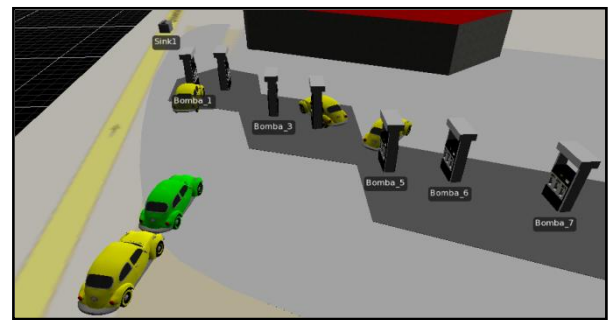


Figure 6: Simulation of Scenario I: 8 servers, the closest to reality

Table 3: Results Simulation of Scenario I

Simulation of System with 8 bombs working	
N°. vehicles generated by the source	217
N°. vehicles that were attended	161
N°. vehicles that were not attended	56
% vehicles that were not attended	25.8%

6.4. Scenario II

We built a second scenario taking into account 10 servers (Figure 7) and we created an "Ideal System", it means, the 10 servers operating according to the parameters that resulted from the data samples, as shown in the table below.

Table 4: Ideal System Parameters

Servers	Queues (max.)	Distributions	
Bombs 1 to 6	3 vehicles	Service time: Uniform	Arrival time: Exponential
Bombs 7 to 10	2 vehicles		

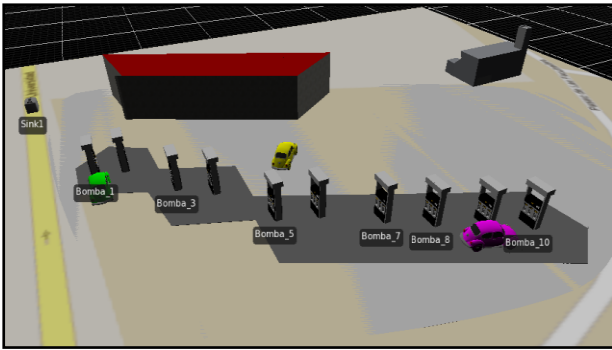


Figure 7: Simulation of Scenario II: "Ideal System"

The next table shows the results for this scenario.

Table 5: Results Simulation of Scenario II

Simulation of System with 10 bombs working	
N°. vehicles generated by the source	202
N°. vehicles that were attended	185
N°. vehicles that were not attended	17
% vehicles that were not attended	8.4%

6.5. Scenario III

In the third scenario (Figure 8), we consider that the 10 pumps are available and they can generate queues (equal that in Scenario II). The difference in this case is the reduction in the time of vehicle arrival.

This decrease was considered by the following:

1. In Scenario II we consider the distributions fitted to the data collected, but those times are more suited to Scenario I, where only 8 servers are available.
2. In this case we consider that there are 10 bombs and they can generate queues, it means, we are considering 2 servers more and therefore the ability of the system under this scenario is greater than in the real system.
3. This reduction is also justified by the fact that it does not affect significantly the waiting time of drivers and does not exceed the limit of the queue, plus the demand exists because University Avenue is very busy at that time.

We suggest an exponential distribution for the arrival time of vehicles with parameter:

$$\lambda = 12 \text{ sec.}$$

It means, a 4 seconds reduction in arrival time, since in this case the vehicles can be distributed in two servers more.

Table 6: Results Simulation of Scenario III

Simulation with 10 servers and a reduction in arrival time	
N°. vehicles generated by the source	255
N°. vehicles that were attended	219
N°. vehicles that were not attended	36
% vehicles that were not attended	14.1%



Figure 8: Simulation of Scenario III: 10 servers considering an arrival time reduction

7. VALIDATION OF THE MODEL

The simulation was validated with a group of data not used in the modeling process. We found that the gap between model and reality is not significant (Table 7), so the data model is closer to reality.

Table 7: Difference between the simulation and the system's data

Validation information	Simulation	Data collected
Average time in the server (<i>minutes</i>)	1.88	1.92
Average number of cars served per server	21	24
System's average time (<i>minutes</i>)	3.7	3

8. RESULTS

After we execute the simulation, we compared the results of the three scenarios. In the Table 8 are shown the results and the graphs below show the comparison of the three scenarios.

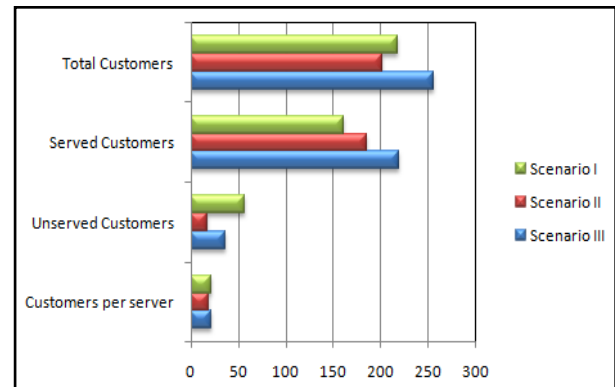


Figure 9: Comparative of three scenarios

Table 8: Results of the three scenarios

Scenarios			
Scenario	I	II	III
No. of servers	8	10	10
Distribution arrival time Parameters	Exponential		
	$\lambda=16$	$\lambda=16$	$\lambda=12$
Time in server	1.8 min.	1.9 min.	1.9 min.
Customers per server	21	19	22
Average time in system	3.7	4	4.2
Total Customers	217	202	255
Served customers	161	185	219
Unserved customers %	56 25.8%	17 8.4%	36 14.1%

We note that if the 10 pumps worked, the number of clients served would be 58 more than the current system, increasing the time in the system only 0.5 minutes, which is acceptable for a client.

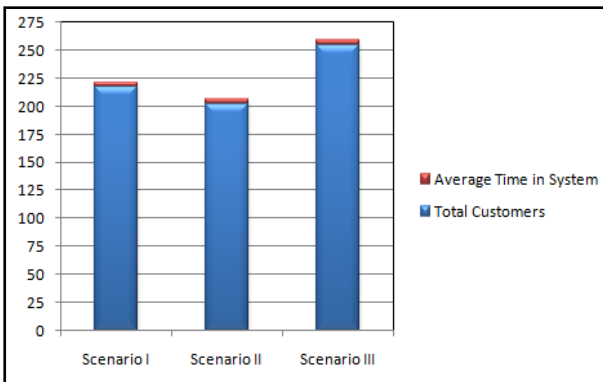


Figure 10: Relation between the customers and their average time in system

8.1. Quantitative Analysis

The gap between scenario I and scenario II indicates that the gas station's service has a loss of 24 customers approximately in the analysis schedule because they have not an allocation policy. Assuming that each car consumes an average of \$100 MXN (it means 7.5 USD, approximately) the University is leaking profits of \$12,000 MXN (923 USD) weekly and \$624,000 MXN (48,000 USD) per year.

By other hand, the gap between scenario I and scenario III indicates that hydrocarbon sales service is not using its full capacity at all because of logistical problems. We estimate that the loss of customers is approximately 58 cars on the busiest schedule. Assuming that each car consumes an average of \$100 MXN the University is leaking profits of \$34,800 MXN

(2,677 USD) weekly and \$1'792,200 MXN (137,862 USD) per year. Table 9 shows these calculations.

Table 9: Quantitative Analysis

Return on equity	
Period	USD
A day	\$580
A week	\$3,480
Per year	\$179,220

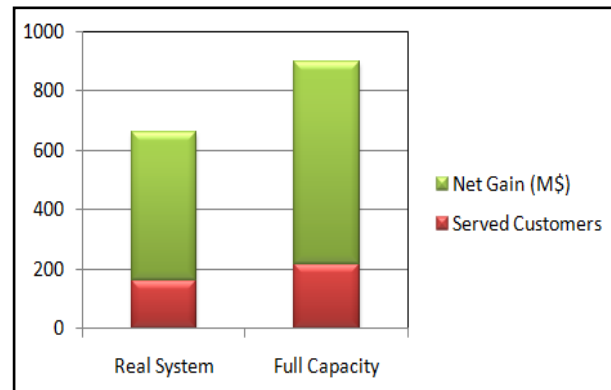


Figure 11: Despite having a small increase in the number of clients served, net earnings are significantly affected

This estimate considers only the days and hours of greatest demand (working days) and does not consider operating expenses. However, it is important to estimate and improve the return on equity.

It is important to note that the accuracy of the estimate is based on the accuracy of the modeling input. If it were necessary a more accurate figure would be necessary to expand the collection of data and use a more robust model and input (Michael 2008).

9. CONCLUSIONS

In this paper, we use Simulation for analyze the performance of the hydrocarbon sales service of the National University of Mexico; we have also could predict what would be the return on equity of the service in its full capacity. However, it should be noted that to make proper use of this tool in a case similar to that proposed in this paper, is necessary to have knowledge of both Statistic as Probability to build a correct input model, as well as an study of the system's behavior to obtain results closer to reality and improve decision-making.

We further consider that the simulation can be used in many services for improve their efficiency within the University such as: medical services, infrastructure and transport.

Thus, we used this tool to analyze and predict the service behavior and estimate information for decision-making with favorable results.

ACKNOWLEDGMENTS

The authors would like to thank to Dra. Idalia Flores for support this research and “Dirección General de Servicios Generales, UNAM” for making available the data.

REFERENCES

- Barton, R.R. 2010. Simulation experiment design. In Proceedings of the *2010 Winter Simulation Conference*, ed. B. Johansson, S. Jain, J. Montoya-Torres, J. Huan, and E. Yücesan: 75-86.
- Billar, B., 2002. Answer to the top ten input modelling questions, Proceedings of the *2002 Winter Simulation Conference*, volume 1: 35 – 40.
- Law, A.M., Kelton W.D., 2000. *Simulation modeling and analysis*. New York: McGraw-Hill.
- Michael E.K., Emily K.L., Natalie M.S., Mary W., James R.W., 2008. Introduction to modeling and generating probabilistic input processes for simulation. *Proceedings of the 40th Conference on Winter Simulation*, December: 07-10.

AUTHORS BIOGRAPHY

Citlalli Dorantes studied Actuary at the Faculty of Sciences of the UNAM. She worked 1 year at BBVA-Bancomer in risk department and 1 year at Banco Azteca in the Information and statistical analysis department. She is currently studying a Master in Operations Research, her line of research is optimization in the transport services.

Israel Andrade studied Computer Engineering at the Facultad de Estudios Superiores Aragón of the UNAM. He worked 3 year at National University’s Computer Emergency Response Team (UNAM-CERT) in risk analysis area. He is currently studying a Master in Operations Research, his line of research is optimization in information security.

DESIGNING PID CONTROLLER FOR 4TH ORDER SYSTEM BY MEANS OF ENHANCED PSO ALGORITHM WITH DISCRETE CHAOTIC DISSIPATIVE STANDARD MAP

¹Michal Pluhacek, ¹Roman Senkerik, ²Donald Davendra, ¹Ivan Zelinka

¹Tomas Bata University in Zlin, Faculty of Applied Informatics
Nam T.G. Masaryka 5555, 760 01 Zlin, Czech Republic
{pluhacek,senkerik,zelinka}@fai.utb.cz

²Department of Computer Science, Faculty of Electrical Engineering and Computer Science
VB-TUO, 17.listopadu 15, 708 33 Ostrava-Poruba, Czech Republic

ABSTRACT

The main aim of this paper is the utilization of discrete chaotic Dissipative standard map based chaos number generator to enhance the performance of PSO algorithm. This paper presents application of proposed algorithm to design PID controller for 4th order system. Results of this application are compared with previously published results in the area of evolutionary PID controller design.

Keywords: PID controller, Optimization, Evolutionary Algorithms, PSO algorithm, Chaos, Dissipative standard map.

1. INTRODUCTION

In the past decades PID controllers became a fundamental part of many automatic systems. The successful design of PID controller was mostly based on deterministic methods involving complex mathematics. Recently (Nagraj et al., 2008) soft-computing methods were used with great results for solving the complex task of PID controller design.

Evolutionary algorithms are important part of soft-computing methods and one of them is particle swarm optimization algorithm (PSO). As proposed in (Davendra et al. 2010) using chaos number generator may improve the performance of an evolutionary algorithm for the task of PID controller design. This paper presents using of Dissipative standard map as a discrete chaotic system for the chaotic number generator and implementation of this chaotic generator into PSO algorithm. This enhanced PSO algorithm is applied on the PID controller design problem for 4th order system.

2. PARTICLE SWARM OPTIMIZATION ALGORITHM

PSO (Particle swarm optimization algorithm) is the evolutionary optimization algorithm based on the natural behavior of bird and fish swarms and was introduced by Eberhart and Kennedy in 1995 (Kennedy, Eberhart 1995, Eberhart, Kennedy 2001) as an alternative to genetic algorithms (Goldberg, David, 1989) and differential evolution (Storn, Price, 1997). Term “swarm intelligence” (Eberhart, Kennedy, 2001) refers to the capability of particle swarms to exhibit surprising

intelligent behavior assuming that some form of communication (even very primitive) can occur among the swarm particles (individuals).

In each generation, a new location of a particle is calculated based on its previous location and velocity (or “velocity vector”). One of PSO algorithm disadvantages is the rapid acceleration of particles which causes them to abandon the defined area of interest. For this reason, several modifications of PSO were introduced to handle with this problem. Within this research, chaos driven PSO strategy with inertia weight was used. Default values of all PSO parameters were chosen according to the recommendations given in (Kennedy, Eberhart 1995, Eberhart, Kennedy 2001). Inertia weight is designed to influence the velocity of each particle differently over the time (Nickabadi et al., 2011). In the beginning of the optimization process, the influence of inertia weight factor w is minimal. As the optimization continues, the value of w is decreasing, thus the velocity of each particle is decreasing, since w is the number < 1 and it multiplies previous velocity of particle in the process of new velocity value calculation. Inertia weight modification PSO strategy has two control parameters w_{start} and w_{ends} . New w for each generation is then given by Eq. 1, where i stand for current generation number and n for total number of generations.

$$w = w_{start} - \frac{((w_{start} - w_{end}) * i)}{n} \quad (1)$$

Chaos driven random number generator is used in the main PSO formula (Eq. 2) that determines new “velocity”, thus the position of each particle in next generation (or migration cycle).

$$v(t+1) = v(t) + c_1 \cdot Rand \cdot (pBest - x(t)) + c_2 \cdot Rand \cdot (gBest - x(t)) \quad (2)$$

Where:

$v(t+1)$ – New velocity of particle.
 $v(t)$ – Current velocity of particle.
 c_1, c_2 – Priority factors.
 $pBest$ – Best solution found by particle.
 $gBest$ – Best solution found in population.
 $x(t)$ – Current position of particle.

Rand – Random number, interval $<0, 1>$. Within Chaos PSO algorithm, the basic inbuilt computer (simulation software) random generator is replaced with chaotic generator (in this case, by using of Dissipative standard map).

New position of particle is then given by Eq. 3, where $x(t+1)$ is the new position:

$$x(t+1) = x(t) + v(t+1) \quad (3)$$

3. DISSIPATIVE STANDARD MAP

The Dissipative Standard map is a two-dimensional chaotic map. The parameters used in this work are $b = 0.1$ and $k = 8.8$ as suggested in (Spratt 2003). The Dissipative standard map is given in Fig. 1. The map equations are given in Eq. 4 and 5.

$$X_{n+1} = X_n + Y_{n+1} \pmod{2\pi} \quad (4)$$

$$Y_{n+1} = bY_n + k \sin X_n \pmod{2\pi} \quad (5)$$

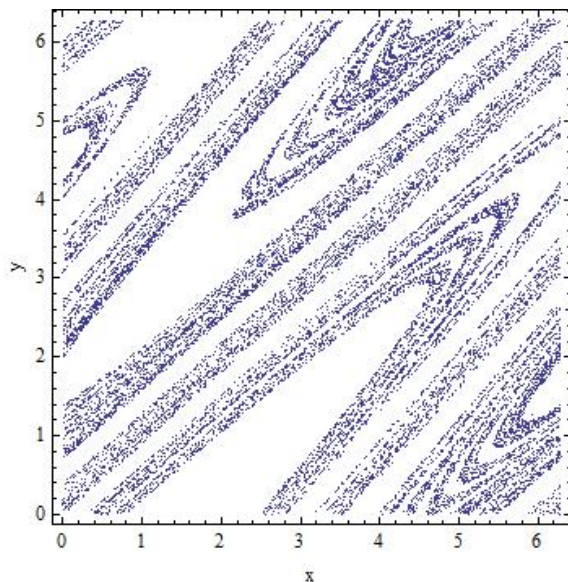


Fig. 1. Dissipative standard map

4. PROBLEM DESIGN

This section contains the description of the PID controller, used model of 4th order system as well as the description cost functions (CF).

4.1. PID Controller and 4th order system

The PID controller contains three unique parts; proportional, integral and derivative controller (Astrom 2002). A simplified form in Laplace domain is given in Eq. 6.

$$G(s) = K \left(1 + \frac{1}{sT_i} + sT_d \right) \quad (6)$$

The PID form most suitable for analytical calculations is given in Eq. 7.

$$G(s) = k_p + \frac{k_i}{s} + k_d s \quad (7)$$

The parameters are related to the standard form through: $k_p = K$, $k_i = K/T_i$ and $k_d = KT_d$. Estimation of the combination of these three parameters that gives the lowest value of the four test criterions was the objective of this research.

The transfer function of used 4th order system is given by Eq. 8 (Davendra et. al. 2010)

$$G(s) = \frac{1}{s^4 + 6s^3 + 11s^2 + 6s} \quad (8)$$

4.2. Cost function

Test criterion measures properties of output transfer function and can indicate quality of regulation. Following four different integral criterions were used for comparison purposes: IAE (Integral Absolute Error), ITAE (Integral Time Absolute Error), ISE (Integral Square Error) and MSE (Mean Square Error). (Nagraj et al., 2008, Davendra et al., 2010).

These test criterions (given by Eq. 9–12) were minimized within the cost functions for the enhanced PSO algorithm.

1. Integral of Time multiplied by Absolute Error (ITAE)

$$I_{ITAE} = \int_0^T t |e(t)| dt \quad (9)$$

2. Integral of Absolute Magnitude of the Error (IAE)

$$I_{IAE} = \int_0^T |e(t)| dt \quad (10)$$

3. Integral of the Square of the Error (ISE)

$$I_{ISE} = \int_0^T e^2(t) dt \quad (11)$$

4. Mean of the Square of the Error (MSE)

$$I_{MSE} = \frac{1}{n} \sum_{i=1}^n (e(t))^2 \quad (12)$$

5. RESULTS

All experiments were focused on the optimization of the four different specification functions as given in previous section. The best results of the optimization with corresponding values of k_p , k_i and k_d together with selected response profile parameters are presented in Table 1.

When tuning a PID controller, generally the aim is to match some preconceived ‘ideal’ response profile for the

closed loop system. The following response profiles are typical (Landau, 2006):

Overshoot: this is the magnitude by which the controlled ‘variable swings’ past the setpoint. 5 - 10% overshoot is normally acceptable for most loops.

Rise time: the time it takes for the process output to achieve the new desired value. One- third the dominant process time constant would be typical.

Settling time: the time it takes for the process output to die between, say +/- 5% of setpoint.

From the statistical reasons, optimization for each criterion was repeated 30 times. The best results in all tables are highlighted by bold number. Results of the simple statistical comparison for the optimizations by means of chaos driven PSO algorithm are given in tables 2 and 3.

Optimized system responses are depicted in Figures 2a - 2d and compared in Figures 3 and 4.

Table 1: The best results for 4th order system

Criterion	CF	Kp	Ki	Kd	Overshoot	Rise Time	Settling time
IAE	12.347900	6.008590	0.007254	11.752400	0.153488	0.016000	0.048100
ITAE	15.533400	5.385930	0.000256	7.902410	0.102804	0.020500	0.034400
ISE	6.405160	5.194300	0.155542	20.815600	0.257472	0.011600	0.064300
MSE	0.032026	5.214940	0.156873	20.840000	0.258542	0.011600	0.064300

Table 2: Average steady state responses for 4th order system

Criterion	Avg. overshoot	Avg. rise time	Avg. settling time
IAE	0.158410	0.015680	0.047500
ITAE	0.133150	0.018297	0.046077
ISE	0.257114	0.011603	0.064340
MSE	0.257894	0.011570	0.064293

Table 3: Statistical overview of the criterions (CF) values for 4th order system

Criterion	Max CF	Min CF	Avg. CF	Median	Std. dev.
IAE	12.614000	12.347900	12.418417	12.395900	0.072049
ITAE	21.534500	15.533400	17.626730	17.401250	1.594303
ISE	6.408370	6.405160	6.405957	6.405765	0.000841
MSE	0.032060	0.032026	0.032032	0.032029	0.000008

Results for PID controller design obtained by chaos driven PSO algorithm are compared in Table 4 with previously published result of evolutionary algorithms

SOMA and DE with chaos implementation (Davendra et al., 2010) and non-heuristic Ziegler-Nichols method.

Table 4: Comparison of other methods and proposed enhanced PSO

Criterion	Z-N	DE Chaos	SOMA Chaos	PSO Chaos
IAE	34.941300	12.330500	12.330500	12.347900
ITAE	137.565000	15.384600	15.384600	15.533400
ISE	17.842600	6.410260	6.410260	6.405160
MSE	0.089213	0.032027	0.032027	0.032026

From the presented results in Table 4, it follows that proposed enhanced PSO was surpassed by other two compared heuristic methods for the two test criterions and for other two it has given better results. Non-heuristic Ziegler-Nichols methods was outperformed in all four cases by all three compared evolutionary algorithms.

System responses are compared in Figure 3. Detailed view on the beginning of simulation interval is depicted in Figure 4. As can be seen from these two Figures, the optimization based on the different criterions led to significantly different system responses; nevertheless the all designed PID controllers were able to quickly and precisely stabilize the system.

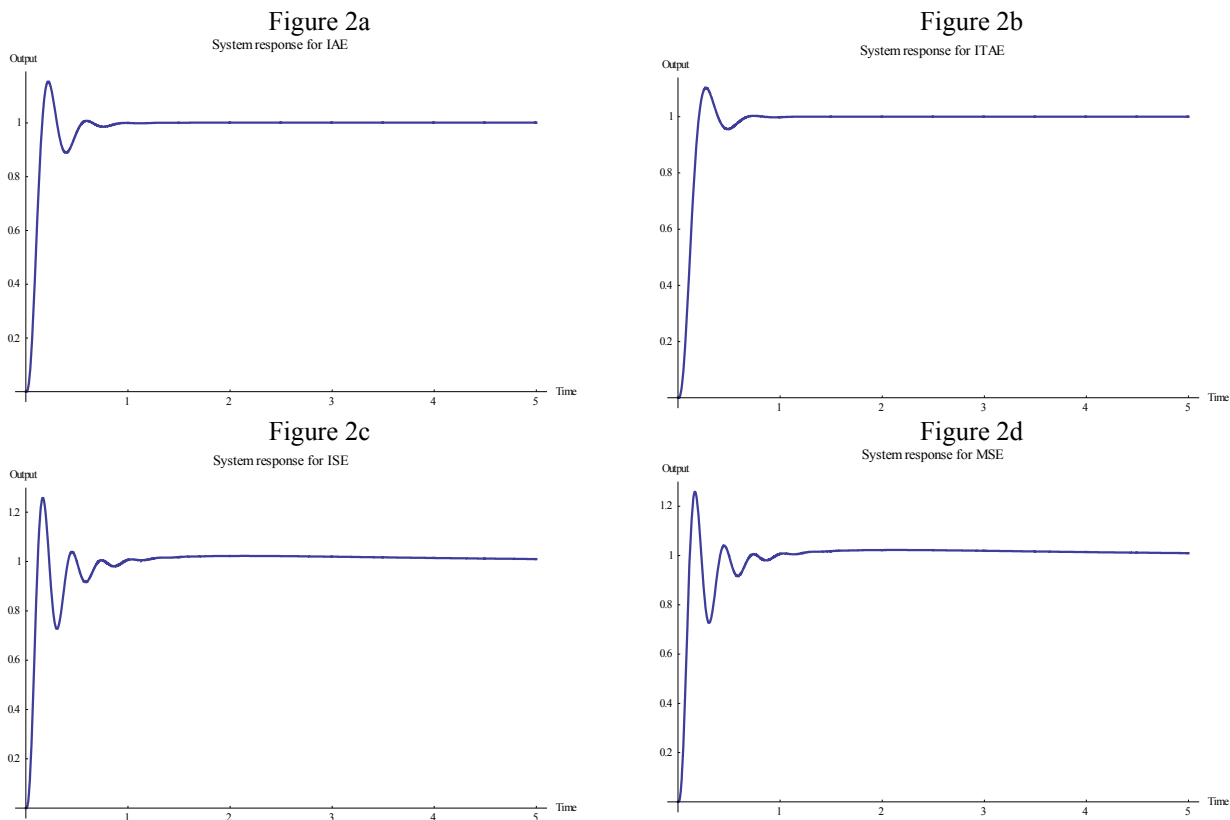


Figure 2: Optimized system responses for K_p , K_i and K_d obtained by four integral criterions.

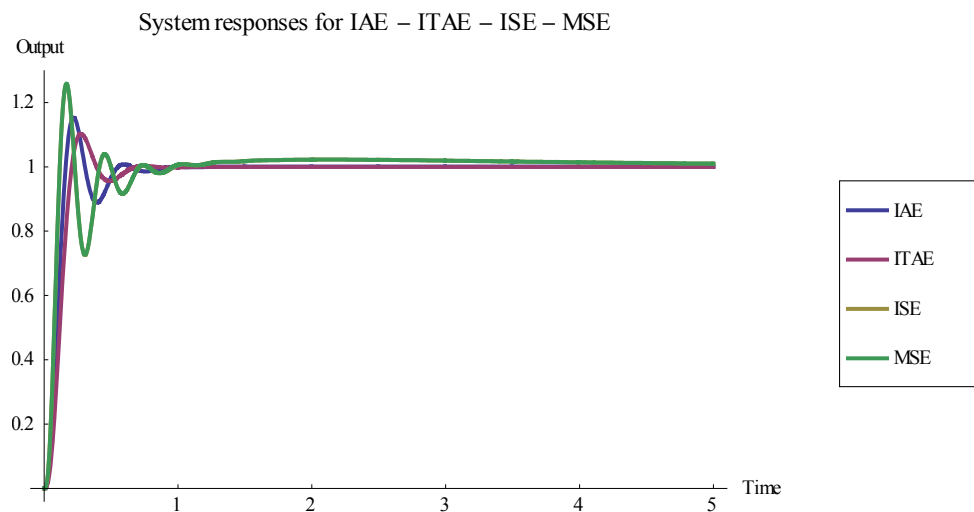


Figure 3: Comparison of optimized system responses for K_p , K_i and K_d obtained by four integral criterions.

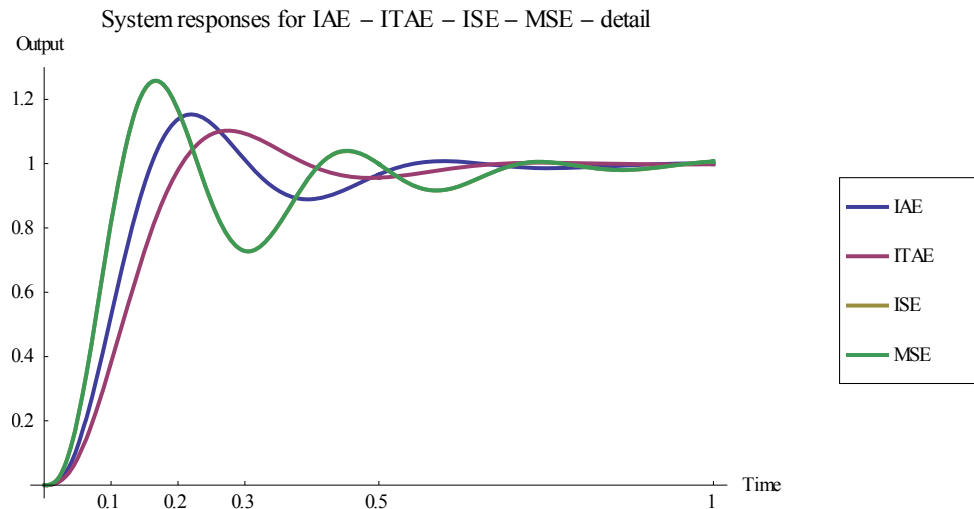


Figure 4: Detailed view on the optimized system responses for K_p , K_i and K_d obtained by four integral criterions.

CONCLUSION

This research was focused on the utilization of chaos driven PSO with discrete chaotic Dissipative standard map in the case of estimation of the PID controller optimal settings for 4th order system.

Presented data and graphical simulation outputs lend weight to the argument that implementation of chaotic Dissipative standard map as a random number generator into PSO algorithm may lead to satisfactory performance in the case of solving the problem of optimal PID controller design for 4th order system.

Future research will be aimed to the possibilities of the development and improvement of the enhanced chaos driven PSO algorithm to achieve better results and explore more possible applications for this promising optimization approach.

ACKNOWLEDGEMENT

This work was supported by European Regional Development Fund under the project CEBIA-Tech No. CZ.1.05/2.1.00/03.0089, and by Internal Grant Agency of Tomas Bata University under the project No. IGA/FAI/2012/037.

REFERENCES

Astrom K., "Control System Design". Santa Barbra, California: University of California, 2002
 Davendra D., Zelinka I., Senkerik R., "Chaos driven evolutionary algorithms for the task of PID control", *Computers & Mathematics with Applications*, Volume 60, Issue 4, 2010, pp 1088-1104, ISSN 0898-1221.

Dorigo, M., *Ant Colony Optimization and Swarm Intelligence*, Springer, 2006.
 Eberhart, R., Kennedy, J., *Swarm Intelligence*, The Morgan Kaufmann Series in Artificial Intelligence, Morgan Kaufmann, 2001.
 Goldberg, David E. (1989). *Genetic Algorithms in Search Optimization and Machine Learning*. Addison Wesley. p. 41. ISBN 0201157675.
 Kennedy, J.; Eberhart, R. (1995). "Particle Swarm Optimization". *Proceedings of IEEE International Conference on Neural Networks*. IV. pp. 1942–1948
 Landau Y., "Digital Control Systems". Springer, London, 2006
 Nagraj B., Subha S., and Rampriya B., "Tuning algorithms for pid controller using soft computing techniques", *International Journal of Computer Science and Network Security*, 2008. 8, pp.278-281.3
 Nickabadi A., Mohammad Mehdi Ebadzadeh, Reza Safabakhsh, A novel particle swarm optimization algorithm with adaptive inertia weight, *Applied Soft Computing*, Volume 11, Issue 4, June 2011, Pages 3658-3670, ISSN 1568-4946
 Sprott J. C., "Chaos and Time-Series Analysis", Oxford University Press, 2003
 Storn R., Price K., Differential evolution—a simple and efficient heuristic for global optimization over continuous spaces, *Journal of Global Optimization* 11 (1997) 341–359.

AUTHOR BIOGRAPHIES

MICHAL PLUHACEK was born in the Czech Republic, and went to the Tomas Bata University in Zlin, where he studied Information Technologies and obtained his MSc degree in 2011. He is now a doctoral student at the same university. His email address is: pluhacek@fai.utb.cz



ROMAN SENKERIK was born in the Czech Republic, and went to the Tomas Bata University in Zlin, where he studied Technical Cybernetics and obtained his MSc degree in 2004 and Ph.D. degree in Technical Cybernetics in 2008. He is now a lecturer at the same university (Applied Informatics, Cryptology, Artificial Intelligence, Mathematical Informatics). His email address is: senkerik@fai.utb.cz



IVAN ZELINKA was born in the Czech Republic, and went to the Technical University of Brno, where he studied Technical Cybernetics and obtained his degree in 1995. He obtained Ph.D. degree in Technical Cybernetics in 2001 at Tomas Bata University in Zlin. Now he is a professor (Artificial Intelligence, Theory of Information). Email address: ivan.zelinka@vsb.cz.



OPERATIONS BY FORKLIFTS IN WAREHOUSES

Aurelija Burinskiene

Vilnius Gediminas technical university

aurelija.burinskiene@vgtu.lt

ABSTRACT

Nowadays the great attention has to be paid to logistics. Theoretical analysis shows the need to improve logistics system. This encourages the search for solutions during warehouse operations. Aiming to determine possible improvements, the operations of forklifts are examined in warehouses.

The study consists of two parts: in the first part of the study possible improvements are analysed, in the second part - the financial evaluation of suggested improvements are presented.

The application of simulation method is presented in the first part of the study, the use of the comparative and financial analysis methods - in the second part of the study.

Simulation results were compared with the results of companies, applying such solutions. This showed labor productivity increased from 27% to 37%. Continuing the investigation, the assessment of financial value is presented. The solution describing how to improve logistics system, gives time savings around 12.5% and cost savings around 9%.

The presented results resemble to the results reached in practise.

Keywords: routing, warehouse, simulation, forklifts, savings

1. INTRODUCTION

Warehousing is becoming critical activity in trade enterprises to outperform competitors on productivity, lead time and customers' service. So, short lead times and productivity are considered in many warehouses as competitive weapon. It becomes more and more difficult to realize short customers' orders throughput times because of factors such as increase in assortment and smaller, not frequent, orders. For the increasing assortment an increasing floor space is needed. This means in increased lead times per order. Smaller orders (less units per line) and higher frequency of ordering lead to some changes: less full pallets are picked and more single item picks are necessary. Also additional activities have to be performed within the short time frame available for handling the customers' orders.

For such activities forklifts are the most important and expensive machines. Requirements for forklifts and costs are crucial for the selection of such operations.

Basically, forklifts are used for moving pallets inside warehouses. The movement of a pallet from point A to point B is not critical itself, but if the wrong pallet is moved or if the right pallet is put in the wrong place, an error will occur.

During the process, driver have to know where to go, how much to pick and where to place it. The construction of least-costs forklift routes can help to increase productivity.

Forklifts are used in environments and applications that require different performance characteristics than other equipments.

Forklifts retrieve products from specified storage locations on the basis of customer orders. The infrastructure needed for a firm to incorporate and handle all movements of forklifts has to be in place.

Forklifts are the most expensive machines due to investments into equipment and other assets, which are used to support their operations.

This shows the importance of such research. In addition, the analysis of scientific literature, which is published by Oxford University Press, Cambridge University Press, Harvard University Press, Springer, M.E. Sharpe, Routledge, etc. shows that only 1% of authors, which analyze logistics issues, give attention to forklifts. The authors that analyze the operations of forklifts mention that minimization of non-productive movements and the construction of less-costly routes can help to increase productivity.

In the paper author analyzes the application of forklifts in trading companies, business cases, the assessment of technology implementation by production companies, their attitudes and interests.

The target of the paper is to determine possible logistics systems improvements in forklifts operations.

To answer to the above mentioned question, study is presented in the paper.

The study is divided into two parts. At the beginning literature review is given, later on experimental study is presented. The literature review is short summary of the application of forklifts in trading companies, business cases, the assessment of technology implementation by production companies, their attitudes and interests. The first part of experimental study is dedicated for the identification of forklift and construction of least-costs forklift routes. The second part of experimental study is dedicated for

the effect related to minimization of costs identification and time savings calculation.

The study is based on simulation, comparative and financial analysis methods.

2. THE SCOPE OF FORKLIFTS APPLICATION IN WAREHOUSES

When purchasing forklift, the purchaser must know, if it can meet handling needs of company. This is where productivity comes in. Speed limits are applicable and they have huge impacts. Usually manufacturers of forklifts can design governors on forklifts that only allow reaching the certain speed (Ryan and Ryan 2006). The speed limit in different warehouses is 10km/h.

A forklift is a powerful tool when used by well trained driver (or operator). It helps to move pallets (or other materials) by eliminating the need to lift and carry boxes by hands.

Forklifts can be classified by different methods including type of power source, driver position, and load engagement method. Electric motors powered by batteries are among the most common type of forklifts seen in industry (Ryan and Ryan 2006). Different manufacturers may offer different models of forklifts. Selection of forklift is often a several-step decision process. First characteristic is volume of material flow - the large volume will require buying the number of forklifts with similar characteristics. Second characteristic is the frequency and scheduling of movements - this relates to the time between movements. Usually, movements are performed due to different batches or continuous. Third characteristic is route factor - this includes distance, conditions along the route, the path of travel (Kasilinga 1998).

In addition, author Kasilinga (1998) mentions important forklift selection factors: purchasing price, operating costs, maintenance costs. The regulation require that a forklift be checked every day that the forklift is used. If forklift is used continuously, then it must be checked at the end of each shift.

Forklift operations require the floor space as well. Traditional wide-aisle pallet storage aisles must have corridors 3.3-3.6 m for forklifts operations. It is necessary to have also barriers that protect walls and racks against forklift damages.

The place of depot in front of aisles or between the two blocks is planned in Caron, Marchet, and Perego (1998) study. This is the position where forklift driver takes task and after which returns back for another one.

Various assignment policies may be used simultaneously within the area of warehouse. Consider, for example, picking and storage areas. The used assignment policy does not have to be permanent and could be switched to another one when conditions are changed. Dedicated storage policy can be used for fast moving products and random storage policy for slow moving items (Hassan 2002).

The number of locations available in storage area usually is smaller than the total number of pallets arriving to warehouse on daily basis. This means that

first, pallets from storage places have to be removed to picking places and after this, new pallets can be placed to storage area. At the end this means increased throughput time per order.

According to De Koster, Roodbergen, and Voorden (1999), the travel time in a warehouse, in general, has a significant impact on throughput time.

The time, needed for forklifts operations can be split in travel time (travelling time), pick and place time, and remaining time. The travel time is required for the movement between locations that have to be visited (where the items are stored that have to be moved). The pick time is associated with stop, finding and picking right pallet. This includes search for the pallet, grabbing it, scanning it and storage location, reading the next location to be visited. Place time is related to the dropping of the pallet to pick location and scanning it. The remaining time is related to time needed to close the task and get next assignment, etc.

2.1. Time savings algorithms

50% of the total travel time spent on unproductive traveling (Dukic and Oluic 2007). Saving algorithms are based on the algorithm of Clarke and Wright (1964) for the vehicle routing problem: a saving on travel distance is obtained by combining a set of small tours into a smaller set of larger tours.

Time savings algorithms are based on the time savings that can be obtained if different tasks are combined instead of being executed separately. For combined tasks the time saving is calculated. Instructions for the next route are given via a computer terminal (De Koster, Le-Duc, and Roodbergen 2006). For reaching next assignment, radio data terminal is used by forklift driver. The forklift driver follows a route designated by reading instructions on a radio data terminal or following commands.

Each route is formed containing many tasks. This process is repeated until all tasks during day have been assigned to a route.

In the calculation of the time savings, a routing algorithm may be used. This may be one of mentioned heuristics: S-shape, Combined, Largest gap, return, mid-point, etc. or optimal (De Koster, Le-Duc, and Roodbergen 2006). Usually optimal method outperforms S-shape method by 7-33 % in single-block random storage warehouses (De Koster and Van der Poort 1998). Several types of the above mentioned algorithms are discussed in De Koster, Roodbergen, and Voorden (1999).

All articles discussed so far assume that the aisles of the warehouse are narrow enough allowing to retrieve pallets from both sides of the aisle without changing position. In Goetschalckx and Ratliff (1988) a polynomial-time optimal algorithm is developed that solves the problem of routing order pickers in wide aisles.

In practice, usually simple routing heuristics are used. No standard warehouse management system package consists that contains the Ratliff and Rosenthal

algorithm. Methods that are used include the 'Largest-gap' return strategy, 'Mid-point' return strategy, 'S-shape' strategy. In the application of 'S-shape' algorithm, a distinction has to be made between single-side and double-side picking (De Koster, Roodbergen, and Voorden 1999).

In many labor-intensive warehouses, there is the constant pressure to reduce travelling time. One of such is Bijenkorf warehouse - warehouse of retail trade organization in Holland with the product assortment of 300 thousand stock-keeping units. Authors De Koster, Roodbergen, and Voorden (1999) have made the case study analysis. The delivered results are as follows: the reduction of total travel time means the reduction in the number of labor units.

Another problem with routing may arise if products are stored at multiple locations in a warehouse (De Koster, Le-Duc, and Roodbergen). In this case a choice by warehouse management system has to be made before directing the forklift to location from which the pallet has to be retrieved.

The travel time is an increasing function of the travel distance (study, for example, Jarvis and McDowell 1991; Roodbergen and De Koster 2001; Petersen and Aase 2004). Consequently, the travel distance is often considered for planning warehouse. Two types of travel distance are widely used in appropriate literature: the average travel distance of tour (or average tour length) and the total travel distance. For a given tasks list (a set of tasks), however, minimizing the average tour length is equivalent to minimizing the total travel distance.

Clearly, the minimization of average travel distance (or, equivalently, total travel distance) is limited for forklift operations. Usually, it is only one of many possibilities. Another important objective would be minimizing the total cost (De Koster, Le-Duc, and Roodbergen 2006) (that may include both investment in to forklifts and related infrastructure and operational costs).

In addition tracking system maybe used that will connected forklifts to the mobile device for the provision of routing information (Giaglis, Minis, Tatarakis, and Zeimpekis 2004).

Eastern Service Company - freight forwarding and logistics service provider in Hong Kong and South China. The company specializes in managing warehouses and providing other cargo logistics services. This company aims to achieve these major service goals to their customers: shorten the lead time; and maintain a higher visibility on the supply chain area. To ensure accuracy scanning is applied to check the right correctness of movement (Cathy, Lam, Choy, and Chung 2011).

3. EXPERIMENTAL STUDY

The objective of experimental study is to calculate how the identification of forklift will help for the construction of least-costs forklift routes; and what will be the effect related to minimization of costs.

The first part of experimental study is dedicated for the identification of forklift and construction of least-costs forklift routes. The second part of experimental study is dedicated for the effect related to minimization of costs identification and time savings calculation.

For the first part of experimental study the Interactive warehouse simulation model is used.

The Interactive Erasmus Logistica Warehouse Website model offers opportunities to discover more ways to perform tasks (Oudijk, Roodbergen, De Koster, and Mekern 2002) in the Microsoft Internet Explorer environment. There are different possibilities to compare different scenarios which depend from the number of aisles and cross-aisles, length of aisles, position of computer station in warehouse. The only limitation of the model is that the maximum number of locations per aisle is limited to 68.

The Interactive warehouse simulation model will be used for optimizing the way of forklift that is done between two transaction points. Each time forklift gets a task, an event (or task) row is recorded in the information system. An event row can include the starting and ending time of task, thus enabling its duration to be calculated. Each consecutive pair of transaction points represents costs of activity (Varila, Seppanen, and Suomala 2007).

The forklift driver starts route at computer station (Oudijk, Roodbergen, De Koster, and Mekern 2002), goes to the front of the particular aisle; drives inside aisle, takes pallet, delivers it to pick location at the same or other aisle in shortest way, and, finally, returns back to the computer station. For calculation of forklift travel distance the optimal route was used mainly (see Figure 1). Each pick and place point is served by only one forklift. In addition, the capacity of forklift is limited. It is possible to handle one pallet on its forks at the same time.

Three assumptions are used for experimental study. The first one is dedicated to optimal routing by assuming that order pickers do not create routes on their own. The next one is dedicated to the wide of the aisle. This means that the aisle has the least floor space where the forklift can pick pallets from both sides of an aisle without covering an additional distance. The third one is dedicated to path and time relationship by assuming that the linear relationship between forklift travel time and distance exists. For the calculation of traveling time the average speed 10 km/h is used (assuming that forklift is travelling in warehouse with the same speed).

This simulation model was used to perform pick and place tests, when:

1. Reserve (pick) and pick (place) locations were in different aisles (see the left side of the picture);
2. Reserve and pick locations were in the front of aisle;
3. Reserve and pick locations were in the end of aisle;
4. The above mentioned is combined (see the middle of the picture).

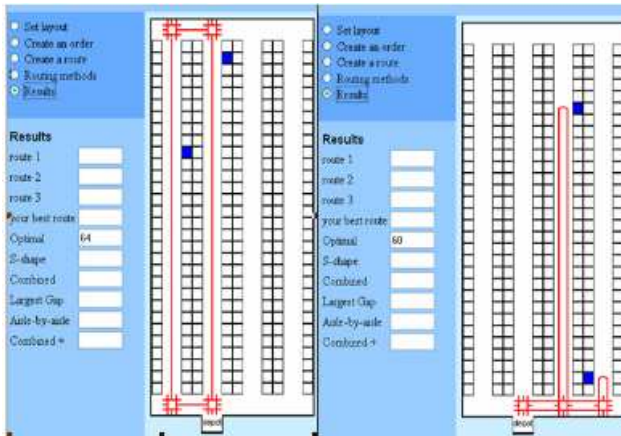


Figure 1: Interactive warehouse simulation model and different tests. Source: Oudijk, Roodbergen, De Koster, and Mekern (2002)

If forklift works according paper-based task list, at first forklift driver moves to depot (where all task lists are placed), then moves to storage location to pick pallet (according task list), takes pallet, delivers it to pick location, and, finally, returns back to the depot to confirm completeness of task and gets assignment for new task. The trip to depot takes some minutes.

If forklift has RF terminal, then new task list is placed on the screen (no need to drive to depot). In such case the driver of forklift has to be equipped with radio control device, such as RF terminal, which is located on the forklift. The terminal of forklift can have real-time communication with warehouse management system. And the portable computer can be used to map out the most efficient route. Operations performed by forklifts with RF terminal require a discrete signal that will ensure only that the desired pallet is identified. RF terminal is used to send messages (SME's) for the driver. The monitor on the forklift typically provides instructions associated with the given task. When the task is finished the driver gives confirmation to warehouse management system over local area wireless (WI-FI) network (see Figure 2, when several or multiple tasks are completed without return to depot).

By running simulation tests with interactive warehouse simulation model it was seen that the best travel distance is when RF-terminal is implemented. This means that the tasks are distributed to forklifts via SME's and forklift drivers don't need to go to depot to give confirmation and get new assignments. In such case, the way decreases by 27-37 % when travelling without depot is implemented and tasks are distributed to forklift drivers on-line.

Talking about costs, these results present the cases with and without RF-terminals. As there are several choices for warehouses - task lists distributed to forklift drivers at depot (computer station) or via SME's.

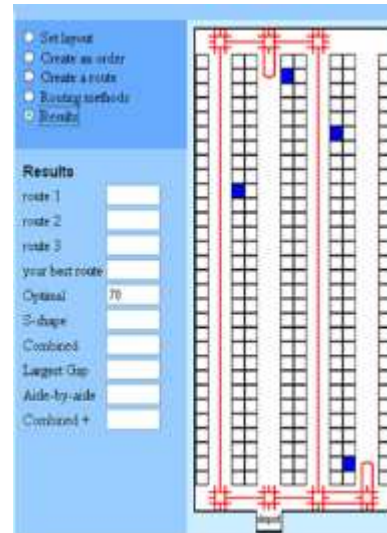


Figure 2: One return to depot for two tasks. Source: Oudijk, Roodbergen, De Koster, and Mekern (2002)

In addition, authors Gray, Karmarkar, and Seidmann (1992) propose to analyse savings in accordance with the components of warehouse operations. The time, needed for forklifts operations, can be split in travel time (travelling time), pick and place time, and remaining time:

- The travel time is required for the movement between locations that have to be visited,
- The pick time is associated with the number of stops, finding and picking right pallet,
- Place time is related to the dropping of the pallet to the right location,
- The remaining time is related to time needed to close the task and get next assignment at computer station.

After each above mentioned component is studied:

- Travel time component. Gray, Karmarkar, and Seidmann (1992) propose to calculate 1,5 minutes per performed task. On average during a day he spends an hour and a half for travelling in order to take a pallet and to place a pallet into new location. Comparing results of two scenarios (Figure 1 and Figure 2) it is seen that the total travel distance of forklift can be reduced by 27-37 %;
- Pick time component. Gray, Karmarkar, and Seidmann (1992) propose to calculate 1 minute per pallet taken from the old place (0.5 minute of this is needed for finding the right pallet and scanning location). If on average the driver of forklift picks 60 tasks, this means that during a day he spends around an hour to pick pallets;
- Place time component. Gray, Karmarkar, and Seidmann (1992) propose to calculate 1.5 minute per pallet placed to new place. On average during a day the driver of forklift spends one hour and a half to place pallets;
- Remaining time component. In paper-based process it takes some forklift driver's efforts to

handle the job at the depot (computer station). Gray, Karmarkar, and Seidmann (1992) propose to calculate 0.5 minutes per task (Gray, Karmarkar, and Seidmann 1992). If on average the driver of forklift picks 60 tasks, this means that during a day he spends around half an hour at the computer station.

The mentioned time components for the first and second scenario are mentioned in Table 1.

Table 1: The time needed for forklift operations

Components	1st scenario	2nd scenario	Effect
Travel time component	1.5	1.5	
Pick time component	1	1	
Place time component	1.5	1.5	
Remaining time component	0.5	0	
Total time	4	3.5	12.5%

The effect 12.5% related to minimization of costs is identified (see Table 1).

And finally, time savings calculation is presented. First, each line of investments is mentioned, later on the comparison for both scenarios is given.

Investments into forklift:

The forklift purchase price - 18113 Euro
 The purchase price of 2 batteries - 2993 Euro
 The purchase price for RF-terminal* - 5000 Euro
 Total purchase price for forklift and its equipments - 26106 Euro

Investments into charging room:

The purchase price for charging room protectors - 23 Euro per sq. meter
 The purchase price for battery change table - 1496 Euro
 The purchase price for 2 battery chargers - 2860 Euro

Investments into warehouse floor:

The purchase price for walls and racks protectors - 2.5 Euro per sq. meter
 The purchase price for WI-FI network* - 3.4 Euro per sq. meter
 Increase of corridor space from 2.5 sq. meter to 3.3 sq. meter for forklifts operations
 One sq. meter of charging room is requested for 135 sq. meter of warehouse floor

* - additional investments needed for second scenario.

The mentioned numbers are presented in Table 2.

Table 2: Total investments required for forklifts operations

Investments		1st scenario	2nd scenario
Investments into forklift	26106 Euro	21106 Euro	26106 Euro
Warehouse space (50 m x 20 m)	1000 sq. m		
Charging room space	7.4 sq. meter		
Investments into charging room	4526 Euro	4526 Euro	4526 Euro
Rent price per sq. meter	5 Euro		
Number of corridors with 3.3 m width and 20 m length	10.5		
Investments into warehouse floor	6740 Euro	3340 Euro	6740 Euro
Forklift driver costs a day	40 Euro	40 Euro	35 Euro
Total costs for 5 years		78372 Euro	80597 Euro
Savings in 5 years			
Savings of driver costs (when 247 working days a year)			6175 Euro
Savings of forklift costs (12.5%)			3263 Euro
Total savings			9438 Euro
Net total costs for 5 years		78372 Euro	71159 Euro

In addition, it should be mentioned that net total costs for second scenario are 91 % lower than for the first scenario. This means that if more forklifts will be included in such calculation, the reduction of travel distance effect would be much higher.

4. CONCLUSIONS

In many labor-intensive warehouses, there is the constant pressure to reduce travelling time. In the literature review short summary of the application of forklifts in trading companies, business cases, the

assessment of technology implementation by production companies, their attitudes and interests. In addition, different time savings algorithms are presented.

In the second part of the study is dedicated to experiments. First, to construction of least-costs forklift route; and second, to effect, related to minimization of costs, estimation.

The experiments demonstrate labor productivity increase from 27% to 37% and reduction of time and costs. The comparison results of both scenarios shows that total time can be reduced by 12.5 % due construction of least-cost forklift routes. In addition, total costs can be reduced by around 9%.

In the paper the travelling of forklift is examined through simulation and experiments with simulation model are undertaken. For saving analyze, the time, needed for forklifts operations, is splitted into travel time, pick and place time, and remaining time. The results of such analysis showed that the yearly savings for each forklift driver are 1235 Euros and for each forklift - 652 Euros.

In addition, it should be mentioned that net total costs for second scenario are 91 % lower than for the first scenario. This means that if more forklifts will be included in such calculation, the reduction of travel distance effect would be much higher. The study results show that the implementation of RF-terminals and related infrastructure is a priority in warehouses. By implementing this managers can have significant savings of warehouse costs, especially for forklifts, which are the most expensive machines used for manual operations in warehouses.

REFERENCES

- Caron, F., Marchet, G., Perego, A., 1998. Routing policies and COI-based storage policies in picker-to-part systems. *International Journal of Production Research*, 36(3), 713-732.
- Cathy, H.Y., Lam, K.L., Choy, S., Chung, H., 2011. A decision support system to facilitate warehouse order fulfillment in cross-border supply chain. *Journal of Manufacturing Technology Management*, 22(8), 972 - 983.
- Clarke, G., Wright, W., 1964. Scheduling of vehicles from a central depot to a number of delivery points. *Operations Research*, 12, 568-581.
- De Koster, R., Van der Poort, E.S., 1998. Routing orderpickers in a warehouse: a comparison between optimal and heuristic solutions. *IIE Transactions*, 30, 469-480.
- De Koster, R., Roodbergen, K.J. and Van Voorden, R., 1999. Reduction of walking time in the distribution center of De Bijenkorf. In: M. G., Speranza, P. Stähly, eds. *New Trends in Distribution Logistics*, Berlin: Springer, 215-234.
- De Koster, R., Le-Duc, T., Roodbergen, K.J., (2006). Design and control of warehouse order picking: a literature review. *ERIM Report series research in management*.
- Dukic, G., Oluic, C., 2007. Order-picking methods: improving order-picking efficiency. *International journal of logistics systems and management*, 4(3), 451-460.
- Giaglis, G.M., Minis, I., Tatarakis, A., Zeimpekis, V., 2004. Minimizing Logistics Risk through Real-Time Vehicle Routing and Mobile Technologies. *International Journal of Physical Distribution & Logistics Management*, 34, 749-764.
- Goetschalckx, M., Ratliff, D.H., 1988. Order picking in an aisle. *IIE Transactions*, 20, 531-562.
- Gray, A.E., Karmarkar, U. S., Seidmann, A., 1992. Design and operation of an order-consolidation warehouse: models and application. *European Journal of Operational Research*, 58, 14-36.
- Hassan, M.M.D., 2002. A framework for the design of warehouse layout. *Facilities*, 20(13/14), 432-440.
- Jarvis, J.M., McDowell, E.D. 1991. Optimal product layout in an order picking warehouse. *IIE Transactions*, 23(1), 93-102.
- Kasilinga, R.G. 1998. *Logistics and transportation - design and planning*. USA: Springer.
- Petersen, C.G., Aase, G., 2004. A comparison of picking, storage, and routing policies in manual order picking. *International Journal of Production Economics*, 92, 11-19.
- Oudijk, D., Roodbergen, K.J., De Koster, R., Mekern, M., 2002. Shelf Area Warehouse Simulation. *Erasmus University Rotterdam and Stichting Logistica*. Available from: <http://www.roodbergen.com/warehouse> [accessed 24 November 2010]
- Roodbergen, K.J., De Koster, R., 2001. Routing methods for warehouses with multiple cross aisles. *International Journal of Production Research*, 39(9), 1865-1883.
- Roodbergen, K.J., De Koster, R., 2001. Routing orderpickers in a warehouse with a middle aisle. *European Journal of Operational Research*, 133, 32-43.
- Ryan, J.L., Ryan, L.D., 2006. *Forklift manual*. USA: Donegal Bay Inc. publishing.
- Varila, M. Seppanen, M., Suomala, P., 2007. Detailed cost modelling: a case study in warehouse logistics. *International Journal of Physical Distribution & Logistics Management*, 37(3), 184-200.

AUTHORS BIOGRAPHY

Aurelija BURINSKIENĖ Dr.Soc.sc., Employee of Vilnius Gediminas technical university, Lithuania; e-mail: Aurelija.Burinskiene@vgtu.lt. Her research is focused on ICT and e-commerce. Her job background covers thirteen years' job experience at wholesale and retail trade logistics and supply chain; for last six years the most of supply chain projects have covered Baltic countries.

SIMULATION OF DYNAMICALLY ADAPTIVE BANDWIDTH ALLOCATION PROTOCOLS USING COLOURED PETRI NETS

J. Asmuss ^(a), V. Zagorskis ^(b), G. Lauks ^(c)

Institute of Telecommunication, Faculty of Electronics and Telecommunication,
Riga Technical University, Azenes str. 12, LV-1048, Riga, Latvia

^(a) Julija.Asmuss@rtu.lv, ^(b) Viktors.Zagorskis@rtu.lv, ^(c) Gunars.Lauks@rtu.lv

ABSTRACT

We consider the problem of resource allocation in a substrate network and suggest a simulation scheme for dynamically adaptive bandwidth allocation protocols using CPN (Coloured Petri Nets) Tools. The proposed simulation scheme based on network virtualization according to DaVinci principles allows us to describe how a single physical network can support multiple traffic classes with different performance objectives by means of multiple virtual networks constructed by subdividing each physical link into multiple virtual links.

Keywords: Bandwidth Allocation Problem, Simulation, Coloured Petri Nets, CPN Tools

1. INTRODUCTION

Network virtualization is a widely applied technique discussed in the networking research community. It is being considered as a good technique to overcome the weaknesses of the current Internet (Anderson, Peterson, Shenker and Turner, 2005). Network virtualization allows multiple virtual networks (VNs) to run parallel on the substrate network (SN). In a virtualization-enabled substrate network resources offered by SN are sharing between all VNs. An optimal allocation of resources is a fundamental problem for virtualization-enabled networking infrastructures (Haider, Potter and Nakao, 2009; Zhu and Ammar, 2006).

DaVinci approach (Dynamically Adaptive Virtual Networks for a Customized Internet) describes a technique of network virtualization, according to which all VNs are constructed over the physical SN by subdividing each physical node and each physical link into multiple virtual nodes and virtual links (He, Zhang-Shen, Li, Lee, Rexford and Chiang, 2008). We consider the problem of bandwidth (BW) resource allocation in a substrate network on the basis of DaVinci architecture of its virtualization-enabled networking infrastructure. In this context it is a maximization problem for the aggregate utility of all virtual networks (Lin and Shroff, 2006), which effective solution depends on the design of dynamically adaptive bandwidth allocation protocols.

We present the design and simulation scheme of dynamically adaptive bandwidth allocation protocols using Coloured Petri Nets.

2. COLOURED PETRI NETS BASED MODELING

The concept of Coloured Petri Nets (CPN) was introduced by Kurt Jensen in 1981. CPN is one of several mathematical modeling languages for the description of Discrete Event Systems. CPN combine a well developed mathematical theory with an excellent graphical representation. This combination is the main reason for the great success of CPN in modeling of the dynamic behavior of systems (Jensen, 1992–1997; Kristensen, Christensen and Jensen, 1998; Jensen, Kristensen and Wells, 2007; Gehlo and Nigro, 2010).

Definition. A Colored Petri Net is a tuple $CPN = \langle P, T, D, Type, Pre, Post, M_0 \rangle$, where

- P is a finite set of places,
- T is a finite set of transitions, $P \cap T = \emptyset$, $P \cup T \neq \emptyset$,
- D is a finite set of types, $D \neq \emptyset$,
- $Type : P \cup T \rightarrow 2^D$ is a type function assigning types to places or transactions,
- $TRANS = \{(t, m) : t \in T, m \in Type(t)\}$ is the set of all transition modes,
- $\mathbb{N}^{PLACE} = \mathbb{N}^{\{(p, q) : p \in P, q \in Type(p)\}}$ is the set (multiset) of all markings,
- $Pre, Post : TRANS \rightarrow \mathbb{N}^{PLACE}$ are the backward and forward incidence functions assigning marking to each transition mode,
- $M_0 \in \mathbb{N}^{PLACE}$ is the initial marking.

Coloured Petri Nets have got their name because they allow the use of tokens that carry data values and can hence be distinguished from each other. Each token could be attached with a colour, indicating the identity of the token. Moreover, each place and each transition has attached a set of colours. A transition can fire with respect to each of its colours. By firing a transition,

tokens are removed from the input places and added to the output places in the same way as that in original Petri Nets, except that a functional dependency is specified between the colour of the transition firing and the colours of the involved tokens.

A CPN model can be effectively applied to describe and analyze multiple virtual networks. CPN model of substrate network describes the states of each virtual network of the system and the events (transitions) that can cause the system to change state.

Our simulation scheme is based on Coloured Petri Nets Tools (Jensen, Kristensen and Wells, 2007). CPN Tools is a discrete event modeling language combining Coloured Petri Nets and the functional programming language ML which is based on Standard ML. Standard ML provides the primitives for the definition of data types, describing data manipulation, and for creating compact and parameterisable models. By making simulations of the CPN model with CPN Tools it is possible to investigate different scenarios and explore the behaviours of the system, to verify properties of the model by means of state space methods and model checking, and to conduct simulation-based performance analysis.

3. DAVINCI PRINCIPLES FOR MODELING OF SUBSTRATE NETWORK

The DaVinci architecture allows us to describe how a single SN can support multiple traffic classes, each with a different performance objective. The problem of bandwidth allocation in SN is a maximization problem for the aggregate objective of multiple applications with diverse requirements. According to the DaVinci approach, each traffic class is carried on its own VN with customized traffic-management protocols. The substrate runs schedulers that arbitrate access to the shared node and link resources, to give each virtual network the illusion that it runs on a dedicated physical infrastructure.

Let the topology of a substrate network SN be described by a graph $G_s = \{V_s, E_s\}$, given by a set V_s of nodes (or vertices) and a set E_s of links (or edges). We suppose that links of E_s are with finite capacities C_l (links are denoted by $l: l \in E_s$). Correspondingly to $G_s = \{V_s, E_s\}$ we consider DaVinci model with N virtual networks, indexed by k , where $k = 1, 2, \dots, N$. Let the key notations be the following:

- $\mathbf{y}^{(k)}$ bandwidth of virtual network k , $k = 1, 2, \dots, N$;
- $\mathbf{z}^{(k)}$ path rates for virtual network k , $k = 1, 2, \dots, N$;
- $\boldsymbol{\lambda}^{(k)}$ satisfaction level degree of virtual network k , $k = 1, 2, \dots, N$;
- $U^{(k)}$ performance objective for virtual network k , $k = 1, 2, \dots, N$.

Bandwidth values $\mathbf{y}^{(k)} = (y_l^{(k)})_{l \in E_s}$ for each substrate link $l \in E_s$ are assigned by the substrate network, taking into account such local information as current satisfaction indicators and performance objectives (Fig. 1). The substrate network periodically reassigns bandwidth shares $\mathbf{y}^{(k)}$ for each substrate link between its virtual links. Thus, values $\boldsymbol{\lambda}^{(k)} = (\lambda_l^{(k)})_{l \in E_s}$ and $U^{(k)}$ are periodically updated by the substrate network and used to compute virtual link capacity $\mathbf{y}^{(k)}$.

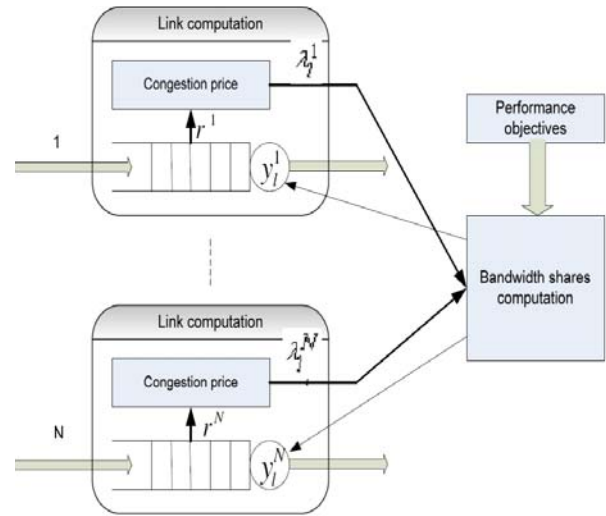


Figure 1: Bandwidth Shares Computation Scheme

At a smaller timescale, each virtual network runs according to a distributed protocol that maximizes its own performance objective independently. Under such combined conditions in a dynamically changing virtual network environment a fundamental problem of resource allocation is the design of dynamically adaptive bandwidth allocation protocols.

4. DESCRIPTION OF BANDWIDTH ALLOCATION PROBLEM

The goal of the substrate network is to optimize the aggregate utility of all virtual networks

$$\sum_{k=1}^N w^{(k)} U^{(k)}(\mathbf{z}^{(k)}, \mathbf{y}^{(k)}),$$

where $w^{(k)}$ is the weight the substrate assigns to represent the importance of VN virtual network k . If the substrate wants to give virtual network k strict priority, then $w^{(k)}$ can be assigned a value several orders of magnitudes larger than the other weights.

First we consider an optimization problem for the performance objective of each virtual network, which represents also constraints of each virtual network k :

$$\begin{aligned}
& \text{maximize} && U^{(k)}(\mathbf{z}^{(k)}, \mathbf{y}^{(k)}) \\
& \text{subject to} && \mathbf{H}^{(k)} \mathbf{z}^{(k)} \leq \mathbf{y}^{(k)}, \\
& && g^{(k)}(\mathbf{z}^{(k)}) \leq 0, \\
& && \mathbf{z}^{(k)} \geq \mathbf{0}, \\
& \text{variables} && \mathbf{z}^{(k)}.
\end{aligned}$$

We suppose that the objective function $U^{(k)}$ depends on both virtual link rates $\mathbf{z}^{(k)}$ and virtual link capacity $\mathbf{y}^{(k)}$. The objective is subject to a capacity constraint and possibly other constraints described in terms of other constraints described in terms of $g^{(k)}(\mathbf{z}^{(k)})$. The capacity constraint requires the link load

$$\mathbf{r}^{(k)} = \mathbf{H}^{(k)} \mathbf{z}^{(k)}$$

to be no more than the allocated bandwidth. To compute $\mathbf{r}^{(k)}$ we use routing indexes

$$H_{lj}^{(k)i} = \begin{cases} 1, & \text{if path } j \text{ of source } i \text{ in virtual} \\ & \text{network } k \text{ uses link } l, \\ 0, & \text{otherwise,} \end{cases}$$

and path rates $z_j^{(k)i}$ that determine for source i the amount of traffic directed over path j .

Now we formulate the optimization problem for the aggregate utility:

$$\begin{aligned}
& \text{maximize} && \sum_{k=1}^N w^{(k)} U^{(k)}(\mathbf{z}^{(k)}, \mathbf{y}^{(k)}) \\
& \text{subject to} && \mathbf{H}^{(k)} \mathbf{z}^{(k)} \leq \mathbf{y}^{(k)}, \quad k = 1, 2, \dots, N, \\
& && \sum_{k=1}^N \mathbf{y}^{(k)} \leq \mathbf{C}, \\
& && g^{(k)}(\mathbf{z}^{(k)}) \leq 0, \quad k = 1, 2, \dots, N, \\
& && \mathbf{z}^{(k)} \geq \mathbf{0}, \quad k = 1, 2, \dots, N, \\
& \text{variables} && \mathbf{z}^{(k)}, \mathbf{y}^{(k)}, \quad k = 1, 2, \dots, N.
\end{aligned}$$

An optimization scheme (Fig. 1) follows directly from DaVinci principles. First, the substrate network determines how satisfied each VN is with its allocated bandwidth. Satisfaction level degree $\lambda_l^{(k)}$ (for link l of VN k) is one indicator that a virtual network may want more resources. In congestion control the link congestion prices are summed up over each path and interpreted as end-to-end packet loss or delay.

Next, the substrate network determines how much bandwidth virtual network k should have on link l : the substrate network increases value $y_l^{(k)}$ proportional to the satisfaction level $\lambda_l^{(k)}$ on link l and proportional to

the relative importance $w^{(k)}$ of virtual network k , taking into account the capacity constraint.

Given that each virtual network is acting independently, the question is whether virtual networks together with the bandwidth share adaptation performed by the substrate network actually maximize the overall performance objective.

5. SIMULATION SCHEME

The aim of our simulation experiment is to get visualization of virtual network switching due to demand for extra link bandwidth. To simplify the problem we simulate the adaptive bandwidth allocation on link level.

We experiment with two nodes topology (Fig. 2) and use the following notations: G1, G2 – packet generators; D1, D2 – destination nodes.

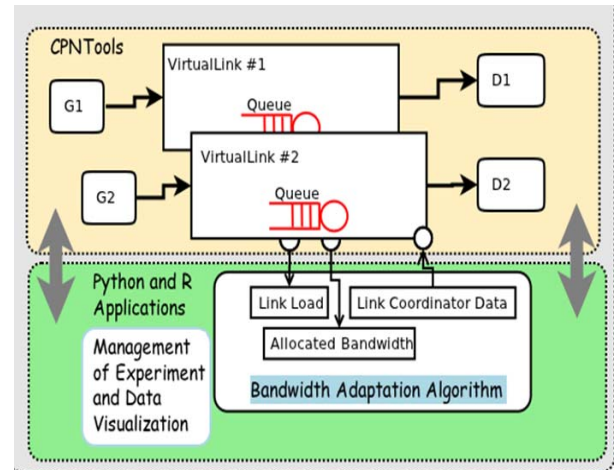


Figure 2: Simulation Scheme Using CPN Tools

According to DaVinci architecture all data packets which are generated by both generators are handled and transmitted over virtual networks. The queuing model of each virtual link (Fig.2) is described independently.

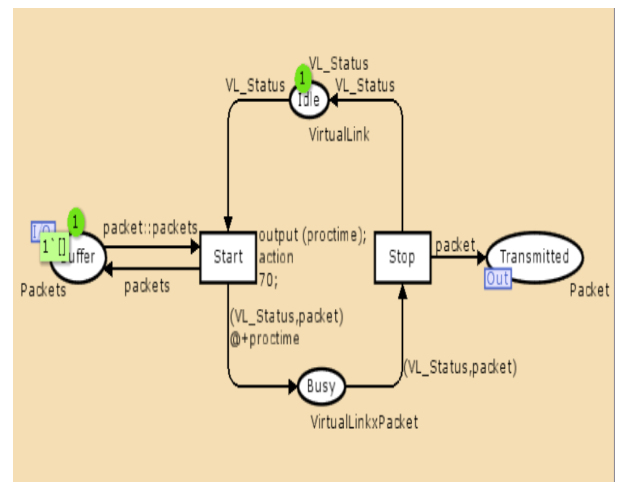


Figure 3: Queuing Model of Virtual Link Using CPN Tools

In our CPN network model packets are generated (Fig. 4) with exponentially distributed inter arrival time.

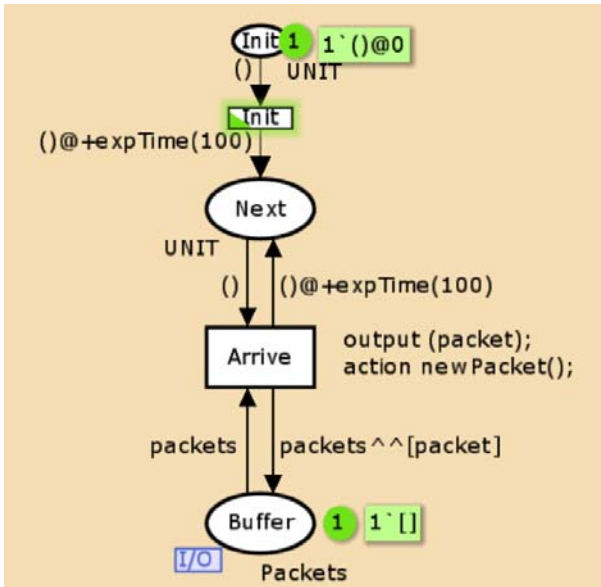


Figure 4: Traffic Simulation Using CPN Tools

Both virtual links (VL) reside on the substrate link (SL) and share the same link bandwidth. Packets are transmitted over corresponding virtual link (Fig. 5) with determined BW, each virtual link is acting independently.

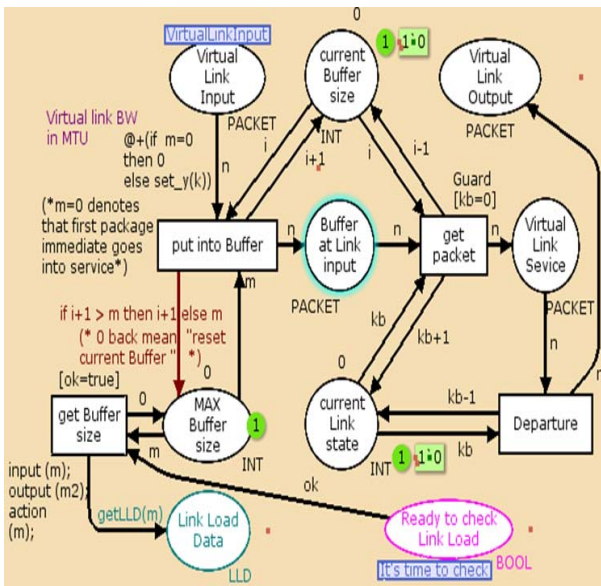


Figure 5: Modelling of a Virtual Link Using CPN Tools

The substrate periodically reassigns bandwidth shares between virtual links based on local information. In our model there is time scheduled monitoring of load of each virtual link (Fig. 6). For instance, if 10 MTU correspond to 10 nS, then for 0.1 sec. time delay in simulator model there should be delay in $10 \cdot 1,000$ MTUs.

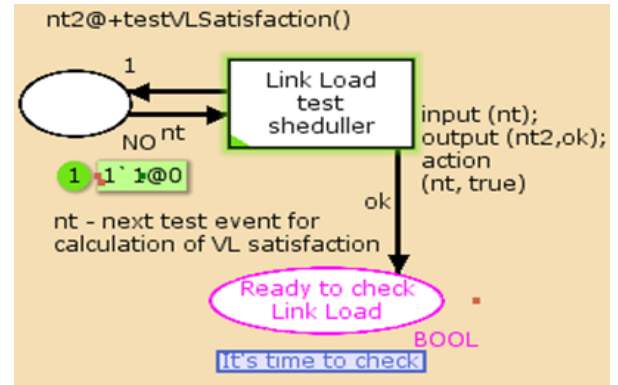


Figure 6: Load Monitoring using CPN Tools

The model involves bandwidth shares adaptation module (Fig. 7). An adaptive scheme can lead to a solution maximizing the aggregate utility of all SL. At the same time small-timescale isolation between VLs ensures the stability of the overall system. Longer-timescale adaptation of resource shares ensures efficiency.

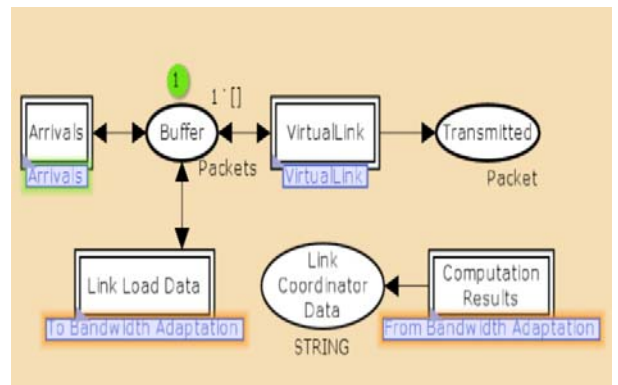


Figure 7: Virtual Network Switching Scheme Using CPN Tools

6. SOME NUMERICAL RESULTS

Up to now there were some experiments with BW adaptation for two virtual links. Bandwidth of SL in our experiment is determined 100 Mbps. In order to present a real network problem, CPN models are using simulation timing determined by Model Time Units (MTU). That gives opportunity to simulate concurrent systems like two or more simultaneously running networks or links. Two columns (Table 1) show network BW corresponding MTU values.

Table 1: Network BW Corresponding MTU Values

Network BW [Mbps]	Network BW [MTU]
100	10
90	11
80	13
70	14
60	17

50	20
40	25
30	33
20	50
10	100

Columns of Table 2 show some combinations how the capacity 100 Mbps can be shared with two different virtual links ($y^{(1)}, y^{(2)}$) in many different ways by means of MTU.

Table 2: Subdividing 100 Mbps of the Virtual Link Capacity in MTU

$y^{(1)}$ [MTU]	$y^{(1)}$ [Mbps]	$y^{(2)}$ [MTU]	$y^{(2)}$ [Mbps]
11	90	100	10
13	80	50	20
14	70	33	30
17	60	25	40
20	50	20	50
25	40	17	60
33	30	14	70
50	20	13	80
100	10	11	90
0	0	10	100

After 10000 MTU since the start of simulation there was a scheduled event to check link load and calculate satisfaction for both links. As a result (Fig. 8, Fig. 9), the first link allocated bandwidth was increased from 10 Mbps to 50 Mbps in order to reduce utilization. For the second link shared bandwidth was reallocated from 90 Mbps to 50 Mbps.

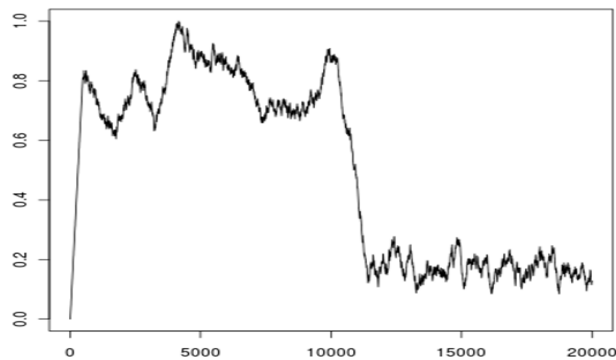


Figure 8: Utility of the First Virtual Link

For computation of the satisfaction level for each virtual link we use the following formula:

$$\lambda^{(k)}(t+T) = \frac{bsa^{(k)}}{y^{(k)}(t+T)} + \frac{y^{(k)}(t+T)}{y^{(k)}(t)},$$

where $bsa^{(k)}$ is a buffer size averaged for the link of virtual network k and T is the time period between bandwidth assignments (the time between iterations).

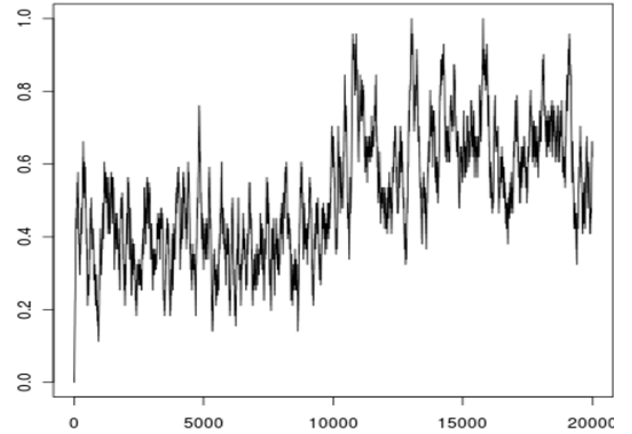


Figure 9: Utility of the Second Virtual Link

At the beginning of the simulation process the utility of the substrate link (Fig. 10) still is a subject for optimization because allocated bandwidth for the first link is more than necessary.

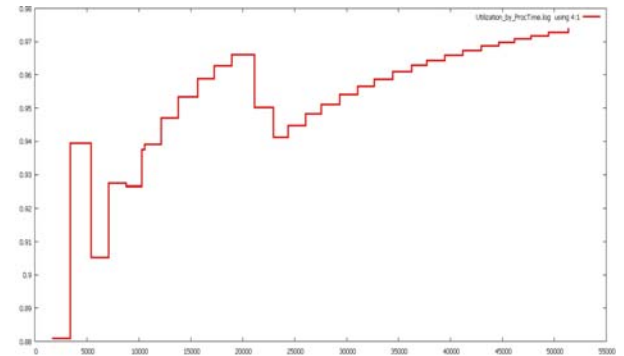


Figure 10: Small-Timescale Utility of the Substrate Link

If the parameters of arriving packets generators are not changed, then adaptive scheme leads to a solution maximizing the aggregate utility of all SL (Fig. 11).

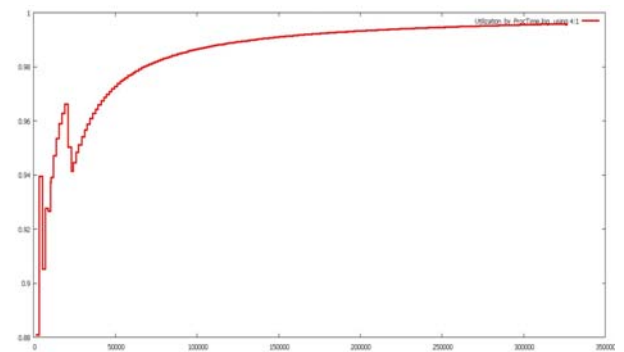


Figure 11: Long-Timescale Utility of the Substrate Link

REFERENCES

- Anderson, T., Peterson, L., Shenker, S. and Turner, J., 2005. Overcoming the Internet impasse through virtualization. *IEEE Computer*, 38 (4), 34–41.
- Gehlo, V. and Nigro, C., 2010. An introduction to system modeling and simulation with Coloured Petri Nets. *Proceedings of Winter Simulation Conference, Baltimore, Maryland, USA*, December, 2010, 104–118.
- Haider, A., Potter, R. and Nakao, A., 2009. Challenges in resource allocation in network virtualization. *20th ITC Specialist Seminar*. May, 2009: Hoi An (Vietnam).
- He, J., Zhang-Shen, R., Li, Y., Lee, C.-Y., Rexford, J. and Chiang, M., 2008. DaVinci: dynamically adaptive virtual networks for a customized Internet. *ACM CoNEXT Conference*, December, 2008: ACM, New York (USA).
- Jensen, K., 1992–1997. *Coloured Petri Nets: Basic Concepts, Analysis Methods and Practical Use*. Volumes 1–3. Springer Verlag.
- Jensen, K., Kristensen, L. and Wells, L., 2007. Coloured Petri Nets and CPN Tools for modelling and validation of concurrent systems. *International Journal on Software Tools for Technology Transfer*, 9, 213–254.
- Kristensen, L., Christensen, S. and Jensen, K., 1998. The practitioner's guide to coloured Petri nets. *International Journal on Software Tools for Technology Transfer*, 2, 98–132.
- Lin, X., Shroff, N., 2006. Utility maximization for communication networks with multi-path routing. *IEEE Trans. Automatic Control*, 51, 766–781.
- Zhu, Y. and Ammar, M., 2006. Algorithms for Assigning Substrate Network Resources to Virtual Network Components. *INFOCOM 2006. Proceedings of the 25th IEEE International Conference on Computer Communications*. April, 2006, 1–12.

SIMULATION MODELS TO SUPPORT GALB HEURISTIC ALGORITHMS AND TO EVALUATE MULTI OBJECTIVE PERFORMANCE INDEX

Sergio Amedeo Gallo^(a), Giovanni Davoli^(b), Andrea Govoni^(c), Riccardo Melloni^(d), Gabriele Pattarozzi^(e)

^(a, b, c, d, e)Department of Mechanical and Civil Engineering (DIMeC), University of Modena and Reggio Emilia, ITALY

Corresponding Author: Sergio A. Gallo e-mail: sgallo@unimore.it, Tel +39-059-2056113, Fax.+39-059-2056126

^(a)sgallo@unimore.it, ^(b)giovanni.davoli@unimore.it, ^(c)andrea.govoni@unimore.it, ^(d)riccardo.melloni@unimore.it,
^(e)gabriele.pattarozzi@gmail.com

ABSTRACT

The following paper deal with an approach to analyze a multi model manual assembly line for oleo dynamic products, and the following **heuristic algorithm** to optimize the scheduling of tasks to the available stations, under the respect of a set of restrictions, as task/station obligation, and with the aim of optimize a multi objective function based on time and line balancing costs elements.

This problem can be considered as belonging to the wide area of **GALB** Problems.

Some strategy about resource scheduling opportunities has been considered.

The original system was an assembly line with six stations, and, in the original and referable configuration, with six operators, but, under the spur of residual margins of the utilization ratios, as a improving evolutive strategy, an idea of evaluate opportunities of improving performances, by assembling coupled mixed items, feeding together the assembly line, have been evaluated, based on a twin mirror counterflowed line.

1. INTRODUCTION

Tasks assignment to stations has to respect efficiency concerns, as the maximization and the balancing of utilization rate, but, furthermore, specific task assignment restrictions to specific station because of the needing of special machines, available just at defined station, for all the items of the production mix.

The line moving is based on a conveyor system, of accumulating type, so that the line is paced, but not synchronized. No inter operational buffer is allowed in the original system, but short accumulation among stations of five pumps is allowed.

Production plan data and configuration derive from a real assembly line. Task times are stochastic, and, based on real observations, and can be considered as triangular or lognormal distributed.

This aspect, has not had opportunity to be considered in the present scheduling problem, because no cost for off line completion can be considered, because task that do not respect line cycle time, cause just the line to increase tack time. No incomplection costs, and no operators moving cost, or costs related to operators training, or changes of the task to operate has

been considered, because we are considering a multi model assembly line, moreover supported with displays showing instructions for tasks to operate. Operators moving costs are supposed be negligible compared to operating cost, because, the short distanced to cover, or the parallel shape of the double line.

A precedence diagram supports technological constrains, very similar among items.

The same tasks require item/size dependent times; times can vary for each item, for the same operation.

Not all operations are performed for all items, depending on item features, and optional.

The assembly line can process a very large variety of items, defined in families, six, but that differ for size, features, optional, under the increasing market competition.

Lot size can varies largely, with a strong tendency to the reducing of assembly quantity for single order.

The performance parameters are tack time, to be reduced, equal to the production rate maximization, and, on an opposite way, optimize the internal balancing of tasks for stations, and labour level among operators.

Under these criteria, a multi objective function based on the whole lot assembly cost, calculated on the effective tack time and on the scheduled resources and their balancing level, has been defined.

The results demonstrate the capability of the proposed algorithm of dealing with the multi objective nature of the re-balancing problem. Solutions with advantages both in tack time reduction, and both on balancing improvement are obtained in any case.

Stations quantity, or, in other words, the assembly line configuration, has been defined to replay with efficiency to all needs for all types belonging to the general production mix, and to respect the assignment of specific tasks to specifically equipped stations.

A virtual model of the assembly line has been built in a simulation environment, to test and measure performances of the heuristic algorithms, but, moreover, also all the algorithm code has been implemented in the same software platform, so simulation has been used not only as a verifying tool, but also as a solving or solution finder, and as task and resource scheduler.

Logics in the heuristic model have been wrote to be as more general and flexible as possible, under the

dimension level, but also to consider the more general problem possible, with easy data configurations.

In the future modular evolution of the model, it should be able to select the configuration asset and the problem type, and choose the algorithm path to apply the best strategy.

The definition of the sequencing in the assembly plan is oriented to the lean production philosophy, so that, first production order has to be produced first. Any way, at least one week, is the planning time horizon an order can be shifted inside the production plan without affect due dates. So, is possible over pass the rule to route assembly orders as they were placed in the order list, to get better system performances.

An early model has been developed. This precedent model, much more simple, represents the "as is" configuration of the firm for strategies and configurations, and is a basic model to be compared with our improved one.

In the first part of the present model, assigning rules have been defined, attempting to fulfil and add tasks to stations in sequence, till total station time doesn't overpass calculated referable tack time. Additional control code check if any constrained task is joined, and in this case, provide to verify the station where to assign that task, if not the actual one, and to calculate all parameters for intermediate stations.

Additional rules evaluate if some operator is idle, and not charged, and the opportunity to re allocate to the more suitable stations, and the recovered time, and all new parameters values.

Just the best allocation will survive, and configuration will be recorded.

More over, if some station is undercharged, a routine defines a recursive increment of the tack time, till all those stations become empties, so freed operators could be re assigned to over charged station.

Also in this case, global efficiency is calculated and compared to the best previous.

Nothing more is possible under this configuration.

After the algorithm implementation to the whole assembly mix plan, output performances has been analyzed, finding, for some item, residual margins for resources utilization rates, no more improvable, because of line configuration, and constrains accomplishment.

As a improving evolutive strategy, based on residual efficiency values, i.e., on the complementary values of the utilization rates, the idea of evaluate opportunities of improving performances, by assembling coupled mixed items, feeding together the assembly line, have been evaluated.

But, because of the constraint position of a special chamfer machine, allocated on a defined station, and because of other operations, just available at other stations, common to the whole items set, opportunities to gain better performances sequencing repeatedly profiled groups of items extracted by the production or assembly plan, PP or AP, conveniently defined for quantity and for typology, has seemed, not so feasible.

In fact, station time profiles, resulted similar for the large part of available items, differing, often, just for the time scale.

Under this observation, the only opportunity to achieve better performances, grouping single units of different available orders, was to couple tasks to be assembled, on two parallel lines, feeding each in counterflow; operators, in this configuration, should be assigned to stations, one for each line, and they should have to complete their operations, alternatively, on both stations of two lines.

This extension of the original system, make possible, with a minimum impact of investment costs and space consuming, to operate more strategies: some items can be processed alone, on a single line, under the tasks assignment rules, or, if it was better, the lot can be processed, half and half, on both the counter flow lines, coupling with itself; finally, some item can be processed coupled with just one other item, in order to improve the performance index.

The choice to test matches of not more than two items only, is based on the consideration that, we are not sure to find, in a specific new assembly/production plan, right combinations, both under the type issue, and both, under the right matching quantity aspect, with the uncertainty level growing up as the matching size grows. But is much more alike finding sets of just two different items that can be coupled and assembled till the quantity of one of the twos ends, and then the remaining quantity can assembled with another further item, available in the AP, or, in the worse case, can be assembled alone with a lower efficiency.

To do this, special matching list have been compiled in a preliminary phase, launching simulation runs to output performance indexes, for each item considered to test all matches with any possible other.

An algorithm, similar to the one used to efficiently assign tasks to station, now adapted to assign, at the same time, tasks of matching items to symmetrical stations, has been wrote and used.

After this, out put results, namely efficiency indexes, and, much more, lot assembly cost reduction, have been listed, for each item, in descending way, to define matching tables.

In a following phase, assembling/production plans have been defined, extracted from the previous one, just items that in the precedent balancing phases showed a significant recovery edges for the efficiency index.

Models can be applied to a wide variety of systems, with a different number of stations, and different constrains positions, just integrating new additional constrains rules. An extension of the actual model to consider other features or restriction is under evaluation, as statistical testing are in progress at this moment to evaluate sensitivity and consistence of the model.

Achieved results show enthusiastic improvements compared with initial solutions, and any time a new strategy is applied.

Keywords: Manual Assembly Lines Balancing, GALB, Modeling and Optimization Heuristic Algorithm.

2. LITERATURE REVIEW

An assembly line is a flow-oriented production system, where the operative location units performing work, referred to as stations, are sequentially aligned. Work pieces move on transportation systems as a conveyor.

Assembly lines are very common in the final phase of industrial production of high quantity of small lots of standardized but customized commodities (mass-customization). They are medium intensive capital systems, so, their configuration planning is relevant.

The Assembly Line Balancing Problem (**ALBP**) means the assignment of tasks to stations and operators on a line, whereas the items are produced at pre-specified production rate. Configuration planning comprises all tasks allocation and decisions which are related to equipping and aligning the productive units for a given production process, including setting the system capacity (cycle time, number of stations, station equipment) as well as assigning the work content to productive units (task assignment, sequence of operations).

Since the times of Henry Ford and the model-T, customer requirements, and consequently, production systems, have changed in a way to increase dramatically customization of their products. Multi-purpose machines with automated tool change, allow, at very low set up cost, for distinct production sequences of varying models. The high level of automation of assembly systems and the fixed movement system make the (re)-configuration of an assembly line critical.

It is easy to find a wide variety of algorithms to solve ALBP in literature, any one facing a partial part of the problem, or oriented to a particular system or configuration.

In spite of the huge academic effort in assembly line balancing, a large distance between requirements of real problems and the status of research, remains.

Many of them consider the problem too much statically, just under a one point of view.

But the increasing need to face continuous changes in customer's requirements, as product design, restyling and lot quantity needed, enforced with high customization and reduction of time-to-market, push to test dynamic versions of ALBP solution procedures.

Those modifications imply a very high flexibility level for the line.

ALBP consists of assigning tasks to stations in such a way that (Salveson, 1955):

- each task is assigned to one and only one station;
- the sum of performance task times assigned to each station does not exceed the cycle time;
- the precedence relationships among the tasks are satisfied;
- some performance measures are optimized.

Most procedures consider the types **I and II ALBP**, based on minimization of the number of stations, given a desired cycle time or minimization of the cycle time, given a desired number of stations, respectively.

Because of the numerous simplifying assumptions of this basic problem, this problem was labelled simple assembly line balancing (**SALB**) in the widely accepted review of Baybars (1986). Subsequent works attempted to extend the problem by integrating practice relevant aspects, like U-shaped lines, parallel stations or processing alternatives (Becker and Scholl, 2006), referred to as general assembly line balancing (GALB).

Scholl (1995), and Pierrelval et al. (2003) proposed a very large and comprehensive reviews of the approaches developed to solve the problem.

Ghosh and Gagnon (1989) proposed a taxonomy to classify ALBP solution procedures under two key aspects, mix or variety of items produced on a single line and the nature of performance task times: single model lines or multi/mixed model lines manufacturing more items in batches or simultaneously; deterministic ALBPs, in with performance task times constant, or stochastic ALBPs, with stochastic task times distributed according to a specific distribution function.

ALBP can be solved to optimize both time - and cost, as reported in Amen (2000, 2001) and Erel and Sarin (1998), which concern the deterministic and stochastic versions of the problem, respectively.

Moodie and Young (1965), Raouf and Tsui (1982), Suresh and Sahu (1994), Suresh et al. (1996) have proposed time-oriented algorithms, improving procedures developed for the single-model deterministic problem, with the aim of minimize stations number and the over time to complete the work off the cycle time.

In any case, in stochastic assembly lines relevant incompleteness costs often occur, and a multi objective cost function often is needed.

Two cases, both described in literature:

- the whole line is stopped till the over work is completed (Silverman and Carter, 1986);
- incomplete products get completed off-line.

Kottas and Lau (1973, 1976, 1981) proposed heuristic procedures to minimize both the total labour cost and the expected incompleteness cost. Extensions of the Kottas and Lau's (1973) method were developed by Vrat and Virani (1976), Shtub (1984)

Sarin et al. (1999) proposed, not so general as Kottas and Lau's (1973), a branch and bound heuristic to minimize the total labour cost and the total expected incompleteness cost with good results.

Erel and Sarin (1998) noticed the difficulty of methods in literature to model real conditions, and suggested that newer works should be oriented at useful studies, with impact on real-life assembly lines.

Rekiek (2000) observed that differences among ALBP and real-life statements were the multi-objective nature of the problem, no so considered in literature.

Some studies deal with the re-balancing problem of an existing line, as Sculli (1979, 1984) and, Van Oyen et al. (2001) considered the re-balancing of an existing line, under fluctuations of operator output rates or equipment failures, in short-term problem. The proposed solution to avoid temporary imbalance on the line has been the dynamic work sharing.

Rekiek et al. (2002) demonstrated that the integration between heuristic approaches and multi-attribute decision making techniques is a proven and efficient way for solving assembly lines problems.

3. SYSTEM AND CONFIGURATION DESCRIPTION

The original assembly mix presents six product families, moreover divided in 127 different versions of items to assembly, depending on optional, features, displacement, etc. The original system based on a conveyor system, shows six work stations, based on original firm evaluations.

Some constrains in the system is based on the needing to have some equipment available at a defined station; also related tasks have to be operated at those stations.

Some further constrains arise from the lean production philosophy, and the FIFO logic: the first order is placed in the system, the first get on the line.

In our model we will overpass the layout constrain, and a model with a coupled double line will be tested; all stations, and all equipments will doubled, except for the chamfer machine, the most relevant, that will be shared to achieve a better balancing, cost reduction and productivity improvement.

Line shall be capable to perform assembly orders very different each from others; just a manual assembly line can face this with negligible set up time.

Task time are triangularly distributed.

Some model parameters (times in hundredth of minute):

Station Number	$k \in [1, n]$
Task Number	$n \in [1, 34]$
N° of tasks assigned to a single station $i \in [1, h]$	
Task Time	T_{op}
Station Time	$T_{Stat} = \sum_{i=1}^h T_{Op}$
$T_{Stat} = UC_S * T_m$	
Operation Unbalancing Coefficient	$UC_{Op} = \frac{T_{Op}}{T_m}$
Station Unbalancing Coefficient	$UC_S = \frac{T_{Stat}}{TT_{Line}} \%$
	$UC_S = \sum_i UC_{Op} = \frac{\sum_i T_{Op}}{TT_{Line}}$
Line Lead Time	$LLT = \sum_{i=1}^k T_{Stat}$
Line Tack Time or Cycle Time	

$$LTT = \text{Max}(\sum_{i=1}^h T_{Op}) = \text{Max}(T_{Stat})$$

Mean or Ideal Tack Time

$$TT_{mean} = \frac{\sum_{l=1}^n T_{Op}}{k}$$

In table 3 original production plan with all descriptions and task times and ideal Tack Time.

Table 1: whole mix production plan with parameters values and task times

Task times ranges from 5% to 80% of the Referable Line Tack Time.

Out of 34 tasks, three are to be operated with constrained equipment, always at fixed stations:

- task 17 (chamferring) at 4 station;
- task 19 (screwing) at 5 station;
- task 33 (air testing machine) at 6 station.

In the basic configuration station 5 is quite always the most charged one: it affects Line Cycle time.

Quite always station 3 is idle, whereas station 2 is often charged, but with a very lower unbalancing Coefficient.

Station 6, depending on the optional presence, can largely varies its station time.

More over, station time shape looks very similar for all station under different items allocation, and stations 1, 2, 4 e 5 seem similarly charged for same family items, also for the station time.

3.1. MALB algorithm

We propose a heuristic method defined by an algorithm logic to achieve feasible and optimized solutions, not necessary the optimal one.

First, we will allocate tasks to stations trying to fulfil the referable cycle time, more over respecting task constrains, to achieve cost minimization, and a better charge balancing.

Our assembly line is a multi mixed model, and then we will face with a **MALBP** (Mixed-Model Assembly Line Balancing Problem).

In particular, will configure our situation as a **MALB-E** problem, given number of K stations, the aim is to maximize the efficiency E_{line} , ie minimizing the direct cost of assembling the lot, given by the product of number of stations K and the cycle time LTT, the production volume of the lot and the cost of labor.

The balance algorithm we will define, through all steps of the model, will be a mixture of Balancing on the work content, through a dynamic allocation of tasks to be performed at each station. In the “as is” situation, the station times were very inhomogeneous, and each row of the production plan wanted peculiar allocation. Resources Balancing, which dynamically assigns operators to stations rather than operations. Balancing on scheduling, by analyzing and optimizing the production plan, or by defining an ideal sequence of orders to be sent into production, or mixing them.

Initially, each operator has been considered bounded to his station, and tasks allocation was made balancing on the content of work; the primary goal the algorithm was designed for is to allocate tasks dynamically to stations, with the ultimate goal of maximize efficiency, but also of minimizing the direct cost of assembly:

$$MAX(E_{time}) \quad \text{where} \quad E_{time} = \frac{\sum_i UC_S}{n} \quad [\%] \quad (1)$$

Efficiency is calculated as the sum of the UC_S divided by the number of charged stations, initially fixed and corresponding to that of resources, thus as you maximize the efficiency as you maximize utilization, or will reduce the unbalance for each individual station (UC_S).

$$MIN(UC_L) \quad \text{where} \quad UC_L = \sum_i UC_S \quad (2)$$

Modified COMSOAL Heuristic

In order to achieve his goals, we will apply a balancing method inspired to the Chrysler heuristic **COMSOAL** (Computerized Method for Sequencing Operations on Assembly Lines), that we adapted to our system.

We can obtain a set of feasible solutions, randomly selecting at each step, from the available tasks, and then going to schedule the best according to a certain criterion.

At each iteration of the algorithm is determined by the set of all tasks that may be assigned to a station k without violating the constraint, ie the tack time LTT , of this. Any task, at any step, is chosen at random, with the same probability of selection.

In our case, the selection of the task to be assigned, can be detected according to a logic which respects the sequence of the assembly operations, and not in a random manner.

Normally, the heuristic is repeated a certain number of times, and each solution found is compared with those found previously. The number of repetitions to be performed depends on the analyst. Note that the same solution can be obtained more than once.

In the modified version of the choice of operations is not random.

In this regard, even the random selection of tasks to be assigned to the first operation is outdated, because in this case the only task for which all of the precedent

are either absent or assigned, is the first, and then go on. Following the precedence diagram, is not possible face with multiplicity of possible situations, but it will lead directly to the case that identifies the optimal balance.

To assembly a model not all the 34 operations are needed for a specific item.

Another parameter used in the preparation of the model is described below.

Reference Tack Time

$$T_m = MAX \left(T_{mean} = \frac{\sum_i T_{Op_i}}{n}; MAX(T_{Op_n}) \right) \quad (3)$$

Minimum time, used as a limitation roof in the allocation of tasks, maximum threshold for the station Time can not overcome. It is the higher value between the tack time average or ideal (**LTT**) on the six stations, and the maximum values of the specific various tasks (T_{OP}) for each line of the production plan. The tack time reference, represents 100% of work time that can be assigned to each station.

In our case, a further control has been added to assure task allocation to the correct stations.

Another specific problem is the highly variable size of the tasks. Some of them, in fact, affect dramatically the ideal tack time, and, where compared to the starting value of T_m , they are often even larger.

As a consequence, in the recursive routine, before T_m was increased enough, for many times the assignment to the current station fails, the current station is closed, and allocation goes tried to the next. In the extreme case, the task can present a particularly high UC_S that causes in the first attempts, with low T_m , its failure to allocate whatever the station is. In this case, a control amplifies the T_m of a defined percentage, and, after resetting all assignments, try to reassign tasks to stations with the new reference T_m , until it reaches.

Our software performs calculations and allocations and defines the values of key parameters (Station tack time, coefficients of imbalance, etc...) of the specific logic block, analysed to define any new further proposals for balancing the line.

3.1.1. Model Description

AP and configuration data, are read from external files.

The code process part that takes care of reading data is called "P_read" program in this part of the main variables are loaded with the values we impose on us from outside.

The conveyor speed is set to a very high value, transferring times are included in the average time of execution of the task, and result very lower when compared to operational times, with no statistical significance.

A first piece of code initializes the model and its parts, to load the variables with the values of the external file and configures the same in accordance with the structured algorithm for assigning tasks to stations.

The first improving strategy provides that the operators that are already no charged, as their stations are empty, are reassigned to the station with the highest tack time so to lower it.

This last configuration (config_2) will be compared with the previous scenario (config_1), but when we calculate the whole direct assembly cost we will care to not consider the resources associated with the empty stations.

The comparison between these two scenarios is based on a cost parameter calculated for each station in each row in both cases. This parameter is calculated by multiplying the number of resources for the reference tack time, for the unit cost of labour and the number of pumps produced. The config_2 is calculated by two procedures that control the stations without assigned operations, storing them on array of pointers, to define the amount of the resulting uncharged operators to free. The second process chooses the most charged station to assign the operator and calculates the decremented tack.

The tack time reduction follows a procedure that takes care of dividing tasks by two operators in the best balanced manner. The procedure, performed for all rows with new assigned operators, is repeated until there are more operators to be assigned.

The better configuration will test the next improvement. Subsequent values of tack time, tasks assigned, imbalance coefficients, efficiency and direct cost for each configuration are stored in distinct array variables.

At this point, the further forced reallocation is attempted.

In the procedure **"P_uncharged_Op_forced_assignment"** all the stations for each line are checked, to trace the presence of under - utilized stations. Once that has been identified a station of this type, it is emptied, and its operator, released by force.

T_m is increased by a defined percentage, all assignment values are placed to zero, a new tasks reallocation starts till under charged station is empty.

In this logical block, in the first phase, operators resulting already uncharged from the previous step, are not reassigned to overcharged stations, otherwise direct cost would be greater, given the increasing number of T_m . In this way, there is a further situation, even at reduced resources, which is compared with the winning one between the previous and the subsequent reallocations, which will be a phase next configuration.

At this point the situation is photographed by saving the various parameters in appropriate variables.

As mentioned earlier, the reallocation of uncharged workers will follow.

We will attempt to reassign available operators to the remaining stations, with the objective to reduce tack time and improve efficiency and costs.

Once again all the characteristic parameters of each situation will be saved for later comparison with those from previous situations.

Fig. 4: uncharged operators search code snapshot

All configuration parameters values, are read from an external file **"configuration.csv"**, making possible to change its value file.

The highest tack time among all various stations, is saved by line.

The position number of the station with two scheduled workers is saved in a pointer array variable.

Fig. 5: new reference tack time code snapshot

Fig. 6: code snapshot to compare direct assembly cost

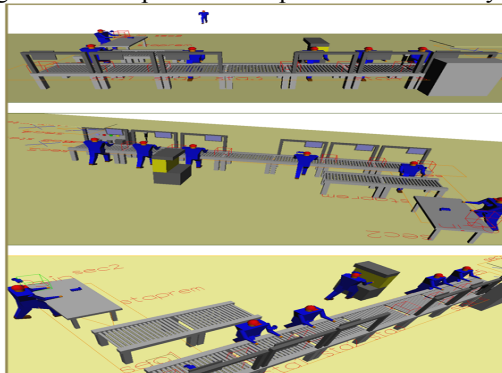


Fig. 7: snapshot of the single assembly line model

3.1.3. Assembly process simulation code

As all possible configurations have been defined, it is possible describe the direct cost objective function calculation and their comparison.

Based on this, all configuration values are tested to be verified on the code part of the assembly line emulation.

A single load activates all the logic and all the code lines that can emulate the assembly line.

The active load acts a process cascade, one for each station, where the presence or needing of the operators is evaluated, and in case, the correct tack time is calculated and charged in a parameters set, respecting the time probability distribution.

A counter takes memory of produced pumps.

3.1.4. The double line

As soon as the best configuration has been outlined for each pump model, we observed that a large margin for the UC_S remains.

Under the last configuration it's very hard to image gaining further improvements. The idea was to evaluate a new balancing opportunity based on a double coupled line, a solution that goes to break the layout constrain, but looks as the only opportunity to start a mixed model balancing policy.

In fact, because of our specific constrains position, all station time profile look very similar and the idea to test any balancing strategy based on scheduling distinct model groups to achieve balancing benefits, since the preliminary observation seems to fail.

On the opposite, it seems possible have a good match, fitting station profile in a counterflowed way, or just considering a single item matched with its self.

Any way, in more general case of distinct constrained stations and tasks, no limitation arises to improve a single or parallel direct flow mixing model balancing strategy.

The possibility of obtaining a clear improvement raises up, under a profile of efficiency and cost, as well as from a point of view of the balance of the loads assigned to resources.

The idea is to abstract from the system under examination, while keeping it as a reference for the data for the model. No investment costs are available for an investment analysis, but if the double line should be proved to be an optimal solution, there are no serious limits to its realization, as the unavoidable costs will be offset by savings in production.

In the new layout, a new twin line will be realized, disposed parallel to the original one, but with the stations arranged in a totally symmetrical way, for example, the station 1 on line 1, it will match to 6 on the second line, the station 2 in the first 5 in line with the second and so on, keeping the number of fixed resources.

In the analysis of the resulting output from the model with the solutions previously applied, some of the stations, in fact, had still space for further optimization because of the presence of stations not well filled, due to the presence of constraints and to the number and features of tasks in which it was divided assembly. To define best configurations and matches to set for the new algorithm implementation, further tests

to try to needed to be conducted. In fact, this configuration requires that distinct pump models could be produced simultaneously.

To determine the best matches between pumps we used simulation software.

By observing results of optimization phase for the single line case, it pops up that there were lines of production plan proposed for the double line. We defined multiple sheets to be read in the program with the following additional information with respect to single - line:

- Production line value: indicates the line the item will be assembled in, first or second.
- Task time: The times are the same as single line, but for item that will result to be assembled on second line, tasks are renumbered in a symmetrical manner, ie, the task number 34, becomes the number 1, number 2, 33, and so on.
- Number of matches: number of rows, subsequent to the current one, who will attempt the match with it.
- New Reference Tack time: average of all coupled items: being twos at a time, the actual value of this will be the sum of the 68 tasks of the two lines, divided by the number of resources (6).

The parameters just defined for each row are then placed into the new files to read in order to verify combinations with all others. Each files show in the first line the data of product to be assembled on the first line, and than those for all others to score the match performances.

The aim is thus to compare each row with the others and define, based on the goodness of each match with the other lines, define for each order line a priority list of coupling with the other in order to improve the joint efficiency.

In order to achieve the best balancing of the line, obtaining a better efficiency and the minimization of costs, a new heuristics has been structured, then checked for the distribution of tasks to the stations of two lines in a dynamic manner, the structure of which will be verified later.

We can observe, first, that it was decided to couple the line 2 to the first in a antisymetric way. So, corresponding to the entrance of the pumps on line 1, is the exit of the assembled pumps in line 2. The number of operators is six, and each operator works on both lines turning him self of 180° and advancing few steps, the possibility of movement is then guaranteed.

In the tasks assigning process, stations will be considered coupled. We will, therefore, face with a pair of stations, and tasks will be assigned to a numbered operator, rather than to station.

The chamfer machine has now been moved in the middle of lines space corresponding to the station 3 and 4, available for the two operators who have to use this

resource: the operator 4 for the first line and the operator 3 for the second.

The task assignment to stations will be based on the operator scheduled to, as tasks of the two order lines are available on the two opposing lines to be allocated to the two stations under operator jurisdiction, respecting each precedence diagram.

The reference total tack time is calculated as average for all tasks of coupled items, or as the sum of the ideal tack times of the lines that try the match.

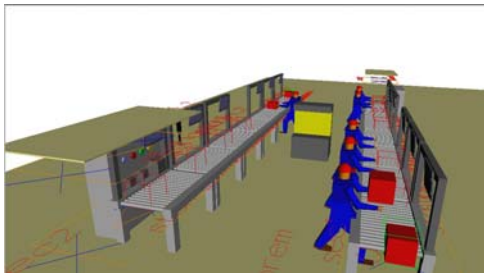


Fig. 7: snapshot of the double assembly line layout

3.1.5. Definition and implementation of heuristic for the double line

In the first part or preliminary phase of the double line algorithm, a pair of rows at a time will be read at the time, considering the first, as the leading one, to be produced in line 1, and the second one, instead, to be tested as mate item on the second line.

At this point, we start to assign tasks to the first operator, or rather the first pair of stations (in our case St_1.1 – St_6.2 where the second index refers to the line on which you are).

The algorithm logic for the allocation, considers that, for each coupled stations/operator, allocation starts with the station, if exists, with constrained tasks till constrained task has been allocated; since that, tasks are allocated alternately to both coupled stations from those of matched order rows, till reference times has got, in respect of priorities.

If the assignment of the task can not be made because of the tack time reference level is exceeded, or if is not possible to assign all tasks within the available stations, an increment of reference Tack Time starts, and the assignment has be done again, as previously.

As the assignment is completed, all the values for tack times, efficiency and cost for subsequent comparison are memorized, and the dominant line with his next match is tested, till the end of the file.

At this point, obtained all the possible configurations for the match with the dominant line, is possible to compare the parameters of best matches with the winning ones in the single line case.

Direct cost and inefficiency, are calculated as in the single line case, just considering the cumulative coefficients of imbalance and a tack time, meaning the added value for the two models matched in the double line.

The improvement combinations are sorted in descending order of saving costs, and this defines the

priority matching lists, available to be used for any production plan. Next matching criterion is the production volume.

```

*===== on task alla stazione corrente della Linea 1 *
if V_operatore_line = 1 and (V_ordi_numero_linea(1) = V_operatore_line * V_operatore_line)
and (V_ordi_numero_linea(2) = V_operatore_line * V_operatore_line)
and (V_ordi_numero_linea(3) = V_operatore_line * V_operatore_line) then
  set V_operatore_line(1) to V_array_tackmatch_linea_num_match(V_linea(1), V_linea(2),
  V_linea(3), V_linea(4))
else if V_operatore_line = 2 begin
  set V_operatore_line to 2
  increment V_operatore_line_numero_linea(1) by 1
end
*===== on task alla stazione corrente della Linea 2 *
if V_operatore_line = 2 and (V_ordi_numero_linea(1) = V_operatore_line * V_operatore_line)
and (V_ordi_numero_linea(2) = V_operatore_line * V_operatore_line)
and (V_ordi_numero_linea(3) = V_operatore_line * V_operatore_line) then
  set V_operatore_line(2) to V_array_tackmatch_linea_num_match(V_linea(1), V_linea(2),
  V_linea(3), V_linea(4))
else if V_operatore_line = 2 begin
  set V_operatore_line to 2
  increment V_operatore_line_numero_linea(2) by 1
end
  
```

Fig. 8: logic for the allocation of alternate operations

For example, if there is an order which requires the production of a different number of pumps belonging to different families and with various optional and drives, by consulting the list of priority can be known, fixing a rule to choose the model to be produced in line 1, which of the remaining ones, mates better produced on line 2.

At this point, one ore more criteria to define the order to assembly in line 1, was requested to combine these results at our disposal, with a specific PP, to obtain a suitable situation to our case to test.

The possible criterions to use priority lists, were:

to respect lean and FIFO logic, was to consider the list position of the rows of the production plan, considering to match to the first matching available one, as it were the time succession of the arrival of the various orders and then define a logic in which each not yet scheduled row, was matched with available sequent ones, under the respect of its priority list, till the quantity ending.

If, however, there is the possibility of delaying the production start of an order, it is possible decide to wait for the arrival of the one that best mates with it, or it can wait until it reaches a number of orders such that their production volume equals that of the order on hold.

Some control code adjusts the emulation of the assembly process, coupled and phased, of the production plan limited to the order lines suitable to be processed in a double line, on the basis of attributes further introduced to manage the routing.

Control code protect the simulation from the possibility that on one of two lines new orders could entry the system if coupled order have been not completed already. The cadence of work considers the operator to work alternately on both coupled items before start a new item following on one of lines.

This has been realized through cross - inhibitions and unlock.

3.2. ANALYSIS AND COMPARISON OF EXPERIMENTAL RESULTS

In the following lines some algorithm and simulation application have been outlined.

Single Line

First, in table 3 it is possible to observe the total absence, in the best configuration case, of stations under-utilized.

It's easy understand that their presence affect the best performances of balancing.

Second, we can see that the stations, under charged at the first instance, have been permanently depleted and erased, as those already empty since first tasks allocation. This means that the final winning situations appear to be those which have a lower number of resources, except in those cases in which stations are all well filled.

Table 4 shows as the final configuration results in an overall improvement in the efficiency and cost. There is no worsening in the final configuration, in fact, but at least, values remain the same. For those rows, it means that the best configuration is the first, the one obtained after the first dynamic allocation. Any way, our new dynamic assignment yield a large improvement for cost and efficiency values, if we should compare these to those corresponding to the first situation, namely that provided by the company, thus obtaining a positive result.

Table 2: unbalance coefficients after dynamic allocation process. In green stations with the maximum coefficient, in orange under charged stations, and red empty ones.

Table 3: UC_L for single line best configuration. In green stations with the maximum coefficient, in orange under charged stations, and red empty ones.

From Table 5 it is evident that the winning configurations are Config_1, corresponding to the initial dynamic distribution, and Config_3, when reference tack time is amplified, and tasks of the under charged station, are reassigned. Before continuing the analysis, it is good to declare that since the Config_2, with operators uncharged since from the beginning, reassigned to overcharged stations, is never successful, it will not be shown in the following charts, as data relating to the configuration number 4.

In other words, since there are no lines which pass configuration 2, there are no rows that will attempt to use the number 4.

Table 4: Global Efficiency and Whole Direct Assembly Cost, Config_1 vs final best configuration. In green, rows showing an improvement.

Table 5: number of winning configurations for all lines.

Conf 1	Conf 2	Conf 3	Conf 4	Conf 5
90	0	37	0	0

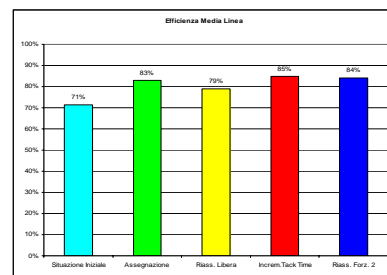


Fig. 9: Average Efficiency for all single line configurations

The efficiency of the line after the first dynamic reassignment grows with a significant increase of 12 percentage points, which leads to 83%.

The following phase, knew as Config_2, with the redistribution of the operators will cause a decrease, while, again, in the Config_3, the efficiency decrease is compensated with the increase of the tack time, that makes possible the elimination of the undercharged - stations which lead to a vertex efficiency of 85%, no more over passed also by Config_4, when redistribution of released workers, then records a decrease, albeit minimal.

But, although the final situation, Config_4, is typically better, from this point of view, if we observe the objective function, the development of costs, it can be observed that it is no more convenient. Since that the objective is to minimize costs, much more than increase efficiency, Config_2 is winning on Config_5.

The cost trend is still fairly close to that one of efficiency, this trend is shown in Figure 9, while in the following figures are the changes in costs and the maximum decrease achieved in various configurations.

The Average Direct assembly Cost undergoes a substantial decrease, both in the case of dynamic allocation, equal to 16.7%, both in the case of depletion of the stations under - utilized, when compared to the initial situation.

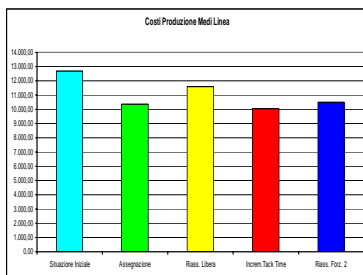


Fig. 10: average Direct assembly Cost for all single line configurations

The reallocation of workers leads to a fall, but is much less important, being equal to 2.9%.

The cost of production was calculated in such a way as to be representative of both the tack time reference of the line for each row, and then for each model, both the number of resources used, as well as the production volume:

Direct Assembly Cost

$$DAC = (Tm \cdot S \cdot LQ \cdot ManWorkCost) \quad (3)$$

where

$LQ = \text{LotQuantity}$

Another evidence is that there is a general tendency that are Station_2 and Station_3 to get empty when we are working to kill under charged stations, indicative of the fact that they appear to be the less loaded. Station_3 has a tendency to be empty already in the case of the first dynamic assignment.

Given the trend of the last three stations, which is almost the same in various assignments, it's possible justify the initial drop of operations on the station 2, in fact offset by the significant increase in allocations to station 1, and this trend is also indicative of the constrained station that creates a bonding allocation in station 4.

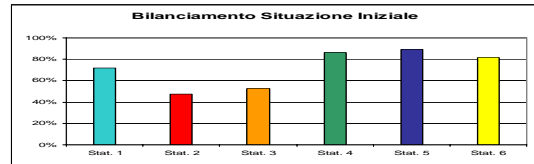


Fig. 10: Initial configuration, Average Station unbalance coefficients, UC_S .

The initial situation presents a quite low balancing level, especially as regards to stations 2 and 3.

All subsequent situations lead to an improvement in percentage for the station, but do not entail a better balance, ie a situation in here there is balance between the various coefficients that should settle to values similar to each other and quite high.

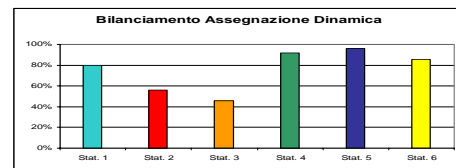


Fig. 11: Config_1, Average UC_S .

We have seen earlier that the resignation of the operators, with subsequent lowering of the tack time, never leads to an advantage compared to the situation where not schedule one or more resources, keeping the same tack time.

Whole UC_S representation for each of all available station as in the initial configuration, any way, is not really well representative, in fact, we are in presence of situations with a variable number of /stations/operators, and therefore, it will be better outline results based on the number of remaining stations/operators.

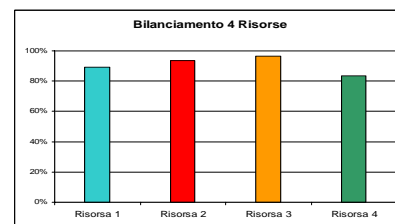


Fig. 12: Final configuration, 4 resources Average Station unbalance coefficients, UC_S .

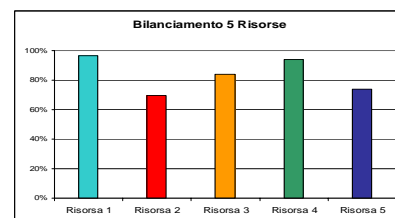


Fig. 13: Final configuration, 5 resources UC_S .

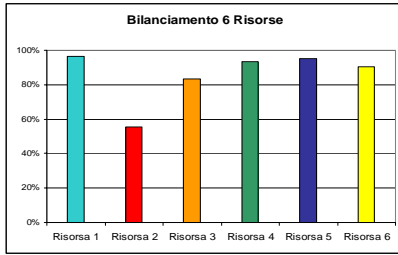


Fig. 14: Final configuration, 6 resources UC_S.

It is now more evident the achieved advantage with the proposed configurations. In cases with a greater number of resources, however, it is noted still the possibility to have an improvement, especially for what concerns the second resource, as the case corresponding to the stations 2 or 3.

In general, however, UC_S coefficients range within a fairly narrow range and values placed around between 70% and 80%.

3.2.1. The analysis of the double line

The double line configurations are all 6 resources.

Two main ranges:

- 0.304 - 0.568: light green, more unbalanced stations;
- 0.568 - 0.7: dark green, less unbalanced stations.

To obtain these ranges, an interval that would go from the minimum value of the coefficients of unbalance (0.304) to a maximum value, chosen by us, equal to 0.7, is considered.

Several possible scenarios were examined to define matches, tested all using the simulator. This solution proved to be the best under speed and efficiency of calculation point of view.

The scheduled lines to be assembled in the double line are 79.

The priorities lists so defined are presented in Table 6.

Table 6: an example of priority list

Marchi UC per riga 4	Marchi UC per riga 5	Marchi UC per riga 6	Marchi UC per riga 7
430 440 450 460 470 480	430 440 450 460 470 480	430 440 450 460 470 480	430 440 450 460 470 480
490 500 510 520 530 540	490 500 510 520 530 540	490 500 510 520 530 540	490 500 510 520 530 540
550 560 570 580 590 600	550 560 570 580 590 600	550 560 570 580 590 600	550 560 570 580 590 600
610 620 630 640 650 660	610 620 630 640 650 660	610 620 630 640 650 660	610 620 630 640 650 660
670 680 690 700 710 720	670 680 690 700 710 720	670 680 690 700 710 720	670 680 690 700 710 720
730 740 750 760 770 780	730 740 750 760 770 780	730 740 750 760 770 780	730 740 750 760 770 780
790 800 810 820 830 840	790 800 810 820 830 840	790 800 810 820 830 840	790 800 810 820 830 840
850 860 870 880 890 900	850 860 870 880 890 900	850 860 870 880 890 900	850 860 870 880 890 900
910 920 930 940 950 960	910 920 930 940 950 960	910 920 930 940 950 960	910 920 930 940 950 960
970 980 990 1000 1010 1020	970 980 990 1000 1010 1020	970 980 990 1000 1010 1020	970 980 990 1000 1010 1020

As the priority list were defined, two defined production plans, extract from the original one just for matching lines, one defined to match the higher-volume lines to all other lines, and one defined to give the leading role to test matches with all other lines, to the rows in the topmost position, as indicative of the sequence of arrival of orders, were tested.

Table 7: final UC_S; in different shades of green worse values.

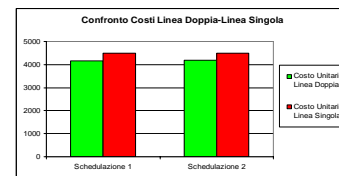


Fig. 14: Comparison of costs in a single line and double line for the two production plans.

As shown by the graph, with the double line is achieved a reduction of costs to produce the same plane vs the single line. Is also observed a higher gain (7.2%) with the first type of scheduling compared to the second (6.8%) even if the difference between the two is minimum, equal to 0.4%.

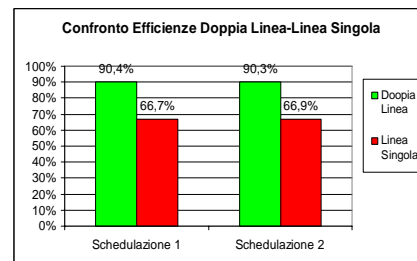


Fig. 15: Comparison of the efficiencies double line vs. single line under two different schedules.

The efficiency implies a remarkable increase, also. The values for both types of scheduling are very good, and the increase compared to the single line best configurations, is 35.5% for the first schedule, while 35% for the second.

The improvement is made even more visible from the observation of the graphs for the UC_S.

With the double line, in both schedules, it is possible observe a very good balance and the range within which falls the various coefficients are very narrow and with excellent values, being included between 85% and 97%.

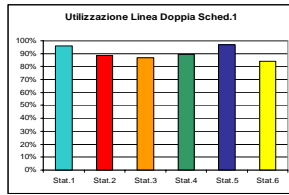


Fig. 15: UC_S for the double line in first scheduling.

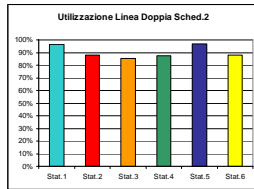


Fig. 15: UC_S for the double line in second scheduling.

3.3. CONCLUSIONS

In this paper a thoroughly research was conducted regarding possible improvements to be applied to the case of an manual assembly line for hydraulic devices.

In this work were identified and then addressed the most critical issues, through an multi phase algorithm definition and consequent simulation of the process.

Preliminarily, we have conducted analyzes that could lead to the definition of the necessary elements to optimize the load balancing of the line, as well as to reduce costs and increase efficiency.

On the basis of data provided by the company, of the imposed constraints and the criticalities, in general, are then created simulation models, which showed the system behaviour depending on the logic strategy applied in each phase.

The aim of this study was to define a global strategy to apply o a wide range of assembling systems, to optimize production.

Therefore, all the relevant parameters have been identified, in order to define all the possible achieved improvements, ie the best balance of stations time distributed on the line, as a certain balance among between the workloads assigned to the operators and avoiding the lack of homogeneity among the various resources, the minimization of production costs of products mix, ie. the maximization of the efficiency.

All strategies have been defined respecting any of the main constraints and considering an appropriate volume production, which could give validity to the model.

The execution of this work has begun with an analysis of manual assembly line specific question, for what regards its characteristics and peculiarities.

Then, a cascade of ameliorative approaches were evaluated, structured as algorithms and heuristics so that they could then translate into a programming language for the implementation and verification of their actual goodness, to the computer.

In conclusion, as verified, considerable improvements in those that were indicated as the objective functions of this work have been got, ie the balance and the production costs (or efficiency), resulting in an improvement in productivity.

Another goal that can be considered reached, the definition of a model that was as versatile as possible. Thanks to the type of structured algorithm and its consequent translation logic programming software, the model can, with its shape, to adapt to other situations of lines of manual assembly with similar characteristics.

A good improvement is definitely the tasks dynamic assignment, useful to assign operations in a flexible way and fully accomplishing with the constraints, structural ones or otherwise, imposed by production statements.

The layout changes for the double line, while going to change the physical structure of the system, and leading to an investment of time and money, can still be considered valid since the benefit obtained.

Thanks to the creation of lists of priorities you have in fact a useful and powerful tool that allows you to go to produce combinations of multiple products minimizing down costs and gain efficiency, and just only when needed, being able to choose among multiple strategies to define double line assembly plans configurations, depending on to ways in which the company prefers replay to market requests and orders. As already mentioned, the costs for the extension can still be reduced by acquiring simple systems to share equipments.

The first part of the study had been inherited from a previous research, much more simple, where the improving strategy has been developed on a spreadsheet.

Future subsequent optimization approaches could include a new data collection and the variation of data of the system randomly with logic, to have a greater validation of the algorithm.

It could be possible also refer to an advancement of multiple products simultaneously on the same line, similar to what we saw in the last part of this work, but without another line, but by simply extending the existing one, with U-Shaped layout, and evaluate, a scheduling strategy but on the double of the stations, with possible assignment of stations even at the same operators, in order to obtain a greater opportunity to balance based on the scheduling of resources, but also to be able to feed as a double line, alternately.

This opportunity is under evaluation.

Finally you could structure the analyzes concerning the study of the cost of any delays on deliveries or completion of the off-line products, evaluating solutions for the optimization of these parameters and the creation of configurations can prevent the emergence of such issues.

In general, the use of solution approaches such as algorithms, heuristics, simulation techniques and classical analytical techniques, opens up a panorama of endless possibilities, which allow to deduce a solution or, more often, a set solutions to the problem to improve the present situation. As there is no best technique, the goodness of one technique over another, is a function of the objectives to be pursued, and the results that we are

provided, as well as the proper structuring of the preliminary steps in the analytical process.

REFERENCES

- Amen, M., 2000. Heuristic methods for cost-oriented assembly line balancing: A survey. *International Journal of Production Economics* 68, 1–14.
- Amen, M., 2001. Heuristic methods for cost-oriented assembly line balancing: A comparison on solution quality and computing time. *International Journal of Production Economics* 69, 255–264.
- Baybars, I., 1986. A survey of exact algorithms for the simple assembly line balancing problem. *Management Science* 32, 09–932.
- Becker, C., Scholl, A., 2006. A survey on problems and methods in generalized assembly line balancing. *European Journal of Operational Research* 168, 694–715.
- Chutima, P. Suphaprugsapongse, H., 2004. Practical Assembly-Line Balancing in a Monitor Manufacturing Company, *Tharnmasat Int. J. Sc. Tech.*, Vol. 9, No. 2
- Ghosh, S., Gagnon, R.J., 1989. A comprehensive literature review and analysis of the design, balancing and scheduling of assembly systems. *International Journal of Production Research* 27, 637–670.
- Erel, E., Sarin, S.C., 1998. A survey of the assembly line balancing procedures. *Production Planning and Control* 9, 414–434.
- Gökçen, H K. Ağpak, R. 2006. “Balancing of Parallel Assembly Lines”, *International Journal of Production Economics*.
- Kottas, J.F., Lau, H.S., 1973. A cost oriented approach to stochastic line balancing. *AIIE Transactions* 5, 164–171.
- Kottas, J.F., Lau, H.S., 1976. A total operating cost model for paced lines with stochastic task times. *AIIE Transactions* 8, 234–240.
- Kottas, J.F., Lau, H.S., 1981. A stochastic line balancing procedure. *International Journal of Production Research* 19, 177–193.
- Jolai, F., Jahangoshai REZAEE M., Vazifeh, A. 2008. Multi-Criteria Decision Making for Assembly Line Balancing, *Springer Science Business Media*.
- Moodie, C.L., Young, H.H., 1965. A heuristic method of assembly line balancing for assumptions of constant or variable work element times. *Journal of Industrial Engineering* 16, 23–29.
- Pierreval, H., Caux, C., Paris, J.L., Viguier, F., 2003. Evolutionary approaches to the design and organization of manufacturing systems. *Computers & Industrial Engineering* 44, 339–364.
- Raouf, A., Tsui, C.L., 1982. A new method for assembly line balancing having stochastic work elements. *Computers & Industrial Engineering* 6, 131–148.
- Rekiek, B., 2000. Design of assembly lines. Memoire presente en vue de l’obtention du grade de docteur en sciences appliquees. *Universite libre de Bruxelles*, Brussels, Belgium.
- Rekiek, B., De Lit, P., Delchambre, A., 2002. Hybrid assembly line design and user’s preferences. *International Journal of Production Research* 40, 1095–1111.
- Salveson, M. E., 1955. The assembly line balancing problem. *Journal of Industrial Engineering* 6, 18–25.
- Sarin, S.C., Erel, E., Dar-El, E.M., 1999. A methodology for solving single-model, stochastic assembly line balancing problem. *OMEGA—The International Journal of Management Science* 27, 525–535.
- Scholl, A., 1995. Balancing and Sequencing of Assembly Lines. *Physica-Verlag, Heildelberg*.
- Scholl, A., Boysen, N., 2009. Designing Parallel Assembly Lines with Split Workplaces: Model and Optimization Procedure. *International Journal of Production Economics*.
- Silverman, F.N., Carter, J.C., 1986. A cost-based methodology for stochastic line balancing with intermittent line stoppages. *Management Science* 32, 455–463.
- Sculli, D., 1979. Dynamic aspects of line balancing. *OMEGA— The International Journal of Management Science* 7, 557–561.
- Sculli, D., 1984. Short term adjustments to production lines. *Computers & Industrial Engineering* 8, 53–63.
- Shtub, A., 1984. The effect of incompleteness cost on the line balancing with multiple manning of work stations. *International Journal of Production Research* 22, 235–245.
- Süer G.A., 1998. Designing Parallel Assembly Lines, *Industrial Engineering Department*, University of Puerto Rico-Mayagüez.
- Suresh, G., Sahu, S., 1994. Stochastic assembly line balancing using simulated annealing. *International Journal of Production Research* 32, 1801–1810.
- Suresh, G., Vinod, V.V., Sahu, S., 1996. A genetic algorithm for assembly line balancing. *Production Planning & Control* 7, 38–46.
- Van Oyen, M.P., Gel, E.S., Hopp, W.J., 2001. Performance opportunity for workforce agility in collaborative and noncollaborative work systems. *IIE Transactions* 33, 761–777.
- Vrat, P., Virani, A., 1976. A cost model for optimal mix of balanced stochastic assembly line and the modular assembly system for a customer oriented production system. *International Journal of Production Research* 14, 445–463.

USING UWB FOR HUMAN TRAJECTORY EXTRACTION

²Gonçalo Vasconcelos, ^{†,3}Marcelo Petry, ^{†,1}João Emílio Almeida, ^{†,1}Rosaldo J. F. Rossetti, ⁴António Leça Coelho

[†]Artificial Intelligence and Computer Science Laboratory (LIACC)

¹Department of Informatics Engineering (DEI)

²Department of Electrical and Computer Engineering (DEEC)

Faculty of Engineering, University of Porto (FEUP)

³INESC TEC – INESC Technology and Science

⁴Laboratório Nacional de Engenharia Civil (LNEC)

{ee03120, marcelo.petry, joao.emilio.almeida, rossetti}@fe.up.pt, alcoelho@lnecc.pt

ABSTRACT

In this paper we report on a methodology to model pedestrian behaviours whilst aggregate variables are concerned, with potential applications to different situations, such as evacuating a building in emergency events. The approach consists of using UWB (ultra-wide band) based data collection to characterise behaviour in specific scenarios. From a number of experiments carried out, we detail the single-file scenario to demonstrate the ability of this approach to represent macroscopic characteristics of the pedestrian flow. Results are discussed and we can conclude that UWB-based data collection shows great potential and suitability for human trajectory extraction, when compared to other traditional approaches.

Keywords: UWB, pedestrian behaviour modelling, emergency planning, evacuation.

1. INTRODUCTION

The safety of people in emergency situations where panic can lead to unexpected or anti-social behaviour has been a subject of interest and study of researchers, engineers and authorities [1]. The study of pedestrian motion and behaviour is thus crucial for assuring the safety of people in situations such as confined spaces with large concentrations of people, which can lead to a large number of wounded and dead people in an evacuation scenario. However, studying crowd behaviour in emergency situations is difficult since it often requires exposing real people to the actual, possibly dangerous, environments [2].

Although models and simulation tools exist to help building designers and emergency planners, results are not generally satisfactory. Scientists and practitioners most of the time must rely on simplified models for which validation is problematic due to the lack of appropriate data, as well as reference models and benchmarks with which to compare. These models must, therefore, be calibrated against reliable data to ensure their validity.

To improve the knowledge related to pedestrian dynamics, it is necessary to develop experiments with volunteers where their movements are recorded and data is subsequently mined in order to extract meaningful information. Towards this goal, this paper reports on a series of experiments performed in different scenarios, using a radio frequency based indoor localization to collect the trajectories of every participant. The data resulting from the experiments will be used in the context of a larger project: “mSPEED” Simulator, an integrated framework constituting a unique tool for agent-based “Modelling and Simulation of Pedestrian Emergent Evacuation Dynamics” under development at LIACC. This tool will be used to validate new and existing building layouts, help planners develop and improve emergency plans and safety systems, train occupants using virtual drills, and help fire-fighters and rescuers develop plans, rescue strategies, and learn how to deal effectively with crowds during emergencies and critical situations.

The remainder of this paper is organised as follows. Section 2 presents some pedestrian data collection technologies, whereas Section 3 is used to detail the UWB-based approach for human trajectory extraction. Experiments are described in Section 4, whose results are discussed in Section 5. We finally draw conclusions and point out directions for further research in Section 6.

2. PEDESTRIAN DATA COLLECTION

Crowds and pedestrians have been empirically studied for the past decades [3,4]. The evaluation methods applied were based on direct observation, photographs, and time-lapse films. Video has been an important tool for observing pedestrians [5]. It is considerably better than direct observation, since the same scene can be studied over and over again, by human observation or using computer software with analysis algorithms.

Some research laboratories have been using video recordings of pedestrians to study and analyse their movement and extract patterns that can provide insight

into theories and mathematical models. One example is the Pedestrian Accessibility Movement Environment Laboratory – PAMELA built to better understand how people interact with the environment and thus how can designers mitigate some of the problems people encounter as they move around (<http://www.ucl.ac.uk/arg/pamela>). Its aim is to study and develop tools for helping people with accessibility problems or some kind of motor disability.

Besides video, other technologies are also used to capture pedestrian behaviour, such as Bluetooth, RFID [6], among others. One possible way of addressing this challenge is by using a combination of various sensors, called “Sensor Fusion”, combining data gathered from various sources, to help understand pedestrian movement and behaviour and thus enabling the creation of better and more complete databases.

In this paper, we propose the use of an ultra-wideband (UWB) radio frequency based indoor localization system for pedestrian dynamics trajectory tracking.

3. USING UWB FOR HUMAN TRAJECTORY EXTRACTION

3.1. UWB

According to Nekoogar [7], the usage of UWB based technology offers several advantages over narrowband communication systems, some of which Corrales, Candelas and Torres [8] claim are beneficial for indoor human tracking:

- Due to the short duration of UWB pulses, receivers are able to differentiate the original signals from the reflected and refracted ones, which make UWB based systems less sensitive to multipath fading.
- The low power UWB signals reside below the noise floor of typical narrowband receivers and enable UWB signals to share the frequency spectrum with other radio services with minimal or no interference.
- There are no line-of-sight restrictions due to the long wavelength, low frequencies included in the broad range of the UWB frequency spectrum ability to penetrate a variety of materials.
- As UWB transmission is carrierless, no modulation is required, and the low-powered pulses eliminate the need for a power amplifier, resulting in simple transceiver architecture and reduced infrastructure.

Although the experiments presented in this paper are very simple and performed under laboratory conditions, the usage of a radio frequency based system allows for a number of advantages over traditional data collection methods like automatic extraction of pedestrian trajectories from video recordings: as previously mentioned, there are no line-of-sight

restrictions and is also suited for low ceiling buildings. It also encompasses a wider breath of simulation scenarios, such as limited visibility situations (e.g. dark or smoke filled rooms), which are very common in emergency situations due to fire.

By assigning identifiable tags to individual participants, we are also able to easily associate some characteristics of the individual pedestrian (e.g. gender, height and age) with its trajectory. This might allow better understanding of the dynamics of heterogeneous crowds and study the effect of outliers like elderly people or people with mobility impairments.

3.2. Ubisense Description

The Ubisense (<http://www.ubisense.net/>) real-time location system is an in-building ultra-wideband radio based tracking system which can obtain accurate information of the positions of people and objects. This system uses small devices (tags) that send UWB pulses to a network of hardware receivers fixated in the localization area, which use a combination of TDOA (Time-Difference of Arrival) and AOA (Angle of Arrival) techniques to estimate the position of each tag [9]. These tags can be attached to objects or carried by personnel. Sensors can also be connected to a computer, and Ubisense also provides a middleware platform which can manage and filter real-time location information and simplify the creation of location aware applications that monitor several localization areas simultaneously.

The system provided by Ubisense has seen wide adoption by the industry, especially in manufacturing plants, providing location services for tracking assets in order to improve and better control processes [10]. Lately, it has also been used to track personnel during military and fire fighter training and operations [11], and as a behaviour analysis tool based on coordinates of body tags [12].

4. EXPERIMENTS

4.1. Aim

Our aim for the experiments described in this document is twofold. First, we aim to provide valid data for pedestrian dynamics model elicitation, as well as model validation in different facilities. Another goal is to evaluate the usage of a UWB based real-time location system for pedestrian movement data collection and trajectory extraction.

4.2. Setup

Experiments were performed in our lab, at FEUP (Fig.1), and were conducted with up to 30 participants, mostly students, whose average age was 21.4 ± 4.5 years and of mixed gender. For all experiments, the test persons were instructed to move with purpose, but not haste. These experiments follow a set of similar experiments performed in Germany at the Jülich Supercomputing Centre (JSC) [13–17], in which pedestrian trajectories were accurately extracted from

video recordings. In contrast, in our experiments automatic data collection is performed by assigning individual tags to participants, whose position was then tracked. Due to the limited number of tags available, our experiments were performed on a smaller scale.



Figure 1: Experiment setup a) Room and sensors b) Christmas hats with tags

After being secured at a height of 2.3 m from the ground, four sensors were placed in the four vertices of the bounding rectangle containing the area where experiments took place (Fig.1a). Within this area, different scenarios were built using tables and a vinyl foldable wall.

Tag placement plays an important role in ensuring that good readings will be achievable. Tags become difficult to read when they are in close proximity to materials that absorb a large amount of radio frequency energy, such as water, that makes up most of the human body. For the purposes of these experiments, tags were attached on top of Christmas hats secured with straps (Fig.1b). Although the system works well without direct line-of-sight, placing tags this way ensures unobstructed path between tags and sensors, which improves measurements and is advised by the Ubisense system setup instructions.

The experiments were divided in three general set-ups: single-file, narrow passage and corner and T-junction. Each set-up aims to provide data suitable to study different phenomena: fundamental relation in a simple scenario, unidirectional pedestrian flow through bottlenecks and more complex configurations like corners and merging of flows respectively. In this paper we are concerned to analyse the single-file scenario only, which is described in detail in the following sections.

4.3. The Single-File Scenario

The reduced degrees of freedom associated with movement along a line helps minimize the effects that might influence the relation between the density and velocity of pedestrian movement. Single-file movement is therefore the simplest system for investigation of this dependency, which is the goal of the first experiment. To avoid boundary effects and limit the amount of test people needed, this first scenario was composed of a looping track. Corridor width was defined such that it does not impede the free movement of arms but enforces single-file movement by preventing passing and the formation of multiple lanes (Fig.2).

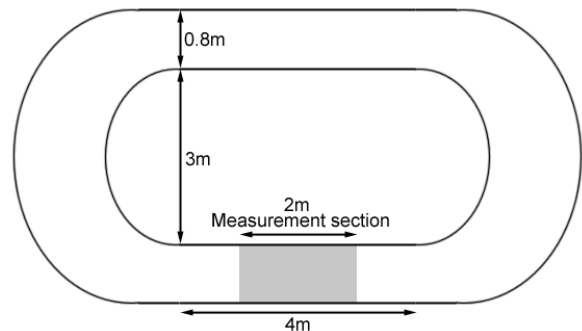


Figure 2: Experimental setup for the single-file scenario

Test subjects were instructed not to overtake and were distributed uniformly in the corridor. Each experiment run had each person complete two full loops before leaving the track. To regulate pedestrian density, three runs with 10, 15 and 20 randomly chosen pedestrians were performed. Ten runs with a single pedestrian were also performed with the purpose of free velocity determination.

Although trajectory data was collected for the whole track, only a section of the straight part with a length of 2 m was analysed, to avoid the influence of curves (shaded area in Fig.2).

5. RESULTS AND DISCUSSION

The UWB system used for data collection asynchronously reads tags' location: a stream of location events is generated over time; each event only contains information about the position of a single tag. Consequently the location of the crowd is updated one pedestrian at a time. Moreover, the system does not ensure a constant frequency of readings for each tag.

The mean frequency of location updates for a single tag in the collected data was 4.74 ± 1.74 Hz. This compares unfavourably with video collection techniques, where frequencies of 25 Hz are common and each frame contains data about all pedestrians.

One of the tags used during the experiments behaved erratically, and therefore was not considered for the purpose of representing trajectories. From the remaining stream of location events, trajectories were constructed for each pedestrian, whose representation for some experiments is presented in Fig.5.

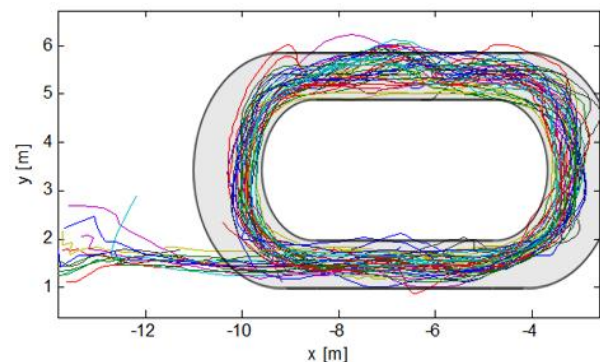


Figure 5: Extracted trajectories for the single-file scenario.

The collected trajectories appear to be jerky and imprecise. Considerable noise seems to affect some measurements as some trajectories are drawn outside the physically delimited track bounds, where pedestrians would be unable to reach.

Although the location system used can, under ideal conditions, achieve an accuracy of up to 20 cm, experiments and test scenarios could only reach sub-meter accuracy [18]. The inaccuracies of the positioning system explain the irregularities in the trajectories, and can be attributed to imprecisions in the calibration process, limitations of the information filter used by the location system framework, background noise, the agglomeration of large number of tags in confined areas and the signal attenuation caused by the presence of a large number of test persons.

5.1. Analysis of the single file experiment

Only a straight section with length $l_m = 2$ m was considered to determine the density-velocity relation of pedestrian movement. Entrance (t^{en}) and exit (t^{ex}) times were recorded for each pedestrian crossing the entrance (x^{en}) and exit (x^{ex}) of this section. From these times, both the average velocity

$$v_i = \frac{l_m}{t_i^{ex} - t_i^{en}} \quad (1)$$

of each crossing i as well as the number of persons inside the measurement section $N(t)$ at each instant t can be obtained. Taking into consideration the large period between consecutive measurements for each tag, a linear interpolation between the positions and instants when each tag is first located inside (x_i^{in} , t_i^{in}) or outside (x_i^{out} , t_i^{out}) the measurement section and the positions and times associated with the previous locations (x_i^{in-1} , t_i^{in-1} , x_i^{out-1} , t_i^{out-1}) are necessary to better estimate the exact entrance and exit times:

$$t_i^{en} = t_i^{in-1} + \left[(t_i^{in} - t_i^{in-1}) \frac{x^{en} - x_i^{in-1}}{x_i^{in} - x_i^{in-1}} \right] \quad (2)$$

$$t_i^{ex} = t_i^{out-1} + \left[(t_i^{out} - t_i^{out-1}) \frac{x^{ex} - x_i^{out-1}}{x_i^{out} - x_i^{out-1}} \right] \quad (3)$$

From the runs with a single pedestrian on the track, the free velocity $v_{free} = 1.33 \pm 0.13$ m/s, was obtained, which matches well with the value from literature (1.34m/s) [19].

Density at each instant t can be obtained from the instantaneous number of pedestrians N inside the measurement section.

$$\rho(t) = N(t)/l_m \quad (4)$$

As the measurement section is short, only small numbers of persons can be inside. Consequently the value of density calculated from the above definition jumps between discrete values. An enhanced definition of the density, calculated through the time headways between successive pedestrians avoids this problem, but

its calculation is a challenging task as the data collection system is unable to provide the location of two tags at the same instant, and also because inaccuracies would increase as error from two different measurements would have to be taken into account.

The density assigned to each pedestrian crossing the measurement section is determined as the mean value of density during the crossing:

$$\rho_i = \frac{1}{t_i^{ex} - t_i^{en}} \int_{t_i^{en}}^{t_i^{ex}} \rho_n dt \quad (5)$$

The differences between the mean value of density over time determined by this method or by the time headway method is negligible [20]. Fig. 6 shows the evolution of the crossings' speed and density in the measurement section over the whole duration of the run with 20 pedestrians.

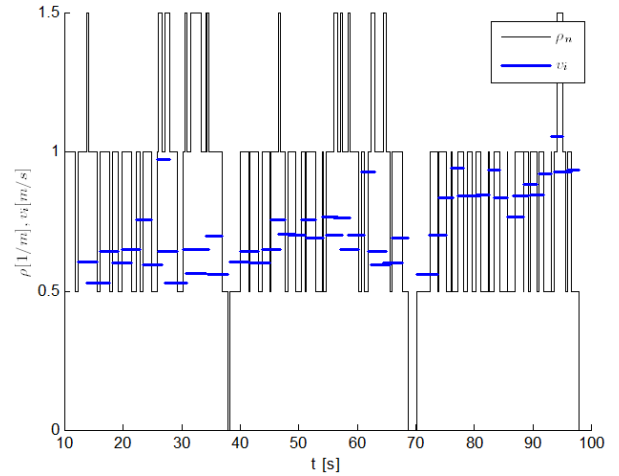


Figure 6: Evolution of speed v_i and density ρ_n over the duration of the experiment composed of 20 participants. Tick blue lines, whose length indicates the time interval a pedestrian is inside the measurement section, represent the mean velocity of the crossing.

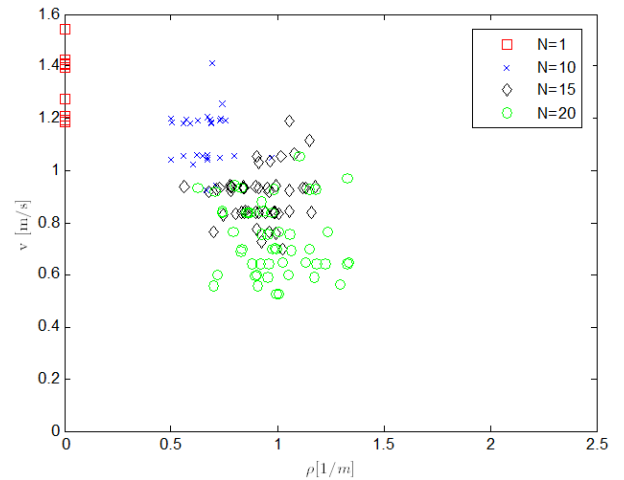


Figure 7: Relation between density and velocity in the single file scenario for the runs with 1, 10, 15 and 20 participants.

A graphical representation of the velocity (v_i) - density (ρ_i) pairs of each crossing is presented in Fig.7. This representation is known as the fundamental diagram of pedestrian movement.

In comparison with the diagrams obtained from similar experiments [13, 20], where data was collected manually from video recordings, similar values for density and velocity are found for runs with the same number of participants. However, our diagram is more disperse as a result of the limited precision of the UWB system. No data is presented for values of density over 1.2 1/m because when the experiment was performed no more than 20 voluntaries were present.

6. CONCLUSIONS

UWB based systems present a great potential for pedestrian data collection. Although more experiments are needed to validate this technique, it shows potential and suitability for human trajectory extraction.

Usage of this technology presents several advantages over traditional data collection techniques, expanding the breath of possible scenarios for experiments, such as situations of limited visibility for which data is inexistent. Compared with video recordings for tracking of people trajectories, UWB allows use in narrower spaces, lower ceilings and areas with line of sight restrictions. Other aspect is related with data collection. UWB based systems record the coordinates of position for each tag directly whereas video recordings must be later analysed and processed in order to extract positions/trajectories. Each tag carried by pedestrians is uniquely identifiable, allowing individual tracking thus enabling investigating both the dynamics of crowds and study the behaviour of specific individuals like child, elderly or people with mobility impairments.

On the down side, it has a lower sample rate than video: about 5 Hz in the case of UWB versus 25 Hz with video. Also, video techniques present synchronized results whilst UWB does not. Moreover, technical limitations such as lack of fine spatial precision make it not optimal for extracting microscopic properties of traffic, such as velocities and densities at a disaggregated level.

In conclusion, and when comparing the drawbacks with the advantages, UWB techniques for human trajectory extraction seems a viable approach. It is particularly suitable for scenarios where video is less applicable and pedestrian fine positioning is not an issue, such as for macroscopic analysis (e.g. egress time, path choice and behaviour scrutiny).

Future work will focus on the analysis of other experiments using different scenarios, following the same methodology. The results of this work will be used to validate and calibrate behaviour models in the "mSPEED" framework. This will constitute a unique tool for agent-based "Modelling and Simulation of Pedestrian Emergent Evacuation Dynamics" under development at LIACC.

ACKNOWLEDGMENTS

Authors would like to thank the volunteers who participated in this study. The second and third authors also acknowledge the financial support from FTC (Fundação para a Ciência e a Tecnologia) in form of PhD scholarships (grants SFRH/BD/60727/2009 and SFRH/BD/72946/2010).

REFERENCES

- [1] Almeida, J. E., Rosseti, R., & Coelho, A. L., 2011. Crowd Simulation Modeling Applied to Emergency and Evacuation Simulations using Multi-Agent Systems. *Proceedings of 6th Doctoral Symposium on Informatics Engineering* (pp. 93-104). Porto, Faculdade de Engenharia da Universidade do Porto.
- [2] Almeida, J. E., Kokkinogenis, Z., & Rosseti, R. J. R., 2012. NetLogo Implementation of an Evacuation Scenario. In: WISA 2012 (Fourth Workshop on Intelligent Systems and Applications), May 20-23, Madrid, Spain.
- [3] Cordeiro, E., Coelho, A. L., Rossetti, R. J., & Almeida, J. E., 2011. Human Behavior Under Fire Situations – Portuguese Population. In: Fire and Evacuation Modeling Technical Conference. August 15-16, Baltimore, Maryland, USA.
- [4] V.M. Predtechenskii and A.I. Milinskii, 1978. *Planning for Foot Traffic in Buildings*. Amerind Publishing Co. Pvt. Ltd., New Delhi.
- [5] D. Helbing, P. Molnar, I. Farkas and K. Bolay, 2001. Self organizing pedestrian movement, in *Environment and Planning B: Planning & Design*.
- [6] S. Sharma and S. Gifford, 2005. Using RFID to Evaluate Evacuation Behavior Models, NAFIPS 2005 Annual Meeting of the North American Fuzzy Information Processing Society, pp. 804-808.
- [7] F. Nekoogar, 2005. Introduction to Ultra-Wideband Communications, in *UltraWideband Communications Fundamentals and Applications*, Prentice Hall, pp. 1-44.
- [8] J. A. Corrales, F. A. Candelas, and F. Torres, 2008. Hybrid tracking of human operators using IMU/UWB data fusion by a Kalman filter, *Proceedings of the 3rd international conference on Human robot interaction HRI 08*, p. 193.
- [9] P. Steggles and S. Gschwind, 2005. The Ubisense smart space platform, in *Adjunct Proceedings of the Third International Conference on Pervasive Computing*, vol. 191, no. May, pp. 73-76.
- [10] J. Cadman, 2003. Deploying commercial location-aware systems, in *Proceedings of the 2003 Workshop on LocationAware Computing*, pp. 4-6.
- [11] U.S. Army Uses UWB to Track Trainees. Available from: http://www.ubisense.net/en/media/pdfs/casestudies_pdf/27863_rfidjournal-usarmy.pdf. [accessed 15 May 2012]
- [12] M. Luštrek, B. Kaluža, E. Dovgan, B. Pogorelc, and M. Gams, 2009. Behavior analysis based on

- coordinates of body tags, in *Ambient Intelligence*, vol. 5859, pp. 14-23.
- [13] A. Seyfried, B. Steffen, W. Klingsch, and M. Boltes, 2005. The Fundamental Diagram of Pedestrian Movement Revisited, *Journal of Statistical Mechanics: Theory and Experiment*, vol. 2005, no. 10, p. 13, 2005.
- [14] A. Seyfried et al., 2008. Enhanced empirical data for the fundamental diagram and the flow through bottlenecks, *Review Literature And Arts Of The Americas*, p. 12.
- [15] A. Seyfried, T. Rupperecht, O. Passon, B. Steffen, W. Klingsch, and M. Boltes, 2007. New insights into pedestrian flow through bottlenecks, *Transportation Science*, vol. 43, no. 3, p. 16.
- [16] J. Zhang, W. Klingsch, T. Rupperecht, and A. Schadschneider, 2011. Empirical study of turning and merging of pedestrians streams in T-junction, *Physics and Society*.
- [17] M. Boltes, J. Zhang, A. Seyfried, and B. Steffen, 2011. T-junction: Experiments, trajectory collection, and analysis. *IEEE*, pp. 158-165.
- [18] J. Xavier, P. H. Abreu, L. P. Reis, and M. Petry, 2011. Location and automatic trajectory calculation of mobile objects using radio frequency identification. *IEEE*, pp. 1-6.
- [19] Kuligowski, E. D., Peacock, R., & Hoskins, B. L. 2010. A Review of Building Evacuation Models, 2nd Edition. *NIST Technical Note 1680*. National Institute of Standards and Technology, U.S. Department of Commerce
- [20] U. Chattaraj, A. Seyfried, and P. Chakroborty, 2009. Comparison of Pedestrian Fundamental Diagram Across Cultures, *Advances in Complex Systems*, vol. 12, no. 3, p. 12.

STUDIES ON THE THERMODYNAMICAL COUPLING OF A MACHINE TOOL AND ITS ENVIRONMENT USING THE OBJECT-ORIENTED MODELLING APPROACH OF MODELICA

Matthias Rößler^(a), Michael Landsiedl^(b), Friedrich Bleicher^(c), Christian Salvatori^(d),
Wolfgang Kastner^(e), Felix Breitenecker^(f)

^{(a)(e)} Vienna University of Technology, Institute of Computer Aided Automation

^(b) dwh Simulation Services

^{(c)(d)} Vienna University of Technology, Institute for Production Engineering and Laser Technology

^(f) Vienna University of Technology, Institute of Analysis and Scientific Computing

^(a) matthias.roessler@tuwien.ac.at, ^(b) michael.landsiedl@drahtwarenhandlung.at, ^(c) friedrich.bleicher@tuwien.ac.at,
^(d) christian.salvatori@tuwien.ac.at, ^(e) wolfgang.kastner@tuwien.ac.at, ^(f) felix.breitenecker@tuwien.ac.at

ABSTRACT

As the necessity of lowering the energy consumption of manufacturing plants rises, the possibility to optimize a planned production hall becomes more and more important. Therefore the research project INFO, a project of the Vienna University of Technology in cooperation with industry partners and supported by the FFG, the Austrian Research Promotion Agency, creates an overall simulation of a cutting factory. This work deals with one aspect of such a simulation by studying the possibilities of coupling different partial models in one simulator. First the two partial models are built and their simulation results are compared to measurement data. The models are kept very simple to avoid numerical problems that could emerge from having an equation system that is too big. Then the two models are coupled and the problems that arise are analysed.

Keywords: thermodynamics, machine tool, Modelica, Dymola, MapleSim

1. INTRODUCTION

As the necessity of lowering the energy consumption of manufacturing plants rises due to increased energy costs and environmental awareness, the possibility to optimize a planned production hall becomes more and more important. Therefore the research project INFO, a project of the Vienna University of Technology in cooperation with industry partners and supported by the FFG, the Austrian Research Promotion Agency, creates an overall simulation of a cutting factory. This includes microscopic and macroscopic processes, like machines, the building hull or influences of the weather, where all manifestations of energy in and the energy flow between the single components are studied (Leobner, Ponweiser, Neugschwandtner and Kastner 2011). Because of the multitude of the used models, one aspect

of the project is to study the possibilities and difficulties of coupling different model parts.

In this paper the coupling of different model parts in one simulator will be studied. Therefore a model of a machine tool and a room model, which are then coupled, are chosen. The models are kept simple to identify the problems that occur because of the coupling of the model parts rather than numerical problems because of the size of the resulting equation system. The model of the machine tool is a linear guiding device and for the room model a compartment model is chosen. For both models exist test rigs, so they can be validated against measurement data.

Additionally a comparison of two different simulators, Dymola and MapleSim, is made. Both simulators rely on the same modelling approach, so their numerical behaviour and efficiency can be studied.

2. SIMULATORS

The Modelica Standard, which is maintained by the Modelica Corporation, uses an object-oriented approach to model physical systems. The system is simulated by building an acausal block-diagram, where every block represents a real component, for instance a linear translational spring. By using the defining equations for each component, which are stored in the representing blocks, and additional equations, that result from combining the blocks with acausal connections, an equation system is built, which can be solved by a simulator. It is important to note, that neither in the components nor in the connections a causality between the variables is assumed.

This approach works in various physical domains such as mechanics, electrical engineering or thermodynamics, which makes it possible to build multi-domain models. The Modelica Standard only provides a language to describe models in such a manner, to simulate the models a simulator, which

understands this language and provides the necessary algorithms to derive and solve the resulting equation system, has to be used. The current version of the Modelica Standard is version 3.2 (Modelica Corporation 2010).

As mentioned before two different simulators are used in this paper: Dymola and MapleSim. These simulators shall now be described briefly laying a focus on the functionalities used in this paper.

2.1. Dymola

The past of Dymola is closely related to Modelica as the Modelica Standard is developed from Dymola. Because of this Dymola can be seen as the simulator who understands the Modelica language best. Models can be built either graphically or textually. The version used in this paper is Dymola 2012, which supports the Modelica Standard 3.2. One of the main advantages is that all dissipative components have an optional heatport, which allows the use of the lost energy in an additional thermodynamical system.

2.2. MapleSim

MapleSim is developed by MapleSoft. Models can only be built graphically, but new components can be defined using either the Modelica language or a built in Maple function, where only the equations and ports have to be defined and a Modelica component is created automatically. MapleSim supports Modelica Standard 3.1, where the optional heatport is only used in the electrical resistor component; this means that for the other dissipative components the lost energy has to be measured to be used in a thermodynamical model.

3. MACHINE MODEL

The linear guiding device is a simple part of a machine tool; it consists of a permanent magnet DC motor that drives a thread bar via a gear belt. The thread bar moves a cart, where the sliding mass is attached. The test setup for the validation of the model is provided by the Institute for Production Engineering and Laser Technology from the Vienna University of Technology (Salvatori 2012) and is shown in Figure 1.

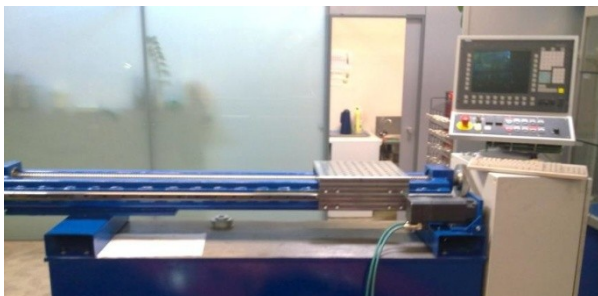


Figure 1: Test setup of linear guiding device

For the model components of the Modelica Standard Library were used, the general structure of the model can be seen in Figure 2. It shows that the structure of the model is very similar to the structure of

the real system, which is an important advantage of this modelling approach.

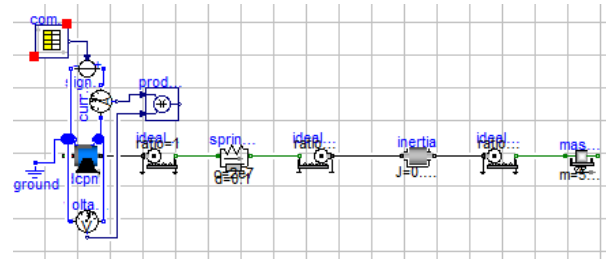


Figure 2: Model of the Machine Tool in Dymola

Due to the graphical representation of the model and the modular structure, the underlying equations are not easy to see, so the individual components of the model are described the following sections.

3.1. Permanent Magnet DC Motor

The electric motor is implemented as a permanent magnet DC motor model (Kral and Haumer 2011). The motor model was updated in version 3.2 of Modelica, so the models in Dymola and MapleSim differ in their complexity. Figure 3 depicts the model in Dymola.

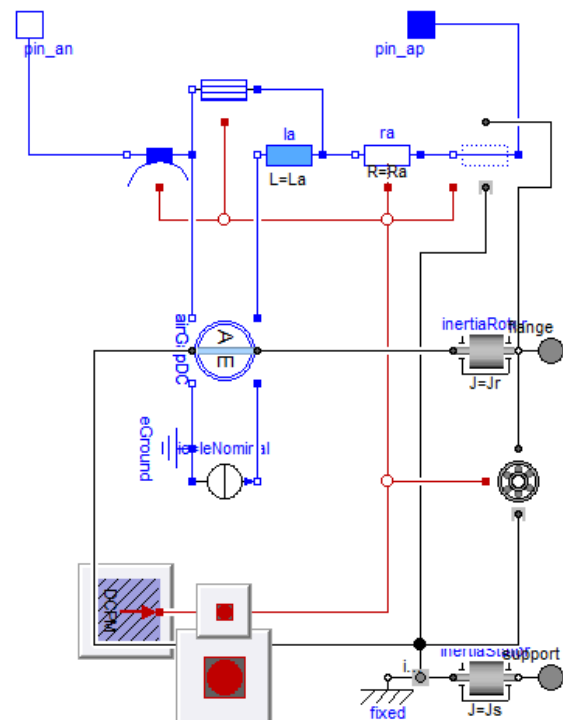


Figure 3: Model of a Permanent Magnet DC Motor in Dymola

It can be seen that many losses are taken into account in the model as many of the components have heatports, which are illustrated as red squares. Besides the heat losses in the armature winding resistance, which is modelled as a resistor component, the other power losses that are considered are

- Brush losses in the armature circuit
- Friction losses
- Core losses
- Stray load losses

The sole purpose of the four components is to model the respective losses, where the power loss depending on the angular velocity or the current is calculated. By setting these dependencies to zero the components have no impact on the simulation results, which will be important to compare the Dymola and the MapleSim model. As mentioned before the MapleSim model of the permanent magnet DC motor is not that complex, here the armature circuit is modelled as a inductor and a resistor connected in series. Because of that the only power losses that can be taken into account are the losses in the resistor component so for comparability reasons the losses in the other components of the Dymola model have to be zero.

The parameters for the component were taken from the datasheets of the motor used in the test setup.

3.2. Gear Belt

The spring constant of a gear belt is always given in a translational manner in the data sheets. Therefore it is modelled as a linear translational spring-damper element, where the damping constant of the component is chosen in such a way that a swinging up of the spring is prevented. The transition between the rotational and translational mechanical domain is made through ideal gears, so no power is lost in this transition.

3.3. Thread Bar

The defining parameters for a thread bar are its inertia and its lead. So the thread bar in this model consists of a inertia component and an ideal gear, where the transition ratio is directly proportional to the lead of the thread bar.

3.4. Cart and Mass

As the cart and the mass that shall be moved are rigidly connected to each other, they can be modelled as one mass. The component chosen for the model is a mass with stop and friction, where also a hard stop can be implemented, but is not considered for this model.

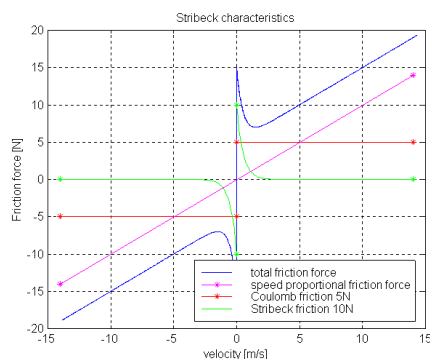


Figure 4: Characteristics of the velocity dependent friction force in Modelica

The friction model that is used in Modelica is called Stribeck friction model. It not only takes into account the static and the velocity dependent friction but also considers the so called Stick-Slip-Effect. This is modelled by an additional term that models the friction decreasing exponentially with rising velocity of the mass. The dependencies between friction force and velocity are depicted in Figure 4, which are taken from the documentation of the Modelica Standard Library.

The parameters of the friction were chosen in such a way, that the measurement data was approximated properly by the simulation results. This can be justified by the fact that the other mechanical components in the model are implemented at least nearly ideal, so the friction component can be seen as a cumulative component, where all the mechanical frictions in the system are considered.

3.5. Voltage Source

The input for the voltage source, that supplies the voltage for the electric motor, is stored in a time table. The entries of the table are derived from measurement data. The data was taken over the course of one displacement process. The measuring equipment was placed in front of the power electronics, so the first step of adjusting the data was to subtract the mean value of the data points in the idle state, because the power electronics is not considered in the model. Additionally, because the measured signal was very noisy, the data was filtered by a very simple algorithm. Every data point v_i is replaced with the mean value of $v_{i-2}, v_{i-1}, v_i, v_{i+1}, v_{i+2}$. This procedure is repeated ten times. The result of the filtering is depicted in Figure 5.

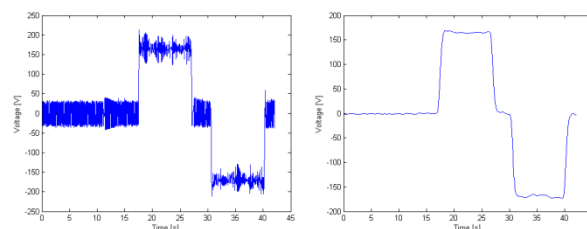


Figure 5: Input-Signal of Voltage Source before and after filtering

3.6. Simulation Results

To compare the simulation results with the measurement data the power consumption of the electric motor was used. Therefore the voltage and current in the armature circuit of the motor was measured in the model and then multiplied.

The first simulation runs were made using the unfiltered noisy signal on the left of Figure 5. The simulation results showed that the two simulators had very big problems to simulate the system. The results of the two simulators were very different depending very much on the solver algorithm, the step sizes. Additionally the simulation results had no real connection to the measurement data, because the noise in the input signal got stronger during the simulation.

Given the model does not account for the power electronics, the power consumption of the controller has to be added to simulation results, so they can be compared to the measurement data. Figure 6 and 7 show the results of the simulation runs in Dymola and MapleSim compared to the measurement data. Additionally the mean values of the power consumptions over time are shown.

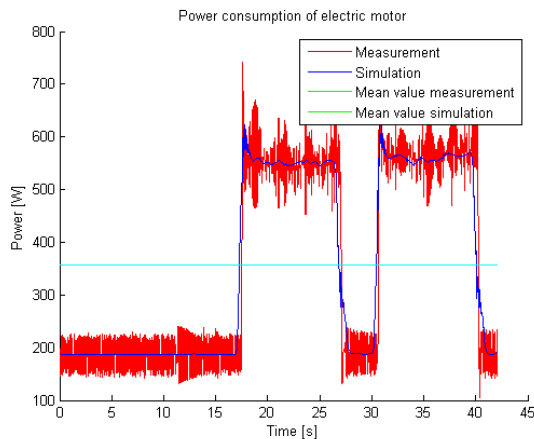


Figure 6: Simulation results in Dymola

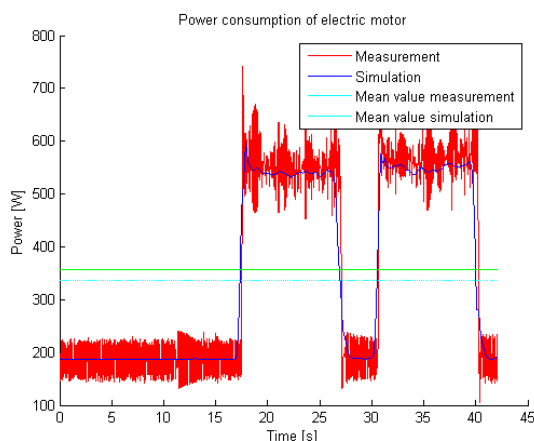


Figure 7: Simulation results in MapleSim

A qualitative analysis shows that the results of both simulators match the measurement data very well. Comparing the two simulators it can be seen that the results are slightly different. Also the mean values over the displacement period are different. Dymola matches the measurement data better in this regard, whereas the machine in MapleSim consumes lesser power over the course of one period.

4. ROOM MODEL

The surrounding of the machine is modelled through a compartment model. This means that the room model is discretized into compartments. The individual compartments can be seen as boxes of a certain size containing air. In reality such a model would have to take into account many things, so several assumptions are made for the model to simplify it:

- The temperature is constant within the compartment
- Heat flow is only permitted over the contact surface of adjacent compartments
- The only way of heat transport is conduction, no convection or radiation is taken into account.
- The walls of the room are perfectly isolated. No heat flow over the boundaries is permitted, so there is no energy lost in the system.
- The thermal parameters of the air are assumed to be independent from the temperature and therefore constant over time.

4.1. Compartments

Each compartment is implemented as a submodel. Figure 8 shows the basic structure of the compartment.

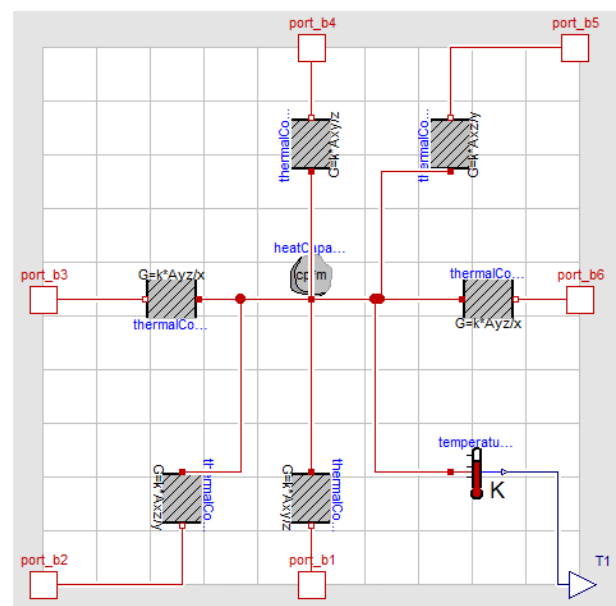


Figure 8: Basic structure of a single compartment in Dymola

In Figure 9 the parameters for the compartment block are shown. The size of the compartment is given by the expansion along the x-, y- and z-axis, which have to be adjusted to the used compartments. Other parameters that are used by the components within the compartment are derived directly like the volume or the area of the faces of the compartment. Also the thermal parameters of the medium, that the compartment is filled with, can be adjusted. The parameters are the specific thermal capacity, the density and the conductivity of the medium. As default the parameters are set to values that correspond to the thermal properties of air at 20°C.

The components used in the compartment submodel use these parameters to calculate the heat flow between the compartments. The heat capacitor which is located in the middle of the block depends on the thermal mass of the compartment, which can be derived from the volume and the specific thermal

capacity. In the heat capacitor component the temperature of the compartment is calculated.

Parameters	
x	0.2675
y	0.17
z	0.12
V	$x*y*z$
Axy	$x*y$
Ayz	$y*z$
Axz	$x*z$
cp	1012
rho	1.204
m	$V*rho$
k	0.0257

Figure 9: Parameters for the Compartment-block

Furthermore six conductor components for all possible directions of the heat transfer are implemented. To derive the heat flow through these components, the simple geometry of the compartment is used. The heat flow is then only dependent on the area of the contact surface between two compartments, the distance between the centres of the two, the thermal conductance of the medium and their temperature difference.

At last a temperature sensor to measure the temperature in the compartment is added.

4.2. Validation

For the validation of the model a test rig was built to see if the assumptions made for this model are too restrictive. Therefore a Styrofoam box was used, where eight temperature sensors were attached inside. As a heat source a soldering rod was used. The parameters of the eight compartments used in this model are depicted in Figure 9, the test rig and the model can be seen in Figure 10.

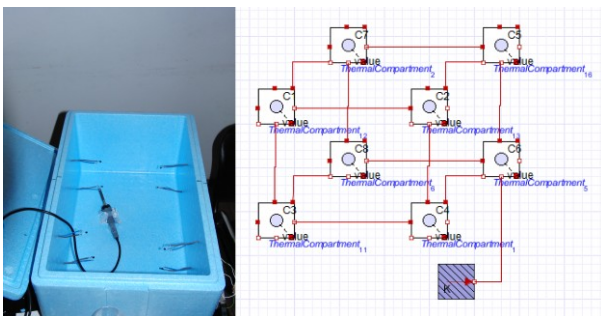


Figure 10: Test rig for the room model and model in MapleSim

The measurement data of the test rig can be seen in Figure 11, the simulation results of Dymola and MapleSim in Figure 12.

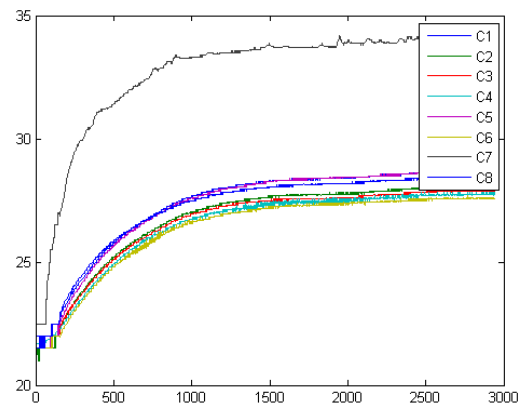


Figure 11: Measurement data of test rig for room model

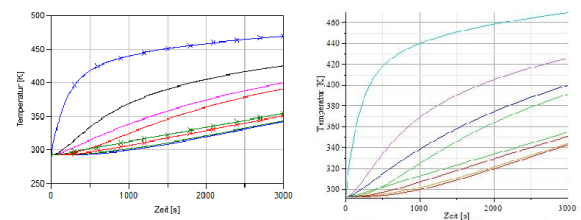


Figure 12: Simulation results from Dymola and MapleSim

It can be seen that the qualitative behaviour of the temperature in the compartment, where the heat source is attached, matches the measurement data, but the magnitude of the temperature rise in the simulation is disproportional. An explanation for this effect can be that the test rig is not isolated well enough, so the assumption of the perfectly isolated walls cannot be met. Further the other compartments heat up much more uniformly in the experiment than in the simulation. This has two main reasons. First in the test rig the heat can flow in any direction, whereas in the simulation it is only permitted in six. Second the convection, which is neglected in the simulation, allows a much smoother heat distribution in the experiment.

The comparison of the simulation results shows that the two simulators work equally good for this model.

5. COUPLING

In a final step the two models are coupled into one model. The energy lost in the dissipative components of the machine model is used as heat source for the room model. In the coupled model the machine stretches across two compartments. The heat loss of the electric motor is a heat source of one compartment and the heat lost through friction in the mechanical parts heats up another compartment. Figure 13 shows the coupled model.

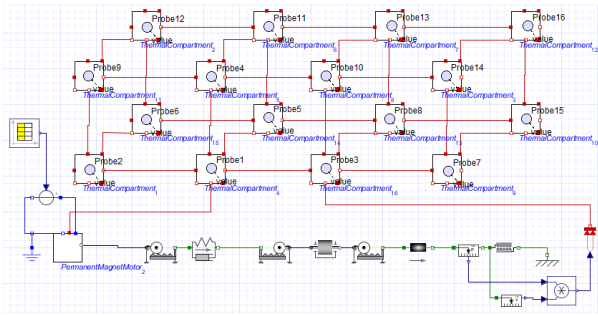


Figure 13: Coupled model in MapleSim

To model a machine hall the compartments in this model are much larger. The machine hall is assumed to have an expansion of 20m x 10m x 6m. Additionally changes in the machine model had to be made. In Dymola it was possible to activate the optional heatports to get the heat loss in the dissipative elements, whereas in MapleSim it was necessary to build a new permanent magnet DC motor component to retrieve the energy lost in the resistor of the armature circuit and to measure force and velocity at the friction component to calculate the heat from this component. Figure 14 depicts the simulation results in Dymola for a simulation time of six hours.

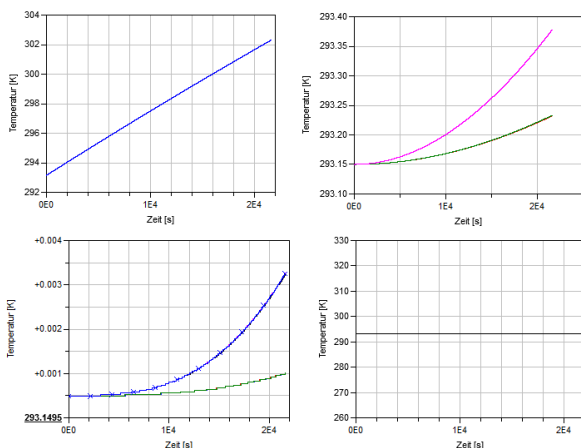


Figure 14: Simulation results of the coupled model in Dymola

More interesting than the simulation results itself are the computation times it took to simulate the model. The two simulators both needed about half an hour to compute this relative simple model. Seeing as the used models are too simplified to represent a real machine or machine hall leads to the conclusion that for more complicated models a coupling in one simulator is nearly impossible even with bigger computational power.

The main problem in coupling the two models arises because of the different time constants of the model parts. As the time constants for the electrical and the mechanical part of the machine model are similar, the thermal time constant is proportional to the thermal mass of the studied system. This has the effect that very small steps have to be made by the solver algorithm

compared to the relatively large simulation time and in each of these time steps the whole thermal model has to be calculated, which would not be necessary because of the slowly changing behaviour of the system. This can also lead to numerical problems through loss of significance.

6. CONCLUSION

For these particular models it is possible to couple them in one simulator, this is due to the simplicity of the models. As mentioned before having bigger, more complex models would take much more computational effort to simulate. To simulate a whole production hall over the course of a year is therefore not advisable with this approach.

For the machine model it is to say, that it provides satisfactory results if the input signal is smooth enough.

The room model is not sophisticated enough to represent a real room, for that the model assumptions are too restrictive. But the modular construction of the room model allows an easy refinement of the discretization of the model.

REFERENCES

- Leobner, I., Ponweiser, K., Neugschwandtner, G., Kastner, W., 2011. Energy Efficient Production – A Holistic Modelling Approach. *WCST2011-Proceedings*, 73-78. 7th–10th November 2011, London.
- Modelica Corporation, 2010. *Modelica – A Unified Object-Oriented Language for Physical Systems Modeling – Language Specification Version 3.2*. Available from: <http://www.modelica.org> [Accessed 9th July 2012]
- Salvatori, C., 2010, *Energieeffizienz von Werkzeugmaschinen - Planung und Aufbau eines Versuchsstandes zur Untersuchung eines Kugelgewindetriebes*, Bachelorthesis, Vienna UT
- Kral, C., Haumer, A., 2011. Object Oriented Modeling of Rotating Electrical Machines, In: Schmidt, M., eds., *Advances in Computer Science and Engineering*, Croatia: InTech.

SEQUENCE OF DECISIONS ON DISCRETE EVENT SYSTEMS WITH STRUCTURAL ALTERNATIVE CONFIGURATIONS

Juan-Ignacio Latorre-Biel^(a), Emilio Jiménez-Macías^(b), Mercedes Pérez-Parte^(c)

^(a) Public University of Navarre. Department of Mechanical Engineering, Energetics and Materials.
Campus of Tudela, Spain

^(b) University of La Rioja. Industrial Engineering Technical School.
Department of Electrical Engineering. Logroño, Spain

^(c) University of La Rioja. Industrial Engineering Technical School.
Department of Electrical Engineering. Logroño, Spain

^(a) juanignacio.latorre@unavarra.es, ^(b) emilio.jimenez@unirioja.es, ^(c) mercedes.perez@unirioja.es

ABSTRACT

The management of certain systems, such as manufacturing facilities, supply chains, or communication networks implies assessing the consequences of decisions, aimed for the most efficient operation. This kind of systems usually shows complex behaviors where subsystems present parallel evolutions and synchronizations. Furthermore, the existence of global objectives for the operation of the systems and the changes that experience the systems or their environment during their evolution imply a more or less strong dependence between decisions made at different time points of the life cycle. This paper addresses a complex problem that is scarcely present in the scientific literature: the sequences of decisions aimed for achieving several objectives simultaneously and with strong influence from one decision to the rest of them. In this case, the formal statement of the decision problem should take into account the whole decision sequence, making impractical the solving paradigm of “divide and conquer”. Only an integrated methodology may afford a realistic solution of such a type of decision problem. In this paper, an approach based on the formalism of the Petri nets is described, several considerations related to this problem are presented, a solving methodology based on the previous work of the authors, as well as a case-study to illustrate the main concepts.

Keywords: Petri nets, sequence of decisions, metaheuristic, discrete event system, alternatives aggregation Petri nets, optimization

1. INTRODUCTION

Real and complex systems, regarded as discrete event systems, may require a decision making process to be useful for certain applications, such as industrial manufacturing, supply chain, computer systems, and communication networks. The decisions may be more or less difficult to take, regarding to the system itself,

the considered application, and the objectives to be achieved. For allowing the decision making, the discrete event system should present one or several freedom degrees or undefined characteristics leading to an undefined discrete event system (Latorre et al, 2011c).

These undefined characteristics may belong to the behavior or to the structure of the system. Several solving methodologies can be considered. In order to develop a more or less general procedure for solving the decision-making problem it is convenient to represent the decision-making problem in a formal language.

Moreover, simulation consists of a technique for trying to foresee the future behavior of the system, under specific initial conditions, that can cope with a broad range of systems and configurations. The result of this formalization of the decision problem is usually an optimization problem, including a model of the system able to perform simulations (Latorre *et al.* 2011c).

1.1. The paradigm of the Petri nets

Different formal languages can be chosen for modeling a given discrete event system. For example, it may be considered queuing networks, finite state machines or automata, Petri nets, or generalized semi-Markov processes (Moody and Antsaklis 1998).

In this case, the paradigm of the Petri nets has been chosen for several reasons. First of all, an undoubted advantage of Petri nets is the double graphical and matrix-based representation. This particular feature of the Petri nets make them very intuitive and powerful, for structural analysis as well as for performance evaluation and simulation.

A second interesting characteristic of the Petri nets is their natural way to represent complex behaviors that include parallelism and synchronizations (Silva 1993), and for the body of knowledge in the field of the Petri nets, which has been developed in the last decades (Balbo and Silva 1998).

The undefined characteristics of the original discrete event system can be expressed in the resulting

model by means of undefined parameters, leading to the concept of undefined Petri net (Latorre *et al.* 2011a). The parameters of a Petri net can play different roles and, subsequently, may be classified accordingly into different types, such as structural, marking, transition-firing, or interpretation parameters.

An overview of different approaches for solving an optimization problem based on an undefined Petri net can be found in (Latorre *et al.* 2011b).

1.2. Optimization processes

The mentioned approaches range from series of optimizations for certain initial conditions chosen manually, including a partial automation of the search for the optimal values associated to the non-structural parameters to the methodology proposed in (Latorre *et al.* 2011b), where a single search for all types of parameters is afforded.

This approach based on a single optimization process has been presented for a decision that corresponds to an instant in the evolution of the discrete event system. This instant may be related to a stage in the design process of the system or a change in the configuration of the freedom degrees of the system or in the freedom degrees themselves.

The optimization process can be solved for the mentioned decision problem focused on an instant in the operation of the DES and a solution can be obtained, where all the undefined parameters will take specific values (Latorre *et al.* 2010). Once a solution for the undefined parameters has been obtained, it is necessary to perform a backwards translation from the undefined parameters to the undefined characteristics of the original discrete event system or freedom degrees, in order to solve the decision problem stated on the original system and not on its model.

The rest of the paper is organized as follows. The section 2 is focused on the statement of the problem aimed to obtain a sequence of decisions based on a discrete event system. The section 3 outlines some approaches aimed to solve the mentioned problem aimed to afford a sequence of decisions. Sections 4 and 5 describe two case studies, while section 6 draws the conclusions and future research lines. The article is completed with a section of acknowledgements and the bibliography.

2. SEQUENCE OF DECISIONS

Some real situations in the design and operation of an undefined discrete event system might lead the decision maker not to a single decision, where some freedom degrees can be specified, but to a sequence of decisions.

This sequence of decisions can be afforded by means of separated optimization processes, following the paradigm of “divide and conquer” or by means of a single optimization.

Examples of this kind of complex problems are the scheduling of tasks, the planning of operations, the routing of conveying parts, and in general the control of

the equipment in a manufacturing facility (Piera and Mušič 2011; Bai *et al.* 2010; Ramirez *et al.* 1993).

It is very usual that this kind of problem requires making a sequence of decisions related to transition-firing parameters. The mentioned parameters, which are the ones that usually appear in this kind of problem, are the priority of firing the transitions involved in conflicts, which arise during the operation of the system.

In order to clarify the concept of undefined parameters and the different types of them, which will be considered in this paper, the following considerations are presented.

2.1. Undefined parameters

The Petri net model of a discrete event system is a formal and quantitative representation of the structure and behavior of the original system. The parameters that configure the Petri net can be classified according to their function in the model. Any of these parameters can be undefined ones, giving place to an ambiguity or non-determinism that can be solved by means of an appropriate decision.

Definition 1. Parameter of a Petri net.

Any numerical variable of a Petri net model or its evolution. □

Definition 2. Undefined parameter.

Any numerical variable of a Petri net model or its evolution that has not a known value but it has to be assigned as a consequence of a decision from a set of at least two different feasible values. The value assigned to the undefined parameter after a decision must be unique. □

Definition 3. Defined parameter.

Any parameter of a Petri net that is not undefined (see **definition 2**). □

Notice that a decision that chooses a feasible value for an undefined parameter transforms the parameter into a defined one.

The undefined parameters of a Petri net can be classified according to their function in the model. A non-exhaustive classification, but useful for many the abbreviations and extensions of the ordinary Petri nets is the following:

Definition 4. Structural parameter.

Numerical value for any element in the input or output incidence matrices of a Petri net. The elements of the incidence matrices determine the weight of the arcs that link the nodes of the Petri net (places and transitions). □

An example of structural parameters arises from the different manufacturing strategies of the case study presented in (Latorre *et al.* 2009). The flow of parts and information (production request) in the manufacturing facility is modelled by weighted arcs between nodes of the Petri net. Different strategies imply diverse weights

in some elements of the incidence matrices; hence, before choosing a manufacturing strategy, some structural parameters are undefined ones.

Definition 5. Marking parameter.

Number of tokens in a particular place of the Petri net in the initial state of its evolution. In the case of a high-level (coloured) Petri net it includes the attributes (colour) of every token.

□

Definition 6. Transition-firing parameter.

Priority of firing a transition involved in a structural conflict or time of firing an enabled transition in the case of free speed firing.

□

Priority is a concept related to priority Petri nets, where the inherent non-determinism related to actual or effective conflicts is solved by associating priorities to the transitions of the net.

In a structural conflict, there is an ordering for firing the involved transitions, which are taken from the priority relation. These priorities determine which transition should be fired when an actual or effective conflict arises. For more information on the different type of conflicts see, for example, (David and Alla 2005).

On the other hand a free speed firing is a topic usually related to the performance improvement of a system by not firing a transition immediately after it becomes fireable (maximal speed) but at the time when, for example, the performance of the system is the best that can be achieved.

An example of undefined parameters related to effective conflicts can be found in a case study described in (Latorre *et al.* 2010). In this example, an optimal sequence of decisions for controlling the operation of a manufacturing facility is searched, as well as a series of decisions related to the design of this system.

Definition 7. Interpretation parameters.

Events, logic conditions, time delays or outputs associated to any node (place or transition) of a certain Petri net.

□

Notice that this kind of parameter might be called synchronization parameters as well.

It is interesting to take into account that the undefined transition firing and interpretation parameters include the usual controllable parameters considered in the classic control theory of DES.

2.2. Outcome of the decision process.

Following with the considerations presented in the previous sections, there are different possibilities to cope with the problem mentioned in the introduction of this section 2.

One possibility consists of giving a sequence of decisions that optimize the objective of the operation of the system.

It is also possible to provide with a summary of this information in the form of a scheduling for the

different machines, a best production mix or sequence of manufacturing, a fixed priority associated to a given transition, a preferred dispatching rule, etc (Mušič 2009, Zimmerman *et al.* 2001).

Another common way to afford this type of problem consists of developing a supervisor, for example in the form of a complementary Petri net model, which is able to prevent the system to reach certain states, such as deadlocks.

In general, it is possible to state that the amount of computational resources required to solve a decision problem depends on the size of the solution space. For real applications, this size is usually very large, no matter if the problem consists of a single decision, giving values to a set of undefined parameters, or a sequence of decisions.

2.3. Methodology for solving sequences of decisions and parameters of the PN

The usual methodologies for solving sequences of decisions may be different regarding the undefined parameters present in the model of the system. Usual undefined parameters in the case of scheduling, planning, or routing are undefined transition-firing parameters, in particular priorities associated to the firing of the transitions involved in conflicts (Piera and Mušič 2011).

However, other type of undefined parameters can be obtained as a result of the translation into a formal language of the undefined characteristics or freedom degrees of the original undefined discrete event systems.

In industrial applications an example in the use of undefined marking parameters can be found when the model of the feeding process of raw materials in a factory is afforded.

Furthermore, undefined interpretation parameters, such as the delay time associated to an enabled transition to become fireable are less usual, but may also be considered to model different layouts of the same machines in a manufacturing facility, which imply diverse conveying time for the parts, when moved from a given machine to another one.

Finally, undefined structural parameters can be associated to the design of a discrete event system or a modification in its structure once the system is in operation (Latorre *et al.*, 2009).

2.4. Parameters that vary over time

The research performed on systems whose parameters vary over time, as is the case of taking a sequence of decisions to modify the values of certain undefined parameters of the Petri net, has been focused mainly on specific topics of the field.

Furthermore, many researches have been devoted to solving efficiently the conflicts that arise in the evolution of a Petri net, for example to perform the scheduling of tasks in a manufacturing facility.

On the other hand, different formalisms for modeling systems with a changing structure have been

developed and deeply studied, such as graph grammars, reconfigurable Petri nets, or self-modifying Petri nets (Ehrig *et al.* 2008; Llorens and Oliver 2004; Badouel and Oliver 1998; Valk, 1978) respectively.

However, these formalisms are not specially defined for solving sequences of decisions or single-decision problems.

Other formalisms, such as a compound Petri net, a mixed set of alternative compound and simple Petri nets, an alternatives aggregation Petri net, or a disjunctive coloured Petri net have been developed for the decision making and can easily be applied for solving sequences of decisions. See for example (Latorre *et al.* 2011c).

3. SOLVING APPROACHES

A sequence of decisions can be required for an undefined discrete event system or, expressed in other language, for its formal counterpart: an undefined Petri net. The undefined Petri net is associated to a set of undefined parameters, also called controllable ones (Latorre *et al.*, 2011c). Two main approaches can be taken into account for making the sequence of decisions.

3.1. The paradigm of “divide and conquer”

On the one hand, the approach of “divide and conquer” may afford the solution of the problem by means of a decomposition of the set of decisions, made for assigning values to specific parameters, into different groups associated to diverse optimization problems.

A natural criterion for grouping the decisions into optimization problems is time. The evolution of the system may require making decisions at certain time points, as a consequence of significant changes in one or several of the elements that define the formal statement of a decision problem: an optimization problem.

The start-up of the operation of an undefined discrete event system requires taking decisions according to the solution of the formal representation of the decision problem: an optimization problem. If one or several elements of this optimization problem are modified, the best solution for the original problem may not be the best for the modified problem or even it might not be a feasible solution. For this reason a new decision problem should be stated and solved.

A given point in time that requires making decisions may be associated to different conditions in the environment of the discrete event system. This situation may happen, for example, in an industrial facility, due to a change in the cost of raw materials, or a variation in the demand.

Furthermore, a change in the system itself may also require making a decision. For example if a machine breaks down or stops its production, or the value assigned as a consequence of a decision to a given undefined parameter is not a feasible value anymore, it is necessary to take the appropriate decision to return as

soon as possible to a normal operation of the discrete event system.

This approach of “divide and conquer” may be useful in case that the decisions in the sequence are independent among them, in the sense that at a certain decision is reactive to a given change in the environment or the system itself and has the purpose of maximizing the objective function, disregarding future decisions.

This situation might arise when the changes in the environment or the system are unforeseen, as happens with the breakdown of a machine or a change in the demand of the manufactured products.

As a consequence, different methodologies, available in the scientific literature, can be applied to solve the required decision making for achieving the objective of the operation of the discrete event system under the new conditions (Piera and Mušič 2011; Latorre *et al.* 2011c; Bai *et al.* 2010; Mušič, 2009; Zimmerman *et al.* 2001; Moody and Antsaklis 1998; Ramirez *et al.* 1993.

3.2. Single-process approach

A second approach for making sequences of decisions consists of stating and solving a single optimization problem. In the statement of this problem, undefined parameters might arise, not only in the model of the system but also in the other elements of the optimization problem, such as the objective function.

This single optimization problem might present a very large solution space, in fact a family of solution spaces, one for every decision, which should be explored in the same solving process.

An approach like this may be more convenient than the “divide and conquer” paradigm, previously mentioned, when the decisions of the sequence are programmable, for example if it is possible to decide the time point and the order of the changes in the environment or the system itself.

In these cases, it is clear that the decisions to be made influence strongly one another, and for this reason it is convenient to make every decision in relation to the others from the same sequence and in relation to the global objective of the operation of the discrete event system.

4. EXAMPLE OF THE PREVENTIVE MAINTENANCE

The industrial field provides with several examples of problems, where a sequence of decisions should be made and it is possible to decide the moment and the order of a series of changes in the environment or the system itself, which lead to the need of a sequence of decisions to keep the system under an efficient operation.

4.1. Programming of the preventive maintenance.

The first of the examples consists in the preventive maintenance programming of the machinery of a manufacturing facility.

This problem requires making the decision of using efficiently the available maintenance resources for minimizing the cost, the time required for the maintenance operations, and the loss of production if the manufacturing facility does not stop the production during the maintenance process.

In this last kind of problem, where the manufacturing facility is in production when the preventive maintenance is already in progress, the structure of the discrete event system changes accordingly to the machines that are stopped for maintenance, while the rest of them are producing.

4.2. Choice of a formalism appropriate for simulation

A methodology based on the simulation of a selected number of feasible configurations requires an appropriate model for the alternative structural configurations, which the factory may have. In order to include this feature in the model of the system, a formalism including a set of exclusive entities is a natural and easy way to represent the original discrete event system.

In particular, a compound Petri net, an alternatives aggregation Petri net, or a disjunctive coloured Petri net are examples of appropriate models for this kind of system. In this kind of models, a sequence of decisions to specify the order of stopping and maintaining the different machines is associated to a sequence of decisions that choose one after another a subset of the exclusive entities related to the model (Latorre-Biel *et al.* 2011c).

4.3. Solving methodology

A test of the most promising of these sequences, for example by means of a search in the solution space guided by a metaheuristic, may lead to the optimal sequence for the maintenance operations. Every maintenance operation will require a decision on the investment of resources. This assignment of maintenance resources will determine the duration of each maintenance operation and the different time points for their beginning.

The methodology presented in this paper to solve this problem includes the following steps:

1. Determine the model of the discrete event system in complete operation.
2. Obtain the diverse alternative structural configurations that correspond to the different maintenance operations that imply to stop different machines.

3. Construct a compact model including all the different alternative structural configurations.
4. Determine the rest of the elements of the optimization problem, including the objective function, which should reward the objectives of the manufacturing process, as well as the goals of the maintenance operations. One critic specification of the problem consists of the completion of all the maintenance operations.
5. Apply a metaheuristic for finding a good solution, that would include the order and type of maintenance operations, their time points, the maintenance resources invested in the operations, and the configuration of the freedom degrees of the remaining manufacturing equipment for producing efficiently during the maintenance operations.

4.4. Structural modification

In fact, this kind of problem can be rewritten as a problem for deciding the structural variation of a Petri net model at certain time points for achieving optimally a goal at the end of the time period, when the structure of the model remains constant or is modified for other reasons, different from the preventive maintenance operations.

An easier version of the previous problem appears when the achievement of two of the objectives, to reach a maximal yield from the manufacturing operations and to obtain a maximal efficiency in the maintenance operations are disengaged in time.

This situation arises when the manufacturing facility stops the production operations in certain periods of time and the duration of the stops can be devoted to the maintenance operations. The usual time for these operations of preventive maintenance are the holidays, weekends, and nights, depending on the manufacturing facility under study.

5. ANOTHER EXAMPLE

A second example of this kind of problem can be found in the change of production in certain manufacturing facilities where this process implies an investment of time and resources.

In these kind of factories it is common that in a certain period of time, different changes of the final products manufactured are performed to obtain a stock of a range of different type of products for satisfying the demand and, perhaps, to store a certain amount of them in the warehouse.

The modification in the production mix may imply a change in the structure of the Petri net model, related to the layout of the manufactured parts or the information required to organize the manufacturing operations.

6. CONCLUSIONS

In this paper, the general problem of defining a sequence of decisions in the design or operation of a discrete event system is afforded. This general problem requires the consideration of a changing structure of the model of the system. Whereas diverse formalisms based on the Petri net paradigm have been developed for representing a variable structure in a Petri net, the problem of deciding what is the optimal evolution for this variation has not been solved yet.

In this paper, some considerations on the statement and solution of this kind of problem have been presented and outlined based on the previous work developed by the authors.

Nevertheless, there already are many issues to be researched before a general statement of this kind of problem can be considered completely solved.

ACKNOWLEDGMENTS

This paper has been partially supported by the project of the University of La Rioja and Banco Santander (grant number API12-11) 'Sustainable production and productivity in industrial processes: integration of energy efficiency and environmental impact in the production model for integrated simulation and optimization'.

REFERENCES

- Bai, Q., Ren, F., Zhang, M. and Fulcher, J., 2010. Using colored petri nets to predict future states in agent-based scheduling and planning systems. *Journal of Multiagent and Grid Systems - Advances in Agent-mediated Automated Negotiations archive*. Volume 6 Issue 5,6. IOS Press Amsterdam.
- Badouel, E., Oliver, J., 1998 Reconfigurable nets: a class of high level petri nets supporting dynamic changes with workflow systems. *Research Report* No. 3339, INRIA (Institut national de recherche en informatique et en automatique).
- Balbo, G. and Silva, M. (editors), 1998 *Performance Models for Discrete Event Systems with Synchronizations: Formalisms and Analysis Techniques*. Editorial Kronos, Zaragoza, Spain.
- David, R., Alla. H., Discrete, 2005 *Continuous and Hybrid Petri nets*. Springer,
- Ehrig, H., Hoffmann, K., Padberg, J., Ermel, C., Prange, U., Biermann, E. and Modica, T., 2008. Petri Net Transformations. In: Vedran Kordic, ed. *Petri Net. Theory and Applications*. I-TECH Education and Publishing, Vienna,
- Latorre, J.I., Jiménez, E., Pérez, M., 2009 Decision taking on the production strategy of a manufacturing facility. An integrated methodology, *Proceedings of the 21st European Modelling and Simulation Symposium* (EMSS 09). Puerto de la Cruz, Spain, vol. 2, pp. 1-7.
- Latorre, J.I., Jiménez, E., Pérez, M., 2010 A genetic algorithm for decision problems stated on discrete event systems. *Proceedings of the UKSim 12th International Conference on Computer Modelling and Simulation*, pp. 86-91. Cambridge, United Kingdom.
- Latorre-Biel, J.I., Jiménez-Macías, E., Pérez, M., 2011. The exclusive entities in the formalization of a decision problem based on a discrete event system by means of Petri nets. *Proceedings of the 23rd European Modelling and Simulation Symposium* (EMSS 11). Rome, Italy, pp. 580-586.
- Latorre, J.I., Jiménez, E., Pérez, M., 2011. Simulation-Based Optimization for the Design of Discrete Event Systems Modeled by Parametric Petri Nets. *Proceedings of the UKSim 5th European Modelling Symposium on Mathematical Modelling and Computer Simulation* (EMS2011), pp. 150-155. Madrid, November.
- Latorre, J.I., Jiménez, E., Pérez, M., 2011 Petri nets with exclusive entities for decision making. *International Journal of Simulation and Process Modeling, Special Issue on the I3M 2011 Multiconference*. Inderscience Publishers.
- Llorens, M. and Oliver, J., 2004. Structural and Dynamic Changes in Concurrent Systems: Reconfigurable Petri Nets. *IEEE Transactions On Computers*, Vol. 53, No. 9.
- Moody, J.O., Antsaklis, P.J., 1998. *Supervisory Control of Discrete Event Systems Using Petri Nets*. Kluwer Academic Publishers, Boston.
- Mušič, G., 2009. Petri net based scheduling approach combining dispatching rules and local search. *Proceedings of the 21st European Modelling and Simulation Symposium* (EMSS 09). Puerto de la Cruz, Spain, vol. 2, pp. 27-32.
- Piera, M.A. and Mušič, G. 2011. Coloured Petri net scheduling models: Timed state space exploration shortages. *Mathematics and Computers in Simulation*. Elsevier.
- Ramírez, A.; Campos, J.; Silva, M., 1993 On Optimal Scheduling in DEDS. *Proceedings of the 1993 IEEE International Conference on Robotics and Automation Atlanta, USA*, pages 821-826.
- Silva, M., 1993. Introducing Petri nets. In: Di Cesare, F., ed. *Practice of Petri Nets in Manufacturing*, pp. 1-62. Ed. Chapman&Hall.
- Valk, R., 1978. Self-Modifying Nets, a Natural Extension of Petri nets. *Proceedings of Icalp'78. Lecture Notes in Computer Science*. Vol 62. Pages 464-476.
- Zimmermann, A.; Freiheit, J.; Huck, A., 2001. A Petri net based design engine for manufacturing systems. *International Journal of Production Research*, Vol. 39, No. 2, pages 225-253..

AUTOMATIC DESIGN BASED ON THE PETRI NETS PARADIGM

Juan-Ignacio Latorre-Biel^(a), Emilio Jiménez-Macías^(b)

^(a) Public University of Navarre. Department of Mechanical Engineering, Energetics and Materials.
Campus of Tudela, Spain

^(b) University of La Rioja. Industrial Engineering Technical School.
Department of Electrical Engineering. Logroño, Spain

^(a): juanignacio.latorre@unavarra.es, ^(b): emilio.jimenez@unirioja.es

ABSTRACT

From ancient times, it has been a dream of human beings the automation of the hardest works to prevent humans from the inconveniences of these tasks. Not only dangerous, remote and repetitive tasks but also mechanical operations that require high precision, speed or repeatability have been automated. The industrialized modern society requires an efficient and sustainable use of the available resources for producing goods and services for the consumers. For achieving this objective, the manufacturing facilities and equipment, chain supplies and products themselves should be designed for verifying certain specifications. In this paper, the design process of a product, such as a production plant, chain supply or a good produced for the final customers is addressed under the light of the modeling paradigm of Petri nets in order to automatize some of the stages of this operation.

Keywords: product design, Petri nets, automation, decision support system

1. INTRODUCTION

From ancient times, it has been a dream of human beings the automation of the hardest works to prevent humans from the inconveniences of these tasks. Not only dangerous, remote and repetitive tasks but also mechanical operations that require high precision, speed or repeatability have been automated.

Along the last decades, a research effort has been devoted to the physical activities and also to the intellectual work performed by humans. The advantages of this approach are many, especially in situations where it is necessary to make difficult decisions due to the influence of a large amount of information, the consideration of systems with complex behavior, etc.

The industrialized modern society requires an efficient and sustainable use of the available resources for producing goods and services for the consumers. For achieving this objective, the manufacturing facilities and equipment, chain supplies and products themselves should be designed for verifying certain specifications.

A global environment for the manufacturing, distribution, commercializing, recycling, and waste

management produces a network of interrelations of multiple actors that makes difficult the decision process in the design of such systems.

For this reason, the development of decision-support systems constitutes a great help in the development of efficient manufacturing facilities, chain supplies and final products. In this paper, the design process of a product, such as a production plant, chain supply or a good produced for the final customers is addressed under the light of the modeling paradigm of Petri nets in order to automatize some of the stages of this operation.

1.1. The paradigm of the Petri nets

The design process involves multidisciplinary work teams, where managers, research and development engineers, sale executives, production engineers, procurement technicians, financial experts, etc. share information, knowledge, a common objective, and should make the best decisions.

The different professional and academic background of the staff involved in the design process make difficult the interchange of information with the accuracy that a critical process, such as the design of a product or a service, requires. However, a fluid interchange of information between design teams and between the members of any of these teams is crucial to develop a successful design process.

A formal language to represent the information concerning the design alleviates the different tasks, where professionals belonging to diverse sectors are involved. Petri nets is a paradigm very well suited for performing this role, since its formal nature and the different interpretations and levels of abstractions allow representing a system in its design process, as well as in the different stages of its life cycle (Silva and Teruel 1997 and Silva and Teruel 1998).

In particular, several Petri net formalisms have been developed for the design process of a discrete event system: alternative Petri nets, compound Petri nets, alternatives aggregation Petri nets, and disjunctive coloured Petri nets (Latorre *et al.* 2011b; Latorre *et al.* 2011d; Latorre *et al.* 2010e).

Moreover, a formal language, such as the ones based on Petri nets, allows the development of a deep analysis of the system in process of being designed, i.e. validation, verification, performance measurement by steady state analysis or simulation.

For this reason, the modeling of the system, by means of Petri nets, may be helpful, not only in the task of representing the system formally and without ambiguity, but also in the process of designing a system free of flaws and optimal according to the criteria set up in the decision problem of choosing the best alternative solution.

1.2. The Petri nets in the design of discrete event systems

Petri nets have been broadly used for the representation of systems in different stages of the design process of a discrete event system and in different technological and industrial sectors. Several are the authors, who have reported applications of this formal language to different case-studies or have developed general or specific methodologies to increase the reliability, automation, and efficiency of certain steps in product and service design.

For example, (Silva and Teruel 1998) surveys and illustrates the utilization of Petri nets in several stages of the life cycle of modern manufacturing systems. Different types of manufacturing systems and usual problems that may arise in the design and operation of these systems are addressed, such as their modeling and control. One of the goals of this reference consists of proving the utility of the paradigm of the Petri nets as the sole formalism to be used during the whole life cycle of the system.

Furthermore, a specific formalism belonging to the family of the Petri nets is considered in (Horváth *et al.* 2000). In this paper it is proposed the application of advanced Petri-net (APN) as a means for modelling design processes together with the decision patterns of designers. According to the reference, the in-process decisions made by designers strongly influence both the process of designing and the manifestation of the designed artefact. An APN is a bi-layer allocated architecture with linked, bipartitioned, directed, and attributed multi-graphs. The case study that presents the conceptualization and design process of a product is described to illustrate the adequacy of APN technique for simultaneous modelling of design actions and decisions.

A more general point of view is given by (Girault and Valk, 2001). This article illustrates the progress in the development and application of formal methods based on Petri net formalisms. It contains a collection of examples arising from different fields, such as flexible manufacturing facilities, telecommunication networks and workflow management systems. The book covers the main phases in the life cycle of the design and implementation of a discrete event system. Some of the stages taken into account are specification of the system, the model checking techniques for verification,

analysis of properties, code generation, and execution of appropriate models.

A more specific approach is provided in (Zimmerman *et al.* 2001). In this paper it is described the Petri net based design engine TimeNET, which is a software tool intended for the efficient design and operation of complex manufacturing systems, integrating modeling, analysis and control methodology. The independent modeling of structural and functional system parts by means of coloured stochastic Petri nets is suggested. TimeNET contains a library of common submodels for this purpose, which includes some parameters, such as processing times or buffer capacities. Qualitative analysis, as well as different evaluation techniques for an efficient performance prediction is implemented: direct numerical analysis, approximated analysis and simulation. The evaluation of different control strategies is also considered. An application example is given to illustrate the use of the mentioned tool and methodology.

Moreover, (Rust *et al.* 2003) introduces a high level Petri net model for real-time systems with dynamically changing structure. The reference describes a load balancing algorithm, implemented as a part of the model itself, for dynamically allocate tasks to computing devices. A design process composed of the modeling, analysis and partitioning and synthesis, is proposed. The high-level Petri net is extended with constructs for self-modification, leading to a self-modifying net, where the transitions are labeled with rules for net transformations and their firing imply a modification in the current net.

The following reference, (Carmona *et al.* 2004), focuses on the application of the Petri nets in designing asynchronous circuits from, for example, specifications in hardware description languages. The described methods avoid using full reachability state space for logic synthesis. On the contrary these methodologies, include direct mapping of Petri nets to circuits, structural methods with linear programming, and synthesis from unfolding prefixes using boolean satisfiability problem solvers.

A different approach is considered by (Lorenz *et al.* 2007), which addresses the synthesis problem for P/T-nets from a behavioral description. According to this methodology, the behavior is given in terms of a finite partial language, as a finite set of labeled partial orders (LPOs). The computed net is a finite representation of the so called saturated feasible net whose places correspond to regions of the given partial language.

An industrial application is presented in (Gradišar and Mušič, 2007), which describes the application of timed Petri nets and the existing production data to the algorithmic modeling of manufacturing systems. Production-data management systems provide information concerning the structure of a production facility and the products that can be produced. The Petri net is built directly following a top-down approach,

from the bill of materials and the routings. This reference describes a timed Petri net simulator developed in Matlab and an application example aimed at the scheduling of an assembly system.

With a similar industrial application, but a different modeling methodology, (Lee and Jeong, 2008) addresses the modeling of a manufacturing system by means of the paradigm of the Petri nets under a bottom-up approach. The presented methodology focuses as well in the design of a controller with deadlock prevention policy. This reference follows a hierarchical procedure that considers a resource model, a process model and a controller. An example is given with the purpose of illustrating the methodology presented in the article.

Furthermore, a different formalism belonging to the family of the Petri nets is considered in (Staines, 2009). This paper describes the modeling, analysis and evolution of a reduced coloured Petri net for fault diagnosis and recovery in embedded and control systems. The reduced coloured Petri net is a compact form of a coloured Petri net having complex token types based on sets containing the structured information for error handling. This approach can reduce the size of the coloured Petri net because information is put in the token by means of the folding of places and transitions. This approach is illustrated with an example of a control system.

An approach outside of the industrial field is presented in (Bergenthum et al., 2009). The authors address the modeling of a business process by means of the Petri nets paradigm as a step in a methodology for decision making. This methodology starts collecting scenarios from domain experts to create a behavioral specification. The reference presents an algorithm for the synthesis of a Petri net, based on refinements, which leads to a model of small size.

In the paper (Latorre et al., 2009) a methodological approach for designing DES is described. The design process from the combinatorial creation of complete solutions for the DES in process of being designed to the choice of the best one for the aimed application is addressed in this methodology. The classic approaches of divide and conquer and the methodology based on the formalism of the alternatives aggregation Petri nets are compared. Some propositions on the alternative aggregation Petri nets are stated, among them the equivalence of the optimization problem based on a set of alternative Petri nets and the one based on an alternative aggregation Petri net constructed from the others.

A large amount of examples can be found in (Labadi and Chen, 2010). This survey stresses the advantages of Petri nets as modeling and analysis tools for the specific field of logistics systems. The paper is organized as a review of the scientific literature on the topic. The reference is focused on the most recent developments in the application of Petri net based approaches for modeling, qualitative or structural

analysis, performance evaluation, and the subsequent optimization.

The main objective of the previous references consists of the development of tools, methodologies, or formalisms that may help in the process of design discrete event systems.

This help may consist on a systematic approach, an environment that ease the development of models of systems, automatic procedures to solve design problems from different type of specifications, the development of new formalisms that allow representing the model of the system in several stages of its life cycle, the improvement of the verification and validation of models of the system in process of being designed, the application of design techniques to different application fields.

In the following, the general procedure of designing a product or a service will be addressed. It will be considered all the important stages, from the gathering of relevant data, obtained from the market, competitors, new technologies, or former design projects, to the beginning of the manufacturing process of the final product.

Section 2 will address the general procedure of designing a product, while in section 3, the problem of automatizing some of the stages involved in the design process are considered. Some conclusions are presented in section 4, as well as some general research lines for the future, related to the automation of the process of designing a product.

2. STAGES OF THE DESIGN PROCESS

In a general case, it is possible to structure the steps involved in the design process of a product or service in four different stages.

These stages are usually developed in a sequential manner, but a process of concurrent engineering may lead to the parallelization of some of them. In fact, some of the steps that compose every one of the mentioned four stages can be developed concurrently by different multidisciplinary teams, which work with the same objectives.

The four mentioned stages are detailed in the following:

2.1. Investigation and definition

This step consists of finding the need that the product or service is aimed to satisfy, as well as analyzing different sources of information for helping in the creative process of developing solutions.

These sources of information may include customers, products sold by the competitors (analyzed by reverse engineering), solutions from other sectors or markets, new technologies, patents, reports, journals, exhibitions, social networking, previous design projects, or a creative process itself.

In this phase of the design, the specifications of the system should be stated in the design brief and the product design specification. Petri nets is a formal paradigm well suited for this task.

2.2. Design and development (conceptualization)

This second stage consists on using the information gathered in the previous phase to create partial solutions able to solve specific subproblems in the design process.

Examples of these kinds of subproblems in product design may be the design of the mechanical components, the electric design, the aesthetic design, or the industrial design. Once this task has been concluded, it is possible to afford the process of generating complete solutions by mixing appropriately the mentioned partial solutions.

Every one of the obtained solutions consists of an alternative system, which can be chosen as a definitive design.

In fact, the process of combining the different subsystems in diverse ways to obtain complete alternative solutions to the design problem can be stated as a combinatorial process. As a consequence, the generation of complete alternative solutions can aim to count on the largest and most varied range of feasible solutions to select the most promising one. It is not unusual, that this process implies a different problem: the combinatorial explosion, where a huge number of complete solutions can be constructed from a relatively small amount of partial solutions.

This important phase leads to the configuration of the solution space of the design problem. In order to state the decision problem, it is necessary to define more elements than the solution space.

One important component of the decision problem is the model of the system in process of being designed. A classical approach for the modeling of the system consists on developing a different model for every one of the complete solutions developed for the design process. When using the paradigm of the Petri nets as modeling formalism, the different models are called alternative Petri nets (Latorre *et al.* 2011a). In a situation, where a huge number of alternative solutions arise, the idea to develop an independent model for every alternative solution is unaffordable by standard methodologies.

Fortunately, other compact formalisms have been developed to represent a system in process of being designed (Latorre *et al.* 2011b). These type of models allow the automation of the decision process in a single step and ease the development of methodologies to construct automatically the complete solutions for a design process from a set of partial solutions.

Other important element of the decision problem is the objective function, usually based on performance measurements of the model of the system. These performance measurements can be calculated by the simulation of the behavior of the system under a set of scenarios, which are chosen from an expected operation of the system.

To complete the statement of the decision problem, some additional constraints can be added. They may be

related to restrictions in the operation of the system in process of being designed.

Once the decision problem is stated, a methodology to solve the decision problem can be afforded leading to the best solution for the product design process as outcome.

The solution of the decision problem usually requires the evaluation of the quality of the complete alternative solutions by means of simulation and the evaluation of the objective function.

In this phase, due to the problem of the combinatorial explosion it may be necessary a previous step of selecting the most promising solutions to be evaluated.

2.3. Planning and production

This stage requires the creation of a production plan and the development of a prototype. Depending on the type of product that is being designed, it may not be possible to develop a prototype and the closest activity to this operation is the development of a model of the system in a formal language, such as the Petri nets. For example, this is usually the case when a manufacturing facility is designed.

On the other hand, the production plan can be developed in parallel to the previous stage in a process called concurrent engineering. Thanks to this approach, it is possible to reduce considerably the time delay from the conception of the idea to design a new product and the start of its manufacturing.

2.4. Evaluation

This step consists of a test of the prototype in order to decide if all the expected specifications are met. Due to the fact that a prototype is not always developed in the design process of a product, this stage of evaluation may be included in the decision process of step 2.

Once the design process of a product has been finished, it is ready to be produced. Consequently, the following stages of the product design are the manufacturing, quality control and storage, distribution, selling, and set up, where some of these steps can be skipped according to the type of product (or service) offered to the customers.

3. AUTOMATION OF THE DESIGN PROCESS

There are, of course, variations on the previous sequence of stages that may alleviate the development of diverse phases of the design process.

For example, if the solution space developed in the second phase is not exhaustive enough or the selection of solutions to be analyzed performed in the third stage is not large enough, it is possible to perform an iterative process of refining a good solution by searching in its vicinity in the solution space, that is, modifying local features that improve the overall quality of the solution. The triggering of this iterative process consists of an evaluation process, such as the one described in the fourth stage of the design process.

The first stage of the design process has received little attention from the research community of modeling and simulation based on the paradigm of Petri nets. In fact, different computer-based tools are available for obtaining information from the market and other sources, in order to detect needs of the potential customers and know alternative solutions for satisfying the needs. Additional information about the regulations and additional constraints are used for developing a set of specifications for the solutions to be chosen. The second stage begins with a data-intensive process of gathering information of alternative products already existing in the market, products with similar specific features, commercial subsystems, and other sources in order to construct new solutions.

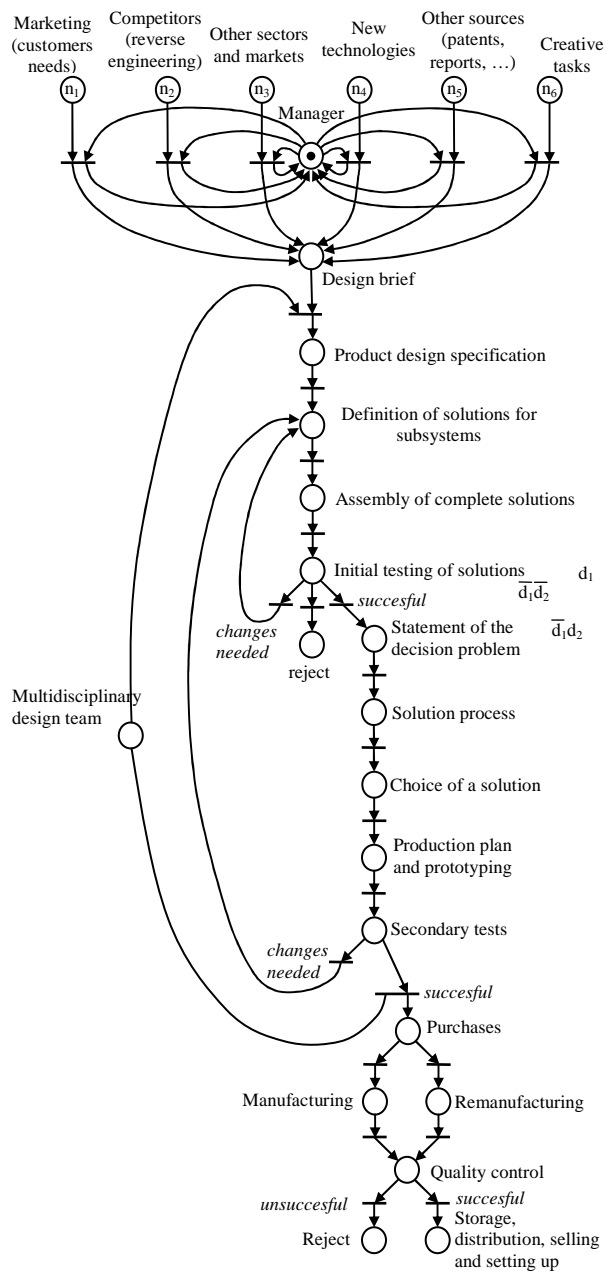


Figure 1: Petri net representing the general process of product and service design.

This process of constructing new solutions from the gathered data is, in part, a combinatorial problem, since partial solutions can lead to adequate solutions to the current design problem. This stage consists in building up the solution space by solving a constraint satisfaction problem, since the valid solutions should verify the specifications defined in the previous stage.

Most of these stages can be alleviated by the use of the paradigm of the Petri nets. However, this particular stage of building up different alternative solutions may show an intensive use of Petri nets in a modeling process, as proven by the bibliography. The different modeling approaches developed for Petri nets lead to the building of formal models. The qualitative analysis techniques, which are applicable to Petri net models, allow developing correct models.

The evaluation of the quality of the different alternative solutions may be afforded by means of formal methods, based on the calculation of performance parameters by means of steady state analysis or simulation. If it is required a previous stage of selecting a subset of the solution space, it is possible to apply different techniques. One of the successful methodologies based on a probabilistic search are the use of metaheuristics to guide the search of the best solutions, in combination with the calculated performance parameters.

In order to obtain the best solution it is possible to construct an objective function with the performance measurements calculated in the previous step and choosing the one that provides with the highest value. This stage and the previous one can be completely automated (Latorre *et al.* 2011b).

4. CONCLUSIONS

In this paper, the automation of the design process of a system is discussed. The diverse stages in the design process are presented and the different degrees of automation, achieved by different authors, are reviewed. Moreover, an approach to automatize a large amount of steps, belonging to different stages in the design process, proposed by the authors of this paper, is described.

Future research lines should afford the detailed analysis of the stages of the design process that have been less analyzed by means of the formalism of the Petri nets, such as the stage of investigation and definition. These stages use to be the ones considered as more creative. Hence, the complete automation of the design process might require a better understanding of the underlying brain processes related to the creative processes.

ACKNOWLEDGMENTS

This paper has been partially supported by the project of the University of La Rioja and Banco Santander (grant number API12-11) 'Sustainable production and productivity in industrial processes: integration of energy efficiency and environmental impact in the

production model for integrated simulation and optimization’.

REFERENCES

- Bergenthum, R.; Desel, J.; and Mauser, S. “Synthesis of Petri Nets for Business Process Design”. *Fundamenta Informaticae - Application of Concurrency to System Design* archive Volume 95 Issue 1. IOS Press Amsterdam, The Netherlands. January 2009.
- Carmona, J.; Cortadella, J.; Khomenko, V.; and Yakovlev, A. “Synthesis of Asynchronous Hardware from Petri Nets”. In Desel, J.; Reisig, W. and Rozenberg, G. (Eds.): *Lectures on Concurrency and Petri Nets: Advances in Petri Nets*, volume 3098 of *Lecture Notes in Computer Science*, pages 345-401. Springer-Verlag, 2004.
- Girault, C. and Valr, R. (Eds.) “Petri Nets for System Engineering: A Guide to Modeling, Verification and Applications”. Springer-Verlag, 2001.
- Gradišar, D. and G. Mušič. “Production-process modelling based on production-management data: a Petri-net approach”. *International Journal of Computer Integrated Manufacturing*, Vol. 20, No. 8, pp. 794-810, 2007.
- Horvath, I.; Vergeest, J.S.M.; and Van der Vegte, W.F. “Modeling design processes and designer decisions with advanced petri-nets”. In Lehoczky, L. and L. Kalmar (Eds.), *International Computer Science Conference* (pp. 81-90). University of Miskolc. Miskolc, Hungary. 2000.
- Labadi, K. and Chen, H. “Modelling, analysis and optimisation of supply chains by using Petri net models: the state-of-the-art”. *International Journal of Business Performance and Supply Chain Modelling*. Vol. 2. Nos. 3/4. 2010.
- Latorre, J.I., Jiménez, E., Pérez, M., Blanco, J., “The problem of designing discrete event systems. A new methodological approach,” *Proceedings of the 21st European Modelling and Simulation Symposium (EMSS 09)*. Puerto de la Cruz, Spain, vol. 2, pp. 40-46, September 2009.
- Latorre, J.I., Jiménez, E., Pérez, M., “Coloured Petri Nets as a Formalism to Represent Alternative Models for a Discrete Event System”. *Proceedings of the 22nd European Modelling and Simulation Symposium (EMSS 10)*. Fez, Morocco, pp. 247-252, October 2010.
- Latorre, J.I., Jimenez, E., Pérez, M., Blanco, J. and Martínez, E. “The optimization problem based on alternatives aggregation Petri nets as models for industrial discrete event systems”. *M&S Optimization Applications in Industry and Engineering*. The Society for Modeling & Simulation International. 2011.
- Latorre-Biel, J.I., Jiménez-Macías, E., Pérez, M., " The exclusive entities in the formalization of a decision problem based on a discrete event system by means of Petri nets ". *Proceedings of the 23rd European Modelling and Simulation Symposium (EMSS 11)*. Rome, Italy, pp. 580-586, September 2011.
- Lee, J.; and Jeong, I. J. “Design of Petri nets based controllers for the synthesis of manufacturing systems”, *Proceedings of SKISE Spring Conference*, May 15, 2008.
- Lorenz, R.; Bergenthum, R.; Mauser, S.; and Desel, J. “Synthesis of petri nets from finite partial languages”. *Proceedings of the 7th International Conference on Application of Concurrency to System Design (ACSD)*, pages 157–166, 2007.
- Rust, C.; Stappert, F.; and Schamberger, S. “Integrating Load Balancing into Petri-Net based Embedded System Design”. *The European Simulation and Modeling Conference (ESMC 2003)*, 1st October 2003.
- Silva, M., Teruel, E. “Petri nets for the Design and Operations of Manufacturing Systems”, *European Journal of Control*, 3, 82–199, 1997.
- Silva, M.; and Teruel, E. “DEDS Along their Life-Cycle: Interpreted Extensions of Petri Nets”. *IEEE International Conference on Systems, Man and Cybernetics*. San Diego, USA. 1998.
- Staines, A.S. “A Compact Colored Petri Net Model for Fault Diagnosis and Recovery in Embedded and Control Systems”. *International Journal of Computers*. Issue 2, Volume 3, 2009.
- Zimmermann, A.; Freiheit, J.; Huck, A. “A Petri net based design engine for manufacturing systems”. In: *International Journal of Production Research*, Vol. 39, No. 2, pages 225-253. 2001.

AUTHORS BIOGRAPHY

Juan Ignacio Latorre, Ph.D. in Industrial Engineering, has developed his professional career in the industry and in educative institutions. He is assistant professor in the Department of Mechanical Engineering, Energetics and Materials in the Public University of Navarre (Spain). His main research interests are factory automation, simulation and modeling of industrial processes and formal methodologies to solve decision problems based on DES. His main research activities have been performed with the modeling, simulation and optimization research group of the University of La Rioja (Spain) in the field of decision-support systems based on models of DES.

Emilio Jiménez is a Professor in the Electrical Engineering Department at the University of La Rioja, where he leads the modeling, simulation and optimization group. His main research interests include factory automation, modeling and simulation of industrial processes and formal methodologies to solve decision problems based on DES.

DECISION MAKING IN THE RIOJA WINE PRODUCTION SECTOR

Juan-Ignacio Latorre-Biel^(a), Emilio Jiménez-Macías^(b), Julio Blanco-Fernández^(c), Juan Carlos Sáenz-Díez^(d)

^(a) Public University of Navarre. Department of Mechanical Engineering, Energetics and Materials.
Campus of Tudela, Spain

^(b and d) University of La Rioja. Industrial Engineering Technical School.
Department of Electrical Engineering. Logroño, Spain

^(c) University of La Rioja. Industrial Engineering Technical School.
Department of Mechanical Engineering. Logroño, Spain

^(a) juanignacio.latorre@unavarra.es, ^(b) emilio.jimenez@unirioja.es,
^(c) julio.blanco@unirioja.es, ^(d) juan-carlos.saenz-diez@unirioja.es

ABSTRACT

The global environment, where many companies compete for their survival, requires a continuous adaptation to changes in the market and to other environment variables. Food industry, agriculture in particular, is a field, where the companies are especially sensitive to modifications in regulations and market requirements. It is very convenient to provide the companies of this sector with a theoretical basis, as well as with practical tools for developing an efficient management that may guarantee not only their survival but also their success. In this area, decision support systems based on the simulation of models, developed by means of the paradigm of the Petri nets, can offer a significant help for improving the efficiency of the farming companies, based on the proper decision making. In this paper, a methodology for decision making, supported by artificial intelligence (and dispatching rules), is applied to the farming field and an application case is analysed for better understanding of the advantages and drawbacks of this approach. In particular, a decision making methodology for improving the management of traditional companies in the farming industry is applied to the wine sector in the region of La Rioja (Spain).

Keywords: workstation design, work measurement, ergonomics, decision support system

1. INTRODUCTION

This section shows the application of the paradigm of the Petri nets to the modelling of business processes in the food industry, performed with success by different authors. The developed methodologies allow modelling and analysing the procedures underlying business processes as a tool for the continuous improvement and even for their complete redesign.

The efficient management of an agricultural corporation constitutes a key strategy for improving farming yield and encourage stable production for small

producers. (Shikanai *et al.* 2008) develops an information system to support the management of the cultivation of sugarcane. By applying this system, the small agricultural producers are able to manage their work systematically and efficiently, accomplishing low-cost and highly-efficient cultivation with full mechanization. The system proposed allows the automatic construction of a farm work database, used for simulating the operation of effective farming.

In the field of the wine industry, (Ferrer *et al.* 2008) develops a methodology, not based on a Petri net model, able to provide with an optimized scheduling for the coordinated activities that correspond to the wine grape harvesting and end in the supply of the crop to a couple of wineries.

(Melberg and Davidrajuh 2009) shows that fish farming industry finds in Petri nets a suitable formalism for the modelling and simulation of the different stages and events related to this field. The work examines the atlantic salmon fish farming processes and the different stages are modelled by a scalable hierarchical structure.

(Guan *et al.* 2010) deepens in the decision making process in intensive farming units for improving profits and reducing costs. The efficient management of the small farming business is performed by means of the strategy of intensive agriculture and a structure of farmers' cooperatives or agricultural corporations. For an efficient management of these farming units, appropriate decisions should be made regarding timeliness in all operations, crop rotations, equipment adjustments, and land rent, leading to an increase of yield, profitability, and work efficiency. The authors have applied a methodology for solving the farm work scheduling problem based on modelling by hybrid Petri nets and optimization. It considers nondeterministic events, such as machine breakdown and labour absence. The optimization methodology is completed by a metaheuristic search in the solution space performed by a genetic algorithm.

The application of a decentralized Petri-net execution engine to a workflow for a wine-production process is presented by (Cicirelli *et al.* 2010). The proposed system allows a smooth transition among the various stages of the process lifecycle. It shows as well the coordination of distributed execution of models and a support for dynamic evolution and reconfiguration.

(Léger *et al.* 2011) addresses one specific but very important process for companies in the farming field: the crop protection using the smallest amount of chemical pesticides. In order of providing a decision support system for allowing farmers handling with large amount of available information, the crop protection decision workflow system is presented and applied to the case of wheat.

The issue of the certification of pollution-free agricultural products is considered in (Wang *et al.* 2011). This paper provides with a Petri-net based model for the pollution-free agricultural regulatory system and a subsequent performance analysis of the mentioned workflow model. The presented methodology allows an easier process management than previous existing techniques.

As a traditional sector, wine production has not received much attention from the scientific community for developing efficient management methodologies based on modelling by Petri nets and simulation for decision support system.

La Rioja is a well-known region of Spain for its long tradition in the production of wine and the high quality of the wine with the qualified designation of origin. Several climate features characterizes the grapes harvested in different parts of the region, in addition to the differences related to the growing of diverse varieties of grapes. Moreover, small farming businesses, scattered in the region, produce relatively reduced quantities of high quality grapes and are usually integrated in farmers' cooperatives. These corporations distribute their crop to the different wineries of La Rioja to produce red, white and rosé wines with the highest standards.

The market for high quality products from the food industry requires keeping the highest standards during every single stage of the farming process, transport of the harvested grapes, storage and production of wine and distribution to the final consumer by a worldwide supply chain. These exigent requirements are also encouraged by the increasing pressure from emergent regions that begin producing wines of quality and export them to the rest of the world.

For this reason, the management of small vineyards, cooperatives, wineries and distribution companies should be very effective and the right decisions must be made at the appropriate time. There are, nevertheless, several handicaps to practise an efficient decision making. On the one hand, the small and traditional business and companies are not well adapted to a changing environment and to proceed using the more advanced and sophisticated strategies and tools for decision making. This fact urges the

development of specific, effective, and simple tools for these applications. On the other hand, the complexity and diversity of the different processes that participate in the complete production cycle of the wine makes almost impossible to follow successful strategies in every step of the farming, transport and production in this network with a large number of actors, without the help of the appropriate decision support systems.

In this regional production system there is a large number of processes that are developed in parallel, are synchronized at certain stages, and compete for limited resources. Petri nets is a modelling paradigm well suited for the modelling, analysis, simulation and optimization of systems whose behaviour verifies these characteristics (Silva 1993).

The authors of this paper have developed a decision making methodology especially suited for this complex environment, where the networks of commercial relations between farmers, cooperatives, wineries, and distribution companies can be arranged in very different ways, leading to models with alternative structural configurations (Latorre *et al.* 2011).

This methodology is based in the modelling of the system in a compact representation made by means of a formalism that includes all the alternative structural configurations in the so called set of exclusive entities (Latorre *et al.* 2011). Several different formalisms allow representing the system, profiting from the features of the different alternative structural configurations to obtain a compact model of the system. This compact representation alleviates the computer requirements of the algorithm that is applied to solve the optimization problem associated to the original decision making (Latorre *et al.* 2010).

The methodology that has been applied to the wine production sector in La Rioja (Spain) is based on a single-staged search in the solution space. This search is guided by a metaheuristic, which has been implemented by means of a genetic algorithm.

As a consequence of the proposed methodology, a decision making support for the different actors that participate in the growing, and harvesting of the grape, the ones that store and distribute them, those that produce the wine and the companies that distribute the resulting product have a tool for efficient decision making adapted to this sector of the food industry. This tool can be used individually or by organizations that supervise and coordinate the interaction of the different businesses and require a global vision of the sector.

In this paper, the specific and critical stage of winemaking in a small or medium-size winery is afforded by the presentation of the model and the proposed methodology for decision making. The decision problem that is aimed to be solved for the presented methodology comprises not only the scheduling or operational choices but also the design of the business, taking decisions that define the structure of the winemaking process.

The following section introduces the modelling formalism, based on Petri nets, which will be used in

the decision support methodology, the section 3 deals with the model of the winery. The fourth section presents the decision problem in detail, while the following section describes the methodology for solving the decision problem. The last section, number six, presents the conclusions and the future research lines.

2. ALTERNATIVES AGGREGATION PETRI NETS

In the previous section, it has been mentioned that the Petri net formalism is suited for the modelling, analysis, simulation, and optimization of discrete event systems. Its graphical representation allows representing, in an explicit and intuitive way, complex behaviours characterized by concurrence and synchronization of subprocesses. Moreover, the matrix-based of a Petri net representation may lead to a very productive structural analysis, as well to the statement and solving of decision problems based on the evaluation of the performance of the system under specific conditions.

Definition 1. A Petri net system is a 5-tuple $R = (P, T, \text{pre}, \text{post}, \mathbf{m}_0)$ such that:

- i) P is a non-empty set of places.
- ii) T is a non-empty set of transitions and $P \cap T = \emptyset$.
- iii) pre and post are functions that associate a weight to the directed arcs between the elements of the sets P and T , in the following way:
- iv) $\text{pre}: P \times T \rightarrow \mathbb{N}^*$ and $\text{post}: T \times P \rightarrow \mathbb{N}^*$, where \mathbb{N}^* is the set of natural numbers, excluding zero.
- v) \mathbf{m}_0 is the initial marking, such that $\mathbf{m}_0: P \rightarrow \mathbb{N}^*$.

This definition does not specify explicitly the mechanisms of the Petri net formalism to represent the controllable parameters, which have a significant influence in the behaviour and performance of the system, and the possibility of making a choice for them among their feasible set of combinations of values.

The design process of a system, modelled by the formalism of the Petri nets, usually requires the development of so many models as alternative structures can be selected for representing different solutions for the structure of the system. These models can be called alternative Petri nets (Latorre *et al.* 2011).

Nevertheless, this approach uses to be ineffective, since the whole set of alternative Petri nets usually shows large amounts of redundant information among the models (Recalde *et al.*, 2004). This redundant information corresponds to shared subsystems.

The alternatives aggregation Petri nets consists of a Petri-net-based formalism, which has the ability of representing in a single model, a complete set of alternative Petri nets removing the redundant information that correspond to shared subsystems. Furthermore, the mechanism for the decision making associated to the choice of one of these alternative structural configurations is represented explicitly by means of the so called choice variables.

A definition of a set of choice variables can be afforded once it is known the number of the alternative structural configurations for the system to be modelled.

Definition 2. Given a discrete event system with n alternative structural configurations, a set of choice variables can be defined as $S_A = \{ a_i \text{ Boolean} \mid \exists! k \in \mathbb{N}^*, k \leq n, \text{ such that } a_k = 1 \wedge \forall j \in \mathbb{N}^*, j \leq n, j \neq k \text{ it is verified } a_j = 0 \}$, where $|S_A| = n$, and the assignment $a_k = 1$ is the result of a decision.

Definition 3. An alternatives aggregation Petri net can be defined as a 10 tuple $R^A = (P, T, \text{pre}, \text{post}, \mathbf{m}_0, S_\alpha, S_{\text{valnstr}\alpha}, S_A, f_A, R_{\text{val}\gamma})$, where

- i) S_α is a set of undefined parameters.
- ii) $S_{\text{valnstr}\alpha}$ is the set of feasible combination of values for the undefined parameters in S_α .
- iii) S_A is a set of choice variables, $S_A \neq \emptyset$ and $|S_A| = n$.
- iv) $f_A: T \rightarrow f(a_1, \dots, a_n)$ is a function that assigns a function of the choice variables to each transition t such that $\text{type}[f_A(t)] = \text{boolean}$.
- v) $R_{\text{val}\gamma}$ is a binary relation between $S_{\text{val}\gamma}$ and R_A .

On the other hand, $f_A: S_A \rightarrow T$, assigns a choice variable to a single or several transitions of the Petri net, and if $S_A' = \{ a_1, a_2, \dots, a_k \}$ is the set of every choice variables associated to the transition t , then the guard function of the mentioned transition is $g_A(t) = a_1 + a_2 + \dots + a_k$.

This formalism, can be used to develop the model of a small or medium-size winery in the region of La Rioja (Spain), with the purpose of its design, improvement or efficient operation.

3. THE MODEL OF THE WINERY

3.1. The winemaking process

La Rioja is a region of Spain, where the wine industry has a long tradition and its influence in the local economy is very important. In fact, La Rioja produces the 6% of all the European wine, being the most important specialty, the red wine.

There exist different methodologies for producing wine, according to the target finished product (red, white rosé, or sparkling wine), with different variants, which depend on the equipment used, the degree of mechanization and automation, the chemical processes, etc.

However, a broadly applied technique for the production of red wine in La Rioja is the traditional Bordeaux method, which has been used in this region since the middle of the XIX century.

According to this winemaking method, the grape clusters can be transported to the winery by different means and in diverse types of containers. At their arrival, the quality of the grapes is measured and they are weighted and transferred to the first stage of destemming, for removing the rachis from the grapes, and of crushing, for liberating their juice.

At this point SO_2 is added to the mixture for antiseptic purposes and the storage of the product for the optional stage of maceration can begin.

The following step is the primary or alcoholic fermentation, where the must is complemented with

yeast for the transformation of the contained sugar into alcohol and carbon dioxide. As a result of this stage an amount of free run wine is obtained by decantation, while the rest of the product is pressed for the separation of the so called press wine and the grape skins. The press wine can be mixed with the free-run wine in order to increase the production.

The next step is the secondary or malolactic fermentation, under bacterial action, which can take place in vats or barrels. An optional ageing or maturing of the wine in oak barrels or in stainless steel barrels with oak chips can be afforded at the end of the secondary fermentation. With the clarification and filtration, most of the large particles, yeast, and bacteria present in the wine are removed, improving the appearance of the product and stabilizing it chemically.

The following stage of bottling and sealing with a cork may be followed, optionally, by a wine ageing in bottle. After the end of the previous process, it is possible to add a capsule to the top of the bottle and to label it. The packing can be made in boxes, stored on pallets. From the warehouse, the pallets with wine are prepared to be distributed around the world.

3.2. The marking controllable parameters

Some controllable parameters, which can be considered and specified for the design and operation of a winery, are presented in the following:

- c₁. Capacity of the available lorries for the transportation of the grape to the winery.
- c₂. Capacity of the available platforms for the transportation of boxes, containing grape clusters, to the winery.
- c₃. Capacity of the chutes for receiving the grapes.
- c₄. Grape conveying capacity to the destemming machine.
- c₅. Processing capacity of the automatic crusher-destemmer.
- c₆. Processing capacity of the stemmer machine.
- c₇. Processing capacity of the centrifugal crusher.
- c₈. Processing capacity of the crusher with rollers.
- c₉. Flow rate of the barrelling pump.
- c₁₀. Capacity for the cold maceration = number of tanks x capacity of every tank.
- c₁₁. Capacity of the winery for the stage of maceration with addition of heat.
- c₁₂. Pipeage pump flow rate.
- c₁₃. Capacity of the hydraulic press after primary fermentation.
- c₁₄. Capacity of the vats for the malolactic fermentation.
- c₁₅. Capacity of the barrels for the malolactic or secondary fermentation.
- c₁₆. Capacity of the barrels for the wine ageing.
- c₁₇. Capacity of the stainless steel tanks with oak chips for wine ageing.
- c₁₈. Capacity of the centrifugal clarification machine.
- c₁₉. Capacity of the machine for precoating.
- c₂₀. Capacity of the clarification filter.

- c₂₁. Capacity of the filter for microbial stabilization.
- c₂₂. Capacity of the facility for ultrafiltration.

More examples of controllable marking parameters are the stock of empty bottles, the stocks of stoppers of cork, metal or plastic, and the processing capacity of the bottling, labelling and packing machine.

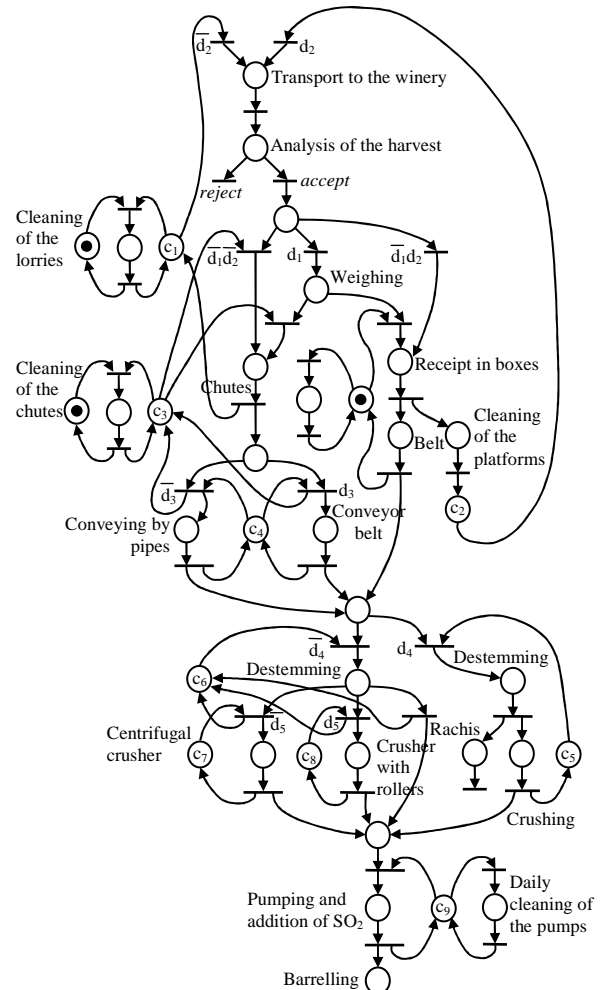


Figure 1: First stages of winemaking

The decision-making methodology, which will be described in the section 5, can afford the choice of the optimal value or a quasi-optimal one for every one of the controllable marking parameters mentioned in this section 3.2, as well as for the structural decisions, which are mentioned in the following section 3.3.

3.3. The structural decisions and choice variables

Some of the stages of winemaking may vary, be combined, or even omitted, according to the quality of the raw materials and the expected finished wine. Furthermore, different equipment and labour force can be used for the diverse winemaking steps. For all these reasons there are many alternative structural configurations for the design of a winery. Hence, there is a large amount of structural decisions that can be made. The most significant ones have been taken into account in the model presented in this paper. They are listed below:

- d1. Double or single weighting process of the incoming grape.
- d2. Receipt of the grape in boxes or in a chute.
- d3. Conveying of the incoming grape by conveyor belts or by pipes.
- d4. Combined or separated destemming and crushing.
- d5. Centrifugal crusher or crusher with rollers.
- d6. Cold maceration.
- d7. Maceration with addition of heat.
- d8. There is not any stage of maceration.
- d9. Secondary fermentation performed in vats or barrels.
- d10. Ageing of the wine in oak barrels or in stainless steel tanks with oak chips.
- d11. Centrifugal clarification or precoating.
- d12. Filtration for clarification.
- d13. Filtration for microbial stabilization.
- d14. Ultrafiltration.
- d15. Normal bottling.
- d16. Aseptic bottling.
- d17. Bottling with addition of heat.
- d18. Ageing of the wine in the bottle.

As a result of these structural decisions, or decisions that condition and specify the structural configuration of the system, it is possible to define a set of choice variables, one for every alternative system that can be built up from the mentioned decisions.

The size of the set of choice variables S_A can be calculated in the following way:

$$|S_A| = 2 \cdot 2 \cdot 2 \cdot 2 \cdot 2 \cdot 3 \cdot 2 \cdot 2 \cdot 2 \cdot 3 \cdot 3 \cdot 2 = 2^9 \cdot 3^3 = 13824.$$

As it can be deduced, analysing a set of 13824 alternative structural configurations to choose the best one as solution of a design process is unpractical. The methodology proposed in this paper has been developed to afford such a problem in an efficient single process.

Moreover, as it will be seen in the following two sections, the proposed methodology can give a solution for the decision making related to the structural and the non-structural controllable parameters. That is to say, the solution of the decision problem specifies the design of the system, as well as its operation.

3.4. The alternatives aggregation Petri net model

In this section, a model of a typical small or medium-sized winery from the region of La Rioja, in process of being designed, is presented.

With the aim of simplifying the representation, the weights of the arcs that represent the change of interpretation of the tokens in relation with physical items do not appear in the Petri nets.

In figure 1, the model of the winemaking process from the receipt of the harvested grapes to the barreling process is presented. In the alternatives aggregation Petri net model, instead of representing the 13824 choice variables, an abbreviated representation based on the 18 decision variables, d_i , has been considered.

Furthermore, in figure 2, the Petri net model for the subsequent stages of maceration, primary and

secondary fermentation, optional aging, clarification, filtering and stabilization is detailed.

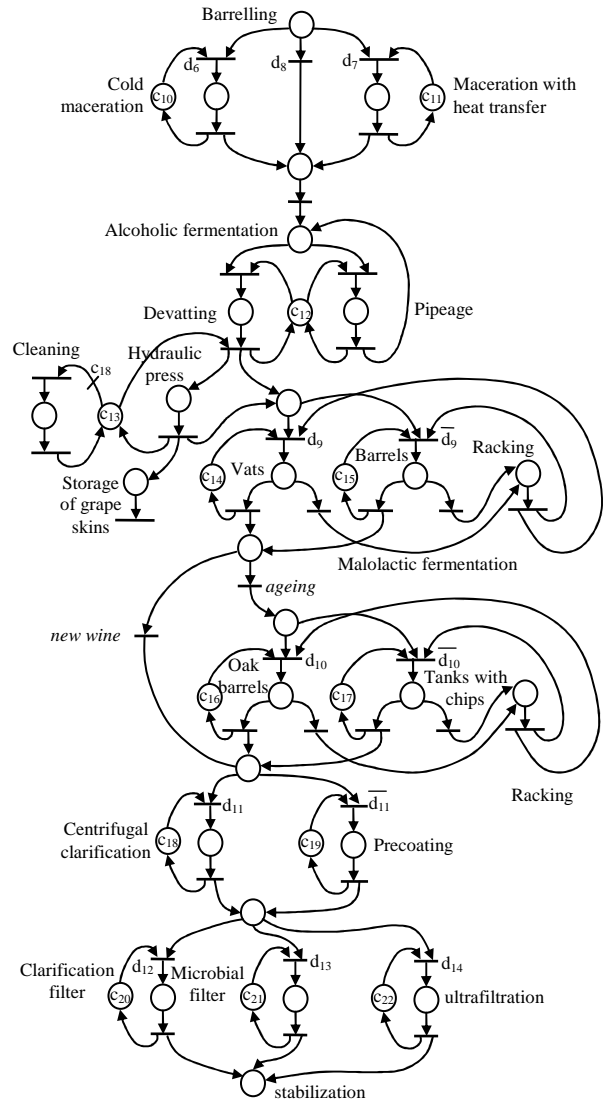


Figure 2: Fermentation and filtration

The Petri net model for the remaining stages of bottling, labelling, and packing, has not been represented in this paper. Nevertheless, as it has been indicated in sections 3.2 and 3.3, this part of the model contains several controllable parameters.

In the next section, the decision problem associated to the model of a winery is presented.

4. THE DECISION PROBLEM

The decision problem stated for the design of the winery aims to optimize the benefit from the facility, hence, it can be written in the form of an optimization problem. This goal implies that a maximal production is expected, with a minimal cost, guaranteeing a high quality standard in the winemaking processes, as well as in the final product.

The solution of the problem is a sequence of optimal values for every controllable marking parameter, as well as a decision, for every structural choices d_i .

The statement of the problem requires an objective function, the consideration of the alternatives aggregation Petri net of the winery as disjunctive constraint and some additional constraints, for example the domain of the controllable parameters.

5. THE SOLVING METHODOLOGY

In order to find the best values for the controllable parameters of the model, a single-staged methodology is proposed (Latorre *et al.* 2010). According to it, a single solution space is constructed, and its exploration can be afforded by means of a metaheuristic, for example a genetic algorithm. Using this search strategy, it is possible to avoid an exhaustive search, usually unfeasible due to the combinatorial explosion and the limited availability of computer resources.

In this exploration, the choice of a given solution to evaluate its quality implies a simulation of the evolution of the Petri net model under the conditions given by the solution and the additional constraints defined in the statement of the optimization problem. This simulation, with the help of the objective function allows characterizing every solution with a performance measurement, which can be used to compare the fitness of the solution as optimal or quasi-optimal solution of the decision problem.

6. CONCLUSIONS AND FURTHER RESEARCH

The traditional but globalized and competitive wine industry may improve by the use of decision support systems, able to improve the design and management of the different business that take part in this sector.

Many actors participate in the winemaking process, from farming and harvesting to conveying the grapes, producing the wine and distributing and commercializing the different type of finished products.

In this paper, a decision-making methodology is described for the efficient design of a small or medium-sized winery. This methodology is aimed to be applied under a more general system, including more alternative items and processes to be considered in the production of wine in the winery, as well as to add more stages of the winemaking, belonging to the external chain supply and farming activities. The goal of this research line consists of developing and proving a general methodology for decision making in the field of wine production, which may help the companies to be more competitive by producing goods and services of higher quality and lower costs.

ACKNOWLEDGMENTS

This paper has been partially supported by the project of the University of La Rioja and Banco Santander (grant number API12-11) 'Sustainable production and productivity in industrial processes: integration of energy efficiency and environmental impact in the production model for integrated simulation and optimization'.

REFERENCES

- Cicirelli F.D., Furfaro A. and Nigro L., 2010. A Service-Based Architecture for Dynamically Reconfigurable Workflows. *Journal of Systems and Software*, Vol. 83, n. 7, pp. 1148-1164.
- Ferrer, J.C., Mac Cawley, A., Maturana, S., Toloza, S., and Vera, J. 2008. An optimization approach for scheduling wine grape harvest operations. *International Journal of Production Economics*, 112, pp. 985-999, Elsevier.
- Guan, S., Nakamura, M., and Shikanai, T. 2010. Hybrid Petri Nets and Metaheuristic Approach to Farm Work Scheduling. In Aized, T. (Ed.) *Advances in Petri Net Theory and Applications*. Chapter 8. Sciyo.
- Latorre, J.I., Jiménez, E., Pérez, M., 2010. On the Solution of Optimization Problems with Disjunctive Constraints Based on Petri Nets. In *Proceedings of the 22nd European Modelling and Simulation Symposium (EMSS 10)*. Fez, Morocco, pp. 259-264.
- Latorre, J.I., Jiménez, E., Pérez, M., 2011. Petri nets with exclusive entities for decision making. *International Journal of Simulation and Process Modeling*, Special Issue on the I3M 2011 Multiconference.
- Léger, B., Naud, O., Gouache, D., 2011. Specifying a strategy for deciding tactical adjustment of crop protection using CPN tools. *Congress of the European Federation for Information Technology in Agriculture, Food and the Environment Efitra 2011*. Pages 1 – 6.
- Melberg, R., Davidrajuh, R. 2009. Modeling Atlantic salmon fish farming industry. In *Proceedings of the IEEE International Conference on Industrial Technology*. ICIT 2009. Pages 1-6.
- Recalde, L.; Silva, M.; Ezpeleta, J.; and Teruel, E. 2004. Petri Nets and Manufacturing Systems: An Examples-Driven Tour. In Desel, J.; Reisig, W.; and Rozenberg, G. (Eds.), *Lectures on Concurrency and Petri Nets: Advances in Petri Nets, Lecture Notes in Computer Science / Springer-Verlag*. Volume 3098, pp. 742-788.
- Shikanai, T.; Nakamura, M.; Guan S.; Tamaki, M. 2008. Supporting system for management of agricultural corporation of sugarcane farming in Okinawa Islands. *World conference on agricultural information and IT, IAALD AFITA WCCA 2008*, Tokyo University of Agriculture, Tokyo, Japan, 24 - 27, pp. 1101-110.
- Silva, M. 1993. Introducing Petri nets. In *Practice of Petri Nets in Manufacturing*, Di Cesare, F., (editor), pp. 1-62. Ed. Chapman&Hall.
- Wang, F., Duan, Q., Zhang, L., and Li, G. 2011. Modeling and Analysis of Pollution-Free Agricultural Regulatory Based on Petri-Net. *Computer and Computing Technologies in Agriculture IV*. IFIP Advances in Information and Communication Technology, Volume 347/2011, 691-700.

UTILIZATION OF ANALYTIC PROGRAMMING FOR THE STABILIZATION OF HIGH ORDER OSCILLATIONS OF CHAOTIC LOGISTIC EQUATION

Roman Senkerik^(a), Zuzana Oplatkova^(a), Ivan Zelinka^(b), Donald Davendra^(b), Michal Pluhacek^(a)

^(a)Tomas Bata University in Zlin , Faculty of Applied Informatics, Nam T.G. Masaryka 5555, 760 01 Zlin, Czech Republic

^(b) Technical University of Ostrava, Faculty of Electrical Engineering and Computer Science, 17. listopadu 15, 708 33 Ostrava-Poruba, Czech Republic

^(a)senkerik@fai.utb.cz, ^(b)ivan.zelinka@vsb.cz

ABSTRACT

This research deals with a utilization of a modern tool for symbolic regression, which is analytic programming, for the purpose of the evolutionary synthesis of a feedback controller for the chaotic system. This synthesized chaotic controller secures the stabilization of high periodic orbit – oscillations between several values of discrete chaotic system, which is Logistic Equation. The paper consists of the descriptions of analytic programming as well as chaotic system, used heuristic and cost function. For experimentation, Self-Organizing Migrating Algorithm (SOMA) and Differential evolution (DE) were used.

Keywords: Chaos Control, Analytic programming, optimization, evolutionary algorithms.

1. INTRODUCTION

During the past five years, usage of new intelligent systems in engineering, technology, modeling, computing and simulations has attracted the attention of researchers worldwide. The most current methods are mostly based on soft computing, which is a discipline tightly bound to computers, representing a set of methods of special algorithms, belonging to the artificial intelligence paradigm. The most popular of these methods are neural networks, evolutionary algorithms, fuzzy logic, and genetic programming. Presently, evolutionary algorithms are known as a powerful set of tools for almost any difficult and complex optimization problem.

The interest about the interconnection between evolutionary techniques and control of chaotic systems is spread daily. First steps were done in (Senkerik et al.; 2010a), (Zelinka et al., 2009), where the control law was based on Pyragas method: Extended delay feedback control – ETDAS (Pyragas, 1995). These papers were concerned to tune several parameters inside the control technique for chaotic system. Compared to previous research, this paper shows a possibility how to generate the whole control law (not only to optimize several parameters) for the purpose of stabilization of a chaotic system. The synthesis of control is inspired by the

Pyragas's delayed feedback control technique (Just, 1999), (Pyragas, 1992). Unlike the original OGY control method (Ott et al., 1990), it can be simply considered as a targeting and stabilizing algorithm together in one package (Kwon, 1999). Another big advantage of the Pyragas method for evolutionary computation is the amount of accessible control parameters, which can be easily tuned by means of evolutionary algorithms (EA).

Instead of EA utilization, analytic programming (AP) is used in this research. AP is a superstructure of EAs and is used for synthesis of analytic solution according to the required behaviour. Control law from the proposed system can be viewed as a symbolic structure, which can be synthesized according to the requirements for the stabilization of the chaotic system. The advantage is that it is not necessary to have some “preliminary” control law and to estimate its parameters only. This system will generate the whole structure of the law even with suitable parameter values.

This work is focused on the expansion of AP application for synthesis of a whole control law instead of parameters tuning for existing and commonly used method control law to stabilize desired Unstable Periodic Orbits (UPO) of chaotic systems.

This work is an extension of previous research (Oplatkova et al., 2010a; 2010b), (Senkerik et al., 2010b) focused on stabilization of simple p-1 orbit – stable state and p-2 orbit. In general, this research is concerned to stabilize p-4 UPO – high periodic orbit (oscillations between four values).

Firstly, AP is explained, and then a problem design is proposed. The next sections are focused on the description of used cost function and evolutionary algorithms. Results and conclusion follow afterwards.

2. PROBLEM DESIGN

The brief description of used chaotic systems and original feedback chaos control method, ETDAS is given. The ETDAS control technique was used in this research as an inspiration for synthesizing a new feedback control law by means of evolutionary techniques.

2.1. Selected Chaotic System

The chosen example of chaotic systems was the one-dimensional Logistic equation in form (1).

$$x_{n+1} = rx_n(1 - x_n) \quad (1)$$

The Logistic equation (logistic map) is a one-dimensional discrete-time example of how complex chaotic behaviour can arise from very simple non-linear dynamical equation (Hilborn, 2000). This chaotic system was introduced and popularized by the biologist Robert May (May, 2001). It was originally introduced as a demographic model as a typical predator – prey relationship. The chaotic behaviour can be observed by varying the parameter r . At $r = 3.57$ is the beginning of chaos, at the end of the period-doubling behaviour. At $r > 3.57$ the system exhibits chaotic behaviour. The example of this behaviour can be clearly seen from bifurcation diagram – Figure 1.

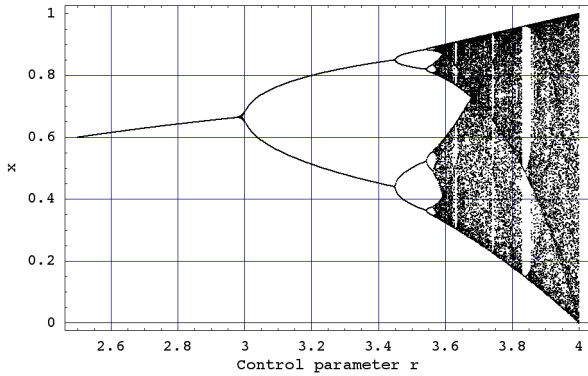


Figure 1: Bifurcation diagram of Logistic Equation

2.2. ETDAS Control Method

This work is focused on explanation of application of AP for synthesis of a whole control law instead of demanding tuning of EDTAS method control law to stabilize desired Unstable Periodic Orbits (UPO). In this research desired UPO is only p-2 (higher periodic orbit – oscillation between two values). ETDAS method was obviously an inspiration for preparation of sets of basic functions and operators for AP.

The original control method – ETDAS has form (2).

$$\begin{aligned} F(t) &= K[(1 - R)S(t - \tau_d) - x(t)] \\ S(t) &= x(t) + RS(t - \tau_d) \end{aligned} \quad (2)$$

Where: K and R are adjustable constants, F is the perturbation; S is given by a delay equation utilizing previous states of the system and τ_d is a time delay.

The original control method – ETDAS in the discrete form suitable for one-dimensional Logistic equation has the form (3).

$$\begin{aligned} x_{n+1} &= rx_n(1 - x_n) + F_n \\ F_n &= K[(1 - R)S_{n-m} - x_n] \\ S_n &= x_n + RS_{n-m} \end{aligned} \quad (3)$$

Where: m is the period of m -periodic orbit to be stabilized. The perturbation F_n in equations (3) may have arbitrarily large value, which can cause diverging of the system outside the interval $\{0, 1.0\}$. Therefore, F_n should have a value between $-F_{\max}$, F_{\max} . In this preliminary study a suitable F_{\max} value was taken from the previous research. To find the optimal value also for this parameter is in future plans.

Previous research concentrated on synthesis of control law only for p-1 orbit (a fixed point). An inspiration for preparation of sets of basic functions and operators for AP was simpler TDAS control method (4) and its discrete form suitable for logistic equation given in (5).

$$F(t) = K[x(t - \tau) - x(t)] \quad (4)$$

$$F_n = K(x_{n-m} - x_n) \quad (5)$$

2.3. Cost Function

Proposal for the cost function comes from the simplest Cost Function (CF). The core of CF could be used only for the stabilization of p-1 orbit. The idea was to minimize the area created by the difference between the required state and the real system output on the whole simulation interval – τ_i .

But another universal cost function had to be used for stabilizing of higher periodic orbit and having the possibility of adding penalization rules. It was synthesized from the simple CF and other terms were added. In this case, it is not possible to use the simple rule of minimizing the area created by the difference between the required and actual state on the whole simulation interval – τ_i , due to many serious reasons, for example: degrading of the possible best solution by phase shift of periodic orbit.

This CF is in general based on searching for desired stabilized periodic orbit and thereafter calculation of the difference between desired and found actual periodic orbit on the short time interval – τ_s (40 iterations) from the point, where the first min. value of difference between desired and actual system output is found. Such a design of CF should secure the successful stabilization of either p-1 orbit (stable state) or higher periodic orbit anyway phase shifted. The CF_{Basic} has the form (6).

$$CF_{Basic} = pen_1 + \sum_{t=\tau_1}^{\tau_2} |TS_t - AS_t|, \quad (6)$$

where:

TS - target state, AS - actual state

τ_1 - the first min value of difference between TS and AS

τ_2 - the end of optimization interval ($\tau_1 + \tau_s$)

$pen_1 = 0$ if $\tau_1 - \tau_2 \geq \tau_s$;

$pen_1 = 10 * (\tau_1 - \tau_2)$ if $\tau_1 - \tau_2 < \tau_s$ (i.e. late stabilization).

3. ANALYTIC PROGRAMMING

Basic principles of the AP were developed in 2001 (Zelinka et al. 2005). Until that time only Genetic Programming (GP) and Grammatical Evolution (GE) had existed. GP uses Genetic Algorithms (GA) while AP can be used with any EA, independently on individual representation. To avoid any confusion, based on the nomenclature according to the used algorithm, the name - Analytic Programming was chosen, since AP represents synthesis of analytical solution by means of EA.

The core of AP is based on a special set of mathematical objects and operations. The set of mathematical objects is a set of functions, operators and so-called terminals (as well as in GP), which are usually constants or independent variables. This set of variables is usually mixed together and consists of functions with different number of arguments. Because of a variability of the content of this set, it is termed the “general functional set” – GFS. The structure of GFS is created by subsets of functions according to the number of their arguments. For example GFS_{all} is a set of all functions, operators and terminals, GFS_{3arg} is a subset containing functions with only three arguments, GFS_{0arg} represents only terminals, etc. The subset structure presence in GFS is vitally important for AP. It is used to avoid synthesis of pathological programs, i.e. programs containing functions without arguments, etc. The content of GFS is dependent only on the user. Various functions and terminals can be mixed together (Zelinka et al. 2005, Zelinka et al. 2008, Oplatkova et al. 2009).

The second part of the AP core is a sequence of mathematical operations, which are used for the program synthesis. These operations are used to transform an individual of a population into a suitable program. Mathematically stated, it is a mapping from an individual domain into a program domain. This mapping consists of two main parts. The first part is called Discrete Set Handling (DSH) (See Figure 2) (Zelinka et al. 2005, Lampinen and Zelinka 1999) and the second one stands for security procedures which do not allow synthesizing pathological programs.

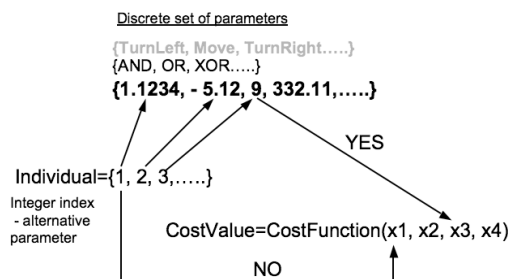


Figure 2: Discrete set handling

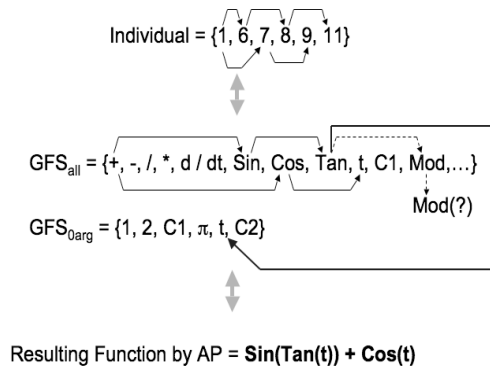


Figure 3: The main principles of AP

The method of DSH, when used, allows handling arbitrary objects including nonnumeric objects like linguistic terms {hot, cold, dark...}, logic terms (True, False) or other user defined functions. In the AP, DSH is used to map an individual into GFS and together with security procedures creates the above-mentioned mapping, which transforms arbitrary individual into a program.

AP needs some EA (Zelinka et al. 2005) that consists of a population of individuals for its run. Individuals in the population consist of integer parameters, i.e. an individual is an integer index pointing into GFS. The creation of the program can be schematically observed in Figure 3. The individual contains numbers which are indices into GFS. The detailed description is represented in (Zelinka et al. 2005, Zelinka et al. 2008, Oplatkova et al. 2009).

AP exists in 3 versions – basic without constant estimation, AP_{nr} – estimation by means of nonlinear fitting package in *Mathematica* environment and AP_{meta} – constant estimation by means of another evolutionary algorithms; meta implies metaevolution.

4. USED EVOLUTIONARY ALGORITHMS

This research used two evolutionary algorithms: Self-Organizing Migrating Algorithm (Zelinka 2004) and Differential Evolution (Price and Storn 2001, Price 2005). Future simulations expect a usage of soft computing GAHC algorithm (modification of HC12) (Matousek 2007) and a CUDA implementation of HC12 algorithm (Matousek 2010).

4.1. Self Organizing Migrating Algorithm – SOMA

SOMA is a stochastic optimization algorithm that is modelled on the social behaviour of cooperating individuals (Zelinka 2004). It was chosen because it has been proven that the algorithm has the ability to converge towards the global optimum (Zelinka 2004) and due to the successful applications together with AP (Varacha and Zelinka 2008, Varacha and Jasek 2011).

SOMA works with groups of individuals (population) whose behavior can be described as a competitive – cooperative strategy. The construction of a new population of individuals is not based on evolutionary principles (two parents produce offspring) but on the behavior of social group, e.g. a herd of

animals looking for food. This algorithm can be classified as an algorithm of a social environment. To the same group of algorithms, Particle Swarm Optimization (PSO) algorithm can also be classified sometimes called swarm intelligence. In the case of SOMA, there is no velocity vector as in PSO, only the position of individuals in the search space is changed during one generation, referred to as 'migration loop'.

The rules are as follows: In every migration loop the best individual is chosen, i.e. individual with the minimum cost value, which is called the Leader. An active individual from the population moves in the direction towards the Leader in the search space. At the end of the crossover, the position of the individual with minimum cost value is chosen. If the cost value of the new position is better than the cost value of an individual from the old population, the new one appears in new population. Otherwise the old one remains there. The main principle is depicted in Figures 4 and 5.

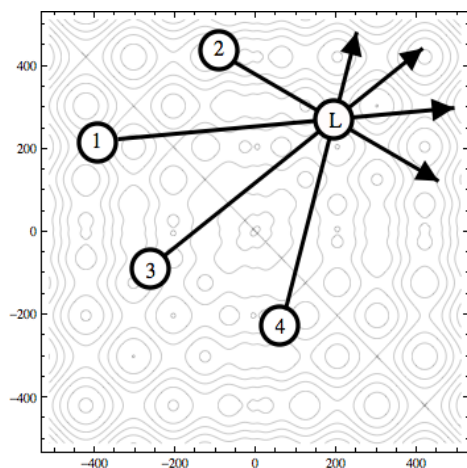


Figure 4: Principle of SOMA, movement in the direction towards the Leader

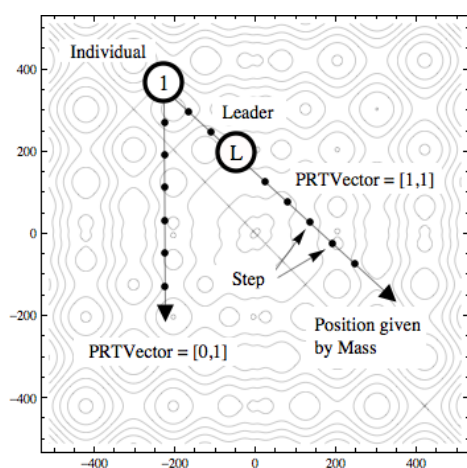


Figure 5: Basic principle of crossover in SOMA, PathLength is replaced here by Mass

4.2. Differential Evolution

DE is a population-based optimization method that works on real-number-coded individuals (Price, 2005). A schematic is given in Figure 6. There are essentially five sections to the code. Section 1 describes the input to the heuristic. D is the size of the problem, G_{max} is the maximum number of generations, NP is the total number of solutions, F is the scaling factor of the solution and CR is the factor for crossover. F and CR together make the internal tuning parameters for the heuristic.

Section 2 outlines the initialization of the heuristic. Each solution $x_{i,j,G=0}$ is created randomly between the two bounds $\bar{x}^{(lo)}$ and $\bar{x}^{(hi)}$. The parameter j represents the index to the values within the solution and i indexes the solutions within the population. So, to illustrate, $x_{4,2,0}$ represents the fourth value of the second solution at the initial generation.

After initialization, the population is subjected to repeated iterations in section 3.

Section 4 describes the conversion routines of DE. Initially, three random numbers r_1, r_2, r_3 are selected, unique to each other and to the current indexed solution i in the population in 4.1. Henceforth, a new index j_{rand} is selected in the solution. j_{rand} points to the value being modified in the solution as given in 4.2. In 4.3, two solutions, $x_{j,r_1,G}$ and $x_{j,r_2,G}$ are selected through the index r_1 and r_2 and their values subtracted. This value is then multiplied by F , the predefined scaling factor. This is added to the value indexed by r_3 .

However, this solution is not arbitrarily accepted in the solution. A new random number is generated, and if this random number is less than the value of CR , then the new value replaces the old value in the current solution. The fitness of the resulting solution, referred to as a perturbed vector $u_{j,b,G}$, is then compared with the fitness of $x_{j,b,G}$. If the fitness of $u_{j,b,G}$ is greater than the fitness of $x_{j,b,G}$, then $x_{j,b,G}$ is replaced with $u_{j,b,G}$; otherwise, $x_{j,b,G}$ remains in the population as $x_{j,b,G+1}$. Hence the competition is only between the new *child* solution and its *parent* solution.

1. Input: $D, G_{max}, NP \geq 4, F \in (0,1+), CR \in [0,1]$, and initial bounds: $\bar{x}^{(lo)}, \bar{x}^{(hi)}$.
2. Initialize: $\forall i \leq NP \wedge \forall j \leq D : x_{i,j,G=0} = \bar{x}^{(lo)} + rand_j[0,1] \cdot (\bar{x}^{(hi)} - \bar{x}^{(lo)})$
 $i = \{1,2,\dots, NP\}, j = \{1,2,\dots, D\}, G = 0, rand_j[0,1] \in [0,1]$
3. While $G < G_{max}$
 4. Mutate and recombine:
 - 4.1 $r_1, r_2, r_3 \in \{1,2,\dots, NP\}$, randomly selected, except: $r_1 \neq r_2 \neq r_3 \neq i$
 - 4.2 $j_{rand} \in \{1,2,\dots, D\}$, randomly selected once each i
 - 4.3 $\forall j \leq D, u_{j,j,G+1} = \begin{cases} x_{j,r_1,G} + F \cdot (x_{j,r_2,G} - x_{j,r_3,G}) & \text{if } (rand_j[0,1] < CR \vee j = j_{rand}) \\ x_{j,j,G} & \text{otherwise} \end{cases}$
 5. Select

$$\bar{x}_{i,G+1} = \begin{cases} \bar{u}_{i,G+1} & \text{if } f(\bar{u}_{i,G+1}) \leq f(\bar{x}_{i,G}) \\ \bar{x}_{i,G} & \text{otherwise} \end{cases}$$
- $G = G + 1$

Figure 6: DE Schematic

DE is quite robust, fast, and effective, with global optimization ability. It does not require the objective function to be differentiable, and it works well even

with noisy and time-dependent objective functions. Description of used DERand1Bin strategy is presented in (7). Please refer to (Price and Storn 2001, Price 2005) for the description of all other strategies. These strategies differ in the way of calculating the perturbed vector $u_{p,i,G}$.

$$u_{i,G+1} = x_{r1,G} + F \cdot (x_{r2,G} - x_{r3,G}) \quad (7)$$

5. SIMULATION RESULTS

As described in section about Analytic Programming, AP requires some EA for its run. In this paper AP_{meta} version was used. Meta-evolutionary approach means usage of one main evolutionary algorithm for AP process and second algorithm for coefficient estimation, thus to find optimal values of constants in the evolutionary synthesized control law.

SOMA algorithm was used for main AP process and DE was used in the second evolutionary process. Settings of EA parameters for both processes were based on performed numerous experiments with chaotic systems and simulations with AP_{meta} (Table 1 and Table 2).

Table 1: SOMA settings for AP

PathLength	3
Step	0.11
PRT	0.1
PopSize	50
Migrations	4
Max. CF Evaluations (CFE)	5345

Table 2: DE settings for meta-evolution

PopSize	40
F	0.8
CR	0.8
Generations	150
Max. CF Evaluations (CFE)	6000

Compared to previous research with stabilization of stable state - p-1 orbit, the data set for AP required only constants, operators like plus, minus, power and output values x_n and x_{n-1} . Due to the recursive attributes of delay equation S utilizing previous states of the system in discrete ETDAS (3), the data set for AP had to be expanded and cover longer system output

history, thus to imitate inspiring control method for the successful synthesis of control law securing the stabilization of higher periodic orbits.

Basic set of elementary functions for AP:

GFS2arg= +, -, /, *, ^
GFS0arg= data_{n-11} to data_n, K

Total number of 200 simulations was carried out. The most simulations were successful and have given new synthesized control law, which was able to stabilize the system at required behaviour (p-4 orbit) within short simulation interval of 200 iterations.

Total number of cost function evaluations for AP was 5345, for the second EA it was 6000, together 32.07 millions per each simulation. All experiments were performed in the Wolfram Mathematica environment. One experiment (simulation) took approx. 72 hours. See Table 3 for simple CF values statistic.

Table 3: Cost Function values

Min	0.0314
Max	8.9088
Average	0.6178

The novelty of this approach represents the synthesis of feedback control law F_n (8) (perturbation) for the Logistic equation inspired by original ETDAS control method.

$$x_{n+1} = rx_n(1 - x_n) + F_n \quad (8)$$

Following Table 4 and Figure 7 contains examples of synthesized control laws. Obtained simulation results can be classified into 2 groups, based on the quality and durability of stabilization at real p-4 UPO, which for unperturbed Logistic equation has following values: $x_1 = 0.3038$, $x_2 = 0.8037$, $x_3 = 0.5995$, $x_4 = 0.9124$. More about this phenomenon is written in the conclusion section.

Table 4 covers direct output from AP – synthesized control law without coefficients estimated, further the notation with simplification after estimation by means of second algorithm DE, corresponding CF value, average error between actual and required system output, and identification of figure with simulation results.

Table 4: Simulation results

Control Law	Control Law with coefficients	CF Value	Avg. output error	Figure
$F_n = -\frac{x_{n-4}}{K_3(x_n^{K_2} - K_1)}$	$F_n = \frac{0.0200224x_{n-4}}{x_n^{50.5239} - 92.1071}$	0.0314	0.0006	7a
$F_n = x_{n-2}^{K_1}$	$F_n = x_{n-2}^{34.6383}$	0.1007	0.0020	7b
$F_n = (x_{n-5}^{x_{n-2}} + x_{n-2})x_{n-2}^{(x_{n-2}^{K_1} - x_{n-11})}$	$F_n = (x_{n-5}^{x_{n-2}} + x_{n-2})x_{n-2}^{\left(\frac{1}{x_n^{35.5805} - x_{n-11}}\right)}$	0.1139	0.0023	7c
$F_n = -\frac{x_{n-3}}{K_1 - x_{n-1}\left(\frac{x_{n-5}x_{n-1} - K_2K_4x_n}{K_3}\right)}$	$F_n = -\frac{x_{n-3}}{-x_{n-1}(0.017878x_{n-5}x_{n-1} - 325.295x_n) - 70.0758}$	0.4814	0.0096	7d

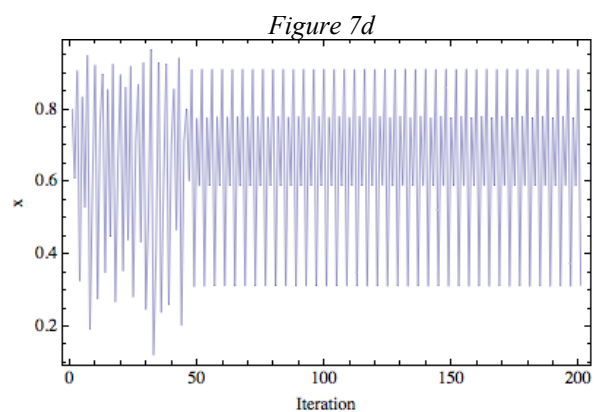
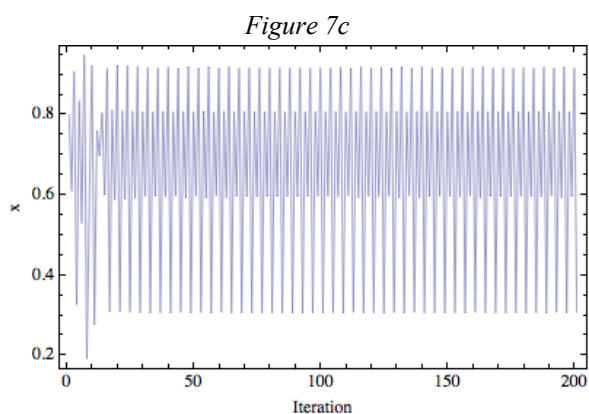
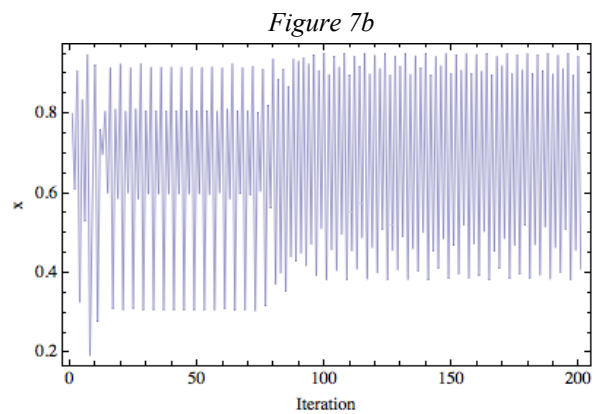
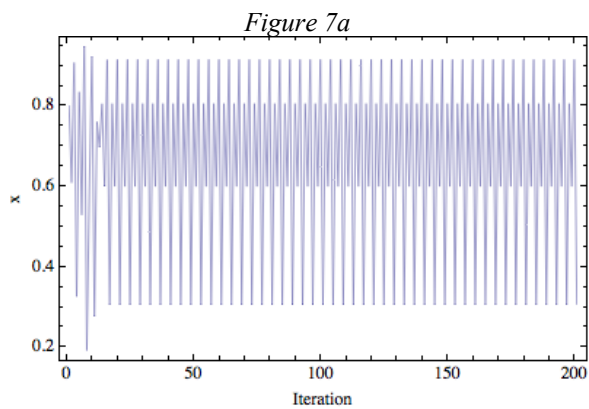


Figure 7: Examples of results – stabilization of p-4 orbit for Logistic equation by means of control laws given in Table 4.

6. CONCLUSION

This paper deals with a synthesis of a control law by means of AP for stabilization of selected chaotic system at high periodic orbit. Logistic equation as an example of one-dimensional discrete chaotic system was used in this research.

In this presented approach, the analytic programming was used instead of tuning of parameters for existing control technique by means of EA's as in the previous research.

Obtained results reinforce the argument that AP is able to solve this kind of difficult problems and to produce a new synthesized control law in a symbolic

way securing desired behaviour of chaotic system and stabilization.

Presented four simulation examples show two different results. Low CF values indicating precise, but unfortunately sometimes unstable and only temporary stabilization, together with simple control law in the first two cases. And according to the higher CF values not very precise, but very stable and relatively complex notation of chaotic controller in the next two cases. This phenomenon is caused by the design of CF, which was borrowed from the previous research focused on the simpler cases, which were stabilization of stable state and p-2 orbit, and it has given satisfactory results. Nevertheless this fact lends weight to the argument, that AP is a powerful symbolic regression tool, which is able to strictly and precisely follow the rules given by cost function and synthesizes any symbolic formula, in the case of this research – the feedback controller for chaotic system.

The question of energy costs and more precise and faster stabilization will be included into future research together with development of better cost functions, different AP data set, and performing of numerous simulations to obtain more results and produce better statistics, thus to confirm the robustness of this approach.

Future research will be also aimed at the time-continuous systems, not only discrete chaotic maps.

ACKNOWLEDGMENTS

This work was supported by the European Regional Development Fund under the project CEBIA-Tech No. CZ.1.05/2.1.00/03.0089 and project IT4Innovations Centre of Excellence No. CZ.1.05/1.1.00/02.0070 and and by Internal Grant Agency of Tomas Bata University under the project No.IGA/FAI/2012/037.

REFERENCES

- Hilborn R.C., 2000. *Chaos and Nonlinear Dynamics: An Introduction for Scientists and Engineers*, Oxford University Press, 2000, ISBN: 0-19-850723-2.
- Just W., 1999, "Principles of Time Delayed Feedback Control", In: Schuster H.G., *Handbook of Chaos Control*, Wiley-Vch, ISBN 3-527-29436-8.
- Kwon O. J., 1999. "Targeting and Stabilizing Chaotic Trajectories in the Standard Map", *Physics Letters A*. vol. 258, 1999, pp. 229-236.
- Lampinen J., Zelinka I., 1999, "New Ideas in Optimization – Mechanical Engineering Design Optimization by Differential Evolution", Volume 1, London: McGraw-hill, 1999, 20 p., ISBN 007-709506-5.
- Matousek R., 2007, „GAHC: Improved GA with HC station“, In *WCECS 2007*, San Francisco, pp. 915-920. ISBN: 978-988-98671-6-4.
- Matousek R., 2010, „HC12: The Principle of CUDA Implementation“. In *MENDEL 2010*, Mendel Journal series, pp. 303-308. ISBN: 978-80-214-4120- 0. ISSN: 1803- 3814.
- May R.M., 2001, "Stability and Complexity in Model Ecosystems", Princeton University Press, ISBN: 0-691-08861-6.
- Oplatková, Z., Zelinka, I.: 2009. Investigation on Evolutionary Synthesis of Movement Commands, *Modelling and Simulation in Engineering*, Volume 2009 (2009), Article ID 845080, 12 pages, Hindawi Publishing Corporation, ISSN: 1687-559.
- Oplatkova Z., Senkerik R., Zelinka I., Holoska J., 2010a, *Synthesis of Control Law for Chaotic Henon System - Preliminary study*, ECMS 2010, Kuala Lumpur, Malaysia, p. 277-282, ISBN 978-0-9564944-0-5.
- Oplatkova Z., Senkerik R., Belaskova S., Zelinka I., 2010b, *Synthesis of Control Rule for Synthesized Chaotic System by means of Evolutionary Techniques*, Mendel 2010, Brno, Czech Republic, p. 91 - 98, ISBN 978-80-214-4120-0.
- Ott E., C. Greboki, J.A. Yorke, 1990. "Controlling Chaos", *Phys. Rev. Lett.* vol. 64, 1990, pp. 1196-1199.
- Price, K. and Storn, R. (2001), *Differential evolution homepage*, [Online]: <http://www.icsi.berkeley.edu/~storn/code.html>, [Accessed 29/02/2012].
- Price K., Storn R. M., Lampinen J. A., 2005, "Differential Evolution : A Practical Approach to Global Optimization", (Natural Computing Series), Springer; 1 edition.
- Pyragas K., 1992, "Continuous control of chaos by self-controlling feedback", *Physics Letters A*, 170, 421-428.
- Pyragas K., 1995. "Control of chaos via extended delay feedback", *Physics Letters A*, vol. 206, 1995, pp. 323-330.
- Senkerik R., Zelinka I., Davendra D., Oplatkova Z., 2010a, "Utilization of SOMA and differential evolution for robust stabilization of chaotic Logistic equation", *Computers & Mathematics with Applications*, Volume 60, Issue 4, pp. 1026-1037.
- Senkerik R., Oplatkova Z., Zelinka I., Davendra D., Jasek R., 2010b, "Synthesis Of Feedback Controller For Chaotic Systems By Means Of Evolutionary Techniques", *Proceeding of Fourth Global Conference on Power Control and Optimization*, Sarawak, Borneo, 2010.
- Varacha P; Jasek, R., "ANN Synthesis for an Agglomeration Heating Power Consumption Approximation". In: *Recent Researches in Automatic Control*. Montreux : WSEAS Press, p. 239-244. ISBN 978-1-61804-004-6.
- Varacha P., Zelinka I., 2008, "Distributed Self-Organizing Migrating Algorithm Application and Evolutionary Scanning". In: *Proceedings of the 22nd European Conference on Modelling and Simulation ECMS 2008*, p. 201-206. ISBN 0-9553018-5-8.
- Zelinka I., 2004. "SOMA – Self Organizing Migrating Algorithm", In: *New Optimization Techniques in Engineering*, (B.V. Babu, G. Onwubolu (eds)), chapter 7, 33, Springer-Verlag, 2004, ISBN 3-540-20167X.
- Zelinka I., Oplatkova Z, Nolle L., 2005. *Boolean Symmetry Function Synthesis by Means of Arbitrary Evolutionary Algorithms-Comparative Study*, *International Journal of Simulation Systems, Science and Technology*, Volume 6, Number 9, August 2005, pages 44 - 56, ISSN: 1473-8031.
- Zelinka I., Senkerik R., Navratil E., 2009, "Investigation on evolutionary optimization of chaos control", *Chaos, Solitons & Fractals*, Volume 40, Issue 1, pp. 111-129.
- Zelinka, I., Guanrong Ch., Celikovskiy S., 2008. *Chaos Synthesis by Means of Evolutionary algorithms*, *International Journal of Bifurcation and Chaos*, Vol. 18, No. 4 (2008) 911–942

TRANSFORMATION ALGORITHM FROM AN ALTERNATIVES AGGREGATION PETRI NET TO A COMPOUND PETRI NET. TWO REPRESENTATIONS OF AN UNDEFINED PETRI NET WITH A NON-EMPTY SET OF EXCLUSIVE ENTITIES

Juan Ignacio Latorre-Biel^(a), Emilio Jiménez-Macías^(b)

^(a) Public University of Navarre. Department of Mechanical Engineering, Energetics and Materials.
Campus of Tudela, Spain

^(b) University of La Rioja. Industrial Engineering Technical School.
Department of Electrical Engineering. Logroño, Spain

^(a)juanignacio.latorre@unavarra.es, ^(b)emilio.jimenez@unirioja.es

ABSTRACT

Simulation, analysis, decision making, and control of discrete event systems, are examples of very common applications in industrial and technological fields. All these operations require the representation of the discrete event system in an appropriate formal language, that is to say obtaining the best suited model for the current application. A very common family of formalisms is the paradigm of the Petri nets. Different Petri net-based formalisms present different modelling power and diverse features, which make them especially suited for a given operation. In the field of decision making, where there exist a number of alternative structural configurations, the alternatives aggregation Petri nets and the compound Petri nets, lead to compact models for describing a discrete event system. This paper describes a transformation algorithm between them and an example to illustrate the application of the different steps. This transformation algorithm allows a fast transformation between both formalisms for applications related to decision making, since it is not necessary to perform a previous transformation to an intermediate set of alternative Petri nets to afford the construction of a compound Petri net from an alternatives aggregation Petri net.

Keywords: Petri nets, transformation, alternatives aggregation Petri nets, compound Petri nets, decision making

1. INTRODUCTION

Petri nets constitute one of the best suited formalisms for representing discrete event systems with complex behaviour. Petri nets (PN) are in fact a family of formalisms, each one of which have been developed for being more suited for a given application. The expressiveness and modelling power of the different formalisms may be related to the constraints imposed to their definitions. Some of the formalisms introduce exogenous elements such as time, in interpreted Petri nets, or random variables, in generalized stochastic Petri

nets, while others transfer information of the static structure from the elements of the incidence matrices, weight of the arcs, to features of the tokens, in coloured Petri nets (Jensen and Kristensen, 2009; David and Alla, 2005; Silva, 1993).

The applications of these particular Petri net-based formalisms range from structural analysis to performance analysis and the compact representation of large systems with shared subsystems. The transformation algorithms allow translating a model of a discrete event system from a given formalism to a different one or simplifying the representation of a given model. This translation is useful for performing certain operations in a model represented by a formalism that is not suited for the aimed application.

Alternatives aggregation Petri nets (AAPN) and compound Petri nets are two Petri net-based formalisms that have been defined for decision making. Both of them are well suited for representing in a compact way a model of a system with alternative structural configurations (Latorre *et al.* 2011b, Latorre *et al.* 2009). In real applications of decision making related to discrete event systems with alternative structural configurations it is common to represent the system by means of a set of alternative Petri nets (Tsinarakis *et al.* 2005, Zimmerman *et al.* 2001). Algorithms have been described to transform a set of alternative Petri nets into an alternatives aggregation Petri net (Latorre *et al.* 2009) and into a compound Petri net (Latorre *et al.* 2011a). In this paper, an algorithm for transforming an alternatives aggregation Petri net to a compound Petri net is described, as well as an example of application to illustrate the different steps. This algorithm is aimed to allow a direct and fast transformation of a model between these two formalisms for applications such as the comparison of the performance of a given model represented in both formalisms when integrated in a decision problem.

In section 2, the definitions that are relevant for the application of the transformation algorithm are given. The section 3 is focussed on the transformation

algorithm itself. Some considerations on a reduction rule to simplify the compound Petri net obtained from the algorithm are presented in the section 4. One important step in the transformation algorithm is explained in the section 5: the translation of the set of exclusive entities associated to the model of the discrete event system from their representation as a set of choice variables to a set of feasible combinations of values for the undefined structural parameters of the resulting compound Petri net. An example of application is detailed in the section 6, while the following section is devoted to the conclusions and future research lines. Finally, the last section lists the bibliographical references of this paper.

2. DEFINITIONS

An alternatives aggregation Petri net can be defined in the following way:

Definition 1. Alternatives aggregation Petri net system.

An alternatives aggregation Petri net system, R^A , is defined as the 8-tuple:

$$R^A = \langle P, T, \text{pre}, \text{post}, \mathbf{m}_0, S_\alpha, S_{val\alpha}, S_A, f_A \rangle$$

where,

- P is the set of places.
- T is the set of transitions.
- pre is the pre-incidence matrix, also called input incidence matrix.
- post is the post-incidence matrix, also called output incidence matrix.
- \mathbf{m}_0 is the initial marking that represents the initial vector of state and is usually a function of the choice variables.
- S_α is a set of undefined parameters.
- $S_{val\alpha}$ is the set of feasible combination of values for the undefined parameters in S_α .
- S_A is a set of choice variables such that $S_A \neq \emptyset$ and $|S_A| = n$.
- $f_A: T \rightarrow f(a_1, \dots, a_n)$ assigns a function of the choice variables to each transition t such that $\text{type}[f_A(t)] = \text{Boolean}$.

□

Where a set of choice variables is given by:

$$\text{Let } c_{str} \in C_{str} = \{1, 2, \dots, m_{strq}\} \subseteq \mathbb{N}^*$$

A set of choice variables can be defined as $S_A = \{a_1, a_2, \dots, a_{mstrq} \mid \exists! a_i=1, i \in C_{str} \wedge a_j=0 \forall j \neq i, j \in C_{str}\}$

Furthermore, the dynamic behaviour of an alternatives aggregation Petri net is given by an enabling rule that differs slightly from most of the formalisms based on Petri nets. The firing rule is the one of a generalized Petri net.

Definition 2. Enabled transition.

Given an alternatives aggregation Petri net R^A with an associated set of choice variables $S_A = \{a_1, a_2, \dots, a_n\}$, let us consider the following decision:

$$a_i = 1 \Rightarrow a_i = 0 \forall j \in \mathbb{N}^* \text{ such that } 1 \leq j \leq n \wedge j \neq i$$

A transition $t_j \in T$ in an alternatives aggregation Petri net is said to be enabled if

$$m_i \geq \text{pre}(p_i, t_j) \forall p_i \in {}^o t_j \wedge f_A(t_j) = 1$$

□

On the other hand, a compound Petri net can be defined from a parametric point of view, as in (Latorre et al, 2011c).

Moreover, a more classic approach (Silva, 1993) for the definition of a compound Petri net can be given as stated below:

Definition 3. Compound Petri net.

A compound Petri net is a 7-tuple

$$R^c = \langle P, T, F, w, \mathbf{m}_0, S_\alpha, S_{val\alpha} \rangle, \text{ where}$$

- i) S_α is the set of undefined parameters of R^c .
- ii) $S_{str\alpha} \neq \emptyset$ is the set of undefined structural parameters of R^c , such that $S_{str\alpha} \subseteq S_\alpha$. Notice that S_α is the set of undefined parameters of R^c .
- iii) $S_{val\alpha}$ is the feasible combination of values for the undefined parameters.

□

A compound Petri net can be considered as a parametric Petri net with undefined structural parameters.

The structural parameters refer to the elements of the incidence matrix of a Petri net. If a Petri net has undefined structural parameters it has a structure with certain freedom degrees that should be specified by a decision from the set of feasible combinations of values for them.

In summary, the undefined structural parameters are present in models that correspond with DES with undefined structure, in process of being designed, modified or controlled.

3. TRANSFORMATION FROM AN AAPN TO A COMPOUND PN

In (Latorre et al. 2011b) it was described a transformation algorithm to obtain an alternatives aggregation Petri net from a compound Petri net. The algorithm presented in this paper solves the opposite transformation and verifies that it is possible to perform a double transformation, using both algorithms sequentially, to return to the initial representation of the discrete event system. As a conclusion it is possible to state that both transformations are reversible.

The algorithm to perform a direct and fast transformation from an alternatives aggregation Petri net RA to a compound Petri net is presented in the following.

Algorithm.

Step 1.

Create a set of variables $S_{valstr\alpha}(R^c) = \{cv_1, cv_2, \dots, cv_n\}$ such that $|S_{valstr\alpha}(R^c)| = |S_A|$,

where $S_A = \{a_1, a_2, \dots, a_n\}$ is the set of choice variables of R^A .

Create a bijection between $S_{valstr\alpha}(R^c)$ and S_A .

This set $S_{valstr}(R^c)$ will contain the feasible combinations of values for the undefined structural parameters of the resulting compound Petri net.

Step 2.

Apply reduction rules to the columns of the incidence matrix of the AAPN, R^A , which have elements in common and are associated to different choice variables, aiming to obtain a more compact matrix.

Step 3.

For every transition $t_i \in T(R^A)$, with a function of choice variables associated to it, $f_A(t_i, a_j)$, transform this function into the sets $S_{str}(t_i)$ and $S_{valstr}(t_i)$.

Step 4.

Represent the resulting compound Petri net R^c . □

4. TRANSFORMATION FROM AN AAPN TO A COMPOUND PN

Reduction rules have been developed for the simplification of Petri net models in order to perform structural analysis or performance analysis in an easier or more efficient way. See for example (Berthelot, 1987) and (Haddad and Pradat-Peyre, 2006). One of the reduction rules is based on the reduction of several identical transitions to a single one (Berthelot, 1987) and (Silva, 1993).

In order to apply this rule to an alternatives aggregation Petri net, it is necessary to consider two or more columns of the incidence matrix of the alternatives aggregation Petri net associated to functions of choice variables, which do not have any choice variable in common. It is possible to merge the mentioned columns by the creation of the appropriate undefined structural parameters if there are elements belonging to different columns but to the same row that are not equal and modifying the function of choice variables.

Furthermore, a simplification rule can also be applied, since according to the Boole algebra if the function of choice variables includes every choice variable in the form $a_1 + a_2 + \dots + a_n$, where $|S_A| = n$, then the function can be removed since it is true after any decision that selects one of the choice variables.

5. TRANSFORMATION OF THE FUNCTIONS OF CHOICE VARIABLES INTO UNDEFINED STRUCTURAL PARAMETERS.

This step is complementary to the previous one. The difference between both operations is that the previous one merges columns of the incidence matrix of the AAPN aiming to obtain a more compact incidence matrix, while this operation manages to eliminate the functions of choice variables and to convert the AAPN into a compound alternative Petri net

In order to proceed as explained, this step develops a reverse operation to a replication of the transitions with associated function of choice variables. Taken a

column with a function of choice variables that does not include a certain choice variable, a new isolated transition is added (a columns of zeros) and associated to this missing choice variable (Latorre et al. 2011b). Then, both transitions are merged by the creation of the appropriate choice variables and increasing the sets of feasible values for the undefined structural parameters if necessary.

On the other hand, the function of choice variables acquires the choice variable of the merged isolated transition.

The resulting function of choice variables might include all the choice variables. In this case, by the application of the simplification rule mentioned in the section 4, the function can be removed. Otherwise, another operation of creation of an isolated transition associated to another missing choice variable and the merge of it can be performed and so on.

As a consequence of the previous explanations it is possible to see that the operation described in this section 5 can be decomposed in the following steps:

a) Replication of the transition associated to functions of choice variables to isolate the individual choice variables. This operation is the opposite to the reduction rule of the transformation described in the previous section.

b) Addition of isolated transitions to complete the choice variables in every transition of the original net.

c) Merging of the transitions with different choice variables and with arcs to the same places and which complete the set of choice variables SA.

Notice that all the operations described in this section are the opposite operation to those applied in the reverse transformation from a compound Petri net into an alternatives aggregation Petri net (Latorre et al. 2011b). Due to the fact that the equivalence between the nets before and after the operations are the same and that they are reversible, their application can be performed in this algorithm.

6. EXAMPLE OF APPLICATION.

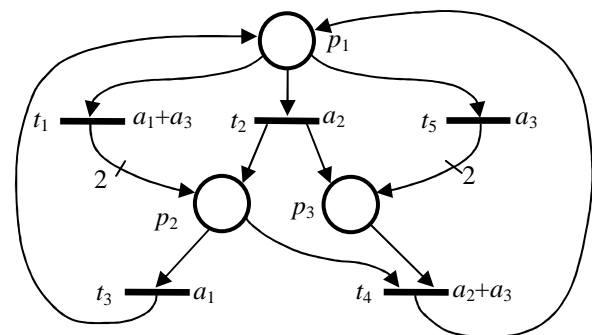


Fig. 1. Graphical representation of the AAPN to be converted into a compound PN.

This example will describe the application of the different steps of the algorithm described in the section

3 for the transformation of an alternatives aggregation Petri net into a compound Petri net. The original alternatives aggregation Petri net to be transformed is shown in the figure 1 in its graphical form and its matrix-based representation is given in the figure 2.

$$\mathbf{W}(R^A) = \begin{pmatrix} t_1 & t_2 & t_3 & t_4 & t_5 \\ -1 & -1 & 1 & 1 & -1 \\ 2 & 1 & -1 & -1 & 0 \\ 0 & 1 & 0 & -1 & 2 \end{pmatrix} \begin{matrix} p_1 \\ p_2 \\ p_3 \end{matrix}$$

$$\begin{matrix} & a_2 & a_1 & & a_3 \\ a_1+a_3 & & & a_2+a_3 & \end{matrix}$$

Fig. 2 Matrix-based representation of the AAPN to be converted into a compound PN.

Step 1.

The set of choice variables of the AAPN is $S_A = \{ a_1, a_2, a_3 \}$.

As a consequence, the set of variables associated to the feasible combination of values for the undefined structural parameters of the resulting compound Petri net, R^c , is created:

$$S_{valstr\alpha}(R^c) = \{ cv_1, cv_2, cv_3 \} \text{ such that } |S_{valstr\alpha}(R^c)| = |S_A| = 3.$$

On the other hand, a bijection between $S_{valstr\alpha}(R^c)$ and S_A is defined and their elements are made correspond, resulting in the following pairs:

$$(cv_1, a_1), (cv_2, a_2) \text{ and } (cv_3, a_3)$$

Step 2.

Apply reduction rules to the columns of the incidence matrix of the AAPN, R^A that have elements in common and are associated to different choice variables, aiming to obtain a more compact matrix.

The first couple of columns to be merged are the 1st and the 2nd ones. In the first case the associated function of choice variables is $f_A(t_1, a_i) = a_1 + a_3$. Moreover, the second column is associated to $f_A(t_2, a_i) = a_2$.

In order to merge both columns, the elements that are placed in the same row are compared and if they are different an undefined structural parameter is created:

$$\text{Row 1: } w_{11} = w_{12} = -1 \Rightarrow w'_{11} = -1$$

$$\text{Row 2: } w_{21} = 2, w_{22} = 1 \Rightarrow w'_{21} = \alpha_4, \text{ where } S_{val\alpha_4} = \{ 1, 2 \}$$

Due to the fact that $w_{21} = 2$ was associated to $a_1 + a_3$ and that there is a bijection that makes the pairs

(cv_1, a_1) and (cv_3, a_3) , then $\alpha_4 = 2$ will be associated to the following combinations of choice variables: cv_1 and cv_3 .

On the other hand, $w_{22} = 1$ was associated to a_2 and the bijection defines the pair (cv_2, a_2) , then $\alpha_4 = 1$ will be associated to the combination of choice variables cv_2 .

Row 3: $w_{31} = 0, w_{32} = 1 \Rightarrow w'_{31} = \alpha_7$, where $S_{val\alpha_7} = \{ 0, 1 \}$ and $\alpha_7 = 0$ is associated to cv_1 and cv_3 , whereas $\alpha_7 = 1$ is associated to cv_2 .

The result of this first merging of columns can be seen in the figure 3.

$$\mathbf{W}(R_1^A) = \begin{pmatrix} t_1 & t_3 & t_4 & t_5 \\ -1 & 1 & 1 & -1 \\ \alpha_4 & -1 & -1 & 0 \\ \alpha_7 & 0 & -1 & 2 \end{pmatrix} \begin{matrix} p_1 \\ p_2 \\ p_3 \end{matrix}$$

$$\begin{matrix} & a_1 & & a_3 \\ a_1+a_3+a_3 & & a_2+a_3 & \end{matrix}$$

Fig. 3. First reduction of transitions.

Where $S_{valstr\alpha} = \{ cv_1, cv_2, cv_3 \} = \{ (\dots, \alpha_4 = 2, \dots, \alpha_7 = 0, \dots), (\dots, \alpha_4 = 1, \dots, \alpha_7 = 1, \dots), (\dots, \alpha_4 = 2, \dots, \alpha_7 = 0, \dots) \}$

Furthermore, the function of choice variables associated to the resulting transition, called t_1 in the figure 3, can be removed since it contains all the choice variables, as it is justified in the section 4.

Another couple of columns in the incidence matrix can be merged. They are the ones associated to the transitions t_3 and t_4 . In the first case the associated function of choice variables is $f_A(t_3, a_i) = a_1$. Moreover, the second column is associated to $f_A(t_4, a_i) = a_2 + a_3$.

In order to merge both columns, the elements that are placed in the same row are compared and if they are different an undefined structural parameter is created:

$$\text{Row 1: } w_{12} = w_{13} = 1 \Rightarrow w'_{12} = 1$$

$$\text{Row 2: } w_{22} = w_{23} = -1 \Rightarrow w'_{22} = -1$$

Row 3: $w_{32} = 0, w_{33} = -1 \Rightarrow w'_{32} = -\alpha_8$, where $S_{val\alpha_8} = \{ 0, 1 \}$ and $\alpha_8 = 0$ is associated to cv_1 , whereas $\alpha_8 = 1$ is associated to cv_2 and cv_3 .

The result of this second reduction of transitions can be seen in the figure 4.

$$\mathbf{W}(R_2^A) = \begin{pmatrix} t_1 & t_3 & t_5 \\ -1 & 1 & -1 \\ \alpha_4 & -1 & 0 \\ \alpha_7 & -\alpha_8 & 2 \\ a_1+a_3+a_3 & a_1+a_3+a_3 & a_3 \end{pmatrix} \begin{matrix} p_1 \\ p_2 \\ p_3 \end{matrix}$$

Fig. 4. Second reduction of transitions.

Where

$$S_{valstr\alpha} = \{ cv_1, cv_2, cv_3 \} = \{ (\dots, \alpha_4 = 2, \dots, \alpha_7 = 0, \alpha_8 = 0, \dots), (\dots, \alpha_4 = 1, \dots, \alpha_7 = 1, \alpha_8 = 1, \dots), (\dots, \alpha_4 = 2, \dots, \alpha_7 = 0, \alpha_8 = 1, \dots) \}$$

Furthermore,

the function of choice variables associated to the resulting transition can be removed since it contains all the choice variables, as it is justified in the section 4.

Step 3.

For every transition $t_i \in T(R^A)$, transform the function of choice variables associated to it, $f_A(t_i, a_j)$, into the sets $S_{str\alpha}(t_i)$ and $S_{valstr\alpha}(t_i)$.

In the case of t_1 and t_3 , the associated function of choice variables has been removed and the subsequent sets $S_{str\alpha}(t_i)$ and $S_{valstr\alpha}(t_i)$ have already been obtained.

On the contrary, t_5 has an associated function of choice variables, which is $f_A(t_5, a_i) = a_3$.

In order to develop this step, two new isolated transitions will be added, associated to the choice variables a_1 and a_2 respectively (Latorre *et al.* 2011a). The result can be seen in the resulting incidence matrix written in the figure 5.

$$\mathbf{W}(R_3^A) = \begin{pmatrix} t_3 & t_5 & t_6 & t_7 \\ -1 & 1 & -1 & 0 & 0 \\ \alpha_4 & -1 & 0 & 0 & 0 \\ \alpha_7 & -\alpha_8 & 2 & 0 & 0 \\ a_3 & a_1 & a_2 \end{pmatrix} \begin{matrix} p_1 \\ p_2 \\ p_3 \end{matrix}$$

Fig.5. Addition of isolated transitions to remove of the function $f_A(t_5, a_i)$.

At this stage, it is possible to reduce the transitions t_5 , t_6 and t_7 .

In order to merge the three columns of the incidence matrix related to these transitions, the elements that are placed in the same row are compared and if they are different an undefined structural parameter is created:

Row 1: $w_{13} = -1$ and $w_{14} = w_{15} = 0 \Rightarrow w'_{13} = -\alpha_3$, where $S_{val\alpha_3} = \{ 0, 1 \}$ and $\alpha_3 = 0$ is associated to cv_1 and cv_2 , whereas $\alpha_3 = 1$ is associated to cv_3 .

Row 2: $w_{23} = w_{24} = w_{25} = 0 \Rightarrow w'_{23} = 0$.

Row 3: $w_{33} = 2$ and $w_{34} = w_{35} = 0 \Rightarrow w'_{33} = \alpha_9$, where $S_{val\alpha_9} = \{ 0, 2 \}$ and $\alpha_9 = 0$ is associated to cv_1 and cv_2 , whereas $\alpha_9 = 2$ is associated to cv_3 .

The result of this step can be seen in the incidence matrix given in the figure 6.

$$\mathbf{W}(R_3^A) = \begin{pmatrix} t_1 & t_3 & t_5 & t_6 & t_7 \\ -1 & 1 & -1 & 0 & 0 \\ \alpha_4 & -1 & 0 & 0 & 0 \\ \alpha_7 & -\alpha_8 & 2 & 0 & 0 \\ a_3 & a_1 & a_2 \end{pmatrix} \begin{matrix} p_1 \\ p_2 \\ p_3 \end{matrix}$$

Fig.5. Addition of isolated transitions to remove of the function $f_A(t_5, a_i)$.

At this stage, it is possible to reduce the transitions t_5 , t_6 and t_7 .

In order to merge the three columns of the incidence matrix related to these transitions, the elements that are placed in the same row are compared and if they are different an undefined structural parameter is created:

Row 1: $w_{13} = -1$ and $w_{14} = w_{15} = 0 \Rightarrow w'_{13} = -\alpha_3$, where $S_{val\alpha_3} = \{ 0, 1 \}$ and $\alpha_3 = 0$ is associated to cv_1 and cv_2 , whereas $\alpha_3 = 1$ is associated to cv_3 .

Row 2: $w_{23} = w_{24} = w_{25} = 0 \Rightarrow w'_{23} = 0$.

Row 3: $w_{33} = 2$ and $w_{34} = w_{35} = 0 \Rightarrow w'_{33} = \alpha_9$, where $S_{val\alpha_9} = \{ 0, 2 \}$ and $\alpha_9 = 0$ is associated to cv_1 and cv_2 , whereas $\alpha_9 = 2$ is associated to cv_3 .

The result of this step can be seen in the incidence matrix given in the figure 6.

$$\mathbf{W}(R_4^A) = \begin{pmatrix} t_1 & t_3 & t_5 \\ -1 & 1 & -\alpha_3 \\ \alpha_4 & -1 & 0 \\ \alpha_7 & \alpha_8 & \alpha_8 \\ a_3 & a_1 & a_2 t_1 \end{pmatrix} \begin{matrix} p_1 \\ p_2 \\ p_3 \end{matrix}$$

Fig.6. Result of the reduction of the transitions t_5 , t_6 and t_7 into a single transition named t_5 .

Where $S_{str\alpha} = \{ \alpha_3, \alpha_4, \alpha_7, \alpha_8, \alpha_9 \}$ and $S_{valstr\alpha} = \{ cv_1, cv_2, cv_3 \} = \{ (0,2,0,0,0), (0,1,1,1,0), (1,2,0,1,2) \}$

Furthermore, the function of choice variables associated to the resulting transition can be removed since it contains all the choice variables, as it is justified in the section 4.

Step 4.

Represent the resulting compound Petri net R^c .

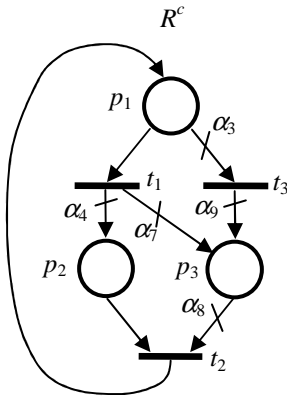


Fig. 7. Graphical representation of the resulting compound Petri net.

$$\mathbf{W}(R^c) = \begin{pmatrix} t_1 & t_2 & t_3 \\ -1 & 1 & -\alpha_3 \\ \alpha_4 & -1 & 0 \\ \alpha_7 & -\alpha_8 & \alpha_9 \end{pmatrix} \begin{matrix} p_1 \\ p_2 \\ p_3 \end{matrix}$$

Fig. 8. Matrix-based representation of the resulting compound Petri net.

The result of this transformation algorithm can be seen in the graphical and matrix-based representations of the resulting compound Petri net, which is equivalent to the original alternatives aggregation Petri net. These representations are shown in the figures 7 and 8 respectively.

$$|S_{valstr\alpha}(R^c)| = |\{ (0,2,0,0,0), (0,1,1,1,0), (1,2,0,1,2) \}| = 3$$

7. CONCLUSIONS

As a conclusion of this paper it can be stated that with this algorithm it has been completed the set of transformations between three common Petri net-based formalisms to represent Petri nets with alternative structural configurations for the main purpose of developing automatic decision support systems: the set of alternative Petri nets, the compound Petri net and the alternatives aggregation Petri net. It is now possible to perform any direct transformation between any pair of formalisms belonging to the mentioned group.

As open research lines it can be considered the analysis of the freedom degrees in these algorithms to adjust them in order to obtain the most compact models for the development of the most efficient optimization problems to solve the original decision problems.

ACKNOWLEDGMENTS

This paper has been partially supported by the project of the University of La Rioja and Banco Santander (grant number API12-11) ‘Sustainable production and productivity in industrial processes: integration of energy efficiency and environmental impact in the production model for integrated simulation and optimization’.

REFERENCES

- R., Alla. H., 2005. *Discrete, Continuous and Hybrid Petri nets*, Springer.
- Jensen, K., Kristensen, L.M., 2009. *Coloured Petri nets. Modelling and Validation of Concurrent Systems*. Springer.
- Berthelot, G., 1987. Transformations and decompositions of nets. In: Brauer, W., Reisig, W., and Rozenberg, G., eds. *PetriNets: Central Models and Their Properties, Advances in Petri Nets. Lecture Notes in Computer Science*, vol. 254-I, pp. 359–376. Springer, 1987.
- Haddad, S. and Pradat-Peyre, J.F., 2006. New Efficient Petri Nets Reductions for Parallel Programs Verification. *Parallel Processing Letters*, pages 101-116, World Scientific Publishing Company.
- Silva, M., 1993. Introducing Petri nets. In: Di Cesare, F., ed. *Practice of Petri Nets in Manufacturing*, pp. 1-62. Ed. Chapman&Hall.
- Latorre, J.I., Jiménez, E., Pérez, M., 2009. Decision taking on the production strategy of a manufacturing facility. An integrated methodology. *Proceedings of the 21st European Modelling and Simulation Symposium (EMSS 09)*. Puerto de la Cruz, Spain, vol. 2, pp. 1-7.
- Latorre, J.I., Jiménez, E., Pérez, M., 2011. Matrix-based operations and equivalence classes in alternative Petri nets. *Proceedings of the 23rd European Modelling and Simulation Symposium (EMSS 11)*. Rome, Italy, pp. 587-592.
- Latorre, J.I., Jiménez, E., Pérez, M., 2011. Petri net transformation for decision making: compound Petri nets to alternatives aggregation Petri nets. *Proceedings of the 23rd European Modelling and Simulation Symposium (EMSS 11)*. Rome, Italy, pp. 613-618.
- Latorre, J.I., Jiménez, E., Pérez, M., 2011. Petri nets with exclusive entities for decision making. *International Journal of Simulation and Process Modeling, Special Issue on the I3M 2011 Multiconference*. Inderscience Publishers.
- Tsinarakis, G. J., Tsurveloudis, N. C., and Valavanis, K. P., 2005. Petri Net Modeling of Routing and Operation Flexibility in Production Systems. *Proceedings of the 13th Mediterranean Conference on Control and Automation*, pages 352-357.
- Zimmermann, A.; Freiheit, J.; Huck, A. 2001. A Petri net based design engine for manufacturing systems. *International Journal of Production Research*, Vol. 39, No. 2, pages 225-253.

OBJECT-ORIENTED MULTI-DOMAIN MODELLING OF MACHINE TOOLS: A CASE STUDY

Bernhard Heinzl^(a), Michael Landsiedl^(b), Niki Popper^(c),
Alexandros-Athanassios Dimitriou^(d), Fabian Dür^(e), Friedrich Bleicher^(f),
Christian Reinisch^(g), Felix Breitenecker^(h)

^{(a) (g)}Institute for Computer Aided Automation, Vienna University of Technology
^{(a) (b) (c)}dwh Simulation Services, Vienna

^{(d) (e) (f)}Institute for Production Engineering and Laser Technology, Vienna University of Technology

^(h)Institute for Analysis and Scientific Computing, Vienna University of Technology

^(a)bernhard.heinzl@tuwien.ac.at, ^(b)michael.landsiedl@drahtwarenhandlung.at, ^(c)niki.popper@drahtwarenhandlung.at,
^(d)dimitriou@ift.at, ^(e)duer@ift.at, ^(f)bleicher@ift.at, ^(g)christian.reinisch@tuwien.ac.at, ^(h)felix.breitenecker@tuwien.ac.at

ABSTRACT

A number of current research projects aim at increasing energy efficiency in production by using comprehensive simulation models of manufacturing plants. In order to gain knowledge about the optimization potential of machine tools, a simulation model of a turning lathe is developed. Using an object-oriented modelling approach allows combining component models of mechanical, electrical and thermal parts in a structural manner in one multi-domain model. This bottom-up approach is combined with stepwise top-down modelling in three stages in order to identify numerical boundaries of the simulation. Simulation results are validated against measurement data. It is confirmed that object-oriented modelling leads to flexible and modular models, but the automatically generated equations are less efficient during simulation, therefore making it necessary to perform manual adjustments in the model. To increase simulation speed, multirate simulation is performed in Simscape using local implicit fixed-step solvers.

Keywords: object-oriented, machine tool, turning lathe, Simscape

1. INTRODUCTION

Rising energy costs and efforts to increase productivity in manufacturing facilities lead to an increased focus on energy efficiency in production. Especially machine tools in metal-cutting manufacturing are among the largest consumers of energy, which have great potential for optimization compared to other energy-intensive manufacturing processes.

For this reason, several current research projects aim at increasing energy efficiency in production by developing comprehensive simulation models of production halls for energy analysis in order to be able to make qualified prediction about the efficiency of different energy saving measures and identify optimization potential (Dorn and Bleicher 2010).

One part of this project investigates the micro-structures of production plants (individual processes and machines) by making extensive energy analysis based on simulation models. Some of these aspects are studied in more detail by developing a multi-domain model of a turning lathe as an example of a machine tool.

A comprehensive approach combines electrical, mechanical as well as thermal aspects of the lathe in one overall model, which afterwards allows for extensive analysis and evaluation regarding energy distribution, comparison of feed and cutting forces as well as dissipated heat.

For modelling we consider a high-level object-oriented approach for physical systems, which provides flexibility and modularity for combining bottom-up modelling with stepwise top-down development in three stages with increasing level of detail. An overview is given in figure 1.

This procedure enables identifying numerical boundaries of the simulation and shows which model complexity can be handled with sufficient performance and which physical components can therefore be taken into account.

Simulation results are validated against real measurement data obtained from an actual turning lathe.

Implementation is done in MATLAB/Simscape as a common simulator for object-oriented modelling of physical systems (MathWorks 2011a; MathWorks 2011b).

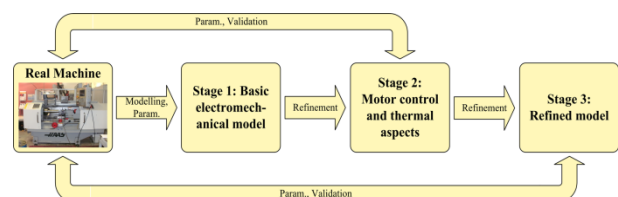


Figure 1: Overview of the Three Stages in the Modelling Process

2. STAGE 1: BASIC ELECTROMECHANICAL MODEL

A first step for model development requires investigation of the turning lathe to be modelled and identification of the main electrical and mechanical components. Although the considered machine tool is rather simple compared to others, it provides sufficient possibilities for our investigations. There are three main drivelines:

- Main drive: Main motor, gear belt drive, spindle with chuck and workpiece
- Longitudinal feed (z-axis): Servomotor, lead-screw drive, linear bearings and slide holding the cross feed
- Cross feed (x-axis): Servomotor, leadscrew drive, linear bearings and cross-slide with tool holder and cutting tool

The main drive sets the workpiece into rotation, longitudinal and cross feed drives allow positioning the tool in z- and x-direction (axial and radial to the workpiece), see figure 2. During machining, the cutting tool penetrates the workpiece and removes material in form of a chip during relative motion. The cutting energy is mostly converted into thermal energy. All three drivelines receive their electric power from an inverter, which is simplified in the first step as ideal voltage sources.

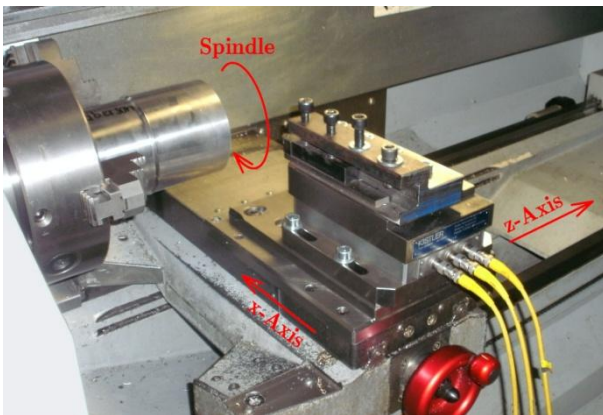


Figure 2: The Three Axes of the Lathe: Spindle for Driving the Workpiece, Longitudinal and Cross Feed for Positioning the Tool in the z- and x-Direction.

For implementing the developed simulation models, we chose Simscape as an extension of MATLAB/Simulink for object-oriented multi-domain modelling and simulation of physical systems (MathWorks 2011a, MathWorks 2011b).

The first overall model is comparatively simple and contains the main mechanical and electrical components of the main drive and the slides for automatic feed and infeed. As part of this first model, figure 3 shows the Simscape model of the main drive with asynchronous engine, voltage supply, gear belt drive, friction components and mechanical loads such as inertias from spindle, chuck and workpiece. The basic structure

of the drive is easy to see which is helpful for further model adjustments and refinements, therefore pointing out one of the big advantages of this object-oriented modelling approach.

The asynchronous motor as well as the servo motors for the remaining drives of the lathe and certain basic mechanical components like gear belt drive, lead screw and linear bearings are modelled as Simscape components using Simscape Language (see MathWorks 2011a) with parameters extracted from available data sheets. A code fragment of this implementation for the asynchronous machine is depicted in figure 4. It shows common equations in normalized space vector description that can be found in relevant literature (e.g. Schröder 2009).

```

component AsynchronousMachine
(...)
parameters (Access = public, Hidden = true)
    M = 2/3*[1,-1/2,-1/2;0,sqrt(3)/2,-sqrt(3)/2];
end
equations
    (...)
    us' == M*[u1;u2;u3]; is' == M*[i1;i2;i3];
    i1 + i2 + i3 == 0;
    %Standardized equations for ASM
    us == is*rs + psis.der/Omegaref_el;
    ur == ir*rr + psir.der/Omegaref_el...
        -[-psir(2),psir(1)]*omegam;
    psis == ls*is + ls*(1-sigma)*ir;
    psir == ls*(1-sigma)*(is+ir);
    ur == [0,0];
    %Torque equation
    mr == is(2)*psir(1)-is(1)*psir(2);
end

```

Figure 4: Code Fragment of the Asynchronous Machine Model Using Simscape Language.

Existing Simscape blocks from the Simscape Foundation library (see MathWorks 2011b) complete the model with components for inertia, friction and sensor blocks for measuring state variables. During the machining process, the cutting force generates an additional torque on the motor. This load is modelled as a torque source, where the value of the torque is calculated externally using common formulas and parameters (like shown in Degner et al. 2009).

In order to keep the first model simple and focus on modelling of electrical and mechanical parts, feedback control for the drive motors is not included. This however limits possible simulation scenarios, for example only cases with constant motor speed can be considered. Also, thermal investigations are not yet provided in this model.

3. STAGE 2: MOTOR CONTROL AND THERMAL ASPECTS

The first modelling stage showed that the object-oriented modelling approach is indeed suitable for basic modelling tasks regarding machine tools. In this next stage we further develop the model and therefore obtain further possible simulation scenarios for observation.

The basic electromechanical model is extended by a number of components:

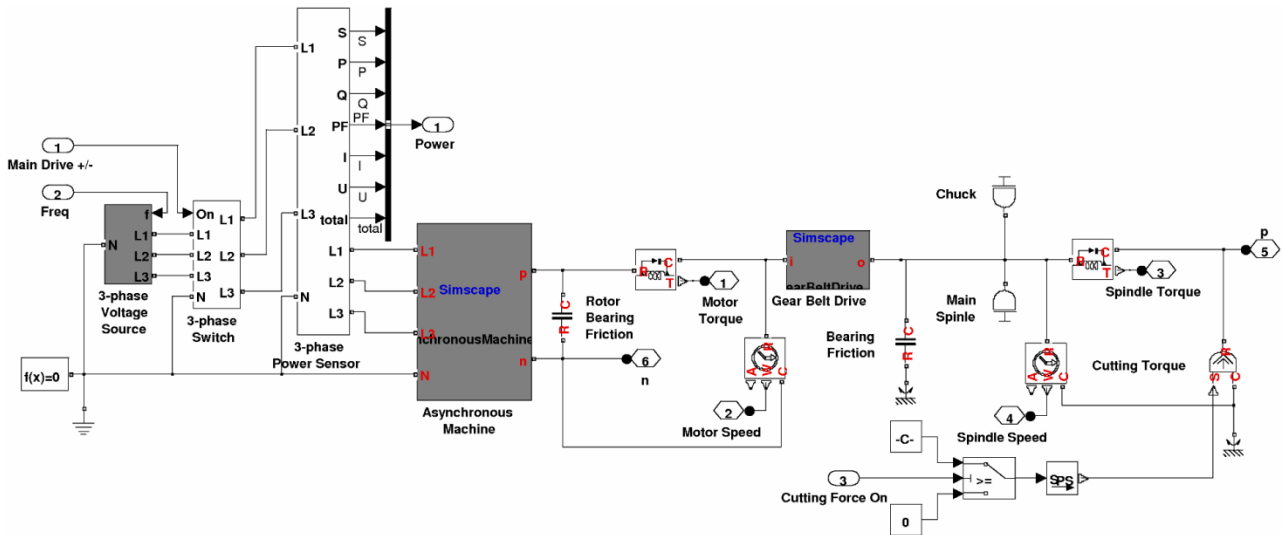


Figure 3: Main Drive of the Turning Lathe Model with Asynchronous Engine, Voltage Supply, Gear Belt Drive and Mechanical Loads.

- Feedback control for all three drive motors
- Calculation of generated heat in lossy components, especially the drive motors
- Heat transition to the environment
- Modelling of energy division in the cutting process

3.1. Modelling

The necessity for appropriate motor control for the overall dynamics is also established in (Heinzl et al. 2012). Figure 5 shows the subsystem for the feedback control implemented in Simulink. Cascaded controllers allow control of position, speed and stator current. Since the stator current is typically controlled in the rotor coordinate system, coordinate transformation with the actual rotor angle has to be performed. Nominal values are created including speed and acceleration limits according to target positions which are defined in advance. For controller design, we made use of available data from data sheets as well as manual iterative adjustment in order for the system to work properly.

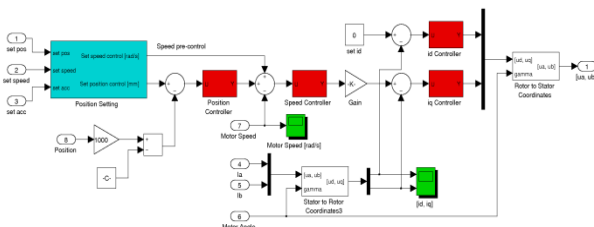


Figure 5: Slide Control with Position, Speed and Current Controller (Red Blocks) and Space Vector Output

The output of the controller subsystem is a vector for the stator voltage, which is then split into phase voltages for an idealized 3-phase converter, which directly supplies the drive motor. The graphical representation of this inverter can be seen in figure 6.

Further model extensions take the waste heat into account that is generated in various components, espe-

cially the drive motors, gear belt drive and friction elements. For that, all necessary components from the model in section 2 are modified with a thermal output port. The waste heat is stored and dissipated into the surrounding environment via convective and radiative heat transfer components, see figure 6. Necessary heat transfer coefficients are taken from available literature (Staton 2008; Boglietti 2003).

In order to increase simulation speed, some adjustments had to be made in the Simscape implementation already in this modelling stage. For that, the three drive trains (main drive, slide and cross-slide) were splint into separate Simscape networks (these are called physical networks or object diagrams), only connected via directed (causal) Simulink signal connections (an overview can be seen in figure 10). This enables more efficient equation generation and handling by the simulator.

3.2. Simulation Results

The modifications now allows for more complex simulation scenarios. As an example, we investigate the turning process sketched in figure 7. Used cutting parameters are:

- Cutting speed: $v_c = 200 \frac{\text{m}}{\text{min}}$,
- Feed: $f = 0.2 \frac{\text{mm}}{\text{U}}$,
- Cutting depth: $a_p = 2 \text{ mm}$,
- Material: C45E.

Figure 8 depicts the respective trajectory of the tool tip and time values. All position values are measured with respect to the coordinate system illustrated in figure 7 (green arrows). The simulation starts at an outside position. First, slide and cross-slide are activated with maximum velocity in order to get to the start position for the turning process. After that, the turning process is started with smaller feed velocity. The impact

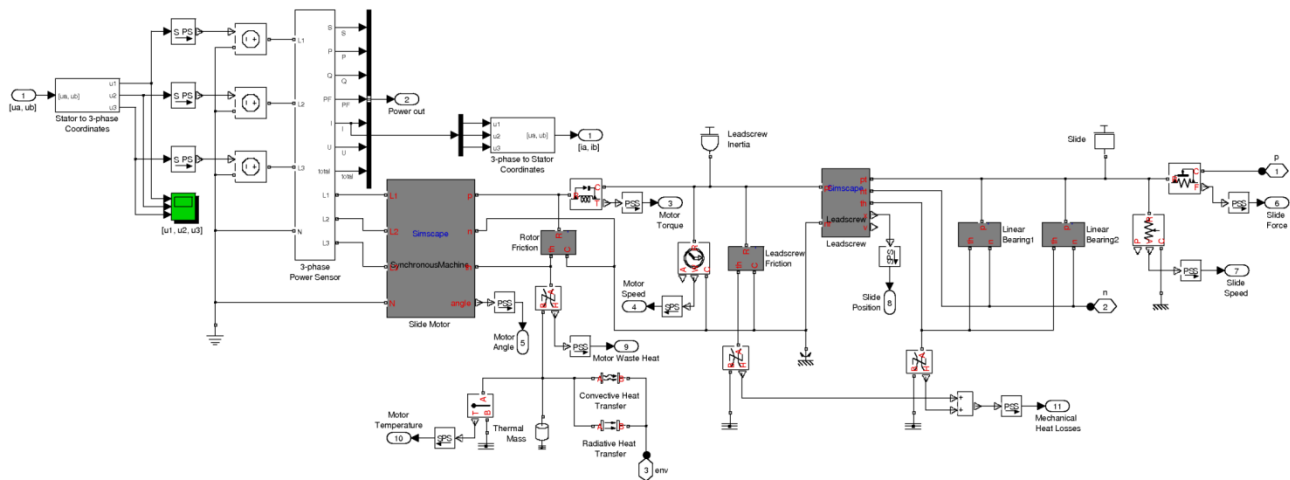


Figure 6: Model of the Slide Drive for the Turning Lathe with 3-phase Voltage Supply, Servomotor, Leadscrew Model, Linear Bearings and Thermal Components.

point between tool and workpiece does not leave any noticeable disturbances. The process is finished with negative infeed to the final position.

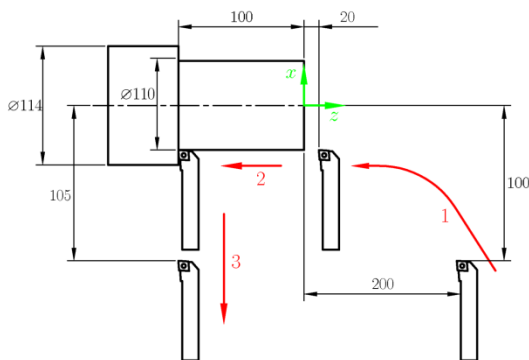


Figure 7: Investigated Simulation Scenario of a Typical Turning Process

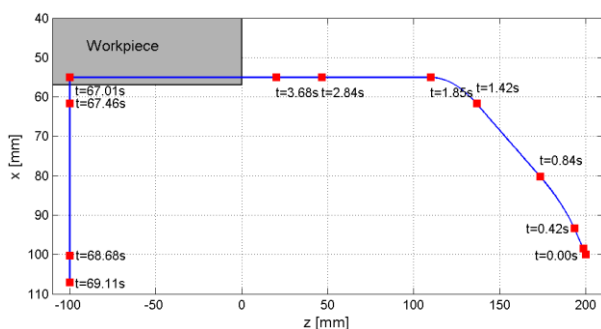


Figure 8: Trajectory of the Tool Tip and Time Values for the Simulation Scenario shown in Figure 7.

For validation, figure 9 compares the calculated total power consumption against measurement data obtained from the turning lathe. Although the cutting parameters were the same for both cases, there is still significant difference in the results, which shows that further model refinement is necessary.

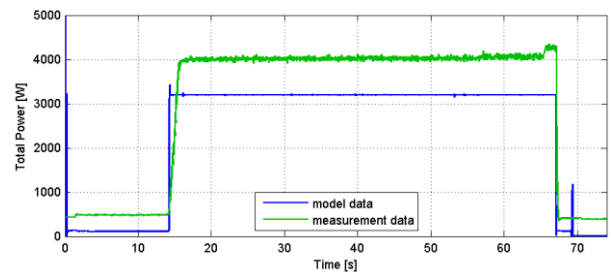


Figure 9: Comparison of Total Power Consumption Between Simulation and Measurement Data.

4. STAGE 3: REFINED MODEL

In the third and final modelling stage, the model is refined by more detailed investigations of the energy supply including power electronic components for a rectifier and inverter.

4.1. Modelling

Since the high-frequency switching operations of an inverter are difficult to realize with sufficient accuracy and simulation speed in a mainly continuous model, the switching inverter is replaced by an idealized version which only implements energy conservation and directly sets desired phase voltages.

Also, additional electrical loads like the control computer or lighting are considered because of their influence on the total power consumption.

For better simulation performance, the division of different drivelines into isolated Simscape networks (which are only connected to each other via directed (causal) Simulink signal connections), which was also mentioned in section 3, is continued and expanded on the new model of rectifier and inverter. Figure 10 given an overview of these Simscape networks. In the top part, the three blocks in the middle represent the subsystems for the drivelines shown in figure 3 and 6, resp., which each belong to a separate Simscape network.

In addition, Simscape allows combining the global solver algorithm with local implicit fixed-step solvers, which can handle isolated Simscape networks and

therefore allow performing multirate simulations for better performance (see also MathWorks 2011b). In the given model, this method is employed for the rectifier subsystem, which made it necessary to isolate the respective part from other Simscape networks based on assumptions for signal causality between these networks (see figure 10 bottom).

The local system appears as a discrete subsystem to the global solver, which triggers an event at each local step. A comparison of solver steps between global and local solver is given in figure 11.

On the one hand this results in loss of accuracy for the specified local part, but on the other hand the global solver does not have to resolve high-frequency oscillations in the inverter, since this part only appears as a discrete subsystem in the global model.

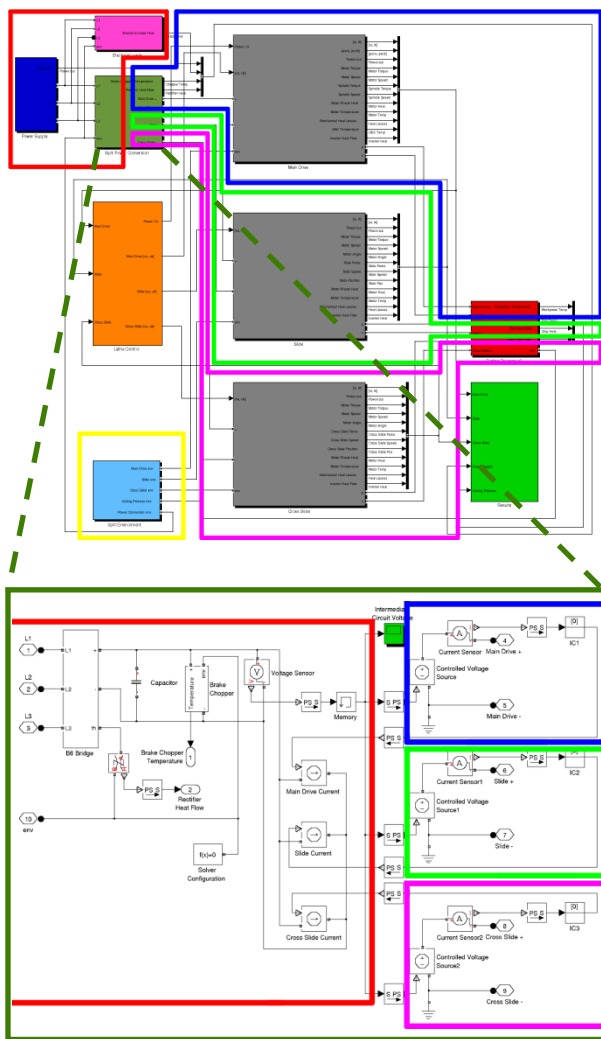


Figure 10: Top: Overview of the Total Simulation Model in Simulink/Simscape. Marked are the Separate Simscape Networks, Which are Only Connected to Each Other via Directed Simulink Signal Connections. Bottom: Detail of the Subsystem for the Electric 3-phase Converter, where the Three Inverters on the Right are Isolated from the Rectifier on the Left. The Left Part (Red) is Handled by a Local Solver Using Backward Euler Method.

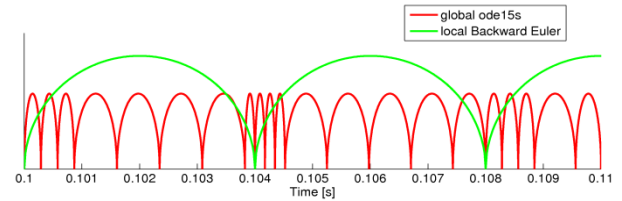


Figure 11: Comparison of Steps Between Local Solver (Backward Euler) and Global Solver (Simulink ode15s).

4.2. Simulation Results

For comparison of simulation results, we again consider the scenario shown in figure 7. The results of a simulation run with the refined model are shown in Figure 12.

Figure 13 visualizes the energy distribution in the system for the given scenario. The input energy is converted into heat mainly in power electronics components, mechanical friction components and in the cutting process. A small part remains as latent energy in the system.

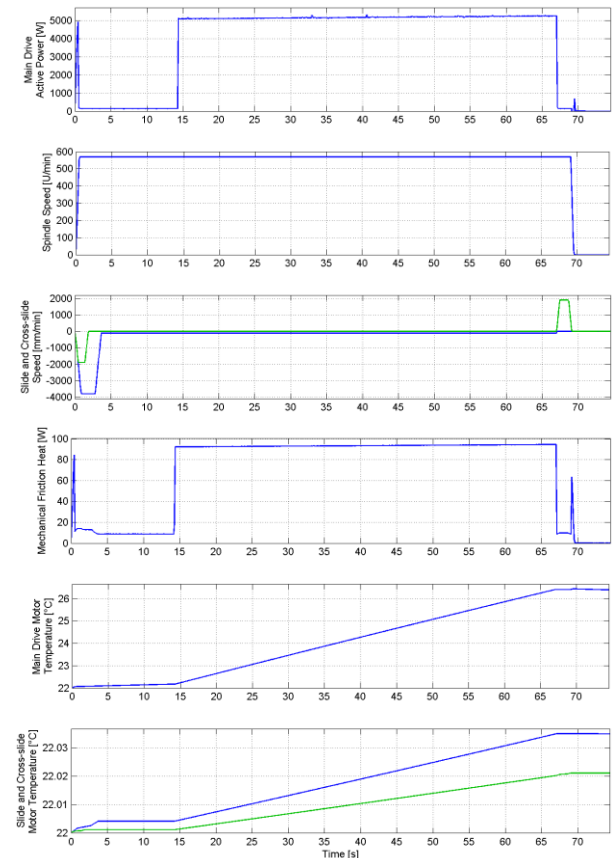


Figure 12: Results of a Simulation Run with the Refined Model. The Plots Show (from Top to Bottom) Main Drive Active Power, Spindle Speed, Slide and Cross-Slide Speed, Mechanical Friction Heat and Main Drive, Slide and Cross-Slide Motor Temperature.

For validation, figure 14 again shows the results for total power consumption compared to respective measurement data. Comparison with figure 9 shows significant better agreement for the refined model. The bottom part of figure 14 compares calculated feed and cutting forces with measurement data.

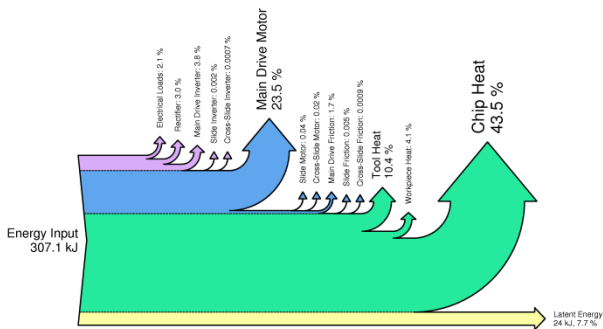


Figure 13: Energy Distribution in the System, Grouped by Parts where Input Energy is Converted into Heat (Power Electronics, Mechanical Friction, Cutting Process, Latent Energy)

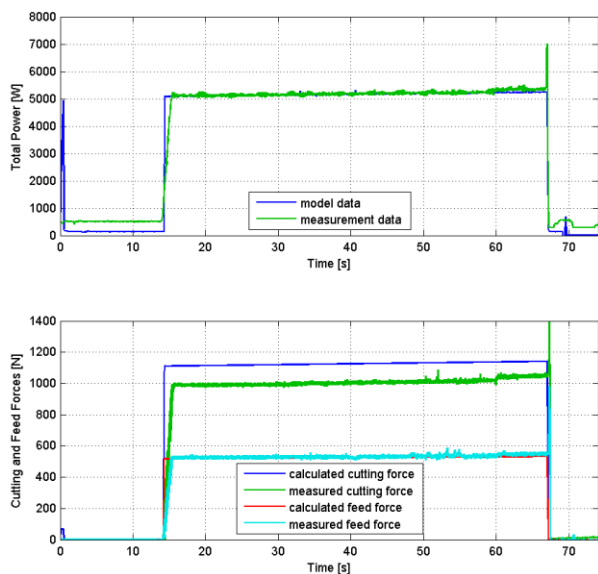


Figure 14: Comparison of Total Power Consumption (Top) as well as Feed and Cutting Forces (Bottom) Between Simulation and Measurement Data.

5. CONCLUSION

It can be said that the advantages of object-oriented modelling of physical systems have been confirmed in application. This approach leads to modular models, which preserve the basic structure of the original system and can easily be modified and adapted. However, this approach results in more complex models with a larger systems of equations, which moreover are less efficient for simulation, so that difficulties with insufficient performance are likely to occur even for models of moderate size.

Manual adjustment can help increasing simulation speed significantly, for example by splitting the model in isolated Simscape networks. This also allows performing multirate simulation using local Simscape solvers. However, splitting the model requires assumptions regarding signal causality, which basically is contradictory to the object-oriented modelling approach.

Comparison of the simulation results with measurement data showed sufficient agreement in principle, however some improvements in the models are still

possible, for example in the models for the drive motors or the cutting process.

REFERENCES

- Boglietti, A., Cavagnino, A. and Staton, D.A., 2003. Thermal analysis of TEFC induction motors. *Industry Applications Conference*, p. 849-856.
- Degner, W., Lutze, H., and Smejkal, E., 2009. *Spanende Formung. Theorie – Berechnung – Richtwerte*. München: Hanser Verlag.
- Dorn, C. and Bleicher, F., 2010. Interdisziplinäre Forschung zur Energieoptimierung in Fertigungsbetrieben. *Junior Science Conference 2010*.
- Heinzl, B., Dorn, C. and Dimitriou, A., 2012. Object-oriented Modelling of Machine Tools for Energy Efficiency Analysis in Production. *In Proceedings of MATHMOD Vienna 2012 – 7th Vienna Conference on Mathematical Modelling*. February 15-17, 2012, Vienna.
- MathWorks 2011a. *Simscape Language Guide*. Available from: http://www.mathworks.com/help/pdf_doc/physmod/simscape/Simscape_lang.pdf. [Accessed May 15, 2012].
- MathWorks 2011b. *Simscape User's Guide*. Available from: http://www.mathworks.com/help/pdf_doc/physmod/simscape/Simscape_ug.pdf. [Accessed May 15, 2012].
- Schröder, D., 2009. *Elektrische Antriebe – Grundlagen*. Berlin Heidelberg: Springer. ISBN 978-3-642-02989-9.
- Staton, D.A. and Cavagnino, A., 2008. Convection heat transfer and flow calculations suitable for electric machines thermal models. *IEEE Transactions on Industrial Electronics*, p. 3509-3516.

DYNAMIC ANALYSIS OF A WORKPIECE DEFORMATION IN THE ROLL BENDING PROCESS BY FEM SIMULATION

Tran Hoang Quan^(a), Henri Champliaud^(b), Zhengkun Feng^(c) and Dao Thien-My^(d)

^(a)PhD student, Mechanical Engineering Department, École de Technologie Supérieure, Quebec, Canada.

^(b)Professor, Mechanical Engineering Department, École de Technologie Supérieure, Quebec, Canada.

^(c)Researcher, Mechanical Engineering Department, École de Technologie Supérieure, Quebec, Canada.

^(d)Professor, Mechanical Engineering Department, École de Technologie Supérieure, Quebec, Canada.

^(a)Email: hoang-quan.tran.1@ens.etsmtl.ca,

ABSTRACT

High strength steel is widely used in the manufacturing of parts dealing with heavy cyclic loads and corrosive environments. But to obtain accurate final shapes for this type of steel by roll bending process is not easy. And it becomes a hard-to-solve problem when the part to produce is large, thick and unrepeated. In order to analyse the dynamic deformation of the workpiece during the roll bending process, Finite Element Method (FEM)–Ansys/LS-Dyna is introduced to do this research. Various dynamic simulations based on 3D element models are performed to provide better understanding of whole deformation history and distribution of stress-strain of the workpiece during this particular process. The results from FE simulation are then compared with corresponding experiment results from an industrial roll bending machine.

Keywords: FE dynamic simulation, roll bending-process, Nonlinear FEM, Elasto-plastic

1. INTRODUCTION

Roll bending is a continuous forming process where plates, sheets, beams, pipes, and even rolled shapes and extrusions are bent to a desired curvature using forming rolls. With the advantages such as reducing the setting up time and material, lowering the cost in tooling investment and equipment and to achieve high final shape quality, over the years, the roll bending process was one of the fundamental process used in metalworking. Moreover, this process is a manufacturing method that is beginning to be taken into serious consideration by industrials for producing large, thick parts such as the thick conical shape of the crown in a Francis turbine runner.

The description of the basic principle and operation for this process can be found in Kohser (2002) and Couture P. (2004). Bouhelier (1982) gives the formulas for calculating the springback, applied forces and the essential required power. Yang (1988) constructed a simulation model for estimating deformation during the

various periods of the roll-bending process. Hua et al (1994-1999) have done a considerable amount of work studying the four-rolls bending process and for understanding the bending mechanism. Based on experiments, they discuss the mechanism of roll-bending process. Analyses of pyramidal three-roll bending process bending can also be found in some publications (Yang (1988), Bassett M. B (1996), Hansen N. E. and Roggendorff S. (1979)), but none of them deals with dynamic analysis of workpiece during the process. The roll bending process on the other hand is a particular bending process where the plate may be assumed as static three points bending, but in the whole process consideration, the deformations of workpiece are dynamic and its single-bending assumption will limit understanding of the bending mechanisms. Therefore, in a more recent article Zeng J., Liu Z., and Champliaud H. (2008) or Feng Z., Champliaud H., Dao.T.M. (2009), or Feng Z., Champliaud H. (2011) developed a 3D simulation model which is based on the elastic-plastic explicit dynamic FEM under the Ansys/LS-Dyna to study the dynamic process of roll plate bending for thick plate conical tubular shape. However, the authors only discuss the deformation of workpiece in the whole process; the distribution of stress-strain leaved in the workpiece of each step of this process has not been studied yet. Hence 3D dynamic FE simulation and dynamic deformation of the workpiece by an asymmetrical roll bending machine will mainly be discussed in this paper.

2. DEFORMATIONS OF WORKPIECE

The axisymmetric roll bending model that consists of three rolls of same radius r is used to shape the flat-plate thickness t into a final radius R as shown in Fig1. During the process, the lateral roll is raised up to a specific position to control the diameter of the final shape while the workpiece is fed and driven forward by two rotating bottom and top rolls. By this relationship, dimension of the final shape depends on the position of the rolls, see Eqn. (1)

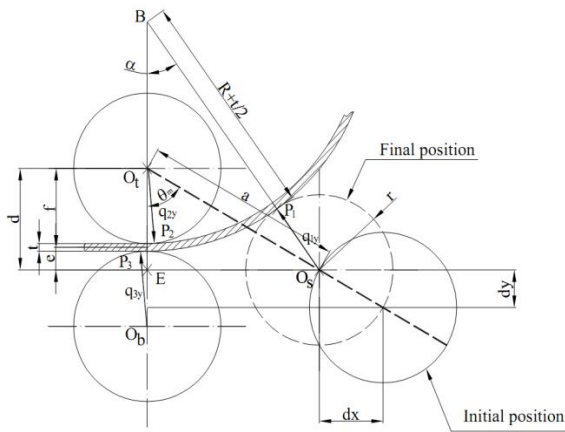


Figure 1: Geometric setup of the asymmetric roll bending process

$$R = \frac{(a^2 + f^2 - (r+t/2)^2 - 2af \cos(\theta_m)) / 2}{(r+t/2 + f - a \cos(\theta_m))} \quad (1)$$

As seen in Fig. 1, the workpiece can be modeled as a beam under three point bending where the plate between P_1P_3 is restricted by contacts with top roll, bottom roll and lateral roll during continuous roll bending mode. If the lateral roll is raised up to a desirable position where the applied stress in the plate is below the yield stress of material, this plate will recover its original shape when loading is removed. Otherwise, the plate will be plastically deformed. The types of these loadings are shown in Fig.2

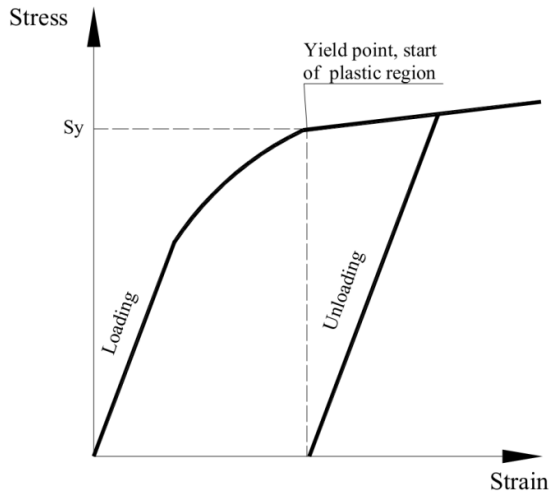


Figure 2: Types of loadings in roll bending process

3. FINITE ELEMENT MODEL AND EXPERIMENTS

In this section, a 3-dimensional numerical FE model of roll bending process described in section 2 was built in the Ansys/ LS-Dyna environment (2011). The FE model consists of four main components: three rolls, and one forming plate which are illustrated in Fig. 3

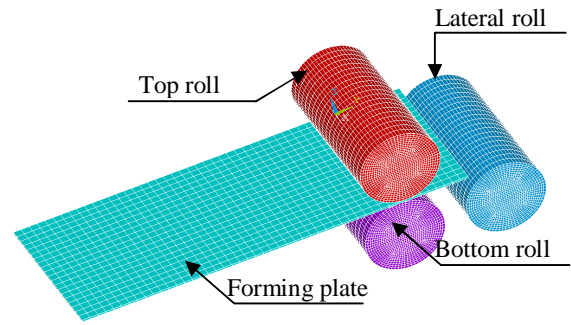


Figure 3: FEM model of roll bending process

The FE simulation involves structural computations for predicting the distribution of stress leaved in workpiece from the initial pass to the final pass of the process. Since the plate thickness is much smaller than its width and the length, this kind of structure is generally modeled with the explicit SHELL163 element of Ansys/LS-Dyna. The rolls are considered as rigid body in comparison with the elasto-plastic deformable plate.

Stainless steel is commonly selected for turbines and hydraulic accessories, so simulation is done with the stainless steel ASTM A743 grade CA-6NM by using the data provided in Zeng J. (2008). In this simulation, bilinear isotropic model (BISO), a material model of Ansys/LS-Dyna that uses two slopes to represent the behavior of material.

The interaction between components is defined by contact surface. In this roll bending process model, the surface of the roll is smaller than the surface of workpiece. Therefore, the automatic node to surface contacts were used to define interaction between rolls and plate. This kind of surface contact is efficient when a smaller surface come into contact with a larger one. There are three main contact surfaces defined between the plate and rolls for our roll bending FE model. The workpiece is driven and deformed to its final shape via these contact surfaces. Besides, two coefficients of friction include static friction and dynamic friction that must be defined for the contact model when defining the contact surface. The values of the two coefficients of friction are available in Zeng J. (2008). For loading condition, in this simulation, the top and the bottom rolls are constrained as rotation and no translation. The lateral roll is constrained as translation and no self-rotation to press the forming plate against the top roll. The plate is not typically constrained, but by the rolls through contacts in this simulation.

For measuring the stress distribution on the plate, a strain gauge, known as a device whose electrical resistance varies in proportion to the amount of strain in the device, is used to record the strain during the bending process. Attached the strain gauge directly to the plate by special glue is shown in Fig.4. Then the plate is fed into machine for bending (Fig.5). The strain gauge will record and export the strain value of plate into a strain recorder when the plate is deformed.

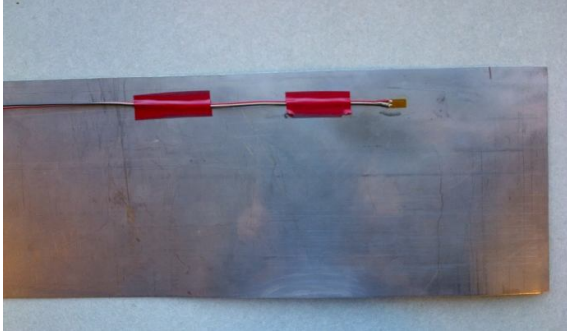


Figure 4: Gluing the strain gauge directly on the plate

From the strain ε read by “The Vishay model P3 strain recorder”, the amount of applied stress σ can be computed using the following formula

$$\sigma = E\varepsilon \quad (2)$$

Where E is modulus of elasticity of material

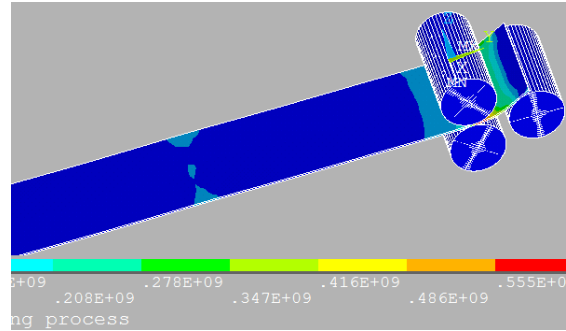


Figure 5: Roll bending process experiment

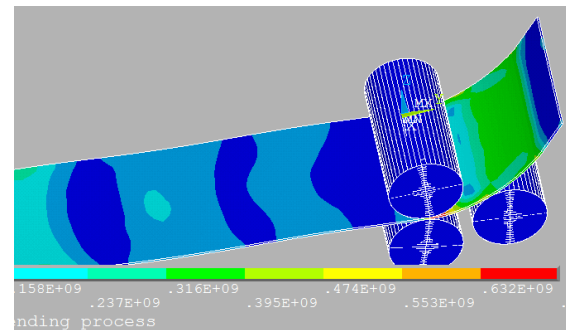
4. RESULTS AND DISCUSSION

The FE model of axisymmetric roll bending machine discussed in section 3 is built in the Ansys/ LS-Dyna environment. The main geometrical data taken from the roll bending machine at École de technologie Supérieure (Canada) includes radius of rolls $r=100$ mm, operating action line angle of lateral rolls $\theta_m = 60^\circ$. The research accomplished to date on this process is preliminary, but very promising. Finite Element Method is quite successful to simulate the roll bending process.

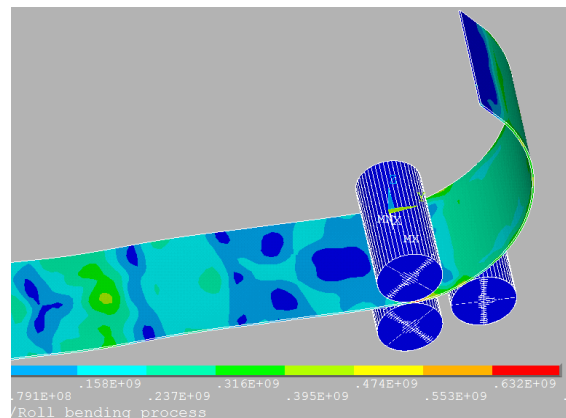
The successive shapes of the forming plate can be plotted at each step of this process as shown in Fig.6.



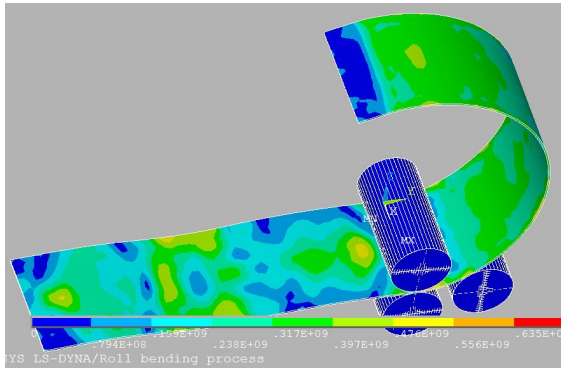
Distribution of stress at the early stage of the process



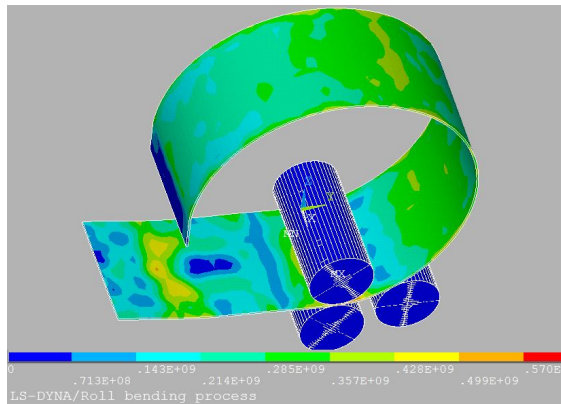
Distribution of stress at 20% of the process



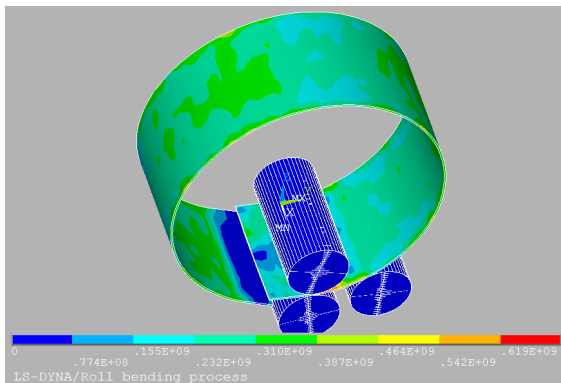
Distribution of stress at 40% of the process



Distribution of stress at 60% of the process



Distribution of stress at 80% of process



Distribution of stress when the process is completed

Figure 6: Shape of workpiece at various steps of the roll bending process

These results are interesting because it assists in establishing and shaping whole working-process in an industrial context. The bending stress results from FE simulation for above different time steps of roll bending process are compared and shown in Fig.7. In the deformation zone P_3P_1 , the bending stress increases when the workpieces is fed into the upper and bottom

rolls. After getting the maximum value at the contact region between the plate and the top roll, this value will reduce and get minimum value in the contact region between plate and lateral roll. However, as can be observed from Fig.7, the curve of stress distribution at the early stage of this process is different with other stages. The maximum bending stress obtained in the deformation zone at this stage is also higher than the steady bending continuous stages.

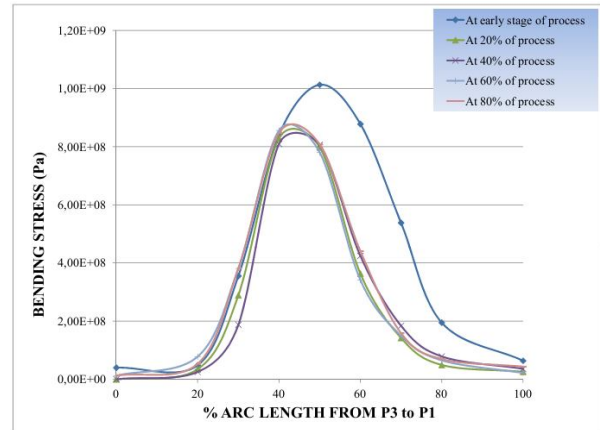


Figure 7: Stress distribution at various steps of the roll bending process

These differences may be explained by changing of contact region between the plate and rolls. The flat workpiece is firstly elastically deformed when the lateral roll is firstly raised up until reaching a desirable position, where the plastic deformation will occur to get a desirable radius. The bending stress value is dependent on material properties and workpiece process parameters (the plate thickness, bending radius etc.). However, in the steady continuous bending stage, under condition of rotating of rolls and moving towards of workpiece, there may occur losing contact between workpiece and upper and bottom rolls and thus the constraint of the bending system becomes less rigid. The combination of these effects would affect the stress distribution leave in the workpiece.

As mentioned, there are many workpiece characteristics that affect formability of the roll bending process such as the plate thickness, the final shape radius, material properties etc. Among them, plate thickness may have the highest influence. Therefore, it is necessary to understand the influences of this parameter on the stress-strain distribution of workpiece during the roll bending process. Comparisons of FE simulation for roll bending flat plates with thickness of 1.0mm, 1.5mm, 2.0mm, 2.5mm and 3mm into 80mm of final shape radius can be seen in Fig.8. Note that in these simulations, only plate thicknesses are changed while other input material properties and workpieces parameters are identical. The curves of FE simulation results for five different plate thicknesses tend to get the maximum bending stress at the position of 40% of arc

length from P_3 to P_1 in the deformation zone (getting start at P_3) as seen in Fig. 8

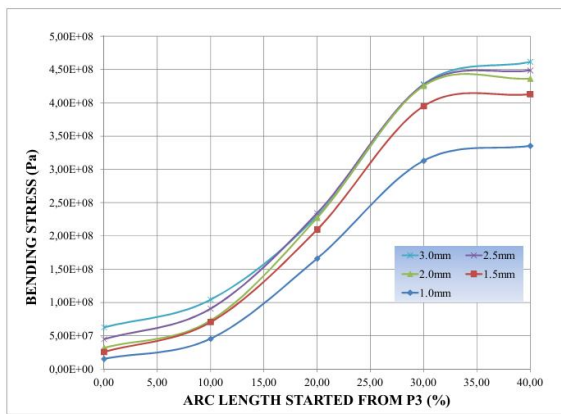


Figure 8: Stress distribution for various plate thicknesses

It can be also observed from Fig. 8 that the bending stress increases quickly when the plate thickness is over 1.0 mm. As expected, the thicker workpiece will get higher stress value. However, as summarized in Fig. 9, the bending stress increases 1.23 times, 1.30 times, 1.34 times and 1.38 times when the plate thickness go up 1.5 times, 2.0 times, 2.5 times and 3.0 times, respectively. In other words, it is a nonlinear changing of bending stress when the plate thicknesses are increased. This simulation results are not only adequately representing the bending process but also help for choosing a machine capacity depending on the plate thickness.

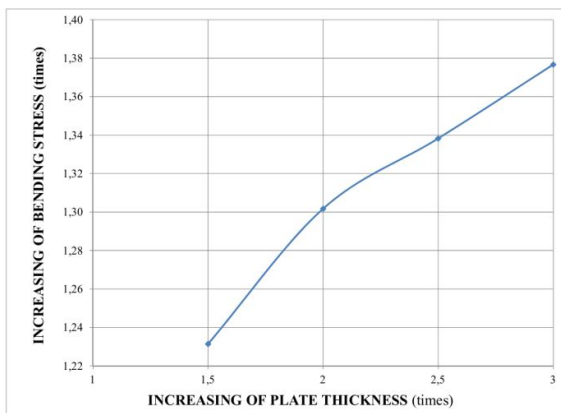


Figure 9: Nonlinear changing of bending stress

In Fig. 10 and Fig. 11, a series of simulations and experiments were performed on 1mm stainless steel with various final radius to study the effects of final radius on bending stress. While the width and thickness of workpiece always remain constants, its radius reduces by rising up the lateral roll. For experiments, all input parameters are kept the same as the input

parameters of FE simulations. It can be seen the curve for two results tends to reduce, from small radius to large radius of final bending shape.

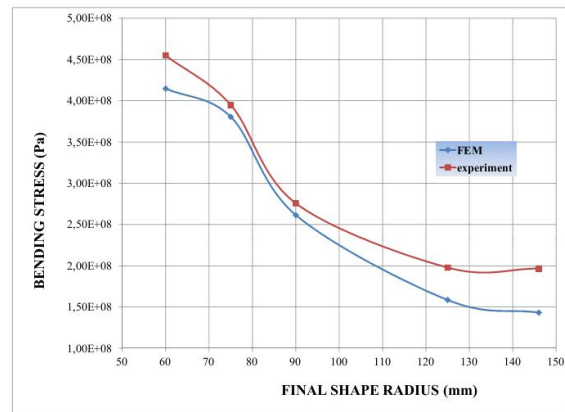


Figure 10: Stress distribution for various final shape radius.

It seems, in general, the FE results compare quite well with value from experiment results. However, the maximum bending stress between 70mm and 90 mm of final shape radius gives better results than the two ends of curves for both FE simulations and experiments. This one can be explained based on the graph of Figure 2. When the radius of final shape is too large, the plastic deformation will not occur. It is also the same problem if the radius of final shape is too small. Plastic deformation gauge cannot be read by the strain gauge for very small radius.

This work is presented in order to get a better understanding of dynamic simulation roll bending process by FEM. Establishing influences that affect formability of the roll bending process will be a part of future works.



Figure 11: Workpiece after roll bending process

CONCLUSION

Based on dynamic FEM simulation and experimental results, the present work analyses the factors that influence the bending stress of plate during roll bending process. It is seen that the bending stress at the early stage of roll bending process is different with continuous bending stage. In addition, by increasing the plate thickness, the maximum bending stress leaved in the workpiece vary non-linearly. Otherwise, with bigger final shape radius, the smaller bending stress is found by both FE simulation and experiment results. It might be useful results for industry for controlling parameters and improve the quality of the final shape.

ACKNOWLEDGEMENT

The authors express their thanks to the Natural Sciences and Engineering Research Council (NSERC) of Canada for financial support during this research.

REFERENCES

- Kohser E.P.D.J.T.B.R.A., 2002. "Materials and Processes in Manufacturing". John Wiley& Sons. 417.
- Couture P., 2004. "Simulation du roulage de tôles fortes, in Mechanical Engineering". École de technologie supérieure, Université du Québec, Montreal.
- Bouhelier C., 1982. "Le formage des tôles fortes", CETIM, pp.101-144.
- Yang M. &Shima S., 1988. "Simulation of Pyramid Type Three-roll Bending Process". International Journal of Mechanical Sciences, 30:12, 877-886.
- Hua M., Baines K. & Cole I.M., 1995. "Bending Mechanisms, Experimental Techniques and Preliminary Tests for the Continuous Four-roll Plate Bending Process".Journal of Material Processing Technology, 2nd Asia Pacific Conf. on Mat. Proc., 48:1-4, 159-172.
- Hua M., Baines K. & Cole I.M., 1999. "Continuous Four-roll Plate Bending: a Production Process for the Manufacture of Single Seamed Tubes of Large and Medium Diameters". International Journal of Machine Tools and Manufacture, 39:6, 905-935.
- Hua M. & al., 1997. "A Formulation for Determining the Single-pass Mechanics of the Continuous Four-roll Thin Plate Bending Process".Journal of Materials Processing Technology, Proceedings of the International Conference on Mechanics of Solids and Materials Engineering, 67:1-3, 189-194.
- Hua M. & Lin Y.H., 1999. "Effect of Strain Hardening on the Continuous Four-roll Plate Edge Bending Process".Journal of Materials Processing Technology, 89-90, 12.
- Hua M., Sansome D.H., Baines K., 1995. "Mathematical Modeling of the Internal Bending Moment at the Top Roll Contact in Multi-pass Four-roll Thin-plate Bending". International Journal of Materials Processing Tech., 52:2-4, 425.
- Hua M. & al., 1994. "Continuous Four-roll Plate Bending Process: Its Bending Mechanism and Influential Parameters". Journal of Materials Processing Technology.
- Hua M., Lin Y. H., 1999. "Large deflection analysis of elastoplastic plate in steady continuous four-roll bending process".International Journal of Mechanical Sciences.
- Bassett M. B., Johnson W., 1966. "The bending of plate using a three roll pyramid type plate bending machine". J. Strain Anal., I(5) 398-414.
- Hansen N. E., Jannerup O.,1979. "Modelling of elastic-plastic bending of beams using a roller bending machine". Journal of Engineering for Industry, Transactions of the ASME, 101(3) 304-310.
- Roggendorff S., Haeusler J., 1979. "Plate bending: three rolls and four rolls compared". Welding and Metal Fabrication, v 47(6) 353-357.
- Zeng J., Liu Z., Champliaud H., 2008. "Dynamic Simulation and Analysis By Finite Element Method for Bending Process of a Conical Tube and Geometric Inspection". Journal of Materials Processing Technology, 198(1-3) 330-343.
- Feng Z., Champliaud H., Dao T. M., 2009. "Numerical Study of Non-Kinematical Conical Bending with Cylindrical Rolls".Simulation Modelling Practice and Theory, 17(10) 1710-1722.
- Feng Z., Champliaud H., 2011. "Modeling and Simulation of Asymmetrical Three-Roll Bending Process". Simulation Modelling Practice and Theory, 19 (9) 1913-1917.
- Kwon Y. W., 1985. "Finite Element Methods for Plate Bending".Ph.D Thesis, Rice University, Ph.D 1985
- ANSYS, 2011. ANSYS, Version 13.

PROCESS MINING OF PRODUCTION MANAGEMENT DATA FOR IMPROVEMENT OF PRODUCTION PLANNING AND MANUFACTURING EXECUTION

Gašper Mušič^(a), Primož Rojec^(b)

^(a)University of Ljubljana, Faculty of Electrical Engineering, Ljubljana, Slovenia

^(b)INEA d.o.o, Ljubljana, Slovenia

^(a)gasper.music@fe.uni-lj.si, ^(b)primoz.rojec@inea.si

ABSTRACT

The paper deals with analysis of data captured within production information systems. Generally, a large amount of data is acquired and stored within these systems, but only a few data are used to support decisions on the production control level. This can be improved by using advanced data analysis techniques, that are capable of building models of other meaningful data representations. Process mining is a technique that results in a discrete state-transition model that can be interpreted as a Petri net. Such a model can be used to improve the understanding of manufacturing processes, improve the processes and assess their conformance to desired operation. The paper presents results of a case study, where a number of product specific routing data were recorded and analyzed in order to detect similarities that would allow for optimization of work order processing.

Keywords: Process mining, Petri nets, simulation, optimization

1. INTRODUCTION

Information technology has a considerable impact on the efficiency and quality of manufacturing especially in terms of enabling better control and optimization. However, the use of computers was in the past due to several reasons limited to the support of business functions on the one hand, and to low level machine and process control on the other. Only a couple of decades ago computers and information technology started to penetrate also into production control level where scheduling, dispatching, plant wide optimizations and coordinations are typically performed. A standard software application in this area is a Manufacturing Execution System (MES), which can be provided as a commercial software package by one of the specialized software companies or can be tailor made for the specific production environment. A common characteristic of these tools is that they are able to collect a vast amount of data and present it in various forms, but are relatively weak in offering more tangible support for decision, optimization and control. And if there are functions which allow advanced data processing and analysis of the production process, only experts are able to extract valuable information.

One can speak about a gap where we have plenty of data about the production on the one side of the gap and very few if any advices (suggestions) how to (re)act in order to achieve better production results on the other side of the gap.

Especially in the plant-wide control in manufacturing the existing challenges require a form of technical intelligence that goes beyond simple data, through information to knowledge (Morel, Valckenaers, Faure, Pereira and Diedrich 2007). Available models and standards are merging traditionally disparate functions and systems across the enterprise. The corresponding information technology solutions allow for access of the right information, in the right place, at the right time and in the right format. But the extraction of the knowledge from the large amounts of collected data and its integration in the production control scheme remains a challenge. The integration of data and process mining methods (Choudhary, Harding and Tiwari 2009, van der Aalst, Pesic and Song 2010, van der Aalst 2011) into the decision making on the production control level is required. The resulting knowledge in the form of static and dynamic models will facilitate new opportunities for collaboration throughout the plant, and across the supply chain. This will enable to meet the increasing demands on flexibility and reactivity within the Intelligence in Manufacturing (IIM) paradigm. The main disadvantage of these approaches is huge complexity, the need to cope with an enormous number of details and low robustness of solutions to changes in the production.

Among modelling formalisms suitable for description of systems with highly parallel and cooperating activities, Petri nets are perhaps the most widely used one. With Petri nets, production systems' specific properties, such as conflicts, deadlocks, limited buffer sizes, and finite resource constraints can be easily represented in the model (Tuncel and Bayhan 2007). The simplicity of model building, the possibility of realistic problem formulation as well as the ability of capturing functional, temporal and resource constraints within a single formalism motivated the investigation of Petri net based knowledge extraction methods. The main results have been achieved in the field of Workflow management where the related Process Mining methodology has been developed (van der Aalst 2011).

The paper investigates the applicability of process

mining methodology in the context of production planning and optimization. This is one of the fields where information technology has an immediate and considerable impact on the efficiency and quality of production control and related manufacturing processes. A case study is presented, where a large set of product routing data was analyzed by basic process mining algorithm and various uses of extracted information were proposed to improve the production planning and manufacturing execution.

2. PROCESS MINING

Information systems are becoming closely interlinked with supported operative processes. This results in logging a high number of events within these systems. Despite the large quantity of available data, organizations have difficulties in acquiring useful information from that data. The aim of process mining is to use the available data to obtain information about underlying processes, e.g., to automatically discover a process model by observing the archived data only.

Process mining represents a technique of obtaining useful process related information from event logs and extends the approaches generally found within Business Process Management (BPM). BPM is a discipline that combines information technology and management science and combines the resulting knowledge for management of business processes.

The relevance of Process mining can be illustrated through BPM life cycle, shown at Figure 1. The design phase creates the process, which becomes operational in the phase of configuration/implementation. Then starts the monitoring phase where the processes are observed to identify required changes. Some of these changes are implemented in the adjustment phase where the process and the related software are not re-designed but only adapted and additionally configured if necessary. In the diagnosis/requirements phase the process is assessed, which can trigger a new cycle in the BPM life cycle.

As shown in Figure 1 models play an important role in design phase and in configuration/implementation phase, while data are important in the monitoring phase and in diagnostic phase. The practice shows that diagnostic phase is not systematically and continuously supported and only some process changes are able to trigger a new life cycle iteration. Process mining enables to establish a true BPM life cycle loop. The archived data contain information that can be used to gain a better insight into the actual process, which means the eventual deviations can be analyzed and the models can be improved.

Process mining can be positioned in between machine learning and data mining on the one hand and between process modelling and analysis on the other (van der Aalst 2011). It aims to identify, monitor and improve real processes by acquiring knowledge from archived data in the contemporary information systems.

Information systems in support of production processes that collect a vast amount of data are ERP systems (SAP Business Suite, Oracle, in Microsoft Dynamics NAV), PDM systems, MES systems. Detailed information about occurring events is stored, which is shown in

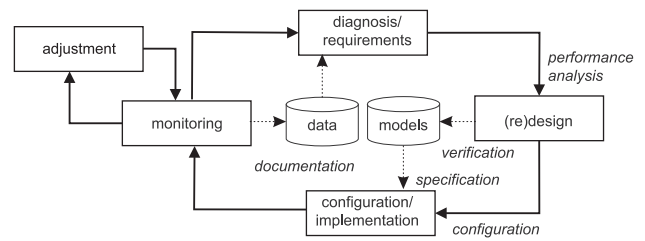


Figure 1: BPM life cycle and the use of process models (van der Aalst 2011)

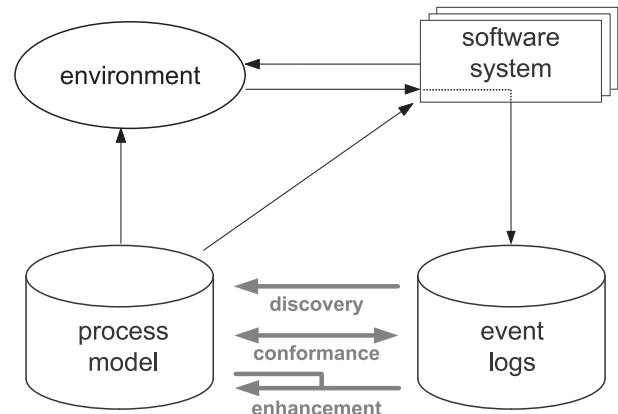


Figure 2: Types and use of process mining (van der Aalst 2011)

Figure 2 under the term event logs. Most information systems collect the data in unstructured form and some preprocessing is required to extract event data. In the following we assume that there is possible to sequentially record events such that each event refers to an activity (i.e., a well-defined step in the process) and is related to a particular case (i.e., a process instance) (van der Aalst 2011). Such a log can then be analyzed by a corresponding process mining algorithm.

Event logs can be used for three types of process mining as indicated in Figure 2. The first is model discovery or process identification. A process model is automatically generated from an event log without any a-priori information. In the sequel such an algorithm is described that generates a Petri net model based on event-log information. The second type of process mining deals with conformance testing. An existing model is compared to the event log in order to detect any deviations. The deviations can be located and also quantified to estimate the severity of changes in the process behavior and related risks. The third type of process mining is related to model improvement or enhancement. An existing model is improved or extended based on the event log information. This can be connected to improving the reflection of reality by the model or to adding new model perspectives. E.g., the initial model may only concern the sequential order of process activities. By adding time information from some event log, such model can be used also to analyze performance, detect bottlenecks, etc.

In general, different mining perspectives can be identified:

- the control-flow perspective is focused on the ordering of activities;
- the organizational perspective deals with resources in the background of recorded activities;
- the case perspective focuses on properties of recorded case instances;
- the time perspective deals with event occurrence times and event frequencies; these can be used to assess performance, locate bottlenecks, measure the utilization, etc.

While the above description implies that the process mining is performed in the frame of an off-line archived data analysis, it is also used in several operational support approaches. E.g., the deviations from the nominal process behaviour can be detected on-line, while the process is running. Process mining is therefore not only relevant in design and diagnosis phases but also in monitoring and adjustment phases (van der Aalst, Pesic and Song 2010).

3. PETRI NETS

Petri nets were introduced by C. A. Petri in his PhD thesis in 1962 and initially had the form of Condition/Event Systems with only binary markings and simple arcs. Later a number of modifications of the basic system model was introduced, including integer markings and weighted arcs. The resulting Place/Transition Petri nets became a central model, which is well explored in terms of analysis and synthesis techniques (Desel and Reisig 1998).

3.1. Place/Transition Petri nets

Informally, a Place/Transition (P/T) Petri net is defined as a bipartite graph, consisting of two types of nodes: places, typically drawn as circles, and transitions, typically represented by bars or rectangles. Nodes are interconnected by directed arcs, which either originate from a transition and end in a place or reversed, i.e., an arc always connects two nodes of different types. An arc can be weighted, which is an abbreviated representation of a set of parallel arcs. An example of a P/T Petri net is shown in Figure 3.

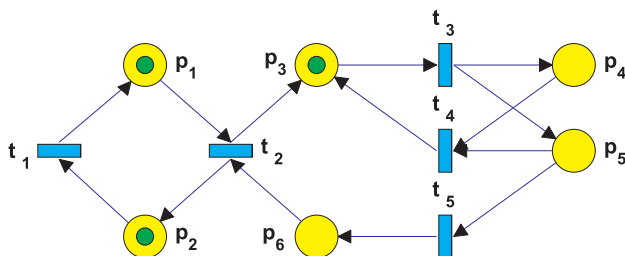


Figure 3: A Place/transition Petri net

Formally, a $PN = (\mathcal{N}, M_0)$ is a P/T Petri net system, where: $\mathcal{N} = (P, T, Pre, Post)$ is a P/T Petri net structure:

- $P = \{p_1, p_2, \dots, p_k\}, k > 0$ is a finite set of places.
- $T = \{t_1, t_2, \dots, t_l\}, l > 0$ is a finite set of transitions (with $P \cup T \neq \emptyset$ and $P \cap T = \emptyset$).
- $Pre : (P \times T) \rightarrow \mathbb{N}$ is the pre-incidence function and defines weighted arcs between places and transitions. It can be represented by a matrix whose element $Pre(p, t)$ is equal to the weight of the arc from p to t . When there is no arc between the given pair of nodes, the element is 0.
- $Post : (P \times T) \rightarrow \mathbb{N}$ is the post-incidence function, which defines weights of arcs from transitions to places. It can be represented by a matrix whose element $Post(p, t)$ is equal to the weight of the arc from t to p or 0 when there is no arc between the given pair of nodes.

$M : P \rightarrow \mathbb{N}$ is the marking of place $p \in P$ and defines the number of tokens in the place p . Net marking M can be represented as a $k \times 1$ vector of integers. M_0 is the initial marking of a P/T Petri net.

Functions Pre and $Post$ define the weights of directed arcs, which are represented by numbers placed along the arcs. In the case when the weight is 1, this annotation is omitted, and in the case when the weight is 0, the arc is omitted. Let $\bullet t_j \subseteq P$ denote the set of places which are inputs to transition $t_j \in T$, i.e., there exists an arc from every $p_i \in \bullet t_j$ to t_j . Transition t_j is enabled by a given marking if, and only if, $M(p_i) \geq Pre(p_i, t_j), \forall p_i \in \bullet t_j$. An enabled transition can fire, and as a result removes tokens from input places and creates tokens in output places. If transition t_j fires, then a new marking is determined by $M'(p_i) = M(p_i) + Post(p_i, t_j) - Pre(p_i, t_j), \forall p_i \in P$.

The switching rule of a Petri net is given as follows:

- a transition is enabled if each of the input places of this transition is marked with at least as many tokens as the weight of the corresponding arc,
- an enabled transition may or may not fire, which may depend on an additional interpretation,
- a firing of a transition is immediate (includes no delay) and removes a number of tokens equal to the arc weight from each of the input places and adds as many tokens to each of the output places as the weight of the corresponding arc.

The basic Place/Transition Petri net model can be extended in different ways, leading to other Petri net classes, e.g. timed models (Bowden 2000).

4. PETRI NETS AND PROCESS MINING

Process Discovery is a central task within process mining. It aims in constructing a process model based on event log. It deals with control-flow perspective and can be defined as follows: Let L denote an event log. A process discovery algorithm is a function that maps L onto a process model that is able to reproduce the behaviour captured in the event log.

This definition does not specify the kind of modelling formalism used to represent the process model. E.g.,

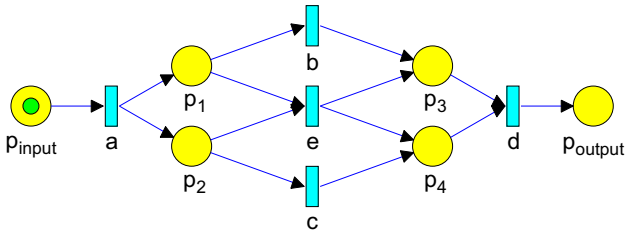


Figure 4: WF-net N_1 discovered from event log L_1

BPMN, EPC, YAWL, or Petri nets can be used. In the following a Petri net representation of the model will be used. Additionally, a simple event log will be used, which is a multi-set of traces over a set of activities \mathcal{A} , i.e., $L \in \mathbb{B}(A^*)$. Example of such a log is:

$$L_1 = [\langle a, b, c, d \rangle^3, \langle a, c, b, d \rangle^2, \langle a, e, d \rangle] \quad (1)$$

L_1 is a simple event log that describes six cases. A process discovery algorithms should generate a PN, that is able to replay all the sequences in L_1 . The PN should belong to the class of sound Workflow net (WF-net), which is safe and contains one input place ($\bullet i = \emptyset$), and one output place ($o \bullet = \emptyset$) (van der Aalst, Weijters and Maruster 2004).

The problem of process discovery can then be reformulated as: A process discovery algorithm is a function γ , that maps a log $L \in \mathbb{B}(A^*)$ into a marked PN $\gamma(L) = (\mathcal{N}, M)$. \mathcal{N} is a sound WF-net and all traces in L correspond to possible firing sequences of (\mathcal{N}, M) .

Based on L_1 , such an algorithm discovers the net shown in Figure 4. There the so called α -algorithm was used (van der Aalst, Weijters and Maruster 2004), which is a basic process discovery algorithm. It is able to discover PN models from a large class of event logs, although it also has some limitations (van der Aalst 2011).

It can be observed that all the possible firing sequences of PN in Figure 4 match the sequences in L_1 . In general this is not the case and the PN generated by the α -algorithm is able to generate a larger set of event sequences. E.g., given the log:

$$L_2 = [\langle a, b, c, d \rangle^3, \langle a, c, b, d \rangle^4, \langle a, b, c, e, f, b, c, d \rangle^2, \langle a, c, b, e, f, b, c, d \rangle^2, \langle a, b, c, e, f, c, b, d \rangle, \langle a, b, c, e, f, b, c, e, f, c, b, d \rangle] \quad (2)$$

the WF-net N_2 shown in Figure 5 is generated. The shown net can generate all the traces from L_2 but also others. E.g., the trace $\langle a, b, c, e, f, c, b, d \rangle$ is feasible but is not contained in L_2 . This complies to the above definition as it is required only that the net is able to generate traces in L while no restrictions related to generation of other traces were given.

Even when the above process discovery algorithm definition is related to WF-nets, other models could also be used. E.g., the WF-net in Figure 4 can be translated into an equivalent BPMN model or equivalent EPC, UML activity diagrams, YAWL models, etc. (van der Aalst 2011).

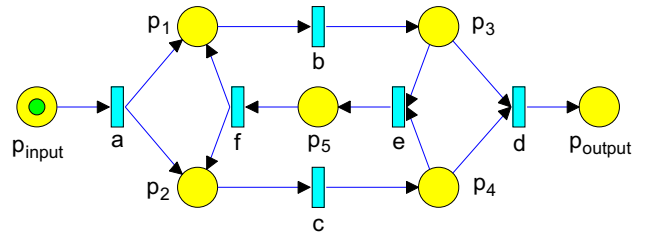


Figure 5: WF-net N_2 discovered from event log L_2

5. PROCESS MINING EXAMPLE

To assess the usability of α -algorithm in conjunction to real production data a testing set of data was collected in cooperation with INEA company. The set comprises technological routing data of over 30.000 door side panel items that were processed in the frame of furniture production.

The data record for an item consists of a set of attribute values followed by a set of time values that correspond to duration of the manufacturing operations. A fixed record length is maintained and in case the attribute is not relevant or certain operation is not performed on an item, the value is NULL.

An item is described by 10 attributes, shown in Table 1. In the routing part there are altogether 67 possible manufacturing operations, such as *Edge processing*, *Lock and hinge holes drilling*, *Chipboard panel assembly*, *Honeycomb panel assembly*, etc. The operation duration table is relatively sparse as only a small subset of operations is typically performed during an item processing.

To derive a suitable event log the data was first pre-processed in a way which separated individual items data and build corresponding cases. Production of each item now represents a production case with operation sequence and timing. In the following only ordering data were used, although the analysis of timing data was later added, too. A simple analysis shows that nearly 98 % of recorded operation sequences only contains two or three operations. These are repeated very often, up to more than 7000 repetitions as shown in Figure 6, while most of the other sequences repeat less than 100 times. A better view is obtained if only different sequences are considered. This is illustrated in Figure 7, which shows the distribution of the lengths (number of operations) of the different processing procedures that correspond to the items in the database.

Table 1: Attributes of manufactured items

Attribute	Meaning
Item ID	Unique item designator
Standard	Internal standard
Core	Type of the panel core
Surface type	Panel surface material
Wood	Panel surface appearance
Surface finish	Type of surface finish
Edge	Edge designation
Groove	Type of additional edge processing
Thickness	Panel dimension
Width	Panel dimension

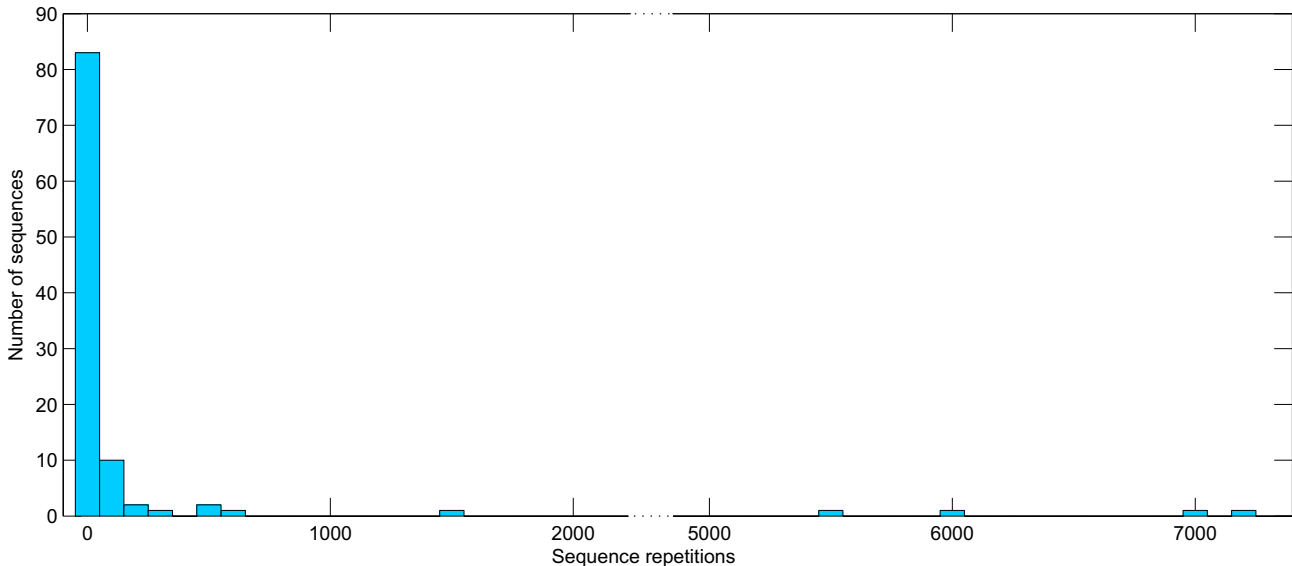


Figure 6: Distribution of the sequence repetitions

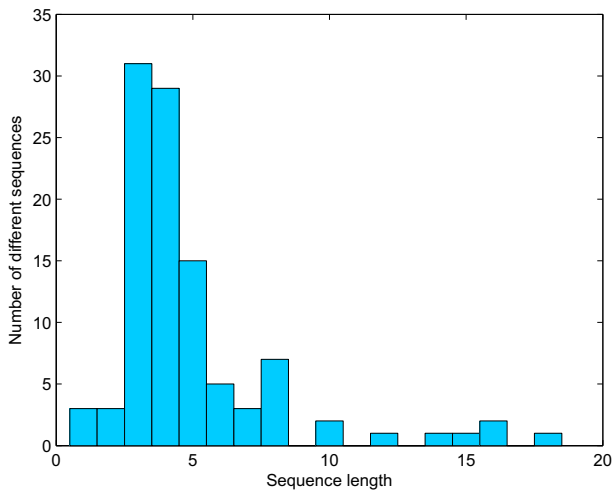


Figure 7: Distribution of the recorded operation sequence lengths in the database

An initial process mining analysis was performed to check the variability of production sequences. Figure 8 shows the resulting model based on 10.000 cases. Clearly we have a large repeatability in the production sequences, i.e., close similarities in item routings. This information could be used to improve the efficiency of work order processing, e.g., by grouping similar items together in larger batches.

Despite the relatively condensed representation of the large number of cases in Figure 8, the analysis of derived net shows that the model is not useful. In contrast to the initial assumption on sound WF-net the derived net does not belong to that class. This can be observed from the graphical representation or shown by analysis of the reachable markings. The analysis shows some non-safe places as well as places that do not receive tokens at all, which indicates dead transitions.

These observations are not a consequence of the anomalous working of the applied α -algorithm but the consequence of the inherent *representational bias* of the al-

gorithm. Such a representational bias is required by any process discovery technique and helps limiting the search space of possible candidate models (van der Aalst 2011). In case of the α -algorithm the technique is able to adequately capture concurrency, but can produce models with livelocks or deadlocks. Limiting the search space to only sound models would limit the expressiveness of the modelling language.

In the addressed case the concurrency is a desired property, as can be exploited to increase equipment utilization. Therefore we tried to circumvent the deficiency of the algorithm by an appropriate data segmentation. First, the number of sequence appearances is considered. Figure 7 shows there are only 8 different sequences with length of 10 or more operations. More detailed analysis shows that these sequences appear at 19 cases all together. These cases are considered exceptions and are filtered out.

The Petri net model obtained by process mining on the reduced set of data is still not acceptable, therefore additional segmentation based on the item attribute values was performed. Here the main problem was a rather poor quality of the data with many missing or questionable attribute values. After a set of experiments with different selection methods a suitable subsets of attributes were determined, which can be used to classify cases into separate groups that can be represented by a set of simple sound WF-type Petri nets. E.g., a combination of *Core*, *Surface type*, *Wood*, and *Surface finish* attributes enables to designate corresponding item routing sequences.

Next, a set of data was used to simulate an on-line conformance testing. At each item processing, the matching between previously developed models and the manufacturing operation sequence was observed. A deviation raised a warning. In practical implementation, such a warning would be used to notify the production operating personnel. Different metrics have been tested, which enable to adjust the warning action according to the degree of deviation.

The main goal of the investigation is to explore the

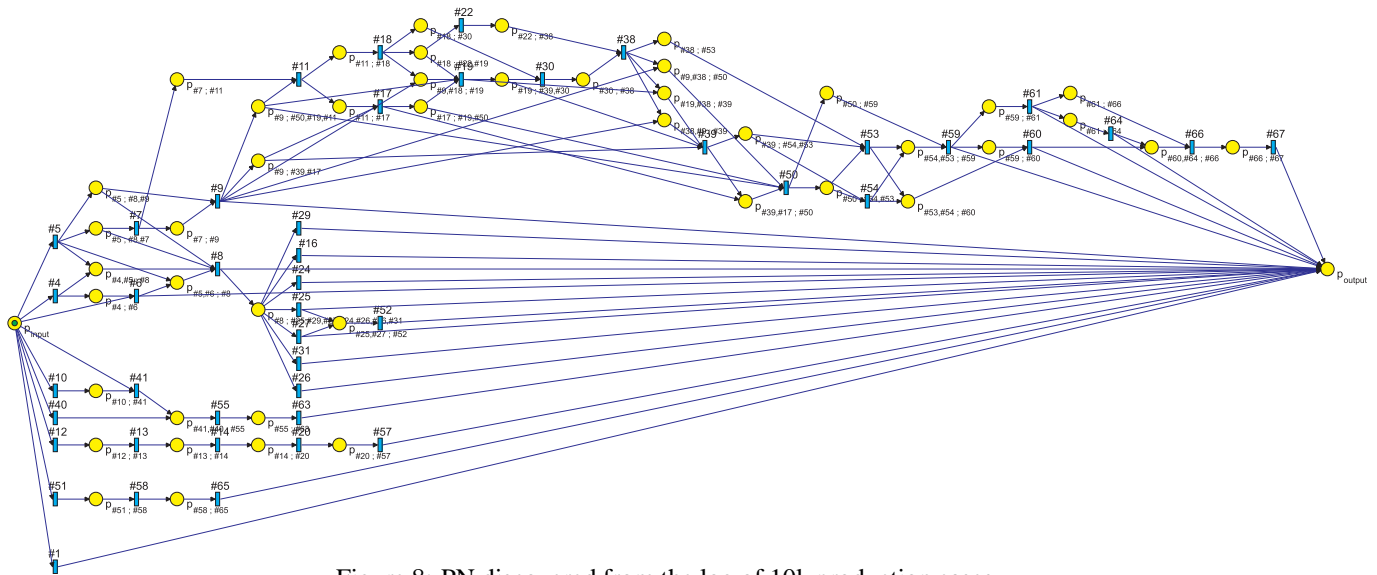


Figure 8: PN discovered from the log of 10k production cases

similarities among processed items in terms of temporal quantities. To achieve this also the time information was included in the models. This way the models can be refined to reflect also the time perspective, which enables to identify groups of items with similar processing times. This information can be used to improve production planning and scheduling.

6. CONCLUSIONS

The presented results indicate that the basic process mining algorithm can be used to analyze certain types of production management data. In particular, the product routing information and corresponding operation durations were used to analyze a large set of production data. Careful data preprocessing and segmentation were required to obtain useful models. The analysis showed similarities and relations among different groups of products that were hardly visible from the data directly, due to the very large number of different production items.

The obtained information will be used to improve the production planning and manufacturing execution.

ACKNOWLEDGMENTS

The presented work has been partially performed within the Competence Centre for Advanced Control Technologies, which is partly financed by the Republic of Slovenia, Ministry of Education, Science, Culture and Sport and European Union, European Regional Development Fund. The support is gratefully acknowledged.

REFERENCES

Bowden, F. D. J., 2000. A brief survey and synthesis of the roles of time in petri nets, *Mathematical & Computer Modelling*, 31, 55–68.

Choudhary, A. K., Harding, J. A. and Tiwari, M. K., 2009. Data mining in manufacturing: a review based on the kind of knowledge, *Journal of Intelligent Manufacturing*, 20, 501–521.

Desel, J. and Reisig, W., 1998. Place/transition petri nets, in W. Reisig and G. Rozenberg (eds), *Lectures on Petri Nets I: Basic Models*, Vol. 1491 of *Lecture Notes in Computer Science*, Springer, pp. 122–173.

Morel, G., Valckenaers, P., Faure, J., Pereira, C. and Diedrich, C., 2007. Manufacturing plant control challenges and issues, *Control Engineering Practice*, 15, 1321–1331.

Tuncel, G. and Bayhan, G. M., 2007. Applications of Petri nets in production scheduling: a review, *International Journal of Advanced Manufacturing Technology*, 34, 762–773.

van der Aalst, W. M. P., 2011. *Process Mining: Discovery, Conformance and Enhancement of Business Processes*, Springer.

van der Aalst, W. M. P., Pesic, M. and Song, M., 2010. Beyond process mining: From the past to present and future, *Lecture Notes in Computer Science*, 6051, 38–52.

van der Aalst, W. M. P., Weijters, T. and Maruster, L., 2004. Workflow mining: Discovering process models from event logs, *IEEE transactions on Knowledge and Data Engineering*, 16 (9), 1128–1142.

AUTHORS' BIOGRAPHIES

GAŠPER MUŠIČ received B.Sc., M.Sc. and Ph.D. degrees in electrical engineering from the University of Ljubljana, Slovenia in 1992, 1995, and 1998, respectively. He is Associate Professor at the Faculty of Electrical Engineering, University of Ljubljana. His research interests are in discrete event and hybrid dynamical systems, supervisory control, planning, scheduling, and industrial informatics. His Web page can be found at <http://mcs.fe.uni-lj.si/Staff.asp>.

PRIMOŽ ROJEC received B.Sc. and M.Sc. degrees in electrical engineering from the University of Ljubljana, Slovenia in 1990 and 2004, respectively. He works at Inea engineering company. His research interests are in planning, scheduling, and manufacturing execution systems.

ACHIEVEMENTS IN RESULT VISUALIZATION WITH THE COMPUTER NUMERIC E-LEARNING SYSTEM MMT

Irene Hafner^(a), Martin Bicher^(b), Thomas Peterseil^(c), Stefanie Winkler^(d), Ursula Fitsch^(e), Nicole Nagele-Wild^(f), Wolfgang Wild^(g), Felix Breitenecker^(h)

(a) - (b), (d) - (h) Vienna University of Technology, Institute of Analysis and Scientific Computing
(c) dwh Simulation Services

(a) irene.hafner@tuwien.ac.at, (b) martin.bicher@tuwien.ac.at, (c) thomas.peterseil@drahtwarenhandlung.at,
(d) stefanie.winkler@tuwien.ac.at, (e) ursula.fitsch@tuwien.ac.at, (f) nicole.nagele@tuwien.ac.at,
(g) wolfgang.wild@tuwien.ac.at, (h) felix.breitenecker@tuwien.ac.at

ABSTRACT

This paper discusses the latest developments of the MMT system. MMT, which stands for Mathematics, Modelling and Tools, represents an e-learning system for teaching basic mathematics as well as modelling and simulation. Since the MMT system got its new interface in summer 2010, the range of examples has reached an impressive amount. Apart from examples concerning Linear Algebra and Analysis which are used in lectures of basic mathematics for students of electrical engineering and geodesy and geomatics engineering, the focus of the MMT system has recently been laid on the extension of examples for teaching modelling and simulation to students of Technical Mathematics. Lecturers use this web-interface to explain the current topic by showing examples on the MMT server. In addition, students receive an account to be able to also access these examples on the server from home to train their newly gained knowledge. Recently the data transfer from MATLAB to the MMT server has been renewed completely. The new render files enable a simple exchange of various output data.

Keywords: E-Learning, MATLAB, Simulink, MMT, rendering

1. STRUCTURE OF THE MMT SERVER

The interface of the MMT server is shown in Fig.1.

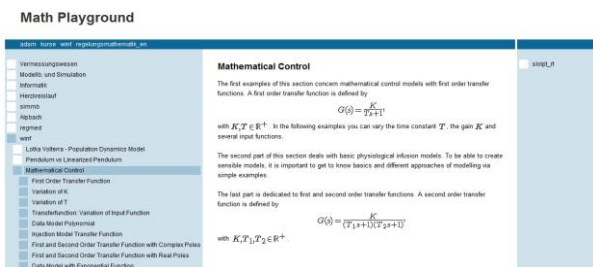


Figure 1: Overview of the MMT Interface

The left section consists of the content tree. Depending on the lecture they are attending, students see a certain selection of examples. The middle section

contains a description of the current section or example and the parameter section. On the right side, all files offered for download can be found.

2. EXAMPLES

2.1. Introductory Example

Each example on the MMT server starts with a description providing information about the current topic. In Addition to the short description in the middle section, pdf documentations and pictures can be uploaded from the lecturers. These documents as well as the underlying source code for an example can be downloaded by following the links on the right side.

All parameters for a simulation or calculation can be defined in the section below the description. By clicking the *ok* button, the MMT parameters are transferred to the referring example's source code which is further executed. Fig.2 shows a MMT MATLAB example consisting of one m-file.

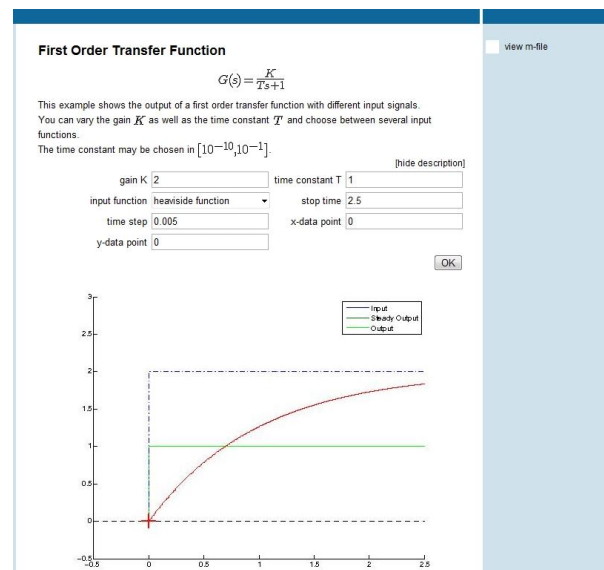


Figure 2: Picture of a MMT Example Accessing One MATLAB File – Description, Parameters and Output

The m-files for a MMT example basically look like usual m-functions consisting of MATLAB code for the

calculation of the example and additional lines to enable the communication with MMT. After clicking the ok – button, the parameters currently selected for the example are converted into strings and stored in a structure variable. This variable is used as input to the m-function. After explanatory comments concerning the topic of the example, authors and last modification date, the strings stored in the structure variable are converted into the desired data formats for further usage (see Fig.3).

```
K = str2double(instruct.var1);
T = str2double(instruct.var2);
number = str2double(instruct.var3);
tend = str2double(instruct.var4);
dt = str2double(instruct.var5);
xxx = str2double(instruct.var6);
yyy = str2double(instruct.var7);
```

Figure 3: Extraction of Input Parameters from the MMT Server in MATLAB

The ensuing code represents the actual code for the respective example. At the end of the m-file, all results are again returned to the MMT server. An overview of the output possibilities on the MMT system is given in section 3.

A MATLAB example for the MMT server can also exist of several m-files. Only the main m-file which has to be the first one to be found in the list of attached m-files contains the additional code for the data exchange with the MMT server. All other m-files needed for the corresponding example are called from the main one and don't have to be adapted in any way.

All MATLAB examples on the MMT server are executed accessing the MATLAB version on the server itself, so it's not necessary to possess a local MATLAB licence.

2.2. Examples Accessing Simulink

The possibility of including examples using several m-files has also enabled the inclusion of Simulink models into the MMT system. Simulink models actually consist of MATLAB code which can also be created graphically using block diagrams. Hence the Simulink model is treated like an additional m-file and called from a MATLAB function which only contains the extraction of input variables, the execution of the Simulink file and the return of the simulation results (see Fig. 4 for the extraction of input parameters from the MMT server and the execution of the mdl-file).

Students can download the source code of the MATLAB function as well as the Simulink model. Since the mdl-file is treated as text file from the browser, it has to be stored locally on the downloader's computer and re-opened with MATLAB to show the corresponding graph model. The successful inclusion of Simulink files also encourages the usage of Simscape on the MMT server, which will open the possibilities of teaching other modelling approaches like Physical Modelling via MMT.

```
phi0 = str2num(instruct.var1);
w0 = str2num(instruct.var2);
k = str2num(instruct.var3);
l = str2num(instruct.var4);
m = str2num(instruct.var5);
t_end = str2num(instruct.var6);

%%%%%%%%%%%%%%%%%%%%%%%%%%%%%%%%%%%%%%%%%%%%%%%%%%%%%%%%%%%%%%%%%%%%%%%%
%% CALCULATIONS, FUNCTION CALLS AND MAIN PROGRAM %%%
% All general calculations and operations come here.
%%%%%%%%%%%%%%%%%%%%%%%%%%%%%%%%%%%%%%%%%%%%%%%%%%%%%%%%%%%%%%%%%%%%%%%%
% set the workspace to give simulink access to the
% variables
option=simset('SrcWorkspace', 'current');
% starting simulation:
[t,x] = sim('pendulumtrial',t_end,option);

%% GRAPHICAL OUTPUT %%%%%%%%%%%%%%%%%%%%%%%%%%%%%%%%%%%%%%%%%%%%%%%%%%%%%%%%%%%%%%%%%%%%%%%%%
% Graphical output is generated here.
```

Figure 4: MATLAB Function Extracting Values from the MMT Server and Simulating a mdl-File

3. NEW RENDER FILES AND CREATION OF MULTIPLE OUTPUT

One of the very recent developments for the MMT server has been the enlargement of possibilities to create output from MATLAB files on the MMT system. Before developing the new rendering routines, returning the output from MATLAB to the MMT system was very unintuitive and rather complicated. Up to March 2012 one could only choose between simple textual output written in html-code or one MATLAB figure. Hence the only possibility to show more than one output plot was using subplots, which of course lead to a very unclear picture for a certain amount of subplots. To improve these options, completely new rendering routines have been developed. These routines allow every MMT example to have as much layers of outputs as needed. For each of these layers a number, written in brackets, occurs in the upper right output corner to enable the navigation between them, see Fig. 5. Every layer consists either of textual output, a static figure or an animated gif with optional title.

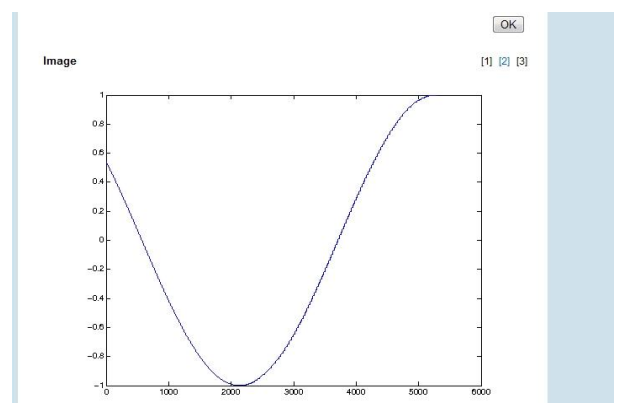


Figure 5: Switching between Multiple Output Layers by Clicking on the Numbers in Brackets

The return variable for the MMT server has to be a string containing html code with the information on the creation of all desired layers. To prevent the manual creation of this string for every single example, a variable *r* of type cell array is used. This array contains cells of strings with information about every layer

which has to be created. To initialize the cell array, the first function to be called in the output section of the MATLAB function is *adamInitialize*. Conventionally the cell array is called *r*, so the function call would be

```
r=adamInitialize();
```

The strings for the creation of all intended layers are created by using the new render files described in the following subsections. After generating as much layers as needed for the referring example, calling

```
retstr=adamComposeResultString();
```

takes the information from the cell array to create an Excel-file containing strings which represent the html-code with the information for the construction of the required layers.

3.1. Rendering Textual Output

In former times, the creation of textual output did require html knowledge, as can be seen in Fig. 6.

```
retstr = 'TEXT';
retstr = [retstr, sprintf('The vector product a x b
results in: ( %s )', num2str(ab))];
retstr = [retstr, sprintf('<br><br>The vector product
b x a results in: ( %s )', num2str(ba))];
retstr = [retstr, sprintf('<br>The vector product
-a x b results in: ( %s )', num2str(minab))];
retstr = [retstr, '<br><br>You see that
-a x b = b x a']
```

Figure 6: Rendering Text without the New Render Functions

Using the new render function *adamRenderText*, common string variables can be used as textual return value. As you see in Fig. 7, *adamRenderText* requires several input parameters.

```
function [r]=adamRenderText(r,instruct,text,varargin)
%Function to render Textual output

%handling with optional parameters
if length(varargin)>0
s.title=varargin{1};
end;

%defining class and adding it to the cell array
s.type='TEXT';
s.text=text;
r{end+1}=s;
end
```

Figure 7: Source Code for the New Text Rendering Function

r is the already allocated cell array being either empty but created with *adamInitialize* or containing the information of previous layers. As seen here the input structure *instruct* of the MMT example has to be used as an input parameter of the render function too as it not only contains the manual chosen parameters of the MMT experiment but also a unique filename extension (*instruct.mlingfilename*) for saving files to a temporary folder. *text* contains the common matlab string which the programmer would like to have displaced on the layer. *varargin* is an optional input which can contain a string with the desired title for the layer. The function

appends a structure variable containing strings with the information about the title (line 6 in Fig.7), type (line 10) and content (line 11) of the output, which would now be *text*, to the cell array. It's important to call this function similar to

```
r=adamRenderText(r,instruct,'sample text',...
'optional title');
```

to make sure the existing cell array is appended.

3.2. Rendering Static Images

As mentioned before, until this year's March the only way to return more than one picture was using subplots in MATLAB. How unclear the resulting picture can get this way is shown in Fig. 8.

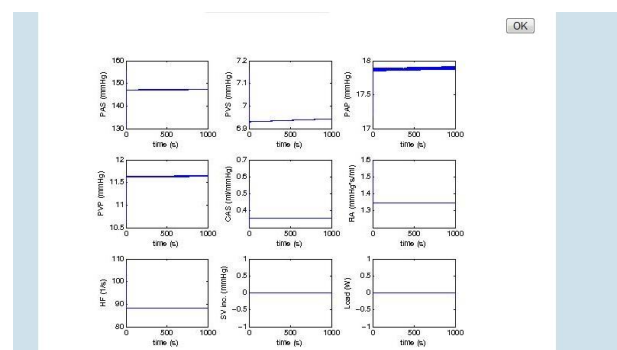


Figure 8: Output of Nine Figures by Using Subplots

In addition, returning this picture to the MMT server required rather unintuitive MATLAB code, as can be seen in Fig. 9.

```
% produces a *.jpeg image for graphical output.
drawnow;
wsprntjpeg(Pic, instruct.mlingfilename);
retstr = 'IMAGE';
```

Figure 9: Former Code for the Submission of a Picture to the MMT Server

Now it's possible to create one layer for every picture the user wants to be returned with much easier code since all additional work is done with the new function *adamRenderImage*. Before calling this function, a MATLAB figure has to be created. Its visibility is usually set to 'off' as graphical output on the server which executes MATLAB in console mode and does not provide a graphical interface, is suppressed anyway. A source code example for this is given below.

```
Pic = figure('visible','off');
plot(sin(0:0.001:2*pi));
```

The figure further has to be transferred to the render function by calling

```
r=adamInitialize();
r=adamRenderImage(r,instruct,Pic,'Sine');
retstr=adamComposeResultString(r);
```

The source code for *adamRenderImage* is shown in Fig.10.

```

function [r]=adamRenderImage(r,instruct,Pic,varargin)
%Routine for image saving to temp folder as .png

%handling with optional parameters
if length(varargin)>0
    s.title=varargin{1};
end;

%Defining class entry for cell array
s.type='IMAGE';
s.imagetype='png';

%Defining filename of .png file
picId=length(r);
filename=sprintf(instruct.mlingmultipath,picId);

%Setting figure position fitting to 576*432 pixels
%72pixels/inch is the default resolution for
nonscreen
%figureoutput
set(Pic,'PaperPositionMode','manual','PaperUnits',...
    'inches','PaperPosition',[0 0 576/72 432/72]);

%Saving process, using filename and
%resolution '-r72' => 72pixels/inch
print(Pic, '-dpng', '-r72',[filename, '.png']);

%saving class to cell array
r(end+1)=s;
end

```

Figure 10: Source Code for the New Rendering Function for Images

The input parameters are basically the same as in *adamRenderText* whereupon the text string is replaced by the MATLAB figure. Besides appending again the information about type and title (lines 6, 11 and 12), this function prints the MATLAB plot to a pre-allocated picture on the MMT server (line 26).

3.3. Rendering Animated Images

```

function
[r]=adamRenderAnimatedCreate(r,instruct,Pic,varargin)
%Routine for image saving to temp folder as .png

%handling with optional parameters
if length(varargin)>0
    delay=varargin{1};
    if length(varargin)>1
        s.title=varargin{2};
    end;
else
    delay=0;
end;

%Defining class entry for cell array
s.type='IMAGE';
s.imagetype='gif';
%Defining filename of .gif file
picId=length(r);
filename=sprintf(instruct.mlingmultipath,picId);

%Setting figure position fitting to 576*432 pixels
%72pixels/inch is the default resolution for
nonscreen
%figureoutput
set(Pic,'PaperPositionMode','manual','PaperUnits','inches',
    'PaperPosition',[0 0 576/72 432/72],'Color',[1 1 1]);

%Saving process, using filename and
%resolution '-r72' => 72pixels/inch
PP = hardcopy(Pic, '-dOpenGL', '-r72');
[P,cm]=rgb2ind(PP,256);
imwrite(P,cm,filename,'gif','Loopcount',inf,'DelayTime',delay);

%saving class to cell array
r(end+1)=s;
end

```

Figure 11: Source Code for the New Rendering Function Creating the First Frame of an Animated gif

For animated gifs, plots have to be created for every frame of the picture. To create the first frame, the picture is initialized with *adamRenderAnimatedCreate* (see Fig.11).

The only significant difference to *adamRenderImage* is the option of a delay-time defining how fast the frames of the gif are intended to change. Setting the delay to zero causes the fastest change of frames. All frames besides the first one are rendered by calling the function *adamRenderAnimatedAppend*, which is shown in Fig. 12.

```

function
[r]=adamRenderAnimatedAppend(r,instruct,Pic,varargin)
%Routine for image appending to an existing animated-
gif

%handling with optional parameters
if length(varargin)>0
    delay=varargin{1};
else
    delay=0;
end;

%Detecting filename of .gif file to append to
picId=length(r);
filename=sprintf(instruct.mlingmultipath,picId-1);

%Setting figure position fitting to 576*432 pixels
%72pixels/inch is the default resolution for
nonscreen
%figureoutput

set(Pic,'PaperPositionMode','manual','PaperUnits',...
    'inches','PaperPosition',...
    [0 0 576/72 432/72],'Color',[1 1 1]);

%Saving process, using filename and
%resolution '-r72' => 72pixels/inch

PP = hardcopy(Pic, '-dOpenGL', '-r72');
[P,cm]=rgb2ind(PP,256);
imwrite(P,cm,filename,'gif','WriteMode','append',...
    'DelayTime',delay)
end

```

Figure 12: Source Code for the New Rendering Function Appending Frames to an Animated gif

An example source code for the creation of an animated gif is given below.

```

Pic = figure('visible','off');

plot(sin((0:0.001:2*pi)*t));

r=adamInitialize();
r=adamRenderAnimatedCreate(r,instruct,Pic,0,'sine');

for t=1:time;
    plot(sin((0:0.001:2*pi)*t/20));
    r=adamRenderAnimatedAppend(r,instruct,Pic,0);
end;

retstr=adamComposeResultString(r);

```

3.4. Example with Multiple Output

The following example shows how multiple output layers can be returned to the MMT server. To enable students downloading the source code from the MMT server to easily convert the file into an executable one

for their own computer, all parts only necessary for the data exchange with the MMT server are framed by

```
%===== BEGIN OF SPECIFIC CODE - CUT HERE =====
and
%===== END OF SPECIFIC CODE - CUT HERE =====
```

The source code of an example creating layers for textual, animated and static images is shown in Fig. 13.

```
1 %% GRAPHICAL OUTPUT %%%%%%%%%%%%%%%%%%%%%%%%%%%%%%%%%%%%%%%%%%%%%%%%%%%%%%%%%%%%%%%%%%%%%%%%%
2 % Graphical output is generated here.
3 %%%%%%%%%%%%%%%%%%%%%%%%%%%%%%%%%%%%%%%%%%%%%%%%%%%%%%%%%%%%%%%%%%%%%%%%%
4
5 %===== BEGIN OF SPECIFIC CODE - CUT HERE =====
6 % disables graphical output on the remote system.
7 Pic1 = figure('visible','off');
8 %===== END OF SPECIFIC CODE - CUT HERE =====
9
10 plot(sin((0:0.001:2*pi)*t));
11
12 %===== BEGIN OF SPECIFIC CODE - CUT HERE =====
13 r=adamInitialize();
14 r=adamRenderAnimatedCreate(r,instruct,Pic1,0,...
15 'Animation');
16 %===== END OF SPECIFIC CODE - CUT HERE =====
17
18 for t=1:100;
19 plot(sin((0:0.001:2*pi)*t/20));
20
21 %===== BEGIN OF SPECIFIC CODE - CUT HERE =====
22 r=adamRenderAnimatedAppend(r,instruct,Pic1,0);
23 %===== END OF SPECIFIC CODE - CUT HERE =====
24
25 end;
26
27 %===== BEGIN OF SPECIFIC CODE - CUT HERE =====
28 % disables graphical output on the remote system.
29 Pic2 = figure('visible','off');
30 %===== END OF SPECIFIC CODE - CUT HERE =====
31
32 plot(cos(1:0.001:2*pi));
33
34 %===== BEGIN OF SPECIFIC CODE - CUT HERE =====
35 r=adamRenderImage(r,instruct,Pic2,'Image');
36 r=adamRenderText(r,instruct,...
37 'To be or not to be...','Text');
38 retstr=adamComposeResultString(r);
39 %===== END OF SPECIFIC CODE - CUT HERE =====
40
41 %% END OF EXAMPLE %%%%%%%%%%%%%%%%%%%%%%%%%%%%%%%%%%%%%%%%%%%%%%%%%%%%%%%%%%%%%%%%%%%%%%%%%
42
43 end
```

Figure 13: Creation of Output Layers for Three Output Types in One Example

In lines 7-10 the first frame for an animated gif is created. Before returning this first output to the MMT server by *adamRenderAnimatedCreate* in line 14, *adamInitialize* has to be called (line 10). Lines 18-25 show the code for creating and appending further frames to this animated image with delay 0. The creation of a static picture with the catching title 'image' is shown in lines 29-35. In line 36, a short text is returned to the third frame. The cell array created by the call of all render functions is further transferred to *adamComposeResultString* (see line 38) which returns the string *retrstr*. This string finally contains all information needed from the MMT system to establish enough output layers with the correct title and contents

while the pictures have already been transferred to the server during the execution of the render functions.

The outputs of this MATLAB function on the MMT server can be seen in Fig. 14. Of course, due to the disability of print media to show animation, the movement for the first output has to be imagined.

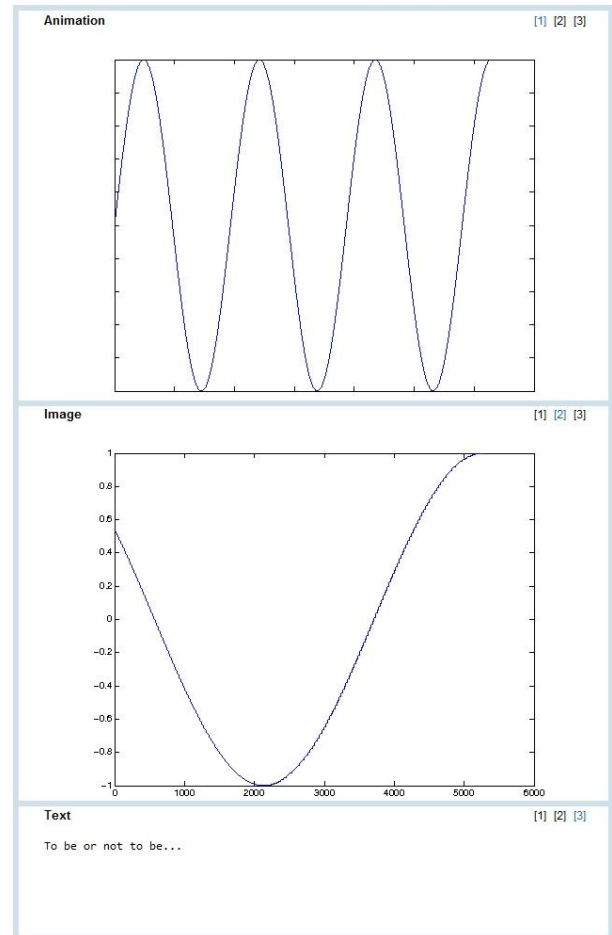


Figure 14: Different Output Layers of One MMT Example

4. USAGE OF THE MMT SERVER IN EXAMS

The MMT system has also become a very helpful tool for exams in lectures about modelling and simulation. The questions for these exams are posed via TUWEL, a moodle based e-learning tool of the Vienna University of Technology. To answer these questions, students have to log in to the MMT server and vary input parameters to achieve a certain result. An example for such a question could be finding the maximum step size for a certain solver algorithm to stay within a given error tolerance. Another question demands the evaluation of the turning point of a PT2 controller for certain input parameters which have to be set on the MMT server. The TUWEL question for this example can be seen in Fig.15.

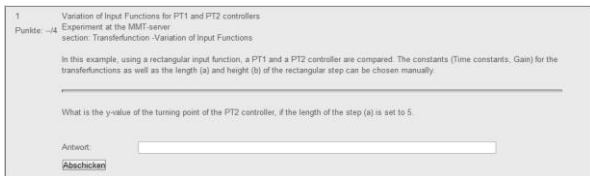


Figure 15: TUWEL Question for an Exam in Cooperation with the MMT System

By following the link in TUWEL, the students find the MMT example corresponding to this question, see Fig.16.

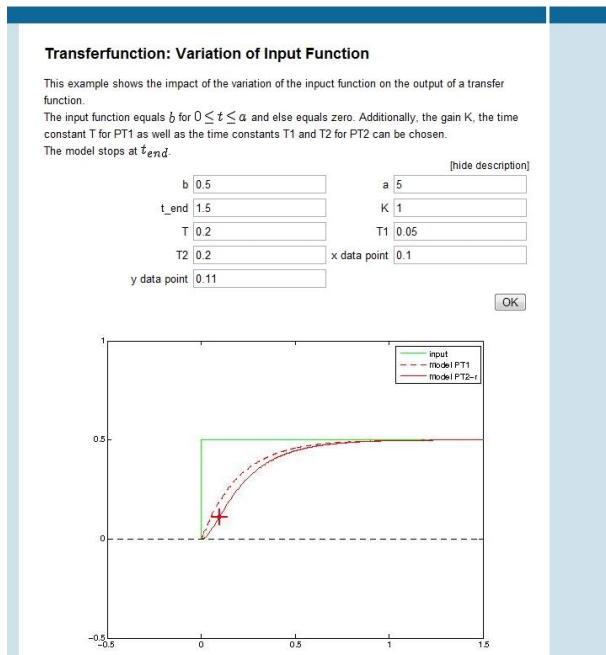


Figure 16: MMT Example Corresponding to a TUWEL Exam Question

For precise reading of the values to be found, additionally to the parameters for the PT controllers a data point can be set. At the chosen point a red cross is plotted which eases spotting certain data. The students further fill in the values they found out to the answer field in the TUWEL question. Grading is done independently by TUWEL.

5. CONCLUSION AND OUTLOOK

While most of the examples currently existing on the MMT server have been implemented by programmers of the Institute of Analysis and Scientific Computing of the Vienna University of Technology, recently many examples which have been developed during projects, diploma and bachelor theses are tested, validated and further included to the MMT system. That way other students are able to profit from those projects which else would probably have been forgotten.

All in all, the MMT server has become a very important tool for teaching basic mathematics as well as modelling and simulation at the Vienna University of Technology. Although all examples currently available

for teaching on the MMT server are implemented in MATLAB, MMT has recently been developed to include also examples implemented in AnyLogic using Java applets which offer way more interesting possibilities for the output. Additionally, to loosen the dependency on the commercial software MATLAB, one of the next developments concerning the MMT system will be the inclusion of examples accessing Octave.

ACKNOWLEDGEMENTS

This work has been realized in the context of the ‘Applied Modelling, Simulation And Decision Making’ project and funded by means of the City of Vienna by the ZIT GmbH - the Technology Agency of the City of Vienna, a subsidiary of the Vienna Business Agency.

The MMT server is administered in cooperation with the dwh Simulation Services.

REFERENCES

- Winkler, S., Körner, A., Hafner, I., 2010. MMT – A web-based e-learning System for Mathematics, Modeling and Simulation using MATLAB. *7th EUROSIM Congress on Modelling and Simulation*, paper 231, Prague (Czech Republic)
- Körner, A., Zauner, G., Schneckreither, G., 2009. Ein e-learning System für MMT – Mathematik, Modellbildung und Tools, Systemerweiterung und Einbindung von graphischer Modellbildung. *20th Symposium Simulation Techniques*, pages 87–94, Cottbus (Germany)
- Körner, A., Hafner, I., Bicher, M., Winkler, S., Breitenacker, F., 2011. MMT - A Web Environment for Education in Mathematical Modelling and Simulation. *ASIM 21. Symposium Simulationstechnik*, Winterthur (Switzerland), ISBN: 978-3-905745-44-3
- Hafner, I., Bicher, M., Winkler, S., Fitsch, U., 2012. MMT - An E-Learning System based on Computer Numeric System for teaching Mathematics and Modelling. *MATHMOD 2012 - 7th Vienna Conference on Mathematical Modelling*, Vienna (Austria)

POSSIBILITIES AND LIMITS OF CO-SIMULATING DISCRETE AND CONTINUOUS MODELS VIA THE BUILDING CONTROLS VIRTUAL TEST BED

Irene Hafner^(a), Matthias Röbner^(b), Bernhard Heinzl^(c), Andreas Körner^(d),
Michael Landsiedl^(e), Felix Breitenecker^(f),
Christian Reinisch^(g)

^(a) ^(d) ^(f) Vienna University of Technology, Institute of Analysis and Scientific Computing
^(b) ^(c) ^(g) Vienna University of Technology, Institute of Computer Aided Automation
^(e) dwh Simulation Services

^(a) irene.hafner@tuwien.ac.at, ^(b) matthias.roessler@tuwien.ac.at, ^(c) bernhard.heinzl@tuwien.ac.at,
^(d) akoerner@asc.tuwien.ac.at, ^(e) michael.landsiedl@drahtwarenhandlung.at, ^(f) fbreiten@osiris.tuwien.ac.at,
^(g) creinisch@auto.tuwien.ac.at

ABSTRACT

This paper discusses the method of cooperative simulation of discrete and continuous models with the Building Controls Virtual Test Bed, a software environment that allows coupling different simulation programs. In the course of a project aiming the energy optimization in cutting factories, models of machines of differing complexity and a building containing them have to be implemented to further simulate the thermal processes. Since all partial models require individual modelling approaches, solver time steps, solvers or even simulators, the method of co-simulation is considered. The partial models will be implemented with Modelica, Matlab, Simulink and Simscape and accessed with the co-simulation tool BCVTB. The simulation results show that this method of co-simulation can be sufficient for the needs of describing thermal systems with large time constants but has to be found insufficient for simulations requiring high accuracy and variable step solvers in the overall simulation.

Keywords: co-simulation, energy optimization, thermodynamics, MATLAB, Dymola

1. INTRODUCTION

1.1. Motivation

To optimize the energy consumption in production halls, it's necessary to model the individual machines as well as the building itself in varying detail. To further install a feedback control keeping the room temperature at comfortable values for human beings which might enter the hall, the heat emitted by the machines and its distribution in the hall have to be simulated. The simulation of the temperature progression in these machine halls is part of the INFO (Interdisziplinäre Forschung zur Energieoptimierung

in Fertigungsbetrieben) project which is supported by the Austrian Research Promotion Agency (FFG).

In this paper a simulation of models implemented with Modelica, MATLAB, Simulink and Simscape will be described. An overview of the intended communication between the simulators is given in Figure 1.

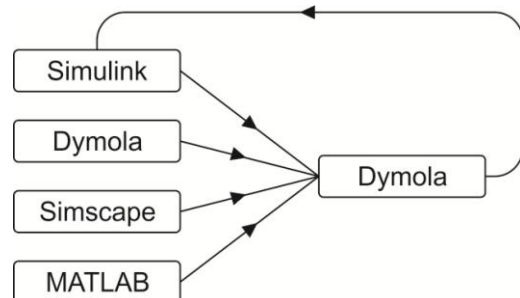


Figure 1: Desired Communication between the Individual Simulators

1.2. Co-Simulation

The basic idea of co-simulation is the parallel simulation of models using different simulators via one overall simulator. This simulator executes a model accessing the individual simulators and lets them synchronize at given time-steps. This way it's possible to match the individual modelling and simulation requirements of all partial models considering the fact that in our case the machine models result in differential algebraic equations describing electrical and mechanical circuits and the room model only deals with systems describing thermal processes, which react much slower and therefore don't require comparably small time steps and can use less complex solver algorithms for the simulation. This also explains why an external simulator is used to combine Simulink and Modelica

models, which could actually be interacting themselves but would use only one solver for the simulation. The overall simulation via BCVTB leads to opening one simulator instance for every model, which means even two models using Dymola can be simulated in parallel with different solver algorithms and solver step sizes.

2. SOFTWARE

2.1. BCVTB

The Building Controls Virtual Test Bed (BCVTB) is a co-simulation tool based on the graphical modelling interface Ptolemy. Though at first glance BCVTB and Ptolemy look exactly the same, BCVTB lacks many Ptolemy blocks (called *actors* in Ptolemy) and in return provides a lot of actors specifically for co-simulation. To supervise the overall simulation, so-called *Directors* are used. Depending on the given problem, one can choose between a *Synchronous Data Flow Director* which allows discrete-time synchronization at fixed time steps and a *Continuous Time Director* offering different variable step solver algorithms for the overall simulation.

Although this might at the first impression sound like an easy way to co-simulate models with a variable step size adapting to the demands of the given problem, it will be shown later in this paper that regarding especially these simulation directors, limits are met very soon. Other actors especially developed for co-simulation with BCVTB are *simulator* actors. These actors access the individual simulators using BSD-sockets, an application programming interface enabling inter-process communication which, like BCVTB itself, also has been developed at the University of California in Berkeley. In the simulator actors the name of the simulator to be accessed as well as the file to be executed has to be defined. All values needed by the respective simulator have to be transferred to the simulator actor as inputs and all values BCVTB gets from the simulator can be accessed at the output port of the actor. BCVTB basically allows co-simulation of Ptolemy, EnergyPlus, Dymola, MATLAB, Simulink, Radiance and BACnet. For further information, see [Wetter, 2012].

2.2. Dymola/Modelica

Modelica constitutes a standard for object-oriented modelling of physical systems using acausal block diagrams. Every block represents an element from one of various physical domains, e.g. *electrical*, *mechanical* or *thermal*. The underlying code contains a set of equations describing the behaviour of the corresponding component. By coupling an arbitrary amount of these components, systems of almost any complexity can be built quite easily without considering causalities of the signals. The solvers from a Modelica simulator like Dymola gather all equations, simplify and rearrange the system of equations and finally solve it.

2.3. MATLAB, Simulink, Simscape

MATLAB is a programming environment offering its own language and various toolboxes meeting the requirements of different modelling approaches. One of these toolboxes is Simulink. Simulink models basically represent signal flow charts and can be built graphically as block diagrams of directed graphs. In block diagrams for Simscape models, acausal connections are used allowing physical modelling similar to Modelica.

3. COMMUNICATION BETWEEN THE INDIVIDUAL SIMULATORS

BCVTB offers several predefined functions to enable communication with the simulators mentioned above. In MATLAB the establishment of sockets, the exchange of data and the closure of the sockets is realized with predefined functions from BCVTB.

For the communication with Simulink BCVTB provides a preimplemented block which basically represents the functions for the communication with MATLAB. To ensure the communication at the time steps given by the overall model despite using an individual solver with variable step size, the block has to be put in an If-Action-Subsystem which is only activated at the given synchronization references. The Simulink block for the communication with BCVTB is shown in Fig. 2:

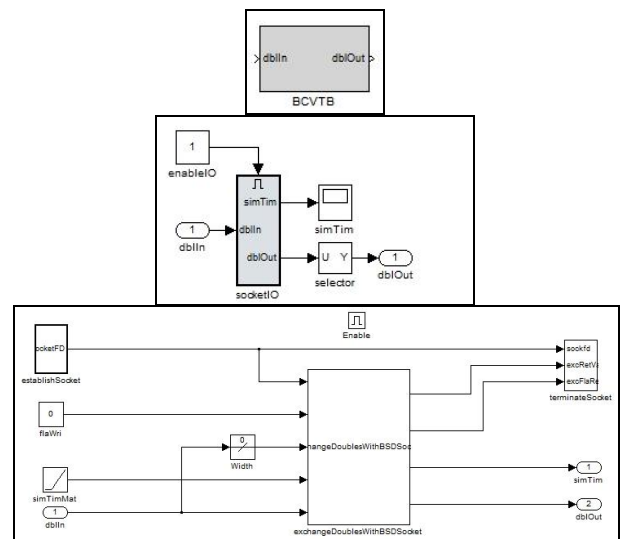


Figure 2: Simulink Block for the Communication with BCVTB

For Dymola, which is used as simulator for Modelica, the Modelica Buildings Library which has also been developed by the inventors of BCVTB has to be downloaded. This Library contains among others a block similar to the one for the communication with Simulink. The parameters and the icon for the BCVTB block in Dymola can be seen in Fig. 3.

Apart from setting the number of values to be read from BCVTB and the number of values to be returned

to BCVTB, the initial return value and the time step for synchronization can be chosen in the block parameters.

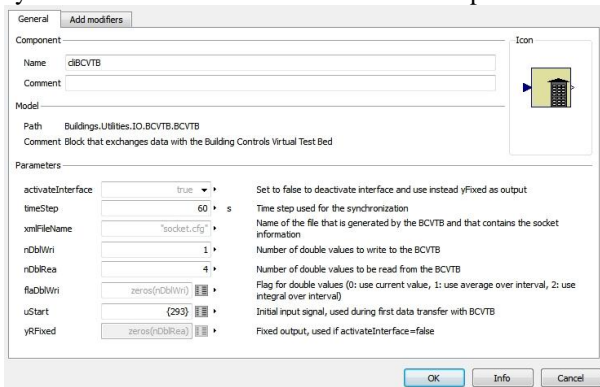


Figure 3: Block for the Communication with BCVTB in Dymola

This shows one of the first weak points of BCVTB: Dymola cannot communicate with BCVTB at variable points in time with the given resources since the synchronization time step in the BCVTB block for Dymola can only be chosen fixed.

4. MODEL DESCRIPTION

To focus again on the problem of simulating the thermal processes in a production hall, the individual models will be described. The machines in the production hall are modelled in Modelica, Simscape and as simple data model in MATLAB. The room itself is implemented as compartment model in Modelica. To keep the room temperature in a tolerable interval around a desired temperature, a discrete-state three-point controller with hysteresis is also included to the model. All these partial models are finally co-simulated by executing an overall BCVTB model.

4.1. Overall Model implemented in BCVTB

The BCVTB model for this problem uses a Synchronous Data Flow Director, which corresponds to a discrete fixed time solver forcing the individual simulators to exchange heat flow and temperature resp. every 60 seconds.

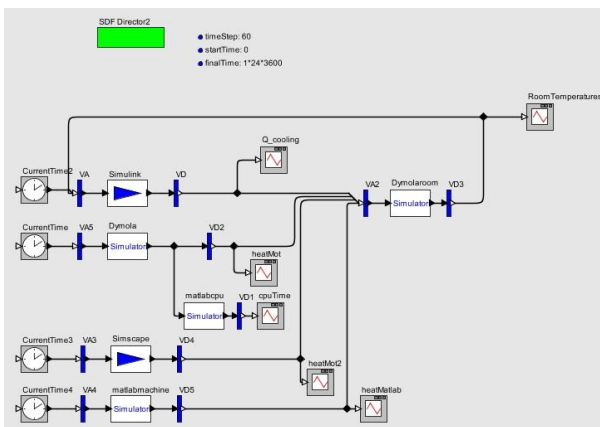


Figure 4: Overall Model for Co-Simulation via BCVTB

As you can see in Fig. 4, the dissipated heat from the machines simulated with Dymola, MATLAB and Simscape is transferred to the room model simulated with Dymola. The temperature in one compartment, where a thermometer can be pictured, is transferred to the control in Simulink. Depending on this temperature, a negative, positive or zero heat flow is returned from Simulink and transferred to the Dymola room model.

4.2. Room Model in Dymola/Modelica

The room model implemented in Modelica is divided into twelve thermal compartments. These compartments have been modelled as cubes basically consisting of a certain heat capacity and thermal elements for heat exchange at the six surfaces. Each surface is represented by a heat port, a thermal conductor block and a thermal convection block. In this simplified model, the convective heat transfer coefficient of air is kept constant as $2 \text{ W}/(\text{m}^2 \cdot \text{K})$, which corresponds to the average value for air at 20 degrees. Additionally, the temperature in the compartment is logged. The model graph as well as the parameters for a thermal compartment can be seen in Fig. 5:

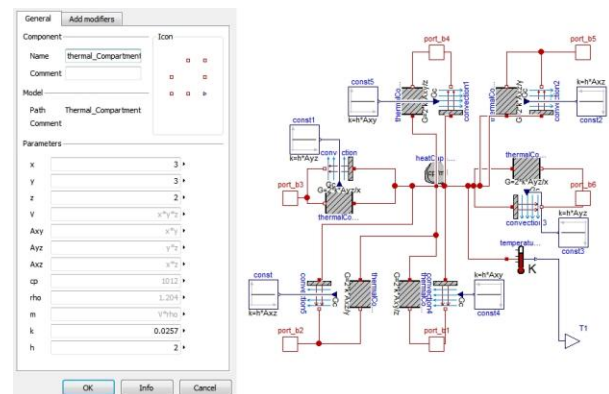


Figure 5: Parameters and Graph of a Thermal Compartment Model in Dymola

Each thermal compartment of the room is chosen to be $3 \cdot 3 \cdot 2 \text{ m}^3$. The whole room, which can be seen in Fig. 6, therefore accounts for $9 \cdot 12 \cdot 4 \text{ m}^3$.

The heat emitted by the individual machines and the output of the control are given as outputs of the BCVTB block. These signals are transferred as heat flow to the compartments where the machines and the cooling system are meant to be found. The first return value from BCVTB corresponds to the heat flow given by the control in Simulink and is sent to two of the upper compartments in the model. The other three outputs from the BCVTB block correspond to the dissipative heat from the machines models in Dymola, Simscape and MATLAB, which are found in three of the lower compartments. Additionally, an open window is represented by a constant temperature of zero degrees at the surface of one of the upper compartments.

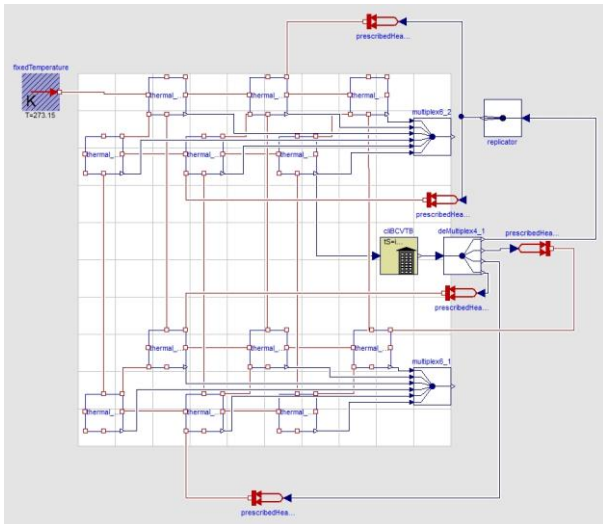


Figure 6: Room Model Implemented in Modelica/Dymola

4.3. Machine Model in Dymola/Modelica

The machine model implemented in Modelica is held rather simple. Basically it consists of a DC motor emitting heat at the resistor and friction element.

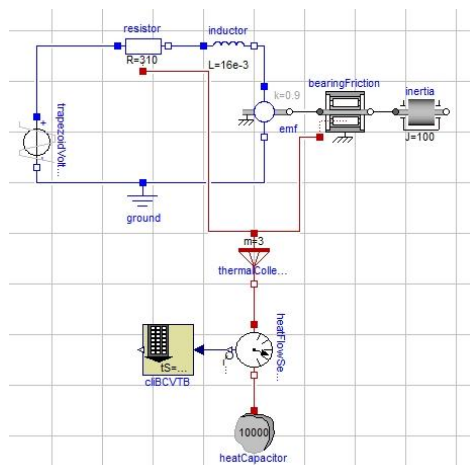


Figure 7: Model of a DC Motor in Modelica/Dymola

Since version 3.2, Modelica provides optional heat ports for further use of the heat emitted by dissipative electrical or mechanical components in thermal circuits. This way the waste heat can easily be diverted and transferred to BCVTB.

4.4. Data Model in MATLAB

The data model in MATLAB accesses an Excel-file containing measured values of the heat emission of a typical machine tool. The file only provides data at every hour, so it is continued uniformly in between.

4.5. Machine Model in Simscape

The machine modelled in Simscape again represents DC motor. In contrast to the Dymola motor, this model

doesn't take into account any friction. Since Simscape doesn't provide any heat ports for dissipative elements, the emitted heat is calculated manually from the voltage drop across the resistor, transferred to a thermal circuit and further to BCVTB (see Fig. 8).

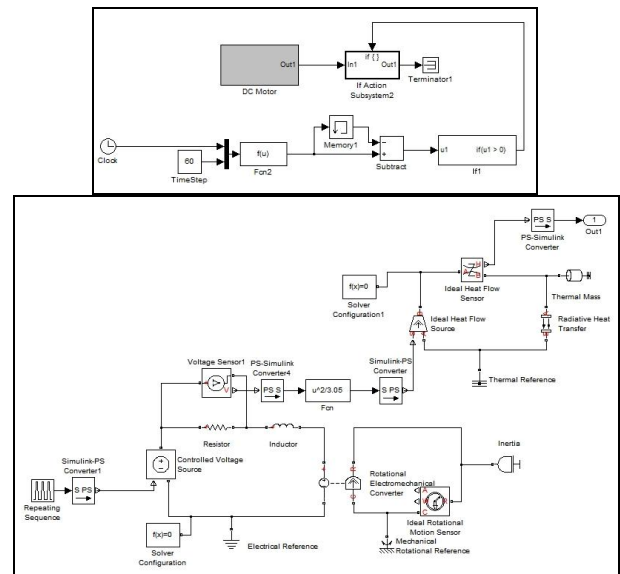


Figure 8: Graph of the DC Motor Model Implemented in Simscape

4.6. Control in Simulink

To keep the temperature in the machine hall bearable for human beings, a three-point control with hysteresis has been implemented in Simulink. Simulink receives the room temperature measured in one compartment (see Fig. 6) and compares it to the desired temperature of 20 degrees.

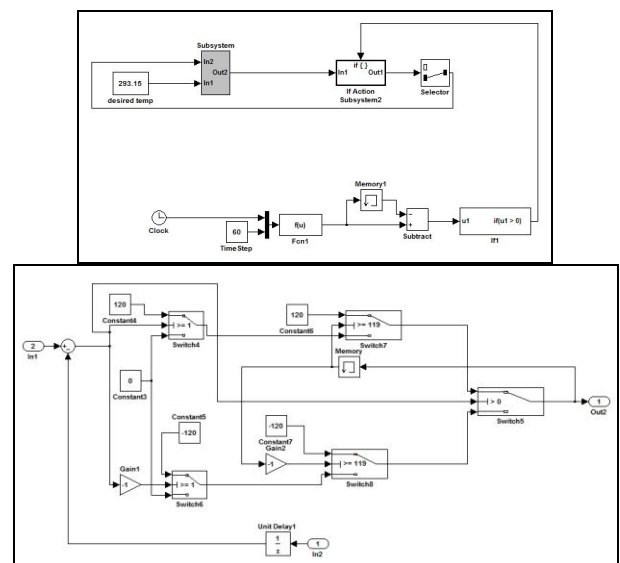


Figure 9: Graph of the Control Model Implemented in Simulink

If the room is warmer than 21 degrees, the system starts to cool by sending a negative heat flow to two

compartments of the room. As soon as the measured room temperature descends again under 20 degrees, the system stops cooling. If the room is cooler than 19 degrees, heating starts until the room is again warmer than 20 degrees. The model graph of this control can be seen in Fig. 9.

5. SIMULATION RESULTS

5.1. Temperature and Heat Flow

Fig. 10 shows the heat emitted by the individual machines over one day. All of the machines are switched on in the morning and turned off at night.

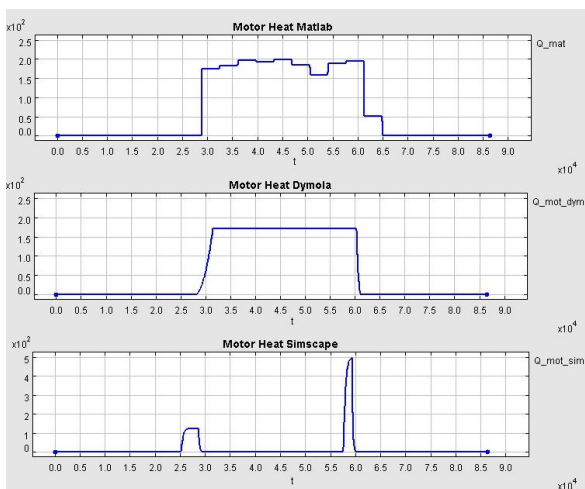


Figure 10: Heat Emission of the Machines Over One Day

The output of the MATLAB machine represents the heat emission of a machine measured every hour. For the Simscape motor, only changes in motor speed (represented by rising or falling supply voltage) cause electrical losses and emission of heat due to the fact that no friction is considered. On the contrary, the emission of the Dymola machine doesn't cease as long as the machine runs.

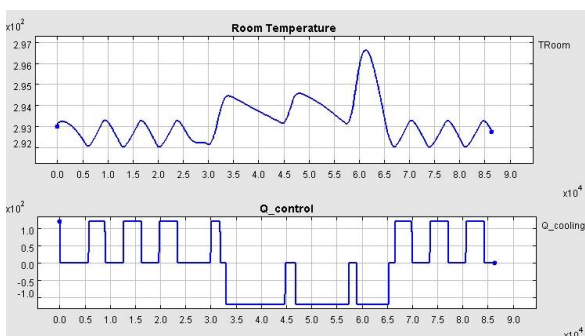


Figure 11: Room Temperature at the Thermometer for the Control and Output of the Control Over One Day

In the first plot of Fig. 11 the progression of the temperature in the compartment with the fictional thermometer for the control can be observed. The legend shows Kelvin, in degrees the temperature range

would be 18 to 24 degrees. As long as the machines are turned off, the room cools down due to the open window so the control has to heat from time to time. As soon as the machines start to work and therefore to emit heat, cooling is necessary. To give an impression on the reaction of this temperature on the output of the control, the latter is shown in the second plot in Fig. 11.

Fig. 12 shows the temperature in the six lower compartments of which three contain a machine and therefore warm up fastest (blue, black and green). The legend again shows Kelvin.

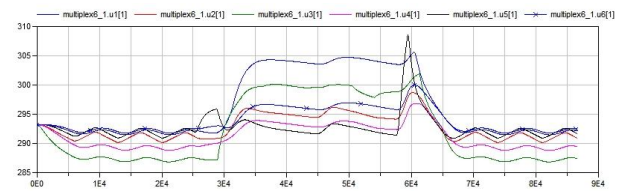


Figure 12: Temperature in the Lower Six Compartments Over One Day

The temperature of the upper six compartments can be observed in Fig. 13. Caused by the output of the Simulink control, two of them react slightly faster (red and black).

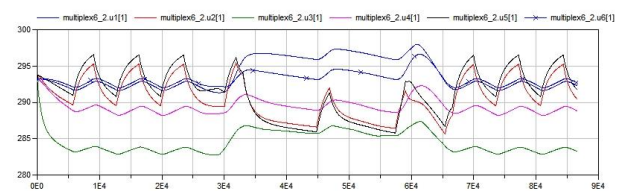


Figure 13: Temperature in the Upper Six Compartments Over One Day

As can be seen in Fig. 14, simulating the same model over one week results in an approximately periodic progression of the room temperature due to the fact that all machines are turned off at night giving the room the possibility to cool down.

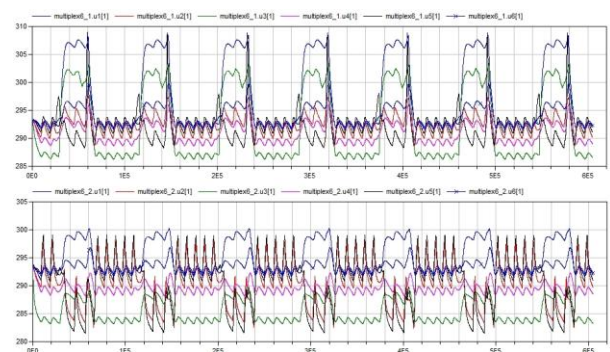


Figure 14: Progression of the Compartment Temperatures Over One Week

5.2. Solver Time Step Documentation

One of the most important and interesting results of a co-simulation is the documentation of the individual

solver step sizes. In this simulation, *DASSL* has been chosen as the solver for the room model in Dymola and the machine model in Dymola. For the Simscape motor *ode15s* was most suitable since it deals with stiff systems. The control in Simulink handles discrete states only, hence a variable step discrete algorithm is used. A significant advantage of co-simulation becomes obvious at one glance at Fig. 15 which shows the time steps taken by the individual solvers during one synchronization interval.

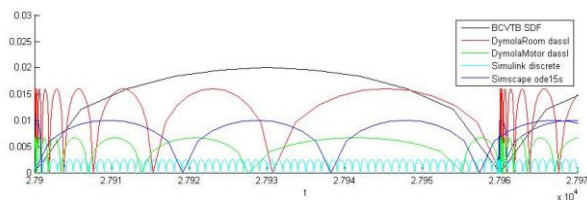


Figure 15: Different Solver Time Steps during One Synchronization Interval

Simulating the machine models requires much smaller solver time steps than simulating the room model. The steps of the *ode15s* solver for Simscape are plotted in blue, those for *Dassl* in the Dymola machine model in green, Simulink discrete in turquoise, *Dassl* for the Dymola Room in red and the overall simulation time step of constant 60 seconds in black.

If for example the machine model in Modelica and the room model were combined in one Modelica model, the simulation would demand many time steps necessary for the machine but superfluous for the needs of the room. Simulating even models which – considering Modelica and MATLAB – could to some extent be coupled without an external interface becomes way more efficient for the same reason.

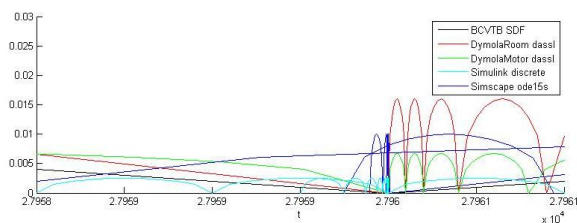


Figure 16: Time steps taken by the individual solvers at a synchronization reference

By looking the time steps in a small interval around one synchronization reference shown in Fig. 16, the redundant steps made by the Simscape solver to iterate the time for synchronization can be seen. In Dymola, the synchronization time is met without iteration since the time step for synchronization can be set in the BCVTB block. On the other hand, the direct setting of this time step prevents the possibility of synchronization at variable points in time as has already been mentioned in section 3.

6. CONCLUSION AND OUTLOOK

The aim of this paper has been to evaluate the possibilities and limits of co-simulating discrete as well as continuous systems with BCVTB.

One of the first important decisions to be made in this regard is the choice of an adequate time step for the overall simulation. Since thermal processes act rather slowly, the synchronization time step for this problem can be chosen comparably big in contrast to the solver time steps of the machine models. On the other hand due to the fact that all values received from BCVTB are kept constant between two synchronization references, the synchronization time step has to be considered small enough to keep the resulting error within adequate tolerances. This shows that for models focusing particularly on precise interaction, the method of co-simulation with BCVTB has to be found insufficient.

As mentioned above, this tool is going to be used for the simulation of the thermal processes in a production hall over one year. The simulation of these rather simple and few partial models for 7 days already takes about eight minutes on an average computer station. In the final model for the production hall, way more detailed and complex machine models are meant to be included. This will lead to very expensive computing times so one might have to consider that this tool is not suitable for co-simulations of such dimension.

All in all, BCVTB can be found as a quite helpful tool to quickly combine models implemented in modelling environments which are executed with different simulators using individual solvers but has to be considered deficient regarding accuracy and requirements of variable step sizes for the overall simulation of complex models.

ACKNOWLEDGEMENTS

This work has partially been supported by the Austrian Research Promotion Agency (FFG).

REFERENCES

- Wetter, M., 2012. *Building Controls Virtual Test Bed User Manual Version 1.1.0.* Building Technologies Department, Environmental Energy Technologies Division, Lawrence Berkeley National Laboratory, Berkeley (California,USA). Available from: <http://simulationresearch.lbl.gov/bcvtb> [Accessed 5th July 2012]
- Heinzl, B., Rössler, M., et al., 2011. Studies on Multi-Domain Modelling and Thermal Coupling of a Machine Tool. *ASIM 21. Symposium Simulationstechnik.* Winterthur (Switzerland), ISBN: 978-3-905745-44-3
- Modelica Buildings Library. Available from: <http://simulationresearch.lbl.gov/modelica> [Accessed 5th July 2012]
- Mathworks. Available from: <http://www.mathworks.com> [Accessed 5th July 2012]

IMPROVEMENT OF ADVANCED MATHEMATICAL SKILLS AND ABILITIES USING THE COMPUTER ALGEBRA BASED E-LEARNING SYSTEM MAPLE T.A.

S. Winkler^(a), A. Körner^(b), V. Urbonaite^(c)

Vienna University of Technology
Institute for Analysis and Scientific Computing
Wiedner Hauptstraße 8-10
1040 Vienna

^(a)stefanie.winkler@tuwien.ac.at, ^(b)akoerner@asc.tuwien.ac.at ^(c)vilma.urbonaite@tuwien.ac.at

ABSTRACT

This paper is about an e-learning environment based on Maple, called Maple T.A. Maple T.A. for stands for Testing and Assessment with Maple. It is used at the Institute for Analysis and Scientific Computing at the Vienna University of Technology. Over the last four years some improvements have been achieved and the number of courses using this tool increased. Also the way of using the e-learning system has changed. At the beginning it was a support for students practicing their mathematical skills. Now it is also a system for testing and assessing. Depending on the course the students have to pass one to three tests each semester to pass the course.

On the other hand Maple T.A. supports the lecturer and organizer as well. All the users and their test results are stored in this system. Therefore using this environment was enhanced through three different courses.

Keywords: Maple, e-learning, mathematics, simulation, testing, assessment

1. INTRODUCTION

At the Institute for Analysis and Scientific Computing the idea of using Maple T.A. was established due to the refresher course. In 2008 the vice-rector of the Vienna University of Technology requested a refresher course supported by an e-learning system. This course should represent the bridging of the gap of knowledge in basic mathematics which comes up between school and university. Most of the male students have to attend military or civilian service. Also some of the students-to-be take time for travelling or au pair. Additionally, pupils from different types of schools graduate with different mathematical levels. For example pupils of tourism schools and pupils of a technical school differ in their mathematical knowledge because of the different focus of their schools. This refresher course should equalize the basic mathematical knowledge and ease the access to university.

To fulfil the requirements the institute was looking for adequate software. One of the advantages of e-learning systems is the availability at any time. On the one hand this tool should help students to coordinate their learning and to give them a feedback about their skills so the students would be able to control their learning progress and success. On the other hand a benefit should be a simplified administration and organization of students and their grading. Therefore Maple T.A. was established.

2. THE DEVELOPMENT (EXPANSION)

Initially the refresher course was only offered in the beginning of September for students of electrical engineering because the Institute for Analysis and Scientific Computing is also involved in all the other mathematical courses for this field of study. Since then, every year another field of study was added to participate of the refresher course. Since two years Maple T.A. is also used for the regular mathematical courses. In 2011 the refresher course was offered additionally in the last week of September for the first time. That year the students of the following fields of studies attended the refresher course.

- Electrical Engineering
- Technical Physics
- Surveying and Geoinformation
- Mechanical Engineering
- Mechanical Engineering - Economics
- Civil Engineering
- Urban and regional planning
- Some students from other fields of study

Because of the simplification due to Maple T.A. and the positive feedback from the students the Institute for Analysis and Scientific Computing started using the system also in the basic mathematical courses. For the first time students had the opportunity to use the

examples on Maple T.A. to understand the subject and to improve their skills.

Up to now Maple T.A. is used in three different ways, the refresher course, two basic mathematical courses and one advanced mathematical course.

3. ABOUT MAPLE T.A.

3.1. In General

Maple T.A. stands for Maple Testing and Assessment. The system is based on Maple, a computer algebra system. On the one hand Maple supports analytic and algebraic calculations. On the other hand it is a very common programming language at the Vienna University of Technology. Currently Maple T.A. version 6.0 is used.

Maple T.A. is designed to simplify the creation of examples and the arrangement of tests. For the examples there are many different possible question types like multiple choice, fill in the blanks, numeric, multipart or true/false questions. The choice of the proper question type depends on the topic of the question and on the aspired goal of the tutor. There are examples which target the logical thinking of the students and some which enhance their numeracy.

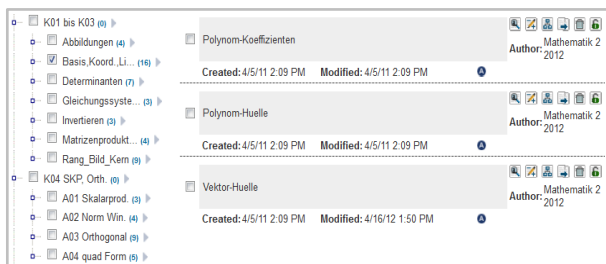


Figure 1: On The Left Side The Question Three Is Shown And On The Right Side The Examples Of The Chosen Subchapter Are Listed.

In general the Maple T.A. system is an interface which contains a Maple kernel. The surface offers many different functions. At first one creates a certain class which is dedicated to the course. This class contains a question repository where all the coded examples are stored and sorted, shown in figure 1. With these questions assignments are created.

Assignment Name	Points	Type
3 UE-Test	16.0	Proctored
2. UE-Test	16.0	Proctored
1 UE-Test	16.0	Proctored
K10 Lokale und globale Verhalten von Funktionen	5.0	Practice
K13 Potenzreihen	5.0	Practice
K12 Integralrechnung	31.0	Practice
K01 Vektorräume	15.0	Practice
K02 Matrizen und lineare Gleichungssysteme	22.0	Practice
K03 Determinanten	7.0	Practice
K04 Skalarprodukt und Orthogonalität	21.0	Practice
K05 Das Eigenwertproblem	11.0	Practice
K06 Differentialrechnung im Mehrdimensionalen Teil 1	12.0	Practice
K06-2 Differentialrechnung im Mehrdimensionalen Teil 2	15.0	Practice

Figure 2: An Overview Of All The Assignments Of Mathematics 2. The First Three Lines Are The Tests.

In figure 2 the assignments, which can help organising the different topics of the lecture, are shown. The students have free access to these assignments if the tutors unlock them. There are different types of assignments. The different topics are anonymous exercises. If one wants to create a test a proctored assignment is necessary. That means that a proctor, in most cases the tutor, has to unlock and close the test again. So the students are not able to make the test at home.

3.2. Maple T.A. Coding

In the Maple T.A. system there are some special commands similar to the Maple ones. But it is also possible and sometimes necessary to use the common and original Maple commands depending on the complexity of the example.

For example an if-command in Maple T.A. looks like the first line of Table 1. The if-query embedded in Maple T.A. including an initialization, which is necessary with an \$-sign, stands below. It is obvious that it is very easy to use the regular Maple commands. The differences are the particular initialization and the active call of Maple. In contrast to the Maple code the same demand within the MTA functions is quite short, as can be seen in the last row of Table 1.

Table 1: The Different Ways For Programming The Same Function In Maple T.A.

Commands	
Maple code	if a<b then a else b end if
Embedded in MTA	\$c = maple("if a<b then a else b end if")
MTA code	\$c:=if(gt(a,b), b, a)

It is also possible to embed a procedure, which means more than one command one after another, separated with a colon, see for example equation 1.

$$\begin{aligned} & \$v1 = \text{maple}("a:=\text{Random}[\text{VecInts}](2,2) : \\ & a(1):=1 : a(2):=0 : \$v1v2.a") \end{aligned} \quad (1)$$

One important advantage of Maple T.A. is that through the creation of one exercise a small pool of different examples results. The principle of the example is every time the same but the numbers or functions are randomized so they change at every request. So the tutors only have to create a few examples to offer a great questionnaire. Additionally the students are not able to cheat at the test that easy because the students sitting next to each other need different results for the same example. The copy of the calculation itself would not help so the student has to think about it although he/she can look at the sheet of paper from the neighbour. So Maple T.A. causes a win-win situation for students, lecturers and tutors.

3.3. Creation Routine

As already mentioned, it is possible to create randomized numbers within Maple T.A. To offer a big variety of examples it is also profitable to create random functions and text as well. Therefore the question designers have developed a new library including some different commands for the creation of examples. There are commands which support the creation of randomized numbers and functions.

For example the command *Random[FromSet]* randomly picks one of the following expressions which are listed in the set like in the following code-line (2).

```
Random[FromSet]({cos(x)^(a), sin(x)^(a)}) (2)
```

For the course Mathematics 2 it was also important to create vectors and matrices in an easy way. In addition to the randomization of the entries of vectors and matrices it is possible to choose the character of the entries as well, for example the amount of zeros or the eigenvalues.

```
Random[MatInts](5, rows = 3, rank = 3) (3)
```

The command above (3) creates a matrix dimensioned 3x3 with integer entries between -5 and 5 except 0. Additionally the matrix will be regular because of the specification *rank=3*, which means the rank of the matrix is the dimension.

This improved library shortens the preparation of examples enormously.

3.4. Grading Routine

Another improvement is the new grading routine. The creating routine supports the designers and tutors more but the development of the grading benefits the students mainly.

This routine enables fair grading for every student. If the question requires a vector with three entries as input one would get no points if only one entry is wrong. The improved grading routine controls every entry so it is possible to get parts of the points. The according command is *Grade[Vec]*. In the same way *Grade[Mat]* works and grades matrices.

The questions concerning the topic of partial fraction expansion causes some complications because they are more difficult to grade. The students enter a long term consisting of many different fractions. The calculation of the factors of these fractions is not so difficult but offers many possibilities for miscalculation. Therefore the improved grading routine checks every single fraction-factor. So the calculation of the students is honoured. This feature makes the e-learning system Maple T.A. more comfortable for the students and so the feedback improves.

4. THE COURSES

As already mentioned, Maple T.A. is used in three different areas. First of all the e-learning system is used in the refresher course in which the mathematical level

of pupils is improved. Secondly there are two basic mathematical courses for the students of Electrical Engineering where this MTA system is used for one year all together. And at last the advanced mathematical course is supported by this system as well. This course is also obligatory for the students of Electrical Engineering. It is obvious, that these students benefit from the system most because they get to know the system in the refresher course. Therefore the usage of MTA in the following lectures does not causes problems or questions anymore.

4.1. Refresher Course

The refresher course was initialized as a “bridging the gap”- course for students of the first semester. The course consists of 8 different topics. They are held in different lectures to offer the students the possibility to visit only the topics, they cannot remember so well. This year there will be ten topics to cover the mathematical requirements of all fields of study.

The course is separated in 2 parts, the lecture and the exercise. The whole course lasts one to two weeks. There are two different timeslots. On the one hand there is the course in the last week of September. An advantage of the September course is that the ordinary courses of the study have not started then. The students can focus on the improvement of their mathematical skills. On the other hand there is one course in the first and second weeks of October. This course is separated in the different fields of study to customize the timetable.

For every module there is a lecture first which takes more than one hour. Afterwards the students have 15 minutes to divide into smaller groups and change the location. There, in the seminar rooms, a tutor is waiting to continue with the exercise part of the module. The practicing takes one and half an hour. The tutor presents many different examples fitting to the lecture. The students also have the possibility to make their first experience at the blackboard in front of the tutor.

Maple T.A. is used in more than one way. On the one hand MTA offers the students the possibility to practice the examples of the different topics whenever they want to. It is also possible to have a look at the examples during the whole semester because the account stays activated. On the other hand there are three voluntary tests. First there is a knowledge test. This test is anonymous so the students have the chance to figure out if they need the refresher course. In the first exercise the students have to make a test to show them and the tutors their current level and knowledge. The last test is in the end of the course. If the students want to receive a mark for that course they have to pass the final exam. Additionally these tests show how much the students profit of this offer.

To get an idea of the level of the Maple T.A. examples the following figure shows a typical example of the refresher course.

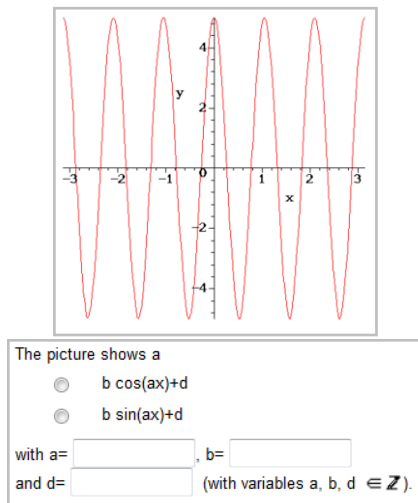


Figure 3: A Typical Example Of The Refresher Course: The Task Of This Question Is The Classification Of The Curve.

In Figure 3 an example is shown which is mostly used in all of the three tests. The identification of mathematical graphs is very important for students of technical fields of studies. There are several variables to figure out. The students have to decide whether the curve is a cosine or a sine. The variables a , b and d stand for the frequency, amplitude and the shift of the sine or cosine. Most of the examples of the refresher course have the same degree of difficulty.

4.2. Basic Mathematical Courses

Another course, where Maple T.A. is used, is obligatory in the first two semesters of Electrical Engineering. Around 300 students attend these two courses, Mathematics 1 and Mathematics 2. Mathematics 1 focuses on Analysis and Mathematics 2 on Linear Algebra. Because of the amount of students the usage of an e-learning system suggests itself, especially an assessment system. It eases the coordination and administration of the students and the verification of their learning progress and skills.

The course itself consists of a lecture and an exercise course. The lecture is held several times a week but is voluntary. The exercise course has more parts. On the one hand they have to prepare eight examples every week. The students should be able to present them at the blackboard and answer questions of the tutor to show their comprehension. If they cannot answer the question they have to correct their achievement with another, hopefully better presentation. On the other hand there are three tests each semester realized in Maple T.A. which are spread over the semester. The students only have to pass two of them. They also get another change with an additional test to achieve two positive results. The points of the test are not important. The minimum to pass the course are fifty percent of the points of each test. For the lecture itself the students have to pass an extra exam. Last year this exam was also supported by the MTA system. In that case there was a written test realized with the Maple T.A. system. about the e-learning

test was basically to check the calculation skills of the students. At the oral exam the students had to prove their theoretical knowledge. Normally the lecture exam consists only of a written exam only containing theoretical question as well as ordinary calculation examples.

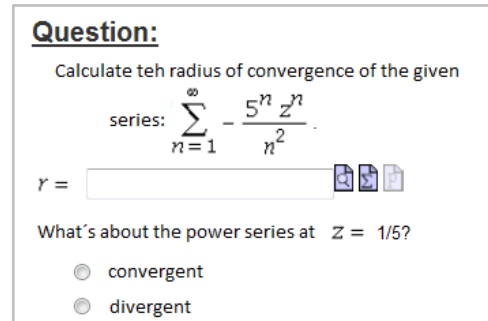


Figure 4: An Example Of The Course Mathematics 1 Which Deals With The Behaviour Of Power Series.

To support the exercises well, the questionnaire in Maple T.A. is enlarged with new examples according to the current topic in the lecture every two weeks. So the students have the facility to practice the fitting examples every time they like to. Additionally the questions on Maple T.A. can help understanding the actual subject. In addition to the questionnaire on Maple T.A. the learning matter for one test usually includes the examples of the last four exercises. Every test consists of four examples.

Figure 4 shows a question of the mathematical course of the first semester. In the first task they have to determine the radius of the convergence of a given power series. In the second part they have to analyse the behaviour of the series at the edge of the convergence area.

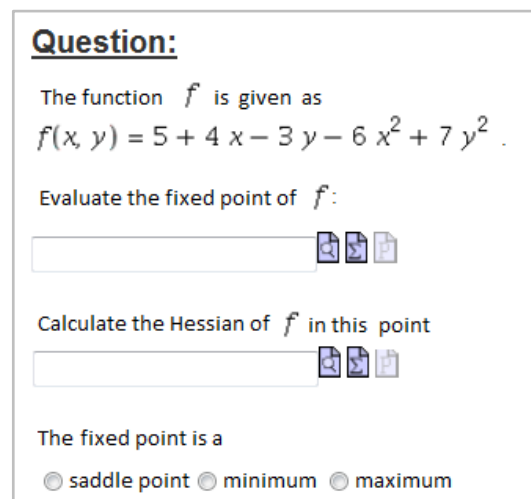


Figure 5: Mathematics 2 Focus On Linear Algebra And Its Usage. The Student Has To Determine The Fixed Point.

In figure 5 an example about the Linear Algebra is given. Given is a function in two variable. The students

have to calculate the fixed point at first. They have to fill in the point as a vector. The second question asks for the Hessian in this certain point. The students should insert a matrix like this, $[a_{11}, a_{12}; a_{21}, a_{22}]$. The last task is a multiple choice question in which the student has to decide if the fixed point is a saddle point, a minimum or a maximum. The vector and the matrix are graded in the way described in chapter three. Most of the examples in the two basic mathematical courses have more than one task so the possibility to earn points without calculating all the right solutions increases.

4.3. Advanced Mathematical Courses

In the last subsection the advanced mathematical course is described. Last year it was the first time that this course was supported with the Maple T.A. system. Last year the examples focused on theoretical knowledge. This year the focus should also be the calculation skills of the students. The questionnaire will be enlarged to offer a greater variety of examples to help the students to cope with the challenges given in the lecture.

This course is a combination of a lecture and an exercise. Most of the time the course is an ordinary lecture and once a week the lecturer calculates some examples in front of the students and explains them. The support of the Maple T.A. is basically voluntary practice at home. The examples which are presented in the lecture can be reconstructed via the questions of Maple T.A. Additionally there are two tests during the course, which are important for the final grade. Additionally there is an oral exam in the end of the course. The final mark consists of the tests and the oral exam.

Question:
Suppose we have a sample of size 12 :
-19, -10, 9, 14, -13, 8, -11, 2, -1, 1, 18, 20.

(1) Calculate:

(a) the sample mean:

(b) the sample variance:

(c) the 0,25-quantile:

(d) the mode:

the 0,75-quantile:

The values must be entered exactly.

Figure 6: An Example For The Advanced Mathematical Course Out Of The Field Of Statistic.

The question in figure 6 shows a task of the statistical part of the lecture. The students receive a

random sample and then have to calculate the mean, the variance and three different quantiles of this sample. Additionally the students have to choose one of the box plots. The right box plot is the one which reflects the random sample.

A random variable Y is given by the transformation of the random variable X :
 $Y = -3X - 6$.

The probability density function of the continuous random variable X is given by

$$f(x) = \begin{cases} \frac{17}{200}, & 1 \leq x < 5, \\ \frac{17}{100}, & 5 \leq x < 7, \\ \frac{8}{175}, & 7 \leq x < 14, \\ 0, & \text{else.} \end{cases}$$

Find the expected value of Y and round your answer to two decimal places.

$E(Y) =$

Figure 7: This Is Another Example Of The Advanced Mathematical Course, One Of The Probability Theory.

Figure 7 presents an example out of the probability theory. The task is the calculation of the expected value of a continuous random variable. This is a very important and common value of the probability theory.

The last example of the advanced mathematical course is one of the chapter vector analysis, shown in figure 8. The students receive a certain function and have to determine the value of the path integral.

Question:

The function f is given as
 $f(x, y) = 5 + 4x - 3y - 6x^2 + 7y^2$.

Evaluate the fixed point of f :

Calculate the Hessian of f in this point

The fixed point is a
 saddle point minimum maximum

Figure 8: This Is Another Example For The Advanced Mathematical Course, One Out Of Probability Theory.

5. SUMMARY AND OUTLOOK

On the left side of the figure 9 the results of the test at the beginning of the refresher course are shown. As already mentioned the students take the test in the first exercise of the refresher course in September before the regular semester starts. The results of the first test of the course Mathematics 1 for electrical engineers are found on the right side. It is remarkable that all the marks enhanced enormously. The refresher course recreates the mathematical basics required for further

mathematical lectures and, as one can see in figure 1, really increases their mathematical skills. Additionally most of the students of electrical engineering attend the refresher course, so they are used to the Maple T.A. system at the beginning of the mathematical course.

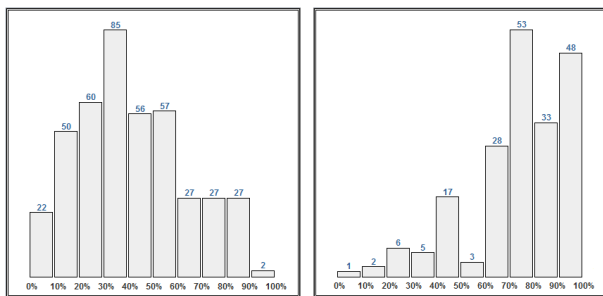


Figure 9: Compares The First Test At The Beginning Of The Refresher Course And The First Test Of Mathematics 1.

The refresher course helps the students to get back their lost mathematical knowledge. In every single technical study mathematic is the basic for all further lectures. Therefore it is very important that the students are aware of all the calculation skills without thinking a lot about it so they can focus on the real challenges of the given problems. With the help of Maple T.A. the students can control their increased skills and can practise also after the end of the courses with immediate feedback from Maple T.A. about the correctness of their calculations.

Figure 10 confirms the gain of mathematical knowledge and shows that the students don't have any big problems handling the e-learning system.

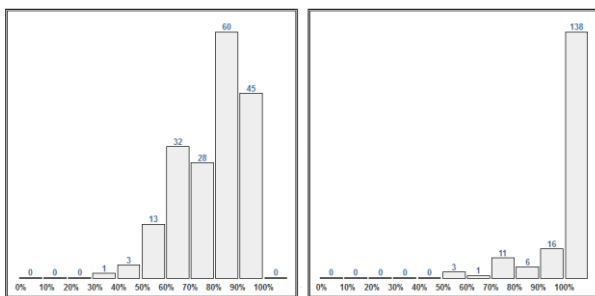


Figure 10: The Two Tests Of The Advanced Mathematical Courses, Left Side – 1st Test And Right Side – 2nd Test.

To put it all in a nutshell the Institute for Analysis and Scientific Computing initiated Maple T.A. to comfort administrators, tutors and students as well. On the one hand it is a time-saving invention for the tutors and lecturers. It eases the creation of the questionnaire which helps students to follow the course by exercising with the examples. The administration and organisation of tests as well as the lecture exam is easier with the support of this e-learning system.

On the other hand the students have the possibility of practicing with immediate control at any time. The obligatory tests should help the students to improve

their numeracy. In the exercise course the students can ask the tutors about incomprehensibilities of the lecture, the examples of Maple T.A. and the examples of the exercises as well. Therefore every student gets any help possible if he uses it. After some primary troubles with the grading of the Maple T.A. system the most important achievement of the improvement concerning the grading routine is a great acceptance by the students.

In the next semester the goal will be the invention of a course for modelling and simulation. Also enlarging and improving the questionnaire of Maple T.A. are important tasks for the next semester.

REFERENCES

- A. Körner, S. Winkler, V. Urbonaite: E-Learning Einsatz im Auffrischkurs Mathematik an der TU Wien, 2011, *4th International eLBA Science Conference*, 145-154.
- A. Körner, S. Winkler, A. Zimmermann, F. Breitenecker, 2009 *Blended-Learning mit Maple T.A. in der Lehre für Mathematik und Modellbildung*, 20th Symposium Simulation Techniques, 62-64.
- A. Zimmermann, V. Urbonaite, A. Körner, S. Winkler, S. Krause, M. Kleinert, *Advanced Randomization and Grading in the E-Learning System Maple T.A.*, EUROSIM 2010 - 7th Congress on Modelling and Simulation, S. 1209 - 1214

MODELLING AND SIMULATION E-LEARNING SET OF HYDRAULIC MODELS

M. Bicher^(a), U. Fitsch^(b), M. Atanasijević-Kunc^(c), N. Nagele^(d), W. Wild^(e), F. Breitenecker^(f)

^{(a),(b),(d),(e),(f)} Vienna University of Technology, Institute of Analysis and Scientific Computing, Austria

^(c) University of Ljubljana, Faculty of Electrical Engineering, Slovenia

^(a) martin.bicher@tuwien.ac.at, ^(b) ursula.fitsch@tuwien.ac.at, ^(c) maja.atanasijevic@fe.uni-lj.si, ^(d) nagele@asc.tuwien.ac.at,
^(e) wild@asc.tuwien.ac.at, ^(f) fbreiten@osiris.tuwien.ac.at

ABSTRACT

As providing e-learning opportunities for students is getting more and more important, the so called MMT system provides a user-friendly online modelling and simulation laboratory. Here a course consisting of a set of experiments is shown to give an example how e-learning can be used in a modern way. A series of tank experiments is used, each of them with different difficulties and increasing complexity, to teach modelling and simulation in fluid dynamics.

Keywords: fluid dynamics, e-learning, MMT, hydraulic, MATLAB, tank

1. INTRODUCTION

Teaching modelling and simulation especially to students who are not permanently confronted with the topic is always a challenge. On the one hand, reasonable models are often too difficult to present them in detail, either for mathematical reasons, lack of programming skills or timing problems. On the other hand presenting a simulation for simplified problems, which cannot be used directly in reality, causes students to suggest, that modelling is a rather theoretical part of science and underestimate the value of good simulations and the complexity and dangers involved.

Thus as a part of the Bologna study a collaborating group of researchers from the University of Ljubljana and the Vienna University of Technology assembled a constructive, well organized e-learning course consisting of a set of high quality simulation models. The course was assembled taking into account the following main ideas:

1. The complexity of the examples is increasing during the course.
2. The examples are strongly related and constructive.
3. Each example deals with different important questions about modelling and simulation.
4. The course can be taught to different fields of study.
5. The examples are available to each student taking part in the course on an internet platform.

6. Students can experiment with the models at home.
7. All students interested in this topic can take part in the course independent from their already existing programming skills.

Especially point 6 and 7 are usually inconsistent or at least hard to manage, so therefore the Vienna University of Technology uses the so called MMT system for teaching, testing and e-learning purposes.

2. MMT SYSTEM

The MMT system - "Mathematics, Modelling and Tools" - is a MATLAB based online simulation platform which provides a user-friendly environment on the one hand for lecturers, who need to present simulation examples in their course, on the other hand for students, who want to experiment with well implemented models at home.

The platform was created in a collaboration between the Drahtwarenhandlung (DWH) and the Vienna University of Technology for many different purposes:

- As an e-learning opportunity for students
- As a virtual modelling and simulation laboratory
- To extend MATLAB, SIMULINK and even JAVA and ANYLOGIC programming skills by downloading and modifying source codes
- As an environment for presentations and lectures
- As a supporting platform for tests and exams
- As a place where well implemented simulation examples by advanced students e.g. for their bachelor or diploma thesis finally get to a good use.

So far about 300 different modelling and simulation examples have been loaded up to the server and the number is steadily increasing. Therefore it is getting more and more difficult for lecturers to find the most appropriate assembly of examples for their course. Thus the upload of a single model or an idealess mix of simulation examples to the server is not enough. A well structured educational aim, e.g. as the one we defined in

the last section, is required to help lecturers taking the correct choice without getting intimidated by the whole variety of the MMT server.

The following set of models shall give an example of how a course can be arranged according to the above mentioned ideas and how the MMT system can be used to assist the lecturer.

3. THE THREE TANK MODEL

The process shown in Figure 1, is located at the Faculty of Electrical Engineering, University of Ljubljana, and consists of three cylindrical plexiglas tanks connected with pipes which can smoothly be closed or opened by valves.

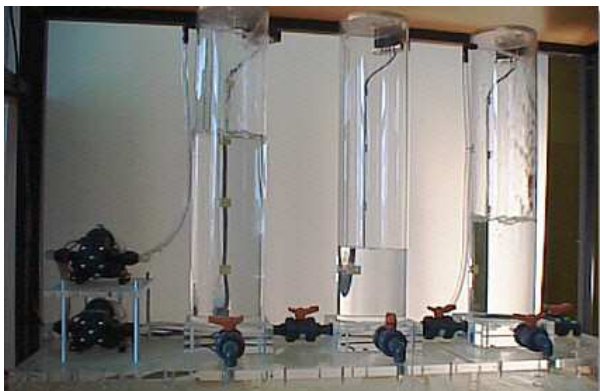


Figure 1: Photograph Of The Process

When water is pumped into the first or the third of the three tanks, assuming that at least those two valves necessary for the flux between the tanks are open, the system complies to the laws of communicating vessels and is thus highly non-linear. Regarding that a model of the whole process is very complex and might be too difficult to explain it is useful to separate the problem.

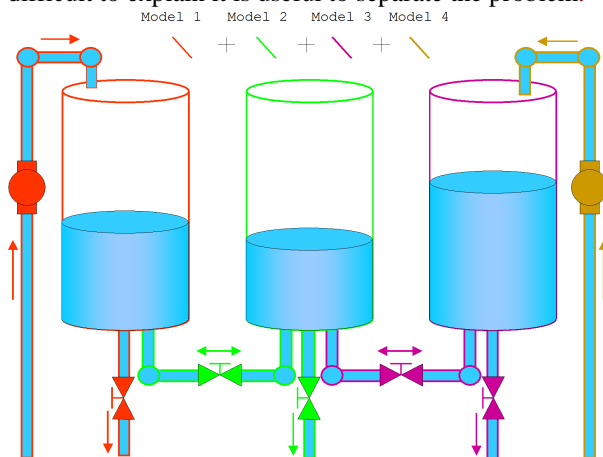


Figure 2: Partition Of The Model

As indicated in Figure 2 the system can be partitioned, hence providing a better understanding of the different subsystems of the tank. The different models discussed later on in the paper are marked in different colours.

3.1. One Tank Model

The easiest model to deal with is defined if the valve, connecting tank one and two, is closed. Though this is a simple first order system it is still non-linear and thus surely a challenge to students inexperienced in modelling. A dynamic model can be found if the relation between the flux into the tank to the derivation of volume and the relation between filling level to the speed of the streaming out liquid are combined:

$$\Phi_{in}(t) - \Phi_{out}(t) = \frac{dV(t)}{dt} = S \frac{dh_1(t)}{dt}$$

$$C\sqrt{2gh_1(t)} = v_{out} = \frac{1}{A}\Phi_{out}(t)$$

In these formulas S donates the cross section area of the cylindrical tank g defines the gravitational acceleration and A donates the cross section area of the valve. The second formula is called Torricelli's Law for water streaming out of a vessel and is a consequence of the famous Bernoulli equation for fluid dynamics. The constant C (close to one) depends on the liquid and on the form of the opening. The resulting non-linear first order differential equation is:

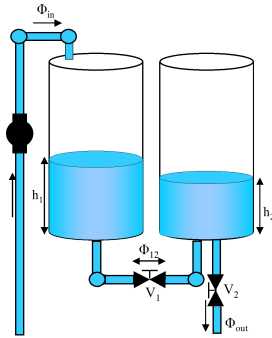
$$\frac{dh_1(t)}{dt} = \frac{\Phi_{in}(t) - C_{V_1}\sqrt{h_1(t)}}{S}, C_{V_1} = AC\sqrt{2g}$$

The following topics are interesting to deal with in a lecture:

- Physical derivation (Torricelli's Law)
- Valve opening \leftrightarrow flux of water (empty tank \leftrightarrow spilling over)
- Linearised model
- Comparison with MATLAB's own *linmod()* function
- Transfer function modelling
- Experimenting equilibrium states with the MMT system
- Experimenting with different kinds of input functions (unsteady, steady, smooth) to the pump
- Comparison to real measured data from the process in Ljubljana (Experiment parameters of the simulation at the MMT system)
- Comparison between measured parameters and theoretical calculated parameters (friction, turbulences, incompressible liquid)
- Controlling e.g. by PID (and other) controller

3.2. Two Tank Model

Adding the second tank leads to a second order system which raises additional issues. First of all linearisation leads to a two dimensional Taylor series expansion which is a really good repetition to students lacking of basic math skills. Also it becomes a little bit more



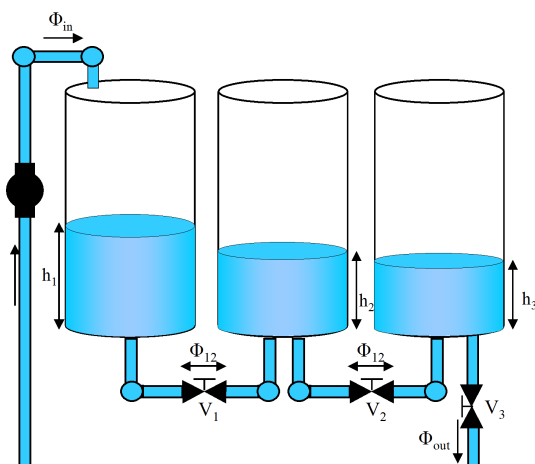
difficult for students to determine steady states, on the one hand due to an unsteady signum function and on the other hand due to the definition of the working point regarding the degrees of freedom. From the physical point of view the determination of the differential equations needs a little bit extension because the flux between the two vessels has to be calculated. The problem can be solved using Bernoulli's equation. This leads to the following system of coupled differential equations:

$$\frac{d}{dt} \begin{pmatrix} h_1 \\ h_2 \end{pmatrix} = \begin{pmatrix} \frac{\Phi_{in} - \text{sgn}(h_1 - h_2) C_{V_1} \sqrt{|h_1 - h_2|}}{S} \\ \frac{\text{sgn}(h_1 - h_2) C_{V_1} \sqrt{|h_1 - h_2|} - C_{V_2} \sqrt{h_2}}{S} \end{pmatrix}$$

Because liquid can pass the valve in both directions the signum function is important here. The following points are taken into account.

- Physical derivation of flux between communicating vessels (Bernoulli's principle, Torricelli's law)
- Calculation of linearised models in form of state-space and transfer function models
- Experimenting with valve openings at the MMT system
- Tuning of the controller
- Difference between SISO and MIMO problems

3.3. Three Tank Models – SISO



Adding the third tank leads to a third order system but is still a SISO problem. The differential equations are quite similar to the two tank system:

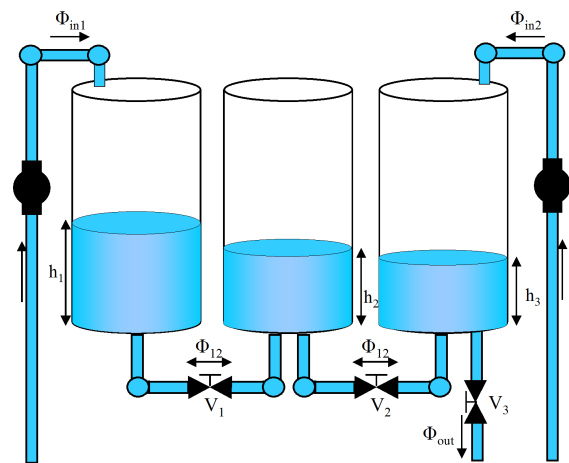
$$\frac{d}{dt} \begin{pmatrix} h_1 \\ h_2 \\ h_3 \end{pmatrix} = \begin{pmatrix} \frac{\Phi_{in} - C_{V_1} \sqrt{|h_1 - h_2|}}{S} \\ \frac{C_{V_1} \sqrt{|h_1 - h_2|} - C_{V_2} \sqrt{h_2 - h_3}}{S} \\ \frac{C_{V_2} \sqrt{h_2 - h_3} - C_{V_3} \sqrt{h_3}}{S} \end{pmatrix}$$

(The signum functions are not shown here)

Due to the fact that the third equation does not depend on h_1 the extension of the two tank model to this third order model is extremely easy. This model can be a perfect example that regarding the modelling point of view a higher order does not always increase the complexity of the problem as the SIMULINK model of the non-linear model needs only to be extended by an additional loop. But the controller needs to be modified and linearisation is getting slightly more difficult. The following points are dealt with.

- Calculate linearised models
- Modification of the controller
- Why is the system SISO

3.4. Three Tank Model – MIMO



In the fourth model the second pump is activated and causes a second input parameter. As a result the system suddenly becomes MIMO and requires completely different controlling. It is important to use and discuss the second degree of freedom which grants that not one but two of the three filling levels can be controlled at once and that there are different options to do so. On the one hand two independent SISO controllers can be used, on the other hand there are several options for really difficult multivariate controllers too. The corresponding differential equation system is:

$$\frac{d}{dt} \begin{pmatrix} h_1 \\ h_2 \\ h_3 \end{pmatrix} = \begin{pmatrix} \frac{\Phi_{in1} - C_{V1} \sqrt{|h_1 - h_2|}}{S} \\ \frac{C_{V1} \sqrt{|h_1 - h_2|} - C_{V2} \sqrt{h_2 - h_3}}{S} \\ \frac{\Phi_{in2} + C_{V2} \sqrt{h_2 - h_3} - C_{V3} \sqrt{h_3}}{S} \end{pmatrix}$$

Model 4 is the most frequently used and simulated experiment also in Ljubljana. Therefore exists a great number of real measurement data from the actual plant. So the comparisons of the simulation to the measurements can be performed at the MMT system which can be a real deal for students which are solely used to deal with theoretical models. Discussing and extending Model 4 and the possibilities for controllers is the final target of the course.

- Comparisons between linearised and non-linear model
- Comparison of different controllers at the MMT system
- Create a linearised model
- Comparison to real measured data at the MMT system
- Experimenting with controller parameters

3.5. Model Summary

Each of the four discussed models has its own special properties and raises additional questions. A short summary is given in the following table.

Model	Order	Type	Controller
One Tank	1	SISO	SISO
Two Tank	2	SISO	SISO
Three Tank	3	SISO	SISO
Three Tank + 2 nd pump	3	MIMO	MIMO/SISO

Table 1: Summary Of The Models

4. RESULTS

4.1. Main Pages

The following screenshot (Figure 3) shows the main page of the course at the MMT system.

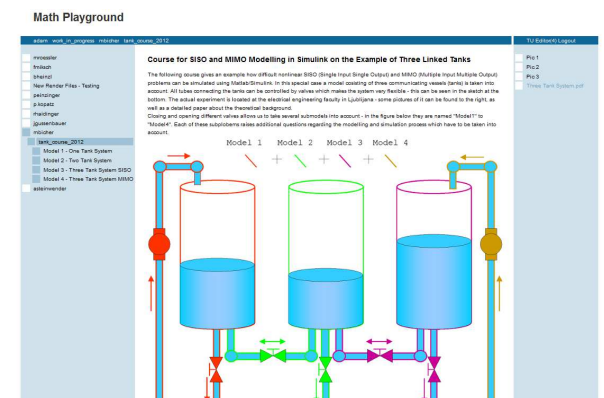


Figure 3: Main Page Of The Course

The area at the left side of the picture respectively of the “Adam-Riese Math Playground”, as the MMT server is called, shows the links to the four model sections with each containing several targeted examples dealing with the already discussed points. It can be seen here, that the MMT system is built up strictly hierarchically using a structure similar to LaTeX:

1. Book
2. Chapter
3. Section
4. Subsection

In this case the whole course constitutes a chapter and the four sub-models are created as sections with each containing several subsection examples.

The centre area of the page contains a first raw explanation for the main topic and the goal of the course and the well known sketch of the three tanks. Due to a LaTeX environment provided by the MMT server also formulas can be included into this part of the page (see Figure 5). As the graphical environment of the page is detailed and colourful, it can also be used instead of slides for an introduction to the course.

The right hand area of the page represents a download section. Files like slides, PDF-files, pictures etc. can additionally be loaded up to the server and offered for download at this area. The links at the main page of this course offer three photographs of the original plant in Ljubljana and a paper containing detailed theoretical information about the system and how to derivate a simulation model.

Using the links in the left hand area lead to the main pages of each sub-model containing more detailed information about each experiment like a sketch of the physical derivation and a short introduction to the different subsection examples.

4.2. Linearisation Examples

Understanding the usage and creation of linearised models poses an important aim of the course. Often linearisation and especially the role of working point and equilibrium state are misinterpreted and used in a wrong way (a correct interpretation can be found in Figure 4).

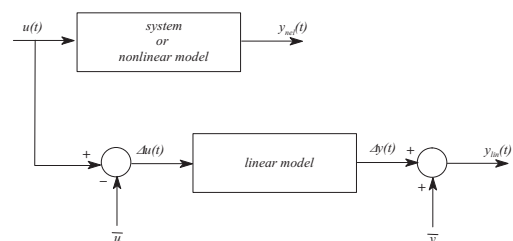


Figure 4: Interpretation Of A Linearised Model

In case of the three tank system, in which all of the differential equations have square-root characteristics and linearisation is not possible or, at least, very bad close to the origin, this is even more important. Figure 5 shows an example of how the process deriving a linearised model could be trained at the example of the one tank system.

The example deals with the calculation of the correct parameters for the linear state space model at a certain working point h_0 :

$$\frac{dh}{dt} = \frac{\Phi_{in} - C\sqrt{h}}{S} \Rightarrow \dot{x} = Ax + Bu$$

So first of all the equilibrium state has to be calculated and afterwards, Taylor series expansion leads to A and B . The calculated parameters can be compared to MATLAB's own $linmod()$ function.

The function $[A,B,C,D]=linmod(Mdl, Wp, Displ)$ calculates the linearised State Space model

$$\dot{x} = Ax + Bu$$

$$y = Cx + Du$$

out of the, usually non-linear, model Mdl at working point Wp with input displacement $Displ$.

As the experiment requires to calculate the correct parameters the user has to put them into the textboxes and press the "ok" button. Doing this, MATLAB is started and the content of the boxes is used as input parameters for a MATLAB function. This function starts SIMULINK, deals with the results and performs the final plots. In this case (Figure 5) the choice for the three input parameters was, taking the output curves compared to the $linmod()$ function into account, not perfectly correct.

As the improvement of MATLAB and SIMULINK programming skills is also a target of the MMT server usage, the links to all source files can be found at the right hand side. As all MATLAB codes also the SIMULINK models can be downloaded in text form (which can easily be converted to the classic .mdl-surface again by just saving the file as "filename".mdl).

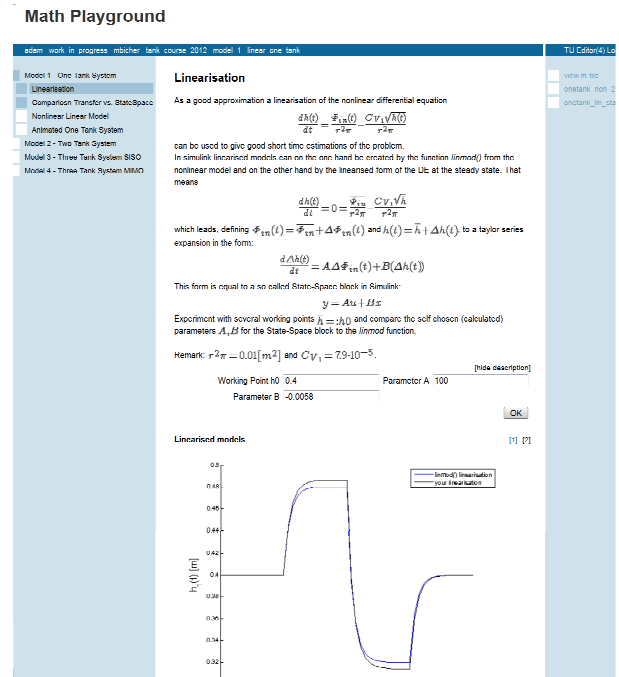


Figure 5: Linearised One Tank model

At the right hand side directly above the figure of the two graphs, a small "<1>" and "<2>" button indicates that there is a second figure available. Switching to the second figure, the graph for the input function (flux into the tank), in this case, a sum of rectangular functions, can be seen. So the MMT server supports multiple output figures represented by a slideshow.

4.3. Non-linear examples

In an example of section "Model 4" several input functions can be tested and the results of the non-linear model is compared to the results of the linearisation. (Indicated in Figure 6)

As there is a choice between a sine-cosine wave function, a sum of rectangular functions (shown in the plot in Figure 6), a sum of sigmoid functions and a pulse of triangular functions, the user can compare the results of steady and unsteady input functions. Because the working points in tank 1 and tank 3 can manually be chosen by the user, comparisons between the non-linear model and the linearisation can also be performed. The plot in Figure 6 shows the results of the non-linear and the linearised model if a sum of rectangular input functions, respectively an unsteady changing but otherwise constant influx into both tanks (one and three), is used.

Playground

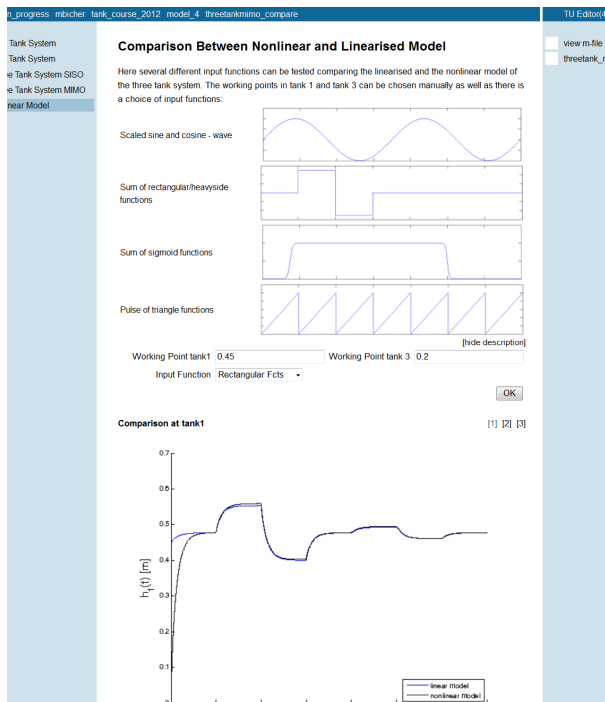


Figure 6: Comparison Between Non-Linear And Linear Three Tank Model Simulation At Tank 1

4.4. Animated examples

As an additional bonus to the graphical plots, the MMT server also supports animated output figures created in MATLAB. In case of the tank system, the scientific value of these examples might not be very high, but they can be used to encourage students and improve the quality of lectures. An example is shown in Figure 7.

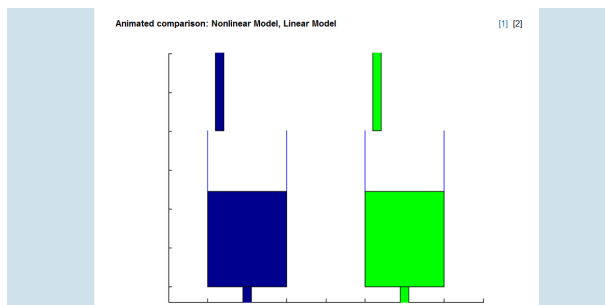


Figure 7: Animated Comparison Between Linear And Non-Linear One-Tank Model

In the animation the water-levels change proportional to the calculated simulation results. A series of plots is used to create a so called animated-“.gif” by a function supported directly in MATLAB.

SUMMARY AND FURTHER DEVELOPMENT

The assembled set of models shall give an example of how flexible the MMT server is used in modelling and simulation lectures as well as in tests or exams.

But yet many developments extending the course are planned too. On the one hand a whole variety of multivariate controllers opens up a very difficult topic

for advanced students e.g. examples dealing with parameterisation of different MIMO controllers and comparisons between them. On the other hand, the University of Ljubljana does studies dealing with remote control of real experiments. Thus the MMT could be used to collect measured data from Ljubljana which could directly be used for model comparisons at the server.

However it has to be kept in mind that none of the mentioned points necessarily require MATLAB or SIMULINK programming skills, hence encouraging students to deal with MATLAB and SIMULINK as the MMT system provides great flexibility. This work has been realized in the context of the ‘Applied Modelling Simulation And Decision Making’ project and funded by means of the City of Vienna by the ZIT GmbH - The Technology Agency of the City of Vienna, a subsidiary of the Vienna Business Agency.

REFERENCES

- Atanasijević-Kunc M., Logar V., Karba R., Papič M., Kos, A. *Remote multivariable control design using a competition game*. IEEE Trans. Ed., Feb. 2011, Vol. 54, No. 1, 97-103.
- Logar V., Atanasijević-Kunc M., Karba R., Papič M., Bešter J. *E-learning game using virtual and remote laboratory environment*. In: Preprints of the 6th Vienna Conference on Mathematical Modelling, 2009, Vienna University of Technology, Austria. MATHMOD Vienna 09 : proceedings, (ARGESIM Report, no. 35). Vienna: ARGESIM, cop. 2009, 2100-2105.
- Körner A., Hafner I, Bicher M., Winkler S., Breitenacker F. *MMT- A Web Environment for Education in Mathematical Modelling and Simulation*, ASIM 2011.
- Winkler S., Körner A., Hafner I. *MMT - A web-based e-learning System for Mathematics, Modeling and Simulation using MATLAB*, In: Preprints of EUROSIM Congress, Prague, Czech Republic, 2010, paper 231.

AUTHORS BIOGRAPHY

Martin Bicher, born 12.05.1988, is currently writing his diploma thesis at the Vienna University of Technology about Agent-Based modelling. He is a member of the ARGESIM Master College and in this position one of the main administrators of the MMT server, responsible for Tuwel (Moodle) based e-learning and math tutor for electrical engineering students. He is currently living in Vienna and this is his second paper.

A MODULAR ARCHITECTURE FOR MODELLING OBESITY IN INHOMOGENEOUS POPULATIONS IN AUSTRIA WITH SYSTEM DYNAMICS – FIRST STEP: A POPULATIONMODEL AND HOW TO INTEGRATE IT IN A DISEASEMODEL

Barbara Glock^(a), Patrick Einzinger^(b), Felix Breiteneker^(c)

^{(a), (c)}Vienna University of Technology, Institute for Analysis and Scientific Computing, Vienna, Austria

^(b)dwh Simulation Services, Vienna, Austria

^(a)barbara.glock@drahtwarenhandlung.at, ^(b)patrick.einzinger@drahtwarenhandlung.at, ^(c)felix.breiteneker@tuwien.ac.at

ABSTRACT

When it comes to modeling diseases with inhomogeneous populations a modular setup can be useful, because specific parts of the model can be easily exchanged or altered. We propose a modular setup consisting of a population model and a separate disease model, which interact on a specifically defined interface. After that an economic cost model can be built and integrated into the modular setup. Aim of this work is to build a population model, in this case with Austrian data, and to define the interface with the disease model, in this case an obesity model. Obesity has become a major problem in Austria. According to (Rieder 2006), over 30% of the Austrian population is overweight and over 9% is obese, resulting in over 227.7 million euro health care costs in 2004.

Keywords: Modular Modeling, Obesity, System Dynamics, Population Model

1. INTRODUCTION

Obesity, defined as the presence of excess adipose tissue, is a health concern of paramount importance in Austria and also worldwide. Next to the long list of comorbidities associated with obesity, like pulmonary disease, coronary heart disease, diabetes mellitus type 2, orthopedic problems, hypertension, etc. obesity is a great cost factor for health care systems because of weight reduction medications, hospitalizations, laboratory costs, inability to work, loss of productivity, early death, pain and reduced quality of life (Dieterle 2006).

A System Dynamics model for the prevalence of obesity in Austria is needed to show the trend of the prevalence of obesity in the next few years and decades, to identify the most important influences on the disease and to test possible political strategies preventing and treating obesity. The usage of System Dynamics is due to a better overview for non-experts and easier administration for the modeler.

Because of the fact that the model will show the prevalence of obesity in the population over at least the next 50 years, a population model, predicting the change of the Austrian population dependent on births,

deaths and migration is necessary. How this affects the population is seen in figure 1. In Austria especially migration is very important, because without it the population would be reduced significantly due to low birth rates.



Figure 1: The Growth Of The Population Is Dependent On Births And Immigration. The Contraction Of The Population is Dependent On Deaths And Emigration.

In this paper we demonstrate why those parts of the model, especially the population model and the disease model, should be independent and therefore a modular setup, as seen in figure 2, is important and how it is done, first by explaining the structure of the disease model and in more detail the structure of the population model and by defining the points of intersection of those two models. Advantages and disadvantages of this modular setup will be discussed too.

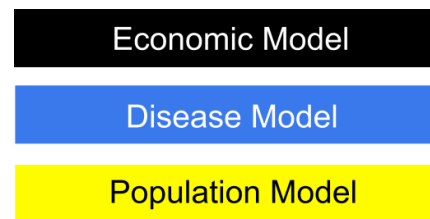


Figure 2: A Modular Setup Of the Simulation Model. An Independent Population Model Is The Basis, Connected Through Defined Points Of Intersection With The Disease Model. Furthermore An Economic Model Can Be Built Individually Based On The Disease Model.

2. THE METHOD: SYSTEM DYNAMICS

The modeling method used for all parts of the whole model is called System Dynamics and was developed in 1956 by Jay W. Forrester (Forrester 1961). It is a top down modeling method, where aggregated states are

looked at and not individuals. For example all male persons aged 15-45 could form a single state, but also all male overweight persons aged 15-45. System Dynamics is a commonly used approach to understand the behavior of complex systems. It is different to other approaches because it allows the usage of feedback loops, which, due to the fact that this is a very descriptive modeling method - easily to be overviewed by non-experts - can be better understood and researched. Sometimes a specific state of the system has an effect (feedback) on itself over (a long) time, which is not recognized easily (Sterman 2000).

Especially the disease model for the prevalence of obesity requires feedback loops, to represent the main influence factors on obesity and how they are influenced in return. An example of a possible reinforcing feedback loop, represented in a *causal loop diagram*, can be seen in figure 3.

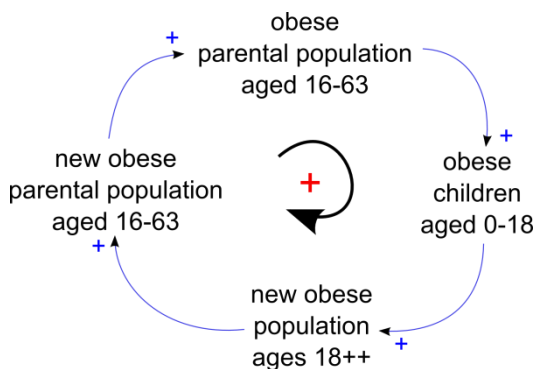


Figure 3: A Causal Loop Diagram Of A Simple Feedback Loop Of the Disease Model.

It shows that the fraction of the obese population, who are parents, has a positive feedback on itself over time: The more obese parents there are, the more obese children they will get, by passing their eating habits on to their children. Therefore the fraction of the obese adult population will increase and also the fraction of the obese parents. Linkages are shown by the blue arrows. A plus-sign represents a proportional effect from quantity at the arrows end to the quantity of the arrows top, as described before.

These causal loop diagrams are a useful tool for developing a model. A System Dynamics model consists of three main elements, described as following and also seen in figure 4:

- *Stocks* describe the state of the system in each time step. They are represented as rectangles.
- *Parameters* are constants.
- *Auxiliaries* are mostly used for mathematical formulas combining stocks and parameters. Special auxiliaries are *flows*, which describe the changes of stocks. Flows are only allowed between two stocks or from a *source* (represents systems of levels outside the boundary of the model) to a stock or from a

stock into a *sink* (where flows terminate outside of the system)

Furthermore most System Dynamics Simulators provide a great number of tools, like delay functions, table functions etc. to allow an easier administration of the modelling process.

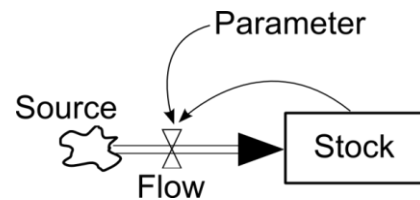


Figure 4: A Simple System Dynamics Stock And Flow Structure With One Parameter And a Source. The Stock Could Represent The Population And The Inflow Births. The Parameter Could Be The Birthrate Depended On The Actual Size Of The Population.

Mathematically System Dynamics models are systems of differential equations with a given simulation time t and initial conditions for the simulation start at t_0 . Each stock represents a single equation. The mathematical formulas for the simple stock and flow structure for time t from figure 4 are shown in equation 1 and 2:

$$Stock(t) = \int Flow(t) dt + Stock(t_0) \quad (1)$$

$$Flow(t) = Parameter \cdot Stock(t - 1) \quad (2)$$

The integral for the stock from equation 1 can be transformed into a differential equation, describing the net change of the stock as seen in equation 3.

$$\dot{Stock}(t) = + Flow(t) \quad (3)$$

When building a system dynamics model, the modeler does not need to know exactly how differential equations work or how they are solved, because the modeling device is graphical and the model can simply be built by dragging and dropping stocks, flows, parameters and auxiliaries onto the main user interface.

3. THE OBESITY DISEASE MODEL

First the main structure of the disease model needs to be discussed shortly. Before starting to build the actual model we specify the research questions as following:

- What are the main factors that influence body weight? As a result: How is the obese (resp. normal-weight and overweight) fraction going to develop in the population?
- What can be changed (after identifying the main influences) and more important what is the effect of those changes in the obese (resp.

normal-weight and overweight) population compared to the costs?

Overweight and obesity are defined as abnormal or excessive fat accumulation that may impair health (WHO 2000). Obesity is measured by the so call *Body Mass Index* (BMI), which is calculated by dividing body mass m (in kg) through the square of body height l (in meters) as shown in equation 4 and categorized as seen in table 1.

$$BMI = \frac{m}{l^2} \quad (4)$$

Table 1: BMI classification: The BMI is divided into 4 main categories of weight classification for adults (WHO 2000).

Classification	BMI
underweight	<18.50
normal weight	18.50 – 24.99
overweight	25.00 – 29.99
obese	≥ 30.00

Furthermore the changes in body weight, and therefore in the BMI are also dependent on the age and sex of the person. For example the basal metabolic rate is different for different ages and also for different gender. Knowing this, we can start to identify the stocks of the System Dynamics disease model: The population is divided by the severity-degree of the disease, age and sex. The idea of this partitioning seen in figure 5 is adapted from Homer et al. (Homer 2006), with the difference that we do not need 100 one-year age-classes, but 12 aggregated five- to ten-year age-classes (except age 0, which is a one-year age-class because of the high infant mortality), because we want to get a look on the trend in general and the main influences on obesity.

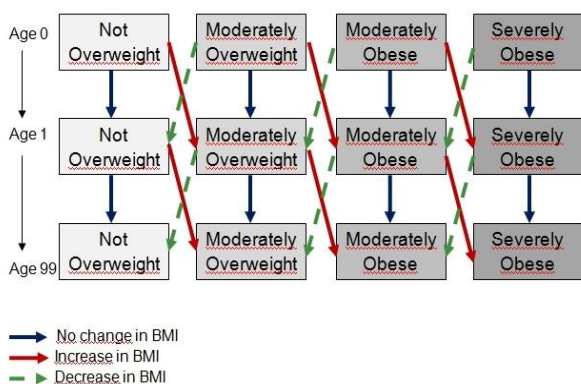


Figure 5: Partitioning Of The Population In The Disease Model (Homer 2006). Persons Of The Same Age, Sex And Severity Degree Of The Disease Build A Separate Stock.

The reasons of crossing over into another BMI-category – which in our model can also be within one age-class, because for example in a 10-year age-class a person can significantly reduce or gain weight – are due to physical activity (caloric expenditure) and eating habits (caloric intake), but they will not be discussed in this paper.

Data is available for the years 1999 and 2006/07 for the partitioning of the population by gender, some age-classes and the four severity degrees of obesity seen in figure 5.

4. THE POPULATION MODEL

As mentioned before the main parts that influence the change of the population are births, deaths and migration. Figure 6 shows the population model as a causal loop diagram. The black loops in the center of such a circle with blue arrows show the polarity of the corresponding feedback loop. A positive feedback portrays a self-reinforcing process, for example: the more people live, the more births will occur and therefore the more people will live in the future. The opposite is a negative feedback loop, or also called a balancing loop, that stabilizes the system. For example: the more people live, the more deaths will occur and the fewer people will live in the future.

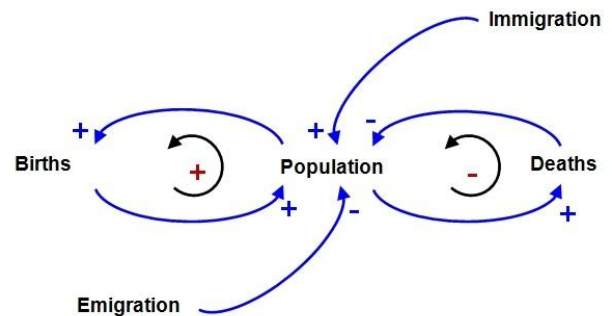


Figure 6: Causal Loop Diagram Of The Population Model Showing The Causal Links And Dependencies Of Variables.

4.1. Available Data

For the partitioning of the population as seen in table 2 data from Statistics Austria (Statistics Austria Database 2012) is available.

The simulation starts in 1999, because for the disease model data is only available since 1999, so the initial partitioning of the population is for this specific year. Due to the fact that migration is not dependent on the population, real data for the years 1999 until 2010 for immigration and emigration (with same partitioning as the population) is also taken from Statistics Austria Database (Statistics Austria Database 2012). The simulation will run 50 years. Therefore the migration data for the next 50 years has to be provided too and a prognosis for immigration and emigration is available in the database, but only for different sexes. To get the partitioning for the age-classes, the distribution of the previous known years is taken, averaged, and assigned to the upcoming years.

Table 2: Partitioning Of The Population By Age And Sex

Age-classes	Sex
Age 0	male
Age 1- 4	female
Age 5 – 9	
Age 10 – 14	
Age 15 – 19	
Age 20 – 24	
Age 25 – 34	
Age 35 – 44	
Age 45 – 54	
Age 55 - 64	
Age 65 – 74	
Age 75+	

The death rate is given for the known years, but for the years from 2010 until 2060 the predicted trend of the life expectancy, which increases by the years and was also taken from Statistics Austria Database (Statistics Austria Database 2012), was used together with a *Weibull* distribution to calculate the death rates for the upcoming years.

Due to the fact that fertility rates did not change significantly over time they were assumed to be constant for the next years as those from 1999. Statistics Austria (Statistics Austria 2011) provides the number of live births per 1000 women per year for the four relevant age-classes in which women can bear a child, namely 15 – 19, 20 – 24, 25 – 34 and 35 – 44. These probabilities $p(i)$, $i=1,2,3,4$, meaning the number of live born singletons divided by 1000 for each of the i age-classes, have to be transformed into rates $r(i)$ as seen in equation 5.

$$r(i) = \ln(1 + p(i)) \quad (5)$$

The aging-rates are calculated to $1/groupsiz$ e for each age-class and sex, where *groupsiz*e is the length of the interval of the age-class.

Furthermore all rates have to have the same, according to the simulation time step, right dimension, in this case months.

4.2. Implementation of the model

The population model is implemented in Anylogic® University 6.5.0 and can be seen in figure 7.

For a better overview and the fact that similar equations and a lot more arrows are saved to be built AnyLogic provides arrays. As seen in figure 5, there would be 12 (for aggregated age-classes) x 2 (for sex) = 24 stocks for the population, but as seen in figure 7, there is only one stock, called *Population*. An array is a container with linear storage of fixed size, called dimension. In this case it is a 2x12 array and holds the 24 entries of the partitioned population. Since the population in general is not the important part of the

model, it is “hidden” in one stock and helps non-experts to understand the model better.

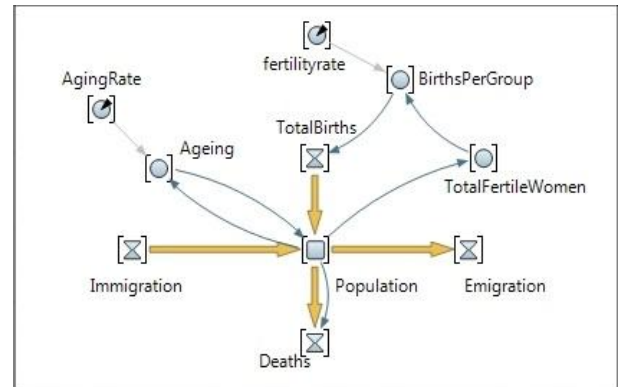


Figure 7: Population Model In Anylogic® University 6.5.0.

Furthermore there are 4 flows, which change the stock (in each dimension of the array). A function provides the input for immigration and emigration and they are not dependent on the population. Two auxiliaries *TotalFertileWomen* and *BirthsPerGroup* are used – also for better overview and understanding, because formally they could be integrated in the equations for *TotalBirths* – in each dimension of the array. *TotalFertileWoman* copies the entries from *Population* that are representative for the fertile women in the previously mentioned four relevant age-classes. *BirthsPerGroup* stores in each time step t the number of total births (male and female together) per age-group of fertile women as calculated in equation 6.

$$\begin{aligned} BirthsPerGroup[FertileWomen](t) \\ = TotalFertileWomen[FertileWomen](t) \\ \cdot fertilityrate[FertileWomen](t) \end{aligned} \quad (6)$$

FertileWomen in the brackets represent the dimension of a sub array from the array for population, which in this case is a 4x1 array for females in the four relevant age-classes of fertile women.

The auxiliary *Ageing* stores the number of people (in each index of the dimension of the array) that cross over into the next age-class within the next time step, which is calculated as seen in equation 7.

$$\begin{aligned} Ageing[Age, Gender](t) \\ = Population[Age, Gender](t) \\ \cdot AgingRate[Age, Gender](t) \end{aligned} \quad (7)$$

Age represents the dimensions of the 12 age-classes and *Gender* represents the dimensions of the two sexes.

The mathematical formulas behind the stock *Population* are stated in equation 8, 9 and 10. Because of the fact that new born enter the population at age 0, there is a separate equation (9) for the first age-class,

including births. And because of the fact that once a person has arrived in the last age-class, he/she stays there or dies, there is a separate equation (10) for the last age-class.

$$\begin{aligned} & \frac{dPopulation[AgeAllBut0_11, Gender]}{dt} \\ &= Immigartion[AgeAllBut0_11, Gender](t) \\ &- Emmigration[AgeAllBut0_11, Gender](t) \\ &- Deaths[AgeAllBut0_11, Gender](t) \\ &+ Aging[AgeAllBut0_11 - 1, Gender](t) \\ &- Aging[AgeAllBut0_11, Gender](t) \end{aligned} \quad (8)$$

$$\begin{aligned} & \frac{dPopulation[Age0, Gender]}{dt} \\ &= Immigartion[Age0, Gender](t) \\ &- Emmigration[Age0, Gender](t) \\ &- Deaths[Age0, Gender](t) \\ &+ Births[Age0, Gender](t) \\ &- Aging[Age0, Gender](t) \end{aligned} \quad (9)$$

$$\begin{aligned} & \frac{dPopulation[Age11, Gender]}{dt} \\ &= Immigartion[Age11, Gender](t) \\ &- Emmigration[Age11, Gender](t) \\ &- Deaths[Age11, Gender](t) \\ &+ Births[Age11, Gender](t) \\ &- Aging[Age11, Gender](t) \end{aligned} \quad (10)$$

The equation for the two flows (one for female newborns entering the population and one for male newborns entering the population) of the *TotalBirths* flow from figure 7 is simply the sum of all births from the *BirthsPerGroup* auxiliary. It is assumed that of all newborns 49% are female and 51% are male.

At last the formula for the flow *Deaths* from figure 7 is calculated as seen in equation 11.

$$\begin{aligned} & Deaths[Age, Gender](t) \\ &= Population[Age, Gender](t) \\ &\cdot Mortality_Function[Age, Gender](t) \end{aligned} \quad (11)$$

Mortality_Function is a function that represents the time dependent, Weibull-fitted mortality rates as mentioned before and is not seen in figure 7.

5. DEFINING POINTS OF INTERSECTION WITH THE DISEASE MODEL

The changes in the stock of the population model (in each age- and sex-class) are calculated continuously. The disease model has the same partitioning concerning age- and sex-classes (also with arrays for sex and age), but is furthermore divided by severity-degrees of the disease (in this case each BMI-category has a separate stock graphically). Therefore an additional auxiliary *PopulationChange*, which is also an array variable with dimensions *Gender* and *Age* as in the population model, receives the changes in the population from the population model continuously as seen in figure 8. The

changes are calculated by the net migration (immigration minus emigration) and the changes within the stock *Population* (Ageing). In the disease model there are flows, as seen in figure 5, from one severity degree to another one, and also from one age-class to the next. The *PopulationChange* affects the flows from one age-class to the next of the disease model, but has to be split up for the different severity degrees for each (Age, Gender)-array-entry. As a result for each severity degree (and (Age, Gender)-array-entry) an additional flow is implemented that calculates the corresponding change by taking into account the current size of the stock and the current size of the part of the population from the population model.

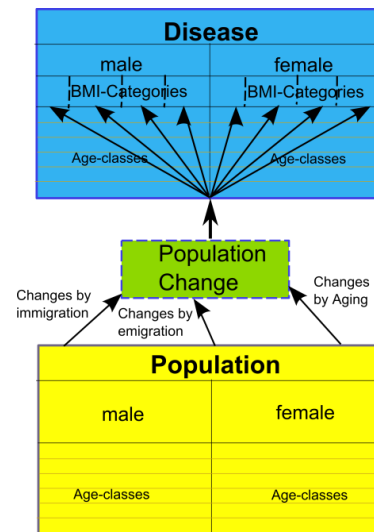


Figure 8: Auxiliary *PopulationChange* is implemented, which has the same structure (dimensions) as *Population*. It stores in each time step the changes of the stocks “hidden” in *Population* and transfers them to the disease model, by splitting them up into BMI-categories.

The equation for the flow *ChangeOverweight*, which calculates the changes within the overweight population (again: the stock *overweight* is an array with dimension *Age* and *Gender* and therefore the calculation is made separately for each entry of this 2x12) is seen in equation 12.

$$\begin{aligned} & ChangeOverweight[Age, Gender](t) \\ &= \frac{PopulationChange[Age, Gender](t) \cdot Overweight[Age, Gender](t)}{Population[Age, Gender](t)} \end{aligned} \quad (12)$$

The changes for the other BMI-Categories are analogue.

This technique leads to some assumptions, which are discussed in the following.

5.1. Assumptions for the disease model

There are some assumptions concerning the points of intersection:

- Obesity (resp. the other BMI-categories) among persons who enter the system of the population model through immigration (resp. exit the system through emigration) is considered equally distributed as in the main population.
- Obesity (resp. the other BMI-categories) among deaths is considered to be distributed as it is in the main population. Obesity-related deaths are not considered here separately.

5.2. Advantages and disadvantages of a modular setup

Keeping in mind that the model should include a separate cost model for calculating the costs assigned to obesity (e.g. costs for hospitalizations, medications, or even surgery as for example gastric banding), we need to research the conditions (concerning the BMI) on which such medications are prescribed or surgeries are done. The evidence based guidelines of the Austrian society for obesity-surgery (Miller 2005) suggest performing surgery only with a BMI > 40 or with BMI > 35 and additional obesity-related co-morbidities, like hypertension or diabetes mellitus type 2. Therefore the classification of “obese” can be split into 3 more categories as seen in table 3.

Table 3: BMI Classification Of The Obese Category: The Obese Can Be Separated Into 4 More Categories For Adults (WHO 2000).

obese	BMI
obese class I	30.00 – 34.99
obese class II	35.00 – 39.99
obese class III	≥ 40.00

The advantages of a modular set up are, that if one wants to change the disease model afterwards, because of new or altered research questions, only the disease model (but with the same assumptions from chapter 5.1.) needs to be altered. In this case, the obese fraction needs to be split up in three stocks and initialized again and no new mortality rates, fertility rates or migration data have to be calculated again.

Furthermore the population model can be used in another disease model where this partitioning of the population is used. If the partitioning of the age-classes is not needed in so much detail, the classes only have to be aggregated.

For some diseases people develop co-morbidities, which result in higher costs for health care systems. The modular setup allows an easy change or integration of additional stocks for people with co-morbidities without changing the population model.

Furthermore an easier change of the population, by changing the rates and initial conditions, can be done, if one wants to calculate the prevalence, costs etc. for another population.

Tests with the separate parts of the model can be done to look for failures more easily.

A disadvantage of this setup is that disease-related fertility rates and mortality rates cannot be tested or modeled.

6. CONCLUSION

A modular structure can be more understandable, especially for non-mathematicians, when they look at two separate models, one concerning the population and the other one concerning the disease. Secondly the modular parts are easily exchangeable, for example if the disease model shall simulate a different kind of disease, with different severity degrees, but the same population. This increases the reusability of models.

REFERENCES

- Dieterle, C., Landgraf, R., 2006. *Folgeerkrankungen und Komplikationen der Adipositas*. Internist (2). 141-149.
- Forrester, J., 1961. *Industrial Dynamics*. Cambridge, MA. ISBN: 9780915299881
- Homer, J., Milstein, B., Dietz, W., Buchner, D., Majestic, E., 2006. *Obesity Population Dynamics: Exploring Historical growth and Plausible Futures in the U.S.*. 24th International System Dynamics Conference, Nijmegen. Available from: <http://www.systemdynamics.org/conferences/2006/proceed/papers/HOMER141.pdf> [Accessed 14 May 2012].
- Miller, K., 2005. *Chirurgische Therapie der Adipositas. Evidenz Basierte Leitlinien der Österreichischen Gesellschaft für Adipositas-Chirurgie*.
- Rieder, A., 2006. *Erster Österreichischer Adipositasbericht 2006*. Altern mit Zukunft. 28-58.
- Statistics Austria, 2011. <http://www.statistik.at> [Accessed December 2011]
- Statistics Austria Database, 2012. <http://sdb.statistik.at/superwebguest/login.do?guest=guest&db=debevstpr> og. [Accessed 24 January 2012].
- Sterman, J.D., 2000. *Business Dynamics - Systems Thinking and Modeling for a Complex World*. McGraw-Hill Companies. USA.
- WHO, 2000. *Obesity: Preventing and Managing the Global Epidemic*. WHO Technical Report Series 894 – Part 1. Geneva. ISBN: 924120894

AUTHORS BIOGRAPHY

Barbara Glock. She was born in Vienna on 5th of March, 1984, started school in 1990 and passed with distinction 2002 from secondary school. After that, she studied Technical Mathematics in Computer Sciences, which she will finish in the end of 2012. Her recent work includes her diploma thesis about a System Dynamics Modeling approach of the prevalence of obesity in Austria.

DATA INDEPENDENT MODEL STRUCTURE FOR SIMULATION WITHIN THE VIENNA UT MORESPACE PROJECT

Benjamin Rozsenich^(a), Salah Alkilani^(b), Martin Bruckner^(c), Štefan Emrich^(d), Gabriel Wurzer^(e)

^{(a)(b)} Institute for Analysis and Scientific Computing, Vienna UT, Austria

^(c) dwh GmbH - Simulation Services, Vienna, Austria

^(d) Chair of Real Estate Development and Management, Vienna UT, Austria

^(e) Digital Architecture and Planning, Institute of Architectural Sciences, Vienna UT, Austria

^{(a)(b)(d)(e)} {benjamin.rozsenich|salah.alkilani|stefan.emrich|gabriel.wurzer}@tuwien.ac.at

^(c) martin.bruckner@drahtwarenhandlung.at

ABSTRACT

The Institute for Analysis and Scientific Computing at Vienna University of Technology (Vienna UT) has created models to simulate lecture room reservations, in order to test strategies for increasing the efficiency of utilisation, increasing booking fairness and perceived capacity without need to add more lecture rooms. Thus, the produced system had to satisfy some tough constraints: (1.) It had to be flexible and multifunctional, meaning that a dynamic code structure was needed so that program logic could depend on the imported data, but simulation algorithms would stay data-independent. (2.) The presentation logic had to be customized to fit the usability needs of the client, who would perform the simulation experiments himself. To report on both programming techniques and architectural decisions that enabled us to achieve these constraints is thus the main goal of this paper.

Keywords: customization, simulation, software architecture

1. INTRODUCTION AND OVERVIEW

For the past years, researchers over various institutions of Vienna UT have been working together on a project that optimises utilisation of lecture rooms, by performing simulations on booking requests instead of having them reserved in a ‘first-come-first-served’ fashion. Together with dwh Simulation Services, this has led to the production of the novel simulation suite, on whose development this paper focuses.

During the initial steps of developing a new simulation, much effort has to be devoted to the correctness of algorithms. Two models had to be produced (see “Simulation Core”, Section 2):

- a *scheduling model*, which performs static scheduling based on a set of heuristic rules (Section 2.1)
- a *pedestrian dynamics model*, which performs physical simulation of students moving within the built environment, according to their lecture timetable (Section 2.2).

Producing a working simulation core is necessary, but not sufficient for a piece of software to become a product (see Section 3, “Building MoreSpace”):

- *Data import and export* have to be tailored to the customer's needs, e.g. reading from and writing to databases that already exist. As a matter of fact, this interfacing aspect becomes a software in its own right, which needs to be written and supported specifically for the client in question (3.1, “Input/Output configuration”).
- Orchestration of the simulation core's algorithms, given the often-changing demands and requirements of the client, can be seen as yet another required task. On the one hand, this means producing code that will call upon the pre-existing algorithms in an order that produces seemingly special-tailored simulations. On the other hand, such models need to have a user interface that meets the requirements of the (not necessarily technically skilled) simulation user. What is thus required is a rather non-technical step in which an analyst *customises* the software so that the inputs needed, simulations performed, and outputs generated clearly reflect what the customer has in mind (3.2, “Simulation customization”).
- Once simulation results have been gained, *analysis* over what scenario gives the best performance has to begin (3.3, “Analysis”). There is, however, no absolute best - only alternative solutions that have to be weighted by the simulation user, according to practicability in implementation. We provide a set of visualisation views, intended for in-depth analysis and justification. The latter aspect is most important when a single result has to be selected and exported for use in a production system on which thousands of users rely (in our case: the reservation system of Vienna UT).

As a side-note for this paper, we wish to state that related work is given directly within the narrative. Additional material is to be found at the end of the paper (see Section 4), before the conclusion (Section 5).

2. SIMULATION CORE

The core of our simulation consists of two models that assign lectures to lecture rooms and let students simulate their would-be passages through the built environment, given the assigned lecture locations and per-term timetables. Both models are implemented in Java, and packed as Java libraries that ship with the application. Changes in the simulation core are thus only possible by using application updates, and only if they affect all clients (not individual customers). For the sake of completeness, we now describe the two models used in some detail:

2.1. Scheduling model

The scheduling model has the task of filling predefined slots, each one measuring half an hour and being within given lecture room of finite capacity, with lectures. In a pre-step, so-called booking requests have to be generated by Vienna UT's reservation system, each one stating *when*, *how long* a room of *what capacity* is needed in which building (*location*), given what *special equipment*. The scheduler then arranges the lectures so as to satisfy one of its implemented constraints, which we give here in simplified form:

- *Greedy scheduling*. Capacity, equipment and location of the booking request have to be satisfied exactly when finding a slot.
- *Tolerant scheduling*. The capacity of the booked room may be more (but not less) than the requested capacity, furthermore, the booker can be tolerant concerning the location.

An additional parameter controls whether the scheduler can *shift* lectures by half an hour plus and minus, in order to see whether the result becomes any better. The same goes for *splitting*, i.e. using multiple rooms for the same event, in case the booking request requires a capacity beyond available rooms.

In all cases, the result of the booking process is a number of successfully booked requests plus any leftover requests that require some (manual) work.

2.2. Pedestrian dynamics model

This model calculates the time that students need to change lecture rooms (see Figure 1). In detail, what is computed are the trails of each virtual student, given his/her timetable as input. This transition between different lecture rooms is governed by three layers of increasing complexity: The movement is calculated with reference to a physical model by (Blue and Adler 2001). Above that, route choice and movement along a circulative network is computed by using graph algorithms, quite similar to (Tabak 2009; Tabak, de Vries and Dijkstra 2010; Wurzer 2011). At the highest level, individual behaviour is governed by the timetable of lectures to visit. If there is more than one lecture that

takes place in an instant, the student's probability of changing rooms is taken into account. This aspect could also be called a fourth layer, that of individual choice or preference. Extended work on this route choice, specifically for urban environments, has been done by (Dijkstra, Jessurun, Timmermans and de Vries 2011). More details on the used pedestrian model can also be found in (Bruckner, Tauböck, Popper, Emrich, Rozsenich and Alkilani 2012; Bruckner 2009).

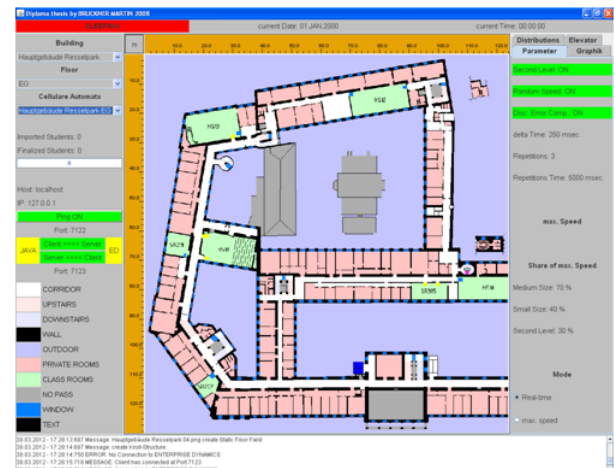


Figure 1: Pedestrian dynamics model

3. BUILDING MORESPACE

The product which we have designed, called MoreSpace, is a platform that glues different simulation algorithms together by making use of a common scripting platform (Rhino for Java). Conceptually, one might think of a common data structure (coined quite paradoxically as *'the data independent model'*) existing as a database and a sequence of simulation algorithms acting on it. The following sections describe, in detail, the setup and workflow connecting the different components of our system, whose reusable and extensible architecture is the main contribution we would like to share. An overview of this workflow is also given in Figure 2:

1. External data stores hold the customer-specific data, which is converted to our data independent model upon import (see Section 3.1).
2. Simulation algorithms acting on our data structure are producing results within the same database (see Section 3.2).
3. These are visualised, in order to select one specific result that fits the end user by whatever criteria he/she sees fit (see Section 3.3).
4. Additional simulation types, such as dynamic simulation using pedestrian dynamics models, can also be incorporated into a post step, if they would take too long to compute to be practical for every simulation run.
5. The export process then records the chosen result as selected by the user, which it then

writes to a data store defined by the client. This might be the same as during import, or a different one (again see Section 3.1).

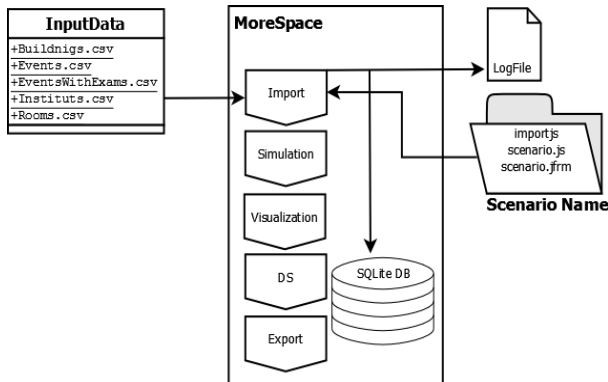


Figure 2: Workflow and outline of MoreSpace App

3.1. Input/Output configuration

Even though our application can have a different user interface and simulation setup for each customer, we rely on a data structure that is static and common to all installations. Once filled, the different simulation models perform their work on this structure, and save their results back into it. We employ the popular SQLite database together with an Object/Relational mapping tool (Apache Cayenne) for this purpose, giving each part of the application easy access to our entities (booking request, space, booked slot, etc.).

The complexity of the import/export process lies in the details of the (external) data stores, whose merging and querying has proved to be a consulting problem of its own. For us, the same application must be able to be used at any university, e.g. the Technical University of Vienna but also in other companies - each having an own data storage type available (e.g. Excel, database, XML). Before being able to simulate, we thus need to import booking requests from whatever source available into our common data structure. The same procedure will be required reverse upon export of the simulation results, either into the same data store or into a different one.

Usually, transformations of data structures are handled by special Extraction/Transformation/Loading (ETL) software packages. We have chosen a different approach, by defining the customer-specific import and export script in Rhino that does the necessary steps, tightly integrated into the application (File>Import and File>Export option). We also have a user interface intended at filtering and selecting data from this external data store so that it fits the scope of the simulation project.

3.2. Simulation customisation

A booking product such as ours must deliver a *project-specific* output, and thus requires also a project specific setup which we call *customisation*. Such a specially tailored approach is not new – it is used e.g. in accounting software (SAP ERP), Hospital Information

Systems and further products that are not by definition finished ‘off the shelf’. Simulation models have been and continue to be an example of such software, being highly specific to the customer and scenario in mind. We extend this notion by introducing a platform in which simulation can be used, i.e. glue between pre-existing models and the customer-specific setup, which is yet unprecedented to the best of our knowledge. In detail, we are using three essential concepts throughout our application:

- *Scenario*: a named sequence of invocations of a variety of simulation and algorithms which has a specially defined user interface where one can define inputs that are not hardcoded but rather given as parameters. Colloquially, each scenario stands for a given problem complex which is due to be analysed.
- *Experiment*: a specific choice of parameters for a given scenario. This scenario can contain several experiments, but at least one (the default experiment having default parameters).
- *Result*: the effect of an invocation of an experiment. Every result is reproducible by using the defined parameters and settings of the experiment again. In this case, the already existing data is overwritten. If two experiment runs with the same parameters are to be compared nevertheless (e.g. for validation), one must duplicate the experiment.

Each scenario is represented by a Rhino script, which invokes all the necessary simulation algorithms iteratively. Multiple simulation runs and aggregation are handled here, as well. As a general rule, scripts do not act directly on the database: They rather call upon algorithms, which load data, compute, and write back into the database, using the experiment ID as conceptual key for the result.

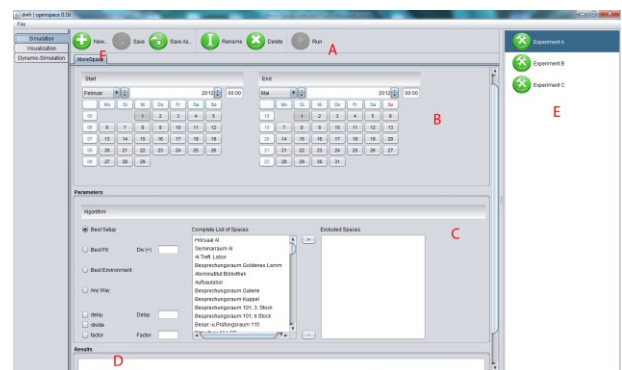


Figure 3: MoreSpace Graphical User Interface. (A) Experiment toolbar for creating and running experiments, (B) filter and (C) parameterisation user interface loaded for each scenario (D) experiment run output console (E) result panel (F) scenario selector.

Each scenario also has a graphical user interface that is dynamic and has been defined to suit the client’s needs (also refer to Figure 3). We employ the Abeille Forms designer for that purpose, which outputs XML that can

be read back to construct Java Swing panels using the jGoodies forms library.

Semantically, a scenario user interface is always divided into two parts: the *filtering part* (Figure 3B) for selecting the data on which the simulation acts, and the *parameter part*, where one can set input data (Figure 3C). Using the experiment toolbar (Figure 3A), one can then create experiments and run them, producing results under the results panel (Figure 3E) and summary console (Figure 3D). This process can be repeated for every scenario that is defined (each being represented by a tab, as in Figure 3F).

3.3. Analysis

Without proper interpretation, the results produced during by the simulation remain useless. Therefore, our application has a visualization dashboard (see Figure 4) in which the produced results can be reviewed and compared by the client or analysts acting on his behalf.

The actual visualisation types used are currently bar charts, line charts, Gantt charts (see Figure 5) and histograms, in both single-experiment and multi-experiment layouts. Each visualisation window retains its position and state even if the program is closed. This enables analysts to show why a certain result was chosen without having to perform data analysis in front of the client.

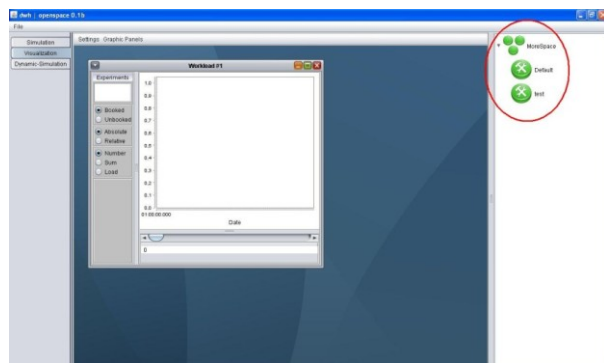


Figure 4: Visualisation dashboard for interpretation of results (circled).

3.4. Summary and big picture

Having presented the core as well as different components of the application, we may now begin to summarise and compact what has been said. One of the interesting aspects of the program, which applies well beyond the borders of our software, is the ability to initialise itself with a completely new user interface and simulation logic specially customised to the client. This means that the system is changing its nature without affecting a single line of java code of the core (which would require recompilation). Technically, this is done by bundling a set of scripts and user interface definitions together with the program, which we read that the programs start.

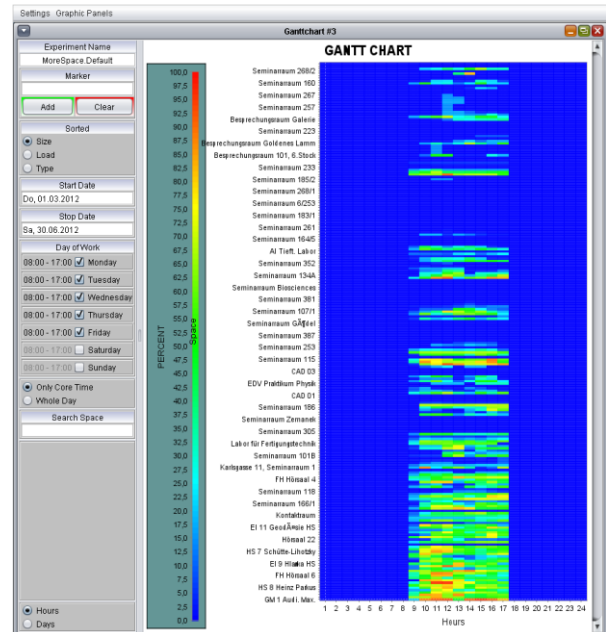


Figure 5: Example resultset visualized as Gantt chart.

In detail, we proceed as follows:

- For every scenario, there must exist a scenario script ('scenario.js') as well as filter ('filter.jfrm') and scenario user interface definition ('gui.jfrm') in a folder having the scenario name.
- Furthermore, we define to special folders containing the same files by the name of 'Importer' and 'Exporter', which contain the logic and user interface necessary for interfacing to the client's data infrastructure.

On start-up, the application knows only how to browse through a set of folders, instantiating scenarios (tabs) and importer/exporter (File>Import and Export) as it goes along. When it has finished doing so, the user is presented with a specially tailored application that is not only customised in its function, but also in language and terminology used. Updates to the functional core are kept at a minimum - what is changed lies mostly in the orchestration part (i.e. scripts), to be elaborated together with the client. The product is thus the executable artefact that incorporates the core library, while everything else belongs to the domain of a project.

3.4.1. Additional implementation notes

Some additional notes given here, although not important for the general picture, might be beneficial when developing a similar application:

- The data structures used for storing experiments and results sacrifice functionality for ease of implementation: One experiment may only have zero or one results. If an experiment has no result (i.e. it is new), its parameters may be updated. In all other cases, the experiment is said to be fixed - no alterations can be made, since that would corrupt the result data. One may, however,

duplicating an experiment (using a Save As.. option), in which case the parameter settings are copied to a new experiment which can be altered.

- The scenarios have a caveat as well: During import, we allocate a special scenario 'Scenario 0' containing a predefined 'Result 0', which is the result of a *manual assignment* of lectures to rooms. This Result 0 of Scenario 0 may not be overwritten; it may only be used for comparison with the actually simulated results.
- Another caveat concerns to input data; should these change, all experiment runs are obsolete. Therefore, a re-import is only possible in order to add data, not for update. Should this be desired, the current database has to be archived and reset (i.e. cleared). This also happens once data has been exported, in order to be ready for another simulation period.

4. BACKGROUND AND RELATED WORK

Our system operates according to the Model-View-Controller (MVC) concept (refer to Figure 6): *Model* objects are the parts of the application that implement the logic for the application's data domain. *Views* are the components that display the application's User Interface (UI). The UI is created using the model data as input. *Controllers* are the components that handle user interaction and update the model (Shelly 2005).

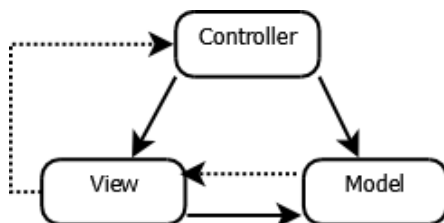


Figure 6: MVC

We take the notion of MVC one step further: Our model is a database with a static structure. The model itself has a delegate which we have called *Importer*, which maps from customer specific data sources to this format. The view and the controller are both put inside the scenario scripts, which are essentially client specific. The meaning of this reflects our project experience in dealing with customisation: a large part of the logic is special tailored and cannot be reused. Instead, we see it all customised called as being yet another delegate to the model, intended for rapid development and (if need arises) redevelopment.

Another topic of which we are well aware is that our base technology *scripting* has large issues with debugging. The used Rhino is an exception here, since there is the excellent Rhino debugger (Oliver and Boyd 2012) that can be utilised. Rhino itself is a Java implementation of JavaScript bundled with the Java Platform, therefore being widely available without additional installation.

Coming to the related work, we are not aware of any approach is similar to our 'glue code scripting' / rapid user interface development technique. It is certainly true that, for example, Anylogic (Borshchev and Filippov 2003) offers a similar experience when coding using the simulation's core library. However, Anylogic is using Java - a compiled language. Thus, customisation can only happen to very limited extent, off-site, where all the development tools are installed. Furthermore, the user interface tools given are very limited, non-scriptable.

As a second contrast point, the application area of Anylogic's core is currently concentrating on ABM, SD, DES. This is certainly an advantage: Functionality exists and can be readily used. At the same time, such closed and pre-existing Application Programmer's Interfaces (APIs) also have a drawback - extending them further might be very complicated, since the source is not available. We are thus taking pure Java as basis, aiming at optimal control of the employed algorithms and source availability rather than functional superiority. The latter may be achieved by incorporating code from a variety of open-source packages such as NetLogo (Wilensky 1999), or put differently: "*An open architecture allows developers to design systems that are made up of many small functional modules interconnected by a common software interface*" (Roschelle, DeLaura and Kaput 1996).

From a development perspective, combining Java and JavaScript also enables new forms of working together among distinct roles: A developer, can implement the core functions of software while a customizer or analyst oversees the design of the application by scripting (*Separation of Concerns*).

5. CONCLUSION

We have presented a simulation called MoreSpace, that is designed to be dynamic in its appearance and in relation to how simulation algorithms are employed. Upon bootstrapping itself, the application looks for specially-named script files together with user interface definitions, which it then goes on to interpret and display. Data is dynamically loaded from proprietary sources into its own common data structure serving all simulation models, which are orchestrated within the script files. Such a high degree of customisation has previously only been found in Enterprise Resource Planning (ERP) and healthcare IT, which is why we see our efforts as being important not only for our application, but also in the light of the ongoing modularisation that modelling packages embrace nowadays.

REFERENCES

- Blue, V.J., Adler, J.L., 2001. Cellular automata microsimulation for modeling bi-directional pedestrian walkways. *Transportation Research Part B* 35 (2001), 293-312.
- Borshchev, A., Filippov, A., 2003. *From System Dynamics and Discrete Event to Practical Agent*

Based Modeling: Reasons, Techniques, Tools. *Proceedings of the 22nd International Conference of the System Dynamics Society*.

- Bruckner, M., 2009. *Modeling of pedestrian dynamics in the university operation using cellular automata in the programming language JAVA*, Master Thesis, Vienna UT.
- Bruckner, M., Tauböck, S., Popper, N., Emrich, Š., Rozsenich, B., Alkilani, S., 2012. A combined Cellular Automata and DEVS simulation, MathMod 2012 Full Paper Preprint Volume, Argesim Report S38, Available from: http://seth.asc.tuwien.ac.at/proc12/full_paper/Contribution356.pdf [accessed 1st June 2012]
- Dijkstra, J., Jessurun, A.J., Timmermans, H.J.P., de Vries, B., 2011. A Framework for Processing Agent-Based Pedestrian Activity Simulations in Shopping Environments, *Cybernetics and Systems*, 42 (7), 526-545.
- Oliver, C., Boyd, N., 2012, Rhino Debugger, Available from: <http://www.mozilla.org/rhino/debugger.html> [accessed 1st June 2012]
- Roschelle, J., DeLaura, R., Kaput, J., 1996. Scriptable Applications: Implementing Open Architectures In Learning Technology, *Proceedings of Ed-Media 96 - World Conference on Educational Multimedia and Hypermedia*, 599-604.
- Tabak, V., de Vries, B., Dijkstra, J., 2010. Simulation and validation of human movement in building spaces, *Environment and Planning B: Planning and Design*, 37 (4), 592-609.
- Tabak, V., 2009, *User Simulation of Space Utilisation*, PhD Thesis, TU Eindhoven.
- Wilensky, U., 1999. Netlogo, Available from: <http://ccl.northwestern.edu/netlogo> [accessed 1st June 2012]
- Wurzer, G., 2011. *Prozessvisualisierung in der Krankenhausplanung*, PhD Thesis, Vienna UT.

AUTHORS BIOGRAPHY

Benjamin Rozsenich got his master degree in medical computer science from Vienna UT in 2010, finishing with his diploma thesis ‘Statistical module of the tumor documentation system "HNOOncoNet" based on JBoss Seam and Hibernate concepts’ for the Vienna General Hospital (AKH Wien). For the Morespace Project, he has been active as lead developer and technical architect, a job which he now continues in the private sector.

Salah Alkilani has a Bachelor in Software Engineering from Vienna UT. During the MoreSpace project, he has been working on the static scheduler, in which topic he has also published first papers. He is also involved in lecturing for the Afro-Asiatic Institute of Vienna

University on the impact of the Arabic spring and the role of Islam in society.

Martin Bruckner studied mathematics at Vienna UT, receiving his master in 2009. His work on ‘Modeling of pedestrian dynamics in the university operation using cellular automata in the programming language JAVA’ has been used in the pedestrian simulation of the MoreSpace project, and beyond, for his PhD thesis that is currently under preparation. He currently works for drahtwarenhandlung simulation services, the company participating in the MoreSpace project.

Štefan Emrich has a master degree in mathematics (2007), where he was focusing on prediction of influenza epidemics using cellular automata and agent based systems in a comparative manner. After his degree, he went on to ETH Zurich, where he was involved in research on modelling workforce and workflow management. Returning to Vienna, he began his PhD on ‘Simulation for Space Management’ in the Real Estate Department of the Faculty of Architecture, in which function he also participated in the MoreSpace project. He is author of numerous articles on evaluation of usage in buildings, and was awarded the Austrian Construction Prize (Baupreis) in the category “best junior scientist” in the year 2011.

Gabriel Wurzer earned his Ph. D. degree in Process Visualization and Simulation for Hospital Planning from Vienna University of Technology in 2011. His research in architectural sciences focuses on tool support for early-stage planning of complex buildings, with regular contributions to both Pedestrian and Evacuation Dynamics conference (PED) and the Education and Research in Computer Aided Architectural Design in Europe conference (eCAADe), from which he was awarded the Ivan Petrovic Prize in 2009. He is also an active researcher in archaeological simulation, together with the Natural History Museum Vienna.

ABOUT THE INTEGRATION OF SIMULINK INTO THE MATLAB-BASED SIMULATION AND EXPERIMENT SERVER MMT

A. Körner^(a), I. Hafner^(b), M. Bicher^(c), S. Winkler^(d), U. Fitsch^(e)

Vienna University of Technology
Institute for Analysis and Scientific Computing
Wiedner Hauptstraße 8-10
1040 Vienna

^(a) andreas.koerner@tuwien.ac.at, ^(b) irene.hafner@tuwien.ac.at ^(c) martin.bicher@tuwien.ac.at
^(d) stefanie.winkler@tuwien.ac.at ^(e) ursula.fitsch@tuwien.ac.at

ABSTRACT

At the Vienna University of Technology, Institute for Analysis and Scientific Computing, the Research Group for Mathematical Modelling uses the MMT-Server for teaching mathematical modelling.

MMT stands for Mathematics, Modelling and Tools. It is based on and a PHP interface, which is responsible for input and output of parameters and results. Most of the currently existing examples on the MMT systems are simulated with MATLAB.

As MATLAB is used for interactive experiments on this server, it's nearby to integrate Simulink as a second simulator in order to have the possibility to compare different modelling approaches. Simulink differs from MATLAB due to its graphical description of models by signal flow graphs.

Simulink works with linear and non-linear time-continuous and time-discrete systems. Therefore, specifications of Laplace- and z-transformations from linear system theory as well as solvers for ordinary differential equations of non-linear systems are available.

Keywords: Simulink, MATLAB, E-learning, Simulation, Mathematical Modelling.

1. BUILD-UP OF THE MMT-SERVER

The existing user interface of the current MMT-Server is illustrated in Figure 1. It is working with examples implemented in MATLAB.

On the left side, there is the Experiment Layer, which organises the structure of the experiments. A higher level denotes a subject out of mathematical modelling and a lower level represents experiments in different scenarios.

In the centre of the user interface, which is the main window, a precise briefing of the actual experiment is given.

The Experiment Description window below shows which parameter should be changed and gives an impression of the expected results.

The right side consists of Files and Source Code and is the important one regarding the experiment's implementation in MATLAB, because the links to the m-files are available there. Users can download these files to learn more about how to program in MATLAB and they can also tune and change the code to experiment with other scenarios.

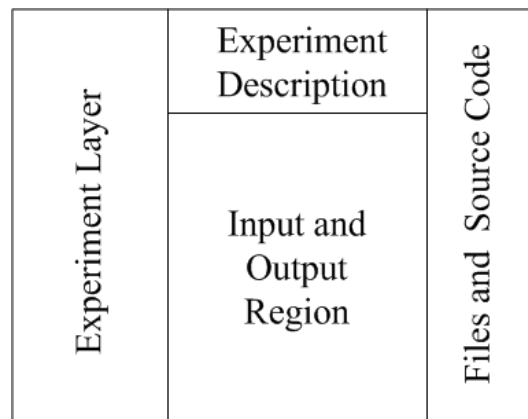


Figure 1: User interface of MMT-Server

The input and output region offers the possibility to enter model and/or simulation parameter. These parameters are available as a string in the MATLAB code, stored in the `instruct.varN` variable. `N` denotes the number of the variable which is assigned from the PHP-based input field in the input region. The `instruct` variable is transformed into a MATLAB variable

```
K = str2double(instruct.var1).
```

After this conversion, the MATLAB specific code follows.

At the end of the MATLAB code, a section for graphical output is offered. Ordinary plots are handled by the system and are displayed in the output region.

The following example illustrates the visual nature of an example or experiment on the MMT-server. Let's observe a mathematical pendulum, described by the ordinary differential equation

$$m \cdot l \cdot \ddot{\varphi}(t) = -m \cdot g \cdot \sin(\varphi(t)) - l \cdot d \cdot \dot{\varphi}(t).$$

l denotes the length of the pendulum, d the damping coefficient and φ is considered as $\varphi(0) \in (-\frac{\pi}{2}, \frac{\pi}{2})$ and the beginning velocity $\dot{\varphi}(0)$ can be chosen. The corresponding look of the example on the MMT-server is shown in Figure 2.

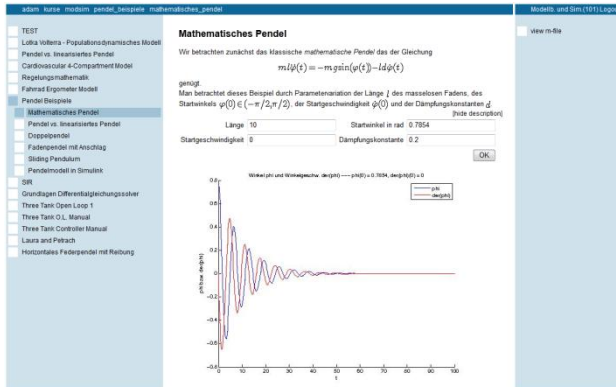


Figure 2: Front-end of MMT-server example of the mathematical pendulum

This structure is important for the integration of Simulink, because Simulink examples on the MMT-server work in the same way focused on the front-end.

2. SIMULINK AT THE MMT-SERVER

To allow comparisons between two or more different simulators, it is necessary to implement more than only MATLAB on the MMT-server. The fact that Simulink is MATLAB-based allows including Simulink on the MMT-server with minimal effort.

2.1. Mathematical description of Simulink Models

A signal flow graph is defined by an oriented graph $G_w = (V, E, w)$, where V is the set of nodes, E is the set of edges and w is a mapping

$$w: E \rightarrow \mathbb{R}_0^+,$$

which relates each edge with a real positive number, the so-called weight of this edge. Furthermore μ defines a mapping

$$\mu: V \rightarrow L^2(\mathbb{R}_0^+),$$

which maps each node to a signal of the signal space $L^2(\mathbb{R}_0^+)$. The mapping w operates along the edge $e_j = \langle v_j, v_l \rangle \in E$ according to

$$x_l(t) = w_{e_j}(x_j(t)).$$

The triple $(G_w, L^2(\mathbb{R}_0^+), \mu)$ is called a (generalised) signal flow graph.

In case of more than one connected edge to one node v_l , that means for $r \in \mathbb{N}$ with the edges

$$e_j = \langle v_j, v_l \rangle, e_{j+1} = \langle v_{j+1}, v_l \rangle, \dots, e_{j+r} = \langle v_{j+r}, v_l \rangle,$$

the mapping w operates according to

$$x_l(t) = \sum_{s=0}^r w_{e_{j+s}}(x_{j+s}(t)).$$

In this definition, $L^2(\mathbb{R}_0^+)$ is used. This is the vector space of quadratic integrable functions.

Because of the fact, that a Simulink model will be implemented on a computer, a closer look to the signals out of $L^2(\mathbb{R}_0^+)$ is appropriate.

Let's assume $I = [a, b] \subset \mathbb{R}_0^+$ and denote

$$Z = \{t_1, t_2, \dots, t_k\}, \quad k \in \mathbb{N},$$

a decomposition of the interval I with $t_1 = a$ and $t_k = b$. fulfils the condition $t_{i+1} - t_i = \Delta t$ for all $i = 1, \dots, k$, is called equidistant. Through

$$x(t_i) = x_i$$

a mapping $\delta_a: L^2(I) \rightarrow \mathbb{R}$ is defined, the sampling function. By this sampling δ_a , a set of values

$$X = \{x_1 = x(t_1), \dots, x_k = x(t_k)\}$$

is defined. In computers only this set of sampled values are available.

This definition allows a mathematical characterisation of Simulink models as signal flow graphs. Simulink offers a graphical interface to build these signal flow graphs in the model editor.

2.2. Some basic signal flow graphs

To emphasise the mathematical characterisation of Simulink models, some basic examples are presented in this subsection.

The multiplication of one signal is represented by the signal flow graph in Figure 3. There, the traditional and an alternative description are depicted.



Figure 3: Signal flow representation of a multiplication in classical and alternative form

In Figure 3, the alternative form of the signal flow representation reminds of the block structure of Simulink. The corresponding mapping is given by

$$x_l(t) = a \cdot x_j(t).$$

For the addition of two signals in a signal flow graph, in case of more than one edge, the mapping w can be adapted.

The weighting is set to be the identity and in case of two signals, the corresponding mapping is given by

$$x_i(t) = x_j(t) + x_{j+1}(t).$$

An even more complex operation is the integration of a signal. In this setting, the construction of the weighting w is visible. It is necessary, that the weighting is a general mapping between the signals without structural limitations. This makes it possible to describe a multiplication as well as an integration. The integration is defined by

$$x_i(t) = \int_0^t x_j(t) dt.$$

After introducing the integration operator into the signal flow concept, a higher operation – the convolution – can be analysed. This operation is very important for linear time invariant systems. Thereby, the description in the time domain is done with the convolution. The convolution is defined on the set of integrable functions on $\Omega \subseteq \mathbb{R}_0^+$, denoted by

$$L^1(\Omega) = \left\{ f: \Omega \rightarrow \mathbb{R}: \int_{\Omega} |f(x)| dx < \infty \right\}.$$

For $f, g \in L^1(\Omega)$, the convolution is defined by

$$(f * g)(t) = \int_{\Omega} f(\tau)g(t - \tau) d\tau.$$

At this point, a problem with the definition of a signal flow graph occurs. Let's assume a signal x_j is related to the signal x_i via convolution by a function $h \in L^1(\Omega)$ through

$$x_i(t) = (x_j * h)(t).$$

This relation is not representable as the mapping w in the definition of a signal flow graph. To handle this problem, a well known transformation for linear time invariant systems is used, the Laplace-transform. It is defined for functions $f: [0, \infty) \rightarrow \mathbb{R}$, which are from exponential order, meaning that the function f fulfils the condition

$$|f(t)| \leq M \cdot e^{s_0 t} \quad \forall t > T,$$

with constants $s_0, M, T > 0$. By the use of

$$\mathcal{L}(f)(s) = \int_0^{\infty} f(t) \cdot e^{-st} dt,$$

a mapping from the set of functions from exponential order to the set of complex functions is defined and called the Laplace-transform. By the use of this Laplace-transform, the description of the convolution in a signal flow graph is realisable. The Laplace-transform offers the Theorem of convolution (see [5]), which transforms the convolution to a multiplication in the s-plane. If capital letters denote the corresponding Laplace-transform, the relation in the s-plane is described by

$$X_i(s) = X_j(s) \cdot H(s).$$

With this extension of the specification of a signal flow graph, the convolution can also be interpreted in this context.

Amongst others, these are basic operations which can be used to construct complex systems in Simulink.

2.3. Implementation of Simulink Models

This graphical representation built in the model editor corresponds to a MATLAB file which stores all used blocks and components and all connections between them. Even constants and possible variables, controlled out of MATLAB, as well as parameters, are stored in this MATLAB-file.

It is possible to run this file in MATLAB without a graphical representation in the Simulink model explorer. The model editor is a more comfortable tool to construct the models in Simulink, but simulation base is the MATLAB executable code in the mdl-file.

Simulink Models are executed via MATLAB on the MMT-Server. The model-file is build up like the schematic sketch in Figure 4.

```

Model {
  Name "simple"

  BlockParameterDefaults {
    [...]
  }

  Block {
    [...]
  }

  [...]
}

```

Figure 4: Cut-out of a (schematic) description of the MATLAB code of a Simulink model

In the MATLAB description of a Simulink model, all names, parameter values, connections, (default) adjustment of all blocks, etc. are stored. This file is executed by a MATLAB file which includes all values and parameters that are required for the simulation at the MMT-server.

The front-end of the MMT-server is equal to the one for MATLAB examples, only the simulator in the background is different. For visualisation, the graphical Simulink model is also available in the file-section, see Figure 1. If users download this file in a normal web browser, only the MATLAB code, as specified in Figure 2, can be observed. The signal flow graph representation of the Simulink model can be observed via local MATLAB/Simulink version. If the file with MATLAB code inside is opened by Simulink, the signal flow graph of the Simulink model is depicted.

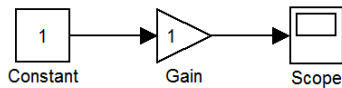


Figure 5: A simple Simulink model

To get an impression, the very simple Simulink model depicted in Figure 5 needs 730 lines MATLAB code to be created. This shows that the model explorer in Simulink is necessary for building more complex systems in Simulink.

3. SIMULINK EXPERIMENTS

Simulink offers a wide range of linear and non-linear time-continuous and time-discrete blocks. Important linear time-continuous block diagrams are the addition and multiplication block, integrator, transfer-function and state space block. These blocks are also available for linear and time discrete system, so-called sampling systems.

Simulink experiments have a wide range of tools with these precast systems. The class of linear systems enables varied methods to describe linear time invariant systems given by the system theory. On the one hand, these systems are characterised via linear ordinary differential equation of n-th order with constant coefficients. These can be transformed into n ordinary differential equations of first order. The differential equation system, combined with an equation, describing the output of a system, formulates the equations of the state space description of a linear time invariant system. An alternative form is a transfer function. Using the Laplace-transform, the state space description is translated in the complex s-plane, where the differential equations appear as algebraic equations. These equations allow formulating an input-output-relation for the linear systems. So a complex system, before specified by a differential equation, is represented in the complex s- plane via rational function.

This is one of the important features of Simulink: different model approaches are not only available for linear systems.

For the numerical simulation, Simulink provides numerical solvers for ordinary differential equations. In this way, linear as well as non-linear systems can be handled.

The following subsections show different examples implemented in Simulink on the MMT-server.

3.1. Binary Data Transmission

The following example shows, that Simulink provides many specialised blocks for a large variety of problems. In this particular case, a binary data transmission is observed. Binary data $\{0,1\}$ is mapped to (abstract) discrete symbols $\{s_0 = -1, s_1 = 1\}$.

After this mapping to discrete symbols, the transmission channel adds Gaussian noise. After the transmission, the

binary data is reconstructed by a decision maker. The whole system is represented in Figure 6.

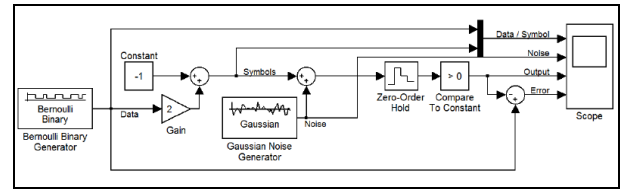


Figure 6: Simulink model of the binary data transmission

3.2. Matter transport of a substance in the human kidney

This example shows the application of a compartment model and its implementation in Simulink. The transport of a substance in the human kidney can be modelled via compartments, shown in Figure 7.

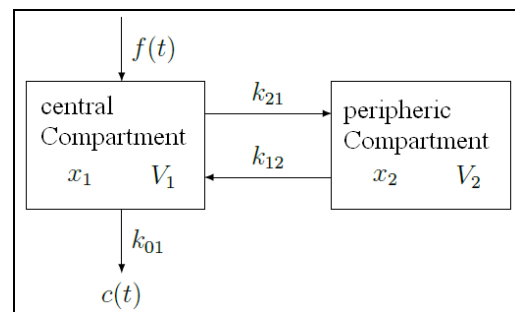


Figure 7: Model of the transport of a substance in the human kidney

The transport process is described by a system of differential equations and a the corresponding injection f . The differential equation system is given by

$$\begin{aligned} \frac{dx_1}{dt} &= f(t) - (k_{01} + k_{21})x_1 + k_{12}x_2 \\ \frac{dx_2}{dt} &= k_{21}x_1 - k_{12}x_2 \end{aligned}$$

and the injection is modeled by

$$f(t) = \frac{D}{\tau} \quad \text{for} \quad 0 \leq t \leq \tau,$$

where D denotes the full amount of the substance.

In the experiment, the influences of the parameters k_{01} , k_{21} and k_{12} can be observed as well as the volume V_1 of the central compartment, the amount of substance D and the injection time .

Mainly, the model is described by a linear differential equation system with constant coefficients, which is managed differently in MATLAB than in Simulink. For these linear systems, MATLAB offers a number of functions and methods. The model implemented in Simulink is shown in Figure 8.

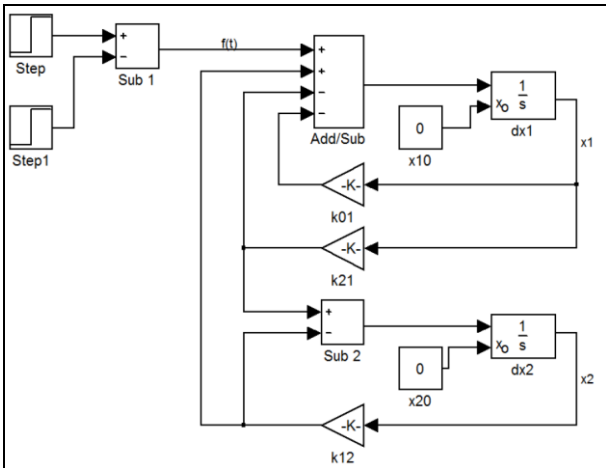


Figure 8: Simulink implementation of the transport model of a substance in the human kidney

This example is a good one to show the differences between the code-oriented implementation in MATLAB and the block-oriented implementation in Simulink.

3.3. Basic Pendulum Models

In section 1, about the built-up of the MMT-server, an example about the mathematical pendulum is used to explain an experiment at the server. This example is suitable to explain the usage of MATLAB and Simulink at the MMT-server.

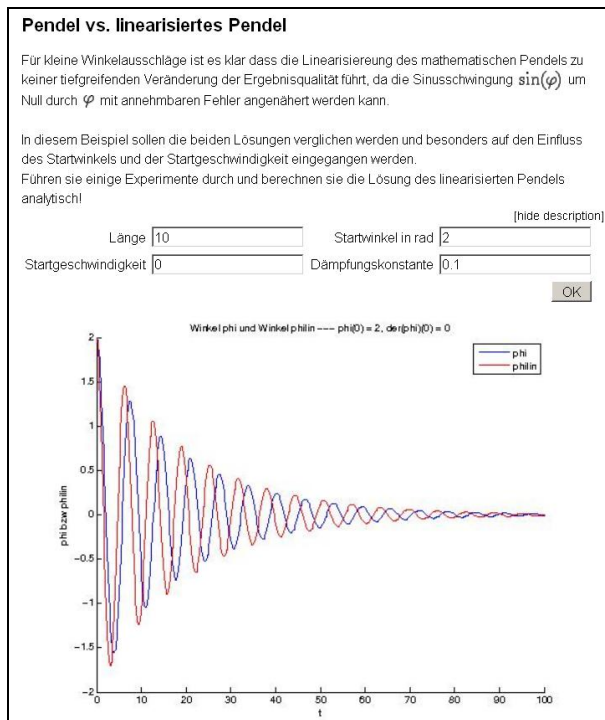


Figure 9: Pendulum experiment to compare linear and non-linear differential equation

The mathematical pendulum is described by a non-linear differential equation, so the second step is to linearise this equation and compare its solution to the non-linearised one. The linearised pendulum equation is received, when the sine function is replaced by the first order Taylor-expansion. The result is

$$m \cdot l \cdot \ddot{\varphi}(t) = -m \cdot g \cdot \varphi(t) - l \cdot d \cdot \dot{\varphi}(t).$$

The experiment at the MMT-server compares the solution of different parameters and different initial values. The result is, that for major starting angles the linear and non-linear solution diverges.

In Figure 9, the example of linear versus non-linear pendulum for a chosen set of values is shown.

Following to this basic example, some experiments with a double pendulum, a constrained pendulum and a sliding pendulum are available.

The last example of this introduction to the topic of modelling and simulation is the pendulum model implemented in Simulink.

In this model, Simulink and some MATLAB functions are compared. The pendulum is a rod pendulum and the example is implemented via Simulink model, shown in Figure 10.

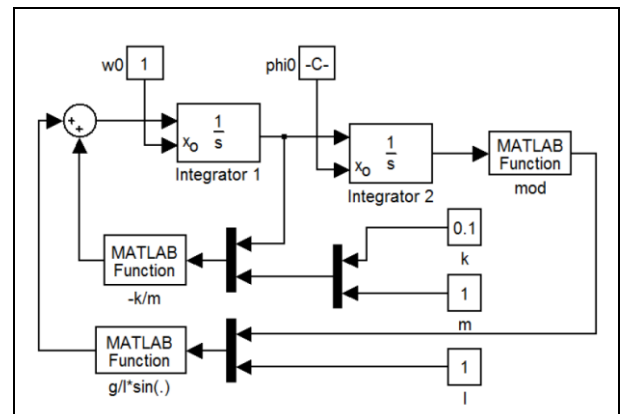


Figure 10: Simulink implementation of a rod pendulum

In this example, a good illustration of the combination of MATLAB functions with Simulink systems is possible. Simulink expands and complements the possibilities to build models at the MMT-server.

3.4. Pendulum with Friction

On the basis of the previous pendulum examples, even a more challenging example in the context of pendulums is available on the MMT-server. The pendulum moves in the horizontal plane and has friction respected. To visualise this specification, Figure 11 shows the pendulum.

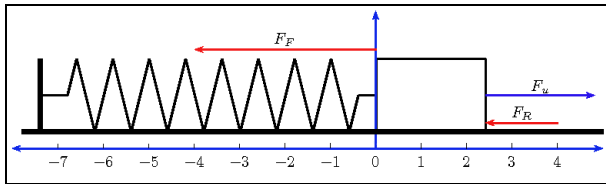


Figure 11: Horizontal pendulum with friction

The goal is to control the position of the mass by a PI-controller, while the process is given by the horizontal pendulum with friction.

This example is exclusively designed in Simulink, both the controller and the process. The controller is a well known structure, simply representable in Simulink. For the process model in Simulink, the pendulum process and the friction are built in two parts. The pendulum part is implemented and as an add-on, the friction process is done in an own model. The friction process depends on the velocity v and the force F , and the Simulink model is shown in Figure 12.

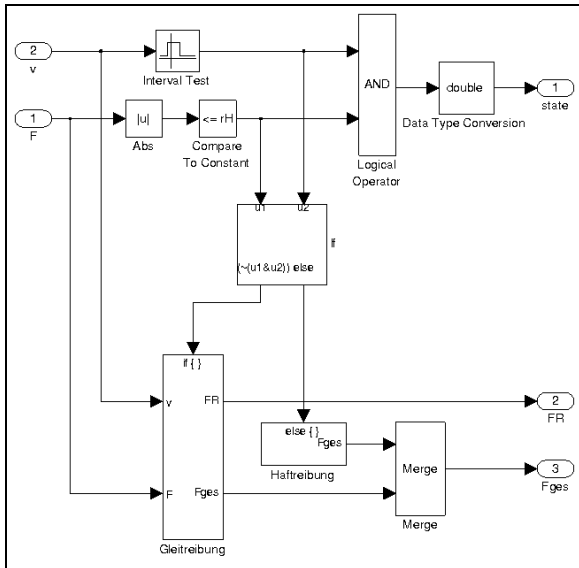


Figure 12: Friction process of the advanced pendulum model

In this case, the model is very large and many subsystems are involved. In that sense, the MMT-server can be used to show how to construct more complex systems in an economic way. Also examples can be offered to analyse the behaviour of several subsystems on their own on the one hand, and working together and influence each other on the other hand.

4. SUMMARY AND OUTLOOK

A long period of development work, which started in 2009, completed a multifaceted experiment server in 2012. The server started containing basic examples implemented in MATLAB to present typical simple tasks of mathematical modelling and simulation.

The initial MMT environment developed to become a multifunctional MATLAB simulation system.

Simulink models are represented as signal flow graphs. These are composed of small prepared blocks, which are offered by Simulink.

In the education of mathematical modelling and simulation, the server is used to teach different model approaches and to illustrate different simulation tools through MATLAB and Simulink.

Future plans include expanding the MMT-server with Simscape examples, as well as other available toolboxes of MATLAB/Simulink.

The MMT-server expands and evolves with every designed example, because each new example creates new ideas to visualise or implement the results in a novel way.

ACKNOWLEDGEMENT

The MMT server, which is introduced and used in this work, is administered in cooperation with the dwh Simulation services.

REFERENCES

- Körner, A., Zauner, G., Schneckenreither, G., 2009. Ein e-learning System für MMT – Mathematik, Modellbildung und Tools, Systemerweiterung und Einbindung von graphischer Modellbildung. *20th Symposium Simulation Techniques*, pages 87–94, Cottbus (Germany)
- Winkler, S., Körner, A., Hafner, I., 2010. MMT – A web-based e-learning System for Mathematics, Modeling and Simulation using MATLAB. *7th EUROSIM Congress on Modelling and Simulation*, paper 231, Prague (Czech Republic)
- Körner, A., Hafner, I., Bicher, M., Winkler, S., Breitenecker, F., 2011. MMT - A Web Environment for Education in Mathematical Modelling and Simulation. *ASIM 21. Symposium Simulationstechnik*, Winterthur (Switzerland), ISBN: 978-3-905745-44-3
- Hafner, I., Bicher, M., Winkler, S., Fitsch, U., Körner, A., 2012. MMT _ A System Offering E-Learning of Modelling and Simulation in a Different Way. *MATHMOD 2012 - 7th Vienna Conference on Mathematical Modelling*, Vienna (Austria)
- Körner, A., 2012, Analyse und Simulation dynamischer Systeme in Simulink mit Web-Interface, diploma thesis, Vienna University of Technology

AUTHORS BIOGRAPHY

Andreas Körner, born on 22.03.1982, is currently phd student at Vienna University of Technology. He is a member of the group Mathematical Modelling and Simulation at the Institute for Analysis and Scientific Computing.

CHANGE OF INDEPENDENT VARIABLE FOR STATE EVENT DETECTION IN SYSTEM SIMULATION - EVALUATION WITH ARGESIM BENCHMARKS

Felix Breitenecker^(a), Horst Ecker^(b), Bernhard Heinzl^(c), Andreas Körner^(d), Matthias Rößler^(e), Niki Popper^(f)

^{(a)(d)} Vienna University of Technology, Institute for Analysis and Scientific Computing, Austria

^{(c)(d)} Institute for Computer Aided Automation, Vienna University of Technology

^(b) Vienna University of Technology, Institute for Mechanics and Mechatronics, Austria

^(e) dwh Simulation Services, Vienna, Austria

^(a) felix.breitenecker@tuwien.ac.at, ^(b) horst.ecker@tuwien.ac.at, ^(c) bernhard.heinzl@tuwien.ac.at,
^(d) andreas.koerner@tuwien.ac.at, ^(e) matthias.roessler@tuwien.ac.at, ^(f) niki.popper@drahtwarenhandlung.at

1. ABSTRACT

In system simulation state event descriptions and state event handling are used to model and to simulation ‘discontinuous’ changes of the system under investigation. State events may cause simple ‘jumps’ of parameters, or complex changes of models, as in case of loss or increase of degrees of freedom. The classical method of state event handling consists of an interpolative and /or iterative method to locate the event with ongoing time – based on the zero of the state event function. This contribution discusses first event classification and time-based event location algorithms, and second, it discusses an alternative method for state event location by change of the independent variable. This method, first suggested by Henon in 1982, makes use of the principles of Poincare mappings. This alternative method is analyzed and sketched with models from the *ARGESIM Benchmarks on Modelling Approaches and Simulation Techniques*.

Keywords: system simulation, state event handling, structural dynamic systems, state event finding, benchmarks

2. STATE EVENT DESCRIPTION IN SYSTEM SIMULATION

Simulation systems for system simulation generate usually an implicit state space description of type

$$\dot{\vec{x}}(t) = \vec{f}(t, \vec{x}(t), \vec{z}(t), \vec{u}(t), \vec{p}), \vec{x}(t_0) = \vec{x}_0 \quad (1)$$

$$\vec{g}(\vec{x}(t), \vec{z}(t), \vec{u}(t), \vec{p}) = \vec{0} \quad (2)$$

For subsequent numerical analysis, an appropriate DAE solver with certain accuracy is to be used.

In models from application it is often necessary to model discontinuities in the model description, because a certain system phenomenon can only be described ‘approximatively’ by a discontinuous change in the model. These discontinuous changes are called *events*; if the time instant of the change is known in advance, the event is called a *time event*.

If the event depends on a certain values or thresholds for state variables or functions of state variables, the time instant of occurrence is not known in advance, and the event is called a *state event*.

For rough numerical analysis these discontinuous changes may be mimicked by *if – then – else* constructs in the right hand side of the system equations. The DAE solver takes these changes into account at the next solver step after the event. For accurate numerical simulation and in case of more complex discontinuous changes it is necessary to synchronise the event with the DAE solver. For time events, this synchronisation is easy. For state events, a relatively complex algorithm – state event handling – must be performed.

A state event is defined

- by an *event function*

$$h(\vec{x}(t), \vec{z}(t), \vec{u}(t), \vec{p}) \quad (3)$$

whose zero determines the time instant \hat{t} of the occurrence of the event,

- and by an *event action*

$$E(\vec{x}(\hat{t}), \vec{z}(\hat{t}), \vec{u}(\hat{t}), \vec{p}) \quad (4)$$

which performs the discontinuous change.

An event function $h(\dots)$ can cause the associated event action $E(\dots)$ several times.

$$h^A(\vec{x}(t), \vec{u}(t), \vec{p}) \stackrel{! \pm}{=} 0 \Rightarrow E^A(\vec{x}(\hat{t}^A), \vec{u}(\hat{t}^A), \vec{p}) \quad (5)$$

The event description (5) is to be read as follows: the event ‘A’ occurs, if the event function (3) associated with the event ‘A’, $h^A(\vec{x}(t), \vec{z}(t), \vec{u}(t), \vec{p})$ has a zero crossing, whose zero \hat{t}^A is to be determined; dependent on the crossing direction, the associated event action $E^A(\vec{x}(\hat{t}^A), \vec{u}(\hat{t}^A), \vec{p})$ has to be performed: only in case of crossing from positive in negative direction, only in case of crossing from negative in positive direction, or in both cases, indicated by the crossing operator:

$$\left(\begin{smallmatrix} ! - \\ = \end{smallmatrix} \right), \left(\begin{smallmatrix} ! + \\ = \end{smallmatrix} \right), \left(\begin{smallmatrix} ! \pm \\ = \end{smallmatrix} \right)$$

The associated event action $E^A(\vec{x}(\hat{t}), \vec{u}(\hat{t}), \vec{p})$ must handle the discontinuous change in the model description, which ranges from simple to very complex. It makes sense to classify events with respect to their complexity of action of change:

- state event – output change – SE-O
- state event – parameter change – SE-P
- state event – input change – SE-I
- state change – state value change – SE-S
- state event – derivative vector change - SE-D
- state event – model change - SE-M

3. CLASSICAL STATE EVENT HANDLING

The primary tasks of event handling are the synchronisation of the state event with the ODE/DAE solver, and the ‘execution’ of the event – i.e. the discontinuous change of parameters, inputs, and states, and the choice of new derivatives or new models. The classical state event algorithm requires the following steps:

- *Detection* of the event
- *Localisation* of event and solver stopping
- *Event Action*
- *Restart* of ODE solver

Event Detection. Observing the algebraic sign of the event function during the time advance of the ODE/DAE solver in each integration interval $[t_k, t_{k+1}]$ allows detection of the event:

$$\text{sign } h(\vec{x}(t_k)) \neq \text{sign } h(\vec{x}(t_{k+1})).$$

On inequality, the event occurred at a time instant $\hat{t}, \hat{t} \in [t_k, t_{k+1}]$. On occurrence, depending on the defined crossing direction, the state event must be handled, or not: in case of crossings into negative direction (‘-’ in (14)) if $\text{sign } h(\vec{x}(t_k)) = +1$, in case of crossings into positive direction (‘+’ in (5)) if $\text{sign } h(\vec{x}(t_k)) = -1$, and in case of crossings in both directions (‘±’ in (5)) in any case.

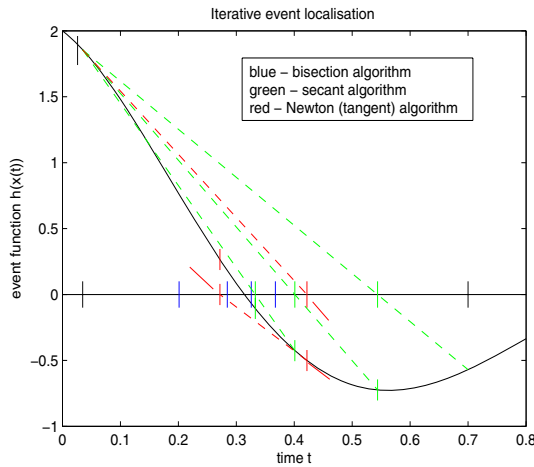


Figure 1: Algorithms for Iterative State Event Location (zero of function $h(\vec{x}(t))$ - black line): Bisection – blue; Secant Method – green; Tangent Method or Newton Algorithm resp. – red.

Classical Event Location. After detection, the event time $\hat{t}, \hat{t} \in [t_k, t_{k+1}]$ must be determined with sufficient accuracy, followed by a ‘closing’ solver step from t_k to \hat{t} . Two related algorithms are used,

Interpolative algorithms $\hat{t} = \Psi_1(t_k, t_{k+1})$

Iterative algorithms $\hat{t}_m = \Psi_1(\hat{t}_m; t_k, t_{k+1})$

A very classical method is bisection (iterative); common method is the secant formula (interpolative or iterative), and advanced method is the tangent formula (interpolative) or the Newton algorithm resp. (iterative.). The iterative event location algorithms stop if the length of the *event window* is less equal a given minimal length:

$$\Delta \hat{t}_m = |\hat{t}_{m-1} - \hat{t}_m| \leq \varepsilon_{event} \rightarrow \hat{t} = \hat{t}_m$$

Figure 1 shows the first steps of the forementioned methods which are given in detail in the following.

Bisection method. The iterative bisection method is the slowest method, but the most ‘stable’:

- The interval $[t_k, t_{k+1}]$ is divided into two halves

$$[t_k, t_{B,1}], [t_{B,1}, t_{k+1}], t_{B,1} = \frac{1}{2}(t_{k+1} - t_k),$$

checking of the algebraic sign determines, in which interval the event happens,

$$\text{e.g. } \hat{t} \in [t_k, t_{B,1}]$$

- Again interval $[t_k, t_{B,1}]$ is divided into two halves

$$[t_k, t_{B,2}], [t_{B,2}, t_{B,1}], t_{B,2} = \frac{1}{2}(t_{B,1} - t_k)$$

and the algebraic sign determines the next ‘event interval’, and so on with further $n-2$ times dividing of the event interval, until event time \hat{t} is sufficiently approximated due to (23) and finally set to $\hat{t} = t_{B,n}$.

- As last step, integration of (2) and (3) on the ‘remaining’ interval $[t_k, t_{B,n} = \hat{t}]$ updates the states until event time.

Another iterative method is the *secant formula*, which determines the zeros of the secant line connecting the event function at the boundaries of the event interval:

- With interval $[t_k, t_{k+1}]$ and values of the event function at the interval borders given by $h_k = h(x(t_k), u(t_k)), h_{k+1} = h(x(t_{k+1}), u(t_{k+1}))$ the first approximation for the event time \hat{t} is the zero of the secant which connects (t_k, h_k) and (t_{k+1}, h_{k+1}) :

$$t_{S,1} = t_k - \frac{t_{k+1} - t_k}{h_{k+1} - h_k} h_k$$

- The time instant $t_{S,1}$ divides the first event interval, and the algebraic sign function determines, where the event happens, e.g. $\hat{t} \in [t_k, t_{S,1}]$; with event function values $h_k, h_{S,1}$ at the interval borders of $[t_k, t_{S,1}]$, the next approximation for \hat{t} is the zero of the connecting secant line:

$$t_{S,2} = t_k - \frac{t_{S,1} - t_k}{h_{S,1} - h_k} h_k$$

- This procedure is further iterated $m-2$ times, until event time \hat{t} is sufficiently approximated due to (23) and finally set to $\hat{t} = t_{S,m}$.
- As last step, integration of (2) and (3) on the ‘remaining’ interval $[t_k, t_{S,m} = \hat{t}]$ updates the states until event time.

A very fast iterative method is the *Newton algorithm*, or simply the *tangent method*:

- With interval $[t_k, t_{k+1}]$ and value and derivative value of the event function at the left border given by

$$h_k = h(x(t_k), u(t_k)), \dot{h}_k = \frac{d}{dt} h(x(t_k), u(t_k)),$$

the first approximation for event time \hat{t} is the zero of the tangent in (t_k, h_k) :

$$t_{N,1} = t_k - \frac{1}{\dot{h}_k} h_k$$

- This procedure is further iterated $r-2$ times, until event the time \hat{t} is sufficiently approximated due to (23) and finally set to $\hat{t} = t_{N,r}$.
- As last step, integration of (2) and (3) on the ‘remaining’ interval $[t_k, t_{N,r} = \hat{t}]$ updates the states until event time.

In principle, this tangent method (Newton algorithm) approximates the event function by a Taylor series expansion of 1st order. Accuracy can be increased by using a Taylor series approximation of 2nd order, requiring the second derivative of the event function, which is available in special cases (event function is threshold of distance, whereby distance and velocity are states). Figure 2 compares the discussed Taylor approximations for the event function; the tangent method is an interesting link to the Henon method (section 4).

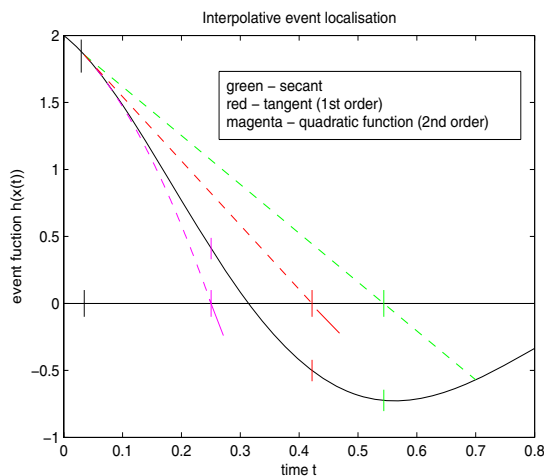


Figure 2: Comparison of interpolative algorithms for state event location (zero of function $h(\vec{x}(t))$) - black

line): secant method – green; tangent method – red, quadratic interpolation - magenta.

Some aspects with respect to event location must be taken into account:

- Iterative methods can give more accurate results. But in case of different event functions with nearby roots, the iterative methods may cause a deadlock, may let events vanish, etc.
- Iterative methods generally cause backstepping in time, which causes problems with not synchronised time events occurring in the iteration interval, and with stepsize control of the ODE solver.
- A general, partly essential and partly philosophical problem comes up with methods which make use of the ‘virtual’ value $h_{k+1} = h(\vec{x}(t_{k+1}))$ of the event function at the time step after the event, which is definitely wrong from viewpoint of physics (in case of bouncing ball example the algorithm accepts, that the ball is flying *in* the ground!). This physical error may give totally wrong results for $h_{k+1} = h(\vec{x}(t_{k+1}))$, or it may be only a strange fact.
- ODE solvers’ stepsize control and event location algorithm are partly ‘competitive’ strategies. If the DAE/ODE solver takes a too long stepsize, an event may vanish, in case the step bridges two zero crossings. In principle, the event time instant \hat{t} is to be seen as so-called *barrier time* for the solver, which limits the stepsize.
- The DAE/ODE solver themselves are approximations of a specific order – if for instance an explicit Euler solver has calculated $\vec{x}(t_{k+1})$ and the event function (3) is a linear function of the states, then the tangent method and secant method for determining the event time coincide with the ODE solver step, so that the event time determined by the cited algorithms is exact, and– further iteration makes no sense. In general, the desired accuracy for determining the event time must be coordinated with the solver’s order and solver’s accuracy.
- Generally, the event function is not really known as formula; as the function depends on the states, which are only known at grid points, also the event function is only known at gridpoints (before and after the event), so that the secant interpolation is the first choice for event location because of genuine accurateness; iteration or more complex methods refine the accuracy of the ODE solvers in behind.

Many advanced DAE/ODE solvers offer the steps *detection* and *localisation* with *solver stopping* as generic feature – so called *root finding* feature. Additionally to system equations (1) and (2) also the event function (3) or (5) resp. with indication of crossing direction can be provided, resulting in a stopping of the ODE/DAE solver at localized event time.

Sometimes tuning parameters for the event location can be chosen, but only in rare cases the location method can be chosen. Simulation systems make either use of a DAE/ODE solver with root finding, or they incorporate the event algorithm into a general event mechanism which controls the ODE solver stopping.

Event Action. Due to the state event classification sketched before, the event actions in (4) consist of discontinuous change of parameter values, of input values, of output values, or of state values, or the actions, switch to new derivative functions (new derivative vector) or to a new model description (with changing dimension). A general view is to interpret a state event as the end of validity of a certain model, and the necessity to restart with a new model, which gets initial values from the previous model. This approach – the *hybrid decomposition* approach -decomposes the system into conditionally consecutive dynamic models, which are interrupted and controlled by discrete events.

The approach, strongly related to *structural-dynamic systems* is recommended for handling *model change* events SE-M and partly *derivative vector* events SE-D. The approach might be an overdo for handling state events of type SE-P, SE-I, SE-S and partly for events of type SE-D, because these events can be handled within one model by specific features like event-synchronised conditions or schedulable discrete segment.

While – If-Then-Else Constructs. The action of state events of type SE-P, SE-I and partly of type SE-D can be handled in *if-then-else* constructs or *while* constructs, which are ‘synchronised’ with the ODE/DAE solver, i.e. which cause implicitly a state event. Most simulation systems offer features for this ‘integrated’ approach which requires artificial constructs for structural dynamic changes and state jumps (frozen states, integrator hold, etc).

4. STATE EVENT DETECTION BY CHANGE OF INDEPENDENT VARIABLE

An unusual, but eventually efficient alternative method for state event location can be based on a method for calculation of Poincare maps, suggested by M. Henon. Henon interprets the state space (1) as (autonomous) dynamical system

$$\begin{aligned} \frac{dx_1}{dt} &= f_1(x_1, x_2, \dots, x_n) \\ \frac{dx_2}{dt} &= f_2(x_1, x_2, \dots, x_n) \\ &\dots \dots \dots \\ \frac{dx_n}{dt} &= f_n(x_1, x_2, \dots, x_n) \end{aligned} \quad (6)$$

which describes curves in the n-dimensional space. A Poincare map is roughly speaking the set of intersections of the curves with (n-1)-dimensional subspace

$$H(x_1, x_2, \dots, x_n) = 0 \quad (7)$$

representing an autonomous event function of type (3):

$$h(\vec{x}(t), \vec{u}(t), \vec{p}) = H(x_1, x_2, \dots, x_n) = 0$$

For simple subspaces of type

$$h(\vec{x}(t), \vec{p}) = H(x_k) = x_k = a \quad (8)$$

in system (6) now the independent variable t can be changed with the dependent variable x_k (e.g. $k = n$) giving a modified system with independent variable x_n and dependent variables $x_1, x_2, \dots, x_{n-1}, t$:

$$\begin{aligned} \frac{dx_1}{dx_n} &= \frac{f_1(x_1, x_2, \dots, x_n)}{f_n(x_1, x_2, \dots, x_n)} \\ \frac{dx_2}{dx_n} &= \frac{f_2(x_1, x_2, \dots, x_n)}{f_n(x_1, x_2, \dots, x_n)} \\ &\dots \dots \dots \\ \frac{dx_{n-1}}{dx_n} &= \frac{f_{n-1}(x_1, x_2, \dots, x_n)}{f_n(x_1, x_2, \dots, x_n)} \\ \frac{dt}{dx_n} &= \frac{1}{f_n(x_1, x_2, \dots, x_n)} \end{aligned} \quad (9)$$

System (9) is usually much more complex, and division by $f_n(x_1, x_2, \dots, x_n)$ might cause severe problems, as well as implicit function theorem must hold, but the systems allows numerical solution of the system with accurate intersection of the subspace $H(x_n) = x_n = a$.

Henon suggest now a clever modification:

- Solution of the original system (6) by an ODE solver until t_m just before the intersection with $H(x_n) = x_n = a$ stopping with $x_n(t_m) \neq 0$.
- Solution of the modified system (9) by the same ODE solver, from $x_n(t_m) = x_{n0}$ with one step of length $\pm x_{n0}$, meeting the intersection almost exactly.

The subspace $H(x_n) = x_n = a$ can be interpreted now as set of zeros of the event function $h(x_1, x_2, \dots, x_n)$ so that the above algorithm can be used as alternative method for state event location without any interpolation and iteration.

For complex subspaces $H(x_1, x_2, \dots, x_n) = 0$ Henon suggests reformulation of the subspace by a differential equation

$$x_{n+1}(t) = H(x_1, x_2, \dots, x_n)$$

$$\frac{dx_{n+1}}{dt} = \frac{d}{dt} H(x_1, x_2, \dots, x_n) =$$

$$\sum_1^n \frac{dH}{dx_i} \cdot f_i(x_1, x_2, \dots, x_n)$$

Henon’s method allows now formulating a modified event location algorithm which meets the zero of the event function $h(x_1, x_2, \dots, x_n)$ ‘exactly’ within the accuracy of the ODE solver used.

Event Detection. Observing the algebraic sign of the event function during the time advance of the ODE/DAE solver in each integration interval $[t_k, t_{k+1}]$ allows detection of the event:

$$\text{sign } h(\vec{x}(t_k)) \neq \text{sign } h(\vec{x}(t_{k+1})).$$

On inequality, the event occurred at a time instant \hat{t} , $\hat{t} \in [t_k, t_{k+1}]$. On occurrence, depending on the defined crossing direction, the state event must be handled.

Event Location by Variable Change. After detection and stopping time integration at t_k with $\vec{x}(t_k)$, the event time \hat{t} , $\hat{t} \in [t_k, t_{k+1}]$ is determined by solving the modified extended state space (9) if $f_{n+1}(x_1, x_2, \dots, x_n)$ does not get zero on $(t_k - \varepsilon, \hat{t} + \varepsilon)$:

$$\begin{aligned} \frac{dx_1}{dx_{n+1}} &= \frac{f_1(x_1, x_2, \dots, x_n)}{f_{n+1}(x_1, x_2, \dots, x_n)} \\ \frac{dx_2}{dx_{n+1}} &= \frac{f_2(x_1, x_2, \dots, x_n)}{f_{n+1}(x_1, x_2, \dots, x_n)} \\ &\dots \dots \dots \\ \frac{dx_n}{dx_{n+1}} &= \frac{f_n(x_1, x_2, \dots, x_n)}{f_{n+1}(x_1, x_2, \dots, x_n)} \\ \frac{dt}{dx_{n+1}} &= \frac{1}{f_{n+1}(x_1, x_2, \dots, x_n)} \\ f_{n+1} &= \sum_1^n \frac{dH}{dx_i} \cdot f_i(x_1, x_2, \dots, x_n) \end{aligned} \quad (10)$$

using the ODE solver on the interval $[x_{n+1}(t_k), 0]$ with

$$x_{n+1}(t_k) = H(\vec{x}(t_k))$$

and stepsize $\pm x_{n+1}(t_k)$ or fractions of $\pm x_{n+1}(t_k)$

resulting in all state values and time instant of the zero of the event function:

$$\hat{t} = t(x_{n+1} = 0)$$

$$\vec{x}(\hat{t}) = \vec{x}(x_{n+1} = 0)$$

In case of simple event functions of type (8) the modified state space simplifies to

$$\begin{aligned} \frac{dx_1}{dx_n} &= \frac{f_1(x_1, x_2, \dots, x_n)}{f_n(x_1, x_2, \dots, x_n)} \\ \frac{dx_2}{dx_n} &= \frac{f_2(x_1, x_2, \dots, x_n)}{f_n(x_1, x_2, \dots, x_n)} \\ &\dots \dots \dots \\ \frac{dx_{n-1}}{dx_n} &= \frac{f_{n-1}(x_1, x_2, \dots, x_n)}{f_n(x_1, x_2, \dots, x_n)} \end{aligned}$$

$$\frac{dt}{dx_n} = \frac{1}{f_n(x_1, x_2, \dots, x_n)} \quad (12)$$

to be solved on the interval $[x_n(t_k), 0]$ with stepsize $\pm x_n(t_k)$ or fractions of $\pm x_{n+1}(t_k)$ resulting in all state values and time instant of the zero of the event function:

$$\hat{t} = t(x_n = 0),$$

$$\vec{x}(\hat{t}) = \vec{x}(x_n = 0)$$

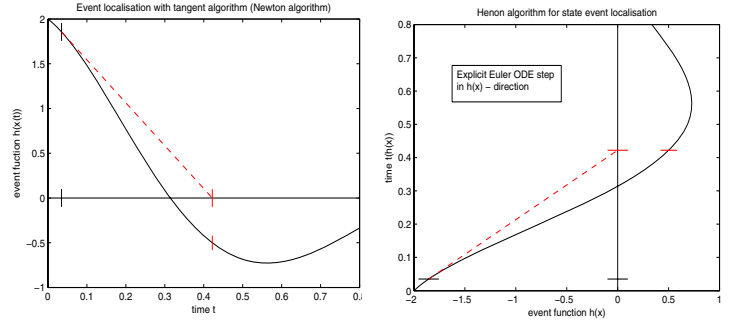


Figure 3: State Event Location with Tangent Method in Time Domain (at left), and State Event Location by Euler ODE Solver in State Domain

The suggested method requires that locally the implicit function theorem holds at least on $(t_k - \varepsilon, \hat{t} + \varepsilon)$, without singularities. Figure 3 shows that indeed uniqueness of inversion can be violated, e.g. as long the function is not monotone. The following evaluation discusses some advantages and disadvantages of this method, and suggests modifications.

- Henon suggest a combination of systems (6) and (9) with a general independent variable and with scaling factors (transformation factors) so that indeed he quotients in equation (12) are used. It might be appropriate to perform symbolical simplifications on these quotients.
- The original method makes one final solver step with the new independent variable – for improving accuracy, or in case of zeros which build up a series of limit points, it might be better to use more than one solver step with fractions of the remaining step, or to continue with the solver in the new independent variable.

Figure 3 shows an interesting link between classical state event location algorithms and Henon’s state event location. The tangent interpolation method in the time domain (at left) makes use of the same tangent line as the Euler ODE solver in the state domain (at right):

$$\begin{aligned} x &= \dot{h}_k t + h_k - t_k \dot{h}_k \\ t &= \frac{1}{\dot{h}_k} x + t_k - \frac{1}{\dot{h}_k} h_k \end{aligned}$$

While in first time domain formula the zero must be calculated, in the second state domain formula simply a zero must be inserted: $t = t_k - \frac{1}{\dot{h}_k} h_k$.

5. EVALUATION WITH ARGESIM BENCHMARKS

The journal SNE – *Simulation Notes Europe* is publishing benchmarks for modelling approaches and implementations of approaches in simulation systems. In these benchmarks, state event handling plays an important role.

At present Henon's method is tested with the models from ARGESIM Benchmark C6 *Constrained Pendulum* and ARGESIM Benchmark C20 *Hybrid and Structural Dynamic Systems*.

Benchmark C6 Constrained Pendulum relates to the physical pendulum described by angle $\varphi(t)$, given by state space

$$\begin{aligned} \frac{d\varphi_1}{dt} &= \varphi_2 \\ \frac{d\varphi_2}{dt} &= -\frac{g}{l} \sin\varphi_1 - \frac{d}{m} \varphi_2 \end{aligned} \quad (13)$$

Task is to model the discontinuous change of pendulum length and angular velocity, if the pendulum hits a pin which is located at angle φ_p . The event function becomes

$$h(\varphi_1, \varphi_2) = \varphi_1 - \varphi_p$$

This event function is of the simple type (8), and for using the method of independent variable change for state event location, the modified system with independent variable φ_1 is

$$\begin{aligned} \frac{d\varphi_2}{d\varphi_1} &= -\frac{g \sin\varphi_1}{l \varphi_2} - \frac{d}{m} \\ \frac{dt}{d\varphi_1} &= \frac{1}{\varphi_2} \end{aligned} \quad (14)$$

Henon's method works well, if φ_2 does not get zero when hitting or leaving the pin. Unfortunately the angular velocity $\dot{\varphi} = \varphi_2$ gets zero, if the pendulum is on point of return – which may happen at pin position φ_p – here a modified event function could help (to be investigated further).

Benchmark C20 Hybrid and Structural Dynamic Systems test more or less complex state event changes in models from mechanical and electrical engineering: bouncing ball, rotating pendulum, and switching circuit.

The bouncing ball model with dynamic contact phase and states ball position, ball velocity, and ball deformation is modelled during flight by

$$\begin{aligned} \dot{x} &= v, & \dot{v} &= -g \\ \dot{w} &= -\frac{k}{d} \cdot w \end{aligned} \quad (15)$$

Flight ends, if the ball gets in contact with the ground, given by the event function

$$h(x, v, w) = x + w \quad (16)$$

Although event function (16) is simple, it must be made a differential equation

$$\frac{dh}{dt}(x, v, w) = \dot{x} + \dot{w} = v - \frac{k}{d} \cdot w$$

The modified system with independent variable h for use of the Henon method is then given by

$$\frac{dx}{dh} = \frac{d \cdot v}{d \cdot v - k \cdot w}$$

$$\frac{dv}{dh} = -\frac{d \cdot g}{d \cdot v - k \cdot w}$$

$$\frac{dw}{dh} = -\frac{k \cdot w}{d \cdot v - k \cdot w}$$

Henon's method only would fail, if flight velocity and deformation change both get zero – which cannot happen or add to zero – which could happen in a very rare case.

Another test model from Benchmark C20, the rotating pendulum, is at present under investigation. Use of Henon's method can range from simple to complex, depending on the chosen coordinate system.

SUMMARY - OUTLOOK

Henon's method offers itself as charming alternative for state event handling. Perhaps the main advantage is the fact, that the ODE solver is not interrupted by a numerical root finding algorithm – whereby both algorithms influence each other. On the other hand, the problem of singularities in the modified state space must not be neglected.

First numerical tests with the cited benchmarks are satisfying and promising because of the 'simpler' algorithms. At present the method is tested within master theses using the ARGESIM Benchmarks and an extended rotor – stator model.

After discussion with experts from mechatronics it is intended to investigate the method within new research project in more detail. There, also possible links to F. Cellier's and E. Kofman's QSS method are to be considered: QSS - Quantized State Systems – integration works with a discretisation of state instead of time, so that state events are determined by a state increment known in advance.

REFERENCES

- Henon, M., 1982. *On the Numerical Computation of Poincare Maps*. Physics 5D, 412-414.
- Henon, M., 1964. *L'evolution Initiale d'un Amas Spherique*. Ann. Astrophys. 27 (1964), 83-91.
- ARGESIM Benchmarks – Benchmark List. www.argesim.org, 2012.

DEVELOPING A MULTIHYPBRID SYSTEM TO SIMULATE A UNIVERSITY CAMPUS

Shabnam Michèle Tauböck ^(a), Felix Breiteneker ^(b), Dietmar Wiegand ^(c), Nikolas Popper ^(d), Gerald Hodecek ^(e)

^{(a), (b)}Institute for Analysis and Scientific Computing, Vienna UT, Austria

^(c)Institut für Städtebau, Landschaftsarchitektur und Entwerfen, Vienna UT, Austria

^(d)dwh GmbH - Simulation Services, Vienna, Austria

^(e)Gebäude und Technik, Vienna UT, Austria

^(a)shabnam.tauboeck@tuwien.ac.at, ^(b)felix.breiteneker@tuwien.ac.at, ^(c)dietmar.wiegand@tuwien.ac.at,

^(d)nikolas.popper@drahtwarenhandlung.at, ^(e)gerald.hodecek@tuwien.ac.at

ABSTRACT

The main focus of this work lies in developing a simulation system that can represent several different points of view in the world defined by a university campus. The primary focus is on the utilization of spaces as well as the capacity utilization and the ability to test different measures to improve both. But these measures should have no negative impact on the quality of the university teaching from the students' point of view.

Keywords: utilization analysis, space management

1. INTRODUCTION

This work focuses on developing a simulation system that can be used to study and evaluate different points of views in the world of a university campus. The strategies for the assignment of spaces to lectures as well as the capacity utilization of rooms and the ability to test different measures to improve both are included in the main usability. But at the same time these measures should have no negative impact on the quality of the university teaching from the students' point of view.

Opposite to several other approaches used to solve the problem of limited space resources at a university that quite often focus on the timetabling problem (S. Abdennadher, M. Marte 2000),(Beyrouthy C., Burke E.K., McCollum B., McMullan P., Landa-Silva D., Parkes A. 2006) this approach focuses mainly on the facility management point of view (D. Wiegand 2005). The problem of generating a timetable for lectures and courses is not the center of interest for this simulation tool. It uses the existing timetable as a basis to evaluate the current situation according to room utilization and room capacity utilization. It also identifies potential solutions that may result in a room assignment that frees space that seemed to be occupied. Possible modifications that can be generated automatically to the given schedule are time shifts within intervals that can be set by the user and the splitting of a lecture into two

parallel events. Further changes to the timetable can only be done with user interactivity. One major condition to be considered that proved to be a major constraint was to not decrease the quality of teaching. That means that the impact of possible modifications to the time schedule on the students has to be reflected in the simulation result.

Instead of trying to generate a timetable to increase the utility of rooms the emphasis of this work lays in the analysis of the space management and the assignment of rooms to lectures is modeled in great detail. Using discrete event simulation in the field of facility management is still a relatively new concept (D. Wiegand, P. Mebes, V. Pichler, 2006). The simulation of the room assignment over time including aspects of the facility management was modeled using a discrete event simulation approach, enabling the user to experiment with changes to the space management rules, including the major aspects of facility management. The integration of other critical aspects required further additions to the model: For the assessment of the quality of the space management and the resulting room assignment students are integrated in the system. These students have a timetable according to their field of study and personal attributes. They behave individually, as they decide which lectures to attend according to their own as well as the lectures characteristics. These students are designed to act as they would in real life, attending lectures, courses and exams and testing the feasibility of the calculated room assignment. It also accounts for the factor of walking times between lectures where a room change is necessary into consideration. All this strongly suggested using an agent based approach. The simulation tool used for implementing the discrete events model is generally suited to also implement an agent based approach (S. Tauböck, F. Breiteneker 2005). But the combination of both approaches as well as the high number of students simulated quickly enforced a split into two different models that interact via a simulation database.

2. BOOKING PROCESS

The first step was to develop a database driven, event based simulation model to simulate the university campus and all events taking place.

A campus is considered to consist of several buildings that may be quite wide spread. Buildings contain rooms that are used for lectures and courses that may be attended by students. This already describes the main components that need to be modeled: Buildings are basically defined by their position and the distance between them. They contain rooms that represent the spaces that can be booked for events. These rooms have a number of attributes that make them usable for certain kinds of events as well as a position within the building. The attributes cover the capacity that depends on the seating as well as the equipment the room provides.

To identify measures that have positive impact on the utilization of spaces the process of assigning spaces to events has to be implemented meticulously but configurable to allow the testing and experimenting with alternative strategies. To represent the booking process a booking manager with variable behavior is modeled. The parameters for this behavior include a selection of different rules that need to be applied for the selection of a room for a certain course, allowances that can be made according to room size or equipment and changes in the behavior that should arise with time or during a particular situation. These parameters define a basically rather rigid set of rules that may ease in the case of a shortage of available space.

The MoreSpace simulation model uses three different data sets as a basis or a simulation run: the list of all events that need a room to be assigned, all information regarding the lecture halls and their status and the information about the number of students attending a course.

The MoreSpace simulation uses this data for calculating a suggestion for the assignment of rooms to these events according to the selected booking management rules. The booking rules define which type of event will be considered of higher priority and therefore will be handled by the booking manager first. It also determines the basic demands a certain event type may have on the setup of the room. The assignment of rooms to events takes place during the whole simulation time – for a University the major part of the room assignment will take place before the semester starts. The simulation tool offers the possibility to use the strategy of pooling opposed to the usual first come first serve policy. That in itself proves to have quite an impact as it allows coordinating the room assignment in a much more efficient way: At the time of actually assigning the rooms the complete situation the overall demand on space is already known.

The simulation of the booking process leads to successful and not successful booking attempts, as not

always a solution can be found where all demands can be fulfilled. Other results are i.e. the utilization of rooms as well as the capacity utilization.

3. STUDENT BEHAVIOR

For the assessment of a tested strategy not only the utilization of spaces but also the impact on the quality of teaching from the students' point of view has to be considered. This is done by actually simulating the students as well. The student behavior can be reduced to two abilities that are of interest for this model: to attend lectures and to move through the campus.

The number of students attending a certain course is an important but generally unknown number. It directly influences the selection of the room as it defines the demand of capacity. But until the course actually starts the number remains unknown. It can be estimated based on the experience of the prior years but this is an ability that only lies with the lecturer. The simulation model needs data and formulas to calculate the expected number of students.

Reviewing the data that could be provided including the number of students enrolled and the number of exams taken for each course did show a certain trend but also indicated another facet to this problem that had to be taken into account: not all lectures are attended by exactly the same students, even within one field of study and semester. In reality a pool of students exists who are enrolled for this certain study and semester and if a lecture takes place some of them will attend it, but not necessarily all of them.

The group that attends one lecture usually is not exactly the same as the group that attends the next one. Fluctuations can be due to personal reasons of the single students or the overlap of two lectures or some unknown reason. Generally students from other fields of study may join the group attending due to their interest in this subject.

To deal with these fluctuations an agent based approach was developed. Students are considered as single individuals with their own behavior that is influenced by their chosen field of study and their progress. Students also have their individual factor of diligence and a certain willingness to move between rooms. These factors define the basic make up of the single students: they affect the decision to remain in the current lecture or to leave early to be in time for the next lecture in the case of overlapping events. It also might result in not attending a lecture if the way between to spaces is too long. The factors also specify the number of courses a certain student will attend during the semester.

Concerning courses several facts are known:

- They can be distinguished in mandatory and non mandatory courses

- Courses in bachelor studies have a higher attendance rate than courses during later semesters
- The number of students attending usually goes down during the semester

Based on the attributes of lectures and courses and the behavioral factors of the students the selections of events they may attend are set. Whether a student actually attends a lecture during the semester is determined shortly before it takes place based on the current 'mood' of the student - this mood is composed of the individual factors, the attributes of the event in question, the current situation of the system and certain randomness.

Moving between lectures proved to be a not-negligible factor for the contemplation of the campus as a whole. On the one hand the time it takes a student to move between two spaces can be considerable as the campus can be quite wide spread and this influences the decision making of students. On the other hand it showed that during times of high utilization of spaces the time for these movements increased considerably as the corridors in the buildings are full of people as shown in Figure 1.

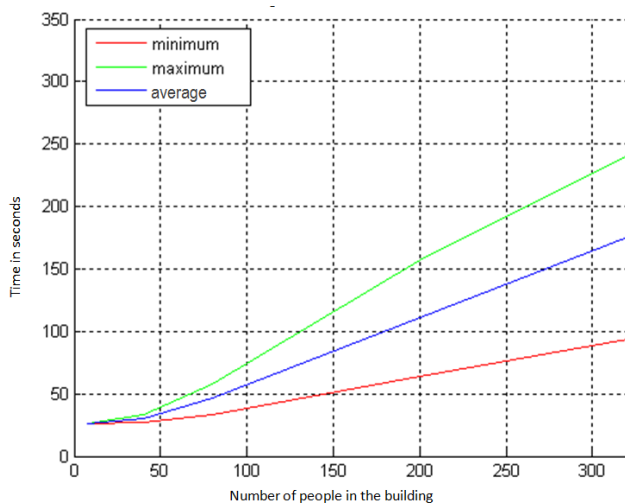


Figure 1: Walking time from room HS1 to room HS2

4. IMPLEMENTATION

Due to the fact that very different requirements must be met by the different parts of the simulation system different modeling approaches are used. The booking process is realized using an event based modeling approach, where each course or lecture is assigned a certain space. The first prototype was implemented in Enterprise Dynamics (Bruckner M., Tauböck S., Wiegand D., Emrich S., Zerlauth S. 2010), to further enhance performance and flexibility the model was further enhanced in details concerning the facility management and then re-implemented in JAVA.

The student simulation uses an agent based approach – in the prototype this was partly integrated in the Enterprise Dynamics simulation model, resulting in a model where agents were integrated into an event based system. Only the movement of students between rooms was calculated in a JAVA model that was connected to the Enterprise Dynamics model moving students between these two models at every entry or leaving of a room (Bruckner et al 2010). In the next step these two models were separated. The process of assigning spaces could be regarded as completely independent from the student simulation. Therefore the simulation models are kept separate; the result of the booking simulation becomes one of the inputs for the student simulation.

The student simulation itself can be run in two different modes: the calculation of travelling times between rooms can be done during the simulation run, enforcing a very exact calculation and therefore resulting in a very high computational effort. It can also run based on prior results regarding the travelling times, allowing much faster calculation in cases where no changes to the travelling times are expected.

5. CONTROLLING THE COMPONENTS

The simulation system is divided into the simulation of the booking process, the student simulation and the simulation of travelling times. All simulation models are controlled by a database that contains the underlying data structure. To enhance reusability of the model the main design is kept as generic as possible.

The goal was to create a system that can be applied to other universities and similar facilities without much further development. Buildings and rooms have attributes that can be adjusted to fit any particular campus or room structure. Courses and lectures can be used arbitrarily to represent any event that takes a certain length of time and needs a certain kind of room. Students and their attributes may represent any person attending an event. The parameterization to create such a system is done via a graphical user interface that is used to define scenarios and experiments. Scenarios contain the basic getup of the simulated system including the definition of the building and room structure, events that will take place and the rules for the assignment of events to spaces. Experiments can be used to change parameters and run experiments within the predefined scenario.

The database acts as the connecting element between the individual models. It contains the input data for the booking simulation as well as its results. These data is provided to the student simulation. The graphical user interface, the scenario manager, allows editing of parameters and controlling the simulation run. It also offers a wide range of analysis tool that have been developed to assess the results of simulation experiments.

6. RESULTS OF THE MORESPACE SIMULATION

6.1. Utilization of Lecture Rooms

This data shows the number of hours each lecture room was booked by the booking procedure. This shows the theoretical utilization, the time the room is booked, but not the time the room is truly used. As past experiences have shown sometimes rooms may be booked for a lecture that does not take place.

Figure 2 shows the utilization of rooms in comparison to the available space separated into room categories.

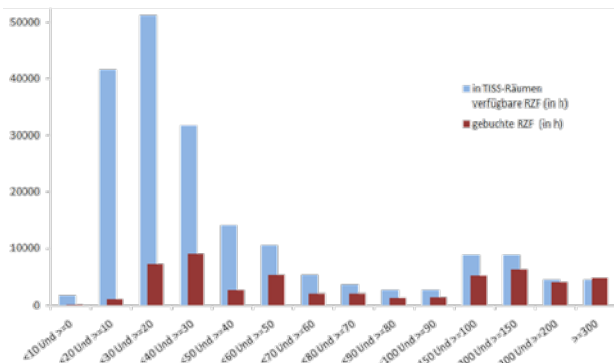


Figure 2: Room Utilization

6.2. Capacity Utilization of Lecture Rooms

This data shows how many students did attend a lecture in the simulation. The number expected is given; the according number of students is assigned. If the number of attending is lower than that it hints at a problem at the accessibility of the course.

6.3. Not Booked Events

The booking procedure tries to find a lecture room for each lecture planned. If it is not able to assign a room the according lecture is listed in this data. For the comparison of several simulation runs one has to make a distinct decision on which aspect to focus the attention.

Depending on this the key data has to be selected. The following example shown in Figure 3 illustrates how easily data can be misinterpreted in the comparison of two scenarios:

Scenario 1: 1 lecture from 11.00 to 15.30 for 56 students could not be booked in any lecture room.

Scenario 2: 2 lectures from 10.00 to 11.30 for 23 students and from 15.00 to 16.00 for 41 students could not be booked in any lecture room.

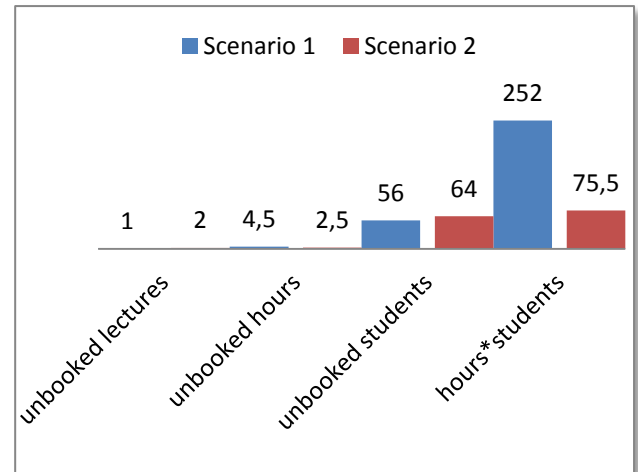


Figure 3: Key Data for Not Successful Booking

This demonstrates the importance of defining the correct key data; Depending on which value is considered the assessment of the simulation results can be interpreted completely different.

Considering the number of not booked lectures Scenario 1 seems to deliver the better result. The number of not booked hours quickly shows another picture: where in scenario 2 both lectures together result in 2.5 hours that could not find a room, Scenario 1's 1 lecture requires 4.4 hours of time.

The picture again changes if one looks at the number of students that cannot attend a lecture without a room: Scenario 1 is the better one in this regard. But taking the hours of lecture each student misses into account Scenario 1 suddenly loses highly against Scenario 2 again.

6.4. Accessibility of Lectures

The accessibility of lectures can be interpreted in two different meanings:

- Temporal accessibility: this indicates if a lecture overlaps with another lecture.
- The spatial accessibility indicates if a lecture can be reached in time: this considers lectures that take place after each other, even with a time gap between them but the location of the rooms is such, that it is not possible to reach the second lecture on time.

While the first kind can be easily determined by evaluating the given data, the second is much more difficult to estimate: the real time it takes from one lecture hall to another depends on far more than the spatial distance: The density of people moving through the corridors, the waiting time at elevators, the distance to staircases influences the walking time. This makes the evaluation of the spatial accessibility to one of the

simulation results as it is able to deliver far more accurate results than estimation by distance.

7. CUSTOMIZING

To make the potential field of application as wide as possible the effort of reusing the MoreSpace model to a new application for a certain institution needs to be kept to a minimum. This is achieved by breaking down the functionality into separate components that work independently and are linked via a database that configures the single parts and controls their working together. Some of these components are generic enough to be integrated in any application without further adaptation.

Others need to be customized: they offer a wide variety of functionality, that can be selected to be included or excluded as needed. The booking process model is divided into the room layout that is created dynamically at the beginning of the simulation run using generic predefined model objects and the space manager that uses the predefined process for room assignment. The simulation of customers is done in a separate model using an agent based approach; the basic input is the result of the booking process simulation and the room layout data.

The structure of the building and room layout and their attributes are given by the data that is stored in the database in a generic data structure that allows mapping every possible topology to the model elements. Both, model objects and database structure are defined in such a way that there will be no further development necessary to reuse them for different institutions. Only the according data needs to be adapted. This part of the model is included by default in the new application at the customizing process.

The behavior of the space manager is used to simulate alternative booking processes. Findings from surveys at different institutions concerning their booking process have resulted in a set of different rules and regulations that are used at different institutions. These rules have been implemented to be selected during the customizing process to be added to an application.

The behavior of the customers can be easily adapted by using certain parameters. The model of the room layout is generated based on the room layout data.

The customizing process builds the new application containing the room layout and the process definition according to the selected features. This is done using an interface without the need to go into the programming level. All selected components are connected and controlled by the simulation database.

The challenging part of customizing is adapting the MoreSpace importer to the new data. One can assume that every institution has their own data management system and therefore the structure of the

data concerning rooms, buildings, organizational units and also the room assignment plans differ greatly from each other. The basic core of MoreSpace is the simulation database, that contains the data requires for analysis, the basic model data, the input data for the simulation experiments, the result data and the data to be exchanged between the different simulation components.

The database acts as a controlling device that defines the individual simulation models based on the data it contains and exchanges information between two separate simulation models and the analyzing tool. This database is designed to stay the same for any application. The importer is used to map any data sets to the internal data structure that corresponds to the setup of the simulation model.

8. MORESPACE DESIGN

To get a basic understanding of the way the MoreSpace concept works two different terms must be defined: the MoreSpace Scenario and the MoreSpace Experiment. The MoreSpace Scenario is used to specify the concrete application. It contains all information about the buildings and their room layout as well as the list of events and the actual space assignment plan. The scenario includes all input data that is needed to initialize the associated simulation database.

A scenario has at least one user defined experiment. The experiment is used to work with the application by modifying configurable parameters for the booking process that influences the assignment of rooms as well as the parameters concerning the behavior of customers.

The user creates an experiment, selects the input data, defines ranges and co-domains and runs the experiment. The results are stored in the database. The setting of the experiment is done by a dynamic graphical user interface that allows a dynamic setting of user – defined parameters. Every result stored in the database and created by an experiment is reproducible by showing the defined parameters and settings. The results of the experiments in one scenario are also comparable because the input data is provided by the scenario.

9. FIRST EXPERIMENTS WITH MORESPACE

MoreSpace was first developed based on experiences and information collected at the Vienna University of Technology (VUT) and expanded in the next step to be able to fit the requirements of any university, school or similar institution. The basic idea behind MoreSpace is enrooted in the situation of many institutions with inner-city location: while the number of people requiring space increases space itself can only increase up to a certain maximum.

At the VUT this maximum has been reached: during the renovation in the last few years the number of rooms has been increased according to the available

space. There are no further reserves to be used in the inner-city location. A simple mathematical calculation seems to prove that the amount of available square meters in relation to the number of students seems to be more than enough. Still it proves to be difficult to find a room for a lecture at short notice.

MoreSpace covers the analysis of the real system based on the current space management, a simulation of alternative space management and a simulation to verify the quality of the alternative results in regard to the customers. The analysis requires data about the current occupancy of rooms as well as detailed data about the room and building topology. It also takes the organization of the institution into account, especially as it concerns the affiliation of rooms to organizational units and therefore may present a restriction according to room availability.

The simulation of alternative space management offers the possibility to experiment with the process of booking and assigning rooms. It shows the effect of changes in the booking process by repeating the room assignment following the experimental process. The result is an alternative space assignment plan that can be compared to the original or other alternative plans.

To compare the quality of these space assignment plans the simulation of customers attending the events that take place in these rooms delivers additional results in regard to the demands of the customers.

Additionally the data analysis based on the high amount of data collected in the controlling database did not only show potential of improvements but very clearly where these potential lay. It allowed a detailed analysis of the current process as well as alternative approaches.

The amount of high quality data also offers the possibility to support decisions concerning the space resources on a daily basis, an added benefit to the daily decision making process in regard to room assignment.

REFERENCES

- S. Abdennadher, M. Marte, 2000, University course timetabling using constraint handling rules, *Applied Artificial Intelligence: An International Journal Volume 14 Issue 4*, pp 311-325
- Wiegand D., 2005, Entwicklung öffentlicher Gebäude und Dienste. *Der Facility Manager Heft 9*, pp. 60-61
- Bruckner M., Tauböck S., Wiegand D., Emrich S., Zerlauth S., 2010, A Combined Cellular Automata - DEVS Simulation For Room Management With Vacation Times, *Proceedings of the EUROSIM 2010 - 7th Congress on Modelling and Simulation*, pp. 555 – 560, 06.09.2010 - 10.09.2010, Prague, Czech Republic
- S. Tauböck, F. Breitenecker, 2005, Simulation of Pedestrian Dynamics in Discrete Event Simulation Systems, *Proceedings IEEE - ERK 14th International Electrotechnical and Computer Science Conference*, Portoroz, Slovenia
- Beyrouthy C., Burke E.K., McCollum B., McMullan P., Landa-Silva D., Parkes A., 2006, Towards improving the utilisation of university teaching space. *Technical Report NOTTCS-TR-2006-5, School of Computer Science & IT, University of Nottingham*
- D. Wiegand, P. Mebes, V. Pichler, 2006, Real Estate und Facility Management – neue Anwendungsbereiche für diskrete ereignisgesteuerte Simulationen. *Proceedings zur ASIM 2006, 19. Symposium Simulationstechnik*, pp. 15-20, 2.–14. September 2006, Hannover, Germany

AUTHORS BIOGRAPHY

Shabnam Michèle Tauböck studied applied mathematics at the Vienna University of Technology. In 2012 she received her PHD for her work in integrating agents in DEVS systems. Her work focuses on using agent based approaches in combination with DEVS in the field of logistic and process optimization.

Felix Breitenecker got a PhD in Applied Mathematics at Vienna University of Technology. After work as research assistant (with habilitation) and guest professor at University Glasgow, Clausthal-Zellerfeld and Hamburg he became Professor at Vienna University of Technology. There he deals with modeling and simulation in research and education in an interdisciplinary area. He has been active in ASIM, the German simulation society for more than 20 years. From 1992 to 1999 he held the position of EUROSIM President. He is head of ARGESIM, a working group providing infrastructure for ASIM, EUROSIM and other simulation activities. He has published three books and more than 200 scientific publications.

Dietmar Wiegand is professor at the Vienna University of Technology at the Institute for Urban Design and Landscape Architecture. His work focuses on research and teaching in the areas of Real estate project development and project management.

Nikolas Popper is working on his PHD at the Vienna University of Technology. He is manager of dwh simulation services and has worked in a wide area of applications in modeling and simulation.

Gerald Hodecek is Head of Facility Management at the Vienna University of Technology.

A SIMULATION MODEL FOR ANALYSING UNMANNED AERIAL VEHICLE FLIGHT PATHS

Halil Cicibas^(a), Kadir Alpaslan Demir^(a), Murat M.Gunal^(b), Nafiz Arica^(a)

^(a) Department of Computer Engineering, Turkish Naval Academy Tuzla, Istanbul, Turkiye

^(b) Department of Industrial Engineering, Turkish Naval Academy Tuzla, Istanbul, Turkiye

^(a) halilcicibas@gmail.com; kadiralpaslandemir@gmail.com; narica@dho.edu.tr, ^(b) mgunal@dho.edu.tr

ABSTRACT

Unmanned Aerial Vehicles (UAVs) are used in a variety of operations in civilian and military domains including search and rescue, surveillance, monitoring, cadastral surveys, and package transportation. Although technological achievements in UAVs made them more intelligent than they were in the past, there is still human factor affecting their operations. Particularly in path planning, operators can improve effectiveness and efficiency of the mission by controlling static and dynamic criteria before the flight and during the flight. However, existence of multiple criteria has made the path planning a difficult task that operators can hardly achieve an optimal path for an UAV. In this paper, we propose a simulation model which can help UAV operators and planners achieve optimal paths. Our model considers environmental factors, performance limitations, basic aviation rules and UAV user requirements.

Keywords: Unmanned Aerial Vehicles (UAV), path planning, A Star Algorithm

1. INTRODUCTION

Intelligent machines have made human life easier than they made in the past. For example, Unmanned Aerial Vehicles (UAVs) are being used for high risk and high cost air-based tasks such as military surveillance, search and rescue, and geographical surveys. However currently, most UAVs are remote-controlled and require a human operator. Therefore, a considerable amount of studies conducted in the UAV domain focus on increasing the level of UAV intelligence and providing more capabilities. Enabling UAVs with autonomous path planning is a key research area in developing intelligent UAVs. Autonomous path planning is defined as the onboard capability of finding navigable sequence of waypoints from an initial location to a target location which minimizes the pre-defined path costs while satisfying several requirements. In addition to increasing the autonomy level of UAVs, autonomous path planning provides continuous satisfaction of flight requirements and objectives in a dynamic operational environment. It also increases the reliability of UAVs

in case of system and communication failure in remote control (Wu et al 2009).

There is extensive literature on UAV autonomous path planning that address several constraints such as flight dynamics, obstacles and environmental factors. However, most of the studies do not address UAV domain-specific operational issues such as employment considerations and aviation rules. Furthermore, most studies are unable to propose solutions to generate suitable and realistic paths that satisfy UAV mission requirements.

We aim to develop a multi-criteria path planning simulation model for Medium Altitude Long Endurance (MALE) UAVs. The model generates paths for online and offline UAV employment. Our model extends the existing models (Wu 2006, Pettersson 2006, Qi 2010, Nikolos 2003) by placing a special emphasis on aviation rules and employment considerations. The distinction of our study compared to the others is that our research includes criteria that are either new or only covered in a few studies. Our simulation model aids in offline and online planning of optimal paths in terms of time, distance and fuel consumption, while taking the described flight criteria, environmental factors, performance limitations, basic aviation rules and UAV user requirements into account. In our study, we also investigated the behavior of various A* based path search algorithms by comparing them in different operational environments.

2. BACKGROUND INFORMATION

UAV path planning problem is a vehicle motion-planning problem under some constraints. It has significant differences from traditional mobile vehicles and manipulator robots (Goerzen 2009). UAV path planning problem is defined as a multi-objective, decision making problem that must take into account flight rules, mission efficiency, operational constraints, environmental conditions and flight limitations.

Modeling for path planning requires a way of representation of the world and its contents. "World space" is defined as the physical space, which contains the vehicle, start location, target location, and obstacles. It is divided into two regions as free-space and obstacle-space (Latombe 1991, LaValle 2006). Free-space

defines the area through which the vehicle can move without collision. Obstacle-space is a set of points that lead to a collision between the vehicle and the obstacle (Hwang and Ahuja 1992). A “configuration” is a vector of parameters defining the shape of the vehicle in the world space. A configuration that is coupled with its rate of change is called a “state”.

These are two types of constraints in the world space: environmental and motion. While environmental constraints consist of obstacles or meteorological factors such as wind or icing; motion constraints defines the maneuver limitations of the vehicle such as climb rate or turning capability. In our study, we use the terms “flight criteria” and “flight objective” instead of “constraints”. While flight objectives are the elements of cost function, flight criteria are the variables that must be implemented for flight safety and mission efficiency during flight.

Path planning in robotics has two major approaches. Although the first approach, combinatorial planning, gives optimal solutions, it is impractical since its computational complexity is high. The second approach, sampling based planning, is preferred since it is a sampling based planning and known to be superior for its efficiency, practicality, and simplicity in high dimensional environments.

Collision Detection (CD) and roadmap generation are the two other terminologies in sampling based path planning. CD algorithms are used to detect obstacles on the path. Roadmap generation is the constructing of a search tree or graph with connecting samples in free space.

Finally, it is noteworthy to mention the UAV path planning flight criteria that are considered in the literature. These are geographical structures, buildings, danger zones, above ground level rules, cruise level rules, mobile objects, cloud, mobile targets, mobile threats, wind, approach angle, and flight dynamics. Additionally, the flight objectives are generally based on distance, time, fuel consumption, risk, path smoothness, and hidability.

3. CONCEPTUAL MODEL

3.1. World Space and Roadmap Generation

Operational environment is represented with a regular grid sampling method. Every sample is represented by a cube in the world space that contains data related to the operational environment. Grid size of the sample cubes defines the level of detail in grids. The number of cubes increases process time and search time significantly.

The size of the sample cubes is determined based on UAV flight performance capabilities and maneuver limitations. Turn radius and ascend/descend angle are the main parameters to identify horizontal and vertical length of sample cubes respectively. In our model, the size of the grid is set depending on the tactical range of the UAV, maximum fly altitude and computational limitations.

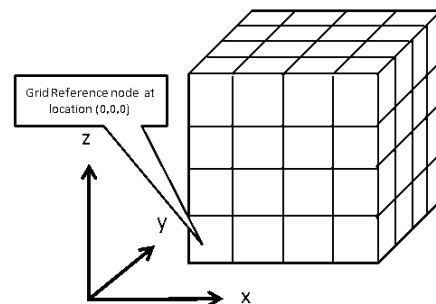


Figure 1: Grid based world space

Each node in the grid has the following fields;

- Latitude/Longitude
- Above Ground Altitude
- Above Mean Sea Level Altitude
- Time Moment
- Wind speed and direction
- Start or Target Indicator Flag
- Obstacle Space Indication Flag
- Cloud Indicator Flag

These fields are initialized with default parameters and then updated based on the information collected from the environment. Furthermore, nodes have additional fields to store the parent node and child nodes. These fields are filled in during adjacency creation process.

When the world space is represented as a 2D or a 3D grid then an algorithm can be applied to find a path in the grid. After moving forward one step on the path, if any change occurs in the operational environment, the path is re-calculated based on the updated grid until the vehicle reaches the goal state. Although this iterative approach runs faster, it produces inconsistent and costly paths in dynamic environments, because this approach is unable to predict the future status of the search space. However, advances in the sensor technology made the UAV's predict ahead in time and therefore it is possible to plan the least cost paths in time varying environments. This can be represented with a “4 dimensional grid (4D)” where the fourth dimension is the time.

4D grid consists of future status of mobile objects and dynamic criteria parameters in the world space. It can be expressed as a combination of 3D grids that represent an instant status of the world space in a time moment. Each time interval (Δt) between moments is equal to a specific duration. This duration is identified from UAV performance specifications and it is measured as the time elapsed during the travel from one hop to another hop, in other words from a parent node to a child node.

In 4D grid generation, as shown briefly in Figure 2, the first step is to detect movements of moving targets and to sense environmental factors. Based on this data, future locations are estimated and projected to 3D grid. These are then combined with 4D grid and least-cost paths are calculated. The UAV proceeds to the next grid. This whole process is repeated until the UAV reaches to the destination.

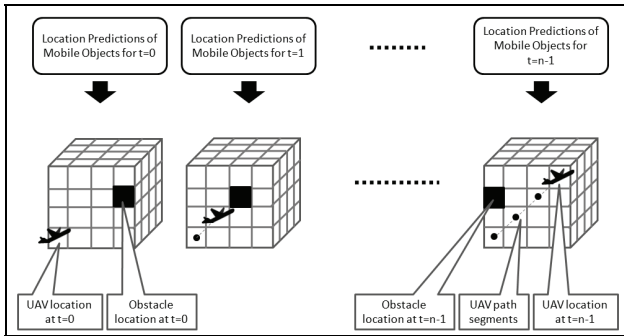
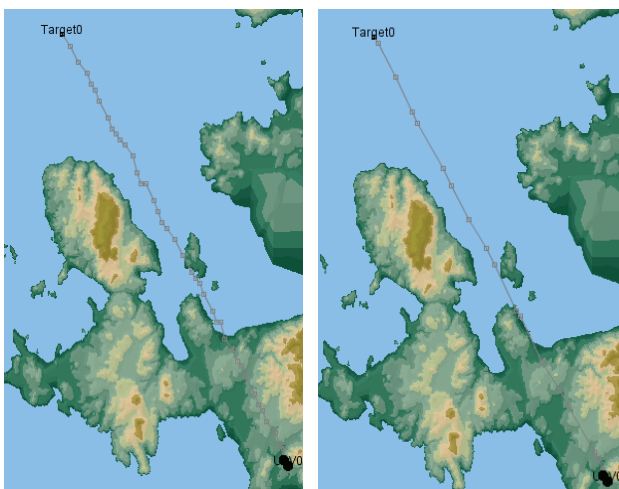


Figure 2: 4D Grid generation

In the roadmap generation phase of the model, multi-resolution grids are used. This is done based on a successor operator. After the partitioning process, the model checks the flag parameters of every node in the regions. If any node in a region is an obstacle node, the model identifies this region as a high-resolution region. Otherwise, the region is classified as a low-resolution region. In other words, the regions without obstacles are marked as low resolution regions.

The distance between node pairs in the high-resolution regions is defined with a successor vector. Nodes in the range of successor distance are adjacency candidate nodes. Successor-based adjacencies provide multiple angular turns for UAVs. Thus, path optimality and path smoothness are achieved in the model. Although multiple angular turns ensure optimality and smoothness, in some cases it may increase computational complexity and graph size. Therefore, there is a trade-off between successor length and computational time. Note that adjacency generation time increases by the successor length, however long successors provide finding least cost paths and more smooth paths compared to a shorter ones. Figure 3 shows how a path changes when max. successor length changes.



Max Successor Length=3 Max Successor Length=12
Figure 3: Paths with different successor lengths

Adjacency creation procedure works as follows; the grid is divided into regions as low and high

resolution. Depending on the node the UAV is located currently, successor length is determined for each node. The nodes are then connected and a graph is formed. Obstacle space indicator of every node pairs are then check to remove the links between obstacle nodes. Travel time is calculated and finally adjacency relations are added to the world space.

3.2. Flight Criteria and Flight Objectives

In our model we have two types of flight criteria that we considered; static and dynamic. Static criteria do not change in time and therefore there is no need to update the locations and other properties during flight time. These include geographical structures, buildings, danger areas, above ground level (AGL) rule, and cruise level rule.

For the geographical structures, the terrain is represented as an obstacle that the UAV cannot pass through. We obtain terrain elevations from Digital Terrain Elevation Data Level 1 (DTED L1) maps. Buildings are represented with polygons which the size and location information are gathered from geographic terrain elevation databases. A danger area is a land region that poses any kind of threat to UAV flight. For example, an anti-air defense system is a kind of threat that a military UAV should stay out of its range. We make a distinction between the aerial threats and the threats on the ground. Danger areas are related to threats found on the ground. In our model, we draw a half-sphere on the location of the threat. The center of this virtual sphere corresponds to the location of the threat.

Dynamic flight criteria include mobile obstacles, mobile threats, mobile targets, cloud, and wind. Properties of these criteria may change in time and therefore the locations and properties of the dynamic criteria should be updated in time until UAV reaches its goal location. The model calculates the future locations of the dynamic criteria based on historical information obtained with UAV sensors.

Other aircrafts in the operational environment are referred as mobile obstacles. Our model prevents the UAV from colliding with other aircrafts by marking mobile obstacles as “obstacle space” in the world space. For the representation of mobile obstacles, flying objects are mapped into cylindrical shapes which the dimensions of the cylinders around mobile targets are computed in such a way that UAV is able to maneuver at an adequate distance to a safe course to avoid a collision with the mobile target.

Clouds may prevent UAVs to accomplish some of its missions such as reconnaissance via photographing or video capturing. In such circumstances, to increase detection quality, UAVs should descend to lower altitudes below the floor level of clouds. Our model enhances mission efficiency by enabling UAVs to go under clouds when the weather is cloudy above the target location. At other times during flight, the UAV can fly through clouds. We represent the clouds with polygonal and cylindrical shapes. Likewise, wind is a significant factor for UAVs’ path planning. In our

model, we assume that in the operational environment there are wind fields with a constant speed and direction.

The objective of the model is to find minimum cost paths in terms of time, distance, and fuel consumption. These terms are included in the objective function with different weights that are determined based on the mission requirements. Details are as follows;

- Flight distance: Distance is a widely used flight objective in similar studies as it can be calculated with simple algorithms. In our model, it is calculated as Euclidian distance such as;

$$f_{dist(s_i, s_j)} = \sqrt{(x_i - x_j)^2 + (y_i - y_j)^2 + (z_i - z_j)^2}$$

- Flight time: Although distance and time objectives seem alike, flight time is not just a function of distance since wind vector effects the flight time. In order to calculate the time cost, we use the following equation. The equation finds the cost of each trajectory between node pairs based on distance and resultant vector of UAV engine and wind speed. \vec{v}_c is UAV engine speed, and \vec{v}_w is wind speed.

$$f_{time(s_i, s_j)} = \frac{f_{dist(s_i, s_j)}}{\left| \begin{matrix} \vec{v}_c & \vec{v}_w \\ \rightarrow & \rightarrow \end{matrix} \right|}$$

- Fuel consumption: We construct a fuel consumption model for the UAV based on EngineSim (NASA, 2012). The UAV uses maximum throttle for climbs, minimum throttle for descents and optimum throttle for the cruise. Similar to aircraft engines, our UAV consumes less fuel in higher altitudes and in lower speeds. Fuel consumption is calculated as follows;

$$F_{fuel}(x_{alt}, x_{spd}, x_{temp}, x_{payload}, x_{rate}) = g(f_{alt}(x_{alt}), f_{spd}(x_{spd}), f_{temp}(x_{temp}), f_{payload}(x_{payload}), f_{rate}(x_{rate}))$$

where $f_{alt}(x_{alt})$ is the fuel consumption at altitude x , $f_{spd}(x_{spd})$ is the fuel consumption at speed x , $f_{temp}(x_{temp})$ is the fuel consumption at temp x , $f_{payload}(x_{payload})$ is the fuel consumption at payload x and $f_{rate}(x_{rate})$ is the fuel consumption at rate x .

4. SIMULATION MODEL

Based on the conceptual model described in the previous section, a simulation model is built in Java using Simkit (Buss 2001) and OpenMap (OpenMap 2012) APIs. Simkit is a Discrete Event Simulation (DES) API in Java and works with Event Scheduling

DES approach. OpenMap is also in Java and an open source Geographical Information System which can process geographical data such as elevations. Gunal (2010) is a latest example of how these two packages can work together.

4.1. Flow of Simulation

Movements of external system entities are handled by methods provided with Simkit. Movement behaviors include start, stop, pause, and accelerate. OpenMap is used to visualize generated paths. A screenshot is shown in Figure 4. It also enables to easily visualize the terrain structure and simulated entities.

Since the simulation provides the movements of entities, static and dynamic criteria parameters are calculated to predict mobile object locations beforehand. This causes the 3D grid to be searchable for a path. In our simulation we used A* algorithm to find the shortest path.

4.2. Inputs

In our model we have three groups of inputs; UAV, Environment, External Systems' parameters.

UAV parameters are;

- weight,
- payload,
- endurance,
- max.speed,
- max.flight
- altitude,
- tactical range,
- fuel consumption,
- turn radius,
- ascend/descend rate.

Environmental parameters are;

- Field size,
- Wind direction and speed,
- Cloud origin,
- Temperature,
- Number of regions,
- High and low resolution,
- Goal and start location altitudes,
- Rules and safe limits.

External systems' parameters are;

- Number of threats,
- Number of aircrafts,
- Mobile target speed,
- Mobile aircraft speed.

4.3. Outputs

Since we wanted to examine the model's performance, our main output variables are grid generation time and search time. Additionally we looked at the path cost for the three objectives; distance, time, and fuel.

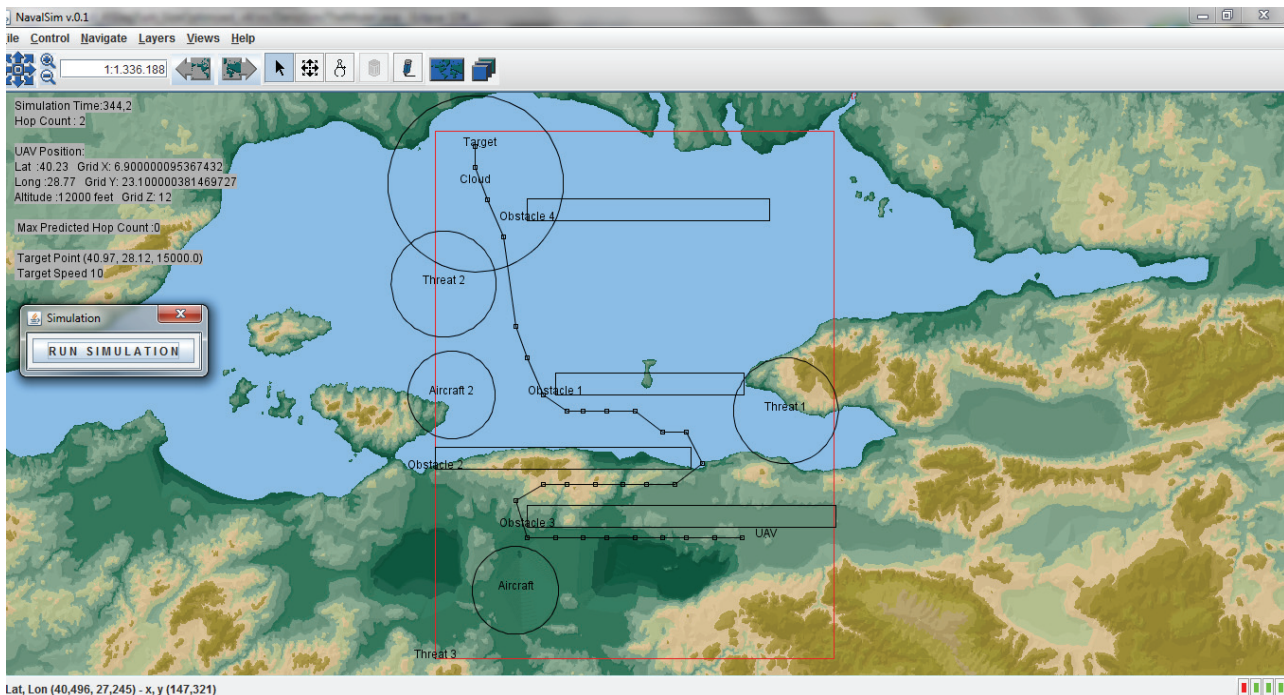


Figure 4: Simulation screen

5. EXPERIMENTAL RESULTS

The model is evaluated with various scenarios containing both static criteria and dynamic criteria. The simulations are conducted with a personal computer (PC) with 2.93 GHz Intel i5 processor and 3 GB RAM. The world space is represented in a 60nm*60nm*31000ft*10t grid which is sampled with nodes in a dimension of 2nm*2nm*1000ft. In Figure 4, dotted line represents UAV optimal path, which is from south to north. Other shapes in the figure represent obstacles such as buildings, threats and aircrafts. UAV geographical location, UAV altitude, target information and simulation parameters are shown in the left side of the OpenMap environment. We created 48 scenarios to achieve the following in our experiments;

- Validate and verify the model in various scenarios,
- Analyze the performance of the model under different constraints,
- Analyze the effects of criteria and grid dimension on path costs,
- Test the modifiability and extendibility properties of the model

Simulation results show that the model is able to generate sensible results. Model architecture provides enhanced modifiability as various scenarios were easily adapted with minor modifications. In addition, the model is able to find collision-free paths in different scenarios. Developed model can generate resolution optimal paths in static and dynamic environments under

different constraints. Besides, it is found that the model reacts properly to the changes in criteria properties and obstacle locations.

We analyzed the simulation performances of 3D and 4D grids in terms of grid generation time and search time in various scenarios for different flight objectives (Table 1). Simulation performance results show that target type does not affect grid generation time and search time in 3D and 4D grids. However, the number of obstacles and obstacle sizes are the main factors on grid generation time. In addition, they increase the search time if obstacles are at locations that intersect with UAV flight path. The search time increases as the number of obstacles increase, since search algorithm needs more time while expanding nodes to find the least-cost path. On the other hand, the increase in the number of obstacles decreases grid generation time as search space becomes smaller. In addition, grid generation time and search time is higher in 4D grid. In fuel consumption objective, search time is longer than search times in other objectives as additional parameters are incorporated in the calculation of fuel consumption. In every scenario, UAV moves from south to north. PNF refers to “Path not found” in the tables. Wind speed is zero.

The model finds the same paths in the calculation of time objective and fuel objective in static environments (Scenario 1, 2, 5 and 6). Besides, path costs in static environments are equal in 3D and 4D grid since there is not any mobile objects in the operational

environment. It is also found that, in fuel consumption objective, UAV climbs to an optimal altitude and proceed in this altitude for a while, then descend to target altitude to reduce the fuel consumption.

Scenario	Number Of Static Obstacles	Number Of Dynamic Obstacles	Target Type	Grid Dimension	Distance		Time		Fuel Consumption	
					Grid Generation Time (sec)	Search Time (sec)	Grid Generation Time (sec)	Search Time (sec)	Grid Generation Time (sec)	Search Time (sec)
					1	0	0	S	3D	2
2	0	0	S	4D	23	1	23	1	23	1
3	0	0	M	3D	2	1	2	1	2	1
4	0	0	M	4D	18	1	23	1	25	1
5	4	0	S	3D	1	2	2	2	1	19
6	4	0	S	4D	8	2	9	3	11	66
7	4	0	M	3D	1	2	2	2	1	14
8	4	0	M	4D	8	2	9	3	10	64
9	4	4	S	3D	2	2	1	2	2	21
10	4	4	S	4D	5	2	6	3	5	58
11	4	4	M	3D	2	2	1	2	2	22
12	4	4	M	4D	5	2	6	3	6	63
13	0	4	S	3D	2	1	2	1	2	1
14	0	4	S	4D	20	1	17	1	15	1
15	0	4	M	3D	PNF	PNF	PNF	PNF	PNF	PNF
16	0	4	M	4D	19	1	15	1	15	1

Table 1: Experimental results (M:Mobile, S:Stationary)

6. CONCLUSION

As the use and application areas of UAVs increase, new challenges and issues arise in developing UAVs. Many studies in UAV domain focus on increasing intelligence capability of these systems. The studies aim to provide UAVs with the capability to perform without human interference opposing different adversities. An important challenge in developing more intelligent UAVs is autonomous path planning.

In this paper, we present a multi-criteria path-planning model for UAVs performing in dynamic environments. The main contribution of the study is the development of a path planning model that provides online and offline planning of resolution-complete, smooth and optimal paths while meeting distance, time and fuel consumption objectives in dynamic environments for Medium Altitude High Endurance UAVs (MALE UAVs). We implement flight criteria and objectives in our model based on employment considerations, environmental factors, performance limitations, basic aviation rules and user requirements. In addition, the presented model takes into consideration of operational efficiency presented in UAV Roadmaps. Operational environment is represented with a 4D grid that includes future status of mobile objects. Taking into consideration of possible changes in the operational field would increase path efficiency and provide least cost paths. In our study, we develop a modular architecture that enables integrating various UAV models, environmental parameters, search

algorithms and various flight criteria/objectives with minimum efforts. In the development of the model and simulation, open source tools and environments are utilized. We simulate our model in multiple scenarios. The model is able to find optimal and collision-free paths in static and dynamic environments under several flight constraints.

ACKNOWLEDGMENTS

The views and conclusions contained herein are those of the authors and should not be interpreted as necessarily representing the official policies or endorsements, either expressed or implied, of any affiliated organization or government.

REFERENCES

- Buss A. 2001. Discrete Event Programming with Simkit, Simulation News Europe, August 2001.
- Goerzen, C., Kong, Z., Mettler.B. 2009. A Survey of Motion Planning Algorithms from the Perspective of Autonomous UAV Guidance. Journal of Intelligent and Robotic Systems, 2009.
- Günel M.M. 2010. Notes on Naval Simulation, Technical Report, Turkish Naval Academy, Istanbul 2010.
- Hwang, Y.K., Ahuja, N. 1992. Gross motion planning - a survey. ACM Computing Surveys (CSUR) Volume 24 Issue 3, Sept. 1992.
- Latombe, J.C. 1991. Robot Motion Planning". Kluwer Academic Publishers, Norwell, MA, USA, 1991.
- LaValle, S. M. 2006. Planning Algorithms. Cambridge University Press (also available at <http://msl.cs.uiuc.edu/planning/>).
- Nikolos,I.K., Valavanis,K.P., Tsourveloudis,N.C., Kostaras, A.N. 2003.Volutionary algorithm based offline/online path planner for UAV navigation, IEEE Trans. Systems, Man Cybernetics, vol 33, pt. B, pp. 898-912, Dec. 2003.
- NASA Glenn Research Center (2012) EngineSim Version 1.7a Official Web site: <http://www.grc.nasa.gov/WWW/K-12/airplane/ngnsim.html> [Access Date: 20 May 2012]
- OpenMap. 2012. BBN Technologies, <http://openmap.bbn.com>. Access Date: 20 May 2012
- Pettersson, P. O. 2006. Sampling-based Path Planning for an Autonomous Helicopter, Thesis, Linkoping University.
- Qi, Z., Shao, Z., Ping, Y.S., Hiot,L.M., Leong, Y.K. 2010. An Improved Heuristic Algorithm for UAV Path Planning in 3D Environment, Second International Conference on Intelligent Human-Machine Systems and Cybernetics, 2010
- Wu, P., Campbell, P.Y., Duncan, A., Merz, T. 2009. On-board multiobjective mission planning for unmanned aerial vehicles, In IEEE Aerospace Conference Montana, 2009.
- Wu, P.2006. Multi-Objective Mission Planning in Civil Unmanned Aerial Systems, PhD Thesis, 2009.

MATHEMATICAL MODELLING FOR EXPERIMENTAL ARCHAEOLOGY: CASE STUDIES FOR MECHANICAL TOOLS IN HALLSTATT SALT MINES

Bernhard Heinzl^(a), Erik Auer^(b), Benedikt Slowacki^(c), Kerstin Kowarik^(d), Hans Reschreiter^(e),
Niki Popper^(f), Felix Breitenecker^(g),

^{(a) (b) (c) (g)}Institute for Analysis and Scientific Computing, Vienna University of Technology

^{(d) (e)}Natural History Museum Vienna, Austria

^{(a) (f)}dwh Simulation Services, Vienna

^(a)bernhard.heinzl@tuwien.ac.at, ^(b)e0926305@student.tuwien.ac.at, ^(c)e0825658@student.tuwien.ac.at,
^(d)kerstin.kowarik@nhm-wien.ac.at, ^(e)hans.reschreiter@nhm-wien.ac.at, ^(f)niki.popper@drahtwarenhandlung.at,
^(g)felix.breitenecker@tuwien.ac.at,

ABSTRACT

In a cooperative project between the Natural History Museum Vienna and the Vienna University of Technology, students are assigned a variety of tasks in modelling and simulation of physical systems. These systems originate from archaeological investigations on the prehistoric salt mines in Hallstatt (Austria) in the Bronze Age. The first example studies different designs of rope pull systems used to hoist the broken salt from the mining halls through shafts to the surface. In the second task, bronze picks for breaking the salt are investigated. The third and last task presents some calculations regarding illumination and air consumption in the mining halls. The calculations and simulation results help archaeologists gain knowledge about the working conditions and technical equipment in the prehistoric salt mines. For the students, the provided examples give interesting insights into practical applications of modelling and simulation.

Keywords: mechanical systems, teaching, mathematical modelling, archaeology

1. INTRODUCTION

The prehistoric salt mines of Hallstatt in Austria are subject of great interest for archaeologists. Salt mining activities are dated to 1458-1245 B.C. in the Bronze Age (Grabner et al. 2006).

A large amount of archaeological finds of technical equipment and organic materials (timber, wooden tools, strings of bast, fur etc.) and the perfect conditions of preservation in the mines due to the conserving properties of salt allow for a reconstruction of the working process in the mines (Reschreiter et al. 2009).

These investigations suggest that mining was organized in an efficient, nearly industrial manner with highly specialized tools. Salt was mined in underground mining chambers using special bronze picks. The resulting small pieces of salt were then collected in buckets and transported to the vertical shaft where it was

hoisted to the surface using a wool sack or cloth attached to a linden bast rope (Kowarik et al. 2012).

The high degree of specialization and functionality observable on certain tools and the design for high efficiency suggest that the workforce had highly specialized knowledge in mining technology and infrastructural processes (Kowarik et al. 2012).

Typically, experimental methods using reconstructions of historical technologies are used in archaeology to provide deeper insights on technological issues. As a new tool, modeling and simulation can also serve as a method for gaining knowledge in different aspects of archaeology.

As part of a collaboration between the Natural History Museum Vienna and the Vienna University of Technology, certain tasks are defined, which were assigned to students as part of their basic training in modelling and simulation. The obtained results will help archaeologists gain knowledge about tools and working processes in the prehistoric salt mines in Hallstatt for a technological reconstruction.

The following sections give a brief description of some current tasks, which investigate certain aspects of the mining process.

2. ROPE PULL SYSTEMS

Rope pull systems were used to hoist the broken salt from the mining halls through shafts to the surface (see figure 1). While there are archaeological findings of bast ropes and other appliances, there are still some matters regarding the construction, length and arrangement of the rope pull systems at issue.

To estimate and compare the time and strength requirements for transporting the salt, various options are investigated using simulation models. For example we compare two variants of the rope design, an open and a closed version, depicted in figure 2. In the closed version, both ends of the rope are connected which enables more uniform distribution of the rope mass and therefore less requirement for external forces. An important issue also concerns modelling of the rope guide, for

which we consider two possibilities, one with sliding friction on a log and one with return pulley.

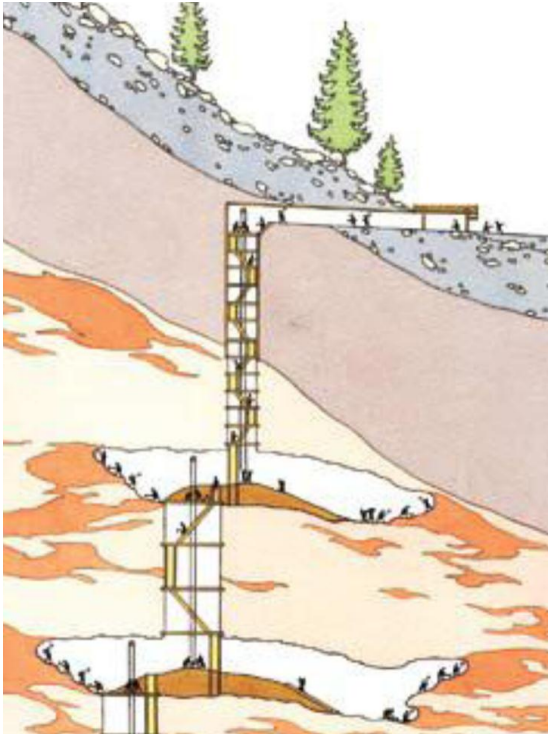


Figure 1: Schematic Reconstruction of the Excavation Chambers and Shaft Structure with Rope Pull Systems (© D. Gröbner, H. Reschreiter, NHM Vienna)

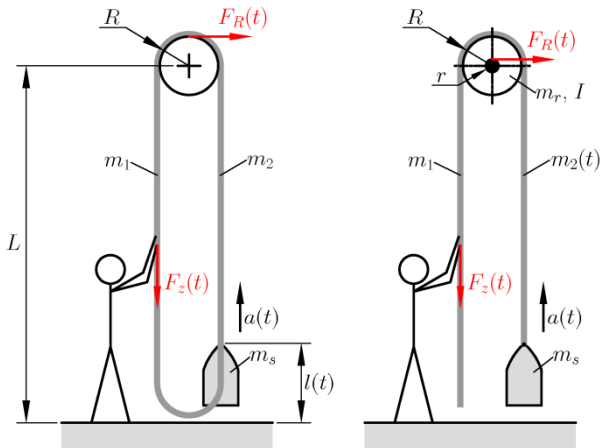


Figure 2: Different Design Options with Closed Rope (Left) or Open Rope (Right) for the Rope Pull System. The Schematic also Shows Two Possibilities for the Rope Guide: Sliding Friction on a Log (Left) and Rotating Return Pulley (Right).

2.1. Rope deflection on a log

Considering simple balance of forces according to figure 2 taking into account mass of the rope on both sides (m_1 and m_2 , resp.) and forces of inertia leads to the following equation:

$$F_z(t) + m_1(g - a(t)) - F_R(t) = m_2(t)(g + a(t)) + m_s(g + a(t)), \quad (1)$$

with external force $F_z(t)$, predefined acceleration $a(t)$ (see equation (4)), acceleration of gravity g and mass of the salt bags m_s . The coulomb friction force $F_R(t)$ is defined as

$$F_R(t) = \mu(v(t))[F_z(t) + m_1(g - a(t)) + m_2(t)(g + a(t)) + m_s(g + a(t))]. \quad (2)$$

The expression in square brackets denotes the total normal force on the log. For the friction coefficient μ , we define the following expression depending on the rope velocity v , also visualized in figure 3:

$$\mu(v) = (\mu_c + (\mu_{brk} - \mu_c) \exp(-c_v|v|) \operatorname{sgn}(v) + fv), \quad (3)$$

with a coulomb friction coefficient μ_c , breakaway friction coefficient μ_{brk} , viscous friction coefficient f and coefficient c_v . This friction model takes into account sticking friction at velocities near zero (μ_{brk}) as well as viscous friction at high velocities (fv).

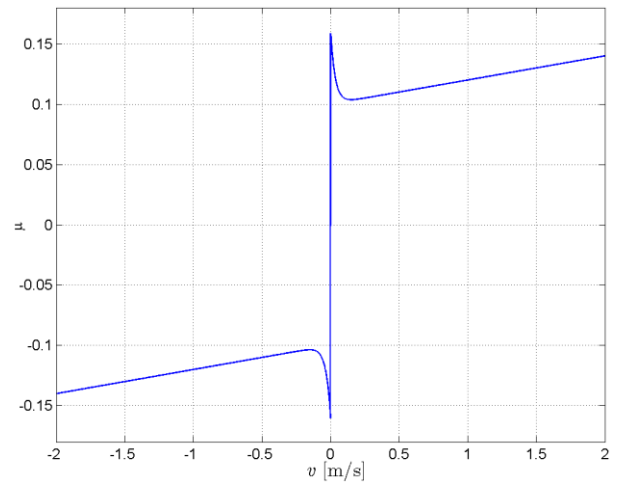


Figure 3: Model of the Friction Coefficient μ with Sticking and Viscous Components for Parameters $\mu_c = 0.1$, $\mu_{brk} = 0.16$, $c_v = 30$ and $f = 1/50$.

In order to determine the forces necessary for hoisting the salt to the surface, the proposed model receives the desired velocity over time as input signal and calculates the necessary external force $F_z(t)$. One possible input signal is depicted in figure 4. It shows a smooth nearly periodic signal with global upward trend.

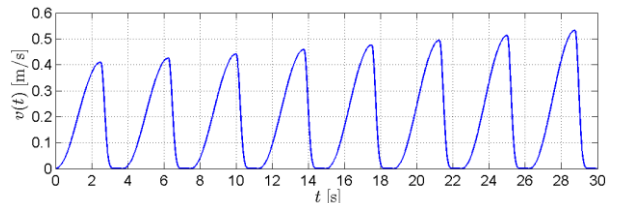


Figure 4: Possible Input Signal $v(t)$ with Smooth Progression and Global Upward Trend.

The external force can then be calculated using equations (1), (2) and (3) and the time derivative

$$a(t) = \frac{d}{dt}v(t) \quad (4)$$

of the input velocity.

For the open rope, the mass $m_2(t)$ of the rope on the right side of the log depends on the current position $l(t)$,

$$m_2(t) = m_{2,0} - \rho l(t), \quad (5)$$

with the assumed density $\rho = 1.5$ kg/m and starting mass $m_{2,0} = \rho L$, and therefore decreases over time according to

$$\frac{d}{dt}m_2(t) = -\rho \frac{d}{dt}l(t) = -\rho v(t) \quad (6)$$

with given input velocity. If the rope is closed (see figure 2 left), then the mass m_2 is constant

$$m_2 = \rho L. \quad (7)$$

In both cases (open and closed rope), the mass m_1 on the left side is assumed constant, also with

$$m_1 = \rho L. \quad (8)$$

The mass of one bag of salt is assumed to be about 28 kg which corresponds to a volume of 20 l. For the value of m_s , one or more bags of salt are considered,

$$m_s = k \cdot 28 \text{ kg}, \quad k = 1, 2, 3, \dots \quad (9)$$

with the number of bags k .

Evaluation of a simulation using the presented equations implemented in MATLAB and parameters $L = 20$ m, $k = 1$ for example for a greased log ($\mu_c = 0.1$, $\mu_{brk} = 0.16$) provide the results given in figure 5. The results show a total duration of about 81 s to hoist one bag of salt over a height of 20 m, maximum external force is about 500 N. The periodic velocity (see figure 4) leads to a pulsating progression of the height $l(t)$.

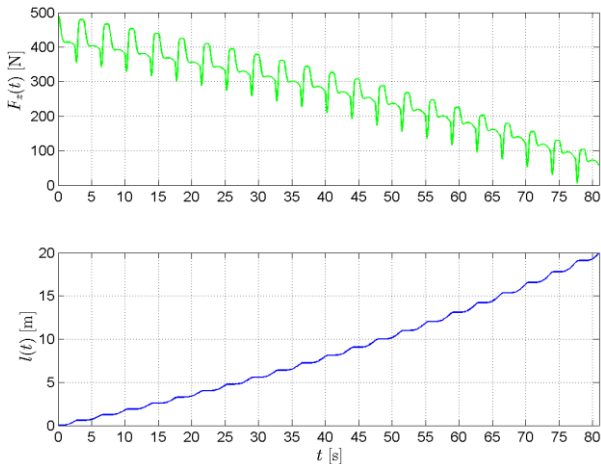


Figure 5: Simulation Results for a Greased Log with Open Rope and $L = 20$ m, $k = 1$.

Similar investigations for different shaft height L as well as different number of bags lead to the results presented in figure 6. It can be seen that each additional bag of salt adds about 400 N to the external force, which is more than the own weight because of additional friction.

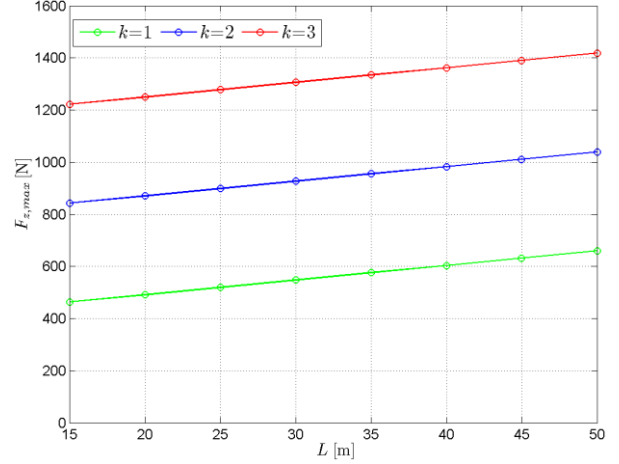


Figure 6: Maximum External Force F_z for the Scenario with Log for Different Shaft Height L and Different Number of Bags k .

2.2. Rope deflection with rotating return pulley

Using a return pulley with outer Radius R and axle radius r instead of a static log adds terms for pulley mass m_r and inertia I to equations (1) and (2), thus, with regard to figure 2, resulting in the new equations

$$F_z(t) + m_1(g - a(t)) - F_R(t) \frac{r}{R} - \frac{Ia(t)}{R^2} = m_2(t)(g + a(t)) + m_s(g + a(t)), \quad (10)$$

$$F_R(t) = \mu(v(t))[F_z(t) + m_1(g - a(t)) + m_2(t)(g + a(t)) + m_s(g + a(t)) + m_r]. \quad (11)$$

Different values can be considered for the parameters of the pulley depending on its material (wood, bronze, etc.). For a pulley made of wood we get for example the following typical parameters:

$$R = 0.6 \text{ m}, \quad r = 0.2 \text{ m}, \quad m_r = 16.3 \text{ kg}, \quad (12)$$

$$I = 3.3 \text{ kgm}^2, \quad \mu_c = 0.06, \quad \mu_{brk} = 0.11.$$

As a simulation result, maximum required external force F_z for the scenario with return pulley and different values for shaft height L and number of bags k is presented in figure 7. Comparison with figure 6 shows significant reduced force requirement due to lower friction.

Figure 8 compares Force input between the version with open rope and with closed rope. Since the moving mass is constant for the variant with closed rope, the required force is also constant in average, whereas in the other case the force requirement decreases steadily.

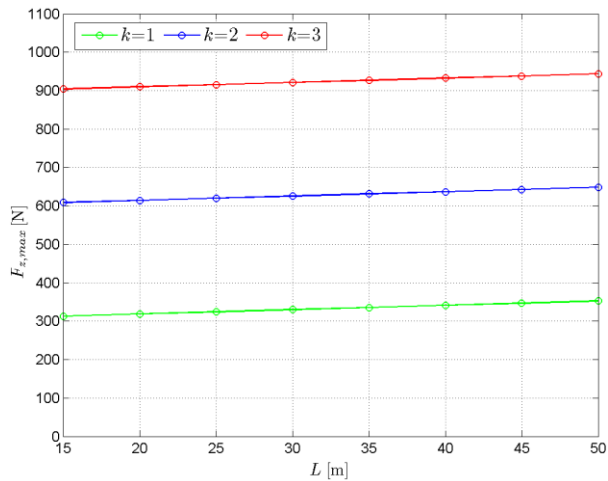


Figure 7: Maximum External Force F_z for the Scenario with Return Pulley for Different Shaft Height L and Different Number of Bags k .

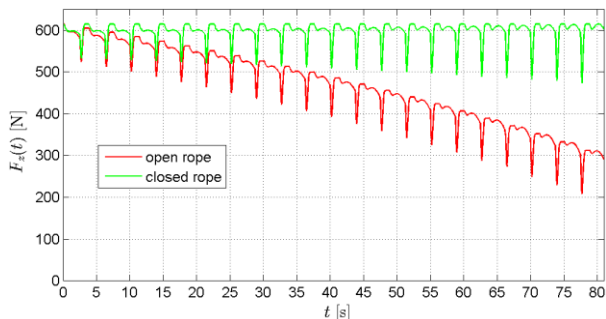


Figure 8: External Force $F_z(t)$ Over Time for the Scenario with Return Pulley and Both Variants of Rope Design.

In summary, it can be said that the simulation results show significant force requirement for the model with sliding friction, especially because of the high mass of the rope. This is also the reason for a limitation regarding the maximum continuous shaft height.

With the presented equations it is also possible to provide the external force $F_z(t)$ and calculate resulting velocity $v(t)$ and position $l(t)$, which will be investigated in further studies.

3. BRONZE PICKS

Salt was mined using bronze picks with wooden handle (see figure 9 left). Highly interesting is the unusual shape of the pick with a typical angle between the shaft and tip of about 55 to 75 degrees. It is believed that this particular shape was adapted to the specific working conditions in the Hallstatt mines, especially since no similar devices have been found at other archaeological sites. The small angle does not allow typical circular hacking motion, which is why it is not yet completely clear exactly how such a pick was used.

Modelling the pick as a rigid body system (figure 9 right) allows evaluation of possible movement scenarios and comparison regarding resulting force and momentum on the tip.

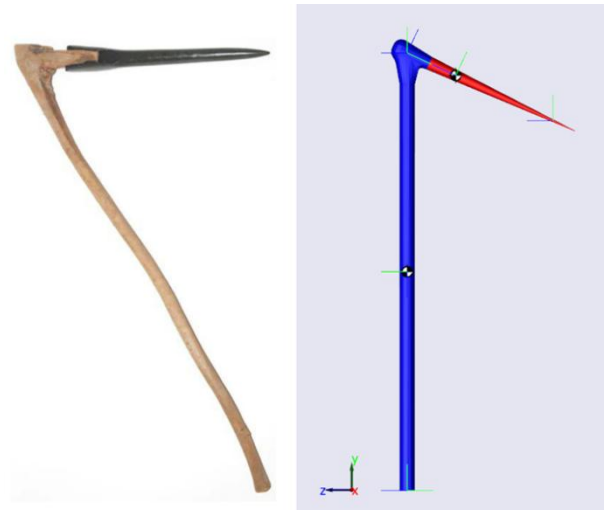


Figure 9: Left: Reconstructed Bronze Age Pick (© A. Rausch, NHM Vienna). Right: Rigid Body Model of the Pick in MATLAB/SimMechanics.

Scenarios of movement are obtained by geometrical considerations, like shown in figure 10. Several points are defined along a trajectory of the tool tip depending on the range of motion for a human. Taking into account the time relation, this trajectory also determines velocity and acceleration behavior. Coordinates for one example trajectory are presented in figure 11. In this figure, impact on the ground occurs at $t = 1$ s. This impact is modeled not as a discontinuous, but as a smoothed transition in velocity.

Special focus is put on the angle, in which the tool tip hits the ground. In order to use the tool effectively, this impact angle is required to be

$$\alpha = 20^\circ \dots 30^\circ. \quad (13)$$

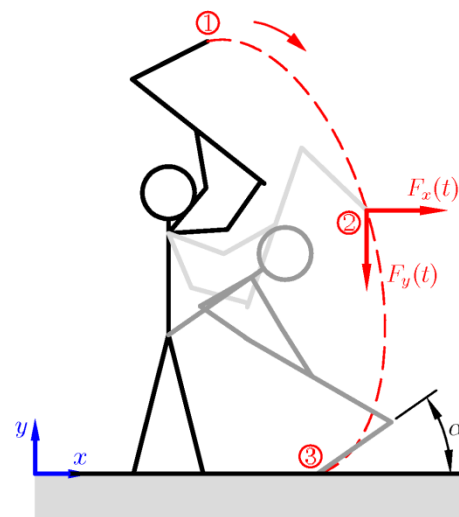


Figure 10: Trajectory for Movement of the Tool Tip and Reaction Forces F_x and F_y .

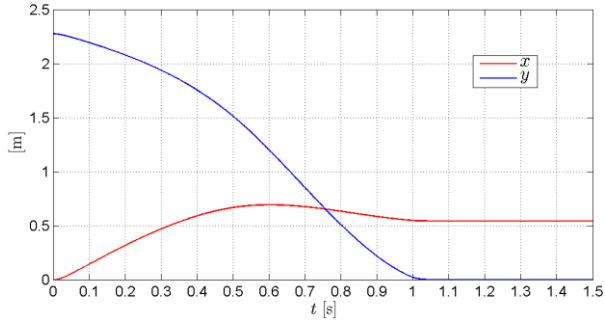


Figure 11: x - and y -Coordinates Over Time for an Example Trajectory.

Using the so defined trajectory as well as geometry and mass data for shaft and tip of the pick, a rigid body model can be set up in MATLAB/SimMechanics, which simulates the movement and provides for example reaction forces (F_x , F_y) on the tool tip as a result, like seen in figure 12.

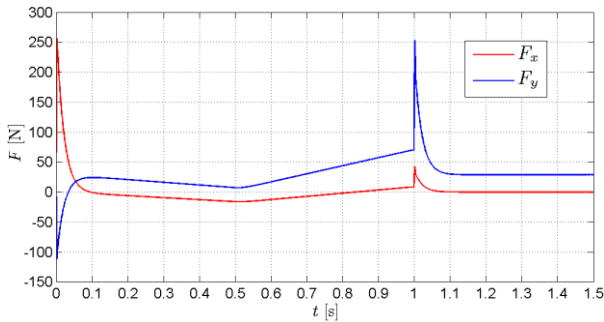


Figure 12: Reaction Forces in x - and y -Direction on the Tool Tip as a Simulation Result for an Example Scenario. At $t = 1$ s, the Impact on the Ground Occurs, Leading to a Peak in the Vertical Force.

In the presented example, salt is mined on the floor, which seems to be rather uncomfortable and unfavorable for body movement and energy requirement. Therefore, future work will investigate mining the salt on vertical surfaces.

4. WOODCHIP FLAME, LIGHTING AND AIR CONSUMPTION

During mining, burning sticks of wood served as the only illumination in the mining halls. Burnt down woodchips were found during excavation in large quantities (Reschreiter et al. 2009).

The resulting light intensity depending on the number of burning woodchips is estimated using a uniform arrangement shown in figure 13. The flame of a burning woodchip is comparable to a flame of a burning candle, therefore we assume a light intensity for each flame of

$$I_v = 1 \text{ cd.} \quad (14)$$

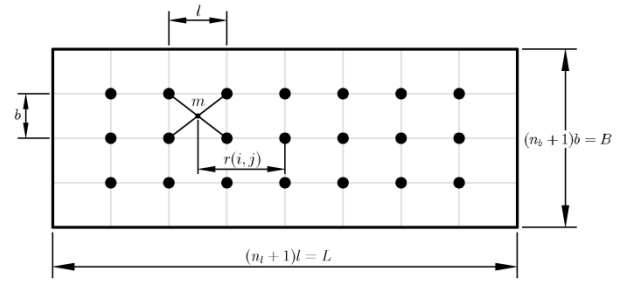


Figure 13: Uniform Arrangement of Burning Woodchips (n_l in Length, n_b in Width) in a Rectangular Mining Hall.

Local minimum illumination occurs at points of maximum distance to the light sources (for example point m in figure 13). For such a point, the distance $r(i, j)$ to each woodchip can be calculated

$$r(i, j) = \sqrt{\left((i-1)l + \frac{l}{2}\right)^2 + \left((j-1)b + \frac{b}{2}\right)^2} \quad (15)$$

and the sum over all positions leads to the illuminance

$$E_{v,m} = \sum_{i=1}^{n_l} \sum_{j=1}^{n_b} \frac{I_v}{r(i,j)^2}. \quad (16)$$

For different density of woodchips in length and width,

$$\rho_l = \frac{n_l}{L}, \quad \rho_b = \frac{n_b}{B}, \quad (17)$$

calculation results are shown in figure 14.

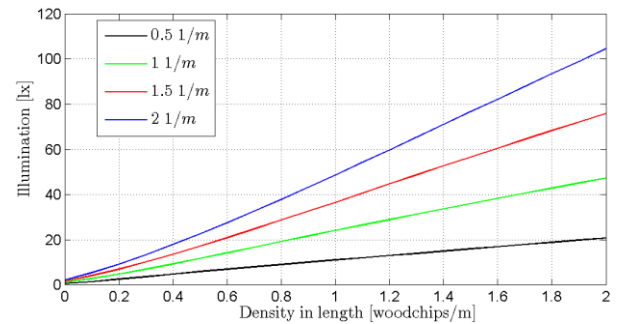


Figure 14: Calculation Results for Illumination for Different Density of Woodchips in Length and Width.

Furthermore, some static calculations are done regarding the oxygen consumption of the flames, which in addition to the oxygen demand of the workers gives information about the necessary air ventilation. For the air consumption of a person doing heavy labour, we assume

$$A_p = 0.81 \frac{\text{m}^3}{\text{h}} \quad (18)$$

at 21% percentage of oxygen in the air. A typical woodchip made of fir wood consumes about

$$A_w = 0.014 \text{ m}^3 \quad (19)$$

of oxygen during burning. Altogether, this data leads to the following formula for the total air consumption:

$$A_{\text{total}} = kA_p + n \frac{A_w}{21\% \cdot T}$$

with the number of workers k , total number of woodchips n ($n = n_i \cdot n_b$) and burning time T of a woodchip. Figure 15 depicts some calculation results.

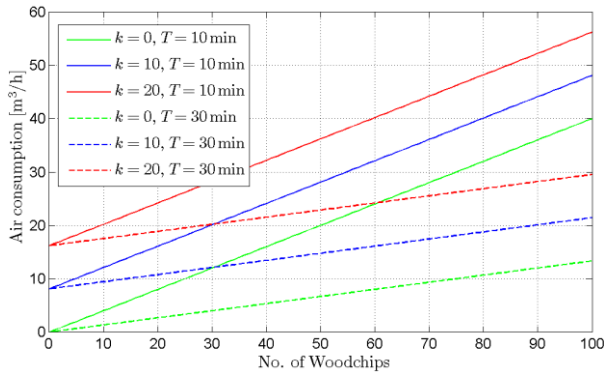


Figure 15: Calculation Results for Air Consumption for Different Number of Woodchips, Burning Time T and Number of Workers k .

This air consumption represents the minimum necessary air exchange in the mining halls in order to keep the oxygen level constant. Taking into account limitations regarding possible air exchange as well as necessary illumination (and therefore necessary number of woodchips), these results also provide reference values for maximum number of workers allowed in the mining halls.

5. CONCLUSION

The calculations and simulation results are visualized graphically. Their evaluations help archaeologists gain knowledge about transport mechanisms and working conditions in the prehistoric salt mines in Hallstatt.

For teaching, these modeling case studies present interesting insights of basic mechanical dynamics including equilibrium of forces, friction or momentum.

In addition, model implementations, which are done in MATLAB, will be included into the MMT system, an e-learning environment for teaching modelling and simulation developed at the Vienna University of Technology (Hafner et al. 2012, Körner et al. 2011).

REFERENCES

- Grabner, M., Reschreiter, H., Barth, F.E., Klein, A., Geihofer, D. and Wimmer, R., 2006. Die Dendrochronologie in Hallstatt. *Archäologie Österreichs*, 17(1): 49-58.
- Hafner, I., Bicher, M., Winkler, S., Fitsch, U., 2012. MMT – An E-Learning System Based on Computer Numeric System for Teaching Mathematics and Modelling. *In Proceedings of the 7th Vienna*

Conference on Mathematical Modelling. February 15-17, 2012, Vienna.

Körner, A., Hafner, I., Bicher, M., Winkler, S., Breitenecker, F., 2011. MMT – A Web Environment for Education in Mathematical Modelling and Simulation. *In Proceedings of ASIM 2011, 21. Symposium Simulationstechnik*. September 7-9, 2011, Winterthur, Switzerland.

Kowarik, K., Reschreiter, H., Wurzer, G., 2012. Modelling Prehistoric Mining. *In Proceedings of the 7th Vienna Conference on Mathematical Modelling*. February 15-17, 2012, Vienna.

Reschreiter, H., Kowarik, K., 2009. The Bronze Age. In: Kern et al. *Kingdom of Salt: 7000 Years of Hallstatt*. Vienna: VPA3, Natural History Museum Vienna, 48-64.

THE TRANSLATION OF CPN INTO NETLOGO ENVIRONMENT FOR THE MODELLING OF POLITICAL ISSUES: FUPOL PROJECT

Miguel Mujica^(a), Miquel Angel Piera^(b)

^(a,b)Autonomous University of Barcelona, Faculty of Telecommunications and Systems Engineering, 08193, Bellaterra, Barcelona

^(a)miguelantonio.mujica@uab.es, ^(b)miquelangel.piera@uab.es

ABSTRACT

The FUPOL project aims in a better way of fostering e-participation through the use of several tools and the social networks. The designed tool will make the citizens participate in the decision-making process in a more active way. The modelling and simulation of social activity is one WP of the project which is in charge of developing multi-agent systems capable of simulating the different actors that participate in the policy process. In order to determine the behaviour of citizens in a unambiguous and formal way the coloured Petri net formalism is used as the modelling framework to govern the agents behaviour. The characteristics of the CPN formalism allow a better understanding of the causal relationships present in systems and in particular in the case of policy process it allows simulating policy domains taking into account the causes of the decisions which contrast with the traditional approach that normally uses data trends or regressions to forecast the future outcomes. In this paper a way to translate the CPN semantic rules into the rules used by the agents called Turtles, links or patches in NetLogo is presented.

Keywords: timed Petri nets, state space, optimization, simulation, manufacturing.

1. INTRODUCTION

The European Commission launched a call under its framework 7 program dealing with ICT solutions for governance and policy modelling (Objective ICT-2011.5.6).

Target Outcomes are ICT solutions for governance and policy modelling. The research focus in the development of advanced ICT tools for policy modelling, prediction of policy impacts, development of new governance models and collaborative solving of complex societal problems.

The main objective of FUPOL is to demonstrate that, with ICT support the whole policy development lifecycle of policy formulation, collaborative stakeholder involvement, policy modelling, scenario generation, visualization of results and feedback is feasible and a core element of future policy development at local, regional, national as well as global level (Figure 1).

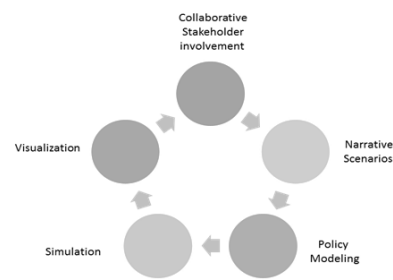


Figure 1: Policy development lifecycle

It will address issues related to the integration of the different components through advanced technical solutions and demonstrate an integrated ICT solution with a collaborative environment for policy modelling to generate different formal scenarios through simulations and scenario-based future development. This will include ICT support based on integrated Web 2.0 / Web 3.0 collaborative tools and policy simulation tools with scenario generation and visualization. It will also assist the long-term strategic planning of governments at all levels and policy operators in any policy area to better address and shape future developments so that the demands of citizens and economy are met.

The overview structure of the FUPOL project is illustrated in figure 2

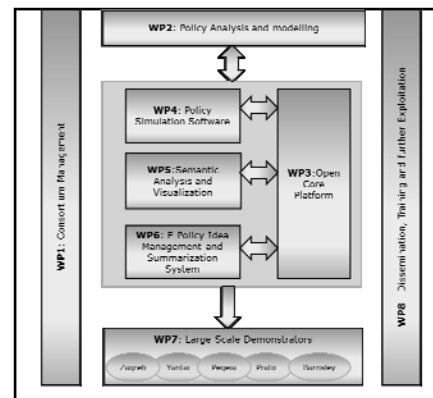


Figure 2: Overview of the WP Structure

The main task of the WP2 is the modelling and validation of policy models of different domains. The selected tools to model the different domains use techniques such as fuzzy cognitive maps (FCM) and coloured Petri nets (CPN) under a multi agent system (MAS) environment which presents great advantages in order to analyse social systems (North and Macal 2007).

2. COLOURED PETRI NETS

Coloured Petri Nets (CPN) is a simple yet powerful modelling formalism which allows to properly modelling discrete-event dynamic systems which present a concurrent, asynchronous and parallel behaviour (Moore et al. 1996, Jensen 1997, Christensen et al. 2001). CPN can be graphically represented as a bipartite graph which is composed of two types of nodes: the place nodes and the transition nodes. Place nodes are commonly used to model system resources or logic conditions, and transition nodes are associated to activities of the real system. The entities that flow in the model are known as tokens and they have attributes known as colours. The use of colours allows modelling not only the dynamic behaviour of systems but also the information flow which is a key attribute in decision making (Mujica and Piera 2011).

The formal definition is as follows.

A Coloured Petri Net can be defined as the tuple (Jensen1997):

$$CPN = (\sum, P, T, A, N, C, G, E, I)$$

Where

- $\sum = \{ C1, C2, \dots, C_{nc} \}$ represent the finite and not-empty set of colours. They allow the attribute specification of each modelled entity.
- $P = \{ P1, P2, \dots, P_{np} \}$ represent the finite set of place nodes.
- $T = \{ T1, T2, \dots, T_{nt} \}$ represent the set of transition nodes such that $P \cap T = \emptyset$ which normally are associated to activities in the real system.
- $A = \{ A1, A2, \dots, A_{na} \}$ represent the directed arc set, which relate transition and place nodes such as $A \subseteq P \times T \cup T \times P$
- $N =$ It is the node function $N(A_i)$, which is associated to the input and output arcs. If one is a place node then the other must be a transition node and vice versa.
- $C =$ is the colour set functions, $C(P_i)$, which specify for the combination of colours for each place node such as $C: P \rightarrow \sum$.

$$C(P_i) = C_j \quad P_i \in P, C_j \in \sum$$
- $G =$ Guard function, it is associated to transition nodes, $G(T_i)$, $G: T \rightarrow EXPR$. It is

normally used to inhibit the event associated with the transition upon the attribute values of the processed entities. If the processed entities satisfy the arc expression but not the guard, the transition will not be enabled.

- $E =$ these are the arc expressions $E(A_i)$ such as $E: A \rightarrow EXPR$. For the input arcs they specify the quantity and type of entities that can be selected among the ones present in the place node in order to enable the transition. When it is dealing with an output place, they specify the values of the output tokens for the state generated when transition fires.
- $I =$ Initialization function $I(P_i)$, it allows the value specification for the initial entities in the place nodes at the beginning of the simulation. It is the initial state of a particular scenario.
- $EXPR$ denotes logic expressions provided by any inscription language (logic, functional, etc.)
- The *state* of every CPN model is also called the *marking* which is composed by the expressions associated to each place p and they must be closed expressions i.e. they cannot have any free variables.

The formalism can be graphically represented by a bipartite graph where the place nodes are represented by circles and the transition nodes by rectangles or solid lines.

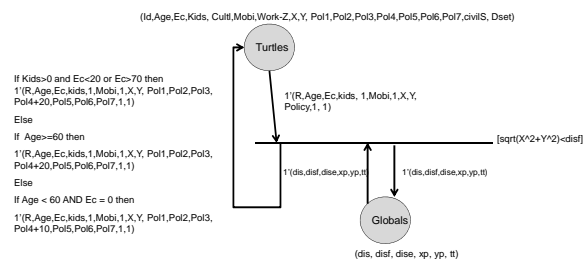


Figure 2: CPN model of land use participation

Figure 2 illustrates a graphical representation of a CPN model with all the described elements.

2.1. Dynamic behaviour of the CPN

The transitions in the CPN models play the role of activities, actions or decisions in the real system. The firing of a transition is caused by the satisfaction of several restrictions imposed by the colours, arc expressions and guards. In the case of social systems the set of conditions or restrictions that cause a particular behaviour or decision are modelled with the

use of colours, arc expressions and guards. In order to enable a transition (i.e. the possibility of an action, activity to occur) It is necessary to satisfy all of the following conditions:

- The number of tokens in the input place nodes are greater than or equal to the arc weight
- There must be at least one combination of tokens within the input place nodes whose colours have the particular values stated in the arc inscriptions. If there are free variables, the variables take the value from the correspondent token colour.
- The Boolean expressions of the guards (generally related to the token variables) must also be satisfied.

Once the restrictions have been satisfied it is said that the transition is enabled and the modelled activity can occur. In such a case the following actions are performed in the input and output place nodes:

- The tokens that enable the transition are consumed (destroyed) from the original input place nodes
- New tokens are created in the correspondent output place nodes based on the values of the variables, the arc expressions attached to the output arcs and the weights of the arcs (there must be created as many tokens as the weight of the output arcs).

The configuration that is obtained after the execution of a transition corresponds to a new state of the original system.

3. NETLOGO

NetLogo is a simulation environment which has been widely used in academia not only for teaching purposes but also for research ones (Romus-Catalin, 2011).

NetLogo is an agent-based model programming environment built on the programming language JAVA and authored by Uri Wilensky. Due to its flexibility it is suited to fully integrate the semantic rules present in CPN using the code available in the procedures window of NetLogo. The implementation of CPN semantic rules allow to govern the agents that interact within the environment in a more transparent way which is useful to understand the emergent dynamics caused by the agent interaction.

3.1. Agents in NetLogo

The NetLogo environment is made up of agents. Agents are beings that can follow instructions. There are four types of agents:

- Turtles. Turtles are agents that move around the NetLogo environment.
- Patches: The world is two dimensional and is divided up into a grid of patches. Each patch is a square piece of "ground" over which turtles can move.

- Links: Links are agents that connect two turtles. Links can be directed (from one turtle to another turtle) or undirected (one turtle with another turtle).
- The observer: The observer does not have a location - one can imagine it as looking out over the world of turtles, links and patches. Generally speaking the observer is the developer and can test instructions over the environment developed in order to verify the behaviour of the different agents.

4. CPN RULES AND THE CODE IN NETLOGO

In order to make a straightforward translation from the CPN formalism into the NetLogo environment, it is necessary to determine a way to code the transitions, the place nodes and the firing rules within the NetLogo environment. The main idea is to combine the capabilities of the CPN formalism with the ability to manage the different agents that interact within the program in such a way that the emergent dynamics are more transparent to the analyst. The implementation of the CPN models will be exemplified with the use of one transition of the Open Space land-use model developed for the FUPOL project.

4.1. Definition of Colours in the NetLogo environment

The CPN of the open space model needs some colours to be defined. These colours are used as part of the different agents with the purpose of tracking down the information flow that takes place when a decision is performed by the agents. The following table illustrates the kind of attributes and colours that are used for the open-space CPN model.

Table 1: Colour attributes of the open space example

Colour	Meaning
Age	Age of the citizen: most urban policies are highly dependent of the population age of citizens that will be affected. Age diversity usually is a problem when trying to devise the benefits of a certain urban policy
Ec	Economical incomes rate: It takes a value between 0% to 100%. 0% means unemployed without subsistence. 100% means a well standing economical position. This information is highly relevant to simulate the economic impact of urban policies.
Kids	Amount of kids bellow 18 years olds: this information is important to evaluate the social impact of urban policies.
CultL	Cultural level: A value between 1 (no studies) until 5 (PhD level). This information is useful not only to evaluate the impact of a policy, but also to describe how his affinities can affect or can be influenced by their neighbourhood 's opinions.
Mobi	Mobility: Describes the preferences of the urban population to access places (working, leisure, shopping, etc.). It is parameterized using 5 values: 1 – Car, 2 – Public urban transport (bus/subway), 3 – Public regional transport (train/buses), 4.- alternative transport means (cycle / by food)
Work -Z	Work place: A discrete value indicating the amount of zones to travel to reach its working company. In this example it is used binary information indicating if the work place is in the area of the study.
X	Vector information (x coordinate with respect to a reference coordinate) which is used to evaluate the impact of a landing change in citizens living close or fare away of the land cell.
Y	Vector information (y coordinate with respect to a reference coordinate) which is used to evaluate the impact of a landing change in citizens living close or fare away of the land cell.
Policy	A value between 0% to 100% to describe de rate of acceptability of policy identified by colour ldp1.
CivilS	Is the civil status of the agent
Dset	this is only an identifier used for taking decisions.

These colours will be used for modelling the information flow within the model. It is possible to define these attributes with the use of lists to define several attributes referenced to the turtles, links or patches (agents). The next figure illustrates the kind of attributes that have been defined for the model within NetLogo.

```
turtles-own [ Age Ec Kids CultL Mobi Work-Z X Y policy civiIS dset]
links-own [turtle-id prox-affin]
patches-own [ usage ] ;; 0 non-usage 1 school 2 health 3 park 4 tran
globals [ dis disf dise xp yp tt]
```

Figure 3: Agents attributes

In the figure it can be appreciated that 4 kinds of agents are being used for the model: Turtles, links, patches and globals. In particular *Globals* is not an agent but a list variable that can be used as a global list which can be accessed by the agents in order to keep track of some global changes of the model. The global attributes can be thought as another place node that participates in all the transitions within the model.

The other attributes are just lists (among brackets) and are attached to any instantiation of an agent class.

4.2. The place nodes

Since the agents in the NetLogo environment can have attributes which can be represented with the use of lists, it is possible to establish a direct relationship (1 to 1) between the coloured tokens and the attributes of the agents. If the modeller make this kind of mapping then the set composed by agents (turtles, patches or links) with common attributes could be representing the entities or tokens that belong to a particular place node. Figure 4 illustrates the association of the attributes of the agents in NetLogo to the colours of the correspondent place nodes.

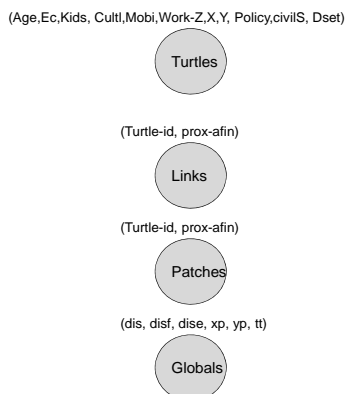


Figure 4: Set Colour association

Despite the fact that different agents have their own predefined attributes, it is possible to perform the particular definition of attributes through the use of lists.

4.3. Transition nodes

As it has been previously mentioned, the transition nodes are modelled through the definition (coding) of the different restrictions that must be satisfied by the set of agents that participate in the evaluation. All the restrictions imposed by the CPN elements (arc expressions, guards, weights) are evaluated in a single procedure that takes into account all of them in order to determine if the selected elements (agents) satisfy the correspondent restrictions.

Figure 5 is an example of a typical transition that has been modelled in NetLogo for the Fupol project.

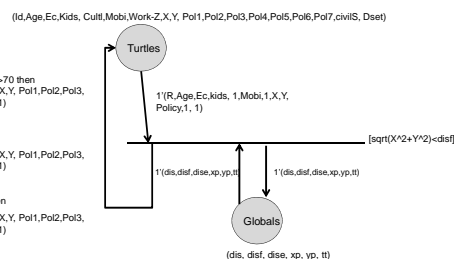


Figure 5: A CPN transition node for land use participation

The transition in

Figure 5 models the decision taken by the agents (turtles) in order to foster the transformation of a particular open space into a green park area within their neighbourhood. This transition uses the sets composed by the turtles and globals and in order to determine if the agents foster or not a particular use of the patch. The key attribute to be satisfied in this example is the proximity of the agents to the land space under study. The latter is evaluated using the global attribute *disf* which evaluate that the distance from their current location to the space under study (assuming that it is located at the 0,0 coordinates) is within reasonable range: $(\text{sqrt}(x^2+y^2) < \text{disf})$. Where *disf* is the distance a normal family walks in order to get to the park. The following table explains the values of the colours that must be fulfilled by the agents in order to fire the transition:

Table 2: Description of the expressions used in the model

Colour Restriction	Description
Dset = 1	The turtles that have the identifier Dset set to 1 will participate in the evaluation. This value indicates that this agent is within one particular radius (in the example is 10)
$\sqrt{x^2+y^2} < \text{disf}$	This guard specifies that the agent is within the acceptable walking distance for a common family
If Kids>0 and Ec<20 or Ec>70 then l'(R,Age,Ec,kids,1,Mobi,1,X,Y, Pol1,Pol2,Pol3, Pol4+20,Pol5,Pol6,Pol7,1,1)	If the agent have kids and has a certain income, it will foster the policy related to the Park with 20 units
If Age>=60 then l'(R,Age,Ec,kids,1,Mobi,1,X,Y, Pol1,Pol2,Pol3, Pol4+20,Pol5,Pol6,Pol7,1,1)	If the agent is older than 60 it will foster the Park development with 20 units
If Age < 60 AND Ec = 0 then l'(R,Age,Ec,kids,1,Mobi,1,X,Y, Pol1,Pol2,Pol3, Pol4+10,Pol5,Pol6,Pol7,1,1)	If the agent is younger than 60 yrs but is in bankruptcy, it will foster with a lower quantity the transformation to a green park.

4.4. NetLogo Code

The previous model can be coded in the *Procedures* window of NetLogo. The correspondent code whose outcome is the one obtained from the previous CPN model is shown in Figure 6

```

to cit-policy-2 ;; Industry ----> Park green
ask turtles [set dset 0]
ask patches with [pcolor = green] [
ask turtles in-radius 10 [set dset 1]
ask turtles with [dset != 1 and (kids > 0 and ((ec < 20) or (ec > 70)))] [
set label ec
dist xp yp xcor ycor
if (dis < disf) [
set color green
set tt (item 2 policy)
set policy replace-item 2 policy (tt + 20)]

ask turtles with [dset != 1 and age >= 60] [
dist xp yp xcor ycor
if dis < disf [
set color green
set tt (item 2 policy)
set policy replace-item 2 policy (tt + 20)]
]
ask turtles with [dset != 1 and age < 60 and ec = 0] [
dist xp yp xcor ycor
if dis < disf [
set color green
set tt (item 2 policy)
set policy replace-item 2 policy (tt + 10)]
]
end

```

Figure 6: The equivalent code to translate the CPN model

The code is a subroutine within a more general program, but it is useful to exemplify the translation of the previous model into the environment.

The name of the procedure is called *cit-policy-2*. The first line *asks turtles [set dset 0]* initializes the value of the *dset* attribute to 0.

The line *ask patches with [pcolor = green] [ask turtles in-radius 10 [set dset 1]]* verifies that the agents (turtles) within a certain distance will participate in the evaluation, if so; the *dset* attribute is set to 1.

The next three lines of the code do not correspond to any expression of the CPN model. The following ones correspond to the restrictions stated in the formalism.

For example the lines

```

ask turtles with [dset != 1 and (kids > 0 and ((ec < 20) or (ec > 70)))] [
set label ec
dist xp yp xcor ycor
if (dis < disf) [
set color green
set tt (item 2 policy)
set policy replace-item 2 policy (tt + 20)]

```

Verify that the *dset* attribute has the value 1 and based on the value of the *kids*, *Ec*, variables, it assigns the new value for the evaluated policy. The function *dist* :

```

set label ec
dist xp yp xcor ycor
if (dis < disf) [
set color green

```

Calculates the distance of the evaluated agent to the studied cell: $(\sqrt{X^2+Y^2})$

Then it assigns this distance to the global variable *dis*. In the next statement, the value of the *dis* variable is compared to that of the global variable *disf*. Finally the new value for the correspondent colour (*item 2 policy*) is updated making use of the auxiliary variable *tt*.

The two remaining *ASK TURTLES* subroutines are the equivalent for the corresponding *IF* expressions of the output arc of the model in Figure 5:

```

If Age>=60 then
l'(R,Age,Ec,kids,1,Mobi,1,X,Y, Pol1,Pol2,Pol3, Pol4+20,Pol5,Pol6,Pol7,1,1)
Else
If Age < 60 AND Ec = 0 then
l'(R,Age,Ec,kids,1,Mobi,1,X,Y, Pol1,Pol2,Pol3, Pol4+10,Pol5,Pol6,Pol7,1,1)

```

It must be clarified that in the case of the variable *Policy*, it is used a list for the attributes *PolX* instead of single variables just for the purpose of code readability.

The previous subsection illustrates how it can be translated a CPN model into a NetLogo environment. The following section presents some parts of an Open Space model which has been implemented in NetLogo in order to be used as part of the module that will simulate the behaviour of societies under particular policies.

5. OPEN SPACE MODEL

The model represents an old industry placed in a town that during last decades has been surrounded by residential habitats, and due to several economic and social factors it has been moved to an industrial area. Different options for the land cell in which this industry was placed are under evaluation under a social and economic perspective.

The main actors that should be modelled to predict the acceptability and the exit of a certain land change are:

1. Set of Land use Policies: For each land entity the set of acceptable land changes should be described as a policy. In this particular problem, a set of acceptable land changes are described in the next table.

Table 3: Different Policies

Policy 1	Industry ---> Park green
Policy 2	Industry ---> Facility : School
Policy 3	Industry ---> Facility: Health
Policy 4	Industry ---> Facility : Leisure area
Policy 5	Industry ---> Facility: Intermodal transport
Policy 6	Industry ---> Commercial Area
Policy 7	Industry ---> Residence Area
Policy 8	Industry ---> Business Area

Each policy is described accordingly to its acceptability by a certain profile of citizens. Thus, considering Policy 1, its acceptability could be fostered by:

- Elderly people: Residents above 65 years old (retired people) with an acceptable healthy conditions (mobility) could be users of a green area close to their homes.
- Family residents: Parents with young kids could be users of a green area during week-ends or after school hours. The green area should be located close to their homes or close to the school.
- Unemployed people: Parks are frequented by people without job obligations.
- Cafe owners: Cafes, pubs and lounges placed close to a small green area use to increase the amount of customers.

There are other aspects that can affect these rules, such as the weather conditions (i.e. rainy area), security conditions in the neighbourhood area, accessibility, amount of green areas located near the proposed area, etc. Some of these aspects can be modelled as boundary conditions which can be seen as predictions that can change on a year basis time. The model proposed, allows an open source policy description, which a parameterized weight influence that can depend on the boundary conditions, which can also be described by end-users.

2. Set of Citizens: Land changes appear because of humans needs. Usually, citizens' needs can be described as a combination of social, economic and environmental needs. Since urban policies will be described in FUPOL considering the effects in citizens' needs (i.e. Citizens' acceptability), citizens should provide all the information and data to predict how an urban policy would fulfil its preferences.

5.1. Coloured Petri Net Description

The description of the causality of the different agent decision making will be defined using the CPN modelling formalism. With the use of the CPN causal models, the land use change can take into account not only the influences by the surrounding areas (adjacent cells) but also by the interaction with other areas or agents that affect the decision of fostering one or another kind of policy.

- Citizen Agents. The attributes or characteristics of the different citizen agents can be described by the colours of the tokens that flow through the model.

In the next table, the attributes are presented for the following colour set which is used for modelling the industrial land-change:

$$Cz = \text{productAge} * Ec * Kids * CultL * Mob * Work * X * Y * Z * idp1 * p1V * idp2 * p2V * idp3 * p3V * ta$$

Table 4: Citizen Attributes

Colour	Meaning
Age	Age of the citizen: most urban policies are highly dependent of the population age of citizens that will be affected. Age diversity usually is a problem when trying to devise the benefits of a certain urban policy
Ec	Economical incomes rate: It takes a value between 0% and 100%. 0% means unemployed without subsistence. 100% means a well standing economical position. This information is highly relevant to simulate the economic impact of urban policies.
Kids	Amount of kids bellow 18 years olds: this information is important to evaluate the social impact of urban policies.
CultL	Cultural level: A value between 1 (no studies) until 5 (PhD level). This information is useful not only to evaluate the impact of a policy, but also to describe how his affinities can affect or can be influenced by their neighbourhood 's opinions.
Mob	Mobility: Describes the preferences of the urban population to access places (working, leisure, shopping, etc.). It is parameterized using 5 values: 1 – Car, 2 – Public urban transport (bus/subway), 3 – Public regional transport (train/buses), 4.- alternative transport means (cycle / by food)
Work	Work place: A discrete value indicating the amount of zones to travel to reach its working company. In this example it is used binary information indicating if the work place is in the area of the study.

Table 4. (cont.)

Colour	Meaning
X	Vector information (x coordinate with respect to a reference coordinate) which is used to evaluate the impact of a landing change in citizens living close or fare away of the land cell.
Y	Vector information (y coordinate with respect to a reference coordinate) which is used to evaluate the impact of a landing change in citizens living close or fare away of the land cell.
Z	Vector information (not used in this example) which can be used to evaluate the impact of a landing change in citizens living close or fare away of the land cell.
Idp1	A citizen should have certain preferences towards certain land changes fostered by some policies. This colour is used to identify a policy for which the citizen could feel a certain degree of acceptability.
P1v	A value between 0% and 100% to describe de rate of acceptability of policy identified by colour Idp1.
Idp2	A citizen should have certain preferences towards certain land changes fostered by some policies. This colour is used to identify a policy for which the citizen could feel a certain degree of acceptability.
P2v	A value between 0% and 100% to describe de rate of acceptability of policy identified by colour Idp2.
Idp3	A citizen should have certain preferences towards certain land changes fostered by some policies. This colour is used to identify a policy for which the citizen could feel a certain degree of acceptability.
P3v	A value between 0% and 100% to describe de rate of acceptability of policy identified by colour Idp3.
ta	The citizen attribute information must be understood as a time stamp data. Thus, some values can change according to a simulation time basis mechanism. This attribute represent the time stamp of the information represented in the attributes.

Next Figure illustrates the CPN model of Policy-1: Industry → Park green, in which the policy impact acceptability is described according to the boundary conditions, the citizen characteristics and the city resources capacities.

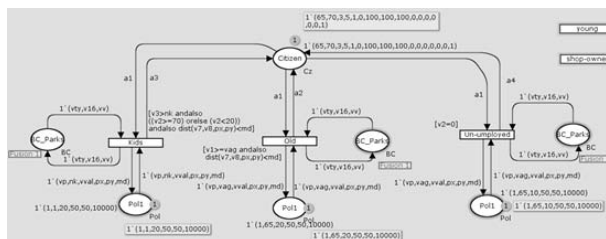


Figure 7: Policy Model1

The arc expressions of the model are presented in the following table.

Table 5: Arc expressions

A1	1*(v1,v2,v3,v4,v5,v6,v7,v8,v9,v10,v11,v12,v13,v14,v15,v16)
A2	if (v10=vp) then 1*(v1,v2,v3,v4,v5,v6,v7,v8,v9,v10,v11+vval,v12,v13,v14,v15,v16) else if (v12=vp) then 1*(v1,v2,v3,v4,v5,v6,v7,v8,v9,v10,v11,v12,v13+vval,v14,v15,v16) else if (v14=vp) then 1*(v1,v2,v3,v4,v5,v6,v7,v8,v9,v10,v11,v12,v13,v14,v15+vval,v16) else if (v11 <= v13) andalso (v11 <= v15) then 1*(v1,v2,v3,v4,v5,v6,v7,v8,v9,v10,v11,v12,v13,v14,v15,v16) else if (v13 <= v11) andalso (v13 <= v15) then 1*(v1,v2,v3,v4,v5,v6,v7,v8,v9,v10,v11,v12,v13,v14,v15,v16) else 1*(v1,v2,v3,v4,v5,v6,v7,v8,v9,v10,v11,v12,v13,v14,v15,v16)
A3	if (v10=vp) then 1*(v1,v2,v3,v4,v5,v6,v7,v8,v9,v10,v11+vval,v12,v13,v14,v15,v16) else if (v12=vp) then 1*(v1,v2,v3,v4,v5,v6,v7,v8,v9,v10,v11,v12,v13+vval,v14,v15,v16) else if (v14=vp) then 1*(v1,v2,v3,v4,v5,v6,v7,v8,v9,v10,v11,v12,v13,v14,v15+vval,v16) else if (v11 <= v13) andalso (v11 <= v15) then 1*(v1,v2,v3,v4,v5,v6,v7,v8,v9,v10,v11,v12,v13,v14,v15,v16) else if (v13 <= v11) andalso (v13 <= v15) then 1*(v1,v2,v3,v4,v5,v6,v7,v8,v9,v10,v11,v12,v13,v14,v15,v16) else 1*(v1,v2,v3,v4,v5,v6,v7,v8,v9,v10,v11,v12,v13,v14,v15,v16)
A4	if (v10=vp) then 1*(v1,v2,v3,v4,v5,v6,v7,v8,v9,v10,v11+vval,v12,v13,v14,v15,v16) else if (v12=vp) then 1*(v1,v2,v3,v4,v5,v6,v7,v8,v9,v10,v11,v12,v13+vval,v14,v15,v16) else if (v14=vp) then 1*(v1,v2,v3,v4,v5,v6,v7,v8,v9,v10,v11,v12,v13,v14,v15+vval,v16) else if (v11 <= v13) andalso (v11 <= v15) then 1*(v1,v2,v3,v4,v5,v6,v7,v8,v9,v10,v11,v12,v13,v14,v15,v16) else if (v13 <= v11) andalso (v13 <= v15) then 1*(v1,v2,v3,v4,v5,v6,v7,v8,v9,v10,v11,v12,v13,v14,v15,v16) else 1*(v1,v2,v3,v4,v5,v6,v7,v8,v9,v10,v11,v12,v13,v14,v15,v16)

In the previous figure there are 3 transitions (driving forces) which evaluate the impact (benefits to the population) of changing the industrial use to a green park.

Elderly People (old transition): There are 3 different entities (agents) that take part when evaluating this driving force: Citizen (Place node *Citizen*), Policy impact on elderly people (Place node *Poll*) and boundary conditions (place node *BC_Parks*). In this transition it is checked the characteristics (arc expression a1 described in precedent tables, of the agent (citizen), using the arc expression:

$$[v1] \geq v_{ag} \text{ andalso } \text{dist}(v7, v8, px, py) < md$$

which tests if the agent is an old citizen (first colour *Age* of the arc expression A1, variable *v1*, which is compared with the estimated age of pensioners which is represented in the variable *vag* in the arc expression $1*(vp, vag, vval, px, py, md)$) and that lives close to the land cell under study obtained using the variables *v7* and *v8* which represent the home location of the agent mapped with the colours X and Y in arc A1, and the variables *px* and *py* which represent the industrial land location in the arc expression $1*(vp, vag, vval, px, py, md)$.

As a consequence of this driving force, the agent acceptability for this policy will be updated with a certain increment represented in arc expression A2. The right increment will be defined partially in the policy definition, but also on the agent affinity to other policies (such as for example a leisure or a commercial area). Thus arc expression A2 allows computing the affinity in

the colour Pv1, Pv2 or Pv3 in case the agent has shown other preferences using as a reference the value of variable *vval* specified in the policy definition.

Next figure illustrates this transition, in which a citizen represented by a token has the following characteristics:

Age	Ec	Kids	CultL	Mob	Work	X	Y	Z	Idp1	P1v	Idp2	P2v	Idp3	P3v	t
65	70	3	5	1	0	100	100	-	0	0	0	0	0	0	

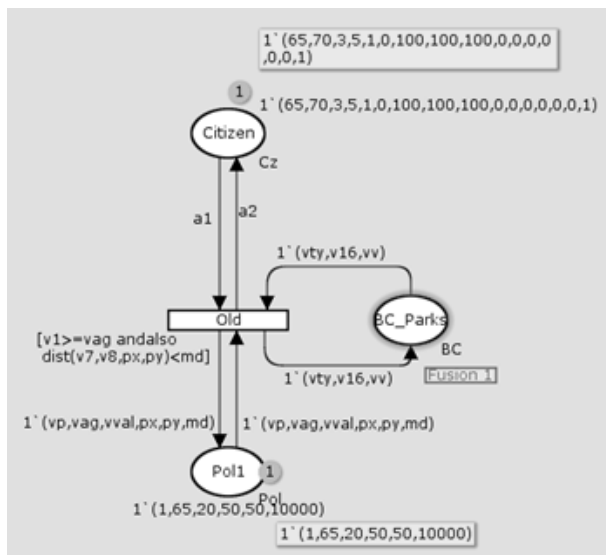


Figure 8: Citizen evaluation

As a result of firing the transition, the new agent state information will be:

Age	Ec	Kids	CultL	Mob	Work	X	Y	Z	Idp1	P1v	Idp2	P2v	Idp3	P3v
65	70	3	5	1	0	100	100	-	1	20	0	0	0	0

In the next figure it is represented the same policy (industrial use → park green) but considering effects on families with kids. The main difference with regards to the previous transition is in the guard expression:

$[v3 > nk \text{ andalso } ((v2 \geq 70) \text{ or else } (v2 < 20)) \text{ and also dist}(v7, v8, px, py) < md]$

In which it is checked the amount of kids (represented in variable *v3* that corresponds to Kids attribute) and the economical capacity of the agent (represented in variable *v2* that corresponds to colour *Ec*).

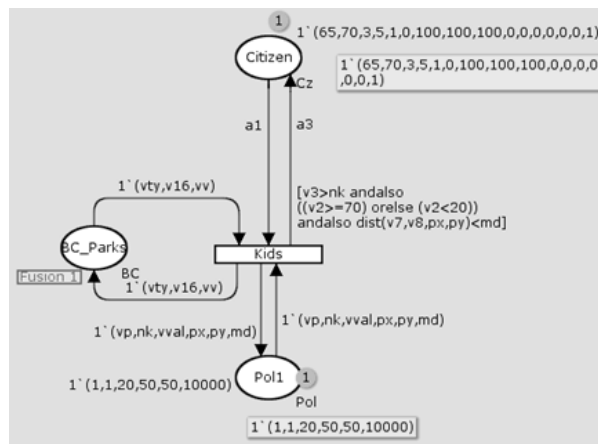


Figure 9: Evaluation of families with kids

Citizen Agent interaction: There are several interactions that can be formalized in a social context, but in this example citizen's interaction has been modelled as a proximity interaction or as an affinity interaction.

Social interaction by proximity has been modelled in such a way, that a policy which is not supported at all by one of the agents and is not highly ranked by the other agent, its acceptability is decreased.

Next figure illustrates the proximity interaction in which 2 citizens explains their opinions to foster or reject a policy. Place node High-op is used to check which one is the policy with highest affinity to each agent.

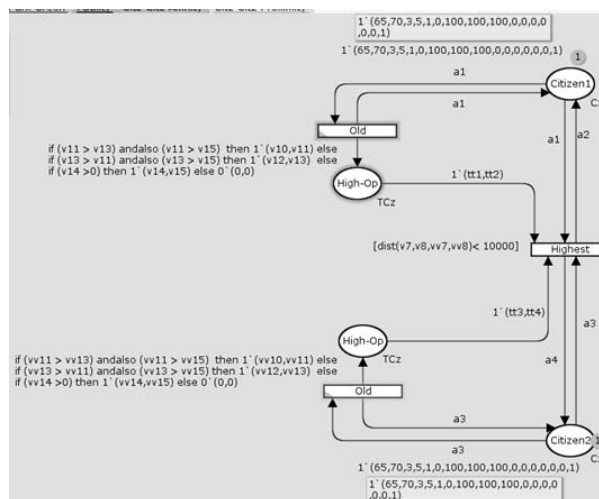


Figure 10: Proximity interaction

As it can be observed in arc expressions *a2* and *a3*, affinity of the citizen to a certain policy is decreased by a certain amount: variables *v11*, *v13* and *v15* represent colours *P1v*, *P2v* and *P3v* for one agent, and variables

vv11, vv13, vv15 represent also the same attributes but for the other agent.

Guard expression attached to *Highest* transition, checks that both agents are candidates for a proximity interaction (i.e. they live in the same area):

$$[\text{dist}(v7,v8,vv7,vv8) < 10000]$$

These are just some examples of the different transitions that rule the behaviour of the correspondent agents.

5.2. Implementation of the Open Space Model in NetLogo Environment

After the causal relationships have been defined through the CPN formalism, it is possible to translate those rules into the MAS environment. It is fair to mention that the rules defined with the CPN formalism can be used for implementing the interaction in any kind of agent architecture or MAS simulation program not only in NetLogo environment.

The causal model for land use relies mainly on three different agent behaviours:

- Citizens: This agent allows evaluating the benefits and shortages of the different policies proposed accordingly to the expected needs of each citizen. All citizens are modelled as turtle agents in NetLogo

- Urban Resources: A City or the urban area under study, is represented by a discretized grid of small areas, each one identified by a reference to a certain location (i.e. georeferenced), and by a functionality. Thus, an area can be characterized by the infrastructures and resources deployed, such as for example: a school (1), a health facility (2), a green park area (3), a transport facility (4), a leisure or a commercial centre (5), a residence area (6) or a business area (7). All areas are modelled as patches agents in NetLogo

- Interactions: Citizens could iterate with other citizens based on:

- Proximity relationship: they are neighbours and can casually share their opinion regarding certain policies that could affect the initial score of each policy.

- Affinity relationship: Citizens that live in different areas share some characteristics that allow them by means of physical interaction or through social IT networks to share their opinions regarding policies. All interactions are modelled as link agents in NetLogo.

- Global Information: There are some data which cannot be represented in the agents, instead they specify global boundary conditions, context scenario information, or experiment hypothesis. In this open space model, it has been setup 4 constants to evaluate different policies for an open space area.

- Disf: The maximum average distance that usually can walk a family with kids from its residence to a green park area.

- Dise: The maximum average distance that usually can walk elderly people to a green park area.
- Xp, Yp: Specify the open space area location under study.
- Global information is formalized by global variables in NetLogo.

In the next figure it is illustrated the NetLogo model implemented using the previous CPN models. There are some *buttons* which allow the user to test different configurations for the same model. The magenta cell represents the open space grid under study.

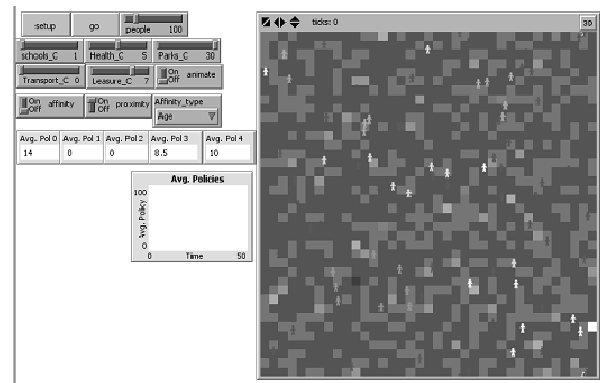


Figure 11: The NetLogo Simulator

The simulator allows also determining which kind of relationship is possible to permit among the agents that participate in the system (e.g. proximity or affinity). The main outcomes that can be obtained from the simulator are the weights of the policies that result more attractive to the general actors within the model (i.e. population). The following table presents some results obtained with the initialization of different parameters which can correspond to particular configurations of an example system.

Table 6: Outcomes for different configurations

Configuration						Outcomes				
People	Schools	Hospitals	Parks	Transport	Leisure	Policy 0 (school)	Policy 1 (health)	Policy 2 (park)	Policy 3 (Transport)	Policy 4 (Leisure)
400	10	5	5	5	5	98	0	45.5	1.3	41.4
400	5	5	5	5	5	100	0	32.4	0	46
400	20	1	10	5	5	52	15	11.7	7	48.5
400	20	1	10	5	10	48	19	20	1	40.4

6. CONCLUSIONS AND FUTURE WORK

Under the framework of the FUPOL project one challenging task is the policy modelling and analysis. The proposed methodology has been performed through a novel approach which models the different actors in a policy process as agents whose behaviour is governed by a causal modelling developed in coloured Petri nets. The translation of the CPN models into the NetLogo environment allows a novel way of understanding the causal relationships that are behind decision making in society. With the use of CPN it is possible to implement the causal relationships that govern the agent behaviour in such a way that more transparency is achieved during the evaluation of a particular policy. The approach presented will be used during the development of a simulation module within the FUPOL framework which will allow the participation of real citizens through social networks to determine the parameters of some characteristics of the simulation model (boundary conditions). With the previous approach it is expected that more transparency and e-participation will be gained for the common population within a city, region or community.

The next steps of the simulation approach are the following ones:

- Verification of the parameters that govern the behaviour of the particular agents through field studies, polls, questionnaires' etc.
- Field testing of the approach with a particular region, city, or community. This step will be performed in the pilot cities of the project.
- The simulation module must be integrated with the IT tool developed by the FUPOL project in order to test or verify that the proposed approach certainly is useful to foster e-participation within a community.

REFERENCES

- Christensen, S., Jensen, K., Mailund, T., Kristensen, L.M., 2001. State Space Methods for Timed Coloured Petri Nets. *Proc. of 2nd International Colloquium on Petri Net Technologies for Modelling Communication Based Systems*, 33-42, Berlin.
- Jensen, K., 1997. *Coloured Petri Nets: Basic Concepts, Analysis Methods and Practical Use*. 1 Springer-Verlag, Berlin.
- Moore, K.E., Gupta, S.M., 1996. Petri Net Models of Flexible and Automated Manufacturing Systems: A Survey. *International Journal of Production Research*, 34(11), 3001-3035.
- Mujica, M.A.; Piera M.A.; 2011. A Compact Timed State Approach for the Analysis of Manufacturing Systems: Key Algorithmic Improvements, *International Journal of Computer Integrated Manufacturing*, Vol.24 (2), February 2011.
- North M. J., Macal C. M., 2007, *Managing Business Complexity Discovering Strategic Solutions with Agent-Based Modelling and Simulation*, Oxford University Press.
- Romulus-Catalin Damaceanu, 2011, *Agent-based Computational Social Sciences using NetLogo: Theory and Applications*, Lambert Academic Publishing.

AUTHORS BIOGRAPHY

Miguel A. Mújica Mota was born in Mexico City. He studied chemical engineering at Autonomous Metropolitan University of Mexico, an MSc in Operations Research in the National Autonomous University of México. He also received a Master's in Industrial Informatics from the Autonomous University of Barcelona and the PhD from the same university. He has professional experience in manufacture and production planning in the cosmetic industry. His research interest focuses on simulation and optimization techniques using the Coloured Petri Nets formalism aiming to solve industrial problems.

Miquel Àngel Piera received his MSc (Control Engineering) from the University of Manchester Institute of Technology in 1990 and his PhD degree from the Autonomous University of Barcelona (Spain) in 1994. He participates in industrial research projects in the logistics and manufacturing field and at present he is Co-director of LogiSim, a Modelling and Simulation Institution sponsored and founded by the local government of Catalonia. Recently, he has published a modelling and simulation book that is being used for teaching in many Spanish universities.

THE EFFECTS OF TRANSIT CORRIDOR DEVELOPMENTS ON THE HEALTHCARE ACCESS OF MEDICALLY FRAGILE VULNERABLE POPULATIONS

Rafael Diaz^(a), Asad Khattak^(b), Joshua Behr^(c), Anna Jeng^(d), Francesco Longo^(e), Jun Duanmu^(f)

^{(a)(c)(f)} Virginia, Modeling, Analysis and Simulation Center, Old Dominion University

^{(a)(b)} College of Engineering, Department Civil & Environmental Engineering, Old Dominion University

^{(a)(c)(d)} College of Health Science, Department of Community and Environmental Health, Old Dominion University

^(e) MSC-LES, University of Calabria, Mechanical Department, Italy

^(a) rdiaz@odu.edu, ^(b) akhattak@odu.edu, ^(c) jbehr@odu.edu, ^(d) hjeng@odu.edu, ^(e) f.longo@unical.it,
^(f) jduanmu@odu.edu

keywords: vulnerable populations, gentrification, simulation, healthy behaviors

ABSTRACT

Transportation has been identified as a major barrier to healthcare access, particularly, within vulnerable population groups. The level of healthcare access that most population segments have in traditional transit systems may be increased with new initiatives that involve complex and large investments in transit oriented developments (TOD) projects. However, the increasing attractiveness of neighborhoods affected by TOD initiatives may result in the gentrification of vulnerable population segments. These vulnerable segments are likely to be relocated into less attractive neighborhoods characterized by inadequate transit systems. This relocation increases the probabilities of reducing healthcare access for these underserved groups leading to an increase in health disparities. The present discussion calls for research to explore relevant factors that affects these dynamics. A framework that enables the identification of individual factors that affect gentrification processes under TOD initiatives as well as quantifying the effects from these processes is suggested in this paper. A system dynamics framework that allows the understanding of the dynamics associated with this system is suggested in this paper. Critical areas for empirical research are highlighted. These are prerequisites for the effective deployment of initiatives that ensure the mitigation of possible negative impacts on vulnerable populations.

1. INTRODUCTION

Transportation has been cited one of the most critical barrier to access to healthcare (Institute of Medicine 1993). A large number of studies indicate the negative impacts of transportation barrier towards access to healthcare, predominantly, for vulnerable population. Rittner and Kirk (1995) report that a majority of low income old people in poor health condition depended

on public transit as their only means of accessing healthcare services. Okoro et al.(2005) report 'lack of transportation' and a possible dependence on public transportation as one of critical barriers to healthcare, especially for women, in a study of overcoming the barriers to preventive care among older population. Similar results are reported by Fitzpatrick et al.(2004). Flores et al.(1998) found that transportation problem was cited by 21 % of the parents as the reason for lack of access to healthcare when studying the barriers to healthcare access among Latino children. Ahmed et al. (2001) report comparable results from studying barriers for non-elderly, poor Americans segments in urban settings. In a study conducted in a community health center settings, Shook (2005) reports that 32 % of the patients reported a transportation barrier within the last year, with most problems related to transit. Consistently, this author finds that this barrier affects the vulnerable populations more severely than the rest. From the discussion above it is evident that transportation remains to be a major barrier to healthcare and that transit is a possibly inefficient but the only (and hence important) means of accessing healthcare especially for the most vulnerable populations.

1.1. Background

The idea of promoting livability through development centered on transit corridors has generated a significant attention from the public opinion in recent times. The concept of livability is centered around the degree of equivalence between the needs of individuals and the provisions within the society/environment to satisfy those needs (Veenhoven and Ouwenel 1995). Livability is concerned with the need of an individual to live in a socially amenable environment that promotes individual as well as collective well-being (Newman and Kenworthy 1999). Public transportation plays a unique and important role in promoting livability. Transportation hubs (stations) become points at which

people meet and interact with each other; stations become centers of commerce and social events and recreation while providing better mobility to people by connecting neighborhoods (Transportation Research Board 1997). Most important elements of TOD include higher density and mixed land use, and ease of access to high quality public transportation in which car rides are replaced by walking and biking and creating a sense of identity within the community (Cervero, Ferrell et al. 2002). During the past decade a large number of major urban centers in the US are planning or implementing some class of mass transit system using TOD as a base (Belzer and Autler 2002). This idea is gaining momentum among local and state governments as well as federal transportation agencies.

A critical consideration that emerges from the discussion above is the effect of transit oriented initiatives on an already weak level of access to healthcare that elderly and medically fragile vulnerable populations have. Particularly, the rising cost of housing in areas that have easy access to public transportation under TOD initiatives are likely to make those housing options unaffordable to these vulnerable segments. The gentrification of low-income neighborhoods due to TOD may cause a reduced access to public transportation for vulnerable populations. This further impedes their access to healthcare.

Gentrification effects due to TOD initiative have already been explored in the literature. Kahn (2007) presents results from an extensive study spanning 14 cities that have implemented TOD initiatives. The author utilizes home price and demographic data for the neighborhoods affected by rail transit access and compared them with similar neighborhoods without rail transit access. Since a large number of factors are shown to affect the degree of gentrification, outcomes from these studies vary significantly. For example, TODs providing *Walk and Ride* access to transit have seen gentrification in Washington DC and Boston metropolitan areas while an absence of effects are observed in Los Angeles and Portland. The empirical evidence indicates that the level of gentrification is associated with the appreciation in the property values due to transit access, and as indicated by Bowes and Ihlanfeldt (Bowes and Ihlanfeldt 2001), this itself is a multi-factorial problem. While acknowledging the potential harmful effects of TOD initiatives in causing gentrification, Poticha (2007) has pointed to the possible lack of mitigation tools in many of the TOD projects. The degree of impact on vulnerable populations is reliant upon the large number of individual factors that intervene in this process as well as their interactions and interrelationships. This makes the problem of accessing and mitigating such effects more complex.

1.2. Critical Factors Underpinning Healthcare and Livability on Transit Corridors

The mobility within the transit corridor is centered on a high quality public transportation system such a rail

(light or heavy) or a bus. Having an easy access to transit stations is fundamental to mobility. This preference is evident from the positive rise in the cost of the properties in the vicinity of the transit stations (Bajic 1983; Armstrong 1994; Gibbons and Machin 2005; Hess and Almeida 2007). A study by Chen et al.(1998) has reported that the positive effect of accessibility on property values dominates the negative impacts due to noise, pollution and criminality in case of Portland, Oregon. However, a study by Bowes and Ihlanfeldt (2001) conducted in Atlanta, Georgia, indicates that the magnitude and direction of the impact of transit access on property values may also depend on other factors such as retail activity, crime, noise, pollution and traffic associated with the stations. Smith and Gihring (2006) call for the resulting value of this positive linkage between transit access and property values to be captured for transit projects financing.

Accessibility is the most important and well-studied issue analyzed in livability communities. A safe, open and convenient pedestrian environment is the basic requirement for a pedestrian friendly transit corridor. For example, Schlossberg and Brown (2004) present 12 geographic information based on walkability measures to visualize and quantify the pedestrian environments. Other important design factors related with walking distance and building site design are found in (O'sullivan and Morrall 1996; Bernick and Cervero 1997; Nelson, Niles et al. 2001; Zimring, Joseph et al. 2005; Samuelson 2009; Miller, Hoel et al. 2010). Various investigations have analyzed the interaction between land use and transportation system (Hanson 1995; Rodrigue 1997) while the model of interaction between transportation and public health and quality life has drawn plenty attention (Frank 2000). Despite the interactions between the transit systems and land use, the topic of gentrification resulting from TOD initiatives has been unexplored.

2. RESEARCH QUESTION

Literature that explores the impact of livable transit corridor development on the healthcare of vulnerable population is limited. This research is extremely important in view of the recent popularity of TOD initiatives and the possibility of adoption of these projects on a larger scale. The purpose of this research is to identify key factors and relationships that impact this process and create a framework wherein this system can be modeled and simulated. An important outcome of this exercise is the identification of areas for empirical research that is not yet available. Further, this model enables a generic understanding of the processes that affect gentrification and hurdles to healthcare access. The proposed model may become a basis for numerous experiments within the cost and practicality constraints.

The system at hand is complex and has a number of intricate feedback effects associated with it. For example, the negative impact of healthcare access may lead to deterioration of health condition which imposes

economic challenges that aggravate vulnerability and lead to further reduction in healthcare access increasing disparity. Similarly, investment in transit system may advance the local economic development for affected neighborhoods and surrounding areas. This may provide more resources for further development of transit systems. The presence of such relationships makes system dynamics an ideal choice as far as the modeling paradigm is concerned.

Maintaining the affordability of the housing in such corridors for medically fragile populations is a potential strategy for mitigating such negative impacts. However the positive pressure on housing prices in the corridor region means increasing subsidies to make such policies feasible. The nature and magnitude of such and other initiatives can only be ascertained when adequate research on the lines as proposed here becomes available. A framework capable of assessing potential interventions in this setting is necessary.

3. RESEARCH APPROACH

The concept *livability* may encompass multiple qualitative attributes of a community's quality of life, including physical and mental well-being, educational and employment opportunity, recreation, built environment, safety, and political efficacy. An ideal characterization of a livable community with a well-being focus includes concepts of representation and responsiveness in the planning and policy generation processes, proximate access to safe public transit, green space, and improved air quality, among others. This includes a supporting system in which vulnerable population groups are protected and intervention strategies may be timely identified. The Partnership for Sustainable Communities Sustainable (2012) describes livable communities as those that promote public health, educational opportunities, and green environmental practices, among others. Thus, the concept of livability is necessarily broad and encompasses a host of economic, social, health, and perceptual characteristics. None of these attributes of transit corridor livability may stand independent, though. That is, the conceptualization of a transit corridor as a *system* necessarily implies that the constituent parts are interrelated to some degree. For example, perceptions of safety may be a function of the built environment and improved air quality may be a function of more transportation choice; both these relationships may, in turn, contribute to a transit corridor's economic competitiveness. However, as indicated before, this generates a variable degree of gentrification of vulnerable groups that depends on the location of each station and the rail line of the corridor.

It is understandable, then, that the study of such a system requires identification of these attributes as well as an understanding of how each attribute may act upon others to promote either reinforcing or balancing behavior of the overall system. It is difficult to conceptualize, let alone empirically capturing, the overall system behavior stemming from the myriad of

causal relationships among these factors. It also difficult to visualize how transit policy interventions may alter livability, and in particular, public health effects, within a system, and even more difficult to understand the disparate impact such interventions may have among population and vulnerable groups or neighborhoods. System Dynamics offers an attractive approach to capturing the complexities inherent within a transit corridor system and how the system may respond to interventions. In addition, since livability is inextricably linked to the experience of place and the surrounding built environment, tools and techniques designed to address issues such as proximity, density, area, and hot spots are also essential to our approach. For example, from the health perspective, the concept of livability may include pedestrian access or walk-ability to transit service station while considering the mobility levels of each pedestrian sub-population such as elderly.

Mental models are unable to accommodate the complexity of interactions that are some distance from the immediate problem. Through a system dynamics approach, the measurement of the dynamic impacts of transit feeder interventions over time are meant to allow stakeholders (especially policy makers and traditionally underserved communities) to interpret the information differently by allowing alteration of mental models. Traditional approaches have not been well suited to anticipate the second and third order health-related consequences of competing policy options upon particular population segments (e.g., underserved communities) and, in some instances, have resulted in policy resistance (e.g., resulting in unanticipated changes in livability). Our system dynamics approach allows us to understand -- as well as anticipate -- the dynamic behavior of the population health dynamics of neighborhoods beyond the transit station area over time, particularly on those vulnerable groups, and allows us to empirically demonstrate changes in the system's behavior which may be counterintuitive or would not have been evident if approached with more traditional causal methodologies. With our proposed approach, decision makers may simulate over time the dynamic interaction and 'ripple effect' of adopting any combination of feeder transit corridor policy options and the sensitivity of various sub-populations to these interventions.

4. CONCEPTUAL MODEL DESCRIPTION

The conceptual model representing the dynamics described and key causal relations is introduced in this section. Figure 1 below illustrates the proposed conceptual model. A description of the dynamic hypothesis that forms the basis of the model follows.

The dynamic hypothesis is developed from the discussion based in the previous section. The causal-loop diagram presented in Figure 1 suggests that the investment in TOD projects enables the deployment of greater number of transportation resources.

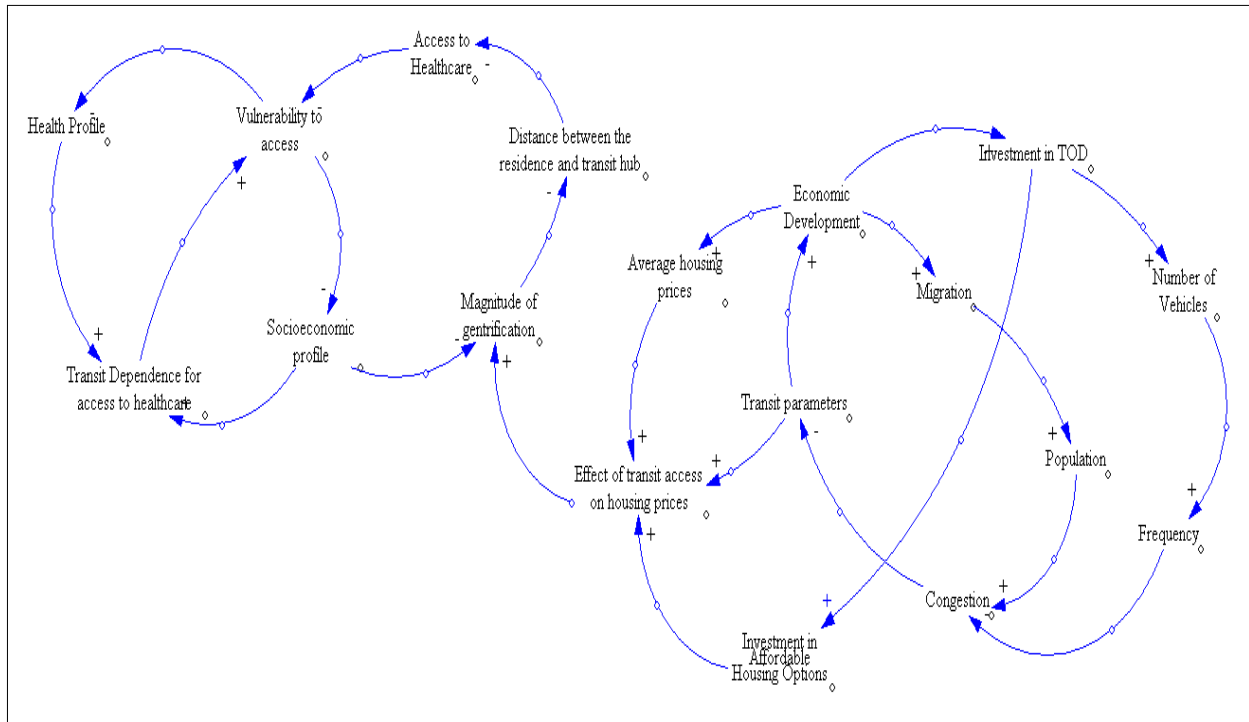


Figure 1. Causal Loop Diagram Representing the Dynamic Hypothesis

This leads to the development of an efficient transportation system. Simultaneously, the availability of efficient transportation becomes an asset for the region that attracts investments and fosters economic activity as indicated in section 1.1 and 1.2. Thus, the areas affected by the TOD solution become centers for commercial activity. The resulting employment opportunities attract migrants to the region which increases the demand for the transit and leads to congestion. However, the increasing commercial activity in the region produces a greater income in form of tax revenues for the local authorities. This income may be reinvested in the TOD or other related project that further transit development.

The effectiveness of the transit determined by the key transit performance parameters is one of the factors affecting the values of home prices in the vicinity of the transit access. Two additional important factors involve the overall trend in housing prices in the region as well as the efforts within the TOD initiatives to maintain the affordability of the housing within the corridor. Affordability of housing within TOD may be maintained by allowing higher density construction and providing subsidies to make affordable housing option available to the low-income populations. The combination of these factors determines the magnitude of change in the housing prices in the corridor.

An increase in the housing prices in the corridor may result in gentrification process of the population having a lower socio-economic profile. This process may occur because of the increasing rents and taxes that result from the increasing house prices will be likely out of reach of these vulnerable classes. The

displaced population is forced to be relocated into areas that have comparatively lower access to public transit. Simultaneously, the gentrification process may occur to those who experience mobility issues, e.g., elderly or those who suffer a chronic disease and are considered a vulnerable population. Since many spaces affected by the TOD solution are purposely design to be walkable spaces, these vulnerable populations may find limited transporting options that cause them to leave to other areas.

As the underserved population relocate, the access to public transit is reduced while experiencing increases in their vulnerability. The reduced access leads to likely neglect their medical care and further deteriorates the health status of these vulnerable individuals. This relocation might lead to a further decline in their socio-economic profile, e.g., a longer commute may increase transportation expenditures jeopardizing job continuity. Figure 2 presents a stock and flow model that implements this dynamic hypothesis. The model is then simulated under hypothetical conditions to determine its behavior. The results of the simulation are presented and discussed in the next section.

5. RESULTS

The model is executed for an experiment wherein the 'Investment fraction in affordable housing' is alternated between 0.001 (scenario 1) and 0.005 (scenario 2). This fraction represents the relative portion in TOD investments dedicated to subsidizing or making available, through a generic theoretical intervention, affordable housing to the disadvantaged. Notice that the values used in these experiments are theoretical.

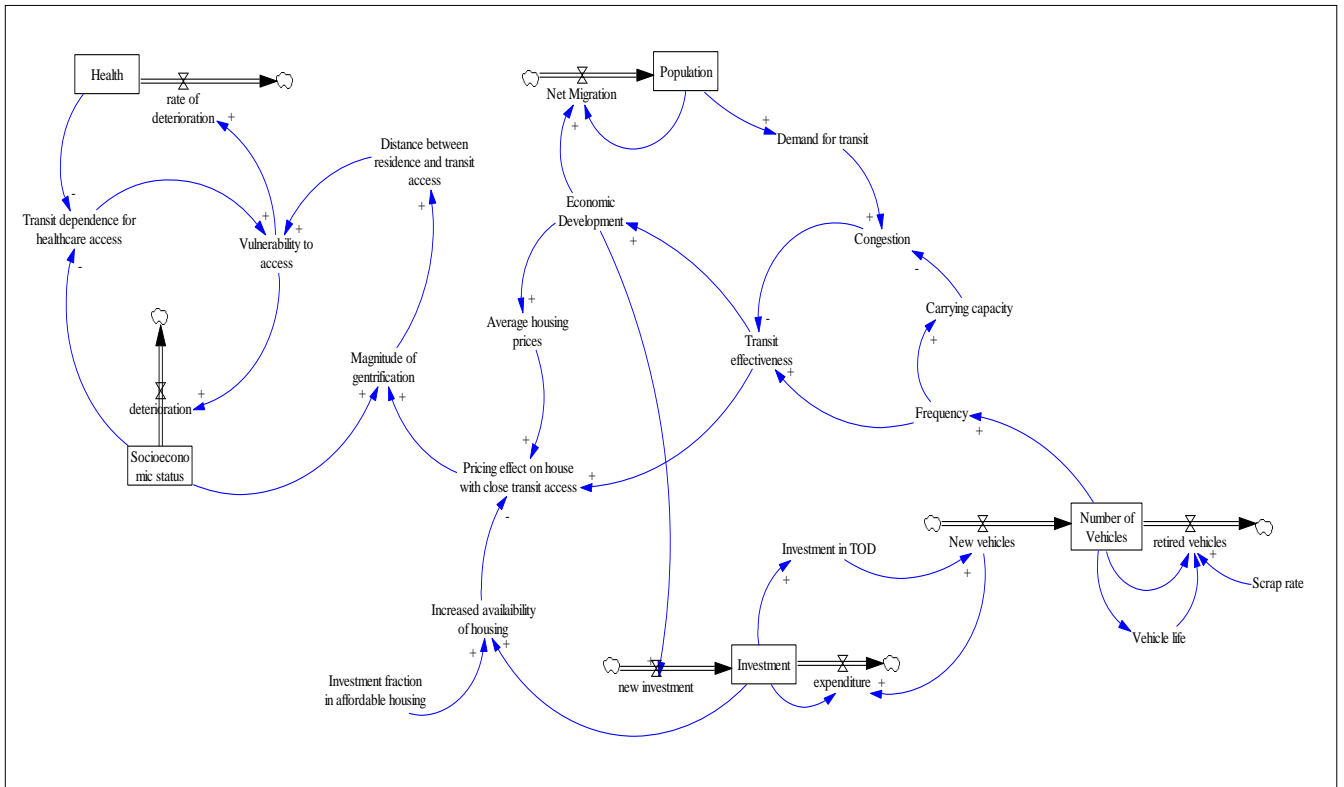


Figure 2. Stock and Flow Model

These hypothetical values do not represent anything and they are just used to explore the theoretical behavior. The resulting system behavior is based on our synthetic representation of a real-world situation. Thus, at this stage, we are seeking to mimic the behavior of each synthetic variable according to its corresponding real-world representation without focusing on accurate levels of the variable. The refinement and calibration of the model will be executed on subsequent research activities.

The fraction indicated above may potentially represent a relative mitigation of the gentrification process. Figure 3 below illustrates the trend in *vulnerability to access* under the scenarios mentioned above where the continuous line represents the scenario 1 while the segmented line represents the scenario 2. As expected in this theoretical model, it is observed that increasing the allocation funds for affordable housing within the TOD projects reduces the vulnerability to healthcare access over time.

The opposite is true when relatively fewer or none funds are allocated for this purpose. A similar trend is seen in the *Socio-economic status*. Availability of affordable housing within the TOD corridor leads to an improvement in the socio-economic status due to increased access to both healthcare and economic opportunities. Conversely, a lack of funding is likely to lead to gentrification and possible deterioration of socio-economic status due to reduced access to

healthcare and the resulting disadvantage from employment perspective.

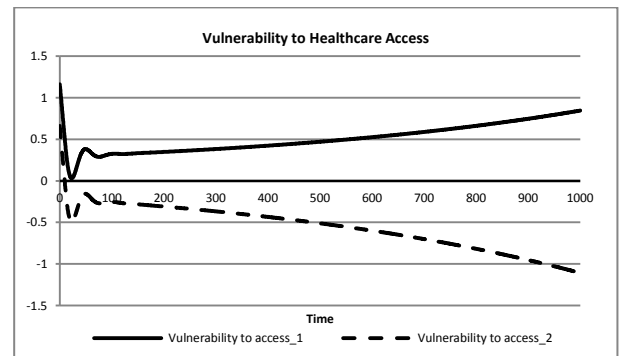


Figure 3. Vulnerability to Reduced Healthcare Access

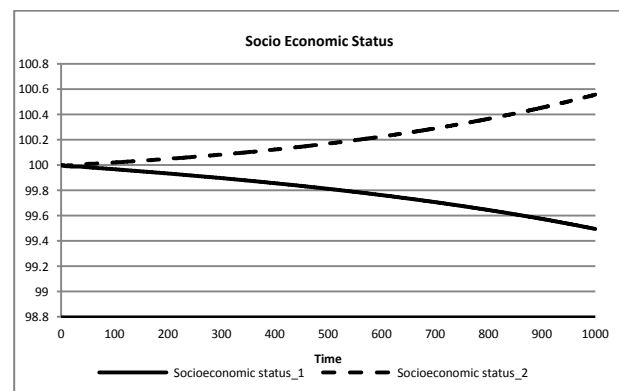


Figure 4. Socioeconomic Status

The level of transit effectiveness within the TOD corridor is reported in Figure 5. The transit effectiveness is expressed as a function of the demand for transit and the available capacity of the transit. The available capacity of transit is characterized as the function of the transit frequency for a constant per trip carrying capacity. Figure 6 illustrates the trend for the price of houses close to the transit locations. The trends are influenced by the proportion of funds available from affordable housing initiatives. Adequate funding levels allocated to affordable housing in the TOD corridor have the capability of mitigating the negative impact of transit access on housing prices and help keeping average housing prices controlled. An absence of such initiatives is likely to result in a price increase in the TOD corridor housings, as transit access is increasingly seen as a useful feature of houses in transit vicinity.

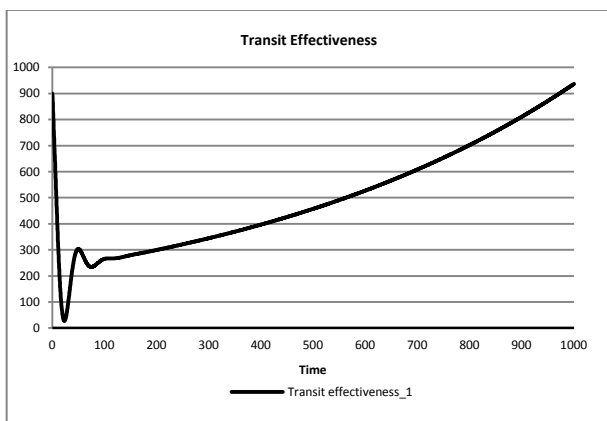


Figure 5. Transit Effectiveness

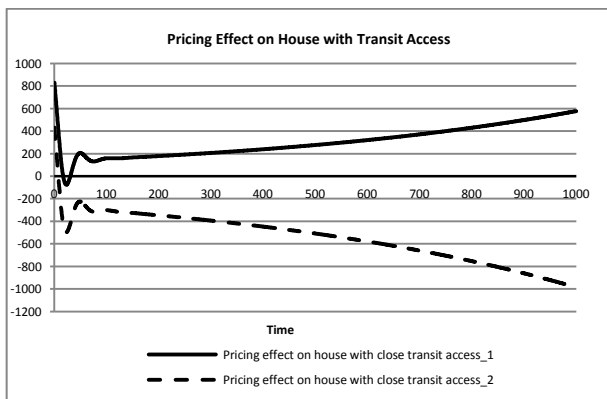


Figure 6. Pricing Effect of Transit Access on Housing Prices

6. CONCLUSIONS

An important linkage between transit oriented development and healthcare access is highlighted in this paper. While TOD is likely to improve healthcare access to the general population by providing reliable transit, its impact on the most vulnerable segments of the population are uncertain. Some studies have shown

that TOD initiatives may potential lead to gentrification under certain conditions. The present study focuses on the modeling of critical factors that characterize this relationship and the characterizing of the links between these factors and their representation using a system dynamics approach. The use of system dynamics as the modeling paradigm is justified by the presence of considerable complexity and feedback in the system under consideration.

The study by Kahn (2007) shows that gentrification in TOD initiatives is not universally observable and depends on numerous factors. Thus, the effect of TOD on the healthcare access of vulnerable populations is likely not to be generic and dependent on numerous variables and their dynamics. A common understanding of effects of a particular set of factors may have on the implementations of TOD projects and potential gentrification processes is lacking. The purpose of the modeling exercise in this paper is to create a platform wherein relevant factors may be modeled and simulated. Thus, a framework that enables a more generic understanding of the effects of TOD on healthcare access of vulnerable population may be created.

While endeavors in the creation of such a model are described in this paper, what is lacking is the empirical analysis necessary to validate the model behavior. Therefore, a critical step in the extension of this work involves development of case studies that empirically analyze the impact of TOD on the healthcare access of vulnerable population. These results may be used to refine and validate the model proposed above. The model may be then used to understand the possible systemic implication (first- and second-order effects) that various scenarios of input factors can create. The model may thus become a useful tool for generalizing the outcomes from these analyses such that they may be employed for predictive studies in future projects. Further, this tool may be prospectively transformed into a training tool that provides an educational platform for understanding the effects of TOD implementations on health inequalities as well as a means for exploring interventions that assist in mitigating the impact of gentrification processes.

In addition this work demonstrates that can be extended to suburban TODs environments (Rodriguez, Khattak et al. 2006; Baran, Rodríguez et al. 2008; Brown, Khattak et al. 2008) which is an ongoing investigation for the authors.

REFERENCES

- Ahmed, S. M., J. P. Lemkau, et al. (2001). "Barriers to Healthcare Access in a Non-elderly Urban Poor American Population." *Health & Social Care in the Community* 9(6): 445-453.
- Armstrong, R. J. (1994). *Impacts of Commuter Rail Service as Reflected in Single-Family Residential Property Values*: 88-98.

- Bajic, V. (1983). "The Effects of a New Subway Line on Housing Prices in Metropolitan Toronto." *Urban Studies* **20**(2): 147-158.
- Baran, P. K., D. A. Rodríguez, et al. (2008). "Space Syntax and Walking in a New Urbanist and Suburban Neighbourhoods." *Journal of Urban Design* **13**(1): 5-28.
- Belzer, D. and G. Autler (2002). *Transit Oriented Development: Moving From Rhetoric to Reality*, The Brookings Institution Center on Urban and Metropolitan Policy.
- Bernick, M. and R. Cervero (1997). *Transit Villages in the 21st Century*. New York, NY, McGraw-Hill.
- Bowes, D. R. and K. R. Ihlanfeldt (2001). "Identifying the Impacts of Rail Transit Stations on Residential Property Values." *Journal of Urban Economics* **50**(1): 1-25.
- Brown, A., A. Khattak, et al. (2008). "Neighborhood Types, Travel and Body Mass: A Study of New Urbanist and Suburban Neighborhoods." *Urban Studies* **45**(4): 963-988.
- Cervero, R., C. Ferrell, et al. (2002). *Transit-Oriented Development and Joint Development in the United States: A Literature Review*, Transit Cooperative Research Program.
- Chen, H., A. Rufolo, et al. (1998). "Measuring the Impact of Light Rail Systems on Single-Family Home Values: A Hedonic Approach with Geographic Information System Application." *Transportation Research Record: Journal of the Transportation Research Board* **1617**(-1): 38-43.
- Communities, T. P. f. S. (2012). "*About Us*." Retrieved June 11, 2012, from <http://www.sustainablecommunities.gov/about/Us.html>.
- Fitzpatrick, A. L., N. R. Powe, et al. (2004). "Barriers to Health Care Access Among the Elderly and Who Perceives Them." *American Journal of Public Health* **94**(10): 1788-1794.
- Flores, G., M. Abreu, et al. (1998). "Access Barriers to Health Care for Latino Children." *Archives of Pediatrics & Adolescent Medicine* **152**(11): 1119-1125.
- Frank, L. D. (2000). "Land Use and Transportation Interaction : Implications on Public Health and Quality of Life." *Journal of Planning Education and Research* **20**(6): 6-22.
- Gibbons, S. and S. Machin (2005). "Valuing Rail Access Using Transport Innovations." *Journal of Urban Economics* **57**(1): 148-169.
- Hanson, S. (1995). *The Geography of Urban Transportation, Second Edition*. New York, NY, Guilford Press.
- Hess, D. B. and T. M. Almeida (2007). "Impact of Proximity to Light Rail Rapid Transit on Station-Area Property Values in Buffalo, New York." *Urban Studies* **44**(5-6): 1041-1068.
- Institute of Medicine (1993). *Access to Health Care in America*. Washington, D.C, National Academies of Science Press.
- Kahn, M. E. (2007). "Gentrification Trends in New Transit-Oriented Communities: Evidence from 14 Cities That Expanded and Built Rail Transit Systems." *Real Estate Economics* **35**(2): 155-182.
- Miller, J. S., L. A. Hoel, et al. (2010). "Evaluating Unplanned Stand-Alone Transportation Projects: Linking Incremental and Comprehensive Planning." *Journal of Urban Planning and Development* **136**(4): 320-329.
- Nelson, D., J. Niles, et al. (2001). *A New Planning Template for Transit-Oriented Development*. San Jose, CA, Mineta Transportation Institute. **MTI Report 01-12**.
- Newman, P. and J. Kenworthy (1999). *Sustainability and Cities: Overcoming Automobile Dependence*. Washington, D.C., Island Press.
- O'sullivan, S. and J. Morrall (1996). "Walking Distances to and from Light-Rail Transit Stations " *Transportation Research Record: Journal of the Transportation Research Board*(1538): 19-26.
- Okoro, C. A., T. W. Strine, et al. (2005). "Access to Health Care Among Older Adults and Receipt of Preventive Services. Results from the Behavioral Risk Factor Surveillance System, 2002." *Preventive Medicine* **40**(3): 337-343.
- Poticha, S. (2007). *Building Housing Near Transit: A Long-Lasting Affordability Strategy*.
- Rittner, B. and A. B. Kirk (1995). "Health Care and Public Transportation Use by Poor and Frail Elderly People." *Social Work* **40**(3): 365-373.
- Rodrigue, J.-P. (1997). "Parallel Distributed Processing of Transportation / Land Use Systems: Theory and Modelling with Neural Networks." *Transportation Research C* **5**(5): 259-271.
- Rodriguez, D., A. J. Khattak, et al. (2006). "Can New Urbanism Encourage Physical Activity? Comparing a New Urbanist Neighborhood With Conventional Suburbs." *Journal of the American Planning Association* **72**(1): 43-56.
- Samuelson, M. (2009). "Reducing Cars and Increasing Development: How the Creation of a Viable Transit Oriented Development Corridor in Arlington, Virginia has Sparked Growth." *Cities in the 21st Century* **1**(1): 1-31.
- Schlossberg, M. and N. Brown (2004). "Comparing Transit-Oriented Development Sites by Walkability Indicators." *Transportation Research Record: Journal of the Transportation Research Board* **1887**: 34-42.
- Shook, M. (2005). *Transportation Barriers and Health Access for Patient Attending a Community Health Center*.
- Smith, J. J. and T. A. Gihring (2006). "Financing Transit Systems Through Value Capture."

American Journal of Economics and Sociology **65**(3): 751-786.

Transportation Research Board (1997). *The Role of Transit in Creating Livable Metropolitan Communities*. New York, NY.

Veenhoven, R. and P. Ouwenel (1995). "Livability of the Welfare-State: Appreciation-of-Life and Length-of-Life in Nations Varying in State-Welfare-Effort." *Social Indicators Research* **36**(1): 1-48.

Zimring, C., A. Joseph, et al. (2005). "Influences of Building Design and Site Design on Physical Activity: Research and Intervention Opportunities." *American Journal of Preventive Medicine* **28**(2): 186-193.

AUTHORS BIOGRAPHY

Rafael Diaz graduated from the Old Dominion University with a Ph.D. in Modeling and Simulation in 2007, and became a Research Assistant Professor of Modeling and Simulation at Old Dominion University's Virginia Modeling, Analysis, and Simulation Center (VMASC). He holds an M.B.A degree in financial analysis and information technology from Old Dominion University and a B.S. in Industrial Engineering from Jose Maria Vargas University, Venezuela. His research interests include operations research, operations management, healthcare and public health policy-making, dependence modeling for stochastic simulation, and simulation-based optimization methods. He is and an Adjunct Assistant Professor in the program of Public Health, at Eastern Virginia Medical School.

Asad Khattak graduated from Northwestern University with a Ph.D. in Civil Engineering in 1991, and is currently Batten Endowed Chair professor at Old Dominion University. He is Director of the Transportation Research Institute at ODU, and has worked nationally and internationally in transportation research, focusing on intelligent transportation system and sustainable transportation. He has authored/co-authored 90 refereed journal articles and managed more than 40 sponsored research projects. He is editor of the Journal of Intelligent Transportation Systems, and associated editor of International Journal of Sustainable Transportation.

Joshua G. Behr received his Ph.D. training at the University of New Orleans specializing in urban and minority politics. He has taught a variety of public policy, state government, and statistical methods courses at the University of New Orleans, Southwestern Oklahoma State University, Eastern Virginia Medical School, and Old Dominion University. His is now a research professor at the Virginia Modeling, Analysis and Simulation Center (VMASC), Suffolk. He has published on a wide range of topics including

presidential approval, times series methodology, minority employment patterns, public health, and emergency department utilization as well as a recent book (SUNY Press) on political redistricting and a book chapter addressing discrete event simulation. Currently, his research interests include modeling and simulating smart grid, transportation systems, and the flow of patients within a regional healthcare system.

Anna Jeng is an Associate Professor of Environmental Health at Old Dominion University. Her research focuses on environmental and public health assessment that identify health effects and diminished quality of life resulting from exposures to environmentally and occupationally hazardous substances in the environment. Her projects have involved site assessment, determination of contaminants of concern in affected communities and identification and evaluation of exposure pathways.

Francesco Longo received his Ph.D. in Mechanical Engineering from University of Calabria in January 2006. He is currently Assistant Professor at the Mechanical Department of University of Calabria and Director of the modeling & Simulation Center – Laboratory of Enterprise Solutions (MSC-LES). He has published more than 80 papers on international journals and conferences. His research interests include Modeling & Simulation tools for training procedures in complex environment, supply chain management and security. He is Associate Editor of the "Simulation: Transaction of the society for Modeling & Simulation International". For the same journal he is Guest Editor of the special issue on Advances of Modeling & Simulation in Supply Chain and Industry. He is Guest Editor of the "International Journal of Simulation and Process modeling", special issue on Industry and Supply Chain: Technical, Economic and Environmental Sustainability. He is Editor in Chief of the SCS M&S Newsletter and he works as reviewer for different international journals. His Web-page can be found at http://www.ingegneria.unical.it/impiantiindustriali/index_file/Longo.htm

Jun Duanmu is a research associate in Virginia Modeling, Analysis and Simulation Center. He got his Ph.D. degree in Clemson University majoring in Industrial Engineering and minor in Transportation Engineering. He also got his master degree in Management of Production from Chalmers University of Technology in Sweden. He worked as a consultant in Norfolk Southern and Swedish Motor Vehicle Inspection Company. Dr. Duanmu has long research experience in simulation and process improvement in public health, freight transportation, logistics and manufacturing.

INNOVATIVE C2 AND SIMULATION FOR CROWDSOURCING AS FORCE MULTIPLIER

Agostino Bruzzone^(a) Henrique C. Marques^(b) Giovanni CANTICE^(c) Michele TURI^(c)

^(a) Genova University

^(b) George Mason University – VA, (US)

^(c) DIME (Department of Mechanic, Energy, Production, Transports and Mathematic Models) PhD Program

^(a)agostino@itim.unige.it ^(b)hmarques@gmu.edu ^(c)cantice@liophant.org ^(c)turi@liophant.org

ABSTRACT

Crowd source isn't a news in the military: its first official appearance as military concept was supported by US Army Brig. Gen. McMaster in 2009 (ARCIC Director), publishing online the 2009 Army Capstone Concept for public comments.

However in this paper the authors aim is to present their studies regarding a project to develop a different generation of C2 processes, inspired by latest technologies, daily applied on Social networks, mobile devices and social cooperation that are addressing also significant researches in the Military Domain, and potentially able to shape the future generation of Simulation and C2 systems.

This paper represents the basic ideas on how to develop a new C2 organization and training simulation approach linked with NCW/NEC concept and strongly oriented to:

- the crowdsourcing phenomena of outsourcing a problem to a large audience;
- translate crowdsourcing into a military environment;
- apply NATO cross functional team concepts in a Virtual/Immersive and interoperable environment;
- define a Crowdsourcing Cross Functional Team;
- evaluating the dispersing leadership concept, self-synchronization and multidimensionality of command;
- analyze information assurance to enable a correct information sharing, using i.e. Augmented Reality;
- model new military dynamic relationships to connect cells and functional areas with neuralgic headquarters;
- applying C2 maturity level N2C2M2 (Alberts et al 2010, Bruzzone et al.2009) and IA (Bruzzone et al 2011, 2010, 2008, 2007).

As the Crowdsourcing has proven a very useful concept in industrial world, adequately adapted, it could serve as a force multiplier in the military.

Keywords: Command and Control, Social Networks, training Simulation, Immersive, NCW/NEC (Net Centric Warfare, Network Enabled Capability), IA (Intelligent Agents), Crowdsourcing, N2C2M2 (Net-centric Command & Control Maturity Model), Augmented Reality, Interoperability.

1. INTRODUCTION

The crowdsourcing concept was officially ascertained in 2006 by an article of Jeff Howe on Wired newspaper "the rise of crowdsourcing". The idea to probe what general people think about any problem is not news, if we think for example at commercial probing or television voting. Avoiding being much generalist, there are two sides to keep in mind:

- crowdsourcing concept is stick to Internet (Networking in general) and the even more spread capability to navigate in different way in almost every country;
- the big leap forward made by the technologies and mobile devices that have made simple to use a lot of daily life applications for the normal people in the last years.

Crowdsourcing as the words explain, is something based on a open request made normally by a digital support, toward a lot of people, especially who has specific knowledge, regarding the solution for a determined problem, asking to give a possible solution and contribute with new ideas, involving not only professionals but also amateurs. That's what defines crowdsourcing "collective intelligence".

Collective intelligence is a business model on which companies can ask for a project or a service development to a distributed group of people working in a virtual community through web and internet support. In this way a lot of companies have the possibility to exploit users and realize products tailored on them, using more resources than they have but costless.

Initially crowdsourcing was based on "digital volunteers" and enthusiast geeks of Internet,

stakeholders from computers and technologies that dedicated spare time to solve problems for others (i.e. the experts that try to answer you on blogs and communities); today crowdsourcing in some countries is considered a “open enterprise” where freelance experts and professionals can offer their abilities and capabilities referring to a “mass cooperation and collaboration”.

Digitalization is changing the life always more and almost every day we can see new items to make easier the people life and passing over a lot of concepts, systems and ways of work and live making them obsolete.

Crowd source isn't completely a news in the military: Its first official appearance as military application concept was supported by US Army Brig. Gen. McMaster in 2009 (ARCIC Director), publishing online the 2009 Army Capstone Concept for public comments; as before, also Lt. Gen. Petraeus wrote in 2006 on US Army Field Manual FM 3/24 “Counterinsurgency”, that “...*insurgents’ capabilities also come from their creative exploitation of commercially available technologies and materials as well as their lack of bureaucratic encumbrance*”.

2. CROWDSOURCING IN THE MILITARY

We can initially define Crowdsourcing as a “distributed problem – solving” and also an application to produce ideas, solutions, answers.

Analyzing this aspect we can immediately view the parallelism with the military problem solving method where an assigned mission from the HQ must be accomplished in cascade by the Unit in all echelons of Command, solving the chained operational problem and proposing to the Commander the possible COAs to apply.

This method, called MDMP (Military Decision Making Process), always has been and it is “the method” used, especially in a conventional and classic scenario, the way to solve operational missions and propose the most probable solutions (COAs – Course of Actions).

In the crowdsourcing the problem is distributed through the network, more or less controlled, to an audience (users) formed normally by specialists or “problem solvers”. The solution is normally owned by an individual that asks help to solve the problem. The contributors to the problem are usually compensated just with the intellectual satisfaction to be the ‘solver’. Should be more than one good solution and the asker will decide which to use.

Making another parallel, in the military, the Commander can receive a mission that he normally translate in a operational problem to submit to his staff through the MDMP and in a modern command post all cells are linked in a

intranet network where all the specialist can operate. Any branches will solve a piece of the operational problem composing few final COAs which will be presented from the chief of staff to the commander. Only he will decide the best COA to use.

In large terms and extrapolating in a well define domain, the MDMP should be considered a sort of primitive Crowdsourcing process where the owner of final solution is the Commander, the audience is represented by the different staffs of units subordinated and the stakeholders that solve the problems are represented by the branches specialist.

But it's not enough. So, how we can apply the distributed and spreading power capability of crowdsourcing in a military operational environment, like a stability mission, to involve huge quantity of different specialists also from distance and solve operational problems?

The new doctrine guidelines to operate in stability missions are normally involving also civilian specialist (engineers, geologists, psychologists, medics, etc.) that any traditional Military Commanding Officer cannot have as “normal capability” from his unit.

2.1. Crowdsourcing possible current example

There are different examples in which this concept was adopted to solve problems related with new technology, medicine, art, research and business through different kind of platform (i.e. Mechanical Turk from Amazon, 2005) but their scope is almost the same: distribute a problem to a audience and get back a solution.

The positive side from using these methods is the large number of solutions and their very low cost. It is not appear just a simple exchange method of ideas; who is using methodically this concept inside a business, company or organization is orienting the power of this concept to create specialized communities, called Community based design or distributed participatory design, able to use software platform to capture, analyze and arrange huge quantity of data.

What is the model to utilize? there are multiple approaches to crowdsourcing concept and application. The principal difference depend from the use of large active cooperation through Internet communities or the searching for specific and controlled interaction from a controlled/interested users.

The primary types of Crowdsourcing (Jeff Howe classification), should be identify as:

- Crowd Wisdom (best practiced form): means using the knowledge of people to find solution for problems, predict future or define strategies;
- Crowd Creation (best known form): concept addressed to encourage and drive people toward creative activities (photos, commercial adv TV, software development – i.e. Linux – etc.), or solve scientific problems as challenge;
- Crowd Voting (best popular form): intended as communities judges for articles, music, movies,
- Crowd Funding (best known form): provide credit and fund to create opportunities or support projects that are not acknowledge.

Other models are build on collective intelligence as Crowd Casting, use put together huge community of experts in various fields of research to face the high cost of researches normally tackled internationally with contribution of multiple researches centers (i.e. Wikipedia).

2.2. Military Crowdsourcing possible current example

Underestimating the raising of new geopolitical and social problems from Intelligence branches, has always been the most reasons why have been developed applications, wargames and algorithms to predict realistic situation developments or possible future events. As in 2011 was founded in U.S. IARPA (Intelligence Advanced Research Projects Activity), working to involve experts by using computer software to make predictions called ACES (Aggregative Contingent Estimation System). The participants are modeled on the ground in real life situation (like soldiers) giving feedback and information about acting situations in real time. This kind of solution is also the concept used in many military projects to digitize information gathered in the battlefield in the last few years, able to speed up and optimize the information's aggregation within C2 and Intelligence systems and digitalize soldiers capabilities on the ground (i.e. Future Soldier program, Future Combat System, etc.), to interact with a complex network, cutting the time to interview on the adversary, etc. Soldier digitization is changing also Doctrine and mission applications as soldiers can have wide access to information, using NCW-NEC concept and application to translate an information advantage in a operational advantage through IT and networking and be able to take more initiative also as dispersed force and

consent to new kind of staff and decisional organization.

Any examples are:

- Military Blogs: it's very easy to find in a lot military headquarters official web pages connections to the principal social networks as Facebook and Twitter; many of these government agencies have official pages and also "discussion corner" for their "friends": at the end, someone have to collect opinions and comments otherwise why spend resources? Looking deeply we can find specific official info-structures like the US AKO (Army Knowledge Online), US ATN (Army Training Network), GTN (Governmental Training Network) and many internal Blogs, etc.; in fact many different training and e-learning Blogs have been created in the last 5 years to involve any ranks and branches soldiers, in pairs with a massive use of e-mails, where they can learn, read, consult, keep them informed, discuss and make opinions about a wide range of issues; strategic and operational too. It is a culture that is changing as they can find some stuff only on the network.
- Crowdsourcing as weapon (Arab spring and social networks): The protests hit Arabic/and Islamic countries in various ways. The riots have in common the use of civil resistance techniques, including strikes, demonstrations, marches and processions, sometimes extreme acts such as suicide and self-injury, but the most innovative elements are the use of technologies like social networks (Facebook and Twitter) and the new era of mobile devices (cell phones, tablet, etc.) to organize, communicate and disseminate events in spite of blaming repressions. The social network drives to a different kind of Command and Control among masses, more light, simple, direct, mutual from commercial HW & SW COTS and without many decisional level; sometimes leveraging people "affiliate" just showing a video and giving direction for the next demonstration, even if they are not interested to the uprising but just to inform people, helping to make re-emerge a new social will, widely supported by technology.
- Civil Defense: during the Japanese tsunami, social network were used giving information and human stories from the flood and dangerous situations.

It's appear that the most important thing in the Decision Making Process of future operational

missions will be manage and predict events; an adapted version of Crowdsourcing should be the process of taking collective opinions, suggestions or information from a group of experts and combining them to predict events more accurately to increase the forecast accuracy, is an opportunity to go beyond the “internet crowdsourcing phenomena” because it transfers value to the singular opinions and producing reliable forecasts. If it is possible to best combine selected experts opinions, it will be possible anticipating and intervening during, or better before, that the events occur and change it or change the enemy course of actions.

3. CONCEPTS TO KEEP IN MIND

Just to have the better landscape to identify a good solution, we wanted highlight few concepts:

3.1. Current MDMP (Military Decision Making Process)

The MDMP is a proven analytical process to problem solving. The MDMP is a tool to assists Commanders and staff to develop mission, analysis and order. It start with the receipt of a mission, and has to product an order to be execute but the analytical aspects of the MDMP continue at all levels during operations. It is a logic process that helps the commander and his staff examines a battlefield situation and reaches logical decisions.

It is configured as a detailed, deliberate and sequential process used, we can say, when the Command post has adequate planning time and sufficient staff support to examine numerous friendly and enemy courses of action (COAs). This situation was typically occurred and occurs when it's necessary to develop operation plans (OPLANs) for entirely new mission, extended operations, and staff training.

The MDMP can be figured out as the foundation of every military mission, classically intended. All documents and conceptual thinking twisted during the process can be used during subsequent planning sessions to re-visiting other changes. Using this process instead of any other methods drive to better analyzes friendly and enemy COAs to identify the best possible friendly COA; it produces great integration, coordination, and synchronization in an operation and minimizes the risk of miss out the critical aspects of mission; it is also detailed as an official document (operation order or operation plan). The MDMP has seven steps and every step begins with input built on the previous steps, driving to the subsequent steps but estimates come on continuously from Commander and staff to give more inputs for the analysis process. Estimates are revised when important new information is received or when the situation changes significantly. They are conducted not only to support the planning process but also during mission execution.

The disadvantage of using this process is that it is a time-consuming process and as a sequential process,

when an errors is committed early in the process will impact also on the later steps.

3.2. NCW/NEC (network Centric Warfare/Network Enable capability)

Is a military Doctrine born in the 1990 and it is coming mature in the current military applications. It's based on the idea to transform the “information advantage” in a “military force advantage” through IT and a massive use of networks to deploy military units in different way than classical doctrine. This kind of wide use of networking and data exchange combined with advanced technology devices and new processes lead through new forms of staff organization.

NCW states the importance of “information” and its power capability based on the relationship that are created with the ignition of tactical information which multiply the ability of a Commander to strike better the enemy.

The doctrine principals are developed around the information sharing, a shared situational awareness, an improved collaboration and synchronization among organizations, singles, flow and correlation of data that enable a faster command and improve geographically the mission efficiency. In that way NWC doctrine is more about personnel and organizations that IT and network and is setting a new way of processing information in a Command and Control organization that is more centric and focalized on the lack of battle space awareness.

3.3. Other new concepts in experimentation:

NATO cross functional team

The development of Cross Functional Team concept is related to build up a new organizational way to lead a specific operational environment like Afghanistan which are more focalized on the efforts on supporting than fighting. This kind of operations are characterized by needs to coordinate, balance and mediate not only military force but also many others activities, often civilian and social, performed for and by different kind of actors. More and more often the operational space where a military force must be introduced is crowded with a lot of different actors (NGO, GO, IO, etc.) that are not always in accordance among them about their reciprocal missions. Any effort is oriented to help building a stable community. The first idea to use cross functional team concept was born with the deploy of Headquarters MNC NE ISAF Joint Command (HQ IJC) in 2010 to combine the Comprehensive Approach, Combined planning and Counterinsurgency because a modern/traditional HQ doesn't allow the best flexibility and agile architecture to face any kind of local needs. The concept was applied to a previous runner scenario to check how the concept could change the general organization and production. The concept doesn't change the basic military planning pillars, execution and also the analyzing principles remain untouched, but there are new and different requirements for information sharing, intensity of social interaction and team work as the cells and branches will continue their

activities in specific small working groups requiring a change of everybody specialists' mindset.

There are other C2 experimentation concepts as AJC2 (Adaptive Joint Command and Control), CROP (Common Relevant Operational Picture), CIE (Collaborative Information Environment), JIP (Joint Interactive Planning) and MNOPS (Multinational Operations) and are all in a research and development phase.

3.4. Cloud Computing

This is set of technologies, content, methods, and communications devices then a process that allocate the activation of a service offered by a provider to a customer to store/archive and process data through the use of resources hardware and software distributed and virtualized on the Network. It can be managed as an evolution of the Internet involvement or a info-structure of resources. The users can work in a simple Internet browser, using software without any local installation and save data in a mass archive on-line managed by the provider. This technology can have 3 levels of complexity:

- SaaS (Software as a Service) - use of programs remotely through a web server. - ASP (Application Service Provider).

- PaaS (Platform as a Service) - similar to SaaS, but instead of programs is performed remotely a software platform that can consist of various services, programs, libraries, etc.

- IaaS (Infrastructure as a Service) - Use of hardware resources remotely. Similar to grid computing, but resources are not allocated, regardless of their actual use but only on demand.

The remote backup and storage are always guaranteed by the server-farm and the operations are increasingly transferred online. The concept provides 3 levels of user:

- Cloud providers: virtual servers, storage, applications, usually according to a comprehensive model demand (pay-per-use);

- administrators: they manages locally the services for a community to integrating software applications which refers to specific audience;

- Cloud users: Use the services according to the level of permits.

As the Cloud can lower the costs of HW, SW, support, maintenance, data storage and can guarantee access everywhere there are some problems about data security to solve as sensitive data exposure, violations, physical residence of servers and mirrors, cyber security, etc.

A server malfunction can affects a large number of users simultaneously since these are shared services. But the most is that everything is based

on the possibility of having a high-speed Internet connection that guarantee the best sharing services.

4. A NEW MODEL: MILITARY CROWD AND SOURCE (SHARING EFFECTIVENESS)

The C2 as we classically know, is part of a decision making practice in a cyclical process. Changes in the way which define decision capabilities affect also doctrine, systems and training. Recent changes in the strategic environment have changed also the point of sight how to have supremacy over the enemy and in an asymmetric theater, information, knowledge and awareness can make difference.

Proposing a new C2 concept we have necessarily remember that it has to be more dynamic, distributed and adequate to different kind of decisions, as the current strategical scenario asking and keeping a large span of manage as the superior situational knowledge remain the pillar of superior capability and awareness.

How to do this? With well prepared personnel, sensors and advanced systems, info-structures, sharing of information and behavior in a coalition environment, information distribution to concept the new operations (SOSO), flattening hierarchies to use experience and background, not only ranks, to defeat enemies that don't know hierarchies and use Facebook and twitter to "hit & run away" conventional and structured forces.

Looking at this detail, dissemination of information is incremented by technologies but the ability to share information and data is the real knot to solve as the most possible way to find solution is decision making decentralization (called edge C2) but supported by adequate resources.

In fact, recent NATO opinion explain that dissemination remain little if decision making is more centralized; this postulate is has been demonstrated in the current peace keeping operations where a classical military operational order is "shaded and adorned" with a crowded and often confusing, humanitarian, civilian, political, diplomatic and re-construction activities. Working on this environments, change the nature of C2 and increase need of trust in the lower level of units.

The medium education level of a generic soldiers and the massive daily use of technological devices let's think that a Military Crowd Source (as Mix of Wisdom, Creation, Voting & Casting), could be a model that must be able to share knowledge and to give effect to all military users the opportunity to resolve their problems, from education to training and up to operational mission capabilities by

exploiting and involving branches' specialists directly, to solve many different problems.

First of all, before to transport this concept in the military, we have to define the borders for a military crowdsourcing model as a parallel world from the rest of possible uses.

That's why in all possible military uses, we could perform, with a crowdsourcing methodology every time problems, situation, training and more, related and dealt with topics that are not normally spread to common people and tied with a complex scale of classified scheme for information. The solution in this case is simple as we can implement the method on the military intranet networks (considering military LAN, MAN, WAN) banned to ordinary people and even accessed controlled to keep secured the exchange of information.

The tactical networks should be even more secure considering that they are used in the battlefield; this condition is more related with the hardware technology and cyber security, considering the wide use of wireless technologies. In any case even the information security is not our focus in this paper, we cannot avoid to mention it.

What we say regarding the bordering of military crowdsourcing model, establish also that we can rely our problems only with military and accredited personnel or at least, with "not-military" accredited qualified experts which could be selected from a specific Governmental basin like Civil Defense, University, research Institutes and more.

The guiding principles in this exploration will be: organization, Methods (i.e. augmented reality, virtual world, IA, etc.), representation (conceptual revision of MDMP) and technology.

4.1. Organizations

Re-visiting the organization should be effective; we just define that Crowdsourcing is like a unique box with partitioned spaces but connected, to contain different approaches to tap into a powerful large and open crowd of stakeholders/experts where there is no methodical understanding for the processes used to source and aggregate the different ideas coming from the crowd.

In our case instead, we'll have a lot of military stakeholders and surely experts, with the same educational background and a lot of specialists and different capabilities, all oriented to military situations or a well chosen civilian experts from specific Governmental basin.

So, before to identify a method we have to spot a possible crowdsourcing organization to apply.

Analyzing some crowdsourcing organizations, we can state that those are all motivated to achieve specific goals and normally they use "crowd

mechanisms" that impact on the organization and the method to decide a specific process to apply.

Recent researches, focusing on the organizational perspective and the mechanisms about crowd sourced, there are more or less 19 distinct process types over 46 official examples just because the Structures that want to adopt crowdsourcing methods have to carefully consider the characteristics of the crowdsourcing process that will be used for their particular aims.

As crowdsourcing could be used for different applications (product design, idea generation, problem solving, etc.), there are different mechanisms applicable to all forms of crowdsourcing processes, like for example:

- based on nature (survey, design, tagging);
- participating consumers with producers for creation of value;
- collective intelligence in the "what", "who", "why", and "how" approach, in a "decide process" for individual or group decisions or a "collection & collaboration" to stimulate selection in a production;
- human computation system evaluating the six components as motivation, quality control, aggregation of results, human skills, chronological order and task request in which the stakeholders are involved.

Proposed organization will not reflect any preview institutions know, but will be defined through crowdsourcing rules adapted to the military environment and needs. The rules will be re-write following these principles:

- Classification of a RESOURCE: a person, institution, organization, that can be both user and resource.
- Initial phase of accreditation resources that can be either single (individuals) or packages of integrated resources (whole Command Posts or parts of it, laboratories, etc..). The resources once accredited by a National Authority will be officially available in list/lists to be included and used in the network environment.
- The resources should not be considered hierarchical, but specialized.
- The resources on the network are authenticated through a system of checks and controls based on the official lists of resources.
- Each user (or resource) can see the other resources available and accessible.

Each resource represents a network node, able to give its capabilities, knowledge and experience to the other nodes.

Just to give some examples it is sufficient to think to info-structures like the US JTEN Network (Joint Training Experimentation Network), which is

representing a critical strategic joint asset for training as realization of JNTC (Joint National Training Capability). JTEN is a global network backbone continental and around the world, that make possible to the US Armed Forces to use everywhere their training capabilities. From 2007 it was also establish a tactical JTEN sub network specific for lower units, using fixed and mobile commercial communication devices to extend the band. This extention allow ti bring services and use all technologies like Virtual, Immersive and 3D as taining solution on site.

Another important example is ATN (Army Training Network) based on a web multichannels portal with a lot of resources for training. The network is focalized on training programs and projects, providing to Commanders and Staffs tools and enabling cooperation, interoperability and resources sharing through trained personnel, materiel to prepare lessons, reharsals and drills and Data Base with training solutions (briefings, SOP, TTP, etc.) ready to be used.

Other training network as reference is GETN (Government Education Training Network) that from 1992 is the training network for many Government Federal Agencies, using satellite channels that allow to the users to share information, training programs and services.

4.2. Methods and Mechanisms to implement

The principal mechanism it's based on the generic potential of crowdsourcing. The resources most suitable are selected by the user and tasked to the problem to be solved. In this way a user can take advantage of the certain resources capacities that it doesn't own, using the intake of experts and stakeholders to solve or help solve and finally share solutions.

The feature of online participation, makes it that once identified the audience of resources involved to solve the problem, the task realization must be done in a modular and variable way as the various resources involved work, make development, use their knowledge and experience, having also crucial contributing to finding a solution that will benefits both parties (applicant and solver) and all the resources that have contributed, in terms of experience and skills gained, in similar problem if it recurs.

Compared to the generic mechanism, in a military case:

- The user that needs to activate the problem solving procedure, he'll performs a task on a number of other specialized resources that may be useful in solving the problem by fixing constrains (time, resources, etc.), and providing the elements that he knows about the mission.
- The solution of the problem or task assigned can be solved in different modes, privileging MDMP expeditious method based on A & A (ask & answer), as the collective intelligence does in a decision process.
- Resources operate in a "flat coordination" environment for constant and dynamic process

elaborating one/more solutions for the decision making/executive level.

Once decision making/executive level have chosen the solution it will puts in place but the tasked resources remain hooked up to the end of mission to check/verify/modify the possible variances.

4.3. Business theories Search theory

The resources group transformation in "collective intelligence", it must meet the requirements related to the ability to solve the problem, able to develop the issue submitted difficulties, standardize procedures for problem development, having a group of resources sufficient making the problem modular and maintaining the various issues independent.

The mechanism requires a strong sense of collaboration and self-synchronization in which there is also a positive competition in advancing the problem development and its potential subjects and participation, and sharing best results (i.e. DARPA 2009).

In a complex environment like a military stabilization operation, the Commander problems are many and are not always related to the typical military sphere. The use of crowdsourcing methodology especially in this sort of work permits in the lack of resources, to assign the development of certain activities of problem-solving to other "geographic" resources or ask for cooperation to solve certain problems if his resources are already committed or to solve complex problems that require the use of valuable and rare resources.

The externalization of problems can be complex, but some specific activities can be given in "external solution" and then assembled in order to ensure the mission achievement.

A conceptual revision of MDMP could be desirable but its needs a specific and dedicated research.

4.4. Representation

The best change we can observe in the current military operations is the strong and advanced use of digital technologies to support the Command and Control networks and in general the Command post activities. The Command Posts today, a part from the kind of missions, are equipped with many different devices and systems that connect to other Centers and nodes to gather information and data.

A possible representation of a crowdsourcing method could use a common operational system and a pre-formatted platform, generically installed in every user's computer or device to connect users and resources in the same network and make easy to use it and collaborate. This software platform could utilize technologies like Augmented Reality, Virtual World, IA-CGF, Avatars and LMSs systems to yield well known technologies and COTS, making simple and open the architecture.

4.5. Technology

As the technologies change every six months, most of the technologies to use to develop a project like this are available just now in the market and also in the Army to realize a prototype. Principal network technologies will

be the Cloud computing concepts applied to the military network.

In particular, using the most advanced technologies HW (Hardware) related to mobile devices and methods of use of Social Networks and Social Cooperation, through the creation of a specific software application, it wants to develop a set of interfaces that allow access to a wide range of individual and collective digital thematic channels from which it can access various types of applications and services, it can federate various types of web server resources in order to foster collaboration and cooperation, you can use simulators situation, compose documents, exchanging and comparing views and resources and find solutions to specific operational problems and, using human and material resources differently and rarely available.

Even more, the crowdsourcing method applied to the military environment could give more meaning to the new projects that Italian Defense for example, is implementing into the training simulation, operational C2 activities and experimental sectors (SIAT, Future soldier and ITB projects) (Amico et al. 2000).

For sure, this kind of project requires a mentality change to be understood like a “step forward, not a menace” by the personnel, before it is implemented and obviously a change in the way we train and educate personnel.

4.6. An example

The construction of a drinking water well in an operational area in which a coalition is conducting humanitarian interventions on the population and where there is also a residual resistance, is a typical scenario for the current mission’ theaters.

Assumptions: the unit Commander, which has received the mission and has already logistic and maneuvering resources involved in other operations, has received the teams able to work with the tools to dig the well but is not able to manage the project. The only hydraulic engineer available in the operating sector is already engaged in other two similar projects.

The Commander can use the crowdsourcing method and the network to set his operational problem, assigning:

- Among the network resources available and tasked, he can involve an engineer from his national Department of Civil Defense, a military engineer unit which has already made a laying of water pipes and a group of engineers from an allied Country University to set the project management.
- He can assign the safety inherent activities for the surrounding area and recognition of his interest area security to his remaining maneuver forces.
- He can task intelligence resources on the network taking them from superior and

parenthetic HQs, to get the intelligence reports, studies and guidelines for the area.

- Assign the logistic and communications problems to their units' support.

The Commander will put together the tasked resources in a workgroup and gives constraints and sharing information that he has. The tasked resources will operate in “flat coordination” exchanging products and studies results about their activities, reaching a final plan composition to follow. The activities may be following by a super-partes coordinator or by an activities' program management. The final plan solutions will be sending to the Commander who will choose the best option.

Generally a plan should contain, for example:

- preliminary contacts with the local political authorities;
- definition of working period and the use of any local personnel;
- definition of the area and reconnaissance;
- securing the area sending personnel to safe area near the well location and sector monitoring;
- definition of logistics support area;
- delivery of equipment and operating personnel;
- starting of activities and monitoring;
- completion of the water pipes and well and organization of population hydraulic services;
- well delivery to the local authorities.

During the plan implementation, the network resources that have helped to design and managing the plan, they will monitor any possible deviations.

5. CONCLUSIONS

Crowdsourcing has found resistance to be used in the Military. Reasons could be found in the digital security of networks and data exchange, and into the “social soul” of this kind of methodology, even if the new developments (Crowdsourcing 2.0) are different and more oriented to a goal, using a specific and determined number of specialists to solve any commercial, business and designing problem.

Only demonize or support crowdsourcing is not the best approach to get on it, as this methodology it's now and even more in the next future, the best way to save human and economical resources into the civilian environment and to make progress in a lot of social fields.

Military Crowdsourcing should be based on the current digitized reality and characterized by high level of sharing resources, an extended networking diffusion and by capabilities and networks, reinforced from the exponential evolution of mobile technologies. If developed in a correct way, Collective Intelligence can be mutual from the

model business as “open enterprise” to product ideas, solutions, answers and analyses but also an educational way for personnel and a collaborative method to practice Command & Control upon projects development.

From this point of view the parallelism with certain military requirements is immediate and can give guidelines about the future developments of multinational activities, Command and Control, Training, information sharing and resolution of operational problems.

This methodology could be applied on various options of operational use to devise an integrated e-learning LMS (Learning Management System) and DMP (Decision Making Process) associated with a Cloud Computing network, able to provide a wide range of applications, resources and services for individual users, institutions, structures and operational training missions, and through software that will enable self-synchronization and multidimensionality of command, information assurance and a correct information sharing.

In the field of training, the extension of the concepts of Crowdsourcing, "open enterprise" and "distributed problem-solving", will allow an optimized use of database management, optimization of the CPX-CAX (Command Post Exercise - Computer Assisted exercise), the collaboration during the exercises and situational update to ensure better integration between the function C2 (Command & Control), training simulation, activities developed with Serious Games and procedural training for users.

In fact, with the application of these concepts, there is also addressed to the world of training Simulation, in particular to the sector of Virtual and IA (Integrated Architecture) by exploiting the possibility of integrating with each other at the distributed level, Virtual Simulators and Serious Games for cultural, linguistic, social, economic training and above all procedural users (Tremori et al. 2012), lowering the cost of personnel and resources and applying the new concepts of Cloud Simulation and Virtualization.

The use of such a platform makes it possible to create an immersive and federable environment where different users are involved and where it constitutes a single "interoperable training environment crowdsourcing based", into which all the resources needed for various educational purposes divided for the base training phases and advanced specialization (e-classroom, e-reading, e-lessons, e-learning, e-capabilities, etc.).

Obviously, there are some critical points as:

- the reliability of digital data;
- the non adequacy of traditional method of control;
- ability to control the knowledge of all experts;
- ability to learn the right information;
- Information control is made from different people;
- Right information published force other users (as competitors, companies, institutional and government agencies, etc.) to answer and to respect rules;
- Focus point should be neutral agreed and consensual to build the participants reliability;
- Goodwill and reliability are fundamental.

The concept application in the Military could solve most of this point, and also allow the development of new forms of collaboration trying to keep up with the evolution of military doctrine and TTPs in the current and most future asymmetric operational environment.

Crowdsourcing will principally allow a new military function identifiable as "military cooperation", able not only to support training in the various levels of military personnel but at the same time provide a basis for establishing a new organization C2, planning, Simulation for training and, operational analysis and decision support is already in use in many industrial and civilian sectors, there are several experiences of such kind of applications (Bruzzzone, 2004, Curcio & Longo 2009).

and that is already being tested in military and NATO allies and other countries thus identifying a form of "distributed Command and Control".

In fact, since 2010 in the military, are studying the possible development trends of the requirements of NATO in the sphere of C2 (or BC-Battle Command), such as "Cross Functional Team", where the traditional concept of Command and Control evolves towards the "Command and Feedback", where the feedback is just a mechanism of monitoring and control the digitized training.

The concept is closely connected with the approach of NCW/NEC (Net Centric Warfare, Network Enabled Capability) and is strongly oriented to:

- To promote the solution of complex problems through the use of resources in a context of crowdsourcing;
- Transport in the military environment the concept of Crowdsourcing as an approach to the available resources in a network;
- Make available specialized resources and valuable, difficult to reallocate and optimize their use and reducing operating costs;

- Apply NATO concepts for Cross Functional Team in a Virtual Immersive and interoperable environment with the use of systems already available, making it more flexible deployment of command posts;
- Define the concepts of Crowdsourcing Cross Functional Team in a national operational environment and their skills, considering the concepts of "Dispersing leadership concept", "self-synchronization" and "multidimensionality of command" in a context like operating SOSO (Stability Operations - Support Operation);
- Define new models of military dynamics relations to connect the cell and functional areas within a "command post geographically" based on the ability to share information and their security;
- Apply the levels of C2 maturity model N2C2M2 (Net-centric Command & Control Maturity Model), IACGF (Computer Generated Forces-Intelligent Agents).

The military importance of operational effects (capabilities) resulting from Crowdsourcing concepts as part of the digitized formation, C2 and Simulation as a collector of resources, designed to support:

- Training of military personnel as a collective but also individual, developing a global Constructive platform consists of a collection of Data Base and digital resources accessible to all users, through Avatar, Serious Game and a virtual environment that can provide, as qualifying technology, training and specialized personnel or to make available resources for research and study in a real training network, information and operational from Army, based on knowledge and training as already happening for example in the U.S. Army;
- C4-ISTAR, limited to the operational function C2 "digitized" as the main enabler of reference for capacity development of the Army and the achievement of the objectives of the ongoing process of transformation and other functions on the basis of the capacity to be expressed and exercisable through the concepts of the Crowdsourcing model;
- Training Simulation LVC-IA, as the dominant tool for training and the achievement of operational readiness of the forces, integrated with the world of C2 and training, but also with government resources available to provide commanders and staff training in the maximum much information as possible on the operational scenarios of reference for enhancing the capacities of departments and individual

components to operate in joint and multinational environments with an operating philosophy "net-centric" and "effect-based".

These concepts and applications will contribute significantly to implement education and digitized training, allowing an ever closer integration of personnel training, skills and individual and collective training in a joint and multinational environment, the use of TTP's in favor of specialists branch and lower levels unit commanders (Pl./Cp.) and crews through the conception, organization and conduct of instructional courses or specific operation done anywhere and eventually useful for preparation of traditional CPX-CAX, accelerating the changes and conceptual culture necessary for a proper implementation of concepts for the Army transformation.

REFERENCES

- Amico Vince, Guha R., Bruzzone A.G. (2000) "Critical Issues in Simulation", Proceedings of SCSC, Vancouver, July
- Baddeley A., (2010), "The future of Command and Control", Military technology review MILTECH - 4.
- Bruzzone A.G., Tremori A., Madeo F., Tarone F, (2011) "Intelligent agents driving computer generated forces for simulating human behaviour in urban riots", International Journal of Simulation and Process Modelling, 2011 Vol. 6 No. 4 p. 308-316, DOI: 10.1504/IJSPM.2011.048011
- Bruzzone A.G., Massei M. Tremori A., Bocca E., Madeo F., Tarone F, (2011) "CAPRICORN: Using Intelligent Agents and Interoperable Simulation for Supporting Country Reconstruction", Proceedings of DHSS2011, Rome, Italy, September 12 -14
- Bruzzone A.G. Tremori A., Massei M. (2011) "Adding Smart to the Mix", Modeling Simulation & Training: The International Defense Training Journal, 3, 25-27
- Bruzzone A.G., Tarone F. (2011) "Innovative Metrics And VV&A for Interoperable Simulation in NEC, Urban Disorders with Innovative C2", MISS DIPTM Technical Report, Genoa
- Bruzzone A.G., Massei M. (2010) "Intelligent Agents for Modelling Country Reconstruction Operation", Proceedings of Africa MS2010, Gaborone, Botswana, September 6-8
- Bruzzone A.G., Frydman C., Cantice G., Massei M., Poggi S., Turi M. (2009) "Development of Advanced Models for CIMIC for Supporting Operational Planners", Proc. of I/ITSEC2009, Orlando, November 30-December 4
- Bruzzone A.G., Cantice G., Morabito G., Mursia A., Sebastiani M., Tremori A. (2009) "CGF for NATO NEC C2 Maturity Model (N2C2M2) Evaluation", Proceedings of I/ITSEC2009, Orlando, November 30-December 4

- Bruzzone A.G., A. Tremori, M.Massei (2008) "HLA AND HUMAN BEHAVIOR MODELS" Proceedings Of MMS2008, April 14 - 17, 2008, Ottawa, Canada
- Bruzzone A.G., Briano A., Bocca E., Massei M. (2007). Evaluation of the impact of different human factor models on industrial and business processes". SIMULATION MODELING PRACTICE AND THEORY, vol. 15, p. 199-218, ISSN: 1569-190X
- BRUZZONE (2004). Preface to modeling and simulation methodologies for logistics and manufacturing optimization . SIMULATION, vol. 80 , p. 119-120 , ISSN: 0037-5497, doi: 10.1177/0037549704045812
- Caussanel J., Frydman C., Giambiasi N., Mosca R. (2007) "State of art and future trend on CGF" Proceedings of EUROS IW2007, Santa Margherita, Italy, June
- Child J., (2011), "Display Tech Advances Overhaul Command Control Systems", COTS journal of military electronics and computing, May.
- CURCIO D, LONGO F (2009). Inventory and Internal Logistics Management as Critical Factors Affecting the Supply Chain Performances. INTERNATIONAL JOURNAL OF SIMULATION & PROCESS MODELLING, vol. 5(4), p. 278-288, ISSN: 1740-2123
- David S. Alberts, Reiner K. Huber, and James Moffat., (2010), "NATO NEC C2 Maturity Model" – SAS 065, C.C.R.P. (Feb.)
- Dan Parsons, (2011), "U.S. Government Turns to Crowdsourcing for Intelligence" National Defence – NDIA Magazine (Dec.)
- David Geiger, Thimo Schulze, Stefan Seedorf, Robert Nickerson, (2011), " Managing the Crowd: Towards a Taxonomy of Crowdsourcing Processes" 17th Americas Conference on Information Systems, Detroit, Michigan (August).
- Le Roux W., (2010) "The use of Augmented reality in Command & Control Situation awareness", (Council for scientific and industrial research – South Africa).
- Mosca R., Giribone P., Bruzzone A.G., Orsoni A., Sadowski S. (1997). Evaluation and Analysis by Simulation of a Production Line Model Built with Back-Propagation Neural Networks. INTERNATIONAL JOURNAL OF MODELLING & SIMULATION, vol. Vol.17, no.2, p. 72-77, ISSN: 0228-6203
- Tremori A., Baisini C., Enkvist T., Bruzzone A.G., Nyce J. M. (2012), "Intelligent Agents and Serious Games for the development of Contextual Sensitivity", Proceedings of AHFE 2012, San Francisco, US, July
- Turi M., Biagini M., (2011) "Command Feedback and response (CFR): Command and Control in an immersive and Interactive Environment (C2I2)" Proceedings of DHSS, Rome (Italy) September.
- Turi M., Biagini M., (2011) "Command Feedback and response (CFR) as a Training Platform" Proceedings of 6th NATO CAX Conference, Rome (Italy) September.
- US Army Field Manual FM 3/24 "Counterinsurgency" 2006.
- Convergence: The International Journal of Research into New Media Technologies Copyright © 2008 Sage Publications London, Los Angeles, New Delhi and Singapore Vol 14(1): 75–90 DOI: 10.1177/1354856507084420 <http://cvg.sagepub.com>
- Headquarters Multinational Corps Northeast (HQ MNC NE) is moving ahead in discovering the essence of Cross-Functional Team concept. Thursday, 21 April 2011 08:17 Veiko Palm

SERIOUS GAMES FOR DEVELOPING INTUITION AND AGILE THINKING FOR DECISION MAKERS

Agostino Bruzzone^(a), Alberto Tremori^(a), Claudia Baisini^(b)

^(a)DIME, University of Genoa, Italy - www.itim.unige.it

^(b)CIM-coach AB, Sweden – www.cim-coach.se

^(a)agostino@itim.unige.it, alberto.tremori@simulationteam.com, ^(b) claudia.baisini@cim-coach.se

ABSTRACT

This paper describes on-going researches about the usage of serious games for training and education of a set of “soft skills” such as intuition and agile thinking. These skills are a critical asset for any kind of decision maker. This work is focused on military officers; however, the authors’ goal is to develop general methodologies and games that could find applications also in the industrial and business world, being decision making and, in particular, strategic decision making critical elements in every sector.

In this paper the theoretical framework and the preliminary ideas on possible games development are illustrated.

Keywords: Serious Games, Contextual Learning

1. INTRODUCTION

The CEO of a company as well as an Officer of our Armed Forces need to be trained to what Napoleon called “Coup d’Oeil” (glance) (Baisini, 2011). Indeed any person with responsibilities, today, has to operate in scenarios that are rapidly evolving and has to deal with huge amount of information to get to the final decision. So, even if the described approaches can be applied to several critical areas (Bruzzone&Longo 2010), the researches described in this paper are specifically focused on the decision making process in the Defense sector. In fact the conflicts in which Armed Forces are engaged are largely characterized by Interactive Complexity: the system is nonlinear, its proportions unstable and cause-effect patterns ambiguous. Large civilian presence and involvement, difficulties in identifying possible threats, high tempo, and dense terrain are typical features of the so called “three block war”, introduced by Gen Krulak, which requires the capability of making a broad range of decisions in little or no time at the micro tactical level. The squad leader has considerable decision making responsibility in this scenario. In order for him to get the best possible situational awareness, it is necessary to provide him with the necessary skill set (not tools, not rules) that allows him to ‘Read’ the operational environment and understand its regulating rules, rather than applying

frames of reference that would work in the Domestic environment. He must be provided with the capability of learning from the Context, stretching his mental models and transcend the obvious (Tremori et al. 2011). Research suggests that visual orientation can be recognized as the important feature for a group leader in urban combat; what one sees and how he interprets can be decisive. However, what has received less attention is the fact that the ability to make fast decisions in a situation of crisis depends also on the ability to make the right judgment of the situation; to perceive and understand context appropriately (Chun, 200). Such ability requires sophisticated training; a context based training that provides an agile mindset and the capability to learn and understand the context appropriately while deployed. Whether focusing on a squad leader of a distributed operation squad in a “three block war” environment, or on a Commander at the Operational Level, or on Intelligence and IOs, what is crucial is the context, which culture of course informs. In particular at the tactical level, it is paramount that a squad leader learns how to watch and interpret what is seen and refer to the local context (understand what he sees in relation to where he is) rather than interpreting it based on preconceived ideas or prior de-contextualized knowledge/information. Furthermore, he must do it fast, which is why the visual dimension and Intuition emerged as so critical: he must get that “Coup d’Oeil” that was considered crucial by Napoleon, and by many after him. He needs to develop that intuition that Gen. Krulak (Krulak, 1999) considers the most important characteristic of young leaders. In this paper is proposed a training philosophy and possible, effective, innovative solutions by Modeling & Simulation, to establish a solid ground for re-framing and creative decision making. To develop such kind of complex and articulated set of skills we are proposing an approach based on Modeling and Simulation and in particular on Serious Games *not* to “teach” new contexts but to stimulate and develop mental agility that help to understand different and every new context. Different scalable architectures and methodologies will be studied, designed, developed, tested, and deployed for decision makers’ education.

As emerged from this introduction, the ‘how to’ enhance the described set of is a particularly complex problem: research on these issues is ongoing (i.e. USMC) but no attempt has yet been made to leverage

on the potential of serious games for this kind of training. The goal of this research, as better explained in the next paragraph, is to investigate how to succeed in training and educating intuitiveness, glance and agile mindset by using serious games. We intend to develop the prototype of a game, which will be tested, and the effectiveness of the training methodology will be verified.

2. INTUITION AND AGILE THINKING

Napoleon referred to the intuitive capability to rapidly assess a situation and make a fast decision as “Coup d’Oeil” or “strike of the eye”: he believed it was a gift of nature. In fact, behavioral psychologists have identified the creative-intuitive personality as being “alert, confident, foresighted, informal, spontaneous and independent. Not afraid of its experiences, accepts challenges readily, unconventional yet comfortable in its role, able to live with doubt and uncertainty, and not afraid of exposing to criticism” (Mrazek, 1972). However, the military believes that although heredity and personality certainly play a role here, intuition can be cultivated and developed.

One definition of intuition is: “intuition is a developed mental faculty which involves the automatic retrieval and translation of subconsciously stored information into the conscious realm to make decisions and perform actions. Organized databases of knowledge gained through education – experiences, memorization, sensations and relationships – are the building blocks for intuitive thought” (Reinwald, 2000, p.86).

While MDMP (Military Decision Making Process) has demonstrated its effectiveness in long term planning, it carries some risks, identified in the literature as “bounded rationality” (Wolgast, 2005). An alternate approach is the one named as Intuitive (or Naturalistic) Theory of decision making based on the premise that individuals often use less formal but much faster decision making strategies (Gigerenzer et al. 2004, 1999; Gilovich et al., 2002) in real time situations (Bryant et al., 2003).

The “Coup d’Oeil” refers to the instant, global understanding of a situation. This refers to what the eye seizes, both literally and metaphorically. It is also the ability to see the whole and also to see what is not there.

Stemming from Klein’s definition of intuition as based on “experience to recognize key patterns that indicate the dynamic of a situation” a problem arises: a soldier has no experience of the local environment in which he is deployed, therefore his intuition would be based on experiences, patterns and dynamics that emerge from, and are applicable to, his prior context and circumstances. Such patterns, however, not necessarily are applicable to the context in which he is deployed and often can be deceptive. These issues are key to “understanding” and “learning” about the operational environment. The way in which an individual sees the world is the product of the

individual’s personal history, experiences, upbringing, personality, and of his social context. However, these frames not necessarily apply to the context in which he is to conduct his operation; in this case they can be misleading, as illustrated in the example below. Both Figure 1 and 2 could be a main road to a rural community anywhere but Figure 2 looks exotic to most Westerners.



Figure 1: Private Photo



Figure 2: Private Photo

3. THE PROJECT

“The human mind’s intuitive process is an irreplaceable determinant of combat success.” (Reinwald, 2000, p.88). Napoleon referred to the intuitive capability to rapidly assess a situation and make a fast decision as “Coup d’Oeil” or “strike of the eye” (glance): he believed it was a gift of nature. In fact, behavioral psychologists have identified the creative-intuitive personality as being “alert, confident, foresighted, informal, spontaneous and independent. Not afraid of its experiences, accepts challenges readily, unconventional yet comfortable in its role, able to live with doubt and uncertainty, and not afraid of exposing to criticism” (Mrazek, 1972). However, the military believes that although heredity and personality certainly play a role, intuition can be cultivated and developed.

From the many definitions of intuition three common traits can be identified:

- it is a phenomenon of subconscious thought
- it relies heavily on experience-based knowledge
- it is a comprehensive, unrestrained thought process

The “Coup d’Oeil” refers to the instant, global understanding of a situation, this is particularly appropriate to the subject discussed here because it refers to what the eye seizes, both literally and metaphorically. It is the ability to see the whole and also to see what is not there, and act.

According to Klein, whose Recognition Primed Decision Model is a milestone in decision making theory, the first source of power is intuition, which he defines as use of experience to recognize key patterns that indicate the dynamics of a situation. (Klein, 1998) This includes recognizing what is happening but also what is not happening, as both can provide clues. The ability to see what others cannot develops with experience. Because of vast experience one is able to see the pieces of the event that are not perceptible to

someone with less experience or expertise. (Wolgast, 2005).

The main goal of this work is first of all to develop a theoretical framework about contextual learning and its application for intuition and glance (“coup d’oeil”). This research will bring to the creation of conceptual models to develop a simulator, based on a serious game approach, which aim is to demonstrate the possibility to effectively train the soft skills described in this document. The simulator will be developed accordingly to a serious games approach: it will stretch over different levels and will be provided with a scoring system for players to create a strong engagement and a better learning experience.

These goals challenge traditional training and simulation paradigms that attempt to reproduce reality (the context) as perfectly as possible, to train the soldier to a sort of automatic “internalized and reflexive response”. We need to take these representations one step further: the role paid by what the subject expects to see cannot be handled well in photorealistic simulations as presently implemented. What is often crucial is to be able to see what we are not conditioned to see. To achieve this, we need to move education, training, and simulation technology beyond a concern with detecting and reinforcing certain rules of behavior or by producing “better” and “better” reproductions of reality.

Moving away from traditional Simulation and Gaming products, where the tendency is that of ‘representing’ reality, we suggest a training that focuses on challenging the player to develop his/her cognitive skills and teach to recognize what is salient in an Operational Context characterized by a high level of Interactive Complexity.

The methodology and the training tools and that we propose are based on the usage of simulation and in particular on Serious Games. In fact, Serious Games provide an opportunity to improve performances with reduced efforts to professional simulation with great attention to interfaces, story, emotional involvement, and graphics, as well as new technologies. The potential application areas for these games usually benefits of the introduction of Artificial Intelligence (Giribone, 1999) and enhanced realism through Human Behaviour (Bruzzone et al. 2011, 2010, 2007). These models are applied also to industrial processes considering both ergonomic (Cimino&Longo 2009, Curcio&Longo 2009) and process-related issues. It is common to develop Intelligent Agents (IA) able to drive several of the active entities in the game. For the purpose of training to the Coup d’Oeil we suggest the study and development of an “educational path” that starts from a simple, portable serious game solution and can move towards more complex and immersive synthetic environments. For all this different levels the basic concept is always to educate the user’s intuitive thought in recognizing key patterns. At the same time we want to increase users’ involvement and recreating some of the key factors in tactical decision making process: speed and stress.

A complete and extended Verification, Validation and Accreditation (VV&A) of the models and a rigorous testing based on the usage of the developed serious game activity will be completed to provide final results.

Among the areas of investigation will be to define how the serious game shall be tailored to specific users, i.e. high ranking officers, non commissioned officers or troop. At this stage we only differentiate with respect to : Tactical level: where the subject (all ranks) is dealing and analyse reality and process real data; for instance the *VTLM-Lince* driver that has to realize that there is something unusual, and consequently, potentially dangerous in the road he’s driving on.

- Operational Level: in this case the user is most likely working on meta-data (i.e. a map or intelligence report) to plan an operation.

Besides tailoring the game to specific users, this project has the goal of, first of all, develop the generic methodology to train people, despite their ranks or task (i.e. officers planning an operation as well a sergeant patrolling a road or a CEO or mid level managers) by:

- Increasing mental agility (capability to re-orient in contexts driven by unfamiliar frames of reference and mental models), flexibility and creative decision making. Particularly flexibility in relating to unknown situations: diminished reliance on familiar categories and stereotypes, increased learning from the context, as a consequence of increased confidence in handling unknown context.
- Diminishing implicit effect of stereotyping.

The prototype should represent logics that do not correspond to familiar categorizations or common sense. Such scenes/images would be created in order to:

- Identify and enhance the effects of existing categories and stereotypes.
- Generate “disconfirmation”
- Require the user to increase attention, observation skills, and interaction with the context in order to learn and identify clues relevant to understanding the logic underlying the scene.
- Relate to the context as a living system, one of constant movement and change rather than having a static picture as often found in Handbooks and briefs.
- Combine the identified cues in multiple ways building different plots in order to challenge common sense and stretch the boundaries of own categories to re-define them (Re-think/Re-frame).
- Identify what is happening in relation to the context.

Purely by way of example we can imagine (see Figure 3) that the prototypal game, running on an a mobile platform (i.e. tablet), will represent a specific geographic scenario (i.e. Afghan village or a Western town road), with incoherent elements in term of objects, people appearance (an Afghan lady with a *burqa*

walking in Bond Street in London), behavior (blond North European guys quarreling excitedly with typical South European gestures), noises (the main Kabul road with New York traffic noise) and even smells (grandma's cookies sweetness in a Middle East bazaar). Two main issues here are to be 'worked through':

- Status Quo Disconfirmation (or Unfreezing): the rules of the competition are not explained and they are not consistent with one's common sense and normal rules. In order to win user has to find the right way to score and so has to re-think his customary behaviors (and the logics underlying them).
- Recognize Key Patterns: while the user is focusing attention on the contest, due to the unusual rules (that create cognitive confusion), we start to inject in the scenario the incongruent elements. This would lead the user to re-create experience in ways that demonstrate the value of re-thinking 'common sense'. One strategy might be to have users become familiar with the game environment, assume that this is a 'stable' reality, and then slowly destabilize the 'taken for granted' order of things.

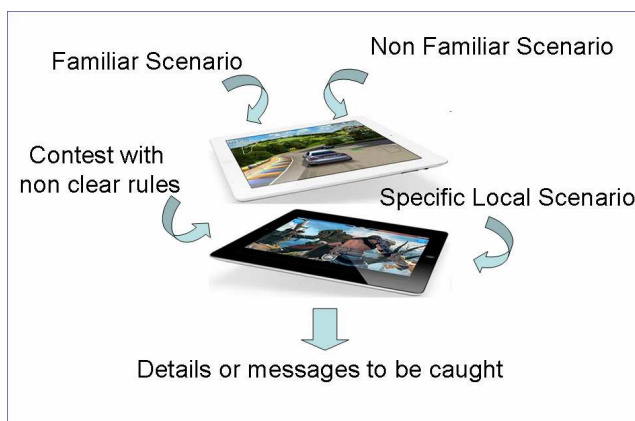


Figure 3 –Solutions for educating to understand stereotypes and develop observation skills

4. IMPACT IN THE DEFENSE SECTOR

As already mentioned our Armed Forces are largely involved in operations characterized by a strong Interactive Complexity, conceptual asymmetry in balance of power, and requiring fast decisions.

The proposed Serious Games for final demonstration of research results is perfectly aligned with the current doctrinal and training framework of Armed Forces. Indeed actual doctrines are the result of deep strategic changes and of new operational approaches increasingly influenced by non military factors (i.e. PMESII, PESTLE) and that influence the symmetry relations between opposite sides.

Training, as well, had to conform, moving from conventional educational program to an increased focus

on smaller units for tactical operations, where the most relevant part of military operations is made by recognition, surveillance, patrolling, specific stabilization operations and, as well, Civil and Military cooperation.

Therefore in this context squad leader has important responsibilities proportional to scenario difficulties but coherent with operation's superior orders. This requires not only a deep knowledge of orders and mission goals, but also a sophisticated training; a context based training that provides an agile mindset and the capability to learn and understand the context appropriately while deployed.

Accordingly to this, MDMP (Military Decision Making Process) has demonstrated its effectiveness in long term planning, by its very nature it carries some risks, identified in the literature as "bounded rationality". Such process improved for classical military doctrine, was re-adapted to current operative conditions but it is, for sure, too complex and onerous for minor units that must be agile and fast in completing assigned tasks.

An alternate approach is the one named as Intuitive (or Naturalistic) Theory of decision making and it is based on the premise that people often use less formal but much faster decision making strategies in real time situations. The "Coup d'Oeil" refers to the instant, global understanding of a situation, this is particularly appropriate to the subject discussed here because it refers to what the eye seizes, both literally and metaphorically. It is the ability to see the whole and also to see what is not there, and act.

According to Klein, whose Recognition Primed Decision Model is a milestone in decision making theory, the first source of power is intuition, which he defines as use of experience to recognize key patterns that indicate the dynamics of a situation. This includes recognizing what is happening but also what isn't happening, as both can provide clues. This ability comes from experience, the ability to see what others cannot. Because of vast experience one is able to see the pieces of the event that are not perceptible to someone with less experience or expertise.

It is important to stress that the training suggested in this project is a complement to efforts that are already taken, particularly within the USMC, to increase Situational Awareness and decision making skills.

The main goal of the proposed Serious Game will be to improve the methodological approach of trained personnel to enhance Contextual Situational Awareness and to refine the capability of using the best available decision making processes to complete assigned task. Finally such training, coherent with actual training needs emerging from operational scenarios, will be a further, important item to the capability of correlating different experiences of deployed personnel and to identify key patterns of the tactical context to understand operational dynamics.

5. CONCLUSIONS

The effort of the on-going research described in this paper is to study a methodology to develop games that educate soft skills such as intuition and agility in thinking despite the specific scenario where the trainees are going to operate. This is an innovative approach in respect to mainstream existing researches, which focus on models that reproduce the reality of a specific operational environment (for critiques of this strategy in a maritime environment see Dekker, 2009). Often training is focused on notional or normative models designed to teach “how things are” or “how they are supposed to be”. The alternative path taken by the authors is to enhance the users’ cognitive systems by teaching them to learn by observing and engaging with operationally relevant field indicators, in more fundamental adaptive ways. The idea is to use a Serious Game approach that supports users, through strong engagement, to become more receptive to the signals sent by specific and generic environments. Further, it will help users “boot strap” from one environment to another without the need to return to first base each time. Most existing learning and training scenarios work off of a set of pre-defined, deterministic categories. This is true even with sense making models. How to reframe and train for beyond the obvious is an issue that has relevance not only in relation to the Modern Operational Environment, but to all branches of Decision Making. Understanding complex environments and to be able to extrapolate from one context to another would strengthen the war fighter’s cognitive assets and help him or her meet the challenges of today’s warfare, providing the ability to succeed also, and particularly, when reality turns out to be different was supposed to be’ (according to the handbook).

REFERENCES

- Abt C.C. (2002) *Serious Games*, University Press of America
- Argyris, C. and Schön, D. (1996) *Organizational learning II: Theory, method and practice*, Reading, Mass: Addison Wesley
- Baisini C., Tremori A., Enkvist T., Bruzzone A.G., James M. N. (2011), White Paper “Agile Intuition An innovative approach for educating Context Sensitive Coup d’Oeil”
- Baisini, C and Deinlein, E (2002) *Knowledge in Knowledge Intensive Organizations. The case of Crime Investigation and Consulting Firms*. Masters Thesis. Gothenburg School of Economics and Law, Graduated Business School.
- Baisini, C. (2009) *USMC and US Army at the Aftermath of OIF and OEF*, Internal Report for Swedish National Defense College, Department of Command & Control Studies
- Baisini, C. and Nyce, JM (2010) *Lethal Modeling*, Military Intelligence Professional Bulletin, June-July
- Baisini, C. Bjurström, E, Gemeinhardt, D. (2010) *Incorporating Contextual Sensitivity and Metacognition into Law Enforcement and Intelligence Activity*, FBI Terrorism Research and Analysis Program, Vol I, US Government Publication
- Bergeron B, (2006) *Developing Serious Games*, Charles River Media
- Bruzzone A.G., Tremori A. Buck W., (2012) “Definition of CD&E cycles to be used in the ”integration test bed (ITB)” to support Italian defence with M&S tools into the new systems development and acquisition processes”, Proceedings ITEC2012 London, May.
- Bruzzone A.G., Tremori A., Madeo F., Tarone F, (2011) "Intelligent agents driving Computer Generated Forces for simulating human behaviour in urban riots", Under Publication on International Journal of Simulation and Process Modelling (IJSPM).
- Bruzzone A.G., Massei M. Tremori A., Bocca E., Madeo F., Tarone, F. (2011) *CAPRICORN: Using Intelligent Agents and Interoperable Simulation for Supporting Country Reconstruction*, Proceedings of DHSS2011, Rome, Italy, September 12 -14
- Bruzzone AG, Longo F (2010). *An Advanced System for Supporting the Decision Process within Large-scale Retail Stores*. SIMULATION, vol. 86, p. 742-762, ISSN: 0037-5497, doi: 10.1177/0037549709348801
- Bruzzone A.G., Frydman C., Tremori A. (2009) *CAPRICORN: CIMIC And Planning Research In Complex Operational Realistic Network MISS DIPTM* Technical Report, Genoa
- Bruzzone A.G., Massei M., Tremori, A. (2009) *Serious Games for Training and Education on Defense against Terrorism - NATO MSG-069 Symposium Use of M&S in: Support to Operations, Irregular Warfare, Defence Against Terrorism and Coalition Tactical Force Integration*", Bruxelles, Belgium October 15, 16
- Bruzzone A.G., Elfrey P., Cunha G., Tremori A. (2009) *Simulation for Education in Resource Management in Homeland Security* Proceedings of SCSC2009, Istanbul, Turkey, July
- Bruzzone A.G., Cantice G., Morabito G., Mursia A., Sebastiani M., Tremori A. (2009) *CGF for NATO NEC C2 Maturity Model (N2C2M2) Evaluation*, Proceedings of I/ITSEC2009, Orlando, November 30-December 4
- Bruzzone A.G. (2009) *Intelligence and Security as a Framework for Applying Serious Games*,

- Proceedings of Serixgame, Civitavecchia, November
- Bruzzone A.G., Briano A., Bocca E., Massei M. (2007). Evaluation of the impact of different human factor models on industrial and business processes". SIMULATION MODELING PRACTICE AND THEORY, vol. 15, p. 199-218, ISSN: 1569-190X
- Bruzzone A.G. (1996) Object Oriented Modelling to Study Individual Human Behaviour in the Work Environment: a Medical Testing Laboratory, Proc. of WMC'96, San Diego, January
- Bryant Dr. D. J, Webb Dr. R. D.G. and McCann C. (2003) Synthesizing two approaches to decision-making in Command and Control Canadian Military Journal Spring
- Chun, M. (2000) Contextual Cueing of Visual Attention Trends in Cognitive Sciences Vol. 4, No. 5 May pp.170-177
- Curcio D, Longo F (2009). Inventory and Internal Logistics Management as Critical Factors Affecting the Supply Chain Performances. INTERNATIONAL JOURNAL OF SIMULATION & PROCESS MODELLING, vol. 5(4), p. 278-288, ISSN: 1740-2123 (almeno 2 volte)
- Cimino A, Longo F, Mirabelli G (2009). A multi measure-based methodology for the ergonomic effective design of manufacturing system workstations. INTERNATIONAL JOURNAL OF INDUSTRIAL ERGONOMICS, vol. 39, p. 447-455, ISSN: 0169-8141, doi: 10.1016/j.ergon.2008.12.004
- Dekker, Dahlstrom, van Winsen, Nyce (2009) Fidelity and Validity of Simulator Training, in Theoretical Issues in Ergonomics Science, Taylor & Francis Ed, 29 January
- Duggan, W. (2005) Coup d'Oeil: Strategic Intuition in Army Planning, SSI Publication, US Army War College
- Gigerenzer, G. (2004). Fast and frugal heuristics: The tools of bounded rationality. In D. Koehler & N. Harvey (Eds.), Blackwell handbook of judgment and decision making. Oxford: Blackwell.
- Gigerenzer, G., Todd, P. M., & the ABC Research Group (1999) Simple heuristics that makes us smart. Oxford: Oxford University Press.
- Gilovich, T., Griffin, D., & Kahneman, D. (2002). Heuristic and biases. The psychology of intuitive judgment. Cambridge: Cambridge University Press
- Giribone P., Bruzzone A, (1999). Artificial Neural Networks as Adaptive Support for the Thermal Control of Industrial Buildings. INTERNATIONAL JOURNAL OF POWER & ENERGY SYSTEMS, vol. 19, No.1, p. 75-78, ISSN: 1078-3466
- Greenwals, A. & Banaji, M. (1995) Implicit Social Cognition: Attitudes, Self-Esteem, and Stereotypes, Psychological Review, Vol. 102, No.1, 4-27
- Iuppa N, Borst T (2006) Story and Simulations for Serious Games: Tales from the Trenches Focal Press
- Klein, G. (1998) Sources of Power: How People Make decisions MIT Press Cambridge MA
- Klein, G. (2007) Flexecution as a Paradigm for Replanning, IEEE Computer Society Vol. 22, No. 5
- Kolb. D. A. and Fry, R. (1975) Toward an applied theory of experiential learning. in C. Cooper (ed.) Theories of Group Process, London: John Wiley
- Krulak Gen , C. (1999) Cultivating Intuitive Decision Making Marine Corps Gazette, May
- Massei M., Tremori A., Pessina A., Tarone F (2011) Competition and Information: Cumana a Web Serious Game for Education in the Industrial World, Proceedings of MAS2011, Rome, Italy, September 12 -14
- Michael D, Chen S (2005) Serious Games: Games That Educate, Train, and Inform, Course Technology PTR
- Mrazek Col, J. (1972) Intuition: an instantaneous backup system? Air University Review January- February
- Reinwald Maj, B. R. (2000) Tactical Intuition Military Review September-October p. 88
- Schein, E. H. (1992) Organizational Culture and Leadership. 2d. Ed. San Francisco, CA.: Jossey Bass
- Tremori A., Baisini C., Enkvist T., Bruzzone A.G., Nyce J. M. (2012), "Intelligent Agents and Serious Games for the development of Contextual Sensitivity", Proceedings of AHFE 2012, San Francisco, US, July
- Wolgast, K. (2005) Command Decision Making: Experience Counts, U.S Army War College Carlisle Barracks

AUTHORS BIOGRAPHY

Agostino Bruzzone since 1991, he has taught "Theories and Techniques of Automatic Control" and in 1992 he has become a member of the industrial simulation work group at the ITIM University of Genoa; currently he is Full Professor in DIPTM. He has utilized extensively simulation techniques in harbour terminals, maritime trading and sailboat racing sectors. He has been actively involved in the scientific community from several years and served as Director of the McLeod Institute of Simulation Science (MISS), Associate Vice-President and Member of the Board of the SCS (Society for Modelling & Simulation international), President of the Liophant Simulation, VicePresident of MIMOS (Movimento Italiano di Simulazione) and Italian Point

of Contact for the ISAG (International Simulation Advisory Group) and Sim-Serv. He has written more than 150 scientific papers in addition to technical and professional reports in partnerships with major companies (i.e. IBM, Fiat Group, Contship, Solvay) and agencies (i.e. Italian Navy, NASA, National Center for Simulation, US Army). He teaches "Project Management" and "Industrial Logistics" at the University for students in the Mechanical Engineering (4th year), Management Engineering (4th year) and Logistics & Production Engineering (3rd Year) Degree Courses. His email address is agostino@itim.unige.it

Alberto Tremori is an Electric Engineer with a PhD in M&S. He acquired an extended experience in technology transfer and management of R&D projects with a particular focus on modeling and simulation (M&S) applied to different areas: process re-engineering in logistics, production and transportation systems; modeling complex non conventional scenarios and human behavior in defense and security. He's also interested in application of M&S to medical and social issues. He participated to several International Conferences as speakers in Europe, Asia and North America.

He worked with IBM as project manager. he had roles in commercial and sales management in Xerox in IDC. He was Site Manager and Project Coordinator for CFLI a Consortium devoted to provide training and education in the Logistic Sector. He was in charge of managing virtual simulation training projects for transportation. He worked also with several IT and Consulting Companies in Technology Transfer, Innovative Hi-Tech Projects and Business Development dealing with Small and Medium and Large Companies and National and International Agencies and Institutions.

He was co-founder and President in MAST a SME devoted to R&D projects with a particular focus to M&S. From 2009 He's faculty member of MIPET (Master in Industrial Plants) at University of Genoa. He's appointed from the Italian MoD to several NATO Research Groups.

He's currently working in the University of Genoa at DIME (former DIPTEM) as technical researcher, managing research projects in M&S and acting as Technology Transfer Manager.

Claudia Baisini started her studies in Economics and Law at the University of Milan. After some years she moved to the University of Aberdeen, King's College, where she focused on Organizational Studies, Cross Cultural Marketing Strategy, International Business, and Organizational Change and Learning. After a course at the Copenhagen Business School in Cross Cultural Marketing Strategy, she took her M.Sc. in International Management at the Graduated Business School of the University of Gothenburg, Sweden. Her Master Thesis' was on "Knowledge in knowledge intensive organizations; the case of crime investigation and consulting firms". After the Master Program she

worked at the University of Gothenburg where she deepened her competence in ethnographic studies and qualitative research. After working with International Humanitarian Operations and Crisis Response, in 2004 she joined the staff of the Swedish National Defense College in Stockholm. The most relevant projects: evaluation of the Planning Under Time pressure method (PUT), research assistant for a simulation program based on System Dynamics theories (STRATMAS, Strategic Management System), and a study focused on Situational Awareness of a squad leader in urban combat (MAC). Since 2007 she has been working as Defense contractor within Concept Development & Experimentation, and leads a project aimed at fostering dynamic decision making, organizational learning, and mental agility. She currently participates at three projects: 1. development of a Context Based Actors' Analysis method to understand the mindset of relevant actors in the Area of Operations, stemming from how our biases and categorizations influence our own understanding; 2. Development of a planning method based on CAS and dynamic decision making, to be used in fuzzy/complex environments; 3. Agility in Expeditionary Operations. Since 2009 she is a member of FBI TRAP (Terrorism Research & Analysis Program), a study group led by FBI Academy Behavioral Science Unit, Quantico, and collaborates with the USMC and NSA. Claudia is a Doctoral candidate at the University of Cambridge, UK.

AN ADVANCED FRAMEWORK FOR INVENTORY MANAGEMENT IN REVERSE LOGISTICS

Francesco Longo

MSC-LES, Mechanical Department, University of Calabria, Via P. Bucci 44C, 87036 Rende, Italy

f.longo@unical.it

ABSTRACT

In the first part of the paper a survey of the most important models used for inventory management in reverse logistics is presented; models are classified according to the approach used for modeling demand and products returns. In the second part of the paper an advanced simulation framework based for inventory management in reverse logistics is proposed. The simulation framework is used to compare different inventory control policies with the aim of understanding their behavior (in terms of total costs) within a supply chain with products return.

Keywords: Reverse Logistics, Inventory Management, Modeling & Simulation

1. INTRODUCTION

Although it has been given increasing attention in the recent years, the origin of research on inventory control with returns can be dated back to the 70's and regards those systems in which customers return products after their leasing, renting or purchasing (Heyman, 1977). Over the years, researchers and practitioners have developed and proposed numerous planning and control methods to integrate the return flow of used products (products recovery) into the producers' material management (Fleischmann et al., 2002). In this context, it seems that the major difficulty is mainly due to the considerable uncertainty with respect to timing, quantity and quality of the return flow (that is often hard to influence by the producer) and to the integration of reverse logistics operations. Kleber et al. (2002) observes that new problems arise both along the supply chain and in each single supply chain node with the integration of reverse logistics and products recovery operations. Among others, the most important are collecting and disassembly of used products, production synchronization and remanufacturing, inventory management. It is worth saying that the meaning of products recovery is different according to the final recovery action: repair, refurbishing, remanufacturing, cannibalization and disposal (see Thierry et al., 1995). As shown later on, in this article the focus is on the multi-echelon inventory system in case of products returns considering two recovery options: products remanufacturing and products disposal.

In effect many authors have proposed quantitative models and approaches for studying single stage and multi-echelon inventory management system with products return. Fleischmann et al. (1997) propose a survey of these research studies by discussing the implications of the emerging reuse efforts, reviewing the mathematical models presented in the literature, and pointing out the areas in need of further research. However, the framework proposed by Fleischmann dates back to more than 10 years ago, therefore the time seems again right for an updated survey on the inventory management problem involving product returns. In this context, the objective of the paper is twofold. First, the article aims at providing the readers with a brief but systematic overview on the main inventory control models proposed (during the last decades) by researchers and practitioners working in this specific area. The authors subdivide the field according to the modeling approaches for demand and returns processes. A first major classification is made into deterministic and stochastic models. Moreover, stochastic models are then classified into periodic and continuous review models. Then, as second and most important objective, the authors present four stochastic models for a multi-echelon inventory management system (within a supply chain) that includes product returns. After presenting and discussing the models, the authors propose the supply chain conceptual model (integrating the multi-echelon inventory system) and implement the conceptual model within an advanced supply chain simulator. The simulator (called IMPRES, Inventory Management with Product REturns Simulator) is used to investigate and compare the behavior of the inventory control models in terms of supply chain costs (total supply chain costs, supply chain echelon costs, supply chain node costs). It is also shown that with respect to the state of the art the treatment proposed in this article considers more flexible and versatile inventory control models.

Before getting into the details of the study, in the sequel a brief overview of each section of the article is presented. Section 2 structures the state of the art on the inventory management with product returns; in particular section 2.1 is dedicated to deterministic models; section 2.2 presents stochastic models and classifies them into periodic and continuous review models. Then, section 3 deals with the supply chain

conceptual model and the four stochastic inventory control models. Section 4 focuses on the IMPRES simulator and proposes an application example for comparing the behavior of the inventory control models in terms of supply chain costs (also discussing the potentials of the IMPRES simulator for investigating supply chain inventory management problems). Finally the last section reports conclusions, summarizes the scientific contribution of the work and the actual research activities still on going.

2. A SURVEY OF THE INVENTORY CONTROL MODELS WITH PRODUCTS RETURN

This section surveys the most relevant articles in the field of inventory management with product returns. The initial bibliographic search involving a huge number of articles were then reduced to about 50 articles based on content and quality. Such relevant articles are studied and considered in the following survey. Section 2.1 and section 2.2 are respectively dedicated to deterministic and stochastic models for single stage and multi-echelon inventory management system with product returns. Deterministic models mainly focus on extensions of Schrady's (1967) model (EOQ model applied to the case of products returns) and on the dynamic lot sizing problem for systems with product returns. Stochastic models are finally classified in periodic review and continuous review.

2.1. Inventory control models with products return: deterministic approach

Here research works dealing with deterministic models for inventory management are presented. These models are usually based on the assumption that demand and return quantities are known with certainty. A first research branch regards models dealing with stationary demand and return flows. The most considered inventory model is usually the Economic Order Quantity (EOQ). Schrady (1967) was the first to consider the EOQ inventory model in which a certain percentage of sold products (under constant demand) comes back, after a known period of time (constant return rate), to be repaired under the hypothesis of infinite production and recovery rates. Nahmias and Rivera (1979) extend Schrady's model by considering the case where the repair rate is finite rather than infinite. Other extensions to the model of Schrady (1967) are presented by Mabini et al. (1992) and Teunter (2001, 2004). Mabini et al. (1992) discuss an extension of Schrady's model to a multi-product inventories system where products share the same repair facility. Teunter (2001, 2004) also generalize Schrady's results. Teunter (2001) assumes infinite production and recovery rates and different holding cost for recoverable, recovered and manufactured products. Teunter (2004) assumes finite production and recovery rates. In both articles, Teunter derives a square-root formula for the optimal production and recovery lot-sizes for each of the two classes of policies: $(M=1, R)$ and $(M, R=1)$, where M manufacturing batches and R

recovery batches succeed each other. The obtained policy is an approximation to the optimal and not the optimal one. However Teunter results are valid for finite and infinite production and recovery rates therefore has to be regarded as more general than those of Nahmias and Rivera (1979) and Koh et al. (2002).

Konstantaras and Papachristos (2004, 2006, 2007) extend Teunter in different cases, finding a solution for Teunter's model that leads to the optimal policy in both cases $(M=1, R)$ and $(M, R=1)$. Also Oh and Hwang (2006) and Chung et al. (2008) and Mitra (2009) extend Teunter (2001, 2004) even if they consider different systems, conditions and constraints. Oh and Hwang still deal with the single echelon case for a recycling system where a fixed fraction of the deterministic demand is returned and used as raw material. Chung et al. consider a multi-echelon inventory system with remanufacturing capability; Mitra consider a two echelon system with returns under more generalized conditions (the assumptions of non-existence or non-relevance of set-up and holding costs at different levels are relaxed).

Richter (1994, 1996a, b) and Richter and Dobos (1999) also consider EOQ models but they differ from Schrady's model because they consider the waste disposal option and the return rate is a variable parameters.

Richter's models are considered and extended by several authors: El Saadany and Jaber (2008) consider the costs associated with switching between production and recovery runs. Jaber and Rosen (2008) propose an extension of the model by proposing a parallel to physical systems and applying the first and second laws of thermodynamics to reduce system entropy. Finally, Jaber and El Saadany (2009) assume different demands for manufactured and remanufactured (repaired) products.

Another important branch of research studies deals with the dynamic lot sizing problem for systems with product returns. Richter and Sombrutzki (2000) propose an extension of Wagner and Whitin (1958) dynamic production planning and inventory control model to the case of reverse logistics. They assume that the number of returns is sufficient to satisfy all demands without delay, and therefore manufacturing is not considered. Richter and Weber (2001) extend the model proposed by Richter and Sombrutzki by considering the manufacturing option and variable manufacturing and remanufacturing costs. However Richter and Weber assume that the number of returns in the first period is at least as large as the total demand over the planning horizon, therefore the manufacturing option is not needed (it is used only for economic reasons). Richter and Gobsch (2003) apply the Richter and Sombrutzki model in a just in time environment.

Golany et al. (2001) extend Richter and Sombrutzki by relaxing restrictive assumptions on the number of returns and they also include the disposal option. Beltran and Krass (2002) relax the assumption on the number of returns but assume that returns can be directly used (no remanufacturing is needed).

Teunter et al. (2006) study the dynamic lot sizing problem by relaxing all the restrictive assumptions of the above models also including set-up costs.

2.2. Inventory control models with products return: stochastic approach

This section is dedicated to the inventory models that deal with demands and returns as stochastic processes. The survey is organized according to the traditional classification into periodic and continuous review models. Section 2.2.1 and section 2.2.2 respectively survey the periodic review models and the continuous review ones that have contributed to well establishing this field through the last four decades.

2.2.1. Periodic Review Models

Literature on periodic review models is abundant. These models aim at deriving optimal control policies over a finite planning horizon (Fleischmann et al., 1997).

The first contribution on stochastic periodic review model was first presented in Simpson (1978), but the research has not been continued. In terms of previous works, the model presented by Simpson is an extension of Veinott's (1966) model in which the dependent relationship between demand and returns is removed. In practice this dependency is rarely modelled because of the small effects and the modelling effort required to consider it (see Fleischmann 2000 for justification of the independence assumption and Kiesmüller and van der Laan 2001 for an additional cases in which returns depend on past demand).

After Simpson, Cohen et al. (1980) present a model where a fixed share of the products is returned after a fixed number of periods. Equations for the optimal policy are proposed, and myopic base stock approximation (that is shown to be optimal in the case of feedback delay is equal to one period) is developed. Inderfurth (1997) extends Cohen et al. model by relaxing the assumption of fixed feedback delay and addressing the problem of product recovery management. In this case, one single product is stocked to fulfill stochastic customers demand that generate, in turns, stochastic product returns (they consider the double options of manufacturing and disposal and assume fixed and different deterministic lead-times for both procurement and remanufacturing).

Kiesmüller and van der Laan 2003 provide the exact computation of the parameters that determine the optimal periodic policy proposed by Inderfurth (1997) and Simpson (1978) in the case of identical lead times. They also provide two different approximations in the case dynamics demand and returns (exact computation is time consuming). Mahadevan et al. (2003), Kiesmueller (2003), and Teunter et al. (2004) explore heuristic approaches for the case of non-identical lead times. Finally Ahiska and King (2009), extending Kiesmueller (2003), conducts an analysis to find optimal policy structure in the existence of fixed cost for manufacturing and/or remanufacturing in the context of periodic-review inventory control.

The above papers consider one products reuse option and one single stage inventory system. The following articles extend the treatment to the case of multiple reuse options and multi-echelon system. Inderfurth (2001) extends Inderfurth (1997) by firstly presenting a periodic review model for product recovery in stochastic remanufacturing systems with multiple reuse options, including a disposal option (still Inderfurth considers one single stage inventory system). DeCroix (2006) focuses on a multi-echelons inventory system but still considers one product reuse option. DeCroix uses the results by Simpson (1978) and by Inderfurth (1997). In effect the system proposed by DeCroix combines the key elements of two simpler systems: (i) the single stage remanufacturing system studied by Simpson and by Inderfurth and (ii) the series system studied by Clark and Scarf (1960). In particular DeCroix investigates whether the optimal policy inherits the basic structural properties of the simpler systems. Note that DeCroix et al.(2005) already investigated the behaviour of a series system in which recovered products are returned directly to stock.

2.2.2. Continous Review Models

In these models the time axis is modeled continuously and the objective is to find optimal static control policies minimizing the long-run average costs per unit of time (Fleischmann et al., 1997).

A first continuous review model was proposed by Heyman (1977). In particular, the author proposes a model with independent demand and return occurrences (with generally distributed quantities and inter-occurrence times), trying to optimize the trade off between additional inventory holding costs and production costs savings and without considering fixed costs (an attempt to consider dependent demand and returns is made by Yuan and Cheung 1998). Muckstadt and Isaac (1981) propose a model similar to the Heyman's model but demand and returns are assumed to be unitary Poisson processes, the model applies to a situation with uncertain manufacturing lead times, finite remanufacturing capacity, nonzero procurement lead time and disposal option is not considered (they deal with both single and multi echelon models and fixed costs are not considered). Korugan and Gupta (1998) consider a model similar to Muckstadt and Isaac but they take into account the disposal option in a two-echelon inventory system with return flows.

Van der Laan et al. (1999) extend Muckstadt and Isaac by relaxing some restrictive assumptions (even if they do not consider disposal option). Van der Laan et al. consider the dependence between demand and returns, allow nonzero fixed remanufacturing costs, consider deterministic manufacturing and remanufacturing lead times and present exact procedures for evaluating the total expected costs.

Fleischmann et al. (2002) aim at presenting a comprehensive analysis of inventory management in a reuse context. The authors come down to the Muckstadt and Isaac model and provide a complete analysis

deriving both an optimal control policy and an optimal control parameter values.

Ching et al. (2003) starting from the Heyman's and Muckstadt and Isaac's models (single-product inventory model with returns), they first include the replenishment costs and then consider two independent identical inventory systems where transshipment of returns from one inventory system to another is allowed.

Finally Mitra (2009) tries to relax most of the assumption of the previous models (such as non-existence or non-relevance of set-up and holding costs at different levels) and considers a two echelons system with returns under more generalized conditions.

All the above papers make the assumption that remanufacturing a return is, on the average, less costly than manufacturing a new product and disposing the return (in other words they made the assumption that remanufacturing is the primary source for satisfying demand). Aras et al. (2006) consider the situation in which returns quality is not always the same and consequently remanufacturing is not the primary source of satisfying demand. The authors establish that a simple average cost comparison is not a reliable basis for priority decisions in hybrid manufacturing and remanufacturing systems.

With respect to the state of the art, the treatment proposed in this article considers more flexible inventory control policies (i.e. respect to Heyman's and Muckstadt and Isaac's models). Different types of continuous and periodic review models (not only based on the s, Q model) are considered. The models are proposed and their behaviour (in terms of supply chain costs) is investigated within a multi echelon supply chain that includes the products return flow (with the double option of remanufacturing and disposal). To this end, an advanced supply chain simulator is developed, presented and used.

3. SUPPLY CHAIN CONCEPTUAL MODEL AND INVENTORY CONTROL POLICIES

Figure 1 shows the supply chain conceptual model: let be N the number of supply chain echelons and N_i the number of node in the i -th supply chain echelon. In addition to the direct flow of product, the supply chain also includes a reverse flow with two options: remanufacturing and disposal. Remanufactured products can join the direct flow in any of the N supply chain echelon. Note that upstream and downstream supply chain boundaries respectively are outside suppliers and customers.

The arrival process of customers demand at stores is Poisson; similarly the products return process to the remanufacturing areas is Poisson. Inventory management system within each supply chain node is based (as explained later on) on inventory control policies that consider both new products (shipped by upstream nodes) and remanufactured products. Stockouts occurrences at each supply chain node can be completely backordered, partially backordered or registered as lost sales.

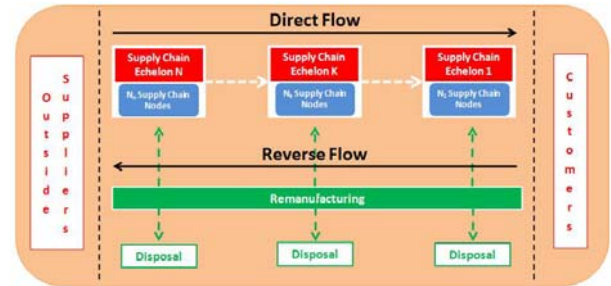


Figure 1: The supply chain conceptual model including the reverse flow of products

The inventory management system at each supply chain node has to answer to five different questions: (i) how often to review the stock status; (ii) when to order new products; (iii) quantity of new products; (iv) quantity of remanufactured products; (v) quantity of products to dispose.

Before getting into inventory policies details let us define the following notations. Note that, where not directly specified, the subscripts i , j and k respectively refer to the supply chain echelon i , to the echelon node j and to the product k .

- N , number of supply chain echelons;
- N_i , number of node in the i -th supply chain echelon;
- $D_{ijk}(t)$, customers' demand at period t ;
- $RT_k(t)$, return at period t ;
- LT_{ijk} , Lead Time (for a new product);
- LT_{rijk} , Lead Time (for a remanufactured product);
- $s_{ijk}(t)$, order point;
- $S_{ijk}(t)$, order-up-to-level;
- $SS_{ijk}(t)$, safety stock;
- h , safety stock factor (used for safety stock and order point evaluation);
- R_{ijk} , review period;
- r_{ijk} , inventory holding cost (for a new product);
- OC_{ijk} , fixed cost per order;
- v_{ijk} , unit value cost (for a new product);
- $B1_{ijk}$, fractional charge per unit short (used to evaluate shortage cost);
- $P1_{ijk}$, fractional part of stockouts backordered;
- $B2_{ijk}$, fractional charge per unit short (used to evaluate backorder costs);
- rc_{ik} , unit remanufacturing cost;
- rr_k , inventory holding cost (for a recoverable product);
- rv_k , unit value cost (for a remanufactured product);
- $P2_{ik}$, fractional part of disposed units;
- dc_{ik} , disposal cost;
- $DF_{ijk}(t)$, demand forecast at period t ;
- $LTD_{ijk}(t)$, lead time demand;
- $\sigma_{ijk}(t)$, standard deviation of the lead time demand;
- $IP_{ijk}(t)$, inventory position;
- $OHI_{ijk}(t)$, on hand inventory;
- $OQ_{ijk}(t)$, on order quantity (new product);

- $OQ_{rijk}(t)$, on order quantity (remanufactured product);
- $BQ_{ijk}(t)$, back order quantity;
- $CQ_{ijk}(t)$, committed quantity;

Decisions about when to order new/remanufacturing products and the orders quantities are taken on the basis of the inventory position $IP_{ijk}(t)$ defined in equation (1).

$$IP_{ijk}(t) = OHI_{ij}(t) + OQ_{ijk}(t) + OQ_{rijk}(t) - BQ_{ijk}(t) - CQ_{ijk}(t) \quad (1)$$

The demand over the lead time (equation 2) is based on demand forecast in the time interval $(t, t + LT)$ where LT is defined as:

$$LT = \begin{cases} LTD_{ijk}(t) \\ LTD_{rijk}(t) \\ \text{Max}(LTD_{ijk}(t), LTD_{rijk}(t)) \end{cases}$$

- The first case is for order placed only for new products
- The second case is for order placed only for remanufactured products
- The last case is order places for new products and remanufactured products

$$LTD_{ijk}(t) = \sum_{k=t+1}^{t+LT_{ij}} DF_{ijk}(k) \quad (2)$$

The Demand Forecast is evaluated by using the single exponential smoothing method. The operations of the four different inventory control policies are presented below.

3.1 Order-Point, Order-Quantity (s, Q) inventory control policy

This inventory control policy is based on continuous review; a fixed quantity Q_{ijk} is ordered when the inventory position, $IP_{ijk}(t)$ drops the order point $s_{ijk}(t)$.

In this case $s_{ijk}(t)$ and Q_{ijk} are determined according to equations for simultaneous determination of s and Q for faster moving products (adapted for Poisson Process), presented in chapter 8 of Silver et al. (1998), chapter 8.

3.2 Order-Point, Order-Up-to-Level (s, S) inventory control policy

As in the previous case the inventory is reviewed continuously and an order is placed whenever the inventory position, $IP_{ijk}(t)$, drops the order point $s_{ijk}(t)$. A variable quantity is ordered to raise $IP_{ijk}(t)$ to the

order-up-to-level $S_{ijk}(t)$. The $s_{ijk}(t)$ is evaluated according to equation (3).

$$s_{ijk}(t) = LTD_{ijk}(t) + SS_{ijk}(t) \quad (3)$$

the safety stock:

$$SS_{ijk}(t) = h * \sigma_{ijk}(t) \quad (4)$$

The order-up-to-level:

$$SS_{ijk}(t) = s_{ijk}(t) + \frac{LTD_{ijk}(t)}{LT} \quad (5)$$

Where the second term of equation 5 is the ratio between the average lead time demand (considering lead time demand for new products and lead time demand for remanufactured products) and the average lead time (considering lead time for new products and lead time for manufactured products). Note that the authors already dealt with the definition of SS in a supply chain without products returns. See Longo and Mirabelli (2008), De Sensi et al. (2008) and Curcio and Longo (2009) for further information. Finally the quantity to be ordered is:

$$Q_{ijk} = S_{ijk}(t) - IP_{ijk}(t) \quad (6)$$

3.3 Periodic Review Order-Up-to-Level (R, S) inventory control policy

This inventory control policy is based on periodic review; every R units of time the inventory is checked and an order is placed that raises the inventory position, $IP_{ijk}(t)$, to the order-up-to-level $S_{ijk}(t)$, according to equation 5.

3.4 Periodic Review, Order-Point, Order-Up-to-Level (R, s, S) inventory control policy

As for the (R, S) inventory control policy, this policy is based on checking periodically the inventory. Every R units of time the inventory position $IP_{ijk}(t)$ is checked. If $IP_{ijk}(t)$ is below the order point $s_{ijk}(t)$ a variable quantity is ordered to raise the inventory position to the order-up-to-level $S_{ijk}(t)$, according to equation 6.

3.5 Supply Chain Total Costs definition

As already mentioned the main objective is to relax most of the assumption made in the stochastic models (both continuous and periodic review) and investigate the multi-echelon inventory system by comparing the behavior of the above inventory control policies in terms of total supply chain costs. This approach requires to specify inventory costs (including ordering costs, holding costs for new and remanufactured products, shortage costs, backordering costs), remanufacturing costs and disposal costs. Equation 7 evaluates the total

expected annual cost for a generic product k at the echelon node j , supply chain echelon i :

$$TC_{ijk} = OC_{ijk}m_{ijk} + v_{ijk}r_{ijk}\Delta T_{ijk} + (1 - P1_{ijk})B1_{ijk}v_{ijk}n_{ijk} + P1_{ijk}B2_{ijk}v_{ijk}n_{ijk} + rv_{ijk}rr_{ijk}\Delta T_{ijk}^{(r)} + (1 - P2_{ik})rc_{ik}rn_{ik} + P2_{ik}dc_{ik}rn_{ik} \quad (7)$$

where:

- ΔT_{ijk} , total time an product is held on the warehouse shelves (serviceable inventory);
- m_{ijk} , number of product orders over 1 year;
- n_{ijk} , number of unit short over 1 year;
- $\Delta T_{ijk}^{(r)}$, total time an product is held on the warehouse shelves (recoverable inventory);
- rn_{ik} , number of recoverable unit over 1 year, intended for remanufacturing process.

The total cost including all products types, inventory costs at all supply chain nodes and echelons, remanufacturing and disposal costs can be written as follows (equation 8)

$$TC = \sum_i \sum_j \sum_k OC_{ijk}m_{ijk} + \sum_i \sum_j \sum_k v_{ijk}r_{ijk}\Delta T_{ijk} + \sum_i \sum_j \sum_k (1 - P1_{ijk})B1_{ijk}v_{ijk}n_{ijk} + \sum_i \sum_j \sum_k P1_{ijk}B2_{ijk}v_{ijk}n_{ijk} + \sum_i \sum_j \sum_k rv_{ijk}rr_{ijk}\Delta T_{ijk}^{(r)} + \sum_i \sum_j \sum_k (1 - P2_{ik})rc_{ik}rn_{ik} + \sum_i \sum_j \sum_k P2_{ik}dc_{ik}rn_{ik} \quad (8)$$

Note that the treatment proposed in this article does not consider most of the common assumptions hold in most of the approaches proposed in literature. Specifically a multi-echelon inventory system with products returns (with the double options: remanufacturing and disposal) is considered and

- the remanufactured products can enter the normal flow of products at any stage of the supply chain;
- remanufactured products are good as new products and economically more convenient but the Lead Time of the remanufactured products is different from zero and different from the Lead Time of the new products.
- products disposal is allowed at any stage of the supply chain
- all the relevant costs are considered and included.

4. THE IMPRES SIMULATOR

In this section an application example, developed by using an advanced supply chain simulator (IMPRES, *Inventory Management with Product RETURNS Simulator*), is presented. The IMPRES simulator recreates the three echelons supply chain conceptual model above presented, the multi-stage inventory system with product returns (including the remanufacturing and disposal options) and the four different inventory control policies. The main aim of the application example is to investigate the multi-echelon

inventory system by comparing the behavior of the above inventory control policies in terms of total supply chain costs. Figure 2 shows the supply chain considered in the application example.

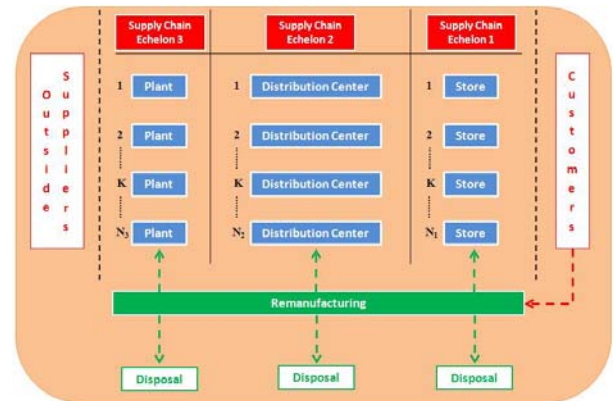


Figure 2: Supply Chain conceptual model considered in the application example

The use of Modeling & Simulation (M&S) is an important part of the proposed approach in order to investigate the multi-echelon inventory system and policies behavior. In effect, a wide range of factors usually affects the inventory management along the supply chain. The ways in which such factors interact and the stochastic nature of their evolution over the time increase the complexity of such system up to critical levels and the use of ad-hoc methodologies, techniques, applications and tools is the only way to tackle problems and succeed in identifying proper and optimal solutions (as already mentioned in the literature survey, analytical approaches mainly require restrictive assumptions).

Simulation has been widely recognized as the best and most suitable methodology for investigation and problem-solving in real-world complex systems (Bruzzone 2002; Bruzzone, 2004) in order to choose correctly, understand why, explore possibilities, diagnose problems, find optimal solutions, train personnel and managers, and transfer R&D results to real systems (Banks, 1998). Moreover, simulation has proved both in Industry and in Logistics its capability to recreate (with high level of accuracy) the intrinsic complexity of real-world systems allows to find out and test alternative solutions under multiple constraints and to monitor, at the same time, multiple performance measures, (Mosca et al., 1997; Giribone and Bruzzone, 1999, Bruzzone and Giribone, 1999, Bruzzone et al., 2007). In effect the author of this paper has a long experience in simulation models development in different areas including industrial plants (Longo et al., 2012), manufacturing systems design (Cimino et al. 2009; Longo and Mirabelli 2009), supply chains and Logistics (Bruzzone and Longo, 2010; Longo 2010) and complex systems training (Bruzzone and Longo, 2012). These considerations has led the author to develop the IMPRES simulator addressing the multi-echelon

inventory management issue along the supply chain in the case of product returns.

The development of the simulator starts with a detailed analysis of the supply chain conceptual model. According to the supply chain conceptual model a single network node is considered as store (ST), distribution center (DC) or plant (PL). A supply chain begins with one or more PLs and ends with one or more STs. STs usually satisfy market demand or demand from other STs, DCs satisfy STs demand or demand from others DCs and PLs satisfy DCs demand and demand from other PLs.

As concerns the inventory management, all the inventory control policies presented in section 3 are implemented within each supply chain node (ST, DC, PL). Obviously the inventory control policies take into account both the traditional forward-oriented product flow as well as the reverse product flow.

The figure 3 shows the IMPRES main frame (the figure depicts a supply chain example with three echelons including 4 plants, 3 Distribution Centers and 4 Stores) and the IMPRES Graphic User Interface (GUI). The GUI provides the user with many commands both for defining the supply chain configuration and for controlling the simulation execution. Number of products, simulation run length, start, stop and reset buttons and a Boolean control for the random number generator (to reproduce the same experiment conditions in correspondence of different operative scenarios) can be controlled and changed. Three different dialog windows can be activated by clicking on the three buttons *Stores*, *Distribution Centers* and *Plants* (see fig. 3). Thanks to these dialog windows, the user can set (in specific tables) the number of supply chain echelons, nodes position in the supply chain, the total number of network nodes and all the numerical values, input parameters and information needed for defining the supply chain configuration.

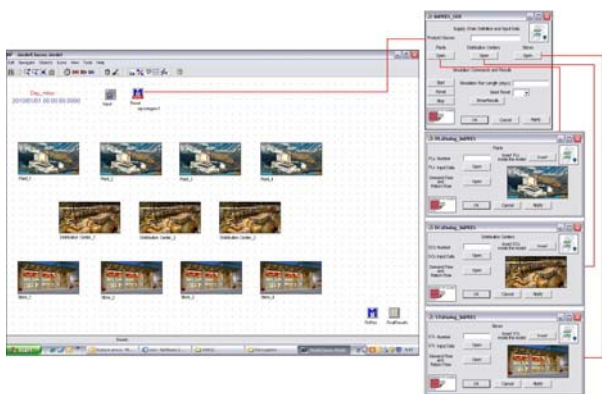


Figure 3: IMPRES main frame and Graphic User Interface

5. INVENTORY CONTROL POLICIES COMPARISON

Note that the high flexibility of the IMPRES simulator in terms of scenarios definition is one of the most important features for using it as a decision making tool. As mentioned above the IMPRES graphic user

interface gives to the user the possibility to carry out a number of different what-if analysis by changing supply chain configuration and input parameters (i.e. inventory policies, demand forecast methods, demand intensity and variability, lead times, inter-arrival times, number of products, number of stores, distribution centers and plants, etc.). The application example proposed below aims at comparing the behavior (in terms of total supply chain costs) of the inventory control policies presented in section 3 in a three-echelons supply chain that includes 6 Plants, 1 Distribution Center, 10 Stores and 20 different products. The application example proposed has to be regarded as an advanced analysis devoted both to investigate inventory control policies behavior in case of products returns (with the double options of remanufacturing and disposal) and to test IMPRES potentials as tool to support supply chain managers decision making. Three different scenarios are considered:

- all the supply chain nodes use the (s, Q) policy;
- all the supply chain nodes use the (s, S) policy;
- all the supply chain nodes use the (R, S) policy;

In effect a complete scenarios investigation requires at least a Design of Experiments (DOE) based on factorial experimental design for checking all inventory control policies combinations.

The figure 4 shows the total supply chain costs (in K€) in the three scenarios. Note that the best policy in terms of total cost is the (s, S) policy, the worst policy is the (R, S). When all the supply chain nodes use the (s, S) policy the total savings, compared to the use of (s, Q) and (R, S) policies, are respectively 1,415 K€ (about 8%) and 828 K€ (about 5%). It should be noted that the (s, S) policy as defined by authors (see equation 3 and 5) performs quite well than the (s, Q) policy.



Figure 4: Total Supply Chain Costs comparison

The figure 5 shows the total costs for each supply chain echelon (Plants, Distribution Centres and Stores) in correspondence of the three different inventory control policies. Once again the best policy is the (s, S). Note that on the whole supply chain the (s, Q) policy performs better than the (R, S). However when considering the single supply chain echelon the (s, Q) policy performs better than the (R, S) only in the Plants echelon and in the Distribution Centres echelon; it

presents greater costs in the store echelon (and this is mostly due to a greater number of stock outs occurrences).

Finally figure 6 shows the different types of cost for the (s, S) policy. The graph reports all the costs defined in equations 7 and 8: ordering cost, carrying cost, shortage cost, backordering cost, carrying cost for remanufactured products, remanufacturing cost and disposal cost. Note that the most important costs are the inventory carrying cost for new products, the ordering cost, the inventory carrying cost for remanufactured products and the remanufacturing cost.

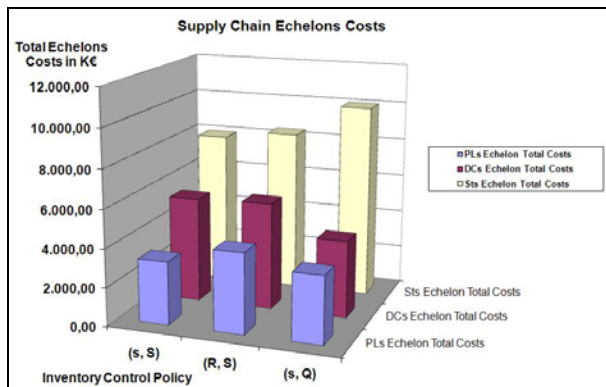


Figure 5: Supply chain Echelon Costs Comparison

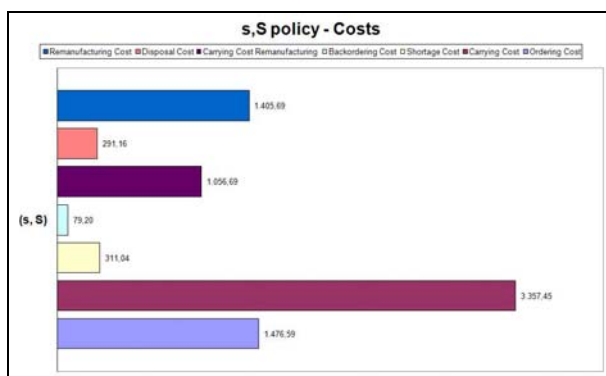


Figure 6: Cost types analysis for the (s, S) policy

Similar results have been obtained for each inventory control policies as well as for each supply chain node. In effect the IMPRES simulator is able to track individually each supply chain node as well as each products (new or remanufactured) within the whole supply chain.

6. CONCLUSIONS

The article addresses the very important issue of multi-echelon inventory management systems with product returns. The authors first propose a detailed state of the art overview on both deterministic and stochastic models proposed by researchers and scientists over the last decades. Then the authors deal directly with the inventory management with products return problem within the supply chain. It should be noted the research effort carried out by the authors in relaxing most of the common assumptions adopted in literature and

presenting and investigating the behaviour of four different inventory control policies in terms of total supply chain costs. To this end the authors develop an advanced simulator, called IMPRES, that can be easily used as decision support tool. Analysis and results are also presented and show how the inventory control policies behave differently in terms of total supply chain costs as well as in terms of supply chain echelon costs.

Further research are still on going carrying out inventory parameters optimization by using Genetic Algorithms (with the aim of total costs minimization) and investigating inventory control policies behaviour with advanced DOE and ANOVA techniques.

REFERENCES

- Ahiska, S.S., King, R.E., 2009. Inventory optimization in a one product recoverable manufacturing system. *International Journal of Production Economics*, In press.
- Aras, N., Verter, V., Boyaci, T., 2006. Coordination and priority decisions in hybrid manufacturing/remanufacturing systems. *Production & Operations Management*, 15(4), 528–543.
- Banks, J., 1998. *Handbook of Simulation*, John Wiley & Sons, New York, pp.3-30.
- Bayindir, Z.P., Erkip, N., Gullu, R., 2003. A model to evaluate inventory costs in a remanufacturing environment. *International Journal of Production Economics*, 81, 597–607.
- Beltran, J.L., Krass, D., 2002. Dynamic lot sizing with returning products and disposals. *IIE Transactions*, 34(5), 437-448.
- Bruzzone A.G., Giribone P, Vio F. (1999). Genetic Algorithms and Simulation for Supporting Layout Re-Engineering of Automotive Component Production Facilities. *International Journal of Flexible Automation And Integrated Manufacturing*, vol. 7, p. 379-391, ISSN: 1064-6345
- Bruzzone A.G. (2002). Introduction to the Special Issue on Simulation in Supply Chain Management. *Simulation*, vol. 78, p. 284-286, ISSN: 0037-5497
- Bruzzone A.G. (2004). Preface to modeling and simulation methodologies for logistics and manufacturing optimization. *Simulation*, vol. 80, pp. 119-120, ISSN: 0037-5497, doi: 10.1177/0037549704045812
- Bruzzone A.G., Briano A., Bocca E., Massei M. (2007). Evaluation of the impact of different human factor models on industrial and business processes". *Simulation Modeling Practice and Theory*, vol. 15, p. 199-218, ISSN: 1569-190X.
- Bruzzone AG, Longo F (2010). An Advanced System for Supporting the Decision Process within Large-scale Retail Stores. *Simulation*, vol. 86, p. 742-762, ISSN: 0037-5497, doi: 10.1177/0037549709348801
- Bruzzone A.G., Longo F., (2012). 3D Simulation as Training Tool in Container Terminals: the

- TRAI^NPORTS Simulator. Journal Of Manufacturing Systems, ISSN: 0278-6125, doi: 10.1016/j.jmsy.2012.07.016
- Buchanan, D.J., Abad, P.L., 1998. Optimal policy for a periodic review returnable inventory system. *IIE Transactions*, 30(11), 1049-1055.
- Cimino A., Longo F., Mirabelli G., (2009). A multi measure-based methodology for the ergonomic effective design of manufacturing system workstations. *International Journal of Industrial Ergonomics*, vol. 39, p. 447-455, ISSN: 0169-8141, doi: 10.1016/j.ergon.2008.12.004
- Ching, W.K., Yuen, W.O., Loh, A.W., 2003. An inventory model with returns and lateral transshipments. *Journal of the Operational Research Society*, 54(6), 636–641.
- Chung, S.L., Wee, H.M., Yang, P.C., 2008. Optimal policy for a closed-loop supply chain inventory system with remanufacturing. *Mathematical and Computer Modelling*, 48(5-6), 867–881.
- Clark, A. J., Scarf, H., 1960. Optimal policies for a multiechelon inventory problem. *Management Science*, 6, 475–490
- Cohen, M.A., Nahmias, S., Pierskalla, W.P., 1980. A dynamic inventory system with recycling. *Naval Research Logistics Quarterly*, 27(2), 289-296.
- Curcio, D., Longo, F., 2009. Inventory and Internal Logistics Management as Critical Factors Affecting the Supply Chain Performances. *International Journal of Simulation & Process Modelling*, vol. 5(4); p. 278-288.
- De Sensi, G., Longo, F., Mirabelli, G., 2008. Inventory policies analysis under demand patterns and lead times constraints in a real supply chain. *International Journal of Production Research*, vol. 46(24); p. 6997-7016.
- DeCroix, G., Jing-Sheng, S., Zipkin, P., 2005. A series system with returns: stationary analysis. *Operations Research*, 53(2), 350–362.
- DeCroix, G.A., 2006. Optimal policy for a multiechelon inventory system with remanufacturing. *Operations Research*, 54(3), 532–543.
- El Saadany, A.M.A. Jaber, M.Y., 2008. The EOQ repair and waste disposal model with switching costs. *Computers & Industrial Engineering*, 55(1), 219-233.
- Fleischmann, M. 2000. Quantitative models for reverse logistics. Ph.D. dissertation, Erasmus University, Rotterdam, The Netherlands.
- Fleischmann, M., Bloemhof-Ruwaard, J.M., Dekker, R., van der Laan, E., van Nunen, J. A.E.E., Van Wassenhove, L.N., 1997. Quantitative models for reverse logistics: A review. *European Journal of Operational Research*, 103(1), 1-17.
- Fleischmann, M., Kuik, R., 2003. On optimal inventory control with independent stochastic product returns. *European Journal of Operational Research*, 151(1), 25-37.
- Fleischmann, M., Kuik, R., Dekker, R., 2002. Controlling inventories with stochastic product returns: A basic model. *European Journal of Operational Research*, 138(1), 63-75.
- Giribone P., Bruzzone A.G. (1999). Artificial Neural Networks as Adaptive Support for the Thermal Control of Industrial Buildings. *International Journal of Power & Energy Systems*, vol. 19, No.1, p. 75-78, ISSN: 1078-3466.
- Golany, B., Yang, J. and Yu, G., Economic lot-sizing with remanufacturing options. *IIE Trans.*, 2001, 33, 995–1003.
- Heyman, D.P., 1977. Optimal disposal policies for a single-product inventory system with returns. *Naval Research Logistics Quarterly*, 24(3), 385-405.
- Inderfurth, K., 1997. Simple optimal replenishment and disposal policies for a product recovery system with leadtimes. *O R Spectrum*, 19(2), 111-122.
- Inderfurth, K., de Kok, A.G., Flapper, S.D.P., 2001. Product recovery in stochastic remanufacturing systems with multiple reuse options. *European Journal of Operational Research*, 133(1), 130-152.
- Jaber, M.Y. Rosen, M.A., 2008. The economic order quantity repair and waste disposal model with entropy cost. *European Journal of Operational Research*, 188(1), 109-120
- Jaber, M.Y. Saadany, A.M.A., 2009. The production, remanufacture and waste disposal model with lost sales. *International Journal of Production Economics*, 120(1), 115-124.
- Kiesmuller, G.P., Minner, S., Kleber, R., 2000. Optimal control of a one product recovery system with backlogging. *IMA Journal of Mathematics Applied in Business and Industry* 11, 189–207.
- Kiesmüller, G.P., Scherer, C.V., 2003. Computational issues in a stochastic finite horizon one product recovery inventory model. *European Journal of Operational Research*, 146(3), 553-579.
- Kiesmüller, G.P., van der Laan, E.A., 2001. An inventory model with dependent product demands and returns. *International Journal of Production Economics*, 72(1), 73-87.
- Kleber, R., Minner, S., Kiesmüller, G.P., 2002. A continuous time inventory model for a product recovery system with multiple options. *International Journal of Production Economics*, 79(2), 121-141.
- Koh S.-G., Hwang H., Sohn K.-I., Ko C.-S., 2002. An optimal ordering and recovery policy for reusable products. *Computers and Industrial Engineering*, 43(1-2), 59-73.
- Konstantaras, I. and Papachristos, S., 2004. Note: Lot-sizing for Inventory Systems with Product Recovery, Department of Mathematics, University of Ioannina, Ioannina, Technical Report No. 13.
- Konstantaras, I. and Papachristos, S., 2006. Lot-sizing for a single-product recovery system with backordering. *International Journal of Production Research*, 44(10), 2031-2045.
- Konstantaras, I. and Papachristos, S., 2007. Optimal policy and holding cost stability regions in a

- periodic review inventory system with manufacturing and remanufacturing options. *European Journal of Operational Research*, 178(2), 433-448.
- Korugan, A., Gupta, S. M., 1998. A Multi-Echelon Inventory System with Returns. *Computer and Industrial Engineering*, 35 (1-2), pp. 145 – 148.
- Longo, F. and Mirabelli, G., 2008. An advanced supply chain management tool based on modeling and simulation. *Computers & Industrial Engineering*, 54(3), 570-588.
- Longo F., Mirabelli G., (2009). Effective Design of an Assembly Line using Modeling & Simulation. *Journal of Simulation*, vol. 3, p. 50-60, ISSN: 1747-7778, doi: 10.1057/JOS.2008.18
- Longo F (2010). Design and integration of the containers inspection activities in the container terminal operations. *International Journal of Production Economics*, vol. 125, p. 272-283, ISSN: 0925-5273, doi: 10.1016/j.ijpe.2010.01.026
- Longo F, Massei M, Nicoletti L (2012). An application of modeling and simulation to support industrial plants design. *International Journal of Modeling, Simulation, and Scientific Computing*, vol. 3, p. 1240001-1-1240001-26, ISSN: 1793-9623, doi: 10.1142/S1793962312400016
- Mabini, M.C., Pintelon, L.M., Gelders, L.F., 1992. EOQ type formulations for controlling repairable inventories. *International Journal of Production Economics*, 28(1), 21-33.
- Mahadevan, B., Pyke, D.F., Fleischmann, M., 2003. Periodic review, push inventory policies for remanufacturing. *European Journal of Operational Research*, 151(3), 536-551.
- Minner, S., Kleber, N., 2001. Optimal control of production and remanufacturing in a simple recovery model with linear cost functions. *O R Spectrum*, 23(1), 3-24.
- Mitra, S., 2009. Analysis of a two-echelon inventory system with returns. *Omega*, 37(1), 106-115.
- Mosca R., Giribone P., Bruzzone A.G., Orsoni A., Sadowski S. (1997). Evaluation and Analysis by Simulation of a Production Line Model Built with Back-Propagation Neural Networks. *International Journal of Modelling & Simulation*, vol. Vol.17, no.2, p. 72-77, ISSN: 0228-6203
- Muckstadt, J.A., Isaac, M.H., 1981. An analysis of single product inventory systems with returns. *Naval Research Logistics Quarterly*, 28(2), 237-254.
- Nahmias, S. Rivera, H., 1979. A deterministic model for a repairable product inventory system with a finite repair rate. *International Journal of Production Research*, 17(3), 215-221.
- Nakashima, K., Arimitsu, H., Nose, T., Kuriyama, S., 2002. Analysis of a product recovery system. *International Journal of Production Research*, 40(15), 3849–3856.
- Oh, Y.H., Hwang, H., 2006. Deterministic inventory model for recycling system. *Journal of Intelligent Manufacturing*, 17(4), 423-428.
- Richter, K. Gobsch, B., 2003. The market-oriented dynamic product recovery model in the just-in-time framework. *International Journal of Production Economics*, 81-82 (1), 369–374.
- Richter, K., 1994. An EOQ repair and waste disposal model. Pre-prints of the Eighth International Working Seminar on Production Economics, 3, 83-91.
- Richter, K., 1996a. The EOQ repair and waste disposal model with variable setup numbers. *European Journal of Operational Research*, 96(2), 313-324.
- Richter, K., 1996b. The extended EOQ repair and waste disposal model. *International Journal of Production Economics*, 45, 443–447.
- Richter, K., Dobos, I., 1999. Analysis of the EOQ repair and waste disposal problem with integer setup numbers. *International Journal of Production Economics*, 59(1-3), 463-467.
- Richter, K., Sombrutzki, M., 2000. Remanufacturing planning for the reverse Wagner/Whitin models. *European Journal of Operational Research*, 121(2), 304–315.
- Richter, K., Weber, J., 2001. The reverse Wagner/Whitin model with variable manufacturing and remanufacturing cost. *International Journal of Production Economics*, 71(1-3), 447-456.
- Roy, A., Maity, K., Kar, S., Maity, M., 2009. A production–inventory model with remanufacturing for defective and usable products in fuzzy-environment. *Computers and Industrial Engineering*, 56(1), 87–96.
- Schrady, D.A., 1967. A deterministic inventory model for repairable products. *Naval Research Logistics Quarterly*, 14(3), 391-398.
- Silver, E. A., Pyke D. F., Peterson R., 1998. *Inventory Management and Production Planning and Scheduling*. Third Edition, Wiley.
- Simpson, V.P., 1978. Optimum Solution Structure for a Repairable Inventory Problem. *Operations Research*, 26(2), 270-281.
- Teunter, R.H., 2001. Economic Ordering Quantities for Recoverable Product Inventory Systems. *Naval Research Logistics*, 48(6), 484-495.
- Teunter, R.H., Bayindir, Z.P., Heuvel, W.V.D., 2006. Dynamic lot sizing with product returns and remanufacturing. *International Journal of Production Research*, 44(20), 4377–4400.
- Teunter, R.H., van der Laan, E., Vlachos, D., 2004. Inventory strategies for systems with fast remanufacturing. *Journal of the Operational Research Society*, 55(5), 475-484.
- Thierry, M.C., Salomon, M., van Nunen, J., Van Wassenhove, L., 1995. Strategic issues in product recovery management. *California Management Review* 37 (2), 114-135.

- Toktay, L.B., Wein, L.M., Zenios, S. A., 2000. Inventory management of remanufacturable products. *Management Science*, 46(11), 1412-1426.
- Van der Laan, E., Salomon, M., Dekker, R., Van Wassenhove, L., 1999. Inventory control in hybrid systems with re manufacturing. *Management Science*, 45(5), 733-747.
- Veinott, A.F. Jr., 1966. The Status of Mathematical Inventory Theory, *Management Science* 12, 745-777.
- Wagner, H.W., Whitin, T.H., 1958. Dynamic version of the economic lot size model. *Management Science* 5, 89-96.
- Yuan, X.-M., Cheung, K.L., 1998. Modeling returns of merchandise in an inventory system. *O R Spectrum*, 20(3), 147-154.

AUTHORS BIOGRAPHY

Francesco Longo received his Ph.D. in Mechanical Engineering from University of Calabria in January 2006. He is currently Assistant Professor at the Mechanical Department of University of Calabria and Director of the Modelling & Simulation Center – Laboratory of Enterprise Solutions (MSC-LES). He has published more than 120 papers on international conferences and journals. His research interests include Modeling & Simulation tools for training procedures in complex environment, supply chain management and security. He is Associate Editor of the “Simulation: Transaction of the society for Modeling & Simulation International”. For the same journal he is Guest Editor of the special issue on Advances of Modeling & Simulation in Supply Chain and Industry. He is Guest Editor of the “International Journal of Simulation and Process Modelling”, special issue on Industry and Supply Chain: Technical, Economic and Environmental Sustainability. He is Editor in Chief of the SCS M&S Magazine (Europe Area). Newsletter and he has served as General Chair and Program Chair for the most important international conferences in the simulation area. His e-mail address is: f.longo@unical.it

SIMULATION BASED ANALYSIS OF A MANUFACTURING SYSTEM DEVOTED TO PRODUCE HAZELNUT BASED PRODUCTS

Agostino G. Bruzzone^(a), Francesco Longo^(b)

^(b) DIME - University of Genoa, via Opera Pia 15 - 16145 Genova, Italy

^(b) MSC – LES, Mechanical Department, University of Calabria, Via Pietro Bucci, Rende, 87036, ITALY

^(a) agostino@itim.unige.it, ^(b) f.longo@unical.it

ABSTRACT

The main goal of this paper is to propose a simulation model that can be used as decision support tool within a manufacturing system devoted to produce hazelnuts based products. The simulation model is capable of investigating different manufacturing systems configurations by considering user-defined input parameters and multiple performance measures. The paper briefly describes the simulation model and proposes an application example to provide evidence on the relevance of the proposed simulation model.

Keywords: Industrial Plants, Modeling & Simulation, Performance Analysis

1. INTRODUCTION

Considering the actual financial crisis (still ongoing in many European countries) manufacturing systems must be able to react at different levels (strategic, tactic and operative) to unexpected changes (both in terms of opportunities and problems). Strategic decisions in manufacturing systems typically concern design problems and resources allocation in the medium/long period (i.e. a new plant lay-out, products assortment, new production machines, etc.). Tactical decisions are related to the planning and control of the manufacturing system resources (manufacturing policies, warehouse and logistics policies, customers' services, etc). Finally, operative decisions are mainly related to the manufacturing system management in the short period (i.e. shop orders scheduling, resources and materials availability, etc.). Usually problems at any of these levels may involve contrasting objectives therefore requiring a strong experience (for people involved in the decision process) as well as advanced decision support tools.

In this context Modeling & Simulation (M&S) is widely used in manufacturing systems design and management to define system requirements, to explain system behavior, to diagnose problems, to take into account the effects of specific constraints, to test different production policies, to investigate different operative scenarios, to evaluate the impact of different human factors on industrial and business processes (Bruzzone, 2002; Bruzzone, 2004, Bruzzone et al., 2007). In fact a survey of the current state of the art

clearly reveals that a tremendous amount of research works have been published (over the last 50 years) in this area (Callahan *et al.* 2006).

Generally speaking, a M&S based approach generally does not provide exact or optimal solutions to problems but it allows users analyzing the behavior of complex systems, performing what-if analysis and choosing correctly among different possible scenarios (Karacal 1998; Banks 1998). In fact, oppositely to analytical approaches, the main advantage of M&S when studying and analyzing manufacturing and logistic systems is the possibility to take into consideration multiple aspects without introducing restrictive assumptions. M&S offers the possibility to generate reliable output results, to describe and analyze the behavior of existing systems while changing initial conditions and operative scenarios.

According to Smith (2003), simulation based approaches can be used both for existing (see for instance Bruzzone et al., 1999) and for new manufacturing systems (still not in existence, Longo and Mirabelli, 2009). Examples of research works in which M&S has been used to support manufacturing systems design and/or management can be found in Berry (1972), Nunnikhoven and Emmons (1977), Stenger (1996), Mullarkey *et al.* (2000), Longo *et al.* (2005), Longo et al. (2012), Ren et al (2012). M&S is also often used in combination with artificial intelligence techniques (above all for solving multi-objective optimization problems). Classifications frameworks for simulation based optimization can be found in Andradottir (2005), Fulcher (2008); examples of applications can be found in Mosca et al. (1997), Giribone and Bruzzone, (1999).

The focus of this paper is a manufacturing system devoted to produce hazelnuts based products. The authors use a M&S based approach to develop a decision making tool that can be used by production managers for investigating different manufacturing system configurations under the effect of multiple critical parameters and by monitoring multiple performance measures. Therefore the goal of this paper is not to find out the best configuration of the manufacturing system but to show the potentials of the simulation approach in the decision making process and how an ad-hoc developed simulation model can be an

advance tool to support decision taken at any level by the company production managers.

The paper is organized as follows: Section 2 reports a description of the hazelnuts market; section 3 presents the hazelnuts production process while section 4 briefly describes the main simulation model features. Section 5 proposes the application examples and the experimental analysis to show the relevance of the proposed approach. Finally, conclusions summarise the main results of the study.

2. THE HAZELNUTS MARKET

According to the Food and Agriculture Organization of the United Nations (FAO), the hazelnuts truck farming covers around 847,435 hectares with an estimated production of 1,052,000 tons per year. Turkey is the major hazelnuts producer (75% of the total hazelnuts production) followed by Italy (11%), USA (3%), Azerbaijan (3%) and Spain (2%).

Therefore hazelnuts' price strongly depends on the international trades and transactions, with Turkey playing the most important role in determining the hazelnuts price. The most important influence on the price is the amount of production placed in international markets from Turkey, which alone represents 70% of the world. However, Turkey usually enters controlled quantities of hazelnuts in the market to keep under control the prices (in order to avoid drastic reduction of international prices with negative consequences on income levels of its farmers).

Even with a strong difference compared to Turkey in terms of total production per year, Italy has a long tradition and experience in the hazelnuts production and today faces the national and international market with a considerable hazelnuts based products assortment. In fact, during the last years, hazelnuts production has received funding and incentives (at both European and national level) for the introduction of innovations for increasing quality standards (i.e. new methods of cultivation have been introduced to optimize harvesting techniques, times and to ensure environment protection). The scenario that characterizes the Italian hazelnuts sector is rather complex: the land dedicated to hazelnuts truck farming is continuously increased during the last 50 years (+126%) as well as the total production passed from about 24,000 tons/year up to 105,000 tons/year. In Italy, most of the land area used for hazelnuts truck farming is located in the South. The first stage is represented by agricultural producers that sell their products to both national and international buyers (mainly represented by the confectionery industry). Hand harvesting affects for about one third the cost of the total crop (in case of mechanized harvesting such percentage drops to 19%). Usually mechanical harvesting can be facilitated by chemical treatments, to promote the maturation and the simultaneous fall of hazelnuts.

Production facilities require complex industrial/manufacturing systems characterized by

different types of operations including sizing, shelling, roasting, grain, packaging and storage. The technical characteristics of the manufacturing system devoted to produce hazelnuts based products considered in this paper are briefly presented in the next section.

Specifically, with regard to Calabrian territory (South Part of Italy) the initiative to design an integrated manufacturing system for processing semi-finished hazelnuts has been undertaken in order to meet the demand of "Pizzo Homemade" ice cream.

3. THE HAZELNUTS PRODUCTION PROCESS

The production process of the manufacturing system considered in this paper consists of several stages. The first phase consists of cleaning and drying operations. Raw hazelnuts are cleaned in two ways: with air jet (to remove impurities) and with water to separate the heavier ones. In particular the raw hazelnuts are placed in a bulk hopper that moves (by gravity) the hazelnuts on a bucket elevator that, in turn, transports them up to the entrance of the impurities separator. Inside the separator hazelnuts are invested by a strong jet of air which ensures the separation of the raw hazelnuts from light impurities such as leaves, twigs, shells, etc. Then the product is conveyed inside a destoner that is used for the elimination of heavier impurities (i.e. stones). In particular, hazelnuts are moved to the subsequent operation by a flow generated by an external unit, while the heavier elements are dragged downwards from the outflow. Another bucket elevator transports the cleaned hazelnuts till the entrance of the dryer.

Within the drying chamber hazelnuts are subject to a jet of hot air (45°C - 60°C) to reduce the moisture (this phase is also useful to guarantee the preservation of the hazelnuts quality over the time) and to prepare hazelnuts to the successive operations. This operation also guarantees bacteria destruction and weakening of the shell. After this phase some of these hazelnuts are directly packed (hazelnuts in shell) while the remaining hazelnuts continue the production process through the pre-calibrating and shelling operations.

At this stage, the hazelnuts are placed again in a bulk hopper and then by gravity in a bucket elevator that moves them till the entrance of a roller sizer. This machine subdivides hazelnuts in different sizes, depending on the shells dimensions. Therefore the hazelnuts are conveyed to the Sheller that deprives hazelnuts for their shells; once deprived of their shells, hazelnuts are subject to further calibration (this time the hazelnuts must respect all the quality standards required in order to proceed with the subsequent operations). Finally, a spiral conveyor moves the hazelnuts to the subsequent phase.

The subsequent phase is the roasting operation; this operation is required to give hazelnuts a complete dehydration, oxidation and therefore more flavors. At the end of the roasting operation a cooling tunnel brings roasted hazelnuts at the environment temperature. The product, deprived of the outer shell, is then moved

through a conveyor belt where operators manually remove the over-burned hazelnuts. At this time, some of the hazelnuts are packed (roasted hazelnuts) while the remaining hazelnuts continue the process through the graining and refining operations. Graining operations are devoted to produce chopped hazelnuts (that will be packaged in a granular form). First the hazelnuts go through the grinder machine, where they are crushed and reduced to chopped hazelnuts. Now, the product, in granular form, passes through a circular vibrating screen that removes dust from chopped nuts. Finally a pneumatic separator separates the granules of different dimensions.

The last phase is the refining operation. The roasted nuts are placed in a flour mill that reduces them into flour. Then the flour is placed in steel tanks where it is mixed with water and sugar and then conveyed into the refiner, where it is continuously kneaded to form the hazelnuts paste. The paste is sieved in the vibrating filter to provide additional smoothness and eliminate possible solid components. At the end the hazelnuts paste is placed in a stainless steel tanks, waiting to be moved with a volumetric pump into stainless steel containers that are successively stored in refrigerators.

Figure 1 shows a schematization of the manufacturing process highlighting the different manufacturing system departments and the transport operations.

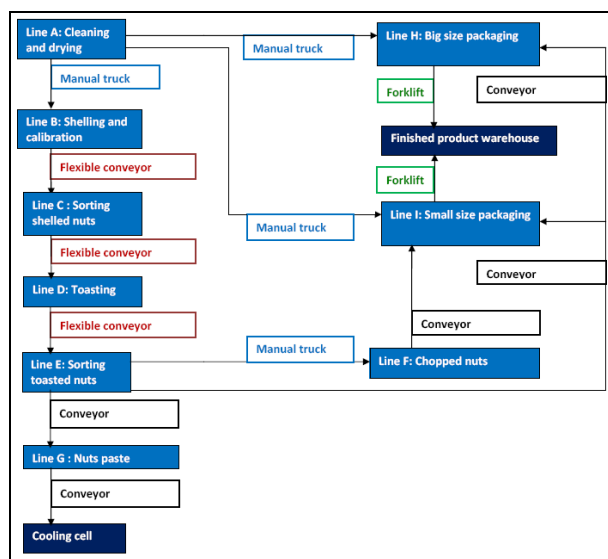


Figure 1: manufacturing process schematization

Information about the estimated production of the manufacturing system considered in this paper are reported in table 1 (expressed in tons per year for each type of product).

4. THE SIMULATION MODEL

Authors have a long experience in developing simulation models (also using advanced approach based on 3D virtual simulation) for supporting the decision process both in the Industry and Logistics area.

Table 1: Estimated production of the manufacturing systems

Product type	Quantity (tons per year)
Hazelnuts in Shell	60
Roasted Hazelnuts	30
Chopped Hazelnuts	60
Hazelnut Paste	37

Example of research works developed by authors in this area can be found in Bruzzone and Longo, (2012), Longo et al. (2012), Bruzzone and Longo (2010), Longo (2010); Cimino et al. (2009); Curcio and Longo (2009), Longo and Mirabelli (2009), Longo and Mirabelli, 2008, De Sensi et al. (2008).

Based on the description reported in the previous section the authors have implemented a java-based simulation model able to recreate the entire hazelnuts production process. The simulation model includes the following elements:

- static entity: workers performing manual operations (i.e. manual sorting of over-burned hazelnuts) and manual transportations.
- dynamic entities: hazelnuts in all the states of transformation (freshly harvested, cleaned, dried, shelled, roasted, chopped nuts, hazelnuts flour, hazelnuts paste), containers used for transportation (canvas bags, stainless steel containers, etc.)
- resources: constituted by machines and conveyor belts that are located within the different manufacturing system departments
- queue: intermediate buffers in which work in process is accumulated

Figure 2 shows the animation the main frame of the manufacturing system simulation model. The mean utilization level of each machine is displayed by means of bar indicators positioned in correspondence of each machine as well as the work in process is displayed by using arc indicators positioned in correspondence of the intermediate buffers. In addition, the mean level of utilization of the intermediate buffers is displayed by using text messages.

The simulation model is equipped with a control panel that provides the user with the possibility to change the most important parameters governing the manufacturing system. In particular it is possible to change the production capacity of each machine, the source rate defined as the amount of raw hazelnuts entering the manufacturing system per unit of time, the number of workers, the products assortment and the amount of each product type to be produced.

The simulation model is also equipped with a section dedicated to display the simulation results. Multiple key performance indicators are displayed: among others, the flow time for each shop order, quantity of quantity of dried, roasted, grained hazelnuts

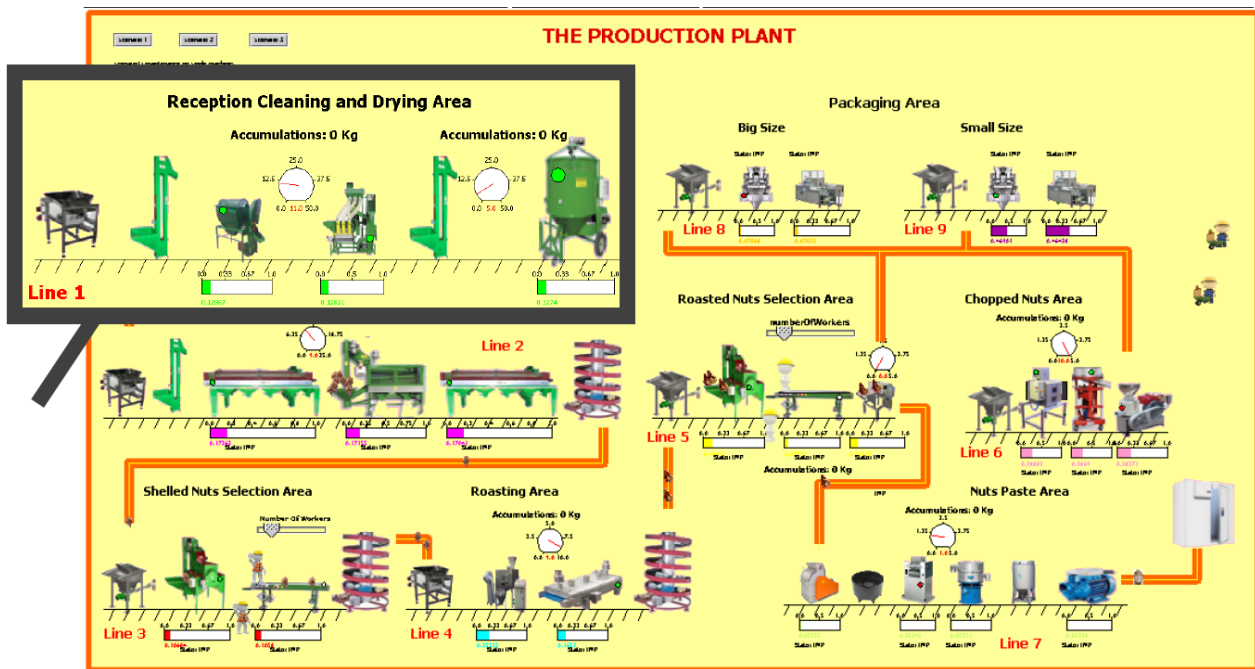


Figure 2: the manufacturing system simulation model

and hazelnuts paste, the number of packages for each product type, machines average utilization level and buffers saturation level.

5. EXPERIMENTAL ANALYSIS

The main idea behind the simulation model proposed in this paper is to provide the production managers operating in the manufacturing system with a decision making tool capable of analyzing different manufacturing system configurations by using an approach based on multiple performance measures and user-defined set of input parameters. Therefore the application example proposed in this section has been developed for understanding tool potentials from the production engineers' perspective.

It is easy to understand that a production manager needs a decision making tool capable of investigating the effects of critical factors on multiple performance measures therefore a decision making tool should provide managers with high flexibility in terms of scenarios definition, critical parameters and performance measures selection.

In the application example proposed in this section the authors decide to use the simulation model to investigate the behavior of several performance indicators under different operative conditions. The simulation model capabilities as decision making tool are strongly amplified if Design of Experiment (DOE) and Analysis of Variance (ANOVA) are respectively used for experiments planning and simulation results analysis. Before carrying out the experimental analysis some preliminary simulations have been executed to test the capability of the simulation model to recreate the real manufacturing system.

The results of these preliminary analyses are reported in table 2 in terms of simulated annual production and real annual production

Table: Comparison between the simulated annual production and the real annual production

Annual Production [tons/year]			
Product Type	Simulated	Real	Difference
Hazelnuts in Shell	60,575	60.0	0.94%
Roasted Hazelnuts	29,580	30.0	1.41%
Chopped Hazelnuts	60,040	60.0	0.06%
Hazelnuts Paste	37,090	37.0	0.24%

The main factors considered as "critical parameters" that can impact the system performances are:

- *Source Rate*, SR, defined as the quantity of raw hazelnuts in input to the production process per unit of time
- *Production Mix*, PM, defined as the mix of products that are currently worked in the manufacturing system
- *Customer Rate*, CR, defined as the number of external customers per unit of time (the Customer Rate simulates the external demand intensity)
- *Working Shifts*, WS, defined as the number of working hours per day.

In this study, we have chosen, for each factor, different number of levels as reported in table 3.

Table 3: Factors and Levels

Factors	Level 1	Level 2
SR	90%	110%
PM	15 %	25%
CR	90%	110%
WS	80%	125%

The meaning of the factors levels can be explained as follows. The minimum level and the maximum level of the source rate are 90% and 110% of the actual value respectively; the actual value of the source rate is the one currently used in the real manufacturing system. The minimum and the maximum level of the production mix are 15% and 25%; the two levels are the percentages of the total raw hazelnuts in input to the manufacturing system that will be stored as hazelnuts in shell while the remaining part will be used for roasted hazelnuts, chopped hazelnuts and hazelnuts paste. The minimum level and the maximum level of the customer rate are 90% and 110% of the actual value respectively; the actual value of the customer rate is the average value of the customer rate in the real system. The minimum level and the maximum level of the working shift are 80% and 125% of the actual value respectively; the actual value of the working shift is the one currently used in the real system.

The following performance measures are monitored during each simulation run:

- Average Utilization Level of each Production line;
- Flow Time of small packages of hazelnuts in shell
- Flow Time of big packages of hazelnuts in shell
- Flow Time of small packages of roasted hazelnuts
- Flow Time of big packages of roasted hazelnuts
- Flow Time of chopped hazelnuts
- Flow Time of hazelnuts paste
- Quantity in output for each product type
- Work in Process
- Average Lead Time
- Percentage of Fulfilled Orders
- Total Back Orders
- Total Probability of Stockout
- On Hand Inventory for hazelnuts in shell
- On Hand Inventory for roasted hazelnuts
- On Hand Inventory for chopped hazelnuts
- On Hand Inventory for hazelnuts paste
- Total On Hand Inventory

Note that the production manager can easily define a different scenario by selecting different factors or different factors levels. To this end the manager can easily implement new factors/parameters thanks to simulator architecture completely based on java programming code. The objective of the application

example is to understand the effects of factors levels on the performance measures reported above.

Checking all possible factors levels combinations (by using a factorial experimental design) requires 16 simulation runs; if each run is replicated 5 times we have 80 replications. To monitor the performances of the manufacturing system requires the collection of a huge number of simulation results. To this end the simulation model has been jointly used with Microsoft Excel and Minitab. At the end of each replication the simulation results are transferred in Excel spreadsheets. By means of routines programmed in Visual Basic the performance measures average values are calculated. Such values can be easily copied on a Minitab project (opportunistly set with the same design of experiments) for statistic analysis. The Microsoft Excel interface has been implemented for correctly working in each scenario (not only in the application example proposed). The results in terms of mean values calculated by Microsoft Excel can be analyzed by using plots and charts (i.e. working in process versus source rate, probability of stock-out versus customer rate, etc.). Therefore the use of the simulation model does not necessarily require Design of Experiments or Analysis of Variance or any kind of statistical methodologies or software.

5.1. Simulation Results and discussion

Considering that currently there are 18 different performance measures implemented within simulation model, we cannot report in this paper all the simulation results of the application example; the following figures summarize some simulation results. The results of the factorial experimental design have been analyzed by using the ANOVA.

The ANOVA allows to evaluating those factors that have a real impact on the performance measures considered by decomposing the total variability of the performance measures into components; each component is a sum of squares associated with a specific source of variation (treatments) and it is usually called treatment sum of squares. Without enter in formulas details, if changing the levels of a factor has no effect on variance of the performance measure, then the expected value of the associated treatment sum of squares will be an unbiased estimator of the error variance (this is known as null hypothesis, H0). On the contrary, if changing the level of a factor has effect on the performance measure, then the expected value of the associated treatment sum of squares will be the estimation of the error plus a positive term that incorporates the variation due the effect of the factor (alternative hypothesis, H1). It follows that by comparing the treatment mean square and the error mean square we can understand which factors have effect on the performance measure (Longo and Mirabelli, 2008). Further information on ANOVA can be found in any statistics handbook (see for instance Montgomery and Runger (2006).

The figure 3 shows the main effects plots (obtained by plotting the meta-model obtained from the analysis of variance) for the average flow time of the chopped hazelnuts. It is possible to observe that both the Source Rate and the Production Mix have an impact on the average flow time. In particular, the average flow time increases roughly of 17% when the Source Rate changes its value from the 90% to 110%, demonstrating as an overuse of the manufacturing system can quickly bring to a rapid increase of the products flow times. Similar results have been obtained from the hazelnuts in shell, roasted hazelnuts and hazelnuts paste.

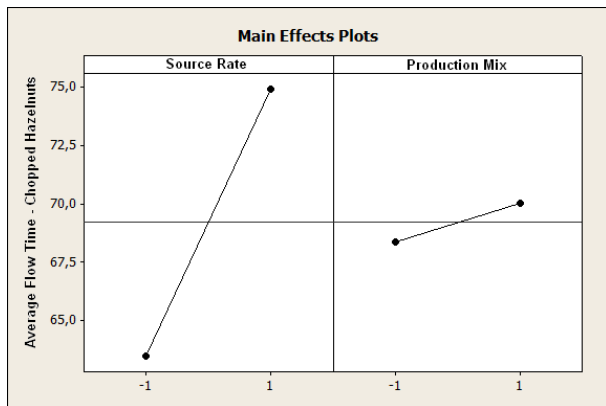


Figure 3: Average Flow time for Chopped Hazelnuts versus Source Rate and Production Mix

The figure 4 shows the main effects plot for the average percentage of fulfilled orders. It is possible to observe that the percentage of fulfilled orders increases up to 97% when the source rate is at its 110% value, while an increase of the customer rate brings to a reduction of the percentage of fulfilled orders (with an increase not shown of orders backordered). The effect of the production mix is smaller compared to the effects of both Source Rate and Customer Rate.

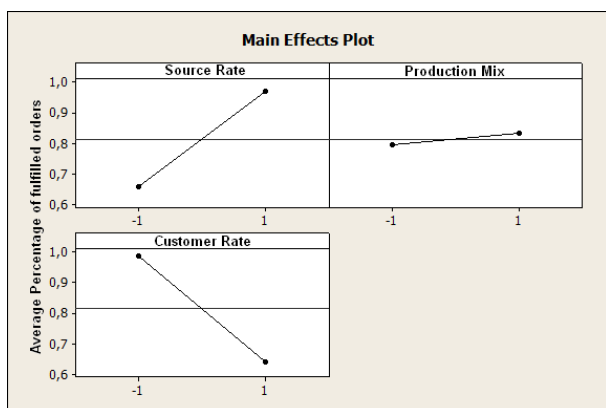


Figure 4: Average Percentage of fulfilled orders versus Source Rate, Production Mix and Customer Rate

Now let us also consider for this second case the interaction effects (shown in figure 5). There are remarkable interaction effects both between the Source Rate and the Production mix and the Source Rate and the Customer Rate. The

percentage of fulfilled orders increases when both the Source Rate and the Production Mix are at their maximum value. In addition, the interaction between the Source Rate and the Customer Rate clearly shows that an increase of the Customer Rate when the Source Rate is at its lowest value may have a tremendous impact on the percentage of fulfilled orders.

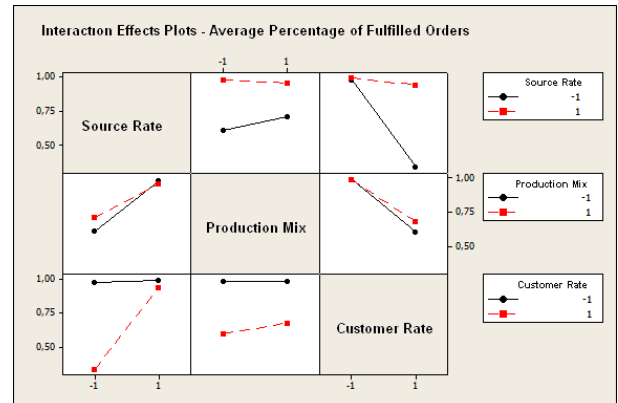


Figure 5: Interaction Effect Plots: Average Percentage of fulfilled orders versus Source Rate, Production Mix and Customer Rate

An additional cas, figure 6 shows how the simulation model can be used to evaluate the effect of Source Rate, Production Mix, Customer Rate and Working Shift on the total On Hand Inventory.

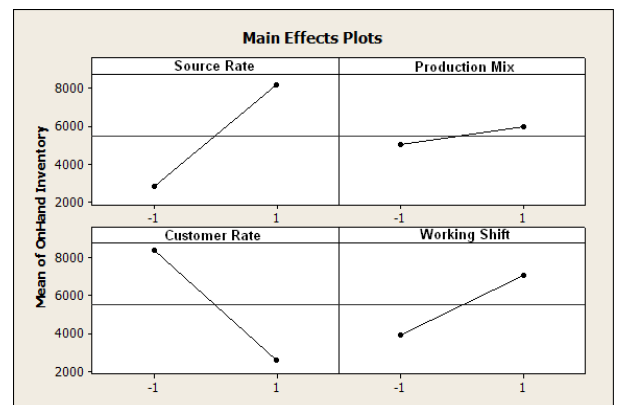


Figure 6: Average On Hand Inventory versus Source Rate, Production Mix, Customer Rate and Working Shift

Needless to say similar results have been obtained for all the other performance measures.

6. CONCLUSIONS

As already stated in the introduction, the aim of the paper is not to find out the best configuration of the manufacturing system but to show the potentials of the simulation model in the decision making process and how the simulation model proposed in this paper can be used by a production manager.

The high level of results detail (analysis of multiple performance measures in correspondence of multiple critical factors) helps in understanding the simulation model capabilities as decision making tool. In effect as reported in literature the decision making process within a manufacturing system requires accurate analysis of the current situation as well as of alternative scenarios. In addition the simulator architecture jointly with Excel and Minitab spreadsheets guarantees high flexibility in terms of scenarios definition, high efficiency in terms of time for executing simulation runs and analyzing simulation results.

REFERENCES

- Balci, O., 1998. Verification, Validation and Testing. In: J. Banks, *Handbook of Simulation*, John Wiley & Sons, Inc., 335–393.
- Banks, J., 1998. *Handbook of Simulation*. John Wiley & Sons, Inc.
- Berry, W.L., 1972. Priority scheduling and inventory control in a job shop lot manufacturing systems. *AIIE Transactions*, 4, 267–276.
- Bocca, E., Curcio, D., Longo, F., Tremori, A., 2008. Warehouse and internal logistics management based on modeling & simulation. *Proceedings of the International Workshop on Modeling & Applied Simulation 2008*, pp. 41–48. September 17–19, Campora S.Giovanni, Cosenza, Italy.
- Bruzzone A.G., Giribone P, Vio F. (1999). Genetic Algorithms and Simulation for Supporting Layout Re-Engineering of Automotive Component Production Facilities. *International Journal of Flexible Automation And Integrated Manufacturing*, vol. 7, p. 379-391, ISSN: 1064-6345
- Bruzzone A.G. (2002). Introduction to the Special Issue on Simulation in Supply Chain Management. *SIMULATION*, vol. 78, p. 284-286, ISSN: 0037-5497.
- Bruzzone A. G. (2004). Preface to modeling and simulation methodologies for logistics and manufacturing optimization . *Simulation*, vol. 80, pp. 119-120, ISSN: 0037-5497, doi: 10.1177/0037549704045812
- Bruzzone A.G., Briano A., Bocca E., Massei M. (2007). Evaluation of the impact of different human factor models on industrial and business processes". *Simulation Modeling Practice and Theory*, vol. 15, p. 199-218, ISSN: 1569-190X.
- Bruzzone, A.G., Curcio, D., Mirabelli, G., Papoff, E., 2009. Warehouse management: inventory control policies comparison. *Proceedings of the International Workshop on Modeling & Applied Simulation 2009*, pp. 148–154. September 23–25, Puerto de La Cruz, Tenerife, Spain.
- Bruzzone A.G., Longo F., (2012). 3D Simulation as Training Tool in Container Terminals: the TRAINPORTS Simulator. *Journal of Manufacturing Systems*, doi: 10.1016/j.jmsy.2012.07.016, ISSN: 0278-6125.
- Bruzzone A.G, Longo F., 2010. An advanced System for supporting the decision process within large scale retail stores. *SIMULATION*, vol. 86, p. 742-762., doi: 10.1177/0037549709348801.
- Callahan, R.N., Hubbard, K.M., Bacoski, N.M., 2006. The use of simulation modelling and factorial analysis as a method for process flow improvement. *Advanced Manufacturing Technology*, 29, 202–208.
- Castilla I, Longo F., 2010. Modelling and Simulation Methodologies, Techniques and Applications: a State of the Art Overview. *International Journal of Simulation & Process Modelling*, vol. 6(1); p. 1-6, ISSN: 1740-2123.
- Cimino A., Longo F., Mirabelli G., 2009. A Multi-Measures Based Methodology for the Ergonomic Effective Design of Manufacturing System Workstations. *INTERNATIONAL JOURNAL OF INDUSTRIAL ERGONOMICS*, vol. 39; p. 447-455, ISSN: 0169-8141, doi: 10.1016/j.ergon.2008.12.004
- Cimino, A., Curcio, D., Mirabelli, G., Papoff, E., 2008. Warehouse inventory management based on fill rate analysis. *Proceedings of the International Workshop on Modeling & Applied Simulation 2008*, pp. 23–30. September 17–19, Campora S.Giovanni, Cosenza, Italy.
- Curcio D, Longo F., 2009. Inventory and Internal Logistics Management as Critical Factors Affecting the Supply Chain Performances. *International Journal of Simulation & Process Modelling*, vol. 5(4); p. 278-288, ISSN: 1740-2123
- De Sensi G, Longo F, Mirabelli G (2008). Inventory policies analysis under demand patterns and lead times constraints in a real supply chain. *International Journal of Production Research*, vol. 46, p. 6997-7016, ISSN: 0020-7543, doi: 10.1080/00207540701528776
- Dunn, R.H., 1987. The quest for software reliability. In: *Handbook of Software Quality Assurance*, Van Nostrand Reynold, 342–384.
- Eben-Chaime, M., Pliskin, N., Sosna, D., 2004. An integrated architecture for simulation. *Computer and Industrial Engineering*, 46, 159–170.
- Fox, D.G., 1981. Judging air quality model performance. *Bulletin of the American Meteorological Society*, 62, 599–609.
- Giribone P., Bruzzone A.G. (1999). Artificial Neural Networks as Adaptive Support for the Thermal Control of Industrial Buildings. *International Journal of Power & Energy Systems*, vol. 19, No.1, p. 75-78, ISSN: 1078-3466.
- Karacal, S.C., 1998. A novel approach to simulation modeling. *Computers & Industrial Engineering*, 34 (3), 573–587.
- Loague, K., Green, R.E., 1991. Statistical and graphical methods for evaluating solute transport models: overview and application. *Contaminant Hydrology*, 7 (1-2), 51–73.

- Longo F, Massei M, Nicoletti L (2012). An application of modeling and simulation to support industrial plants design. *International Journal of Modeling, Simulation, and Scientific Computing*, vol. 3, pp. 1240001-1-1240001-26, ISSN: 1793-9623, doi: 10.1142/S1793962312400016
- Longo F (2010). Design and integration of the containers inspection activities in the container terminal operations. *International Journal of Production Economics*, vol. 125, p. 272-283, ISSN: 0925-5273, doi: 10.1016/j.ijpe.2010.01.026
- Longo, F., Mirabelli, G., Papoff, E., 2005. Material flow analysis and plant lay-out optimization of a manufacturing system. *International Journal of Computing*, 1 (5), 107–116.
- Longo F., Mirabelli G., 2009. Effective Design of an Assembly Line using Modeling & Simulation. *Journal of Simulation*, vol. 3; p. 50-60, ISSN: 1747-7778, doi: 10.1057/JOS.2008.18.
- Longo F., Mirabelli G., 2008. An Advanced Supply Chain Management Tool Based on Modeling & Simulation. *COMPUTERS & INDUSTRIAL ENGINEERING*, vol. 54/3; p. 570-588, ISSN: 0360-8352, doi: 10.1016/j.cie.2007.09.008.
- Montgomery D.C., Runger G.C., 2006. *Applied Statistics and Probability for Engineers*. John Wiley & Sons.
- Mosca R., Giribone P., Bruzzone A.G., Orsoni A., Sadowski S. (1997). Evaluation and Analysis by Simulation of a Production Line Model Built with Back-Propagation Neural Networks. *International Journal of Modelling & Simulation*, vol. Vol.17, no.2, p. 72-77, ISSN: 0228-6203
- Mullarkey, P., Gavirneni, S., Morrice, D.J., 2000. Dynamic output analysis for simulations of manufacturing environments. *Proceedings of the 2000 Winter Simulation Conference*, pp. 1290–1296. December 10–13, Orlando, Florida (USA).
- Nunnikhoven, T.S., Emmons, H., 1977. Scheduling on parallel machines to minimize two criteria related to job tardiness. *AIIE Transactions*, 3, 288–296.
- Ren, L., Zhang, L., Tao, F., Zhang, X., Luo, Y., Zhang, Y. (2012). A methodology towards virtualisation-based high performance simulation platform supporting multidisciplinary design of complex products. *Enterprise Information Systems*, Volume 6, Issue 3, pp. 267-290.
- Smith J. S., Survey in the use of simulation for manufacturing system design and operation, *J. Manuf. Syst.* 22(2):157–171, 2003.
- Stenger, A.J., 1996. Reducing inventories in a multi-echelon manufacturing firm: a case study. *Production Economics*, 45, 239–249.
- Andradottir S., 2005. An overview of simulation optimization via random search, in Henderson S. G., Nelson B. L. (eds.), *Handbooks in Operations Research and Management Science: Simulation*, Chapter 21, Elsevier, 2005.
- Fulcher J., 2008. Computational intelligence: An introduction, *Studies in Computational Intelligence* 115:3–78

AGOSTINO BRUZZONE

Agostino Bruzzone since 1991, has taught "Theories and Techniques of Automatic Control" and in 1992 he has become a member of the industrial simulation work group at the ITIM University of Genoa; currently he is Full Professor in DIPTM. He has utilized extensively simulation techniques in harbour terminals, maritime trading and sailboat racing sectors. He has been actively involved in the scientific community from several years and served as Director of the McLeod Institute of Simulation Science (MISS), Associate Vice-President and Member of the Board of the SCS (Society for Modelling & Simulation international), President of the Liophant Simulation, VicePresident of MIMOS (Movimento Italiano di Simulazione) and Italian Point of Contact for the ISAG (International Simulation Advisory Group) and Sim-Serv.

FRANCESCO LONGO was born in Crotona (Italy), on February the 08th, 1979. He took the degree in Mechanical Engineering from University of Calabria (2002). He received the PhD in Industrial Engineering (2005). He is currently researcher at the Mechanical Department (Industrial Engineering Section) of University of Calabria and scientific responsible of the Modeling & Simulation Center – Laboratory of Enterprise Solutions (MSC-LES) in the same department. His research interests regard modeling & simulation of manufacturing systems and supply chain, DOE, ANOVA.

MODELING AND SIMULATION OF A ONE-WAREHOUSE, N -RETAILER INVENTORY SYSTEM: REASSESSING A NEGATIVE BINOMIAL APPROXIMATION

Adriano O. Solis^(a), Francesco Longo^(b), Pietro Caruso^(c), Elisa Fazzari^(d)

^(a) School of Administrative Studies, York University, Toronto, Canada

^(b) ^(c) ^(d) Department of Mechanical, Energy, and Management Engineering, University of Calabria, Rende, Italy

^(a) asolis@yorku.ca, ^(b) f.longo@unical.it, ^(c) pietrocaruso21@libero.it, ^(d) elisa_fazzari@libero.it

ABSTRACT

Some studies in the multi-echelon inventory systems literature have used a negative binomial distribution to approximate that of a critical random variable arising in the inventory model. Graves (1996) developed a model with fixed replenishment intervals where each site follows a base stock policy. He proposed – in the one-warehouse, N -retailer case – a negative binomial distribution to approximate a random variable which he referred to as “uncovered demand”. Computational evidence was provided to demonstrate the effectiveness of the approximation. Graves then suggested search procedures for approximately optimal base stock levels at the warehouse and N identical retailers under two customer service criteria: (i) probability of no stockout and (ii) fill rate. A separate analytical evaluation of the negative binomial approximation has also been reported elsewhere. In the current study, we apply a modeling and simulation approach to assess whether the approximation-based search procedures, in fact, lead to optimal stock levels.

Keywords: one-warehouse and N -retailer inventory system, multi-echelon inventory model, base stock policy, negative binomial approximation, modeling and simulation

1. INTRODUCTION

Since the seminal work by Clark and Scarf (1960), many studies on multi-echelon inventory systems have appeared in the literature. These systems involve two or more levels of entities handling or storing inventory of an item or items. Typical entities in a distribution network, for example, would be distribution centers or warehouses, at national, regional, or sub-regional levels, as well as retail sites.

Simplifying assumptions which have been made in some multi-echelon models have allowed for mathematical tractability. However, in order to better capture the complexities of multi-echelon systems that actually exist in practice, those restrictive assumptions have had to be relaxed in favor of more realistic ones (e.g., random demand or stochastic leadtimes). Some of the more complex elements of the resulting models have sometimes required the introduction of

approximations to continue to permit analytical investigation.

The negative binomial distribution (NBD), with discrete density function (e.g., Mood, Graybill, and Boes 1974):

$$f(x; r, p) = \binom{r+x-1}{x} p^r (1-p)^x I_{\{0,1,2,\dots\}}(x), \quad (1)$$

has parameters p and r . The parameter p is a probability of “success” ($0 < p \leq 1$) and the parameter r (a positive integer) is a target number of successes. A realization x of the random variable X represents a number of failures before the r^{th} success is attained.

An NBD was earlier used by Graves (1985) as an approximation to the distribution of outstanding orders for a repairable item under one-for-one replenishment in a two-echelon system involving N operating sites supported by a repair depot. The distribution of $Q_i(t)$, the outstanding orders at operating site i at time t , is observed to be unimodal, with its variance greater than its mean. Graves proposed to approximate the distribution of Q_i by a negative binomial distribution with the same mean and variance as the exact distribution. He reported that the approximation erred in only 0.9% of 1,968 test cases in specifying stockage levels that would minimize inventory holding and shortage costs. Graves reported that, in comparison, the METRIC model developed by Sherbrooke (1968) understated stockage requirements in 11.5% of the cases.

Lee and Moinzadeh (1987) confirmed the effectiveness of the negative binomial approximation under a more general setting: a two-echelon model for a repairable item with batch ordering at the operating sites. The approximation is excellent, with a maximum percentage of cost deviation of 2% for the special case when the batch size is one, which corresponds to the one-for-one replenishment policy assumed by Graves (1985). The performance of the approximation appears to deteriorate for larger batch sizes, but the maximum cost deviations are below 9% up to a batch size of seven.

Graves (1996) reported the negative binomial approximation of a random variable referred to as

uncovered demand to be “a very accurate approximation.” However, he provided only an illustration of the accuracy of the approximation, while citing that the effectiveness of such an approximation had been shown by Graves (1985) and Lee and Moinzadeh (1987) for the systems they considered.

In all three multi-echelon inventory studies cited above that have proposed a negative binomial approximation, *computational* evidence has been offered in support of the proposed approximation. A first *analytical* evaluation of the negative binomial approximation was reported by Solis, Schmidt, and Conerly (2007), applying to the latest of the three models (Graves, 1996). In the current study, we apply the modeling and simulation approach to evaluate Graves’ NBD approximation. In effect, Modeling and Simulation have proved to be one of the most powerful approaches when dealing with complex stochastic systems (Bruzzone, 2002; Bruzzone, 2004); in particular, the authors have a long experience in using Modeling and Simulation based approaches for inventory management problems (see for instance, De Sensi et al., 2008; Longo and Mirabelli, 2008; Curcio and Longo, 2009).

This paper is organized as follows. In section 2, we present a summary of Graves’ (1996) model. We discuss our modeling and simulation approach, as well as our preliminary simulation results, in section 3. In the final section, we present our conclusion and expected directions for further study.

2. GRAVES’ MODEL

In this section, we present a slightly modified version of a summary, as earlier prepared by Solis and Schmidt (2009), of the major assumptions and results in Graves’ (1996) model.

The model involves an arborescent system with M inventory sites each having a single internal supplier, with the exception of site 1, a central warehouse (CW) whose inventory is replenished by an external supplier. Customer demand occurs only at retail sites, at the lowest echelon. All other sites are storage and/or consolidation facilities, called transshipment sites. The unique path linking a retail site to the CW is the *supply chain* for the retail site.

The analysis involves a single item of inventory. The demand at each retail site j is an independent Poisson process with demand rate λ_j . $D_j(s,t)$ represents the demand over the time interval $(s,t]$ for site j . The item under study is included in a multi-item distribution system, with each shipment being a consolidation of orders for various items. Site j places its m^{th} replenishment order on its supplier at preset times $p_j(m)$ with fixed intervals. Fixed positive leadtimes τ_j are assumed for shipments to site j from its supplier; the m^{th} order is thus received at time $r_j(m) = p_j(m) + \tau_j$. When inventory is in short supply, the supplier will ship less than the quantity ordered and make up for the shortfall on later shipments. Customer demand is fully backordered. The external supplier is fully reliable and

fills every order by the CW with a fixed leadtime τ_1 . Each site j follows a base stock policy. Initial inventory (at time 0) at site j is the base stock level B_j for site j . $T_j(m)$ represents the *coverage* provided by the supplier to site j on its m^{th} order, with $D_j[T_j(m-1), T_j(m)]$ units shipped by the supplier.

Graves’ model assumes *virtual allocation*. Whenever a unit demand occurs at the retail site, each site on the supply chain increases its next order quantity by one. At the same time, each site on the supply chain commits one unit of its inventory, if available, for shipment to the downstream site on the latter’s next order occasion. Virtual allocation, while possible under current information technology, is not the common practice but is assumed for mathematical tractability. It is found by Graves to be near-optimal in many cases.

A random variable requiring attention is $A_j(t)$, which denotes the *available inventory at site j* at time t —on-hand inventory not yet committed for shipment to another site. $A_j(t) < 0$ indicates backorders. Graves establishes that, if $r_j(m) \leq t < r_j(m+1)$, then

$$A_j(t) = B_j - D_j[T_j(m), t]. \quad (2)$$

Let site i be the internal supplier to site j . If $T_j(m) < p_j(m)$, then $T_j(m)$ equals the time when site i would run out of available inventory to allocate to site j . Consider the *relevant* shipment to the supplier i such that, at $p_j(m)$, site i has received its n^{th} shipment but not yet its $(n+1)^{\text{th}}$ shipment. Suppose that, based upon its receipt of this n^{th} shipment, site i is able to cover the demand processes of its successor sites up through time $S_i(n)$. We call $S_i(n)$ the *depletion* or *runout time* for this n^{th} shipment to site i . It follows that

$$T_j(m) = \min\{p_j(m), S_i(n)\}. \quad (3)$$

Then $S_i(n) - T_i(n)$ is the *buffer time* provided by B_i , and

$$S_i(n) - T_i(n) \sim \text{gamma}(\lambda_i, B_i). \quad (4)$$

Graves then focuses on a two-echelon system consisting of sites 1 (the CW) and j (N retailers). A *single-cycle* ordering policy is in place: each retailer orders a fixed number of times for every order placed by the CW. If θ_1 and θ_j respectively denote the CW and retail site order cycle lengths, θ_1/θ_j is a positive integer. The ordering policy is also *nested*: every time the CW receives a shipment, all retail sites place an order.

Consider an arbitrary (n^{th}) CW order cycle. Graves simplifies the analysis by setting time zero equal to $p_j(n)$. Graves draws attention to the last, or $(\theta_1/\theta_j)^{\text{th}}$, retail site order within the CW order cycle, placed at time $p_j = \tau_1 + \theta_1 - \theta_j$ and received at time $p_j + \tau_j$. The resulting available inventory will be used to cover demand until the next order, placed at time $p_j + \theta_j$, arrives at the retail site at time $t_r = \tau_1 + \theta_1 + \tau_j$. The instant of time t_r^- just before this replenishment proves crucial to the analysis. In this case, $r_j(m) \leq t_r^- < r_j(m+1)$ holds.

Treating this $(\theta_1/\theta_j)^{\text{th}}$ order as the m^{th} order for the retail site j within the n^{th} CW order cycle, the indices m and n are henceforth dropped for notational convenience. Rewriting (3), $T_j = \min\{p_j, S_1\}$ is the coverage provided by the $(\theta_1/\theta_j)^{\text{th}}$ shipment to retail site j . From (4), $S_1 \sim \text{gamma}(\lambda_1, B_1)$.

Graves defines a random variable $D_j[T_j, t]$, which he calls *uncovered demand* (up to some specified point in time t): demand at retail site j not covered by the $(\theta_1/\theta_j)^{\text{th}}$ shipment from the CW. He derives the following mean and variance:

$$E\{D_j[T_j, t]\} = \lambda_j (t - E[T_j]) \quad (5)$$

$$\text{Var}\{D_j[T_j, t]\} = \lambda_j (t - E[T_j]) + \lambda_j^2 \text{Var}[T_j]. \quad (6)$$

He reports computationally finding the NBD having the same first two moments to be a fairly accurate approximation to the distribution of $D_j(T_j, t)$. Graves presents very limited evidence in support of his assertion, however. Based on (5) and (6), the parameters of the NBD approximation are determined as follows:

$$r = (t - E[T_j])^2 / \text{Var}[T_j] \quad (7)$$

$$p = (t - E[T_j]) / \{(t - E[T_j]) + \lambda_j \text{Var}[T_j]\}. \quad (8)$$

Graves proposes a procedure for each of the two most commonly specified service level criteria (Silver, Pyke, and Peterson 1998) that would search for a base stock policy $\langle B_1, B_j \rangle$ that minimizes expected on-hand inventory in the system. The first service criterion is an average *probability of no stockout* α . The other service measure is an average fraction of demand to be satisfied from stock on hand, or *fill rate* β .

2.1. Probability of No Stockout as Service Criterion

The probability of the retail site stocking out is greatest for the $(\theta_1/\theta_j)^{\text{th}}$ retail order within the CW order cycle. To set base stock levels to achieve a given probability α of the retail site *not* stocking out within the CW order cycle,

$$\Pr\{A_j(t_r^-) \geq 0\} \geq \alpha, \quad (9)$$

needs to be assured. The distribution of uncovered demand $D_j(T_j, t_r)$, where $t_r = \tau_1 + \theta_1 + \tau_j$ as discussed above, comes into play and leads to a computational procedure that searches over possible settings of the CW base stock level B_1 . For each B_1 , the minimum retail site base stock level B_j that would yield (9) is to be determined. The antecedent $r_j(m) \leq t_r^- < r_j(m+1)$ of (1) being satisfied, it follows that requirement (9) translates into

$$\Pr\{D_j(T_j, t_r) \leq B_j\} \geq \alpha. \quad (10)$$

We apply the negative binomial approximation $\sum_{x=0}^{B_j} \binom{r+x-1}{x} p^r (1-p)^x$ for the left hand side of (10) – starting with $B_j = 1$, and incrementing B_j by 1 until (10) is first satisfied. The base stock level B_1 which yields the lowest average system inventory is selected. (In the case of ties, the smallest value of B_1 is preferred, there being no difference assumed between holding costs at the CW and the retail sites.)

Graves provides an approximation to expected system on-hand inventory:

$$\text{Avg. inventory} = B_1 + \sum_1^N B_j - 0.5\lambda_1\theta_1 - \lambda_1\tau_1. \quad (11)$$

Strictly speaking, (11) should be corrected for counting retail backorders at negative inventory. For reasonable service levels, however, the expected backorder component is very small and is ignored.

2.2. Fill Rate as Service Criterion

For “realistic” fill rates (> 0.95), expected backorders over a CW order cycle may be approximated by expected backorders pertaining to the $(\theta_1/\theta_j)^{\text{th}}$ retail order, since effectively all backorders occur at this last retail order. $E[\{A_j(t_r)\}^-]$, where $y^- = \max\{0, -y\}$, represents expected backorders at time t_r (just before the next order arrives). A computational procedure similar to that in sub-section 2.1 arises. For each B_1 , a minimum retail site base stock level B_j is sought that would yield

$$E[\{A_j(t_r)\}^-] = \left\{ \sum_{x=0}^{B_j} [(B_j - x)f(x)] \right\} - \{B_j - \lambda_j(t_r - E[T_j])\} \leq (1 - \beta) \lambda_j \theta_1, \quad (12)$$

where $\lambda_j \theta_1$ represents mean demand at the retail site over the CW order cycle. The base stock level B_1 which yields the lowest average system inventory is chosen.

2.3. Graves’ Computational Study

In his computational study, Graves used test scenarios all based on a single system demand rate $\lambda_1 = 36$. Identical retail sites are assumed, with the number N of retail sites being 2, 3, 6, or 18. Hence, the retail site demand rates λ_j are 18, 12, 6, or 2, respectively. The length of the retail site order cycle is fixed at $\theta_j = 1$ time unit. Four different parameter combinations $\langle \theta_1, \tau_1, \tau_j \rangle$ are tested. This resulted in 16 test scenarios, summarized in Table 1.

Table 1: Summary of Graves’ Test Scenarios

Scenario	θ_1	τ_1	τ_j	N	λ_j
1	2	1	1	18	2
2				6	6
3				3	12
4				2	18
5	2	1	5	18	2
6				6	6
7				3	12
8				2	18
9	5	4	1	18	2
10				6	6
11				3	12
12				2	18
13	5	4	5	18	2
14				6	6
15				3	12
16				2	18

For the probability of no stockout criterion, four levels of α were used: 0.80, 0.90, 0.95, and 0.975. Similarly, four fill rate levels β were tested: 0.95, 0.98, 0.99, and 0.999. Thus, for each service criterion, 64 test cases were considered by Graves.

3. MODELING AND SIMULATION

3.1. Simulation Models

Solis, Schmidt, and Conerly (2007) reported the very first *analytical* evaluation of the effectiveness of the negative binomial approximation used in Graves' (1996) model. Prior to their analytical evaluation, only *computational* evidence had been offered in all three multi-echelon inventory studies earlier cited (Graves 1985; Lee and Moinezadeh 1987; Graves 1996) in support of the proposed NBD approximation to a crucial random variable.

In the current study, we apply the modeling and simulation (M&S) approach to evaluate the NBD approximation as proposed by Graves (1996). We create simulation models using the AnyLogic platform for the sixteen scenarios as summarized in Table 1. For each simulation model, we test the "optimal" base stock policy $\langle B_1, B_j \rangle$ as determined by Graves' search procedure (based upon the NBD approximation of uncovered demand). Each simulation run is over 100 CW order cycles – i.e., 200 retail site order cycles for scenarios 1-8 or 500 retail site order cycles for scenarios 9-16. Our simulation experiments involve 100 replications each; hence, 20,000 or 50,000 retail site order cycles for scenarios 1-8 or 9-16, respectively. Depending upon whether the simulated service level is below or above the target service level, we increase or decrease B_1 or B_j one unit at a time until the simulated α or β is at or just over the target level. The "optimal" base stock policy from Graves' search procedure is then compared against the optimal policy obtained using M&S. To attain comparability of simulated service levels under different pairs of B_1 and B_j values being assessed, we apply fixed random number seeds in

generating the Poisson demand streams at the retail sites.

3.2. Simulation Results for the Probability of No Stockout Criterion

In Table 2, we compare Graves' "optimal" base stock policies $\langle B_1, B_j \rangle$ under the probability of no stockout criterion for scenarios 4, 8, 12, and 16 (where $N = 2$ retail sites) against the optimal policies using the M&S approach. In our simulation experiments, we find that Graves' "optimal" policies meet the target (minimum) α in only seven of the 16 test cases, and are thus equal to the M&S optimal policies. For the remaining nine test cases, the simulated α from Graves' optimal policy is below the target α . However, the echelon base stocks arising from the M&S optimal policy is not more than two units over that resulting from Graves' "optimal" policy.

Table 2: Comparison of Simulation Results under the Probability of No Stockout Criterion when $N = 2$

$\alpha = 0.80$										
Scenario	"Optimal" Policy Using Graves' Search Procedure				Simulated α	Optimal Policy Using Simulation				Simulated α
	B_1	B_j	Ech Base St			B_1	B_j	Ech Base St		
4	44	56	84	0.7996	45	56	85	0.8164		
8	7	150	235	0.8045	7	150	235	0.8045		
12	245	66	143	0.7959	246	66	144	0.8085		
16	248	139	292	0.7991	249	139	293	0.8092		
$\alpha = 0.90$										
Scenario	"Optimal" Policy Using Graves' Search Procedure				Simulated α	Optimal Policy Using Simulation				Simulated α
	B_1	B_j	Ech Base St			B_1	B_j	Ech Base St		
4	53	55	91	0.9000	53	55	91	0.9000		
8	37	140	245	0.9019	37	140	245	0.9019		
12	272	57	152	0.8942	273	57	153	0.9015		
16	268	135	304	0.8962	269	135	305	0.9017		
$\alpha = 0.95$										
Scenario	"Optimal" Policy Using Graves' Search Procedure				Simulated α	Optimal Policy Using Simulation				Simulated α
	B_1	B_j	Ech Base St			B_1	B_j	Ech Base St		
4	55	57	97	0.9520	55	57	97	0.9520		
8	61	132	253	0.9499	62	132	254	0.9540		
12	283	55	159	0.9411	283	56	161	0.9524		
16	272	138	314	0.9496	273	138	315	0.9529		
$\alpha = 0.975$										
Scenario	"Optimal" Policy Using Graves' Search Procedure				Simulated α	Optimal Policy Using Simulation				Simulated α
	B_1	B_j	Ech Base St			B_1	B_j	Ech Base St		
4	60	57	102	0.9762	60	57	102	0.9762		
8	53	140	261	0.9759	53	140	261	0.9759		
12	287	56	165	0.9681	290	56	168	0.9757		
16	271	143	323	0.9755	271	143	323	0.9755		

For scenario 3 (with $N = 3$ retail sites), Graves' "optimal" policies meet the target α in all four test cases. However, we have found that Graves' optimal policies meet the target α in only about one-fourth of all the 64 test cases. Moreover, we have observed that the deviations between simulated and target service levels tend to become larger as N increases – and are thus largest for scenarios 1, 5, 9, and 13 (with $N = 18$ retail sites) than in corresponding scenarios with fewer retail sites. These deviations also tend to be larger with a longer CW order cycle (i.e., when $\theta_1 = 5$, as compared to $\theta_1 = 2$). Furthermore, these deviations become more pronounced with lower target α levels, particularly when $\alpha = 0.90$ and 0.80 .

3.3. Simulation Results for the Fill Rate Criterion

We show in Table 3 the comparisons between Graves' "optimal" and the M&S optimal base stock policies under the fill rate criterion for scenarios 4, 8, 12, and 16

(with $N = 2$ retail sites). In our simulation experiments, the policies determined using Graves' search procedure meet the target β in only five of the 16 test cases. The simulated β from Graves' "optimal" policy is below the target β in the remaining 11 test cases. In one of these test cases, the echelon base stocks arising from the M&S optimal policy is four units more than that from Graves' "optimal" policy, but not more than two units in the remaining cases.

None of Graves' "optimal" policies meets the target β in any of the four test cases under scenario 3 (where $N = 3$). The echelon base stocks for the M&S optimal policies in these four test cases, however, are only either one or two units more than for Graves' "optimal" policies.

We have found that Graves' optimal policies meet the target β in only five of the 64 test cases. As in the probability of no stockout service criterion, we have observed that the deviations between simulated and target β levels tend to become larger as N increases – and are thus largest for scenarios 1, 5, 9, and 13 (where $N = 18$) relative to corresponding scenarios with smaller N . These deviations also tend to be larger with a longer CW order cycle. Moreover, these deviations are less pronounced with higher target β levels, and are more pronounced as target β levels become lower.

Table 3: Comparison of Simulation Results under the Fill Rate Criterion when $N = 2$

$\beta = 0.95$										
Scenario	"Optimal" Policy Using Graves' Search Procedure				Simulated β	Optimal Policy Using Simulation				Simulated β
	B_1	B_2	Ech Base St	β		B_1	B_2	Ech Base St	β	
4	56	47	150	0.9477	57	47	151	0.9523		
8	53	125	303	0.9460	52	126	304	0.9504		
12	259	50	359	0.9486	260	50	360	0.9513		
16	207	151	509	0.9506	207	151	509	0.9506		

$\beta = 0.98$										
Scenario	"Optimal" Policy Using Graves' Search Procedure				Simulated β	Optimal Policy Using Simulation				Simulated β
	B_1	B_2	Ech Base St	β		B_1	B_2	Ech Base St	β	
4	55	52	159	0.9804	55	52	159	0.9804		
8	51	132	315	0.9798	52	132	316	0.9813		
12	267	53	373	0.9795	268	53	374	0.9810		
16	259	133	525	0.9791	260	133	526	0.9803		

$\beta = 0.99$										
Scenario	"Optimal" Policy Using Graves' Search Procedure				Simulated β	Optimal Policy Using Simulation				Simulated β
	B_1	B_2	Ech Base St	β		B_1	B_2	Ech Base St	β	
4	64	50	164	0.9892	65	50	165	0.9906		
8	47	138	323	0.9904	47	138	323	0.9904		
12	275	53	381	0.9891	276	53	382	0.9900		
16	269	133	535	0.9888	269	134	537	0.9905		

$\beta = 0.999$										
Scenario	"Optimal" Policy Using Graves' Search Procedure				Simulated β	Optimal Policy Using Simulation				Simulated β
	B_1	B_2	Ech Base St	β		B_1	B_2	Ech Base St	β	
4	65	57	179	0.9991	65	57	179	0.9991		
8	58	143	344	0.9991	58	143	344	0.9991		
12	288	56	400	0.9984	288	58	404	0.9990		
16	279	141	561	0.9988	280	141	562	0.9990		

4. CONCLUSION AND FURTHER WORK

Departing from the traditional computational and analytic approaches to looking into the effectiveness of distributions used to approximate exact distributions of random variables arising in multi-echelon inventory models, we have applied the M&S approach in the evaluation of a negative binomial approximation as proposed by Graves (1996) in a one-warehouse, N-retailer inventory system.

Computational evidence offered by Graves (1996) suggests the NBD approximation to be fairly accurate,

and an analytical investigation (Solis, Schmidt, and Conerly 2007) has suggested why the approximation is effective in certain instances.

In our simulation studies to date, we have found Graves' search procedures, based on his NBD approximation, to be less effective when the number of retail sites is larger, the CW order cycle is longer, or when the target service level is lower. At the time of the conference, we will provide a more thorough report of our findings.

Solis and Schmidt (2007, 2009) have introduced stochastic leadtimes τ_j between the CW and the retail sites and investigated how optimal base stock policies differ between deterministic and stochastic leadtime cases when the CW does not or does carry stock. In the former situation where the CW does not carry stock (as in a distribution center with cross-docking), an analytical investigation was reported (Solis and Schmidt 2007). In the latter situation where the CW actually carries stock, with the model becoming mathematically intractable, Solis and Schmidt (2009) applied an M&S-based heuristic taking off from Graves' search procedures. We will soon apply the M&S approach to the stochastic leadtime τ_j case, whether the CW carries stock or not.

Further, we will also use the M&S approach to investigate the implications of stochastic leadtimes τ_1 between the external supplier and the CW. In practice, τ_1 is probably more prone to randomness than the internal leadtimes between the CW and retail sites, over which retail firms would expectedly be able to exercise greater control. In investigating stochastic leadtimes τ_1 , we would be interested in finding out whether the model is more sensitive to randomness in τ_1 or to randomness in τ_j .

REFERENCES

- Bruzzzone A.G., (2002). Introduction to the Special Issue on Simulation in Supply Chain Management. *Simulation*, vol. 78, p. 284-286, ISSN: 0037-5497.
- Bruzzzone A.G. (2004). Preface to modeling and simulation methodologies for logistics and manufacturing optimization. *Simulation*, vol. 80, p. 119-120, ISSN: 0037-5497
- Clark, A.J. and Scarf H., 1960. Optimal policies for a multi-echelon inventory problem. *Management Science*, 6 (4), 475-490.
- Curcio D., Longo F., (2009). Inventory and Internal Logistics Management as Critical Factors Affecting the Supply Chain Performances. *International Journal of Simulation & Process Modelling*, vol. 5(4), p. 278-288, ISSN: 1740-2123
- De Sensi G, Longo F, Mirabelli G (2008). Inventory policies analysis under demand patterns and lead times constraints in a real supply chain. *International Journal of Production Research*, vol. 46, p. 6997-7016, ISSN: 0020-7543, doi: 10.1080/00207540701528776
- Graves, S.C., 1985. A multi-echelon inventory model for a repairable item with one-for-one

- replenishment, *Management Science*, 31 (10), 1247-1256.
- Graves, S.C., 1996. A multiechelon inventory model with fixed replenishment intervals. *Management Science*, 42 (1), 1-18.
- Lee, H.L. and Moinzadeh, K., 1987. Two-parameter approximations for multi-echelon repairable inventory models with batch ordering policy. *IIE Transactions*, 19, 140-149.
- Longo F., Mirabelli G., (2008). An advanced supply chain management tool based on modeling and simulation. *Computers & Industrial Engineering*, vol. 54, p. 570-588, ISSN: 0360-8352, doi: 10.1016/j.cie.2007.09.008.
- Mood, A.M., Graybill, F.A., and Boes, D.C., 1974. *Introduction to the Theory of Statistics*, 3rd ed. New York, USA: Mc-Graw-Hill.
- Sherbrooke, C.C., 1968. METRIC: A multi-echelon technique for recoverable item control. *Operations Research*, 16 (1), 122-141.
- Silver, E.A., Pyke, D.F., and Peterson, R., 1998. *Inventory Management and Production Planning and Scheduling*. New York, USA: John Wiley & Sons.
- Solis, A.O. and Schmidt, C.P., 2007. Stochastic leadtimes in a one-warehouse, N-retailer inventory system with the warehouse not carrying stock. *European Journal of Operational Research*, 181 (2), 1004-1013.
- Solis, A.O. and Schmidt, C.P., 2009. Stochastic leadtimes in a one-warehouse, N-retailer inventory system with the warehouse actually carrying stock. *International Journal of Simulation and Process Modelling*, 5 (4), 337-347.
- Solis, A.O., Schmidt, C.P., and Conerly, M.D., 2007. On the effectiveness of the negative binomial approximation in a multi-echelon inventory model: a mathematical analysis. *Proceedings of the International Conference of Numerical Analysis and Applied Mathematics*, American Institute of Physics Conference Proceedings 936, pp. 531-534, September 16-20, Corfu (Greece).

AUTHORS BIOGRAPHY

Adriano O. Solis is an Associate Professor of Logistics Management and Management Science at York University, Canada. After receiving BS, MS and MBA degrees from the University of the Philippines, he joined the Philippine operations of Philips Electronics where he became a Vice-President and Division Manager. He went on to obtain a PhD degree in Management Science from the University of Alabama. He was previously Associate Professor of Operations and Supply Chain Management at the University of Texas at El Paso. He has been a Visiting Professor in the Department of Mechanical, Energy, and Management Engineering, at the University of Calabria, Italy. He has published in *European Journal of Operational Research*, *International Journal of Simulation and Process Modelling*, *Information Systems*

Management, *International Journal of Production Economics*, *Journal of Forecasting*, *Computers & Operations Research*, and *Journal of the Operational Research Society*, among others.

Francesco Longo obtained his degree in Mechanical Engineering, *summa cum laude*, in 2002 and his Ph.D. in Mechanical Engineering in 2005 from the University of Calabria, Italy. He is currently an Assistant Professor in the Department of Mechanical, Energy, and Management Engineering at the University of Calabria, where he also serves as Director of the Modeling & Simulation Center – Laboratory of Enterprise Solutions (MSC-LES). He is an Associate Editor of *Simulation: Transactions of the Society for Modeling and Simulation International*. He has also been Guest Editor of two issues of *International Journal of Simulation and Process Modelling*. He has been active in the organization and management of a number of international conferences in modeling and simulation, serving as General Chair, Program Chair, Track Chair, and/or member of the International Program Committee. He has published in *International Journal of Production Economics*, *Computers & Industrial Engineering*, *International Journal of Production Research*, *International Journal of Computer Science Issues*, *Simulation*, *Journal of Simulation*, *International Journal of Simulation and Process Modelling*, and other publications.

Pietro Caruso and **Elisa Fazzari** are students in the *Laurea Magistrale* (master's degree) program in Management Engineering at the Department of Mechanical, Energy, and Management Engineering of the University of Calabria, Italy. They obtained their first degrees in Management Engineering at the same university in 2010.

FPGA, PHYSICS-BASED MODELING OF IGBT AND PIN DIODE FOR HARDWARE CO-SIMULATION OF COMPLEX POWER ELECTRONIC CONVERTERS AND SYSTEMS

P. Aristidou^(a), P.R. Palmer^(b)

^(a)Department of Engineering University of Cambridge, Cambridge, UK

^(b)Department of Engineering University of Cambridge, Cambridge, UK

^(a)pa297@cam.ac.uk, ^(b)prp@eng.cam.ac.uk

ABSTRACT

This paper presents the steps and the challenges for implementing analytical, physics-based models for the insulated gate bipolar transistor (IGBT) and the PIN diode in hardware and more specifically in field programmable gate arrays (FPGAs). The models can be utilised in hardware co-simulation of complex power electronic converters and entire power systems in order to reduce the simulation time without compromising the accuracy of results. Such a co-simulation allows reliable prediction of the system's performance as well as accurate investigation of the power devices' behaviour during operation. Ultimately, this will allow application-specific optimisation of the devices' structure, circuit topologies as well as enhancement of the control and/or protection schemes.

Keywords: FPGA, hardware co-simulation, IGBT, power device analytical electro-thermal modeling

1. INTRODUCTION

In the field of power electronics, circuit and system computer simulation has become a vital tool for developing successful designs, first prototypes and final products with minimal experimental work. Ideally such a simulation needs to be sufficiently accurate in order to permit a reliable examination of the detailed circuit/system operation and fast enough in order to allow quick identification of the required performance trade-offs, and thereby be utilised for design optimisation. Satisfying both of the above requirements for any level of design complexity, however, is still a major challenge that today with the increased application of power electronic converters in large scale power systems, exercises the power electronics industry more than ever before.

There are many reasons accounting for this great challenge. First of all the characteristic times within a power electronic system may be different by many orders of magnitude, ranging from nanoseconds and microseconds for the switching transitions of the power semiconductor devices and the typical switching cycles, through several seconds for the load or fault transient responses to several minutes/hours/days for complete load/thermal cycles (Pejovic and Maksimovic 1994).

Thus simulating the full time-domain response of a power electronic circuit/system with high resolution may require trillions of time steps to be calculated. In addition to this, the simulation should be able to faithfully capture the switching behaviour of the power devices via the use of accurate/detailed models and robust enough for handling their inherent nonlinearities. At present, implementing such a long-time, detailed simulation is infeasible or -in the best case- extremely time consuming and therefore impractical.

Generally the required time for each time step computation scales with the detail of the power devices representation as well as the circuit/system complexity; hence depending on the objective of the simulation, different devices' models, software packages and circuits are being used in order to make it practical. On the one extreme we have the numerical models constructed in 2D or 3D finite differences or finite element packages, such as Silvaco Atlas and Sentaurus Device. These models can provide a precise picture of the devices' physical phenomena and can be utilised in mixed-mode circuit simulations to give accurate results regarding the devices' switching operation, namely power losses, transition durations and voltage/current overshoots. This kind of simulation however, is extremely computationally expensive typically requiring several minutes or even hours to simulate just few switching cycles (~100-200 μ s) of simple test circuits comprised only of one or two power devices. As such this approach is of limited applicability for circuit/system designers and is mostly restricted to device manufacturers whose objective is mainly the enhancement of general device characteristics. However, even for this latter application there is difficulty in drawing useful conclusions about the effects that several structural parameters have on the device's performance since the link of the parameters with the simulation output is purely numerical. On the other extreme we have the behavioural and average device or converter models (e.g. Oh and Nokali 2001, Jin 1997) that simulate a device or converter behaviour based on databases, curves, expressions or components fitted to experimental or datasheet output device or converter characteristics. These models can be constructed in any circuit or equation solver package

and their use can significantly speed up the simulation, allowing thereby investigation of complex circuits/systems or long load/thermal cycles. However the results lack any sort of accuracy and are thus of limited creditability. Even when a behavioural model claims giving precise results for the certain circuit topology used for its experimental extraction, its validity in different or more complex topologies is extremely limited due to the change of the values of several stray components (e.g. capacitances and inductances). Furthermore, since these models do not consider any device physics or internal parameters, they cannot be used for device optimisation.

Clearly the quest for general-application accurate and computationally efficient power semiconductor device models has a solution lying somewhere in the middle. More specifically the models should be physics based (as opposed to behavioural models) and analytical (as opposed to numerical models). However, especially for the case of high voltage power bipolar devices, such as the PIN diode and the IGBT, there has been a great difficulty in constructing truthful analytical models. This is mainly due to the distributed nature of the charge transport which combined with the large base thickness (required to achieve high voltage capability) amplifies the effects of charge dynamics and thereby makes any simple charge control approaches failing (Leturcq 1997). On the other hand, however, solving analytically the full set of semiconductor charge transport equations is impossible. In order to evade the issue the full equations' set is simplified into one equation: the ambipolar diffusion equation (ADE); which is solvable and still retains the essentials of the distributed nature of charge transport. The only way to solve this equation without assuming an initial solution shape or making oversimplifications is a Fourier-based one, proposed by Leturcq (Leturcq 1997). With this approach it became possible to develop and validate accurate and fairly robust electrothermal, circuit simulator (e.g. PSpice) and Simulink p-i-n diode and IGBT models [Palmer et al. 2003, Bryant et al. 2007a], together with easy parameter extraction procedures [Bryant et al. 2007b]. The use of these compact models enables reasonably fast simulation times: for the inductive chopper circuit case, it typically takes 5-10s for every switching cycle (~50µs). This is a great improvement against numerical models (~400 times faster); however for simulations of more than few tens of milliseconds or of more complex circuit topologies, the computational time is still prohibitive.

Nowadays, FPGAs have millions of hardware resources and are capable of performing thousands of operations in parallel, allowing complicated functions to be executed within a single-clock cycle. As such FPGAs can be deployed in computationally intensive simulations or other processes in order to carry out the most intense tasks and thereby increase the overall speed of execution.

This paper presents a new step towards the ultimate solution of the power bipolar device modelling

and simulation challenge, which comes in the form of the FPGA implementation of the abovementioned Fourier-based, analytical models. The second section of the paper provides an overview of the main features of the available FPGA technologies and identifies the benefits, the constraints and the challenges of using FPGAs in our application. The third section provides an explanation of the chosen PIN diode and IGBT physics-based models along with a detailed solution of the electrothermal ADE. In the fourth section the strategy for implementing the device modeling in parallel FPGA programming is presented while conclusions and plans of future work are being given at the end.

2. FEATURES, BENEFITS, LIMITS AND CHALLENGES OF FPGAs

2.1. FPGA Basics

The basic layout of an FPGA chip is shown in fig.1.

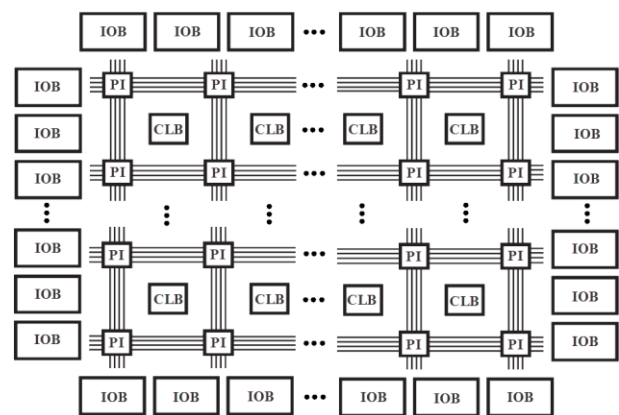


Figure 1- Basic layout of an FPGA

Simplistically this layout can be seen as consisting of three main components. First and most important one is a large two-dimensional array of configurable logic blocks, CLBs, each of which can be programmed to perform a combinatorial and/or sequential operation. The other basic component is a number of input/output blocks (IOBs) at the chip periphery whose purpose is to handle the interfacing between the internal chip resources and the external circuitry, including the signals to and from the CLBs and the signals required for programming the necessary logic configurations. Finally there is a large interconnection network consisting of wires and programmable interconnection matrices (PIs) which are responsible for the connection of the CLBs to the IOBs and/or with each other. (Xilinx Inc. 2012a-b, Altera Corp. 2012a-b)

Besides the above basic features today's FPGAs also include a number of higher level functionality elements such as block RAM blocks, hardwired digital signal processing (DSP) blocks, communication blocks and clock manager systems. These dedicated resources generally speed up the execution of some common functions and save the usage of primitive resources for other application-specific operations.

2.2. Benefits of FPGAs

It is evident from the FPGA architecture that the CLBs (and the embedded DSPs) can be set up to perform arithmetic and logic functions like a microprocessor's arithmetic logic unit (ALU). However, in contrast with microprocessors where the arithmetic logic unit is fixed and configured for general purpose use, the CLBs can be customized to implement only application-specific tasks, resulting in improved computational efficiency and optimum hardware resources use.

Moreover due to the numerous available resources it is possible to construct a vast number of tailored ALUs and use them in parallel in order to enable higher computational throughput and vastly superior performance. FPGAs can even outperform cluster or massively parallel supercomputers with thousands of CPUs (and thus ALUs) since in FPGAs there are no processor cache misses, there is ultralow latency and the execution of operators is efficiently pipelined via point-to-point interconnects (Zack et al. 2004). As a practical proof of the computational accelerations offered by FPGAs is the experience with several complex algorithms. Comparisons of execution times of FPGA hardware co-simulations against offline simulations on single or multiple processors show that the use of the former results to speed-ups ranging from 10x to 1000x, with the mode value lying within 120-200x (Xilinx Inc. 2009, Gonzalez and Nunez 2009). It should therefore be expected that the use of the FPGA technique in our device modeling application will result to improved computational times as well.

Besides giving higher speeds, FPGAs also consume much less power since they can operate at a lower clock frequency than microprocessors (e.g. at 500MHz instead of 3GHz) and still achieve improved performance due to parallelism. This is very advantageous in our case since the FPGA device models are also intended to be utilized as the basis for real time circuit control, and less power consumption means amongst others lower running costs and improved reliability. Furthermore FPGAs can be considered as cost effective, since their average DSP function cost of less than \$2 is much less than that of DSP devices and no more than that of processors (Zack et al. 2004).

2.3. Limitations and Challenges

From the above it is clear that FPGAs can offer significant benefits, however they also exhibit limitations and challenges which must be considered in order to minimize their effect as much as possible.

2.3.1. Representation of Real Numbers

The first limitation is the use of fixed-point arithmetic instead of floating point one since the latter -though possible to implement- results to highly inefficient usage of the hardware resources. More specifically, in order to enable the representation and handling of the standard IEEE-754 floating point structure of the form $(-1)^{(\text{sign})} \times (\text{normalized mantissa}) \times (\text{base})^{(\text{exponent})}$, shown in figure 2 (IEEE 2008), each instruction data input and

output requires the use of special mantissa normalisation / denormalisation circuitry employing many interconnections, multiplexers, shifters and counters, ultimately leading to excessive logic usage and slow clock rates.

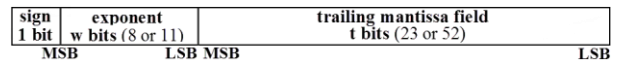


Figure 2 - IEEE-754 floating point number

On the contrary the use of fixed-point arithmetic, where a number is represented as a scaled integer by a fixed number of digits before and after a radix point, is well suited for FPGA implementation since conventional 2's complement can be used with only the location of the radix point required to be specified. However, achieving adequate precision might be challenging. First the quantization noise can be much larger than in single or double precision floating-point arithmetic due to the fact that the represented numbers are now uniformly spaced and possibly implemented with fewer bits. Also fixed point operations can produce results having more bits than the operands resulting to information loss due to rounding, truncation or saturation. Therefore in order to enable high precision with fixed-point arithmetic while at the same time achieving optimal utilization of the hardware resources, the bit width of each variable needs to be optimized for the dynamic range and accuracy of the specific algorithm.

2.3.2. Numerical Integration Considerations

Another challenge in using FPGAs in a simulation of a system like ours is the choice of the most appropriate numerical integration method, classically distinguished by three main properties: (i) fixed time-step size/variable time-step size (ii) explicit/implicit and (iii) single-step/multi-step. The choice should be made after considering accuracy, convergence, stability, and speed issues in conjunction with the co-simulation objective and constraints. Below we present the major considerations. Details about the choices and the overall integration methodology are given later in section 4.

Fixed time-step size methods use a constant step size throughout the simulation, whereas variable ones adjust the step size in every time step depending on the model dynamics, namely reducing the size to increase accuracy when the model's states are changing rapidly and increasing it when they are changing slowly in order to avoid taking unnecessary steps (Greenberg 1998). In variable step size methods the solution's truncation error is estimated in every step computation and is used in order to evaluate the largest allowable step size that will keep the error bounded below some specified limits. This means that in a variable step size technique an additional computational overhead is present in every time step, but this is more than compensated by the reduction in number of steps. For this reason variable step size are the methods of choice, however only for offline co-simulations. For real-time co-simulations, the integration method should use fixed-

step size in order to assure synchronisation of the data exchange between the co-simulation nodes and meet the real-time related constraints (i.e the computations to be completed within an interval less than or equal to the simulation clock period). The use of fixed time-step size, however, in an event-based system like ours where discrete events (such as control switching pulses) take place in an otherwise continuous model, introduces inaccuracies whenever these events occur at non-integer multiples of the fixed time step and as the simulation proceeds the accumulated error might become large enough to cause non-characteristic harmonics, switching mistakes and other abnormal behaviour (Strunz 2004). Using a sufficiently small time step size solves the abovementioned problem, but this also requires the computational time of the single step to be less than the step interval. Here the difference of our co-simulation fidelity objective to that of real-time power system platforms should be highlighted. The latter concern only with the simulation of the behaviour and response of the overall power system (e.g. detection of voltage sags or fault propagation) thus their models of the power electronic converters are behavioural with no concern of what is happening at the device level. On the contrary our purpose is to increase the simulation fidelity to the level of the exact device operation. This means that the use of small time step sizes (<100ns) is not only for improved accuracy but a requirement in order to capture the switching waveforms.

Regarding the choice between explicit and implicit methods the decision is taken primarily by stability and stiffness considerations. Explicit methods evaluate a state at the next time step as an explicit function of the state values only up to the current time step, whereas implicit ones evaluate the next time-step state as an implicit function of the state values up to the value of the next time step as well (Greenberg 1998). Therefore for dynamic systems, implicit methods require the solution of a system of equations, meaning a higher computational cost in every time step. On the other hand implicit methods offer much greater stability, producing bounded numerical solutions with much larger time steps than those required by explicit methods for maintaining numerical stability. As our system is also stiff –i.e. with time constants ranging various orders of magnitude- and the use of small time steps is nonetheless mandatory, using explicit methods would require extremely small time step sizes (~ps) resulting to the evaluation of an extremely large number of steps. Off course for real time co-simulations this would also call for equivalently small computational times. Even assuming the best case scenario of a single step calculation requiring just a single FPGA clock cycle, the minimum time step size would be limited by the FPGA clock frequency (typically up to 500MHz) to about 2ns. But even for off-line co-simulations the smaller computational cost per step offered by explicit methods will almost certainly be well overcompensated by the huge increase in number of steps, resulting thereby to prohibitive overall simulation times. It

should also be noted here that with the FPGAs calculation parallelism the difference in the computational cost per step between implicit and explicit methods is greatly nullified. Furthermore it should be taken into account that a round-off error is introduced in every time step because of the finite word length employed in the calculations. For example for 32bit/64bit floating point words (fig. 2) or equivalently fixed-point words with 23/52 bits in the fractional part, the accuracy is restricted at best to approximately 7/13 decimal places. Therefore if the step size is extremely small, the small differences in the calculated numbers will most likely be rounded and since the number of steps is large, the accumulated round-off errors will have a significant impact on accuracy (and even on numerical stability).

Multi-step and single-step methods can both be used in our case provided they are stable with sufficiently high order (i.e. rate of decrease of the accumulated truncation error (global error) with the time step size). Single-step methods evaluate the value of a state at the next time step using the solution of the present time point and estimated values at points between the present and next time step (minor points). Multi-step methods, on the other hand, approximate the state derivatives by polynomials and thereby use many past state solutions for the next-time-step state-value calculation. Provided that the state trajectories are smooth the greater the number of points employed (either minor or past) the higher the achievable integration order. Therefore since single-step methods require evaluation of the state derivative functions at many minor points their computational cost per time step is generally higher than that of multi-step ones which use only past values that are already available. And since these minor point single-step calculations are primarily sequential, the use of FPGAs cannot nullify this burden. It should be mentioned, however, that multi-step methods are not well suited when the states exhibit discontinuities, since fitted polynomials based on past values are not valid in the neighbourhood of a discontinuity and their use in such case will lead to inaccuracies.

Lastly it should be highlighted that there is a fundamental trade-off between stability and accuracy properties with only second order methods being unconditionally stable - i.e producing bounded solution for any time step size (Hoffman 2001). Generally stability is a requirement in order to damp numerical oscillations and keep the solution bounded. However the initial amplitude of these oscillations depends on the order of the numerical integration method. In any case it would be undesirable to produce an under-damped but still oscillatory response because of large numerical errors. Also the existence of oscillations means that a small time step size is required to capture them making the method highly inefficient and computationally expensive. Therefore it is usually beneficial to trade some stability for higher order and there are some techniques which attempt to find the best compromise.

3. PHYSICS-BASED, ANALYTICAL PIN DIODE AND IGBT MODELS

This section first gives an overview of the basic geometric structure of the considered power electronic devices and then provides a detailed analytical solution and modelling of the relevant equations.

3.1. Basic Device Structure

The basic non-punch-through (NPT) structure of the considered devices is shown in figures 4(a) and 4(b) for the PIN diode and the IGBT respectively.

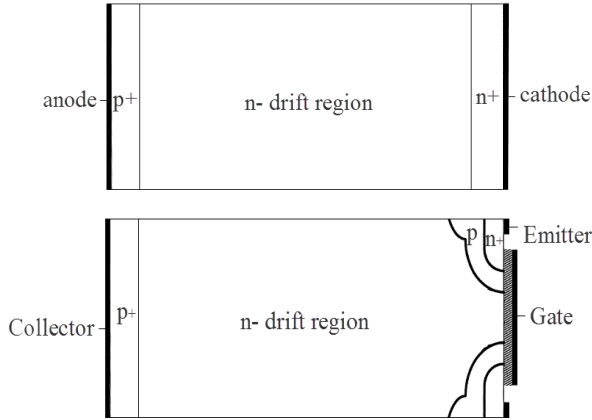


Figure 4 - Structure of NPT (a) PIN diode, (b) IGBT

The NPT PIN diode consists of a wide N- doped or intrinsic (nb denoted by I) drift region (nb also called base region) sandwiched between a thin P doped anode and a thin N⁺ doped cathode. The resulting P⁺N⁻ and N⁺N⁻ (or N⁺I) junctions are referred to as junctions J₁ and J₂ respectively. Similarly to diode at the one end, the NPT IGBT is featuring a P⁺ anode (collector) and a wide N⁻ drift region forming a P⁺N⁻ junction (junction J₁). However the IGBT is a gate controlled device with a MOSFET-like structure at the other end –i.e. P well, N⁺ emitter/source and MOS gate. The P well/N⁻ drift region and the N⁺ source/P well junctions are referred to as junctions J₂ and J₃ respectively.

3.2. Bipolar Device 1D Modeling

Generally circuit simulation works by solving a system of linear or linearized differential equations describing the circuit states (voltages/currents of each component). Main purpose of device modeling is to dynamically relate the voltage across the device with the current flowing through it so that the necessary values can be calculated at each time step.

For both the PIN Diode and the IGBT the device voltage can be considered as the voltage across the base; which in turn can be divided into the voltage across the carrier-storage-region (CSR), the junction (Boltzmann) voltages and the voltages across the space charge regions. The latter includes the depletion layers formed around reversed biased junctions and the non-conductivity modulated regions in the base (known as drift regions). In order to realistically model these two bipolar devices, the distributed nature of the charge

storage in the drift region as well as the floating nature of the borders of the CSR have to be accounted. Nonetheless, a dynamic solution is required only for the base region. All the other device parts can be considered as behaving quasi-statically; as suppliers/collectors of charge carriers to and from the drift region (Leturcq, P., 1997) or in mathematical terms as dynamic boundary conditions for the evaluation of the borders' positions and the CSR charge concentration profile. Knowledge of the latter two enables the computation of the voltages across the CSR and the space charge regions. The following sub-sections describe in detail the analytical evaluation of all the required quantities.

3.2.1. Model of the Carrier Storage Region (CSR)

The charge profile and the depletion layers are primarily one-dimensional (nb for the diode for almost 100% while for the IGBT for over 90% of the drift region), thus a 1-D solution is adequate. Also as a convention in both devices a 1D base region width can be assumed, denoted by W_B. Under the conditions of quasi-neutrality and high levels of injection, the charge dynamics are described by the ambipolar diffusion equation (ADE), which in 1D is:

$$D \frac{\partial^2 p(x,t)}{\partial x^2} = \frac{p(x,t)}{\tau_{hl}} + \frac{\partial p(x,t)}{\partial t} \quad (1)$$

where D is the ambipolar diffusion coefficient, τ_{hl} is the high-injection-level carrier lifetime and p(x,t) is the ambipolar charge carrier density (nb excess holes (Δp) and excess electrons (Δn) in equal concentrations).

Since the carrier distribution inside the CSR can be written as a continuous function, the solution of (1) can be expressed as a cosine Fourier series (Leturcq 1997):

$$p(x,t) = v_0(t) + \sum_{k=1}^{\infty} v_k(t) \cos\left(\frac{k\pi(x-x_1)}{x_2-x_1}\right) \quad (2)$$

where v₀ is the DC component of p(x,t) at time t, v_k is the amplitude of the kth harmonic and x₁ & x₂ are the abscissae of the floating borders of the charge storage region. Furthermore, the Fourier series coefficients v_k (for k=0, 1, 2, 3, ...) can be expressed as follows:

$$v_k(t) = \frac{1}{x_2-x_1} \int_{x_1}^{x_2} p(x,t) \cos\left(\frac{k\pi(x-x_1)}{x_2-x_1}\right) dx \quad (4)$$

Multiplying (1) by the cosine term, then integrating it w.r.t. x from x₁ to x₂ while using (4), the ambipolar diffusion equation transforms into the infinite system of first-order differential equations described by (5):

$$\frac{dv_0(t)}{dt} = -\frac{v_0(t)}{\tau} + \frac{1}{(x_2-x_1)} D \left(\frac{\partial p(x,t)}{\partial x} \Big|_{x_2} - \frac{\partial p(x,t)}{\partial x} \Big|_{x_1} \right) - \frac{1}{(x_2-x_1)} \sum_{n=1}^{\infty} v_n(t) \left[\frac{dx_1}{dt} - (-1)^n \frac{dx_2}{dt} \right] \quad (\text{for } k=0) \quad (5)$$

$$\begin{aligned} \frac{dv_k(t)}{dt} = & - \left(\frac{1}{\tau} + \frac{Dk^2\pi^2}{(x_2-x_1)^2} + \frac{1}{4} \frac{d(x_1-x_2)}{dt} \right) v_k(t) \\ & + \frac{2}{(x_2-x_1)} D \cdot \left((-1)^k \frac{\partial p(x,t)}{\partial x} \Big|_{x_2} - \frac{\partial p(x,t)}{\partial x} \Big|_{x_1} \right) \\ & - \frac{2}{(x_2-x_1)} \sum_{\substack{n=1 \\ n \neq k}}^{\infty} \frac{n^2}{n^2-k^2} v_n(t) \left[\frac{dx_1}{dt} - (-1)^{n+k} \frac{dx_2}{dt} \right] \quad (\text{for } k \neq 0) \end{aligned}$$

The evaluation of the Fourier coefficients from system (5) requires the boundary conditions at the two ends of the CSR, namely the abscissae of the borders $x = x_1$ and $x = x_2$, their time derivatives $\frac{dx_1}{dt}$ and $\frac{dx_2}{dt}$, and the carrier concentration gradients at these points $g_1(t) = \frac{\partial p(x,t)}{\partial x} \Big|_{x_1}$ and $g_2(t) = \frac{\partial p(x,t)}{\partial x} \Big|_{x_2}$. The charge carrier distribution and the associated boundary conditions are illustrated in figure 5 for the case of static conduction and turn off transient (for the PIN diode fig. 5(a,b) and for the IGBT fig. 5(c)).

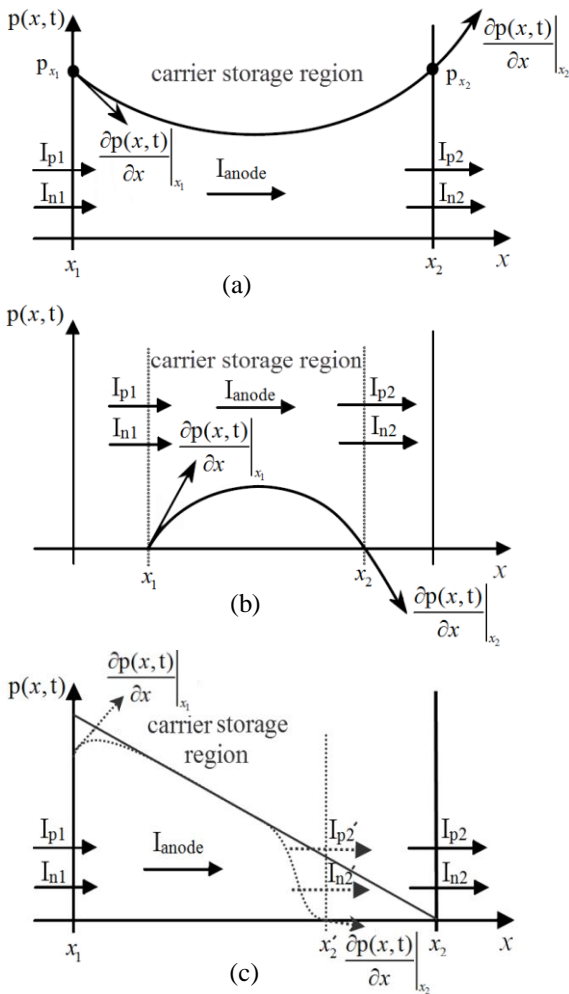


Figure 5 - Charge carrier profile & boundary conditions for (a) Diode during static conduction (b) Diode during turn-off (c) IGBT during static conduction and turn-off

The gradients $g_1(t)$ and $g_2(t)$ can be calculated from the boundary hole and electron currents (i.e. I_{n1} , I_{p1} at $x=x_1$ and I_{n2} , I_{p2} at $x=x_2$) as in (6) where q is the electron charge, A is the junction area and D_n and D_p are respectively the electron and hole diffusion coefficients (Palmer et al. 2003). The coefficients D_n , D_p and D are calculated by equation (7) where μ_n and μ_p are the electron and hole mobilities, k is the Boltzmann constant and T is the junction temperature in K.

$$g_1(t) = \frac{1}{2qA} \left(\frac{I_{n1}}{D_n} - \frac{I_{p1}}{D_p} \right) \quad g_2(t) = \frac{1}{2qA} \left(\frac{I_{n2}}{D_n} - \frac{I_{p2}}{D_p} \right) \quad (6)$$

$$D_p = \frac{kT}{q} \mu_p \quad (i) \quad D_n = \frac{kT}{q} \mu_n \quad (ii) \quad D = \frac{2D_n D_p}{D_n + D_p} \quad (iii) \quad (7)$$

3.2.2. Diode Boundary Conditions

For the diode, the emitter layers (i.e. the P^+ anode and the N^+ cathode layers) act as recombination sinks for the minority carriers. Thus the resulting minority currents I_{n1} , I_{p1} can be characterised by the conventional “h parameters” (Schlangenotto et al. 1969) and calculated using equation (8) where h_p is the recombination parameter at the P^+ layer, h_n is the recombination parameter at the N^+ layer and p_{x1} & p_{x2} are respectively the excess carrier concentrations at $x=x_1$ and $x=x_2$. The majority currents I_{p1} , I_{n2} can then be calculated by equation (9) where I_A is the total anode current and I_{disp1} & I_{disp2} are the displacement currents charging respectively the capacitances of the depletion layers around junctions J_1 and J_2 (nb if applicable). The latter can be evaluated using equation (10) where ϵ is the material’s electric permittivity, W_{d1} and W_{d2} are the widths of the respective depletion regions and V_{d1} and V_{d2} are respectively the voltages across them. W_{d1} and W_{d2} are related to V_{d1} and V_{d2} according to equation (11) which is classically derived from the Poisson equation. In (11) an effective base region doping concentration is considered which comprises of the background doping, N_B , and the density of free carriers moving through the region at their saturated velocity v_{sat} . The depletion layer voltages V_{d1} and V_{d2} are in turn calculated from the boundary carrier densities using equation (12) which is derived by applying proportional control with feedback (similar to op-amp circuits) from the boundary carrier densities p_{x1} & p_{x2} . The feedback is such that whenever the depletion layers are active, the concentrations p_{x1} & p_{x2} are kept equal to zero as physically expected. In control theory terms the values of p_{x1} & p_{x2} are equivalent to error signals and the motion of the boundaries x_1 and x_2 (via the change of the depletion region widths) is equivalent to the action for compensating that error. In our case the depletion layer widths are linked to p_{x1} and p_{x2} indirectly via the depletion layer voltages. It is possible to link them directly (proportionally) but this has been found causing convergence and accuracy issues (Bryant et al. 2007a). Finally, the abscissae of the CSR borders can be found from the depletion layer widths as in (13).

Equations for the Diode boundary conditions:

$$I_{n1} = qAh_p(p_{x_1})^2 \quad I_{p2} = qAh_n(p_{x_2})^2 \quad (8)$$

$$I_{p1} = I_A - I_{n1} - I_{disp1} \quad I_{n2} = I_A - I_{p2} - I_{disp2} \quad (9)$$

$$I_{disp1} = \frac{\varepsilon A}{W_{d1}} \frac{dV_{d1}}{dt} \quad I_{disp2} = \frac{\varepsilon A}{W_{d2}} \frac{dV_{d2}}{dt} \quad (10)$$

$$W_{d1} = \sqrt{\frac{2\varepsilon V_{d1}}{qN_B + \frac{|I_{p1}|}{Av_{sat}}}} \quad W_{d2} = \sqrt{\frac{2\varepsilon V_{d2}}{qN_B + \frac{|I_{n2}|}{Av_{sat}}}} \quad (11)$$

$$V_{d1} = \begin{cases} 0 & p_{x_1} \geq 0 \\ -K_{FP} p_{x_1} & p_{x_1} < 0 \end{cases} \quad V_{d2} = \begin{cases} 0 & p_{x_2} \geq 0 \\ -K_{FP} p_{x_2} & p_{x_2} < 0 \end{cases} \quad (12)$$

$$x_1 = W_{d1} \quad x_2 = W_B - W_{d2} \quad (13)$$

3.2.3. IGBT Boundary Conditions

The boundary conditions for the NPT IGBT are identical to that of the diode at the end $x=x_1$ with the P⁺ IGBT collector layer serving as a recombination sink for the electrons. Therefore, I_{n1} and I_{p1} can be found by equation (14) with I_C being the collector current and the rest of the symbols having the same meaning as before. It should be noted here that there is no displacement current I_{disp1} since the junction J_1 is always forward biased and thereby no depletion layer is present there. This also means that the boundary x_1 is always fixed at $x=0$. At $x=x_2$ the situation is different from the diode with I_{n2} now being the MOS channel electron current, and the I_{p2} the hole current collected by the P-well. The value of I_{n2} can be calculated by the typical MOSFET equations (15(i)-(16)) where V_{GE} is the voltage applied to the gate (G) w.r.t the IGBT N⁺ source/emitter (E), V_{TH} is the threshold voltage for channel inversion, V_{DE} is the voltage between the “virtual drain” (D) and the emitter, K_p is the MOS transconductance and λ is the channel shortening parameter. The value of I_{p2} can then be found from (15(ii)) i.e. by subtracting I_{n2} and the two displacement currents at $x=x_2$ from I_C . The latter-namely I_{disp2} and I_{CG} represent respectively the current charging the collector-emitter capacitance, C_{CE} , (formed by the depletion region under the p-well) and the current charging the collector-gate (Miller) capacitance, C_{CG} (nb. or equivalently collector- “virtual-drain” capacitance). The values of I_{disp2} and I_{CG} are calculated from (17), (18) where C_{ox} is the oxide capacitance per unit area, α_i is the ratio of the intercell area (nb. area between P-wells) to the total die area, A is the total die area, l_m is the half intercell width and W_{d2} is the depletion region width formed under the P-wells. The latter is associated with the voltage across the layer, V_{d2} , as in the case of the diode via equation (19(i)) with V_{d2} again serving as the control actuator (equation (20)) for keeping the concentration p_{x_2} equal to zero (nb in this case the time). Equations (17)-(18) can be derived respectively from $I_{disp2} = C_{CE} \frac{dV_{DE}}{dt}$ & $I_{CG} = C_{CG} \frac{dV_{DG}}{dt}$

and the expressions of the relevant capacitances (Palmer et al. 2003). It should be noted here that the value of V_{DE} is assumed to be equal to V_{d2} since typically the potential at the edge of the depletion layer around the P-

well is approximately equal to that at the end of the MOS channel. Lastly, x_2 is found by equation (19(ii)).

Equations for the IGBT boundary conditions:

$$I_{p1} = I_C - I_{n1} \quad I_{n1} = qAh_p(p_{x_1})^2 \quad (14)$$

$$I_{p2} = I_A - I_{n2} - I_{disp2} - I_{GC} \quad (i) \quad I_{n2} = \begin{cases} I_{MOS} & \text{if } V_{GE} \geq V_{TH} \\ 0 & \text{if } V_{GE} < V_{TH} \end{cases} \quad (ii) \quad (15)$$

$$I_{MOS} = \frac{K_p}{2} [2V_{DE}(V_{GE} - V_{TH}) - V_{DS}^2] \quad \text{if } V_{DE} \leq V_{GE} - V_{TH} \quad (16)$$

$$\text{or } = \frac{K_p}{2} [(V_{GE} - V_{TH})^2 (1 + \lambda(V_{DE} - (V_{GE} - V_{TH})))] \quad \text{otherwise}$$

$$I_{disp2} = \frac{\varepsilon A(1 - \alpha_i)}{W_{d2}} \frac{dV_{d2}}{dt} \quad (17)$$

$$I_{CG} = \frac{C_{ox} A \alpha_i}{1 + \frac{C_{ox}}{\varepsilon} \left(W_{d2} - l_m - \sqrt{\frac{2\varepsilon V_{GE}}{qN_B}} \right)} \left(\frac{dV_{d2}}{dt} - \frac{dV_{GE}}{dt} \right) \quad (18)$$

$$W_{d2} = \sqrt{\frac{2\varepsilon V_{d2}}{qN_B + \frac{|I_C|}{Av_{sat}}}} \quad (i) \quad x_2 = W_B - W_{d2} \quad (ii) \quad x_1 = 0 \quad (iii) \quad (19)$$

$$V_{d2} = \begin{cases} 0 & p_{x_2} \geq 0 \\ -K_{FP} p_{x_2} & p_{x_2} < 0 \end{cases} \quad (20)$$

3.2.4. Charge Storage Region (CSR) Voltage Drop

The voltage drop across the quasi-neutral CSR region, V_B , can be found by calculating the integral expression (21) where J is the total device current density. In physical terms the first integral represents a purely ohmic voltage drop, V_{Ω} , whilst the second one is the Dember voltage, V_{Dember} , which is much smaller than V_{Ω} and is therefore safely neglected.

$$V_B = V_{\Omega} + V_{Dember} = \frac{J}{q(\mu_n + \mu_p)} \int_{x_1}^{x_2} \frac{dx}{p_x} - \frac{kT}{q} \left(\frac{\mu_n - \mu_p}{\mu_n + \mu_p} \right) \int_{p(x_2)}^{p(x_1)} \frac{dp}{p} \quad (21)$$

where $p_x = p_T(x) = p(x) + \mu_n N_B / (\mu_n + \mu_p)$ for a time t

Since an analytical evaluation of V_{Ω} is impossible with p_x expressed in Fourier series, a piecewise linear approximation of p_x is instead considered. More specifically the concentration is evaluated (using the Fourier series) at $M+1$ equidistant points and then assumed to vary linearly between them as in figure 6.

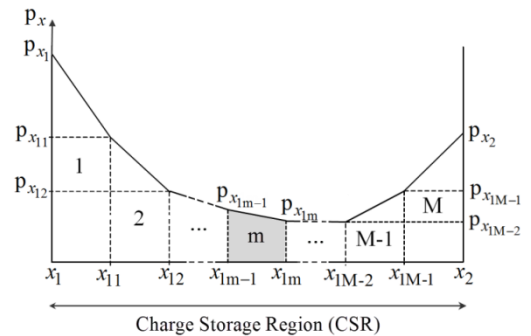


Figure 6– Discretisation of charge carrier profile in CSR

The total base voltage can then be calculated by (22):

$$V_B = \frac{J(x_2 - x_1) / M}{q(\mu_n + \mu_p)} \times \sum_{m=1}^M \left(\gamma \frac{\ln \left[\frac{N_B + p(x_{1m})}{N_B + p(x_{1m-1})} \right]}{p(x_{1m}) - p(x_{1m-1})} - (\gamma - 1) \frac{1}{p_{x_{1m}}} \right)$$

where $\gamma = \begin{cases} 1 & \text{if } p(x_m) \neq p(x_{m-1}) \\ 0 & \text{if } p(x_m) = p(x_{m-1}) \end{cases}$ and $x_{1m} = x_1 + m(x_2 - x_1) / M$

Note: p_{x1} and p_{x2} are respectively equivalent of p_{x10} and p_{x1M} . Similarly for $p(x_1)$ and $p(x_2)$

It should be noted that for the case of the IGBT the assumption of a purely 1D profile needs to be treated carefully at the MOS end of the device. As described previously in the evaluation of the boarder position, x_2 , the model assumes an effective depletion region width equal to that formed under the p-well and controlling p_{x2} to be equal to zero. However for the calculation of the ohmic drop, V_Ω , the effect of the accumulation charge under the gate overlap should be taken into account as otherwise an unrealistically high resistance will be predicted. To account for this effect the value of $p(x_2)$ used in equation (22) is derived from the penultimate one according to $p(x_2) \approx \alpha_i p(x_{M-1})$.

3.2.5. Calculation of the Devices' Terminal Voltages

For the diode the terminal anode-cathode voltage, V_{AK} is given by equation (23), i.e. it is equal to the sum of the following voltages: (i) the two Boltzmann junction voltages V_{J1} and V_{J2} (equation 24), (ii) the two space charge region voltages V_{d1} and V_{d2} (equation 12) and (iii) the CSR voltage, V_B , (equation 22 where $J=I_A/A$).

$$V_{AK} = V_{J1} + V_{J2} + V_{d1} + V_{d2} + V_B \quad (23)$$

$$V_{J1} = \frac{kT}{q} \ln \left(\frac{p_{x1} N_B}{n_i^2} \right) \quad V_{J2} = \frac{kT}{q} \ln \left(\frac{p_{x2}}{N_B} \right) \quad (24)$$

For the IGBT the terminal collector-emitter voltage, V_{CE} is given by equation (25), i.e. it is equal to the sum of the following voltages: (i) the Boltzmann junction voltage V_{J1} (equation 24), (ii) the space charge region voltage V_{d2} (equation 20) and (iii) the CSR voltage, V_B , (equation 22 where $J=I_C/A$).

$$V_{CE} = V_{J1} + V_{d2} + V_B \quad (25)$$

The terminal gate-emitter voltage, V_{GE} , can be found by solving the differential equation (26) where I_G is the gate current, C_{GE} is the gate-emitter capacitance (constant) and C_{GC} is the non-differential part of equation (18). The differential equation (26) can be derived by considering Kirchoff's current law (KCL) at the gate i.e. $I_{GE} = I_G + I_{CG}$.

$$\frac{dV_{GE}}{dt} = \frac{1}{C_{GE} + C_{GC}} \left(I_G + C_{GC} \frac{dV_{d2}}{dt} \right) \quad (26)$$

3.2.6. Temperature Dependency

The models include temperature effects through the temperature dependency of the various physical

parameters. The required device temperature can be calculated via a thermal model (e.g. RC network) of the device packaging. More details about temperature dependency can be found in (Palmer et al. 2003).

4. STRATEGY FOR FPGA IMPLEMENTATION

4.1. Co-simulation Method

As described in section 2.3.2 when simulating stiff systems like power electronic circuits, an implicit method should be preferred due to its stability. However, a true implicit approach would call either for the system states to be processed all in one platform or in the case of co-simulation it would call for a mixed, concurrent processor/FPGA evaluation of the involved matrices ultimately leading to a very time-consuming simulation due to the huge number of (different) data exchanges and thereby communication overheads during a single time step. The solution to the problem is system partitioning i.e. decoupling of the system to at least two portions, one or more for processing in FPGA and one or more for processing in software.

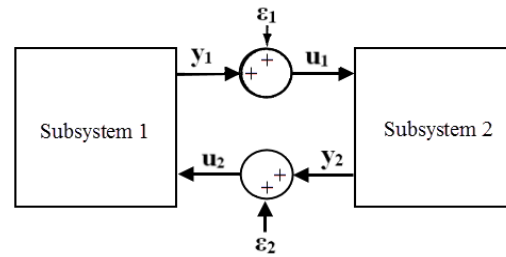


Figure 7 – Block diagram representation of system partitioning into two subsystems

Without any loss of generality figure 7 shows a functional diagram of the considered method where the circuit is divided into two subsystems passing to each other the required coupling state variables y_1 & y_2 augmented by unavoidable errors ϵ_1 and ϵ_2 (due to sampling as well as due to truncation and rounding by the selected integration method) into inputs u_1 and u_2 . Once the system is decoupled, different integration methods and/or time step sizes can be used in order to ensure stability (Gear et al. 1984). Furthermore, because of partitioning the matrices are less sparse resulting to only few unnecessary zero-element multiplications and hence more efficient usage of the hardware resources.

For illustration purposes the generalised chopper circuit of figure 8 is chosen to be modeled. Although it is possible to split the system by pure numerical considerations, here for simplicity the system is partitioned naturally. In particular the system is separated into four subsystems: (i) the PIN diode model with internal states x_{diode} as defined by equation (5), (ii) the IGBT model with internal states x_{igbt} as defined by equations (5) and (26), (iii) the main circuit with states $x_{circuit}$ and (iv) the gate drive circuit with states x_{drive} . The first two subsystems are chosen to be implemented in FPGA (since they are the most computationally intensive) while the other two in software.

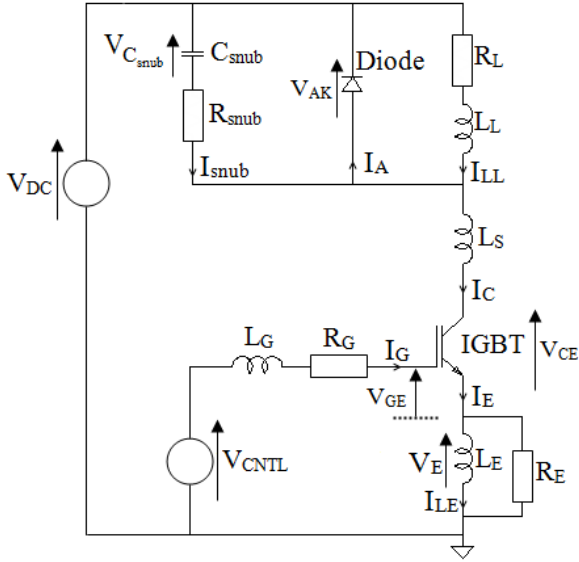


Figure 8 – The generalised chopper cell circuit

With the considered approach the entire system with states \mathbf{x} can be decomposed as follows:

$$\dot{\mathbf{x}} = \begin{bmatrix} \dot{\mathbf{x}}_{\text{diod}} \\ \dot{\mathbf{x}}_{\text{igbt}} \\ \dot{\mathbf{x}}_{\text{circ}} \\ \dot{\mathbf{x}}_{\text{driv}} \end{bmatrix} = \begin{bmatrix} \mathbf{f}_{\text{diod}}(\mathbf{x}_{\text{diod}}, \mathbf{w}_{\text{diod}}, t) \\ \mathbf{f}_{\text{igbt}}(\mathbf{x}_{\text{igbt}}, \mathbf{w}_{\text{igbt}}, t) \\ \mathbf{f}_{\text{circ}}(\mathbf{x}_{\text{circ}}, \mathbf{w}_{\text{circ}}, t) \\ \mathbf{f}_{\text{driv}}(\mathbf{x}_{\text{driv}}, \mathbf{w}_{\text{driv}}, t) \end{bmatrix} \quad (27)$$

where \mathbf{f}_{diod} , \mathbf{f}_{igbt} , \mathbf{f}_{circ} , \mathbf{f}_{driv} and \mathbf{w}_{diod} , \mathbf{w}_{igbt} , \mathbf{w}_{circ} , \mathbf{w}_{driv} are respectively the vector functions and vector inputs of the diode, IGBT, main circuit and gate drive circuit subsystems including the coupling variable(s) passed into them. More specifically: $\mathbf{w}_{\text{diod}} = \mathbf{y}_{\text{circ}_1}$, $\mathbf{w}_{\text{driv}} = \mathbf{y}_{\text{igbt}_2}$,

$\mathbf{w}_{\text{igbt}} = [\mathbf{y}_{\text{circ}_2}, \mathbf{y}_{\text{driv}}]^T$, $\mathbf{w}_{\text{circ}} = [V_{\text{DC}}, \mathbf{y}_{\text{igbt}_1}, \mathbf{y}_{\text{diod}}, \mathbf{y}_{\text{driv}}, \mathbf{y}_{\text{circ}_2}]^T$ with the coupling variables being $\mathbf{y}_{\text{diod}} = V_{\text{AK}}$, $\mathbf{y}_{\text{igbt}_1} = V_{\text{CE}}$, $\mathbf{y}_{\text{igbt}_2} = V_{\text{GE}}$, $\mathbf{y}_{\text{circ}_1} = I_{\text{A}}$, $\mathbf{y}_{\text{circ}_2} = I_{\text{C}}$, $\mathbf{y}_{\text{driv}} = I_{\text{G}}$

It should be noted here that to the internal states of the devices' subsystems it is required to add extra states for the calculation of the derivatives as required by system (5) and its internal functions (10), (17) and (18).

4.2. Numerical Integration

The decomposed states of the several subsystems are calculated in parallel using a suitable numerical integration method. As explained in section 2.3.2 the preferred methods should be (i) fixed time step-size, (ii) implicit and (iii) multistep. For such methods the general solution equation for the value of the next-time-step subsystems' states can be written as in (28)

$$\mathbf{x}_{\text{sub}}^{n+1} = \sum_{i=0}^p \alpha_i \cdot \mathbf{x}_{\text{sub}}^{n-i} + \Delta t_{\text{sub}} \sum_{i=1}^p \beta_i \cdot \mathbf{f}_{\text{sub}}^{n-i} \quad (28)$$

where $\mathbf{x}_{\text{sub}}^m$ and $\mathbf{f}_{\text{sub}}^m = \mathbf{f}_{\text{sub}}(\mathbf{x}_{\text{sub}}^m, \mathbf{w}_{\text{sub}}^m, t^m)$ are respectively the state and function vectors of the subsystem at the m^{th} time step, α_i and β_i are method-dependent

polynomial coefficients (with $\beta_i \neq 0$ for implicit methods), and Δt_{sub} is the subsystem's integration time-step size. Based on stability, efficiency, accuracy and real-time constraints considerations the chosen method for the devices' subsystems is the 3rd order Gear Method (Gear 1971) while that for the circuit subsystems is the 3rd order Brayton method (Brayton 1972) with some modifications as proposed by Shampine (Shampine 1980) and others.

In order to solve equation (28) explicitly in terms of $\mathbf{x}_{\text{sub}}^{n+1}$, the vector function \mathbf{f}_{sub} must be linear. For the cases of the diode and the IGBT subsystems where \mathbf{f}_{sub} is non-linear, this should be linearized according to:

$$\mathbf{f}_{\text{sub}} = \frac{\partial \mathbf{f}_{\text{sub}}}{\partial \mathbf{x}_{\text{sub}}} \mathbf{x}_{\text{sub}} + \frac{\partial \mathbf{f}_{\text{sub}}}{\partial \mathbf{w}_{\text{sub}}} \mathbf{w}_{\text{sub}} = \mathbf{A}_{\text{sub}} \mathbf{x}_{\text{sub}} + \mathbf{B}_{\text{sub}} \mathbf{w}_{\text{sub}} \quad (29)$$

Then the evaluation of the time advanced states can be done as in (30):

$$\mathbf{x}_{\text{sub}}^{n+1} = \Delta t_{\text{sub}} \left(\mathbf{I} - \Delta t_{\text{sub}} \beta_{-1} \mathbf{A}_{\text{sub}}^{n+1} \right)^{-1} \times \left[\beta_{-1} \mathbf{B}_{\text{sub}}^{n+1} \mathbf{w}_{\text{sub}}^{n+1} + \sum_{i=0}^p \left(\alpha_i \mathbf{x}_{\text{sub}}^{n-i} + \beta_i \mathbf{f}_{\text{sub}}^{n-i} \right) \right] \quad (30)$$

where $\mathbf{f}_{\text{sub}}^{n+1}$ has been substituted by its linear/linearized form as in (29) with $\mathbf{A}_{\text{sub}}^{n+1}$, $\mathbf{B}_{\text{sub}}^{n+1}$ being the Jacobian matrices of the next time step (nb these are calculated numerically using the small perturbation theory). The inverse of the matrix $\mathbf{M} = (\mathbf{I} - \Delta t_{\text{sub}} \beta_{-1} \mathbf{A}_{\text{sub}}^{n+1})$ is found using LU decomposition followed by forward and backward substitution.

4.3. FPGA Parallel Programming

In FPGAs the matrix multiplications involved in equation (30) can all be performed in parallel in two steps as a sum of products (SOP) resulting to great computational speed ups compared to serial processing. For example for a matrix-matrix \mathbf{MN} multiplication, where \mathbf{M} and \mathbf{N} are $m \times m$ and $m \times n$ matrices, the computational cost reduces from $mn(2m-1)$ sequential operations to m^2n parallel multiplications and $m(m-1)n$ parallel additions. Besides from the number of calculation steps the simulation speeds also depend on the overheads imposed by the several processing equipment and communication links. Since the most critical overhead is that of software-hardware data transactions, the considered methodology reduces the number of software-FPGA interactions via the use of frame signals, i.e. data transaction parallelism. In particular a series of input/output data values are stored in a data vector which is transferred in one burst into/from an input/output buffer residing on the FPGA.

4.4. Practical Implementation

The targeted hardware platform is a Digilent Atlys development board with Xilinx Spartan 6 FPGA. The co-simulation environment is set up in Simulink with the software-hardware interface being provided by

Xilinx System Generator (XSG), (Xilinx Inc., 2012c), and the communication between the PC and the board done via 1Gbit Ethernet. An important advantage of this method is that it enables rapid implementation and verification of the algorithms employed as opposed to the more classical approach. The entire system development requires the following steps:

1. Floating-point algorithm development and verification in Matlab/Simulink via the use of embedded Matlab functions.
2. Design elaboration for FPGA implementation by including the use of fixed point arithmetic and other hardware constraints. The former requires selection of the appropriate bit widths and radix point position for each block in order to enhance/maximise the signal to noise ratio (SNR). A safety margin of four bits is also added to avoid overflows. It should be noted here that the several state variables require appropriate scaling in order to reduce the effect of round off errors and increase precision.
3. Design adjustment for bottleneck removal and efficient exploitation of the hardware resources via critical paths' pipelining and time division multiplexing for resource sharing of unutilized functional blocks.
4. Generation/writing of HDL (VHDL/Verilog) code for the several hardware subsystems (nb only the device models for the circuit of figure 8). Placement of the relevant HDL codes into XSG "black boxes".
5. Set up of the software-hardware interfacing via Xilinx Gateway blocks as well as FIFO buffers and control for frame-based processing. For the latter the FPGA is used in free run mode.
6. Automatic generation of BIN file using the System Generator with Xilinx ISE.

5. CONCLUSIONS

In this paper the strategy for the FPGA implementation of analytical power device models incorporated in a circuit has been described. A detailed comparison of the co-simulation results and the achieved computational accelerations will be presented in a later publication. Further work is required towards the development of a multi-FPGA platform in order to achieve hardware implementation of larger circuit systems employing multiple power devices. Furthermore apart from co-simulation purposes the device models will also be exploited for real-time model-based control.

REFERENCES

Altera Corp., 2012. *Cyclone IV Device Handbook*. Available from: <http://www.altera.com/literature/hb/cyclone-iv/cyclone4-handbook.pdf> [accessed 12 July 2012]

Altera Corp., 2012. *Stratix IV Device Handbook*. Available from: http://www.altera.com/literature/hb/stratix-iv/stratix4_handbook.pdf [accessed 12 July 2012]

Brayton, R.K, Gustavson, F.G., Hachtel, G.D., 1972. A new Efficient Algorithm for Solving Differential-Algebraic Systems Using Implicit Backward Differentiation

Formulas, *IEEE Transactions on Industry Applications*, 60 (1): 98–108.

Bryant, A.T., Palmer, P. R., Santi, E., and Hudgins, J.L., 2007. Simulation and optimization of diode and Insulated Gate Bipolar Transistor interaction in a chopper cell using MATLAB and Simulink, *IEEE Transactions on Industry Applications*, 43 (4): 874–883.

Bryant, A.T., Santi, E., Palmer, P. R., and Hudgins, J.L., 2007. Two-step parameter extraction procedure with formal optimization for physics-based circuit simulator IGBT and p-i-n Diode Models, *IEEE Transactions on Power Electronics*, 21 (2): 295–309.

Hoffman, J.D., 2001. *Numerical Methods for Engineers and Scientists*. 2nd Ed. New York: Marcel Dekker Inc.

Gear, C.W., 1971. Simultaneous Numerical Solution of Differential-Algebraic Equations, *IEEE Transactions on Circuit Theory*, 18 (1): 89-95

Gear, C.W. and Wells, D.R., 1984. Multirate linear multistep methods, *BIT Numerical Mathematics*, 24 (4): 484–502.

Gonzalez J. and Nunez R., 2009. LAPACKrc: Fast linear algebra kernels/solvers for FPGA accelerators. *Journal of Physics: Conference Series, SciDAC 2009*, IOP Publishing, 180012042.

Greenberg, M.D., 1998. *Advanced Engineering Mathematics*. 2nd Ed. New Jersey: Prentice Hall.

IEEE, 2008. *754-2008 IEEE Standard for Floating-Point Arithmetic*. Available from: <http://ieeexplore.ieee.org> [accessed 12 July 2012]

Jin, H., 1997. Behavior-Mode Simulation of Power Electronic Circuits, *IEEE Transactions on Power Electronics*, 12 (3): 443-452.

Leturcq, P., 1997. A study of distributed switching processes in IGBTs and other power bipolar devices Circuit simulator models for the diode and IGBT with full temperature dependent features, *Proceedings of Power Electronics Specialists Conference*, pp. 139-147. June 22-27, St. Louis (Missouri, USA).

Oh, H.-S, Nokali M. El., 2001. A new IGBT behavioural model, *Solid-State Electronics*, 45 (12): 2069-2075.

Palmer, P. R., Santi, E., Hudgins, J. L., Kang, X., Joyce, J. C. and Eng, P. Y., 2003. Circuit simulator models for the diode and IGBT with full temperature dependent features, *IEEE Transactions on Power Electronics*, 18 (5): 1220–1229.

Pejovic, P. and Maksimovic, R., 1994. A Method for Fast Time-Domain Simulation of Networks with Switches, *IEEE Transactions on Power Electronics*, 9 (4): 449-456.

Schlangenotto, H. and Gerlach W., 1969. On the effective carrier lifetime in p-s-n rectifiers at high injection levels, *Solid State Electronics*, 12: 267-275.

Shampine, L.F., 1980. Implementation of implicit formulas for the solution of ODE's, *SIAM Journal on Scientific and Statistical Computing*, 1(1): 103-118.

Strunz, K., 2004. Flexible Numerical Integration for Efficient Representation of Switching in Real Time Electromagnetic Transients Simulation, *IEEE Transactions on Power Delivery*, 19 (3): 1276-1283.

Xilinx Inc., 2009. *Hardware Co-Simulation Basics using System Generator for DSP*. Available from: Xilinx webinars [accessed 12 July 2012]

Xilinx Inc., 2012. *DS150, Virtex-6 Family Overview*. Available from: http://www.xilinx.com/support/documentation/data_sheets/ds150.pdf [accessed 12 July 2012]

Xilinx Inc., 2012. *DS160, Spartan-6 Family Overview*. Available from: http://www.xilinx.com/support/documentation/data_sheets/ds160.pdf [accessed 12 July 2012]

Xilinx Inc., 2012. *System Generator for DSP*. Available from: http://www.xilinx.com/support/documentation/sw_manuals/xilinx13_4/sysgen_user.pdf [accessed 12 July 2012]

Zack S. and Dhanani S., 2004. DSP Co-Processing in FPGAs: Embedded High-Performance, Low-Cost DSP Functions. *Xilinx White Paper*, ver.1.0, (March): 1–8.

Authors' Index

- Abourizk, 180
Accorsi, 129
Affenzeller, 265, 340, 362, 368
Akimoto, 138
Alkilani, 519
Allocca, 328
Almeida, 428
Andersen, 163
Arica, 543
Aristidou, 616
Asmuss, 408
Atanasijevic-Kunc, 283, 507
Auer, 549
Bachler, 316
Baisini, 584
Bal, 241
Barrera, 210
Baumgartner, 156
Beham, 379
Behr, 565
Bicher, 489, 507, 525
Blanco-Fernandez, 452
Bleicher, 434, 471
Bogner, 21, 74, 115
Bogner
Bolanos, 390
Bolshakov, 226
Borgmann, 271
Bortolini, 129
Breitenecker, 434, 471, 489, 495, 507, 513, 531, 537, 549
Bruckner, 519
Bruzzone, 573, 584, 602
Bubevski, 59
Burinskiene, 402
Burlacu, 362, 368
Canades, 390
Cantice, 573
Cao, 109
Cappannoli, 334
Caruso, 610
Catapano, 346
Champlaud, 27, 477
Cicibas, 543
Coelho, 204, 428
Costa, 328
Costantino, 334
Davendra, 396, 458
Davoli, 414
De Nicola, 256
Dejax, 80
Demir L., 44
Demir A., 543
Di Gravio, 334
Diaz, 565
Dimitriou, 471
Drazdilova, 169
Drinovec, 283
Duanmu, 565
Dür, 471
Ecker, 531
Eichert, 198
Einzinger, 513
Ekyalimpa, 180
Eldemir, 189
Eliiyi, 44
Ematinger, 74
Emrich, 519
Fanti, 150
Fazzari, 610
Feng, 27, 477
Ferrari, 129
Fitsch, 489, 507, 525
Flores, 309
Forstenlechner, 340
Gallo, 414
Gamberi, 129
Garcia, 309
Garredu, 216
Georgoulas, 150
Gertsbakh, 68
Gira, 316
Glock, 513
González, 210
Govoni, 414
Graziani, 129
Gudundsdottir, 163
Gunál, 543
Hafner, 489, 495, 525
Hametner, 316, 322
Hamri, 385
Heinzl, 471, 495, 531, 549
Helgason, 163
Hodecek, 537
Hoffmann, 293
Iacobellis, 150
Il Bae, 97
Jacak W., 232, 265
Jacak J., 271
Jacob, 204
Jeng, 565
Jiménez-Macías, 440, 446, 452, 465
Kaczorek, 1
Karakaya, 189
Kastner, 434
Kenne, 80
Khattak, 565
Kiesling, 90
Kim, 97
Kommenda, 265, 340, 362
Körner, 495, 501, 525, 531
Kose, 44

Kouedeu, 80
 Kowarik, 549
 Kronberger, 265, 340, 362, 379
 Kropf, 316, 322
 Landsiedl, 434, 471, 495
 Lanza, 32
 Latorre-Biel, 440, 446, 452, 465
 Lauks, 408
 Lee, 97
 Legato, 248
 Lewis, 6
 Liu, 38
 Longo, 565, 591, 602, 610
 Luo, 38
 Maio, 144
 Maksoud, 293
 Manzo, 256
 Marques, 573
 Martinovic, 169
 Mastaglio, 6
 Mathew, 6
 Mayer, 316, 322
 Mazza, 248
 Melloni, 414
 Merkurjeva, 226
 Messouci, 385
 Moccia, 256
 Mohamed, 180
 Monhof, 198
 Montanaro, 346
 Morin, 27
 Mujica, 555
 Muñoz D.F., 15
 Muñoz D.G., 15
 Music, 483
 Nagele, 489, 507
 Nascimento, 144
 Nonino, 334
 Oplatkova, 458
 Oren, 277
 Osintsev, 156
 Palmer, 616
 Pan, 109
 Parragh, 322
 Pasquino, 352
 Pattarozzi, 414
 Pérez-Parte, 440
 Peterseil, 489
 Petry, 428
 Piera, 555
 Pitzer, 368
 Pluhacek, 396
 Pluhacek, 458
 Pomorski, 103
 Popa, 237
 Popper, 471, 531, 537, 549
 Premier, 293
 Proell, 232
 Quan, 477
 Rarità, 352
 Reinisch, 471, 495
 Ren, 38, 373
 Renken, 198
 Reschreiter, 549
 Rodrigues, 204
 Rojec, 483
 Rong, 121
 Rossetti, 204, 428
 Rößler, 434, 495, 531
 Rozenich, 519
 Saba, 180
 Sabourin, 27
 Sáenz-Díez, 452
 Salvatori, 434
 Santucci, 216
 Sauer, 32
 Schaller, 271
 Scheibenpflug, 368
 Schiller, 115
 Schütz, 21
 Schumann, 293
 Selberherr, 156
 Sementa, 328
 Senkerik, 396, 458
 Sentocnik, 283
 Shi S., 121
 Shi W., 121
 Shpungin, 68
 Silva, 144
 Silvestri, 334
 Slaninova, 169
 Slowacki, 549
 Solis, 610
 Songmene, 80
 Sorge, 346
 Sperka, 169
 Stanojevic, 156
 Stekel, 265, 340
 Stummer, 90
 Stylios, 150
 Sverdlov, 156
 Takizawa, 138
 Tanaka, 138
 Tao, 38
 Tauböck, 537
 Thien-My, 477
 Tomažič, 283
 Torres-Jardón, 210
 Toy, 50
 Tremori, 584
 Tufano, 256
 Tunali, 44
 Turi, 573
 Ukovich, 150

Urbani, 216
Urbonaite, 501
Ustundag, 241
Vaglieco, 346
Valtýsdóttir, 163
Vasconcelos, 428
Viamonte, 144
Vindel, 303
Vittori, 216
Vymetal, 169
Wagner, 265 340, 368
Wassertheurer, 316, 322
Weghuber, 271
Wei, 109
Wellens, 210
Wiedemann, 176
Wiegand, 537
Wiesinger, 21, 74, 115
Wild, 489, 507
Winkler S.M., 265, 271, 340, 362
Winkler S., 489, 501, 525
Wurzer, 519
Yilmaz, 277
Zagorskis, 408
Zelinka, 396458
Zennir, 103
Zhang G., 121
Zhang, J.138
Zhang L., 38
Zhou, 109